Qiaohong Zu
Bo Hu
Atilla Elçi (Eds.)

LNCS 7719

Pervasive Computing and the Networked World

Joint International Conference, ICPCA/SWS 2012
Istanbul, Turkey, November 2012
Revised Selected Papers

Springer

Lecture Notes in Computer Science 7719

Commenced Publication in 1973
Founding and Former Series Editors:
Gerhard Goos, Juris Hartmanis, and Jan van Leeuwen

Qiaohong Zu Bo Hu Atilla Elçi (Eds.)

Pervasive Computing and the Networked World

Joint International Conference, ICPCA/SWS 2012
Istanbul, Turkey, November 28-30, 2012
Revised Selected Papers

Springer

Volume Editors

Qiaohong Zu
Wuhan University of Technology
Heping Road 1178, Wuchang District, Wuhan, Hubei 430081, P.R. China
E-mail: zuqiaohong@foxmail.com

Bo Hu
Fujitsu Laboratories of Europe Ltd.
Hayes Park Central, Hayes End Road, Hayes, Middlesex UB4 8FE, UK
E-mail: bo.hu@uk.fujitsu.com

Atilla Elçi
Aksaray University
Department of Electrical and Electronics Engineering
Merkez Kampüsü, Aksaray 68100, Turkey
E-mail: atilla.elci@gmail.com

ISSN 0302-9743 e-ISSN 1611-3349
ISBN 978-3-642-37014-4 e-ISBN 978-3-642-37015-1
DOI 10.1007/978-3-642-37015-1
Springer Heidelberg Dordrecht London New York

Library of Congress Control Number: 2013933046

CR Subject Classification (1998): C.2.0-1, C.2.4-6, C.5.3, C.3, F.2.2, H.2.8, H.3.3-5, H.5.3, I.2.4

LNCS Sublibrary: SL 5 – Computer Communication Networks and Telecommunications

Typesetting: Camera-ready by author, data conversion by Scientific Publishing Services, Chennai, India

Printed on acid-free paper

Springer is part of Springer Science+Business Media (www.springer.com)

Preface

As sensory and mobile products roll out with increasing speed, research foci in pervasive computing are shifting gradually from technology to interaction and coalescence between computing devices on one hand and humans as well as human societies on the other hand. Thus far, the technical merits of pervasive computing are highly appreciated: on-demand, on-device, and on-the-move information access offering unprecedented business and social engagement opportunities. However, neither the resulting mid-term and long-term social impact nor the mechanisms and processes creating that impact are sufficiently understood.

Against this background, the goal of the Joint Conference of ICPCA7 and SWS4 is to bring together people from different research communities (e.g., computer science, sociology, psychology, etc.) to further explore both theoretical and practical issues in and around the emerging computing paradigms, e.g., pervasive collaboration, collaborative business, networked societies.

The ICPCA community has a long history dating back to 2006 when the first conference in the series was held in Urumqi, China. This was followed by five successful events in Birmingham (UK 2007), Alexandria (Egypt 2008), Tamkang (Taiwan 2009), Maribor (Slovenia 2010), and Port Elizabeth (South Africa 2011). SWS reflected the growing interest in understanding how technology infiltrates human society. Past SWS events were held in Lanzhou (China 2009) and Beijing (China 2010). In 2012, the merging of ICPCA and SWS gave birth to a cross-disciplinary forum, Pervasive Computing and Networked World. Its intention is to highlight the unique characteristics of the "everywhere" computing paradigm and promote awareness of its potential social and psychological consequences.

This year ICPCA7/SWS4 received 143 submissions from authors in 10 countries. All papers were peer-reviewed by Program Committees whose members are from USA, Canada, Japan, UK, Germany, France, Turkey, Austria, Italy, The Netherland, and China. Based on these recommendations, the Program Co-chairs made acceptance decisions and classified the accepted papers into two categories:

Full papers: 53 papers passed the most stringent selection criteria. Each paper is allocated up to 15 pages in the conference proceedings. The acceptance rate for selected papers is 37%.

Short papers: 26 additional papers were selected because of their good quality. Each paper is allocated up to 4 pages.

We invited two renowned speakers for keynote speeches:

- Albert Levi, Sabanci University, Turkey
- Tingshao Zhu, Chinese Academy of Science, China

Many people contributed to the organization of ICPCA7/SWS4. We would like to take this opportunity to thank those who worked behind the scenes. First, we are

grateful to all members of the Technical Program Committee (TPC). It was their hard work that enabled us to identify a set of high-quality submissions reflecting the trends and interests of the related research fields. We would like to extend our gratitude to the Steering Committee and international Advisory Committee for their invaluable advice and guidance. Our special thank also goes to the non-TPC reviewers, student volunteers, and members of the local organization team who are the key elements that made ICPCA7/SWS4 a successful event.

Last but not least, we would also like to thank all the authors of the submitted papers; we appreciate and sincerely thank you for your contributions.

November 2012

Qiaohong Zu
Bo Hu
Atilla Elçi

Organization

Honorary Chairs

Mustafa Aydin	Chairman of The board of Trustees of Istanbul Aydin University, Turkey
Yadigar İzmirli	Rector of Istanbul Aydin University, Turkey

General Conference Chairs

Hai Jin	Huazhong University of Science and Technology, China
Atilla Elçi	Aksaray University, Turkey

Steering Committee

Lin, Zongkai	ICT, CAS, China
Bin Hu	Lanzhou University, China
Vic Callaghan	University of Essex, UK
Bo Hu	Fujitsu Laboratories of Europe Limited, UK

Organizing Committee Co-chairs

Ali Güneş	Istanbul Aydin University, Turkey
Osman Nuri Uçan	Istanbul Aydin University, Turkey
Duygu Çelik	Istanbul Aydin University
Qiaohong Zu	Wuhan University of Technology, China

International Advisory Committee

Alcaiz, Mariano	Human Lab, Technical University of Valencia, Spain
Baldoni, Roberto	University of Rome "La Sapienza", Italy
Callaghan, Vic	University of Essex, UK
Chen, Dingfang	Wuhan University of Technology, China
Chen, Li	A*STAR, Singapore
Compatangelo, Ernesto	University of Aberdeen, UK
Greiner, Russ	University of Alberta, Canada
Greunen, Darelle van	NMMU, South Africa

Guo, Yurong	Temple University, USA
Gutknecht, Jörg	ETH Zurich, Switzerland
He, Daqing	University of Pittsburgh, USA
Holzinger, Andreas	TU-Graz, Austria
Hu, Bin	Lanzhou University, China
Li, Kuan-Ching	Providence University, Taiwan
Lin, Zongkai	ICT, CAS, China
Lindner, Maik	SAP Research, USA
Luo, Junzhou	Southeast University, China
Malyshkin, Victor	Russian Academy of Science, Russia
Majoe, Dennis	ETH Zurich, Switzerland
Reynolds, Paul	France Telecom, France
Riss, Uwe	SAP Research, Germany
Shi, Yuanchun	Tsinghua University, China
Song, Junde	Beijing University of Posts and Telecommunications, China
Salvadores, Manuel	Stanford University, USA
Terada, Tsutomu	Osaka University, Japan
Wang, Shaojun	Wright State University, USA
Zhang, Yanchun	Victoria University, Australia
Zhu, Tingshao	Chinese Academy of Science, China
Zou, Gang	ST-Ericsson, Sweden

Publication Co-chairs

Jizheng Wan	Birmingham University, UK
Bo Hu	Fujitsu Laboratories of Europe Limited, UK

Program Committee

Natasha Alechina	University of Nottingham, UK
Angeliki Antoniou	University of the Peloponnese, Greece
Juan Carlos Augusto	University of Ulster, UK
Roberto Barchino	University of Alcala, Spain
Paolo Bellavista	DEIS - University of Bologna, Italy
Adam Belloum	Universiteit van Amsterdam, The Netherlands
Luis Carriço	University of Lisbon, Portugal
Yiqiang Chen	Chinese Academy of Science, China
Tianzhou Chen	Zhejiang University, China
Aba-Sah Dadzie	University of Sheffield, UK
Marco De Sá	University of Lisbon, Portugal
Luhong Diao	Beijing University of Technology, China
Monica Divitini	IDI-NTNU, Norway
Talbi El-Ghazali	University of Lille, France

Henrik Eriksson	Linköping University, Sweden
Xiufen Fu	Guangdong University of Technology, China
Mauro Gaspari	University of Bologna, Italy
Bin Gong	Shandong University, China
Horacio Gonzalez-Velez	National College of Ireland, Ireland
José María Gutiérrez	University of Alcala, Spain
Fazhi He	Wuhan University, China
Bin Hu	Birmingham City University, UK
Changqin Huang	Zhejiang University, China
Wenbin Jiang	Huazhong University of Science and Technology, China
M. Lourdes Jimenez	University of Alcala, Spain
Hai Jin	Huazhong University of Science and Technology, China
Romain Laborde	IRIT/SIERA, France
Thomas Lancaster	Birmingham City University, UK
Victor Landassuri-Moreno	University of Birmingham, UK
Bo Lang	Beihang University, China
Aggelos Lazaris	University of Southern California, USA
Wenfeng Li	Wuhan University of Technology, China
Shaozi Li	Xiamen University, China
Hua Li	Chinese Academy of Sciences, China
Xiaofei Liao	Huazhong University of Science and Technology, China
Hong Liu	Shandong Normal University, China
Yongjin Liu	Tsinghua University, China
Shijun Liu	Shandong University, China
Junzhou Luo	Southeast University, China
Yasir Malkani	University of Sussex, UK
Mohamed Menaa	University of Birmingham, UK
Marek Meyer	Technische Universität Darmstadt, Germany
Maurice Mulvenna	University of Ulster, UK
Mario Muñoz	Universidad Carlos III de Madrid, Spain
Tobias Nelkner	Universität Paderborn, Germany
Sabri Pllana	University of Vienna, Austria
Klaus Rechert	University of Freiburg, Germany
Andreas Schrader	ISNM - International School of New Media at the University of Luebeck, Germany
Stefan Schulte	Technische Universität Darmstadt, Germany
Beat Signer	Vrije Universiteit Brussel, Belgium
Junde Song	Beijing University of Posts and Telecommunications, China
Mei Song	Beijing University of Posts and Telecommunications, China
Meina Song	Beijing University of Posts and Telecommunications, China

Yuqing Sun	Shandong University, China
Xianfang Sun	Cardiff University, UK
Xianping Tao	Nanjing University, China
Shaohua Teng	Guangdong University of Technology, China
Yan Huang	Cardiff University, UK
Yunlan Wang	Northwestern Polytechnical University, China
Qianping Wang	China University of Mining and Technology, China
Hongan Wang	Chinese Academy of Science, China
Yun Wang	Southeast University, China
Hans Friedrich Witschel	FHNW, Switzerland
Gang Wu	Shanghai Jiaotong University, China
Toshihiro Yamauchi	Okayama University, Japan
Yanyan Yang	University of Portsmouth, UK
Yanfang Yang	Wuhan University of Technology, China
Chenglei Yang	Shandong University, China
Chen Yu	Japan Advanced Institute of Science and Technology, Japan
Xiaosu Zhan	Beijing University of Posts and Telecommunications, China
Yong Zhang	Beijing University of Posts and Telecommunications, China
Gansen Zhao	South China Normal University, China
Shikun Zhou	University of Portsmouth, UK
Tingshao Zhu	Chinese Academy of Sciences, China
Zhenmin Zhu	Chinese Academy of Sciences, China

Wireless Sensor Network Security: Trends and Challenges

Keynote Talk

Albert Levi

Sabancı University, Faculty of Engineering and Natural Sciences
Computer Science and Engineering Program
Orhanlı, Tuzla, İstanbul, Turkey
levi@sabanciuniv.edu

Abstract. Wireless sensor networks (WSNs) are composed of resource-constrained and tiny sensor nodes with sensing and/or short-range communication capabilities. Due to the limited capacities and capabilities of the sensor nodes, especially due to computational power restrictions, sensor network functionalities must be performed in effective way. Among those, providing security in WSNs requires lightweight solutions with no costly (in terms of memory, communication and computational) mechanisms for the sensor nodes. Moreover, the self-organizing characteristic and distributed nature of WSNs pose extra challenges for the security solutions. Fulfillment of classical security requirements is via lightweight adaptation of classical cryptographic techniques. However, WSNs are vulnerable to other network level and routing related attacks, such as selective forwarding, sinkhole, sybil and wormhole attacks, for which network level solutions are needed in addition to cryptographic solutions. On top of these, a secure and resilient key distribution mechanism is the main enabler of all security solutions.

In the first half of this talk, after a brief introduction to WSNs, major threats and proposed security solutions for WSNs will be discussed. In the second half of the talk, the relevant research results of the presenter, which includes thwarting network-level spamming, key distribution in single and multiphase static WSNs and mobile WSNs will be summarized.

Computational CyberPsychology
Keynote Talk

Tingshao Zhu

Institute of Psychology, Chinese Academy of Sciences
Beijing, China
tszhu@psych.ac.cn

Abstract. In the past few years, Internet has become increasingly popular. Because of its richness in personal daily information available from large and diverse population, Internet has been regarded as an ideal laboratory for conducting psychological research. In this talk, I will introduce our work on behavior analysis on the web and mobile devices. We propose to train psychological computing models based on user behavior.

Personality plays a key role in human behavior, including web behavior. We propose to predict web user's personality based on her/his web behavior on Sina Weibo (a leading microblog service provider in China, http://weibo.com). We recruit 563 participants, and measure their personality with Big Five Inventory. After extracting 845 behavioral features from the usage data, we train two continuous value prediction model (ZeroR and GaussianProcesses), with mean absolute error of 0.08-0.11. Further, we train a classifier (SVM) for distinguish high score group and low score group in each personality trait, with the accuracy of 70%-75%. The result demonstrates that web user's personality could be predicted based on his/her Weibo behavior.

We also conduct an user study by recruiting 104 graduate students using Five-Factor Inventory and 75 students using Cattell's 16 Personality Factor Questionnaire simultaneously (dependent variable measurement), and their web behavior were recorded by web gateway automatically (independent variable measurement). Then, computational personality models were built by using machine learning method (Support Vector Machine algorithm). Results indicate that based on either theory of Cattell's 16 personality factors or Five-Factor Personality, computational personality models all have satisfying classification accuracy.

Our preliminary results indicate that it is very promising to build computational psychological models on behavior. I will also present our CBT-based systems for mental health self-help intervention. For more information, please visit us at http://wsi.gucas.ac.cn.

Table of Contents

Online and Offline Determination of QT and PR Interval and QRS Duration in Electrocardiography 1
Martin Bachler, Christopher Mayer, Bernhard Hametner, Siegfried Wassertheurer, and Andreas Holzinger

Predicting Reader's Emotion on Chinese Web News Articles 16
Shuotian Bai, Yue Ning, Sha Yuan, and Tingshao Zhu

Clustering Algorithm Based on Triple-Stranded and 3-armed DNA Model 28
Xue Bai, Xiaoling Ren, and Xiyu Liu

Synthesis of Real-Time Applications for Internet of Things 35
Sławomir Bąk, Radosław Czarnecki, and Stanisław Deniziak

iScope – Viewing Biosignals on Mobile Devices 50
Christian Breitwieser, Oliver Terbu, Andreas Holzinger, Clemens Brunner, Stefanie Lindstaedt, and Gernot R. Müller-Putz

CloudSVM: Training an SVM Classifier in Cloud Computing Systems 57
F. Ozgur Catak and M. Erdal Balaban

A Document-Based Data Warehousing Approach for Large Scale Data Mining 69
Hualei Chai, Gang Wu, and Yuan Zhao

Smart Navigation for Firefighters in Hazardous Environments: A Ban-Based Approach 82
Mhammed Chammem, Sarra Berrahal, and Nourreddine Boudriga

Personalized Recommendation Based on Implicit Social Network of Researchers 97
Cheng Chen, Chengjie Mao, Yong Tang, Guohua Chen, and Jinjia Zheng

Effect on Generalization of Using Relational Information in List-Wise Algorithms 108
Guohua Chen, Yong Tang, Feiyi Tang, Shijin Ding, and Chaobo He

The Optimization of Two-Stage Planetary Gear Train Based on Mathmatica 122
Tianpei Chen, Zhengyan Zhang, Dingfang Chen, and Yongzhi Li

Mobi-CoSWAC: An Access Control Approach for Collaborative Scientific Workflow in Mobile Environment 137
Zhaocan Chen, Tun Lu, Tiejiang Liu, and Ning Gu

A Survey of Learning to Rank for Real-Time Twitter Search 150
Fuxing Cheng, Xin Zhang, Ben He, Tiejian Luo, and Wenjie Wang

An Ontology-Based Information Extraction Approach for Résumés 165
Duygu Çelik and Atilla Elçi

Measure Method and Metrics for Network Characteristics in Service Systems 180
Haihong E, Xiaojia Jin, Junjie Tong, Meina Song, and Xianzhong Zhu

AIM: A New Privacy Preservation Algorithm for Incomplete Microdata Based on Anatomy 194
Qiyuan Gong, Junzhou Luo, and Ming Yang

An Overview of Transfer Learning and Computational CyberPsychology 209
Zengda Guan and Tingshao Zhu

A Formal Approach to Model the Interaction between User and AmI Environment 216
Jian He and Fan Yu

Multi-Robot Traveling Problem Constrained by Connectivity 231
Cheng Hu, Yun Wang, and Fei Ben

An Application Study on Vehicle Routing Problem Based on Improved Genetic Algorithm 246
Shang Huang, Xiufen Fu, Peiwen Chen, CuiCui Ge, and Shaohua Teng

Cost-Effective and Distributed Mobility Management Scheme in Sensor-Based PMIPv6 Networks with SPIG Support 259
Soonho Jang, Hana Jang, and Jongpil Jeong

The Research on Virtual Assembly Technology and Its Application Based on OSG 274
Jia Li, Guojin Li, Wen Hou, Li Wang, Yanfang Yang, and Dingfang Chen

An Enhanced Security Mechanism for Web Service Based Systems 282
Wenbin Jiang, Hao Dong, Hai Jin, Hui Xu, and Xiaofei Liao

Data-Apart Hybrid Centralized Scheduling in Coordinated Multi-Point System with Non-ideal Backhaul Link 297
Huiqin Li, Wenan Zhou, Xiaotao Ren, Xianqi Lu, and Guowei Wang

Geo-Ontology-Based Object-Oriented Spatiotemporal Data Modeling ... 302
Jingwen Li, Yanyan Liang, and Jizheng Wan

A New Object-Oriented Approach towards GIS Seamless Spatio-Temporal Data Model Construction ... 318
Jingwen Li, Jizheng Wan, Yanling Lu, Junren Chen, and Yu Fu

Mechanical Research of the Planet Carrier in Wind Turbine Gear Increaser Based on Co-simulation of ADAMS-ANSYS ... 332
Taotao Li, Dingfang Chen, Pengfei Long, Zhengyan Zhang, Jiquan Hu, and Jinghua Zhang

PAPR Reduction for 802.16e by Clipping and Tone Reservation Based on Amplitude Scale Factor ... 339
Tianjiao Liu, Xu Li, Cheng Chen, Shulin Cui, and Ying Liu

A DCaaS Model of DNA Computing for Solving a Class of Nonlinear Problems ... 350
Xiyu Liu, Laisheng Xiang, and Xiaolin Yu

How to Dynamically Protect Data in Mobile Cloud Computing? ... 364
Hongliang Lu, Xiao Xia, and Xiaodong Wang

Enriching Context-Oriented Programming with Structured Context Representation ... 372
Jun Ma, Xianping Tao, Tao Zheng, and Jian Lu

Analysis of the Square Pillar Electromagnetic Scattering under the PML Absorbing Boundary Condition ... 389
Xiangfang Mao, Jie Jin, and Jinsheng Yang

A Framework Based on Grid for Large-Scale Risk Files Analysis ... 396
Jiarui Niu, Bin Gong, and Song Li

A Cache-Sensitive Hash Indexing Structure for Main Memory Database ... 400
Xiaoqing Niu, Xiaojia Jin, Jing Han, Haihong E, and Xiaosu Zhan

SCADA System Security, Complexity, and Security Proof ... 405
Reda Shbib, Shikun Zhou, and Khalil Alkadhimi

Cranduler: A Dynamic and Reusable Scheduler for Cloud Infrastructure Service ... 411
Xuanhua Shi, Bo Xie, Song Wu, Hai Jin, and Hongqing Zhu

Multi-objective Virtual Machine Selection for Migrating in Virtualized Data Centers ... 426
Aibo Song, Wei Fan, Wei Wang, Junzhou Luo, and Yuchang Mo

Study on Virtual Simulation of the New Screw Pile Hammers Based on a Combination of Multi-software Platforms 439
Yangyang Su, Li Bo, and Dingfang Chen

The Interference Effect of Group Diversity on Social Information Foraging 447
Guichuan Sun, Wenjun Hou, and Yu Cui

Hierarchical Clustering with Improved P System 454
Jie Sun and Xiyu Liu

A New Positioning Algorithm in Mobile Network 461
Shaohua Teng, Shiyao Huang, Yingxiang Huo, Luyao Teng, and Wei Zhang

Performance Analysis with Different Sensing Results in the Cognitive Radio Networks 477
Yinglei Teng, Yanan Xiao, Gang Cheng, Yong Zhang, and Mei Song

QoS Routing for LEO Satellite Networks 482
Aida Nathalie Urquizo Medina and Gao Qiang

A Slot Assignment Algorithm Based on Nodes' Residual Energy 495
Qianping Wang, Xiang Xu, Jin Liu, and Liangyin Wang

Heterogeneity-Aware Optimal Power Allocation in Data Center Environments 513
Wei Wang, Junzhou Luo, Aibo Song, and Fang Dong

A Discussion on Intelligent Management System for Centralized Plotting and Filing of Railway Design Institute 529
Xiangqing Wang, Dingfang Chen, and QiaoHong Zu

Optimizing Interactive Performance for Desktop-Virtualization Environment 541
Xiaolin Wang, Binbin Zhang, and Yingwei Luo

Design and Implementation of Clusters Monitor System Based on Android 556
Yan Wang, Bin Gong, and Song Li

An Empirical Comparative Study of Decentralized Load Balancing Algorithms in Clustered Storage Environment 562
Yun Wang, Xiangyu Luo, Feifei Yuan, and Cong Li

A Contact-History Based Routing for Publish-Subscribe Scheme in Hierarchical Opportunistic Networks 575
Zhen Wang, Yong Zhang, Mei Song, Yinglei Teng, and Baoling Liu

Study of E-commerce-Based Third-Party Logistics Alliance System 586
Zhengguo Wang, Guoqian Jiang, and Hanbin Xiao

A Fast Indexing Algorithm Optimization with User Behavior Pattern ... 592
Zhu Wang, Tiejian Luo, Yanxiang Xu, Fuxing Cheng, Xin Zhang, and Xiang Wang

An FPGA Real-Time Spectrum Sensing for Cognitive Radio in Very High Throughput WLAN 606
Zhigang Wen, Zibo Meng, Qing Wang, Lihua Liu, Junwei Zou, and Li Wang

Trust Services-Oriented Multi-Objects Workflow Scheduling Model for Cloud Computing 617
Wenan Tan, Yong Sun, Guangzhen Lu, Anqiong Tang, and LinShan Cui

Scalable SPARQL Querying Processing on Large RDF Data in Cloud Computing Environment 631
Buwen Wu, Hai Jin, and Pingpeng Yuan

Iterative Receiver with Joint Channel Estimation and Decoding in LTE Downlink 647
Weijie Xiao, Qiong Li, Xinxue Zhao, and Qiang Gao

The Research and Design of an Applied Electronic Lottery System 653
Yuhong Xing

Scheme of Cognitive Channel Allocation for Multiple Services without Spectrum Handover 659
Haoman Xu, Yinglei Teng, Mei Song, Yifei Wei, and Yong Zhang

A Content Aware and Name Based Routing Network Speed Up System 672
Ke Xu, Hui Zhang, Meina Song, and Junde Song

Solving Directed Hamilton Path Problem in Parallel by Improved SN P System 689
Jie Xue and Xiyu Liu

Application of TDMI in Government Informatization 697
Liyou Yang, Hongyu Zhao, and Yongqiang Wang

Design of Control System for Hydraulic Lifting Platform with Jack-Up Wind-Power Installation Vessel 711
Xuejin Yang, Dingfang Chen, Mingwang Dong, and Taotao Li

Research on Motion Control Technology for Virtual Assembly Platform 719
Yanfang Yang, Wengeng Guo, Jia Li, and Dingfang Chen

Efficient Data Collection with Spatial Clustering in Time Constraint WSN Applications 728
Zhimin Yang, Kaijun Ren, and Chang Liu

The Effect of Critical Transmission Range in Epidemic Data Propagation for Mobile Ad-hoc Social Network 743
Hong Yao, Huawei Huang, Qingzhong Liang, Chengyu Hu, and Xuesong Yan

Waveform Decreasing Multi-copy Based Routing in Low Node Density DTNs 757
Chen Yu, Longbo Zhang, and Hai Jin

Research on Cooperative Scheduling at Container Terminal under Uncertainties 769
Meng Yu, Yun Cai, and Zhangye Zhao

A New Hyper-parameters Selection Approach for Support Vector Machines to Predict Time Series 775
Yanhua Yu, Junde Song, and Zhijun Ren

Location Context Aware Collective Filtering Algorithm 788
Wenjun Yue, Jing Han, Haihong E, and Meina Song

Clustering Analysis Research Based on DNA Genetic Algorithm 801
Wenke Zang, Xiyu Liu, and Yanlong Wang

Massive Electronic Records Processing for Digital Archives in Cloud 814
Guigang Zhang, Sixin Xue, Huiling Feng, Chao Li, Yuenan Liu, Yong Zhang, and Chunxiao Xing

Research and Analysis of Method of Ranking Micro-blog Search Results Based on Binary Logistic Model 830
Jing Zhang and Wenjun Hou

A Kinect Based Golf Swing Reorganization and Segmentation System 843
Lichao Zhang, Jui-Chien Hsieh, and Shaozi Li

An EEG Based Pervasive Depression Detection for Females 848
Xiaowei Zhang, Bin Hu, Lin Zhou, Philip Moore, and Jing Chen

Opportunistic Networks Architecture with Fixed Infrastructure Nodes 862
Yong Zhang, Zhen Wang, Jin Li, Mei Song, Yinglei Teng, and Baolin Liu

An Improved DNA Computing Method for Elevator Scheduling Problem 869
Hong-Chao Zhao and Xiyu Liu

Campus Network Operation and Maintenance Management and Service Based on ITIL Service Desk 876
Hong-yu Zhao, Yong-qiang Wang, Xue-yan Zhang, and Li-you Yang

Research on the Application of the P System with Active Membranes in Clustering 883
Yuzhen Zhao, Xiyu Liu, and Jianhua Qu

Enhanced ALOHA Algorithm for Chirp Spread Spectrum Positioning 891
Zhengwen Yang, Qiang Wu, Yongqiang Lu, Pei Lu, Yinghong Hou, and Manman Peng

A Case Study of Integrating IoT Technology in Bridge Health Monitoring 904
QiaoHong Zu and Xingyu Xu

Author Index 919

Online and Offline Determination of QT and PR Interval and QRS Duration in Electrocardiography

Martin Bachler[1,2], Christopher Mayer[2], Bernhard Hametner[2], Siegfried Wassertheurer[2], and Andreas Holzinger[3]

[1] Vienna University of Technology, Institute for Analysis and Scientific Computing, Wiedner Hauptstr. 8, 1040 Vienna, Austria
Martin.Bachler@student.tuwien.ac.at
[2] AIT Austrian Institute of Technology, Health & Environment Department, Donau-City-Strasse 1, 1220 Vienna, Austria
[3] Institute of Medical Informatics, Statistics & Documentation, Medical University Graz, Auenbruggerplatz 2, A-8036 Graz, Austria

Abstract. Duration and dynamic changes of QT and PR intervals as well as QRS complexes of ECG measurements are well established parameters in monitoring and diagnosis of cardiac diseases. Since automated annotations show numerous advantages over manual methods, the aim was to develop an algorithm suitable for online (real time) and offline ECG analysis. In this work we present this algorithm, its verification and the development process.

The algorithm detects R peaks based on the amplitude, the first derivative and local statistic characteristics of the signal. Classification is performed to distinguish premature ventricular contractions from normal heartbeats. To improve the accuracy of the subsequent detection of QRS complexes, P and T waves, templates are built for each class of heartbeats.

Using a continuous integration system, the algorithm was automatically verified against PhysioNet databases and achieved a sensitivity of 98.2% and a positive predictive value of 98.7%, respectively.

Keywords: Electrocardiography, ECG, QRS complex, P wave, T wave, QT interval, PR interval, real time.

1 Introduction

Coronary heart diseases are the most common cause of death in Europe [1] and the second most in the United States, respectively [2]. In the diagnosis and monitoring of these diseases, electrocardiography (ECG) plays an important role. ECG measurements can be recorded fairly easily using skin electrodes on the chest or limbs and thus are widespread, non-invasive and painless [3].

The shape of one heartbeat in an ECG signal can be divided into a P wave representing the atrial depolarization, a QRS complex indicating the ventricular depolarization and a T wave displaying the ventricular repolarisation [4].

Q. Zu, B. Hu, and A. Elçi (Eds.): ICPCA-SWS 2012, LNCS 7719, pp. 1–15, 2013.

Segments and intervals between these features are well defined and established indicators in the diagnosis of cardiac diseases [4]. The most important of these intervals are [4]

- the PR interval, ranging from the beginning of the P wave to the beginning of the QRS complex,
- the QT interval, starting from the onset of the QRS complex to the offset of the T wave, and
- the duration of the QRS complex itself, ranging from the onset to the offset of the QRS complex.

Additionally, some non-antiarrhythmic drugs are found to cause an undesired prolongation of the QT interval. Therefore newly developed drugs are required to be assessed with respect to this effect [5]. The automation of the annotation of the ECG using signal analysis algorithms offers several advantages over manual methods. They are immune to observer related errors and operator fatigue, show higher accuracy in repeated measurements or allow for a faster or more extensive testing at lower cost.

A lot of ECG analysis methods have been developed in the last decades. Especially the rapid development of powerful computing hardware led to a widespread application of software ECG annotation algorithms in the last 30 years. Despite the usage of many different approaches such as signal derivatives [6], digital filters, wavelets and neural networks, most methods focus only on the detection of the QRS complex [7]. Other software algorithms combine existing QRS detectors with the evaluation of QT intervals [8,9] or P waves [10], but these methods are only suitable for offline ECG analysis. The challenge of correctly classifying biomedical signals is widespread and can be found, for example, in similar ways in the field of EEG analysis [11]. This paper presents an algorithm combining some of these methods and adopting them for online (real time) measurements.

2 Development Process

In this work we are addressing two fields of application of ECG annotation at the same time. One is the analysis of previously recorded signals using a common personal computer (offline) and the other one is the detection of features in the ECG in real time using an embedded system (online, real time). To avoid unnecessary complexity during the development process, we combined the work towards these goals as long as possible. Also, to relief the developer of repetitive tasks, we utilised the continuous integration system *Jenkins* [12,13]. Figure 1 shows the process of development split into its stages.

2.1 Offline Prototyping

The actual algorithm was developed and tested using the scientific computing environment MATLAB® as the first step of the process. MATLAB® allows easy matrix and vector manipulations, therefore it is perfectly suited for the

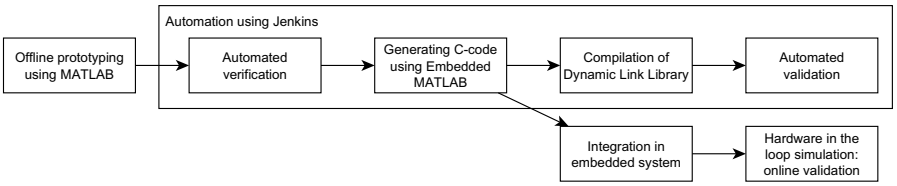

Fig. 1. Overview of the development process

rapid development of signal processing algorithms. Also, it can interface with other programming languages, including C, thus allowing an easy porting of the developed algorithm to digital signal processors in embedded systems or the compilation of dynamic link libraries (DLLs). Besides, MATLAB® allows the automation of the verification process using its scripting features, making it easy to integrate with continuous integration systems.

2.2 Continuous Integration Using Jenkins

Continuous integration tools help to implement "best practices" in software development by automating the whole building process (code generation, compilation, testing and verification) and the documentation thereof [14]. They mainly focus on the principles of centralisation, "test early, test often", automation of build and documentation, and feedback. A continuous integration system usually features

- a version control repository,
- a continuous integration server,
- build scripts, and
- a feedback mechanism.

Version control repositories such as the *Concurrent Versions System* (CVS) or *Apache Subversion* (SVN) keep track of all changes made to the source files during development. The continuous integration system *Jenkins* monitors the CVS or the SVN and starts the building process as soon as a change in the source code is detected.

Automated software tests are performed by *Jenkins* after each successful build. Since developers are encouraged to commit changes in the source code after each single change, these changes are immediately integrated and tested by *Jenkins*. This approach narrows down bug tracking and facilitates to resolve errors [12,14].

2.3 Automated Verification

During the development process, the algorithm was continuously verified against ECG signals manually annotated by medical experts from different PhysioNet

databases [15,16] with respect to sensitivity, positive predictive value and the differences in time between features detected by the algorithm and annotations of the medical experts.

2.4 Generation of C-Code

After the successful verification of the algorithm, C-code was automatically generated from the MATLAB®-code. Since it allows efficient code generation, mainly to be used for embedded systems, but also suitable for ordinary PCs, Embedded MATLAB® was used for this task. It is a subset of the MATLAB® scientific computing language and can be easily automated using scripts. Therefore it was easy to integrate in *Jenkins* [12].

2.5 Compilation and Validation of PC Software

Using a standard C-compiler, a dynamic link library was built from the generated C-code by *Jenkins*.

In the next step, this library was validated using an established software testing environment. To ensure that the results are comparable, the same ECG signals that had been used for the verification were also used for validation. The library was considered to be valid only if the test reported no errors and if the results of verification and software tests matched completely.

2.6 Integration and Validation in the Embedded System

After all automated steps were carried out by the continuous integration system and verification and validation of the library were successfully finished, the C-code was manually integrated in an existing embedded system.

To validate this embedded system, a hardware-in-the-loop simulation was used. At this point, the embedded system was ready to use, but instead of measuring real ECG signals, they were simulated using a signal generator controlled by MATLAB®. In this simulation the signals previously used for verification were reproduced. This approach allows an efficient verification of the results as well as a validation of the final device.

3 Measurement Algorithm

R peaks are the most distinctive feature in ECG signals due to their high amplitude and steep slope. Therefore, they are easy to detect and can be used as a reference for other additional features. Thus, as shown in the overview in figure 2, the first step of the algorithm is to determine the R peaks as starting point for further signal analysis. The measurement algorithm detects R peaks in real time by continuously monitoring the amplitude and the first derivative of the signal [6]. Additionally, statistic characteristics of the signal are evaluated to prevent the algorithm from detecting motion artefacts as R peaks. After the

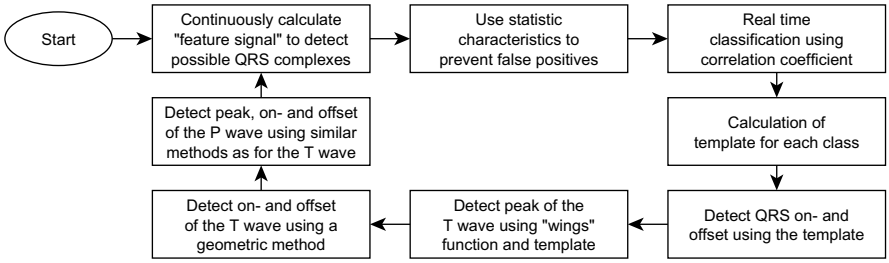

Fig. 2. Overview of the measurement algorithm

identification of an R peak a classification is performed to distinguish between premature ventricular contractions and normal QRS complexes. To reduce noise and enhance the accuracy of the detection of further features, templates are created by averaging each class of R peaks. The template's local amplitude is subsequently used to detect the QRS on- and offset. The peaks of T and P waves are found by analysing the signals first derivative [9]. Finally, the detection of the on- and offsets of T and P waves is based on a geometric method. These steps are described in more detail in the following subsections.

3.1 R Peak Detection

R peaks usually show a high signal amplitude, although sometimes the P wave can have an even higher amplitude. However, in contrast to the P wave, R peaks also show a steep slope of the signal. Therefore, R peaks can be detected by combining amplitude and first derivative of the signal and comparing them to a certain threshold.

To localise R peaks in the ECG tracing, a feature signal is continuously calculated as follows:

- Determine the first discrete derivative D_t of the signal S_t

$$D_t = S_t - S_{t-1}\,. \tag{1}$$

- Calculate amplitudes SA_t of S_t and DA_t of D_t within a moving window (w = 60 ms)

$$SA_t = max\left(S_{(t-w)\ldots t}\right) - min\left(S_{(t-w)\ldots t}\right) \tag{2}$$

$$DA_t = max\left(D_{(t-w)\ldots t}\right) - min\left(D_{(t-w)\ldots t}\right)\,. \tag{3}$$

- Derive C_t as a combination of SA_t and DA_t

$$C_t = SA_t^2 \cdot DA_t\,. \tag{4}$$

- Calculate feature signal FS_t within a moving window (w = 100 ms)

$$FS_t = max\left(C_{(t-w)\ldots t}\right)\,. \tag{5}$$

– Use the mean value of the last 2 seconds of FS_t as threshold Th_t ($w = 2$ s)

$$Th_t = \frac{1}{w} \cdot \sum_{k=t-w}^{t} FS_k \,. \tag{6}$$

– Continue with the signal analysis only if

$$FS_t > Th_t \,. \tag{7}$$

Figure 3 shows different ECG signals with noise, small artefacts, high T waves and motion artefacts with their corresponding feature signals. The feature signal is robust regarding noise, small artefacts and prominent T waves, but does respond to sudden motion of the subject.

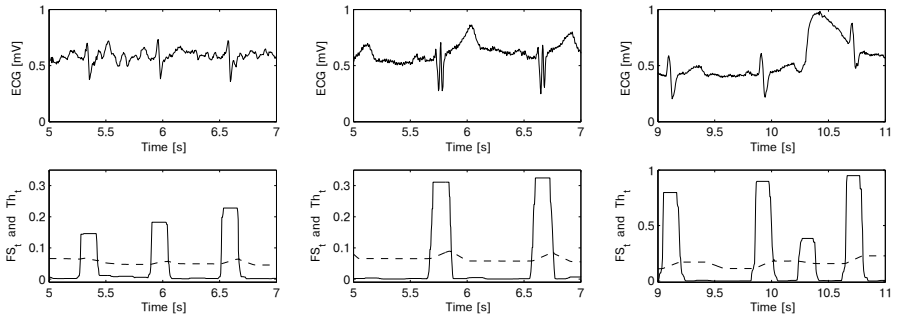

Fig. 3. Differently shaped ECG signals (top) and the response of feature signal FS_t (equation 5, bottom, solid line) and threshold Th_t (equation 6, dashed line)

Whenever the condition in equation 7 is fulfilled, the following statistic parameters are calculated. If these criteria are not reached, the evaluated part of the signal is considered as an artefact:

– Standard deviation σ within the last 400 ms

$$FS_t > Th_t + 6 \cdot \sigma^3 \,. \tag{8}$$

– Kurtosis β_2 within the last 2.5 seconds

$$\beta_2 > 4 \,. \tag{9}$$

To find the R peak within each region of the QRS complex, local minima and maxima are calculated. The exact position of the R peak is chosen at the maximum with the biggest difference to its surrounding minima.

After the detection of more than two R peaks, a template is built by averaging them (see figure 4 (b) for an example). The correlation of the newly detected R

peak with the template is calculated to measure the similarity. If the correlation is below a certain threshold, the R peak is discarded.

To avoid false negative detections, the RR interval (interval between two consecutive R peaks) is calculated. If it exceeds 1.8 times the previous RR interval, this intermediate section is searched again, but with lower thresholds.

Subsequently, a real time classification of the R peaks is performed. The tracing of the last detected heartbeat is correlated with a predefined number of classes and is assigned to the class with the highest correlation. In the case that classes correlate better among each other than with the last detected heartbeat, these two classes are merged and a new class is created from the current heartbeat. Thus, in the real time version of the algorithm, classes evolve dynamically over time, continuously enhancing with the duration of the measurement. Figure 4 (a) shows the result of the classification of an ECG signal with pulsus bigeminus, a cardiovascular phenomenon where every second heartbeat is caused by a premature ventricular contraction [17]. The figure shows a complete separation of these two classes of heartbeats.

Furthermore, templates are created by averaging each class to reduce noise. Figure 4 (b) shows the template of a particularly noisy signal. As the level of noise exceeds the amplitude of the P wave, it would be impossible to detect this feature without the template. Therefore, the templates are used to detect all subsequent features (QRS on- and offset, P and T wave as well as their on- and offsets).

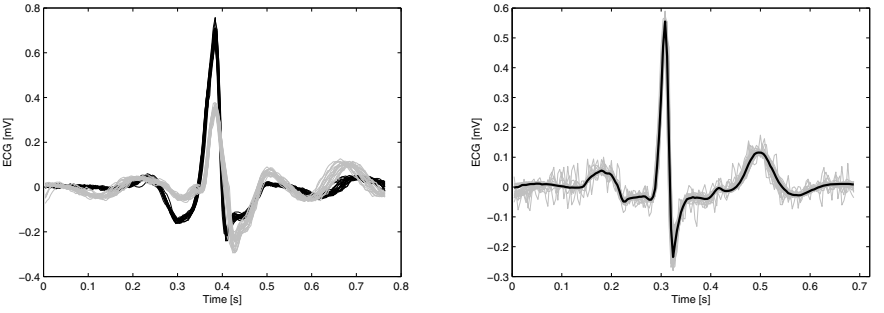

(a) (b)

Fig. 4. (a) Result of the real-time classification of an ECG signal with pulsus bigeminus (every second heartbeat is a premature ventricular contraction [17]). (b) Template (black) of several heartbeats (grey) in a noisy signal.

3.2 On- and Offset of the QRS Complex

The onset of the QRS complex is the the point preceding the R peak, where the signal's slope is flat and its amplitude approaches the baseline. Similarly, the offset shows the same qualities after the R peak. Therefore, amplitude and first derivative of the signal are suitable measures to determine these points.

An interval of 150 ms right before the R peak is analysed to detect the onset of the QRS complex. This analysis is performed using the template as follows:

- Calculate the amplitudes TA_t and TDA_t of the template T_t and its first discrete derivative within a moving window ($w = 30$ ms)

$$TA_t = max\left(T_{(t-w)\ldots t}\right) - min\left(T_{(t-w)\ldots t}\right) \tag{10}$$

$$TDA_t = max\left(T'_{(t-w)\ldots t}\right) - min\left(T'_{(t-w)\ldots t}\right), \text{ whereas} \tag{11}$$

$$T'_t = T_t - T_{t-1}\,. \tag{12}$$

- Calculate a threshold TT and TD for the amplitudes TA_t and TDA_t

$$TT = c_1 \cdot (max\,(TA_t) - min\,(TA_t)) + min\,(TA_t) \tag{13}$$

$$TD = c_2 \cdot (max\,(TDA_t) - min\,(TDA_t)) + min\,(TDA_t) \tag{14}$$

  with c_1 and c_2 being predefined constants.
- The point closest to the R peak, where TA_t is below TT or TDA_t is below TD, is annotated as the QRS onset.

The QRS offset is detected in the same way as the QRS onset, with two exceptions:

- The QRS complex might be pathologically prolonged, therefore a larger interval is chosen to be the analysed.
- In equation 10 and 11, window w is 60 ms.

3.3 Peak of the T Wave

The T wave succeeds the QRS complex. The amplitude of its peak differs considerably from the baseline, however no general statement can be given about its absolute values or the amplitude relative to the R peak. Also, its polarity depends on the location of measurement of the ECG signal [4]. Therefore, a function detecting peaks independently of their polarity has to be used for the detection of the peak of the T wave.

A special "wings" function W, described by Christov and Simova [9], is used to detect the peak of the T wave. It is calculated as follows ($w = 40$ ms):

$$W1_t = T_{t-w} - T_t \tag{15}$$

$$W2_t = T_t - T_{t+w} \tag{16}$$

$$W_t = W1_t \cdot W2_t\,. \tag{17}$$

This "wings" function is calculated for the Template T_t in the interval between the last QRS offset and the end of the template. As shown in Figure 5, the minimum of the "wings" function corresponds to the peak of the T wave, regardless of the polarity of the T wave. Therefore, the point of the minimum of the "wings" function is used as reference for the detection of the T wave's peak. Subsequently, the exact position of the peak is determined on the original signal by finding the next local minimum or maximum, depending on the T wave's polarity.

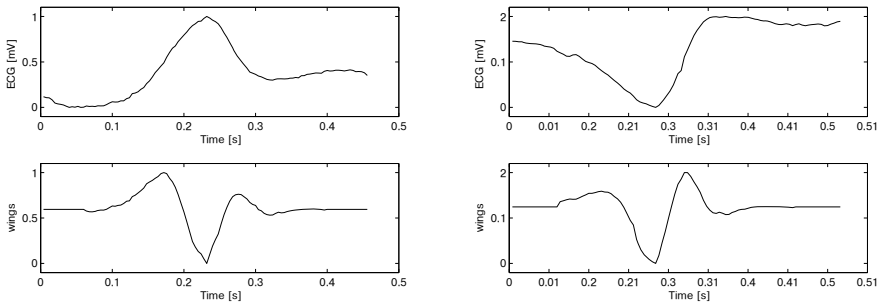

(a) (b)

Fig. 5. Top: differently shaped T waves ((a) positive T wave, (b) negative T wave). Bottom: Corresponding "wings" function.

3.4 On- and Offset of the T Wave

The onset of the T wave precedes the peak of the T wave and is located in the area where the amplitude of the signal approaches the baseline or its slope flattens. The offset succeeds the peak of the T wave in the same way. Since there is no guarantee that the signal's value or first derivative reach certain thresholds, a geometric method is utilised for the detection of these points.

Figure 6 illustrates the geometric method used to detect the onset of the T wave. It is calculated as follows:

– Determine the straight line g_t connecting the QRS offset and the peak of the T wave of the signal S_t:

$$k = \frac{S_{T\_peak} - S_{QRS\_offset}}{T\_peak - QRS\_offset} \tag{18}$$

$$d = S_{QRS\_offset} - k \cdot QRS\_offset \tag{19}$$

$$g_t = k \cdot t + d\,. \tag{20}$$

– Subtract g_t from the signal S_t:

$$S_t^* = S_t - g_t\,. \tag{21}$$

– The minimum of S_t^* is annotated as the onset of the T wave.

The offset of the T wave is determined in the same way by using a straight line between the peak of the T wave and the end of the template.

3.5 P Wave

The P wave precedes the QRS complex and is very similar to the T wave, therefore it can be analysed using similar methods. In contrast to the P wave, it can only have positive polarity and its amplitude is usually very low.

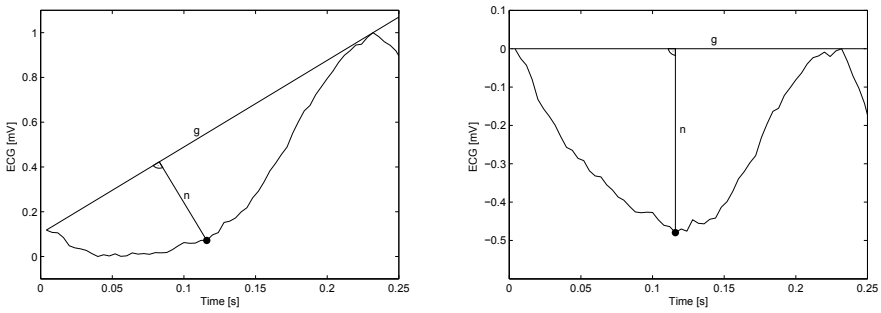

Fig. 6. Geometric method to determine the onset of the T wave. (a) Connecting the QRS offset and the peak of the T wave by the straight line g. Finding the longest line n intersecting g and the signal with a right angle between g and n. (b) Simplification of the calculation by subtraction of g from the signal. The intersection of n with the signal corresponds to the minimum of the signal.

The interval between the previous offset of the T wave and the current onset of the QRS complex is analysed on the template to detect the peak of the P wave. A slightly altered version of the "wings" function (equations 15, 16, and 17), which only reacts to positive waves, is used for this analysis. Onset and offset of the P wave are detected with the same method as on- and offset of the T wave.

4 Differences between Online and Offline Algorithm

Both, the online and the offline version of the algorithm, follow the steps described in the previous section. The only differences are the order of the classification, the calculation of the template for the detected classes, and the available memory.

The online version of the algorithm has no information about future signal values, therefore the classification is performed every time an R peak is detected. Also, the template is rebuilt whenever a class receives new information, thus after each new R peak. Hence, in the beginning of the measurement, the online algorithm has very little information about possible different waveforms to be analysed. In the first few seconds, the template is built based on only a few heartbeats and therefore cannot develop its full capabilities of signal smoothing and noise reduction. As the measurement continues the online version of the algorithm receives more information and produces better results.

The offline version of the algorithm on the other hand is able to analyse the whole signal at once. It classifies all detected heartbeats prior further investigation and is thus able to build the template from all available information. Therefore, the quality of the annotations stays constant throughout the whole measurement.

Considering the memory available for the analysis, the offline version of the algorithm has the advantage of being carried out on an ordinary personal computer. It can receive an arbitrary amount of memory and can access all values of the signal at any time. Contrary, the online version of the algorithm is designed to be used on an embedded system with very limited amount of memory. The online algorithm hence will not store all signal values in the memory, but only the templates of the classes based on previously detected heartbeats. Thus, the memory needed depends only on the numbers of classes that are to be distinguished. Since this value is predefined, the amount of memory needed by the online version of the algorithm can be predicted and adapted to the resources of the embedded system.

5 Results

The verification of the results of the algorithm was performed by comparing them to the results of medical experts. The PhysioNet databases provide recordings of different physiological modalities and corresponding annotations by medical experts, hence these databases are an ideal data source for the verification [15,16].

Due to the different original purpose of these databases, the amount and quality of these annotations varies. After assessing the signals and the annotations, the following four databases were chosen for the verification:

- QT Database, created to evaluate algorithms detecting the QT interval [18].
- AF Termination Challenge Database, designed to be used in the "Computers in Cardiology Challenge 2004" [19].
- MIT-BIH Arrhythmia Database, test material for evaluation of arrhythmia detectors [20].
- Fantasia Database, originally used for testing automated arrhythmia detection [21].

All four databases where used in the assessment of the detection rate of R peaks of the algorithm. The following two parameters are recommended by the American National Standards Institute (ANSI) for the evaluation of the detection rate [22]:

- The sensitivity Se

$$Se = \frac{TP}{TP + FN} \tag{22}$$

- and the positive predictive value PPV

$$PPV = \frac{TP}{TP + FP}, \tag{23}$$

where TP is the number of true positive, FN the number of false negative and FP the number of false positive detections.

Table 1. Means and standard deviations of differences in time between annotated and detected points as well as between different expert annotations. "Online" refers to the features detected by the online version of the algorithm executed on the embedded system in real time, whereas "Offline" refers to the offline version of the algorithm executed on a PC.

	Online vs. Experts		Offline vs. Expert		Inter-expert diff.	
Feature	μ	σ	μ	σ	μ	σ
P Onset	1.9 ms	19.0 ms	1.2 ms	19.2 ms	*	*
P Peak	0.2 ms	16.1 ms	0 ms	10.3 ms	*	*
P Offset	-0.9 ms	17.9 ms	-0.2 ms	14.1 ms	*	*
QRS Onset	0.5 ms	10.2 ms	-2.2 ms	10.3 ms	3.8 ms	14.2 ms
R Peak	-9.1 ms	14.3 ms	-9.4 ms	14.4 ms	0.1 ms	2.4 ms
QRS Offset	4.3 ms	12.6 ms	8.3 ms	13.6 ms	2.7 ms	17.0 ms
T Onset	24.9 ms	43.4 ms	4.4 ms	45.4 ms	9.5 ms	44.9 ms
T Peak	-3.4 ms	32.9 ms	-1.7 ms	33.9 ms	3.5 ms	30.0 ms
T Offset	-4.0 ms	38.7 ms	0.3 ms	40.4 ms	5.8 ms	39.9 ms

* Annotated by one expert only

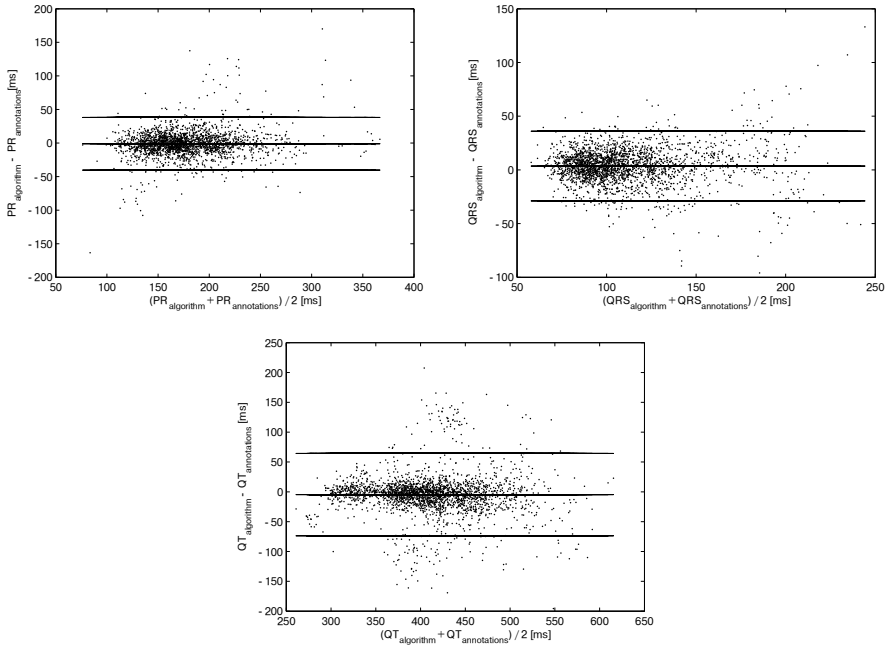

Fig. 7. Bland-Altman diagrams showing the differences between results of the algorithm and results of medical experts

A sensitivity of 98.2% and a positive predictive value of 98.7% were achieved in the verification of the detection rate by the offline as well as the online version of the algorithm.

On- and offset of the QRS complex and P and T wave were only annotated by medical experts in the QT database. Hence, this was the only database used for the verification of these features. The time differences between detected and corresponding annotated points are shown in Table 1.

Finally, the durations of the QT and the PR intervals and the QRS complexes were calculated from the results of the algorithm and the expert annotations, respectively. Figure 7 shows Bland-Altman diagrams comparing the results of the algorithm with those of the medical experts [23]. Means and standard deviations of the differences are -1.1 $\pm$ 10.0 ms for the PR interval, 3.6 $\pm$ 16.5 ms for the QRS complex and -4.7 $\pm$ 35.2 ms for the QT interval. These results are satisfying and match existing offline algorithms [7,8,24].

6 Discussion and Conclusion

The majority of the means of differences found in Table 1 are smaller than the sampling interval of 4 ms, suggesting an insignificant error. The standard deviations of the differences between the results of the medical experts and the algorithm are also very similar to those of inter-expert differences. As they reflect the uncertainty in the annotation of the features among experts, these results suggest that the algorithm performs approximately as well as humans.

Two outliers can be identified in Table 1: The R peak and the T onset. These findings can be traced back to unusual annotations in the QT Database. Sometimes, negative peaks within the QRS complex are marked as R peaks, whereas they ought to be positive by definition. Due to the occasional overlapping of T waves with QRS complexes the exact position of the onset of the T wave can be ambiguous. The comparatively high standard deviation of the inter-expert differences also reflects this fact.

The detection rates of the offline and the online version of the algorithm are identical as both versions use the same detection strategy for R peaks. However, comparing their accuracy as shown in Table 1, the offline algorithm achieves slightly better results. This outcome was to be expected due to the fact that the offline algorithm is able to analyse the whole signal at once whereas the online algorithm has no information about future signal values.

In the analysis of the Bland-Altman diagrams in Figure 7 no trends or shifts can be found, therefore not suggesting any methodical error. Their means are in the range of the sampling interval and therefore indicate only a minimal error. Since the standard deviations are in the same range as those in Table 1, they show no abnormalities.

7 Future Work

The algorithm presented in this paper only works on one ECG signal, thus the next step of the development will be an extension to several ECG leads. This enhancement will allow for a better detection of motion artefacts or even a continuous analysis despite incomplete data. Therefore, the enhanced algorithm

can be used on data from 24 hour ECG measurements. This will allow the evaluation of the heart rate variability (HRV) and dynamic changes in all other detected features and intervals as well as the analysis of the approximate entropy of ECG signals [25].

Acknowledgements. This work was partly supported by a grant of the Government of Lower Austria and the EC (EFRE), contract number WST3-T-81/015-2008.

References

1. Allender, S., Scarborough, P., Peto, V., Rayner, M., Leal, J., Luengo-Fernandez, R., Gray, A.: European cardiovascular disease statistics. Brussels: European Heart Network (2008)
2. Roger, V.L., Go, A.S., Lloyd-Jones, D.M., Adams, R.J., Berry, J.D., Brown, T.M., Carnethon, M.R., Dai, S., de Simone, G., Ford, E.S., et al.: Heart disease and stroke statistics–2011 update: A report from the american heart association. Circulation 123(4), e18–e209 (2011)
3. Rangayyan, R.M.: Biomedical Signal Analysis: A Case-Study Approach. IEEE Press (2002)
4. Luthra, A.: ECG made easy. Jaypee Brothers Medical Pub. (2012)
5. U.S. Department of Health and Human Services - Food and Drug Administration and Center for Drug Evaluation and Research (CDER) and Center for Biologics Evaluation and Research (CBER). Guidance for industry: E14 clinical evaluation of qt/qtc interval prolongation and proarrhythmic potential for non-antiarrhythmic drugs. Regulatory Information (October 2005)
6. Chouhan, V.S., Mehta, S.S.: Detection of qrs complexes in 12-lead ecg using adaptive quantized threshold. IJCSNS 8(1), 155 (2008)
7. Köhler, B.U., Hennig, C., Orglmeister, R.: The principles of software qrs detection. IEEE Engineering in Medicine and Biology Magazine 21(1), 42–57 (2002)
8. Hayn, D., Kollmann, A., Schreier, G.: Automated qt interval measurement from multilead ecg signals. In: Computers in Cardiology, pp. 381–384. IEEE (2008)
9. Christov, I., Simova, I.: Fully automated method for QT interval measurement in ECG. In: Computers in Cardiology, pp. 321–324. IEEE (2006)
10. Diery, A., Rowlands, D., Cutmore, T.R.H., James, D.: Automated ecg diagnostic p-wave analysis using wavelets. Computer Methods and Programs in Biomedicine (2010) (in Press, Corrected Proof)
11. Holzinger, A., Scherer, R., Seeber, M., Wagner, J., Müller-Putz, G.: Computational Sensemaking on Examples of Knowledge Discovery from Neuroscience Data: Towards Enhancing Stroke Rehabilitation. In: Böhm, C., Khuri, S., Lhotská, L., Renda, M.E. (eds.) ITBAM 2012. LNCS, vol. 7451, pp. 166–168. Springer, Heidelberg (2012)
12. Bachler, M., Hametner, B., Mayer, C., Kropf, J., Gira, M., Wassertheurer, S.: Automated verification of cardiovascular models with continuous integration tools. In: Breitenecker, F., Bruzzone, A., Jimenez, E., Longo, F., Merkuryev, Y., Sokolov, B. (eds.) The 24th European Modeling & Simulation Symposium, pp. 316–321. DIME Universitá di Genova (September 2012)
13. Berg, A.: Jenkins Continuous Integration Cookbook. Packt (2012)

14. Duvall, P., Matyas, S., Glover, A.: Continuous integration: improving software quality and reducing risk. Addison-Wesley Professional (2007)
15. Goldberger, A.L., Amaral, L.A.N., Glass, L., Hausdorff, J.M., Ivanov, P.C., Mark, R.G., Mietus, J.E., Moody, G.B., Peng, C.-K., Stanley, H.E.: Physiobank, physiotoolkit, and physionet: Components of a new research resource for complex physiologic signals. Circulation 101(23), e215–e220 (2000), Circulation Electronic Pages, http://circ.ahajournals.org/cgi/content/full/101/23/e215
16. PhysioNet, Physiobank, http://physionet.org/physiobank/database/
17. Iaizzo, P.A.: Handbook of Cardiac Anatomy, Physiology, and Devices. Humana Press, a part of Springer Science+ Business Media, LLC, Totowa, NJ (2009)
18. Laguna, P., Mark, R.G., Goldberg, A., Moody, G.B.: A database for evaluation of algorithms for measurement of qt and other waveform intervals in the ecg. In: Computers in Cardiology 1997, pp. 673–676 (1997)
19. PhysioNet and Computers in Cardiology. Spontaneous termination of atrial fibrillation - a challenge from physionet and computers in cardiology (2004), http://www.physionet.org/challenge/2004/
20. Moody, G.B., Mark, R.G.: The impact of the mit-bih arrhythmia database. IEEE Engineering in Medicine and Biology Magazine 20(3), 45–50 (2001)
21. Iyengar, N., Peng, C.K., Morin, R., Goldberger, A.L., Lipsitz, L.A.: Age-related alterations in the fractal scaling of cardiac interbeat interval dynamics. American Journal of Physiology-Regulatory, Integrative and Comparative Physiology 271(4), R1078–R1084 (1996)
22. Ansi/aami ec57: Testing and reporting performance results of cardiac rhythm and st segment measurement algorithms (October 1998), http://www.aami.org, Order Code: EC57-293
23. Bland, J.M., Altman, D.G.: Statistical methods for assessing agreement between two methods of clinical measurement. The LANCET 1, 307–310 (1986)
24. Schreier, G., Hayn, D., Lobodzinski, S.: Development of a new qt algorithm with heterogenous ecg databases. Journal of electrocardiology 36, 145–150 (2003)
25. Holzinger, A., Stocker, C., Bruschi, M., Auinger, A., Silva, H., Gamboa, H., Fred, A.: On Applying Approximate Entropy to ECG Signals for Knowledge Discovery on the Example of Big Sensor Data. In: Huang, R., Ghorbani, A.A., Pasi, G., Yamaguchi, T., Yen, N.Y., Jin, B. (eds.) AMT 2012. LNCS, vol. 7669, pp. 646–657. Springer, Heidelberg (2012)

Predicting Reader's Emotion on Chinese Web News Articles

Shuotian Bai[1], Yue Ning[1], Sha Yuan[2], and Tingshao Zhu[1,⋆]

[1] Institute of Psychology,
University of Chinese Academy of Sciences, CAS
Beijing 100101, China
tszhu@psych.ac.cn
[2] Institute of Acoustics, CAS,
Beijing 100190, China
{baishutian10,ningyue09,yuansha10}@mails.gucas.ac.cn

Abstract. Currently, more and more information are spreading on the web. These large amounts of information might influence web users' emotion quite a lot, for example, make people angry. Thus, it is important to analyze web textual content from the aspect of emotion. Although much former researches have been done, most of them focus on the emotion of authors but not readers. In this paper, we propose a novel method to predict readers' emotion based on content analysis. We develop an emotion dictionary with a selected weighting coefficient to build text vectors in Vector Space Model, and train Support Vector Machine and Naive Bayesian model for prediction. The experimental results indicate that our approach performs much better on precision, recall and F-value.

Keywords: Reader Emotion, Emotion Classification, Emotion Dictionary.

1 Introduction

More and more information spread on the web with the rapid development of Internet. The amount of online information increases dramatically, including news, blogs, etc.. On one hand, these large amounts of information can meet people's information need with the help of information retrieval techniques; On the other hand, people would like to express their emotion or meet their emotional needs on the web. For example, a severely depressive fan of rock and roll needs heartwarming stories more than rock music. Traditional search engines focus on meeting informational needs to retrieve the music immediately but not heartwarming ones. Therefore, they can not meet the user's emotional needs sometimes.[8]

To identify people emotional needs, we need to identify their emotion after accessing web content, that is, their emotional preference. Emotion plays an important role in human intelligence which helps people adapt to environment,

⋆ Corresponding author.

Q. Zu, B. Hu, and A. Elçi (Eds.): ICPCA-SWS 2012, LNCS 7719, pp. 16–27, 2013.

arouse individual motivation, organize mental activities and smooth the process of interpersonal communication. Contents on the web may trigger different moods of readers, which will influence their life at the end. It is very useful to detect the users affective state, thus to improve the performance and user interfaces of various web applications. Nowadays, affective information is pervasive on the web, especially online news.[23] Although much research have been done on text emotion classification, they focus on the sentiment of content, instead of readers' emotion triggered by the content. It is a challenging task to predict the reader's emotion on web information [12]. In this paper, we propose to build a reader emotion classification system based on emotion dictionary and machine learning, and evaluate its performance on simplified Chinese News.

The rest of this paper is organized as follows. Section 2 will describe some related work by other researchers. We elaborate our experiment method and system in section 3, and Section 4 shows the experiment results and analyzes of different algorithms. At last, Section 5 provides the conclusion of our work and the future work.

2 Related Work

Text emotion classification is a emerging topic on Data Mining (DM)[4] and Information Retrieval (IR)[3]. Much research has been done on this direction.

Yue Ning et al. [20] introduced a Chinese text emotion classifier with five sentiment categories. They added an emotion lexicon in feature extraction process which would increase the weight of emotion tokens and decrease the weight of non-emotion tokens. However, a part of tokens will be ignored in there system in the process of feature extraction which makes the predictor function badly on short text dataset.

Kevin et al. [21] built a classification system on reader emotion[8] on news articles of Yahoo. They classified news articles into different emotion categories using various combinations of feature sets. There feature sets contains the Chinese character bigrams and metadata. But reader emotion of a news article didn't have a strong correlation with metadata such as publishing time or event location. Therefore, the accuracy of the implemented eight-category SVM classifier was even lower than 60% for some categories.

Hu et al. [15] implemented a Naive Bayesian text classification model. Their results show that the Naive Bayesian classification can achieve a good performance on pure text classification. However, this classifier just categorizes texts into two classes, positive and negative. Emotion of a reader contains a lot such as happy, angry, sad, moving. A more detailed prediction of emotion is needed.

Plaban et al. [22] presented a method for classifying news sentences into multiple emotion categories. The corpus contained 1000 news sentences and the emotion labels are considered as anger, disgust, fear, happiness, sadness and surprise. They compared the performance between machine classification and human classification of emotion. In both the cases, it is observed that some ambiguous emotion (emotion which combining anger and disgust) is hard to predict

in human classification. They used words present in the sentences and the polarity of the subject, object and verb as features. In this experiment, the best average precision was computed to be 79.5% and the average class wise micro F1 is found to be 59.52% when anger and disgust classes are combined and surprise class is removed.

Some other research on Chinese text classification[16][2] use the similar method. Most of their works are based on traditional text classification. Some researchers conducted experiment on the massive web blog information[9][11] as corpus. They analyze both author or reader emotion[6][7], but with low precision.

All the above workings indicate that building an emotion classification system is quite important for sentiment analysis. The emotion classification is a fundamental work which can be used in other system. But the accuracy of them can not satisfy further application.

3 Methods

In this paper, we propose to predict the reader's emotion on Chinese news articles using Support Vector Machine(SVM)[14] and Naive Bayesian(NB)[13] based on emotion dictionary. The system flow chart is shown in Fig. 1.

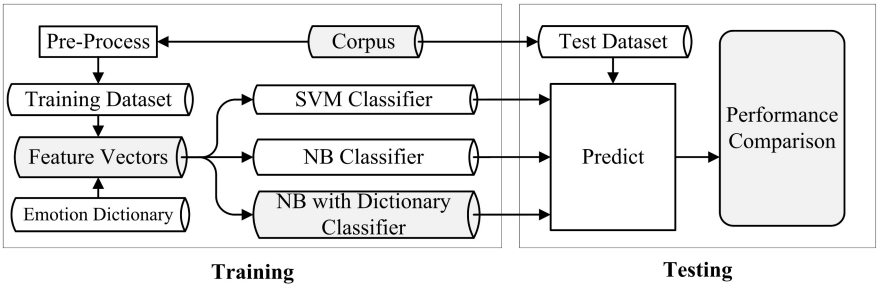

Fig. 1. System flow chart

We download the online society news articles as the corpus and divide it into training data set and testing data set. Before training the classifier, we run preprocessing on the training data set, including HTML tags removing, Chinese word segmentation and stop word removing. Using the emotion dictionary, we can construct the text vector for each news article. After training with different algorithms, we get different classifiers. In the testing part, we use the classifiers on the prediction of reader emotion on testing data set. Finally, we compare the performance of the different classifiers.

3.1 Dataset

Our corpus comes from Sina society news articles[10]. Sina society news web page supports an emotion voting function. After reading each news article, the reader

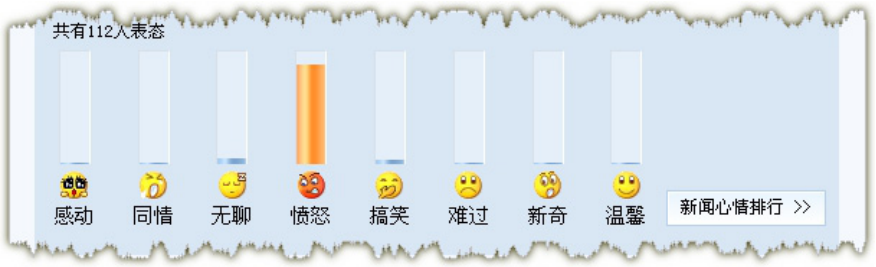

Fig. 2. Eight Moods of Sina Society News

can vote an emotion label: *Moving, Pity, Sad, Boring, Funny, Heartwarming, Surprised or Angry* that best describes his/her feeling shown in Fig.2. Therefore, we implement a crawler to download the corpus from Sina society news.

However, this corpus contains some noisy samples which would be useless for model training. In order to get a high-quality dataset, we need to make a sampling on the corpus. Our sampling strategies are shown below:

- Some ambiguous news which makes no sense or makes reader get multi-emotions should be neglected.
- Some out-of-fashion news which has vote count lower than a threshold (500) should be neglected.
- News articles with too many words or too few words should be neglected.
- Some categories should be neglected if the article number of this category is small.

With the four strategies, we can get a high-quality dataset with less noises. We download 14000 social news articles from Sina.com networking services between April, 2007 to November, 2009. Then we manully filter out some samples according to strategies 1 to 3. Finally, the article number distribution table of each category is listed in Tab. 1.

In Tab. 1, Boring, Sad, Pity and Heartwarming news articles make up a tiny proportion of the corpus. Based on strategy 4, we do not consider them and omit these 4 weak categories. Therefore, our further emotion predictions are all based on the remaining four categories, *angry, moving, funny and surprised.*

Until now, we get a better dataset, named imbalanced dataset with different sample number of 4 categories. In order to get a better performance of classification, a balanced dataset is necessary. Using strategies 1 to 3 again, we select 200 news articles from each category and build a balanced dataset.

3.2 Pre-process

The simplified Chinese documents need some pre-processes before training. Since the corpus comes from the webpage crawler, it is necessary to remove HTML tags first. Then we make a sampling according to strategies listed in the previous section.

Table 1. Emotion Distribution Samples

Category	Proportion	Number
Angry	75.26%	6255
Moving	13.58%	1129
Funny	6.94%	577
Surprised	3.36%	279
Boring	0.47%	39
Sad	0.24%	20
Pity	0.12%	10
Heartwarming	0.02%	2

Chinese articles need to be segment into tokens which is different from English articles. ICTCLAS[5], developed by Institute of Computing Technology(ICT) is one of the most popular tools of Chinese word segmentation. It performs quickly, and researcher can add customized dictionary based on the training purpose. The tool give each article an output of bag of tokens. These tokens are then filtered with a strop word list. This step removes the stop words in the simplified Chinese which appear frequently but have no actual meaning. After the above processes, each news article is represented as a bag of meaningful tokens.

3.3 Emotion Dictionary

The core idea of our method is to increase the weight of emotion tokens and decrease the weight of the other tokens. The emotion dictionary we use comes from four parts: the extended lexicon of TongYiCi CiLin[17], the original TongYiCi CiLin[19], HowNet[18] and corpus key tokens. CiLin was firstly published in 1996 by Shanghai CiShu, then extended by HIT-IRLab during 2006 to 2009. Emotion words in HowNet come from actual corpus corresponding with artificial screening. We also calculate χ^2 statistic for each token in corpus. The formula of χ^2 is shown as following:

$$\chi^2 = \frac{N \times (AD - CB)^2}{(A + C) \times (B + D) \times (A + B) \times (C + D)}$$

where A is the frequency that a term and a category occur together, B is the times that a term occurs while a category does not occur, C is the occurrences of a category without a term, D is the count that a term or a category neither occurs and N is the number of the total text set. χ^2 test is based on hypothesis test and measures the positive interdependency and negative interdependency between a word and a categorization. That is how irrelevant between a word and a categorization. We select the top 100 χ^2 statistic tokens.

In sum, we get an emotion dictionary with more than one thousand four hundred emotion words shown in Fig. 3.

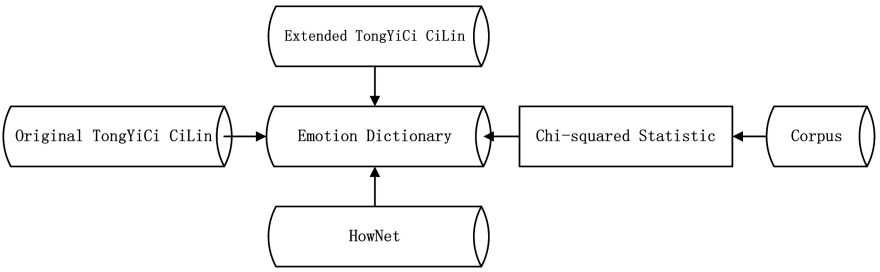

Fig. 3. System flow chart

Then we begin to build the text vector of each article in vector space model where articles are represented as

$$document = (token_1, weight_1; token_2, weight_2 ... token_n, weight_n); \quad (1)$$

An intuitive idea is to increase the weight of emotion words that appears in training dataset and decrease the weight of all the other non-emotion words. Therefore, we take the Bayesian conditional probability into consideration. For each token, the Bayesian conditional probability is

$$weight_{t,c} = \frac{T_{c,t} + 1}{\sum_t T_{c,t} + B} \quad (2)$$

where $T_{c,t}$ is the term frequency(the appearing time of the token) of token t in category c, B is the total number of tokens in all the categories. The "1" term is a smooth factor to avoid zero weight.

Therefore, we revised the formula of Naive Bayesian conditional probability with a weighting coefficient shown in the following:

$$weight_{t,c} = \begin{cases} \frac{(K_t+1)\times T_{c,t}+1}{\sum_t T_{c,t}+B+K_t\times N_c} & \text{if t is an emotion token;} \\ \frac{T_{c,t}+1}{\sum_t T_{c,t}+B} & \text{otherwise.} \end{cases} \quad (3)$$

where N_c is the total term frequency of emotion tokens in category c, K_t is a non-negative emotion word weighting coefficient. If token t is non-emotion word, then set $K_t = 0$. Otherwise, we set K_t a non-negative number. The classification will be back to traditional Naive Bayesian classification if K_t is always set zero shown in Fig. 4.

If K_t is positive infinity, the conditional probability is

$$weight_{t,c} = \begin{cases} \frac{T_{c,t}}{N_c} & \text{if t is an emotion token;} \\ 0 & \text{otherwise.} \end{cases} \quad (4)$$

This case with a positive infinity K_t will only take emotion tokens into account and omit all the other non-emotion tokens. Therefore, we need to build a balance between emotion tokens and non-emotion tokens and find the optimal value of K_t.

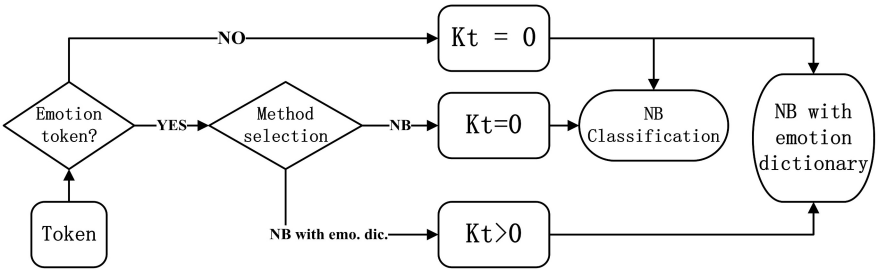

Fig. 4. Weight coefficient selection

Algorithm 1. TrainNBwithEmotionDictionary

Require: Class, C; Documents, D; Token set, V; Emotion dictionary, E;

$N_c \leftarrow CountEmotionTokenAppearing(D, E)$;
$B \leftarrow |V|$;
for $c \in C$ **do**
  $prior[c] \leftarrow \frac{N_c}{N}$;
  $text_c \leftarrow ConcateTextOfAllDocsInClass(D, C)$;
  for $t \in V$ **do**
    $T_{ct} \leftarrow CountTokensOfTerm(text_c, t)$;
  end for
  for $t \in V \&\& t \in E$ **do**
    $condprob[t][c] \leftarrow \frac{(K_t+1)\times T_{c,t}+1}{\sum_t T_{c,t}+B+K_t\times N_c}$;
  end for
  for $t \in V \&\& t \notin E$ **do**
    $condprob[t][c] \leftarrow \frac{T_{c,t}+1}{\sum_t T_{c,t}+B}$;
  end for
end for
return $V, prior, condprob$;

4 Experiments

In order to test the importance of emotion dictionary, we design two comparable experiments. Experiment 1 tests the classification without emotion dictionary. This experiment uses the classic algorithms(*SVM, NB*) in machine learning. The performance can be the baseline of our work. Experiment 2 works on the classification with emotion dictionary. This experiment uses our method when constructing text vectors. We also list the precision, recall and F-value of the two experiments.

4.1 Experiment 1

Experiment 1 focus the classification without emotion dictionary. While constructing the text vectors, we use formula (2) where K_t is always set zero for

any token. We firstly test the performance with Support Vector Machine. An SVM model is a representation of the examples as points in space. The core idea is to find a biggest clear gap that can divide examples of the separate categories. Test samples are then predicted to belong to a category based on which part they fall in. Since Support Vector Machine(SVM) is insensitive to data distribution, we choose it as training algorithm on imbalanced dataset. To simplify calculation, we use the method of chi-squared feature extraction. We select the top 500 keywords as features to do the training. We chose the C-SVC as the SVM type with $C = 40$. Using 10 fold cross-validation, the testing results are shown in Tab. 2.

Table 2. Results of SVM on imbalanced dataset

Category	Recall	Precision	F-value
Angry	0.912	0.963	0.937
Moving	0.873	0.690	0.771
Funny	0.575	0.460	0.511
Surprised	0.818	0.720	0.766

We also test the performance with Naive Bayesian Classification. Since Naive Bayesian can get a good performance in balanced dataset, we use the balanced dataset. The main idea of Naive Bayesian Classification is the conditional probability which means the probability of a token appears in a category. We use both Support Vector Machine and Naive Bayesian with formula (2) methods on the balanced dataset and take a five-fold cross validation to get the average results in the following Tab. 3.

Table 3. Results of SVM and NB on balanced dataset

	SVM			NB		
Category	Recall	Precision	F-value	Recall	Precision	F-value
Angry	0.806	0.83	0.818	0.933	0.63	0.752
Moving	0.904	0.88	0.891	1	0.279	0.436
Funny	0.790	0.76	0.745	0.740	0.9	0.812
Surprised	0.832	0.83	0.831	0.535	0.93	0.679

From the results, the precision of category "Moving" is lower(0.279) compared to other categories(0.535 at least). The reason may be the contents in this class. Since the news articles in the moving class involve many different kinds of aspects of topics, it is an ambiguous emotion for an automatic classifier. This two systems can be the baseline of our work.

4.2 Experiment 2

In experiment 2, we add the emotion dictionary and compare the classification results with experiment 1.

To minimize the bias from other factors, experiment 2 tests on the balanced dataset. As explained in formula 3, we take emotion dictionary into consideration. The first question is how to set the weighting degree K_t of the dictionary. As discussed above, the system turns back to traditional text classification if K equals to zero (formula 2). On the other side, the system will be over-fit if K_t is equal to infinity(formula 4). Therefore, we give K_t several values and run a series of experiments on the examination of K_t. For each given value of K, we can calculate the average precision, average recall and average F-value.

We show three curves of weighting coefficient on precision, recall and F-value in Fig. 5. In Fig. 5, the horizontal axis is K_t and we find a local optimal value at K_t equaling to 1.2.

Table 4. Results of NB with Emotion Dictionary

Category	Recall	Precision	F-value
Angry	0.902	0.87	0.886
Moving	0.980	0.88	0.972
Funny	0.831	0.87	0.849
Surprised	0.877	0.94	0.907

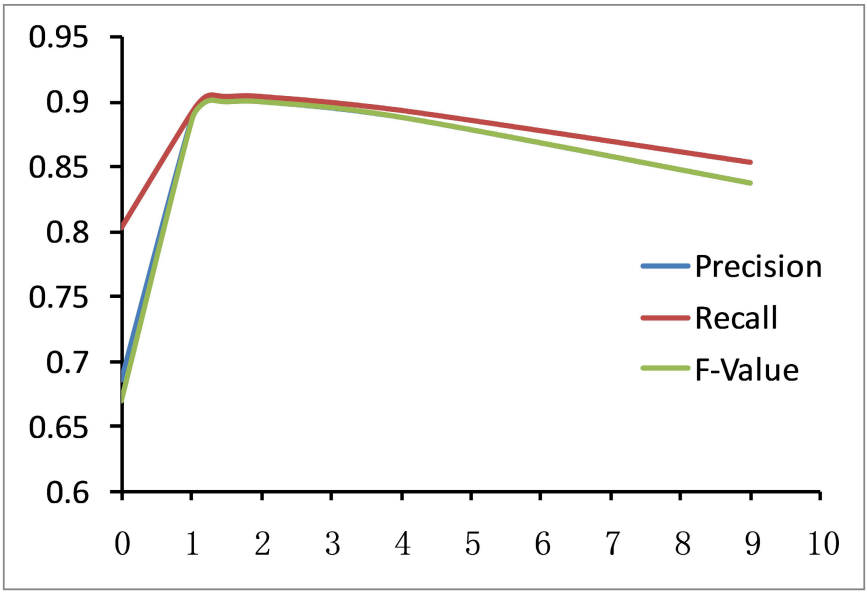

Fig. 5. Weighting coefficient experiment

From this result, we set $K_t = 1.2$ in the following experiments. The results with $K_t = 1.2$ are shown in Tab. 4.

In Tab. 4, the average precision reaches 90% which is much beyond the precision of the baseline. It means that our method performance well in simplified Chinese.

5 Conclusion

In this paper, we propose to build a classifier which is able to predict the reader emotion with emotion dictionary on news articles in simplified Chinese. We tune the Naive Bayesian conditional probability formula and add a new coefficient which stands for the weight of the emotion dictionary. From the experiment results, it is obvious that the system performances better with emotion dictionary. That high accuracy means that the classifier can seize the emotion tendency correctly for each news article and classify news article according to the emotion tendency precisely.

After investigating the experiment results, we find that most wrongly-classified samples are more likely to be judged as angry, which means the emotions of news articles have a large component of anger. This may lead to some mental illnesses or social instabilities. This situation results from the news itself. The purpose of reporters of writing news articles is to attract the reader's attention. People may pay less attention to boring news, instead they may prefer to news with strong emotions, angry or surprised.

Our work still has some limitations. First, the sample set contains 800 news articles in all. If we can download much more documents, the precision will get a rise. Second, since the articles are all long text, the classifier cannot work well on short text dataset. We will continue to work on the emotion classification on micro-blog. Third, our classifier can only predict reader emotion into four categories. For the other emotions, we cannot make the prediction because of the lack of the training dataset.

In the future, we may improve our research in two possible ways. For the classifier itself, we will refine training method to increase the accuracy and make some update of emotion dictionary. Web users create many new web words each day, it is necessary to keep the developing step. On the other hand, we would like to use our classifier into other systems such as web personality analysis system.

Acknowledgments. The authors gratefully acknowledges the generous support from NSFC (61070115), Institute of Psychology(113000C037), Strategic Priority Research Program (XDA06030800) and 100-Talent Project(Y2CX093006) from Chinese Academy of Sciences.

References

1. Bhowmick, P.K., Basu, A., Mitra, P.: Classifying emotion in news sentences: When machine classification meets human classification. International Journal on Computer Science and Engineering, 98–108 (2010)
2. Bracewell, D.B., Minato, J., Ren, F., Kuroiwa, S.: Determining the Emotion of News Articles. In: Huang, D.-S., Li, K., Irwin, G.W. (eds.) ICIC 2006. LNCS (LNAI), vol. 4114, pp. 918–923. Springer, Heidelberg (2006)
3. Christopher, H.S., Manning, D., Raghavan, P.: Introduction to Information Retrieval. Cambridge University Press (2008)
4. Han, J., Kamber, M.: Data Mining Concepts and Techniques, 2nd edn. China Machine Press (2008)
5. Zhang, H.: Ictclas chinese segmentation tool (2010)
6. Zhou, L., He, Y., Wang, J.: Survey on research of sentiment analysis. Computer Applications 4, 2725–2728 (2008)
7. Hsin, K., Lin, Y., Chen, H.H.: Ranking reader emotions using pairwise loss minimization and emotional distribution regression. In: Proceedings of the 2008 Conference on Empirical Methods in Natural Language Processing, vol. 9, pp. 136–144 (2008)
8. Lin, K.H.-Y., Yang, C., Chen, H.-H.: What emotions do news articles trigger in their readers? In: SIGIR 2007 Proceedings, vol. 2, pp. 733–734 (2007)
9. Quan, C., Ren, F.: Construction of a blog emotion corpus for chinese emotional expression analysis. In: Proceedings of the 2009 Conference on Empirical Methods in Natural Language Processing, vol. 8, pp. 1446–1454 (2009)
10. Sina.com. Sina society moodrank (2010), `http://news.sina.com.cn/society/`
11. Tokuhisa, R., Inui, K., Matsumoto, Y.: Emotion classification using massive examples extracted from the web. In: Proceedings of the 22nd International Conference on Computational Linguistics (Coling 2008), pp. 881–888 (2008)
12. Weare, C., Lin, W.Y.: Content analyis of the world wide web: opportunities and challenges
13. Wikipedia. Naive bayes classifier, `http://en.wikipedia.org/wiki/Naive_Bayes_classifier`
14. Wikipedia. Support vector machine, `http://en.wikipedia.org/wiki/Support_vector_machine`
15. Hu, Y., Zhou, X., Ling, L., Wang, X.: A bayes text classification method based on vector space model. Computer and Digital Engineering 32, 28–30 (2004)
16. Zhang, Y., Li, Z., Ren, F., Kuroiwa, S.: A preliminary research of chinese emotion classification model. IJCSNS International Journal of Computer Science and Network Security, 127–132 (2008)
17. HIT-IRLab. Extended tongyici cilin, `http://ir.hit.edu.cn/demo/ltp/Sharing_Plan.htm`
18. HowNet, `http://www.keenage.com/`
19. Mei, J., Zhu, Y., Gao, Y., Yin, H.: TongYiCi CiLin. Shanghai CiShu Press (1996)
20. Ning, Y., Zhu, T., Wang, Y.: Affective word based chinese text sentiment classification. In: Proceedings of 5th International Conference on Pervasive Computing and Applications, ICPCA 2010 (2010)

21. Lin, K.H.-Y., Yang, C., Chen, H.-H.: What emotions do news articles trigger in their readers? In: SIGIR 2007 Proceedings, vol. 2, pp. 733–734 (2007)
22. Bhowmick, P.K., Basu, A., Mitra, P.: Classifying Emotion in News Sentences: When Machine Classification Meets Human. International Journal on Computer Science and Engineering 2(1), 98–108 (2010)
23. Ning, Y., Li, A., Zhu, T.: Are Online Mood Labels A True Reflection of Our Experiences? In: Proceedings of 2011 3rd Symposium on Web Society (SWS 2011), pp. 21–26 (2011)

Clustering Algorithm Based on Triple-Stranded and 3-armed DNA Model

Xue Bai[1], Xiaoling Ren[2], and Xiyu Liu[2]

[1] East of Wenhua Road No. 88, Jinan, Shandong, 250014
sdnubaixue@163.com
[2] School of Management Science and Engineering, Shandong Normal University, Jinan, China

Abstract. The quality of traditional grid-clustering and pure hierarchical clustering methods suffers from some limitations, especially the inability of hierarchical clustering to perform adjustment on once merge or split decision. However, DNA computations can be introduced here to do global search and find the best clusters. Since the grid-clustering can be transformed into HPP (Hamilton Path Problem) and the other one equals to MST (Minimal Spanning Tree) algorithm while using the minimum distance measure, this paper proposes to solve grid-clustering using triple-stranded DNA model and nearest neighbor clustering by 3-armed DNA model based on the above thought. Firstly, it is needed to get the initial data pool containing all the possibilities, then screen those owning all data points to be clustered, and finally get the best one(s). Accordingly, under the special designed biological algorithm, both of the DNA algorithms have the time complexity of $O(n)$, which n represents the number of processed data waiting to be clustered. In fact, the way of using triple-stranded structures to select solutions satisfying the paticularly restricted conditions could be further extended to more DNA algorithms using double-helix. Meanwhile, if other applications are on the basis of binary tree constructions, 3-armed DNA molecules designed here can be made more use.

Keywords: DNA computing, Grid-clustering, Hierarchical clustering, Triple-stranded DNA, 3-armed DNA.

1 Introduction

DNA computing has made great achievements since 1994 and has solved several NP problems which are transformed into permutations and combinations or graph theory problems. Since DNA computing provides a better way of data processing, it can also be used to solve clustering problems. So far, there have been some theoretical attempts on applying DNA computing to clustering [1-2] and in this paper, we focus on two clustering algorithms using triple-stranded and 3-armed DNA model.

With the mesh data structure of multi-resolution, grid clustering quantifies the object space into limited units and makes all the clustering operations be carried out on the grid. Grid clustering applies to processing large amounts of data in different resolution levels and the CLIQUE algorithm, a gird clustering based on density and

Q. Zu, B. Hu, and A. Elçi (Eds.): ICPCA-SWS 2012, LNCS 7719, pp. 28–34, 2013.

grid, will be used in our paper. Hierarchical clustering was first put forward by Kaufman in 1990, including agglomerative hierarchical clustering and divisive hierarchical clustering. In recent years, the agglomerative hierarchical clustering has various applications in like Web services [3], processing of document datasets, improved design of neural network and community detection in complex network.

The purine-rich strand in double-stranded DNA connects the new third chain with Hoogsteen-type or reversed Hoogsteen-type hydrogen bonds to become triple-strand. Literature [4] preliminarily confirmed the feasibility of molecular computation with triple-stranded nucleic acids mediated by RecA-protein. *K*-armed DNA structure has long existed in nature. Research shows that fairly stable 3-armed and 4-armed molecules can be obtained and under certain conditions, the 8 and 12-armed can also be gained [5]. Just by intuition, The 3-armed molecules are feasible to construct a binary tree, which can be added on flexible operations of enzyme digestion [6].

2 Basic Algorithm

The discussion here limits to two-dimensional plane, and we use similarity measure between two objects or points of data. The idea of DNA computing is to design special DNA fragments to represent data points and the similarity, put them into tubes for ligation reaction to get all kinds of combinations, and find the final best ones. Accordingly, the basic DNA algorithm is shown as below:

Step1 Converse the data points and similarity between them into an empowering undirected complete graph, and then encode them with four kinds of DNA bases;

Step2 Generate the initial solution space;

Step3 Select and retain the DNA fragments covering all the vertices;

Step4 Find the optimal solution to be the preliminary clustering results;

Step5 Divide all the vertices into several clusters and read them at last.

3 Grid Clustering Algorithm Based on Triple-Stranded DNA

3.1 Problem Description

The procedure of two-dimensional CLIQUE algorithm is firstly dividing the two-dimensional data plane into grid cells, mapping the objects into them and calculating the density of each cell. Then determine if each cell is a high-density unit by the threshold *MinPts* and clusters will be formed by the adjacent dense units finally.

Based on the idea of CLIQUE, we define each cell as a node in the graph and transfer the clustering of cells into the clustering of nodes. Then these adjacent nodes will cluster into one class and those non-adjacent nodes won't belong to the same class after the clustering. In the graph, all the vertices are linked with weighted edges. We limit the weight of edge between adjacent nodes under the threshold τ and set the weight of the non-adjacent beyond τ. Then the original problem is equivalently transformed into HPP in a connected undirected graph, which the path includes all the

vertices and the sum of edges' value is minimized. After that, the graph is cut into k pieces by cutting the edges with weights beyond τ. By that we'll get k clusters as the final results. Specific description of HPP is as follows: Given the empowering undirected complete graph $G=(V,E)(v_i \in V,\ e_{ij} \in E)$ and $w_{ij}(w_{ij} \geq 0)$ of e_{ij}, the target Hamilton path is in $G'=(V',E')(V'=V,\ E' \subseteq E)$ where the sum of weights in G' is minimum. The expression is $W' = \sum_{e_{ij} \in E'} w_{ij} = \min \sum_{e_{ij} \in E} w_{ij}$.

3.2 Encoding

There are only two kinds of relationships between two points. In Fig. 1, if v_i and v_j are adjacent, w_{ij} of e_{ij} is 1 or $\sqrt{2}$, else it's above $\sqrt{2}$.In the first case, weight sequences are encoded in the same way. Otherwise, the restriction endonuclease should be introduced in them. 20mer oligonucleotide fragments are used to encode v_i and record it as S_i. The coding $M_{ij}(1 \leq i,j \leq n)$ of e_{ij} has three parts: first part is the complement strand of last 10 base pairs of S_i, and third part is complamentary to the first 10 bases of S_j. The second part consists of bases showing the weight of e_{ij}.

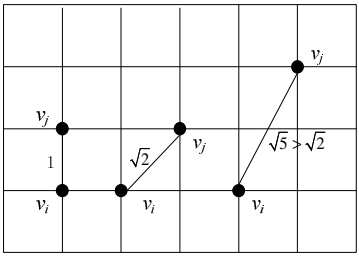

Fig. 1. The relative position of two nodes after the transformation

3.3 Biological Algorithm

Step1 Structure some single DNA fragments to represent all the vertices and edges in graph G, put them into solution for full reaction and gain those double-stranded DNA as original data pool.

Step2 Mix RecA-protein with the complement strands of v_1's DNA fragments under certain conditions. Thus nucleoprotein filaments will come into being.

Step3 Use nucleoprotein filaments of v_1 as probes and preserve the triple-stranded DNA structures corresponding to v_1.

Step4 Take advantage of the high affinity of biotin-streptavidin interaction, separate the triple-stranded DNA structures containing v_1 from other library chains and change them into double-strand. After that, all desired chains in data pool will contain the DNA fragments of v_1.

Step5 Repeat steps 2, 3 and 4 for each of the remaining vertices and the finally acquired double strands will include all the vertices of graph G.

Step6 Make use of gel electrophoresis to measure the shortest double-stranded DNA and gain the Hamilton paths with smallest weights.

Step7 Have the aid of restriction endonuclease to disconnect the edges with weights above threshold. After PCR amplification, choose amplified products and strands with different sizes of nanoparticles to have hybridization reaction on the slide. As different vertices are marked with distinct nanoparticles, they will scatter differ colors under proper circumstances [7] and the final grid clustering results could be found.

4 Nearest Neighbor Clustering Algorithm Using 3-armed DNA

4.1 Problem Discription

The nearest neighbor clustering algorithm is the most simple hierarchy clustering algorithm and the distance between two objects is measured by Euclidean distance. In addition, distance between two classes is decided by distance of the most recent points from two classes. At the beginning, each object is treated as one class and Euclidean distance between each pair of them is computed. Then it is needed to combine the nearest two objects into one group and measure the distance between two classes by combining the nearest two until all the objects are gathered into only one cluster.

Nearest neighbor clustering problem can be transformed into MST, which is defined as following: Given a connected and undirected graph $G=(V,E)$, a spanning tree of $G=(V,E)$ is a subgraph that is a sub-tree connecting all the vertices together. A single graph can have many different spanning trees. e_{ij} is the edge joining vertex v_i and v_j together($e_{ij}\in E$, $v_i\in V$, $v_j\in V$). We assign a weight w_{ij} to each edge e_{ij}, and define the weight to a spanning tree by computing the sum of the weights of edges in that tree. A minimum spanning tree has the weight less than or equal to every other spanning trees. The mapping from nearest neighbor clustering into MST is as follows:

The objects or points of data are mapped into the vertices of a graph. The Euclidean distance between two objects is transformed into the weight or distance between two vertices. The algorithm will generate a binary tree because it is trying to combine two classes during every step.

4.2 Encoding

Since what we'll get is a binary tree, 3-armed DNA molecules are perfect as the basic structure to construct a binary tree structure. And the encoding of each arm of the 3-armed DNA molecule lists below.

Vertices arms: Two of the 3 arms are selected to represent two different vertices. All the double-stranded part of these vertices arms are labeled all the same.

Distance arm: If two arms of a 3-armed DNA molecule are labeled with the sequence of v_i and v_j, correspondingly, the distance w_{ij} is coded only with bases G and C into the double-stranded part of the rest one arm, with the extended single part encoded the complement sequence of v_i or v_j. We have to notice that the distance has

to be integer. If not, by using the method in [1], integer distance can be obtained. A restriction endonuclease sequence needs to be coded into the double-stranded section of distance part if the weight is larger than threshold.

For example, if the distance between *A* and *B* is 2, 3-armed DNA molecules needed are in Fig. 2. In addition, hairpin structures are also needed to make extended single parts to be closed ends. With respect to a graph of *n* vertices, $n(n-1)$ kinds of 3-armed molecules and $2n$ kinds of hairpin structures are demanded.

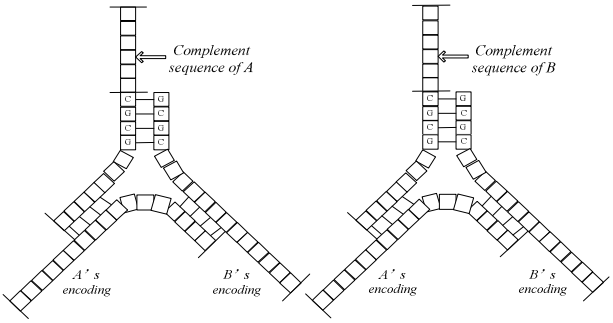

Fig. 2. Two kinds of 3-armed DNA molecules coded with two vertices

4.3 Biological Algorithm

Step1 Prepare sufficient 3-armed DNA molecules, hairpin structures, as well as corresponding sequences of single strands for reaction and it's possible to get the original pool containing all the 3-dimentional DNA graph structures with closed ends.

Step2 Remove those 3-dimentional DNA molecules which are partly formed, not fully matched and have open ends and also remove redundant hairpin structures, thus getting the data pool waiting to be screened.

Step3 Mix RecA-protein with compliment strands of vertices under certain conditions. Then, the corresponding nucleoprotein filaments are obtained.

Step4 Do the same operations in 3.2 to get 3D graph structures containing all the vertices.

Step5 Select the lightest 3D-DNA molecules and reserve products with smallest weights. Carry out detection process with the help of restriction endonuclease and nanoparticles.

5 Example

For simplicity, we just give one graph of four vertices in Fig. 3 to show how these two DNA algorithms make work. The points are viewed as dense cells whose density of points are more than the threshold, as well as the normal two-dimensional data needed to be clustered. Since we treat the length of one edge of a cell as per unit length, we can get the length of all edges between all pair of points. What is given in Fig. 3 is an undirected complete graph with $V=\{v_1,v_2,v_3,v_4\}$ and $E=\{e_1, e_2, e_3, e_4, e_5,e_6\}$.

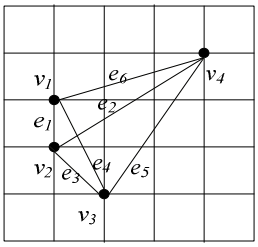

Fig. 3. An undirected complete graph of four vertices

Grid-clustering: Encode DNA sequences expressing v_i and $e_{ij}(1 \le i,j \le 4)$, combine multiple copies of all corresponding DNA strands in a single tube and allow the complementary ends to hybridize and ligate in the first place. In vitro, all the possible Hamilton paths can be formed automatically. There are two Hamilton path satisfying the conditions: $v_1 \rightarrow v_2 \rightarrow v_3 \rightarrow v_4$ and $v_4 \rightarrow v_1 \rightarrow v_2 \rightarrow v_3$. Finally, cut the edges with endonuclease recognition sites and then get the result of clusters. There are two clusters, one cluster containing v_1, v_2, v_3, the other containing v_4.

Hierarchy clustering: First of all, make 12 kinds of three-armed DNA molecules and form three-dimensional graph structures. Then screen those containing all the vertices by using triple-stranded DNA structure. Use gel electrophoresis to find the three-dimensional graphs that are lighter than others. One possible structure is given in Fig. 4 and the result is as same as the above one.

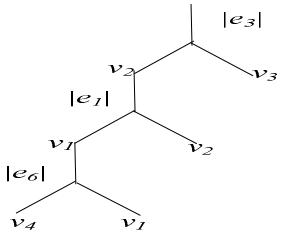

Fig. 4. One possible MST structure chosen by 3-armed DNA model

6 Conclusion

When the ClIQUE algorithm, based on grid-clustering, is transformed into Hamilton path problem, and the nearest hierarchical clustering is mapped into MST, two DNA algorithms are provided to solve them, using triple-stranded and 3-armed DNA model respectively. The good point is that using triple-stranded molecules in the process of screening the possible solutions can avoid mismatch between DNA strands and the possible hairpin structures, thus making the biochemical reaction more efficient compared with the common probes. With the advantage of the structure of 3-armed molecules, the tree structure is created directly. According to algorithms in section 3 and 4, the time complexity is $O(n)$.

Although it is believed that the theoretical procedures here are empirically possible, there are also some technical problems to be studied further. For instance, the DNA strands or DNA molecules could be too long or too big to realize when the amount of data or the weight of edges is larger and larger. The way to code the weight is restricted to integer. In fact, we could consider using binary or quaternary coding to encode weight with real number under certain precision.

Despite of the troubles, DNA computing still has broad prospects. We are encouraged by the progress of DNA computing and the repid development of biological technologies.

Acknowledgements. This work was supported by National Natural Science Foundation of China (61170038), Shandong Province Natural Science Foundation (ZR2011FM001), Humanities and Social Sciences project of Ministry of Education (12YJA630152).

References

1. Abu Bakar, R.B., Watada, J.: A Biologically Inspired Computing Approach to Solve Cluster-based Determination of Logistic Problem. Biomedical Soft Computing and Human Sciences 13, 59–66 (2008)
2. Zhang, H.Y.: The Research on Clustering Algorithm Based on DNA Computing. Shandong Normal University, Jinan (2011)
3. Liu, X.W., Yao, S.H.: A DHCS-based Discovery Mechanism of Semantic Web Services. Chinese Journal of Computer Applications and Software 24, 173–178 (2006)
4. Fang, G., Zhang, S.M., Zhu, Y., Xu, J.: The DNA Computing Based on Triple Helix Nucleic Acid. Chinese Journal of Bioinformatics 3, 181–185 (2009)
5. Wang, X., Seeman, N.C.: Assembly and Characterization of 8-Arm and 12-Arm DNA Branched Junctions. Journal of the American Chemical Society 129, 8169–8176 (2007)
6. Li, W.G., Ding, Y.S., Ren, L.H.: Design and Implementation of Generalized List in DNA Computer. Chinese Journal of Computers 31, 2215–2219 (2008)
7. Sun, W., You, J.Y., Jiang, H., Jiao, K.: Preparation and Detection Application of Nanoparticle Tagging DNA Probe. Chinese Journal of Health Laboratory Technology 15, 1008 (2005)

Synthesis of Real-Time Applications for Internet of Things

Sławomir Bąk[1], Radosław Czarnecki[1], and Stanisław Deniziak[1,2]

[1] Cracow University of Technology, Department of Computer Engineering
Warszawska 24, 31-155 Cracow, Poland
{sbak,czarneck,sdeniziak}@pk.edu.pl
[2] Kielce University of Technology, Department of Computer Science
Al. Tysiaclecia Panstwa Polskiego 7, 25-314 Kielce, Poland
s.deniziak@tu.kielce.pl

Abstract. This paper presents the methodology for synthesis of real-time applications working in the Internet of things environment. We propose the client-server architecture, where smart embedded systems act as clients, while the Internet application is a server of the system. Since centralized systems are prone to contain bottlenecks, caused by accumulation of transmissions or computations, we propose the distributed architecture of the server and the methodology which constructs this architecture using available Internet resources. We assume that the function of the server is specified as a set of distributed algorithms, then our methodology schedules all tasks on existing network infrastructure. It takes into account limited bandwidth of communication channels as well as limited computation power of server nodes. If available network resources are not able to execute all tasks in real-time then the methodology extends the network by adding necessary computation nodes and network components, minimizing the cost of required reconstruction. We also present a sample application for adaptive control of traffic in a smart city, which shows benefits of using our methodology.

Keywords: Internet of things, real-time system, system synthesis, embedded systems.

1 Introduction

Internet of Things (IoT) is a concept in which the real world of things is integrated with internet technologies [1]. More and more internet-enabled devices are now available (mobile phones, smart TVs, navigation systems, tablets, etc.). It is expected that in a few years almost each product may be identified and traced in Internet using RFID (Radio Frequency IDentification), NFC (Near Field Communication) or other wireless communication methods. This will make possible the development of huge number of Internet applications. But enormous growth of devices connected to Internet may cause additional problems relative to computational complexity of IoT-based systems and the communication bottleneck. Existing Internet technologies may be

Q. Zu, B. Hu, and A. Elçi (Eds.): ICPCA-SWS 2012, LNCS 7719, pp. 35–49, 2013.

insufficient for dealing with IoT systems, thus new web architectures, communication technologies and design methods should be developed to enable development of efficient IoT systems[2][3][[4].

One of the most interesting domain is the Internet of Smart Things, where IP-connected embedded systems built in our environment may interact with Internet. Smart device not only incorporates sensing/monitoring and control capabilities but also may cooperate with other devices and with internet applications. For example an adaptive car navigation system may interact with an internet system, controlling and monitoring the traffic in a city, to avoid traffic jam. In such case Internet acts as a distributed server which process requests sent by smart devices implementing client applications. Usually responses to the device should be sent during the limited time period. Therefore, this class of IoT application is a real-time system.

Current work concerning Internet of Things mainly concentrates on 3 domains: developing new wireless communication technologies and protocols, adopting existing web technologies to this new paradigm and developing software architectures for IoT applications. Except low range communication systems based on RFID like RFID sensor networks [7] or WISP (Wireless Identification and Sensing Platform) [8] also IP-based communication systems were developed. 6LoWPAN [9] or Internet Ø [10] approaches implement low-power light IP protocols, that may be built in almost any object, therefore the vision that any thing may be addressable and reachable from any location may be realistic in the nearest future. Communication systems define lowest layer of the IoT system, upon this layer the software layers consisting of middleware and application are defined. Middleware defines the software architecture and it is composed of a set of Internet and web technologies. Most approaches adopt existing web technologies to IoT applications. Usually architectures based on SOA (Service Oriented Architecture) or REST (REpresentational State Transfer) [11] are applied. Integration of smart things with the web is also called Web of Things (WoT).

In [3] the problem of real-time requirements in WoT applications was discussed. Authors observed that a lot of WoT systems interact with embedded devices and expect real-time data, thus development of WoT application that satisfy real-time requirements is one of the main challenge. Although some technologies for real time communication (e.g. RTP/RTSP, XMPP) or real-time interaction (e.g. Comet[12]) were developed, but still more developments and standards are required for real-time WoT and IoT systems.

In this paper we present the methodology for synthesis of reactive, real-time applications accordant with the Internet of Things concept. We assume that each thing is represented as an embedded system that may send requests to Internet application and expects the response in the specified time. The goal of our methodology is to find the distributed architecture of the application which will satisfy all user requirements and will best fit to the existing Internet infrastructure.

Next section presents our assumptions and the definition of real-time Internet of things (RTIoT) application. In section 3 the method of synthesis will be described. Section 4 presents example demonstrating the advantages of the methodology. The paper ends with conclusions.

2 Problem Statement

System synthesis is a process of automatic generation of the system architecture, starting from the formal specification of functional and non-functional requirements. Functional requirements define functions that should be implemented in the target system. Non-functional requirements usually define constraints that should be fulfilled, e.g. time constraints define the maximal time for execution of the given operations, cost requirements define the maximal cost of the system, etc.

Functions of distributed systems are usually specified as a set of communicating tasks or processes. We use similar model for specification of IoT applications, details are given in p.2.1. Since we consider real-time systems, hence the main set of requirements are time requirements. IoT uses existing network infrastructure, consisting of servers, routers and connections. Therefore, the target architecture of the IoT system should fit into existing network architecture, but it may not guarantee that all time requirements will be met. In this case the infrastructure should be extended by adding some components. Thus it should be possible to specify architectural requirements that should be satisfied by the target system. The model of the target architecture is described in p.2.2, while requirements that are used in our methodology are presented in p.2.3.

2.1 Functional Specification

Reactive IoT system should be able to process thousands of requests in a short time period. It will be possible only if massive parallel computing will be applied. Therefore, the functional specification of the system should represent the function as a distributed algorithm [6], developed according to the following requirements:

1. parallel model of computations: system should be specified as a set of parallel processes using message passing communication,
2. parallel request handling: huge number of requests may couse the communication bottleneck, to avoid this, simultaneous requests should be handled by different processes.

We assume that the system is specified as a collection of sequential processes coordinating their activity by sending messages. Specification is represented by a graph $G=\{V, E\}$, where V is a set of nodes corresponding to processes and E is a set of edges. Edges exist only between nodes corresponding to comunicating processes. Tasks are activated when required set of events will apear. As a result task may generate other events. External input events will be called requests (Q), external output events are responces (O) and internal events correspond to messages (M). Function of the system is specified as finite sequences of activation of processes. There is a finite set of all possible events $\Lambda = Q \cup O \cup M = \{\lambda_i : i = 1,..., r\}$. For each event λ_i communication workload $w(\lambda_i)$ is definied. System activity is defined as a function:

$$\Phi : C \times V \rightarrow \omega \times 2^{\Lambda} \tag{1}$$

where C is an event expression (logical expression consisting of logical operators and Boolean variables representing events) and ω is the workload of the activated process.

Using function Φ it is possible to specify various classes of distributed algorithms. Fig. 1 presents sample echo algorithm [13] consisting of 5 processes. The algorithm consists of 10 actions. Each action is activated only once, when the corresponding condition will be equal true. All actions except A_1 and A_6 contain alternative sub-actions, only the first action, for which the condition will be satisfied, will be activated. According to the echo algorithm specification, process v_1 is the initiator, messages $m1_1$, ..., $m14_7$ are explorer messages, while $m15_1$, ..., $m25_7$ are echo messages (indices are added only for readability, mx_i means that message mx is associated with edge e_i in the graph, for the same reason, edge names in the event expressions mean any received message corresponding to this edge, e.g. $e_1 = m1_1 \mid m4_1 \mid m15_1$, $e_2 = m2_2 \mid m9_2 \mid m20_2$, etc.). Events x_1, ..., x_{11} are internal events, used for storing the state of processes between successive executions.

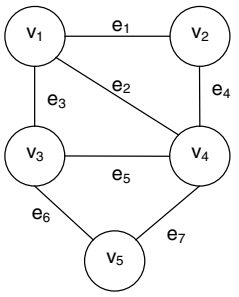

A_1: $\Phi(v_1,\{q_1\}) \rightarrow (5, \{m1_1,m2_2,m3_3\})$

A_2: $\Phi(v_2,\{m1_1\}) \rightarrow (4,\{x_1,m5_4\}) \mid \Phi(v_2,\{m10_4\}) \rightarrow (4,\{x_2,m4_1\})$

A_3: $\Phi(v_3,\{m3_3\}) \rightarrow (7,\{x_3, m7_5,m8_6\}) \mid \Phi(v_3,\{m11_5\}) \rightarrow (7,\{x_4,m6_3,m8_6\})$
$\mid \Phi(v_3,\{m13_6\}) \rightarrow (7,\{x_5,m6_3,m7_5\})$

A_4: $\Phi(v_4,\{m2_2\}) \rightarrow (6,\{x_6,m10_4,m11_5,m12_7\})\mid$
$\Phi(v_4,\{m5_4\}) \rightarrow (6,\{x_7,m9_2,m11_5,m12_7\})\mid$
$\Phi(v_4,\{m7_5\}) \rightarrow (6,\{x_8,m9_2,m10_4,m12_7\})\mid$
$\Phi(v_4,\{m14_7\}) \rightarrow (6,\{x_9,m9_2,m10_4,m11_5\})$

A_5: $\Phi(v_5,\{m8_6\}) \rightarrow (5,\{x_{10},m14_7\}) \mid \Phi(v_5,\{m12_7\}) \rightarrow (5,\{x_{11},m13_6,\})$

A_6: $\Phi(v_1,\{e_1\&e_2\&e_3\}) \rightarrow (10, \{r_1\})$

A_7: $\Phi(v_2,\{x_1\&e_1\&e_4\}) \rightarrow (4,\{m15_1\}) \mid \Phi(v_2,\{x_2\&e_1\&e_4\}) \rightarrow (4,\{m16_4\})$

A_8: $\Phi(v_3,\{x_3\&e_3\&e_5\&e_6\}) \rightarrow (3,\{m17_3\}) \mid$
$\Phi(v_3,\{x_4\&e_3\&e_5\&e_6\}) \rightarrow (3,\{m18_5\}) \mid$
$\Phi(v_3,\{x_5\&e_3\&e_5\&e_6\}) \rightarrow (3,\{m19_6\})$

A_9: $\Phi(v_4,\{x_6\&e_2\&e_4\&e_5\&e_7\}) \rightarrow (5,\{m20_2\}) \mid$
$\Phi(v_4,\{x_7\&e_2\&e_4\&e_5\&e_7\}) \rightarrow (5,\{m21_4\}) \mid$
$\Phi(v_4,\{x_8\&e_2\&e_4\&e_5\&e_7\}) \rightarrow (5,\{m22_5\}) \mid$
$\Phi(v_4,\{x_9\&e_2\&e_4\&e_5\&e_7\}) \rightarrow (5,\{m23_7\})$

A_{10}: $\Phi(v_5,\{x_{10}\&e_6\&e_7\}) \rightarrow (2,\{m24_6\}) \mid \Phi(v_5,\{x_{11}\&e_6\&e_7\}) \rightarrow (2,\{m25_7\})$

Fig. 1. Sample specification of the echo algorithm

Since different requests may be processed by distinct algorithms, the function of a system may be specified using a set of functions Φ sharing the same processes. Each function has only one initiator (process activated by the request). Processes may be activated many times but the algorithm should consists of the finite number of actions and infinite loops are not allowed.

2.2 Target Architecture

The proposed architecture of RTIoT system is composed of four layers: Things Layer (*QL*), Wireless Layer (*WL*), Network layer (*NL*) and Server Layer (*SL*). The dependencies between layers are shown in Fig. 2.

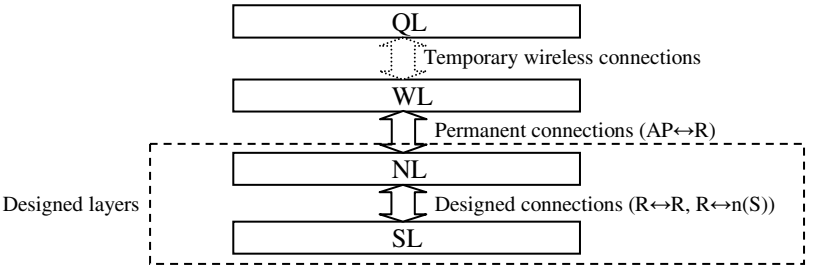

Fig. 2. Layers in RTIoT system

Layer *QL* consists of embedded systems (smart things) managed by RTIoT. We assume that things are mobile systems (q_i), thus the number of things N_q may change in time but it is limited to Q_{max}. Let $Q(t_i)=\{q_j;\ j=1, \ldots, N_q(t_i)\}$ be the set of things available in RTIoT system at time frame t_i. Each q_x has connection with the nearest access point *AP* in layer *WL*, i.e.

$$\forall t_i \forall q_j \exists AP_k^j : q_j \mapsto AP_k \tag{2}$$

where t_i is the time frame, AP_i^j is the access point nearest to q_j at time t_i and $\mapsto$ means the connection. Since q_j is a mobile system than it may change location in time. This may cause that the nearest access point also will be changed in the following time frames, thus for some time frames it may appear that $AP_i^j \neq AP_{i+1}^j$.

Layer *WL* includes access points (*AP*). Access points should guarantee that each q_i can communicate with the system at any time. Therefore all *AP*s should cover all possible geographical locations of q_i and the number of *AP*s is constant. For each AP_i we may identify the maximal number of *q*s that may appear in the region covered by this AP_i. Each AP_i is permanently connected to just one router R_j from the network layer (*NL*). We assume that layer *WL* will also satisfy the following condition:

$$\forall AP_i : \sum_j B(q_j^i) \leq B(AP_i) \tag{3}$$

where $B(q_j^i)$ is the peak transmission rate for q_j connected to AP_i, and $B(AP_i)$ is the bandwidth of the communication link between AP_i and a router.

Layer *NL* consists of routers (*R*) and communication links (*CL*). For each CL_i the maximal bandwidth $B(CL_i)$ is defined. Each router may be connected with any numbers of access points, other routers and servers.

Layer *SL* contains servers (*S*) consisting of computational nodes N_i. Each N_i is characterized by performance P_i reserved for RTIoT system, and it may be equipped with a network interface. Thus each computational node may be connected to another router.

The goal of our methodology is to find the system architecture that fulfills all time constraints and uses existing network infrastructure. All network resources (servers, routers, access points and communication links) that may be used in the system define the initial architecture $\Pi_I=\{S', R', AP', CL'\}$. But Π_I may have performance that is not sufficient for the given system. In such case some modifications of Π_I may be required. Our methodology minimizes the cost of such modifications by optimizing the target architecture to best utilize available network resources and to minimize the total cost of all required modifications. Each resource is characterized by properties defining the cost and the performance. Specifications of all available resources constitute the database of resources $L=\{R'', CL'', S''\}$.

R'' is a set of available routers. Each router r_i is defined by the following properties:

- $C(r_i)$ - cost of the router,
- $n_p(r_i)$ - the number of ports,
- $P(r_i)$ - set of ports, for each port p_i (i=1,..., $n_p(r_i)$) the maximum available bandwidth of the port ($B(p_i)$), is defined.

Communication links $cl_i \in CL''$ are characterized by the maximal available bandwidth $B(cl_i)$ and the cost of link $C(cl_i)$. Communication link connects any route port with: port of another router, access point port or network interface port. The final bandwidth for such connection c_j is defined as:

$$B(c_j) = MIN(B(p_s), B(cl_i), B(p_d)) \tag{4}$$

where: p_s and p_d are ports connected by communication link cl_i. Thus, the time of transmission of packet D_i through connection c_j is the following:

$$T(D_i) = \frac{l(D_i)}{B(c_j)} \tag{5}$$

where $l(D_i)$ is the length of packet D_i.

We assume that each server s_i is configurable and may consist of any number of nodes i.e. a multiprocessor or a cluster architecture. Each node may execute all assigned tasks sequentially. Thus, the following properties characterize the server:

- n_S - the number of nodes, hence server s_i may be represented as a set $\{N_1, \ldots, N_{n_S}\}$ of nodes,
- n_{MAX} - the maximal number of nodes,

- $C(s_i)$ - the cost function, the cost depends on the number of nodes, but usually the function is not linear. Sample function for a cluster server is presented on Fig.3,
- $\{P_1,\ldots,P_{n_S}\}$ - performance of each node,
- $\{B_1,\ldots,B_{n_S}\}$ - maximal bandwidth of each network interface.

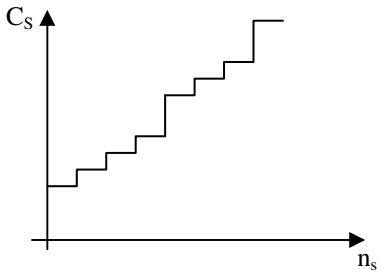

Fig. 3. Sample cost function for cluster server

The time required for executing process τ_i by the node N_j equals:

$$T(\tau_i)=\frac{w(\tau_i)}{P_j} \tag{6}$$

where $w(\tau_i)$ is the workload of task τ_i.

If the performance of Π_I is not sufficient, then if for any server $n_S < n_{MAX}$ then the performance of this server may be increased by adding new nodes, otherwise new servers should be added to the system. Fig. 4 presents sample target architecture of the RTIoT system.

2.3 Requirements and Constraints

Let $\rho(\lambda_x,\lambda_y)$ be a sequence of actions $A_1,\ldots,A_s$ such that λ_x is the request, λ_y is the response, and:

$$A_1=\Phi(v_i,\lambda_x), A_s=\Phi(v_j,\lambda_s)\rightarrow\{\omega_s,\{\lambda_y\}\}, \bigvee_{1<k<n} A_k \rightarrow A_{k+1} \tag{7}$$

where v_i, v_j are any processes and $A_k \rightarrow A_{k+1}$ means that action A_k generates events activating action A_{k+1}. Then, the time of execution of the given sequence of actions is defined as a sum of the following times: time required for transmitting the request, execution times of all processes, time of inter-process communication and transmission time of response:

$$t(\rho(\lambda_x,\lambda_y))=\frac{\omega(\lambda_x)}{B(\lambda_x)}+\sum_{i=1}^{s}\frac{\omega(A_i)}{P(A_i)}+\sum_{i=1}^{s}\frac{\omega(m_i)}{B(m_i)} \tag{8}$$

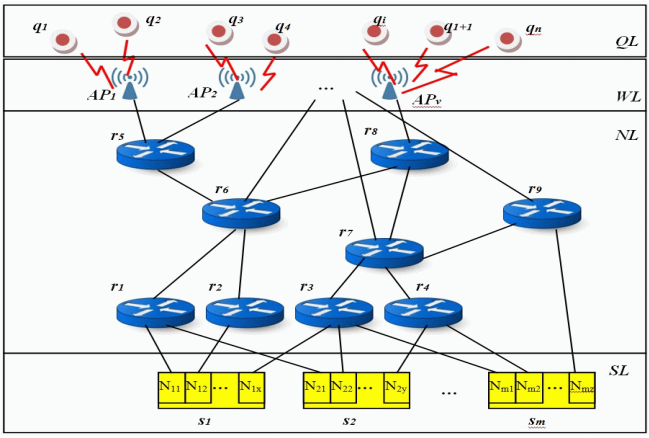

Fig. 4. Sample target architecture

where: $\omega(A_i)$ is the workload of the process activated by action A_i, $P(A_i)$ is the performance of the server executing this process, $\omega(m_i)$ is the communication size and $B(m_i)$ or $B(\lambda_y)$ is a bandwidth of the connection used for sending the message or request. If processes activated by actions A_k and A_{k+1} are executed by the same server, then $\omega(m_k)$=0 for any message sent between these processes.

Time constraint is the maximal period of time that may elapse between sending request by the smart thing and receiving the response. Since the request may activate different sequences of actions until the response will be obtained, therefore the time constraint (deadline) is defined as:

$$t_{\max}(\lambda_x, \lambda_y) = \underset{i}{MAX}(\rho_i(\lambda_x, \lambda_y)) \tag{9}$$

During the synthesis, processes and transmissions are scheduled and assigned to network resources. But if it will be not possible to perform this task without violating time constraints then a new resource should be added to the network infrastructure. The following modifications are considered:

- new communication link *cl*, then the cost equals *C(cl),*
- new router *r*, then the cost equals *C(r),*
- new server *s*, then the cost equals *C(s),*
- additional node *N* in existing server *s*, since the cost function for clusters is not linear then the cost should be computed as $C(s \cup N)$-$C(s)$.

Hence, the total cost of all modifications will be the following:

$$C_M = \sum_i C(cl_i) + \sum_j C(r_i) + \sum_k C(s_k) + \sum_l (C(s_l \cup \bigcup_m N_m) - C(s_l)) \tag{10}$$

The goal of our methodology is to minimize C_M.

3 Synthesis

Our method of synthesis starts from the formal specification of the RTIoT system (as described in p. 2.1) and produces the target architecture of the system, that satisfies all constraints. The method minimizes also the extra cost required to increase the performance of the existing network infrastructure.

3.1 Assumptions

The method is based on the worst case design. We assume that the workload of each action and sizes of all transmissions are estimated for the worst cases. All time constraints should also satisfy the following condition:

$$t_{\max}(\lambda_q, \lambda_o) \leq \frac{1}{f_{\max}(\lambda_q)} \tag{11}$$

where $f_{max}(\lambda_q)$ is the maximal frequency of requests λ_q. Otherwise, the system will be not able to process requests in real-time.

The system specification consists of a set of distributed algorithms (tasks). Our scheduling method is based on the assumption that the worst case is when all tasks will start at the same time, this corresponds to simultaneous appearance of all requests. Thus, all tasks are scheduled in fixed order and are activated in certain time frames. When the system will receive new request, it will be processed during the next activation of the corresponding task. Therefore, time constraints should include this delay, i.e. task should be scheduled with period equal $t_{max}(\lambda_q)/2$.

The main goal of optimization is the minimization of the additional cost. But if it is possible the method schedules tasks and transmissions on available resources. Since in each step it should decide which resource use to execute the next process or next transmission, it should take into consideration other preferences. In our method the least utilized resource is chosen, this corresponds to minimization of the peak workload of servers or communication links. In this way we may avoid blocking the resource by our application and it may be used also for other applications.

3.2 Algorithm of Synthesis

Synthesis is performed using the greedy algorithm, that schedules processes according to their priority. If scheduling violates any time constraint then the network infrastructure is modified by adding new resources to increase the system performance. Presented methodology repeats the following steps, until all processes and transmissions will be scheduled:

- selects the next process, schedules it and schedules all transmissions of messages sent to this process, next the dynamic task graph created,
- if any time constraint is violated in the task graph then new resources are added to the existing architecture, first, resources with minimal cost are considered.

The algorithm is constructive, thus in each step it should be able to verify if after scheduling next task, it is still possible to obtain the valid system. For this purpose the dynamic task graph (DTG) is created. All tasks are simultaneously analyzed according to their order of execution, assuming that processes and transmissions will be executed by the fastest resources. Since in the system specification, only first message received by a process is relevant, all other messages are temporarily neglected. In this way the specification is converted into task graph. Next, the task graph is scheduled using ASAP (As Soon As Possible) method. All paths in the DTG which are embraced by time constraints will be called critical paths. For each critical path p_i the laxity is defined as follows:

$$L(p_i) = t_{\max}(p_i) - t(p_i) \tag{12}$$

where $t(p_i)$ is the time when the last task on the path finish its execution. Each process has assigned priority in reverse order of the laxity of the path containing this process.

Processes are scheduled according to their priorities. After scheduling each task, the DTG is modified and verified against time requirements. If any deadline is overrun then the network infrastructure is modified to enable earlier schedule of the last task and the method proceeds with the next tasks.

Details of the algorithm are presented on Fig. 5. First, the DTG_i for each task is created, all processes are assigned to the best resources and scheduled using ASAP method. Next, critical paths are computed and if any path will overrun deadline then algorithm stops (it is not possible to construct the system even using the fastest resources). Next, initial list L of processes is created and sorted according to descending order of priorities. Initial list contains only initiators. In the main loop of the algorithm, consecutive processes are removed from list L and scheduled. After successful scheduling, DTG graph is reconstructed, new priorities are computed and all successors of the scheduled task are added to list L. If it is not possible to find feasible schedule then the set of the resources Ψ', required for finding the schedule is added to the system. As a result the final network infrastructure Π and the statically scheduled DTG are received.

The algorithm for minimizing the cost of resources that must be added to the network is presented on Fig. 6. The system performance may be increased by adding new server or one node to existing servers (for faster execution of task T_i) and/or by adding new connections (to earlier finish transmissions incoming to task T_i). First all possible single modifications are analyzed, for each one the cost is computed. If exists a modification for which violation of the deadline will be compensated (i.e. $\Delta T \geq \Delta T_r$) then the modification with minimal cost is returned. Otherwise all combinations of single modifications are analyzed, according to ascending order of costs. Algorithm will finish when the first set of modifications, compensating the deadline overrun, will be found.

```
/* Construction of DTG graphs for each task */
Π=available network infrastructure;
Find the best performance of resources available in the database: P(n(S))best, b(cl)best;
for each task Ai do
    for each process Tj in Ai do assign t(Tj)=w(Tj)/P(n(S))best to Tj;
    for each message mj in Ai do assign t(cj)=l(mj)/b(cl)best to mi;
for each task Ai do
    Create temporary dynamic graph DTGi;;
ASAP scheduling and assigning priorities to each process Ti in all DTGs;
for each DTGi do
    for each critical path p_k^i in DTGi do
        if t(p_k^i)>tmax(p_k^i) then stop - it is not possible to find the solution;
Create an ordered list of initiator processes starting from the highest priority L={T1,...,Tn};
/* Scheduling */
while list L≠φ do
    Ti = first(L); Remove Ti from L;
    Find Ψ={n(Sf), {CLf}} in Π, such that te(Ti) is minimal;
    Assign Ti to n(Sf) and incoming messages of Ti to {CLf};
    Reschedule processes in each DTGi,;
    for each TDGi do
        for each critical path p_k^i in DTGi do
            if t(p_k^i)>tmax(p_k^i) then
                Find Ψ'={n(Sc), {CLc}, {Rc}} from the database, such that all time constraints are
                satisfied and C(Ψ') is minimal;
                Π= Π ∪ Ψ';
                Assign Ti to n(Sc) and incoming messages of Ti to {CLc};
                Reschedule processes in each DTGi,;
        Compute new priorities and update L;
```

Fig. 5. Algorithm of synthesis

4 Example

As an example demonstrating our methodology we present the design of an adaptive navigation system for a smart city. We assume that all cars are equipped with GPS navigation devices (GD), that are able to communicate with the Internet using wireless communication (we assume that the network of access points covers the whole city). GD devices send requests to RTIoT system. Requests contain information about current position, the destination and user preferences. Then, the system finds the optimal route and sends response to GD device. Since GD expects response in reasonable time then the system should satisfy real-time constraints. The idea of such system is based on the adaptability, i.e. the system may take into consideration traffic information, traffic impediments (e.g. car accidents) and it may construct different routes for the same destinations to avoid traffic jams.

```
Cost_min=0;
ΔT_r= t( p_k^i )-t_max( p_k^i );
Ω=φ;
for each cl_i in the database do
  for each incoming transmission m_j do
    Temporarily add cl_i (and router if required) to Π and assign m_j to it;
    ΔT= t'( p_k^i )- t( p_k^i );
    if ΔT>0 then Ψ={ cl_i } ∪ {r_i}; Ω= Ω ∪ Ψ;
for each s_l and N_j in the database do
    Temporarily add s_l or N_j to Π and assign T_i to it;
    ΔT= t'( p_k^i )- t( p_k^i );
    if ΔT>0 then Ψ={ cl_i }; Ω= Ω ∪ Ψ;
if exists Ψ_i ∈ Ω such that ΔT≥ ΔT_r then
  return MinCost(Ψ_i);
for each subset σ={Ψ_a ,..., Ψ_b } from Ω do
   Temporarily add σ to Π and assign T_i and icoming trasmissions to it;
    ΔT= t'( p_k^i )- t( p_k^i );
    if ΔT>0 then return σ;
```

Fig. 6. Algorithm for cost minimization

Since the system may receive thousands of requests per second the centralized system may not be able to handle all request due to the communication bottleneck. Therefore, we propose the distributed system. The city is partitioned into sectors, routes through each sector are computed by different processes (Fig. 7). Each process also receives requests and sends responses from/to positions inside the corresponding sector. Thus, the function of the system may be specified as a set of distributed algorithms, similar to the echo algorithm. In our example the specification consists of 8 tasks, in each task another process is the initiator. Initiator receives all requests coming from the corresponding sector, computes all possible routes to adjacent sectors and sends the information about routes to adjacent processes. When messages will reach the destination sector, then the best route is selected and information about it is sent back to the initiator.

Assume that the available network infrastructure, which may be used for our system consists of 3 servers (Fig. 8a) and that execution times for all processes are presented in Table 1. After applying our method it occurred that the performance of the system is sufficient, the final task assignment is given on Fig. 8b. Next, we try to map our application onto the network presented on Fig. 9a. In this case allocation of new nodes for cluster was required, the final system is presented on Fig. 9b. Part of the schedule is presented on Fig.10.

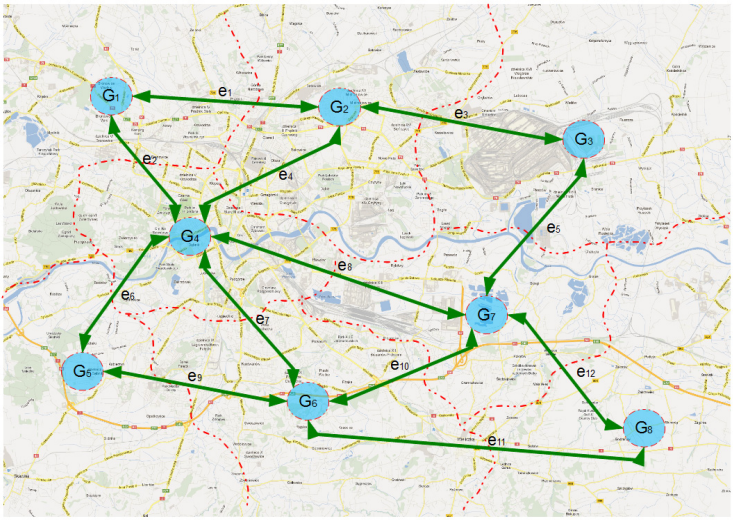

Fig. 7. Processes assigned to sectors of a city

Table 1. Execution times for 3 servers

	Server S1	Server S2	Server S3
Process	T_i[ms]	T_i[ms]	T_i[ms]
G1	54	67,5	90
G2	153	191,25	255
G3	37	46,25	61,67
G4	160	200	266,7
G5	28	35	46,7
G6	95	118,75	158,34
G7	63,8	79,75	106,34
G8	80	100	133,34

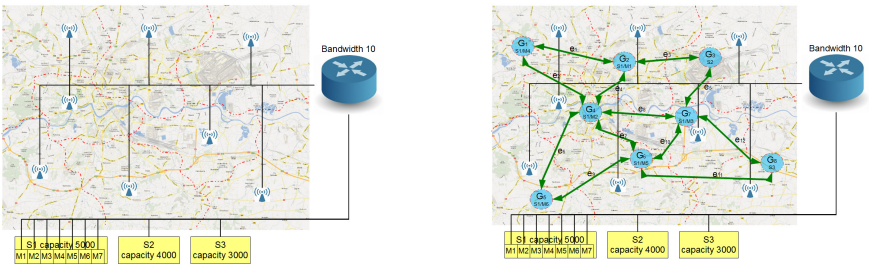

(a) (b)

Fig. 8. Initial network infrastructure 1 (a) and the target architecture (b)

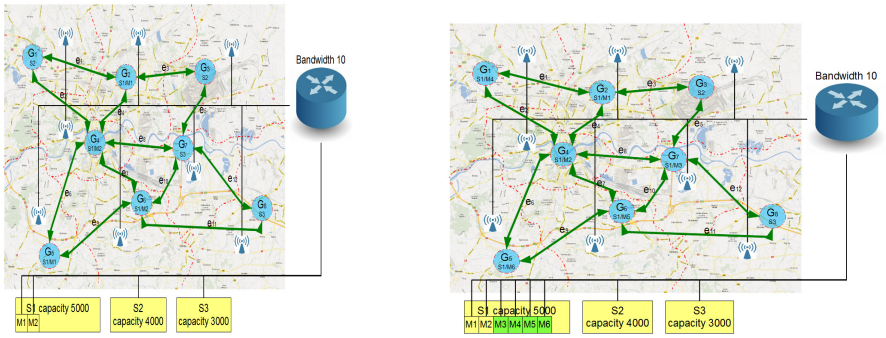

(a) (b)

Fig. 9. Initial network infrastructure 2 (a) and the target system architecture (b)

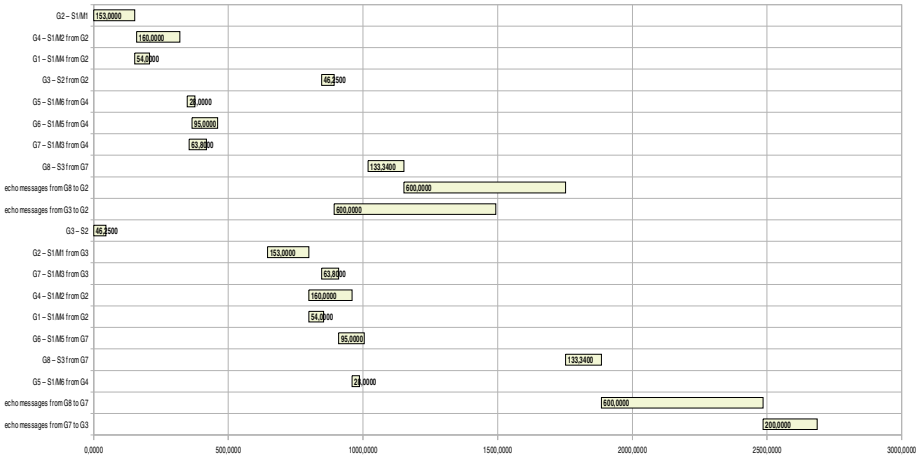

Fig. 10. Part of the schedule

5 Conclusions

In this paper the methodology for synthesis of reactive, real-time applications accordant with the Internet of Things concept, was presented. We developed the architectural model of the reactive RTIoT system and we proposed the method of specification for such systems, in the form of a set of distributed algorithms. Next, the method of synthesis that guarantees the fulfillment of all time requirements was proposed. The method schedules all processes and transmissions on available network resources, and if it is not possible, then adds new resources minimizing the cost of

such enhancements. Finally we presented the design process of the sample RTIoT system, which underlines the advantages of our methodology. To the best of our knowledge it is the first methodology of synthesis for real-time IoT systems.

In our approach we use heuristic greedy algorithm for scheduling and allocation of new resources. In the future work we will consider developing a more sophisticated methods of optimization as well as more advanced methods for the worst case analysis. Reactive RTIoT systems are a new challenge for future IoT. We believe that in the future, RTIoT systems will constitute an important class of IoT systems, thus efficient design methods will be very desirable.

References

1. Atzoria, L., Iera, A., Morabito, G.: The Internet of Things: A survey. Computer Networks 54(15), 2787–2805 (2010)
2. Uckelmann, D., Harrison, M., Michahelles, F.: An Architectural Approach Towards the Future Internet of Things. In: Uckelmann, D., Harrison, M., Michahelles, F. (eds.) Architecting the Internet of Things. Springer, Heidelberg (2011)
3. Guinard, D., Trifa, V., Mattern, F., Wilde, E.: From the Internet of Things to the Web of Things: Resource Oriented Architecture and Best Practices. In: Uckelmann, D., Harrison, M., Michahelles, F. (eds.) Architecting the Internet of Things. Springer, Heidelberg (2011)
4. Guinard, D., Trifa, V., Wilde, E.: A Resource Oriented Architecture for the Web of Things. In: IEEE International Conference on the Internet of Things (2010)
5. Trifa, V., Wieland, S., Guinard, D., Bohnert, T.M.: Design and Implementation of a Gateway for Web-based Interaction and Management of Embedded Devices. In: 2nd International Workshop on Sensor Network Engineering, IWSNE 2009 (2009)
6. Tel, G.: Introduction to Distributed Algorithms, 2nd edn. Cambridge University Press (2001)
7. Buettner, M., Greenstein, B., Sample, A., Smith, J.R., Wetherall, D.: Revisiting smart dust with RFID sensor networks. In: Proceedings of ACM HotNets (2008)
8. Yeager, D.J., Sample, A.P., Smith, J.R.: WISP: A Passively Powered UHF RFID Tag with Sensing and Computation. In: Ahson, S.A., Ilyas, M. (eds.) RFID Handbook: Applications, Technology, Security, and Privacy. CRC Press (2008)
9. Hui, J., Culler, D., Chakrabarti, S.: 6LoWPAN: Incorporating IEEE 802.15.4 Into the IP Architecture – Internet Protocol for Smart Objects (IPSO) Alliance, White Paper #3 (January 2009), `http://www.ipso-alliance.org`
10. Gershenfeld, N., Krikorian, R., Cohen, D.: The internet of things. Scientific American 291(4), 76–81 (2004)
11. Fielding, R.T., Taylor, R.N.: Principled Design of the Modern Web Architecture. ACM Transactions on Internet Technology 2(2), 115–150 (2002)
12. Crane, D., McCarthy, P.: Comet and Reverse Ajax: The Next-Generation Ajax 2.0. Apress (2008)
13. Chang, E.J.H.: Echo Algorithms: Depth Parallel Operations on General Graphs. IEEE Transactions on Software Engineering 8(4) (1982)

iScope – Viewing Biosignals on Mobile Devices

Christian Breitwieser[1], Oliver Terbu[1], Andreas Holzinger[2], Clemens Brunner[1], Stefanie Lindstaedt[3], and Gernot R. Müller-Putz[1]

[1] Institute for Knowledge Discovery, Graz University of Technology, Inffeldgasse 13/IV, 8010 Graz, Austria
{c.breitwieser,clemens.brunner,gernot.mueller}@tugraz.at, o.terbu@gmail.com
[2] Institute for Medical Informatics, Statistics and Documentation, Medical University Graz, Auenbruggerplatz 2/V, 8036 Graz, Austria
andreas.holzinger@meduni-graz.at
[3] Know Center GmbH, Inffeldgasse 13/VI, 8010 Graz, Austria
slind@know-center.at

Abstract. We developed an iOS based application called iScope to monitor biosignals online. iScope is able to receive different signal types via a wireless network connection and is able to present them in the time or the frequency domain. Thus it is possible to inspect recorded data immediately during the recording process and detect potential artifacts early without the need to carry around heavy equipment like laptops or complete PC workstations. The iScope app has been tested during various measurements on the iPhone 3GS as well as on the iPad 1 and is fully functional.

Keywords: biosignal, ECG, EEG, iOS, monitoring, application, visualization.

1 Introduction

Recording, processing, storing, and analyzing biosignals is a major part within the broad field of neuroscience or health informatics. Common biosignals in this case include the electroencephalogram (EEG), the electrocardiogram (ECG), and many others. Such biosignals are often either recorded, stored and processed later on or directly processed online during the recording process. In both cases, a clean and artifact free signal is a crucial requirement; a recording heavily contaminated with biological and/or technical artifacts could render the recorded data useless. Thus, online monitoring of the recorded signals is an important aspect during biosignal recording processes.

Many companies already provide tools to monitor such signals like the Brainvision recorder from BrainProducts (Brain Products, Gilching, Germany) or their open-source acquisition program PyCorder. Other open-source tools [1] include the BCI2000 Source Signal Viewer [2], the OpenViBE Signal Display [3] or the tools4BCI TiAScope[1]. All these viewers provide the user with the possibility to

[1] tools4bci.sf.net

Q. Zu, B. Hu, and A. Elçi (Eds.): ICPCA-SWS 2012, LNCS 7719, pp. 50–56, 2013.

monitor the acquired signals. However, they are partly bound to hardware from one manufacturer or restricted to single operating systems, and they all require a running personal computer to display the recorded signals. Often, in case of patient measurements and other measurements out of the lab, a full-blown measurement system can be a high burden. This might be due to limited space, safety regulations or just the inconvenience to carry around an array of laptops.

Furthermore, as presented in [5,6], flexibility and standardization are important, in the field of brain-computer interface (BCI) research [7]. BCIs, as described with a functional model by Mason et al. [8], rely on realtime processing of brain signals, or in the case of hybrid BCI systems [9], also on processing of other types of input signals like buttons, joysticks, and many more. Reliable processing and an early detection of artifacts or other disturbances in the recorded data are a crucial requirement to provide accurate feedback to the user.

To cope with these issues, we present a lightweight and portable app running on iOS devices (iPhone, iPad,...) to monitor recorded biosignals online, using the tools4BCI TiA (TOBI interface A) protocol [4]. Figure 1 shows a schematic illustration of the data flow and at which point the iScope is used to display the acquired signals. With this application, it becomes possible to monitor the biological signals in realtime and immediately determine the signal quality, hence avoiding recording useless data due to bad signal quality.

2 Methods

2.1 Requirement Analysis

As presented in [4], biosignal acquisition can be subdivided into different signal types such as EEG, ECG, and many more. Such a distinction is a meaningful way to transmit and display signals, as different signal types like EEG or ECG have different characteristics (amplitude, vulnerability to interferences, ...). Thus, individual treatment for different signal types is further also a meaningful way to design the iScope. Due to a limited resolution and display size of iPods, iPads and others, the selection of individual channels is an important feature too, as it might become a problem to draw all signals at once [10]. Additionally, a user should be free to choose the signals to display.

Signals can be analyzed in the time as well as in the frequency domain. Often, the observation of a signal in the frequency domain reveals information, hardly visible in the time domain. As the fast fourier transform (FFT) is a powerful and relatively low resource consuming way to transfer a time domain signal into the frequency domain, this feature is a valuable requirement too.

Usually it is desired to inspect a certain time window of recorded data, e.g., the last 10 seconds, but this requirement can change during a recording out of various reasons. Thus, a time-zoom function is a crucial requirement. With this function it is possible to steplessly change the timeframe of the displayed signals. Additionally, the possibility to zoom exactly one channel to full screen is implemented, as a detailed inspection of single channels is a necessary feature too.

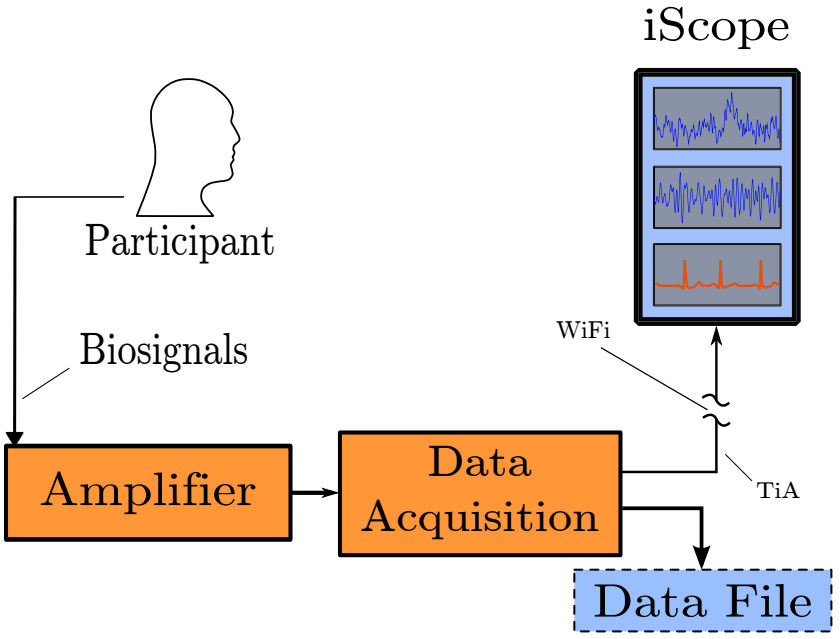

Fig. 1. Schematic illustration of the data flow to the iScope. Biosignals are recorded from a participant by an amplifier and acquired by a data acquisition module. This module then delivers the recorded data via the TiA protocol to the iScope, where it can be monitored in realtime in different ways.

2.2 Design Principles

iOS devices are usually designed to fulfill low power consumption requirements, which are unfortunately usually related to limited processing power of the respective device. Thus, especially in case of data acquisition with many channels or high sampling rates, an iOS device might be to slow to display all channels at once. Furthermore, the resolution is also restricted in some way. A meaningful way to cope with those two problems is the introduction of a fixed amount of graphs visible on the display and the possibility to scroll through all signals. Hence, only a fixed number of signals has to be displayed at once, resulting in a scalable behavior based on the number of displayed channels and their sampling rates.

To avoid freezing of the device in case of insufficient processing power, the only supported protocol is the user datagram protocol (UDP), which is also offered by TiA. In case of a full network buffer, samples are automatically dropped, reducing the amount of samples to process. In case of any sample loss, the user will be notified with red lines in the individual graphs, padding the lost samples.

To fulfill the usual look-and-feel of the iOS environment, the whole control of iOS is realized with finger gestures. Moving one finger up or down on the display is used to scroll through the different graphs, a two finger pinch gesture is used

to in- or decrease the displayed timeframe and double taps are used to zoom the tapped channel to full screen mode.

3 Results

3.1 The iScope App

Figures 2 and 3 show different user screens of the iScope app, either presenting acquired signals in the time- or the frequency domain.

It can be seen, that the channel selection is functional and also the the distinction of different signal types is properly supported. Furthermore, this selection can be modified during the running app. iScope is able to display multiple graphs at once, also from different signal types, as visible in Figure 2(b), where EEG signals are shown together with an ECG signal. Figure 2(c) illustrates the zoomed ECG signal for a timeframe of 1.7 s with additional information.

Figure 3(a) shows FFT spectra of multiple channels, which are computed and plotted in realtime. The zoomed FFT view mode is presented in Figure 3(b), which provides additional information compared to the multi graph view. In this case, the spectrogram is computed for a time period of one second and updated every 0.2 s. This parameters can be changed in the iScope configuration to fit the individual users needs.

A mobile application is not just the pure 1:1 transformation of a possible desktop solution, instead a complete adaptation on the mobile context of use, as it is essential in the medical area to consider the aspects of mobility and to bring a clear added value for the end user [11]. One possible solution is to adapt to the individual context automatically, so to say making the App smart [12].

iScope further supports various other little features, as re-grouping of graphs, automatic or manual scaling, the possibility to take screenshots, save them to the device or send them per email and other little things.

4 Discussion

iScope was successfully tested and evaluated on different iOS devices. It has already been used in various measurements within and outside the lab and has proved its usefulness. It is easy and intentional to use, as common iOS apps. It further proved it's stability during measurements with a duration longer than two hours.

The current iScope implementation is based on iOS 4, but porting to newer iOS versions should become no problem and will be a straight forward process [13]. Furthermore, it has mainly been tested on different iOS devices like the iPhone 3GS or the iPad 1. Considering this two devices, a main difference in computational power could be recognized. While the iPhone 3GS was merely able to process and display 3 channels (while receiving 10 channels) at once without juddering, the border of the iPad 1 was much higher. Due to the higher

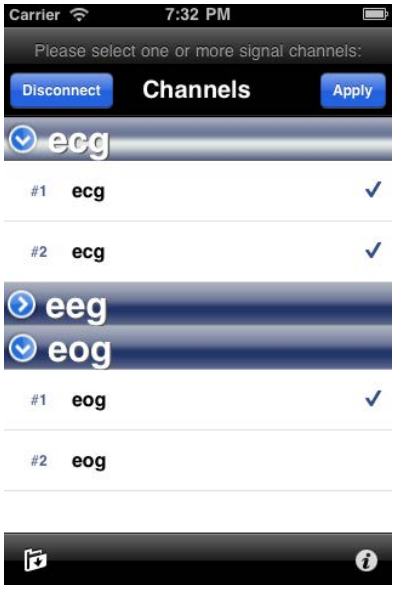

(a) Selection Screen

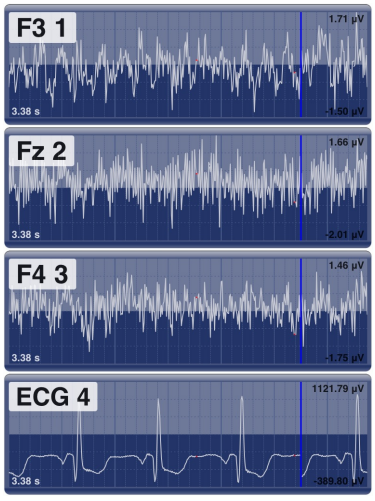

(b) Visualization Screen

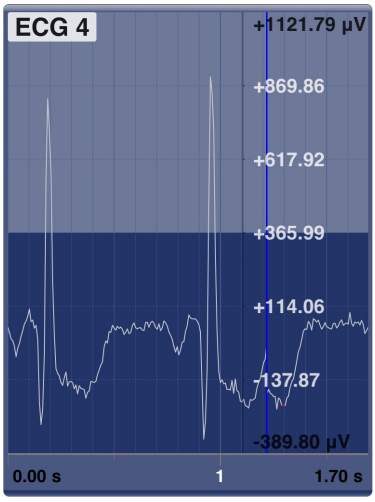

(c) Detailed Visualization

Fig. 2. User screens within the iScope app. The first screen shows the selection screen, where individual channels or entire signal types can be switched on or off. The second screen shows the usual visualization screen in the time domain with four signal graphs. Screen number three presents the zoomed mode of the fourth signal graph.

computational power of the iPad 1, it was smoothly possible to show 4 channels and calculate the FFT view at the same time, while receiving 32 channel with 128 Hz sampling rate without any sample loss.

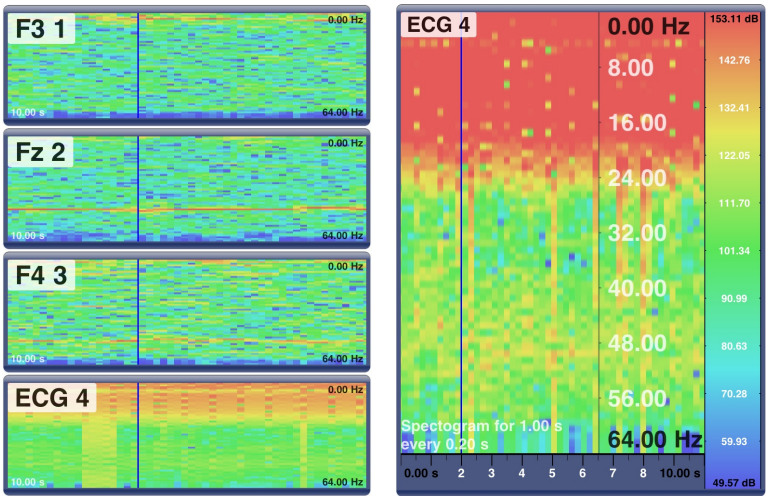

(a) Frequency domain view for multiple channels

(b) Zoomed frequency domain view for a single channel

Fig. 3. Multi graph and zoomed FFT view within the iScope app. Red colors illustrate a higher power and blue colors a lower power. Concrete values are visible in the zoomed presentation mode.

Due to the rapid development of such mobile devices, higher sampling rates and a higher number of channels will become possible because of the increase of computational power. Better display resolutions will further facilitate the presentation of more signal graphs at once.

However, distribution of the iScope is not a trivial process. A main component of the iScope, the TiA library, is licensed under the lesser GNU public license (LGPL), which creates some issues, uploading the iScope to Apple's app store. Thus, the iScope is currently only available on request, as it has to be built for individual devices manually. However, after resolving the licensing issues, caused by the TiA lib, the iScope app is planned to be published in the app store, to distribute this useful tool to a broader community.

Acknowledgements. This work is supported by the European ICT Programme Project FP7-224631. This paper only reflects the authors' views and funding agencies are not liable for any use that may be made of the information contained herein. The authors are further grateful to the KnowCenter for financial and technical support during the development of the iScope app.

References

1. Brunner, C., Andreoni, G., Bianchi, L., Blankertz, B., Breitwieser, C., Kanoh, S., Kothe, C.A., Lécuyer, A., Makeig, S., Mellinger, J., Perego, P., Renard, Y., Schalk, G., Susila, I.P., Venthur, B., Müller-Putz, G.R.: BCI Software Platforms. In: Allison, B., Dunne, S., Leeb, R., Del, R., Millán, J., Nijholt, A. (eds.) Towards Practical Brain-Computer Interfaces: Bridging the Gap from Research to Real-World Applications (2012) (in press)
2. Schalk, G., McFarland, D.J., Hinterberger, T., Birbaumer, N., Wolpaw, J.R.: BCI 2000: a general-purpose brain-computer interface (BCI) system. IEEE. Trans. Biomed. Eng. 51(6), 1034–1043 (2004)
3. Renard, Y., Lotte, F., Gibert, G., Congedo, M., Maby, E., Delannoy, V., Bertrand, O., Lécuyer, A.: OpenViBE: An open-source software platform to design, test, and use brain-computer interfaces in real and virtual environments. Presence-Teleop. Virt. 19(1), 35–53 (2010)
4. Breitwieser, C., Daly, I., Neuper, C., Müller-Putz, G.R.: Proposing a Standardized Protocol for Raw Biosignal Transmission. IEEE. Trans. Biomed. Eng. 59(3), 852–859 (2012)
5. Müller-Putz, G.R., Breitwieser, C., Cincotti, F., Leeb, R., Schreuder, M., Leotta, F., Tavella, M., Bianchi, L., Kreilinger, A., Ramsay, A., Rohm, M., Sagebaum, M., Tonin, L., Neuper, C., Millán, J.d.R.: Tools for Brain-Computer Interaction: A General Concept for a Hybrid BCI. Front Neuroinform 5(30), 1–10 (2011)
6. Brunner, P., Bianchi, L., Guger, C., Cincotti, F., Schalk, G.: Current trends in hardware and software for brain-computer interfaces (BCIs). J. Neural. Eng. 8(2), 1–7 (2011)
7. Wolpaw, J.R., Birbaumer, N., McFarland, D.J., Pfurtscheller, G., Vaughan, T.M.: Brain-computer interfaces for communication and control. Clin. Neurophysiol. 113(6), 767–791 (2002)
8. Mason, S.G., Birch, G.E.: A general framework for brain-computer interface design. IEEE Trans. Neural. Syst. Rehabil. Eng. 11(1), 70–85 (2003)
9. Pfurtscheller, G., Allison, B.Z., Brunner, C., Bauernfeind, G., Solis-Escalante, T., Scherer, R., Zander, T.O., Müller-Putz, G., Neuper, C., Birbaumer, N.: The hybrid BCI. Front Neurosci. 4(30), 1–11 (2010)
10. Holzinger, A., Treitler, P., Slany, W.: Making Apps Useable on Multiple Different Mobile Platforms: On Interoperability for Business Application Development on Smartphones. In: Quirchmayr, G., Basl, J., You, I., Xu, L., Weippl, E. (eds.) CD-ARES 2012. LNCS, vol. 7465, pp. 176–189. Springer, Heidelberg (2012)
11. Holzinger, A., Kosec, P., Schwantzer, G., Debevc, M., Frühwirth, J., Hofmann-Wellenhof, R.: Design and Development of a Mobile Computer Application to Reengineer Workflows in the Hospital and the Methodology to Evaluate its Effectiveness. J. Biomed. Inform. 44(6), 563–570 (2011)
12. Holzinger, A., Geier, M., Germanakos, P.: On the development of smart adaptive user interfaces for mobile e-Business applications: Towards enhancing User Experience some lessons learned, pp. 3–16. SciTePress, INSTICC, Setubal (2012)
13. Holzinger, A., Errath, M.: Mobile computer Web-application design in medicine: some research based guidelines. Universal Access in the Information Society International Journal 6, 31–41 (2007)

CloudSVM: Training an SVM Classifier in Cloud Computing Systems

F. Ozgur Catak[1] and M. Erdal Balaban[2]

[1] National Research Institute of Electronics and Cryptology (UEKAE), Tubitak
ozgur.catak@tubitak.gov.tr
[2] Quantitative Methods, Istanbul University
mebalaban@gmail.com

Abstract. In conventional distributed machine learning methods, distributed support vector machines (SVM) algorithms are trained over pre-configured intranet/internet environments to find out an optimal classifier. These methods are very complicated and costly for large datasets. Hence, we propose a method that is referred as the Cloud SVM training mechanism (CloudSVM) in a cloud computing environment with MapReduce technique for distributed machine learning applications. Accordingly, (i) SVM algorithm is trained in distributed cloud storage servers that work concurrently; (ii) merge all support vectors in every trained cloud node; and (iii) iterate these two steps until the SVM converges to the optimal classifier function. Single computer is incapable to train SVM algorithm with large scale data sets. The results of this study are important for training of large scale data sets for machine learning applications. We provided that iterative training of splitted data set in cloud computing environment using SVM will converge to a global optimal classifier in finite iteration size.

Keywords: Support Vector Machines, Distributed Computing, Cloud Computing, MapReduce.

1 Introduction

Machine learning applications generally require large amounts of computation time and storage space. Learning algorithms have to be scaled up to handle extremely large data sets. When the training set is large, not all the examples can be loaded into memory in training phase of the machine learning algorithm at one step. They are computationally expensive to process. It is required to distribute computation and memory requirements among several connected computers for scalable learning.

In machine learning field, support vector machines (SVM) offer most robust and accurate classification method due to their generalized properties. With its solid theoretical foundation and also proven effectiveness, SVM has contributed to researchers' success in many fields. But, SVM's suffer from a widely recognized

Q. Zu, B. Hu, and A. Elçi (Eds.): ICPCA-SWS 2012, LNCS 7719, pp. 57–68, 2013.

scalability problem in both memory requirement and computational time [1]. SVM algorithm's computation and memory requirements increase rapidly with the number of instances in data set, many data sets are not suitable for classification [14]. The SVM algorithm is formulated as quadratic optimization problem. Quadratic optimization problem has $O(m^3)$ time and $O(m^2)$ space complexity, where m is the training set size [2]. The computation time of SVM training is quadratic in the number of training instances.

The first approach to overcome large scale data set training is to reduce feature vector size. Feature selection and feature transformation methods are basic approaches for reducing vector size [3]. Feature selection algorithms choose a subset of the features from the original feature set and feature transformation algorithms creates new data from the original feature space to a new space with reduced dimensionality. In literature, there are several methods; Singular Value Decomposition (SVD) [4], Principal Component Analysis (PCA) [5], Independent Component Analysis (ICA) [6], Correlation Based Feature Selection (CFS) [7], Sampling based data set selection. All of these methods have a big problem for generalization of final machine learning model. Generalization accuracy of supervised learning algorithms like SVM will increase as the training data set scale increases. The more training data given to SVM algorithm, the more evidence the learning algorithm has about the classification problem. Training data would contain every possible example of classification problem, and then classifier function would generalize perfectly.

Second approach for large scale data set training is chunking [13]. Collobert et al. [12] propose a parallel SVM training algorithm that each subset of whole dataset is trained with SVM and then the classifiers are combined into a final single classifier. Lu et al. [8] proposed distributed support vector machine (DSVM) algorithm that finds support vectors (SVs) on strongly connected networks. Each site within a strongly connected network classifies subsets of training data locally via SVM and passes the calculated SVs to its descendant sites and receives SVs from its ancestor sites and recalculates the SVs and passes them to its descendant sites and so on. Ruping et al. [9] proposed incremental learning with Support Vector Machine. One needs to make an error on the old Support Vectors (which represent the old learning set) more costly than an error on a new example. Syed et al. [10] proposed the distributed support vector machine (DSVM) algorithm that finds SVs locally and processes them altogether in a central processing center. Caragea et al. [11] in 2005 improved this algorithm by allowing the data processing center to send support vectors back to the distributed data source and iteratively achieve the global optimum. Graf et al. [14] had an algorithm that implemented distributed processors into cascade top-down network topology, namely Cascade SVM. The bottom node of the network is the central processing center. The distributed SVM methods in these works converge and increase test accuracy. All of these works have similar problems.

They require a pre-defined network topology and computer size in their network. The performance of training depends on the special network configuration. Main idea of current distributed SVM methods is first data chunking then parallel implementation of SVM training. Global synchronization overheads are not considered in these approaches.

In this paper, we propose a Cloud Computing based novel SVM method with MapReduce [18] technique for distributed training phase of algorithm. By splitting training set over a cloud computing system's data nodes, each subset is optimized iteratively to find out a single global classifier function. The basic idea behind this approach is to collect SVs from every optimized subset of training set at each cloud node, and then merge them to save as global support vectors. Computers in cloud computing system exchange only minimum number of training set samples. Our algorithm CloudSVM is analyzed with various UCI public datasets. CloudSVM is built on the LibSVM and implemented using the Hadoop implementation of MapReduce.

This paper is organized as follows. In section 2, we will provide an overview to SVM formulations. In Section 3, presents the Map Reduce pattern in detail. Section 4 explains system model with our implementation of the Map Reduce pattern for the SVM training. In section 5, convergence of CloudSVM is explained. In section 6, simulation results with various UCI datasets are shown. Thereafter, we will give concluding remarks in Section 7.

2 Support Vector Machine

Support vector machine is a supervised learning method in statistics and computer science, to analyze data and recognize patterns, used for classification and regression analysis. SVM uses machine learning theory to maximize generalization accuracy while automatically avoiding overfit to the training dataset. The standard SVM takes a set of input data and predicts, for each given input, which of two possible classes forms the input, making the SVM a non-probabilistic binary linear classifier. Note that if the training data are linearly separable as shown in Figure 1, we can select the two hyper planes of the margin in a way that there are no points between them and then try to maximize their distance. By using geometry, we find the distance between these two hyper planes is $2/\|\boldsymbol{w}\|$. Given some training data, D, a set of n points of the form

$$D = \{(\boldsymbol{x}_i, y_i) | \boldsymbol{x}_i \in R^m, y_i \in \{-1,1\}\}_{i=1}^n \quad (1)$$

where $\boldsymbol{x}_i$ is an m-dimensional real vector, y_i is either -1 or 1 denoting the class to which point $\boldsymbol{x}_i$ belongs. SVMs aim to search a hyper plane in the Reproducing Kernel Hilbert Space (RKHS) that maximizes the margin between the two classes of

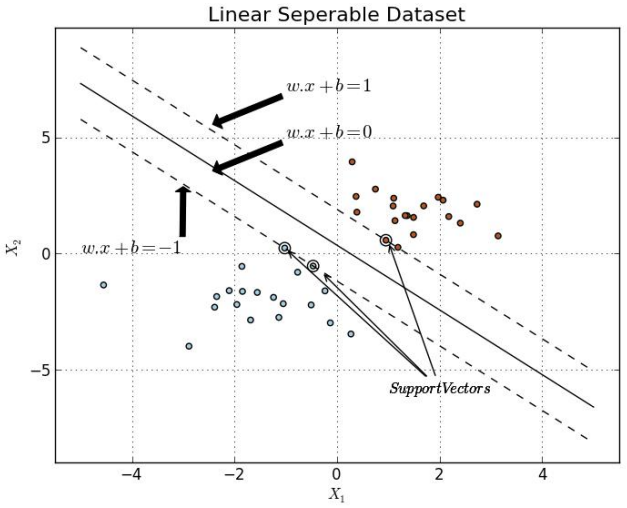

Fig. 1. Binary classification of an SVM with Maximum-margin hyper plane trained with samples from two classes. Samples on the margin are called the support vectors.

data in D with the smallest training error [13]. This problem can be formulated as the following quadratic optimization problem:

$$\begin{gathered} minimize : P(\boldsymbol{w}, b, \xi) = \frac{1}{2}\|w\|^2 + C \sum_{i=1}^{m} \xi_i \\ subject\ to : y_i(\langle \boldsymbol{w}, \phi(\boldsymbol{x}_i) \rangle + b) \geq 1 - \xi_i \\ \xi_i \geq 0 \end{gathered} \tag{2}$$

for i = 1,... , m, where ξ_i are slack variables and C is a constant denoting the cost of each slack. C is a trade-off parameter which controls the maximization of the margin and minimizing the training error. The decision function of SVM is $f(\boldsymbol{x}) = \boldsymbol{w}^T \phi(\boldsymbol{x}) + b$ where the $\boldsymbol{w}$ and b are obtained by solving the optimization problem P in Equation (2). By using Lagrange multipliers, the optimization problem P in Equation (2) can be expressed as

$$\begin{gathered} min: F(\alpha) = \frac{1}{2}\alpha^T \boldsymbol{Q}\, \alpha^T - \alpha^T \mathbf{1} \\ subject\ to : \mathbf{0} \leq \alpha \leq \boldsymbol{C} \\ \boldsymbol{y}^T \alpha = 0 \end{gathered} \tag{3}$$

Where $[Q]_{ij} = y_i\, y_j\, \phi^T(x_i)\phi(x_j)$ is the Lagrangian multiplier variable. It is not need to know ϕ, but it is necessary to know is how to compute the modified inner product which will be called as kernel function represented as $\$\, K(\boldsymbol{x}_i, \boldsymbol{x}_j) = \phi^T(\boldsymbol{x}_i)\phi(\boldsymbol{x}_j)$. Thus, $[Q]_{ij} = y_i y_j K(x_i, x_j)$. Choosing a positive definite kernel

K, by Mercer's theorem, then optimization problem P is a convex quadratic programming (QP) problem with linear constraints and can be solved in polynomial time.

3 MapReduce

MapReduce is a programming model derived from the map and reduce function combination from functional programming. MapReduce model widely used to run parallel applications for large scale data sets processing. Users specify a map function that processes a key/value pair to generate a set of intermediate key/value pairs, and a reduce function that merges all intermediate values associated with the same intermediate key [18]. MapReduce is divided into two major phases called map and reduce, separated by an internal shuffle phase of the intermediate results. The framework automatically executes those functions in parallel over any number of processors [19]. Simply, a MapReduce job executes three basic operations on a data set distributed across many shared-nothing cluster nodes. First task is Map function that processes in parallel manner by each node without transferring any data with other notes. In next operation, processed data by Map function is repartitioned across all nodes of the cluster. Lastly, Reduce task is executed in parallel manner by each node with partitioned data.

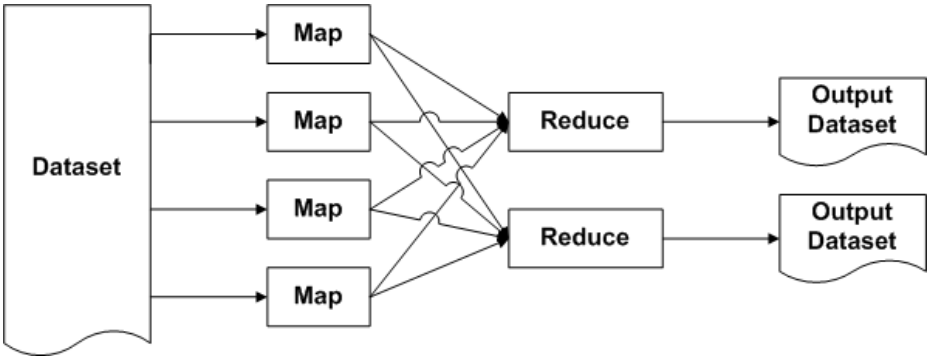

Fig. 2. Overview of MapReduce System

A file in the distributed file system (DFS) is split into multiple chunks and each chunk is stored on different data-nodes. A map function takes a key/value pair as input from input chunks and produces a list of key/value pairs as output. The type of output key and value can be different from input key and value:

$$map(key_1, value_1) \Rightarrow list(key_2, value_2)$$

A reduce function takes a key and associated value list as input and generates a list of new values as output:

$$reduce(key_2, list(value_2)) \Rightarrow list(value_3)$$

Each Reduce call typically produces either one value v_3 or an empty return, though one call is allowed to return more than one value. The returns of all calls are collected as the desired result list. Main advantage of MapReduce system is that it allows distributed processing of submitted job on the subset of a whole dataset in the network.

4 System Model

CloudSVM is a MapReduce based SVM training algorithm that runs in parallel on multiple commodity computers with Hadoop. As shown in Figure 3, the training set of the algorithm is split into subsets and each one is evaluated individually to get $\boldsymbol{\alpha}$ values (i.e. support vectors). In Map stage of MapReduce job, the subset of training set is combined with global support vectors. In Reduce step, the merged subset of training data is evaluated. The resulting new support vectors are combined with the global support vectors in Reduce step. The CloudSVM with MapReduce algorithm can be explained as follows. First, each computer within a cloud computing system reads the global support vectors, then merges global SVs with subsets of local training data and classifies via SVM. Finally, all the computed SVs in cloud computers are merged. Thus, algorithm saves global SVs with new ones. The algorithm of CloudSVM consists of the following steps.

1. As initialization the global support vector set as $t = 0, V^t = \emptyset$
2. t = t + 1;
3. For any computer in $l, l = 1, \ldots, L$ reads global SVs and merge them with subset of training data.
4. Train SVM algorithm with merged new data set
5. Find out support vectors
6. After all computers in cloud system complete their training phase, merge all calculated SVs and save the result to the global SVs
7. If $h^t = h^{t-1}$ stop, otherwise go to step 2

Pseudo code of CloudSVM Algorithm's Map and Reduce function are given in Algorithm 1 and Algorithm 2.

Algorithm 1 Map Function of CloudSVM Algorithm

$SV_{Global} = \emptyset$ //Empty global support vector set
while $h^t \neq h^{t-1}$
  for $l \in L$ **do** //For each subset loop
    $D_l^t \leftarrow D_l^t \cup SV_{Global}^t$
  end for
end while

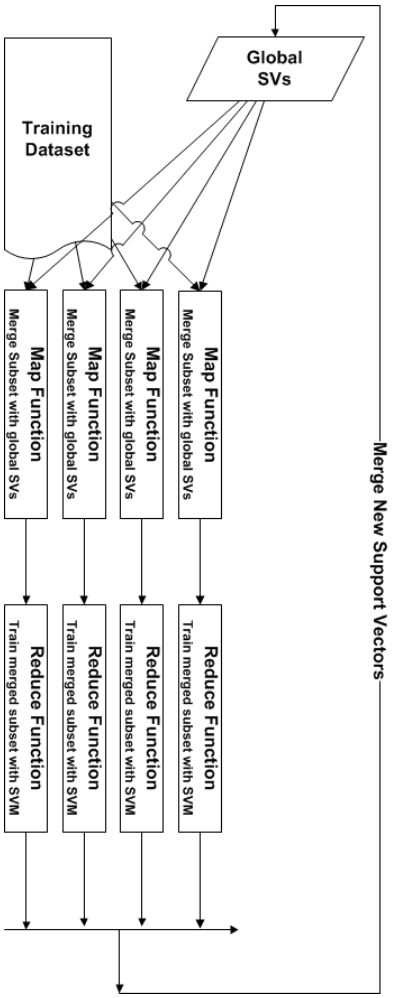

Fig. 3. Schematic of Cloud SVM architecture

Algorithm 2 Reduce Function of CloudSVM Algorithm

while $h^t \neq h^{t-1}$ **do**
  for $l \in \boldsymbol{L}$
    $SV_l, h^t \leftarrow svm(D_l)$ // Train merged Dataset to obtain Support Vectors and Hypothesis
  end for
  for $l \in \boldsymbol{L}$
    $SV_{Global} \leftarrow SV_{Global} \cup SV_l$
  end for
end while

For training SVM classifier functions, we used LibSVM with various kernels. Appropriate parameters C and γ values were found by cross validation test. We used 10-fold cross validation method. All system is implemented with Hadoop and streaming Python package mrjob library.

5 Convergence of CloudSVM

Let S denotes a subset of training set D, $F(S)$ is the optimal objective function over data set S, h^* is the global optimal hypothesis for which has a minimal empirical risk $R_{emp}(h)$. Our algorithm starts with $\boldsymbol{SV}^0_{Global} = \mathbf{0}$, and generates a non-increasing sequence of positive set of vectors $\boldsymbol{SV}^t_{Global}$, where $\boldsymbol{SV}^t_{Global}$ is the vector of support vector at the t.th iteration. We used hinge loss for testing our models trained with CloudSVM algorithm. Hinge loss works well for its purposes in SVM as a classifier, since the more you violate the margin, the higher the penalty is [20]. The hinge loss function is the following:

$$l(f(x), y) = max\{0, 1 - y.f(x)\}$$

Empirical risk can be computed with an approximation:

$$R_{emp}(h) = \frac{1}{n}\sum_{i=1}^{n}\big(l(h(x_i), y_i)\big)$$

According to the empirical risk minimization principle the learning algorithm should choose a hypothesis $\hat{h}$ which minimizes the empirical risk:

$$\hat{h} = \arg\max_{h \in H} R_{emp}(h)$$

A hypothesis is found in every cloud node. Let X be a subset of training data at cloud node i where $X \in R^{mxn}$, $\boldsymbol{SV}^t_{Global}$ is the vector of support vector at the t. th iteration, $h^{t,i}$ is hypothesis at node i with iteration t, then the optimization problem in equation 3 becomes

$$\begin{aligned} &maximize\ h^{t,l} = -\frac{1}{2}\begin{bmatrix}\alpha_1\\ \alpha_2\end{bmatrix}^T \begin{bmatrix}\boldsymbol{Q}_{11} & \boldsymbol{Q}_{12}\\ \boldsymbol{Q}_{21} & \boldsymbol{Q}_{22}\end{bmatrix}\begin{bmatrix}\alpha_1\\ \alpha_2\end{bmatrix} + \begin{bmatrix}1\\ 1\end{bmatrix}^T \begin{bmatrix}\alpha_1\\ \alpha_2\end{bmatrix} \\ &subject\ to: 0 \le \alpha_i \le C, \forall i\ and \sum_{i}^{I} \alpha_i y_i = 0 \end{aligned} \tag{4}$$

where $\boldsymbol{Q}_{12}$ and $\boldsymbol{Q}_{21}$ are kernel matrices with respect to

$$Q_{12} = \left\{ K_{i,j}\left(x_{ij}, SV^t_{Global(i,j)}\right) \middle|\ i = 1, \dots, m, j = 1, \dots n \right\}.$$

α_1 and α_2 are the solutions estimated by node i with dataset X and $\boldsymbol{SV}_{Global}$. Because of the Mercer's theorem, our kernel matrix $\boldsymbol{Q}$ is a symmetric positive-

definite function on a square. Then our sub matrices $\boldsymbol{Q}_{12}$ and $\boldsymbol{Q}_{21}$ must be equal. We can define $\boldsymbol{Q}_{11}$ and $\boldsymbol{Q}_{22}$ matrices such that

$$\boldsymbol{Q}_{11} = \left\{ K_{i,j}\left(x_{i,j}, x_{i,j}\right) \middle| x_{i,j} \in X, i = 1, \dots, m, j = 1, \dots, n \right\}$$
$$\boldsymbol{Q}_{22} = \left\{ K_{i,j}\left(SV_{Global}, SV_{Global}\right) \middle| i = 1, \dots, m, j = 1, \dots, n \right\}$$

at iteration t.

Algorithm's stop point is reached when the hypothesis' empirical risk is same with previous iteration. That is:

$$R_{emp}(h^t) = R_{emp}(h^{t-1}) \tag{5}$$

Lemma : Accuracy of the decision function of CloudSVM classifier at iteration t is always greater or equal to the maximum accuracy of the decision function of SVM classifier at iteration $t-1$. That is

$$R_{emp}(h^t) \leq arg \min_{h \in H^{t-1}} R_{emp}(h) \tag{6}$$

Proof: Without loss of generality, Iterated CloudSVM monotonically converges to optimum classifier.

$$\boldsymbol{SV}_{Global}^{t} = \boldsymbol{SV}_{Global}^{t-1} \cup \{ \boldsymbol{SV}_{i}^{t-1} \mid i = 1, \dots n \}$$

where *n* is the data set split size(or cloud node size). Then, training set for svm algorithm at node *i* is

$$d = X \cup \boldsymbol{SV}_{Global}^{t}$$

Adding more samples cannot decrease the optimal value. Generalization accuracy of the sub problem in each node monotonically increases in each step.

6 Simulation Results

We have selected several data sets from the UCI Machine Learning Repository, namely, German, Heart, Ionosphere, Hand Digit and Satellite. The data sets length and input dimensions are shown in Table 1. We test our algorithm over a real-word data sets to demonstrate the convergence. Linear kernels were used with optimal parameters (γ , C). Parameters were estimated by cross-validation method.

Table 1. The datasets used in experiments

Dataset Name	Train. Data	Dim.
German	1000	24
Heart	270	13
Ionosphere	351	34
Satellite	4435	36

We used 10-fold cross-validation, dividing the set of samples at random into 10 approximately equal-size parts. The 10 parts were roughly balanced, ensuring that the classes were distributed uniformly to each of the 10 parts. Ten-fold cross-validation works as follows: we fit the model on 90% of the samples and then predict the class labels of the remaining 10% (the test samples). This procedure is repeated 10 times, with each part playing the role of the test samples and the errors on all 10 parts added together to compute the overall error.

Table 2. Performance Results of CloudSVM algorithm with various UCI datasets γ

Dataset Name	γ	C	No. Of Iteration	No. Of SVs	Accuracy	Kernel Type
German	10^0	1	5	606	0.7728	Linear
Heart	10^0	1	3	137	0.8259	Linear
Ionosphere	10^8	1	3	160	0.8423	Linear
Satellite	10^0	1	2	1384	0.9064	Linear

Table 3. Data set prediction accuracy with iterations

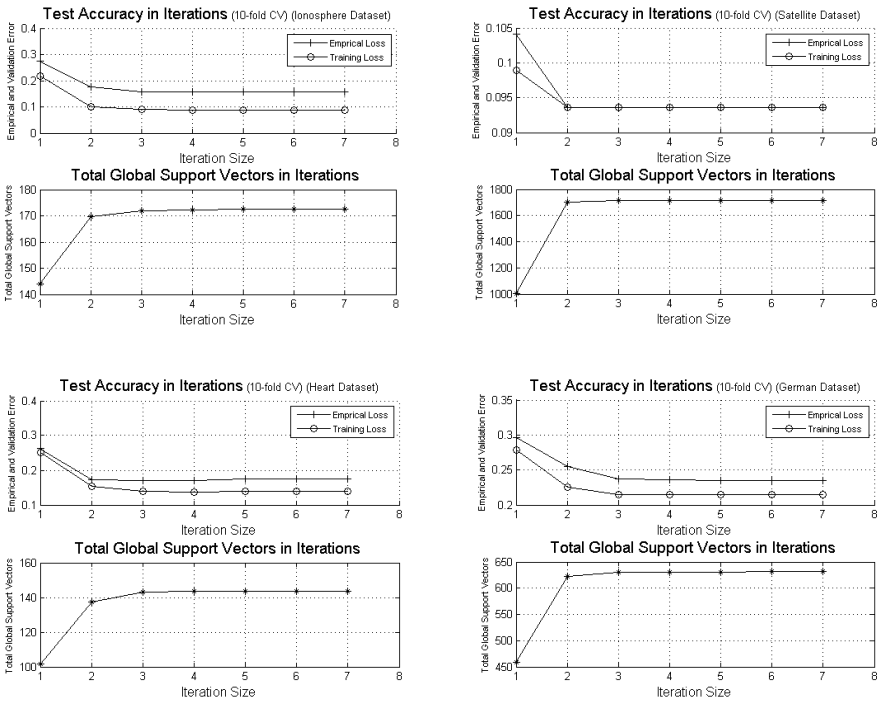

To analyse the CloudSVM, we randomly distributed all the training data to a cloud computing system with 10 computers with pseudo distributed Hadoop. Data set prediction accuracy with iterations and total number of SVs are shown in Table 3. When iteration size become 3 - 5, test accuracy values of all data sets reach to the highest values. If the iteration size is increased, the value of test accuracy falls into a steady state. The value of test accuracy is not changed for large enough number of iteration size. As a result, the CloudSVM algorithm is useful for large size training data.

7 Conclusion and Further Research

We have proposed distributed support vector machine implementation in cloud computing systems with MapReduce technique that improves scalability and parallelism of split data set training. The performance and generalization property of our algorithm are evaluated in Hadoop. Our algorithm is able to work on cloud computing systems without knowing how many computers connected to run parallel. SVM algorithm's training problem for large scale data set is solved with the designed algorithm referred to as CloudSVM. It is empirically shown that the generalization performance and the risk minimization of our algorithm are better than the previous results.

References

1. Chang, E.Y., Zhu, K., Wang, H., Bai, H., Li, J., Qiu, Z., Cui, H.: PSVM: Parallelizing Support Vector Machines on Distributed Computers. In: Advances in Neural Information Processing Systems, vol. 20 (2007)
2. Tsang, I.W., Kwok, J.T., Cheung, P.M.: Core Vector Machines: Fast SVM Training on Very Large Data Sets. J. Mach. Learn. Res. 6, 363–392 (2005)
3. Weston, J., Mukherjee, S., Chapelle, O., Pontil, M., Poggio, T., Vapnik, V.: Feature selection for SVMs. In: Advances in Neural Information Processing Systems, vol. 13, pp. 668–674 (2000)
4. Golub, G., Reinsch, C.E.: Singular value decomposition and least squares solutions. Numerische Mathematik 14, 403–420 (1970)
5. Jolliffe, I.T.: Principal Component Analysis, 2nd edn., New York. Springer Series in Statistics (2002)
6. Comon, P.: Independent Component Analysis, a new concept? Signal Processing 36, 287–314 (1994)
7. Hall, M.A.: Correlation-based Feature Selection for Discrete and Numeric Class Machine Learning. In: Proceedings of the Seventeenth International Conference on Machine Learning, pp. 359–366. Morgan Kaufmann Publishers Inc., San Francisco (2000)
8. Lu, Y., Roychowdhury, V., Vandenberghe, L.: Distributed parallel support vector machines in strongly connected networks. IEEE Trans. Neural Networks 19, 1167–1178 (2008)

9. Stefan, R.: Incremental Learning with Support Vector Machines. In: IEEE International Conference on Data Mining, p. 641. IEEE Computer Society, Los Alamitos (2001)
10. Syed, N.A., Liu, H., Sung, K.: Incremental learning with support vector machines. In: Proceedings of the Fifth ACM SIGKDD International Conference on Knowledge Discovery and Data Mining (KDD), San Diego, California (1999)
11. Caragea, C., Caragea, D., Honavar, V.: Learning support vector machine classifiers from distributed data sources. In: Proceedings of the Twentieth National Conference on Artificial Intelligence (AAAI), Student Abstract and Poster Program, pp. 1602–1603. AAAI Press, Pittsburgh (2005)
12. Collobert, R., Bengio, S., Bengio, Y.: A parallel mixture of SVMs for very large scale problems. Neural Computation 14, 1105–1114 (2002)
13. Vapnik, V.N.: The nature of statistical learning theory. Springer, NY (1995)
14. Graf, H.P., Cosatto, E., Bottou, L., Durdanovic, I., Vapnik, V.: Parallel support vector machines: The cascade SVM. In: Proceedings of the Eighteenth Annual Conference on Neural Information Processing Systems (NIPS), pp. 521–528. MIT Press, Vancouver (2004)
15. Chang, C.C., Lin, C.J.: LIBSVM: a library for support vector machines. ACM Transactions on Intelligent Systems and Technology 2, 27–27 (2011)
16. LeCun, Y., Bottou, L., Bengio, Y., Haffner, P.: Gradient-based learning applied to document recognition. Proceedings of the IEEE 86, 2278–2324 (1998)
17. Bertsekas, D.P.: Nonlinear Programming, 2nd edn. Athena Scientific, Cambridge (1999)
18. Dean, J., Ghemawat, S.: Mapreduce: Simplified data processing on large clusters. In: Proceedings of the 6th conference on Symposium on Operating Systems Design & Implementation(OSDI), p. 10. USENIX Association, Berkeley (2004)
19. Schatz, M.C.: CloudBurst: highly sensitive read mapping with MapReduce. Bioinformatics 25, 1363–1369 (2009)
20. Rosasco, L., De Vito, E., Caponnetto, A., Piana, M., Verri, A.: Are loss functions all the same. Neural Computation 16, 1063–1076 (2011)

A Document-Based Data Warehousing Approach for Large Scale Data Mining

Hualei Chai, Gang Wu, and Yuan Zhao

School of Software,
Shanghai Jiao Tong University, Shanghai, China
{joestone_chai,zhaoyuan}@sjtu.edu.cn
wugang@cs.sjtu.edu.cn

Abstract. Data mining techniques are widely applied and data warehousing is relatively important in this process. Both scalability and efficiency have always been the key issues in data warehousing. Due to the explosive growth of data, data warehousing today is facing tough challenges in these issues and traditional method encounters its bottleneck. In this paper, we present a document-based data warehousing approach. In our approach, the ETL process is carried out through MapReduce framework and the data warehouse is constructed on a distributed, document-oriented database. A case study is given to demonstrate details of the entire process. Comparing with RDBMS based data warehousing, our approach illustrates better scalability, flexibility and efficiency.

Keywords: Data Warehousing, Document-based, Big Data, MapReduce.

1 Introduction

Data mining has always been a hotspot issue in computer science. Having the rapid development in IT industry in the past two decades, data mining techniques are now widely applied in almost every aspect of our economic and social life and have enjoyed an explosive growth. From scientific research to Business Intelligence systems, data mining is an irreplaceable part of the Knowledge Discovery process.

Data warehouse is the basis of data mining, and is playing an important role in modern IT industry and has evolved into an unique and popular business application class. Early builders of data warehouses already consider those systems to be key components of their data mining and even decision-support system architecture [1].

Since the emergence of cloud computing, the demand of mining massive data has become relatively urgent. In order to obtain valuable information hidden in the ocean of data, data mining techniques are being applied to almost every aspect of modern society. The ability of handling big data is so crucial that no one could neglect. However, big data poses more challenges, among which, both scalability and efficiency have always been the most important issues and have

Q. Zu, B. Hu, and A. Elçi (Eds.): ICPCA-SWS 2012, LNCS 7719, pp. 69–81, 2013.

attracted tremendous interests. In recent years, large-scale data mining has been extensively investigated [2], and many approaches have been proposed [3][4][5][6].

Traditional data warehousing is more like constructing a larger database, and follows certain steps including requirements analysis, data modeling, normalization or denormalization and so on [7]. However, as a RDBMS based data warehouse, it is facing tougher challenges today. First of all, the problem comes from scalability. The collected data is getting bigger and bigger, and even beyond the tolerance of a traditional DBMS. Second, dealing with heterogeneous data sources is complex. The schema of data sources could change more frequently than before as the real business keep changing. The corresponding modification job is a great burden, as redesign and reconstruction of the data warehouse may take place from time to time. This could be tremendous time and money consuming. Third, efficiency has become the bottleneck of RDBMS based data warehouse. Data mining usually calls for millions of aggregation operations and mathematical computations. Those operations are very likely to be inefficient and complex because all data is organized as linked tables in RDBMS, thus each query leads to several operations like projection and OUTER-JOIN. As a result, the operating efficiency is sacrificed.

This paper focuses on presenting a better solution of data warehousing in the big data era. We explore a document-based data warehousing approach. This approach includes three phases, namely documentization phase, aggregation phase and data loading phase. In the documentization phase, we extract all the data from respective heterogeneous data sources, and write them to basic text files. In the aggregation phase, a MapReduce process is applied to accomplish ETL of data from multiple sources, and transform all the results into JSON objects [8]. The main difference between our approach and the traditional ones is that after the aggregation phase we keep all the data as recursive key/value pairs, getting rid of their original schema which includes the table format and foreign keys. The data loading phase is responsible for putting all the output JSON objects into a document-oriented data warehouse. In order to demonstrate details of the entire process, a case study is given in Section 4 and the result of our experiments shows that our data warehouse is more scalable, efficient and flexible.

The rest of this paper is organized as follows. Section 2 presents the background and related work. The Third section gives our solution and the fourth section is a real case study in order to show details of the whole process. Evaluations and discussions are also given in Section 4. Section 5 presents our future plans and conclusion of this paper.

2 Background

2.1 Difference between Database and Data Warehouse

Data warehousing is an essential element of data mining or decision-support system and has always been a focus in the database industry. Data warehouse is a "subject-oriented, integrated, time-varying, non-volatile collection of data

that is used primarily in organizational decision making" [9]. The main difference between a data warehouse and a database is that the former one is targeting at collecting useful data from heterogeneous sources, and seeking information and patterns hidden behind the data. Whereas the later one is used to record data generated during a transaction process. Therefore the ability of handling a huge amount of data is more critical for a data warehouse and database emphasis more on the atomic operation, which refers to accuracy and consistency in a single operation.

Figure 1 is used to demonstrate different requirements for a data warehouse and an ordinary database application. Data warehouse is a basic support for data mining, whereas transaction process, for example, OLTP, is a typical application of a database. In general, data mining is usually read-intensive and calls for complex mathematical operations, but transaction processes are write-intensive with simple operations. Therefore operating efficiency, including throughput and response time, is more important for data warehouses and consistence and accuracy is prior to an ordinary database.

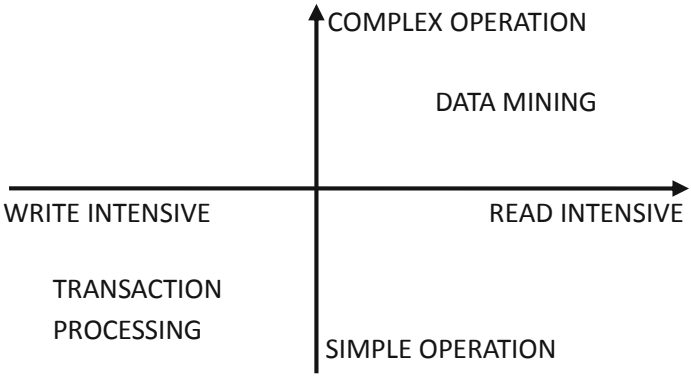

Fig. 1. Different Database Application Characteristics

2.2 Challenges in Data Warehouse

Considering both the different characteristics between data warehouses and databases, and the demand of big data, we conclude the following three features for a data warehouse as the most critical requirements.

Scalability

The data warehouse should have full support for dynamic scaling. When dealing with big data, any database server would have the risk of running out of storage and there is not a "large-enough-ever" storage. In the coming cloud era, dynamic scaling is definitely the best solution.

Efficiency

This word here refers to two aspects, the efficiency of construction and maintenance of the data warehouse, and operating efficiency of the data warehouse

responds to each query. Data mining usually studies large data set from multiple sources. How convenient is the data immigration? How fast does the data warehouse respond for millions of queries from data mining engine? Efficiency is always of great concern.

Heterogeneity

In a real data mining application, data sources are usually heterogeneous. Data sources may be RDBMS with different schema, or even different types of data set, like XML files, logs or other NoSQL databases. Furthermore, changes in data sources may take place at any time, including introducing new data sources, or adjustment of schema due to commercial reasons. If the data warehouse is not flexible enough to deal with heterogeneous sources, it will lead to reconstruction of the data warehouse, which is really both money and time consuming. The only solution is to put heterogeneity into consideration in designing your data warehouse.

2.3 Related Work

Traditional data warehouse is constructed based on RDBMS, following certain steps includes defining architecture of storage, integrating servers, designing warehouse schema and views, implementing data extraction, cleansing, transformation, loading and so on [10].

Even though Entity Relationship diagrams and other RDBMS techniques are popularly used for database design in OLAP, the database designs recommended by ER diagrams are inappropriate for decision support systems [10]. On one hand, heterogeneous data sources are difficult to be integrated in one schema, which is flexible enough to face possible adjustments of sources in the long run. On the other hand, the RDBMS based data warehouse can not transcend limitations of dynamic scaling due to the fixed schema.

The problem is so important that there have been lots of engineers working on it and they have proposed lots of solutions. Yang Lai and Shi Zhongzhi proposed an indexing method, aiming at more efficient data accessing for large scale data mining [3]. Jane Zhao, proposed an optimization which adds a OLAP service layer in between the data warehouse and data mining application [4]. Vuda Sreenlvase Rao focus on distributed storage and has made some improvements on the hardware [5]. Jin Han, et. al. believed that applying a shared-memory in order to store temporary data, just like the idea of MemCache, would greatly improve accessing efficiency [6].

These works have made some progress, yet they are still facing challenges. On one hand, scalability remains a problem. When collected data gets larger than the origin infrastructure thus corresponding hardware should be extended, but that is not easy for these added in shared-memory [6] or OLAP query layer [4]. On the other hand, heterogeneity is making the problem harder. Both the schema design and indexing system [3] lead to great modification job, because neither has a support of incremental modification. And real business world changes rapidly, any fixed schemas or indexes have problems adjust to any structural updates.

3 Approach

This section gives a document-based data warehousing approach to tackle challenges in big data era. The entire process consists of three phases, namely documentization phase, aggregation phase and data loading phase, and is demonstrated in Fig.2.

3.1 Glossary

MapReduce is a programming model and associated implementation for processing and generating large data sets [11]. It is proposed by Google and used for handling large data analyze tasks. MapReduce consists of two functions: Map and Reduce. The Map function takes input key/value pairs and produces intermediate data, also key/value pairs. The Reduce function collects the intermediate data and produces the final output. This framework is a high efficient distributed programming model and has been validated in recent years.

DFS (Distributed file system) is a file system that allows access to files from multiple hosts via a shared computer network. This makes it possible for multiple users on multiple machines to share files and storage resources. There are various implementations, such as Google File System [12], BigTable [13] and Hadoop's HDFS [14].

JSON (JavaScript Object Notation) is a lightweight data-interchange format [8]. It is based on a subset of the JavaScript Programming Language, Standard ECMA-262 3rd Edition - December 1999. JSON is a completely language-independent text format, and is built on a collection of name/value pairs and an ordered list of values.

3.2 Documentization Phase

The first challenge to tackle is heterogeneous data sources, varying from traditional RDBMS, to XML files, even log files and so on. Documentization refers to extract data from original sources and transform them into independent documents. In this phase, we export all the data from each original sources into a set of typical text files, and an extra document indicating corresponding structure or format of each text file. This is a very important step which guarantees the flexibility of our approach. After this phase, the overall system shall deals with documents only, as shown in Fig.2.

3.3 Aggregation Phase

The core idea of our data warehousing approach is carried out in this phase. In the big data era, thanks to distributed file systems, storage capacity is no

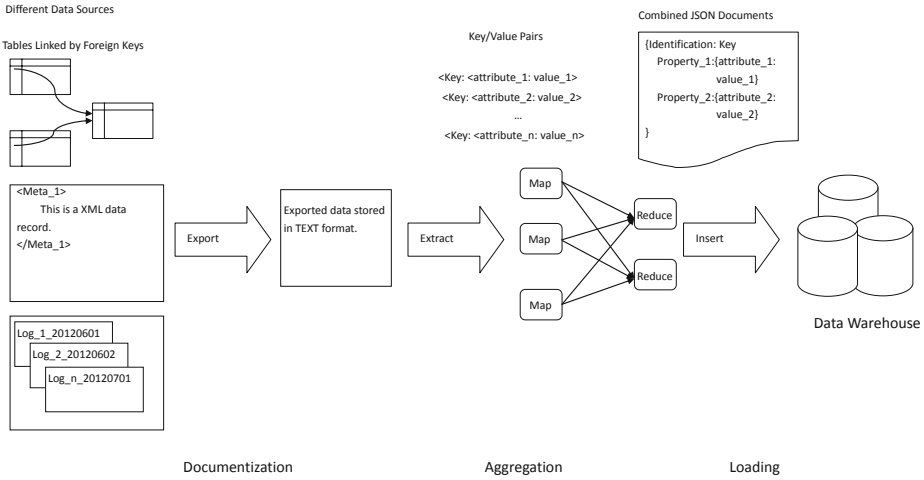

Fig. 2. Document-Based Data Warehousing Process

longer a tough constraint. And the aggregation phase is aimed at promoting query efficiency of the overall system.

Before getting started, all data exported from original databases are uploaded on DFS. And afterwards, a MapRedeuce process is applied. The Map function is applied to read through the data set by line, and transform each line into recursive key/value pairs, having each attribute name as keys and its correspond data as values, thus the intermediate output is produced. The Reduce function is used to collect all the lines by separate identification key, as shown in Fig.2. Lines from different table, which were linked by foreign keys in its previous sources, are now gathered into one JSON object, and written to a document file on DFS. Since data originally from different tables are now gathered via each primary key, it is also convenient to kick out inconsistent data, wrong type data and many other types of dirty data. The algorithm is given in Algorithm 1.

3.4 Data Loading Phase

For load balance and query efficiency considerations, we gather all the JSON objects produced in last phase into multiple documents. In this phase, we read all these files and insert the JSON objects into a document-oriented database. Since all data are stored as JSON objects, which has a nature support for Object-Oriented programming languages, such as JAVA and C++. All need to do in future data mining process is to implement analyze algorithms in any Object-Oriented programming languages without considering any SQL queries. This is both agile and high efficient.

Algorithm 1: MapReduce Data Preparation

```
   Input: FileNames, OutputDirectory
   Output: OutputFile
 1 Procedure Mapper(key=Line Number, value=Line String)
 2 begin
 3     foreach attribute_item in each Line do
 4         if attribute_item is not primary key then
 5             attribute_item ← {"attibute_name:", "attribute_item"}
 6         end
 7         transform Line String into JSON Object
 8         output(key=collect_key, value=Line String in JSON format)
 9     end
10 end
11 Procedure Reducer(key=collect_key, value=Line String in JSON format)
12 begin
13     collect all Line String with same collect_key
14     make new JSON Object: {"collect_key: property"}
15     foreach Line String do
16         add Line String to {"collect_key": {Line String}}
17     end
18     output(key=NULL, value= {"collect_key": {Line String},...,{Line String}})
19 end
```

4 Case Study

In this section, we use a real case in order to show the details of our approach and validate it.

4.1 Data Set

The dataset we use is released in KDD Cup 2012, provided by Tencent, one of the largest micro-blog websites in China [15]. The entire data set is over 10 Gega Byte, consists of 13 entity-relationship tables. The dataset is a subset of basic customer information of Tencent Weibo users, including personal information, such as tweeting activity, comments and each person's Follower and Followee list, and advertisement information. The basic logic view of the dataset is demonstrated in the Fig.3.

In order to estimate a big data input, we replicate this data set 100 times to build a large data collection, which is over 1 TB. We use this data set for two reasons. First, social networks have become tremendously popular in recent years. Popular social network websites like Facebook, Twitter, and Tencent Weibo are adding thousands of enthusiastic new users each day to their existing billions of actively engaged users. Currently, there are more than 200 million registered users on Tencent Weibo, generating over 40 million messages each

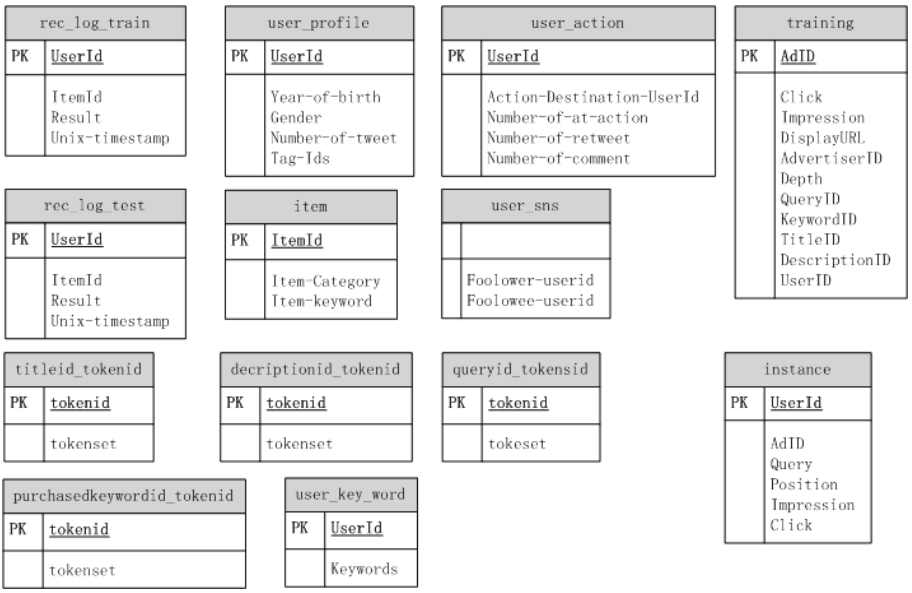

Fig. 3. OR mode of original dataset

day [15]. Valuable information interfering with almost every aspect of social life, including economic, social and political issues, state and regional security issues, scientific and technological researches and so on. As a result, there is an urgent demand of studying this kind of data. Second, the dataset also shares the features of Web 2.0 service, which is a new trend in IT industry and needs to be further investigated. One of the most unique characters of Web 2.0 is that the database stores customer-provide data, therefore the database must be heterogeneous-tolerant and robust enough in order to face customers' different requirements. Under this scenario, our approach is given full play.

4.2 System Environment

The experiment is carried out on a distributed Cluster consists of seven machines. Environmental Parameters of each node is shown in Table 1.

Hadoop is an opensource implementation of MapReduce by Apache Foundation [14]. The Apache Hadoop project consists of many subprojects, among which HDFS(Hadoop DFS) and MapReduce are the most commonly used.

MongoDB is a C++ implemented, opensource document oriented database, developed by 10gen [16]. It is a BSON(Binary JSON) based high performance database, features its schema-free structure, well support for dynamic scaling, powerful Javascript-like query language and high accessing speed.

Table 1. System Environment Parameter

Environment	Parameter
CPU	Intel(R)Xeon(R)CPU E5405@2.00GHZ (2 cores)
Memory	8 GB RAM
Hard Disk	1 TB
Operating System	Ubuntu 12.04 64-bit
JAVA Runtime Environment	JDK 1.7
Hadoop Version	Apache Hadoop 0.20.2
Database	MongoDB 2.0.6 (Linux 64-bit)

4.3 Implementation

The structure of the overall system is shown in Fig.4. There are three parts, data source, MapReduce Cluster and MongoDB Cluster.

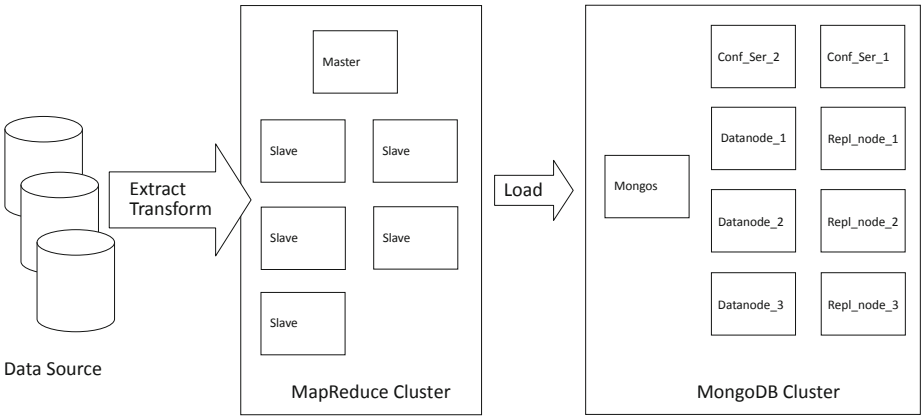

Fig. 4. System Structure of Implementation

In our case, the data source consists of 100 subsets, each of which is a document collection exported from Tencent Weibo's operating database. As for the MapReduce cluster, we built a 6-node Hadoop cluster. One acts as the master and the other five as slaves. Slave node can be dynamically dropped out or added in, in order to validate the system's scalability. The entire experiment is carried out on this cluster separately with 3 nodes and 6 nodes. The last part of Fig.4 is MongoDB Cluster, based on which we constructed our data warehouse. The logical view of the data warehouse's structure is demonstrated in this figure.

- *Mongos* is the accessing node of the cluster.
- *Conf_ser_i* is the ith Configuration Server, maintaining name space, data servers' information and index.

- *Datanode_i* is the ith Data Server.
- *Repl_node_i* is the replica of the ith Data Server.

We choose MongoDB for two reasons. First, it has a very agile support of dynamic scaling. If the data warehouse run out of storage, it is very easy to add in a new node into the distributed storage environment. Second, MongoDB has a special key/value storage mechanism which has a nature support of MapReduce framework. Since the data extraction and loading job is carried out in MapReduce framework, the data loading phase doesn't need to wait till the aggregation phase is totally finished. Therefore, much time and memory is saved.

4.4 Experiment Result and Discussion

Scalability

Definition 1. *Scale Sensitivity (ScaS) measures a system's sensitivity facing changes of workload. ScaS equals to the average value of the multiples of processing time changes divided by the corresponding growth of input data size in multiples. A system with a lower ScaS is less sensitive to workload change, therefore this system features better scalability.*

$$ScaS = Ave(\frac{T/t}{F/f}) \tag{1}$$

where F *is the size of input file and* f *is the size of standard input file, and we use the average size of input subsets as* f *in this case.* T *and* t *are the corresponding running time of input* F *and* f *respectively.*

In our experiment, we implement the entire process as mentioned in Fig.2, using our MapReduce approach, marked as MR in Fig.5. As for comparison, we also implement the same function as a none-MapReduce Java program, which is named SoleJava here. SoleJava runs on single node, while MR is implemented respectively on a 3-node and 6-node cluster. We use ScaS to compare the scale sensitivity of each system.

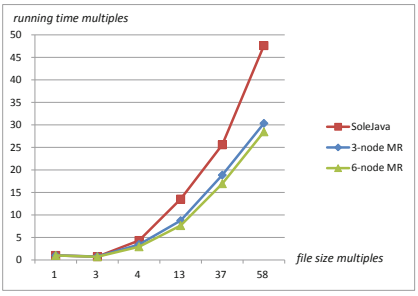

(a) Sensitivity Curve

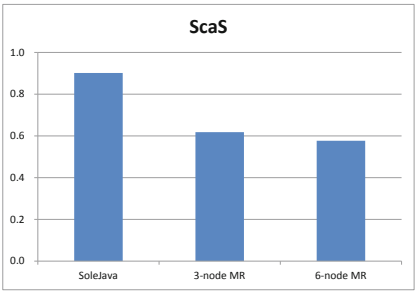

(b) System ScaS

Fig. 5. System Scalability

In Fig.5(a), the horizontal axis marks multiples of input data size of *f*, and the vertical axis records the corresponding running time multiples. As input data set gets larger, the running time multiples of both methods increase. However, the Curve of MR grows always slower than SoleJava. And Fig.5(b) demonstrates the ScaS of SoleJava, 3-node MR and 6-node MR. Facing increasing workload, running time of SoleJava has almost a linear growth of almost the same speed, while ScaS of MR is about two thirds of that of SoleJava. Therefore, facing growing workload, data warehouse built through our approach is less sensitive. That is to say, our approach is more scalable.

Efficiency

We evaluate overall system's efficiency from two perspectives, the efficiency of constructing and operating the data warehouse. As for constructing the data warehouse, Table 2 shows a comparison between traditional approach and our document-based approach. It is straightforward that our approach requires fewer work to do and the process is very agile.

Table 2. Comparison of Data Warehousing Approaches

Phases	Rational DW	Document-based DW
Preparation	Requirement Analysis	Requirement Analysis
	Data Modeling	Data Modeling
Design	Design Table Format	
	Choose Foreign Keys	
Construction	Data Extraction	Documentization
	Data Cleansing	
	Transformation	Aggregation
	Loading	Loading
Operating	SQL query	Object Operation
	OUTTER-JOIN, Projection	
Modification	Change Schema	(Not Affected)
	Possible Reconstruction	

As for operating efficiency, we use an experiment to estimate accessing the data warehouse and validate its performance. Figure 6 shows the efficiency comparison between the MongoDB based data warehouse and a MySQL Cluster based data warehouse, both are build on the same physical machines. A write experiment and a query experiment are carried on both data warehouses. The pillar graph (a) shows the comparison of data insertion performance and the graph (b) shows the QPS (query per second) curve of both system. As demonstrated in Fig.6, the average processing capacity of MongoDB based data warehouse is 50,000 requests per second while that of MySQL based data warehouse is less than 30,000. Therefore our data warehouse is more efficient.

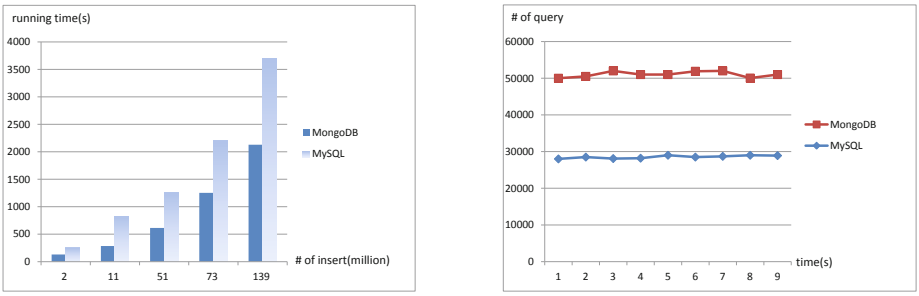

(a) System Respond Time (b) QPS Curve

Fig. 6. Efficiency Comparison

Heterogeneity

Heterogeneity, as mentioned in Section 2, refers to the overall system's flexibility facing both heterogeneous structure and changes of data source. In our experiment, the format of data source is given to our program as an input configuration document, which is read automatically. The unique key/value storage format and schema-free designment the flexibility of our data warehouse. Our data warehouse has no dependence on the schema of data source. When input file is changed, very few lines of code are changed. Also we find this approach to be convenient enough facing similar kinds of data mining requirements.

5 Conclusion

This paper presents a better solution for data warehousing in the big data era. Comparing with traditional RDBMS-based data warehousing, our approach shows better performance in scalability, efficiency and heterogeneity. The approach consists of three phases, namely documentization, aggregation and data loading. Our data warehouse is constructed on a distributed environment and the MapReduce framework is applied for efficiency consideration. Even though it is agreed to all that there is not, and will never be, a "one-fits-for-all" solution, our approach definitely boosts its unique characteristic.

In future, we will introduce more data mining applications based on this data warehouse structure under the similar scenario. More data mining algorithms will be implemented on this platform. We will also work on more friendly documentization tools for different data sources.

References

1. Gupta, V.R.: An Introduction to Data Warehousing. System Services Corporation (1997)
2. Tan, A.X., et al.: A Comparison of Approaches for Large-Scale Data Mining. Technical Report UTDCS-24-10 (2010)
3. Yang, L., Shi, Z.: An Efficient Data Mining Framework on Hadoop using Java Persistentce API. In: 10th IEEE International Conference on Computer and Information Technology (2010)
4. Zhao, J.: Designing Distributed Data Warehouses and OLAP Systems. In: ISTA 2005, pp. 254–263 (2005)
5. Sreenivasa Rao, V., Vidyavathi, S.: Distributed Data Mining And Mining Multi-agent Data. International Journal on Computer Science and Engineering (IJCSE) 02(04), 1237–1244 (2010)
6. Han, J., et al.: A Novel Solution of Distributed Memory NoSQL database for Cloud Computing. In: 2011 10th IEEE/ACIS International Conference on Computer and Information Science (2011), 978-0-7695-4401-4/11$26.00
7. Sen, A., Sinha, A.P.: A comparison of data warehousing methodologies. Communications of The ACM 48(3) (2005)
8. JSON, `http://www.json.org/`
9. Inmon, W.H.: Building the Data Warehouse. John Wiley (1992)
10. Chaudhuri, S., Dayal, U.: An Overview of Data Warehousing and OLAP Technology. ACM Sigmod Record (1997)
11. Dean, J., Ghemawat, S.: MapReduce: Simplified Data Processing on Large Clusters. In: OSDI (2004)
12. Ghemawat, S., et al.: The Google File System. In: SOSP 2003. ACM (2003)
13. Chang, F., et al.: BigTable: A Distributed Storage System for Structured Data. In: OSDI (2006)
14. Apache Hadoop, `http://hadoop.apache.org/`
15. KDD Cup 2012, `http://www.kddcup2012.org/`
16. MongoDB, `http://www.mongodb.org/`

Smart Navigation for Firefighters in Hazardous Environments: A Ban-Based Approach

Mhammed Chammem, Sarra Berrahal, and Nourreddine Boudriga

Communication Networks and Security (CNAS) Laboratory,
University of Carthage, Tunisia
{m.chammem,berrahal.sarra,noure.boudriga2}@gmail.com

Abstract. Recent advances in integrated electronic devices motivated the use of Body Area Networks in many applications including monitoring, localization, tracking and navigation. In this paper we introduce an indoor navigation approach based on Body Area Network to assist firefighters in finding their way to save human lives and to combat fires. For this we develop a technique based on a real-time graph called Temporal Weighted Graph that provides some special functions such as localization, navigation, communication, and hazard estimation. Then we implement a real time solution aiming to predict firefighters' isolation time in an indoor space by estimating the horizon of risk deterioration in the graph. And finally, we demonstrate the importance of the presented technique in assisting firefighters during the navigation process. A set of simulation scenarios are conducted to evaluate the performance of the solution.

Keywords: Indoor navigation, navigation, localization, BAN, sensor network, firefighting, real time, hazard estimation.

1 Introduction

The navigation through indoor environment is a novel area for the deployment of body area networks (BANs) [1] which became essential and more than more important to use in Security and Emergency works such as firefighting sector in order to fight incident and save human lives [2]. In fact, firefighters are one of the first users group interested by indoor navigation because despite all technical advances firefighting still remain a dangerous job and one of the most physically demanding and exhausting activities that a human body can perform. The dangers associated with this activity are the result of a number of factors such as a lack of information regarding firefighters (location and state of health) and the environment surrounding them (size and spread of the fire, surrounding temperature) and the high level of mental and physical stress which might cause lost and disorientation especially in a burning building. This can lead to fatal consequences for both the firefighter operators and the building's occupants. Indoor navigation in firefighting sector deals with guiding firefighter from its present location by avoiding obstacles and hazardous regions. The related works that address the navigation for firefighters hold the following issues that must be taken into account and resolved in the navigation system:

Q. Zu, B. Hu, and A. Elçi (Eds.): ICPCA-SWS 2012, LNCS 7719, pp. 82–96, 2013.

- Firefighting operations take place in unfamiliar, complex, and hazardous environments characterized by the presence of heat, smoke, dust, and noise. This environment is marked by its sudden change.
- Firefighters do not have real-time maps with them when they enter in the building to combat the hazard. During firefighting operations there is a lack of real- time information regarding the environment surrounding firefighters.
- The environmental disruptions and the signal attenuation through walls in indoor environments inhibit the use of some localization technologies [3]; the Global Positioning System (GPS) has problems locating in altitude because it cannot receive the satellite signals indoor.

Due to all these issues, it remains essential to connect, control, locate, and protect firefighters during their missions and analyze their environment in real time manner. Thus, firefighting system should provide a real-time maps managing system that supports some tasks such as navigation, localization, firefighter protection, environment monitoring, and hazard estimation.

The objective of our paper is to address the several tasks and issues mentioned previously. In fact the different problems can be solved if a BAN system is viewed as a part of the firefighting system. The BAN will gather and evaluate information regarding the current situation and location of the firefighters and the indoor environment. The collected data will be sent to the incident commander in order to take decision. So, the major contributions of the paper are listed in the following:

- Build and study a real-time graph, to help firefighters in the rescue operation.
- Predict the possible isolation moments of firefighters based on an estimating function that predicts the risk in the graph.
- Implement an evacuation procedure that proceeds through the path less risky.

The rest of the paper is organized as follows. Section 2 reviews the state of the art of the indoor navigation task in firefighting sector and presents current indoor navigation solutions. The build of the real-time graph for firefighting navigation will be done in section 3, in this section we will explain semantics of this graph, and the specific functions of it. Section 4 gives an explanation of how use the proposed graph to provide smart navigation in hazardous environment. In Section 5, we present the simulation results. The last section concludes the work.

2 State of the Art

The navigation during firefighting operations has been the subject of many researches. Nonetheless the available works don't address in an efficient manner the issues presented above.

In [4] Matthew Barnes, Hugh Leather, and D. K. Arvind, address the presence of hazard throughout the building by finding exit paths from all locations. The progress of hazard is modeled by a Hazard Graph in which the weight of edges corresponds to the fastest time for a hazard to traverse the edge. The progress of the evacuees operation is modeled by a Navigation Graph formed by the human navigable paths between

sensor locations. In this graph the weight of the edge is equal to the lowest time taken by firefighter to move between two locations.

The Fire Information and Rescue Equipment (FIRE) project [5] consists of a fixed wireless sensor network deployed throughout the building, called "SmokeNet", and used to track firefighters during the fire rescue operation. The SmokeNet system is sensitive to the various changes in the environment and it may degrade over time. This degradation can lead to mapping imperfections and limitations.

LifeNet project [6] provides the functionality of traditional lifelines. It is composed with sensor nodes that provide relative positioning and a wearable system that processes some special data from the sensor network and shows navigational guidance on a head-mounted display in order to provide support to the firefighters. Each sensor node acts as a way point to guide the firefighters when they navigate along the area of the incident. The different sensors deployed by firefighters constitute the different escape routes.

Table 1. Comparison between some related works

Solution	Technology used	Mapping			Hazard graph monitoring
		Type	Firefighting management	Services supported	
Emergency Evacuation	WSN	Predefined floor plan map with navigation and hazard graphs.	Real time	- Navigation - Rescue	Yes
LIFENET	BAN WSN	Egocentric representation.	Real time	- Navigation -Localization	Yes
FIRE	WSN	Predefined floor plan map with current locations of the firefighter agent.	Non Real time	-Navigation -Tracking	No
Landmarke	BAN WSN		Non Real time	-Navigation -Tracking	No
Our solution	BAN	Generated map with current agent's location.	Real time	-Navigation -Localization -Tracking -Rescue	Yes

Landmarke project [7] is another navigational support in which a set of nodes called "Landmarke nodes" deployed either in an automatic way or completely by the firefighters themselves; act as way points with special capabilities to find the closest exit, to find a lost firefighter, to tag important places and to collect information regarding the progress of the firefighting mission.

The limitations linked to [4], [6] and [7] are the result of the possible destruction of the deployed sensors under very harsh conditions. This problem can lead to mapping imperfections and erroneous information.

Our method should address the different limitations mentioned above. We aim to support real time navigation for firefighters in hazardous environments through the maintenance of a graph named Temporal Weighted Graph (TWG) in which the hazard conditions are valued in real-time manner.

3 Temporal Weighted Graph for Hazard Management

We aim to support navigation for firefighters in hazardous environments through the maintenance of a graph in which the risk parameters are collected, in a real-time, while firefighters are progressing. We assume that the firefighters are organized into teams; each team is assigned a team leader (or a reference point). The building model is represented as a set of edges E, a set of nodes N, and a set of communication links C defining a Graph $\mathrm{G(t)} = (\mathrm{N}, \mathrm{E}, \mathrm{C})$ named Temporal Weighted Graph TWG, where: N is a set of data structures built at every slot of time and reporting on the slot of time of collection, the place where the reference point is located and information related to risk in the surrounding environment. Therefore, N counts the number of places, in the building, where teams collect information every slot of time.

E represents straight lines between two successive nodes and is referring to paths followed by a team between two successive collections of information. These paths are effective displacements that teams perform between a place where the reference point is found at time and the place where the same reference point is found at instant $t + 1$. However, we assume that when two teams collect their information, at the same place, the data structure reported in the graph is the recent one. Therefore, we formally define a link e by

$$e = (n(t), n'(t')) \quad for \;\; n, n' \in \mathrm{T}$$

where T is the set of teams.

C is a set of communication links between two terminal nodes (in the graph). A presence of communication link indicates that the team leaders of the related teams can communicate.

Typically, a data structure in N defines the time t of information collection made by a team n, whose reference point is located at a place $rp(t)$. The collected information includes two parts: local information, and collected information. A node is represented by:

$$message\ (n, t) = (t, id, rp(t), r, locinf(t), collectinf(t)), n \in \mathrm{N}.$$

where:

id is the team identification. A given id always refers to one particular team inside the building.

r is the maximum radius that firefighters in a same team should not exceed to guarantee direct visibility between them and their team leader. This distance can vary over time.

$locinf(t)$ reflects the localization of all firefighters belonging to the same team relatively to their leader at instant *t*. It also reflects metrics regarding the health status of the firefighter. In fact, every firefighter in the team will transport a BAN system that will locate him and report on their body's features (e.g., temperature, blood saturation and oxygen level).

$collectinf\ (t)$ is a set of data referring to the environmental information collected at every moment by the firefighters. The complexity of the data varies significantly from one environment to another. Typically, the collected data includes environmental parameters having an immediate impact on: (a) the fire-fighter's health status such as humidity, surrounding temperature, smoke density and toxicity level; and (b) the management of the firefighting and rescue operations within the building. These parameters will be analyzed and used by the system during the prediction process.

Our Temporal Weighted Graph is a dynamic graph in which the collected information varies over time. In fact, at each node the different parameters mentioned previously are updated when a new passage from this position is performed. Then, the previous data will be stored and only the most recent observations will be taken into account.

Fig. 1 shows an example of a temporal weighted graph. As illustrated we dispose of three types of node. The dark node is a fixe node referring to the Incident Commander (IC) position located at the entrance of the building. The red nodes reproduce the different locations of firefighter teams inside the building and reflect information regarding the environment conditions corresponding to this location at the recent moment where a team passed by it. The information reproduced by the red nodes is updated each time the location is revisited. The circle nodes are terminal nodes including yellow nodes referring to current positions occupied by firefighters belonging to a given team and red node that reflects the reference point position. Then, the terminal node provides instantaneous information such as the position of a given team, the health status and position of firefighters belonging to this team and the conditions of the surrounding environment.

The dashed lines are communication links between two terminal nodes. One may see in this particular graph that the radio communication is done either in inter-team or intra-team manner.

In the frame of our Temporal Weighted Graph (TWG), we describe some useful definitions such as Radio Connected TWG, route, safe route and safest shortest route.

When any team leader can communicate with the post advanced node directly or indirectly through other team, the graph is called Radio Connected TWG. We assume that connectivity of a TWG is always guaranteed in order to keep a continuous protection of firefighters. When such feature is provided, one can say that every firefighter can communicate with his leader and with the post advanced node through of the form:

$$P = (n_1, n_2), (n_2, n_3), \dots, (n_{exit-1}, n_{exit}), \qquad (n_i, n_{i+1}) \in E$$

where (n_i, n_{i+1}) characterizes a physical segment within the building for which two recent information sets have been collected to report on the risk perceived at the ends

of the segment. Since, in general, the segment is short, these information sets can indicate the risk on the whole segment (usually, the most recent set). In this context, we say that a route P is a safe route for team A at time t, for horizon h, if it connects the current place of the reference point of A to the post advanced node through segments where the risk management are accepted until horizon h. The shortest safe route is therefore defined as the shortest route among the set of safe route.

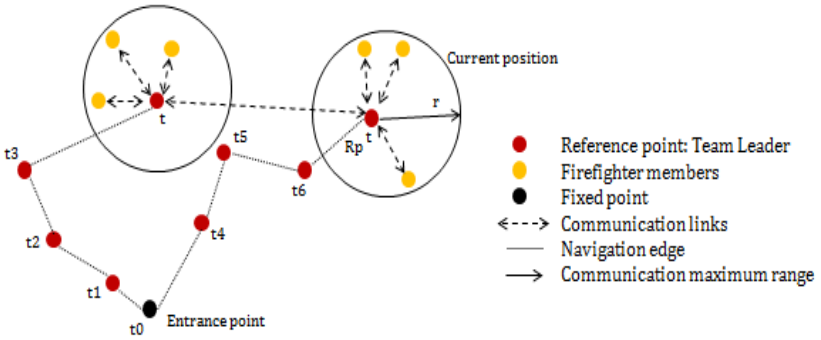

Fig. 1. Typical Example of the Temporal Weighted Graph TWG

To be able to manage safe routes, we provide the firefighting system with a library of prediction models that are able to check whether the risk related to any parameter involved in the collection is acceptable in the interval of time $[t, t + h]$. We also assume that an algorithm is provided to estimate the length of any segment and provide the shortest route.

4 Smart Navigation in Hazardous Environment

In this section we detail the description of a smart navigation approach based on the TWG introduced previously. In fact, the graph will provide some functions aiming to assist firefighters during the navigation process.

4.1 Requirements and Constraints for Smart Navigation

For the TWG to efficiently perform its purposes, we assume that the firefighting system should be equipped with functions such as navigation, localization, communication visibility, hazard monitoring and protection of firefighters, and prediction functions. A set of requirements should be met by these functions to provide efficiency and accuracy. Among the major requirements, one can mention the following:

N*avigation requirements*: The navigation function should be implemented at the incident commander and at team leader BAN system. It involves two scenarios: visibility

and discovery. The visibility format should be operational at the team leaders to allow them to know how far they can go in the indoor space by identifying barriers and risk factors. It is also performed at the incident commander in order to assist and manage the different team motions in an efficient manner. The discovery navigation is done in case of poor (or no visibility) in order to provide assisted navigation to firefighter teams. It should rely on a progressive construction of a map describing the discovered hallways of the indoor space as the firefighters move.

Localization requirements: The navigation through the building can be performed only if the location of the firefighter is known. The localization function should be made in real-time manner to take into account the hazard phenomenon. It is made either in absolute or relative way. In an absolute localization, the incident commander must be able to locate each firefighter working in the indoor space with good accuracy and little error. In a relative localization the incident commander deduces the location of a given firefighter team relatively to the location of other teams in its vicinity or relatively to the points constructed when he progresses in the building.

Communication requirements: Communication must be provided by the firefighting system. Any team leader must be directly or indirectly radio connected to the post-advanced node (i.e. the incident commander). In fact, the team leader should be able to communicate with the incident commander directly or through other team leaders acting as way points. In addition, the location of firefighters belonging to the same team is in general done through the exchange of communication messages between them and their correspondent team leader. The members of the same team must be in *direct visibility* with each other and with their team leader. For this reason, the radius 'r' should be adapted to ensure communication in whatever condition (e.g. in case of lack of energy in the firefighter's BAN equipment, the communication can be made through another member from the same team). The cell around the team leader of radius r must be safe, at any time and a given horizon h.

Hazard monitoring and Protection of firefighters requirements: The path leading to the current position of a team of firefighters must be safe at least for a given horizon h to allow them to exit, when necessary. Then, we should supervise the hazard phenomenon through the graph in real-time manner by the collection of enough environmental information (e.g., surrounding temperature and the smoke density). On the other hand, some physical phenomenon should be supervised by measuring some vital parameters of the firefighters during firefighting operation. This monitoring must be done for all actors of the navigation process, including the firefighter members, the team leaders and the incident commander.

Prediction requirements: In fact, the system needs to monitor continuously the evolution of the risk parameters collected by firefighters in order to be able to predict the occurrence of unacceptable events. The prediction function is crucial to avoid eventual damages like firefighter's injuries or death and to facilitate the selection of the shortest path that leads to a given destination from the current position of a given team. For this reason, the hazard measurements should be close in time and space to provide efficient prediction. The estimation should be based on three estimation models:

- Temporal prediction: the different observations are time dependent and are collected periodically. Then, the system tries to predict when a hazardous situation is detected in a zone and for how long the team could stay in this zone before being injured.
- Spatial prediction: since the system can predict when a harmful hazard will occur at a specific (reference) point in the zone covered by the graph, one can assume that the system is able to predict how the hazard is distributed around the reference point.
- Spatio-temporal prediction: Such a model should take into account temporal correlations as well as spatial correlations to monitor the occurrence of hazards in a reduced zone and through a limited interval of time. In fact by relating the spatial position of the nodes in the network with the instant of risk occurrence, one can track the displacement of the risk instantaneously.

4.2 Temporal Weighted Graph (TWG) Based Navigation

In this section we describe the prediction function based on the TWG and provided by our system. It assumes that a library of mechanisms that allows the prediction of health-based parameters and environment measurements is available. The prediction mechanism should take into account the nature of the managed risk.

A. A Prediction Model for Hazard Management

The hazard in firefighting has a dynamic evolution that needs to be estimated continuously. Since the substructure $'collectinf'$ reports on the risk features of a given zone covered by the graph, one needs to estimate the time of deterioration of the risk conditions based on the knowledge of the history of the different collections and the current measurements. For this, we define an example of prediction based on the traditional model called double exponential smoothing method [6,7,8,9,10]. This method is simple to implement, the forecasting equations are easy to understand and compute, and it takes into account the trend of the studied series of risk measurements. Several other models can be added to our library or adapted from known ones. Assume that $\{R_1, R_2, \dots, R_T\}$ is a set of T observations reflecting risk measures taken at a given node in the graph taken by a given node at instant $t \geq T$. For an horizon h with $h \in \mathbb{N}^*$, we aim at predicting the future value of the risk that the node may have at instant $t + h$. We note this prediction by $\hat{R}_T(h)$. The proposed method using the double exponential smoothing method operates as follows:

The observation R_t is expressed at time t by $R_t = b + (t - T)a$, where b are real numbers changing with the evolution of observations. Then the prediction made at instant T for horizon h, $(1 \leq h \leq T)$ is:

$$\hat{R}_T(h) = \hat{a}(T)h + \hat{b}(T) \quad (1)$$

where $\hat{b}(T)$ is the smoothed value at time T and $\hat{a}(T)$ is the smoothed value for the trend which is the difference between two adjacent smoothed values. The two coefficients $\hat{a}(T)$ and $\hat{b}(T)$ are obtained by minimizing:

$$F = \sum_{j=0}^{T-1} \beta^j \left(R_{T-j} - b + a * j\right)^2 \quad (2)$$

where β is a weight called the smoothing constant such that $\beta \in]0,1[$. Let with $\alpha = \frac{1-\beta}{1+\beta}$, parameters $\hat{a}(T)$ and $\hat{b}(T)$ are given by, :

$$\begin{cases} \hat{a}(T) = \dfrac{(1-\beta)}{\beta}[S_1(T) - S_2(T)] \\ \hat{b}(T) = 2S_1(T) - S_2(T) \end{cases} \quad (3)$$

Where $S_1(T)$ and $S_2(T)$ are the smoothed series given by:

$$S_1(T) = (1-\beta)\sum_{j=0}^{T-1} \beta^j R_{t-j} \quad \text{and} \quad S_2(T) = (1-\beta)\sum_{j=0}^{T-1} \beta^j S_1(t-j)$$

By performing simple algebraic manipulations, we obtain finally the expressions of $\hat{a}(T)$ and $\hat{b}(T)$:

$$\begin{cases} \hat{a}(T) = \alpha\,(\hat{b}(T) - \hat{b}(T-1)) + (1-\alpha)\hat{a}(T-1) \\ \hat{b}(T) = \beta^2\left(\hat{a}(T-1) + \hat{b}(T-1)\right) + (1-\beta^2)\,R_T \end{cases} \quad (4)$$

Choice of the Smoothing Constant β: The smoothing constant β is usually very subjective and varies with the context of the desired prediction. It measures how much the observations influence on the future prediction. In general, the best value for the smoothing constant $\beta$is the one that results in the smallest mean of the squared prediction error:

$$\sum_{t=1}^{T-h} (R_{t+h} - \hat{R}_t(h))^2 = \sum_{t=1}^{T-h} (R_{t+h} - (\hat{a}(T)h + \hat{b}(T)))^2$$

With mathematical manipulations of formulas (2) we obtain for h=1:

$$\sum_{t=1}^{T-1} (R_{t+1} - (1-\beta)^2 \sum_{j=0}^{T-1} \beta^j R_{t-j} - (1-\beta)\sum_{j=0}^{T-1} \beta^j S_1(t-j))^2$$

B. Prediction Applications

Since the system can predict when a harmful situation will occur, the system is able to apply prediction models to offer more protection.

Monitoring of Safe Route: Route monitoring takes into account all the routes in the TWG including unsafe routes $P_t = \{S(t), U(t)\}$. In fact, the risk measurements of an unsafe route may decrease over time until being acceptable and in consequence the correspondent route will be considered safe. Monitoring the safe route is based on two steps: route initialization and route update:

Route initialization: Initially, the route is reduced to a point that corresponds to the initial node in the graph, where the taken values are not risky. This initial point is fixe and corresponds to the incident commander position located at the entrance of the building. It collects at this point the first risk measurements. The first team can traverse the initial point only if the risk deduced from the collected information is acceptable. Then we can assume that at time t_0, the firefighting operation is marked when the first team traverses the initial point.

$$P_{t_0} = \{S(t_0), U(t_0)\}, S(t_0) = n_{exit}\ , U(t_0) = \emptyset$$

Route Update: At a given instant t, we have a set of paths $P_t$including safe and unsafe routes, $S(t)$ and $U(t)$. To deduce the set P_{t+1} from P_t, the system should look at the set of measurements corresponding to each path in each set. The set of safe paths at instant $t+1$ will be composed by the elements of $S(t)$ that will still be safe and elements $U(t)$ that will become safe minus the elements of S(t) that will become unsafe. In a similar way, the set of unsafe paths at instant $t+1$ is obtained. Thus, we have:

$$P_{t+1} = \{S(t+1), U(t+1)\}$$
$$S(t+1) = S(t)_{safe} - S(t)_{unsafe} + U(t)_{safe}$$
$$U(t+1) = U(t)_{unsafe} - U(t)_{safe} + S(t)_{unsafe}$$

Selection of Shortest Safe Route for the Evacuation Process: The shortest path always uses safe paths. Then the shortest path at instant t is the shortest path among all the path in the set $S(t)$. The safety of the path depends on the time of the deterioration of the risk. The concept to introduce here is the function $Time(P_t)$ that defines the time taken for a firefighter team to travel along the path P_t.

$$P_t = \left(n_1^{t_1}, n_2^{t'_1}\right), \left(n_2^{t_2}, n_3^{t'_2}\right), \ldots, \left(n_{e-1}^{t_i}, n_e^{t'_i}\right)$$

$n_1^{t_1}$: The current position of the reference point with $t_1 \leq t$. This function can be generated by using a simple traversal of the graph. We start from the current position of the firefighter team then:

$$Time\left(n_1^{t_1}, n_2^{t'_1}\right) = |t_1 - t'_1|$$

If the time to travel the distance separating the nodes $n_1$and n_2 is less than the horizon needed for this zone to become hazardous (i.e.,$Time\left(n_1^{t_1}, n_2^{t'_1}\right) < h$), then the route is safe and can be used for the evacuation process to get out; else, this segment is considered unsafe. The time cost of the path P_t between n_1, n_{exit} at time t is:

$$Time(P_t) = (t - t_1) + Time\left(n_1^{t_1}, n_2^{t'_1}\right) \ldots + Time\left(n_{exit-1}^{t_p}, n_{exit}^{t'_p}\right)$$

Thus, the shortest path between two nodes at the time t is the path that minimizes the time cost. The function $Shortest\_Path\ (n_1, n_e)$ defines the path leading to the exit node from the current position of a given team in the fastest time possible.

Path Discovery based on TWG: Path discovery operation aims at constructing segments inside the building to allow better visibility of a given floor to assess the

damages related to this floor and to rescue building's occupants blocked in this floor. It can be an assisted or a non assisted operation. Assisted path discovery is done when there is enough visibility in the monitored zone or based on a map of the building. However, the non assisted path discovery is done in situation where there is poor or no visibility. For this reason we propose some heuristic approaches based on the hazard managing function described previously, in particular, to help firefighter team to discover new routes in the building.

In Case of Visibility. We have selected three heuristics that can be used to assist firefighter's navigation in case of visibility.

*Heuristic*1: Assume that the firefighter is in a hallway, where the risk is acceptable ($R_t < Th$). If there are some doors and the prediction of the risk for a given horizon h at this floor is acceptable ($\widehat{R}_t(h) < Th$). Then, after checking what's behind the doors, the firefighter can progress in the floor.
Heuristic 2: Assume that the risk at a given zone is high but still less than the threshold value ($R_t \approx Th$). A firefighter team moves in this zone to fight the detected incident. Once the incident is managed and controlled ($R_{t+1} < Th$ and $\widehat{R}_{t+1}(h) < Th$) the firefighter can progress in the floor.
Heuristic 3: We assume that, in case of distressed call, the firefighter team enters in a hallway where some occupants are blocked, following a given route. If the risk measurements indicate that this route is safe ($R_t < Th$) and it will still be safe for horizon h ($\widehat{R}_t(h) < Th$), then the firefighter team progresses in the hallway.

In Case of no Visibility. Three heuristics can be used by the firefighters during navigation in case of no or poor visibility.

Heuristic 4: We assume a firefighter in position A, where the risk measurements are acceptable ($R_t < Th$), and that he wants to progress to position B located at a distance d meters from A. If the estimation of the risk measurement for horizon h that allows him to traverse the distance between A and B is acceptable ($\widehat{R}_t(h) < Th$), then the firefighter allowed; else, he should move back to find new acceptable routes to exit.
Heuristic 5: We assume that the firefighter is in an intersection of hallways, where different risk measurements are available. If the firefighter wants to exit from the building, he takes the route corresponding to the lowest risk value. If the firefighter wants to fight the incident, he takes the route corresponding to the highest value.
Heuristic 6: We assume that in a hallway, the risk measure indicates that the route taken by a team is no longer safe, then the firefighter moves back to find new routes.

5 Simulation

In this section, we describe a simulation model to show how our scheme and system perform using TWG. Our numerical results will be analyzed using Matlab.

5.1 Simulation Model

An illustration of the simulation model is depicted in Fig. 2, where we consider a rectangular area of width W=30meters and length L= 200meters. We assume three

sources of fire. Each fire has its own velocity $\rho(t)$ of expansion. To fight the fronts of fire, three teams enter into the building. Each team can move from its location following a given velocity $v_i = l_i/x_{i,i=\{1,2,3\}}$. '$l_i$' is the distance separating two node positions in TWG. To prove the efficiency of our navigation approach to avoid the critical conditions faced by firefighter teams, using the exponential smoothing method, we assume that the first and the third teams succeed to stop the evolution of the first and the third sources of fire. However, the second team is less efficient than the other and he only decreases the velocity of the medium source of fire. Then, the task here is to compute the time needed for the third team of firefighters to reach a safe position before the second source of fire can damage the risk of the second location. Let us notice, however, that the time can be easily computed mathematically.

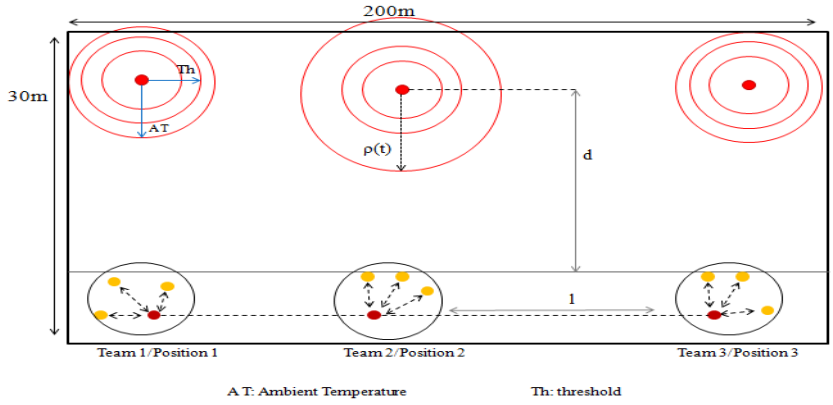

Fig. 2. Environment model

5.2 Simulation Results

Fig. 3 and Fig. 4 depict the variation of the exit time as a function of the length 'l' when 'x' is tuned and the time 'x' when 'l' is tuned, respectively. We assume that $x=x_3$ and $l=l_3$. In these figures, 'tsafe' corresponds to the time for which the hallway is blocked by the second source of fire. We remark that the impact of "x" on the time of exit is similar to the impact of "l". In Fig. 3, it is remarkable that a small increase of the value of x considerably increases the time to reach the safe position and in consequence decreases the performance of our approach in term of safety. For a given x, the time of exit is proportional to the distance 'l'. We notice that for a given x, the curve decreases with the growth of the distance. This decay is more visible when x is large. We remark that the more x is large, the more the curve is pronounced. In consequence, more x is large, more the firefighters are unlucky to reach the safe position in safe manner. In the same way, in Fig. 4, we conclude that "l" has the same impact on the time of exit as "x". Then, the more the distance "l" is important, the more the time of exit is large and the firefighter team is unlucky to reach the safe position in safe manner.

Fig. 5 illustrates the impact of the velocity of displacement of the firefighter team on the blockage status. For some velocities, there are some instants when the firefighters can be blocked. In fact, if the team reaches the safe position before the source of fire, the blockage status is set to '0', else it is set to '1'. A little decay in the velocity of displacement increases the probability of the blockage of the team. Then more the velocity is important more the firefighters are unfortunate to be found blocked.

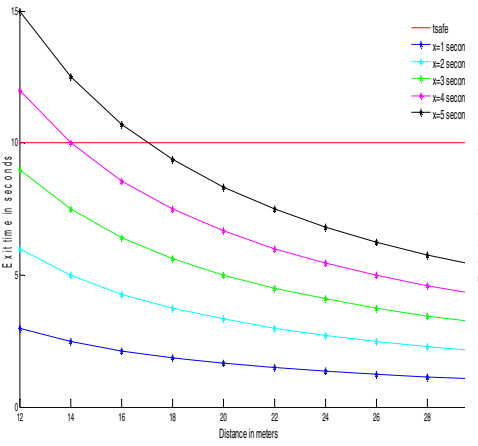

Fig. 3. Impact of 'x' on the time of exit

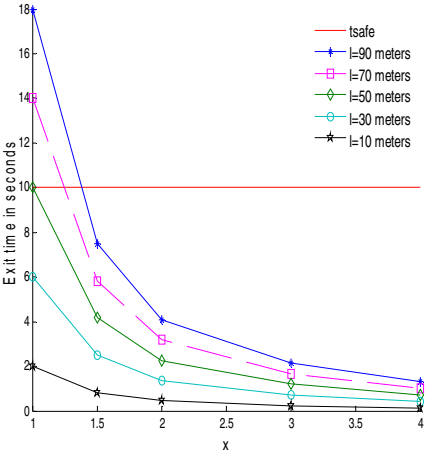

Fig. 4. Impact of 'l' on the time of exit

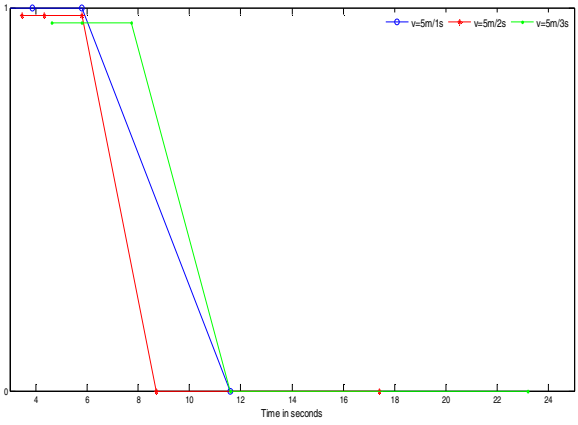

Fig. 5. Impact of the velocity of displacement of the firefighters on the blockage status

The management of the hazard throughout the TWG, should not be limited to the control of the evolution of the source of fire, the observations collected by the different teams should be taken into account also. Then, the task in the simulation depicted

in Fig. 6 is to predict the future surrounding temperature that a given node may take. In other words, we need know at each time the risk will be detected by the system. The predicted values will be compared to the threshold value assumed in our simulations to be 60°C. As mentioned in the simulation scenario only the second source of fire evolves. Then, by applying the prediction method for different horizons, for the collected information at the second node we obtain the illustrated curves. Fig. 6(a) illustrates the results obtained for a smoothing constant β=0.5; whereas Fig. 6(b) illustrates the results corresponding to β=0.9. We notice that for all horizons, the temperature increases with time. This increase is explained by the availability of new observations for each new passage by the position 2. Then each new prediction takes into account of the most recent observation. For a given β, there is a difference between the values predicted for each horizon. This difference increases with time and in consequence the detection of hazard is done more early for an important horizon. The impact of the horizon on the prediction and on the detection time is more visible in Fig. 6 (a). We remark also a difference between the predicted value for the same horizon and the two values of β; for example at t=5 second the predicted temperature for β=0.5 is equal to 55°C whereas for β=0.9 it is equal to 60°C.

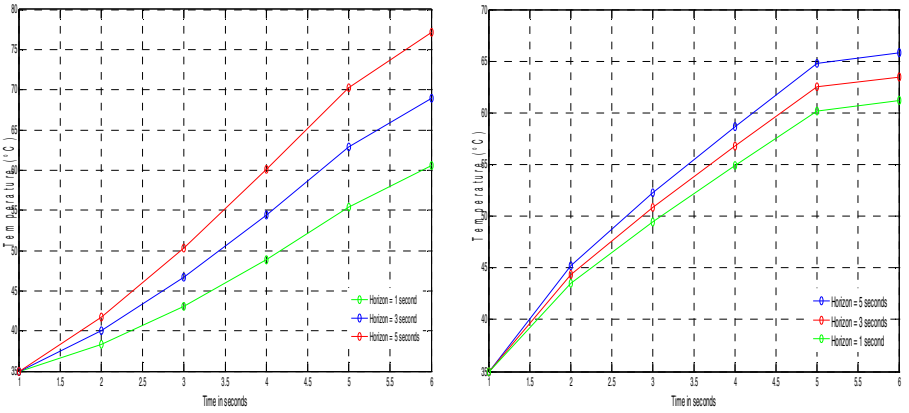

(a) β=0.5 (b) β=0.9

Fig. 6. Impact of the value of β on hazard detection

6 Conclusion

In this work, we described a smart navigation approach in indoor space for firefighters. This approach is based on a novel concept of graph called the Temporal Weighted Graph, where information regarding the firefighters and the surrounding environment are collected. Based on the history of the collected data, the hazard is managed using a library of mechanisms allowing the application of a real-time technique that aims to predict the isolation moments of firefighters. On each node in the graph, the prediction method is applied for a given horizon, reflecting the time needed to stay safe. A simulation is conducted to analyze the efficiency of the proposed solution.

Directions for future works includes the use of a risk library in order to introduce more technicality in the management of the risk, the minimization of communication overloads and the monitoring of firefighter's physiological conditions.

References

[1] Barnes, M., Leather, H., Arvind, D.K.: Emergency Evacuation using Wireless Sensor Networks. In: Pro. of the 32nd IEEE Conf. on Local Computer Networks, Dublin, Ireland, pp. 851–857 (October 2007)

[2] Filippoupolitis, A., Gelenbe, E.: A distributed decision support system for building evacuation. In: Pro.of the 2ndIEEE Int. Conf. on Human System Interaction, Catania, Italy, pp. 323–330 (May 2009)

[3] Fischer, C., Gellersen, H.: Location and Navigation support for Emer-gency Responders: A Survey. IEEE Pervasive Computing 9(1), 38–47 (2010)

[4] Klann, M.: Tactical Navigation Support for Firefighters: The LifeNet Ad-Hoc Sensor-Network and Wearable System. In: Löffler, J., Klann, M. (eds.) Mobile Response. LNCS, vol. 5424, pp. 41–56. Springer, Heidelberg (2009)

[5] Scholz, M., Riedel, T., Decker, C.: A flexible architecture for a robust indoor navigation support device for firefighters. In: Pro. of the 7th International Conf. on Networked Sensing Systems (INSS 2010), pp. 227–232 (June 2010)

[6] LaViola Jr., J.J.: An experiment comparing double exponential smoothing and Kalman filter-based predictive tracking algorithms. In: Pro. of the IEEE Virtual Reality 2003, RI, USA, pp. 283–284 (March 2003)

[7] Channouf, N., L'Ecuyer, P., Ingolfsson, A., Avramidis, A.N.: The application of forecasting techniques to modeling emergency medical system calls in Calgary, Alberta. Health Care Management Science 10(1), 25–45 (2006)

[8] Hu, S., Li, Y., Zhang, W., Fan, S.: Adaptive Outlier-tolerant Exponential Smoothing Prediction Algorithms with Applications to Predict the Temperature in Spacecraft. International Journal of Advanced Computer Science and Applications (IJACSA) 2(11), 126–129 (2011)

[9] LaViola, J.J.: Double Exponential Smoothing: An Alternative to Kalman Filter-Based Predictive Tracking. In: Pro. of the Workshop on Virtual Environments 2003, Zurich, Switzerland, pp. 199–206 (May 2003)

[10] Clay, G.R., Grange, F.: Evaluating Forecasting Algorithms and Stocking Level Strategies Using Discrete-Event Simulation. In: Proceedings of the 29th Conference on Winter Simulation, Atlanta, Georgia, United States, December 07-10, pp. 817–824 (1997)

Personalized Recommendation Based on Implicit Social Network of Researchers

Cheng Chen[1], Chengjie Mao[1], Yong Tang[1,*], Guohua Chen[1,2], and Jinjia Zheng[1]

[1] School of Computer Science, South China Normal University, Guangzhou, China
[2] School of Mathematical Science, South China Normal University, Guangzhou, China
chengchen202@gmail.com, maochj@qq.com, {ytang4,chengh3}@qq.com, zhengjinjia@yeah.net

Abstract. In this paper we discuss the importance of social network of researchers for personalized recommendation of researchers and papers. We begin by briefly describing collaborative filtering method for personalized recommendation and its cold start problem of the new uses. We present the related studies which have used social network information to provide personalized recommendation. Then, we introduce our original method of extracting implicit social network of researchers from the published papers and paper recommendation algorithm. We test the presented algorithm on real world datasets from Chinese social network site. The result indicates the advantage of recommendation based on implicit social network.

Keywords: social network, personalized recommendation, data mining.

1 Introduction

Social network sites (SNSs) have been popular all over the world and have acquired a great amount of attention. Various kinds of social network sites (SNSs) have emerged to meet the need of persons in the different fields. However, people are flooded with information from many resources. This might lead to Information Overload, meaning that the information is too much to handle for us.

One way to solve this problem is to provide users with personalized recommended items. The goal of such recommendations is to present to users the most relevant items. In this work, we study personalized recommendations within a social network site called Scholat, which is oriented to the researchers' need. We focus on recommending new researchers and papers to researchers.

Traditionally, there are two main methods to fulfill the task of personalized recommendation. They are typically based on(1)content, i.e., recommend items with content that is similar to the content of the items already consumed by the target users;(2)collaborative filtering(CF), i.e., providing items related to people who are

* Corresponding author.

Q. Zu, B. Hu, and A. Elçi (Eds.): ICPCA-SWS 2012, LNCS 7719, pp. 97–107, 2013.

related to the target user by some kind of similarity[2]. Collaborative Filtering (CF) [5] has become one of the most popular techniques of personalized recommendation. It is based on the assumption that similar users share the same interest. However, for the new users who hardly have interacted with others, there isn't enough information to use collaborative method to find similar users.

In this paper, we propose personalized recommendation that is based on the users' implicit social network to help solve the cold start problems of new users. We demonstrate how we extract the similarity social network. We assume that the researchers' papers reflect their interests, and the preferences of other similar researchers provide a good prediction for the preferences of the researcher.

Our measure of tie strength differs from previous work in that we use co-occurrence information to calculate the similarity between the researchers and extract the similarity social network. We recommend new users and papers based on the extracted social network. Finally, the personalized recommendations are evaluated by an off-line evaluation and a live-user survey.

The rest of the paper is organized as follows. Section 2 discusses related work on recommendation technique and social network method. Section 3 describes details and algorithm of our recommender system. Section 4 describes our experiment and the results we obtained. Section 5 concludes and suggests future work.

2 Related Work

Collaborative Filtering (CF) [5] is one of the most successful recommendation techniques. CF suggests items to the users based on the opinions of other similar users and their previous likings. The traditional CF techniques calculate the users' similarity by using similar tags, consuming similar documents, or having similar interest as expressed in item rating. One drawback of CF is the search for neighbors among a large population of potential neighbors, so CF needs intensive computation which influences the efficient of the system [6]. Hence, Fengkun and Hong [9] show that combining social network relationships from a social network website and k-nearest neighbor algorithm makes prediction more accurate than traditional CF techniques. Groh and Ehmig [8] reveal that using social network information for neighborhood generation improves regular CF algorithm in taste related domains.

A Few studies have discussed the method of using social network information for personalized recommendation. Guy et al. [1] compare between the personalized recommendation that are based on the familiarity and similarity network, and indicates that the familiarity network outperforms similarity network as a basis for recommendations. Carmel et al. [2] show that using the familiarity-based network and similarity-based network improves personalized social search.

Referral Web [9] addresses a method to extract social network by the co-occurrence of names on Web pages using a search engine. The relevance of two person X and Y is estimated by putting a query "X and Y" to a search engine. Yutaka developed a social network extraction system from the Web called POLYPHONET [10]. The system extracts person-to-person relations and person-word matrix from the Web using a search engine.

Roth et al.[11] address a friend-suggestion algorithm that assists users to find contact groups in the email network. This algorithm is based on the implicit social graph, which is formed by user's interaction with contacts and group of contacts. The implicit social graph differs from explicit social graphs that are formed by users explicitly adding other individuals as friends. They build a weighted social graph, where edge weights are determined by the frequency, recency, and direction of interaction and cluster contacts into groups. Some related work use interaction of users site to measure the tie strength. Gilbert and Karahalios[13] explore different features to predict the tie strength between a user and his Facebook friends.

Bar-Yossed *et al*.[19] address a novel cluster ranking algorithm called C-Rank. The C-Rank algorithm is based on email egocentric social network, consisting of contacts with whom an individual exchanges email. Edges between contacts represent the frequency of their co-occurrence on message header. In this work, we propose a method to extract users' implicit social network using co-occurrence information in users' papers with the help of a search engine.

3 Recommender System Description

3.1 System Architecture

The basic assumption of this work is that a user's implicti social graph (their published papers, and their collaboration) provides a powerful source of profile information that can be used as the basis for recommendatioin. In this section we describe our *Scholarmender* recommendar system, focusing on the system architecture, how the users' implicit social network information can be used to suggest papers to the users. *Scholarmender* system has been developed as a Web service. It provides users with access to two basic functions, as follows:

1. Academic Paper Search. The user provides query terms to receive a ranked-list of relevant papers. Figure 1 shows the result of a search for paper corresponding to the query "Badrul Sarwar". Each result contains the relevant information such as the paper's title, authors, author organizations, journal, keywords and abstract.
2. Paper Recommendation. The system recommends a list of papers to the users who are researchers in the college or institution. We first extract implicit social network relation of the user in the web site Scholat[21] with the help of the search engine mentioned above. The extracted social network information are harnessed to calculate the similarity between the users in the SNS website. The system recommends papers based on the top similar users in the social network of a given user. The interface of paper recommendation is showed in the Figure 2.

Fig. 1. The Search Result for The Query “Badrul Sarwar”

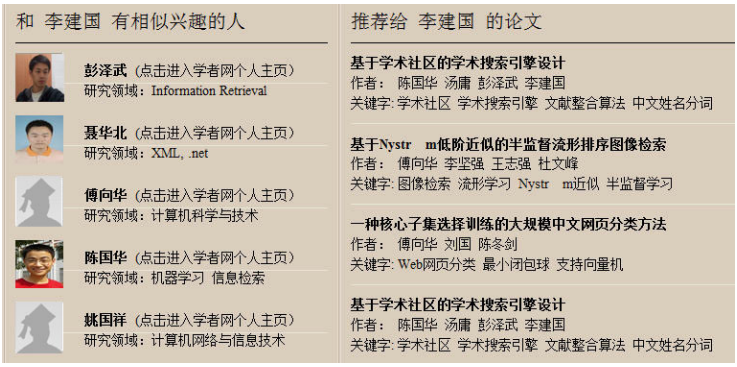

Fig. 2. An example of the recommendation interface

In what follows we will focus on how we extract the users' implicit social network and how the users’ social network information are used to recommend papers in the recommender system. We will return to the *Scholarmender* system towards the end of this paper when we describe the result of a live-user trial of the system.

3.2 Keywords Extraction

In this work, we firstly extract the keywords representing the researchers in order to extract the social network. One commonly used approach to obtain keywords for a researcher is to search the researcher’s homepage and extract words from the page. But homepages of researchers do not always exist. Moreover, a great quantity of information about a researcher is not included in homepages, but is included in the papers that he or she published and co-authored.

As a result, we extract a person-word matrix using the academic search engine mentioned in the above. In the researchers' papers, a particular researcher's name co-occurs with some keywords which represent the person's major research topic.

If we use the content of the whole papers of researchers, the computation is expensive. Using the content of papers involves the patent of the researchers. Therefore we use the abstract of papers for keywords extraction. We collect the abstract of all the papers which are obtained by retrieving a researcher's name, and extract a set of words and phrases as keywords. In this mode, we use Termex[14] which is the tool for term extraction in Chinese and English. (For details of the algorithm and its evaluation, see [15]) Fig.3 shows an example of some extracted keywords that represent a researcher.

Description logic
Temporal logic
Temporal index
Access Control Model
Temporal relational operators
Collaboration Work

Fig. 3. An example of some extracted keywords representing "Tang Yong" using co-occurrence

3.3 Extracting the Researchers' Implicit Social Network

We suggest a novel approach to extract the researchers' similarity social network. From the perspective of the researchers, we figure out a hypothesis that the more similar the research topics of two researchers are, the stronger is their context similarity in the preferences. Our procedure is that we firstly extract the keywords representing the researchers, secondly compute the social network by measuring the co-occurrence of keywords and names, and plus the co-occurrence of names.

From the perspective of the researchers, we base on the hypothesis that the more similar the research topics of two researchers are, the stronger is their context similarity in the preferences. And Co-occurrence information of words and persons form a matrix. We have a person-word co-occurrence matrix W= (w_{ij}) (i,j=1,…,n), and w_{ij} represents the o-occurrence indice of a person's name X_i and a keyword W_j. In this work, we use the overlap coefficient to measure co-occurrence because the previous study [10] proved that overlap coefficient is better to weight the co-occurrence. The formula is as follow:

$$f(n_X, n_Y, n_{X \wedge Y}) = \begin{cases} \dfrac{n_{X \wedge Y}}{\min(n_X, n_Y)} & if \quad n_x > k \quad and \quad n_Y > k \\ 0 & otherwise \end{cases} \tag{1}$$

```
Algorithm 1: GetKeywordWeightVector(n)
     Comment: calculate each weight of the keywords vector
     input: n denotes the name of researcher
     output: (v1,…vi,…,vk) , vk is the weight of the k-th
keyword
Vector kwl = {}
   retrieve all the papers of the researcher n
   keywordList • extract the keywords from the abstract of
papers
   for k : keywordList
       kweight • calculate the weight of keyword based on the
formula (1)
       add kweight in the kwl
   end for
return (kwl)
```

where n_X denotes the hit counts of name X, and n_Y denotes the hit counts of keyword Y, and $n_{X \wedge Y}$ denotes the hit counts of "X AND Y". We set some absolute threshold for n_X and n_Y in actual use because the co-occurrence indices described above are based on ratios that can change considerably if the number is low. And we set k=10 for our case. Algorithm 1 shows the brief pseudo-code for calculating co-occurrence indices of a researcher's name and keywords.

We assume that the more keywords do two persons have in common, the more similar they are in the research interest, and the more frequent do they co-author, the more related they are. In order to calculate the context similarity of two researchers, we not only use the co-occurrence information of two persons' name, but also consider the cosine similarity between two co-occurrence vectors in the person-word matrix (i.e., two rows of the matrix W), which respectively represent two persons. The similarity of two persons X and Y is determined by the following formula:

$$sim(X, Y) = a\cos(a_X, b_Y) + b\frac{n_{X \wedge Y}}{\min(n_X, n_Y)} \tag{2}$$

where x and y are two researchers' names; a_X denotes the keyword vector of the researcher X; b_Y denotes the keyword vector of the researcher Y; n_X denotes the hit counts of name X, and n_Y denotes the hit counts of name Y, and $n_{X \wedge Y}$ denotes the hit counts of "X AND Y"; a and b are parameters which is set to the relative weight of the two parts in the formula. Then we find the most suitable value of a, b in our special case.

```
Algorithm 2: CalSimilarityContext (NameList)
      comment: calculate similarity based on Double List
Graph     structure
      input:  NameList = {n_1,…,n_i,…n_k}, n_i denotes the i-th
researcher name
      output: graph G with similarity weigh
for name : NameList
    add the node representing name to the graph G.
end for
for i=0 to length of NameList
    for j=i+1 to length of NameList
        kwl1 • calculate keywordweightVector of NameList[i].
        kwl2 • calculate keywordweightVector of NameList[j].
       calculate the similarity of n_i and n_j based on the
formula(2)
       add the edge with similarity weight to the graph G.
       end for
   end for
   return (G)
```

Algorithm 2 shows the brief pseudo-code for calculating the similarity between the researchers. Then we calculate the cosine similarity of two vectors and plus the co-occurrence index of two researchers. Even if no direct relation exists between two researchers, it is thought that if they have similar interests it implies a kind of intellectual relation or potential social relation [10]. From this perspective, we obtain the implicit social network of the researchers, which is utilized to recommend in the following part. Fig 4 shows an example of social network graph extracted in the SNS website Scholat, which nodes represent the users, edges represent the relationship of users and distance represents the similarity of the users.

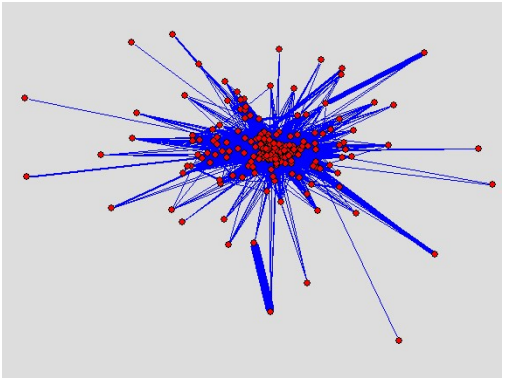

Fig. 4. Social network graph extracted using the above method

3.4 Paper Recommendation Algorithm

For the extracted similarity social network, we use the system to obtain the list of top 10 similar people and their corresponding similarity to the user. Then we recommend the user papers which are related to persons in his or her social network. We use the item recommendation algorithm which is proposed by Ido Guy [1]. To measure the relevance between a paper and a user, we use the following user-paper relationship types in the website and weights: authorship(0.6) , collecting(0.3), share(0.3). The recommendation score of paper p to user u is determined by the following formula:

$$R(u, p) = \sum_{t \in L(u)} S[u,t] \sum_{r \in R(t,p)} W(r) \tag{3}$$

where L(u) is the list of the top 10 related users in the user u's implicit similarity network; S[u, t] is the similarity weight between user u and t in the extracted social network; R(t, p) is the set of all the relationship types between user t and paper p (authorship, collecting, etc.); and W(r) is the corresponding weight of the relation type between user t and paper p as described above. For example, if only one researcher in the user's similarity network is related to this paper and this person is the author of the paper, has collected it, and has a 0.5 similarity weight with the user, then the corresponding recommendation score of the paper will be calculated by 0.5*(0.6+0.3).

Fundamentally, the recommendation score of a paper reflects the probability the user has interest in the paper. The score is related to the following factors: the number of people related to the paper in the user's social network, the similarity score of these people to the user and the relationship score of these people to the paper. Additionally, we exclude papers that are found to be related to the recommended user, so we do not recommend a paper that the user has already collected or has co-authored.

4 Off-line Evaluation and Live-user Trial

The success of our recommender will ultimately depend on its ability to suggest new researchers and papers that the target users are likely to be interested in. In this section we describe an offline evaluation based on a dataset generated from real SCHOLAT[17] users, and a live-user study of Scholatmender. The particular approach to evaluation is commonplace amongst recommender systems research.

For the purpose of this evaluation, we imported 100 users and their friend relation from SCHOLAT website as a test set. The recommendation lists of researches contain top similar researchers in the target users' extracted social network. For each target user we count how many of the recommendations are in the user's known friends list. We look to see how often the recommender suggests people who the

target user has already known. Our basic measure is the average percentage overlap between a recommendation list of researchers and the target user's actual friends list; and it is a precision measure. And we do this for different recommendation list sizes (k) from the top-5 recommendations to the top-20 recommendations. Figure 5 graphs the average precision versus recommendation-list size based on the 100-user test-sets.

The recommendations appear to perform not very well, generating precision scores around 10% in the 100-user test-sets. For example, for recommendation lists of size 10, it delivers a precision score of 0.11; so mostly 1 of these 10 recommendations is actually friend of the target user. The fact contributing to the low precision score is that the friend relationships of the users in the website are not rich. Many users have two or three friends obviously in the website.

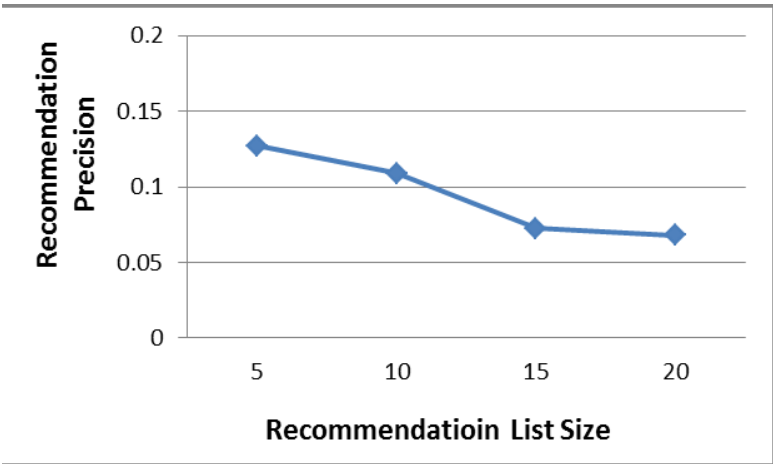

Fig. 5. Average precision vs. recommendation-list size using the 100-user test sets

In the off-line evaluation, precision is calculated as the percentage overlap between recommendations and the target user's existing friends-list. However, the non-overlapping recommendations may indeed be of great interest to the user. As such we view these results as providing a useful baseline concerning likely recommendation precision in a live-user context, and we conduct a user survey of 20 trial participants in our group during December 2011. These participants were all existing users of the website. Each participant was presented with a list of 10 recommended SCHOLAT users and 25 recommended papers and the user was asked to indicate which of the recommended and papers they would likely have interest.

On average, the 20 participants indicated an interest with an average of 2.5 users and an average of 3.6 papers per recommendation-list. We view this result to be positive. Every participant found at least some users and papers that would be of interest to him or her.

5 Conclusion and Future Work

In this paper we propose a new method to extract the users' implicit similarity social network. We have demonstrated how the users' social network can be used as the basis for a friend and paper recommender called Scholarmender. Although the results of off-line evaluation are not ideal, we see the core contribution of this paper is providing an approach to deal with the cold start problem of new users. As the similarity network is acquired using an academic search engine that is an external source to the website, it is able to provide recommendation to new users, who do not complete their profile or take part in any activity within the website.

Also, it suggests that the combination of social method and content-based methods may be effective. We also plan to extend our recommended item types to other social resources like community and shared files, and use the users' profile besides papers to extract social network.

Acknowledgements. This work is supported by the National Nature Science Foundation of China (No.61272067, 60970044), Guangdong Province Science and Technology Foundation (No.7003721, S2012030006242) and the Program for New Century Excellent Talents in University (NCET-04-0805).

References

1. Guy, I., Zwerdling, N., Carmel, D.: Personalized Recommendation of Social Software Items Based on Social Relations. In: RecSys, pp. 53–60. ACM Press (2009)
2. Carmel, D., Zwerding, N., Guy, I.: Personalized Social Search Based on the User's Social Network. In: CIKM, pp. 1227–1236. ACM Press (2009)
3. Amitay, E., Carmel, D., Har'el, N., Soffer, A., Golbandi, N., OfekKoifman, S., Yogev, S.: Social search and discovery using a unified approach. In: Proc. HT 2009, pp. 199–208 (2009)
4. Guy, I., Jacovi, M., Shahar, E., Meshulam: Harvesting with SONAR: the value aggregating social network information. In: Proc. CHI 2008, pp. 1017–1026 (2008)
5. Goldberg, D., Nichols, D., Oki, B.M., Terry, D.: Using collaborative filtering to weave an information tapestry. Commun. ACM 35(12) (December 1992)
6. Badrul, S., George, K., Joseph, K., John, R.: Item-Based Collaborative Filtering Recommendation Algorithm. In: WWW 2010, May 1-5, ACM Press (2001)
7. Liu, F., Lee, H.J.: Use of social network information to enhance collaborative filtering performance. Expert Systems with Applications (2009)
8. Groh, G., Ehmig, C.: Recommendations in Taste Related Domains: Collaborative Filtering vs. Social Filtering. In: Proc. GROUP 2007, pp. 127–136 (2007)
9. Kautz, H., Selman, B., Shah, M.: The hidden Web. AI Mag. 18(2), 27–35 (1997)
10. Matsuo, Y., Mori, J., Hamasaki, M.: POLYPHONET: An advanced social network extraction system from the Web. Journal of Web Semantics (2007)
11. Roth, M., Ben-David, A., Deutscher, D., Flysher, G., Horn, I., Leichtberg, A., Leiser, N., Matias, Y., Merom, R.: Suggesting Friends Using the Implicit Social Graph. In: 16th ACM SIGKDD Conference on Knowledge Discovery and Data Mining KDD (2010)

12. Hannon, J., Bennett, M., Smyth, B.: Recommending Twitter Users to Follow Using Content and Collaborative Filtering Approaches. In: RecSys 2010, pp. 199–206 (2010)
13. Gilbert, E., Karahalios, K.: Predicting tie strength with social media. In: Proceedings of Computer Human Interaction, CHI (April 2009)
14. Nakagawa, H., Maeda, A., Kojima, H.: Automatic term recognition system termextract (2003), http://gensen.dl.itc.utokyo.ac.jp/gensenwebeng.html
15. Mori, J., Matsuo, Y., Ishizuka, M.: Finding user semantics on the Web using word co-occurrence information. In: Proceedings of the International Workshop on Personalization on the Semantic Web, PersWeb 2005 (2005)
16. Jannach, D., Zanker, M., Felfernig, A., Friedrich, G.: Recommender systems: an introduction. Cambridge University Press (2011)
17. Kuhn, M., Wirz, M.: Cluestr: Mobile social networking for enhanced group communication. In: Proceedings of the International Conference on Supporting Group Work, GROUP (May 2009)
18. Pal, C., McCallum, A.: CC prediction with graphical models. In: Proceedings of the Third Conference on Email and Anti-Spam, CEAS (July 2006)
19. Bar-Yossef, Z., Guy, I., Lempel, R., Maarek, Y.S., Soroka, V.: Cluster ranking with an application to mining mailbox networks. In: Proceeding of the IEEE International Conference on Data Mining, ICDM (December 2006)
20. Ting, I.-H., Wu, H.-J., Chang, P.-S.: Analyzing multi-source social data for extracting and mining social networks. In: Proceedings of the International Conference on Computational Science and Engineering (2009)
21. SCHOLAT, http://www.scholat.com

Effect on Generalization of Using Relational Information in List-Wise Algorithms

Guohua Chen[1,2], Yong Tang[3,⋆], Feiyi Tang[4], Shijin Ding[1], and Chaobo He[3]

[1] School of Mathematical Sciences, Souch China Normal University Guangzhou, 510631, Guangdong, China
[2] Shenzhen Engineering Laboratory for Mobile Internet Application Middleware Technology, Shenzhen, 518060, Guangdong, China
[3] School of Computer Science, Souch China Normal University Guangzhou, 510631, Guangdong, China
[4] School of Computing and Information Systems, Univerisity of Melbourne Victoria, 3010, Australia
{chengh3,ytang4}@qq.com, f.tang2@student.unimelb.edu.au, dingsj@scnu.edu.cn, hechaobo@gmail.com

Abstract. Learning to rank became a hot research topic in recent years and utilizing relational information in list-wise algorithms was discovered to be valuable and was widely adopted in various algorithms. These algorithms' empirical performances were usually given, but few of them conduct theoretical analysis on the generalization bound. Based on the theory of Rademacher Average, we derive the generalization bound of ranking relational objects algorithms and discuss the effect on the generalization bound of using this method. Especially, an interesting property of ranking relational objects algorithms for Topic Distillation was discovered: the generalization bound does not depend on the size of documents in each query in training set. Experiments are conducted to verify this property.

Keywords: Learning to Rank, Relational Information, Generalization Analysis, Rademacher Average.

1 Introduction

Learning to rank became a hot topic in the field of Information Retrieval (IR) and Machine Learning communities [1–14]. It is a task that aims to learn a ranking function to sort a set of documents using machine learning techniques. In learning, we are given a training set that consists of queries, the corresponding documents and their manually labeled relevance judgments, then a ranking model is created using machine learning techniques. The ranking model is then used to score documents in the test set and presents the reverse sorted documents to the user.

⋆ Corresponding author.

Q. Zu, B. Hu, and A. Elçi (Eds.): ICPCA-SWS 2012, LNCS 7719, pp. 108–121, 2013.

In the past several years many learning to rank algorithms have been proposed. They can be categorized into 3 groups: point-wise[6], pair-wise [3, 8–10] and list-wise algorithms [11–15]. The point-wise algorithms assume the document labels to be scores or have no order information and then transform the ranking problem into conventional regression or classification problem respectively. The pairwise approaches assume the document pairs to be independent of each other and convert ranking into binary classification. However, ranking in IR has some unique properties: it's commonly accepted that the relative order information among documents is more important than single document's score or category, and that the position is sensitive: the top-ranked documents are more important than others. To fit these properties better, various list-wise approaches are proposed.

The performances of these algorithms have been verified empirically. Yet, few of them conduct a thorough theoretical analysis and a comparison among these algorithms until recently, some researchers start to analyze the algorithms' stability and generalization bound, which measure the consistent performance when the ranking model learned from the training set is applied to the test set. With generalization bound, we can know how well we can enhance the test performance by boosting the accuracy in training. Since the point-wise and pair-wise approaches can be transformed to regression and classification, many existing methods can be applied. However, little analysis on list-wise algorithms are proposed except [16, 17].

There are many relationships between documents, such as the similarity and link information between pages. The information is valuable and it could and should be utilized besides the document content in ranking results in a search engine . The Page-Rank [18] and HITS [19] algorithms purely analyzed the link information and get a great success, so why . The relation information is first analyzed independently without learning in link-analysis based methods and then , in recent year, it is incorporated into the data set along with the content of documents and they are trained together to get a ranking model in learning to rank algorithms. In [20], Qin *et al.* exploits relational information between the documents as well as the content information to learn a ranking function; Jin *et al.* uses users' feedback to refine the base ranker's performance in [21], and in [22–25] *et al.*, relational information is incorporated into the graph structure to learn a ranking function by keeping the vertices consistent. However, there is no generalization analysis for these algorithms and we have no idea of how they would perform if given more queries or increasing the number of documents in each query.

[20] is a representative work among these using relational information algorithms. In this paper, taking [20] as an example, we focus on the effect of using relational information on the generalization ability, i.e., we aim to answer the following question: whether it's useful to enhance generalization ability by using relational information in learning to rank algorithms?

This paper is organized as follows: first, we recall the existing generalization bound study in learning to rank. Next we describe how to apply the theory of Rademacher Average to obtain the generalization bound of a list-wise ranking

algorithm. Then we discuss the effects on generalization bound of using relational information by comparing the upper bound when using and not using relational information. In the end, we make some discussions on the tightness of generalization bounds between our result and [16, 17].

2 Related Work

To the best of our knowledge, the first study of generalization properties of the learning algorithms was that of Vapnik and Chervonenkis [26], who derived generalization bounds for classification algorithms based on uniform convergence. Since then, a large number of methods were proposed to analyze the generalization bounds for classification and regression problems. Recently, some work about generalization bound of learning to rank algorithm has been addressed, for example, [10] analyzed the bound of Rankboost using VC-dimension analysis techniques. Then Agarwal *et al.* studied generalization bound of Area Under the ROC Curve based on uniform convergence in [27] and then applied the algorithmic stability to reveal the generalization behavior of bipartite ranking algorithms in [28]. Considering the property of IR, Lan *et al.* used query-level stability to analyze generalization ability of learning to rank algorithms [29]. These methods can only be applied to point-wise or pair-wise approach, and no generalization theory is proposed for list-wise approach until more recently, a novel probabilistic framework was developed based on Rademacher Average technique in [17]. Using the same idea, we analyze the effect of using relational information on generalization ability in learning to rank algorithms by computing the generalization upper bound of algorithm that not use relational information and two ranking relational objects algorithms proposed in [20].

3 Generalization Analysis on Ranking Relational Objects Algorithm

In this section, we will first briefly introduce the general framework of ranking relational objects algorithm and review the Rademacher Average theory, then we apply the theory to compute the upper bound of 3 algorithms: not using relational information algorithm, using relational information in Pseudo Relevance Feedback and using relational information in Topic Distillation.

3.1 An Introduction to Ranking Relational Objects Algorithm

It's stated in [20] that besides the documents content, the relational information between documents also plays an important role in search ranking. For instance, if two documents are similar with each other and one document is relevant to the query, then it's very probable that the other document is also relevant. Therefore, the relational information should be effectively utilized.

The problem of ranking relational objects is formulated as: given N queries $Q = \{q^1, q^2, \ldots q^N\}$, each query $q^i \in Q$ is associated with n_i documents $\boldsymbol{D}^i =$

$\{D_1^i, D_2^i, \ldots, D_{n_i}^i\}$. Each document $D_j^i \in \boldsymbol{D}^i$ has a label y_j^i representing the relevance with query q^i, and $\boldsymbol{y}^i = \{y_1^i, y_2^i, \ldots, y_{n_i}^i\}$ is the label list for $\boldsymbol{D}^i$. D_j^i is represented as a d-dimensional real vector x_j^i which is calculated using the query-document pair (q^i, D_j^i). Then, for query q^i, the associated documents $\boldsymbol{D}^i$ can be represented as a $n_i \times d$ matrix X^i. The $n_i \times n_i$ matrix R^i is used to denote the relations between any two documents D_j^i and D_k^i. Then $(X^i, R^i, \boldsymbol{y}^i)$ forms a sample.

In learning, we are given N training samples:$\{(X^i, R^i, \boldsymbol{y}^i)\}_{i=1}^N$. Suppose f to be a ranking function $y = f(X, R)$, the goal of learning is to select the best function $\widehat{f}$ from a function space $\mathcal{F}$ using the training data. Define a loss function $L(f(X, R), \boldsymbol{y})$ to evaluate the performance of the ranking function f, then the problem of ranking relational objects can be represented as minimizing the total loss with respect to the training data:

$$\widehat{f} = \arg\min_{f \in \mathcal{F}} \sum_{k=1}^{N} L(f(X^k, R^k), \boldsymbol{y}^k) \tag{1}$$

In [20] two different loss functions are proposed for different application fields: one is in Pseudo Relevance Feedback (we denote this algorithm as RRSVM-PRF) and the other Topic Distillation(RRSVM-TD). The two loss functions share a similar structure:

$$f(h(X;\omega), R) = \arg\min_{\boldsymbol{z}} \{l_1(h(X;\omega), \boldsymbol{z}) + \beta l_2(R, \boldsymbol{z})\} \tag{2}$$

where $\boldsymbol{z}$ denotes any possible ranking scores, h is a function of X which can be learned using any learning-to-rank algorithms without consideration of document relations R, ω is the parameter used in h. The first objective $l_1(h(X;\omega), \boldsymbol{z})$ is a loss function of $h(X;\omega)$ and the second objective $l_2(R, \boldsymbol{z})$ measures the inconsistency between elements in $\boldsymbol{z}$ under relation R. β is a non-negative coefficient representing the trade-off between the two objectives. When $\beta = 0$, the loss function reduces to conventional ranking algorithms.

In [20], $l_1(h(X;\omega), \boldsymbol{z})$ is defined as:

$$l_1(h(X;\omega), \boldsymbol{z}) = \|h(X;\omega) - \boldsymbol{z}\|^2 \tag{3}$$

To compare our result with [16, 17], we make the same assumptions:

1. For every x, the feature vector of a query-document pair, $\|x\| \leq W$.
2. The ranking function to be learned $f(x)$ as well as $h(x)$ are from the linear function class: $\mathcal{F} = \{x \to wx : \ \|w\| \leq B\}$.
3. To conduct a meaningful comparison of the generalization abilities of different algorithms, we need to normalize the loss functions. Each loss function should be normalized to be in the range of [0, 1].

3.2 Rademacher Average Based Generalization Bound

We will use empirical Rademacher Averages as our analysis tool, so we first review the definition of Rademacher Average[30] as follows.

Defination 1. *The empirical Rademacher Average of a function class $\mathcal{F}$ on i.i.d. random variables $x_1, \ldots, x_n$ is defined as*

$$\widehat{\mathcal{R}}(\mathcal{F}) = E_\sigma \sup_{f \in \mathcal{F}} \frac{1}{n} \sum_{i=1}^{n} \sigma_i f(x_i) \tag{4}$$

where $\sigma_i, i = 1, \ldots, r$ are i.i.d random variables with probability 1/2 of taking value 1 or -1.

Several properties on Rademacher Average have been proposed in [30] below, we restate three important properties, which our generalization bound is based on.

1. For every $c \in \mathbb{R}$, $\mathbb{R}$ stands for the space of real numbers, then $\widehat{\mathcal{R}}_n(c\mathcal{F}) = |c|\widehat{\mathcal{R}}_n(\mathcal{F})$.
2. If $\phi : \widehat{\mathbb{R}} \to \mathbb{R}$ is Lipschitz with constant λ and satisfies $\phi(0) = 0$,then $\widehat{\mathcal{R}}_n(\phi \circ \mathcal{F}) \leq \lambda \widehat{\mathcal{R}}_n(\mathcal{F})$.
3. $\widehat{\mathcal{R}}_n(\Sigma_{i=1}^k \mathcal{F}_i) \leq \sum_{i=1}^k \widehat{\mathcal{R}}_n(\mathcal{F}_i)$.

We now cite an important result about the Rademacher Average in the list-wise ranking problem.

Theorem 1. *Given a training set $S = (z_i, y_i), i = 1, \ldots, n$, let A denote a list-wise ranking algorithm , $l_A(f; z, y)$ be its list-wise loss, $l_A(f; z, y) \in [0, 1]$, then with probability at least $1 - \delta$, the following inequality holds:*

$$\sup_{f \in \mathcal{F}} (\mathcal{R}_{l_A}(f) - \widehat{\mathcal{R}}_{l_A}(f; S)) \leq 2\widehat{\mathcal{R}}(l_A \circ \mathcal{F}) + \sqrt{\frac{2 \ln \frac{2}{\delta}}{n}} \tag{5}$$

where $\widehat{\mathcal{R}}(l_A \circ \mathcal{F}) = E_\sigma[\sup_{f \in \mathcal{F}} \frac{1}{n} \sum_{i=1}^n \sigma_i l_A(f; z_i, y_i)]$.

With theorem 1, we can find that generalization bound of a particular list-wise algorithm depends on Rademacher Averages of compound function which operators on loss function and ranking model, smaller Rademacher Average of the compound function class corresponds to tighter generalization bound.

3.3 Upper Bound When Not Using Relational Information

We first consider the Rademacher Average upper bound of the algorithm that does not use relational information(the RRSVM-None algorithm). There can be many various loss functions for this algorithm, for comparison with the other two ranking relational objects algorithms, we take the same loss function with l_1 defined in RRSVM-PRF and RRSVM-TD.

$$l_{RRSVM-None}(f; X, \boldsymbol{y}) = \|h(X; \omega) - f(X)\|^2 \tag{6}$$

By applying Rademacher Average, we have the following theorem:

Theorem 2. *The upper bound of Rademacher Average of the algorithm that does not use relational information is:*

$$\widehat{\mathcal{R}}(l_{RRSVM-None} \circ \mathcal{F}) \leq 4mBW\widehat{\mathcal{R}}(\mathcal{F}) \tag{7}$$

Proof. Substituting the definition of $l_{RRSVM-None}$ into $\widehat{\mathcal{R}}(l_A \circ \mathcal{F})$, we have

$$\begin{aligned} &\widehat{\mathcal{R}}(l_{RRSVM-None} \circ \mathcal{F}) \\ =&E_\sigma[\sup_{f\in\mathcal{F}} \frac{1}{n}\sum_{i=1}^{n}\sigma_i \sum_{j=1}^{m}(h(x_j^i;\omega) - f(x_j^i))^2] \\ \leq&\sum_{j=1}^{m} E_\sigma[\sup_{f\in\mathcal{F}} \frac{1}{n}\sum_{i=1}^{n}\sigma_i(h(x_j^i;\omega) - f(x_j^i))^2] \end{aligned} \tag{8}$$

Define $\varphi(t) = t^2$, $t = h(x_j^i;\omega) - f(x_j^i)$. Then $\varphi(0) = 0, \varphi'(t) = 2t$. Since both $h(x)$ and $f(x)$ are assumed to be linear models, we can get $-BW \leq h(x) \leq BW, -BW \leq f(x) \leq BW$, therefore $-2BW \leq t \leq 2BW$. According to the property of Rademacher Average, the following inequality holds:

$$\begin{aligned} &\sum_{j=1}^{m} E_\sigma[\sup_{f\in\mathcal{F}} \frac{1}{n}\sum_{i=1}^{n}\sigma_i(h(x_j^i;\omega) - f(x_j^i))^2] \\ \leq&\sum_{j=1}^{m} 4BWE_\sigma[\sup_{f\in\mathcal{F}} \frac{1}{n}\sum_{i=1}^{n}\sigma_i(h(x_j^i;\omega) - f(x_j^i))] \end{aligned} \tag{9}$$

$h(x_j^i;\omega)$ will not change once the function h of content information X is specified, and it does not depend on $f(x)$, so $h(x_j^i;\omega)$ can be viewed as a constant, then we can get the following inequality:

$$\begin{aligned} &\sum_{j=1}^{m} E_\sigma[\sup_{f\in\mathcal{F}} \frac{1}{n}\sum_{i=1}^{n}\sigma_i(h(x_j^i;\omega) - f(x_j^i))^2] \\ \leq&\sum_{j=1}^{m} 4BWE_\sigma[\sup_{f\in\mathcal{F}} \frac{1}{n}\sum_{i=1}^{n}\sigma_i f(x_j^i)] \\ =&4mBW\widehat{\mathcal{R}}(\mathcal{F}) \end{aligned} \tag{10}$$

■

3.4 Upper Bound of Loss Function in Pseudo Relevance Feedback

The loss function RRSVM-PRF is defined as follows:

$$\begin{aligned} l_{RRSVM-PRF}(f;X,\boldsymbol{y}) &= \|h(X;\omega) - f(X)\|^2 + \frac{\beta}{2}\sum_{i=1}^{m}\sum_{j=1}^{m} R_{ij}(f(x_i) - f(x_j))^2 \\ &= \sum_{i=1}^{m}(h(x_i;\omega) - f(x_i))^2 + \frac{\beta}{2}\sum_{i=1}^{m}\sum_{j=1}^{m} R_{ij}(f(x_i) - f(x_j))^2 \end{aligned} \tag{11}$$

where R is the relational information matrix with each element R_{ij} representing the similarity between x_i and x_j.

We apply Rademacher Average to the loss function $l_{RRSVM-PRF}(f; X, Y)$ and get its generalization bound in the following theorem:

Theorem 3. *The upper bound of empirical Rademacher Average of loss function* $l_{RRSVM-PRF}(f; X, Y)$ *is:*

$$\widehat{\mathcal{R}}(l_{RRSVM-PRF} \circ \mathcal{F}) \leq 4mBW(1 + \beta m)\widehat{\mathcal{R}}(\mathcal{F}) \tag{12}$$

Proof. Substituting the definition of $l_{RRSVM-PRF}$ into $\widehat{\mathcal{R}}(l_A \circ \mathcal{F})$, we have

$$\begin{aligned}
&\widehat{\mathcal{R}}(l_{RRSVM-PRF} \circ \mathcal{F}) \\
=&E_\sigma[\sup_{f\in\mathcal{F}} \frac{1}{n}\sum_{i=1}^{n} \sigma_i(\|h(x^i;\omega) - f(x^i)\|^2 + \frac{\beta}{2}\sum_{j=1}^{m}\sum_{k=1}^{m} R_{jk}(f(x_j^i) - f(x_k^i))^2)] \\
\leq&E_\sigma[\sup_{f\in\mathcal{F}} \frac{1}{n}\sum_{i=1}^{n} \sigma_i \sum_{j=1}^{m}(h(x_j^i;\omega) - f(x_j^i))^2] \\
&+ E_\sigma[\sup_{f\in\mathcal{F}} \frac{1}{n}\sum_{i=1}^{n} \sigma_i \frac{\beta}{2}\sum_{j=1}^{m}\sum_{k=1}^{m} R_{jk}(f(x_j^i) - f(x_k^i))^2)] \\
\leq&\sum_{j=1}^{m} E_\sigma[\sup_{f\in\mathcal{F}} \frac{1}{n}\sum_{i=1}^{n} \sigma_i(h(x_j^i;\omega) - f(x_j^i))^2] \\
&+ \frac{1}{2}\sum_{j=1}^{m}\sum_{k=1}^{m} \beta R_{jk} E_\sigma[\sup_{f\in\mathcal{F}} \frac{1}{n}\sum_{i=1}^{n} \sigma_i(f(x_j^i) - f(x_k^i))^2]
\end{aligned} \tag{13}$$

The first term is the same with RRSVM-None, now consider the main part of the second term in Eq. 13: $E_\sigma \sup_{f\in\mathcal{F}} \frac{1}{n}\sum_{i=1}^{n} \sigma_i(f(x_j^i) - f(x_k^i))^2$. Define function $\varphi(t)$ to be the same with the first term while t changes to $f(x_j^i) - f(x_k^i)$, then $t \in [-2BW, 2BW]$. Therefore, the following inequality holds:

$$\begin{aligned}
&E_\sigma[\sup_{f\in\mathcal{F}} \frac{1}{n}\sum_{i=1}^{n} \sigma_i(f(x_j^i) - f(x_k^i))^2] \\
\leq&4BW E_\sigma[\sup_{f\in\mathcal{F}} \frac{1}{n}\sum_{i=1}^{n} \sigma_i(f(x_j^i) - f(x_k^i))] \\
\leq&8BW\widehat{\mathcal{R}}(\mathcal{F})
\end{aligned} \tag{14}$$

Combining Eq. 13, Eq. 14 and Theorem 2, we can obtain the following inequality:

$$\begin{aligned}
&\widehat{\mathcal{R}}(l_{RRSVM-PRF} \circ \mathcal{F}) \\
\leq&(\sum_{j=1}^{m} 4BW + \frac{1}{2}\sum_{j=1}^{m}\sum_{k=1}^{m} \beta R_{jk} 8BW)\widehat{\mathcal{R}}(\mathcal{F}) \\
\leq&4mBW(1 + \beta m)\widehat{\mathcal{R}}(\mathcal{F})
\end{aligned} \tag{15}$$

3.5 Upper Bound of Loss Function in Topic Distillation

The loss function used in topic distillation(denoted as RRSVM-TD) is defined as:

$$l_{RRSVM-TD}(f; X, \boldsymbol{y}) = \|h(x;\omega) - f(x)\|^2 + \beta \sum_i \sum_j R_{ij} e^{f(x_i)-f(x_j)} \tag{16}$$

where R_{ij} is a binary variable {0,1} and indicates whether object i is the parent of object j.

In a similar way we can get the upper bound of the empirical Rademacher Average of the loss function $l_{RRSVM-TD}(f; x, y)$:

Theorem 4. *The upper bound of empirical Rademacher Average of loss function* $l_{RRSVM-TD}(f; x, y)$ *is:*

$$\widehat{\mathcal{R}}(l_{RRSVM-TD} \circ \mathcal{F}) \leq (4(\beta+1)BW + 2\beta)m\widehat{\mathcal{R}}(\mathcal{F}) \tag{17}$$

Proof. Substituting the definition of $l_{RRSVM-TD}$ into $\widehat{\mathcal{R}}(l_A \circ \mathcal{F})$, we have

$$\begin{aligned}
&\widehat{\mathcal{R}}(l_{RRSVM-TD} \circ \mathcal{F}) \\
=&E_\sigma[\sup_{f\in\mathcal{F}} \frac{1}{n}\sum_{i=1}^{n} \sigma_i(\|h(x^i;\omega) - f(x^i)\|^2 + \beta \sum_{j=1}^{m}\sum_{k=1}^{m} R_{jk} e^{f(x_k)-f(x_j)})] \\
\leq&E_\sigma[\sup_{f\in\mathcal{F}} \frac{1}{n}\sum_{i=1}^{n} \sigma_i \sum_{j=1}^{m}(h(x_j^i;\omega) - f(x_j^i))^2] \\
&+ E_\sigma[\sup_{f\in\mathcal{F}} \frac{1}{n}\sum_{i=1}^{n} \sigma_i \beta \sum_{j=1}^{m}\sum_{k=1}^{m} R_{jk} e^{f(x_k)-f(x_j)}] \\
\leq&\sum_{j=1}^{m} E_\sigma[\sup_{f\in\mathcal{F}} \frac{1}{n}\sum_{i=1}^{n} \sigma_i (h(x_j^i;\omega) - f(x_j^i))^2] \\
&+ \sum_{j=1}^{m}\sum_{k=1}^{m} \beta R_{jk} E_\sigma[\sup_{f\in\mathcal{F}} \frac{1}{n}\sum_{i=1}^{n} \sigma_i e^{f(x_k)-f(x_j)}]
\end{aligned} \tag{18}$$

It's difficult to find the upper bound directly, here we use Taylor expansion to approximate $e^{f(x_k)-f(x_j)}$:

$$\begin{aligned}
e^{f(x_k)-f(x_j)} &\approx 1 + (f(x_k) - f(x_j)) + \frac{1}{2}(f(x_k) - f(x_j))^2 \\
&= \frac{1}{2}(f(x_k) - f(x_j) + 1)^2 + \frac{1}{2}
\end{aligned} \tag{19}$$

Eq. 16 then changes to:

$$l_{RRSVM-TD}(f; x, y) = \|h(x;\omega) - f(x)\|^2 + \beta \sum_i \sum_j R_{ij} (\frac{1}{2}(f(x_i) - f(x_j) + 1)^2 + \frac{1}{2}) \tag{20}$$

And Eq. 18 changes to:

$$\begin{aligned}
&\widehat{\mathcal{R}}(l_{RRSVM-TD} \circ \mathcal{F}) \\
\leq &\sum_{j=1}^{m} E_\sigma[\sup_{f\in\mathcal{F}} \frac{1}{n}\sum_{i=1}^{n} \sigma_i(h(x_j^i;\omega) - f(x_j^i))^2] \\
&+ \sum_{j=1}^{m}\sum_{k=1}^{m} \beta R_{jk} E_\sigma[\sup_{f\in\mathcal{F}} \frac{1}{n}\sum_{i=1}^{n} \sigma_i(\frac{1}{2}(f(x_k) - f(x_j) + 1)^2 + \frac{1}{2})] \\
= &\sum_{j=1}^{m} E_\sigma[\sup_{f\in\mathcal{F}} \frac{1}{n}\sum_{i=1}^{n} \sigma_i(h(x_j^i;\omega) - f(x_j^i))^2] \\
&+ \frac{1}{2}\sum_{j=1}^{m}\sum_{k=1}^{m} \beta R_{jk} E_\sigma[\sup_{f\in\mathcal{F}} \frac{1}{n}\sum_{i=1}^{n} \sigma_i(f(x_k) - f(x_j) + 1)^2]
\end{aligned} \tag{21}$$

The first term of Eq. 21 is the same with RRSVM-None too, so we only need to consider the main part of the second term $E_\sigma \sup_{f\in\mathcal{F}} \frac{1}{n}\sum_{i=1}^{n} \sigma_i(f(x_k) - f(x_j) + 1)^2$. The function $\varphi(t)$ remains the same while t changes to $f(x_k) - f(x_j) + 1$, then $-2BW + 1 \leq t \leq 2BW + 1$. According to the property of Rademacher Average, we have:

$$\begin{aligned}
&E_\sigma[\sup_{f\in\mathcal{F}} \frac{1}{n}\sum_{i=1}^{n} \sigma_i(f(x_k) - f(x_j) + 1)^2] \\
\leq &2(2BW+1)E_\sigma[\sup_{f\in\mathcal{F}} \frac{1}{n}\sum_{i=1}^{n} \sigma_i(f(x_k) - f(x_j) + 1)] \\
= &2(2BW+1)E_\sigma[\sup_{f\in\mathcal{F}} \frac{1}{n}\sum_{i=1}^{n} \sigma_i(f(x_k) - f(x_j))] \\
\leq &4(2BW+1)\widehat{\mathcal{R}}(\mathcal{F})
\end{aligned} \tag{22}$$

Combining Eq. 21, Eq. 22 and Theorem 2, we finally have:

$$\widehat{\mathcal{R}}(l_{RRSVM-TD} \circ \mathcal{F}) \leq (\sum_{j=1}^{m} 4BW + \frac{1}{2}\sum_{j=1}^{m}\sum_{k=1}^{m} \beta R_{jk} 4(2BW+1))\widehat{\mathcal{R}}(\mathcal{F})$$

Note that $R_{jk} \in \{0, 1\}$ and represents whether object j is the parent of k, and as mentioned in [20], in site map hierarchy a web page has at most one parent page, so there is at most one element 1 in each column in matrix R. Therefore, $\sum_{j=1}^{m}\sum_{k=1}^{m} \beta R_{jk} 4(2BW+1) \leq 4(2BW+1)\beta m$. The following inequality holds:

$$\begin{aligned}
&\widehat{\mathcal{R}}(l_{RRSVM-TD} \circ \mathcal{F}) \\
\leq &(4mBW + (4BW+2)\beta m)\widehat{\mathcal{R}}(\mathcal{F}) \\
= &(4(\beta+1)BW + 2\beta)m\widehat{\mathcal{R}}(\mathcal{F})
\end{aligned} \tag{23}$$

To conduct a meaningful comparison among RRSVM-None, RRSVM-PRF and RRSVM-TD, we need to normalize the loss functions. For algorithms $\mathcal{A}$ (e.g., RRSVM-None, RRSVM-PRF or RRSVM-TD), we normalize the original loss function $l_{\mathcal{A}}(f; X, \boldsymbol{y})$ to be $l'_{\mathcal{A}}(f; X, \boldsymbol{y}) = \frac{l_{\mathcal{A}}(f;X,\boldsymbol{y})}{Z_{\mathcal{A}}}$, where $Z_{\mathcal{A}}$ is the maximum of the corresponding loss function. It can be easily seen that:

$$\begin{aligned} Z_{RRSVM-None} &= 4mB^2W^2 \\ Z_{RRSVM-PRF} &= (4+2m\beta)mB^2W^2 \\ Z_{RRSVM-TD} &= (4+2\beta)mB^2W^2 + m\beta(2BW+1) \end{aligned} \tag{24}$$

Note that all of the normalizers are constants, with the property of Rademacher Average, we can get the new upper bound for normalized loss functions RRSVM-None, RRSVM-PRF and RRSVM-TD:

$$\widehat{\mathcal{R}}(l'_{RRSVM-None} \circ \mathcal{F}) \leq \frac{1}{BW}\widehat{\mathcal{R}}(\mathcal{F}) \tag{25}$$

$$\widehat{\mathcal{R}}(l'_{RRSVM-PRF} \circ \mathcal{F}) \leq \frac{2+2m\beta}{(2+m\beta)BW}\widehat{\mathcal{R}}(\mathcal{F}) \tag{26}$$

$$\widehat{\mathcal{R}}(l'_{RRSVM-TD} \circ \mathcal{F}) \leq \frac{4(\beta+1)BW+2\beta}{(4+2\beta)B^2W^2+\beta(2BW+1)}\widehat{\mathcal{R}}(\mathcal{F}) \tag{27}$$

To have a comparison with other list-wise algorithms, we list the currently available conclusions: the generalization ability of ListMLE, ListNet and RankCosine demonstrated in [16, 17].

$$\widehat{R}(l_{listMLE} \circ \mathcal{F}) \leq \frac{2}{(b-aBM)(\log m + \log\frac{b+aBM}{b-aBM})}\widehat{R}(\mathcal{F}) \tag{28}$$

$$\widehat{R}(l_{listNet} \circ \mathcal{F}) \leq \frac{2m!}{(b-aBM)(\log m + \log\frac{b+aBM}{b-aBM})}\widehat{R}(\mathcal{F}) \tag{29}$$

$$\widehat{R}(l_{listCosine} \circ \mathcal{F}) \leq \frac{\sqrt{m}}{2(b-aBM)}\widehat{R}(\mathcal{F}) \tag{30}$$

4 Experiments and Discussions

Theorem 4 shows that the upper bound for RRSVM-TD does not depend on m, which is very valuable in practical learning problems. To verify this property, we conduct experiments using the TREC 2003/2004 topic distillation dataset which can be extracted from *.Gov* collection in LETOR 3.0. We implement the RRSVM-TD algorithm on the basic of Primal-SVM[31].

There are about 1000 documents per query. To verify the property proposed above, we randomly select a subset from the training set for each query with increasing number 50, 100, 150,... ,1000. To ensure there are positive instances to learn, we make sure that there are at least 3 positive instances for each query in the experiment. Then we run the algorithm and observe the gaps between

training and testing performances. Fig. 1 and 2 illustrate the result we get. As can be seen from the two figures that the gaps between training and testing performances decrease with the size of subset when it's less than 400, and the subset size grows above 400, the gaps remain stable around 0.

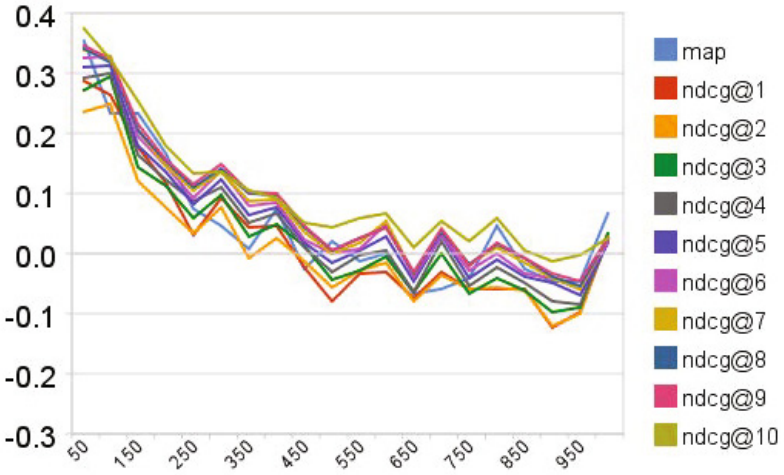

Fig. 1. Gaps between training and testing error on TD-2003

We can get the following conclusions:

- The bound of RRSVM-TD is irrelevant with m, thus we need not worry about overfitting if we increase the number of documents for each query. The reason lies in the uniqueness of the relational matrix R. If the sum of R_{ij} does not exceed m, then this property holds.
- When $BW < \frac{1}{\sqrt{2}}$, the bound of RRSVM-TD is looser than RRSVM-None. To enhance the generalization ability for RRSVM-TD algorithm, we should make BW small enough.
- The bound of RRSVM-PRF is looser than RRSVM-None and increases monotonously w.r.t. m, thus it may bring some risks of overfitting. However, it does not increase infinitely: the limit is $2/BW$. It's looser than ListMLE but tighter than ListNet and RankCosine[17].
- The generalization bound of both RRSVM-PRF and RRSVM-TD algorithms decreases with n.

5 Conclusions and Future Work

In this paper, we study effect of using relation information on the generalization ability for ranking algorithms. We use Rademacher Average as a tool to analyze the generalization bound of RRSVM-None, RRSVM-PRF and RRSVM-TD and

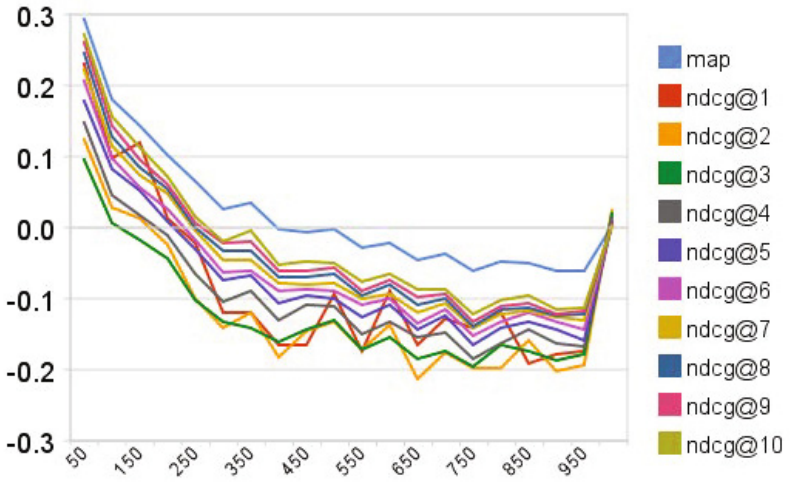

Fig. 2. Gaps between training and testing error on TD-2004

find that: (1) The generalization bound of RRSVM-PRF is not better than that of RRSVM-None, thus it may cause over fitting in training set; (2) The generalization of RRSVM-TD is tighter than that of RRSVM-None when $BW < \frac{1}{\sqrt{2}}$, so we need to limit the value of BW if we want to get better generalization performance.

For the future work, we want to analyze generalization ability on more algorithms. Further more, we plan to make other theoretical analysis on learning to rank algorithms, such as stability and complexity.

Acknowledgments. This paper is supported by National Nature Science Foundation of China (No. 61272067 and 60970044), Guangdong Province Science and Technology Foundation(No.S2012030006242, 2011B080100031, 2011168005 and 2011A091000036).

References

1. Lai, H., Pan, Y., Liu, C., Lin, L., Wu, J.: Sparse learning-to-rank via an efficient primal-dual algorithm. IEEE Transactions on Computers (2011)
2. Pan, Y., Luo, H., Qi, H., Tang, Y.: Transductive learning to rank using association rules. Expert Systems with Applications 38, 12839–12844 (2011)
3. Rigutini, L., Papini, T., Maggini, M., Scarselli, F.: SortNet: Learning to Rank by a Neural Preference Function. IEEE Transactions on Neural Networks 22, 1368–1380 (2011)
4. Chapelle, O., Chang, Y.: Yahoo! Learning to Rank Challenge Overview. Journal of Machine Learning Research 14, 1–24 (2011)

5. Lubell-Doughtie, P., Hofmann, K.: Learning to Rank from Relevance Feedback for e-Discovery. In: Baeza-Yates, R., de Vries, A.P., Zaragoza, H., Cambazoglu, B.B., Murdock, V., Lempel, R., Silvestri, F. (eds.) ECIR 2012. LNCS, vol. 7224, pp. 535–539. Springer, Heidelberg (2012)
6. Li, P., Burges, C., Wu, Q.: Mcrank: Learning to ank using multiple classification and gradient boosting. In: Advances in Neural Information Processing Systems, vol. 20, pp. 897–904 (2007)
7. Xu, J., Chen, C., Xu, G., Li, H., Abib, E.R.T.: Improving quality of training data for learning to rank using click-through data. In: Web Search and Data Mining, pp. 171–180 (2010)
8. Joachims, T.: Optimizing search engines using clickthrough data (2002)
9. Burges, C., Shaked, T., Renshaw, E., Lazier, A., Deeds, M., Hamilton, N., Hullender, G.: Learning to rank using gradient descent. In: Proceedings of the 22nd International Conference on Machine Learning (ICML), pp. 89–96. ACM Press (2005)
10. Freund, Y., Iyer, R., Schapire, R., Singer, Y.: An efficient boosting algorithm for combining preferences. The Journal of Machine Learning Research 4, 933–969 (2003)
11. Xia, F., Liu, T.Y., Wang, J., Zhang, W., Li, H.: Listwise approach to learning to rank: theory and algorithm. In: Proceedings of the 25th International Conference on Machine Learning, pp. 1192–1199. ACM Press (2008)
12. Cao, Z., Qin, T., Liu, T.Y., Tsai, M.F., Li, H.: Learning to rank: from pairwise approach to listwise approach. In: Proceedings of the 24th International Conference on Machine Learning (ICML), pp. 129–136. ACM Press (2007)
13. Qin, T., Zhang, X.D., Tsai, M.F., Wang, D.S., Liu, T.Y., Li, H.: Query-level loss functions for information retrieval. The Journal of Information Processing and Management 44(2), 838–855 (2007)
14. Qin, T., Liu, T.Y., Li, H.: A general approximation framework for direct optimization of information retrieval measures. MSR-TR-2008-164, Microsoft Research (2008)
15. Shi, Y., Larson, M., Hanjalic, A.: List-wise learning to rank with matrix factorization for collaborative filtering. In: Conference on Recommender Systems, pp. 269–272 (2010)
16. Liu, T.Y., Lan, Y.: Generalization analysis of listwise learning-to-rank algorithms using rademacher average. Technical Report MSR-TR-2008-155, Microsoft Research (2008)
17. Lan, Y., Liu, T.Y., Ma, Z., Li, H.: Generalization analysis of listwise learning-to-rank algorithms. In: Proceedings of 26th International Conference on Machine Learning (2009)
18. Brin, S., Page, L.: The anatomy of a large-scale hypertextual web search engine. Comput. Netw. ISDN Syst. 30, 107–117 (1998)
19. Kleinberg, J.M.: Authoritative sources in a hyperlinked environment. J. ACM 46, 604–632 (1999)
20. Qin, T., Liu, T.Y., Zhang, X.D., Wang, D.S., Xiong, W.Y., Li, H.: Learning to rank relational objects and its application to web search. In: Proceeding of the 17th International Conference on World Wide Web, pp. 407–416. ACM, New York (2008)
21. Jin, R., Valizadegan, H., Li, H.: Ranking refinement and its application to information retrieval. In: Proceeding of the 17th International Conference on World Wide Web, pp. 397–406 (2008)

22. Zhou, D., Bousquet, O., Lal, T.N., Weston, J., Schölkopf, B., Olkopf, B.S.: Learning with local and global consistency. In: Advances in Neural Information Processing Systems, vol. 16, pp. 321–328. MIT Press (2003)
23. Zhou, D., Huang, J., Schölkopf, B.: Learning from labeled and unlabeled data on a directed graph. In: ICML 2005: Proceedings of the 22nd International Conference on Machine Learning, pp. 1036–1043. ACM, New York (2005)
24. Zhou, D., Schölkopf, B., Hofmann, T.: Semi-supervised learning on directed graphs. In: Saul, L.K., Weiss, Y., Bottou, L. (eds.) Advances in Neural Information Processing Systems, vol. 17, pp. 1633–1640. MIT Press, Cambridge (2005)
25. Deng, H., Lyu, M.R., King, I.: Effective latent space graph-based re-ranking model with global consistency. In: WSDM 2009: Proceedings of the Second ACM International Conference on Web Search and Data Mining, pp. 212–221. ACM, New York (2009)
26. Vapnik, V.N., Chervonenkis, A.: On the uniform convergence of relative frequencies of events to their probabilities 16, 264–280 (1971)
27. Agarwal, S., Graepel, T., Herbrich, R., Har-Peled, S., Roth, D.: Generalization bounds for the area under the roc curve. Journal of Machine Learning Research, 393–425 (2005)
28. Agarwal, S., Niyogi, P.: Stability and Generalization of Bipartite Ranking Algorithms. In: Auer, P., Meir, R. (eds.) COLT 2005. LNCS (LNAI), vol. 3559, pp. 32–47. Springer, Heidelberg (2005)
29. Lan, Y., Liu, T.Y., Qin, T., Ma, Z., Li, H.: Query-level stability and generalization in learning to rank. In: Proceedings of 25th International Conference on Machine Learning, pp. 512–519 (2008)
30. Bartlett, P.L., Mendelson, S.: Rademacher and gaussian complexities: Risk bounds and structural results. Journal of Machine Learning Research, 463–482 (2002)
31. Chapelle, O.: Training a Support Vector Machine in the Primal. Neural Computation 19, 1155–1178 (2007)

The Optimization of Two-Stage Planetary Gear Train Based on Mathmatica

Tianpei Chen, Zhengyan Zhang, Dingfang Chen, and Yongzhi Li

Wuhan University of Technology, Hubei Wuhan 430063
jasongervin@163.com, zzy0309@yahoo.com.cn,
dfchen@whut.edu.cn, whlgd.lyz@263.net

Abstract. Planetary gear reducer has a lot of advantages, such as high transmission and efficiency, compact structure, and has a variety of applications in construction machinery and equipment, hoisting and conveying machinery and so on,. The optimization design of the planetary gear train could make the volume at minimum(as well as the weight at minimum) under the conditions of carrying capacity. This paper focus on the optimization of two stage planetary gear train with the differential evolution algorithm, based on Mathmatica. The author established mathematical model and source program is present in this paper. After the optimization, the author verifies the optimal result, including the contact fatigue stress and tooth bending strength fatigue stress. The verification infers that the optimization based on Mathmatica with differential evolution algorithm is effective and correct.

Keywords: Mathmactica, optimization and design, planetary gear reducer, verification and validation of gear.

1 Introduction

Planetary gear trains take a very important place among the gear transmissions which are used in many branches of industry. Under similar operating conditions, planetary gear train have a number of advantages as comparing to the standard transmission with shafts: light weight, compact size, large speed ratio, high efficiency, long service life, low noise and so on. Therefore a special attention should be taken to its design [1].

The optimal design of planetary gear trains is a complex engineering problem and a multi-objective optimization problem because of very complicated calculations, a great number of conditions, geometrical and functional constraints and a large number of solution variants. In this paper, based on Mathmatica, we used differential evolution algorithm in the optimization of two stage planetary gear train.

Q. Zu, B. Hu, and A. Elçi (Eds.): ICPCA-SWS 2012, LNCS 7719, pp. 122–136, 2013.

2 The Optimal Model of Planetray Gear Train

For the given kinematics scheme of the planetary gear train (Figure1), kinematics parameters of the input shaft and the overall gear ratio, find a solution (basic constructional parameters as number of teeth, modules), which simultaneously the following objective functions: Weight of the planetary gear train.

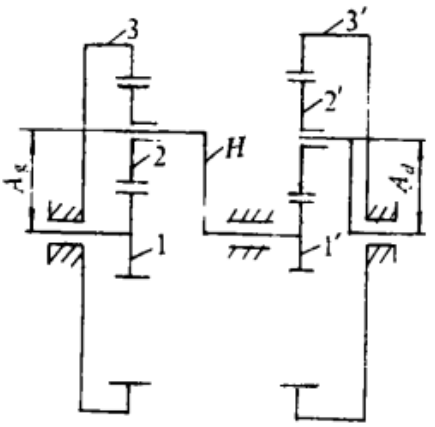

Fig. 1. Planetary gear train

The vector of design variables is identified as follows:

$$\mathrm{Z}=\left\{x_1,x_2,x_3,x_4,x_5;x_6,x_7,x_8,x_9\right\}^T=\left\{Z_1,m_1,b_1,X_1,i_1;Z_{1'},m_2,b_2,X_2\right\}^T \quad (1)$$

Where: $Z_1,Z_{1'}$ are the numbers of teeth of the first stage sun gear and the second stage sun gear , m_1,m_2 are the modules of the gear wheels respectively, b_1,b_2 are the tooth width of the gear respectively, X_1,X_2 are the modification coefficient of the sun gear respectively, i is the transmission ratio of the first stage.

2.1 Determine the Objective Function

To design the planetary gear reducer with minimal weight, the total volume of all sun gears and planetary gears can be taken as the objective function.

$$\mathrm{F}=\frac{\pi}{4}\left[b_1\left(d_{a1}^2+3d_{a2}^2\right)+b_2\left(d_{a1}^{'\,2}+3d_{a2}^{'\,2}\right)\right] \quad (2)$$

Where: $d_{a1}, d_{a2}, d_{a1'}, d_{a2'}$ are the addendum circle diameter of the gear wheels respectively, b_1, b_2 are the tooth width of the gear respectively.

Simultaneously, these variables are involved in the following equations.

$$d_a = \left(Z + 2h_a\right)m \tag{3}$$

So the objective function is

$$\begin{aligned} f(x) = \frac{\pi}{4}x_3\left(\left(\left(x_1 + 2(1+x_4)\right)x_2\right)^2 + 3\left[\left(\frac{1}{2}(x_5-2)x_1 + 2(1+x_4)\right)x_2\right]^2\right) \\ + x_8\left(\left(\left(x_6 + 2(1+x_9)\right)x_7\right)^2 + \left[\left(\frac{1}{2}(\frac{u}{x_5}-2)x_6 + 2(1+x_9)\right)x_7\right]^2\right) \end{aligned} \tag{4}$$

Where: u is the overall transmission ratio of the planetary gear train.

2.2 Determine Constrain Conditions

The constraint conditions are expressed as follows.

(a) Contact fatigue stress conditions:

$$\begin{aligned} \sigma_1 &= Z_{H1}Z_{E1}Z_{\varepsilon 1}\sqrt{\frac{2K_1T_1(u_1+1)}{b_1d_1^2u_1}} \le \sigma_{HP1} \\ \sigma_{1'} &= Z_{H2}Z_{E2}Z_{\varepsilon 2}\sqrt{\frac{2K_2T_2(u_2+1)}{b_2d_{1'}^2u_1}} \le \sigma_{HP2} \end{aligned} \tag{5}$$

Where: Z_H --- node region coefficient, Z_E ---elastic coefficient, Z_ε ---contact ratio coefficient; d_1 , $d_{1'}$ are the pitch diameter of the sun gear respectively; $\sigma_{HP1}, \sigma_{HP2}$ are the permitted contact fatigue stress of the sun gear respectively; b_1, b_2 are the tooth width of the gear respectively; u_1, u_2 are the ratio of tooth number respectively; T_1, T_2 are the input torque respectively; K_1, K_2 are the load factor respectively and load factor $K = K_AK_VK_\alpha K_\beta$, where K_A --- application

factor; K_V ---dynamic factor, K_α --- load distribution factor, and K_β --- valve of load partition factor.

(b) Tooth bending strength fatigue stress conditions:

$$\begin{aligned}\sigma_{F1} &= \frac{2K_1T_1}{b_1d_1m_1}Y_{Fa1}Y_{Sa1}Y_{\varepsilon 1} \le \sigma_{FP1} \\ \sigma_{F1'} &= \frac{2K_2T_2}{b_2d_{1'}m_2}Y_{Fa2}Y_{Sa2}Y_{\varepsilon 2} \le \sigma_{FP2}\end{aligned} \tag{6}$$

Where: Y_{Fa} --- tooth form factor, Y_{Sa} ---stress concentration coefficient, Y_ε ---contact ratio coefficient; b_1, b_2 are the tooth width of gear respectively. $d_1, d_{1'}$, are the pitch diameter of the sun gear respectively; m_1, m_2 are the modules of the gear wheels respectively ; T_1, T_2 are the input torque respectively; $\sigma_{FP1}, \sigma_{FP2}$ are the permitted bending fatigue stress of the sun gear respectively; K_1, K_2 are the load factor respectively.

(c) Transmission ratio condition

According to Mechanical Principle, the number of annular gear and sun gear must meet the following equations:

$$\begin{aligned}i_1 &= \frac{Z_3}{Z_1} + 1 \\ i_2 &= \frac{Z_{3'}}{Z_{1'}} + 1\end{aligned} \tag{7}$$

(d) Meshing of the gears

According to Mechanical Principle, the sum of tooth number of annular gear and sun gear has to be integral multiple of the number of planetary gear.

$$\begin{aligned}\frac{Z_1 + Z_3}{3} &= \text{int} \\ \frac{Z_{1'} + Z_{3'}}{3} &= \text{int}\end{aligned} \tag{8}$$

(e) Parallelism of distance between axes of the input and output shafts

$$\begin{aligned}\frac{Z_1+Z_2}{\cos\alpha_{12}^{'}}&=\frac{Z_3-Z_2}{\cos\alpha_{23}^{'}}\\ \frac{Z_{1'}+Z_{2'}}{\cos\alpha_{1'2'}^{'}}&=\frac{Z_{3'}-Z_{2'}}{\cos\alpha_{2'3'}^{'}}\end{aligned}\tag{9}$$

Where: $\cos\alpha_{12}^{'},\cos\alpha_{23}^{'},\cos\alpha_{1'2'}^{'},\cos\alpha_{2'3'}^{'}$ are the meshing angles of the gears respectively.

(f) Adjacent conditioned

$$\begin{aligned}\mathrm{d}_{a2}&<2a_{12}^{'}sin60°\\ \mathrm{d}_{a2'}&<2a_{1'2'}^{'}sin60°\end{aligned}\tag{10}$$

Where: $d_{a2},d_{a2'}$ are the outside diameters of the planetary gear; $a_{12}^{'}$, $a_{1'2'}^{'}$ are the actual center distance of gear wheels 1 and 2 , gear wheels $1^{'}$ and $2^{'}$.

(g) Module conditions

$$\begin{aligned}2\le \mathrm{m}_1\le 9;\\ 2\le \mathrm{m}_2\le 9\end{aligned}\tag{11}$$

(h) Tooth width conditions

$$\begin{aligned}0.6Z\le\frac{b_1}{m_1}\le 1.3Z\\ 0.6Z\le\frac{b_2}{m_2}\le 1.3Z\end{aligned}\tag{12}$$

3 Optimal Example

Given the total transmission ratio is 55.46, the total input torque of the first stage $T_1=5.69\times10^5 N\bullet mm$ and the total input torque of the second stage $T_2=4.78\times10^6 N\bullet mm$, gear material is 20CrMnMo and heat treatment is quenching surface and its rigidity is HRC57-61.

According to Mechanical Design Handbook, the coefficients above are selected respectively.

3.1 The First Stage

Node region coefficient $Z_{H1}=2.22$, elastic coefficient $Z_{E1}=189.98\sqrt{MPa}$, contact ratio coefficient $Z_{\varepsilon 1}=0.95$, $K_1=2.89$, tooth form factor $Y_{Fa1}=2.29$, stress correction coefficient $Y_{Sa1}=1.73$, contact ratio coefficient $Y_{\varepsilon 1}=1.12$, the permitted contact fatigue stress $\sigma_{HP1}=1033.41MPa$, the permitted bending fatigue stress $\sigma_{FP1}=499.39MP\text{a}$.

3.2 The Second Stage

Node region coefficient $Z_{H1}=2.25$, elastic coefficient $Z_{E1}=189.98\sqrt{MPa}$, contact ratio coefficient $Z_{\varepsilon 1}=0.94, K_1=2.95$, tooth form factor $Y_{Fa1}=2.32$, stress correction coefficient $Y_{Sa1}=1.73$, contact ratio coefficient $Y_{\varepsilon 1}=1.08$, the permitted contact fatigue stress $\sigma_{HP1}=1104.47MPa$, the permitted bending fatigue stress $\sigma_{FP2}=521.53MP\text{a}$.

4 The Realization of Optimization Based on Mathmatica and Results

4.1 Simplification

In order to solve the question better, with high speed and high efficiency, we simplified the constraint conditions (the modules, the tooth number, and the tooth width) in smaller range artificially. The advantage is less iterations, higher solving speed, and higher efficiency in the solution of the mathematical model.

$$\begin{cases} z_1 \geq 13 \\ 2 \leq m_1 \leq 9 \\ 55 \leq b_1 \leq 61 \\ \frac{4}{17} \leq x_1 \leq 1 \\ 5 \leq i_1 \leq 50 \\ z_1^{'} \geq 13 \\ 2 \leq m_2 \leq 9 \\ 110 \leq b_2 \leq 140 \\ \frac{4}{17} \leq x_2 \leq 1 \end{cases} \tag{13}$$

4.2 The Method of Differential Evolution

The differential Evolution (DE) method of Storn and Price (1995) is perhaps the fastest evolutionary computational procedure yielding most accurate solutions to continuous global optimization problems. It consists of three basic steps: (i) generation of (large enough) population with individuals in the m-dimensional space, randomly distributed over the entire domain of the function in question and evaluation of the individuals of the so generated population by finding f(x), where x is the decision variable; (ii) replacement of this current population by a better fit new population, and (iii) repetition of this replacement until satisfactory results are obtained or the given criteria of termination are met.

The strength of DE lays on replacement of the current population by a new population that is better fit. Here the meaning of 'better' is in the Pareto improvement sense. A set Sa is better than another set Sb ***iff*** : (i) no xi $\in$Sa is inferior to the corresponding member of xi$\in$Sb ; and (ii) at least one member xk $\in$Sa is better than the corresponding member xk $\in$ Sb. Thus, every new population is an improvement over the earlier one. To accomplish this, the DE method generates a candidate individual to replace each current individual in the population. A crossover of the current individual and three other randomly selected individuals obtains the candidate individual from the current population. The crossover itself is probabilistic in nature. Further, if the candidate individual is better fit than the current individual, it takes the place of the current individual else the current individual passes into the next iteration.

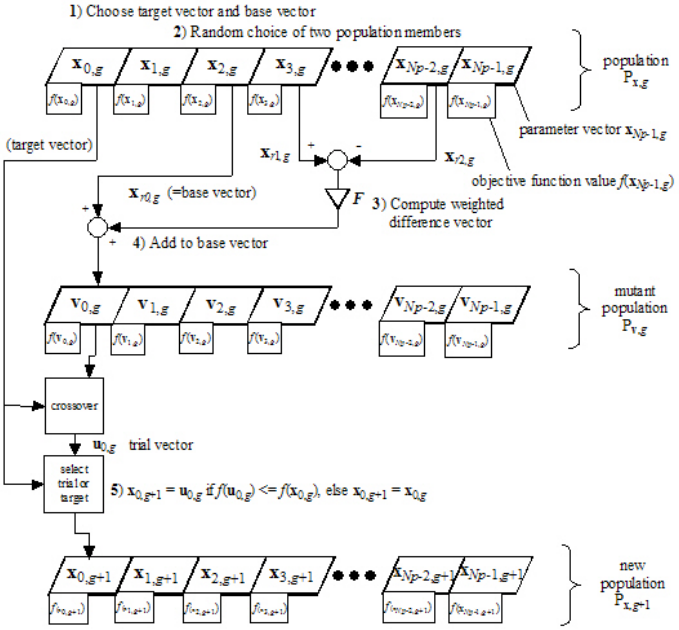

Fig. 2. The method of differential evolution

4.3 Source Program

After the treatment of objective function and constraints conditions, we input the mathematical models to Mathmatica 7.0 and the source program is as follows:

```
NMinimize[
  {3.1415926/4*(x3*(((x1+2*(1+x4))*x2)^2+3*((0.5*(x5-
     2)*x1+2*(1+x4))*x2)^2)+x8*(((x6+2*(1+x9))*x7)^2+
     ((0.5*(55.46/x6-2)*x6+2*(1+x9))*x7)^2)),
  (5.69*10^5)/((x3*(x1*x2)^2)*(x5/(x5-2))-1.1541•0,
  (5.69*10^5/x8*(x6*x7) ^2 *(55.46/(55.46/x5-2))-
     1.2975•0,
  5.69*10^5/(x1*x2^2*x3)-19.4420•0,
   (5.69*10^5*x5)/(x6*x7^2*x8)-20.4021•0,
  -√3/2*x1*x5+(0.5*(x5-2)*x1+2*(1+x4))*x2<0,
  -√3/2*55.46*x7/x6+(0.5*(55.46/x5-2)*x6+2*(1+x9))*x7<0,
  0.6*x1*x2-x3•0,
  x3-1.3*x1*x2•0,
  0.6*x7*x8-x9•0,
  x9-1.3*x7*x8•0,
  x1≤13,
  x2≤2,
  x2≤9,
  x3≤55,
  x3≤61,
  X4≤4/17,
  x4≤1,
  5-x5≤0,
  x5≤50,
  x6≥13,
  x7≥2,
  x7≤9,
  x8≥110,
  x8≤140,
  X9≥4/17,
  x9≥1},
 {x1,x2,x3,x4, x5,x6,x7,x8 ,x9},
  Method {"DifferentialEvolution",
            …
           "RandomSeed" 20},
  MaxIterations 2000]
```

4.4 Results and Analysis

After the processing of Mathmatica, the result of optimization is obtained as following:

{x1 13.0071,x2 2.47044, x3 60.7104, x4 0.238434, x5 12.9891, x6 13.0407, x7 6.9805, x8 110.067, x9 0.2408021}.

For the nine variables above are practical physical quantities, they are not numbers continuous; these variables have to be rounded to integer or in accordance with the standard series. So the result after rounded is

$$z_1 = 13, Z_2 = 71, Z_3 = 155, m_1 = 3.5, b_1 = 60, x_1 = 0.23,\ i_1 = 12.9231,$$
$$z_{1'} = 13, z_{2'} = 15, z_{3'} = 44, m_2 = 7, b_2 = 110,\ x_2 = 0.24.$$

Table 1. Parameters Before Optimization

Stage	Type	Tooth Number	Module	Width	Pitch Diameter
First Stage	Sun Gear	13	3.5	73	45.5
	Planetary Gear	43	3.5	73	150.5
	Annular Gear	101	3.5	73	353.5
Second Stage	Sun Gear	18	5.5	139	99
	Planetary Gear	32	5.5	129	176
	Annular Gear	84	5.5	129	462
Total Volume (mm^3)		15229548.97			

Table 2. Parameters After Optimization

Stage	Type	Tooth Number	Module	Width	Pitch Diameter
First Stage	Sun Gear	13	3.5	60	45.5
	Planetary Gear	71	3.5	60	248.5
	Annular Gear	155	3.5	60	542.5
Second Stage	Sun Gear	13	8	110	104
	Planetary Gear	15	8	110	136
	Annular Gear	44	8	110	376
Total Volume (mm^3)		14555831.29			

$$Percentage = \frac{15229548.97 - 14555831.29}{15229548.97} \times 100\% = 4.42\% \tag{14}$$

4.5 The Verification and Validation of the Result

In order to assure the effectiveness and reliability of the result，we would better verify the contact fatigue stress and the tooth bending strength fatigue stress using formula (5) and (6).

(a) Contact fatigue stress:

According to Mechanical Design Handbook, the coefficients above are selected respectively.

(i) First Stage

With a uniform power source (an electronic motor) and a uniform load (an output shaft), we find the application factor $K_{A1} = 1.5$; we have the dynamic factor $K_{V1} = 1.1$, and the load distribution factor $K_{\beta 1} = 1.0$; the valve of load partition factor $K_{\beta 1}$ depend on the tooth width of gear b and the pitch diameter d_1.

$$K_{\beta 1} = 0.99 + 0.31 \times \left(\frac{b}{d_1} \right)^2 + 0.00012 \times b = 1.54 \tag{15}$$

Then, compute the load factor

$$K_1 = K_{A1} K_{V1} K_{\alpha 1} K_{\beta 1} = 1.5 \times 1.5363 \times 1.0 \times 1.1 = 2.54 \tag{16}$$

According to Mechanical Design Handbook, we find node region coefficient $Z_{H1} = 2.48$; elastic coefficient $Z_{E1} = 189.98\sqrt{MPa}$, contact ratio coefficient $Z_{\varepsilon 1} = 0.9139$.

So the contact fatigue stress

$$\sigma_1 = Z_{H1} Z_{E1} Z_{\varepsilon 1} \sqrt{\frac{2K_1 T_1 (u_1 + 1)}{b_1 d_1^2 u_1}} = 1301.94\text{MPa} \tag{17}$$

The permitted contact fatigue stress

$$\sigma_{HP} = \frac{\sigma_{H\lim}}{S_{H\min}} Z_N Z_W \tag{18}$$

Where: $\sigma_{H\lim}$ --- endurance limit for contact strength; Z_N ---life factor; Z_W --- hardness ratio factor; $S_{H\min}$ ---factor of safety.

According to Mechanical Design Handbook, we find endurance limit for contact strength $\sigma_{H\lim}=1500MPa$; life factor $Z_N=0.8562$; hardness ratio factor $Z_W=1.1841$; factor of safety $S_{H\min}=1$

Then, compute the permitted contact fatigue stress

$$\sigma_{HP}=\frac{\sigma_{H\lim}}{S_{H\min}}Z_N Z_W=1521.11MPa>\sigma_1 \tag{19}$$

(ii) Second Stage

With a uniform power source (an electronic motor) and a uniform load(an output shaft),we find the application factor $K_{A2}=1.5$;we have the dynamic factor $K_{V2}=1.1$,and the load distribution factor $K_{\beta 2}=1.0$; the valve of load partition factor $K_{\beta 2}$ depend on the tooth width of gear b_2 and the pitch diameter $d_{1'}$.

$$K_{\beta 2}=0.99+0.31\times\left(\frac{b_2}{d_{1'}}\right)^2+0.00012\times b_2=1.35 \tag{20}$$

Then, compute the load factor

$$K_2=K_{A2}K_{V2}K_{\alpha 2}K_{\beta 2}=1.5\times 1.35\times 1.0\times 1.1=2.23 \tag{21}$$

According to Mechanical Design Handbook, we find node region coefficient $Z_{H1}=2.22$; elastic coefficient $Z_{E1}=189.98\sqrt{MPa}$, contact ratio coefficient $Z_{\varepsilon 1}=0.9491$.

So the contact fatigue stress

$$\sigma_{1'}=Z_{H2}Z_{E2}Z_{\varepsilon 2}\sqrt{\frac{2K_2T_2(u_2+1)}{b_2d_{1'}^2u_1}}=1584.67MPa \tag{22}$$

According to Mechanical Design Handbook, we find endurance limit for contact strength $\sigma_{H\lim}=1500MPa$; life factor $Z_N=0.9388$; hardness ratio factor $Z_W=1.1853$; factor of safety $S_{H\min}=1$.

Then, compute the permitted contact fatigue stress

$$\sigma_{HP} = \frac{\sigma_{H\lim}}{S_{H\min}} Z_N Z_W = 1669.14MPa > \sigma_{1'} \tag{23}$$

(b) Tooth bending strength fatigue stress

According to Mechanical Design Handbook, the coefficients above are selected respectively.

(i) First Stage

With a uniform power source (an electronic motor) and a uniform load (an output shaft), we find the application factor $K_{A1} = 1.5$; we have the dynamic factor $K_{V1} = 1.1$, and the load distribution factor $K_{\beta 1} = 1.0$; the valve of load partition factor $K_{\beta 1}$ depend on the tooth width of gear b and the pitch diameter d_1.

$$K_{\beta 1} = 0.99 + 0.31 \times \left(\frac{b}{d_1} \right)^2 + 0.00012 \times b = 1.54 \tag{24}$$

Then, compute the load factor

$$K_1 = K_{A1} K_{V1} K_{\alpha 1} K_{\beta 1} = 1.5 \times 1.5363 \times 1.0 \times 1.1 = 2.54 \tag{25}$$

According to Mechanical Design Handbook, we can find tooth form factor $Y_{Fa1} = 2.32, Y_{Fa2} = 2.29, Y_{Sa1} = 1.78, Y_{Sa1} = 1.74$, contact ratio coefficient $Y_{\varepsilon 1} = Y_{\varepsilon 2} = 1.09$.

So the bending fatigue stress

$$\begin{aligned} \sigma_{F1} &= \frac{2K_1 T_1}{b_1 d_1 m_1} Y_{Fa1} Y_{Sa1} Y_{\varepsilon 1} = 324.60MPa \\ \sigma_{F1'} &= \frac{2K_2 T_2}{b_2 d_{1'} m_2} Y_{Fa2} Y_{Sa2} Y_{\varepsilon 2} = 299.69MPa \end{aligned} \tag{26}$$

The permitted contact fatigue stress

$$\sigma_{FP} = \frac{\sigma_{F\lim}}{S_{F\min}} Y_N Y_{ST} \tag{27}$$

Where: $\sigma_{F\lim}$ --- endurance limit for bending strength; Y_N ---life factor for bending strength; Y_{ST} ---stress correction factor ,usually $Y_{ST}=2.0$; $S_{F\min}$ ---factor of safety for bending strength.

According to Mechanical Design Handbook, we find endurance limit for contact strength $\sigma_{F\lim 1}=\sigma_{F\lim 2}=460MPa$; life factor for bending strength $Y_{N1}=0.87, Y_{N2}=0.91$; factor of safety $S_{F\min}=1.6$.

Then, compute the permitted bending fatigue stress

$$\begin{aligned}\sigma_{FP1}&=\frac{\sigma_{F\lim 1}}{S_{F\min}}Y_{N1}Y_{ST}=499.39MPa>\sigma_{F1}\\ \sigma_{FP2}&=\frac{\sigma_{F\lim 2}}{S_{F\min}}Y_{N2}Y_{ST}=522.62MPa>\sigma_{F2}\end{aligned} \tag{28}$$

(ii) Second Stage

With a uniform power source (an electronic motor) and a uniform load(an output shaft),we find the application factor $K_{A2}=1.5$;we have the dynamic factor $K_{V2}=1.1$,and the load distribution factor $K_{\alpha 2}=1.0$; the valve of load partition factor $K_{\beta 2}$ depend on the tooth width of gear b_2 and the pitch diameter $d_{1'}$

$$K_{\beta 2}=0.99+0.31\times\left(\frac{b_2}{d_{1'}}\right)^2+0.00012\times b_2=1.35 \tag{29}$$

Then, compute the load factor

$$K_2=K_{A2}K_{V2}K_{\alpha 2}K_{\beta 2}=1.5\times 1.35\times 1.0\times 1.1=2.2275 \tag{30}$$

According to Mechanical Design Handbook, we can find tooth form factor $Y_{Fa1}=2.34, Y_{Fa2}=2.32, Y_{Sa1}=1.81, Y_{Sa1}=1.76$, contact ratio coefficient $Y_{\varepsilon 1}=Y_{\varepsilon 2}=1.29$ ..

So the bending fatigue stress

$$\begin{aligned}\sigma_{F1}&=\frac{2K_1T_1}{b_1d_1m_1}Y_{Fa1}Y_{Sa1}Y_{\varepsilon 1}=416.45MPa\\ \sigma_{F1'}&=\frac{2K_2T_2}{b_2d_{1'}m_2}Y_{Fa2}Y_{Sa2}Y_{\varepsilon 2}=397.31MPa\end{aligned} \tag{31}$$

According to Mechanical Design Handbook, we find endurance limit for contact strength $\sigma_{F\lim 1} = \sigma_{F\lim 2} = 460MPa$; life factor for bending strength $Y_{N1} = 0.91, Y_{N2} = 0.94$; factor of safety $S_{F\min} = 1.6$.

Then, compute the permitted contact fatigue stress

$$\begin{aligned} \sigma_{FP1} &= \frac{\sigma_{F\lim 1}}{S_{F\min}} Y_{N1} Y_{ST} = 521.58MPa > \sigma_{F1} \\ \sigma_{FP2} &= \frac{\sigma_{F\lim 2}}{S_{F\min}} Y_{N2} Y_{ST} = 539.06MPa > \sigma_{F2} \end{aligned} \tag{32}$$

5 Conclusion

Directed by theory of differential evolution algorithm the optimal design mathematical model of planetary gear train is established. This mathematical model with nine design variables and sixteen constraints conditions is a complex optimal design problem. When simulated in Mathmatica, minimal volume (also minimal weight) of the planetary gear train can be obtained, and optimal values of variables can be obtained too.

Then, we verify the optimal result using strength conditions in mechanisms and machine theory, including the contact fatigue stress and tooth bending strength fatigue stress. The verification infers that the optimization based on Mathmatica with differential evolution algorithm is effective and correct. The result of simulation shows that by using differential evolution algorithm, the weight of the planetary gear train can be reduced; the design quality and efficiency can be improved greatly. Differential evolution algorithm is a new method in solving the complex optimal design problem. The fundamental idea, simulation process and data-processing method of planetary gear train can be used for reference to other similar optimal design.

Acknowledgment. This research was supported by “the Fundamental Research Funds for the Central Universities”.

References

1. Xue, Y., Lv, G.M., Chen, S.: Optimum design of the planetary g ear box based on MATLAB. Construction Machinery (5) (2005)
2. Liu, L.M., Li, Y.X.: The optimization of planetary gear reducer based on Mathlab. Mechanical Engineer. (9) (2009)
3. Sun, Z.L., Li, C.: The research on Multi-objective reliability optimization method of planetary gear reducer. Machinery & Electronics (10) (2007)
4. Guan, H.J., Zhang, N.H., Liu, B.G.: The optimal design of three stage planetary gear reducer. Journal of Mechanical Transmission 32(3) (2008)

5. Zhu, H.L., Mao, Y., Zhu, B.S., Miao, W.M.: The minimum volume optimal design of planetary gear reducer in construction machinery and equipment. Construction Machinery and Equipment 40(11) (2009)
6. Shigley, J.E., Mischke, C.R., Budynas, R.G.: Mechanical Engineering Design, 7th edn. McGraw-Hill (2004)
7. Mott, R.L.: Machine elements in mechanical design. Prentice Hall, Inc. (2004)
8. Juvinall, R.C., Marshek, K.M.: Fundamentals of Machine Components Design, 3rd edn. John Wiely & Sons, Inc. (2000)
9. Smith, E.H.: Mechanical Engineer's Reference Book, 12th edn. Butterwort-Heinemann, Oxford (1998)
10. Spoots, M.F., Shoup, T.E.: Design of Machine Elements. Prentice-Hall, Inc. (1992)
11. Edwards Jr., K.S., Mckee, R.B.: Fundamentals of Machine Components Design. McGraw Hill (1991)
12. Norton, R.L.: Design of Machinery, An introduction to the synthesis and analysis of mechanisms and machines. McGraw Hill (1999)
13. Oberg, E., et al.: Machinery's Handbook, 25th edn. Industrial Press, New York (1996)
14. Ye, Z., Lan, Z., Smith, M.R.: Mechanism and Machine Theory, Beijing (2001)
15. Eckhardt, H.D.: Kinetic Design of Machines and Mechanisms. McGraw Hill (1998)
16. Erdman, A.G., Sandor, G.N., Kota, S.: Mechanism Design: Analysis and Synthesis. Prentice-Hall, Inc., New Jersey (1997)
17. Dimarogoneas, A.D.: Machine Design. John Wiley & Sons, Inc. (2001)
18. Mishra, S.K.: The nearest correlation matrix problem: Solution by differential evolution method of global optimization (2007)
19. `http://www1.icsi.berkeley.edu/~storn/code.html`

Mobi-CoSWAC: An Access Control Approach for Collaborative Scientific Workflow in Mobile Environment

Zhaocan Chen, Tun Lu, Tiejiang Liu, and Ning Gu

School of Computer Science, Fudan University
chenzhaocan@gmail.com, {lutun,liutiejiang,ninggu}@fudan.edu.cn

Abstract. With the development of mobile technology and popularity of pervasive applications, more and more scientific collaborative research works are carried out *in the wild* or *on the move*. How to make an optimal tradeoff between deep collaboration and strict access control in mobile environments is a challenging work. In this paper, we propose *Mobi-CoSWAC*, an access control approach for collaborative scientific workflow in mobile environments. In our approach, ranked access permissions will be provided to users for continuous collaboration in disconnected settings, as well as the owned access permissions can be dynamically assigned according to the role's evolution in various mobile contexts. The model and access control algorithms of *Mobi-CoSWAC* are elaborated and a prototype is implemented on Android mobile devices in collaborative proteomics research platform *CoPExplorer* to demonstrate its effectiveness.

Keywords: Role-based Access Control, Collaborative Scientific Workflow, Role Evolution, Mobile Environment.

1 Introduction

In the past decades, scientific workflow systems (e.g. Kepler, Taverna and Triana) have been critical infrastructure to fully support all scientific research phases, such as design, schedule, operation, monitoring, analysis and synthesis [1, 2]. With the quick development of mobile technology, more and more scientific research works are carried out in the wild or on the move, which are gradually facilitated by the advantages of mobile devices' portability, convenience and pervasiveness [3]. But mobile environment also brings instable network connection and high network latency problems, to alleviate which, data replication is always used to provide high local responsiveness and enhance scientific research throughout by introducing local replicas [4].

In the traditional scientific workflow, on the basis of users' different capabilities, responsibilities and domains, the administrator will assign them different roles to perform different tasks, and hence to ensure the complete, efficient, secure and collaborative completion of the scientific research. *Access control* (*AC*) is one of the

Q. Zu, B. Hu, and A. Elçi (Eds.): ICPCA-SWS 2012, LNCS 7719, pp. 137–149, 2013.

foundations and facilities underpins the scientific workflow system to specify and control at what time which roles have what permissions to access what data. *Role-based access control* (*RBAC*) [5, 6], *task-based access control* (*TBAC*) [7], *task and role-based access control* (*T-RBAC*) [8] and their extended models are developed for different scientific workflow systems. RBAC model is the most prevalent methodology for specifying and applying authorization policies. It has many advantages, such as least privileges, separation of duty and reducing the cost of administration. The concept of tasks was explicitly described in TBAC or T-RBAC model, where the notion of a lifecycle for an authorization-step is supported. Further, TBAC keeps track of the usage of permissions, thereby preventing the abuse of permissions through unnecessarily and malicious operations.

Though the mentioned AC models can partly reduce the administration's burden, however, collaborative scientific workflows in mobile environment challenge the access control in the following two aspects. 1) *More cooperative and dynamic access control policies*: Users cooperatively participate in various tasks and work of scientific workflows, where their states, tasks, environments and mobile devices change constantly. Accordingly, the user roles need to change continually according to the de facto situation, which needs a more flexible, dynamic access control policies. 2) *More responsive and automatic conflict resolution methods*. Instable mobile network connection may block users from any operations due to non-timely update of workflow states and access control policies. Therefore, the access control should support smooth scientific work experience when in disconnected occasions and automatic conflict resolution when network connection opportunity comes.

In this paper, based on the basic *CA-RBAC* model [9], we propose a novel access control approach for collaborative scientific workflow in mobile environment (*Mobi-CoSWAC*), where four types of *contexts* are introduced to address the above challenges. Its corresponding AC model supports *dynamic role evolution* and *virtual role prediction* in case of disconnected mobile network. Our initial rationales of virtual role are HBAC model [10-11] and SBAC model [14]. Virtual roles policy can remedy the shortcomings of traditional AC in mobile environment and enable users to concurrently perform tasks in real time with high responsiveness. As a concept-of-proof, *Mobi-CoSWAC* is implemented in our collaborative proteomics analysis platform- *CoPExplorer* [12], to demonstrate its efficiency and which result in good performance of our prototype and security guarantees.

The remainder of this paper is organized as follows: Section 2 gives a typical scenario of our research motivation. In Section 3, we present details of *Mobi-CoSWAC* model, followed by proposed algorithms in Section 4. We discuss the design and implementation issues in Section 5. Related work is surveyed in Section 6, and conclusion is drawn in Section 7.

2 Typical Scenario

In recent years, proteomics research [12] has achieved great development with workflow technology. A typical proteomics data analysis process and architecture is

described in Fig. 1. First, the administrator establishes a workflow instance, which consists of the tasks(T_1, T_2, T_3, T_4, T_5), and maps each task to appropriate services and resources by service discovery & matching. Replicas are created to achieve high responsiveness. For example, task T_1 takes services Ser_1, Ser_2 and resources Res_1, Res_2 to create a replica for task T_1. Next, the administrator assign task T_1 to users U_1, U_2, U_3 with specified role. Finally, users can download the corresponding replicas from the server to perform part or the whole task.

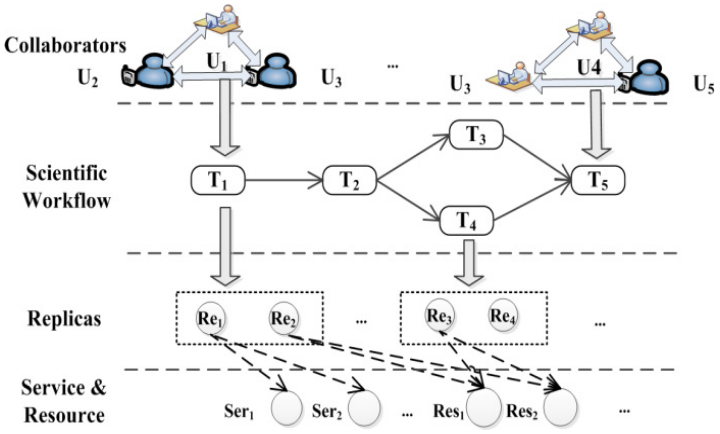

Fig. 1. A typical proteomic analysis workflow in mobile environments

Taking the task T_1 process as an example, its requirements are specified in mobile settings. Roles R_0, R_1, R_2, R_3 are associated with different permissions: role R_0 only has the basic rights to participate in task T_1; role R_1 can modify replicas; role R_2 can use (i.e. execute, abort, commit) the software (one type of replica); and role R_3 can submit task when finished. And their hierarchical relation is $R_0 \rightarrow R_1 \rightarrow R_2 \rightarrow R_3$. If contexts of the task or/and users change, user's role would be evolved automatically. For instance, the transition of $R_1 \rightarrow R_2$ need to be done at time node t_1, and user should fulfill 10 hours' participation. Only one user can be assigned to R_3 and execute software Ser_1 to complete task when lab's network is connected. When uses U_2, U_3 perform T_1 in mobile devices, they want to continuously modify Res_1 with high responsiveness even he cannot connect to the server.

From the above description, the research questions in this paper are summarized as follows:

- What kind of contexts in mobile collaborative scientific workflow should be specified?
- How to enable roles evolution in a flexible and dynamic way?
- How to associate activation of roles or permissions with rich contexts?
- How to address the access control and achieve final consistency of replicas in intermittent mobile network connections?

3 *Mobi-CoSWAC* Model for Collaborative Scientific Workflow in Mobile Environment

3.1 Collaborative Scientific Workflow in Mobile Environment

In mobile envrionments, due to the instability of network and the storage, computing and power limtations of mobile devices, scientific workflows' states and access control policies can not be acquired by the client timely. Therefore, replicas are usually introduted into the tasks to reach high responsiveness. In the following, we formally define the scientific workflow model and its basice elements:

Definition 3.1 [*Replica*] Replica Re is 2-tuple $\langle Obj, \langle op, Constraints \rangle \rangle$, where Obj is a service or a resource object; op is the operation set on the object; and $Constraints$ are operating conditions.

In our workflow model, operations include read-only, insert, delete, write (modify) and execute. $Constraints$ are defined as the maximum number of concurrent operation on the object or required resources.

Definition 3.2 [*Task*] Task T is defined as a 3-tuple $\langle Re_T, P_T, Id_T \rangle$, where Re_T is the replica set of services and resources; P_T represents set of permissions required to perform the task T; and Id_T is a identifier of task T in the workflow.

Definition 3.3 [*CoSW*]: Collaborative scientific workflow $CoSW$ is defined as $\langle T, \leq, TA \rangle$, where T is a task set to assemble a scientific workflow; $\leq$ specifies a partial order of T, namely $T_i \leq T_j$ $(i < j)$ means the task T_i was executed before T_j. Tasks T_i and T_j are parallel if and only if none of the relations ($T_i \leq T_j$ and $T_j \leq T_i$) exists.

3.2 Mobi-CoSWAC Model

Our basic *Mobi-CoSWAC* model for collaborative scientific workflow in mobile environments is composed of two parts as shown in Fig. 2.

The first part is contexts management of tasks, users, environment and interaction in collaborative scientific workflow, respectively denoted as TCM, UCM, ECM and ICM. TCM manages task-specific states, including the time nodes, replica context and other information. UCM manages the state of user's attributes and her/his history of participation. ECM manages current environmental state, including device attributes, time and location etc. ICM manage the information of user interaction with his collaborators. These contexts of awareness form the basis of our dynamic and flexible access control approach.

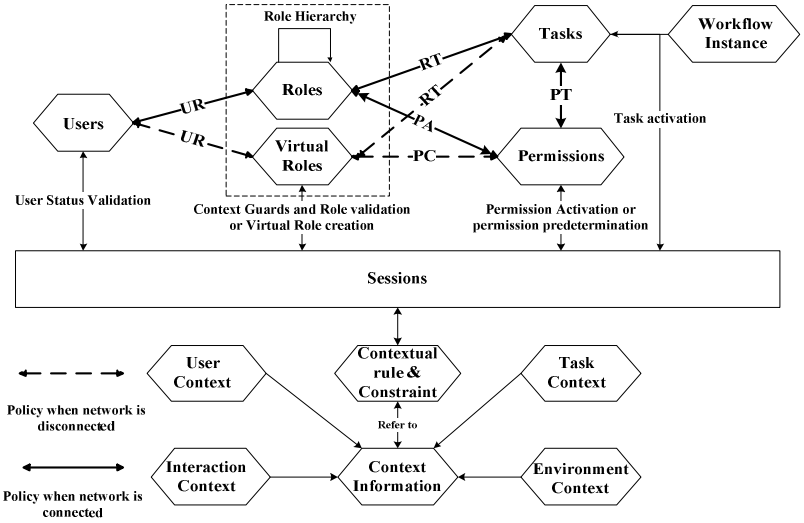

Fig. 2. Components and relations in *Mobi-CoSWAC* Model

The other part is access control policy based on the above contexts, mainly including evolution of roles, generation of virtual role, rules and constraints specification for above processes and activation roles or permissions. An administrator combines workflow contexts and user contexts to specify evolution rules. Therefore, permissions available to user would change with her/his roles evolution correspondingly. When the user participates in a task in network disconnected case, generation of virtual roles will assign user with some ranked permissions. Higher ranked permissions are more approximate to user's real permissions and its effects will be more likely to be admitted and submit to the server. The more contexts of interaction and participation are provided, the more accurate the prediction of virtual role is made. Further, activation of roles or permissions is also determined by rules specified with related contexts. Our model maintains context guards to guarantee the execution of context-based rules.

Definition 3.4 [*Mobi-CoSWAC Model*] *Mobi-CoSWAC* model's components and corresponding relations between them are defined as follows:

- $U(users)$, subjects who can perform tasks in scientific workflow;
- $R(roles)$, a set of user roles, including *role* in traditional *RBAC* and virtual *role* in our model;
- $T(tasks)$, a set of tasks in workflow;
- $P(permissions)$, a set of permissions, where permission is the right to perform an operation on one or more protected objects in the task (formally as $P = 2^{(OPS \times OBS)}$);

- $Op(p: P) \rightarrow \{op \subseteq OPS\}$, the permission-to-operation mapping granting the set of operations associated with permission p;
- $Ob(p: P) \rightarrow \{ob \subseteq OBS\}$, the permission-to-object mapping granting the set of objects associated with permission p, where Ob is equal to Obj described in *replica*;
- $CI(Context\ Information)$, a set of context information in collaborative scientific workflow, including user contexts, task contexts, environmental contexts and interaction contexts;
- $UC(User\ Context)$, a set of user contexts reflecting user's state;
- $TC(Task\ Context)$, a set of task contexts related to a collaborative scientific workflow instance;
- $EC(Environment\ Context)$, a set of environmental contexts reflecting the user's current research environment (e.g. location);
- $IC(interaction\ Context)$, a set user interaction contexts;
- $S(sessions)$, a set of sessions, where a role is assigned to a specific user when her/his context information CI satisfying the requirement of the role's activation;
- $UA \subseteq U \times R$, a many-to-many mapping of user-to-role assignment relation;
- $RT \subseteq R \times T$, a many-to-many mapping of role-to-task assignment relation;
- $PT \subseteq P \times T$, a many-to-many mapping of permission-to-task assignment relation;
- $PA \subseteq P \times R$, a many-to-many mapping of permission-to-role assignment relation;
- PC $\subseteq$ P $\times$ R, a many-to-many mapping of permission-to-virtual role assignment relation;
- $taskroles(t: T) \rightarrow 2^{ROLES}$, the roles that can perform the task t;
- $assigned\_permissions(r: ROLES) \rightarrow 2^{PERMS}$, the permission belongs to the role r, i.e. $assigned\_permissions(r) = \{p \in PRMS | (p, r) \in PA || (p, r) \in PC\}$;
- $CI \subseteq UC \times TC \times EC \times IC$, a many-to-many mapping among user context, task context, environmental context and interaction context;
- $user\_sessions(u: U) \rightarrow 2^{SESSIONS}$, the mapping of user u to a set of sessions;
- $session\_roles(s: S) \rightarrow 2^{R}$, the mapping of session s to a set of roles, i.e. $session\_roles(s_i) \subseteq \{r \in R \mid (session_{user(s_i)},\ r) \in UA\}$;
- $session_{tasks(s:S)} \rightarrow 2^{T}$, the mapping of session s onto a set of tasks, i.e. $session_{tasks(t_i)} \subseteq \{t \in T \mid (session\_roles(t_i)r) \in RT\}$
- $avail\_session\_permssions(s: S) \rightarrow 2^{p}$, the permissions available to a user in a session s, i.e. $\cup_{r \in session\_roles(s)}\ assigned\_permissions(r)$.

Definition 3.5 [*Rule*] In *Mobi-CoSWAC* model, $Rule$ is a 4-tuple $\langle r, c, t, p \rangle$, where $r \in R, c \in CI, p \in P$, $(r, t) \in RT$, and $(t, p) \in PT$.

For instance, $< R_3, (Network = connected\ \&\&\ Location = Lab), Task_1, Execute\ pFind\ on\ Server >$ means a user acted as role R_3 can make use of *pFind* software to execute task $Task_1$ when she/he is at lab and network is connected.

Definition 3.6 [*Constraint*] $Constraint$ is a 3-tuple $\langle s, c, x \rangle$, where s is the (constraint) scope, c is the constraint set and x is the context (taking one of the following values: *static* (s), *dynamic* (d) [13]).

For example, the constraint $\langle U, \langle taskroles(T_1), taskroles(T_2) \rangle, s \rangle$ is a static separation of *duty*, which requires that no user can be assigned to both roles in task T_1 and T_2.

Definition 3.7 [*PH*] *Participant History* (PH) is a 6-tuple $\langle u, f, re, c, tp, t \rangle$, describing that user u at the time t participate in the use of replica re on the workflow f for tp time when the context information c is satisfied.

Definition 3.8 [*CH*] *Contribute History* (CH) is a 5-tuple $\langle u, f, t, p, c \rangle$, which measures the contribution and participation of the user u in the task t of the workflow f.

In our model, contribution c is based on the evaluation of each user in the same task after the task completion, and its value will be normalized as a *real* in [0, 1] range.

Definition 3.9 [*IH*] *Interaction History* (PH) is a 6-tuple $\langle u_i, u_j, f, re, ts, t \rangle$ and can be interpreted as the user u_i interact with user u_j at the time t for p long time during the use of replica re on the workflow f and the context information c is satisfied.

4 Access Control Algorithms

In this section, related AC algorithms of *Mobi-CoSWAC* model, e.g. role & task detection, role evolution, virtual role generation & detection, rule & constraint detection, are proposed.

4.1 Role and Task Detection

After a workflow is established, the administrator assigns particular roles to users to enable performing the corresponding task. Since a user role in the task will evolve, so we need validate if all the reachable roles in the task could finish the task with minimum privileges. First, all reachable roles in the task are identified. Secondly, all required permissions in the task and available permissions of reachable roles are obtained. Finally, the completeness of permissions is checked by the subtraction of above two sets. The administrator can adjust assignments based on the checking results.

4.2 Role Evolution

A user role evolves continuously according to user's context and the related task context. The participation degree for user role evolution in current workflow should be

close to that of its average participation for the role evolution in history, which is measured by participation time. In addition, the more contribution a user makes, the faster a role evolves. Algorithm 1 and Algorithm 2 depicts the configuration of role evolution and the checking procedure of role evolution respectively. In Algorithm 1, RoleEvolutionAveTime returns user participation time of role evolution in research history, and AverageHistoryContribution obtains user average contribution. At running time, current task context TC and user context UC will be obtained for checking the rule of role evolution. As shown in Algorithm 2, the CheckCondition verifies if role evolution conditions hold or not to evolve or activate user current role.

```
Algorithm 1: UserRoleEvolutionConfig(task)
{
  Users ← TaskUsers(task)
  For each u in Users
{
    R_Time ← RoleEvolutionAveTime(u)
    C_Index ← AverageHistoryContribution(u)
    RealTime ← R_Time×(1-C_Index)
    Config(task,u,RealTime)// Configure each user's
participation time for evolution of her/his roles.
  }
}


Algorithm 2: CheckRoleEvolution(user,role,task)
{
    NewRole ← role
    RCI ← RoleEvolveContext(role,user)//obtain context
information for the evolution of user role.
    TC ← TaskContext(task)
    UC ← UserContext(user)
    Result ← CheckCondition(RCI,TC,UC)
    If(Result = true)//Assign new role to current user.
      NewRole ← RoleEvolution(user,role,RCI)
    Return NewRole
  }
```

4.3 Virtual Role Generation and Detection

Disruption in collaborative research will bring users uncomfortable interaction experiences, especially in disconnected network situation. Since a user role is similar to that of other participants with whom they often interacts with during execution of the

same task, one's permissions at current contexts can be predicted according to the operation history and interaction records.

Generation rules of user virtual roles should be configured first. It determines which collaborator's role is similar to current user role, and then configures the threshold of the interaction and participation time in the task. At running time, Algorithm 3 will generate a virtual role for users if network is disconnected. The permissions of virtual role consist of history permissions the user has used and the permissions ranked by his collaborators. *ConnectUsers* obtains the connected users in the current session, whose permission history will be used for prediction. If a connected user participates in the same replicas and interacts with a current user, their permissions will be added to ranked permissions *RankPerms*. Finally, the client generates virtual role with *RankPerms* and assigns it to current user automatically, and then user can perform appropriate operations. Once the network is reconnected, the server will check the conflicts between virtual roles and its actual user role, which validates and keeps the operations' effects.

```
Algorithm 3: UserVirtualRole(user,task)
{
  I_Time ← InteactiveTime(task)//obtain the interaction
time with collaborators, which is configured at the
beginning.
  P_Time ← ParticipationTime(task) //obtain the configured
participaion time in the task.
  Add HistoryPermssion(user) to RankPerms
  Users ← ConnectUsers(user,task)
  For each u in Users
{//get each connected user's permissions for prediction
    Perms ← PeerExcutePermissions(user,u,I_Time,P_Time)
    Time ← InteractiveTime(user,u)
    Rank ← UserRank(user,u)//relatiohship rank was
configured first, deciding whose role is similar to user.
    add <Perms,Time×Rank> to RankPerms
  }
  Sort(RankPerms)
  Return CreateVirtualRole(RankPerms)
  }
```

4.4 Rule and Constraint Detection

In an active session, the system will first obtain the constraints and rules related to the request, as well as context information (*CI*) of current user. Then, the rules and constraints will be checked according to *CI*. The checking result determines whether the corresponding permissions or roles are active or not.

4.5 Complexity Analysis of Algorithms

For the role evolution algorithm, if appropriate hash function is applied to context variables, the cost is $O(N_c + N_t + N_u)$, where N_c, N_t, N_u represent the number of context information, task contexts and user contexts, respectively. The cost of generating a virtual role is $O\left(N_{p1} + N_u \times N_{p2} \times N_t\right)$, where N_{p1}, N_u, N_{p2}, N_t represent the number of permissions used by a user, current connected partners, permissions used by its partners and their interaction, respectively. The cost of activation is $O\left(N_c \times (N_{uc} + N_{rc})\right)$, where N_c, N_{uc}, N_{rc} represent the number of rules and constraints, context information and contexts of each rule or constraint, respectively. Therefore, the cost for a user to obtain appropriate privileges is polynomial, which is acceptable for computing capacity of mobile devices.

5 The Design and Implementation of *Mobi-CoSWAC*

This section describes the system architecture (in Fig.3) and implementation (in Fig.4) of *Mobi-CoSWAC*.

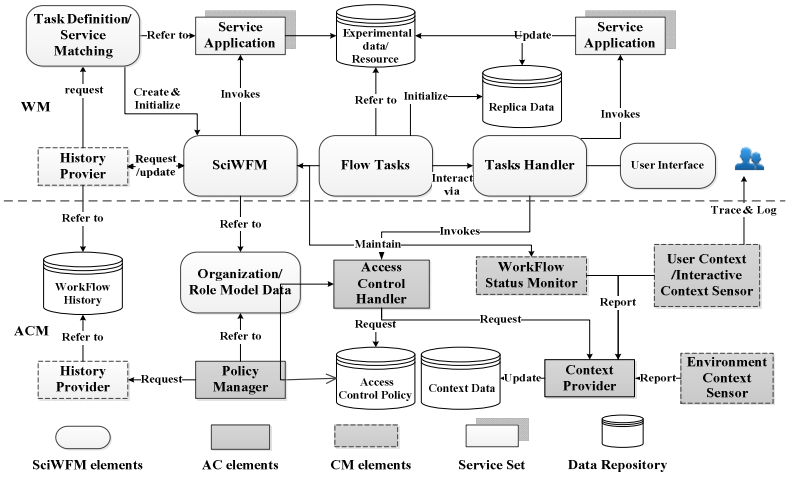

Fig. 3. Architecture for Implementation of *Mobi-CoSWAC*

The first part is the Workflow Management (*WM*) module. At the beginning, *WM* defines the scientific workflow and the relationship between tasks, thereafter maps services and resources to each task to instantiate the workflow and replicas. *WM* provides an interface, namely tasks handler, for researcher to participate in the task.

The second part is the Access Control Management (*ACM*) module (described in section 3.2). Context Provider (*CP*) is responsible for constructing and reasoning based on contexts, which translates low-level context information into high-level semantic context. Task handler makes decision based on Policy Manager (*PM*), followed by checking corresponding contexts of the rules and constraints.

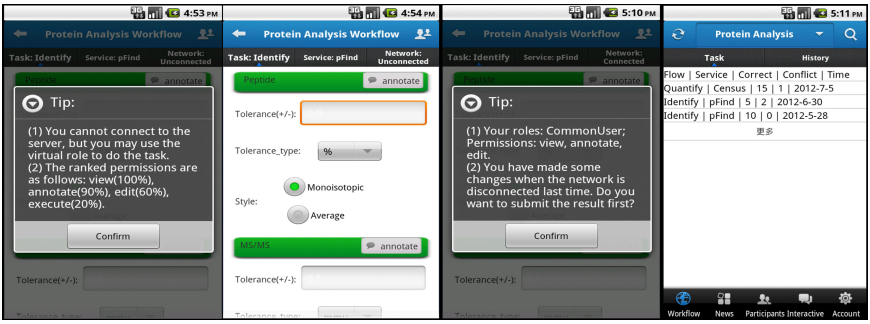

Step 1. Participating in the task when the client is not connected to the server. **Step 2. Performing the task via the virtual role.** **Step 3. Participating in the task when the network is reconnected.** **Step 4. Reviewing user's participation in the task history.**

Fig. 4. Participating in a workflow on mobile phones under different network conditions

We have applied *Mobi-CoSWAC* to our proteomics analysis workflow CoPExplorer [12] on mobile phone. After creating a workflow, the administrator first conducts access control management and configuration; and users participate in the task with the evolving roles in the mobile environment at run time. Fig. 4 depicts the process how users perform task under different network conditions.

6 Related Work

In pervasive computing environments, a number of spatial and location-aware access control models have been developed [15, 16, 17]. The concept of location in their models enables a flexible access control for mobile applications. However, more contexts for collaborative scientific workflow needed for consideration in mobile environments. We extend the *CA-RBAC* [9] model to meet the requirements of pervasive computing tasks in mobile scientific workflows. Similar with other context-aware models, rich context information will be reasoned to a high-level semantic data and integrated into access policies. But these models cannot be simply applied in our workflow model due to undefined collaborative contexts.

In order to integrate dynamic context during workflow execution, many new access control methods have been put forward. Some models, such as *RB-WAC* [18] and *AW-RBAC* [19], consider contexts of the workflow to improve the flexibility of access control strategy. The *RB-WAC* offers adaptive policies to deal with dynamic

contexts, while the *AW-RBAC* enables a priority concept to resolve the conflicts, resulting from new rules specified by the contexts. The *WCRBAC* model enables security administrator to configure authorization policy considering both security-related context information and the workflow-related data, as well as organization's structural information [20]. Wang et. al. combine teamwork with workflow information to define bridging entities and contribution property and proposed an Enhanced RBAC model[21]. However, these work did not take user interaction, request history and contribution information into consideration, which have important implications on the administration of access control policies in mobile environment.

7 Conclusion and Future Work

With the rapid development of mobile technology, scientists have gradually accommodated to carry out research activities in the wild. In order to adapt to dynamic changes in mobile collaborative scientific workflow, we propose MCA-RBAC model. It takes advantage of workflow history, current user status and environment information to achieve an automatic evolution of user roles in the mobile environment, as well as the generation of virtual roles. Our model guarantees security of workflow and reduces the overhead of administration, at the same time supports sustainable, collaborative, real-time and efficient scientific research even the network goes down. Our model will be more meaningful with upcoming tablet PCs, such as "Surface Pro", equipped with Windows 8 Pro operating system and Intel CPU. It will remedy some limitations in current mobile devices and the research environment in the wild much closer to the lab environment. In the future, we will incorporate privacy issues into our model that guarantees security on the premise of not violating user's privacy.

Acknowledgements. The work is supported by the National Natural Science Foundation of China (NSFC) under Grants No. 61272533 & No. 61233016, and the Shanghai Science & Technology Committee Key Fundamental Research Project under Grant No. 11JC1400800 and Soft Science Research Project under Grant No. 12dz1508600.

References

1. Deelman, et al.: Workflows and e-Science: An overview of workflow system features and capabilities. Future Generation Computer Systems 25(5), 528–540 (2009)
2. Goecks, J., Nekrutenko, A., Taylor, J.: Galaxy: a comprehensive approach for supporting accessible, reproducible, and transparent computational research in the life sciences. Genome. Biol. 11(8), R86 (2010)
3. Saito, Y., Shapiro, M.: Optimistic replication. ACM Computing Surveys (CSUR) 37(1), 42–81 (2005)

4. Alexander, M., Christiane, M., Manfred, T., Erika, R.: Mobile work efficiency: enhancing workflows with mobile devices. In: Proc. HCIMDS (2011)
5. Ferraiolo, D.F., Sandhu, R., et al.: Proposed NIST Standard for Role-Based Access Control. ACM Trans. Inf. Syst. Secur. 4(3), 222–274 (2001)
6. Bertino, E., Ferrari, E., Atluri, V.: The specification and enforcement of authorization constraints in workflow management systems. ACM Trans. Inf. Syst. Secur. 2(1), 65–104 (1999)
7. Thomas, R., Sandhu, R.: Task-based Authorization Controls (TBAC): A Family of Models for Active and Enterprise-oriented Authorization Management. Database Security 11, 166–181 (1998)
8. Oh, S., Park, S.: Task-role-based access control model. Information Systems 28(6), 533–562 (2003)
9. Kulkarni, D., Tripathi, A.: Context-aware role-based access control in pervasive computing systems. In: Proc. of SACMAT 2008, pp. 113–122 (2008)
10. Banerjee, A., Naumann, D.A.: History-Based Access Control and Secure Information Flow. In: Barthe, G., Burdy, L., Huisman, M., Lanet, J.-L., Muntean, T. (eds.) CASSIS 2004. LNCS, vol. 3362, pp. 27–48. Springer, Heidelberg (2005)
11. Abadi, M., Fournet, C.: Access control based on execution history. In: Proceedings of the 10th Annual Network and Distributed System Security Symposium, pp. 107–121 (2003)
12. Zhai, G., Lu, T., et al.: PWMDS: A system supporting provenance-based matching and discovery of workflows in proteomics data analysis. In: CSCWD 2012, pp. 456–463 (2012)
13. Crampton, J.: Specifying and enforcing constraints in role-based access control. In: Proc. of SACMAT 2003, pp. 43–50 (2003)
14. Barker, S., Sergot, M.J., Wijesekera, D.: Status-based access control. ACM Trans. Inf. Syst. Secur. 12(1), 1 (2008)
15. Hansen, F., Oleshchuk, V.: Spatial role-based access control model for wireless networks. In: Proc. of VTC 2003, vol. 3, pp. 2093–2097 (2003)
16. Kirkpatrick, M.S., Bertino, E.: Enforcing spatial constraints for mobile rbac systems. In: SACMAT 2010, pp. 99–108 (2010)
17. Cruz, I.F., Gjomemo, R., Lin, B., Orsini, M.: A location aware role and attribute based access control system. In: Proc. of GIS 2008, p. 84 (2008)
18. Hanane, E.-B., Hamid, H.: RB-WAC: New Approach for Access Control in Workflows. In: AICCSA, May 10-13, pp. 637–640 (2009)
19. Leitner, M., Rinderle-Ma, S., Mangler, J.: AW-RBAC: Access Control in Adaptive Workflow Systems. In: ARES, pp. 27–34 (2011)
20. Park, S.-H., Eom, J.-H., Chung, T.-M.: A Study on Access Control Model for Context-Aware Workflow. In: 2009 Fifth International Joint Conference on INC, IMS and IDC, August 25-27, pp. 1526–1531 (2009)
21. Le, X.H., Doll, T., Barbosu, M., Luque, A., Wang, D.: An Enhancement of the Role-Based Access Control Model to Facilitate Information Access Management in Context of Team Collaboration and Workflow. Biomedical Informatics (2012)

A Survey of Learning to Rank for Real-Time Twitter Search

Fuxing Cheng, Xin Zhang, Ben He, Tiejian Luo, and Wenjie Wang

[1] Information Dynamic and Engineering Applications Laboratory,
[2] Key Laboratory of Computional Geodynamics
University of Chinese Academy of Sciences
{chengfuxing07,zhangxin510}@mails.ucas.ac.cn,
{benhe,tjluo,wangwj}@ucas.ac.cn

Abstract. Recently learning to rank has been widely used in real-time Twitter Search by integrating various of evidence of relevance and recency features into together. In real-time Twitter search, whereby the information need of a user is represented by a query at a specific time, users are interested in fresh messages. In this paper, we introduce a new ranking strategy to rerank the tweets by incorporating multiple features. Besides, an empirical study of learning to rank for real-time Twitter search is conducted by adopting the state-of-the-art learning to rank approaches. Experiments on the standard TREC Tweets11 collection show that both the listwise and pairwise learning to rank methods outperform baselines, namely the content-based retrieval models.

Keywords: Learning to rank, twitter search, recency.

1 Introduction

Twitter, a popular microblogging platform, is attracting more and more people to capture the fresh events and other messages. That an overwhelming amount of updates are generated everyday leads to the difficulty for users who tend to interest in fresh news, to find the most relevant and recent messages.

There have been researches on achieving the real-time Twitter search by introducing time factor into the traditional content-based models [21,10].

Despite the improvement brought by these methods, multiple intrinsic features in social networks are unable to integrated into the models [19], such as authority, retweets, mentions and so on.

By combining various sources of evidence of relevance, learning to rank has been widely applied in Twitter search. Learning to rank, a family of learning approaches, aims at learning the ranking model automatically from a training dataset and it has been broadly used in information retrieval and machine learning. There are multiple intrinsic features of tweets, such as user authority, mentions, retweets, hashtags, etc. The application of learning to rank by incorporating diverse sources of evidence of recency and relevance has shown beneficial in previous studies, especially as demonstrated in the TREC 2011 Microblog

Q. Zu, B. Hu, and A. Elçi (Eds.): ICPCA-SWS 2012, LNCS 7719, pp. 150–164, 2013.

track [27]. Among the 59 participating research groups and organizations, Metzler and Cai use ListNet to combine the evidence from multiple features, where recency is represented by difference in time between the query's temporal point and tweet's timestamps [25]. Miyanishi et al. apply an unspecified learning to rank method by clustering the tweets retrieved for given topics [26]. Besides, Duan et al. employ RankSVM to rank the tweets which output the matched tweets based on their relevance to the query in content [8].

In this paper, we introduce a ranking strategy for the real-time Twitter search by incorporating diverse evidence into learning to rank algorithms.Paper [19] shows author authority plays an important role in Twitter search. According to this paper, we exploit features to indicate the influence of an author. Besides, we also introduce other evidence to represent the recency and content richness of the given tweet.

The major contributions of the paper are two-fold. First, we combine diverse sources of evidence into learning to rank, especially the author authority and recency evidence. Second, we carry out an empirical study of learning to rank for Twitter search by adopting the state-of-the-art pairwise and listwise algorithms. Extensive experiments on the standard TREC Tweets11 collection demonstrate the effectiveness by applying learning to rank.

The rest of the paper is organized as follows. In Section 2, we briefly survey the existing research on Twitter search and learning to rank. Sections 3 and 4 give a detail description about the algorithms applied during the learning process and the features exploited for the tweet representation, which is evaluated in Section 5. Finally, we conclude this research and suggest future research directions in Section 6.

2 Related Work

Real-time Twitter search is a service that returns real-time posts, links to images or videos fetched from the microblogging platform according to the user's information need which is represented by a query issued at a specific time. Thus freshness plays an important role in capturing the real-time messages. Twitter search engine ranks tweets according to the posting time of a tweet and the popularity of the topic that the tweet is talking about. However, this can not guarantee that the most interesting messages are top-ranked [8].

To achieve real-time Twitter search, some research extend the content-based weighting models to tackle this problem. Li and Croft incorporate the time factor into the classical language model. Instead of the uniform document prior distribution, a conditional probability is assumed by taking the publishing time of the document into consideration [21]. Efron and Golovchinksy propose to maximize the posterior estimation in the query likelihood model by integrating the issuing time of the top-ranked documents to improve the rate parameter of the assumed exponential distribution of the document's existing life [10]. Similarly, Efron and Golovchinksy introduce a temporal factor into pseudo-relevance feedback. Thus, the smoothing of the document generation probability is biased towards the

document's timestamps, and consequently, feedback terms in the recent documents are favored [10].

Despite the improvement over the classical content-based weighting models, the above described approaches ignore the many aspects and characteristics of the social features in microblogging services [19,5,8]. For example, the authoritative features, indicating a user's influence on others, may have significant impact on relevance; the temporal features, indicating whether the tweet is timely to a given query topic, is important in real-time Twitter search. Besides, Twitter has its unique characteristics, such as mentions, retweets and hashtags. All these characteristics and aspects have their potential influence on the relevance of the tweets. However, using the traditional Twitter search approaches, it is rather difficult to properly integrate the variety of features into the retrieval model.

Recently, there have been research in applying learning to rank (LTR) approaches for real-time Twitter search for its advantage in combining different features to automatically learn a ranking model from the training data.

Learning to rank, is a family of methods and algorithms, in which machine learning algorithms are used to learn this ranking function. A typical setting in learning to rank is that feature vectors describing a query-document pair are constructed and relevance judgments of the documents to the query are available. A ranking function is learned based on this training data, and then applied to the test data.One of the major advantages of LTR is its flexibility in incorporating diverse sources of evidence into the process of retrieval [23]. Categorized by the input representation and loss function, there are in general three types of LTR algorithms, namely the pointwise, pairwise, and listwise approaches. Empirical results suggest that the latter two approaches usually outperform the former [17,40,36]. The main difference between the pairwise and listwise approaches are the training instances and the loss functions [23]. In the pairwise approach, it takes the object pair as instances in learning; in contrast, the document lists rather than the document pairs is taken as the learning instances in the listwise approach. The objective of the pairwise learning is to minimize the errors of disclassification of the document pairs, while in the listwise approach, the objective is the optimization of the ranking list using any metric between the probability distributions as the loss function.

In this paper, we apply two state-of-the-art LTR approaches, including the pairwise Ranking SVM (RankSVM) approach [17], and the recent listwise approaches, LambdaMART [36].

RankSVM is one of the most popular pairwise methods, which improves the traditional formulation of the SVM optimization problem, namely exhibiting a different form of sparsity. Rather than taking pair instances during the training process, list instances are handled to learn a ranking model of the listwise approaches. Among the many listwise algorithms proposed in literature, ListNet [40] and LambdaMART [36,13] are two popular approaches.

There have been efforts in applying learning to rank for real-time Twitter search, especially as demonstrated in the TREC 2011 Microblog track [27]. Metzler and Cai use ListNet to combine the evidence from multiple features, where

recency is represented by difference in time between the query's temporal point and tweet's timestamps [25]. Miyanishi et al. apply an unspecified learning to rank method by clustering the tweets retrieved for given topics [26].

In addition to the above described approaches in the Microblog track. Hong et al. propose to apply affinity propagation, a non parametric clustering algorithm, to cluster the initial ranked list of tweets [15]. Li et al. apply the Word Activation Force algorithm and Term Similarity Metric algorithms to mine the connection between the expansion terms and the given topic [22]. Louvan et al. apply query expansion from dataset with different weighting schemes and then incorporate timestamps of the tweets for real-time search [24]. We refer to [27] for an overview of all the other techniques and approaches evaluated in Microblog track 2011.

In this paper, we conduct an empirical study of learning to rank for real-time Twitter search by integrating diverse sources of evidence of recency and relevance into both the pairwise and listwise approaches.

3 Learning to Rank for Twitter Search

Section 3.1 introduces the types of features that are used to represent the given tweet, which are described in detail in Section 4; Section 3.2 represents the algorithms which are used in our learning to rank algorithms. Section 3.3 introduces the labeling strategy for facilitating learning to rank.

3.1 Feature Extraction for Tweets Ranking

It is significantly important to select the feature set to represent the given tweet during the learning to rank process. In this paper, we exploit five types of features to develop the ranking strategies to rerank the tweets. Our features are organized around the basic entities for each query-tweet tuple to distinguish between the relevant and irrelevant messages, some of which have been widely used in previous work on Twitter search [8,26,25]. Table 2 presents all the features exploited in this paper. More specifically, five types of features are defined as follows.

- **Content-based relevance** is the content-based relevance score.
- **Content richness** indicates how informative a tweet is.
- **Recency** refers to those features that indicate the temporal relationships between the query's submitted time and the tweet's posted time.
- **Authority** measures the influences of the author's tweets to others.
- **Tweet specific** features are those specific to given tweets, like RT, mentions and hashtags.

3.2 Learning to Rank Algorithms

Many learning to rank approaches have been proposed in the literature [23], which can be applied for learning the ranking model. Among them, in this paper, we choose to use two popular learning to rank algorithms, namely RankSVM

Table 1. Target values used for learning a ranking model

Target value.	Temporal distance (days)
4	0
3	1-5
2	6-10
1	others

[17] and LambdaMART [36,13]. RankSVM [17] is a classical pairwise learning to rank approach, which adopts the traditional formulation of the SVM optimization problem by taking the document pairs and their preferences as the learning instances. LambdaMART [36,13] is a state-of-the-art listwise learning to rank approach. Instead of learning from pairwise instances, LambdaMART integrates also the evaluation result of the list instances into its loss function. LambdaMART is a combination of the ranking model LambdaRank with the boosted tree optimization method MART and it has shown to be a robust algorithm for solving real world ranking problems. For example, an ensemble of the LambdaMART rankers achieved the top runs in the recent Yahoo! Learning To Rank Challenge [6].

3.3 Tweet Labeling

In the learning process, after the positive and negative examples are appended to the labeled set by making use of the relevance assessments information, we empirically assign preference values according to the temporal distance between the timestamps of the tweet and the query. The larger the preference value is, the higher the tweet is relevant to the given query. This labeling strategy is mainly due to the fact that recency is a crucial factor of relevance in real-time Twitter search. The fresh tweets are favored over those outdated.

The target values of RankSVM define the order of the examples of each query. We arbitrarily reassign the target values of the relevant tweets with an interval of 1, as shown in Table 1, according to the temporal distance in days between the timestamps of the tweet and the query.

Similar to the labeling for RankSVM, the target values of training data in LambdaMART define the relevance degree of the tweet to the given query, in association to the temporal factor. In this paper we use the same target values for LambdaMART.

4 Feature Description

In this section, we will give a detailed description about the five types of features used in learning to rank approaches, including content-based relevance features (Section 4.1), content richness features (Section 4.2), recency features (Section 4.3), authority features (Section 4.4) and Twitter specific features (Section 4.5).

Table 2. Features extracted for the tweet representation

Feature Type	Feature Name	Description
Content-based	BM25	relevance score given by BM25
	PL2	relevance score given by PL2
	DirKL	relevance score given by the KL-divergence language model with Dirichlet smoothing
	KLIM	scores applying the KLIM model
	BM25QE	relevance score given by query expansion on top of BM25
	PL2QE	relevance score given by query expansion on top of PL2
	DirKLQE	relevance score given by query expansion on top of DirKL
	KLIMQE	relevance score given by query expansion on top of KLIM
Content richness	Content Length	the length of a tweet in words
	URL [8]	whether the tweet contains URL
	OOV [8]	the ratio of the unique words in the tweet
	RTRATIO	the ratio of appended comments after retweet
Authority	Global RT Count	the number of the retweets given an author, no matter what topic the author is talking about
	Number of tweets	the number of the tweets the author has posted
Recency	DAY_QUERY_DIF [25]	difference in days between the time of the query's issuing and the tweet's posted time
	DAY_BURST_DIF	differences in days between the burst time of an event and a tweet's posted time
	Ratio_DAY_QUERY_DIF	the ratio of DAY_QUERY_DIF of a given tweet in a day
	Ratio_DAY_BURST_DIF	the ratio of DAY_BURST_DIF of a given tweet in a day
Sentiment	Ratio_Positive_Sentiment	the ratio of positive sentiment words in the tweet
	Ratio_Negative_Sentiment	the ratio of negative sentiment words in the tweet
Tweet specific	BEGIN RT	whether the tweet begins with a RT tag
	CONTAIN RT	whether the tweet is retweeted with appended comments
	BEGIN AT [8]	whether the tweet is a replied tweet, i.e. beginning with an @
	AT COUNT	how many users are mentioned in the tweet with an @
	English?	whether the tweet is written in English

4.1 Content-Based Relevance Features

Four popular content-based retrieval models and their corresponding query expansion or pseudo relevance feedback methods are applied in this paper.

BM25 is a classical probabilistic model based on the two-Poisson assumption [29]. On top of BM25, *BM25QE* applies a query expansion mechanism [37] derived from Rocchio's relevance feedback algorithm [30].

PL2 is derived from the divergence from randomness (DFR) framework. It is based on the Poisson approximation for the term frequency distribution and Laplace succession for the aftereffect with a term frequency normalization component [2]. On top of PL2, the Bo1 query expansion model is applied to yield the relevance score of *PL2QE* [2].

DirKL is the KL-divergence language model with Dirichlet smoothing [38]. The RM3 pseudo-relevance feedback method [20] is applied to produce the relevance score *DirKLQE*.

KLIM is parameter-free model derived a Kullback-Leibler based product of information measures. In combination with the Bo1 query expansion model, *KLIMQE* achieves one of the top runs in the Microblog track 2011 [3].

The parameters in the above content-based models are optimized using Simulated Annealing [18] on the Blogs06 collection, which is a median crawl of blog posts and feeds used by the TREC Blog track 2006-2008 [28]. The choice of the

collection for the parameter tuning is mainly due to the intuition that the blog posts to some extent share the characteristics of the online social media with the tweets, although the difference between the two, especially in length, is apparent.

4.2 Content Richness Features

It is believed that more information a tweet conveys, more interested a user will be in the tweet. Twitter is a bench where every registered user can post messages. However, the messages generated by different users may vary in different quality. We regard that the lower quality the content is , the less valuable information the tweet conveys. Thus, we exploit several features to measure the content quality. *Content Length*: Intuitively, the longer the tweet, the more information the tweet may convey.

URL : As each tweet has the a maximum limit of 140 characters, extra details have to be expressed via redirects. A tweet containing URL may convey more information, and is therefore more valuable.

OOV : The ratio of unique words in the given tweet indicates the quality of its content. Intuitively, the higher the value of OOV, the better quality the tweet is.

RTRATIO: Retweet is a unique characteristic of Twitter. In some cases, people just retweet their interested tweets without any comments. Retweets with appended comments may convey extra information.

4.3 Recency Features

Messages on Twitter regarding a sudden event tend to exhibit a burst period within given hours or days. We hypothesize that the tweets posted in those burst periods are likely to be relevant. We also hypothesize that, the more recent the tweet is, the more likely it is relevant. Description of the recency features are listed in Table 2. In particular, *Ratio_DAY_QUERY_DIF* is computed as follows:

$$Ratio\_DAY\_QUERY\_DIF = \frac{DAY\_QUERY\_DIF}{\sum_{day} DAY\_QUERY\_DIF}$$

where the denominator is the sum of *DAY_QUERY_DIF* of the retrieved tweets posted in the same day with the given tweet.

Ratio_DAY_BURST_DIF is computed in a similar way:

$$Ratio\_DAY\_BURST\_DIF = \frac{DAY\_BURST\_DIF}{\sum_{day}(DAY\_BURST\_DIF)}$$

where the denominator is the sum of *DAY_BURST_DIF* of the retrieved tweets posted in the same day with the given tweet.

4.4 Authority Features

Intuitively, users who have posted more tweets and whose tweets have been retweeted, are infulential, namely authoritative.

We simply use the number of retweets an author receives and the number of tweets an author has posts.

4.5 Twitter Specific Features

If a tweet is retweeted or replied to someone [8], then the tweet may be more valuable than others. The five tweet specific features extracted are detailed in Table 2. All the features are binary values.

BEGIN RT: whether the tweet is retweeted.
CONTAIN RT: we believe that if a tweet is retweeted with appended comments, it may be more informative.
BEGIN AT: A tweet begins with an @ and a twitter account is regarded as a reply tweet, which is denoted as 1.
AT COUNT: the number of mentions in a tweet.
English ?: the language a tweet uses. For the language filter, the LC4j package is used to detect whether a tweet is English or not. It is a language categorization library designed for the Java programming language. It has been designed to be a compact, fast and scalable Java library that implements the algorithms to identify languages using n-grams [43]. In our runs, the detected non-English tweets are removed.

5 Experiments

5.1 gives an introduction to the dataset and preprocessing of Tweets11. 5.3 describes how to obtain the optimized parameters for RankSVM and LambdaMART which are used in the learning stage. 5.4 introduces the three levels of evaluating our proposed methods.

5.1 Dataset and Indexing

We experiment on the Tweets11 collection, which consists of a sample of tweets over a period of about 2 weeks spanning from January 24, 2011 to February 8, 2011 [27]. In the TREC 2011 Microblog track, this collection is used for evaluating the participating real-time Twitter search systems over 50 official topics. Participants are required to download the tweets from Twitter.com using the feeds distributed by the track organizers. Our crawl of the Tweets11 collection consists of 13,401,964 successfully downloaded unique tweets. Note that because of the dynamic nature of Twitter, there is a discrepancy between the number of tweets in our crawl and the figures reported by other participants in the Microblog track 2011. This does not affect the validity of the conclusions drawn from our experiments as the proposed approach and the baselines are evaluated on the same dataset with consistent settings. Standard stopword removal and Porter's stemmer are applied during indexing and retrieval. The official measure in the TREC 2011 Microblog Track, namely precision at 30 (P30), is used as the evaluation metric in our experiments. All of the indexing and retrieval experiments are conducted on the open source platform, namely Terrier [1].

5.2 Pre-processing and Indexing

The corpora used in our experiments is in the format of HTML. Before further using it, we first convert the corpora to the TREC format. In particular, in TREC-formatted files, documents are delimited by<DOC></DOC> tags, as in the following example:

<DOC>
<DOCNO> 28968126875963392 <DOCNO>
<AUTHOR> TonyFranceOH </AUTHOR>
<TIME> Sun Jan 23 00:11:54 +0000 2011 </TIME>
<AT> </AT>
<BODY> Oh, my GOD </BODY>
<RTAT> </RTAT>
<RT> if today was a boring slop day </RT>
</DOC>

In the above example, DOCNO is the tweet id; AUTHOR is the author of the tweet; TIME is the posted time of the tweet; AT contains all the mentioned users in the tweet, except those occurring in RT tweet; RT is the reposted tweet; RTAT indicates the author from which the tweet is retweeted; BODY means the remaining tweet content after removing AT, RTAT, RT.

In our experiments, we build the index using Terrier, version 3.5 [42]. Both direct index and inverted index are built to support retrieval and query expansion. Standard stopword removal and Porter's stemmer are applied.

5.3 Parameter Tuning

The choice of the hyperparameter C, the regularization parameter for RankSVM, plays an important role in the retrieval performance. C can be selected by carrying out cross-validation experiments through a grid search from 1 to 40 on the training queries.

The LambdaMART algorithm has five parameters that need to be tuned to achieve the best results: "Max number of leaves", "Min percentage of observations per leaf", "Learning rate", "Sub-sampling rate" and "Feature sampling rate". We apply a greedy boosting algorithm for the parameter tuning, as described in Figure 1. Firstly, we optimize each of the five parameters, while keeping the other four parameters to the default values. Then, we set the parameter that has the highest optimized retrieval performance to its optimized value. This process repeats until all the parameters are optimized. We apply grid search to optimize each parameter. Values we scan for each of the parameters are listed in Table 3.

5.4 Evaluation Design

The aim of our experiments is to evaluate the effectiveness of learning to rank methods based on pairwise and listwise ranking functions which incorporating

Input
P={P1, P2, P3, P4, P5}: the 5 parameters

Output
V={V1, V2, V3, V4, V5}: the optimized parameter values

Method
1. Set each parameter to be the default value
2. For each unoptimized parameter pi, optimize Pi and keep the other parameters unchanged
3. Select the parameter Pi and its value Vi that obtains the best retrieval effectiveness
4. Set the value of Pi to Vi
5. For the remaining parameters, repeat steps 2-4 until all the parameters are optimized

Fig. 1. The greedy boosting algorithm for the parameter tuning of LambdaMART

Table 3. Values used in grid search for LambdaMART parameter tuning

Parameter.	Values
Max Number of Leaves	2, 3, 5, 7, 10
Min Percentage of Obs. per Leaf	0.05, 0.12, 0.15, 0.75
Learning rate	0.01, 0.04, 0.045, 0.05, 0.07, 0.2
Sub-sampling rate	0.05, 0.1, 0.3, 0.5, 0.7, 1
Feature Sampling rate	0.1, 0.3, 0.5, 0.7, 1

diverse evidence of relevance and recency. In particular, two state-of-the-art learning to rank approaches, namely Ranking SVM (RankSVM) [17], a classical pairwise learning to rank algorithm and LambdaMART [36], a tree-based listwise learning to rank algorithm which has the best performance in the 2010 Yahoo! Learning to Rank challenge, are applied. Our proposed combined learning to rank framework is evaluated at two different levels as follows.

1. Comparison to the content-based retrieval models with query expansion. Four popular weighting models, including BM25 [29], PL2 [2], the KL-divergence language model with Dirichlet smoothing [38] and KLIM [3], with their corresponding query expansion or pseudo relevance feedback mechanisms [37,2,20,3] are used as the baselines. In particular, KLIM with query expansion (KLIMQE) is a strong baseline that provides one of the top runs in the TREC 2011 Microblog track [3]. Indeed, latter in the next section, our proposed approach is only compared to KLIMQE as it turns out to have the best retrieval performance among all four content-based baselines. In our experiments, we adopt the recommended query expansion setting in [3] by adding 10 expansion terms from the top-30 tweets to the original query.

   We examine if learning to rank algorithm (**LTR**) is able to improve the retrieval effectiveness over the classical content-based weighting models. At this stage, different granularities of cross-validation experiments are conducted, namely the 2-fold (**LTR_2**), 5-fold (**LTR_5**) and 10-fold (**LTR_10**)

Table 4. Results obtained by four baseline content-based models with query expansion

	BM25QE	PL2QE	DirKLQE	KLIMQE
P30	0.3429	0.3537	0.3571	**0.3782**

Table 5. Comparison of the learning to rank approaches with the KLIMQE baseline

RankSVM			
KLIMQE	LTR_10	LTR_5	LTR_2
0.3782	**0.4061, 7.38%**∗	**0.3980, 5.24%**∗	0.3823, 1.08%
LambdaMART			
KLIMQE	LTR_10	LTR_5	LTR_2
0.3782	0.3864, 2.17%	0.3837, 1.45%	0.3925, 3.78%

cross-validation, respectively. The training and test queries are partitioned by the order of the topic numbers of the 50 official queries of the TREC 2011 Microblog track.

2. Comparing the pairwise learning to rank approach to the listwise LTR method.

   In our experiments, both RankSVM and LambdaMART, based on pairwise and listwise respectively, are adopted as the ranking functions, where the ranking models are learned from the official relevance assessments from the Microblog track 2011, since they represent the conventional application of the state-of-the-art learning to rank algorithms. Extensive experiments are conducted to examine the effectiveness of the learning to rank algorithms adopting different ranking functions.

5.5 Results and Discussion

We firstly compare different learning to rank algorithms to the content-based retrieval models with query expansion. Table 4 outlines the precisions at 30 given by the four baselines. As shown in this Table, KLIMQE turns out to have the best effectiveness over other baselines. This observation is consistent with the experimental results reported in the TREC 2011 Microblog track, where KLIMQE provides one of the best runs among all participants [27].

Figures 2 and 3 plot the retrieval effectiveness of the pairwise and listwise learning to rank algorithms, respectively. As shown by the figures, we can see that the results obtained by applying LTR is better than the content-based models, no matter what kinds of learning to rank algorithm is applied. The results obtained by applying different learning to rank approaches are shown in Table 5. In all the following tables, a $*$ indicates a significant improvement over the baseline according to the matched-pairs signed-rank test at the 0.05 level. For example, in Table 5, LTR_5 adopting RankSVM as the learning algorithm, leads to a statistically significant difference over KLIMQE, which has the best retrieval performance among the four content-based baselines. As shown by the results, LTR_5 and LTR_10 using RankSVM lead to significant improvement over the baseline. On the other hand, while applying LambdaMART as the learning

Table 6. Comparison of the pairwise learning to rank approach with the listwise approach

2-fold	
LambdaMART	RankSVM
0.3925	0.3823, -2.60%
5-fold	
LambdaMART	RankSVM
0.3837	**0.3980,+3.73%**
10-fold	
LambdaMART	RankSVM
0.3864	**0.4061,+5.10%**

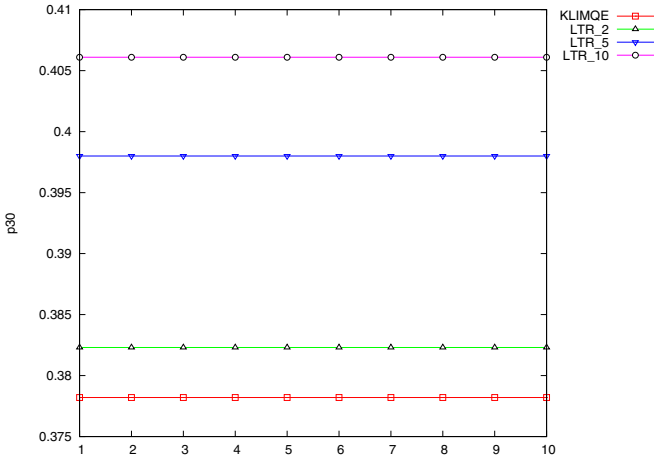

Fig. 2. Comparision of LTR using RankSVM with KLIMQE baseline

algorithm, no significant improvement is observed on all the cross-validation experiments.

From Table 6, we also notice that the retrieval results obtained using RankSVM is better than using LambdaMART as the LTR algorithm, in most cases. We analyze that it is the target values we used in the learning process, that leads to no significant improvement while applying the listwise approach.

One of the major contributions of this paper is an exploration of a variety of features. Finally, Table 7 lists the important features that affect the most on the retrieval performance in the experiments. We can see that recency and Twitter specific play the most important role in learning an effective ranking model. The content richness and content-based relevance are the next to affect the effectiveness.

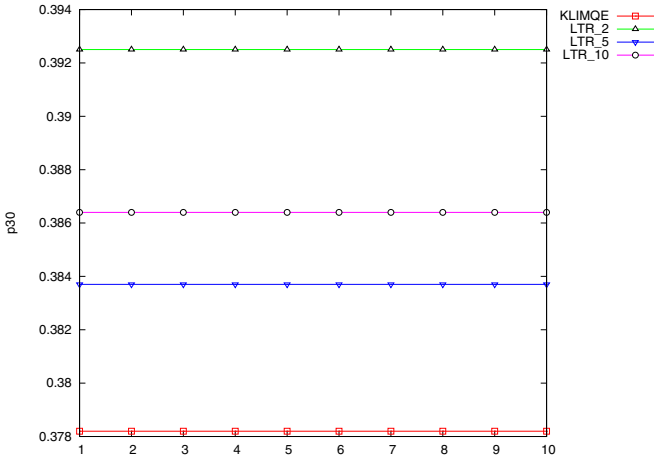

Fig. 3. Comparision of LTR using LambdaMART with KLIMQE baseline

Table 7. List of the top features sorted by their importance

Feature name	Type
Ratio_DAY_QUERY_DIF	Recency
BEGIN RT	Twitter specific
OOV	Content richness
Ratio_DAY_BURST_DIF	Recency
RTRATIO	Content richness
DirKL	Content-based relevance

6 Conclusion and Future Work

In this paper, we rerank the tweets utilizing a ranking strategy which combines diverse sources of evidence into together, including content-based relevance, content richness, authority, recency and Twitter specific features. In particular, two of the state-of-the-art learning to rank approaches, namely RankSVM and LambdaMART, are adopted to achieve real-time Twitter search, where the ranking function is learned from the relevance assessment information. Extensive experiments have been conducted on the standard Tweets11 dataset to evaluate the effectiveness of our proposed approach. Results show that the learning to rank approach is able to outperform strong baselines, namely the KLIM model with query expansion, which is one of the top runs in the TREC 2011 Microblog track, and the state-of-the-art learning to rank algorithms. Moreover, our study in this paper suggests the ranking strategy plays an important role while utilizing learning to rank algorithm.

In future, we plan to make a complete investigation on the target values used both in the pairwise and listwise methods, which we believe are able to affect the retrieval effectiveness in some extent.

References

1. Ounis, I., Amati, G., Plachouras, V., He, B., Macdonald, C.: Terrier: A high performance and scalable information retrieval platform. In: SIGIR OSIR (2006)
2. Amati, G.: Probabilistic models for information retrieval based on divergence from randomness. PhD thesis, DCS, University of Glasgow (2003)
3. Amati, G., Amodeo, G., Bianchi, M., Celi, A., Nicola, C.D., Flammini, M., Gaibisso, C., Gambosi, G., Marcone, G.: Fub, iasi-cnr, UNIVAQ at TREC 2011. In: TREC (2011)
4. Blum, A., Mitchell, T.M.: Combining labeled and unlabeled data with co-training. In: COLT, pp. 92–100 (1998)
5. Cha, M., Haddadi, H., Benevenuto, F., Gummadi, K.P.: Measuring user influence in twitter: The million follower fallacy. In: ICWSM (2010)
6. Chapelle, O., Yang, Y.: Yahoo! Learning to Rank Challenge Overview. In: JMLR (2011)
7. Dong, A., Chang, Y., Zheng, Z., Mishne, G., Bai, J., Zhang, R., Buchner, K., Liao, C., Diaz, F.: Towards recency ranking in web search. In: WSDM, pp. 11–20 (2010)
8. Duan, Y., Jiang, L., Qin, T., Zhou, M., Shum, H.-Y.: An empirical study on learning to rank of tweets. In: COLING, pp. 295–303. Tsinghua University, Beijing (2010)
9. Duh, K., Kirchhoff, K.: Learning to rank with partially-labeled data. In: SIGIR, pp. 251–258 (2008)
10. Efron, M., Golovchinksy, G.: Estimation methods for ranking recent information. In: SIGIR, pp. 495–504 (2011)
11. El-Yaniv, R., Pechyony, D.: Stable Transductive Learning. In: Lugosi, G., Simon, H.U. (eds.) COLT 2006. LNCS (LNAI), vol. 4005, pp. 35–49. Springer, Heidelberg (2006)
12. Esuli, A., Sebastiani, F.: Sentiwordnet: A publicly available lexical resource for opinion mining. In: LREC, pp. 417–422 (2006)
13. Ganjisaffar, Y., Caruana, R., Lope, C.: Bagging gradient-boosted trees for high precision, low variance ranking models. In: SIGIR, pp. 85–94 (2011)
14. Geng, X., Liu, T.-Y., Qin, T., Arnold, A., Li, H., Shum, H.-Y.: Query dependent ranking using k-nearest neighbor. In: SIGIR, pp. 115–122 (2008)
15. Hong, D., Wang, Q., Zhang, D., Si, L.: Query expansion and message-passing algorithms for TREC microblog track. In: TREC (2011)
16. Huang, X., Huang, Y., Wen, M., An, A., Liu, Y., Poon, J.: Applying data mining to pseudo-relevance feedback for high performance text retrieval. In: ICDM, pp. 295–306 (2006)
17. Joachims, T.: Optimizing search engines using clickthrough data. In: KDD, pp. 133–142 (2002)
18. Kirkpatrick, S., Gelatt, C., Vecchi, M.: Optimization by simulated annealing. Science 220(4598) (1983)
19. Kwak, H., Lee, C., Park, H., Moon, S.: What is Twitter, a social network or a news media? In: WWW, pp. 591–600 (2010)
20. Lavrenko, V., Croft, W.B.: Relevance-based language models. In: SIGIR, pp. 120–127 (2001)
21. Li, X., Croft, W.B.: Time-based language models. In: CIKM, pp. 469–475 (2003)
22. Li, Y., Zhang, Z., Lv, W., Xie, Q., Lin, Y., Xu, R., Xu, W., Chen, G., Guo, J.: PRIS at TREC 2011 microblog track. In: TREC (2011)
23. Liu, T.: Learning to rank for information retrieval. Foundations and Trends in Information Retrieval (3), 225–331 (2009)

24. Louvan, S., Ibrahim, M., Adriani, M., Vania, C., Distiawan, B., Wanagiri, M.Z.: University of Indonesia at TREC 2011 microblog track. In: TREC (2011)
25. Metzler, D., Cai, C.: Usc/isi at TREC 2011: Microblog track. In: TREC (2011)
26. Miyanishi, T., Okamura, N., Liu, X., Seki, K., Uehara, K.: TREC 2011 microblog track experiments at KOBE university. In: TREC, Gaithersburg, MD (2011)
27. Ounis, I., Macdonald, C., Lin, J., Soboroff, I.: Overview of the TREC 2011 microblog track. In: TREC, Gaithersburg, MD (2011)
28. Ounis, I., Macdonald, C., Soboroff, I.: On the TREC blog track. In: ICWSM, Seattle, WA (2008)
29. Robertson, S.E., Walker, S., Hancock-Beaulieu, M., Gatford, M., Payne, A.: Okapi at TREC-4. In: TREC (1995)
30. Rocchio, J.: Relevance feedback in information retrieval, pp. 313–323. Prentice-Hall, Englewood Cliffs (1971)
31. Sellamanickam, S., Garg, P., Selvaraj, S.K.: A pairwise ranking based approach to learning with positive and unlabeled examples. In: CIKM, pp. 663–672 (2011)
32. Vapnik, V.N.: Statistical learning theory. Wiley, New York (1998)
33. Veloso, A.A., Almeida, H.M., Gonçalves, M.A., Meira Jr., W.: Learning to rank at query-time using association rules. In: SIGIR, pp. 267–274 (2008)
34. Witten, I., Frank, E.: Data Mining: Practical machine learning tools and techniques, 2nd edn. Morgan Kaufmann, San Francisco (2005)
35. Wu, J., Yang, Z., Lin, Y., Lin, H., Ye, Z., Xu, K.: Learning to rank using query-level regression. In: SIGIR, pp. 1091–1092 (2011)
36. Wu, Q., Burges, C., Svore, K., Cao, J.: Ranking boosting and model adaptation. Technical report, Microsoft (2008)
37. Ye, Z., He, B., Huang, X., Lin, H.: Revisiting Rocchio's Relevance Feedback Algorithm for Probabilistic Models. In: Cheng, P.-J., Kan, M.-Y., Lam, W., Nakov, P. (eds.) AIRS 2010. LNCS, vol. 6458, pp. 151–161. Springer, Heidelberg (2010)
38. Zhai, C., Lafferty, J.D.: Model-based feedback in the language modeling approach to information retrieval. In: CIKM, pp. 403–410 (2001)
39. Zheng, Z., Zha, H., Sun, G.: Query-level learning to rank using isotonic regression. In: Allerton, pp. 1108–1115 (2008)
40. Cao, Z., Qin, T., Liu, T.-Y., Tsai, M.-F., Li, H.: Learning to rank: from pairwise approach to listwise approach. In: ICML, pp. 129–136 (2007)
41. Ounis, I., Macdonald, C., Lin, J., Soboroff, I.: Overview of the TREC 2011 microblog track. In: TREC, Gaithersburg, MD (2011)
42. OunIs, I., Amati, G., Plachouras, V., He, B., Macdonald, C., Lioma, C.: Terrier: A High Performance and Scalable Information Retrieval Platform. In: Proceedings of ACM SIGIR 2006 Workshop on Open Source Information Retrieval (OSIR), Seattle, Washington, USA, August 10 (2006)
43. `http://olivo.net/software/lc4j/`

An Ontology-Based Information Extraction Approach for Résumés

Duygu Çelik[1,*] and Atilla Elçi[2]

[1] Computer Engineering Department, Istanbul Aydin University, Turkey
[2] Dept. Electrical-Electronics Engineering, Aksaray University, Turkey
duygucelik@aydin.edu.tr
atilla.elci@gmail.com

Abstract. A Curriculum Vitae (CV) or a résumé, in general, consists of personal information, education information, work experience, qualifications and preferences parts. Scanning or making structural transformation of the millions of free-formatted résumés from the databases of companies / institutions with human factor will result in the loss of too much time and human effort. In the literature, a limited number of studies have been done to change the résumés of the free-format to a structural format. The overall objective of the study is to infer required information such as user's experience, features, business and education from résumés of the potential user of a human resources system. In this article, we proposed an ontology driven information parsing system that is planned to operate on few millions of résumés to convert them structured format for the purpose of expert finding through the Semantic Web approach.

Keywords: Web Semantics, Web Ontology Language, Résumé, Semantic Search Agents, Information Extraction.

1 Introduction

When a résumé is mentioned, a written document comes to mind containing a person's education, work experience, skills, and personal information and so on. The résumés are created and sent as individual free-format, to make a job application via a brokerage firm or directly to companies which call for recruitment of staff. The purpose of the study is to elicit the requested information from each section, by dividing the résumés which may come from various sources on the Internet into the above sections with the semantic-based information extraction system and to make this information presentable in the form of relational data.

Owing to the fact that forming a general system which will be able to extract information from any kind of document is a very difficult application data mining systems is being developed specifically for the collapsed spans. Data acquisition which can be saved to the database from the *Résumés* or *Curriculum Vitaes (CVs)* written in free format is also one of the areas studied on. Therefore, Natural Language

* Corresponding author.

Q. Zu, B. Hu, and A. Elçi (Eds.): ICPCA-SWS 2012, LNCS 7719, pp. 165–179, 2013.

Processing (NLP) methods require a separate study for each language as the rules of language, semantic and grammatical structures are different from each other. Although, there are many studies on this issue in particular English language but not adequate study implemented such that has been found by considering concept-based semantics of résumés for English language in the literature. In fact, NLP algorithms without semantic consideration can be applied successfully however which can be more effective with semantic consideration if it also is applied on the résumé documents having semantic content.

On the database of Kariyer.net[1] company, there are more than 6,000,000 unstructured, written in both English and Turkish languages and free-style résumés as MS Word[2] documents. Therewithal the contents of the résumés are similar to their aims, the classification, the collection under the titles and the presentation of information can be totally different. Information gathering from each of these résumés to the existing system's database into a searchable form will be increasing the possible losses in terms of human factor. Therefore, there are many difficulties of résumé servicing by such governmental/commercial companies or unions, which consume too much their crucial resources such as time, capacity, human effort, money etc. Moreover, filtered résumés are the most important resource for employment in human resources departments of the governmental/commercial companies. Hundreds of applications can be made by mail online or fax and by hand to the ads of a member position that published by a company for its employees search. So, all the résumés other than online ones are filed and their chance of recall and being found becomes almost impossible. As the information contained in résumés is the only way for a company to employ suitable candidates, structurally organized and searchable résumés, regardless of the size of each are important for the company's human resources department. Other than the résumés uploaded by the candidates applying for a job, the request for evaluating the résumés accumulated in their hands over time and from different channels have emerged.

In the files and storage environments of companies making intensive recruitment, ten thousands of résumés are suspended without evaluation. In order for NLP algorithms to operate properly, intended scope must be determined in advance and the algorithm need to be developed specifically for this scope. With this study, development of a semantic-based information parsing system is considered which is first productized for the both languages English and Turkish language and which is targeted to have commercial value is presented. Therewithal formal analysis of the application prepared according to résumé scope, semantic analyzer part is designed in a way appropriate for the linguistics rules and structure for both languages separately and its adaptation with different scopes will be possible by this approach.

The rest of this paper is organized as follows: In Section 2 presents recent researches of IE applications on résumés in the literature. In Section 3 investigates the Ontology Knowledge bases used in the system. While Section 4 presents the architecture of the system through a case study, Section 5 is dedicated to conclusions.

[1] www.kariyer.net

[2] http://office.microsoft.com/tr-tr/word/

2 Related Works

Free format texts are being operated together with context interpretation and information debugging constitutes one of the major parts of information management systems. Semantic Web (SW)[3] provides to produce results appropriate with human communication from the information in the computer format or in contrast, the use of standardized methods for data generation from the resource documents written in free style. In fact, the SW is an extension of current Web technology that was developed in order to share and integrate information not only in natural language, but also by the associated software to be understood, interpreted and can be expressed in a way, so that makes easier to find the required data in the software. Additionally, ontologies are considered one of the pillars of the SW which can be developed through ontology languages that are a type of knowledge representation used for describing the concepts, properties and relationships among concepts of a domain.

Table 1. DOAC And Résumé RDF Comparison

Ontology Structure	*DOAC*	*Résumé RDF*
Classes/Concepts	15	16
Properties/Relationship s	17	73
Year	2005	2002

A SW based word treasure (vocabulary) can be considered as a special form of (usually light-weight) ontology, or sometimes also simply as a set of URIs with an (usually informally) described meaning. Recently, many ontology languages have been proposed and standardized such as RDF(S)[3] , Web Ontology Language (OWL)[4] and its new version OWL 2.0[5] etc. The OWL expresses the concepts in a specific space, terms and features in the form of ontology. In this way, it is possible to adapt the heterogeneous information from the distributed information systems. Additionally, each described concept in ontology encapsulates a subset of instance data from the domain of discourse [1].

A résumé, in general, consists of personal information, education information, work experience, qualifications and preferences parts and is kept somewhere and used during job interview. Scanning or making structural transformation of the millions of free-formatted résumés from the company/institution repositories with human factor will result in the loss of too much time and human effort. In addition, a limited number of studies have been done to change the résumés of the free-format to a structural format. Recently, most of the researches were designed for résumé ontology/vocabulary in English and some of them are presented below:

Bojārs and Breslin proposed Résumé RDF ontology in order to identify résumés semantically. The purpose of this ontology was designed for the systems which reveal

[3] `http://www.w3.org/RDF/`, 1999
[4] W3C Recommendation, `http://www.w3.org/tr/owl-features/`, 2004.
[5] W3C Recommendation, `http://www.w3.org/TR/owl2-overview/`, 2009.

the structure of “authority finder”. With this ontology structure, it is possible to describe information about people, features and skills etc. semantically [2].

Another similar study is Description of a Career (DOAC). In this study, a vocabulary is suggested by R. A. Parada to describe résumés [3]. In DOAC concepts about information, features, capabilities or skills of people were depicted. However, a limited number of concept descriptions were done. In the Résumé RDF ontology basic topics like, jobs, academic knowledge, experiences, skills, publications, certificates, references and other information were discussed. In the Résumé RDF two different namespaces were described that are:

```
http://purl.org/captsolo/résumé-rdf/0.2/cv
http://purl.org/captsolo/résumé-rdf/0.2/base
```

In the first namespace, there are a variety of concepts about résumés (such as work experience, education etc.). In the second namespace (base), the values of the general characteristics of résumés are defined (such as BS, MS, PhD or foreign language level etc.). However, the DOAC is in the form of word treasure (vocabulary) rather than ontology. With this vocabulary generally “professional skills” features about people are defined that has a namespace and is given in the below:

```
http://ramonantonio.net/doac/0.1/personal
```

Both of them can define a person's résumés and can describe experience of the capabilities of that person and similar information such as personal information of that person can be described with the help of common facilities or important differences. However, as in the Résumé RDF a greater number of properties (73) are defined, in information extraction semantically, more information can be obtained from queries. In contrast with the Résumé RDF, in the DOAC less semantic feedback can be achieved as a smaller number of properties (17) are defined.

Another research has been proposed by E. Karaman and S. Akyokuş [4] that is also IE based system model that can do the finding dismantling operation from résumés in four different sequential steps. These are called as *Text Segmentation, Scanning and Identifying Name Property, Classifying Name Property,* and *Text Normalization*. In the proposed system by E. Karaman and S. Akyokuş, a set of résumés written in the English language are considered to parse through a syntactic-based matching algorithm instead of the semantic matching [5-8]. While matching, the system matches the extracted information from a document with the predefined résumé vocabulary. For example, the system can see that the abbreviation *"IAU"* is *"Istanbul Aydin University"* but it can’t understand the semantics of ‘It is a university’, in other words "IAU is a university".

To combine several different methods as a hybrid approach from some studies are also discussed in the literature [9-12]. For example, in K. Yu, G. Guan and M. Zhou [13] studies HMM modeling is presented with a statistical approach, also, J. Piskorski and his group’s [14], SVM modeling is presented with learning based approach [15].

In this study, the proposed ontology driven information extraction system that is called ***Ontology-based Résumé Parser (ORP)*** will be operated on few millions English language and Turkish language résumés to convert them ontological format. The system will also assist to perform the expert finding/discovery and aggregation of skill information among résumé repository through its involved semantic approach.

The *Ontology Knowledge Bases (OKBs)* of the ORP system contain many domain ontologies each that contain concepts, properties and relationship among them for each type of résumé segments (Section 4.1). Moreover, OKBs is generated in English but also contains `<Literal xml:lang="tr">` declaration that is created for indicating the Turkish equivalent concept of each English concept in the OKBs that is shown in below OWL example.

```
<Declaration>
<Class IRI="#LanguageSkill"/>
<Literal xml:lang="en">Language Skill</Literal>
<Literal xml:lang="tr">Dil Becerileri</Literal>
</Declaration>
```

The OKBs provide to associate along concepts, relations and properties that may profit to solve some special cases of relationships among concepts (i.e. a Résumé Ontology in the OKBs is required for the both segments: work experiences and education segments, since a person's work place or company/institution information can be a university who works for and also studies in the same university).

3 Ontology Knowledge Bases (OKBs)

The system uses its own ontologies that are *Education, Location, Abbreviations, Occupations, Organizations, Concepts* and *Résumés Ontologies* in its OKBs. The functionality and the purpose of OKBs with its ontologies are described below and also the parentheses are used to keep Turkish meanings of the ontologies;

- *Education Ontology (Eğitim Ontolojisi –EO):* It keeps the concepts of comprehending the words of the education domain in Turkish such as 'University' (Üniversite), 'High School' (Lise) etc. and some properties among concepts such as '*hasDegree'* i.e. 'Honour degree' (Onur Derecesi) that is related for the education domain. The ontology also keeps the individuals that are instances of entire education institutes such as *'Istanbul Aydin University'*. The IAU is an individual of the 'University' concept in the ontology. Beside this, each concepts of this ontology indicates a relational concept in the Résumé Ontology. i.e. the system can understand the mean of the term 'University' in a candidate's résumé that is parsed from the education/work/other segments through the pre-declared concept 'University' in the Education Ontology.
- *Location Ontology (Konum Ontolojisi –LO):* It keeps the concepts of the location domain in Turkish such as 'Country' (Ülke), 'City' (Şehir), 'Village' (Köy) etc also some properties are declared such as '*hasPostalCode*' property of a city. The ontology is also associated some other ontologies through URIs such as Résumé Ontology, Concepts Ontology so on.
- *Abbreviations Ontology (Dil Kısaltmaları Ontolojisi –AO):* The ontology for abbreviations of certain word groups in the English or Turkish Languages such as *'Istanbul Aydin University'* as a single concept and also keeps its properties such as

'hasAbbreviation' property value is IAU. The ontology is also associated the Education Ontology, Concepts Ontology, Occupations Ontology so on.

- *Occupations Ontology (Meslekler Ontolojisi –OCCO):* It contains entire concepts of the used terms for the types of occupations in Turkish such as 'Doctor' (Doktor), 'Chef Assistant' (Şef Yardımcısı), 'Academician' (Akademisyen) and also includes their relations such as *'subClass'* i.e. 'Chef Assistant' is a subclass of the concept 'Chef'.
- *Organizations Ontology (Organizasyonlar Ontolojisi –OO):* contains entire concepts for the types of Companies/Institutions in Turkish language such as 'Pastryshop' (Pastane), 'University' (Üniversite) or 'Hospital' (Hastane) so on.
- *Concepts Ontology (Kavramlar Ontolojisi –CO):* It contains common concepts in general such as 'Date' (Tarih), 'Year' (Yıl), 'Month' (Ay), 'Day' (Gün) or 'Currency' (Para Birimi) and their relationships. The ontology almost has association entire OKBs in the system.
- *Résumés Ontology (Özgeçmiş Ontolojisi –RO):* While there is no single correct format or style for writing a résumé in English or Turkish as well as other languages, therefore we can summarize the following types of information that are generally used terms by a résumé owner, and typically organized through ontologies for processing and understanding by machines in the following way as listed in Section 4.1.

Effective detailing of the OKBs will help understanding of the mechanics of the system. The most important one is Resume Ontology that is only explained with detail in the following section and also discussed the association ship among others.

3.1 Résumé (Özgeçmiş) Ontology

The Résumé (Özgeçmiş) ontology, the RO, is developed in order to express on the semantic data contained in a résumé, such as personal information, business and academic experience, skills, publications, certifications, etc. A résumé individual is described in ontology form via a résumé upper ontology. It is possible to annotate semantically the information of personal, work experiences, academic or educational life, skills, taken courses, certificates, publications, personal/professional references and other information in the résumé of the person.

Personal information keeps many concepts such as 'Name', 'Address', 'Email', 'Mobile', 'Home Phone', 'Military State' etc of a person. The 'Education' concepts contains the sub concepts such as 'dissertation', 'certificates', 'fellowships/awards', 'areas of specialization', 'areas of research', 'teaching interests', 'teaching experience', 'research experience', 'publications/presentations', 'related professional experience' and their properties. The education segment in the RO is mostly associated with the Education Ontology –EO.

The ***'Work Experiences'*** involves the semantic annotations for current work, previous works and goal works, namely, the information personal work preferences for future. Furthermore, the RO is designed with querying in mind and is able to extract a better semantic information from résumés e.g. 'Company' is a concept in the RO, may related to the person's current work, previous work or targeted work that are

annotated via a 'ro:employedIn' (ro:Gecmis_is) property used for work history, 'ro:isCurrentWork' (ro:halen_is) used for the company information of current work, and 'ro:isGoalWork' (ro:Hedef_is) used for information of the person's target.

Additionally, the ***Skill*** is also considered in the RO and that is designed as in Resume RDF [5]. The skill data can be described semantically by 'ro:skillName' (ro:yetenekAdı) concept in RO. In addition, skill levels is also semantically described through owl:objectProperty that is named as 'ro:skillLevel' (ro:yetenekSeviye) from 'bad' (kötü) to 'excellent' (mükemel). Moreover, the 'ro:skillLastUsed' (ro:yetenekSonKullanım), 'ro:skillHasCertificate' (ro:yetenekSertifika) and 'ro:skillYearsExperience' (ro:yetenekYılSayısı) are used since it allows to quantify of skill levels particularly on foreign languages or used software tools.

Table 2. A Small Portion of the Résumé (Özgeçmiş) Ontology-RO

Personal Information	
Education	
Dissertation	
Fellowships/Awards	
Areas of Specialization	
Research and Teaching Interests	
Teaching Experience	
Research Experience	
Publications/Presentations	
Certificates	
Related Professional Experience	
Work Experiences	
Current Work	
Previous Works	
Skill	
Language	
Used Computer Software	
Driving License	
Activities	
References	
Other	
.	
.	

```
1   <!—A portion of the Résumé Ontology in English Language-->
2   <owl:Class rdf:ID="Resume"/>
3   <owl:Class rdf:ID="Employee"/>
4   <owl:Class rdf:ID="Company"/>
5   <owl:Class rdf:ID="Skill"/>

6   <owl:Class rdf:ID="Software_Skill">
7       <rdfs:subClassOf rdf:resource="#Skill"/>
8   </owl:Class>
9   <owl:Class rdf:ID="Driving_Skill">
10      <rdfs:subClassOf rdf:resource="#Skill"/>
11  </owl:Class>
12  <owl:Class rdf:ID="Language_Skill">
13      <rdfs:subClassOf rdf:resource="#Skill"/>
14  </owl:Class>

15  <owl:ObjectProperty rdf:about="#hasSoftware_Skill">
16      <rdfs:range rdf:resource="#Resume"/>
17      <rdfs:domain rdf:resource="#Tool"/>
18        <owl:inverseOf>
19          <owl:ObjectProperty rdf:about="#isSoftware_SkillOf"/>
20        </owl:inverseOf>
21  </owl:ObjectProperty>

22  <owl:DatatypeProperty rdf:ID="#hasDriversLicense">
23      <rdfs:domain rdf:resource="#Resume"/>
24      <rdfs:range  rdf:resource="&xsd:boolean"/>
25  </owl:DatatypeProperty>

26  <owl:ObjectProperty rdf:ID="WorksInCompany">
27      <rdfs:domain rdf:resource="#Employee"/>
28      <rdfs:range rdf:resource="#Company"/>
29          <owl:inverseOf rdf:resource="#CompanyMembers"/>
30  </owl:ObjectProperty>
```

Furthermore, the ontology uses literals to describe skills in the form of ***owl:datatypeProperty*** since avoid uncertainty of skill identification and enabling straight skill matching. The concept ***'skill'*** has many subclasses for language skill, driving skill, software skill, tool or machine skill etc. and allows to semantically describing if a person has foreign language ability, a driver license or used softwares/tools/machines and their levels respectively. The semantic declaration by the

RO will assist to perform the expert finding/discovery and aggregation of skill information among résumé repository. As shown in Table 2, a portion of the upper ontology of Résumé Ontology is depicted.

In fact, a résumé is characterized by its skills. The hasSoftware_Skill and isSoftware_SkillOf relations join the two classes together through a bidirectional link. They are inverseof one another, so they have inverted domain and range. The owl:inverseOf construction can be used to define such an inverse connection between relations through the *owl:ObjectProperty* (Lines 15-21, Table 2). Skill assertion should be considered since people mostly have mentioned their software/language/driving skill information on their résumés.

To the addition of the contributions of the RO, these kind of semantic declarations provide to infer another meaningful data from pre-asserted data for a résumé through an inferencing mechanism. The mechanism is able to give an opportunity to discover an appropriate résumé for a specific job position of a company.

Through semantic based inferencing rules declaration based on the resume ontology, a person with a university degree who has *Java knowledge* and has experience more than *three years* will be suitable candidate for some companies that are looking for a *'Java Supervisor'*. The conceptualizations of a person and a university can be captured from OWL classes called *'Person' (p)* and *'University' (u)*. The experience year, degree and computer skill conditions can be expressed from *hasExperienceYR, hasdegreefrom (if p has degree from university) and hasComputerSkill (if p has JAVA knowledge)* object properties. This rule could be written as:

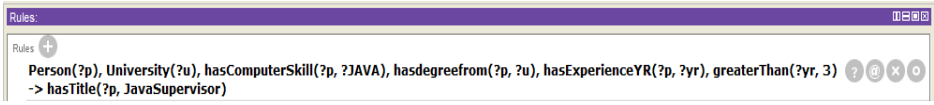

Fig. 1. Rule syntax form semantic rule tab of Protégé ontology tool [16]

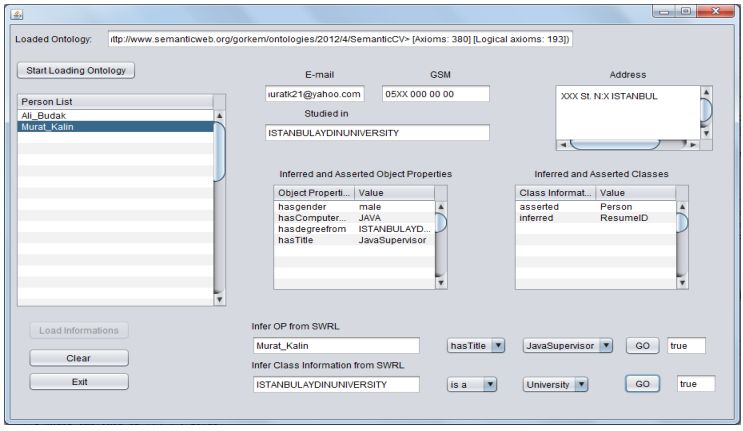

Fig. 2. System finds a person with a university degree who has *Java knowledge* and has experience more than *three years*. Also it infers Istanbul Aydin University is a University.

Through the inferencing mechanism of the system, a significant information stack is obtained from a résumé that can be stored separately in OWL form through the RO upper ontology model. Therefore, with a résumé scanning module, it can be possible to get information whether the résumé is eligible for a required criterion. A semantic search agent can easily access in its semantic descriptions and examine the suitability the résumé. In next section, the working mechanism of the system on a sample free formatted résumé is analyzed as a case study.

4 Working Mechanism of ORP

The system detects and extracts the desired information from the unstructured résumé after using its ontology parsing mechanism applied on the terms of the résumé and the concepts in OKBs. After that, the system transfers the parsed unstructured data from the focused résumé to the suitable place of the system's database and also structures it in the OWL form to a separate personal résumé ontology file.

The ORP system performs five major steps that are *converting an input résumé*, *dividing the résumé to some specific segments*, *parsing meaningful data from the input résumé*, *normalize it* and finally *applying classification and clustering task* to structure the résumé. The steps are described through a case study in below:

-Converter: It will carry out the process of converting for the given as .doc, .docx, .pdf, .ps etc. form of résumés into plain text. In case study, as a first step a free formatted sample résumé (i.e. Mr. Ali Budak résumé on the right in Figure 2) is presented to the system as an input (.doc, .pdf, .txt etc.) which will be converted to plain text format through a converter (for example: .txt, Figure 2 step 1 to 2).

-Segmenter: With the help of a Segmenter, the produced plain text will be segmented into parts like personal information, education, work experience, personal experience etc. Then, the necessary parts will be cut out and send to the ORP Parser Engine. The semantic-based segmentation process of the working experiences segment of the considered case study is shown in the figure below (Figure 2 step 3 to 4).

Table 3. Eng/Tr Translatıon of the Given Résumé Above (For Fıgure 1)

SEGMENTS	***ONROLOGY KNOWLEDGE BASES***	***A SAMPLE RÉSUMÉ GIVEN ABOVE***
Tur_ish/Eng_ish	**Turkish/English**	**Turkish/English**
Kişisel Bilgiler/Personal Information	Eğitim Ont./Education Ont.	'Bostancı' is a location in Istanbul city.
Eğitim/Education	Yer Ont./Location Ont.	'Migros' is a market company in Turkey.
İş Tecrübeleri/Working Experience	Kıslatmalar Ont./Abbreviation Ont.	'Torta' is an ignored unnecessary data.
Kişisel Becerile-ri/Personal Skills	Meslekler Ont./Occupations Ont.	'Pastane' is an organization that is pastry-shop.
	Özgeçmiş Ont./Resume Ont.	'Şef Yardımcısı' is a title of occupation that is called Assistant of Chef.
	Kavramlar Ont./Concepts Ont.	'Altınkek' is a name of a company.
	Organizasyonlar Ont./Organizations Ont.	'San.' is abbreviation of the industry that same as 'Ind.' in English and same for others: 'Tic.' is Trade 'Trd.', 'Ltd.' is Limited 'Ltd.' and 'Şti.' is company 'Co.' so on…

As shown in the Figure 2, the input résumé (belong to Mr. Ali Budak) is transferred to the Segmenter in the format of plain text (Step 3), the system separates the segments (such as personal information, work experiences, education etc.) by using its OKBs (Step 4 and 5) that are shown above in yellow boxes (Step 6). During segmentation, the ORP Segmenter takes a number of sample terms from the résumé to differentiate particular segments of the résumé.

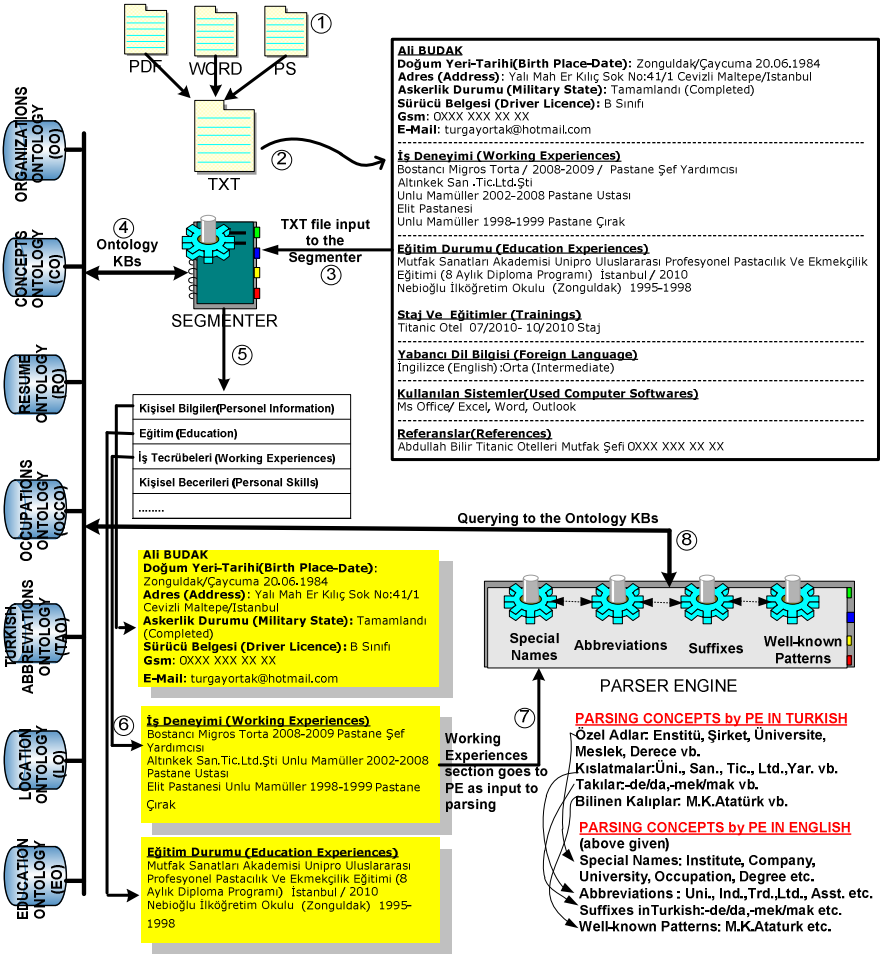

Fig. 3. A sample CV in Turkish and the system's *Segmenter* and *Parser Engine* working on it

-Parser Engine: At this step, the system does parsing process of proper names/ concepts, the abbreviations, suffixes and prefixes well-known patterns in sentence. During this decomposition process, as shown above, the OKB will be used. OKB of the proposed system is consisted of education, place / space, abbreviations, personal information, concepts, and companies' ontology. In the example below, "work experience" section is sent to a Parser Engine as an input (Figure 2 Step 7 or Figure 3 Step

8). One by one, each section will be separated and turned in to formatted form in Parser Engine. The obtained output from the Parser Engine is shown in Figure 3. The system can infer which concept is the piece scanned in a sentence from ontologies, and also can keep the information of start and finish lines for the next sentence.

In Figure 3, a yellow box contains the working experience segment of the sample résumé that is analyzed by the parser engine of the system. The segment contains the sentence ***'Bostancı Migros Torta / 2008-2009 / Pastane Şef Yardımcısı'***. The system starts to detect each terms of the sentence in concept base and tries to find each concept's URI information (ontology location) and appropriate place in the system's database (Figure 3 Step 8 to 11).

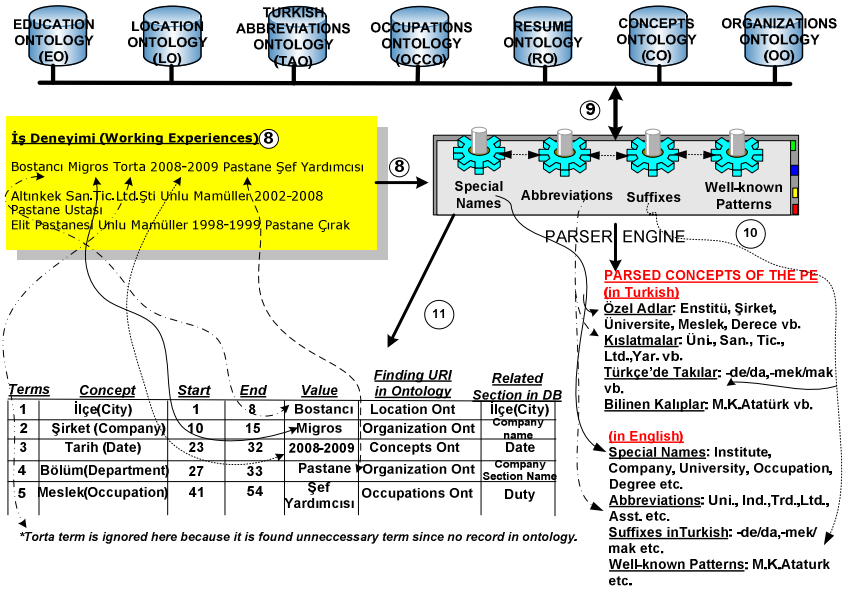

Fig. 4. The system's *Parser* continues to analyze *Working Experiences* section of the same résumé according to *Special Names*, *Abbreviations*, *Suffixes*, and *Well-known patterns*

-The next process is text normalization though a Transformation Module. The system will scan the abbreviations in the latest result table and turn them into standard usage (Figure 4 Step 12). For example, above in the 2nd row in the working experience segment in Figure 3, the work experience knowledge includes many abbreviations such as San. Tic. etc. The system converts these abbreviations into normal state (Figure 4 Step 11 to 13). The transformation module detects the abbreviated concepts and retransforms to normal form and assigns them in to another table that does not involve any abbreviation concept. For instance, table may include 'Ltd.' abbreviation then the transformation module will convert it into normal state 'Limited' with its indicated concept in OKB. In final table, the transformation module always keeps the URIs of the fitting full concepts of abbreviations.

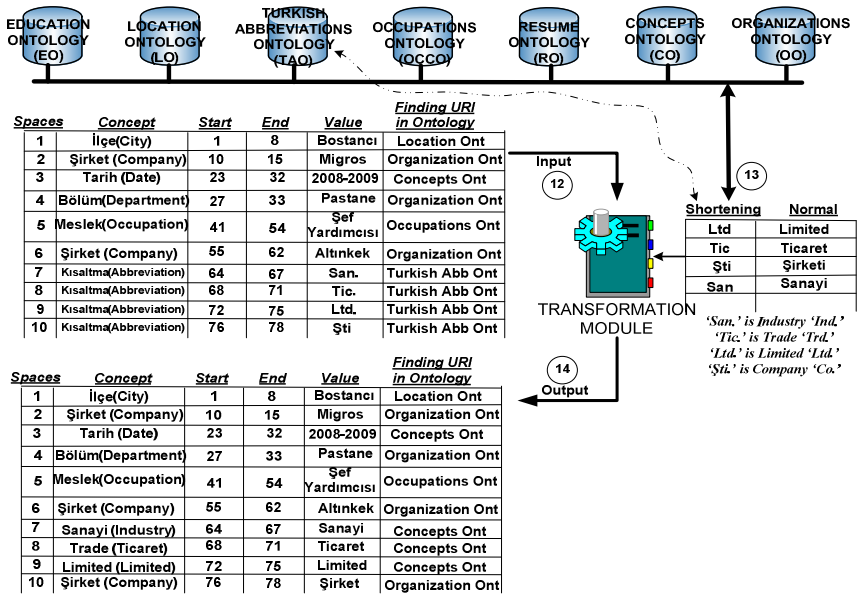

Spaces	Concept	Start	End	Value	Finding URI in Ontology
1	İlçe(City)	1	8	Bostancı	Location Ont
2	Şirket (Company)	10	15	Migros	Organization Ont
3	Tarih (Date)	23	32	2008-2009	Concepts Ont
4	Bölüm(Department)	27	33	Pastane	Organization Ont
5	Meslek(Occupation)	41	54	Şef Yardımcısı	Occupations Ont
6	Şirket (Company)	55	62	Altınkek	Organization Ont
7	Kısaltma(Abbreviation)	64	67	San.	Turkish Abb Ont
8	Kısaltma(Abbreviation)	68	71	Tic.	Turkish Abb Ont
9	Kısaltma(Abbreviation)	72	75	Ltd.	Turkish Abb Ont
10	Kısaltma(Abbreviation)	76	78	Şti	Turkish Abb Ont

Spaces	Concept	Start	End	Value	Finding URI in Ontology
1	İlçe(City)	1	8	Bostancı	Location Ont
2	Şirket (Company)	10	15	Migros	Organization Ont
3	Tarih (Date)	23	32	2008-2009	Concepts Ont
4	Bölüm(Department)	27	33	Pastane	Organization Ont
5	Meslek(Occupation)	41	54	Şef Yardımcısı	Occupations Ont
6	Şirket (Company)	55	62	Altınkek	Organization Ont
7	Sanayi (Industry)	64	67	Sanayi	Concepts Ont
8	Trade (Ticaret)	68	71	Ticaret	Concepts Ont
9	Limited (Limited)	72	75	Limited	Concepts Ont
10	Şirket (Company)	76	78	Şirket	Organization Ont

Fig. 5. The system's *Transformation Module* converts involved abbreviations in the *Working Experiences* segment

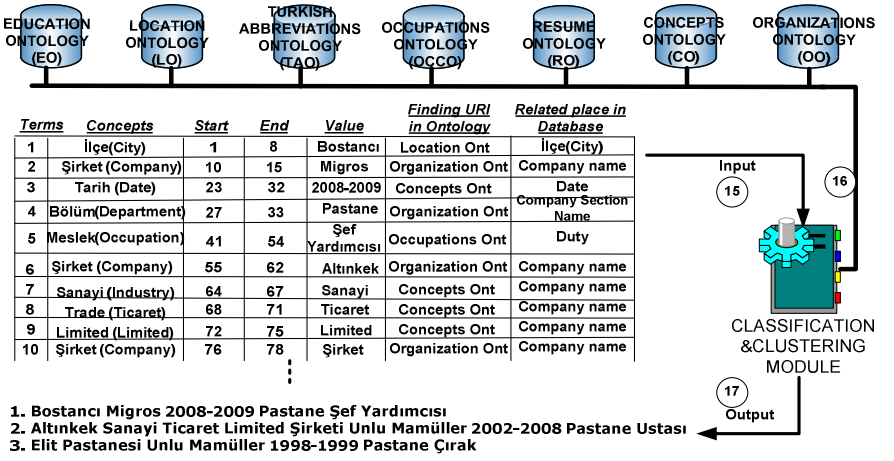

Terms	Concepts	Start	End	Value	Finding URI in Ontology	Related place in Database
1	İlçe(City)	1	8	Bostancı	Location Ont	İlçe(City)
2	Şirket (Company)	10	15	Migros	Organization Ont	Company name
3	Tarih (Date)	23	32	2008-2009	Concepts Ont	Date
4	Bölüm(Department)	27	33	Pastane	Organization Ont	Company Section Name
5	Meslek(Occupation)	41	54	Şef Yardımcısı	Occupations Ont	Duty
6	Şirket (Company)	55	62	Altınkek	Organization Ont	Company name
7	Sanayi (Industry)	64	67	Sanayi	Concepts Ont	Company name
8	Trade (Ticaret)	68	71	Ticaret	Concepts Ont	Company name
9	Limited (Limited)	72	75	Limited	Concepts Ont	Company name
10	Şirket (Company)	76	78	Şirket	Organization Ont	Company name

Fig. 6. The system's *Classification and Clustering Module* detects involved meaningful sentences in the *Working Experiences* segment of the résumé

-Classification and Clustering of Concepts: In this step, the combination of obtained concepts from the concept stack returned from the Parser Engine (as shown in the table) operation will be carried out. As shown in the figure above, three different phrases exist in the business experiences have been shown in section of business.

The system uses the concepts of found suitable OKBs at that moment to carry out meaningful sentences during its classifications processes (Figure 5 Step 15 to 17). The Classification and Clustering module detects each individual sentence in the working experiences segment of the résumé according to the generated table of transformation module in previous step. The Classification and Clustering module starts to detect start and stop point of each sentence according to the generated table. Each typical working experience sentence may contains some possible concepts a 'City', a 'Date', a 'Company', a 'Department name', an 'Occupation', and some abbreviations etc. The Classification and Clustering module will able to define start and stop points in a typical working experience sentence. In Figure 5, the system finds three different working experience sentences and then the system performs structuring its OWL ontology that is keeping reuse during expert finder searching in future (Table 4).

4.1 Generated Personal Résumé Ontology for Individuals

End of the *Classification and Clustering of Concepts* step, the system is able to generate its OWL form of the input résumé. For instance, personal information section in a résumé may involve *hasBirthCity, hasBirthTown, hasBirthDate, hasCurrentAddress, hasCurrentTown, hasEMail* etc. Similarly, the past working experience section is able to declare through some crucial properties such as *WorkingExperience, hasWorkCity, hasWorkCompany, hasWorkDate, hasStartWorkDate, hasEndWorkDate, hasWorkDuty* so on. The values of these properties are kept in the OWL form for the person (Mr.Ali Budak) that is shown in Table 4. For our example, first working experience is depicted in OWL form through the ***WorkingExperience property*** *(WorkingExperience_1, Line 17-24 in Table 4).* The property contains ***hasWorkCity*** property that indicates a city concept. The city concept keeps a value that is ***"Bostancı"*** under the ***"&Location"*** ontology.

Table 4. A Sample of a Person Résumé (Özgeçmiş)

Resume No: R-0000001		
Name: Ali Budak	1	<!— A portion of the Résumé (Özgeçmiş) Ontology in English Language -->
Doğum Yeri-Tarihi(Birth Place-Date): Zonguldak/Çaycuma 20.06.1984	2	<Resume rdf:ID=" R-0000001">
	3	<hasBirthCity rdf:resource="&Location;Zonguldak"/>
	4	<hasBirthTown rdf:resource="&Location;Çaycuma"/>
Adres (Address): Yalı Mah Er Kılıç Sok No:41/1 Cevizli Maltepe/Istanbul	5	<hasBirthDate rdf:datatype="&Concept;Date">20.06.1984
	6	</hasBirthDate>
	7	<hasCurrentAddress rdf:resource="&Location;Street"/>Yalı Mah Er Kılıç Sok
Askerlik Durumu (Military State): Tamamlandı (Completed)	8	No:41/1 Cevizli</ hasCurrentAddress>
	9	< hasCurrentTown rdf:resource="&Location; Maltepe"/>
Sürücü Belgesi (Driver Licence): B Sınıfı(B Class)	10	<hasCurrentCity rdf:resource="&Location;İstanbul"/>
	11	<hasMilitaryState rdf:resource="#Completed"/>
Gsm: 0XXX XXX XX XX	12	<hasDirverLicence rdf:resource="#B Class"/>
E-Mail: turgayortak@hotmail.com	13	<hasCurrentGSM rdf:datatype="&Concept;GSMNumber">0XXX XXX XX XX
İş Deneyimi (Working Experiences)	14	</hasCurrentGSM>
	15	<hasEMail rdf:datatype="&Concept;EMail">turgayortak@hotmail.com
-Bostancı Migros Torta / 2008-2009 / Pastane Şef Yardımcısı	16	</hasEMail>
	17	<WorkingExperience rdf:about="WorkingExperience_1">
-Altınkek San.Tic.Ltd.Şti Unlu Mamuller 2002-2008 Pastane Ustası	18	<hasWorkCity rdf:resource="&Location;Bostancı"/>
	19	
	20	

Table 4. (*Continued.*)

-Elit Pastanesi Unlu Mamuller 1998-1999 Pastane Çırak ……..	<hasWorkCompany rdf:datatype="&Organization;SuperMarket">Migros </hasWorkCompany>
In English:	<hasWorkDate rdf:resource="&Concepts;Date"/>2008-2009</hasWorkDate>
'Bostancı' is a location in Istanbul city.	<hasWorkDepartment rdf:resource="&Organization;Pastane"/>
'Migros' is a market company in Turkey.	<hasWorkDuty rdf:resource="&Occupation;Şef_Yardımcısı"/>
'Torta' is an ignored unnecessary data.	</WorkingExperience>
'Pastane' is an organization that is pastry-shop.	<WorkingExperience rdf:about="WorkingExperience_2">
'Şef Yardımcısı' is a title of *an* occupation type that is called Assistant of Chef.	<hasWorkCompany rdf:datatype="&Organization;Pastane">Altınkek San. Tic. Ltd. Şti Unlu Mamuller</ hasWorkCompany>
'Pastane Ustası' is a type of occupation that is called Pastry-shop Chef.	<hasWorkDate rdf:resource="&Concepts;Date"/>2002-2008</hasWorkDate>
'Çırak' is a title of *an* occupation type that is called footboy.	<hasWorkDepartment rdf:resource="&Organization;Pastane"/>
'Altınkek' is a name of a company.	<hasWorkDuty rdf:resource="&Occupation;Pastane Ustası"/>
'San.' is abbreviation of the industry that same as 'Ind.' in English and same for others: 'Tic.' is Trade 'Trd.', 'Ltd.' is Limited 'Ltd.' and 'Şti.' is company 'Co.' so on.	</WorkingExperience>
'Elit Pastanesi Unlu Mamuller' is a name of a company.	<WorkingExperience rdf:about="WorkingExperience_3">
	<hasWorkCompany rdf:datatype="&Organization;Pastane">Elit Pastanesi Unlu Mamuller </hasWorkCompany>
	<hasWorkDate rdf:resource="&Concepts;Date"/>1998-1999</hasWorkDate>
	<hasWorkDepartment rdf:resource="&Organization;Pastane"/>
	<hasWorkDuty rdf:resource="&Occupation;Çırak"/>
	</WorkingExperience>
	</Resume>
	</rdf:RDF>

5 Conclusion

In this article, an ontology driven information extraction system is considered that is called Ontology-based Résumé Parser (ORP) is operated on few millions English language and Turkish language résumés to convert them automatically ontological format. The system is also assist to perform the expert finding/discovery and aggregation of skill information among résumé repository through its involved semantic approach. To do this, the system has its own ontological semantic based inferencing rules during its inferring mechanism. Therefore, the system has able to learn and keeps the inferred new relationships after inferring new information and uses them in the next steps when it requires again that makes the system is a learning-based system. As a conclusion, some of above mentioned properties of the ORP are not discussed here since taking too much space and are detailed separate studies as future studies of the project.

Acknowledgement. This project is supported by the Kariyer.net Company[1] that is titled as *"Document-based Semantic Information Extraction System from Turkish Résumés through Ontology"*.

References

1. Hu, B., Kalfoglou, Y., Alani, H., Dupplaw, D., Lewis, P., Shadbolt, N.: Semantic metrics. In: Proceedings of the 15th International Conference on Knowledge Engineering and Knowledge Management, pp. 166–181 (2006)
2. Bojars, U., Breslin, J.G.: RésuméRDF: Expressing Skill Information on the Semantic Web. In: The 1st International Workshop on ExpertFinder, Berlin, Germany (January 2007)
3. Parada, R.A.: DOAC Vocabulary Specification (July 08, 2006), http://ramonantonio.net/doac/0.1/
4. Karamatlı, E., Akyokuş, S.: Résumé Information Extraction with Named Entity Clustering based on Relationships. In: INISTA 2010, Kayseri (2010) (last visited: April 12, 2010)
5. Paolucci, M., Kawamura, T., Payne, T.R., Sycara, K.: Semantic Matching of Web Services Capabilities. In: Horrocks, I., Hendler, J. (eds.) ISWC 2002. LNCS, vol. 2342, pp. 333–347. Springer, Heidelberg (2002)
6. Çelik, D., Elci, A.: Towards a semantic-based workflow model to the composition of OWL-S Atomic Processes-through process based similarity matching and inferencing Techniques. J. of Internet Technology, Taiwan Academic Network Executive Committee (2010) ISSN: 1607-9264, Published by: Taiwan Academic Network Executive Committee (Accepted, SCI-E)
7. Çelik, D., Elçi, A.: Ontology-Based Matchmaking and Composition of Business Processes. In: Elçi, A., Koné, M.T., Orgun, M.A. (eds.) Semantic Agent Systems. SCI, vol. 344, pp. 133–157. Springer, Heidelberg (2011)
8. Çelik, D., Elci, A.: OWL-S Semantic-Based Workflow Model Based on Atomic Processes Unification. Journal of the Science and Engineering University of Cankaya, Ankara, Turkey (submitted, June 2010)
9. Sovren Résumé / CV Parser, http://www.sovren.com/ (last visited: April 12, 2010)
10. ALEX Résumé Parsing, http://www.hireability.com/ALEX/ (last visited: April 12, 2010)
11. Résumé Grabber Suite, http://www.egrabber.com/résumégrabbersuite/ (last visited: April 12, 2010)
12. Daxtra CVX, http://www.daxtra.com/ (last visited: April 12, 2010)
13. Yu, K., Guan, G., Zhou, M.: Résumé information extraction with cascaded hybrid model. In: ACL 2005: Proceedings of the 43rd Annual Meeting on Association for Computational Linguistics, Morristown, NJ, USA, pp. 499–506 (2005)
14. Piskorski, J., Kowalkiewicz, M., Kaczmarek, T.: Information Extraction from CV. Information Retrieval and Filtering, 185–192 (2005)
15. Chieu, H.L., Ng, H.T., Lee, Y.K.: Closing the Gap: Learning-Based Information Extraction Rivaling. In: Proceedings of the 41st Annual Meeting of the Association for Computational Linguistics, Sapporo, Japan (2003)
16. Protégé, OWL-S Ontology Editor CS / AI Department, University of Malta (2004), http://owlseditor.semwebcentral.org/ (last visited: April 2009)
17. Gruber, T. (N.d.): What is Ontology? http://wwwksl.stanford.edu/kst/what-is-an-ontology.html (last visited: April 15, 2007)
18. Onder, P., Ozen, N., Unlu, S., Orhan, Z.: A Framework for Building a Turkish Lexicon and Knowledge Base. In: Proceedings of IKE 2008, The 2008 International Conference on Information and Knowledge Engineering, Monte Carlo Resort, Las Vegas, Nevada, USA (July 2008)

Measure Method and Metrics for Network Characteristics in Service Systems

Haihong E[1], Xiaojia Jin[2], Junjie Tong[1], Meina Song[1], and Xianzhong Zhu[3]

[1] PCN&CAD Center Lab, Beijing University of Posts and Telecommunications, China
{ehaihong,jjtong,mnsong}@bupt.edu.cn
[2] China Mobile Group Hebei Co.Ltd., China
jinxiaojia@he.chinamobile.com
[3] China Digital Library Corp. Ltd., Beijing, China
zhuxianzhong@gmail.com

Abstract. As the development of Service-oriented architecture and service engineering, they have been generally adopted as the architecture and engineering method of software. More and more service applications and systems are constituted by distributed resources and web services which means more challenges in dynamic, varied and complex network environment. At the same time, the dependence and interactivity between the elements of networked service systems result in faults and difficulties in understanding and upgrading system and making the systems much more weakness. In this paper, according to the dynamic characteristics of the networked service system, we propose a network characteristics measure method and metrics for service system (MSS). Service system is defined by the descriptions of six important parameters at system level, which include service complexity, service cooperation relationship factor, service node factor, service cooperation factor, and service composition factor. Then the corresponding simulation is introduced by using the characteristics measure method and the analysis of the simulation results is also given. At last, a dynamic on-demand service composition algorithm based on MSS is designed and its feasibility and effectiveness are verified.

Keywords: service systems, network characteristic measure, service cooperation relationship.

1 Introduction

Various resources on the network are accessible, on-demand available and reusable combining with third-party professional services delivered by the service provider. Based on reuse and integration of these resources, the service system has become a complex networked application. Dependence and interactivity between elements of the networked service system and networked software, not only increase the difficulty of operation and transformation of the system, but also bring weakness that a small fault is likely to lead to the collapse of the entire system. Therefore, there is an urgent need to study new methods to meet the demands of system testing, monitoring and credible protection, in a dynamic network environment [1]. On the other hand, online

Q. Zu, B. Hu, and A. Elçi (Eds.): ICPCA-SWS 2012, LNCS 7719, pp. 180–193, 2013.

service system composed by the interoperable network elements included internally with control and externally without control, , means complexities on monitoring, evaluating, maintaining and upgrading. And that fat has brought many problems for the foreseeable bound large-scale third-party, fourth party (the convergence of third-party service integration services operators) service system operators.

Studying the service system or service-oriented networked applications under the traditional software engineering view, people often overly concerned with the software in the local structural characteristics of the lower surface, such as the implementation and integration of the component, while ignoring the global structure and overall properties of the system under the network view. This has led the developers and engineers to the lack of accurate measure structure and essential characteristics of the entire service system, and the overall assessment. And consequently, it is difficult for them to grasp the large-scale system operation and sustainable delivery.

According to the dynamic characteristics of networked service system, a network characteristics measure method and metrics for service systems (MSS) have been presented. Service system is defined by the description of six important parameters, including: service complexity, service cooperation relationship factor, service node factor, service cooperation factor, and service composition factor. Then the simulation is introduced by using the metrics method and the result's meaning is also analyzed.

2 The Perspective of Networked Service System

As the overwhelmed increasing in size and complexity of the elements of the networked services, quality of service is difficult to be effectively controlled. Meanwhile the complexity is the network's inherent properties. The research of service system is a typical complex issue. On the other hand, the structure of the service system has a very close relationship between the quality and function. Exploring and discovering the global perspective of the structural properties of the complex service system will give a comprehensive awareness and understand the essential characteristics of the service. Consequently, it can be used for discovering the natural law of service evolution and the behavioral characteristics, to quantify the service system complexity.

As the software systems have been expanding in the field of software engineering, many researchers analysis software system through network science perspective. As thinking about the object-oriented software system modeling, many researchers found that certain characteristics of the existing software systems follow the small world model or scale-free model. The relationship between classes composition of the network shows small-world effect in object-oriented software systems. Average distance between classes is still small, and the class of the distribution law follows the power law distribution, even in the smaller coupling degree between classes case, Sergi Valverde[2][3]. Alessandro P. S. de Moura [4] and Christopher R. Myers [5] analyzed variety of open source software, then found the software system modules, classes and methods in line with small-world model and scale-free model. Alex Potanin [6] studied object graph characteristics, and found object graph according with scale-free model. Panagiotis Louridas [7] analyzed the statistics data of languages such Java, Perl, Ruby, Tex, and the original Unix command library, the Window dynamic link library, and the FreeBSD ports system libraries. And he believed that software system did not strictly follow of the power law distribution, while the prevalence of the long tail effect. Giulio Concas [8] studied 10 kinds of distribution features Smalltalk

system, and believed that system follows the Pareto distribution, which were showed strong dependence of the organization, and demonstrate applicability Yule process.

At the software systems evolution characteristic research, S. Jenkins [9] used the directed graph to model software update process. And he used complex network segmentation method to describe software evolution properties. Kai-Yuan Cai [10] regarded the execution process of the software as evolving complex networks, by measuring the software implementation process, showing a small-world effect. Sudeikat et al. [11] analyzed the structural differences between the Object-oriented software systems and agent-oriented systems. He found the different development methods would affect the system structures. I.Turnu [12] based on Yule process, analyzed the evolution properties of four kinds of object-oriented software system.

At the software complexity metrics, Ma Yu tao et al. [13] [14] based on software metrics, compared to traditional measurement methods, some measure of system characteristics were very important. For example: the metrics of overall complexity of the system structure and behavior, which can be used to analyze and reuse of legacy systems; a class be deleted or failure of the entire system, which can be used for fault-tolerant design of the system; system organization level metrics, which can be used for the optimization of the software architecture. Jing Liu [15] proposed that using the proportion of the average spread to measure the degree of change of the software system.

To look at and research services system, the networked service system is regarded as a typical complex adaptive system from the network characteristics. Complex network theory can provide a way for service science and engineering research [16]. The research team of Seog-Chan Oh, through figure theory, using the Web service data set collected in the real world, established a number of different network topologies through flexible matching. The study found that these network topologies with small world characteristics, and to some extent, showing the power-law distribution [17].

Wei Tan, and others used the association rule mining and matrix-based search algorithm, on the basis of the myExperiment, proposed Service Map architecture, by undirected workflow-services network and directed operating networks to facilitate discovery service composition in the biological field, in order to facilitate biological experiments carried out and co-operation [18 19]. Chantal Cherifi, who through the establishment of a network based on syntax and three semantic-based networks, founded that these four networks had small world properties, but the nodes degree not showing power-law distribution. In addition, comparing the network based on syntax with semantic-based network on average path and network radius, researcher found that semantic-based network more conducive to service composition [20].

To response the new challenges networked service system, existing single theory (software engineering) and methods (object-oriented software metrics) to be ineffective, needs to be encouraged interdisciplinary convergence [21,22]. More and more researchers use service ecosystem, network thinking and generative holistic guide analysis and research networked software [1]. Therefore we may understand the structural features and behavioral characteristics of and networked service system, to break shackles of software technology development, and bottleneck of service system networked delivery.

To explore and discover a global perspective the structural properties of complex service system and the behavioral characteristics, it can provide manageable and controllable means assessment and quantitative data. For the further improvement service engineering methodology, our work maybe can expand the research point of view.

3 Service System Network Characteristics Measure Method

3.1 The Suite of Service System Network Characteristics Metrics

Service system run-time goal can be summarized as demands the following aspects:

- Open framework for aggregation of disparate services;
- Be able to shield heterogeneity network, information, resources;
- Able to respond quickly to services demand change ;
- On-demand service composition;
- Capable of supporting complete life cycle of the ecosystem;
- High service efficiency;
- Better survival.

Based on the services features and needs analysis, the authors proposed a service system metrics method and the metrics set (metrics for service system, MSS), as following table 1 shown. Service system metrics set, defines six key parameters that describe the system from the service system level. Include: Service complexity、Service coupling factors、Service cooperation relationship factor、Service node factor、Service cooperation factor and Service composition factor, namely:

$$MSS= \{SC, SCF, SCRF, SNF, SCOF, SCPF\}$$

Service system metrics and the metrics set MSS proposed six parameters, by five aspects of the complexity of the service system, service coupled, service survivability and service composability. These established a set of metrics of a service system. From the level of service system characteristics and the level combined elements to analyze the various characteristics of the system, provides an effective quantitative method and indicators for the service system managers and developers.

Table 1. Metrics service system

Metric	Abbrev-iations	Characteristics of service systems	Service system portrayed
Service complexity	SC	Complexity	The complexity of service system
Service coupling factor	SCF	Coupling	The service cohesion in net-worked system
Service cooperation relationship factor	SCRF	Survivability	The importance of the collabora-tion relationship between the services in system
Service node factor	SNF	Survivability	The importance of the service node in system
Service cooperation factor	SCOF	Composability	The stability of service collabo-ration in system
Service composition factor	SCPF	Composability	The service system hierarchy and stability of service composition

Definition 1: Service Complexity
Service system complexity (SC) is the entropy of system. SC assesses the service node complexity from a systemic perspective. The higher entropy of the system composed by the service node, indicates that the higher randomness of the service nodes organizational structure. This parameter characterizes the uncertainty of the service system structure, to assess its complexity.

$$\mathrm{SC} = -\sum_{i=1}^{n} p_i log p_i \,, i = 1 \ldots n, \tag{1}$$

Where i is the service node degree, n is the number of non-zero degree node, p_i is the probability of degree i , p_i is the probability of occurrence degree equal to i.

Definition 2: Service Coupling Factor
Service coupling factor (SCF) is the average clustering coefficient C of the service nodes in the service system. k is the degree of service node v_i, E is the actual number of edges , between the k neighbor nodes of the node v_i.

$$SCF = C = \frac{1}{\mathrm{N}}\sum_{\mathrm{i}=1}^{\mathrm{N}} C_i \;, \quad C_i = \frac{2\mathrm{E}}{k(\mathrm{k}-1)} \tag{2}$$

Definition 3: Service Cooperation Relationship Factor
Service cooperation relationship factor (SCRF) is the edge betweenness B_{mn} of relationship between the service nodes in the service system.

Services cooperation relationship factor SCRF reflects the role and influence in the entire network of collaboration services relationships (edges). According to the value, it is able to analyze the influence of any collaboration service relationship be deleted or less effectiveness, which can provide guidance for the protection and optimization of the system at run time.

All edges in the network as e_{ij} (i≠j) , there are B different shortest path between nodes, and b paths go through e_{mn} , then the connectivity impact of the edge e_{mn} in this node as g_{ki}. While e_{mn} edge betweenness B_{mn} as follows:

$$SCRF = B_{mn} = \sum_{i \neq j} \mathrm{g_{mn}(i,j)} \tag{3}$$

Definition 4: Service Node Factor
Service node factor (SNF) is service node betweenness B_k in the service system. Service node factor SNF reflects influence of the service node in the network service system. The value is capable of analyzing the influence of any service node be deleted or less effectiveness, which can be an accurate assessment of the service node importance in the system. This will provide guidance to redundant design and system services survivability guarantee.

In the networked system, service nodes couple is (i, j). There are B different shortest paths between nodes, and b paths go through node v_k, then the connectivity

impact of the node v_k for this nodes couple *(i, j)* is $B\ g_k(i\ ,\ j) = \frac{b}{B}$. While v_k node betweenness B_k as follows:

$$SNF = B_k = \sum_{i \neq j} g_k(i,j) \tag{4}$$

Definition 5: Service Cooperation Factor
Service collaboration factor (SCOF) is the service nodes connectivity correlation, *corr* $(k_i\ ,\ k_j)$, in the service system. Service collaboration factor SCOF can be used to analyze the service collaboration and hierarchy of composite services and atomic services in service life-cycle process.

$$SCOF = corr(k_i, k_j) = (k_i - \bar{k})(k_j - \bar{k})/k_i k_j \tag{5}$$

Definition 6: Service Composition Factor
Service composition factor (SCPF) is the service node degree and clustering coefficient in service system, *corr* $(k_i\ ,\ C_i)$.

$$SCPF = corr(k_i, c_i) = (k_i - \bar{k})(c_i - \bar{c})/k_i c_i \tag{6}$$

Service composition factor SCPF can be used to analyze the structure of service systems and stability in service composition. It seems that small services tend to cluster together to form stable composed services as the atom service for reuse in service composition.

Additionally, by analyzing the dependence between node's degrees and clustering coefficient of the complex network, we can conclude one principle for recognizing common services. And the principle is that in common services positive dependences between nodes' degree and minus dependences between node's degree and clustering coefficient. As the common services mostly come up in general processing, such as identification, authentication management and commutation, these services are reusable in various environment and service systems, which mean the positive dependences. And as its high reusability and lack of particularity, the common services are often not used in important business processing, which means the minus dependences.

3.2 Analysis of the Service System Network Characteristics Metrics

In this section, we will analyze the existing service system based on the network characteristics measure method and metric for service systems (MSS) which have been proposed. To simplify the processing, we make an assumption that certain web services on a specific domain can be considered as an independent service system. And then we calculate and analyze the metrics on the view of complex networks.

3.2.1 Collecting and Preprocessing in WSDL Files

In this step, it aims to collect enough data sets and filter and preprocess them for ensuring their availability to construct the service system network.

1. Gathering the data set. First, we download 1,544 files collected by Fan et al. [23] who downloaded the files form public repositories such as XMethods.org or BindingPoint.com. Second, we collect WSDL files from the repositories such as XMethods.org and WebServicelist and Google by using the keynotes "wsdl fieldtype:wsdl". At last, we have 130 WSDL files on four domains, including book, weather, finance and music.
2. Filtering the data set. We have to remove the duplicated WSDL files and make WSDL files available according to WSDL standards.
3. Preprocessing the data set. As the different naming mechanisms on the parameter's type and name, we have to do type flattening for less ambiguity on both syntax and semantic. First, we change the capital letters in the message parameter type and name to the lowercase letters. Second, we cut and abstract the parameter's type and name into a single word to facilitate calculating the similarity.
4. Collecting the input and output. In this step, we extract the parameters in the messages into inputs and output. And maybe there are several pairs of input and output in a single WSDL file.

In the information about the data set and processing is illustrated in Table 2.

Table 2. Information of the data set

Domain(Service System Type)	WSDL Downloaded	WSDL Adopted (after filtering and preprocessing)	Input and Output Extracted
book	32	27	5
weather	35	22	7
finance	30	28	14
music	33	12	3
Total	130	89	29

3.2.2 Parameter Matching and Network Construction

In this step, the association between web services (WSDL) by calculating the similarity of parameter, and we will built the service system network based on the association.

1. Parameter matching and similarity calculating. As we have extracted the input and output pairs from messages in WSDL file for a single web service, for example, for services w_i and w_j, and w_i have m inputs, the similarity between the two web services is calculated as follows:

$$\text{Similarity}(w_i, w_j) = \begin{cases} 0, \text{if } \text{Input}_i.\text{type} \neq Output_j.\text{type} \\ \sum_{i=1}^{m} \text{sim}(\text{Input}_i.\text{name}, Output_j.\text{name}), \text{ for each } Output_i.\text{type} = Output_j.\text{type} \end{cases} \quad (7)$$

And we use wordnet to calculate $\text{sim}(\text{Input}_i.\text{name}, \text{Output}_j.\text{name})$. The smaller the value is, the less similarity between the two words is.

2. Constructing the service system network. Considering the WSDL file as the node of web service, and adding the unweight and undirected link between two web services if their similarity is less than a threshold (eg. ten), we construct the service system on finance domain as the pure nodes and association of the other domain web services.

Corresponding information in this step are shown in Table 3.

Table 3. Information about parameter matching

Type of service system (domain)	Nodes with link	links number	links number with duplicated ones
book	3	6	3
weather	5	23	7
finance	9	144	31
music	2	1	1

3.2.3 Analysis and Conclusion

From Table 2, we can easily figure out that the number of WSDL files adopted is small, and the reasons include the limited use of WSDL standard, infrequency of interoperations between web services which we have collected and the limited number downloaded. And from Table 3, the average nodes and links in different domains are low, and we will analysis the finance as its considerable number of nodes and links.

By using *networkx*, we build the finance service system network, which is an undirected graph in which the node is web service and link means the interoperation. As illustrated in Figure 1, there are nine nodes and thirty-one links in the finance service system network. And its distribution of the degrees can be illustrated in Figure 2.

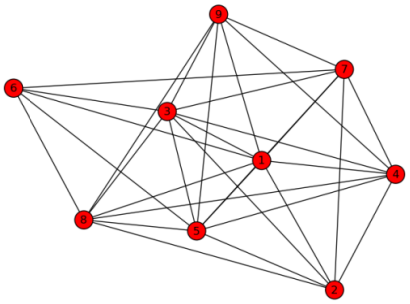

Fig. 1. The finance service system network

Then we calculate the entropy of the service system which means the SC of the system is 0.57, and its SCF is 0.86, the average path is 1.14. In the scale-free network, while there are nine nodes and three links, its SC is 0.57 and its SCF is 0.42, the average path is 1.53. And from Figure 2, we know that although the distribution of the network is not powerful, it has low average path and large clustering coefficient. There means the interoperations between web services are highly centralized and function similarity means the frequency of the interoperations at some extend.

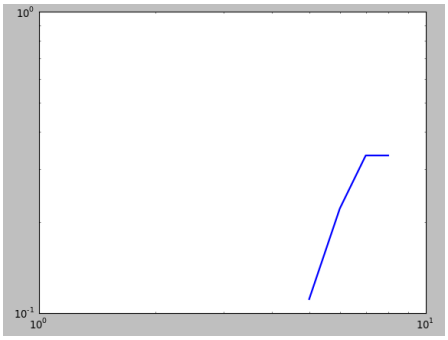

Fig. 2. The degree distribution of the network

4 Case Study

In service engineering, service has become the basic element of building a service system, In order to meet the needs of complex enterprise applications, how to effectively combine various functions in distributed network to achieve service integration to form business processes, has become an important step in the development process of the service project. Service itself is stateless [24~26], and cannot support the complex interactions between services. And meanwhile, a dynamic service composition is expected to meet the characteristics including the autonomous and loosely coupled to achieve reasonable and flexible service composition under specific service environment and demands, which determines runtime service dynamic discovery, binding and calling. Therefore, in the study of service computing, service composition is a challenging problem. Service composition is to combine multiple autonomous services through service discovery and integration of the interface based on users' needs to form new, more powerful composed services, so as to provide value-added services to consumers. Domestic and foreign scholars research different aspects of service composition on modeling language, the service composition, composite service execution, Portfolio of services authentication, and many research projects are launched, the research results are also emerging. And corresponding researches can be divided into two main aspects: QoS-based service composition and authentication in service composition.

In the environment of SaaS, users pay more attention to non-functional properties in services, such as service response time, service reliability. How to dynamically select the most suitable one for users' needs from the numerous services is widely concentrated. Among them, the QoS (Quality of Service, QoS) will become an important factor in the dynamical service selection. A highly dynamic service composition model is required to provide more available and flexible services for users and software service providers. [27]considers the performance requirements of the dynamic service composition on both service quality and the structure. It calculates QoS of the service considering the QoS evaluation model. It divides service composition into different types on the inner structure of composed service and that provides preconditions for the dynamic service selection. At last, it presents corresponding strategies on service discovery and service composition. [28] proposes a QoS-based dynamic web

services composition model, and the model supports thepublish and selection of Web services with QoS descriptionAnd through the service agent, it combines the services which meet the demands to provide candidates as large as possible. [29] proposes a web service composition algorithm based QoS while considering individual adaption, variation optimism of services and service reselection in service running. [30] proposes QoS context model for the dynamic service composition. Using the QoS feedback control mechanism, according to the user's QoS requirements, the model can provide dynamic selection, composition and operation on candidate services in changing QoS environment.[31] proposes a QoS-based web service composition framework (QWSCF) and its corresponding methods for the deployment and implementation. In [32], it proposes a quality-driven web service composition (DQos). And this model includes an extendable QoS decide mode to optimism the service selection. Current researches on service discovery and selection focus on QoS of service without considering the QoS of runtime environment and users' demands. And researches on dynamic service composition model do not consider the monitor and control of service composition. That may lead uncontrolled failure in the processing of service composition to have unavailable service composition results. And there is hardly any research in this area.

At present the formal description and verification of Web services and combinations is an important research direction in the Web service. Currently, many description languages of web service and its service composition are semi-structure which easily leads to fault hardly detected. And we need structure methods to test the correctness of service composition model. The correctness of model is the correctness in structure which means security, bounded and none dead locks. The corresponding details are described in service context. Web service composition can be described and proved in several ways. Generally speaking, current researches on web service composition proving mostly use three ways including Petri network, automaton theory and process algebra [33]. The above three ways are varied on describing way and mathematical theory, but the proving ability is same for web service composition. But there are differences on calculating costs. Adopting Petri network or automaton theory to describe service composition, it can be directly understood. But it will lead place blooming with increasing in service scale, service number and service complexity. So the complexity of the two methods will increase overwhelmingly with the increase in service scale. Meanwhile, the description of the methods based on process algebra is more powerful and concise. But as the abstraction of Pi calculus, it is not suitable for describing service composition directly as its low ability on graphical expression. Therefore, based on the study and explore the complexity of network and services system complexity metrics, In order to verify the service system to measure the feasibility of the parameter set MSS, author differs from the existing service composition algorithm, Designed based on the perception of dynamic on-demand service composition algorithm. The algorithm described in natural language as follows:

1. Generating the Initial Service Composition

(a) According to the service demands and service contract description to generate the composite service processes, service contract needs to reflect the service interface, the metric of capability, quality, capability, trust, and to reflect user needs;

(b) As illustrated in Figure 3, Service contract description (SCD) include: service interface, service capability, quality of service, service attributes, service trust. SCD realize the agreement description of the context-aware content, which is a dynamic service composition required. SCD contains five elements: $SCD= \{D_{si}, D_{sc}, D_{Qos}, D_{sa}, D_{st}\}$.

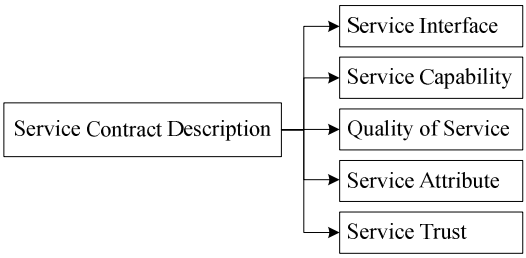

Fig. 3. Five Elements Service contract description

(c) Based on the service path structure of the SCD consistency
$SCD_{out} << SCD_{in}$ (" <<" indicates that satisfy the relation)
A service of SCD_{out} must meet the follow-up services SCD_{in}, and focus on the existing combination of path reuse;

(d) If there are a number of service paths to satisfy the SCD, the shortest path is selected. To calculate the average shortest path (d) of the alternative service paths (non-weighted case), and choose the path of least of the average shortest path to reduce small composite service response time.

$$d = \frac{\sum_{i \neq j} \mathrm{d_{ij}}}{N(\mathrm{N}-1)} \tag{8}$$

(e) To generate a service composition topology $U=<L, V>$, where L is the relationship between service to the set of edges $L=\{(v_i, v_j)\}$, V is the service node set $V=\{v_i\}$.

2. Dynamic Perception of Service

(a) To calculate the service node factor (SNF) of node sets $V=\{v_i\}$, and sort the sets of nodes by SNF : $sort\ V=\{V_i, V_j, \ldots | B_{Vi} > B_{Vj}\}$;

(b) To calculate the service cooperation factor (SCRF) of edge sets $V=\{v_i\}$, and sort the sets of edges by SCRF : $sort\ L=\{L_i, L_j, \ldots | B_{Li} > B_{Lj}\}$;

(c) According to the order of importance, perception-based Agent describe the perception of important nodes and edges (P_i), the service interface response time S_i, service capacity performance perception C_i, the quality of service value Q_i and service trust degree of T_i, form perception results, $P_i (S_i, C_i, T_i, Q_i)$.

(d) To contrast perception results P_i with the initial contract description SCD_i, and then judge whether the combination state of the running services compliance with the initial statute, in order to maintain the consistency of the service level.

$$SLA= \{ D_{si} * S_i, D_{sc} * C_i, D_{Qos} * Q_i, D_{st} * T_i \}$$

3. Updating of the Service Path

(a) Based on SLA agreements, the service path can adjust dynamically by policy mechanism, as well as system dynamic adaptive update or restore.

(b) To calculate the service path correlation to determine the stability of the service composition path.

(c) Calculate the service path of service collaboration between the various service nodes factor SCOF (Service cooperation factor) $corr\ (k_i\ ,\ k_j\ )$; come to cluster nodes in the path of the combination set the $Cluster\ V=\{\ (\ V_i,\ V_j\ )\ |\ max\ corr\ (\ k_i\ ,\ k_j\ )\ \}$;

(d) In the cluster nodes sets, to compute service composition factor (SCPF) of nodes, $corr\ (k_i\ ,\ C_i\ )$, and then obtain the stability composite services from combination paths, generate higher granularity combination of services, the next iteration as a high-granularity atomic services to be elected.

Service composition algorithm based on the perception of dynamic demand has changed the traditional dynamic service composition model only consider service QoS limitations, and introduced the SCD five-tuple, $SCD=\{D_{si},\ D_{sc},\ D_{Qos},\ D_{sa},\ D_{st}\ \}$. Algorithm attempts to measure the service interface, ability, quality, property and trust, and thereby to achieve monitor multifaceted combination services, which reflect user demands.

At the same time, the perception of dynamic on-demand service composition algorithm has introduced $MSS=\{SC,\ SCF,\ SCRF,\ SNF,\ SCOF,\ SCPF\}$, attempted to optimize service system starting from the networked characteristics. In the large-scale service systems, faced the case of that the size of the service process, more number of services, service interaction complicated, *SCRF and SNF can be used.* Using the statistical properties of complex networks, introduction the node, $sort\ V=\{V_i,\ V_j,\ldots|\ B_{Vi}>B_{Vj}\ \}$, and the edge, $sort\ L=\{L_i,\ L_j,\ldots|\ B_{Li}>B_{Lj}\ \}$, can realize monitor that the dynamic perception importance node and edge. The introduction of node connectivity correlation $corr\ (k_i\ ,\ k_j\ )$ and degree and clustering coefficient $corr\ (k_i\ ,\ C_i\ )$, can achieve the choice of cluster node sets, $Cluster\ V=\{\ (\ V_i,\ V_j\ )\ |\ max\ corr\ (\ k_i\ ,\ k_j\ )\ \}$. Large service systems stabilize composition services generate high granularity of atomic services to be selected to achieve optimization service composer efficiency.

5 Conclusion and Future Research

In this paper we first analyze the new research ideas of service system and service engineering in the networked trend. And based on network characteristics of the service system measurable goals, service metrics method and metric sets (MSS) were proposed. We identified and described six important parameters, including: service complexity, service cooperation relationship factor, service node factor, service cooperation factor, and service composition factor. And the simulation introduced the metrics method and meaning. Furthermore, this paper gave a case study by the dynamic on-demand combination algorithm based on MSS.

In the network characteristics of the service system is has just started. The authors' goal is to look at from an overall and global perspective and quantify the essential characteristics of the service system, positive and beneficial to explore the service engineering. In the future, the authors will improve the service system metrics and the metrics set. Through the data set collection and measurement, summed up a reference indication. This work can be used for the service system run-time optimization and dynamic evolution management.

Acknowledgement. This work is supported by the National Key project of Scientific and Technical Supporting Programs of China (Grant No.2008BAH24B04, 2009BAH39B03); the National Natural Science Foundation of China (Grant No.61072060); the Program for New Century Excellent Talents in University (No.NECET-08-0738); the National High Technology Research and Development Program of China(863 Program) (Grant No. 2011AA100706); the Research Fund for the Doctoral Program of Higher Education(Grant No. 20110005120007); the Co-construction Program with Beijing Municipal Commission of Education; Engineering Research Center of Information Networks, Ministry of Education.

References

1. Ma, Y.T., He, K., Li, B., Liu, Q.: Empirical Study on the Characteristics of Complex Networks in Networked Software. Journal of Software (03) (2011)
2. Valverde, S., Solé, R.V.: Scale-free networks from optimal design. Europhysics Lett. 60(4), 512–517 (2002)
3. Valverde, S., Solé, R.V.: Hierarchical small worlds in software architecture. Working Paper 03-07-044, Santa Fe Institute, Santa Fe, NM (2003)
4. de Moura, A., Lai, Y., Motter, A.: Signatures of small-world and scale-free properties in large computer programs. Phys. Rev. E 68 (2003)
5. Myers, C.: Software systems as complex networks: structure, function, and evolvability of software collaboration graphs. Phys. Rev. E 68 (2003)
6. Potanin, A., Noble, J., Frean, M., Biddle, R.: Scale-free geometry in OO programs. Communications of ACM 48(5), 99–103 (2005)
7. Louridas, P., Spinellis, D., Vlachos, V.: Power laws in software. ACM Transactions on Software Engineering and Methodology 18(1), 1–26 (2008)
8. Concas, G., Marchesi, M., Pinna, S., Serra, N.: Power-Laws in a Large Object-Oriented Software System. IEEE Transactions on Software Engineering 33(10), 687–708 (2007)
9. Jenkins, S., Kirk, S.R.: Software architecture graphs as complex networks: A novel partitioning scheme to measure stability and evolution. Information Sciences 177(12), 2587–2601 (2007)
10. Cai, K.-Y., Yin, B.-B.: Software execution processes as an evolving complex network. Information Sciences 179(12), 1903–1928 (2009)
11. Sudeikat, J., Renz, W.: On Complex Networks in Software: How Agent–Orientation Effects Software Structures. In: Burkhard, H.-D., Lindemann, G., Verbrugge, R., Varga, L.Z. (eds.) CEEMAS 2007. LNCS (LNAI), vol. 4696, pp. 215–224. Springer, Heidelberg (2007)

12. Turnu, I., Concas, G., Marchesi, M., Pinna, S., Tonelli, R.: A modified Yule process to model the evolution of some object-oriented system properties. Information Sciences 181(4), 883–902 (2011)
13. Ma, Y.T., He, K., Du, D.: A qualitative method for measuring the structural complexity of software systems based on complex networks. In: 12th Asia-Pacific Software Engineering Conference, APSEC 2005, December 15-17, p. 7 (2005)
14. Ma, Y.T., He, K., Li, B., Liu, Q., Zhou, X.: A Hybrid Set of Complexity Metrics for Large-Scale Object-Oriented Software Systems. Journal of Computer Science & Technology (06), 1184–1201 (2010)
15. Liu, J., Lü, J., He, K., Li, B., Tse, C.K.: Characterizing the Structural Quality of General Complex Software Networks. International Journal of Bifurcation and Chaos 18(2), 605–613 (2008)
16. Zhang, R., Zhu, X.: Services science overview. Electronic Industry Press (2009)
17. Kil, H., Seog-Chan, O., Elmacioglu, E., Nam, W., Lee, D.: Graph theoretic topological analysis of web service networks. WWW 21(3), 321–343 (2009)
18. Tan, W., Zhang, J., Foster, I.T.: Network Analysis of Scientific workflows: A gateway to reuse. IEEE Computer-COMPUTER 43(9), 54–61 (2010)
19. Tan, W., Zhang, J., Madduri, R., Foster, I.: ServiceMap: providing map and GPS assistance to service composition in bioinformatics. In: SCC 2011, pp. 632–639 (2011)
20. Cherifi, C., Labatut, V., Santucci, J.-F.: Benefits of Semantics on Web Service Composition from a Complex Network Perspective. In: Second International Conference on Networked Digital Technologies, Prague (2010)
21. Barabási, A.L.: Taming complexity. Nature Physics 1(2), 68–70 (2005)
22. Merali, Y.: Complexity and information systems: The emergent domain. Journal of Information Technology 21(4), 216–228 (2006)
23. Jianchun, F., Subbarao, K.: A snapshot of public web sercie. ACM SIGMOD Record 34(1), 24–32 (2005)
24. Wu, Z.H., Deng, S.G., Wu, J.: Service Computing and Service Technology. Zhejiang University Press, Zhejiang (2009)
25. Gu, Y.: SOA Principles of Service Design. Posts & Telecom Press, Beijing (2009)
26. Wang, H.B.: Service Computing Application Development Technology. Zhejiang University Press, Zhejiang (2009)
27. Liu, W., Yu, B.: QoS-based Dynamic Service Composition. Computer Technology and Development 17(5), 140–143 (2007)
28. Wang, P., Hou, H., Shan, Y.: QoS-based Web services, dynamic combination model. Computer Engineering and Design 28(10), 2494–2497 (2007)
29. Gong, X.Y., Zhu, Q.S., Wu, C.L.: Improved QoS-based genetic algorithm in Web service composition. Computer Application Research 25(10), 2922–2924 (2008)
30. Xu, X.W., Ding, Q.L.: Context-based QoS Dynamic Composition of Web services. South China University of Technology (Natural Science Edition) 35(1), 106–110 (2007)
31. Mao, Y., Le Research, J.: on QoS-Based Web Service Composition. In: Advanced Computer Control, ICACC 2009 (2009)
32. Hu, J., Guo, C., Wang, H., Zou, P.: Quality driven Web services selection. In: e-Business Engineering, ICEBE 2005 (2005)
33. Foster, H., Uehitel, S., Magee, J., Kramer, J.: A tool for model-based verification of web service compositions and choreography. In: Proceeding of the 28th International Conference on Software Engineering (2006)

AIM: A New Privacy Preservation Algorithm for Incomplete Microdata Based on Anatomy

Qiyuan Gong, Junzhou Luo, and Ming Yang

School of Computer Science and Engineering
Southeast University, Nanjing, P.R. China
{gongqiyuan,jluo,yangming2002}@seu.edu.cn

Abstract. Although many algorithms have been developed to achieve privacy preserving data publishing, few of them can handle incomplete microdata. In this paper, we first show that traditional algorithms based on suppression and generalization cause huge information loss on incomplete microdata. Then, we propose AIM (anatomy for incomplete microdata), a linear-time algorithm based on anatomy, aiming to retain more information in incomplete microdata. Different from previous algorithms, AIM treats missing values as normal value, which greatly reduce the number of records being suppressed. Compared to anatomy, AIM supports more kinds of datasets, by employing a new residue-assignment mechanism, and is applicable to all privacy principles. Results of extensive experiments based on real datasets show that AIM provides highly accurate aggregate information for the incomplete microdata.

Keywords: Incomplete data, Anonymity, Anatomy.

1 Introduction

A number of organizations publish microdata for purposes such as demographic and public health researches. For example, a hospital may release patients' diagnosis records so that researchers can study the characteristics of various diseases. The raw data, also called microdata, contains the identities and sensitive information of individuals, which may cause privacy leakage. However, simply removing the identities from microdata is insufficient due to the possibility of *linking attacks*. There may exist other attributes that can be used, in combination with an external database, to recover the identities. According to a microdata published by Group Insurance Commission (GIC) in 1990, approximately 87% of the population of the United States can be uniquely identified on the basis of their 5-digit Zipcode, gender, and birthday[1].

To reduce the risk of linking attacks, k-anonymity[2] has been proposed. A table satisfies k-anonymity if each record in the table is indistinguishable from at least $k-1$ other records. However, even with large k value, k-anonymity may still allow an adversary to infer the sensitive value of the individual with high confidence in some situations. Hence, l-diversity[3] was proposed to overcome the weakness of k-anonymity, which provides stronger privacy protection. Although

Q. Zu, B. Hu, and A. Elçi (Eds.): ICPCA-SWS 2012, LNCS 7719, pp. 194–208, 2013.

Table 1. Incomplete Microdata

ID	Age	Gender	Zipcode	Disease
1	*	Male	12000	Gastric ulcer
2	*	Male	14000	Dyspepsia
3	26	Female	18000	Pneumonia
4	28	Male	19000	Bronchitis
5	32	Male	*	*
6	39	Male	24000	Pneumonia
7	41	*	*	Flu
8	36	Female	22000	Gastritis
9	48	Female	*	Pneumonia
10	*	Female	21000	Flu

Table 2. Tradition Released Dataset

Age	Gender	Zipcode	Disease
[20,30)	Person	[15000,20000)	Pneumonia
[20,30)	Person	[15000,20000)	Bronchitis
[30,40)	Person	[20000,25000)	Pneumonia
[30,40)	Person	[20000,25000)	Bronchitis

lots of algorithms have been proposed to achieve l-diversity, few of them can handle microdata with missing values. Even worse, most of existing algorithms delete records with missing value, causing huge information loss.

1.1 Motivation

To explain the difficulty of the problem, consider a scenario that a hospital is tending to release patients' diagnosis records, meanwhile some patients do not want their personal information to be published, shown in Table 1.

Table 3. Published Data Based On Generalization

Age	Gender	Zipcode	Disease
*	Male	[10000,15000)	Gastric ulcer
*	Male	[10000,15000)	Dyspepsia
[20,30)	*	[15000,20000)	Pneumonia
[20,30)	*	[15000,20000)	Bronchitis
[30,40)	Male	*	*
[30,40)	Male	*	Pneumonia
*	Female	[20000,25000)	Gastritis
*	Female	[20000,25000)	Flu
[40,50)	*	*	Flu
[40,50)	*	*	Pneumonia

Example 1. *Patients 5, 7, 9 do not want data recipient to know their locations, so they hide their Zipcode values. Meanwhile, patients 1, 2 do not want anyone to know their ages, so they mask the age values, and so on. Then, we get a serious situation shown in Table 1, up to 60% of recodes have missing vales.*

Table 4. Published Data Based On AIM

(a) QIT

Age	Gender	Zipcode	GID
*	Male	12000	1
*	Male	14000	1
26	Female	18000	2
28	Male	19000	2
32	Male	*	3
39	Male	24000	3
41	*	*	4
36	Female	22000	4
48	Female	*	5
*	Female	21000	5

(b) SAT

GID	Disease
1	Gastric ulcer
1	Dyspepsia
2	Pneumonia
2	Bronchitis
3	*
3	Pneumonia
4	Flu
4	Gastritis
5	Pneumonia
5	Flu

If we remove all incomplete records in Example 1 like former algorithms, 60% of records will be lost, shown in Table 2. Suppressing incomplete records caused much more information loss than anonymization. Even worse, the statistics in Table 2 is totally different from Table 1, which may mislead data recipients. Obviously, situation could be worse when people are unwilling to provide their personal information. We examine a number of online datasets, most microdata published after 2002 bear high incomplete rate, some of them even up to 97%.

1.2 Contributions

We first show that traditional record suppression and generalization are insufficient for incomplete microdata, then we propose AIM, a new liner-time algorithm based on anatomy that will solve these drawbacks. Combined with a new residue-assignment mechanism, this algorithm is applicable to more kinds of datasets than anatomy. AIM treat missing values as normal value, which greatly reduce the number of records being suppressed. Compared to traditional generalization and record suppression, it ensures the same level of privacy guarantee but preserves significantly more information in microdata. To the best of our knowledge, this paper presents the first complete study on privacy preserving data publishing for incomplete microdata. Our experiments demonstrated that AIM is better than previous algorithms.

The rest of the paper is organized as follows. Section 2 formalizes the underlying concepts and the missing value problem. Section 3 presents a new linear-time algorithm for maintaining l-diversity called AIM. Section 4 experimentally demonstrates the inadequacy of existing algorithms and the effectiveness of AIM. Section 5 reviews the previous work related to ours. Section 6 concludes the paper with directions for future work.

2 Model and Notation

In this section we will introduce some basic notations that will be used in the remainder of the paper. We will also discuss how a table can be anonymized and how to measure incompleteness of microdata.

Let T be the microdata that needs to be published. T' denote the published version of T, * denote the missing value. Attributes in T are classified into 4 categories: ID, QI, SA and other attributes.

1. **Identifier Attribute(ID).** Attributes that uniquely identify an individual in microdata (e.g. Social Security Number), written as A^{id}.
2. **Quasi-Identifier Attribute(QI).** Attributes that, in combination, can be linked with external information to re-identify individuals in T (e.g. Age, Gender, Zipcode), written as A^{qi}.
3. **Sensitive Attribute(SA).** Attributes may be confidential for an individual (e.g. Disease), written as A^{sa}.
4. **Other Attributes.** Attributes do not fall into the previous three categories.

A^{id} must be removed when T' is released to the public. A^{qi} can be published in T' after anonymization. A^{sa} can be published when the attacker cannot re-identify any individual in the T'. Other attributes are not relevant to our discussion. We split T into d dimensional A^{qi} and a single A^{sa}, each $A_i^{qi}(1 \leq i \leq d)$ can be either numerical or categorical, but A^{sa} should be categorical. Following the notation of anatomy[4], for each tuple $t \in T$, we denote $t[i](1 \leq i \leq d)$ as the A_i^{qi} value of t, and $t[d+1]$ as A^{sa} value. As a result, t can be regarded as a point in a $(d+1)$-dimensional data space.

Definition 1 (Equivalence Class). *Equivalence classes (EC) for T with respect to attributes $A_i^{qi}(1 \leq i \leq d)$ is the sets of all tuples in T containing same values for each $A_i^{qi}(1 \leq i \leq d)$. We denote them as $EC_1, EC_2, ..., EC_m(1 \leq m \leq |T|)$, $\bigcup_{j=1}^{m} EC_j = T$.*

Definition 2 (L-diversity). *The published version T' is said to be of l-diversity if each EC in T' have at least l distinct SA values.*

l-diversity requires each EC to contain at least l "well-represented" sensitive values. While providing higher anonymity than k-anonymity, l-diversity causes much more information loss. Even in the suppression status, l-diversity is a NP-hard problem[5].

Definition 3 (Suppression). *Suppression refers to removing part of information in T to achieve anonymity, e.g. remove entire tuple t or some values of t.*

In some situations, some records cannot be grouped during l-diversity, which should be suppressed. In this paper, we denote suppression as a serious status of generalization.

Definition 4 (Generalization). *Generalization refer to replace specific values with their parent values in the taxonomy tree of $A_i^{qi}(1 \leq i \leq d)$.*

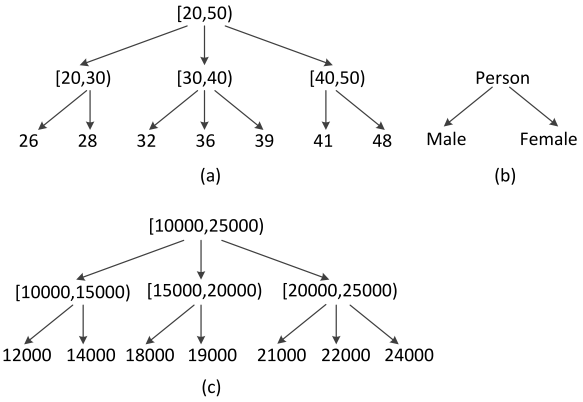

Fig. 1. Taxonomy Tree

Figure 1 shows possible taxonomy tree for age, Gender and Zipcode. In generalized Table 2, QI values are generalized to satisfy k-anonymity (k=2). For instance, tuple 3 in Table 1 is generalized to tuple 1 in Table 2. Age value 26 is generalized to [20,30), gender value Female is replace by Person, Zipcode 18000 is generalized by [15000,20000), disease value Pneumonia remains unchanged. However, due to the "curse of dimensionality"[6], generalization will lose considerable information, when the number of QI attributes is large. To overcome the weakness of generalization, Xiao et al.[4] proposed anatomy.

Definition 5 (Anatomy). *Given a l-diverse partition with m groups, anatomy produces a QI table (QIT) and a SA table (SAT) as follows. The QIT has schema*

$$(A_1^{qi}, A_2^{qi}, ..., A_d^{qi}, GID). \tag{1}$$

For group in T, $T = \bigcup_{j=1}^{m} QI_j (1 \leq j \leq m)$ and each tuple $t \in QI_j$,QIT has a tuple of the form:

$$(t[1], t[2], ..., t[d], j). \tag{2}$$

The ST has schema

$$(GID, A^{sa}, Count). \tag{3}$$

For each group $QI_j (1 \leq j \leq d)$ and each distinct A^{sa} value v in QI_j, the SAT has a record of the form:

$$(j, v, c_j(v)). \tag{4}$$

Anatomy can achieve anonymity smartly without generalization for microdata adapting l-eligible[1]. However, l-eligible is too strick for most datasets.

[1] Anatomy require the microdata satisfying l-eligible: at most n/l tuples are associated with the same A^{sa} value, where n is the cardinality of T.

Definition 6 (Information Loss Rate). *Given an microdata T and published vision T', the information loss rate of T is*

$$ILossRate(T') = \frac{ILoss(T')}{ILoss(ALL)} \tag{5}$$

where $ILoss(T')$ denotes the information loss caused by anonymization, and $ILoss(ALL)$ denotes the information loss caused by suppressing all records.

Although there are many metrics for information loss, we cannot figure out, what percentage of information are lost during anonymization. Information loss rate can help us solve this problem.

Definition 7 (Value Missing Rate). *Given an incomplete microdata T, we have*

$$VMR(T) = \frac{\sum_{i=1}^{|T|}\sum_{j=1}^{d+1} g(t_i[j])}{|T| \times (d+1)} \tag{6}$$

For each $t_i[j] \in t_i$,

$$g(t_i[j]) = \begin{cases} 1, & t_i[j] = * \\ 0, & otherwise \end{cases} \tag{7}$$

VMR denotes the proportion of missing value in T ($0 \leq VMR(T) \leq 1$). Most previous algorithms can only support datasets with $VMR(T) = 0$.

Definition 8 (Record Missing Rate). *Given an incomplete microdata T, we have*

$$RMR(T) = \frac{\sum_{i=1}^{|T|} f(t_i)}{|T|} \tag{8}$$

For each $t_i \in T$,

$$f(t_i) = \begin{cases} 1, & \sum_{j=1}^{d+1} g(t_i[j]) > 0 \\ 0, & otherwise \end{cases} \tag{9}$$

RMR denotes the proportion of records in T with missing value, all of which may be suppressed in previous algorithms. As each $t \in T$ could contain $d+1$ missing values, we have $VMR(T)/(d+1) \leq RMR(T) \leq VMR(T)$. Given a microdata with missing value, the information loss cause by suppressing incomplete records is relative to RMR.

3 Privacy Preservation for Incomplete Microdata

In this section, we first quantify the information loss of suppressing incomplete records and generalization for incomplete microdata. Then, we propose a new anonymization algorithm called AIM that overcomes all the above problem. Compared to traditional generalization and record suppression, it preserves significantly more information in microdata with the same privacy guarantee.

3.1 Record Suppression and Generalization

We first talk about the drawback of record suppression for incomplete records. As previous algorithms delete records with missing value during data pretreatment, information in these records are completely lost. Here we introduce Theorem 1.

Theorem 1. *Suppressing records with missing values will cause huge information loss rate, which equals to RMR(T).*

Proof. Let's define suppressing records with missing values as one kind of anonymization. According to the *data metric* proposed by Xiao et.al[7], suppressing a entire record will cause information loss: δ (including A^{sa}) .

$$\delta = \sum_{j=1}^{d+1} \frac{|A_j| - 1}{|A_j|} \tag{10}$$

Here $|A_j|$ denotes the domain size of A_j. Then, suppressing all records with missing value will cause $ILoss(SRMV)$.

$$ILoss(SRMV) = \delta \times \sum_{i=1}^{|T|} f(t_i) \tag{11}$$

Meanwhile, suppressing all records will cause $ILoss(ALL)$

$$ILoss(ALL) = \delta \times |T| \tag{12}$$

In the end, we define $ILossRate(SRMV)$ to denote the information loss rate for microdata.

$$ILossRate(SRMV) = \frac{ILoss(SRMV)}{ILoss(ALL)} = \frac{\sum_{i=1}^{|T|} f(t_i)}{|T|} = RMR(T) \tag{13}$$

Theorem 2. *Traditional generalization with incomplete microdata may increase VMR of the dataset.*

$$VMR(T') \geq VMR(T). \tag{14}$$

Proof. As shown in Section 1.1, generalization with missing value will lead to value suppression. Consider a scenario, when $VMR(T') = VMR(T)$, which means that only missing value is generalized together. In this special situation, T must satisfy a condition:

$$VMR(T) = \frac{\sum_{i=1}^{d} w_i |EC|}{|T|} (0 \leq w_i \leq d) \tag{15}$$

In k-anonymity, we have $|EC_i| = k$. So $VMR(T) = \frac{wk}{|T|} (w > 0)$. If T do not satisfy this condition, some of * will generalized with other values, suppressing their values. So after generalization, $VMR(T') > VMR(T)$.

As shown in Theorem 1 and Theorem 2, suppressing incomplete records and generalization with missing value will lead to considerable information loss. To avoid the drawbacks of generalization and record deletion, we introduce an improved algorithm for incomplete microdata based on anatomy (AIM). AIM can publish anonymized microdata without generalization, while minimizing the record suppression during anonymization.

3.2 AIM Algorithm

The algorithm we proposed here is an extension of anatomy. Anatomy is a popular algorithm for privacy preserving in data publication. However, anatomy supports limited number of datasets. To overcome these drawbacks, we propose AIM. Unlike anatomy, AIM supports more kinds of datasets, and can handle microdata with missing value very well.

The main difference between anatomy and AIM is that, AIM do not require the datasets to obey l-eligible, which makes it support more datasets than anatomy. AIM separates microdata into two tables: QIT and SAT. AIM first computes a l-diversity partition of T, and then, produces the QIT and SAT from the partition. Since calculation of QIT and SAT is already clarified in [4], we concentrate on finding the partition and residue-assignment. As the missing values in QI do not make sense the anatomy, we only talk about '*' in SA. We treat missing value in SA as normal value, which will be hashed to bucket with other values. Missing values in SA will help us efficiently reduce the number of records being suppressed. Concerning Table 1, our algorithm will achieve low information loss, as shown in Table 4.

Partition. Partition phase of AIM is performed in iterations, and continues as long as there are at least l non-empty buckets (Line 3). Each iteration creates a new group G_i (Line 4) as follows. First, AIM obtains a set S consisting of the l hash buckets that currently have the largest number of tuples (Line 5). Note that bucket with missing value may be selected in this step, and the selection of S may vary in different iterations. Then, a random tuple is selected (Line 7) from each bucket in S, and added to G_i (Line 8). Therefore, G_i contains l tuples with distinct A^{sa} values.

Residue-Assignment. The same as anatomy, after partition phrase, there may be at most $l-1$ buckets (Line 12). For each residue bucket S_i^r, AIM collects a set S' of groups, where no tuple has the same A^{sa} value as S_i^r (Lines 13). However, without the restraint of l-eligible (see in [4]), tuples in S_i^r may be more than one. Consequently, assignment phase of AIM is performed in iterations, and continues as long as there are at least one tuple in S_i^r and at least one group in S' (Line 14). In each iteration, AIM assigns tuple in S_i^r to a random group in S' (Lines 15-19). However, after these iterations, some tuples cannot be assigned, which must be suppressed (Lines 20). Residue-assignment phrase for AIM is more complex than anatomy. Then, we have Property 1.

Property 1. *After residue-assignment phase, each G_i has at most one missing values in SA.*

AIM algorithm

Data: Microdata T and l
Result: QIT, SAT and suppcount

```
1  QIT=∅; SAT=∅; i=0; suppcount=0;
2  hash the tuples in T by their A^sa(* included) values(each bucket per
   A^sa);
   /* Lines 3-10 are the group-creation step                          */
3  while there are at least l non-empty hash buckets do
       /* Lines 4-9 form a new group                                  */
4      i = i + 1; G_i =∅;
5      S = the set of l largest bucket;
6      foreach bucket in S do
7          remove an arbitrary tuple t from the bucket;
8          G_i = G_i ∪ {t};
9      end
10 end
   /* Lines 11-21 are the residue-assignment step                     */
11 S^r= the residue non-empty buckets(0 ≤ S^r ≤ l − 1);
12 foreach i=0 to |S^r| do
13     S'= the set of groups that do not contain the A^sa value of S_i^r;
14     while S' ≠ ∅and S_i^r ≠ ∅ do
15         t = an arbitrary tuple in S_i^r;
16         assign t to a random group G_r in S';
17         remove G_r from S';
18         remove t from S_i^r;
19     end
       /* suppress the rest tuple in |S_i^r|                          */
20     suppcount = suppcount + |S_i^r|;
21 end
   /* Line 22-30 populate QIT and ST                                  */
22 foreach j = 1 to gcount do
23     foreach tuple t ∈ G_j do
24         insert tuple(t[1],...,t[d],j) into QIT;
25     end
26     foreach distinct A^sa value v in G_j do
27         c_j(v) = the number of tuples in G_j with A^sa value v;
28         insert record(j, v, c_j(v)) into SAT;
29     end
30 end
31 return QIT and SAT;
```

Proof. In partition phase, every tuple in G_i is obtained from different hash buckets (missing value is hashed to one of buckets). Hence, each G_i have at most one missing value in SA after partition step. In the residue-assignment phase, the assignment of tuples into G_i ensures that all tuples in the group still have distinct SA values. Hence, missing value in G_i will not increase. Property 1 is correct.

Privacy Guarantee. AIM will publish a QIT and a SAT, both tables contain missing values. * in SAT was treated as normal value. Then we have Property 2.

Property 2. *After residue-assignment phase, each G_i has at least l tuples. Furthermore, all tuples in each G_i have distinct A^{sa} values.*

Proof. After the partition phase, every G_i has l tuples with distinct A^{sa} values (these tuples are obtained from different buckets). In the residue-assignment phase, the assignment of tuples into G_i ensures that all tuples in the group still have distinct SA values. Hence, Property 2 is correct.

Theorem 3. *Given a pair of QIT and SAT published by AIM, an adversary can correctly infer the SA value of any individual with probability at most $1/l$.*

Proof. According to Property 2, each G_i after residue-assignment has at least l distinct SA values (satisfying l-diversity). Following the theorem in anatomy, an adversary can correctly infer the SA value of any individual with probability at most $1/l$.

Table 5. Summary of attributes

Attribute	Number of distinct values	Generalization method (inapplicable to anatomy)
Age	74	Free interval
Work-class	8	Taxonomy tree(4)
Education	16	Free interval
Marital	7	Taxonomy tree(3)
Race	5	Taxonomy tree(2)
Gender	2	Taxonomy tree(2)
Country	41	Taxonomy tree(3)
Occupation	14	NA(sensitive)

4 Experiments

This section experimentally evaluates the effectiveness of AIM. We utilize American Census Income of 1996 (also called adult data[2]), from the UC Irvine machine learning repository. The dataset contains 48,842 records (5.5 MB), 3,620 of which have missing values. The RMR of adult data is 7.41%, and the VMR is 1.65%. All

[2] Downloadable at `http://archive.ics.uci.edu/ml/datasets/Adult`

programs are implemented in Java. All experiments were run under Linux (Ubuntu Core 11.04) on a Pentium IV 3.00GHz machine with 1.5GB physical memory.

From the adult data, we create three sets of microdata, in order to examine the influence of dataset. All attributes are listed in Table 5. Specially, "free interval" means that the generalized interval can fall on any value in the domain of the corresponding attribute. "Taxonomy tree(x)", on the other hand, indicates that the end points must lie on particular values, conforming to a taxonomy with hight x. The first set has adult-5, adult-7, respectively. Specifically, adult-d ($4 \leq d \leq 7$)treats the first d attributes in Table 5 as the QI, and Occupation as the SA. The second set has p-adult-5, p-adult-7,they do not contain missing value but violate l-eligible. The third set has e-adult-5, e-adult-7, they do not have missing value and satisfy l-eligible.

Table 6. Support for datasets

Algorithm	adult-d	p-adult-d	e-adult-d
AIM	✓	✓	✓
Anatomy	×	×	✓

We compare AIM with anatomy on three sets of dataset. For anatomy, we employ the algorithm proposed in [4]. As shown in Table 6, AIM supports all kinds of dataset, while anatomy only handles l-eligible dataset. In fairness, we try to compare AIM with anatomy on e-adult-d. However, AIM turns back to anatomy on e-adult-d. In the rest of experiment, we examine the performance of AIM.

Security. Security is the main property of privacy preserving data publishing. As show in Property 3, our algorithm will publish T' achieving l-diversity requirement. Following the privacy guarantee by l-diversity, the adversary can correctly inferring a tuple in T with a probability at most $1/l$.

Data Quality. We measure the data quality by answering aggregate queries[4] on published data, since they are the basic operations for numerous mining tasks (e.g., decision tree learning, association rule mining, etc.). Specifically, we use queries of the following form:

```
SELECT COUNT(*) FROM Unknown-Microdata
WHERE pred(A_1^qi) AND ... AND pred(A_qd^qi) AND pred(A^sa)
```

Specifically, a query involves qd random QI-attributes A_1^{qi},...,A_{qd}^{qi} (in the underlying microdata), and the sensitive attributes A^{sa}, where qd is a parameter called *query dimensionality*. For instance, if the microdata is adult-3 and $qd = 2$, then $\{A_1^{qi}, A_2^{qi}\}$ is a random 2-sized subset of {*Age,Gender,Education*}

$$b = \lceil |A| \cdot s^{1/(qd+1)} \rceil \tag{16}$$

where $|A|$ is the domain size of A. s denotes the selection proportion of dataset, and a higher s leads to more selection conditions in *pred(A)*.

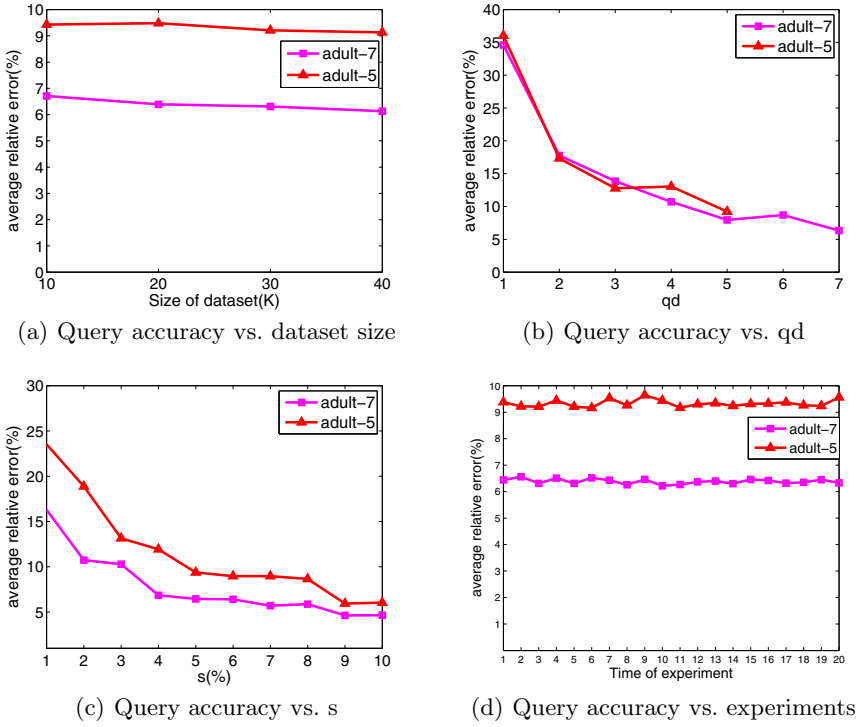

Fig. 2. Query accuracy of AIM

The first set of experiments investigates the effect of dataset size on query accuracy. Figure 2(a) examine how the accuracy of AIM scales with the dataset cardinality. AIM achieves significantly lower error for $d = 7$ in all cases, and the precision AIM improves as the size of microdata increases.

Next, we concentrate on two values of $d = 5$ and 7. For each d, we measure the accuracy of AIM using different query dimensionalities qd. Figure 2(b) plots the error of AIM as a function of qd. As expected, AIM permits significantly accurate aggregate analysis, since it captures a larger amount of correlation in the microdata. The effectiveness of AIM is not affected by d. In particular, for $d = 7$, the error of AIM is low to 6.33%. Interestingly, the error of AIM goes down when qd increases. To explain this, recall the query form of aggregate query. When qd becomes larger, the number b (Equation 16) of values queried on each attribute increases considerably, leading to a more sizable search region, which in turn reduces error.

Finally, to study the impact of query selectivity s, we examine the adult-d with $d = 5$ and 7. Figures 2(c) plots the error of both datasets as a function of s, respectively. AIM achieves lower error for $d = 7$ in all cases, and the precision of AIM improves as s increases.

Stability. Both AIM and anatomy use random variables, and aggregate queries are also computed with random variable. Figure 2(d) repeats the above experiments on adult-7 and adult-5. Notice that, the results of AIM are slightly influenced by random variable.

Efficiency. Finally, we evaluate the overhead of anonymization. As the microdata is huge, high complex algorithms will need huge time and I/O overhead. While inheriting the efficiency of anatomy, our algorithm has linear complexity O(n). AIM cost a little more I/O overhead than anatomy during residue-assignment. All experiments on adult-d can be finished within 1 second.

5 Related Work

This section surveys the previous work on privacy preserving data publishing. We will first introduce the known anonymization approaches, then review the existing anonymization principles.

Since the introduction of k-anonymity in[1,8], numerous algorithms have been proposed to achieve anonymization. These algorithms are mainly based on generalization. Samarati et al.[9] first introduced "full-domain generalization". Then, Sweeney et al.[8] developed the exhaustive search method. LeFevre et al.[10] propose the apriori-like dynamic programming approach. Specifically, a genetic algorithm is developed by Iyengar[11] and the branch-and-bound paradigm is employed on a set-enumeration tree by Bayardo[12]. These approaches, however, do not minimize information loss. Bayardo and Agrawal[6] remedy the problem with the power-set search strategy.

The above works focus on generalization. A serious drawback of generalization is that, when the number of QI attributes is large, any generalization necessarily losses considerable information in the microdata, due to the "curse of dimensionality"[6]. To overcome this drawback, Xiao et al.[4] propose anatomy, which publishes QI and SA separately. However, Anatomy support limited number of datasets. Tao et al.[13] proposed ANGEL to achieve marginal publication without generalization. Aggarwal and Yu[14] design the condensation method, which releases only selected statistics about QI-group.

Machanavajjhala et al.[3] observe the first drawback of k-anonymity. They propose l-diversity to enhance privacy protection. Meanwhile, Truta et al.[15] propose p-sensitive to overcome this drawback. Later, Li et al.[16] observed that when the overall distribution of a sensitive attribute is skewed, l-diversity does not prevent attribute linkage attacks, then they introduce t-closeness.

Several other works investigate the characteristics of anonymization principles. For example Aggarwal[6] discusses the curse of dimensionality related to k-anonymity. Meyerson et al.[17] prove two general versions of optimal k-anonymity is NP-hard, even in the suppression version. Yao et al.[18] propose a solution for checking whether a set of views violate k-anonymity. Xiao et al.[5] show that optimal l-diverse generalization is NP-hard even when there are only 3 distinct sensitive values in the microdata.

The seminal work by Mehmet et al.[19], is the first to treat incomplete data as one part of microdata, and develop a solution to handle these incomplete records. Although they consider incomplete databases in bitmap anonymization based on suppression, their results are unsatisfied because anonymization based on suppression for incomplete microdata may cause huge generalization loss.

6 Conclusions

This paper presents the first study on privacy preserving data publishing for incomplete microdata. We introduce AIM, a liner-time algorithm based on anatomy, aiming to retain more information in incomplete microdata. Different from previous algorithms, in AIM, we treat missing values as normal value, which greatly reduce the number of records being suppressed. Compared to anatomy, AIM supports more kinds of datasets, by employing a new residue-assignment mechanism, and is applicable to all privacy principles. Extensive experiments confirm that AIM permits highly accurate aggregate information on incomplete microdata.

This work also initiates several directions for future work. In this paper, we proposed the l-diversity version of AIM. Applying AIM to other principles will be an interesting topic. Furthermore, we focused on the case where there is a single sensitive attribute. Extending AIM to multiple sensitive attributes is a challenging topic. Finally, there may be other algorithms that can be modified for privacy preserving data publishing on incomplete microdata(e.g. ANGEL).

Acknowledgments. This work is supported by National Key Basic Research Program of China under Grants No. 2010CB328104, National Natural Science Foundation of China under Grants Nos. 60903162, 60903161, 61070161, and 61003257, China National Key Technology R&D Program under Grants Nos. 2010BAI88B03 and 2011BAK21B02, China Specialized Research Fund for the Doctoral Program of Higher Education under Grants No. 20110092130002, Jiangsu Provincial Natural Science Foundation of China under Grants No. BK2008030, Jiangsu Provincial Key Laboratory of Network and Information Security under Grants No. BM2003201, and Key Laboratory of Computer Network and Information Integration of Ministry of Education of China under Grants No. 93K-9.

References

1. Sweeney, L.: K-anonymity: a model for protecting privacy. Int. J. Uncertain. Fuzziness Knowl.-Based Syst. 10(5), 557–570 (2002)
2. Pierangela Samarati, L.S.: Protecting privacy when disclosing information: k-anonymity and its enforcement through generalization and suppression. In: IEEE Symposium on Research in Security and Privacy (1998)
3. Machanavajjhala, A., Kifer, D., Gehrke, J., Venkitasubramaniam, M.: L-diversity: Privacy beyond k-anonymity. ACM Trans. Knowl. Discov. Data 1(1), 3 (2007)

4. Xiao, X., Tao, Y.: Anatomy: simple and effective privacy preservation. In: Proceedings of the 32nd International Conference on Very Large Data Bases, VLDB 2006, pp. 139–150 (2006)
5. Xiao, X., Yi, K., Tao, Y.: The hardness and approximation algorithms for l-diversity. In: Proceedings of the 13th International Conference on Extending Database Technology (EDBT), New York, NY, USA, pp. 135–146 (2010)
6. Aggarwal, C.C.: On k-anonymity and the curse of dimensionality. In: Proceedings of the 31st International Conference on Very Large Data Bases, VLDB 2005, pp. 901–909 (2005)
7. Xiao, X., Tao, Y.: Personalized privacy preservation. In: Proceedings of the 2006 ACM SIGMOD International Conference on Management of Data (SIGMOD), New York, NY, USA, pp. 229–240 (2006)
8. Sweeney, L.: Achieving k-anonymity privacy protection using generalization and suppression. Int. J. Uncertain. Fuzziness Knowl.-Based Syst. 10(5), 571–588 (2002)
9. Samarati, P.: Protecting respondents identities in microdata release. IEEE Transactions on Knowledge and Data Engineering 13(6), 1010–1027 (2001)
10. LeFevre, K., DeWitt, D.J., Ramakrishnan, R.: Incognito: efficient full-domain k-anonymity. In: Proceedings of the 2005 ACM SIGMOD International Conference on Management of Data(SIGMOD), New York, NY, USA, pp. 49–60 (2005)
11. Iyengar, V.S.: Transforming data to satisfy privacy constraints. In: Proceedings of the eighth ACM SIGKDD International Conference on Knowledge Discovery and Data Mining(SIGKDD), New York, NY, USA, pp. 279–288 (2002)
12. Bayardo, R.J., Agrawal, R.: Data privacy through optimal k-anonymization. In: Proceedings of International Conference on Data Engineering (ICDE), Los Alamitos, CA, USA, pp. 217–228 (2005)
13. Tao, Y., Chen, H., Xiao, X., Zhou, S., Zhang, D.: Angel: Enhancing the utility of generalization for privacy preserving publication. IEEE Transactions on Knowledge and Data Engineering 21(7), 1073–1087 (2009)
14. Aggarwal, C.C., Yu, P.S.: A Condensation Approach to Privacy Preserving Data Mining. In: Bertino, E., Christodoulakis, S., Plexousakis, D., Christophides, V., Koubarakis, M., Böhm, K. (eds.) EDBT 2004. LNCS, vol. 2992, pp. 183–199. Springer, Heidelberg (2004)
15. Truta, T.M., Vinay, B.: Privacy protection: p-sensitive k-anonymity property. In: Proceedings of the 22nd International Conference on Data Engineering Workshops (ICDEW), Washington, DC, USA, p. 94 (2006)
16. Li, N., Li, T., Venkatasubramanian, S.: t-closeness: Privacy beyond k-anonymity and l-diversity. In: Proceedings of International Conference on Data Engineering (ICDE), pp. 106–115 (2007)
17. Meyerson, A., Williams, R.: On the complexity of optimal k-anonymity. In: Proceedings of the Twenty-Third ACM SIGMOD-SIGACT-SIGART Symposium on Principles of Database Systems (PODS), New York, NY, USA, pp. 223–228 (2004)
18. Yao, C., Wang, X.S., Jajodia, S.: Checking for k-anonymity violation by views. In: Proceedings of International Conference on Very Large Data Bases (VLDB), pp. 910–921 (2005)
19. Ghinita, G., Kalnis, P., Tao, Y.: Anonymous publication of sensitive transactional data. IEEE Transactions on Knowledge and Data Engineering 23(2), 161–174 (2011)

An Overview of Transfer Learning and Computational CyberPsychology

Zengda Guan and Tingshao Zhu*

University of Chinese Academy of Sciences, Beijing 100049, China
Institute of Psychology, Chinese Academy of Sciences, Beijing 100101, China
tszhu@gucas.ac.cn

Abstract. Computational CyberPsychology deals with web users' behaviors, and identifying their psychology characteristics using machine learning. Transfer learning intends to solve learning problems in target domain with different but related data distributions or features compared to the source domain, and usually the source domain has plenty of labeled data and the target domain doesn't. In Computational CyberPsychology, psychological characteristics of web users can't be labeled easily and cheaply, so we "borrow" labeled results of related domains by transfer learning to help us improve prediction accuracy. In this paper, we propose transfer learning for Computational CyberPsychology. We introduce Computational CyberPsychology at first, and then transfer learning, including sample selection bias and domain adaptation. We finally give a transfer learning framework for Computational CyberPsychology, and describe how it can be implemented.

Keywords: Computational CyberPsychology, transfer learning, machine learning.

1 Introduction

The internet develops rapidly and plays an important role in people's life, thus it becomes important to understand how people behave on the web. CyberPsychology focuses on the association between virtual behaviors and psychological characteristics on internet. However, most research use questionnaires to assess individual psychological traits, which is a bit time-consuming and expensive. To cope with this problem, we propose to use machine learning and other techniques to build computational models of web behavior and psychological characteristics [1], i.e., Computational CyberPsychology(CCP).

In traditional machine learning, instances in training and testing dataset are presumed to follow independent identical distribution(IID). However in CCP, it is quite often that training data(source domain) and testing data(target domain) follow different distributions, thus cannot meet the IID assumption. For this reason, traditional machine learning techniques perform poorly. Transfer learning is designed to transform data and knowledge from source domain to target domain

* Corresponding author.

Q. Zu, B. Hu, and A. Elçi (Eds.): ICPCA-SWS 2012, LNCS 7719, pp. 209–215, 2013.

to make better predictions on target domain, which motivates us to explore the possibility to adapt it on CCP.

The rest of paper is organized as follows: in Section 2, we introduce CCP and the necessity using transfer learning on CCP. We then describe transfer learning briefly in Section 3. In Section 4, we present a transfer learning framework for CCP. Finally, we conclude the paper and refer to our future work in Section 5.

2 Computational CyberPsychology

For years, psychologists have been studying the association between web behavior and psychological characteristics by questionnaires [2]. However, the self-report method can be negatively influenced by participants' subjective involvement [3]. Technically, we can obtain a large quantity of web behavior data [3], and use machine learning to build computational model for predicting users' psychological characteristics [1]. The recent research results is inspiring [1], [4].

Following a general CCP procedure, we collect web user's behaviors on the internet, preprocess and extract behavioral features, and build users' computational psychology models, which then can be used to predict psychological characteristics. Psychological characteristics include personality, mental health status, society well-being, etc. The web behavior has various types of web data, including interaction on SNS and microblogs, searching, communicating with Emails, chatting with IM, playing games and users' behaviors recoded as logs on gateway servers or browsers, and etc [3].

To build a model for identifying association between users' web behaviors and the psychological characteristics, supervised learning methods would be used as the first choice. However, if the training and test data are drawn from different feature space or different distributions, the supervised learning methods usually do not work well. In such cases, we can use information of related domains and bring in transfer learning to train a better classifier. For example, if we want to predict graduate students' personality based on their web behaviors, but unfortunately few labeled samples available. So the traditional classification methods perform poorly. Meanwhile, we have plenty of labeled data of undergraduate students. Graduate students and undergraduate students have similar on-line time, related working behaviors, and other similar web behaviors. Thus, it would be helpful for training a better classifier on graduate students that we transfer the undergraduate students' classification knowledge to the graduate students domain through transfer learning.

3 Transfer Learning

In recent years, transfer learning becomes an important research area in machine learning, which is originally introduced in NIPS95 workshop [5]. Since there is much difference in data distributions and data features between training and testing data set, traditional supervised or semi-supervised methods perform

poorly. We can make use of these different but related dataset in a transfer learning way to improve the performance of classifiers for target task. Transfer learning was defined by Pan et al. [5] as:

Definition. *Given a source domain D_S and learning task T_S, a target domain D_T and learning task T_T, transfer learning aims to help improve the learning of the target predictive function f_T in D_T using the knowledge in D_S and T_S, where $D_S \neq D_T$ or $T_S \neq T_T$.*

In the above definition, the data difference between source domain and target domain usually includes, the difference of data distributions, the difference of data features, and the difference of label criteria. In CCP, we focus on problems that source domain differs from target domain, but following the same label criteria. They consist of two types of problems: one is distribution transfer, to solve problems with different distributions between source and target domain, i.e., sample selection bias or data shifting; the other is feature transfer, for different features between source domain and target domain, i.e., domain adaptation.

3.1 Sample Selection Bias

Most distribution transfer approaches are motivated by importance sampling [5]. The distribution transfer solution is to learn the optimal value of unknown parameter by minimizing the expected risk on all instances of target domain. A common representation is as follows [5]:

$$\theta^* = \arg\min_{\theta \in \Theta} \mathbb{E}_{(x,y)\in P}[l(x, y, \theta)].$$

where x is the input sample data, y is the corresponding label, P is the labeled data set, θ is the optimal model parameters that will be determined, and $l(x, y, \theta)$ is the risk. In reality, we finally calculate $P(x_{S_i})/P(x_{T_i})$ as follows [5]:

$$\theta^* \approx \arg\min_{\theta \in \Theta} \sum_{i=1}^{n_S} \frac{P(x_{S_i})}{P(x_{T_i})}[l(x_{S_i}, y_{S_i}, \theta)].$$

where $P(x_{S_i})$ is probability of a instance in source domain, while $P(x_{T_i})$ is probability of a instance in target domain.

To estimate the ratio, Huang et al. [6] proposed a kernel-mean matching (KMM) algorithm, which directly produces resampling weights by distribution matching between training and testing sets in feature space. Sugiyama et al. [7] further proposed an algorithm Kullback-Leibler Importance Estimation Procedure (KLIEP) to estimate $P(x_{S_i})/P(x_{T_i})$ directly, which behaved well due to add an automatic model selection procedure. In CCP, we can directly apply the above framework for distribution transfer problems.

For more related recent research about data set shift, Storkey[8] represented a number of data shift models, including covariant shift, prior probability shift, sample selection bias, shift on imbalanced data, domain shift and etc. Bickel et al. [9] proposed a integrated optimization method for discriminative learning problem under covariant shift.

3.2 Domain Adaptation

To cope with domain adaptation, Blitzer et al. [10] proposed a method in Structural Correspondence Learning(SCL) framework. The method begins with extracting some relevant features(called pivot features) to bridge source and target domain. Then it constructs some auxiliary classification tasks, and obtains a projection from the original feature space to shared feature representation. Finally, it trains a classifier on augmented feature space combining the shared features and the original features. Daume III et al. [11] proposed a very easy algorithm, which put source domain feature, target domain feature and shared features into one structure, and then used a standard discriminative method to train classifiers. Chang et al. [12] argued that adaptation combining both unlabeled adaptation frameworks and labeled adaptation frameworks would perform better. These methods depend on extracting explicated or implicated common features of the two domains, but their disadvantages lie that, these common features usually can't be obtained in a simple way. So the algorithms can only be adapted to limited situations. All above algorithms were developed for NLP problems. When we deal with CCP problems, to find pivot features of SCL framework would be domain dependent, and Daume III's algorithm remind us to construct an augmented feature representation.

For another type of transfer learning called heterogeneous transfer learning where features of both domains have totally different feature spaces, there have been no general solution. However, these heterogeneous transfer learning methods may provide ideas and choices to solve some CCP problems. Yang et al. [13] proposed an algorithm, which improved unsupervised learning by transferring knowledge from auxiliary heterogeneous data and using an extended PLSA method. Zhu et al. [14] proposed a heterogeneous transfer learning framework for knowledge transfer between text and images. They used collective matrix factorization (CMF) to learn a common latent semantic space for image and text data, and trained a classifier in the new space. Argyriou et al. [15] considered a heterogeneous environment in which tasks could be divided into groups, and proposed an algorithm which could group tasks and computed a common representation for all groups in a low dimensional feature space.

4 Transfer Learning Framework for Computational CyberPsychology

Here, we propose a framework for transfer learning in CCP. Firstly, we measure web users in source domain and label their psychological characteristics such as personality through psychology assessment. Then, we collect web log and other information of these labeled users and other few-labeled users from a different domain(target domain), and preprocess the data according to researcher-defined web features. After that, transfer learning is used to learn association between data of both domains, and train a better classifier to predict what unlabeled users' psychological characteristics are.

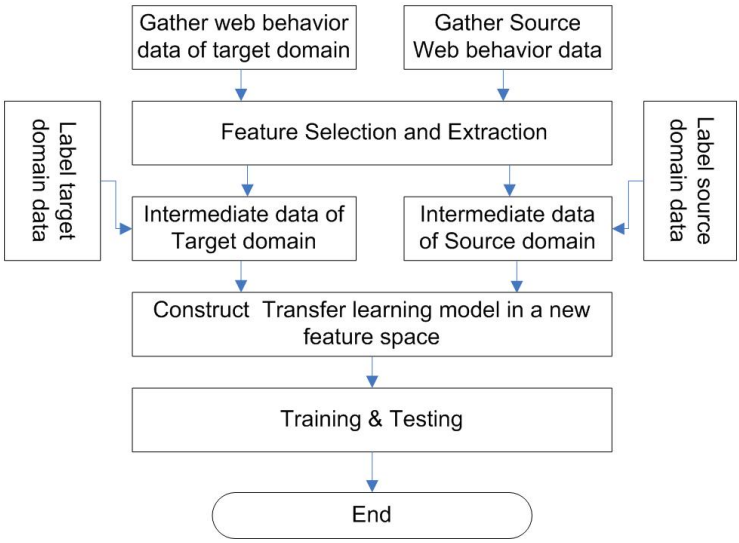

Fig. 1. A procedure of a transfer learning framework

We show a general framework to do transfer learning for CCP in Fig. 1, in which various transfer methods can be analyzed and compared more conveniently and more completely. The framework is as follows:

$$\min_{w_t, w_s, \Phi} R(x_t, y_t, w_t) + \mu R(\Phi(x_s, y_s, w_s, x_t, y_t, w_t)) + \lambda \|(w_t, w_s, \Phi)\|_f.$$

Where x_t, y_t and w_t, is the sample, the responding label, and the parameter that will be learned in target domain, x_s, y_s and w_s is x_t, y_t and w_t's correspondence in source domain, μ and λ are ratio-constant terms, Φ is a transfer function or transfer operator, and $\|(w_t, w_s, \Phi)\|_f$ is a f-norm of combining w_t, w_s, Φ. There are three parts separated by sign "plus". The first part represents a risk function over inadequate labeled samples in the target domain, which can be acquired by supervised learning. The second part is transfer risk, and it represents distribution-transfer risk and feature-transfer risk. The third part controls the complexity of transfer and training function, and it is often regarded as a regular term. In some particular situation, the equation should be adapted or just simplified.

We can utilize transformations of those methods described in Section 3 to apply this transfer learning framework. As the graduate example in Section 2, if graduate students and undergraduate students have identical features, but different distributions, we would choose distribution transfer methods to solve the problem. In fact, we should firstly test whether distributions of both domains are identical by T-test or other method. If they are identical, then supervised learning can meet the requirement. Otherwise, we can try using Sugiyama's

method or other method to represent transfer risk for this problem. We usually face the situation that users in target domain are labeled only a few, and these users data can put into the first part to work. As to the third part, it indicates a prior of the optimal model parameters, or can be omitted.

Another example, suppose we collect users' web-behavior data and extract feature information from social network sites (SNS) and gateway independently, and use these data to predict users' personality. Gateway has much less samples than SNS and is taken as the target domain, while SNS is the source domain. In this case, the features from each domain have different categories. Facing this problem, we can introduce extend PLSA method to transfer data from the original features space to a common latent variable representation, and then train a model over both domains under the transfer risk. In addition, we represent the transfer (function) complexity and training function complexity over latent variable representation in the third part. Much more, if there are some features in both domains having equivalent semantics, we can apply Daume III's method in some way.

5 Conclusion

CCP concerns about users' psychology characteristics through their web behaviors. Due to the complexity of web psychological phenomenon, it brings many challenges to machine learning especially transfer learning. We discussed the necessity of transfer learning for CCP, gave an overview about CCP, briefly surveyed sample selection bias issue and domain adaptation issue in transfer learning, and finally gave a transfer learning framework for CCP. In the future, we will construct a more specific transfer learning framework for CCP, and develop new transfer learning algorithms corresponding psychological analysis methods.

Acknowledgment. The authors gratefully acknowledges the generous support from NSFC(61070115), Research-Education Joint Project(110700EA02) and 100-Talent Project(110700M202) from Chinese Academy of Sciences.

References

1. Zhu, T., Li, A., Ning, Y., Guan, Z.: Predicting Mental Health Status Based on Web Usage Behavior. In: Zhong, N., Callaghan, V., Ghorbani, A.A., Hu, B. (eds.) AMT 2011. LNCS, vol. 6890, pp. 186–194. Springer, Heidelberg (2011)
2. Hamburger, Y.A., Ben-Artzi, E.: The relationship between extraversion and neuroticism and the different uses of the internet. Computers in Human Behavior 16, 441–449 (2000)
3. Li, Y., Zhu, T., Li, A., Zhang, F., Xu, X.: Web Behavior and Personality: A Review. In: 3rd International Symposium of Web Society (SWS), Port Elizabeth, South Africa (2011)
4. Zhu, T., Ning, Y., Li, A., Xu, X.: Using Decision Tree to Predict Mental Health Status based on Web Behavior. In: 3rd International Symposium of Web Society (SWS), Port Elizabeth, South Africa (2011)

5. Pan, S.J., Yang, Q.: A Survey on Transfer Learning. IEEE Transactions on Knowledge and Data Engineering 22(10) (2010)
6. Huang, J., Smola, A., Gretton, A., Borgwardt, K.M., Scholkopf, B.: Correcting Sample Selection Bias by Unlabeled Data. In: Proc. 19th Ann. Conf. Neural Information Processing Systems (2007)
7. Sugiyama, M., Nakajima, S., Kashima, H., Buenau, P.V., Kawanabe, M.: Direct Importance Estimation with Model Selection and its Application to Covariate Shift Adaptation. In: Proc. 20th Ann. Conf. Neural Information Processing Systems (2008)
8. Storkey, A.: When Training and Test sets Are Different: Characterizing Learning Transfer. In: Dataset Shift in Machine Learning, pp. 3–28. MIT Press (2009)
9. Bickel, S., Bruckner, M., Scheffer, T.: Discriminative Learning under Covariate Shift with a Single Optimazation Problem. In: Dataset Shift in Machine Learning, pp. 161–177. MIT Press (2009)
10. Blitzer, J., McDonald, R., Pereira, F.: Domain Adaptation with Structural Correspondence Learning. In: Proc. Conf. Empirical Methods in Natural Language, pp. 120–128 (2006)
11. Daume III, H.: Frustratingly Easy Domain Adaptation. In: Proc. 45th Ann. Meeting of the Assoc. Computational Linguistics, pp. 256–263 (2007)
12. Chang, M., Connor, M., Roth, D.: The Necessity of Combining Adaptation Methods. In: Proceedings of the 2010 Conference on Empirical Methods in Natural Language Processing, pp. 767–777 (2010)
13. Yang, Q., Chen, Y., Xue, G., Dai, W., Yu, Y.: Heterogeneous transfer learning for image clustering via the social web. In: Proceedings of the 47th Annual Meeting of the ACL and the 4th IJCNLP of the AFNLP, pp. 1–9 (2009)
14. Zhu, Y., Chen, Y., Lu, Z., Pan, S.J., Xue, G., Yu, Y., Yang, Q.: Heterogeneous Transfer Learning for Image Classification. In: Proceedings of the Twenty-Fifth AAAI Conference on Artificial Intelligence, pp. 1304–1309 (2011)
15. Argyriou, A., Maurer, A., Pontil, M.: An Algorithm for Transfer Learning in a Heterogeneous Environment. In: Daelemans, W., Goethals, B., Morik, K. (eds.) ECML PKDD 2008, Part I. LNCS (LNAI), vol. 5211, pp. 71–85. Springer, Heidelberg (2008)

A Formal Approach to Model the Interaction between User and AmI Environment

Jian He[1] and Fan Yu[2]

[1] School of Software Engineering, Beijing University of Technology, Beijing 100022, China
Jianhee@hotmail.com
[2] Cyber Object Corp, Suite 530 Norcross, 6525 The Corners Pkwy, Atlanta, Georgia 30092, USA
yufan21cn@gmail.com

Abstract. According to the decentralization of modeling tasks caused by user who is essentially nondeterministic and highly individual in Ambient Intelligence (AmI) environment, the mental model, plan model and behavior model are introduced to describe both static features and dynamical behavior of user in AmI environment. With the interactive model based on multi-agent, a formal approach to model user is proposed at first. Meanwhile, the relations between agents and AmI system are discussed in detail. The path which maps the natural scenario of an AmI environment into a real system shows that our models can help designers capture user's static features and dynamic behavior, and these relations between agents and AmI system can help designer to manage and track AmI system from its requirements to implementation through as well.

Keywords: Ambient Intelligence, multi-agent, knowledge, interactive model.

1 Introduction

The concept of Ambient Intelligence is presented by the Information Society Technology Advisory Group (ISTAG). It describes a vision of the information society where the emphasis is on greater user friendliness, more efficient services support, user-empowerment and support for human interactions [1]. Since the complexity associated with the varieties and uses of computer-based artifacts requires that researchers should design and develop a system that lets intelligence disappear into the infrastructure of AmI system, and automatically learns to carry out everyday tasks based on the users' habitual behavior [2]. The AmI system has introduced new research challenges in the field of distributed artificial intelligence.

An agent is an abstract of a real system, which can independently carry out some actions in order to achieve its design performance. In general, an agent has the characters of entity, autonomy, cooperation, reaction and intelligence. So agents are naturally introduced to build AmI systems. However, agents that operate in such environments are probably expected to have different goals, experiences and perceptive capabilities, limited computation capabilities, and use distinct vocabularies to describe their context [3]. It is very hard for them to typically know a priori all other entities

Q. Zu, B. Hu, and A. Elçi (Eds.): ICPCA-SWS 2012, LNCS 7719, pp. 216–230, 2013.

that are present at a specific time. So far, AmI systems have not managed to efficiently deal with these challenges. As it has been already surveyed in [4], most of them follow reasoning approaches that assume perfect knowledge of context, failing to deal with inaccurate or dynamic information. Regarding the distribution of reasoning tasks, a common approach followed in most systems assumes the existence of a central entity, which is responsible for collecting and reasoning with all the available context information [5]. However, AmI systems have much more demands, especially on user's natural interaction. User in AmI environment is essentially nondeterministic and highly individual. The deference in user's habitual behavior, knowledge and interests require researchers not only model the user's static characters, but also dynamic behavior. This inevitably leads to the decentralization of modeling tasks. As a result, it is very necessary to find a way that help researcher model user's static features and dynamic behaviors, and map AmI system into different agents conveniently.

The rest of the paper is structured as follows. Section 2 presents background information and an interactive mode based on multi agent. Section 3 introduces three models to cooperatively describe user's static features and dynamic behaviors so as to formal model the interaction between user and AmI system. Section 4 deeply describes the relations between agent and AmI system in order to help researchers conveniently develop AmI system. Section 5 the path of mapping from the natural scenario of an AmI environment into a real system (namely AmI-Space) is outlined. The last section summarizes the main results and discusses future work.

2 Related Work

2.1 Background

At present, AmI is still an open research field, not bounded for what certainly concerns topics of interest and related issues. Despite of this, lots of intelligent environments have been built up by some famous institutes and universities to demonstrate intelligent space solutions. Most of these projects initially focus on realizing prototypes or scenarios to show the potentiality of this technology. The first AmI system presented by Trivedi et al. uses several cameras and microphones to acquire information on the surrounding environment [6]. The Oxygen project developed at Massachusetts Institute of Technology (MIT) shows computational power will be freely available everywhere, not be necessary to carry computers or personal communication terminals to access it [7]. More recently, at the Artificial Intelligence Lab, MIT, an intelligent room has been designed and developed to research on natural and reliable vocal interfaces, context specific user-transparent system reactions, dynamic resource allocation, and natural cooperation among different contiguous environments [8], [9]. At the Georgia Institute of Technology, a long-term research group is developing a project called the Aware Home Research Initiative (AHRI) to address the fundamental technical, design, and social challenges presented by the creation of the context-aware home environment [10], [11]. The RUNES [12] supported by the 6th Framework Program (FP6) puts more attention on the creation of large scale, widely distributed and heterogeneous embedded systems that can interoperate and adapt to the environments. The RUNES is based on the component technology, and quite suitable for the disaster management, industrial control and automation.

The computing units in AmI system have features of modularization, distribution and complexity, which is quite suitable to be modeled by Agent. Hence, more and more AmI systems are designed and developed based on agent. Project DALICA [13] supported by the FP6 introduces multi-agent system (MAS) to model the cultural-assets-fruition (CAF) scenario, and a hierarchical structure is designed to satisfy the application goal. The AMIGO [14] also supported by FP6 focuses to develop open and interoperable middleware and intelligent services for the home environment. Meanwhile, it aims to offer users intuitive, personalized and unobtrusive interaction by providing seamless interoperability of services and applications. The Essex intelligent dormitory uses embedded agents to create the AmI system which has the ability of learning user behavior and adapting to user needs [2]. ScudWare [15] synthesizes the multi-agent, context-aware and adaptive component technology to build a semantic and adaptive middleware platform for intelligent space in vehicles. It supports autonomy, adaptability, scalability and semantic integration. Smart Classroom developed by Tsinghua University [16] also uses agent to model each module that has its own goal and cooperates with others. A software architecture based on multi-agent for AmI system is proposed in AmI-space, and message-oriented middleware (MOM) is developed to support the communication and data transmission among agents [17][18].

Nowadays a major focus in AmI is in recognizing human activity in the smart environments. There are lots of papers recognizing a variety of human activities such as medicine taking [19], tracking movement in a house [20], and micro-payments [21] in recent Ubicomp, Pervasive Computing and Ambient Intelligence conferences. The ability to model user's activities of daily living and to accurately infer the intent from user's behavior is the holy goal of AmI. However, the ability of accurately modeling user's behavior is limited at present to simple activities and intent cannot be sufficient inferred [22]. While developing and evaluating ambient intelligent systems, a formal model can help researchers pay attention to outlining the boundary of what can be built, and building more interesting applications.

2.2 Interactive Model between User and the AmI System

How do we ever think of seeing a given object? The answer can be described in terms of two key roles, the organism and the object, and the relationships which those roles hold in the course of their natural interactions. Here, the organism in question can be considered as the AmI system, whereas the object is the user so that we can concentrate on modeling the interaction between user and AmI system. The relationships between organism and object are the contents of the knowledge.

User is surrounded by smart devices in AmI environment, so it is natural to introduce agent to model the interaction. A software architecture based on multi-agent is proposed in AmI-Space [17]. Meanwhile, biologically inspired by neurobiological model [23] [24], a multi-agent-based interactive model is designed. Fig. 1 shows it.

As can be seen from Fig. 1, user interacts with AmI system through *portable devices*, *wearable sensors* and *embedded sensors*. Both *Mobile Agent* and *Multi-sensor Agent* transfer the interactive information to the *Context-ware Agent* which devotes to the analysis of heterogeneous data and the generation of contextual information. *Database Agent* is responsible for the storage under the form of long-term data produced by *Context-ware Agent*. Some of the context relating with user's interactive

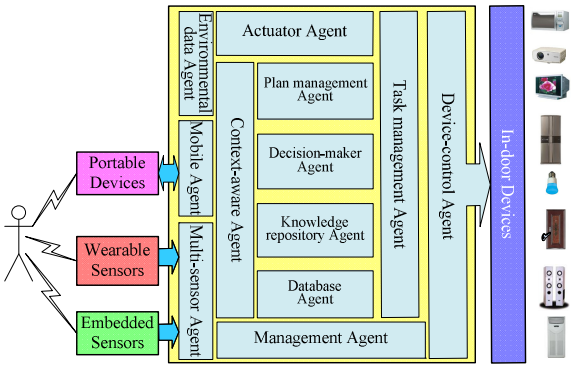

Fig. 1. The interactive model between user and AmI system

policy transform into rules of plan for the *Plan management Agent*. Other context relating with user's habitual behaviors forms knowledge for higher level *Knowledge repository Agent*. Both *Plan management Agent* and *Knowledge repository Agent* constitute of growing experience that can be implemented with associative techniques [25].

The *Decision-maker Agent* produces action sequence for *Task management Agent* which dispatches actions to different *Device-control Agent* according to the resource states. The decision-making step takes place in a decision engine that can be represented by a rule-based system [26]. To provide its results, the decision logic also relies on the direct observations form *Context-aware Agent,* on new predicting data from *Plan management Agent*, *Knowledge management Agent* and on the past data provided by *Database Agent*. The decisions for internal environment can be transferred to *Actuator Agent* which directly controls mechanical tools, such as thermostatic devices, or physical part of the doors to open or close.

The Management Agent is responsible for the communication and data transmission among agents through multimode communication channel based MOM [18]. The Environmental data Agent monitors the internal parts of the AmI system (such as heat and light), and transforms environmental variables to Context-aware Agent which analyze the relation between environmental (external) events and internal state condition.

Since the user and agents are the key roles in the AmI environment, the way to model user and the relation between agent and AmI system are discussed successively.

3 Model User in AmI Environment

Different user shows different mental and behavior features during the interaction with the AmI system, due to the difference in individual character, knowledge background and habitual behavior. The traditional AmI model which describes user's features in a coarse granularity is very hard to describe user's mental activities and behavior transition. We introduce mental model, plan model and behavior model to cooperative describe user's static features and dynamic behaviors. Each model cooperates with other models. Fig. 2 shows the relations among different models. Among them, *MS'* is a mental state, *plan_effect* is the effect after executing the plan, and *behavior_effect* is the effect after doing the behavior. *m* is an element of *M* which is a set of variable about the environment. *M* can be considered as a message queue.

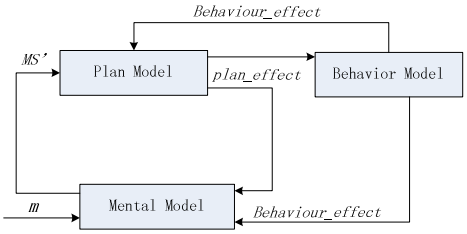

Fig. 2. Relations among the models

3.1 Mental Model

Referring to the BDI model in artificial intelligence [27][28], The mental model of user in AmI environment is composed of a mental state set MS which can be defined as 7-tuples.

MS=< *M, G, T, B, I, K, R*>, then

G: G×*T*×*M*→*G*, *G* is a set of goal which describes objectives to be accomplished. Since the goal of user is dynamically changed according to the time and environmental event, *G* is a function of time and environmental event. The set of goal is automatically generated by tracking the change of goal.

B: B×*T*×*M*→*B*, *B* is a set of user's belief which embodies user's knowledge about the environment. The user's belief is always changed according to the time and environmental event, so *B* is a function about time and environmental event. The set of belief is automatically produced by recording the change of belief.

I*: I*×*T*×*M*→*I*, *I* is a set of user's intention which describes the currently chosen course of action. Because the user's intention is dynamically changed according to the time and environmental event, *I* is a function about time and event of environment. The intention set is automatically generated by tracking the change of intentions.

K: K×*T*×*M*→*K*, *K* is knowledge repository which consists of information about user's experience. It is a function about time and user's experience. Since the user's knowledge is dynamic updated along with the time and interaction, the knowledge repository is automatically modified by tracking the change of knowledge.

User's mental state is unstable. It always transits from one state to another when user interacts with the AmI system. For instance, user often stops doing exercise when he is attracted by a video during the period of exercise in AmI environment. We introduce a tetrad <MS^0,*next_act*,*next_ms*> to describe the transition of user's mental state, and each element is defined as follows.

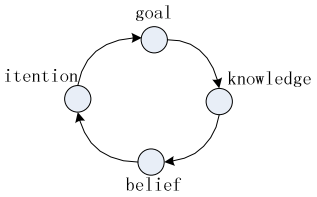

Fig. 3. The transition between the elements of the mental model

User's mental state is unstable. It always transits from one state to another when user interacts with the AmI system. For instance, user often stops doing exercise when he is attracted by a video during the period of exercise in AmI environment. We introduce a tetrad $<MS^0,next\_act,next\_ms>$ to describe the transition of user's mental state, and each element is defined as follows.

MS^0 is the initial state of the mental state, which is composed of goal, belief, intention and knowledge.

next_act : $MS \times ACT \rightarrow ACT$. *next_act* is a function which selects an action from atomic action sets according to current mental state.

next_ms : $MS \times ACT \rightarrow MS$ *next_ms* is a function which generates the next new mental state according to the finished action.

The scripts describing the flow of the mental state transition is as follows.

```
Step1: MS^0 = InitMetalState(), n=0;
Step2: a=next_act(MS^n);
Step3:Do(a);
Step4:MS^(n+1)=next_ms(MS^n, a),n=n+1;
Step5:goto step2.
```

3.2 Plan Model

User should always consider about the mental state, the goal and the available resources at first, and then makes a plan which specifies both the means of achieving the goals and the available options, so as to execute actions and accomplishes the goal. According to the model presented by presented by CHEN Jian-zhong *et al* [29], user's plan can be described as a tetrad *Act_plan*.

Act_plan=<plan_goal, plan_premise, plan_body, plan_result>, then
plan_goal is the goal of actions.
plan_body is a sequence of actions or scripts of actions.
plan_premise is the preconditions for the *plan_body*.
plan_resul is the expected effect after executing the *plan_body*. When the *plan_premise* is satisfied, the *plan_body* will be executed and produce new state and effect. The BNF expression of the *Act_plan* is as follows.

Act_plan::= <plan_goal><plan_premise> <plan_body> <plan_result>
plan_goal::= goal_list;
plan_premise::= resourse_list and *knowledge_list;*
resource_list::= any resource element or *a subset of the resource;*
knowledge_list::=any knowledge element or *a subset of the knowledge repository;*
plan_body::= act_list || *<plan_exp>*;*
act_list::= any action or *a subset of the actions*;
plan_exp::= event_list;
plan_effect::=effect_list;
effect_list::= any element or *a sub set in the effect set.*

"*<a>*" means one or many of *a*. "*" means iteratively composite. "||" means concurrence. *goal_list* is a list of goal description. *resourse_list* is a list of resource

description. *knowledge_list* is a list of knowledge description. *act_list* is a list of the action description. *result_list* is a list of effect description according to the action. *event_list* is a list of environmental event.

3.3 Behavior Model

User generally selects and executes an action sequence according to the plan made before interaction so as to achieve the goal. Therefore, the behavior model can be defined as a 5-tuples BM.

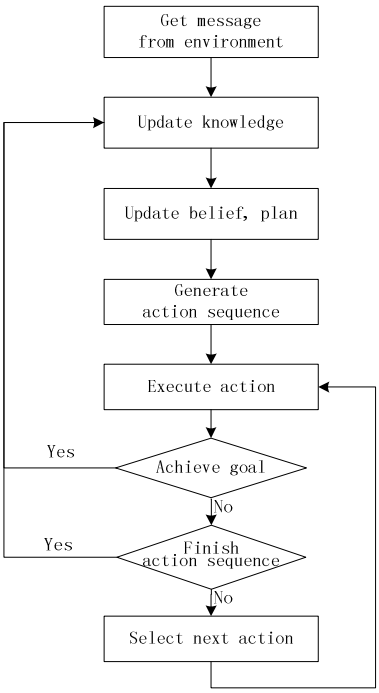

Fig. 4. Flow chart of three models cooperation together

$BM=<Q,\Sigma,\delta,q_0,F>$, then

Q is a definite set which specifies all possible actions of user.

$\Sigma=MS\times PS$ Σ is a definitely alphabetic list which is a Cartesian product of *MS* (the set of mental state) and *PS* (the set of plan).

$q_0 \in Q$, q_0 is one of initial actions for users.

$F \in Q$, F is a set of final actions for users.

δ is a transition function ($Q\times\Sigma\rightarrow Q$), which outputs new actions for user.

Though the mental model, plan model and behavior mode are separately introduced to describe user's static features and dynamic behavior clearly, they cooperate with each

other to accomplish the interaction between user and AmI system. Fig. 4 is the flow chart of which these models cooperatively achieve the interaction.

During the realization of AmI system, the three models can be mapped into different agents. For example, in Fig. 1, they are mapped into Plan management agent, Knowledge repository agent, Data agent and Decision-maker agent. However, in AmI-Space [17], besides Data agent, the Smart agent implements most functions of three models.

4 The Relations between Agent and AmI

Since AmI system finally is composed of different agents. Finding the clear relations between agents and AmI system is very helpful for successfully developing the system. During the development of an AmI system, there always should be goals which define objectives to be accomplished, plans which describe policies to achieve goals, function specifications which specify functions or services provided by the AmI system. An AmI system can be regarded as a tetrad *AE*.

AE =<*G, P, F, R*>, then
G is a set of goals of the AmI system;
P is a set of plans of the AmI system;
F is a set of functions of the AmI system;

R is the relations between different agents in AmI system. Generally there are 3 kinds of relations between two agents: *Negotiation relation of* which means two agents have different goal, and need to negotiate about some resource so as to achieve each goal respectively. *Help relation* of which means two agents have common goal, and need to help each other so as to achieve the goal. *Peer relation* of which means two agents have different goal, and can work independently at the same time.

Given *AS* is the set of agents in AmI system, we candescribe the relations between AmI system and agents according to the aspects of goal, plan and function.

4.1 Goal Relation between Agent and AmI System

Given $agent_i$ is a member of *AS*, g_i is a goal of $agent_i$, and *G* is the set of goals of the AmI system. The goal relation between $agent_i$ and AmI system is as follows.

Compatibile-goal If any goal of $agent_i$ is a member of *G*, then the relation is called *Compatibile-goal*.

Conflicting-goal If there is a goal of $agent_i$ which is not a member of *G*, then the relation is called *Conflicting-goal*.

And-goal The *g* being a member of *G* is achieved iff $agent_i$ accomplishes g_i. Namely, *g* depends on g_i, it is marked as $AndG(g, g_i)$.

Or-goal If $agent_i$ accomplishes g_i, then AmI system achieves *g* being a member of *G*. That is, there is a *OR* relation between g_i and *g*, and it is marked $OrG(g_i, g)$.

Structure-goal There is a *and/or* tree between the set of goals of AmI system and the set of goals of its agents. The *and/or* tree has some unique features.

a) The relation between any child node and its parent node is either *and-goal* or *or-goal*.

b) The root node of the *and/or* tree embodies of the total goals of AmI system. Traversing all the child nodes provides a resolution to disassemble the total goals of the AmI system into different sub-goals accomplished by its agents.

c) The leaf node means that the goal can be achieved by a specific agent alone in AmI environment.

d) The other node between root and leaf means that the goal should be cooperatively achieved by multiple agents.

Based on those goal relations, we can draw three properties about the goal relation.

Completeness: if $G = \bigcup_{agent_i \in AS} g_i$, then the relation is called completeness.

Incompleteness: if $G \supset \bigcup_{agent_i \in AS} g_i$, then the relation is called incompleteness.

Redundancy: if $G \subset \bigcup_{agent_i \in AS} g_i$, then the relation is called redundancy.

4.2 Plan Relation between Agent and AmI

Given $agent_i$ is a member of AS, p_i is a plan of $agent_i$, and P is the set of plans of the AmI system. The plan relation between $agent_i$ and AmI system is as follows.

Compatibile-plan If any plan of $agent_i$ is a member of P, then the relation is called *Compatibile-plan*.

Conflicting-plan If there is a plan of $agent_i$ which is not a member of P, then the relation is called *Conflicting-plan*.

And-plan The p being a member of P is achieved iff $agent_i$ has the the plan p_i. Namely, p depends on p_i, it is marked as $AndP(p, p_i)$.

Or-goal If $agent_i$ has the plan p_i, then AmI system has p being a member of P. That is, there is a *OR* relation between p_i and p, and it is marked $OrP(p_i, p)$.

Structure-plan There is a *and/or* tree between the set of plans of AmI system and the set of plans of its agents. The *and/or* tree has some unique features.

a) The relation between any child node and its parent node is either *And-plan* or *Or-plan*.

b) The root node of the *and/or* tree embodies the total plans of AmI system. Traversing all the child nodes provides a resolution to divide the total plans of the AmI system into detail plans of its agent.

c) The leaf node means that the plan applies to the specific agent alone in AmI environment.

d) The other node between root and leaf means that the plan can be refined to for different agent.

Based on those plan relations, we can draw three properties about the plan relation.

Completeness: if $P = \bigcup_{agent_i \in AS} g_i$, then the relation is called completeness.

Incompleteness: if $P \supset \bigcup_{agent_i \in AS} g_i$, then the relation is called incompleteness.

Redundancy: if $P \subset \bigcup_{agent_i \in AS} g_i$, then the relation is called redundancy.

4.3 The Function Relation between Agent and AmI

Given $agent_i$ is a member of AS, f_i is a function of $agent_i$, and F is the set of functions of the AmI system. The function relations between $agent_i$ and AmI system is as follows.

Compatibile-function : If any function of $agent_i$ is a member of F, then the relation is called *Compatibile-function*.

Conflicting-function: If there is a function of $agent_i$ which is not a member of F, then the relation is called *Conflicting-function*.

And-function The f being a member of F is achieved iff $agent_i$ accomplishes f_i. Namely, f depends on f_i, it is marked as *AndF(f, f_i)*.

Or-function If $agent_i$ accomplishes f_i, then AmI system achieves g being a member of G. That is, there is a *OR* relation between g_i and g, and it is marked *OrG(g_i ,g)*.

Structure-function There is a *and/or* tree between the set of functions of AmI system and the set of functions of its agents. The *and/or* tree has some unique features.

a) The relation between any child node and its parent node is either *And-function* or *Or-function*.

b) The root node of the *and/or* tree embodies the total functions of AmI system. Traversing all the child nodes provides a resolution to accomplish the total functions of the AmI system.

c) The leaf node means that the function can be accomplished by the specific agent alone in AmI environment.

d) The other node between root and leaf means that the function can be refined and cooperatively implemented by multiple agents.

Based on those function relations, we can draw three properties about the function relation.

Completeness: if $F = \bigcup_{agent_i \in AS} f_i$, then the relation is called completeness.

Incompleteness: if $F \supset \bigcup_{agent_i \in AS} f_i$, then the relation is called incompleteness.

Redundancy: if $F \subset \bigcup_{agent_i \in AS} f_i$, then the relation is called redundancy.

5 Application

In this section, the path from the natural scenarios to a real AmI system (AmI-Space) is outlined to show how to use our model to guide the development of AmI system.

5.1 AmI-Space Scenarios

In AmI-Space, there are different kinds of electric appliance (such as TV, fridge, microwave oven, projector, etc.), which are distributed in different areas in invisibly computing form and can provide user with service automatically. As soon as the user enters into the AMI-Space, the authentication system for AmI will automatically authenticate the user. After authentication, the system searches the user database, obtains the user privilege and historical experiences. Then the system analyzes such data and environmental data, and generates a list of personalized services according to the service policy. The list of personalized services is pushed to user's PDA through WLAN. The facial orientation recognition (namely FO) system will verify the user's face orientation, and instruct the projector to projects the content of service to the wall against user's face as soon as user selects an service items through the PDA, The air condition will turn on and adjust the rooms' temperature according to the environmental temperature and user's favorite. At last, on user's departure from the environment, the AmI Center will sense this event, stop the service and log the user out.

5.2 User Model in AmI-Space

In AmI-Space, the mental model describes static data coming from user and environment, and the objective the user wants to achieve. It is mapped into database which store the static data about user and environment, and knowledge repository which stores user's historical experience and potential objective. Besides, the sequence diagram is introduced to describe the transition of mental state. The plan model describes the policy of which services are provided by the system. It is mapped into a smart planner which is mainly composed of Knowledge repository and a rule set of plan. The behavior model depicts the dynamic behavior of user which is mainly mapped into action sequence, decision engine and action executer, and the sequence diagram is introduced to describe the interaction between user and AmI environment as well.

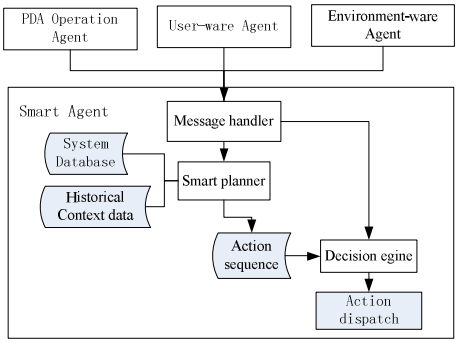

Fig. 5. The structure of Smart Agent

During the design of AmI-Space, three models are mapped into Smart Agent, Fig.5 show its structure. The Smart agent mainly consists of Message handler, Smart planner, Decision engine, System database, Historical context data and Action sequence. The System database stores the static data about user and environment. Historical context stores historically interactive experience of the user. Message handler gets environmental parameters (i.e. time and temperature) and user ID at first. The Smart planner deuces user's habitual behavior and favorites according to the data from knowledge repository, and generates action sequence which is a list of active services.

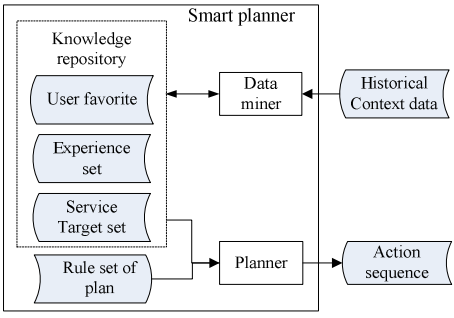

Fig. 6. The structure of Smart planner

At last, the decision engine judges whether the condition of active service is satisfied or not according to environmental variable. The action sequence of active service will be ignited as long as the condition is satisfied, and each action is dispatched to a special function agent to provide personalized service to user.

Fig. 6 describes the structure of Smart planner. Based on the historical context data, the data miner apply the fuzzy-logic-based incremental learning algorithm to find new knowledge, and add to the knowledge repository respectively. Planner produces action sequence according to the rules of plan and data from knowledge repository. The production for each element of the action sequence is as follow.

If <condition: time, user Id > then <action: service Id, service parameters>

The skeleton of the Smart Agent can be described in pseudo code as follows:

```
function Skeleton-SmartAgent
  static:memery  /*storing the historical information*/
  memory←Update-Memorr /*getting new sensing data*/
  action←Choose-Best-Action /*Generating action plan*/
  memory←Update-Memory
return action   /*returning the action */
```

5.3 Agents in AmI-Space

According to the scenarios of AmI-Space, we design User-aware Agent, PDA operation-aware Agent, Environment-aware Agent, Appliances control Agent, Multimedia Agent, FO Agent, Smart Agent, Management Agent and Data Agent[17][18]. Different agents work together which they not only aim to accomplish their own work, but also interacts with each other, and provide useful data for other agents. For example, Data Agent plays the role of packing the data in XML, and provides data service to other agents so as to make sure they work well. Meanwhile, the smart Agent indirectly gets information from User-Aware agent, PDA Operation-aware Agent. After dealing with such information and intelligent plan, the Smart Agent produces the action sequence to drive the function agents which control the household appliance to provide user with services through appliance agent.

Table 1 shows the goals and functions of different agent in AmI-Space, and different plans to implement each agent. Since the authentication based on wireless badge is just one of methods to implement automatic authentication, there is an *Or-goal* relation between AmI-Space and User-aware Agent. Besides, the goal of *Display media according to Facial Orientation of user* is achieved if and only if *FO Agent* can project media against user's face, so there is And-goal relation between *AmI-Space* and *FO Agent.* Fig. 7 shows the and/or tree for goal relation between AmI-Space and agents. Accordingly, it is easy to get the and/or tree of the plan relation and the and/or tree of the function relation respectively.

Table 1. The goal, plan and function of each agents

Agent Name	Goal of the Agent	Plan of the Agent	Function of the Agent
User-aware Agent	Automatic Authentication based on wireless badge.	Wearable Blu-etooth badge	Automatic authentication based on Blue-tooth
PDA operation-aware Agent	User-centered interaction	Wi-Fi technology	Capturing user's input and display-ing result friendly
Environment-aware Agent	Automatically capture environmental context	Embedded Sensor	Automatically capture and process environmental variables.
Appliance Agent	Automatically control appliance	Network	Generate commands to make the appliance work based on network.
Multimedia Agent	Play user's favorite media	Media stream	Manage the multimedia resource, and play the specific media.
FO Agent	Project media against user's face	HMM	Recognize facial orientation based HMM, and project media against user
Management Agent	Manage communication and data transmission	MOM	Manage the communication and data transmission among agents by realizing MOM.
Smart Agent	Make decision and schedule the task	Decision Engine	Make decision according user's habitual behaviors and plan, and schedule the specific task.
Data Agent	Manage static data	SQL Server	Store and query the static data

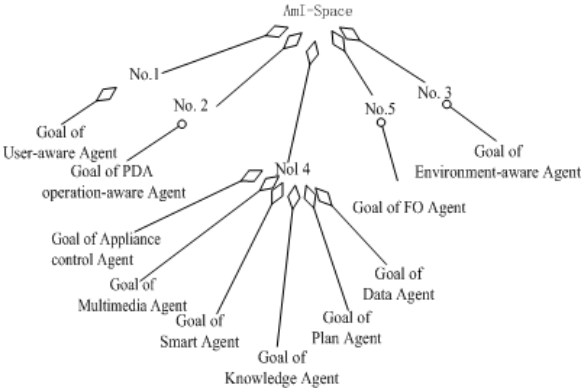

Fig. 7. The and/or tree of goal relations between Agents and AmI-Space

6 Conclusions

Since AmI system focuses on naturally Human-centered interaction, the way to model user plays a key role for the development AmI system. With the interactive model based on multi-agent, a formal approach which mode the mental, plan and behavior of user is proposed to describe both static features and dynamical behavior of user. This work will enable and empower designers to capture the nondeterministic and highly

individual feature of user in AmI environment. Besides, while more and more AmI system is implemented by Agent, the relations between Agent and AmI system is discussed at detail. These relations not only help designers understand the AmI system better, but also help them keep tracking how an AmI system is implemented in Agents. Based on such relations, we will develop a toolkit being similar to Rational RequisitePro to help designers to manage and track AmI system from its requirement to implementation in the future.

Acknowledgments. This work has been supported by the Beijing natural science foundation under grant No. 4102005, and partly supported by the National Nature Science Foundation of China (No. 61040039). The authors also wish to express their appreciations to all the participants of the AmI-Space project.

References

1. ISTAG, Scenarios for Ambient Intelligence in 2010, http://www.cordis.lu/istag.html
2. Hagras, H., Callaghan, V., Colley, M., et al.: Creating an Ambient-Intelligence Environment Using Embedded Agents. IEEE Intelligent Systems 19(6), 12–20 (2004)
3. Henricksen, K., Indulska, J.: Modelling and Using Imperfect Context Information. In: Proceedings of PERCOMW 2004, Washington, DC, USA, pp. 33–37. IEEE Computer Society, Los Alamitos (2004)
4. Bikakis, A., Patkos, T., Antoniou, G., Plexousakis, D.: A Survey of Semantics-based Approaches for Context Reasoning in Ambient Intelligence. In: Mühlhäuser, M., Ferscha, A., Aitenbichler, E. (eds.) AmI 2007 Workshops. CCIS, vol. 11, pp. 14–23. Springer, Heidelberg (2008)
5. Bikakis, A., Antoniou, G.: Defeasible Contextual Reasoning with Arguments in Ambient Intelligence. IEEE Transactions on Knowledge and Data Engineering 22(11), 1492–1506 (2010)
6. Trivedi, M., Huang, K., Mikic, I.: Intelligent environments and active camera networks. IEEE Transactions on Systems Man and Cybernetics (October 2000)
7. MIT Project Oxygen, http://oxygen.lcs.mit.edu/
8. Coen, M., Dang, D., De Bonet, J., Kramer, J., et al.: The intelligent room project. Presented at the 2nd Int. Cogn. Technol. Conf., Aizu, Japan (August 1997)
9. Lorigo, L.M., Brooks, R.A., Grimson, W.E.L.: Visually guided obstacle avoidance in unstructured environments. In: Proc. IROS, Grenoble, France, pp. 373–379 (September 1997)
10. Aware Home Research Initiative (AHRI), http://www.cc.gatech.edu/fce/ahri/
11. Kidd, C.D., Orr, R., Abowd, G.D., Atkeson, C.G., et al.: The aware home: A living laboratory for ubiquitous computing research. In: 2nd Int. Workshop Cooperative Buildings (October 1999)
12. RUNES, http://www.ist-runes.org/
13. Costantini, S., Mostarda, L., Tocchio, A., Tsintza, P.: DALICA: Agent based ambient intelligence for cultural-heritage scenarios. IEEE Intell. Syst. 23(2), 34–41 (2008)
14. AMIGO, http://www.hitech-projects.com/euprojects/amigo/

15. Wu, Z., Wu, Q., Cheng, H., Pan, G., et al.: ScudWare: A semantic and adaptive middleware platform for smart vehicle space. IEEE Trans. Intell. Transp. Syst. 8(1), 121–132 (2007)
16. Shi, Y., Xie, W., Xu, G., Shi, R., et al.: The smart classroom: Merging technology for seamless tele-education. IEEE Pervasive Comput. 2(2), 47–55 (2003)
17. He, J., Dong, Y., Zhang, Y., Huang, Z.: Creating an Ambient-Intelligence Environment Using Multi-Agent System. In: 2008 International Conference on Embedded Software and Systems Symposia (ICESS Symposia), pp. 253–258 (2008)
18. Chen, R., Hou, Y.-B., Huang, Z.-Q., He, J.: Modeling the Ambient Intelligence Application System: Concept, Software, Data, and Network. IEEE Transactions on Systems, Man, and Cybernetics—Part C: Applications and Reviews 39(3), 299–324 (2009)
19. Vurgun, S., Philipose, M., Pavel, M.: A Statistical Reasoning System for Medication Prompting. In: Krumm, J., Abowd, G.D., Seneviratne, A., Strang, T. (eds.) UbiComp 2007. LNCS, vol. 4717, pp. 1–18. Springer, Heidelberg (2007)
20. Patel, S.N., Reynolds, M.S., Abowd, G.D.: Detecting Human Movement by Differential Air Pressure Sensing in HVAC System Ductwork: An Exploration in Infrastructure Mediated Sensing. In: Indulska, J., Patterson, D.J., Rodden, T., Ott, M. (eds.) PERVASIVE 2008. LNCS, vol. 5013, pp. 1–18. Springer, Heidelberg (2008)
21. Reddy, S., Estrin, D., Hansen, M., et al.: Examining Micro-Payments for Participatory Sensing Data Collections. In: Proc. Ubicomp 2010, pp. 33–36 (2010)
22. Dey, A.K.: Modeling and intelligibility in ambient environments. Journal of Ambient Intelligence and Smart Environments 1(1), 57–62 (2009)
23. Damasio, A.R.: The Feeling of What Happens Body, Emotion and the Making of Consciousness. Harvest Books, London (2000)
24. Marchesotti, L., Piva, S., Regazzoni, C.: Structured Context-Analysis Techniques in Biologically Inspired Ambient-Intelligence Systems. IEEE Transactions on Systems, Man, and Cybernetics-Part A: Systems and Humans 35(1), 106–120 (2005)
25. Du, T.C.: Implementing Association Rule Techniques in Data Allocation of Distributed Database. Chung Yuan Christian Univ., Taiwan (2000)
26. Jess, the Rule Engine for the Java Platform, `http://herzberg.ca.sandia.gov/jess/`
27. Kushmerick, N.: Software agents and their bodies. Minds and Machines 7(2), 227–247 (1997)
28. Hu, S.-L., Shi, C.-Y.: Agent-BDI Logic. Journal of Software 1(10), 1351–1360 (2000) (in Chinese)
29. Chen, J.-Z., Liu, D.-Y., Tang, H.-Y., Hu, M.: An Extended BDI Logic for Modeling Multiagent Communication. Journal of Software 10(7), 778–784 (1999) (in Chinese)

Multi-Robot Traveling Problem Constrained by Connectivity

Cheng Hu, Yun Wang, and Fei Ben

School of Computer Science and Engineering Southeast University, Nanjing, China
{chhc,yunwang,benfei}@seu.edu.cn

Abstract. Multi-robot system provides more advantages over a single robot. In certain situations, robots need to maintain global connectivity while proceeding tasks such as traveling some interested spots in an area. This paper formulates the *Multi-Robot Traveling Problem Constrained by Connectivity*, and proposes a *Connected Nearest Neighbor* solution aiming to minimize the total traveling distance of the robots, which performs nearly twice better than previous work. Additionally, it is load balancing, fast in response, and robust to environmental dynamics and robot failures. Further improvements of the solution are also discussed and developed. Simulations are designed to investigate the cost of maintaining connectivity, the influence of different environments, and the comparison among the algorithms.

Keywords: Traveling problem, traveling salesman problem, multi-robot system, global connectivity, nearest neighbor.

1 Introduction

In recent years, research on control of *Multi-Robot Systems* (MRS) has gained a lot of attention due to the advantages provided by a robot network with respect to a single robot. A MRS is composed of a network of robots that interact with each other to achieve a common goal. It may provide more efficiency, redundancy, fault tolerance, and even the ability that one robot cannot achieve.

In situations where static infrastructures are not available, MRS can be quickly deployed and can provide sensing and actuating abilities. It thus can be used in a variety of missions such as surveillance in hostile or severe environments (i.e. border patrol, disaster sites, areas contaminated with biological, chemical or even nuclear wastes), large area environmental monitoring (i.e. air quality monitoring, forest monitoring, wild animals monitoring), etc.. Generally, in these missions, the area of interest cannot be covered by robots, which give rise to the problem of traveling the *Interested Spots* (ISs).

This paper presents and solves a *Multi-Robot Traveling Problem Constrained by Connectivity* (MRTPCC). Informally speaking, given several robots and predetermined positions (i.e. ISs) on a map, this problem is to assign travel paths to the robots for them to traverse all the ISs while make sure that they can communicate with one another via wireless radio all the time. Although this problem seems very similar to

Q. Zu, B. Hu, and A. Elçi (Eds.): ICPCA-SWS 2012, LNCS 7719, pp. 231–245, 2013.

the multi-depot multiple traveling salesmen problem, the connectivity constraint makes it more difficult to solve. Firstly, some robots will have to move to non-interested spots to keep the robot network connected, so it significantly expands the searching scope and thus makes traditional heuristic searching method impractical. Secondly, the robots have to be connected instantly, it means that the solution has to take temporal factors into consideration. While traditional methods are merely time-sensitive. Last but not the least, network partition has to be prevented, which increases the communication and computation burdens of the solution.

To solve this problem, a nearest neighbor based method is proposed, which ensures connectivity in rounds. In each round, robots reach to as many ISs as possible. These ISs are selected based on their distance to robots. Some robots have to move to positions which are not ISs to maintain connectivity of the robot system.

This work is motivated by a practical monitor mission, in which a network of robots equipped with cameras patrol in the school and send the videos back to a sink computer through wifi. The data rate generated by a camera is up to 2Mbps, however the storage space on each robot is only 256MB, which means if a robot loss connection to the sink computer for a period of about 20 minutes, the data will be lost. In outdoor environment, the transport range of wifi is typically 20--30 meters, thus data loss is constant if the paths of robots are not properly scheduled. Solving MRTPCC is also helpful to prevent network partition which leads to inconsensus states of the robots, and to disperse real-time commands which have to be executed immediately and causing great lose if not.

The contributions of this paper are summarized as follows: (1) To the best of our knowledge, it is the first formulation of MRTPCC; (2) A nearest neighbor based planning method is proposed, which is load balancing, fast in response, and robust to environmental dynamics and robot failures. Some improvements are also investigated; (3) Simulations are designed to investigate the cost of maintaining connectivity, the influence of different environments, and the comparison among the algorithms.

The remainder of this paper is organized as follows: in next section, related work in multi-robot systems are reviewed. Section III gives the system model and problem formulation. Then the *Connected Nearest Neighbor* (CNN) algorithm and three of its improvement are proposed in Sect. 4. Simulations are introduced in Sect. 5, and Sect. 6 concludes this paper.

2 Related Work

Traveling ISs is part of patrolling planning problem, or persistent surveillance planning problem [1], based on whether the visits should be regular. Generally, the solutions to this problem can be divided into two classes depending on how they categorize the problem.

Stump et al. [2, 3] considered a persistent surveillance problem in which ISs are periodically visited over a long period of time. They approximated the problem to a *Vehicle Routing Problem with Time Windows*. By properly modifying the original problem, they got a Mixed Integer Linear Problem formulation, which is further decomposed into sub-problems by using Lagrange multipliers to relax the constraint that

each site can only be visited by one vehicle. The proposed method is centralized and robust to mission dynamics. However, it has to compute for each time window, and it does not consider connectivity of the robots.

Another viewpoint is to take it as a *Multiple Depot Multiple Traveling Salesmen Problem* (MMTSP). Trevai et al. [4] considered multi-robot surveillance in unknown environments, where the boundary and obstacles are not known. By robots' sweeping through a bounded region to perform a search requiring maximum coverage, the iterative surveillance paths are planned, aiming to minimize the cyclic path. A simple but not effective method is to find a TSP cyclic path along all the observation points, and then make the robot repeat this travel cycle over and over. Khamis et al. [5] solved the problem of task allocation in mobile surveillance systems applying market-based approach. *Shortest Sequence Planning* (SSP) algorithm is used to find the minimum cost path for each robot given the ISs. The solution needs to perform a centralized SSP algorithm first, and to adjust the scheme in a distributed way. Furthermore, both [4] and [5] did not take connectivity into consideration.

Yang [6] presented a complete transformation of MMTSP to the standard TSP. Thus, the resulting problem can be solved by any algorithm devised for the TSP. This transformation makes copies of depots and results in an expanded graph which increases the problem scale and complexity. Xu et al. [7] developed a 3/2-approximation algorithm for MMTSP, which partially fill the gap between the existing best approximation ratios for the TSP and for the MMTSP in literature. The problem of TSP has been intensively studied for decades, and many exact and approximate solutions have been proposed [8]. However, to the best of our knowledge, none of them considers the connectivity among the salesmen.

In many multi-robot applications, maintaining connectivity is essential to their performance and even the results. Sugiyama et al. [9] investigated a multi-robot rescue system consisting of a base station and autonomous mobile robots. These robots coordinately form a chain network to explore a disaster area and send the video back to the base station. So the connectivity of this chain network is essential for the reconnaissance. In this work, robots are divided into relay robots and search robots depending on whether they are at the end of the chain network. Relay robots keep their master search robot connected to the fixed base station. Arkin et al. [10] investigated how a team of robotic agents self-organize for the exploration of a building, subject to the constraint of maintaining line of sight communications. Based on the information available, three different behavioral strategies were developed and tested. Two behavioral assemblages were involved: Wander-Avoid-Past and Living-In-Past. Vazquez et al. [11] presented a behavior-based architecture for multi robot exploration and mapping. In this architecture, if the signal strength among the robots on the bridge of the robot network falls below a threshold, the Achieve-Connectivity action will be executed. Otherwise, robots moves to their goals in a distributed manner while avoiding collisions. However, this strategy cannot guarantee global connectivity when one sets of robots lose connect with another set simultaneously. Hsieh et al. [13] implemented a neighbor based method. In this method, robots keep connect to certain neighbors. If the link quality among the robots falls below a certain threshold, they move to these neighbors. And robots move to their goals when the link quality is at an acceptable

level. Anderson [14] and Derbakova [15] considered repair of a broken robot network due to robot failures. In these works, robots wander to reach their goals instead of moving cooperatively, which increases the total traveling distance to keep connectivity or avoid collision with each other.

Global connectivity preserving in MRS is also intensively studied by Ji [16], Dimarogonas [17], Sabattini [18] et al. In these works, algebraic graph theoretic tools are used. Each robot is assigned a control law, in which parameters are to be adaptively and locally estimated. Obeying the control law, robots can ensure that they keep connected to others, and thus applications like rendezvous and formation control while preserving connectivity can be achieved. However, these literatures only consider one goal position for each robot, leave the allocation of all ISs to be unmentioned.

3 System Model and Problem Formulation

Consider a planar rectangular area with no obstacles, where N robots are randomly deployed. These robots are equipped with a wireless communication module, a computing module, a GPS module and a moving module. Each robot can communicate with any robot within distance r directly, and with those outside its communication range in an ad hoc way if relay robots exist.

Note that r is the effective communication distance rather than the maximum communication range r_{max}, for the communication model is actually not an ideal circle [19, 20]. Additionally, each robot occupies a circle of radius r_0. Suppose that initially these robots can communicate with each other, i.e. they are connected. Robots can move at a maximum speed V, and turning time is neglected.

This paper considers the traveling problem in wild and severe environment, where obstacles are few in number and easy for robots to cross over. And since generally ISs are far away from each other, collision among robots rarely occurs. Even if it happens, a simple avoidance procedure will be executed automatically by the robots. So it is reasonable to omit obstacles and robot size r_0 in the model.

In a traveling mission, there are M ISs to be traversed, whose coordinates are predetermined. Generally, $N < M$. Both ISs and Robots can be viewed as points on the plane, which is characterized by its position. By constantly exchanging information with others, robots are available to global knowledge about the mission and the map.

Formally speaking, ISs are the positions on the plane which have to be visited by robots at least once, and any other positions on the plane are called *Auxiliary Spots* (ASs). Robot R_i is called connected with R_j if (1) $D(R_i, R_j) \leqslant r$, where $D(x, y)$ calculates the distance of x and y; or (2) there exists a robot R_k, such that $D(R_i, R_k) \leqslant r$ and R_k is connected with R_j. We denote $C(R_i, R_j) = 1$ if R_i is connected with R_j, and $C(R_i, R_j) = 0$ otherwise. A robot network S is a set of robots such that for $\forall R_i, R_j$ in the set, $C(R_i, R_j) = 1$. A robot R_i is said to be connected with a robot network S if $\exists R_j \in S$, such that $C(R_i, R_j) = 1$.

MRTPCC is formulated as follows. Given M ISs, i.e., IS_1, IS_2, … , IS_M, and N Robots, i.e., R_1, R_2, … , R_N, try to designate a path $P_i(t)$ for each robot R_i, to minimize:

$$\sum_{i=0}^{N} \int_{t=0}^{\infty} D(P_i(t+dt), P_i(t))dt \tag{1}$$

s.t.

$$\forall j, \exists t = t_0, i, such\ that\ P_i(t_0) = IS_j \tag{2}$$

$$\forall t, i, k, such\ that\ C(R_i, R_k) = 1 \tag{3}$$

$$\forall t', t'', i, such\ that\ \int_{t'}^{t''} D(P_i(t+dt), P_i(t))dt \le V \cdot (t'' - t') \tag{4}$$

where $i, k \in \{1,2, \dots, N\}$, $j \in \{1,2, \dots, M\}$, t_0, t',t'' $\in[0, \infty]$, and $P_i(t)$ is the position of robot i at time t.

Constraint (2) illustrates that each IS should be visited by some robots within finite time. Constraint (3) demands that the robot network should be connected at any time. Constraint (4) declares that robots cannot move beyond speed V. And the goal is to minimize the *Total Traveling Distance* (TTD) of all the robots according to (1).

4 The Solution

4.1 Connected Nearest Neighbor Algorithm

In this subsection, *Connected Nearest Neighbor* (CNN) algorithm is proposed. Algorithm CNN works in rounds to find the next goal position and corresponding arriving time for each robot until all ISs are visited. In each round, a *Search Phase* is firstly performed to find a pioneer robot and IS pair based on nearest neighbor strategy, which means the robot will move to the IS in this round. Then *Restore Phases* are performed to find proper robots and assign their goal positions to gain connection with the pioneer robot. The robots whose goal positions are connected with that of the pioneer robot forms a set S_{VR}. The *Restore Phase* repeats until all the robots are added to S_{VR}, i.e. global connectivity are achieved in this round.

Algorithm 1 CNN: A multi-robot traversing planning using nearest neighbor method while reserving connectivity.

Require:
  $\{IS\}$, $\{R\}$, V_{II}
Ensure:
  $Path[M][C]$, $Time[C]$;

01. $S_{VI} \leftarrow \Phi$, $S_{II} \leftarrow \{IS\}$, $Time[0]=0$, $C=1$;
02. **while** $S_{II} \neq \Phi$ **do**
03. $S_{VR} \leftarrow \Phi$, $S_{IR} \leftarrow \{R\}$;

```
04.   for all R_i∈S_IR, IS_j∈S_II do
05.     Find R_x and IS_y which minimize D(R_i,IS_j);
06.   end for
07.   Path[x][C]=Pos(IS_y), Pos(R_x)=Pos(IS_y);
08.   S_VR←R_x, S_VI←IS_y, S_IR←R_x, S_II←IS_y;
09.   while S_IR≠Φ do
10.     for all R_i∈S_IR, R_k∈S_VR do
11.       if R_i is connected with R_k then
12.         Path[i][C]=Path[i][C-1];
13.         S_VR←R_i, S_IR←R_i;
14.       end if
15.     end for
16.     S_tmp←Φ;
17.     for all IS_j∈S_II do
18.       if ∃ R_i∈S_IR such that D(R_i,IS_j)←r then
19.         S_tmp←IS_j;
20.       end if
21.     end for
22.     if S_tmp≠Φ then
23.       for all R_i∈S_VR, IS_j∈S_II do
24.         Find R_x and IS_y which minimize D(R_i,IS_j);
25.       end for
26.       Path[x][C]=Pos(IS_y), Pos(R_x)=Pos(IS_y);
27.       S_VR←R_x, S_VI←IS_y, S_IR←R_x, S_II←IS_y;
28.     else
29.       for all R_i∈S_VR, R_k∈S_IR do
30.         Find R_x and R_y which minimize D(R_i,R_k);
31.       end for
32.       Find AS between R_x and R_y such that D(AS,R_y)=r;
33.       Path[x][C]=Pos(IS_y), Pos(R_x)=Pos(AS);
34.       S_VR←R_x, S_IR←R_x;
35.     end if
36.   end while
37.   for all R_i, R_j whose path intersects do
38.     Path[i][C]←Path[j][C];
39.   end for
40.   D_max= maximum length of all paths in this round;
41.   Time[C]=D_max/V_max;
42.   C++;
43. end while
```

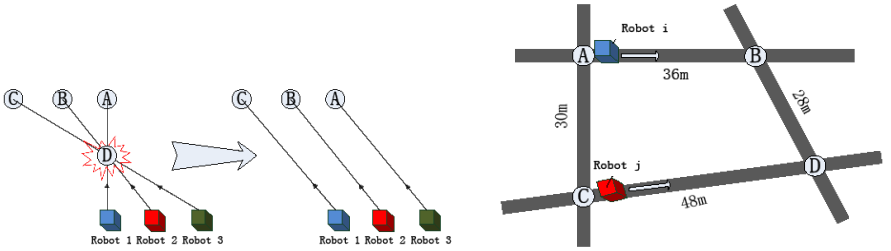

(a) A demonstrative example of collision avoidance by exchanging the goals of crossing paths

(b) A demonstrative example of lemma 1, where R = 30m and V_{max} = 4m/s

Fig. 1. Demonstrative examples

The detail of CNN is shown in Alg. 1. In the *Search Phase*, the algorithm finds out the shortest route from robots to the remaining ISs and makes a virtual move (line 4-8). The virtual move means the robot does not physically move until the end of this round. After this step, the robot network maybe disconnected, so a *Restore Phase* is followed (line 9-36). In this phase, robots which have virtually moved form a set S_{VR} (line 10-15), and these robots are viewed to be located at their target positions. All other robots which are connected with S_{VR} are also added in, and they will stand still in this round (line 16-27). If there still exists robots outside S_{VR}, the algorithm selects the one which is nearest to S_{VR}, and finds its target position to make it connected with S_{VR} (line 29-34). Then it adds this robot into S_{VR}, and repeats previous process until all robots are in S_{VR}. In case that robots crash into each other, the goal positions of cross paths are exchanged (line 37-39), as Fig. 1(a) shows. Note that if the cost of paths satisfies triangle inequality, the exchange will decrease the total cost. Suppose that the longest moving distance of the robots is D_{max} in this round, then sets the arriving time of all robots to $T = D_{max} / V_{max}$, and enables actual move. It means that for any robot i with moving distance d_i, it will move at the speed of $V_i = d_i / T$.

We will show that algorithm 1 provides a valid solution for MRTPCC.

Lemma 1. *Let A, B, C, D be four points on a plane, such that D(A,B) ⩽ r and D(C,D) ⩽ r. For ∀E on segment AC and ∀F on segment BD,*

$$If \quad \frac{D(A,E)}{D(A,B)} = \frac{D(B,F)}{D(B,D)}, \ then \ D(E,F) \leqslant r.$$

Proof. Suppose that O is a reference point on the plane, and let $\lambda = \frac{D(A,E)}{D(A,B)} = \frac{D(B,F)}{D(B,D)}$,

Then $\overrightarrow{EF} = \overrightarrow{OF} - \overrightarrow{OE}$

$$= \left[\lambda\overrightarrow{OC} + (1-\lambda)\overrightarrow{OD}\right] - \left[\lambda\overrightarrow{OA} + (1-\lambda)\overrightarrow{OB}\right]$$

$$= \lambda\overrightarrow{AC} + (1-\lambda)\overrightarrow{BD}$$

Without loss of generality, let $\left|\overrightarrow{AC}\right| \geq \left|\overrightarrow{BD}\right|$, then $\left|\overrightarrow{EF}\right| \leq \left|\lambda\overrightarrow{AC} + (1-\lambda)\overrightarrow{AC}\right| \leq r$ ■

Lemma 1 demonstrates that for any two robots, if the distances of their initial and goal positions are less than R, and if they move straight forward at the speed proportional to their moving distance, then they will remain connected in the whole process.

For instance, in Fig. 1(b), if robot i moves from A to B at the speed of 3m/s, and robot j moves from C to D at the speed of 4m/s, then they will be connected while they are moving.

Corollary 1. *Let A, B, C be three points on the plane, such that* $D(A,B) \leqslant r$ *and* $D(A,C) \leqslant r$. *Then for* $\forall E$ *on segment BC,* $D(A,E) \leqslant r$.

Corollary 1 is a direct use of lemma 1. It shows a scenario in which one robot is at a standstill.

Corollary 2. *Let* A_1B_1, A_2B_2, … , A_nB_n *be n segments on the plane, such that* $D(A_1,A_2) \leqslant r$, $D(A_2,A_3) \leqslant r$, … , $D(A_{n-1},A_n) \leqslant r$ *and* $D(B_1,B_2) \leqslant r$, $D(B_2,B_3) \leqslant r$, … , $D(B_{n-1},B_n) \leqslant r$. *For* $\forall E_i$ *on* A_iB_i *and* $\forall E_{i+1}$ *on* $A_{i+1}B_{i+1}$, *if* $\frac{D(A_i,E_i)}{D(A_i,B_i)} = \frac{D(A_{i+1},E_{i+1})}{D(A_{i+1},B_{i+1})}$, *then for* $\forall E_j$, E_k *on* A_jB_j, A_kB_k *and* $\frac{D(A_j,E_j)}{D(A_j,B_j)} = \frac{D(A_k,E_k)}{D(A_k,B_k)}$, *such that* $C(E_j,E_k)=1$, *where* $i, j, k \in \{1,2, \dots, n\}$.

Corollary 2 is obvious according to lemma 1. It reveals that if N robots are connected at the beginning as well as in the end, and they move straight forward at the speed proportional to their moving distance, then they will remain connected in the whole process.

Theorem 1. *Algorithm 1 provides a valid solution for MRTPCC, in which robots moves C rounds, and in round c, robot i moves from Path[i][c] to Path[i][c+1] at the speed of* $V_{ic} = D(Path[i][c], Path[i][c+1])/T[c]$.

Proof. We prove by induction.

At the beginning of the algorithm, the robot system is connected by definition, and at the end of first round, the robot system is also connected according to algorithm description. Since robots move in straight lines, the robot system is connected during the first round applying corollary 2.

Suppose that at the beginning of round i, the robot system is connected, then it will also be connected in the end. Since robots move in straight lines, the robot system is connected during the round i.

In summary, the robot network keeps connected during all C rounds.

On the other hand, in each round, at least one IS is visited, so the algorithm ensures termination. ■

4.2 Improvements

Algorithm CNN is easy to understand and implement. However, it performs poorly because only local optimal decisions are made. It can be improved in many aspects to reduce TTD at the cost of higher computation complexity. In this section, two of them are presented (CANN and CRNN), as well as one considering load balancing among robots (CBNN).

Connected All Nearest Neighbors Algorithm (CANN). Algorithm CANN constructs N initial states based on the nearest neighbor of each robot. Under each initial state, CNN is then applied to find a solution. The best one with minimum TTD will be selected as the final solution. On average, CANN is better than CNN, for the initial state of CNN is included in that of CANN.

Connected Random Near Neighbors Algorithm (CRNN). Algorithm CRNN constructs M initial states based on all the neighbors of a random selected robot. Under each initial state, CNN is then applied to find a solution. The best one with minimum TTD will be selected as the final solution. On average, CRNN is better than CNN, for the initial state of CNN is included in that of CRNN.

Connected Balanced Nearest Neighbor Algorithm (CBNN). Algorithm CBNN is very similar to CNN except that in CBNN, when choosing the next robot to put into S_{VR}, robots with minimum traveling distance will be given higher priority. This rule aims to make the robots have similar traveling distance (TD), in case that some robot will exhausts its energy if moving a much longer TD than others. The performance of CBNN will be evaluated compared to CNN in Sect. V.

4.3 Discussion

The computation complexity of the proposed algorithms are easy to analyze, which is $O(M^2N^3)$ for CNN, $O(M^2N^4)$ for CANN, $O(M^3N^3)$ for CRNN and $O(M^2N^2)$ for CBNN. Furthermore, the connectivity is held for CANN, CRNN and CBNN. The proof is similar to that of CNN, and be omitted here. The reduce of TTD caused by the increase in complexity will be shown in Sect. V, together with comparison of balancing parameters between CNN and CBNN.

The proposed algorithms can be implemented in either centralized manner or decentralized manner. In former case, a leader robot is elected to run the program and broadcasts goal positions for each robot. Other robots memorize the broadcasted information and moves to their own goals. Heartbeat messages are regularly exchanged between leader and the rest robots to monitor possible failure of the robots. While in later case, each robot executes the same copy of the algorithm to find a strategy most beneficial to itself. A voting procedure is then performed to find a global best solution. Then the robots will agree on the solution and move to their goals. Heartbeat messages are also used to keep the latest information of the environment.

Although environmental dynamics is not considered in the system model, to which the proposed algorithms can be certainly adapted. If some ISs are dynamically added in or wiped out, the robots will recalculate the next goal position according to the updated map. Since our algorithms ensure that robots are connected at any time, the changed environment can be viewed as a new initial state, and thus correctness is preserved. The algorithms are also robust to robot failures, for no fixed structure is needed. So if network partition occurs, any robot can move to the goal position of the failed robot to regain global connectivity.

These algorithms aim to minimize the TTD, which scarifies other important aspects such as *Total Traveling Time* (TTT). As described above, a round ends once the robot network gains connectivity, resulting that some robots do not move in this round. And these algorithms are best suit for planar areas that are obstacle-free and with a convex boarder. In these situations, the algorithms are load balancing, fast in response and robust to environmental dynamics and robot failures while ensuring connectivity. In other situations, such as in indoor environment and rugged terrain, these algorithms do not work.

5 Simulations

5.1 Simulation Setup

In practice, the scale of environment ($X \times Y$), the number of ISs (M) and their distribution, the number of robots (N) as well as their communication range (r) are the key parameters that influence the final results. Here $\frac{M}{X \times Y}$ decides the density of the IS, $\frac{r}{X \times Y}$ decides the relative coverage of robots. So the influence of the scale of environment can be simulated by changing other parameters, and thus it is by default set to $1000 \times 1000 m^2$ hereafter. And since the absolute velocity of the robots do not influence the results, it is set to a very large value to accelerate the simulation.

The simulation consists of two parts. In the first part, CNN, CANN, CRNN and CBNN are compared varying these parameters. Another important and interesting issue is how connectivity influences the planning scheme. Thus algorithms in this paper are also compared to *Nearest Neighbor* (NN) method which is very similar to CNN except that NN takes no consideration of connectivity. The reason to use NN as a benchmark algorithm is that it also applies nearest neighbor strategy, which minimizes its distinctions with CNN etc., so that the differences of the results can be viewed as the cost of considering connectivity.

In the second part, another comparing algorithm LQCN [13] is adopted. In this algorithm, each robot keeps connect with certain neighbors. For simplicity, a tree structure is constructed through a DFS procedure, and each robot keeps connect with its parent robot in the tree. For comparison, the simulations assume the acceptable range of each robot as r. Since LQCN considers only one goal for each robot, we adopt allocation method in [11] and [12] to solve the whole traveling problem. Each robot automatically select its goal position (an IS) to maximize the information gain: $G = \frac{1.5^x}{1.5^y \cdot d}$, where x and y are IS number and robot number within the sensing range of the IS, and d is the distance from the robot to the IS.

All the results in the simulations are averaged by 200 runs.

5.2 Simulation Results and Analysis: Part I

Simulation 1: Varying Robot Numbers. In this simulation, r=100m, M=100, and ISs subject to uniform distribution, N varies from 2 to 20.

Figure 2(a) shows TTD of CNN, CANN and CRNN compared to NN. As the number of robots increases, the TTD planned by CNN, CANN and CRNN all increases relative to NN. This is because more TTD be generated to keep the robot network connected. However, the increase trend becomes softened as N increases. It means that there may exist an up-bound of increase which is cost by connectivity for each environmental configuration. I.e., given the same mission and environment, a highest ratio exists regardless of the robots number. As expected previously, TTD of CRNN and CANN is less than that of CNN. And CRNN achieves even less TTD than CANN. As robots number increases, the better CRNN and CANN perform over CNN. However, the absolute decrease in TTD is less than 10%, which is at the cost of much more computation. So in practice, CRNN or CANN shall be carefully selected based on the computing ability of robots and delay demand of a specific application.

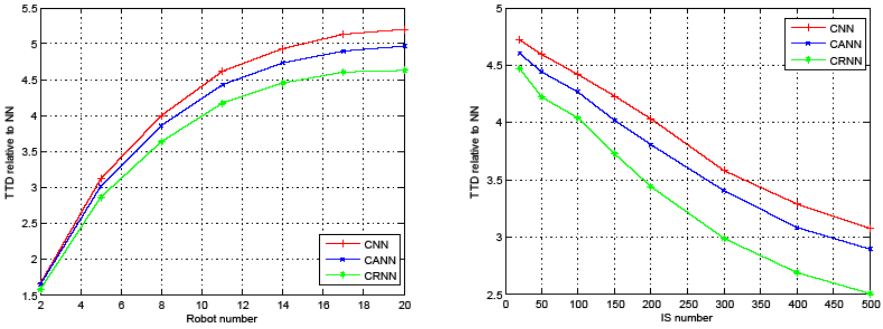

(a) Varying *M* (b) Varying *N*

Fig. 2. TTD comparison among CNN, CANN, CRNN and NN varying M and N

Simulation 2: Varying IS Numbers. In this simulation, r=100m, N=10, and ISs subject to uniform distribution, M varies from 20 to 500.

As depicted in Fig. 2(b), as the number of IS increases, the TTD planned by CNN, CANN and CRNN all decreases relative to NN. This is because the higher density of ISs, the less traveling distance is wasted for connectivity. And the theoretical low bound of the ratio is 1. In this simulation, similar results are obtained as previous where CRNN performs better than CANN, and CANN performs better than CNN.

Simulation 3: Varying Distribution of ISs. To investigate how the distribution of ISs influences the results, three controlled distributions are presented. They are: (1) Grid distribution, where ISs are distributed on the vertexes of grids, whose side length is 100m. This distribution corresponds to the street surveillance. (2) Circular distribution, where ISs are uniformly distributed along a circle, whose radius is 495m. This distribution corresponds to boarder surveillance. (3) Normal distribution, where ISs subject to normal distribution. This distribution corresponds to priority based surveillance.

In this simulation, N=10, M=100, while r ranges from 25m to 125m. The results are depicted in Fig. 3. Generally, CNN, CANN and CRNN perform poorest in Fig. 3(b), it is because almost all the robots are passively moved along the circle to keep connectivity. The most interesting part of the results is the turning point of curves in Fig. 3(a) and Fig. 3(b). In Fig. 3(a), the turning point appear at r=100m, which is exactly the side length of the grids. And the ratio decrease slightly when r>100m. This phenomena may reveal the relationship between the ratio and mean number of ISs' neighbors which are not r far away. Analogical results shown in Fig. 3(b). The distance between neighboring ISs on the circle is 31m, thus an obvious turning point appear at r=50m. It will be very helpful if such law really exists, however it is beyond the scope of this paper, and will be left to the future work.

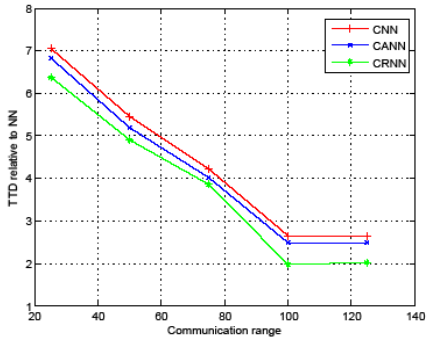

(a) Grid distribution

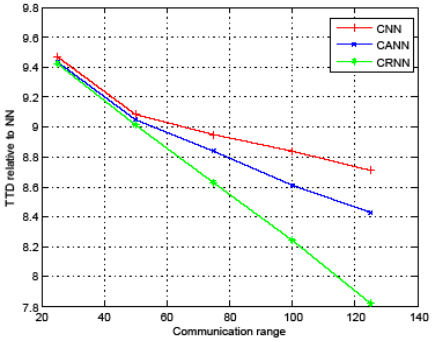

(b) Circular distribution

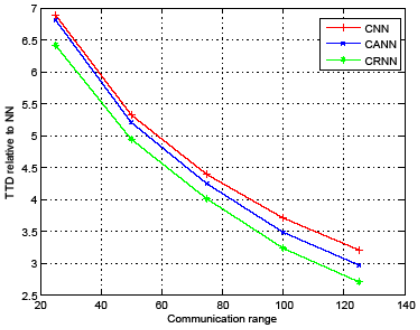

(c) Normal distribution

Fig. 3. TTD comparison among CNN, CANN, CRNN and NN varying M and N varying distribution of ISs

Simulation 4: Comparing CNN with CBNN. To investigate the load balance performance of CNN, CBNN is used for comparison. TTD of all the robots, the maximum TD among the robots and variance of TD among the robots are considered. Fig. 4 shows the compare results on varying N and varying M. From these results, it can be concluded that there is no need to use CBNN, despite its low variance over CNN. Because in most circumstances, the maximum TTD of CBNN is much the same as CNN, while the total TTD is much larger. The reason is that in CNN, load balance has been achieved to some extant due to the connectivity constraint, which forces robots to move to follow the leading robots.

5.3 Simulation Results and Analysis: Part II

In this part of simulation, M=100, and ISs subject to uniform distribution. The TTT and TTD are considered.

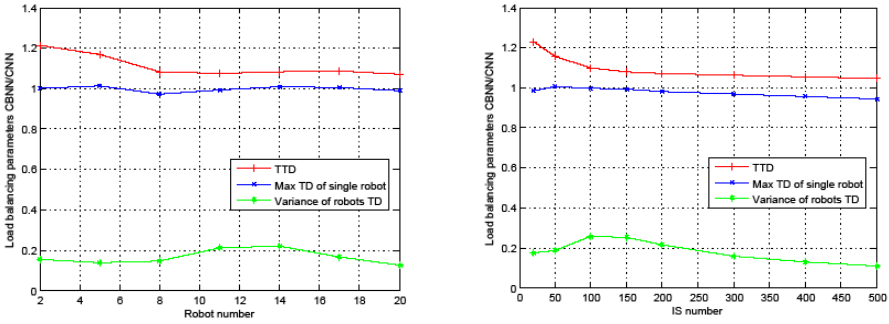

(a) Varying M (b) Varying N

Fig. 4. Comparison between CNN and CBNN

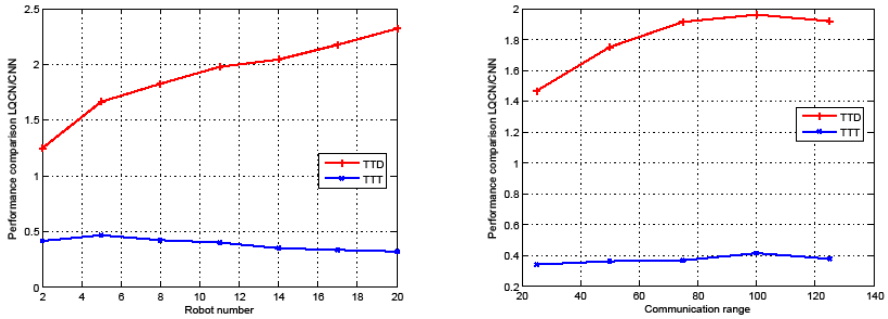

(a) Varying M (b) Varying R

Fig. 5. Performance comparison between CNN and LQCN

Simulation 5: Varying Robot Number. This simulation compares the performance of CNN and LQCN when r=100m and N varies from 2 to 20.

As shown in Fig. 5(a), as the number of robots increases, LQCN generates more and more TTD than CNN. There are two main reasons for larger TTD of LQCN. Firstly, robots act in a distributed manner in LQCN resulting that two or more robots may set the same goal position. And only one of them will achieve the goal, leaves the others turn to other goals. Secondly, the selection of goals does not make sure that robots will keep connected in the whole process. Instead, *Achieve-Connection Behavior* is constantly carried out which further increase the TTD. On the other hand, TTT of LQCN is much smaller than that of CNN. This is because one round in CNN ends once the robot network achieves connection, despite of whether each of the robots moves in this round. This strategy is designed for decreasing TTD, while increasing the TTT as a tradeoff. Again, we should note that the main target of this paper is to minimize the TTD. However, it is easy for CNN to reduce TTT, if robots always make a move in each round.

Simulation 6: Varying Communication Range. In this simulation, N=10 and r ranges from 25m to 125m.

Similar results are shown in Fig. 5(b). However, communication range seems not influence as much as robot number whether on TTD or TTT according to the results. This is because in LQCN, there is a better chance of collision if robot number increases. On the contrary, the collision rate decreases as the communication range expands.

6 Conclusion

This paper formulated the *Multi-Robot Traveling Problem Constrained* by *connectivity*, and proposed the *Connected Nearest Neighbor algorithm* which works in rounds to ensure connectivity of the robot network. It is load balancing, fast in response, and robust to environmental dynamics and robot failures. Three improvements were also developed to improve the performance. Simulation results showed that the proposed algorithms performed better when *Interested Spots* number increases, and worse when robots number increases, relative to the nearest neighbor method. It generated only half *Total Traveling Distance* of LQCN, while spent double *Total Traveling Time*. Influences of different distribution of ISs were also studied.

In future works, environment with obstacles and of irregular shapes will be studied, and real-world experiments are in progress. The proper number of robots to tackle a certain surveillance task while reserve connectivity will also be investigated. And several local networks connectivity will be considered instead of one global network connectivity. In each local robot network, a certain number of robots shall be guaranteed.

Acknowledgements. The authors sincerely thank the anonymous reviewers for their valuable comments that have led to the present improved version of the original manuscript.

This research work is partially supported by the Natural Science Foundation of China under grant No. 60973122, the 973 Program in China under grant No. 2009CB320705, and 863 Hi- Tech Program in China under grant No.2011AA040502.

References

1. Bonnet, F., Défago, X.: Exploration and Surveillance in Multi-robots Networks. In: International Conference on Networking and Computing (ICNC), pp. 342–344. IEEE Computer Society, Osaka (2011)
2. Stump, E., Michael, N.: Multi-robot persistent surveillance planning as a Vehicle Routing Problem. In: IEEE Conference on Automation Science and Engineering (CASE), pp. 569–579. IEEE Computer Society, Trieste (2011)
3. Michael, N., Stump, E., Mohta, K.: Persistent Surveillance with a Team of MAVs. In: IEEE/RSJ International Conference on Intelligent Robots and Systems, pp. 2708–2714. IEEE Computer Society, San Francisco (2011)

4. Trevai, C., Ota, J., Arai, T.: Multiple Mobile Robot Surveillance in Unknown Environments. Advanced Robotics 21, 719–749 (2007)
5. Khamis, A.M., Elmogy, A.M., Karray, F.O.: Complex Task Allocation in Mobile Surveillance Systems. Journal of Intelligent & Robotic Systems 64, 33–55 (2011)
6. Yang, G.X.: Transformation of Multidepot Multisalesmen Problem to the Standard Travelling Salesman Problem. European Journal of Operational Research 81, 557–560 (1995)
7. Xu, Z., Rodrigues, B.: A 3/2-Approximation Algorithm for Multiple Depot Multiple Traveling Salesman Problem. In: Kaplan, H. (ed.) SWAT 2010. LNCS, vol. 6139, pp. 127–138. Springer, Heidelberg (2010)
8. Gutin, G.: The Traveling Salesman Problem. Springer (2009)
9. Sugiyama, H., Tsujioka, T., Murata, M.: Integrated Operations of Multi-Robot Rescue System with Ad Hoc Networking. In: Wireless VITAE, pp. 535–539. IEEE Computer Society (2009)
10. Arkin, R.C., Diaz, J.: Line-of-Sight Constrained Exploration for Reactive Multiagent Robotic Teams. In: 7th International Workshop on Advanced Motion Control, pp. 455–461. IEEE Computer Society (2002)
11. Vazquez, J., Malcolm, C.: Distributed Multirobot Exploration Maintaining a Mobile Network. In: Intelligent Systems, pp. 113–118. IEEE Computer Society (2004)
12. Simmons, R., Apfelbaum, D., Burgard, W., Fox, D., Moors, M., Thrun, S., Younes, H.: Coordination for Multi-Robot Exploration and Mapping. In: Proceedings of the National Conference on Artificial Intelligence, pp. 852–858. AAAI Press (2000)
13. Hsieh, M.A., Cowley, A., Kumar, V., Taylor, C.J.: Maintaining Network Connectivity and Performance in Robot Teams. Journal of Field Robotics 25, 111–131 (2008)
14. Anderson, S.O., Simmons, R., Golberg, D.: Maintaining Line of Sight Communications Networks Between Planetary Rovers. Intelligent Robots and Systems 3, 2266–2272 (2003)
15. Derbakova, A., Correll, N., Rus, D.: Decentralized Self-Repair to Maintain Connectivity and Coverage in Networked Multi-Robot Systems. In: Robotics and Automation, pp. 3863–3868. IEEE Computer Society (2011)
16. Ji, M., Egerstedt, M.: Distributed Coordination Control of Multiagent Systems While Preserving Connectedness. IEEE Transactions on Robotics 23, 693–703 (2007)
17. Dimarogonas, D.V., Kyriakopoulos, K.J.: Distributed Coordination Control of Multiagent Systems While Preserving Connectedness. IEEE Transactions on Robotics 24, 1213–1223 (2008)
18. Sabattini, L., Chopra, N., Secchi, C.: Distributed control of multi-robot systems with global connectivity maintenance. In: IEEE/RSJ International Conference on Intelligent Robots and Systems (IROS), pp. 2321–2326. IEEE Computer Society (2011)
19. Zhou, G., He, T., Krishnamurthy, S., Stankovic, J.A.: Impact of Radio Irregularityon Wireless Sensor Networks. In: Proceedings of the 2nd International Conference on Mobile Systems, Applications, and Services, pp. 125–138. ACM (2004)
20. Zhou, G., He, T., Krishnamurthy, S., Stankovic, J.A.: Models and Solutions for Radio Irregularity in Wireless Sensor Networks. ACM Transactions on Sensor Networks (TOSN) 2, 221–262 (2006)

An Application Study on Vehicle Routing Problem Based on Improved Genetic Algorithm

Shang Huang, Xiufen Fu, Peiwen Chen, CuiCui Ge, and Shaohua Teng

School of Computer, Guangdong University of Technology, Guangzhou 510006, China
{dragoneightgogo@163.com,peiwenc,gecuicui1988}@163.com,
{xffu,shteng}@gdut.edu.cn

Abstract. The Vehicle Routing Problem of Logistics and Distribution is a hot and difficult issue in current field of combinatorial optimization, therefore this paper presents an improved genetic algorithm. The algorithm which applied the idea of Saving Algorithm to the initialization of groups, and improved algorithm on selection operator and cross operator, In the meantime, it proposes a new way to calculate the adaptive probability in the cross operator. In addition, it also introduces a novel CX crossover operator .By the way of simulating experiments of the Vehicle Routing Problem, it demonstrates that the improved genetic algorithm enhanced the ability of global optimization, moreover it can significantly speed up convergence efficiency.

Keywords: logistics and distribution, Vehicle Routing Problem, calculate adaptive probability, genetic algorithm.

1 Introduction

With the rapid development of e-commerce, the logistics industry is becoming more and more important, which attracts extensive concern of various industries as the third profit source. The vehicle routing problem holds the count for much status in logistics, which has become the most important research to low the distribution cost. Therefore, the optimization of vehicle routing has been a hot area of research in the field of logistics and distribution. The Vehicle routing problem (VRP) was first proposed by Dantzig and Ramser in 1959, belonging to a class of problems of combinatorial optimization field with multiple constraints. VRP can be described as such a problem that the vehicle can pass a series of customer points by organizing proper driving route, meanwhile satisfying the constraints(such as goods demand, vehicle capacity restriction, etc.), which is to reach a certain goal (such as the shortest distance, cost at least, etc.).In recent years, Domestic and foreign scholars utilized the heuristic algorithms and intelligent algorithm to solve VRP [1]. As a result of the particular frequency use of genetic algorithms, researchers attempted to overcome the 'premature convergence' issue by improving the genetic algorithm [2].

Because genetic operator is the key to the genetic algorithm, improving the operation of the genetic operators becomes the most important part of improved genetic algorithm. The CX crossover operator was cited in [3], the thought of the crossover operator, which is still able to produce a new individual even if two of the

Q. Zu, B. Hu, and A. Elçi (Eds.): ICPCA-SWS 2012, LNCS 7719, pp. 246–258, 2013.

same individual cross, meets the requirements of the traditional crossover operator in the diversity of the population, while avoiding the precocious phenomenon, and reducing the possibility of local optimal solution. In [4], a new selection strategy was proposed to control a specific number of individuals, which accelerates the speed of the convergence rate based on maintaining the diversity of the population. Abbattista F firstly proposed the idea of the integration of genetic algorithm and ant colony algorithm, Reference [5] proposed an improved ant colony and genetic integration of optimization algorithms, which apply adaptive crossover probability.

However, in population initialization process, randomly generating the initial population with a random number generator is customarily adopted. The resulting individual has the features of random and multi-point investigation, which is not easy to fall into the regional optimal when solving the optimal solution. Whereas randomly generated initial population has great influence on the convergence rate [6]. Mileage-saving method, also known as VSP (Vehicles Scheduling Program), applies to the situation that the satisfying quasi optimum value or the approximate value of all optimal solutions, not necessarily the optimal value is required in a practical application [7]. The author who combines the idea of saving mileage algorithm, proposed a new initialization way trying to accelerate the convergence speed. As the key link of genetic algorithm, crossover operator maintains the excellent individual characteristics in the original group to some extent, as well as enabling the algorithm to search the new solution space ensuring the diversity of individuals in a population. Therefore the selection of Crossover Concept will directly affect the convergence of genetic algorithm. Also, we present a new computational method for adaptive crossover probability based on the recent one in reference [6]. The final part of this paper is the test of the performance of the algorithm by the MATLAB simulations and experiments.

2 Vehicle Routing Problem Description

2.1 Specific Description

The name of vehicle routing problem was first proposed in the late 1950s by two linear programming masters Dantzig and Ramser, it is mainly used to solve the problem that how to send a car and how many cars should be sent and what kind of route should the cars take to ensure that meeting the customer requirements and making the cost lowest when the customer location and demand for goods was given.

The vehicle routing problem expressed as follows: The number of car in distribution centers is K, and the vehicle's maximum load is Q, the existing transport task of the N client nodes (1,2, ..., N) need to be completed, the demand for the client node of i is d_i (i = l, 2, ..., N) and $\max\ d_i \le Q$,and each client is just only served by one car once transported tasks. Each vehicle will start from the distribution center, and return the distribution center after the completion of certain tasks. The ultimate goal is to calculate the minimum distribution costs of vehicle routing under the vehicle capacity constrains using as few vehicles as possible [1]. The VRP with one distribution be shown in the Figure 1.

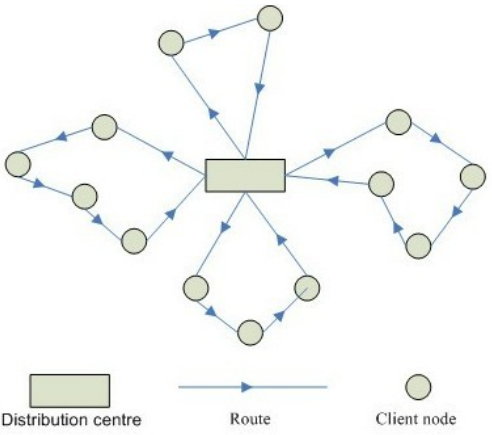

Fig. 1. Schematic Diagram of VRP

2.2 Mathematic Model of Vehicle Routing Optimization

By the above mentioned description, the mathematical model which regards the total cost of the minimum distribution as the objective function establish as follows [3]:

$$\min \quad F(i,\ j,\ k) = \alpha \sum_{k=1}^{k} \sum_{i=0}^{i} \sum_{j=0}^{j} c_{ij}\, x_{ijk} + \beta \sum_{k=1}^{k} \sum_{j=0}^{j} x_{ojk} \tag{1}$$

$$\sum_{k=1}^{k} \sum_{j=1}^{j} x_{ijk} \le K \qquad i = 0 \tag{2}$$

$$\sum_{j=1}^{N} x_{\mathrm{ijk}} = \sum_{j=1}^{N} x_{\mathrm{jik}} \le 1 \quad i = 0, \mathrm{k} \in \{1,2,\ldots,\mathrm{K}\} \tag{3}$$

$$\sum_{k=1}^{k} \sum_{j=0}^{j} x_{ijk} = 1 \ \text{或} \sum_{k=1}^{k} \sum_{i=0}^{i} x_{ijk} = 1 \quad i,\ j \in \{1,2,\ldots,\mathrm{N}\} \tag{4}$$

$$\sum_{i=o}^{N} \sum_{j=0}^{N} d_i\, x_{ijk} \le Q \qquad k \in \{1,2,\ldots,\mathrm{K}\} \tag{5}$$

$$x_{ijk} \in \{0,1\} \quad i, j \in \{1,2,\ldots,\mathrm{N}\}, k \in \{1,2,\ldots,\mathrm{K}\} \tag{6}$$

The formula (1) demonstrates the smallest total distribution cost, which is the objective function. It consists of the costs of vehicle distance and the number of vehicles enabled. Ci, j: the transportation cost of vehicles from customer i to customer j (distance); formula (2) means the number of vehicles from the distribution center is no more than K units; Formula (3) presents that each vehicle starting from the distribution center and eventually return to the distribution center; Formula (4) denotes that each customer point happens to be accessed by a vehicle once; formula

(5) said that the sum of the task assumed by each vehicle does not exceed the load capacity limit of the car the amount of Q(the vehicle's maximum load); formula (6): integer constraint, which restricts the number to be 0 or 1.

3 Improved Genetic Algorithm

3.1 Encoding and Decoding on Chromosome

In the genetic algorithm, the selection of encoding method often depends on the actual situation of the problem to be solved. In vehicle routing problem, feasible solutions should be composed of customers and access path, while the genetic algorithm can not deal directly with the solution data of the solution space. In this paper, in order to calculate conveniently, with the method of natural number encoding mechanism, the form of solutions for the vehicle routing problem is converted to genetic algorithm of genotype string data, and then forms chromosomes.

Supposing there are customers in the distribution center, the resulting production of chromosomes with a length of N, each gene in the chromosome corresponds to a customer; there is no gene locus of separation point between clients. So, there is no need to consider the impact of the separation point in the crossover and mutation operations. When decoding, what need to be done is just to put the customer of the corresponding gene point into the path in order as much as possible until a point against the constraints. For example, eight clients individual coding (51273684) can be interpreted as:

Sub path l: 0-5-1-2-0;

Sub path 2:0-7-3-6-0;

Sub path 3:0-8-4-0; (0 stands for the distribution center)

3.2 Improved Population Initialization

When the population is initialized, we will introduce a new mechanism based on the idea of mileage-saving method in order to produce part of the individual. Saving algorithm is one of the most classic heuristic algorithms for VRP. The idea of the algorithm is that according to the principle of the connection distance between the customers points will be the most economical. Then inserting the absence customer to line in proper order, it will be finished after all points are arranged into the line [7]. The formula to calculate the conservation value between two nodes of the save algorithm was shown in Figure 2, and its significance is shown in Equation (8):

$$S(i,j)=2(d(i,0)+d(0,j))-(d(i,0)+d(0,j)+d(i,j)) \tag{7}$$

That is: $$S(i,j)=d(i,0)+d(0,j)-d(i,j) \tag{8}$$

At the beginning, the algorithm to calculate the savings value of any two nodes and rank conservation values in descending order. Then according to the results, as well as the feasibility conditions, merger path until you can not find a better solution under constraints to some conditions.

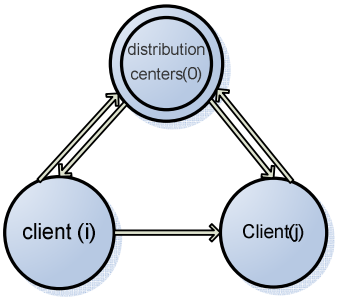

Fig. 2. The idea of Saving Algorithm

For example, for eight customers, we will get three sub paths as follow under the premise that satisfies the constraints by saving algorithm: sub path l: O-5-1-2-0; sub path 2:0-7-3-6-O; sub path 3:0-8-4-0. Then the realignment of three sub paths can produce the following individuals: 51273684, 51284736, 73651284, 73684512, 84736512, 84512736; these will be a part of the initial population, the other part will be randomly generated.

The individuals produced by the saving algorithm is generally more excellent than that produced random, but research shows that when encountering the huge number of customers or a complex service point distributed network, this algorithm will lead to huge computing workload and computational complexity. When facing the small scale, the algorithm shows its superiority comparing with the huge one to be dealt with. Of course, we can also divide the complex network randomly into a number of simple networks. When the problem that the little difference between individuals will easily fall into the "premature convergence" is taken into account, we will also randomly generate initial population as the probability of the saving initialization is too large.

3.3 Genetic Operators

(1) Selection Operator

Selection operator is similar to the natural evolution "natural selection, survival of the fittest". Its purpose is to turn the optimize individual in the population by means of cross-matching or inheriting directly into the next generation, and eliminate the least suitable individuals.

The idea of this paper is based on individual fitness. Part of the individual which have the highest individual fitness will do not participate in the crossing and mutation and directly get into the next generation, but for the individual with a very low degree will directly discarded. This will ensure that the best individual will be able to enter the next generation of genetic manipulation successfully, which can improve the operating efficiency of the algorithm and speed up the convergence rate of the population. For the rest, the roulette wheel selection operator which is easy to operate will be adopted [1].What roulette wheel selection describe is choosing a few

individuals from the group, these individuals probability that are selected are proportional to their relative fitness, the higher individual relative fitness value, the greater the probability that is to be selected. But it does not guarantee the individual that has higher relative fitness value can be elected to the next generation, which simply means that it has big probability to be selected. So we directly save the individual that has higher fitness value to the next generation, so that it can make up for the deficiency of the roulette wheel selection to a certain extent.

(2) The Improved Crossover Operator

The crossover operation is the most critical aspect in the genetic algorithm, which mimics the natural evolution process that two chromosomes form a new chromosome by mating to produce a new individual. Not only does the operation provide new individuals, but also it can generate new genes, so that crossover operator protects the individual diversity.

In the process of cross operations, the CX crossover operator is introduced as follow [3]:Randomly generate two bit string cross points, define the area between the two points as intersection, add the intersection in front of the first gene, and then remove the original individual parts of the same genes as the intersection of genes one by one, getting the individual as a result. An example for the crossover process is as follows:

(1) Randomly choose a cross area from parent individuals, If two father generation individual and cross area that were selected are describe as: Parent1="29|1674|538"， Parent2="734|2596|18", in which the symbol "| |" means cross area;

(2) Add the cross area of Parent2 to the front of the Parent1, and adding the cross area of Parent1 to the front of the Parent2, then we can get two provisional individuals: A="2596291674538",B="1674734259618";

(3) In A and B, deleting the same genes as that in cross area in the order after increase area, and then get the final two individual: Child1 = "259617438", Child2 = "167432598".

The cross operation process is as shown in figure 3.

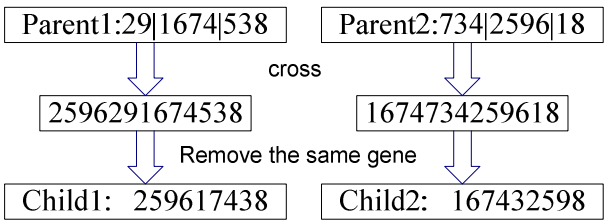

Fig. 3. Crossover operator

Compared with traditional single-point crossover and multi-point crossover, CX Cross ensure that even if two of the same individual cross, it was still able to produce a new individual, So that it gets rid of shortage of the traditional crossover operator on

the diversity of the population and avoids premature convergence and reduces the possible results for the local optimal solution.

Studies have shown that the crossover probability of the genetic algorithm have a direct impact on the convergence of the algorithm.

When the value of p_c remain the same, the higher the value, the faster of the new individuals generated by, with a too large p_c ,the possibility of genetic patterns breakage is increased and high-fitness individuals structure will soon be destroyed. If the value is too small, the search process will become slow or even be stagnant. When using adaptive crossover probability, different individuals have different values, as shown in the figure 4. In order to meet the above requirements, the paper uses adaptive crossover probability formula as follow:

$$P_c = \begin{cases} P_k & f < \bar{f} \\ \dfrac{P_k (f_{\max} - f)^2}{(f_{\max} - \bar{f})^2} & f \geq \bar{f} \end{cases} \tag{9}$$

In the above equation, $f_{\max}$ is the maximum fitness value in groups and $\bar{f}$ is the average fitness value of each generation group and f is the individual fitness and P_k is the crossover probability that has preset.

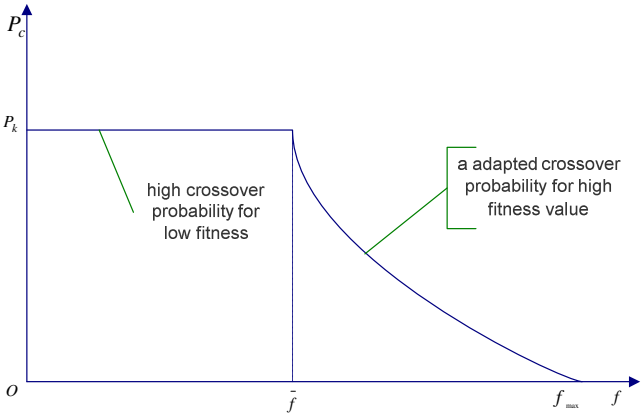

Fig. 4. Adaptive crossover probability

Setting the value of as 0.8, by the formula 9 and Figure 4, we can find that the cross probability is 0.8 when the individual's fitness is less than or equal to the average cross probability; the probability of cross adapt reduced accordingly when the individual's fitness greater than the average cross probability. In this way, we will ensure excellent individuals were reserved to the next generation. On the contrary, the poor individual will be implemented crossover operation with larger probability. The value of can be appropriately adjust according to specific needs in order to achieve the effect of to keep the best individual as much as possible.

(3) Mutation Operator

What the variation describe as randomly select a individual from the population at first, with regard to the selected individuals, randomly changing a string value in the string data structure with a certain probability.The mutation operator of genetic algorithm will be conducive to jump off a fixed area to search a broader space. In this paper, the inversion mutation operator is that selecting two points as the mutation point randomly at first,then invert the area between mutation points into a chromosome and make a new individual. And inversion mutation describe that in the evolutionary process we can effectively adjust the individuals of the population in order to prevent the premature convergence problem, as well as improving the genetic operation of the global optimization performance. The example of inversion mutation process is shown as follows:

(1) Randomly choose two change points in the individuals of father generation, so as to determine a variation area, for example: Temp = "29 | 16745 | 38", in which the symbol "| |" represents variation area;
(2) Inversing gene in genetic variation area, then replace the original position, thus we can obtains the new individual: Temp1 = "295476138";

The mutation process is shown in Figure 5.

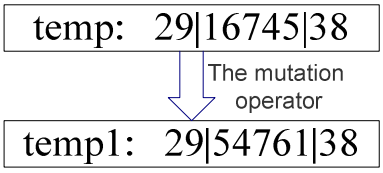

Fig. 5. Mutation operator

4 The Flowchart of Genetic Algorithm

The execution process of genetic algorithm is typical of iteration process, as shown in figure 6, and the process is described below:

Setp1 : Construct chromosomes satisfying the criteria. Genetic algorithm can not directly handle the solution space, so it must express the solution of the space as the corresponding chromosome by means of encoding. There are many chromosomes encoding method in practical problems, and natural number coding mode is adopted in this paper.

Setp2 : Generate the initial population and select the appropriate number, then set the relevant parameters. Such as the maximum generation, population size (N), crossover probability (Pc), mutation probability (Pm), and the dead-weight of every vehicle (Q) and so on.

Setp3 : Calculate the fitness of chromosomes. As an important evaluating index reflecting the quality of chromosomes, fitness is associated with the solution, and the individual with the largest fitness is the optimal solution of the genetic algorithm to be solved.

Setp4 : Produce new individuals by means of using selection, crossover and mutation operator.

Setp5 : Repeat step 3 and step 4, stopping evolution until meeting termination conditions, and then get the final result.

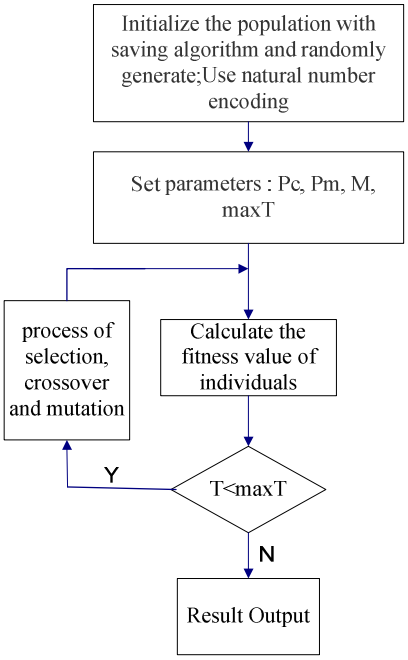

Fig. 6. The flowchart of Genetic algorithm

5 The Experimental Results and Analysis

In order to verify the feasibility of the algorithm, Benchmark Problems R101 examples designed by Solomon were selected as test data in this experiment. The basic parameters of the experiments be used in table 1 , and the test data showed in table 2. The first column figures in Table 2 represent distribution centers and customer node numbers, the figure 0 stands for distribution center; Data in the second and the third column represent x-axis and y-axis of distribution center or customer respectively, the fourth column figures mean the customers demand for goods . Each set of data is corresponding with one node shown in figure 7.

Table 1. Relevant parameter

Parameters	value
maximum generation	200
population size (N)	100
The number of customers	25
crossover probability(Pc)	0.8
mutation probability(Pm)	0.01
The unit cost	1.5
Enable fixed costs	10
Deadweight（Q）	60

Table 2. The Message of clients

Client (i)	Axis (x)	Axis (y)	Demand (Gi)	Client (i)	Axis (x)	Axis (y)	Demand (Gi)
0	35	35	0	13	30	25	23
1	41	49	10	14	15	10	20
2	35	17	7	15	30	5	8
3	55	45	13	16	10	20	19
4	55	20	19	17	5	30	2
5	15	30	26	18	20	40	12
6	25	30	3	19	15	60	17
7	20	50	5	20	45	65	9
8	10	43	9	21	45	20	11
9	55	60	16	22	45	10	18
10	30	60	16	23	55	5	29
11	20	65	12	24	65	35	3
12	50	35	19	25	65	20	6

Table 3. Experimental results

Objective / results	The best value	Generation number	Vehicle number
Calculation results	912	89	7
path number	Service order		
1	0-19-4-22-0		
2	0-15-11-1-23-0		
3	0-24-5-2-9-0		
4	0-13-20-7-14-0		
5	0-25-12-21-3-0		
6	0-18-17-16-10-8-0		
7	0-6-0		

After several tests, we list the optimal experimental results in the table 3 and the corresponding distribution path scheme be shown in Figure 7. From the table 3 we can see that we get the optimal solution 912 in the 89th generation.

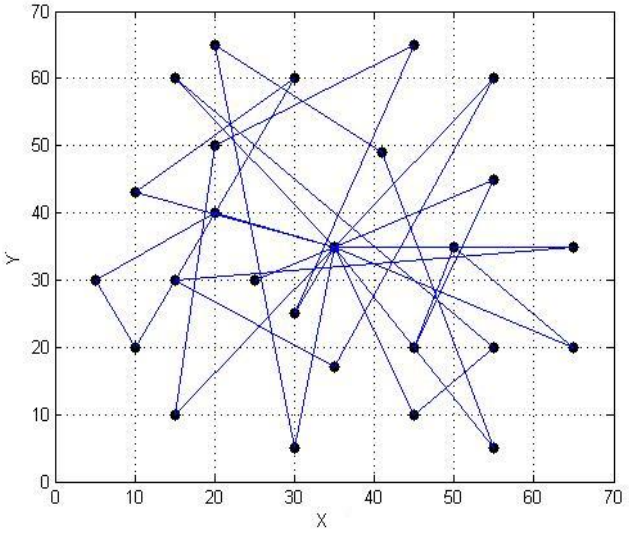

Fig. 7. Distribution path

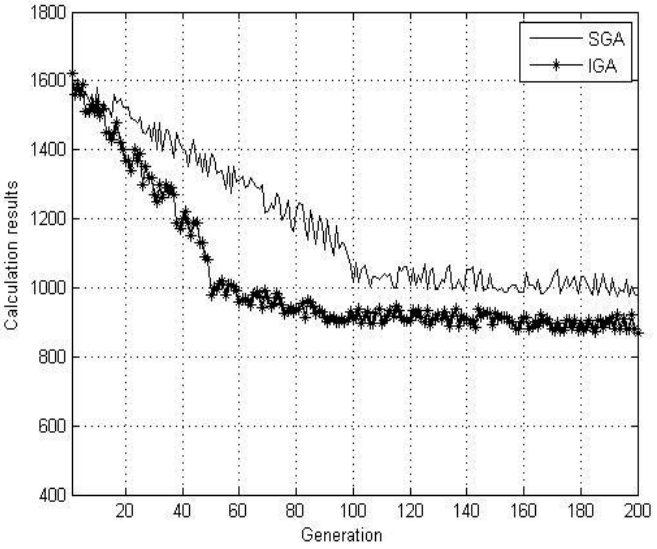

Fig. 8. Compared with the basic algorithm

From the Figure 8 we can see that, in the beginning stage of the optimizations in the process the curve falls relatively steep. Carry on with the conduct of the process, the curve which is optimized would become flatten and get the optimal solution 912 in the 89th generation. Since initial population is generated randomly, fitness of population in the beginning stage of the optimizations in the process is poor. Carry on with the conduct of the process, the mechanism which can find best solution automatically would conduct the convergence procedure convergent to the direction which is more optimized so that the solution would approach the optimal solution gradually. Since 60th generation, the volatility of the solution got relatively stable, and got the optimal solution in 89th generation.

We can find that the improved genetic algorithm is superior to the basic genetic algorithm in solution quality, speed, and stability, and it is a feasible and effective way to solve a vehicle routing problem. Additionally, different parameters may obtain different performance during solving process, therefore generally require repeated adjustments or setting the parameters according rule of thumb because of their great unpredictability. The reason is that the genetic algorithm is guidance of a randomized search technical. The operation of the genetic operators needs to randomly generate the corresponding random number. The good or bad numbers have effect on the research performance of genetic algorithm to some extent. So even if the same question, we may get different test results by using the same parameter setting. Additionally, because different parameters may obtain different performance during solving process , generally require repeated adjustments or according rule of thumb to set the parameters, As a result, the search solutions become great uncertain.

6 Conclusion and Future Work

This paper mainly studies the application of the genetic algorithm for vehicle routing optimization problems. Aimed at the characteristics of the VRP problem based on the results of many researchers, we modifie the process of initial population and cross operator, and proposes a new adaptive adjustment method for crossover probability, moreover puts forward the improved genetic algorithm. The experimental results show that the improved method proposed in this paper can effectively speed up the convergence and reduce the possibility of the results for the local optimal solution. But in the course of the study, we did not consider the influence of real-time traffic information and personalized service time requirements for the customer, but to analyze the feasibility of the proposed algorithm from a theoretical point of view. We will focus on analyzing the superiority of the algorithm from the point of view of practical application in the next research.

Acknowledgements. This work was supported by Guangdong Provincial Natural Science Foundation (Grant No.10451009001004804 & 9151009001000007), and Key Laboratory of the Ministry of Education project (Grant No. 110411).

References

1. Jiang, B.: Study of Vehicle Routing Problem with Time Windows Based on Genetic Algorithm. Beijing Jiaotong University (2010)
2. Cai, Z.: Research on logistics vehicle routing problem based on genetic algorithm. In: 2011 IEEE 3rd International Conference on Communication Software and Networks (ICCSN), pp. 232–235 (2011)
3. Huang, X., Zou, S., Zhang, H.: Improved genetic algorithm and its application to the optimization of physical distribution routing. Journal of Southwest University for Nationalities (Natrual Science Edition) 34(4) (2008)
4. Ren, C., Wang, X.: Research on Vehicle Scheduling Problem Based on Improved Genetic Algorithm for Electronic Commerce. In: 2007 Second IEEE Conference on Industrial Electronics and Applications, pp. 1887–1891 (2007)
5. Gong, G., Hu, X.-T., Wei, K.-X., Hao, G.-S.: Optimized Performance Research of the Vehicle Routing Problem in Industry Logistics. Computer Science & Engineering (2011)
6. Lang, M.X.: Study of the optimizing of physical distribution routing problem based on genetic algorithm. China Journal of Highway and Transport 15(3) (2002)
7. Zhang, Y.-M.: Research on Routing Optimization of Logistics Distribution Based on Saving Algorithm and its Improved. South China Normal University of Zengcheng College, Guangzhou (2011)
8. Lang, M.: Vehicle routing problem model and algorithm. Publishing House of Electronics Industry, Beijing (2009)
9. Kunkel, M., Schwind, M.: Vehicle Routing with Driver Learning for Real World CEP Problems. In: 2012 45th Hawaii International Conference on System Science (HICSS), pp. 1315–1322 (2012)
10. Calvete, H.I., Gale, C., Oliveros, M.J.: A goal programming approach to vehicle routing problems with soft time windows. European Journal of Operational Research 177, 1720–1733 (2007)
11. Alvarenga, G.B., Mateus, G.R., de Tomi, G.: A genetic and set portioning two-phase approach for the vehicle routing problem with time windows. Computers & Operations Research 34, 1561–1584 (2007)
12. Ge, H., Wang, Y.: Improved simulated annealing genetic algorithm for VRPSDP problem. Computer Engineering and Applications 46(30), 36–39 (2010)
13. Nazif, H., Lee, L.S.: Optimized crossover genetic algorithm for vehiclerouting problem with time windows. Amer. J. Appl. Sci. 7(1), 95–101 (2010)
14. Ghoseiri, K., Ghannadpour, S.F.: Hybrid genetic algorithm for vehicle routing and scheduling problem. J. Appl. Sci. 9(1), 79–87 (2009)
15. Kulkarni, R.V., Venayagamoorthy, G.K.: Bio-inspired algorithms for autonomous deployment and localization of sensor nodes. IEEE Trans.Syst., Man, Cybern. C, Appl. Rev. 40(6), 663–675 (2010)
16. Amini, S., Javanshir, H., Tavakkoli-Moghaddam, R.: A PSO approach for solving VRPTW with real case study. Int. J. Res. Rev. Appl. Sci. 4(3), 118–126 (2010)
17. Cheng, L., Wang, J.: Improved gentic algorithm for vehicle routing problem. Computer Engineering and Applications 46(36), 219–221 (2010)
18. Zhang, J., Fang, W.: Improved gentic algorithm for vehicle routing problem with time window. Computer Engineering and Applications 46(32), 228–231 (2010)
19. Gendreau, M., Tarantilis, C.D.: Solving large-scale vehicle routing problems with time windows - the state-of-the-art. Technical report, Universite de Montreal, CIRRELT (2010)

Cost-Effective and Distributed Mobility Management Scheme in Sensor-Based PMIPv6 Networks with SPIG Support

Soonho Jang[1], Hana Jang[1], and Jongpil Jeong[2,*]

[1] Graduate School of Information and Communications, Sungkyunkwan Univeristy
Seoul, 110-745, Korea
[2] College of Information and Communication Engineering, Sungkyunkwan Univeristy
Suwon, Kyunggi-do, 440-746, Korea
{prolike,hnsh77}@naver.com, jpjeong@skku.edu

Abstract. Due to limited resources, the slow progressive development of wireless sensor networks (Wireless Sensor Network) through the development of hardware and power management technology is currently in progress for the development of the latest IP-based IP-WSN. Those with low-power devices on IPv6 can mount the 6LoWPAN (IPv6 over Low power WPAN) this is getting attention. In these IP-based sensor networks, existing IP-based schemes, which were impossible in wireless sensor networks, become possible. 6LoWPAN is based on the IEEE 802.15.4 sensor network and is a technology developed for IPv6 support. The host-based mobility management scheme in IP-WSN is not suitable due to the additional signaling; the network-based mobility management scheme is suitable. In this paper, we propose an enhanced PMIPv6 route optimization, which considers the multi-6LoWPAN network environment. All SLMA (Sensor Local Mobility Anchor) of the domain 6LoWPAN is connected to the SPIG (Sensor Proxy Internetworking Gateway) and perform cross-domain distributed mobility control. All information of SLMA in the 6LoWPAN domain is maintained by SMAG (Sensor Mobile Access Gateway) and route optimization is performed quickly and the route optimization status information from SPIG is stored to SLMA and is supported without additional signaling.

Keywords: Mobile Networks, Distributed Mobility Control, Proxy Mobile IPv6, Wireless Sensor Networks.

1 Introduction

Standardized IP-based 6LoWPAN [1] is IPv6 packets transmission technology at wireless sensor networks (WSNs) over the IEEE 802.15.4 Standard MAC and Physical layer. However, there are existing sensor networks in 6LoWPAN limited resources (low-power, limited storage space, a small packet size, and so on), which will present the same limitations, too. The current IP-WSN is a wireless sensor

* Corresponding author.

Q. Zu, B. Hu, and A. Elçi (Eds.): ICPCA-SWS 2012, LNCS 7719, pp. 259–273, 2013.

network and the integration of IPv6 technology is widely recognized as the global sensor network infrastructure and is applied to health care systems, surveillance systems and a variety of applications, such as real-time requirements. Therefore, fast and seamless handover supports are an important 6LoWPAN research issue.

To support mobility in the 6LoWPAN standard mobility protocol, MIPv6, [3] is that IETF 6LoWPAN WG [2] has been proposed, but did not consider the handover. Also, in order to support the Intra-PAN handover for the proposed LoWMo [4] to reduce delays in handover MN for the parent node by estimating the location after the move of the new parent node, information should be transferred to the preset. Mobility management is one of the most important research issues in 6LoWPAN, which is a standardized IP-based WSNs (IP-WSN) protocol.

In this paper, the SPMIPv6 (Sensor Proxy Mobile IPv6) [6] domain managed by SPIG (Sensor Proxy Internetworking Gateway) is separated to manage control between domains. SPMIPv6 domain managing SLMA (Local Mobility Anchor Sensor) and the cost of the SPIG domain is the sum of mobility costs within the existing simple distributed mobility of the PMIPv6 [5] domain. Therefore, our scheme shows the optimized distributed mobility control in the PMIPv6 domain.

The rest of the paper is organized as follows. Chapter 2 reviews background data related to PMIPv6, 6LoWPAN and SPIG. The proposed SPIG architecture, along with its mobility scenarios, sequence diagram and message formats are presented in Chapter 3. Chapter 4 describes performance analysis and evaluation, and finally Chapter 5 concludes the paper.

2 Related Work

2.1 PMIPv6

The main idea of PMIPv6 is that the mobile node is not involved in any IP layer mobility-related signaling. The Mobile Node is a conventional IP device (that is, it runs the standard protocol stack). The purpose of PMIPv6 is to provide mobility to IP devices without their involvement. This provision is achieved by relocating relevant functions for mobility management from the Mobile Node to the network. PMIPv6 provides mobility support within the PMIPv6 domain. While moving within the PMIPv6 domain, the Mobile Node keeps its IP address, and the network is in charge of tracking its location. PMIPv6 is based on Mobile IPv6 (MIPv6), reusing the Home Agent concept but defining nodes in the network, which must signal the changes in the location of a Mobile Node on its behalf.

Figure 1 represents the PMIPv6 domain architecture. The functional entities in the PMIPv6 network architecture include the following:

• Mobile Access Gateway (MAG): This entity performs mobility-related signaling on behalf of the Mobile Nodes attached to its access links. The MAG is usually the access router for the Mobile Node, that is, the first-hop router in the Localized Mobility Management infrastructure.

• Local Mobility Anchor (LMA): This entity within the core network maintains a collection of routes for each Mobile Node connected to the LMD. The routes point to the MAGs managing the links where the Mobile Nodes are currently located. Packets sent or received to or from the Mobile Node are routed through tunnels between the LMA and the corresponding MAG.

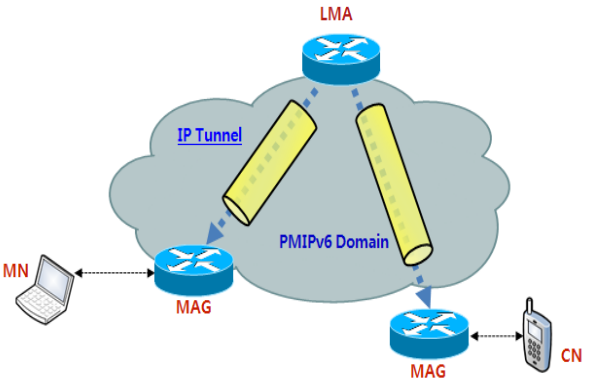

Fig. 1. PMIPv6 Domain

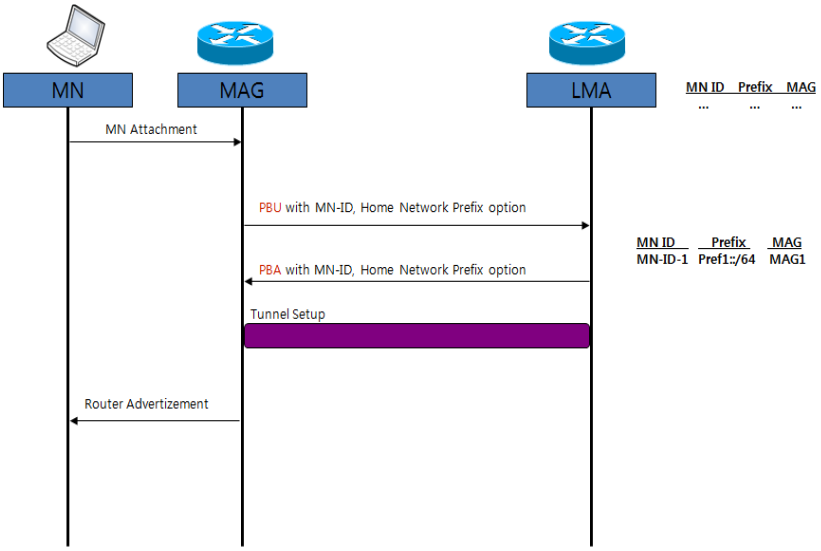

Fig. 2. PMIPv6 Basic Operation

Figure 2 shows PMIPv6 basic operation. That is as follows. When a Mobile Node enters a PMIPv6 domain, it attaches to an access link provided by a MAG. The MAG proceeds to identify the Mobile Node and checks if it is authorized to use the network-based mobility management service. If it is, The MAG performs mobility

signaling on behalf of the Mobile Node. Also, the MAG sends a Proxy Binding Update (PBU) to the LMA associating its own address with the identity of the Mobile Node. Upon receiving this request, the LMA allocates a prefix to the Mobile Node. Then, the LMA sends a Proxy Binding Acknowledgment (PBA) to the MAG including the prefix allocated to the Mobile Node. It also creates a Binding Cache entry and establishes a bidirectional tunnel to the MAG. The MAG sends Router Advertisement messages to the Mobile Node, including the prefix allocated to the Mobile Node, so the Mobile Node can configure an address.

2.2 6LoWPAN

The 6LoWPAN working group of the IETF has defined an adaptation layer for sending IPv6 packets over IEEE 802.15.4.[7,8] The goal of 6LoWPAN is to reduce the sizes of IPv6 packets in order to make them fit into 127 byte IEEE 802.15.4 frames. The 6LoWPAN proposal consists of a header compression scheme, a fragmentation scheme, and a method for framing IPv6 link local addresses into IEEE 802.15.4 networks. The proposal also specifies enhanced scalabilities and mobility of sensor networks. The challenge to 6LoWPAN lies in the sizable differences between an IPv6 network and an IEEE 802.15.4 network. The IPv6 network defines a maximum transmission unit as 1,280 bytes, whereas the IEEE 802.15.4 frame size is 127 octets. Therefore, the adaptation layer between the IP layer and the MAC layer must transport IPv6 packets over IEEE 802.15.4 links. The adaptation layer is responsible for fragmentation, reassembly, header compression and decompression, mesh routing, and addressing for packet delivery under the mesh topology. The 6LoWPAN protocol supports a scheme to compress the IPv6 header from 40 bytes to 2 bytes.

2.3 Sensor Mobility over 6LoWPAN

The network-based mobility management approach, PMIPv6, is more suitable than the host-based approach for supporting the mobility for 6LoWPAN since there are no mobility related signaling messages over the wireless link. Accordingly, the performance of the network-based mobility scheme in terms of energy consumption, signaling costs, and handoff latency can certainly be reduced compared to the host-based mobility scheme. However, the single-hop-based PMIPv6 protocol of the network-based mobility scheme cannot be applied to the multi-hop-based 6LoWPAN.

2.4 SPMIPv6

To introduce an efficient addressing and routing scheme in our proposed global IP-WSN, we use sensor proxy mobile IPv6 (SPMIPv6) architecture. Figure 3 shows the proposed architecture. That has different functional components. The architecture mainly consists of a sensor network-based localized mobility anchor (SLMA). It also contains a sensor network-based mobile access gateway (SMAG). For end-to-end communications, it contains many full functional devices (FFDs) and reduced functional devices (RFDs).

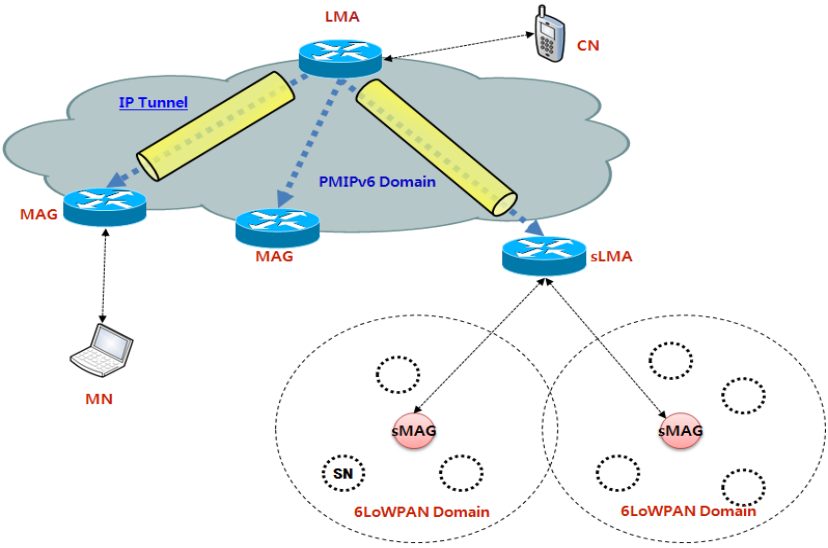

Fig. 3. Sensor Mobility over 6LoWPAN

3 Proposed SPIG Scheme

The SLMA acts as a topological anchor point for the entire IP-WSN domain. The main role of the SLMA is to maintain accessibility to the sensor node while the node moves in or outside the IP-WSN domain. The SLMA includes a binding cache entry for each sensor node, both encapsulation and decapsulation sections and a SMAG information table. The binding cache entry at the SLMA is used for holding the information of the mobile sensor node. It includes different information such as the sensor node's address, the sensor node's home network prefix, and a flag bit indicating sensor proxy registration. It also acts as the interfacing device between the IP-WSN domain and the Internet domain.

The SMAG acts like a sink node in a traditional sensor network. With regards to the proposed IP-WSN based on SPMIPv6 it acts like an access gateway router with the main function of detecting sensor node movement and initiating mobility-related signaling with the sensor node's SLMA on behalf of the sensor node. It can move with its member sensor node as a SMAG domain within or outside an IP-WSN domain similar to the body sensor network of a patient. It consists of different functional modules such as routing, neighbor discovery, sensor information table, adaptation module and interfacing modules to the sensor node and border router. The routing module performs efficient data transmission among individual sensor nodes and facilitates the end to end communication. The neighbor discovery module performs neighbor discovery and duplicate address detection functionality. The adaptation module performs the task of transmitting IPv6 packets over IEEE 802.15.4 link as mentioned in the 6LoWPAN adaptation layer. The sensor information table provides the up to date information about the sensor nodes to the SLMA.

The IP-WSN domain is comprised of numerous sensor nodes based on IPv6 addresses. We consider the domain as a federated IP sensor domain. There are two types of sensor nodes. One type contains the tiny TCP/IP communication protocol stack with an adaptation layer and an IEEE 802.15.4 interface. This type can forward information to other nodes of similar type as well as information sensing from the environment. Actually, this type of sensor node acts as a mini sensor router and is considered a fully functional device. The other type of sensor node has the protocol stack and environment sensing capability, but can only forward the sensed information to nearby mini sensor router nodes. These types of sensor nodes are considered reduced functional devices. Nevertheless, both types are able to perform end to end communication.

3.1 SPIG Architecture

Figure 4 shows the architecture of SPIG including SPIG, SLMA, SMAG and IP sensor node. The SPIG acts as a topological anchor point for the entire SPMIPv6 domain. The main role of the SPIG is to maintain accessibility to the sensor node while the node moves in or out of the SPMIPv6 domain. The SPIG includes a binding cache entry for each sensor node, encapsulation and decapsulation sections and a SLMA information table. The binding cache entry at the SPIG is used for holding the information of the mobile sensor node.

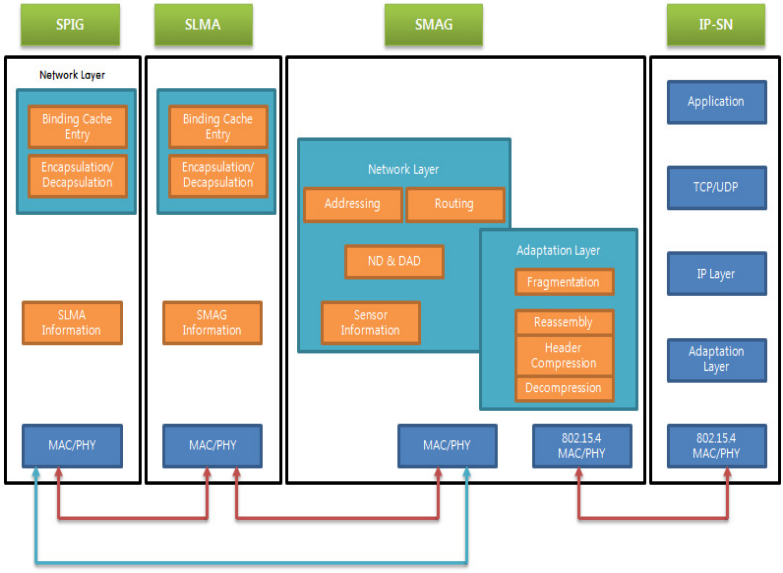

Fig. 4. Operation Architecture of SPIG

3.2 SPIG Message Flow

Figure 5 shows message flow in SPIG architecture. All data transfers flow through the SPIG. In the packet delivery, the control operation for the binding query is separated from the data packet delivery. The data passed from CN to IP-WSN includes several stages. First, IP-WSN acquires access to the network and sends a Router Solicitation message to the SMAG. Second, the RS message is received within the SMAG and then the SMAG saves IP-SN information and sends the PBU message to the SLMA. Third, the LBU and LBA message is sent to the SLMA. Fourth, The SLMA will send PBA messages. Fifth, the PBA message received by SMAG was sent to the RA command IP-SN. And then IP-SN can respond CN request. CN is the PMIPv6 network for MAG and LMA, SPIG acquires the information from the IP-SN, and then you may be able to submit data through the SMAG.

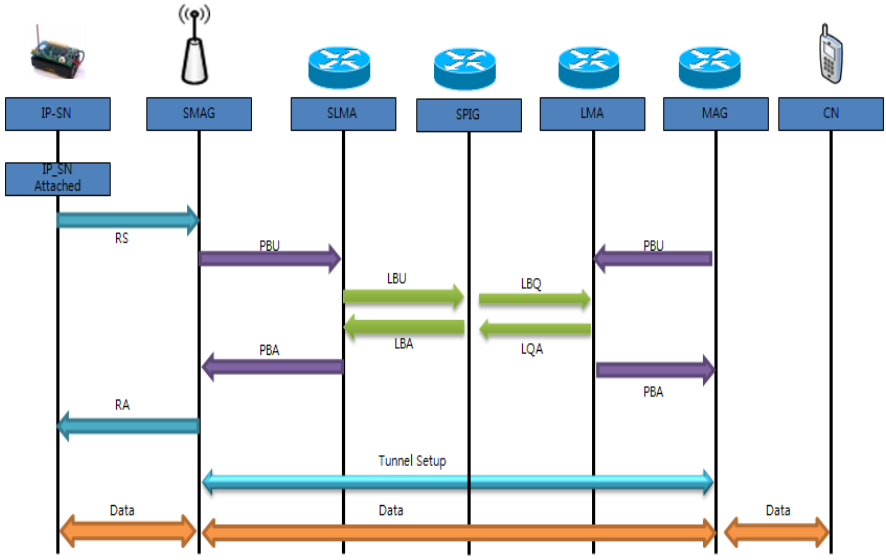

Fig. 5. SPIG Message Flow

4 Performance Analysis

4.1 Network Mobility Model

Mobility of the IP-sensor node and the SMAG domain network are the major advantages of IP-WSN over the static wireless sensor networks. In this paper, mobility is the key concern in the design and performance analysis of the SPIG. Most wireless network performance studies assume that the coverage areas are configured as a hexagonal or square shape. We assume that IP-WSN networks are to be configured with a square topology. Sensor nodes for an IP-WSN area are assumed to

have identical movement patterns within and across IP-WSN. A 2D square shaped random walk mobility model can be used to study the movement pattern of the movable sensor nodes. In this paper, we used a network model subject to some modification for the five-layer personal area network model, with n = 5. In our network model, an IP-WSN consists of a cluster of 2D square shaped sensor nodes, as shown in Figure 6. Each macro-cell covers n × n micro-cells (n = 5). Each macro-cell coverage area is one location area (LA). Firstly, we can aggregate the states of cells based on their symmetrical positions. Cells belonging to such an aggregated state have the same properties. There are six aggregated states for the 5 × 5 square shaped micro-cell/macro-cells. The corner states (S11, S15, S51 and S55) are grouped into state S1. State S2 consists of (S12, S14, S21, S25, S41, S45, S52 and S54), state S3 consists of (S13, S31, S35 and S53), state S4 consists of (S22, S24, S42 and S44), state S5 consists of (S23, S32, S34 and S43), and state 6 consists of S33. In this figure, aggregate states S1, S2 and S3 are the boundary states. We define asterisk boundary states, S1*, S2* and S3*, which are in the LAs adjacent to the LA under consideration. Figure 7 also demonstrates the state transition diagram for the Markov chain. Movement into any boundary state indicates inter-IP-WSN mobility, which can be used to study binding update costs [9].

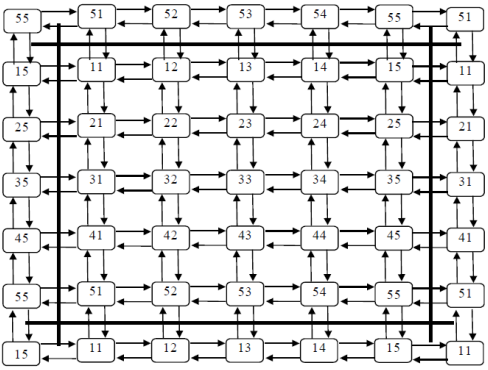

Fig. 6. Square shaped cell layout of a five-sublayer

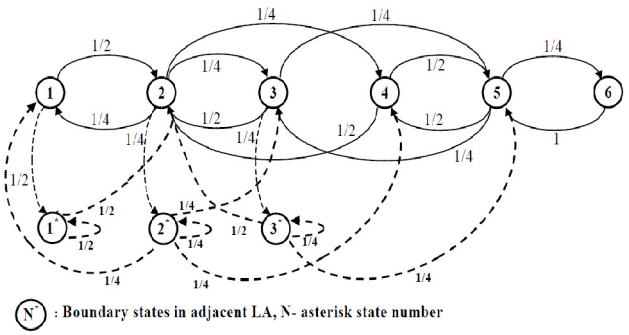

Fig. 7. State transition diagram for a 5 * 5 square cell model

The state transition diagrams in Figure 7 demonstrates that there are no transient sets in the model but only a single ergodic set with only one cyclic class, hence the regular Markov chain properties can be applied to analyze the behavior of the proposed model. As long as the SN moves within cells in a location area, SN is in one of the main aggregate state. Let *P* be the regular transition probability matrix, then the steady state probability vector π can be solved by the following equations:

$$\pi P = \pi \text{ and } \sum_{i=1}^{m} \pi_i = 1$$

Where m is the number of states *P*, the fundamental matrix for the regular Markov chain is given by:

$$Z = [Z_{ij}] = (I - P + A)^{-1}$$

Where *A* is the limiting matrix determined by *P*, and the powers *Pn* approach the probability matrix *A*. Each row of *A* comprises the same probability vector $\pi = \{\pi_1, \pi_2, \ldots, \pi_n\}$, i.e. $A = \xi\pi$, where ξ is column vector with all entries equal to 1. *I* mean the identity matrix. The matrix *Z* can be used to study the behavior of the regular Markov chain and through the use of this matrix one can compute the mean number of times the process is in a particular state. Let $y_j^{(k)}$ be the number of times that a process is in the state S_j in the first *k* steps, then if $M_i\left[y_j^{(k)}\right]$ is the mean number of times the process is in the state S_j starting from the state S_i is given by:

$$M_i\left[y_j^{(k)}\right] \rightarrow (Z_{ij} - \pi_j) + k\pi_j$$

The total number of boundary updates in *k* steps starting from state S_i can be computed by the total number of times that the process is in the asterisk states (for e.g. 1*, 2* and 3* in Figure 7) starting from state S_i – the initial state. Hence, if UA_LA is the average number of location updates in the analytical model, this is given by:

$$U_{A\_LA} = M_i\left[y_{1*}^{(k)}\right] + M_i\left[y_{2*}^{(k)}\right] + M_i\left[y_{3*}^{(k)}\right]$$

Generalizing,

$$U_{A\_LA} = \sum_{n=1^*}^{N^*} M_i\left[y_n^{(k)}\right]$$

Where 1*, 2* ….N* are the asterisk states in the model. The geometric random variable arises when we count the number *M* for the independent Bernoulli trials until the first occurrence of a success. *M* is called the geometric random variable and it takes on values from the set {1,2, ...}. We found that the *pmf* of *M* is given where $p = P[A]$ as the probability of "success" in each Bernoulli trial. Note that $P[M = k]$ decays geometrically with *k*, and that the ratio of consecutive terms is $\frac{p_{M(k+1)}}{p_{M(k)}} = (1 - p) = q$. As *p* increases, the *pmf* decays more rapidly.

If $M \leq k$ can be written,

$$P[M \leq k] = \sum_{j=1}^{k} pq^{j-1} = p\sum_{j=0}^{k-1} q^{j} = p\frac{1-q^{k}}{1-q} = 1 - q^{k}$$

From the above expression, we can obtain intra-mobility cost.

$$M_{intra-IP-WSN} = 1 - (1 - \frac{1}{U_{bu}})^{k}$$

If we get intra-mobility cost, also we get inter-mobility cost. Inter-mobility cost is intra-mobility cost and inter-domain binding update cost.

$$M_{inter-IP-WSN} = 1 - (1 - \frac{1}{U_{bu}})^{k} * \frac{1}{U_{bu}}$$

4.2 Cost Analysis

Figure 8 show SPIG architecture over SPMIPv6. SPMIPv6 structure combine intra-Domain Mobility control model and inter-Domain mobility control model. SPMIPv6 of all domains are combined with SPIG, and SPMIPv6 domains oversee the SLMA and are composed of SMAG. Global mobility can control through SPIG.

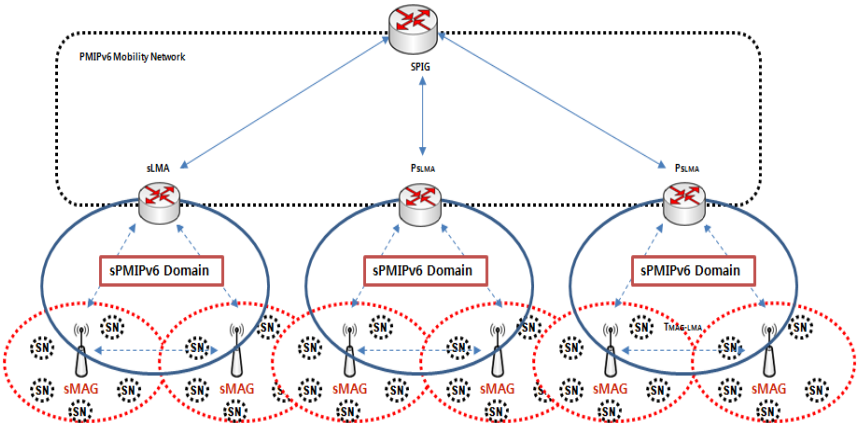

Fig. 8. SPIG over SPMIPv6

The total cost of IP-WSN in internal move costs and the signaling of IP-WSN are available as the sum of an inter-domain move. Table 1 explains the symbols used.

The PMIP inter-domain binding update operation is done as follows. When IP-SN enters a new SMAG region, IP-SN is in the Router Solicitation SMAG messages. Following this, the IP-SN of the SMAG is the PBU and the PBA control messages, which can be exchanged in the SLMA, and then the SLMA sends a message to IP-SN in the Router Advertisement. As a result, the cost of updating the cross-binding domain of the PMIP can express the following:

$$BUC_{PMIP} = M_{inter-IP-WSN} + S_{CONTROL} * 2T_{SMAG-SLMA} + P_{SLMA}$$

Thus, the packet delivery cost from CN to IP-SN can be calculated as follows. First, a data packet of CN is passed to the MAG. Then the MAG of CN and LMA exchange PBQ and PQA messages, and then the MAG receives a CoA from IP-SN. The MAG of CN delivers data packets in LMA. LMA of CN is LBQ and LQA messages sent to the SLMA. LMA of CN is delivers packets of data to the SMAG of IP-SN. SLMA of IP-SN delivers packets to the SMAG of IP-SN. Finally, the SMAG of IP-SN delivers data packets to IP-SN. The cost regarding the inter-domain for the PMIP packet forwarding is as follows:

$$PDC_{PMIP} = S_{DATA} * \begin{pmatrix} T_{CN-MAG} + T_{MAG-LMA} + T_{LMA-SLMA} + \\ T_{SLMA-SMAG} + T_{SMAG-SN} \end{pmatrix} + S_{CONTROL} * (2T_{MAG-LMA} + 2T_{LMA-SLMA}) + P_{LMA} + P_{SLMA}$$

So, we obtain the total cost of PMIP as follow:

$$TC_{PMIP} = BUC_{PMIP} + PDC_{PMIP}$$

The SPMIPv6 Inter-domain binding update operation is done as follows. When IP-SN enters a new SMAG region, IP-SN is in the Router Solicitation SMAG messages. Following this, the IP-SN of the SMAG is the PBU and the PBA control messages, which can be exchanged in the SLMA, and then the SLMA sends a Router Advertisement message to the IP-SN. As a result, the cost of updating the cross-binding domain of the SPMIP is as follows:

$$BUC_{SPMIP} = M_{inter-IP-WSN} + S_{CONTROL} * 2T_{SMAG-SLMA} + P_{SLMA}$$

Thus, the packet delivery cost from CN to IP-SN can be calculated as follows. First, a data packet of CN is passed to the MAG. Then the MAG of CN and LMA exchange PBQ and PQA messages, and then the MAG receives a CoA from IP-SN. The MAG of CN delivers data packets in LMA. LMA of CN is LBQ and LQA messages sent to SLMA. LMA of CN delivers packets of data to the SMAG of IP-SN. Finally, the SMAG of IP-SN delivers data packets to IP-SN. The cost regarding the inter-domain of the SPMIP packet forwarding is as follows:

$$PDC_{SPMIP} = S_{DATA} * (T_{CN-MAG} + T_{MAG-LMA} + T_{LMA-SMAG} + T_{SMAG-SN}) + S_{CONTROL} * (2T_{MAG-LMA} + 2T_{LMA-SLMA}) + P_{LMA} + P_{SLMA}$$

So, we obtain the total cost of SPMIP as follow:

$$TC_{SPMIP} = BUC_{SPMIP} + PDC_{SPMIP}$$

The SPIG inter-domain binding update operation is done as follows. When IP-SN enters a new SMAG area, IP-SN is in the Router Solicitation SMAG messages.

Following this, the IP-SN of SMAG is the PBU and the PBA control messages, which can be exchanged in the SLMA, and then the SLMA sends a Router Advertisement message to the IP-SN. The SLMA send LBU message to SPIG, and then SLMA can update SPIG latest information. SPIG is the LBA control messages sent to the SLMA. As a result, the cost of updating the cross-binding domain of the SPIG is as follows:

$$BUC_{SPIG} = M_{inter-IP-WSN} + S_{CONTROL} * 2T_{SMAG-SLMA} + P_{SLMA}$$

The packet delivery cost from CN to IP-SN can be calculated as follows. First, a data packet from CN is passed to the MAG. The MAG of CN and the LMA of CN exchange PBQ and PQA messages. The LMA of CN receives IP-SN information of the SLMA from SPIG. SPIG sends an LQA message to the LMA of CN then the LMA of CN receives the SLMA of IP-SN information. The MAG of CN sends a PBQ message to the SLMA of IP-SN. Then, the SLMA of IP-SN sends a PQA message to the MAG of CN. The MAG of CN is as a data packet should pass IP-SN of SMAG. Finally, IP-SN as the IP-SN of the SMAG delivers data packets. SPMIPv6 the cost of packet forwarding cross-domain as follows:

$$PDC_{SPIG} = S_{DATA} * (T_{CN-MAG} + T_{MAG-SMAG} + T_{SMAG-SN}) + S_{CONTROL} * (2T_{MAG-LMA} + 2T_{LMA-SPIG}) + P_{LMA} + P_{SLMA}$$

So, we obtain the total cost of SPIG as follow:

$$TC_{SPIG} = BUC_{SPIG} + PDC_{SPIG}$$

4.3 Numerical Results

Figure 9 shows the cost with respect to the number of nodes in the IP-WSN in term of the PMIPv6, SPMIPv6 and SPIG. PMIPv6 and SPMIPv6 compared with SPIG showed to be more cost effective.

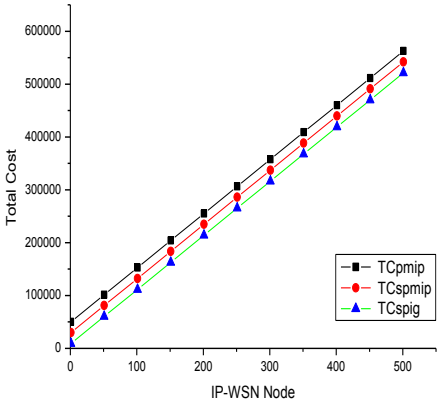

Fig. 9. Number of IP-WSN Node

Figure 10 is the hop count to reach the destination nodes according to the cost analysis number. The maximum hop count is 15. The increase in the number of hop count cost in accordance with the methodology proposed increased linearly and SPMIPv6 compared to PMIPv6 demonstrated good performance.

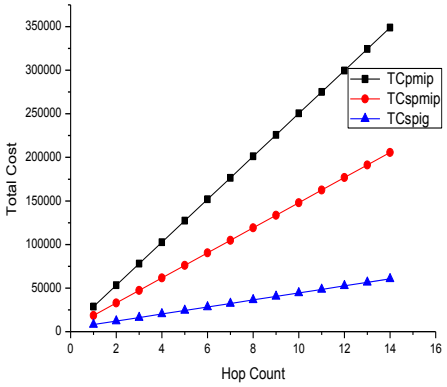

Fig. 10. Number of Hop Count

Figure 11 and Figure 12 are the binding updates and show the sum of the cost lookup behavior. All techniques shown in the picture are almost unaffected. This is the total cost of the binding update and lookup behavior is an important, you might find that does not affect.

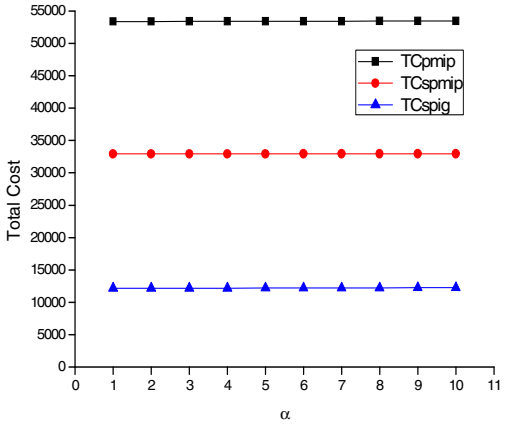

Fig. 11. Cost Analysis as Binding Update

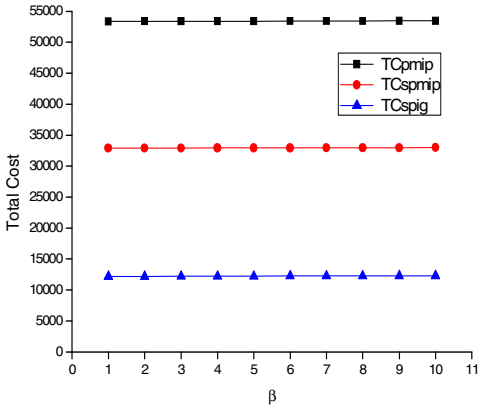

Fig. 12. Cost Analysis as Lookup

Figure 13 is the number of hosts contained in the MAG, and the total cost of the analysis. As shown in comparison to host MAG count, almost all the schemes do not affect.

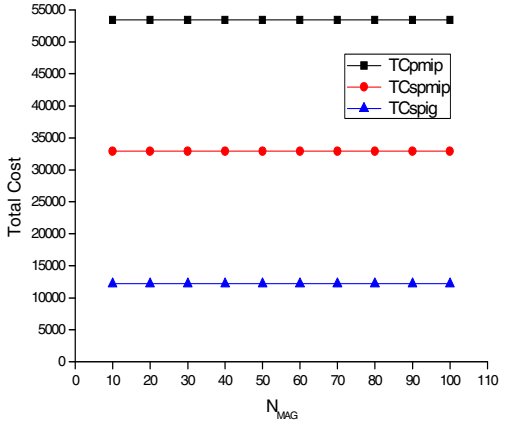

Fig. 13. Number of MAG vs. Total Cost

Looking at all of the results of the analysis, the expansion of the existing domain distributed mobility control, and apply the techniques suggested in this paper than the techniques in the analysis showed that the performance of all cost effective. In particular, signal distributed control technique SPIG full figured most effectively in terms of cost.

5 Conclusions

SPIG was proposed in order to resolve the issue regarding IP-SN hand-over excessive signal transport problems and delays, recent 6LoWPAN within a domain, for efficient data processing and distributed control study. This paper discusses recent research in the PMIPv6 domain regarding the mobility of IP-SN and the SPMIPv6 techniques presented in this paper are applied rather than a separate hand-over procedure, even if they are not for LMA and SLMA information is included in the SPIG has continuous network. If you look at the cost side, by the analysis of the existing SPMIPv6 techniques using distributed control techniques than SPIG performance will prove to be excellent.

Acknowledgments. This research was supported by Basic Science Research Program through the National Research Foundation of Korea(NRF) funded by the Ministry of Education, Science and Technology(2011-0027030).

References

1. Mulligan, G., Group, L.W.: The 6LoWPAN architecture. In: Proc. of the EmNets, Cork, Ireland, pp. 77–82 (June 2007)
2. IETF WG 6lowpan, IPv6 over low-power WPAN (6LoWPAN), http://www.ietf.org/html.charters/6lowpan-charter.html
3. Silva, R., Sa Silva, J.: An Adaptation Model for Mobile IPv6 support in lowPANs. Internet-Draft, IETF (May 2009)
4. Bag, G., Raza, M.T., Kim, K.-H., Yoo, S.-W.: LoWMob: Intra-PAN Mobility Support Schemes for 6LoWPAN. IEEE Sensors Journal 9(7), 5844–5877 (2009)
5. Gundavelli, S., et al.: Proxy Mobile IPv6. RFC 5213 August (2008)
6. Motaharul Islam, M., Huh, E.-N.: Sensor Proxy Mobile IPv6 (SPMIPv6)—A Novel Scheme for Mobility Supported IP-WSNs Sensors 11(2), 1865–1887 (2011)
7. Montenegro, G., Kushalnagar, N., Hui, J.W., Culler, D.E.: Transmission of IPv6 Packets over IEEE 802.15.4 Networks. IETF RFC 4944 (2007)
8. Kushalnagar, N., Montenegro, G., Schumacher, C.: IPv6 over Low-Power Wireless Personal Area Networks (6LoWPANs): Overview, Assumptions, Problem Statement, and Goals. IETF RFC 4919 (2007)
9. Akyildiz, I.F., Lin, Y.B., Lai, W.R., Chen, R.J.: A new random walk model for PCS networks. IEEE J. Sel. Area Commun., 1254–1259 (2004)

The Research on Virtual Assembly Technology and Its Application Based on OSG

Jia Li[1], Guojin Li[2], Wen Hou[2], Li Wang[2], Yanfang Yang[2], and Dingfang Chen[2]

[1] Navy Submarine Academy, Shandong Qingdao 266042
[2] Research Institute of Intelligent Manufacture & Control Wuhan University of Technology, Hubei Wuhan 430063

Abstract. This system is a virtual assembly one of a type of cylinder cover which based on OSG. The system uses OSG the 3Dgraphics engine to realized model rendering, human-computer interaction, stereoscopic displaying, parts dragging, animation path and other related technologies. At the same time using CEGUI to achieve the interaction of the virtual scene and a graphical interface .Users can directly use the mouse or keyboard to realize some operations such as translation, rotation. The system better achieved virtual simulation of training and teaching of a type of cylinder cover for the user to save costs and improve work efficiency.

Keywords: OSG, Virtual Assembly, Virtual Reality, CEGUI.

1 Introduction

The Virtual Assembly is a new concept proposed in recent years. Chen Ding fang et al, which are in Research Institute of Intelligent Manufacture & Control Wuhan University of technology hold that the virtual assembly has two definitions of narrow and broad. Narrow sense of the virtual assembly is that assembles quickly individual parts to form products in a virtual environment. The generalized virtual assembly is in a virtual environment, how structural design and modify product design, allows designers to focus more on the product features the perfect [1]. According to different functions and purposes of the study of virtual assembly can be divided into the following three categories: product design-centric virtual assembly, the virtual assembly center of process planning and virtual prototyping as the center of virtual assembly [2]. The virtual assembly overcome the lag of physical verification, can greatly shorten the development cycle, saving development costs, and control problems that may arise in the assembly, operations jobs in advance. Essentially, virtual assembly, the actual assembly process achieves the progress of the actual assembly in the computer and used to guide production planning assembly sequence, training assembly workers, thus shortening the development cycle and saving development costs.

In real life, because of the mechanical parts with diverse parts and shapes, assembly constraints and other causes result that the process of assembly and disassembly is cumbersome and complex. Especially complex assembly and disassembly of

Q. Zu, B. Hu, and A. Elçi (Eds.): ICPCA-SWS 2012, LNCS 7719, pp. 274–281, 2013.

expensive parts is not only time-consuming and inefficient, loss, and the resulting series of questions. The emergence of virtual assembly technology can effectively solve the above problems. Virtual assembly (VA) is one of the important part of computer virtual manufacturing (VM) in the technology of virtual reality, is also currently a hot research. It is a computer-aided design, graphics, assembly and manufacturing processes, virtual simulation technology, virtual reality, visualization techniques, such as the comprehensive use of various technologies. Has a broad application prospects.

The most significant application of virtual assembly is the aircraft of Boeing 787. The process of aircraft assembly, the whole machine assembly process digitized analog simulation, designers can wear 3D glasses in the laboratory, and to operate and control the actual aircraft assembly process [3]. Digitized virtual assembly simulation is shown in figure 1.

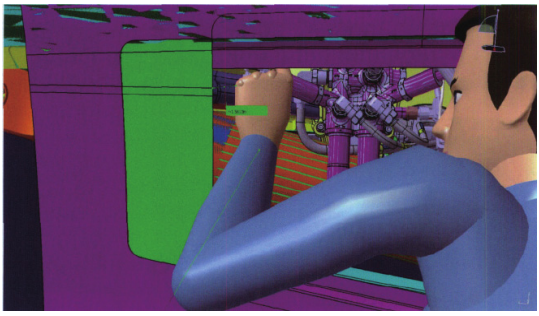

Fig. 1. Digitized model of the people

Shanghai Institute of Satellite Engineering Houpeng et al use DELMIA to develop a digital prototype assembly sequence and prototype simulation. They have studied the basic processes of satellite assembly process planning and its key technology [4].

Many institutions at home and abroad have developed their own virtual assembly system, a type of Washington State University VADE system, University of Maryland's VTS system, VDVAS system of Zhejiang University [5].

In this paper, using the three-dimensional graphics engine OSG and CEGUI graphics interface library to build a virtual assembly simulation platform, implementation of a certain type of cylinder head based on the path animation of the virtual assembly simulation platform.

2 Development Tools of System Introduced

2.1 Overview of OSG

OSG is a development library of open-source scene graph management, mainly for the development of graphics application program to provide scene management and the function of graphic rendering optimization. It uses portable ANSI C++ prepared,

with the ability of cross-platform [6]. The hierarchy diagram as shown in figure 2. It provided an object-oriented framework over the OpenGL. Make full use of STL and design patterns. OSG focuses on the scene graphics rendering, most of its operating independently of the local GUI (Graphical User Interface, a graphical user interface), but OSG provides for the support of certain functions of window system. For example: CEGUI (Crazy Eddie's GUI), MFC (Microsoft Foundation Classes, Microsoft Foundation Class Library). This paper of realizing the graphics window is CEGUI.

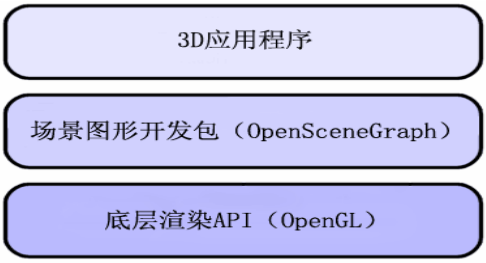

Fig. 2. OSG hierarchical diagram

OSG mainly includes four libraries: core library, tool magazine, plug-in library, introspection library. Its composition module is as shown in figure 3.

OSG after many years of development, the latest version is OSG3.0.1.

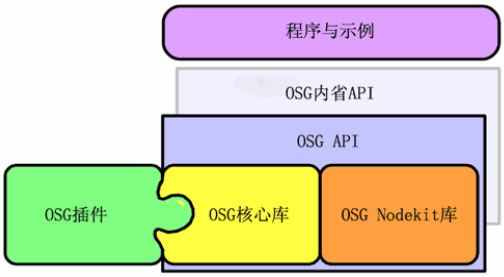

Fig. 3. OSG composition module chart

2.2 CEGUI Introduction

CEGUI (Crazy Eddie's GUI) is a free, open GUI graphical interface library, and the organization of its components in a tree knot. It provides a procedural framework for object-oriented design and uses the C + + to implement. CEGUI rendering needs the help of 3D graphics API, such as OpenGL or Direct3D. Through with a script to cooperate, can realize flexible window appearance, layout characteristics setting. The interfaces of The Eight Creatures and a giant game are used of CEGUI development.

2.3 OSGAL Introduction

OsgAL is a three-dimensional graphics rendering engine of 3D sound effects library that is used in the OpenSceneGraph. It contains OpenAL + + (based on the OpenAL) and OsgAL two separate library. Which OpenAL + + library handles the sound source, the listener, the sound stream; OsgAL library uses OpenAL + + sound integration in OSG [7].

3 The Overall Framework of the Virtual Assembly System

3.1 The Composition of the System

The entire virtual assembly simulation platform consists of the following modules: the scene rendering module, input and output modules, three-dimensional sound module, animation path module, stereoscopic display modules. The system block diagram is shown in figure 4.

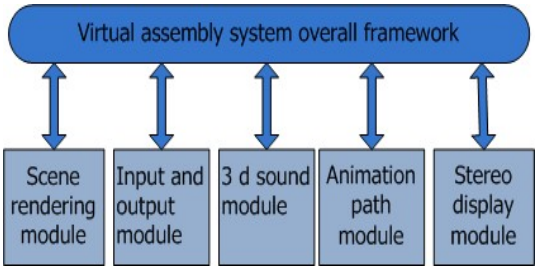

Fig. 4. The virtual assembly system

The functions of each module are as follows:

1. Scene rendering module: it mainly uses the internal renderer mechanisms of the OSG to display and destruct of the three-dimensional scene model.
2. Input and output module: it is responsible for all input and output devices (data gloves, force feedback, keyboard and mouse, ECT) to respond to and to examine the display and acquisition of information.
3. Three-dimensional sound module: responsible for the operation of loading, playing, uninstalling of sound.
4. The animation path module: it is responsible to constraint the trajectory of the parts.
5. Stereoscopic display module: responsible for stereoscopic display for three-dimensional scene.

3.2 System Architecture Design

A virtual assembly system is divided into hardware and software. The hardware of the system composed by two projectors, polarizing plates, 3D glasses, graphics workstations. Through the independent research and development of the simulation engine will each module effectively integrated. The system hardware structure is shown in figure 5.

Fig. 5. System hardware connection diagram

4 The Realization of the Key Technologies of Virtual Assembly

The software part of the system consists of two parts: (1) the operation of the components; (2) a graphical interface based CEGUI. The following will detail the implementation of the various parts.

4.1 Technology Parts Dragging

In OSG, there are eight dragging apparatus. The commonly used are TBD (TabBoxDragger), TPD (TabPlaneDrAgger), TBTD (TabBoxTrackballDragger) and TranslateAxisDragger (TAD).

The system uses TranslateAxisDragger drag. It can be in three directions XYZ axis parts to pan. Will drag apparatus and parts node joint added to the father node, can be realized on the components of the drag. The part of the code is as follows:

```
Selection - > addChild (scene);
/ / according to name produce towing apparatus
OsgManipulator:: Dragger * Dragger = createDragger
(name);
Osg :: Group * root = new osg :: Group;
Root - > addChild (selection);
Root - > addChild (dragger);
```

Finally will root variable return and added to the scene to parts can be realized the drag.

4.2 Animation Path

This system is mainly used to operating personnel's teaching and training. Assembly simulation process is an important part of it. Therefore, this system through the animation displays various parts disassembling sequence. Users can from different Angle to observe the movement of parts. The part of the code is as follows:

```
/ / set starting point
ChannelAnimation - > getOrCreateSampler () - > getOrCrea-
teKeyframeContainer () - > push_back (osgAnimation: :
Vec3Keyframe (0, osg: : Vec3 (0, 0)));
ChannelAnimation - > getOrCreateSampler () - > getOrCrea-
teKeyframeContainer () - > push_back (osgAnimation: :
Vec3Keyframe (10, osg: : Vec3 (x, y, z)));
Anim - > addChannel (channelAnimation);
/ / setting playback modes
Anim - > setPlaymode (osgAnimation: : Animation: : ONCE);
MNG - > registerAnimation (anim); / / registered
```

Through the above steps, for each need operation part set starting point and end point, can realize the corresponding animation. Enables operators to parts of the disassembly sequence know more intuitive. By setting can be opposite motion path let parts from the termination point moves to the starting point, the user can be repeated to watch a parts characteristics of the movement.

4.3 The Realization of Stereo Display Technology

In OSG, the stereo display attributes set and operation basically by OSG::DisplaySettings class to realize. The common control: display type (displayType) set; The display mode (stereoMode) set; viewport of the around eyes rendering; papillary distance, etc. To display mode as an example, the realization to realize a total of 9 kinds of display mode, the commonly used are a square body buffer, complementary color, vertical (horizontal) segmentation, vertical staggered. Its effect is as shown below.

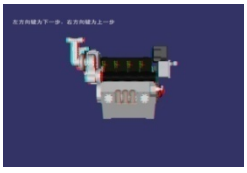

Fig. 6. Complementary color

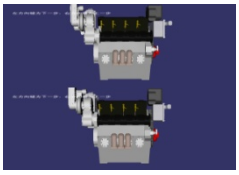

Fig. 7. Vertical segmentation

Part of Its Code as Follows:

```
/ / Open stereoscopic display
osg :: DisplaySettings :: instance () -> setStereo
(true);
osg :: DisplaySettings :: instance () -> setStereoMode
(osg :: DisplaySettings :: VERTICAL_INTERLACE);
viewer-> addEventHandler (new CMyStereoEvent (osg :: Dis-
playSettings :: instance ()));
```

4.4 The Realization of the Three-Dimensional Sound

Hearing is in addition to visual outside, people get information from outside of the second main way. In the real virtual assembly site can't be a silent environment. In the assembly process, when two rigid bodies in the operation process of the collision happened over-application voice. For more real simulation assembly environment, 3 d sound realization appears more important. Part of its code as follows:

```
std::string file=wave_vector[index%wave_vector.size()];
osgAL::SoundManager::instance()>removeSoundState(file);
file = wave_vector[index%wave_vector.size()];
bool add_to_cache = true;
osg::ref_ptr<openalpp::Sample> sam-
ple=osgAL::SoundManager::instance()
->getSample(file.c_str(),add_to_cache);
```

5 Conclusion

The cylinder head virtual assembly system realized the path animation, drag and other related technologies. Introducing stereo display, 3d audio technology, enhance the virtual assembly of the immersive and sense of reality. With the combination of using OSG and CEGUI method, has realized the virtual scene and graphics interface interaction, make the user's operation more intuitive. Final rendering is as shown in figure 8.

Fig. 8. Virtual assembly system operation rendering

And in OSG 3 d graphics engine, wrap the common effects, font and particle system class library, shorten the system development cycle. The system is successfully applied to the cylinder head simulation training and assessment. Operators of virtual training environment more realistic, training efficiency improved.

Acknowledgements. Project 2012-ZY-080 supported by exploring and innovating project of Graduate students and Project 2011-1V-079 supported by NSFC.

Reference

1. Chen, D., Luo, Y.: Virtual design, p. 172. Mechanical Industry Press, Beijing (2007)
2. Xia, P., Yao, Y.: Virtual assembly of Research and Analysis (I). Harbin Institute of Technology 40(5) (2008)
3. Fan, Y.: General assembly line of Boeing 787 aircraft and its characteristics. Aeronautical Manufacturing Technology (Z2) (2011)
4. Houpeng, Zhang, L., Yang, B., Yang, G.: Particular model satellite aviation manufacturing technologies. Virtual Assembly Technology Research and Application (22) (2011)
5. Pengtao, Li, S., Wang, J., Xu, C.: Based on an enhanced virtual assembly technology of human-computer interaction. Aided Design and Computer Graphics (3) (2009)
6. Xiao, P., Liu, G., Xu, M.: OpenSceneGraph dimensional graphics rendering engine Programming Guide, vol. 2. Tsinghua University Press, Beijing (2010)
7. Guo, L., Tan, T., Zhao, H., Zhang, W.: Based on the design and realization of the three-dimensional virtual sound osgAL. To Micro Computer Information Magazine (4) (2009)

An Enhanced Security Mechanism for Web Service Based Systems

Wenbin Jiang, Hao Dong, Hai Jin, Hui Xu, and Xiaofei Liao

Services Computing Technology and System Lab
Cluster and Grid Computing Lab
School of Computer Science and Technology
Huazhong University of Science and Technology,
Wuhan, 430074, China
wenbinjiang@hust.edu.cn

Abstract. Web service technologies have been widely used in diverse applications. However, there are still many security challenges in reliability, confidentiality and data nonrepudiation, which are prominent especially in some Web service systems that have massive resources in diverse forms. An enhanced mechanism for secure accesses of Web resources is presented and implemented based on the combination of modules of identity authentication, authorized access, and secure transmission to improve the security level of these systems. In the identity authentication, the highly safe and recognized authentication method U-Key is used. For the aspect of authorized access, the integration of an improved Spring Security framework and J2EE architecture is applied to ensure authorized access to Web resources, while the security interceptor of Spring Security is extended and a series of security filters are added to keep web attacks away. Moreover, some improvements of the XML encryption and XML decryption algorithm are made to enhance the security and speed of data transmission, by means of mixing RSA and DES algorithm. The above security mechanism has been applied to an online virtual experiment platform based on Web services named *VeePalms*. The experimental results show that most security problems with high severity in the system have been solved and medium-low severe problems degreased dramatically.

Keywords: Web service, Spring Security, U-Key authentication, XML encryption.

1 Introduction

More and more e-learning, electronic businesses and e-governance projects tend to apply Web services to build systems. Although the availability is one of essential issues of Web service, some other key issues, such as security, reliability, interoperability, are also indispensable for enterprise applications based on Web services. Among all these issues, security is an inevitable key issue for all applications. Only secure Web services can guarantee the safety of diversified web applications. However, at present, *SQL* injection, cross-site scripting and other Web

Q. Zu, B. Hu, and A. Elçi (Eds.): ICPCA-SWS 2012, LNCS 7719, pp. 282–296, 2013.

service attacks are still constantly emerging because of various security holes [1]. Most communications between applications based on Web service require trust of their partners, which reduces the widespread of Web services [2]. Since Web services are based on *XML* and rely on Internet for information exchange, there are considerable number of unsolved security problems such as data eavesdropping and wiretapping, illegal access, which bring about serious potential safety risks in data exchange and transmission [3].

VeePalms is a representative Web service based system [4], which provides multi-discipline virtual experiments for massive learners in a unified platform. It can support tens of thousands of students to do experiments concurrently with the aid of high-performance distributed computing technologies and Web services.

As a classic Web service based system, *VeePalms* also faces diverse web security vulnerabilities, such as illegal changes of the experimental data, falsifications of students' experimental scores, important resources exposed to unauthenticated users. How to design and implement a safe and stable web security mechanism is an urgent problem.

In this paper, an enhanced security mechanism for Web service based system is presented. It can ensure the security requirements of Web services by combining identity authentication, authorized access and secure transmission. At the same time, some security interceptors of the security architecture are modified so that some kinds of web attacks are prevented from damaging the system. It has been applied in *VeePalms* that approves its effectiveness.

2 Background

2.1 Web Service Security

So far, security researches of Web services mainly focus on establishment of service safety regulations, combining with Web service protocol stacks. For example, many researchers build new safety mechanisms by modifying and extending *SOAP* head. A number of standard organizations, companies and social groups have carried out a lot of research work. Some organizations such as *W3C*, *IETF*, and *OASIS* set a series of standards for *XML* and Web service safety [5].

Most of deployed Web services rely on the security mechanism in the transport layer by using the combined authentication of *SSL* and *HTTP*, which can provide security guarantees for Web service to some extent. *SSL*, *TLS*, and *IPSec* are often used for email, e-commerce, bank web sites, etc. Some international mail services, such as *Gmail*, *Yahoo Mail*, and *Live,* adopt *SSL* security mechanism. These large web applications generally apply direct point-to-point data transmission without the participation of third party services, which can ensure the nonrepudiation of these applications. However, this simple and one-fold security solution is short of following characteristics: end-to-end protection, selective protection, sound and flexible authentication mechanism, as well as environmental support of message level safety. For example, *SSL/TLS* can only encrypt all *SOAP* messages, instead of the selected ones. One of what a comprehensive Web service security system needs is an end-to-end security mechanism [6].

2.2 Access Control Level

Access control of Web services resources can be generally divided into following three types: the access control of *URL* resources, the one of operation methods, and the one of domain objects. Access control of *URL* resources can be implemented by interceptor mechanisms, such as filters of Servlet. For the access control of operation functions, all authorization logic codes are mixed in business logic ones. Since the codes of authorization logic are scattered in many parts of the system, it makes them with low maintainability. Access control of domain objects can be achieved in the database by writing a set of triggers for each data sheet which can achieve row-level data access. However, because many tables are required to be handled while changing permissions, a number of codes involved should be altered, which also reduce the maintainability of the system.

3 Related Work

XML is a cornerstone of the Web service standard. It forms the basis of safe Web services. Traditional work for reliability including *XML* document encryption, data integrity testing, and sender confirmation is a simple process relatively. However, more and more documents require particular operations for certain parts according to different security levels. The security-related *XML* methods involve *XML* encryption, *XML* signature [7], *XACL* (expanded access control language), *SAML* (security assertions markup language) and *XKMS* (*XML* Key Management Standard). *XML* signature and *XML* encryption can ensure the confidentiality, integrity, authentication, nonrepudiation as well as the end-to-end security [8]. *XML* encryption and *XML* signature generally adopt asymmetric encryption, using public and private key authentication. The data encrypted by one's public key can only be decrypted by one's private key, which can guarantee the data security. However, for massive data, these asymmetric encryption and decryption will take lots of computation resources, which gives rise to performance degradation [9].

JGuard [10] provides easy security (authentication and authorization) in Web and other applications. It is built over *JAAS* (Java Authentication and Authorization Service) framework, which is part of Java APIs on security. But *JGuard* does not use the concept of *AOP* (Aspect-Oriented Programming), which makes it not easy to be integrated with low coupling.

JSecurity [11], a project of the Apache Software Foundation, is a powerful and flexible open-source Java security framework, which implements authentication, authorization, enterprise session management, and cryptography services well. However, it does not provide access control mechanism for domain objects.

Spring Security [12] provides powerful and flexible security solutions for enterprise applications. It is a stable and mature approach based on Spring Framework, using Spring dependency injection. Meanwhile, it provides comprehensive authorization services, which is also easily integrated with existing databases. What's more, it provides access control of three levels, which are the access controls of *URL* resources, of operational approaches, and of domain objects. Therefore, *Spring Security* is selected as our research base. However, this security architecture does not provide the

security mechanism for blocking web attacks. Although *Spring Security* can effectively ensure authorized accesses to resources, security interceptor mechanism cannot filter those illegal access requests and prevent systems from being damaged by illegal users. Moreover, *Spring Security* provides an access control list (*ACL*) to achieve the access control of domain objects. But it needs to add a new table to manage the *ACL*. It usually takes considerable long time to query this table.

4 Design and Implementation

The enhanced web security mechanism presented here is achieved from three aspects that are identity authentication, access control and secure transmission. Since this security mechanism takes *VeePalms* as a representative application, the following discussion about the mechanism focuses on it. However, those ways mentioned below are also suitable for many other Web service based systems.

Usually, there are multi-role users in this system. The *U-Key* authentication is used only for logins of important roles, such as teachers, academic deans, administrators. Meanwhile, other roles of users, such as students and guests need another way to ensure security authentication. Thus, the key of the mechanism lies in the integration of all kinds of user authentications, and the combination of identity authentication with access control modules.

The *Spring Security* framework has its own set of identity authentication methods, including *HTTP* basic authentication, digest authentication, and form authentication. However, all these authentication methods cannot meet the security requirements of the system enough. Worse still, *Spring Security* framework only focuses on banning unauthorized resources accesses. It cannot solve web attacks such as *SQL* injections, cross-site scripting, insecure *HTTP* methods, from illegal users and users with partial rights.

4.1 Architecture

Figure 1 shows the security architecture. According to characteristics of the Web service based systems, the enhanced security mechanism is based on the *Spring Security* framework, and some improvements are made on the safety intercept module of *Spring Security*. Different requests are processed distributed through the security interceptor: for login authentication requests, they will be sent to identity authentication module; for encrypted requests, data security transmission module will deal with them; for requests of other types, the access control manager module is in charge of them to decide whether the requests have permissions to access resources [13]. The access control manager queries an *ACL* to judge whether the requests are legal or not. *ACL* maintains a mapping table about the relationship between resources and authority, through which the access control manager can estimate whether the user is authorized to access resources or not.

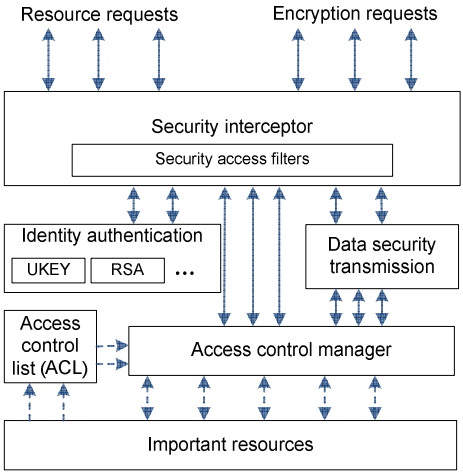

Fig. 1. Security mechanism architecture

The identity authentication module adds *U-Key* identity authentication and *RSA* (Rivest-Shamir-Adleman) encryption authentication to improve the reliability of the authentication module. As shown in Figure 1, some security filters are added at the security interceptor in the *Spring Security* framework, so as to ensure the safety of the system resources accesses, integrating the data security transmission and identity authentication modules.

4.2 Access Control Model

Figure 2 illustrates the architecture of the access control model in the system. The architecture consists of three parts: resource requests from clients, requested resources, and access control policies. In this architecture, role-based access control (*RBAC*) model is used to implement access control policies [14].

The role-based access control model consists of following five components: users, roles, permissions, resources, and sessions. As shown in Figure 2, there are also five assignment relations between components. When a user tries to access an object, the system checks the rights owned by the user and decides whether to allow the access or not.

Some abbreviations are explained as follows:

U (Users): a set of operators who can independently access information system data or other resources expressed by data. In *VeePalms*, users are virtual experiment designers, managers, consumers, and others. If u is used to denote a particular user, $U=\{u_1, u_2, u_3, u_4, \ldots, u_n\}$.

R (Roles): a set of participators who have same access operations to some data with same types. There are five roles in *VeePalms,* which are teacher, administrator, academic dean, student, and guest visitor. When a role is assigned to a user, its permissions to resources are also assigned to the user. Thus, role is a medium of assigning permission rights to users. If r is used to denote a particular role, $R=\{r_1, r_2, r_3, r_4, \ldots, r_n\}$.

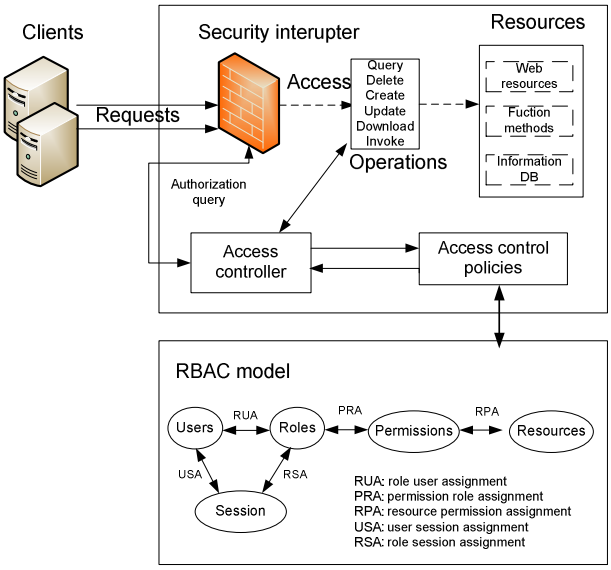

Fig. 2. Architecture of access control model

P (Permissions): a set of rights that are used to access resources. Permission is the right of operating resource objects. These operations include creating, updating, deleting, querying, viewing, invoking, and downloading. So, P = {*create, update, delete, query, view, download, invoke*}.

W (Resources): a set of entity objects that are various organizing forms of resources saved and accessed by users, such as a file, a page, database record, function methods. In *VeePalms*, objects are multiform experimental resources. If w is used to denote a particular resource, W= {w_1, w_2, w_3, w_4, … , w_n}.

S (Sessions): a set of mappings between users and roles. When a user activates a role, a session is created. A session is a unit of access control. Each session is associated with a single user, and each user is associated with one or more sessions. Session and role are a many-to-many relationship.

In *RBAC*, key relations are related to role, user, and permission. Two important relations with them are shown as follows:

RUA (*Role User Assignment*): a many-to-many mapping of the role-to-user assignment relation. $RUA = R \times U$.

PRA (*Permission Role Assignment*): a many-to-many mapping of the permission-to-role assignment relation. $PRA = P \times R$.

The access control in this model is determined by roles, permissions, and resources. After *RUA, PRA*, and *RPA* are completed, users can access resources appointed according to corresponding permissions. The implementation of the mechanism is introduced in next section.

4.3 Strategy and Implementation

A safe Web service system should meet five security requirements that are authentication, authorization, confidentiality, integrity, and nonrepudiation. All those five requirements fall into three parts according to their actions: the secure transfer of data which ensures confidentiality, integrity, and nonrepudiation; the authentication mechanism used for guaranteeing the authorization; and the authorized access mechanism for ensuring the authentication. To sum up, in order to ensure the security of Web service, there are three security modules need to be achieved, which are the identity authentication module, the access control module, and the data security transmission module.

The identity authentication module discussed in this paper adopts *U-Key* authentication and *RSA* encryption for authentication mechanism. A user's *CA* certificate is stored in *U-Key* hardware, which is used as the only identifier of user's identity. When a user uses the *U-Key* to login, after encrypted with the private key, the authentication information is sent to a certificate server. Its security authentication module decrypts the information to get the user's identity.

The access control module is built based on *Spring Security* framework. Although the identity authentication mentioned above can guarantee users' legitimacy, it is not able to ensure authorized accesses to resources yet. Here, we construct a new access control module by improving *Spring Security* framework.

Data security transmission module encrypts users' core data selectively, adopting the hybrid encryption by combining *RSA* and *DES*. The server-side maintains a pair of *RSA* keys, which are the private key and the public key, and transmits the public key messages back to the client-side. Then, the client-side generates *DES* key which is used to encrypt vital data, and the *RSA* public key is applied to encrypt the *DES* keys.

In the following, we are going to discuss the identity authentication and the access control in details.

1) Authentication and Authorization

A. Identity Authentication Based on U-Key

The identity authentication module adopts *U-Key* authentication mechanism, which is implemented by a public-key infrastructure (*PKI*). The *PKI* provides a mechanism to support both identity certificates and access control. The core of the *PKI* is that of the certification authority (*CA*) that mainly deals with key pairs (a private and a corresponding public key) issuing. The private key must remain secret, under the control of its owner, while the public key must become available to anyone who wishes to have some type of transactions with the owner of the private key. A typical *PKI* consists of *PKI* policy, software and hardware, *CA*, *RA* (Register Authority), and *PKI* application. The purpose of the *CA* is to ensure the digital certificates to be used by other parties. The jobs of the *RA* are to process users' requests, confirm their identities, and induct them into the user database.

User's *CA* certificate, which identifies the only identity of users, is stored in the *U-Key* hardware. The authentication information is encrypted by private key and sent to the authentication server, in which the security authentication module decrypts the

identity of the user by public key. The public key of users should be under the unified management by authentication server. After the authentication succeeds, the *U-Key* owner is granted the permissions assigned to his/her role.

In the identity authentication based on *U-Key*, the main function of the server is to verify the identity of the *U-Key*. There are two steps in this process: verifying the validity of user certificate in the *U-Key* and verifying the validity of private key of the *U-Key*. Figure 3 shows the authentication process of *U-Key*.

The premise of the first step is that the server has already had dependable *CA* certificate. The process of the steps is listed as follow.

Step1: The server receives the user certificate from *U-Key* client.

Step2: The server gets the public key from user certificate and decrypts the *CA* signature part of user certificate, which is named *Digest-A*, while the server digests the other part of user certificate, which can be named *Digest-B.*

Step3: Compare *Digest-A* with *Digest-B*. If *Digest-A* equals *Digest-B,* the user certificate is issued by *CA*. Otherwise, the authentication is failed.

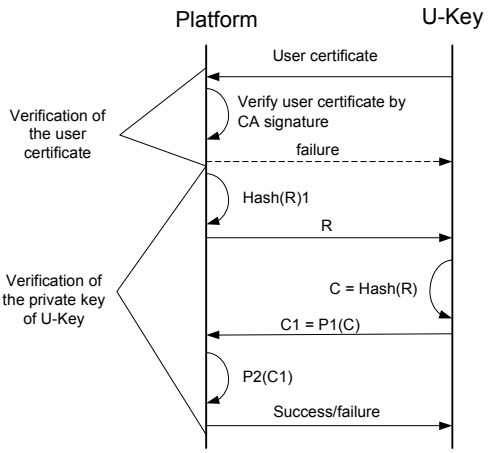

Fig. 3. Process of U-Key authentication

Due to the possibility of falsifying user certificate, verifying the validity of user's certificate is not enough for security. It also requires that the client should match with the certificate provided by the user. Because the private key of user is exclusive, the user's identity can be confirmed by digital signature.

The premise of the second step is that the server has already verified the validity of user certificate, which is issued by *CA*. The process of the second step is described in details as follows.

Step1: The server generates a random string *R*, and deal with it by hash function, named *Hash(R)1*.

Step2: The server sends *R* to the client, and the client also processes *R* by hash function, named *C.* Then the *U-Key* encrypts *C* with private key, named *C1*. Then *C1* is sent to the server.

Step3: The server receives *C1* and decrypts it with the public key of user certificate, called *Hash(R)2*. Compare *Hash(R)1* with *Hash(R)2*. If *Hash(R)1* equals to *Hash(R)2,* the *U-Key* authentication is successful, otherwise, it fails.

B. Identity Authentication Based on RSA Encryption

Due to the special requirements of the system, it is impossible to ensure every user having a *U-Key*. For the *non-U-Key* users, the system adopts *RSA* encryption to ensure the safety of their authentications. *RSA* encryption algorithm is an asymmetric cryptographic algorithm, widely used in the public key cryptography standards and electronic businesses.

When someone first visits the system, the system generates a pair of *RSA* public and private keys, which are stored in the session of the request, and sends the *RSA* public key to the client. Then the client logs in, using the password and account encrypted by the *RSA* public key. Meanwhile, it sends the encrypted cipher text to the server. After receiving the login request, the server searches for *RSA* private key from the session and decrypts the password by *RSA* algorithm. Even if this kind of ciphertext encrypted by *RSA* is wiretapped through Internet, it is useless for the reason that *RSA* algorithms should be decrypted by public key, and it will become more and more difficult to decrypt with *RSA* key lengthening.

C. Authorization after Success Authentication

After the user is successfully authenticated by the server, the server grants all permissions of the role to the user. These relations between components of access control model have been shown above. The permissions assigned to the user are stored in the global session of the user by the form of key-value: <*"grantedauthority", authorities*>. The key is named *grantedauthority* and the value is a list of authorities: *authorities*= $\{p_1, p_2, p_3, \ldots p_n\}$. So, it is unnecessary to query the database to get the permissions of the user again. Moreover, once the permissions are assigned to the user, they cannot be changed until the user logs out.

Not all permissions are stored in the session. In most cases, just the identifier of permission is recorded, which can reduce memory space of the client effectively.

2) Security Access Control

A. Authorized Access

Although the identity authentication can guarantee users' legitimacy, it cannot ensure authorized accesses to resources. *Spring Security* framework is a suitable choice to control the authorized accesses of users, which has excellent expansibility and portability. *Spring Security* adopts the thought of *AOP*, which has weak coupling with system integration. As shown in Figure 4, *Spring Security* and the group frame *SSH* (Structs+Spring+Hibernate) are integrated.

Spring Security achieves three levels of access controls: *URL*-level access control, method-level access control, and domain object-level access control, which are corresponding to the presentation layer, business logic layer, and the persistence layer, respectively.

Users usually visit system sources through *HTTP* protocol. *HTTP* request is the basic unit of the access control target. It is made up of following components.

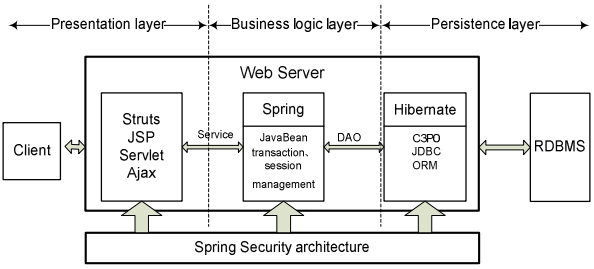

Fig. 4. Integration of *Spring Security* and *SSH*

Request Line: It is composed of request method, request *URI*, and *HTTP* version, which are separated by a blank space, such as "*GET /news.asp HTTP/1.1"*.

Message Header: It is composed of domain name and value pairs, which are separated by a colon. For example, "*Host: http://dome.com:80"* expresses the host and port of the requested resource.

Entity Body: It carries the data related to request, such as some potentially needed parameters. It is indicated by *Content-Length* or *Transfer-Encoding*. *Content-Type* expresses the type of transport data.

(1) URL-Level Access Control

What the *URL*-level access control achieves is to make users to access *URL* resources safely, such as a picture, a *JSP* page, a *XML* file. The domain name of *Message Header* takes the information of the requested resource, such as "*http://ip:80/beginExperiment.jsp, http://ip:80/sport.xml"*.

(2) Method-Level Access Control

During the response process for a user's request, it is necessary to call business logic method under safety control. At this moment, the safety interceptor of *Spring Security* is triggered, which estimates whether the user has the authority to call this method.

Spring Security takes the concept of *AOP*. It can be realized by the mechanism of Java annotation. There are four comments: *@PreAuthorize, @PreFilter, @PostAuthorize*, and *@PostFilter*. They can be invoked by global-method-security namespace elements. For example:

```
@PreAuthorize("hasPermission('Create_User')")
  public void create(User user);
```

It means that only the user granted the permission *Create_User* can invoke the method above. *@PreAuthorize* is the most frequently used comment.

(3) Domain object-level access control

For the domain object-level access control, *Spring Security* achieves it through an access control list (*ACL*), by which users can modify and delete specified data lines.

However, the line-level access control of *Spring Security* brings some negative influences on the system performance. It needs to create a new record in *ACL* for every record to be protected. When the record protected is accessed, the new record is checked to judge whether the request has the right or not.

However, we find that the tables protected have the field of owner identifier. So it is not necessary to create *ACL*. Based on this characteristic, the domain object-level access control can be implemented by judging whether the user is the owner of this domain object. The information of the user can be stored in the global session when the user logs into the system.

Usually the persistence layer just needs to finish four functions, including *update, delete, create*, and *find*. These functions should add two more parameters, which are *HttpSession* of the user and the owner field of the table. Figure 5 shows the architecture of the domain object-level access control.

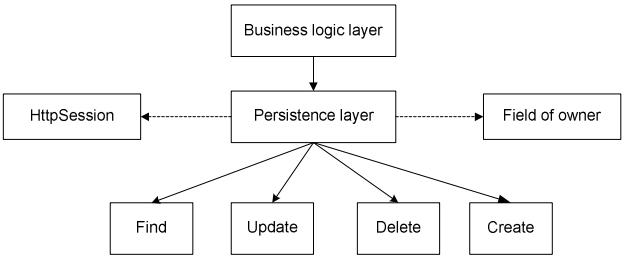

Fig. 5. Architecture of the domain object-level access control

B. Security Filter Chain

Although Spring Security can ensure authorized accesses to resources effectively, the security interceptor mechanism cannot get good performance on filtering those illegal access requests. Therefore, a series of security access filters for the system are desired to be added to intercept the illegal access requests and fix the high-severity security bugs, in order to improve the system security.

The *U-Key* authentication can ensure the safety of authentications of important roles. After being authenticated, users can get what they want through *HTTP* requests. Therefore, it is necessary to make a filter chain to filter illegal requests by detecting every parts of the *HTTP* requests, including *Request Line, Message Header*, and *Entity Body*.

Figure 6 shows the improvement of Spring Security access control by adding a series of security access filters. *HTTP* method filter can filter out illegal accesses brought by *Request Line*, such as *delete, move, search, copy*. Meanwhile, the invalid character filter can filter out requests containing illegal visiting characters in the parameters of *Entity Body*, such as *script*, *alert*, *window*, *open*, *where*, which can avoid *SQL* injection attacks, cross site scripting, and other web attacks effectively. More other filters, such as invalid session filter, have been also realized for preventing system from other more illegal accesses.

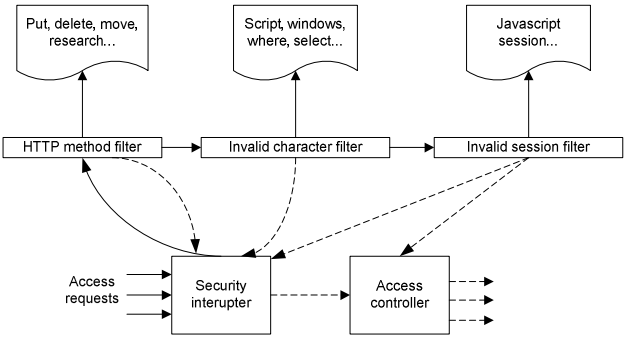

Fig. 6. Process of access control of Spring Security

5 Performance Evaluation

To approve the effectiveness of the mechanism presented in this paper, we test it in *VeePalms* by adopting IBM Rational AppScan [15]. The *VeePalms* architecture is shown in Figure 7.

The system is deployed in a high-performance cluster. Its nodes are divided into four categories. The details of them are shown in Table 1.

Here, the centre management server and computer nodes are in charge of virtual experiment simulations, which are not related to data security of the enhanced security mechanism. So we focus on the web servers and DB servers.

The data in the virtual experiment platform are in multiple forms, such as experimental components (*XML*), experimental guidelines (video, Word), lists of scores (*TXT*), experimental scenes (*XML*), Simulation sources files (*MO*).

First, we make comparisons of encryption performances of *DES*, *RSA*, and *DES&RSA*. Selected four files have different sizes: *10KB*, *30KB*, *60KB*, and *100KB*. The detail encryption time is shown in Table 2.

Table 1. Servers and parameters of the VeePalms

Servers	Parameters	Type
Web servers	2×Intel Xeon E5520, Memory 16GB, Hard Disk 2×146GB SAS	NF5220
DB servers	2×Intel Xeon E5520, Memory 32GB, Hard Disk 2×300GB SAS	NF560D2
Centre Management Server	4×Intel Xeon E7450, Memory 16GB, Hard Disk 2×146GB SAS	NF5120
Computing nodes	2×Intel Xeon E5520, Memory 16GB, Hard Disk 2×146GB SAS	NF5120

As seen in Table 2, although DES&RSA has more time in encryption compared with DES, it has an obvious time advantage compared with RSA. At the same time, DES&RSA can provide securer guarantee than DES.

Second, the Rational AppScan is used to test the security holes of the system with and without the security mechanism (*SM* as abbreviation). There are five roles in the *VeePalms* which are administrator, academic dean, teacher, student, and guest visitor. The security test results of every user space are shown in Table 3. The number of

security holes in every user space is reduced more than 60%. The ratios of security holes of different user spaces are shown in Figure 8. The test results of different severity levels are shown in Figure 9. For convenience, the names of roles are written in abbreviations: administrator as Adm., academic dean as Acd., teacher as Tea., student as Stu., and guest visitor as Vis.

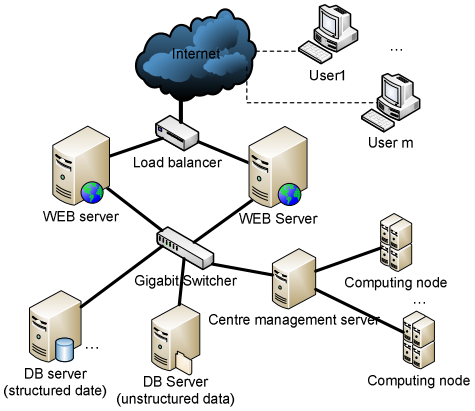

Fig. 7. Architecture of VeePalms

Table 2. Time of encryption by DES, RSA, and DES&RSA

Size / *Algorithm*	***10KB***	***30KB***	***60KB***	***100KB***
DES	*4ms*	*10ms*	*19ms*	*35ms*
RSA	*1209ms*	*3542ms*	*7080ms*	*11744ms*
DES & RSA	*96ms*	*111ms*	*160ms*	*586ms*

As seen in Figure 9, after applying the security mechanism, all security holes with high severity in the system have been fixed and medium and low severe holes decreased dramatically. In details, the presented web security mechanism can solve most systematic bugs of extremely high severity, such as incomplete account blockade, cross-site scripting establishment. Moreover, it also solves lots of bugs of medium severity, including enabling unsafe *HTTP* method, decrypted login request, and so forth.

Table 3. Test results of every user space

Role	Sum. of URLs	Num. of security holes		Reduction ratio
		Without SM	With SM	
Adm.	89	49	17	65.9%
Acd.	24	17	4	72.7%
Tea.	42	15	3	78.3%
Stu.	20	17	3	78.8%
Vis.	30	19	4	62.0%

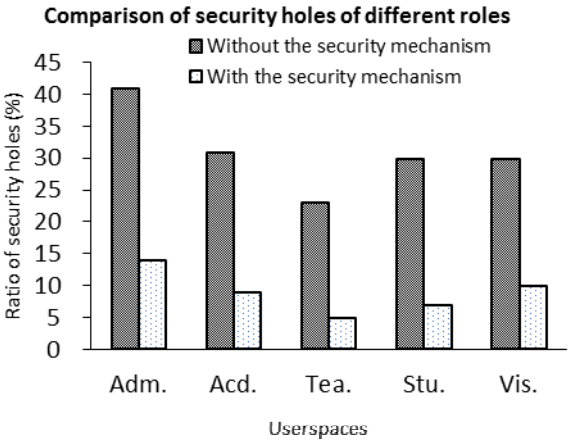

Fig. 8. Ratios of security holes of different user spaces

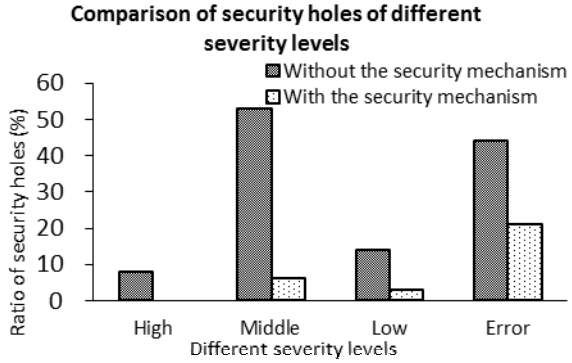

Fig. 9. Test results of different severity levels

6 Conclusion

This paper presents a new web security mechanism for Web service based systems, which ensures the security requirements of the systems from identity authentication, access control, and safety transmission. The identity authentication adopts *U-Key* authentication combined with *RSA* encryption. By improving the *Spring Security* safety interceptor mechanism and its authentication mechanism, various kinds of illegal access requests are intercepted. The experimental data shows that this security mechanism can fix all kinds of bugs with high-severity existing in the Web service based applications, and decrease the numbers of web security bugs with medium and low severity effectively. Due to the excellent expansibility of *Spring Security* and web security mechanism, the safety of the web system has been improved obviously.

Acknowledgments. This paper is supported by National Natural Science Foundation of China under grant No.60903173 and the Key Project in National Science & Technology Pillar Program of China under grant No.2008BAH29B00.

References

1. Roberts-Morpeth, P., Ellman, J.: Some Security Issues for Web Based Frameworks. In: 7th IEEE, IET International Symposium on Communication Systems Networks and Digital Signal Processing (CSNDSP 2010), pp. 726–731. IEEE Press, Piscataway (2010)
2. Xie, W., Ma, H.: A policy-based security model for Web system. In: 2003 International Conference on Communication Technology (ICCT 2003), vol. 1, pp. 187–191. IEEE Press, Piscataway (2003)
3. Peng, S., Han, Z.: Trust of User Using U-Key on Trusted Platform. In: 8th International Conference on Signal Processing (ICSP 2006), pp. 3023–3026. IEEE Press, Piscataway (2007)
4. Jiang, W., Li, H., Jin, H., Zhang, L., Peng, Y.: VESS: An unstructured data-oriented storage system for multi-disciplined virtual experiment platform. In: Park, J.J., Jin, H., Liao, X., Zheng, R. (eds.) HumanCom and EMC 2011. LNEE, vol. 102, pp. 187–198. Springer, Heidelberg (2011)
5. Park, E., Kim, H., Lee, R.Y.: Web Service Security Model Using CBD Architecture. In: Fifth ACIS International Conference on Software Engineering Research, Management, and Applications (SERA 2007), pp. 346–352. IEEE Press, Piscataway (2007)
6. Chess, B., McGraw, G.: Static analysis for security. IEEE Security & Privacy 2(6), 76–79 (2004)
7. Chen, Y., Guo, W., Zhao, X.: Study of XML digital signature for resource document fragment. In: 2nd International Conference on Information Science and Engineering (ICISE 2010), pp. 1541–1544. IEEE Press, Piscataway (2010)
8. Xiao, Z., Yang, Y., Zhang, W.: XML-based information security technology study. In: 2nd International Conference on Software Technology and Engineering (ICSTE 2010), pp. 236–239. IEEE Press, Piscataway (2010)
9. Nordbotten, N.A.: XML and Web Services Security Standards. IEEE Communications Surveys and Tutorials 11(3), 4–21 (2009)
10. Prunicki, A., Elrad, T.: Aclamate: An AOSD Security Framework for Access Control. In: 2nd IEEE International Symposium on Dependable, Autonomic and Secure Computing (DASC 2006), pp. 293–300. IEEE Press, Piscataway (2006)
11. Jsecurity (2011), `http://www.jsecurity.org/`
12. Spring Security (2011), `http://static.springsource.org/spring-security/`
13. Sidharth, N., Liu, J.: IAPF: A framework for enhancing web services security. In: 31st Annual International Computer Software and Applications Conference (COMPSAC 2007), pp. 23–30. IEEE Press, Piscataway (2007)
14. Oh, S., Park, S.: Task-role-based access control model. Information Systems 28(6), 533–562 (2003)
15. Tang, K., Chen, S., Levy, D., Zic, J., Yan, B.: A Performance Evaluation of Web Services Security. In: 10th IEEE International Enterprise Distributed Object Computing Conference (EDOC 2006), pp. 67–74. IEEE Press, Piscataway (2006)

Data-Apart Hybrid Centralized Scheduling in Coordinated Multi-Point System with Non-ideal Backhaul Link

Huiqin Li[1], Wenan Zhou[1], Xiaotao Ren[2], Xianqi Lu[1], and Guowei Wang[1]

[1] ICN&SEC Center, Beijing University of Posts and Telecommunications, Beijing, China
{Lihuiqinbupt,luxianqi}@gmail.com, zhouwa@bupt.edu.cn, guoweiwang007@hotmail.com
[2] HUAWEI TECHNOLOGIES CO.,LTD, Beijing, China
renxiaotao@huawei.com

Abstract. Coordinated Multi-Point (CoMP) transmission is a promising technique to improve the coverage of high data rates, the cell-edge throughput in cellular networks, in which centralized CoMP can obtain global optimal cooperation when CU can gather CoMP information (including CSI) and send scheduling decisions without delay. However, due to the imperfect channel characteristic, there is CSI latency during the cooperation, which will decrease the CoMP gain. In this paper, we propose a modified centralized CoMP scheme called DAHCS (Data-Apart Hybrid Centralized Scheduling), in which user data process is set apart from CU and a hybrid structure scheduling is adopted to schedule CoMP UEs intensively and non CoMP UEs locally. Simulation results show that the proposed DAHCS CoMP outperforms the traditional method when a lower capacity/higher latency backhaul link is considered.

Keywords: CoMP, latency, hybrid scheduler, X2 interface.

1 Introduction

Coordinated Multi-Point (CoMP) technology has attracted people's attention for its capability to improve the coverage of high data rates, the cell-edge throughput and/or to increase system throughput [1]. However, this performance can only achieved when the backhaul links connected several coordinated points have low latency. In practice, X2 interface latency is in an order of 10 to 20 milliseconds [2]. Thus, the scheduler always uses the outdated CSI for scheduling which leads to system performance deterioration. Several research institutions had demonstrated the performance deterioration using simulation results [3-4].

In this paper, the traditional centralized CoMP scheme and the corresponding analysis are given firstly. And then a modified centralized CoMP named DAHCS (Data-Apart Hybrid Centralized Scheduling) is described, which set user data processing apart from CU and a hybrid structure scheduling is introduced at the same time. The rest of the paper is organized as follows. Section 2 analyzed the drawbacks of

Q. Zu, B. Hu, and A. Elçi (Eds.): ICPCA-SWS 2012, LNCS 7719, pp. 297–301, 2013.

traditional centralized CoMP and described the modified DAHCS CoMP detail. Simulation results are provided to evaluate the performance of our method in Section 3, followed by conclusions in Section 4.

2 A Traditional Centralizrd CoMP and The Modified Dahcs CoMP

The architecture of a traditional centralized CoMP is illustrated in Fig.1.

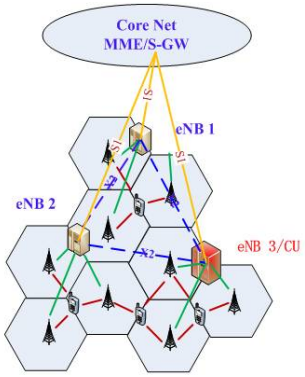

Fig. 1. Architecture of traditional centralized CoMP

CU collects all users' information and data, executes centralized scheduling, scheduling non-CoMP UEs and CoMP UEs simultaneously. Scheduling decision and processed UEs' data (MAC PDUs) are distributed over the X2 interface to all relevant eNBs. In fact, X2 interface is not suitable to undertake too much cooperation work due to its limited performance, mainly containing the following three reasons. Firstly, X2 interface has a lower bandwidth compared with S1 interface, about 5% of the S1 bandwidth is a generous allowance [5-6]. Secondly, both control plane signaling and user plane data need to be shared to support CoMP technique, and it is the latter which dictates the bandwidth requirement [7-8]. Thirdly, X2 latency is in an order of 10 to 20 milliseconds, while S1 U-plane has a latency of 5 ms [9], there will be less latency if user data are achieved via S1. We can easily conclude from the previous analysis that the X2 interface is not appropriate for a heavy traffic, which means that the traditional centralized CoMP needs to be modified.

The DAHCS COMP improved from the following two aspects. On one hand, modify the centralized scheduler into a hybrid structure, which means that non-CoMP UEs are scheduled locally by a distributed scheduler while CoMP UEs are scheduled intensively by a centralized scheduler. On the other hand, separate the U-plane from CU. CU only take charge of control plane signaling, leaving user data managed locally by distributed eNBs. User data are directly sent from the S-GW via S1 interface to relevant cooperation eNBs. The corresponding procedure is given in Fig.2.

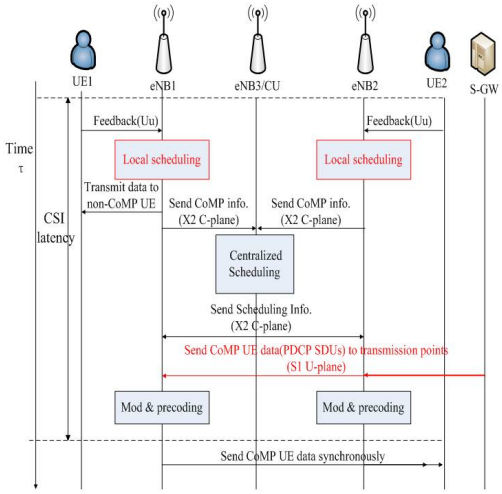

Fig. 2. The procedure of CoMP JT under DAHCS CoMP

Each cell's frequency is divided into two parts: CoMP frequency zone to schedule cell-edge UEs (CoMP UEs) jointly and non-CoMP frequency zone to schedule cell-center UEs (non-CoMP UEs) individually by each cell.

In our example, eNB3 is preconfigured as CU, eNB1 and eNB2 are the ordinary eNBs. Only two UEs (UE1、UE2) are portrayed for simplification, UE1 is a non-CoMP UE belongs to eNB1, while UE2 is a CoMP UE belongs to eNB2. In the initialization stage, CU obtains all user information and schedules CoMP UEs on the CoMP frequency zone first, and then sends the resources allocation information to other eNBs for next local scheduling. eNBs can schedule its own cell-center UEs on these remaining available RBs. The procedure mainly contains the following steps:

Step1: UE1 and UE2 report the CoMP information including CSI to their serving eNBs, i.e. eNB1 and eNB2.

Step2: eNB1 and eNB2 classify their attached UEs as CoMP UEs and non-CoMP UEs, and schedule locally on the remaining RBs of last centralized scheduling.

Step3: For a non CoMP UE (UE1), data are transmitted only from its serving eNB.

Step4: eNB1 and eNB2 forward the CoMP information of CoMP UEs (UE2 in this example) to CU (eNB3) via X2 C-plane.

Step5: CU schedule CoMP UEs intensively on the CoMP frequency zone.

Step6: Scheduling information like allocated RBs, transport block size, MCS, the segmentation/concatenation information of the radio link control (RLC) protocol etc. are then transmitted from CU to the individual transmission points.

Step7: The raw user data (PDCP SDUs) are transmitted to the transmission eNBs from the S-GW via S1-U interface. Then transmission eNBs pre-code separately.

Step8: The serving eNB and coordinated eNB transmit data to the CoMP UE synchronously.

3 Simulation Results

In order to evaluate the impact of CSI latency and the performance of the proposed DAHCS CoMP, we consider the situation of centralized CoMP based on the deployment scenario 2 given in TR 36.819. The LTE-A CoMP simulation platform was designed based on the LTE system level simulation platform [10]. Four modules were added: CoMP UE judging module, coordinated point selection module, resource allocation module and latency generation module.

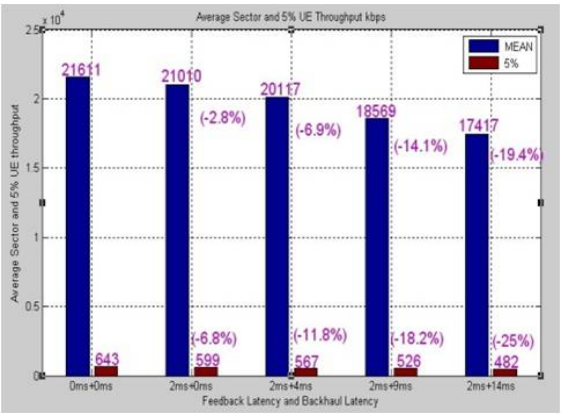

Fig. 3. Average sector and 5% UE throughput loss under different latency

Fig .3 shows the average sector and 5% UE throughput loss under different latency used the traditional centralized CoMP.The result illustrates that the increasing latency will damage the system performance. Especially, when the latency increases to 16ms, performance enhancement with CoMP is hard to be expected.

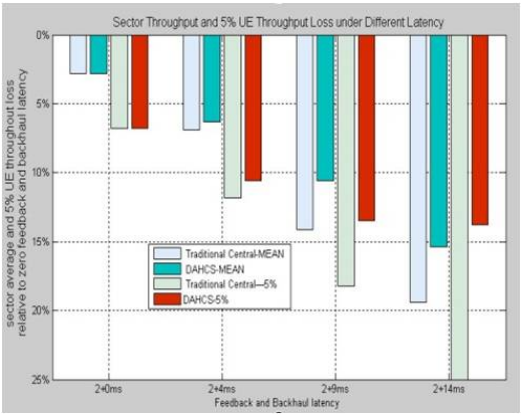

Fig. 4. System performance loss comparison between two CoMP schemes

Fig.4 shows the comparison of cell average and cell edge throughput between the traditional centralized CoMP and the DAHCS CoMP scheme. We can see from the result that when the latency is small, there is little difference on system performance between the traditional centralized CoMP and the DAHCS CoMP scheme. However, with large latency, the DAHCS CoMP outperforms the traditional centralized CoMP.

4 Conclusion

CoMP technique can achieve significant system gain in comparison with non CoMP. However, CoMP performance is somewhat sensitive to CSI latency. When latency increases to a certain extent, the performance degradation will be unacceptable. In this paper, we introduce a modified centralized CoMP scheme that can take the advantage of centralized scheduling and decrease the latency at the same time. Simulation results demonstrate that the modified DAHCS CoMP achieves higher cell average and cell edge throughput than the traditional centralized CoMP schemes when practical CSI latency is considered.

Acknowledgment. This work is supported by the funds of HuaWei, under NO.YJCB2011060WL.

References

1. 3GPP TR 36.819. Coordinated Multi-Point Operation for LTE Physical Layer Aspects (Release 11), V2.0.0 (September 2011)
2. 3GPP: Evolved universal terrestrial radio access network (e-utran): X2 general aspects and principles. TSG RAN TS 36.420 V9.0.0 (2009)
3. 3GPP TSG RAN WG1 Meeting #66.R1-112339. CoMP Performance Evaluation under Low-capacity/High-latency Backhaul (August 2011)
4. Rate Loss Caused by Limited Feedback and Channel Delay in Coordinated Multi-point System, 07 VTC (2011)
5. Unell, P.: Ericsson, Right Sizing RAN Transport Requirements. Transport Networks for Mobile Operators (2010)
6. Widjaja, I., La Roche, H.: Sizing X2 Bandwidth For Inter-Connected eNodeBs, Bell Labs, Alcatel-Lucent. In: IEEE VTC 2009-Fall (September 2009)
7. Brueck, S.: Backhaul Requirements for Centralized and Distributed Cooperation Techniques. Presented at ITG Heidelberg, Qualcomm (July 8, 2010)
8. Cambridge Broadband Networks Limited. Backhauling X2
9. 3GPP TR R3-018: E-UTRA and E-UTRAN Radio Access Architecture and Interfaces, v0.3.0 (March 2006)
10. Ikuno, J.C., Wrulich, M., Rupp, M.: System level simulation of LTE networks. In: 2010 IEEE 71st Vehicular Technology Conference, Taipei, Taiwan, pp. 1–5 (May 2010)

Geo-Ontology-Based Object-Oriented Spatiotemporal Data Modeling

Jingwen Li[1,2], Yanyan Liang[1,*], and Jizheng Wan[3]

[1] College of Geomatic Engineering and Geoinformatics,
Guilin University of Technology, Guilin, China
[2] Guangxi Key Laboratory of Spatial Information and Geomatics, Guilin, China
GIS@glite.edu.cn
[3] Birmingham City University, Birmingham, The United Kingdom

Abstract. Spatiotempoal data model is fundamental to geospatial data representation, organization, analysis and applications. Due to the absence of geospatial semantic modeling and its logical structure, the spatiotemporal data may be interpreted mistakenly by other users or by other systems. For multi-purpose urban geospatial information development and sharing, spatial entities and their semantics should be modeled carefully. This paper presents strategy in geo-ontology-based object-oriented spatiotemporal data modeling to design a geospatial data model which can solve the problems of semantic conflict, and is ease of backtracking query and data sharing. A new approach is proposed to enterprise-level urban geospatial data integration, management and sharing. Modeling experiences show that it is easy to storage, manage and distribute spatiotemporal data for urban enterprise-level GIS applications in the network environment.

Keywords: Geo-ontology, Object-oriented, Spatiotemporal data model.

1 Introduction

As a direction of geographic information science research, geo-ontology has been put forward since the 1990s, people know the geographical phenomena again from the point of view of origin, and develop the technology of GIS [1-2]. Spatiotemporal data model, as a real characteristic abstraction of geospatial data and temporal data, is the way that people understand and express the geographical phenomena in the real world and the basis of GIS spatiotemporal data organization and data processing algorithm design [3-4]. With the construction of smart city and the accelerated pace of urban information technology, higher requirements are post in geospatial data model for description of geographical entities and expression of semantic information. How to change the geographical data and geographical information into geographical knowledge and how to use the geo-ontology realize the reconstruction of geography in human brain by computer, realize network intelligence information retrieval, cross-platform treatment, semantic fusion, integration and intelligent decision, how to solve the data mining processing of masses of geographic information are all hot spot

Q. Zu, B. Hu, and A. Elçi (Eds.): ICPCA-SWS 2012, LNCS 7719, pp. 302–317, 2013.

problems of geo-ontology and GIS spatiotemporal data model research [5]. In recent years, in order to solve the problems of data organization, storage and sharing, many scholars [6-11] made deeply researches from many kinds of models, such as the semantic GIS data model, entity-oriented spatial data model, object-oriented spatiotemporal data model, geo-ontology logical structure for 3D geology modelling and database model based on spatiotemporal ontology. Unfortunately, they mainly focus on the problems of the data, semantic model and data storage and few studies concentrate on the expression of the geographical entities semantic and logical structure. Two main issues remain unsolved: a lack of good understand in semantic between different systems and can not fully satisfied the needs of geographic information sharing in different industries. Therefore, a new model which can overcome these two issues is needed to be constructed [12].

In this paper, on the basis of the semantics of geographic entities, we combined with the integrity of geospatial and the time process of geographic entities from birth to death to construct geo-ontology-based spatiotemporal data model. The researches involved two main scientific objectives: one is the spatiotemporal semantics description of entity, the logical expression and geographic information retrieval to solve the problems of semantic sharing and providing reference for data integration and sharing in many fields. An example of the application of this model was presented in the road in Lingui County, Guilin, Guangxi, to realize road-based ontology spatiotemporal data retrieval and spatial information interoperability. The other objective is the introduction of variable weight synthesis theory to travel decision analysis which is more close to the human ontology decision in making selection and application.

2 Methods

Considering the complexity of geospatial data, the data organization and storage issues have been well explored in recent years. Therefore, we concentrate on the design of a geographic spatiotemporal data model which can solve the problems of semantic conflict, and is ease of backtracking query and data sharing.

2.1 Ontology-Based Theory and Data Abstract Processing

Ontology derive from the field of philosophy ontology [13], is a shared conceptual model of the formal specification and the description of the recognized and concepts set within the field [14]. Ontology-based geo-spatial cognition is a continuous understanding and the decomposition process, as well as the bridge to connect the real world and the computer world.

Object-oriented cognitive theory puts forward that the real world is consist of different ‘objects’ which have vary forms, regular movement and different internal state. ‘Object class’ is called by a group of same or similar objects collections and any objects belong to an "object class". According to some rules, simple object is composited to complex objects. Objects combination and interaction constitutes the

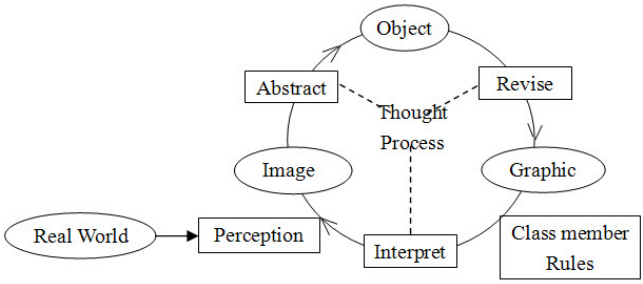

Fig. 1. The object-oriented-based cognitive method (Ma, R.H., 2002)

objective world [15].It is more suitable for human to form a way of thinking to understand and simulate the real world by using cognitive mode of object-oriented-based methodology. The object-oriented-based cognitive method can be seen in Fig1.

As seen in Fig.1, object is defined as the result of real world perception and concept abstraction in the method of object-oriented cognitive. Objects establishment can revise and refining the schema which can be improved to interpret images. On one hand, people have applied semantics in geographic database expression since the relation data model appeared [16], on the other hand, the cognitive theory put to use in geographic database expression study. Object-oriented cognitive methods simulated the process of objective world people understanding naturally. Based on the cognitive method, the concept of software system and mechanism are easier to understand completely, and can describe geographical space perfectly for user understanding.

Having clear definition, ontology provides concept support for co-construction and data sharing in different areas. However, it must be linked with data. A lot of advantages of object-oriented technology are obvious in data organization and data sharing, but it is easy to produce semantic ambiguity between different industries in data exchange and understanding, and lead to data sharing is prevented. If the two kinds of technology combine with each other and learn from each other, it can provide new train of thought for co-construction and data sharing in different industries and different areas.

Geo-ontology is the theory and methods which abstract the science of the geographical knowledge into one with a consensus by the object (or entity) and the composition of the system in accordance with a certain relationship. It is also carried out the process of conceptualization and clearly defined simultaneously and finally expression in the form of formalization [17]. The geographical cognition process based on ontology is shown in Fig.2.

The description of geo-ontology included the relation between geographic entities and entity description. Among them, the description of geographic entities included the temporal features, spatial features and non-spatial attribute features. Spatial features be partitioned into two parts—the geographic entity space position and geometric shape. Temporal features depict the change processes of the geographic entities in time axis. While the features except geographic entity features of temporal

and spatial features belong to the non-spatial attribute features. The geographical entity attributes were packaged as a whole in the process of ontology- based geo-spatial cognition. This process achieves the concept of temporal features, spatial features and non-spatial attribute features of integration, which not only realize the semantic sharing, but also realize a good understanding of the real world following human thought process.

The construction of geographic ontology is a conceptual model of geographic sciences domain. Based on object-oriented method, this model abstracted geographical things which have the same properties to form class or a concept. Through the process to building the abstraction, definition, classification, hierarchical and logical relationship of the concept, this paper described the connotation and denotation of the geographic things in the real world. The ontology-based geospatial abstract not only followed the thought process of the human understanding to the world, but also explained and defined the geospatial object together that lay a firm foundation for in the process of semantics sharing.

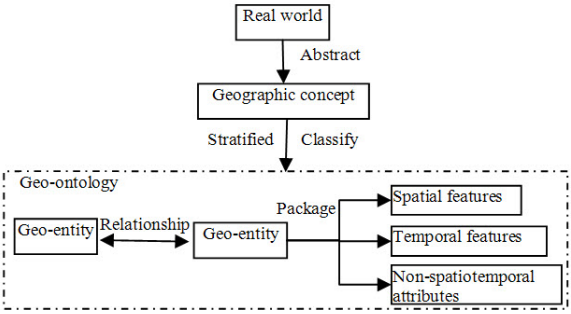

Fig. 2. Geographical cognition process based on ontology

Definition 1. The sum of directly or indirectly related to the distribution of the surface things, phenomena and the characteristics and the description of them as geographic reality. A point set is expressed as space dimension, and then the geographic reality performed as a multi-tuple [18]:

$$(p,a1,a2,\ldots,an) \tag{1}$$

Where p is any point of space-dimensional, {a1, a2, …, an} represents the collection of geographic things, geographical features and geographical phenomena.

Definition 2[19]**.** Geographic entity is the smallest logical unit with entire geographic significance. There are many kinds of methods to describe the structure of the geographic entity information, while the mainstream description methods is conceptual model. A typical conceptual model of geographic entity can be described as a six-tuple array:

$$E=\{ID,\ N,\ G,\ A,\ R,\ M\} \tag{2}$$

Where ID is the unique identification code to identify an unique geographical entity, N is the name of the geographical entity and G is the geometric properties of the geographical entity to describe the characteristics of the geographical entity such as size and shape, A is the property of the geographical entity, A={a1,a2,…,an}(n=1,2,3,…); R describes the relations between geographic entities, M is the entities operation.

Definition 3[20]**.** Geographic ontology model is a five-tuple, denoted by On=(T, X, TD, XD, H). Where T is the term set. The term in T is called the atom in terms of terminology, including the atomic C and atomic properties term P, denoted by T=(C, P). Body has two types of attributes: class attributes and attributes values. The former represents the relationship between classes and the latter represents the properties of that class; X as the set of instances; TD is a set of definitions of terms, definitions of terms in T; XD set for the instance declaration to declare an instance of T; H is the hierarchical relationship between the concepts; T×T is a subset, H(T1, T2) means T1 is the sub-concept of T2.

The geographic ontology model not only distinguished each object but also contacted each object, and it reflects the hierarchy of the real things and internal relations to achieve the requirement of geographical space integrity. Meanwhile, the geo-ontology, describes the logical expression, has a foundation of logical reasoning. In practical application domains, data were stored into the corresponding database through establishing ontology model related to the objective world and describing application formalization language to relate to the instance of the object-oriented in order to integrate object-oriented method and ontology.

2.2 Description of Geo-spatiotemporal Data Model

In real life, time and space is inseparable. However, the ontology-based discussion of the relationship between time and space is still in exploration stage. From the point of view of the theory, it will be more perfect to make the time and space as a whole and construct the spatiotemporal model. In addition, from another perspective of the realization, it adds the temporal support based on the existing special model which has relative more research foundation and is easier to be realized [21].

Any geographic objects die with the change in spatial and attribute at a point of time because of a certain events, there must be a new object is created simultaneously. The spatial and temporal variation of geographic object can be divided into space change and attribute changes. Furthermore, the space changes consist of three circumstances: position change, shape change, position and shape all change [10]. No matter which kind of change, the death or the birth of geographic object is a relative state, and the existence of geographic objects is relative stability of a process during the period of birth to death, and the space and attributes have no change. The relationship during the birth, the existence and the death of geographic objects are showing in the following in Fig.3.

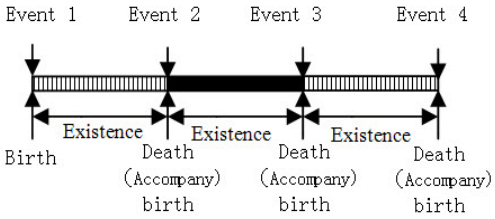

Fig. 3. The relationship of spatial object's creation, existence and death

Confronted with the complex geographical reality, people no longer satisfies with the management and display to geographic entity object data, while pay more attention to the analysis and decision-making of geographical reality problem. It is important to capture the semantic information accurately to build ontology-based object-oriented of spatiotemporal data model with the integration functions of management, sharing, decision-making and temporal information, spatial information and attribute information have been contained.

The real world is abstracted in ontology-based geographic spatiotemporal data model based on the concept of semantic to obtain the information described for data storage and description. This paper defined the conceptual model of ontology-based geographic spatiotemporal data through continuous ontology modelling process.

Definition 3. geographic spatiotemporal data model can be described by tribasic array: M= (On, Ob, Ti, L), denoted by ontology-based geographic spatiotemporal data conceptual model. On = (T, X, TD, XD, H) represents geographic ontology model, details on Definition 2; Ob represents the geographic entity object model and the geographic entity is described by object-oriented model; Ti represents time set, described the geographic object changes with time process[22], L is defined by representing the layer. The model construction is shown in Fig.4.

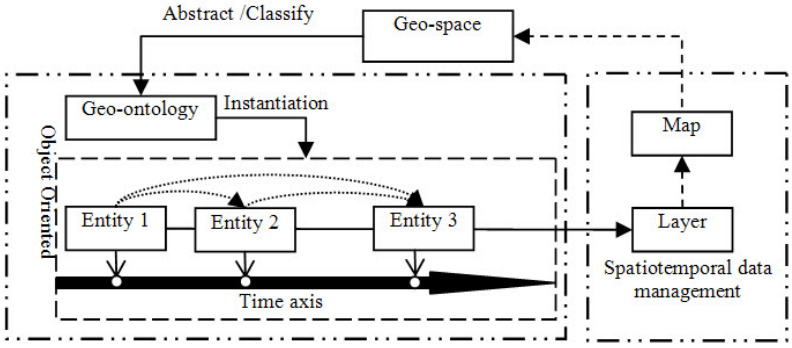

Fig. 4. Geographic spatial data concept model based on ontology

The model is organized based on geographic information as a unit entity. The real world is viewed as a whole. On the basis of ensuring the advantages of traditional model which can be understand and implement relative simply, this model is the further expansion of the traditional model which added the logical relationship between entities and semantic links and introduce the temporal attribute.

3 Model Design and Construction

This paper propounds geo-ontology-based objected-oriented spatiotemporal data model from the logic models construction, abstraction, organization and variable weights synthesizing.

3.1 The Construction of Logical Model

For the establishment of geographic ontology, geographic ontology is the knowledge base established based on certain norms, a clear definition and description of geographical concepts. Thus the definition of entity is made within the area and the logical relationship of the studied object is abstracted simultaneously.

The organization of the concepts and the relationship of the abstracted geographical entities using geographic ontology model and description with the ontology published by W3C are used to describe OWL (Web Ontology Language) which is the language based on description logies. It has advantages and solid theoretical foundation in ontology formalizing description and semantic expression. Meanwhile, OWL supported the logical semantic reasoning in knowledge base and rule base with powerful semantic expression function for helping to gain new knowledge. This paper adopted OWL to describe logic relationship, and finally to store data in Oracle XML/OWL.

3.2 Organization and Storage

Because of the comprehensive domain knowledge ontology covered widely, contented mass data, we should store ontology reasonably and efficiently to improve ontology-based searching efficiency as the premise and guarantee for knowledge reasoning, semantic query retrieval, analysis and decision-making.

This paper applied the object-oriented method to abstract geographic reality into geographic entities and the logical relations. According to Geometric shape of geographic entities, the geographical entities are abstracted for three simple objects (SIO): dot, line, polygons. And two or more simple objects compose to complex object. The object-oriented method to store data is adopted in this paper. Due to the different between the spatiotemporal data and general data, traditional relation database can't satisfy with unified storage and management of graphic and attribute data. Therefore, this article presents a method to store and manage the temporal data, spatial data and attribute data by using Oracle Spatial relational database, and it also can stored parts of attribute information independently.

The geographic ontology is constructed based on the entity concept and the logical relationship during concepts and described using OWL language. The specific geographical entity objects encapsulate the data using hierarchical expression, organization while the ultimate of body and physical data are stored in Oracle Spatial-relationship database. The organization of the ontology-based geospatial logical model is depicted in Fig.5.

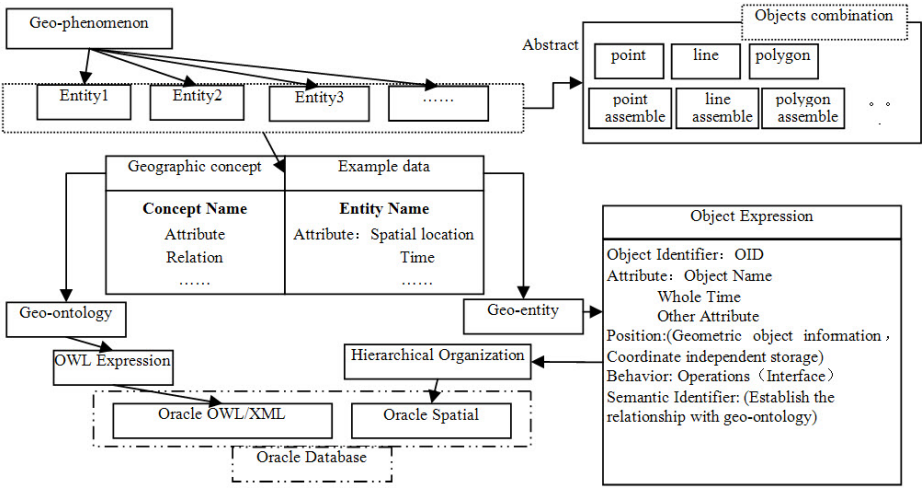

Fig. 5. Abstraction and organization of geographic spatial data logical model based on ontology

3.3 Semantic Reasoning Query and Decision-Making

Semantic query is based on the actual work in specific areas with powerful pertinence, and the habit of user and query in the field should be satisfied enough in the process of interface design. To make sure the inquire contents comprehensive and reliable with rapid response speed, query speed improving is also helpful for users in the professional field. [23-27].

The traditional semantic query module is mainly based on matching keywords entered by users, but the query results are often unable to accurately describe the user's query intention that is difficult to meet the semantics requirement of the user. This paper designed semantic reasoning query module based on ontology. Common query pattern libraries were established on the basis of simple processing of natural language, and pattern matching in the process of user queries that improves query efficiency and makes query results easier to meet the requirements of the user's semantics.

When users enter keywords or natural language as query contents, key words will be extracted and marked firstly. The marked words are converted into a query which can be handled by computer through pattern matching. The computer handled the data simply according to the query content user input, then converted into computer language for related content searches in order to present the query results to users.

ontology-based geographical spatiotemporal data query model support natural language query, and the query results based on ontology obtained, comparing with the results obtained by the common query system, can be more satisfied by users' demand. The ontology-based geographical spatiotemporal data semantic query process is shown in Fig6.

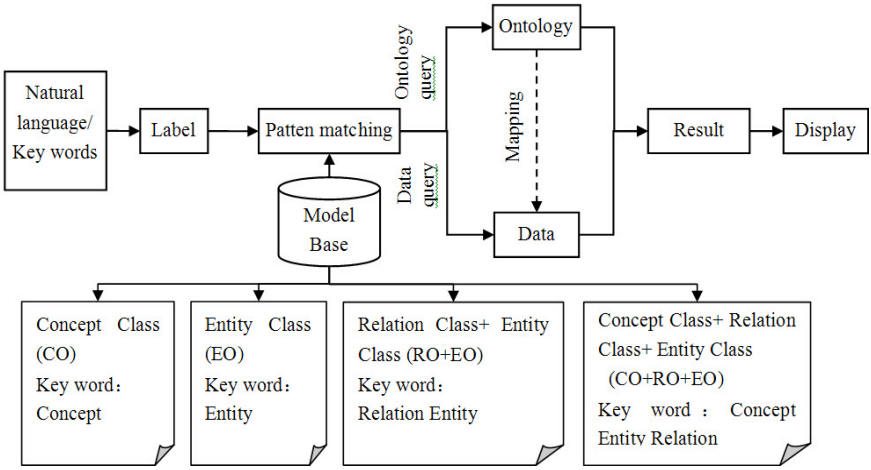

Fig. 6. The semantic query process of ontology-based geographical spatiotemporal data

Ontology-based geospatial spatiotemporal data query processing flow is as follows: First, input the content for querying. The query content can be the form of a natural language or keywords; Second, filter the input, remark the vocabulary and remove the useless information; Third, match the marked results and the pattern in the pattern libraries; Fourth, inquiry semantic query and semantic extension to get semantic query results; Fifth, returned the result to users.

To some extent, decision-making is based on the human mind with uncertainty in some practical applications and semantic reasoning query of ontology model for example fuzziness description of the traffic concept [28], service satisfaction degree and user needs, the decision-maker's preference and value judgment always affects the final decision results. Decision-maker do our best to choose "the best" feasible scheme, this needs to range up the given solutions in order to identify good or bad. This paper introduces the theories and methods of variable weight synthesizing into the spatiotemporal ontology model in consideration of the balance of many elements of the synthetic decision to make the selection and the application decision-making closer to the human ontology mind. Based on variable weights theory the feasibility model of decision-making is [29] as follows:

(1)Standardized index: in order to facilitate to calculate and optimize analysis, eliminate the comparison difficulties of dimensional difference between indexes, it is necessary to transform the indexing formula $R = (r_{ij})_{m\times n} (i = 1,2,...,m; j = 1,2,...,n)$ into standardized matrix through formula in the following.

$$r_{ij} = \frac{r_{ij}^{'}}{r_i} \tag{3}$$

Each scheme index constructs the matrix R later through the standardized processing.

$$R = (r_{ij})_{m\times n} (i = 1,2,...,m; j = 1,2,...,n) \tag{4}$$

Where $r_{ij}^{'}$ is the index value and r_{ij} is the index value after the standardization, n is the number of scheme, m is the number of index, r_i is general objective value. R is the matrix of r_{ij}

(2)Subjective weight: In the decision-making process, the subjective weight can reflect the decision index preference of decision makers. The subjective weight of the index is given in the following through expert evaluation:

$$w_{ij} = \frac{w_{ij}^{(0)} / r_{ij}}{\sum_{i=1}^{m} w_{ij}^{(0)} / r_{ij}} \qquad (j = 1,2,\cdots,n) \tag{5}$$

w_{ij} is the subjective weight value of decision maker.

(3)Calculate the distance between solutions and the ideal point. Ideal point defined as $X^* = (1,1,\cdots,1)^T$, is these ideal point of decision index after standardization process, the dimension of X^* is m, the solutions to the ideal point distance is:

$$d_p = \left[\sum_{i=1}^{m} \lambda_i^p (1 - r_{ij})^p \right]^{\frac{1}{p}} \tag{6}$$

(4)Quality decision scheme : sort d_1 from high to low were, the minimum d_1 correspond optimal model. When d_1 are equal, sort d_2 from high to low, differentiate d_2 to scheduled scheme priority.

4 Case Study

From the construction of geo-ontology spatiotemporal data model above, we can find that this model can be modified easily, convenient to query and spatial analysis. The following context take the smart city road in Lingui County, Guilin, Guangxi as an example to validate the effectiveness of the proposed model used in the practical analysis and decision.

4.1 Road Entities and Ontology of Abstract

The road-ontology-based spatiotemporal analysis expend to the traditional road-ontology description structure. The unknown information is deduced from the analysis of the known concept and the relations. According to users' defined rules, it

can also be used in inferential analysis. The essence of the road and the relations of the concept is shown clearly and comprehensively when using the proposed model to describe the concept of road domain and the relationship between concepts and a unit, normative road domain knowledge framework is created to provide decision-making and service of personalized requirements for travelers and road management organizations.

To take the smart city road an example, the roads in this region were split by entities, and the results mainly include pavement, roadway, blind road, bridge, tunnel components. According to the geo-ontology-based spatiotemporal data model, this paper will abstract city road entities in four levels: Transportation Network, Road section, Road and Location.

City road ontology is the expression of geographical entity and the logical relationship between entities. The logical relationship refers to the city road entity relationship and the internal factors relationship of road entity which can be divided into 3 parts: kind-of, part-of, instance-of, as shown in Fig.7. Kind-of is used to express the relationship between road sections and roadway, pavement, blind line, bridge and tunnel. Part-of describes the relationship between the roads and road network, road junctions, the relationship between the road and the road sections, the relationship between road parts and road sections. The relationship between entity and road parts is described by instance-of.

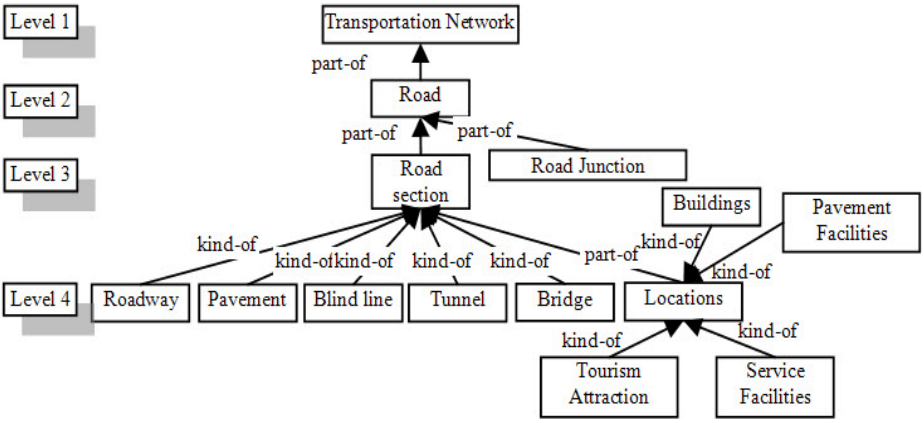

Fig. 7. Conceptual level of road

4.2 Road Spatiotemporal Data Management

According to the requirements of the model, geo-ontology-based spatiotemporal data model divides the city road-ontology into three layers for users' interaction and decision-making. It contains user layer, description layer and decision-making layer.

(1) User layer

Due to different user have different purpose to travel, different vehicles and any other factor, the demand for road conditions varies from each other. It is difficult for users to choose a suitable spatiotemporal data model to make decisions to travel. Comparatively, interactive questionnaires, incorporating most of questions related to users' knowledge, are easily understood and responded by users [30]. Meanwhile, the weight of users' demands on environment, traffic volume, safety and other factors are different in road choosing. Therefore, through user questionnaires (Fig.8), this paper obtains the users' demands on the road traffic from the personal perspective. The questionnaire includes the feasibility demand of road traffic as much as possible, such as: purpose of travel, vehicle, starting road, ending road, travel time and road selection priority level, and the demand for road facilities etc. From the weight division of road selection priority level about traffic conditions, safety index, environmental index, the system recommends one or more balanced, reasonable models according to the variable weight theory to provide spatiotemporal information which users required.

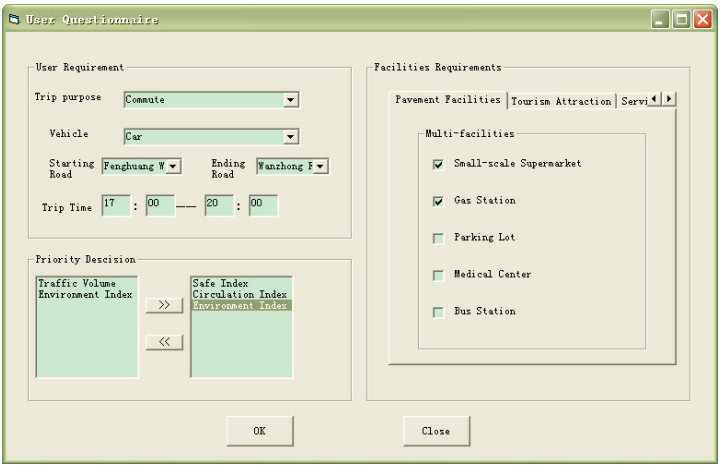

Fig. 8. Road-ontology-based user questionnaire

(2) Description layer

Description layer is structuring personalized road-ontology according with the needs of the user, its model UML diagrams are depicted in Fig.9. In this manner, personalized road-ontology services using object-oriented, semantic and ontology to satisfy user demands [31]. Through the abstraction and organization of geo-ontology-based spatiotemporal data model of, describe layer stored the road-ontology in object-relational database in Oracle Spatial according to the requirements of the model. Each road entity occupies a record which the graphical information stored in field of class SDO_GEOMETRY. Using the object's ID to establish the connection between the database tables.

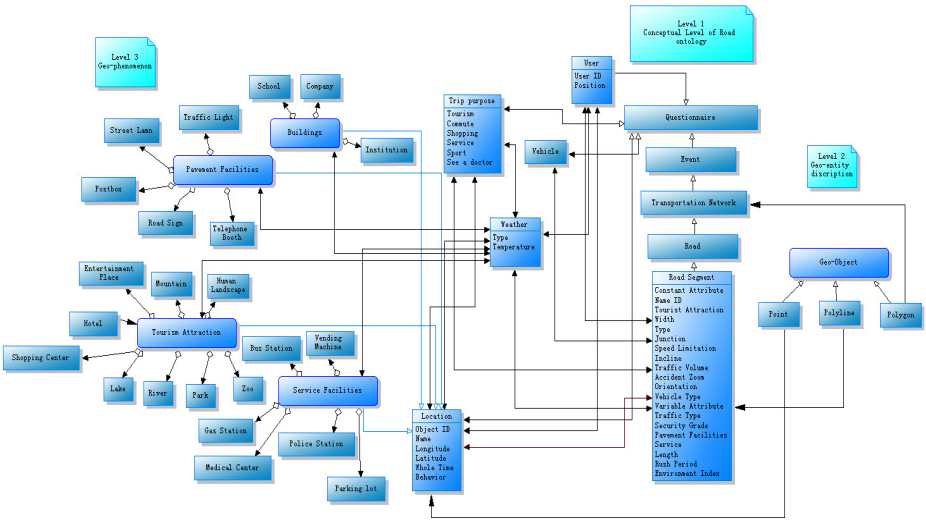

Fig. 9. The UML of road-ontology-based model

Database tables mainly include road tables, sections tables, road junction tables, road parts tables and road entity relationship table. The road junction tables and road parts tables store simple objects information; Road tables and sections tables don't store objects position information, only store address information of combination objects and simple objects; Road entity relationship tables store the logical relations between entities. The relationship between tables of city roads is showing in Fig.10 shows.

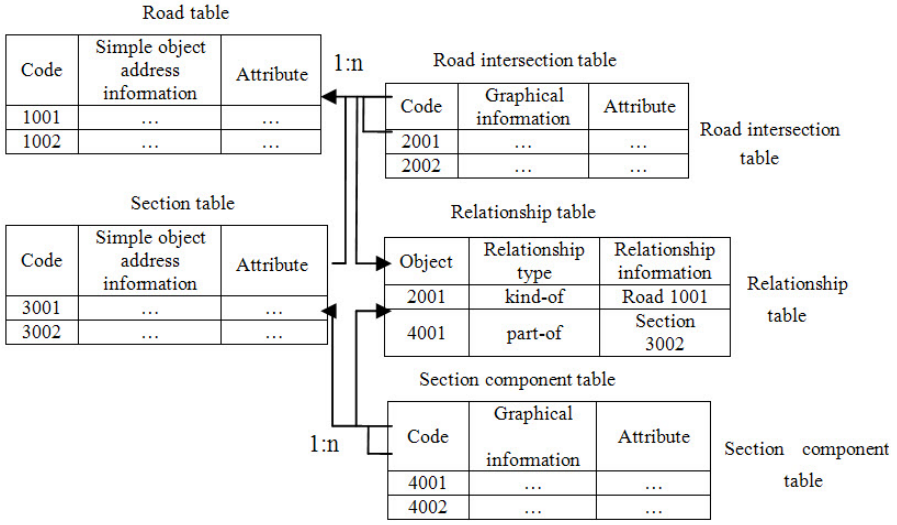

Fig. 10. Organization and management of city roads

(3) Decision-making layer

Variable weights synthesizing theory is introduced into travelling in city road decision-making. The application of variable weight synthesis theory is to analyze different travel factor weight from different users according to user questionnaires survey for the purpose of getting a set of optimal results. In the user questionnaire stage, the user presented: 17:00-20:00, self-driving back home, from Guilin centre hospital in Fenghuang West Road to Huayang housing estate in Wanzhong Road, and need for passing small-scale supermarket and gas station, road selection priority level is: the safety index > circulation index > environment index.

At the beginning, we should make sure that the starting and ending road section respectively is Fenghuang West Road and Wanzhong Road, the road parts are small-scale supermarkets and gas stations. And travel time is in rush hour: 17:00-20:00. The deduce process as following:

Step 1: system analysis all optimal path from Fenghuang West Road to Wanzhong Road road, and get set C1;

Step 2: Traverse all the road parts of path in C1, from which passed by small-scale supermarket and the gas station, and get set C2;

Step 3: According to the users road selection priority, system distributes the weight of road safety index, circulation index, environmental index for comprehensive variable weights analysis during 17:00 to 20:00, get set C3;

Step 4: Traverse all the small-scale supermarkets and gas stations in each section of the route in set C3, then get the name and corresponding attributes of the existing small-scale supermarkets and gas stations, get set C4.

The conclusion shows that: the road section, Fenghuang West Road -Wanping Road-Wanfu Road-Wanbei Road-Wanzhong Road, is optimal choice, which passed by the small-scale supermarkets are: Huimei department. And the passed by gas stations are: Wanfu Road gas station.

5 Conclusion

Geo-ontology-based object-oriented spatiotemporal data model is designed to study the description and expression of the semantic and logical relationship in geographical world from the perspective of human mind. The real world geographical phenomenon is described using geographic entities and the relationship between entities. That has changed the traditional geospatial cognitive approach which only described from the geometry shape. In information management, geographic entity is stored in the way of object-oriented with the advantages such as entity management method, easy to modify, query retrieval and realize spatial analysis easily. More importantly, any complex geographical entity that from user's requirements can be relative simply constructed. The storage method of the proposed model realizes the integrated management of geographical entities' spatial data, attribute data and temporal data. And the model highlights the management of the semantic information, while expands the existing data model. Furthermore, the introduction of the variable weights synthesizing theory makes the model more close to the human ontology mind and provides a reference in the expression, storage and sharing of the smart city geographic information.

Acknowledgements. This work has been supported by the Natural Science Foundation of Guangxi (NO. 2011GXNSFD018003).

References

1. Agarwal, P.: Ontological considerations in GIS science. Geographical Information Science 19(5), 501–536 (2005)
2. Smith, B., Mark, D.M.: Ontology with Human Subjects testing:An empirical investigation of geographic categories. Geographical Information Science 15(7), 591–612 (2001)
3. Chen, J.: Key issue and reseach direction in GIS's spatial data models. Acta Geographic Sinica 50, 24–32 (1995) (in Chinese)
4. Wu, L.X., Gong, J.Y., Xu, L., et al.: On spatial data and spatial data modeling. Geomatics World 3(2), 41–51 (2005) (in Chinese)
5. Song, J., Zhu, Y.Q., Wang, J.L., Li, R.: A Study on the model of Spatio-temporal Geoontology based on GML. Journal of Geo-Information Science 11(4), 442–451 (2009) (in Chinese)
6. Chen, C.S.: The function of classification of geographical information system in the GIS semantic data model design. Bulletin of Surveying and Mapping 8, 17–20 (1998) (in Chinese)
7. Chen, C.S., He, J.B.: A GIS semantic data model for the purpose of data sharing. Journal of Image and Graphics 4(1), 13–18 (1999) (in Chinese)
8. Ye, Y.Q., Zuo, Z.J., Chen, B.: Orient-Entity Spatial Data Model. Earth Science Journal of China University of Geosciences 31(5), 595–560 (2006) (in Chinese)
9. Li, J.W., Liu, J.F., Zhou, W.T., Yan, S.J.: Description method of spatial data model based on geography cognition. Geotechnical Investigation & Surveying 1, 59–63 (2009) (in Chinese)
10. Chen, X.B., Li, S.N., Zhu, J.J.: Database Model Based on Spatio-temporal Ontology. Geography and Geo-Information Science 26(5), 1–6 (2010) (in Chinese)
11. Hou, W.H., Liu, X.G., Wu, X.C., Zhou, Y.Z.: Geo-ontology Logical Structure and Development Technology for3D Geology Modeling. Geography and Geo-Information Science 25(1), 27–31 (2009)
12. Wand, Y.D., Gong, J.Y., Wu, X.H.: Geospatial Semantic Interoperability Based on Ontology. Geo-spatial Information Science 10(3), 204–207 (2007) (in Chinese)
13. Wang, X.J.: Ontology of Social Science Research. Journal of Henan Normal University 34(5), 76–78 (2007)
14. Borst, W.N.: Construction of engineering ontologies for knowledge sharing and reuse. PhD thesis. University of Twente, Enschede (1997)
15. Ma, R.H.: The research on Geographical spatial cognition and GIS spatial data organization. Ph.D. Thesis, Nanjing University (2002) (in Chinese)
16. Jeremy, L.M., Donna, J.P., Qian, L.J.: A Conceptual Framework for Incorporating Cognitive Principles into Geographical Database Representation. Geographical Information Systems 14(6), 501–520 (2000)
17. Chen, J.J., Zhou, C.H., Wang, J.G.: Advances in the study of the geo-ontology. Earth Science Frontiers 13(3), 81–90 (2006) (in Chinese)
18. Goodchild, F.: Geographic data modeling. Computer and Geo-sciences 18(4), 401–408 (1992)
19. Chen, C.S., He, J.B.: A GIS Semantic Data Model for the Purpose of Data Sharing. Journal of Image and Graphics 4(1), 13–18 (1999) (in Chinese)

20. Wang, H.W.: The ontology-based metadata model research. Doctor's thesis. Shanghai Jiaotong University, Shanghai (2004)
21. Min, M., Tan, C.F., Jiang, L., Fan, C., Hu, C.F.: Research progress in geographical spatio-temporal ontologies. Journal of Central China Normal University (Nat. Sci.) 40(1), 132–137 (in Chinese)
22. Li, J.W., Zhou, W.T., Liu, J.F.: Design of object-oriented vector model based on geo-entity. Geography and Geo-Information Science 24(4), 29–31 (2008)
23. Steffen, S., Jurgen, A.: AI for the web-Ontology-based Community Web Portals. In: AAAI 2000/LAAI 2000, pp. 1034–1039. AAAI Press/MIT Press (2000)
24. Doan, A.H., Natalya, F.N., Alon, Y.H.: Introduction to the Special Issue on Semantic Integration. SIGMOD Record 33(4), 11–13 (2004)
25. Wache, H., Vogele, T., Visser, U.: Ontologies-based Integration of Integration—A Survey of Existing Approach. In: Proc. of the Workshop on Ontologies and Information Sharing at the Intl. Joint Conf. on Artificial Intelligence, pp. 108–117 (2001)
26. Doan, A.H., Alon, Y.H.: Semantic Integration Research in the Database Community: A Brief Survey. AI Magazine 26(I), 83–94 (2005)
27. Natalya, F.N.: Semantic Integration: A Survey of ontology-based Approach. SIGMOD Record 33(4), 65–70 (2004)
28. Li, D.R., Wang, Q.: Transportation Knowledge Modeling Based on Spatio-temporal Fuzzy Ontology. Geomatics and Information Science of Wuhan University 34(6), 631–635 (2009) (in Chinese)
29. Yue, C.Y.: Decision-making theory and method. Science Press, Beijing (2003) (in Chinese)
30. Chau, K.W.: An ontology-based knowledge management system for flow and water quality modeling. Engineering Software 38, 172–181 (2007)
31. Niaraki, A.S., Kim, K.: Ontology based personalized route planning system using a multi-criteria decision making approach. Expert Systems with Applications 36(2), 2250–2259 (2009)

A New Object-Oriented Approach towards GIS Seamless Spatio-Temporal Data Model Construction*

Jingwen Li[1,2], Jizheng Wan[3,4,**], Yanling Lu[1,2], Junren Chen[1,2], and Yu Fu[1,2]

[1] School of Geomatics and Geoinformation, Guilin University of Technology, Guilin, China, 541004
lijw2008@glite.edu.cn
[2] Guangxi Key Laboratory of Spatial Information and Geomatics, Guilin, China, 541004
[3] Corporate ICT, Birmingham City University, Birmingham, UK, B42 2SU
Jizheng.Wan@bcu.ac.uk
[4] School of Computer Science, University of Birmingham, Birmingham, UK, B15 2TT
JXW178@bham.ac.uk

Abstract. Spatio-temporal data model has been recognized as the foundation of the description of spatiotemporal characteristic for geographic entity. In this paper we present a new way to construct seamless spatio-temporal data model and explore the spatiotemporal evolution and the data storage process for a spatial object from both space and time point of view. In addition, this data model has been used to organize and manage city cadastral information for evaluation purpose. It will improve the ability to construct, save and query integrated spatio-temporal data during the dynamic evolution process of geographic entity in our physical world.

Keywords: object-oriented, seamless spatio-temporal data model, cadastral, information organization.

1 Introduction

In the cycle of the geographical environment system, development and evolution of regional environment are promoted by the interactions between geographic entities. From the dynamic evolution point of view, space and time seamless and characteristic of multi-attributes apply to all geographic entities. Regard to direction, distance, level and geographical location, space seamless feature represents the geometric continuity to geographic entities. In the meantime, time seamless feature of geographical entities described as migration behavior and state of continuous change and causal association. The relationship of complex logic and the inheritance among geographical entities, could be described by the multi-attribute characteristics. Therefore, GIS spatio-temporal data model is the foundation of data storage, reproduction and dynamic analysis during the description process of geographical entities.

* This reseach was supported by Guangxi Natural Science Foundation;The project was funded by Guangxi Key Laboratory of Spatial Information and Geomatics.
** Corresponding author.

Q. Zu, B. Hu, and A. Elçi (Eds.): ICPCA-SWS 2012, LNCS 7719, pp. 318–331, 2013.

Appeared in the early 1990s, the object-oriented data model joined effectively together the geometric data and attribute data which solve the problem of tiered storage of spatial data in traditional GIS data model research. These data models have a relatively strong ability to deal with complex geographic entities. For example, [1] analyzed the state integrated packaging method; [2]created an object-oriented GIS data model which unified the storage of spatial data and attribute data. All these models, however, use static and single phase method to organize and manage space data, therefore cannot describe and manage time characteristic properly. Nowadays, research about spatio-temporal data model includes: spatio-temporal cube model [3], sequent snapshots model [4], ground-state correction model [5], spatio-temporal composite model [6], non-first normal form (N1NF) relationship spatio-temporal data model [7], object-oriented spatio-temporal data model [8], event based spatio-temporal data model [9], Voronoi-based spatial data model [10], process based spatio-temporal data model [11] [12] and spatio-temporal data model based on graph theory [13], etc. All these models are based on snapshot description, therefore the following disadvantage can be identified:

1. Unable to manage timeline seamlessly.
2. The management of geographic entities' space characteristic and time characteristic cannot be unified.
3. Only deal with space data statically without record and manage the evolution process of geographic entities in any period of time.

With the development of GIS technology and the research of geographic environment, higher requirements for comprehensive information about the change causalities on geographical environment and the dynamic management of the spatiotemporal evolution process have been put forward by researchers. In this paper, the spatiotemporal logic relationship of the key elements of geographical environment has been clarified. Then classify and abstract spatiotemporal information, and transfer geographical entity into space object. In the following sections, a new object-oriented description method for geographical entity has been introduced, which solve the problem of managing historical data and dynamic data for geographical spatio-temporal information.

2 Object-Oriented Description Method for Geographical Entity

In the physical world, geospatial information is a specific description of the geographical entity and expression. It changes with the disappearance, creation or combination of the geographical entity. Geographical entity can be abstracted to spatial object, and the integrated storage and distributed management for the geographical entities' time, space and attribute information can be achieved by package each spatial object [14].

2.1 Geospatial

Definition 1: The set of directly or indirectly related to things, phenomena and characteristics of the surface distribution, together with their description known as the geographic reality [15]. It shows as two-tuples if the space has been represented by point set.

$$\big((x, y, z), (a_1, a_2, \cdots, a_n)\big)$$

Where (x, y, z) represent arbitrary point in space, $(a_1, a_2, \cdots, a_n)$ is the set of geographical items, geographical features and geographical phenomenon on this point.

Definition 2: Use $P_i = (x_i, y_i, z_i)$ to represent an arbitrary point in space, $S = \{P_1, \cdots, P_i, \cdots, P_n\}$ as the space for research objects. $b_i = f\big(P_i, (a_1, a_2, \cdots, a_n)\big)$ is the effect of comprehensive function which geographic reality $(a_1, a_2, \cdots, a_n)$ affects on P_i. Set $B = (b_1, b_2, \cdots, b_i, \cdots, b_n)$ represents the effect of comprehensive function which geographic reality affects on the space S. Then (S, B) represents a generalized geospatial [16].

2.2 By This Definition, the Geospatial Is a Continued and Generalized Space, and Its Geo-graphical Sense Expressed by the Set B. Geographical Entity

Definition 3: *Geographical entity* is the minimal independent logical unit in the geospatial with complete geographical significance. If the space S is a discrete space on variable A_i, s is an independent unit in S, $F(s, A_i)$ is the value of A_i in S, then s and F called geographical entity [17 [18]. It has the following features:

1. Any geographical entities can be marked with a unique identifier.
2. Geographical entity can be distinguished. All geographical entities should have a set of properties which could be used to identify their existence.
3. A complete description about geographical entity should include:
    a. The domain of spatiotemporal property and its value.
    b. The domain of non-spatiotemporal property and its value.
    c. The description of basic relationship and method for geographical entities.

    The domain of property is a set of description which express all the possible properties contained by the geographical entity. The range is the possible value range of each property.
4. Geographical entities can be divided or combined into a new geographic entity with the difference of research purpose and scope.

2.3 Spatial Object [19] [20]

Definition 4: *Meta Object* (MO) is the object abstracted from the smallest geographic entities in the geospatial. MO is constituted by point, line and surface. It cannot be divided anymore.

Definition 5: Point, line and surface which make up MO called *Element*. Point element $P = \{P_{id}, X, Y, Z\}$, line element $L = \{L_{id}, P_{id1}, P_{id2}, P_{id3}, \cdots, P_{idn}, \cdots\}$, surface element $A = \{A_{id}, L_{id1}, L_{id2}, L_{id3}, \cdots, L_{idn}, \cdots\}$. As MO is constructed by those elements, so $MO.G = \{\{P\}, \{L\}, \{A\}\}$.

Definition 6: Physical or virtual object to which spatial information applies called Spatial Object (SO). It separates into entity object and semantic object. The entity object refers to the objective existence object. For example, when dealing with building information management, building itself is the entity object. Semantic object is defined by people according to the actual needs of non-objective existence of objects. Such as management of a company, the company as a semantic object.

2.4 Abstract Process of Spatial Object

The dynamic object packaging process of spatiotemporal data model is based on the spatial, temporal and property characteristic of the geographic entity. Each geographic entity has been abstracted to object based on the geometric and semantic characteristics. Then use the object ID to record the logic relationship between spatial objects, and use a combined way to describe the evolution process. Shown as figure 1.

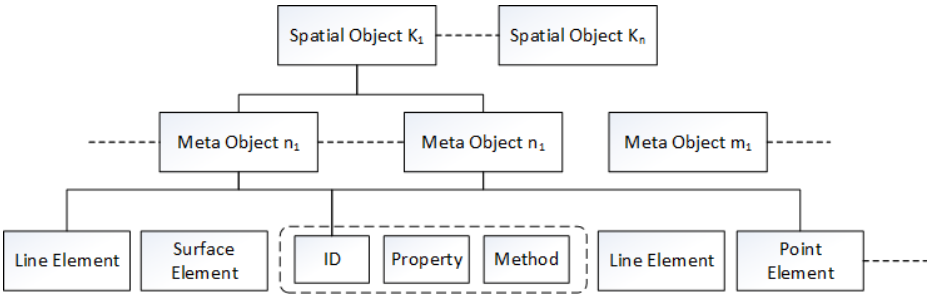

Fig. 1. The constitute of spatial objects

Items constituted by multi-point, multi-line and multi-surface have been recognized as *Meta Object*; *Spatial Object (SO)* is constructed by at least two *Meta Objects*; in addition, several *Spatial Objects* can be combined into a new spatial object. Any *SO* can be expressed as [19]:

$$SO = \cup_{i=1}^{n} MO_i$$

MO_i. is one of the components which construct the *Spatial Object*. *Meta Object* belongs to *Spatial Object* as well, and it's the minimal *SO* in geographic entity.

2.5 Model Description for Spatial Object

Due to the indivisible of *MO*, the data model should contain the properties of the spatial geometric features. Therefore, the model structure expresses as:

$$\langle Object, \{OID, (Spatial, Temporal, Attribute, Event), Operation\}\rangle$$

For other Spatial Objects:

$$\langle Object, \{OID, (Relation, Temporal, Attribute, Event), Operation\}\rangle$$

OID is the unique identifier for the *Spatial Object*. *Spatial* describe the spatial distribution, location and other related attributes of the *Meta Object.*

Temporal represents the description of object from the time point of view, it also reflects a life cycle of an object from the generation, development until the disappearance.

$$\langle Temporal\rangle := \langle Ts\rangle\langle Te\rangle\langle Td\rangle$$

Ts is the initial time when the stage of the object change, *Te* represents when it's finished and *Td* is the system time. When record the events which causing changes in the state of the object, *Ts* represents time; when record the process of the change, *Temporal* is the discrete points about time.

Generally speaking, *Attribute* reflects non-spatial information about the object, and it is the semantic definition about geographical entity and its characteristic.

Relation describes the logic relationship between *Spatial Object* and *Meta Object.*

Event represents the event which case the object state change.

$$\langle Event\rangle := \langle EID\rangle\langle ETS\rangle\langle Proi\rangle\langle ETE\rangle\langle EN\rangle \ \ (i \geq 1)$$

<*EID*> is the event identifier, <*ETS*> and <*ETE*> represent start time and end time of the event. <*EN*> is the name of the event, <*Proi*> describes the process of the event.

Operation is a set of operations on the *Spatial Object* and it separates into two different types of operations: qualitative change operation and quantitative change operation. Qualitative change operation focus on the relationship, topology and geometry modification which includes: creation, disappear, reincarnation, merging and splitting. Quantitative change operation is the operation which only changes the spatial feature or attribute feature of the object, without modifying the unique identifier. It includes maintenance, cessation and alteration.

3 Method for Constructing Seamless Spatiotemporal Data Model

Object-Oriented Seamless Spatiotemporal Data Model (OOSSDM) aimed on expressing the evolution process of the spatial object and solving the problem of information inquiry, history review and spatiotemporal analysis during this process. With this model, geographic entities could be abstracted into spatial object with specific time scale. Then the relationship between each spatial object can be built and therefore the attributes change along with the timeline series can be recorded.

With the help of OOSSDM, the characteristics of time and space can be integrated properly, and a seamless expression of the geographic entity from time and space point of view can be achieved.

3.1 The Tense of the Spatial Object

Time is one of the objective attributes of all natural things and every geographic entity will go through the cycle of creation and disappear. In the meantime, time and space connect closely, therefore the temporal characteristics of geographic entity can be expressed by spatial characteristics and attribute characteristics together. In other words, temporal semantic can be expressed by the geographic time series which change the spatial or attribute state of the object.

In OOSSDM, three states can be identified for the temporal change of a spatial object caused by spatial and attribute characteristics change: creation (birth), existence and disappearance (death).

The Creation and Disappear: any existing spatial object will disappear once its spatial and attribute characteristics change. Accompany with the disappearance, a new spatial object must be created simultaneously. There are three different types of disappearances:

1. Attribute information change, but the spatial geometric information remains same.
2. Spatial geometric information change, but attribute information remain same.
3. Both attribute information and spatial geometric information change.

The creation of a spatial object is a relative state of the disappearance in all three types above. Therefore, in order to guarantee the seamlessness of the geospatial, the spatial characteristics in both created spatial object and disappeared spatial object must be consistent.

Geographical entity's state changing is the most direct reflection of how human understand and transform the geographical environment. The creation and disappearance of the spatial object are instantaneous state, and the spatial object itself always appeaser as a relatively stable state. Their relationship shows as fig 2.

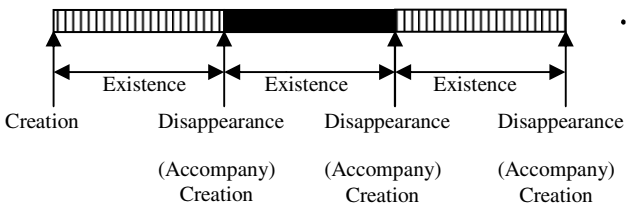

Fig. 2. The relationship of Creation, Existence and Disappearance

3.2 The Construction Process of OOSSDM

The construction of spatiotemporal data model must be consistent with human cognitive rules. It should be able to express *What*, *Where* and *When*, etc. In OOSSDM, the change of spatial object can be summarized as merging, splitting, merging and splitting, and inheriting. Shown as Fig 3.

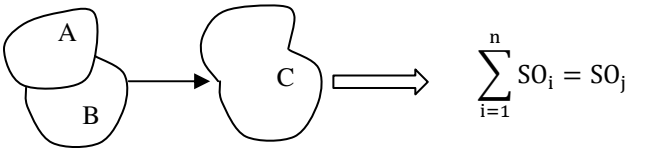

(a) Spatial objects merging

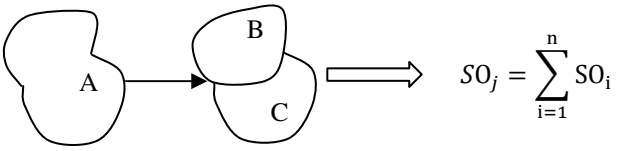

(b) Spatial objects splitting

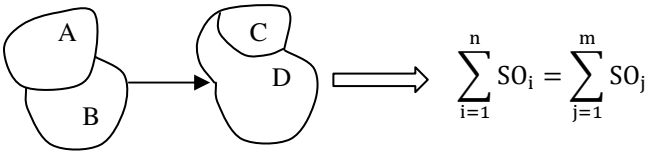

(c) Spatial objects merging and splitting

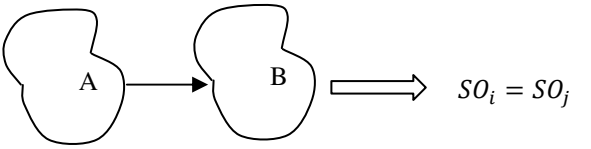

(d) Spatial objects inheriting

Fig. 3. Four basic types of spatial object change

Geospatial is composed by a series of spatial objects. Each spatial object has different state in different time. A series of time constitutes the evolution process of geographical information. In Fig 4, during the period of $T_1 \sim T_4$, new spatial objects have been created while old spatial objects disappeared due to the change of spatial geometrical information or attributes information.

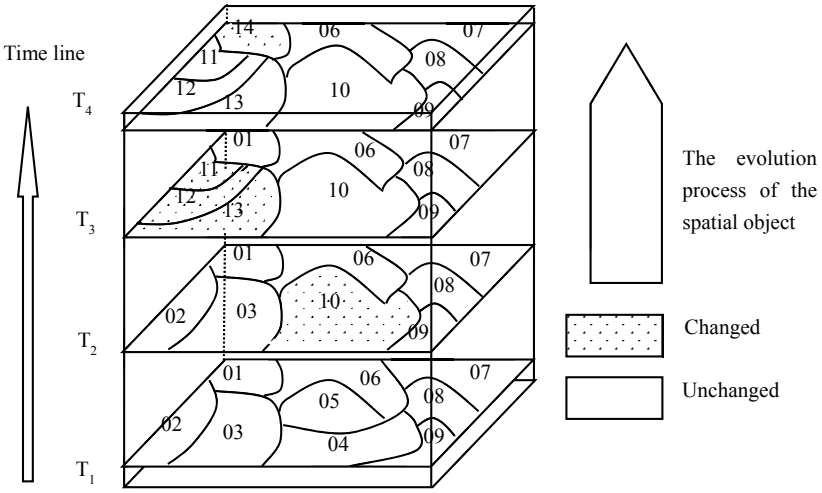

Fig. 4. Spatiotemporal relationship

Fig 4 shows that, the change of spatial object can be recorded by the evolution process. For example, 04 and 05 disappear at T_2, and 10 has been created simultaneously; 02 and 03 disappear at T_3, and 11, 12, 13 have been created; At T_4, 01 disappear due to the attribute change, and therefore 14 has been created.

The changing process of spatial object could be expressed by OOSSDM in a simple and direct way. In the whole process, the model only save changed spatial objects information. For the unchanged information, it only saves once. So it reduces the amount of data which need to be saved for every change.

3.3 Data Management for OOSSDM

Based on the requirement of the spatial object data model, OOSSDM transform the geometrical information and attributes information of the geographical entity into objects and then save to a relational database like Oracle Spatial, Sybase, etc. Each record in the database table reflects to one object, and the graphical information saved in a GEOLOC type of field called SDO-GEOMETRY. Object ID is used to connect between tables.

The design of the table includes: *Meta-Object* table, *Combined Object* (also known as *Spatial Object*) table and the Logic Relationship table. *MO* table used to save simple object information. Based on the principle of OOSSDM, *CO* table designed for the information of combined object and the address information about simple object which constitute the combined object.

The relationship between *MO* table, *CO* table and *LR* table shows in fig 5. Some object in *CO* table is formed by *Meta-Objects* in *MO* table. These *Combined Objects* also inherit the attributes from the *Meta-Objects*. The logic relationship will be created automatically during the process and saved in LR table.

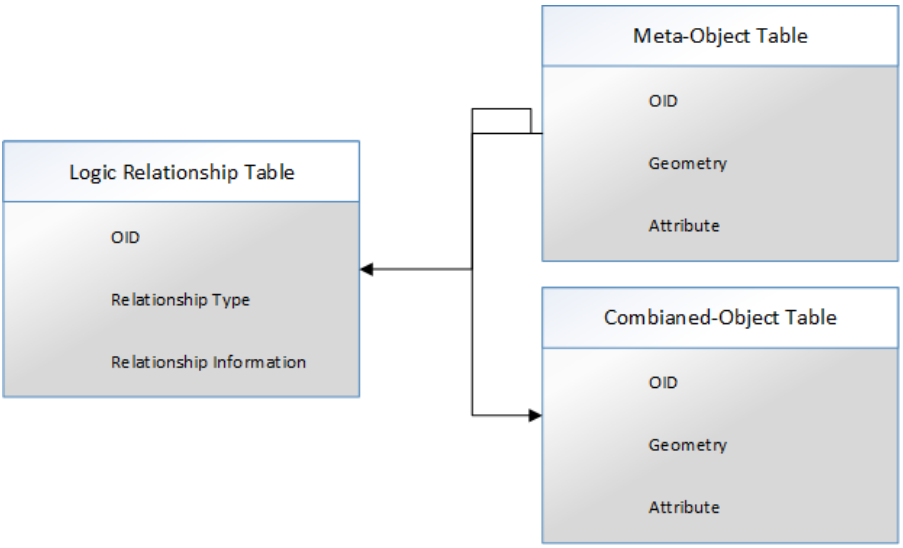

Fig. 5. Storage method for the relationship of spatial objects

During the model construction process, the system will generate the creation time, disappearance time and build the relationship table for the spatial object automatically. Please refer to Table 1 and Table 2.

Table 1. Relation of Combined Object

Object ID	Creation Time	Disappearance Time	Geometric Data	Attribute Data
01	2009.7.25	2009.7.30	…	…
02	2009.7.25	2009.7.28	…	…
03	2009.7.25	2009.7.28	…	…
04	2009.7.25	2009.7.27	…	…
05	2009.7.25	2009.7.27	…	…
…	…		…	…
10	2009.7.27		…	…
11	2009.7.28		…	…
12	2009.7.28		…	…
13	2009.7.28		…	…
14	2009.7.30			
…	…		…	…

Table 2. Logic Relationship Table

Before Change	Change Type	After Change
04, 05	Merging	10
02, 03	Merging and Splitting	11, 12, 13
01	Inheriting	14
…	…	…

3.4 The Inquiry Process of OOSSDM

In OOSSDM, the creation time and disappearance time of the spatial object have been saved in the format of object. Therefore, in order to inquire about the data on T_i, just get rid of the data when despaired before T_i and created after T_i. In Fig 6, spatial objects 01, 02, 03, 06, 07, 08, 09 and 10 are the result we expected.

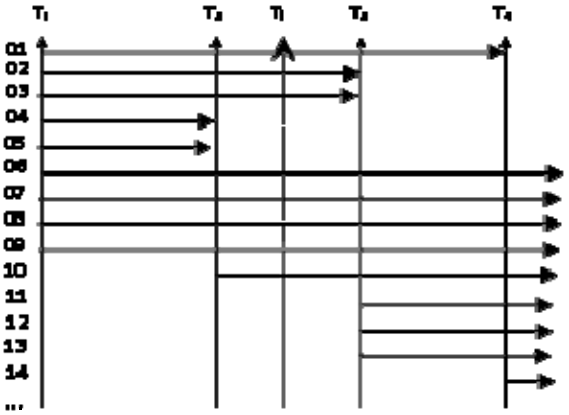

Fig. 6. Presence of spatial object at Ti time

OOSSDM can improve the inquiry performance, because the inquiry here is based on the relation change of the spatial objects which is irrelevant with the graphics and attributes.

4 Information Organize Method Based on OOSSDM

4.1 The Cadastral Spatial Object

Cadastral spatial objects can be constructed by the following method: Abstract the cadastral elements, and package the attribute characteristic, spatial characteristic and dynamic action information into an object based on OOSSDM. Each type of object has a separate packaging process, and contains a unique identification that can determine its creation or disappearance state.

In the cycle of creation, existence and disappearance, the dynamic change process of the cadastral object is mainly reflected on the land splitting, merging, creation, change the usage of the land and change the ownership. It can be summarized as [21]: 1. Attribute changes but spatial information remain same. 2. Spatial information changes but attribute remain same. 3. Both attribute and spatial information change.

4.2 The Description of Cadastral Spatial Object Changes

The relationship between cadastral change process and cadastral spatial object is very complex. In this paper, 4 types of events can be identified based on the number of cadastral spatial object: 1. only one cadastral spatial object change once. 2. a single cadastral spatial object changes several times. 3. Several cadastral spatial objects involve in one change process. 4. Several cadastral spatial objects involve in more than one changes.

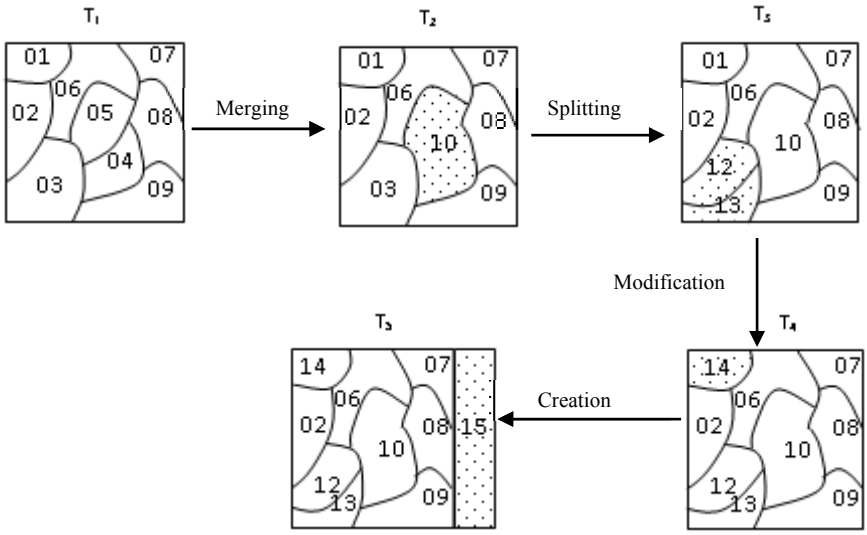

Fig. 7. The change events of cadastral spatial objects [14]

In Fig 7, 5 state changes and the relevant events have been presented. However, the temporal relation and the causal relationship of the cadastral spatial object cannot be described properly. With OOSSDM, we can represent this into *Table 3*. *EID is* the event id, *Ename* is the event name. *B_OID* is the identifier of the cadastral spatial object before the change and *A_OID* is the identifier after the change. *ST* is the start time, *ET* is the end time. *PID* is the process id.

Table 3. The change processes of cadastral spatial objects

EID	Ename	B_OID	A_OID	ST	ET	PID
E1	Merging	04,05	10	2004..4.15	2005.2.15	P1
E2	Splitting	03	12,13	2005.10.20	2006.9.10	P2
E3	Modification	01	14	2007.8.10	2008.7.20	P3
E4	Creation		15	2009.6.25	2011.3.5	P4

Because the cadastral spatial object is described by the attribute data and the geometric data which have the same target identification code [22]. Therefore, all cadastral change events share with one unique *EID, PID* and other characteristics. With OOSSDM, data in table 3 have been saved as objects, and each one contains their own attributes and actions. In addition, they can perform some operations independently and simultaneously.

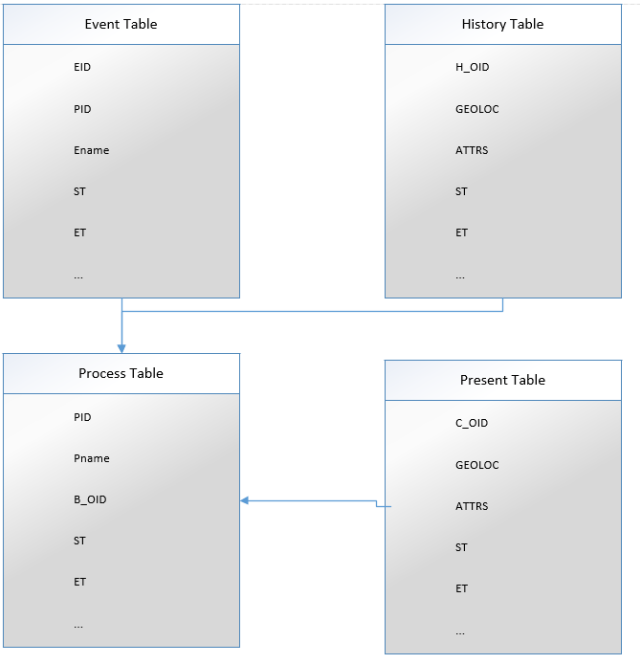

Fig. 8. The physical organization chart of cadastral space-time data basing on OOSSDM

4.3 Organize the Cadastral Data

The cadastral spatial geometric information and attribute information contained by the cadastral entities can be integrated and save in the SDO_GEOMETRY field in Oracle Spatial. The cadastral spatial object modification and inquiry can be performed in the following way: Create *Present Table, History Table, Process Table* and *Event Table* for every single cadastral object. Then build the connection between each table. Shown as Fig 8.

5 Conclusion

Spatial objects with spatial geometric information, attributes information and temporal information can be abstracted from geographic entities with OOSSDM. It also brings the temporal dimension concept into the spatial object. By recording the creation, existence and disappearance of the spatial object, OOSSDM can easily handle with the recording and inquiry about when, why and how geographic entities change. Therefore, it can effectively and dynamically manage the cadastral change and help to do the spatiotemporal analysis and decision make. In addition, it can also be used by spatiotemporal tools to simulate the change process, exploring and mining information and potential rules inside the spatiotemporal data.

References

1. Li, G., Zhuang, Y., Wang, Y.: The Object-Oreinted GIS Data Model-GeoDatabase. Bulletin of Surveying and Mapping, 37–39 (2006)
2. Xie, Q., Zhao, H.: Research on object-oriented GIS data model. Computer Engineering and Applications (25), 224–226 (2007)
3. W.M.F: Object -oriented models of spatiotemporal information. In: The Proceedings of the GIS/LIS (1992)
4. Langran, G.: Time in Geographic Information System. Taylor & Francis London, Washington, DC (1992)
5. Peuquet, D., Niu, D.: An event-based spatiotemporal data model (ESTDM) for temporal analysis of geographical data. International Journal of Geographical Information Science 9(1), 7–24 (1995)
6. Yang, M.: Temporal GIS and Spatiotemporal Modeling (1996), http://www.ncgia.ucsb/conf/SANTA_FE_CD-ROM/sf_papers/yuan_may/may.html
7. Shu, H., Chen, J., Du, D., Zhou, Y.: An Object oriented Spatio temporal Data Model. Journal of Wuhan Technical University and Mapping (WUHAN) 3, 229–233 (1997)
8. Pelekis, N., Theodoulidis, B., Kopanakis, I.: Literature review of spatio-temporal database models. The Knowledge Engineering Review 19(3), 235–274 (2005)
9. Cheng, C., Zhou, C., Lu, F.: The Improved Base State with Amendments Spatio-temporal Model in the Object-relation GIS. Journal of Image and Graphics 6, 687–702 (2003)
10. Yan, Y.: The Research of The Voronoi-based Spatial Data Model. Journal of Image and Graphics 1, 115–120 (2003)

11. Reitsma, F., Albrecht, J.: Implementing a new data model for simulating processes. International Journal of Geographical Information Science 19, 1073–1090 (2005)
12. Mcintosh, J., Yuan, M.: Assessing similarity of geographic processes and events. Transaction in GIS 2, 223–245 (2005)
13. Huang, Z., Feng, X.: A Study of Spatio-temporal Process Modeling Based on Petri Net for Land Alteration. Acta Geodaetica Et Cartographic Sinica 3, 239–245 (2005)
14. Li, J., Fu, W., Ye, L., Ma, X., Tian, L.: Design Method of GIS Spatio-Temporal Data Model Based on Object. Geography and Geo-Information Science 6, 11–14 (2010)
15. Good, C.: Geographical data modeling. Computers and Geosciences 4, 401–408 (1992)
16. Chen, C., He, J.: A GIS Semantic Data Model for the Purpose of Data Sharing. Journal of Image and Graphics 1, 13–17 (1999)
17. Tangay, Adamst, Useryel.: A Spatial data model design for feature – based geographical information system. Geo-graphical Information System 5, 643–659 (1996)
18. Lynneu: Category theory and the structure of featureinge- ographic information system. Cartography and Geographic Information System 20(1), 5–12 (1993)
19. Li, J., Zhou, W., Liu, J.: Design of Object-Oriented Vector Model Based on Geo-entity. Geography and Geo-Information Science 4, 29–31 (2008)
20. Le, X., Yang, C., Yu, W.: Spatial Concept Extraction Based on Spatial Semantic Role in Natural Language. Editorial Board of Geomatics and Information Science of Wuhan University 12, 1100–1103 (2005)
21. Li, J., Zou, W., Tian, L.: Organization Method of City Cadastral Comprehensive Information Using Process-Based Object-Oriented Spatial Data Model. Geography and Geo-Information Science 3, 32–35 (2012)
22. Shen, C.: Temporal Data Structure Model of Cadastral Parcel Alternation. Journal of Nanjing Normal University (Natural Science Edition) 2, 107–114 (2000)

Mechanical Research of the Planet Carrier in Wind Turbine Gear Increaser Based on Co-simulation of ADAMS-ANSYS

Taotao Li, Dingfang Chen, Pengfei Long, Zhengyan Zhang, Jiquan Hu, and Jinghua Zhang

Research Institute of Intelligent Manufacture & Control, Wuhan University of Technology, Hubei, China
taotaoliwhtu@163.com, cadcs@126.com, zzy0309@yahoo.com.cn

Abstract. As one of the most important parts in the wind turbine gear increaser, the planet carrier plays a role that is irreplaceable in the whole machine equipment. Co-simulation technology is one kind of new method which owes the characteristic of higher accuracy than the traditional safety coefficient method. Because the planet carrier has the features of irregularly shaped and working in alternating dynamic environment, co-simulation technology of ADAMS-ANSYS is applied to the mechanical research of the planet carrier in wind turbine gear increaser. The dynamic simulation of the whole gear increaser system is conducted based on the ADAMS platform in which the compact force、friction force and step driving are taken into consideration, with the maximum forces which are forced on the planet carrier calculated out. In the process of finite element analysis, there are three important steps which are modeling、meshing process、force application and result calculation. Strength check of the planet carrier with all kinds of dynamic elements into consideration is completed by taking the calculated maximum forces as the load inputs in the force application process. The planet carrier designed through the co-simulation method is lighter and more material-saving than it is through the safety factor method.

Keywords: Co-simulation, planet carrier, Gear Increaser, dynamic simulation, finite element analysis.

1 Introduction

As the core equipment of wind turbine system, the gear increaser plays an important role of transporting driving force and increased motion which are input by the wind wheel to the generator. Because of the random characteristic of the driving wind force, the planet carrier structure of the gear increaser is always in the complex working condition in which many dynamic elements such as impact、friction、alternate loading、variable acceleration and so on exist. In the traditional design of planet carrier, a related safe safety factor is always chosen to offset the complex effects of the dynamic working elements using the safety coefficient method. How much the safe

Q. Zu, B. Hu, and A. Elçi (Eds.): ICPCA-SWS 2012, LNCS 7719, pp. 332–338, 2013.

factor is chosen greatly depends on the design experience of the engineer. Even if the most experienced engineers won't have the ability to get accurate safety factor which can make the part meet the strength requirement just right. Thus, the safety coefficient method is a sketchy and imprecise method which last leads a larger and heavier planet carrier, resulting in material wasting and a bad rotation characteristic.

To make an improvement on the deficiency of the safety coefficient method, the co-simulation technology of ADAMS-ANSYS which is more reliable and scientific is used in the design of the planet carrier of a megawatt wind turbine which is independent developed.

2 The Co-simulation Technology Based on ADAMS and ANSYS

Aimed at making full use of the advantage of different software, the co-simulation technology creates connections high-quality interfaces between two or more different software. In the co-simulation process of the megawatt wind turbine gear increaser transmission, the dynamic model is created in the ADAMS platform, and the output calculated data is set as the maximum forces that are applied on the planet carrier. Then, in the ANSYS platform, using the output maximum forces as the load input in the process of finite element analysis, the strengthen check is finished successfully.

As it is shown in the co-simulation method description, the strengthen-checking load comes from the dynamic simulation in ADAMS. The load forces have taken all the dynamic elements including acceleration、 inertia force and so on into consideration, evading the action of choosing safety factors by experience smartly. Thus more reasonable mechanical analysis is conducted. Figure1 presents the structure of the ADAMS and ANSYS co-simulation.

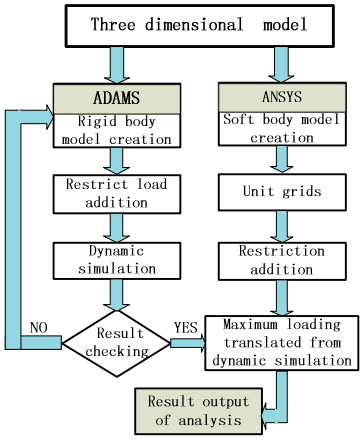

Fig. 1. Co-simulation flow diagram based on ADAMS and ANSYS

3 Dynamic Research of Megawatt Turbine Gear Increaser Planet Carrier Based on ADAMS

In the process of operating, the forces applied on the planet carrier are mostly translated from the planet gear in the circumference direction. As a result, the planet gears circumference force which is calculated in the ADAMS is applied on the planet carrier as the load with the action and reaction relation between the planet gear and planet carrier.

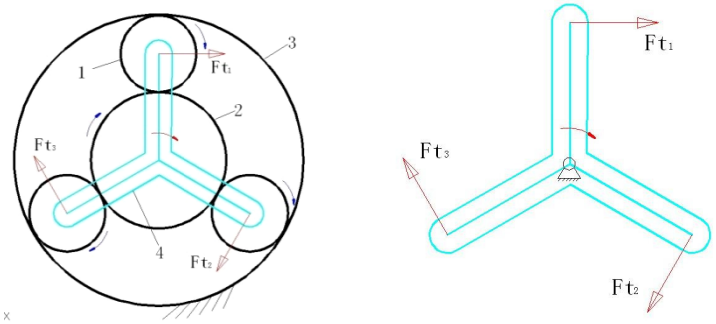

Fig. 2. The force analysis of planet carrier with three planet gears

3.1 The Theoretical Analysis of Planet Carrier

Floating shaft technology is adapted to assure the forces evenly distributed between the three planet gears which are placed as a central symmetry system. Figure2 shows the function of the planet carrier forced. A result can be conducted that the forces applied on planet carrier are zero with a torque equivalent calculated.

The torque applied on planet carrier can be derived from the power formula:

$$T_{center} = 9550\frac{P}{n}$$

$$T_{center} = 573000\text{N}\cdot\text{m}$$

The equivalent force at the axis of planet gears on the planet carrier in z-axis direction can be calculated:

$$F_t = \frac{1000T_{center}}{\text{r}\cdot\text{n}_\text{w}}$$

Thus the two equivalent forces applied on the two planet carriers are:

$$F_{t1}=252644N \quad F_{t2}=44954N$$

3.2 Dynamic Models Creation of the Gear Transmission Equipment

Real-time function is used to simulate working process of the gear transmission system which is simplified appropriately because of the complex working condition. A loading torque which is opposite in direction to the input axis is added at the output axis and the contact force between two meshing gears is calculated with the different gear parameter into consideration. The dynamic model created in the ADAMS platform is showed in the figure3.

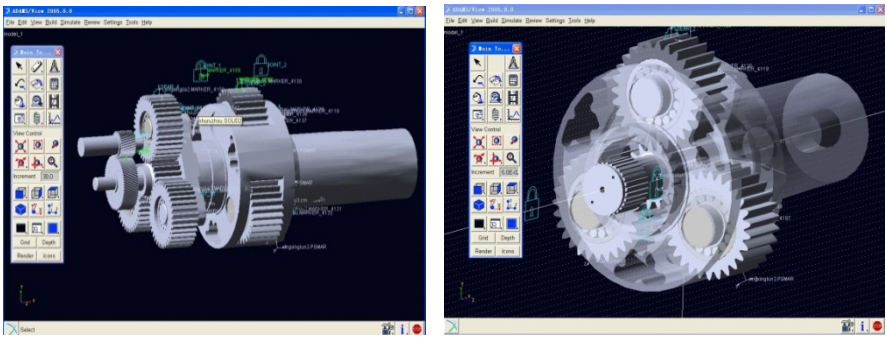

（a）Inner perspective of the equipment （b）The first gear stage dynamic mode

Fig. 3. The rigid dynamic model of the megawatt turbine gear transmission

3.3 Dynamic Simulation Result and Analysis of the Planet Carrier

In the equivalent force calculation conditions, the circumferential forces of the two stage planet carriers are conducted based on the dynamic simulation showed the simulated curves in figure4.

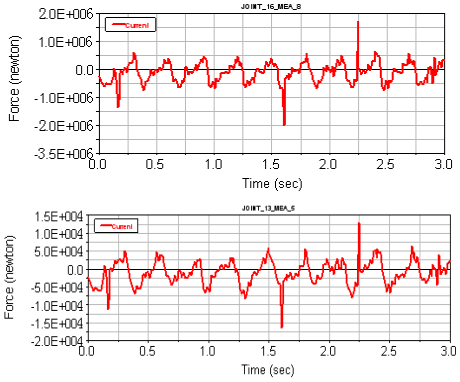

（a）The circumferential force time domain figure of the first stage planet carrier
（b）The circumferential force time domain figure of the first stage planet carrier

Fig. 4. The circumferential force curves of the planet carriers

Analysis is as follows after comparing the simulated result with the theoretical ones.

- 1）Analysis from the force direction aspect

As it is shown in figure4, the force curves is almost distributed around the zero axis symmetrically, waving in a proper positive and negative arrange regularly. It is the special working process of planet gear transmission in which planet gear rotates around the sun gear and meshes with the annular gear regularly that leading the planet gear meshing force direction changed in a circle degree regularly. On the other hand, positive and negative force value is related to the force direction. Therefore, the simulation results accord with the real working characteristic of the planet gear in the force direction, verifying the reliability of the simulation in the force direction aspect.

- 2）Analysis from the force value aspect

In the simulated curves, the forces wave by a stable cycle and amplitude after 0.2second which is the starting process time and the positive force is calculated ignoring the outliers.

The maximum circumferential force of the first stage planet carrier is 652479N, and also with the minimum value 0N and average value 253428.3N simulated. Comparing the theoretical value 252644N with the simulated average value 253428.3N, the simulated value comes near the theoretical one with a tiny relative error which can even be ignored, verifying the reliability of dynamic simulation. So is the second stage planet carrier simulation, shown in table 1 follows.

Table 1. Circumferential force compare of the theoretical and simulated average value

Circumferential force /N	Simulated value	Theoretical value	Relative error
The first stage planet carrier	253428.3	252644	0.003
The second stage planet carrier	45236.8	44954	0.006

4 Finite Element Analysis in Dynamic Environment of the Planet Carrier Structure

The maximum loading of the planet carrier structure is calculated in the dynamic simulation process in which the dynamic elements of velocity and acceleration are taken into consideration to simulate the maximum meshing force. Therefore, the problem that choosing the safety coefficient by experience of the traditional safety coefficient method is avoided skillfully, achieving the effect that planet carriers with minimum volume and mass is designed under the safe premise. Figure5 presents the two stages planet carriers finite element analysis results.

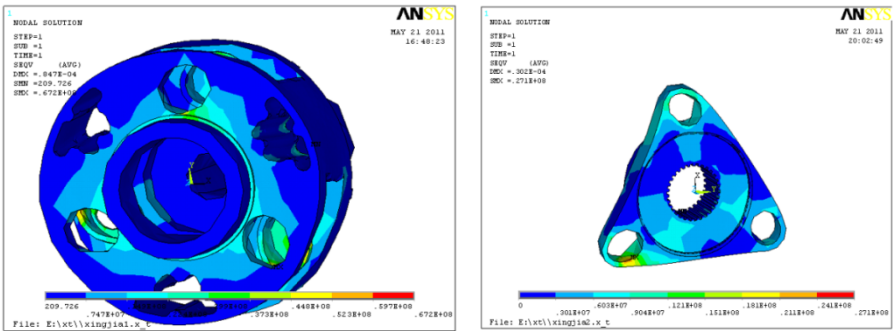

(a)The finite element analysis result of the first planet carriers
(b)The finite element analysis result of the second planet carriers

Fig. 5. The effective stress cloud charts of planet carriers

As is shown in the effective stress cloud charts of the two carriers, the maximum effective stress located around the area of the hinge hole with the maximum stress 67.2MPa and 27.1MPa value respectively which are both less than the allowable stress350MPa, satisfying the strength requirement in the uniform load working condition.

5 Conclusion

Based on the ADAMS platform, dynamic simulation is accomplished after the virtual prototype created including restriction、driving、loading addition. The simulated result is verified reliable with a tiny relative error between the simulated value theoretical value. In the highly reliable dynamic simulation basis, the strength check to the two stages of planet carriers is completed taking the dynamic simulated maximum force as the finite element analysis loading input, achieving the goal of mechanics property analysis to the planet carriers based on the co-simulation technology of ADAMS-ANSYS.

Acknowledgment. This research was supported by “the Fundamental Research Funds for the Central Universities”.

References

1. Jie, D., Ding, W., Wang, H., Li, T.: Dynamic simulation and analysis for high-speed punch guide based on ADAMS & ANSYS. Machinery Design & Manufacture 4, 182–185 (2012)
2. Sun, Z.: Dynamic simulation of gear reducer based on ADAMS. Technology and Economy in Areas of Communications (9), 77–79 (2007)
3. Ren, J., Guan, H., Liu, Z.: Simulation analysis of backhoe loader working device based on ADAMS & ANSYS. Design & Research 38, 1–3 (2011)

4. Zhu, J., Chen, Z., Shen, J.: The Application of Pro/E, Adams, Ansys in the Glass Gathering Robot Design. Mechanical Engineer 7, 2–5 (2008)
5. Ahn, K.-Y., Ryu, B.-J.: A modeling of impact dynamics and its application to impact force predicition. In: Proceedings of ACMD, pp. 448–453 (2004)
6. Wilcox, P.A., Burger, A.G., Hoare, P.: Adanced Distributed Simulation: a Review of Development and their Implication for Data Collection and Analysis. Simulation Prctice and Theory (8), 201–231 (2000)
7. Kahraman, K.: Planetary gear train dynamics. Journal of Me2 Chanical Design 116(9), 712–720 (1994)

PAPR Reduction for 802.16e by Clipping and Tone Reservation Based on Amplitude Scale Factor

Tianjiao Liu, Xu Li, Cheng Chen, Shulin Cui, and Ying Liu

State Key Lab. of Rail Traffic Control and Safety, Beijing Jiaotong University, Beijing, China
{11120128,xli,09120108,11120073,liuying}@bjtu.edu.cn

Abstract. IEEE 802.16e is a widely used standard for mobile broadband wireless access system and Orthogonal Frequency Division Multiplexing (OFDM) is employed in this system. So, it can perform well in anti-multipath fading and spectrum utilization. But there are also several critical problems, one of major drawbacks of this system is the high Peak-to-Average Power Ratio (PAPR) of the transmit signal. Thus the power amplifier in the transmitter requires a wide dynamic range or to be backed off, to prevent spectrum spreading issued from nonlinear distortion and BER rising issued from in-band distortion. But that will increase the system cost or lead to low power efficiency.

This paper firstly gives a brief of some important PAPR reduction techniques for multicarrier transmission, and then proposes a new PAPR scheme for 802.16e Wireless OFDM physical layer by using clipping and tone reservation (TR), and also considering the amplitude scale factor to reduce the computation cost and the system complexity. This new scheme has a very low out-of-band distortion, requires no side information and gains better PAPR performance by sacrificing fewer sub-carriers. At last, the performance of this new technique on PAPR reduction, BER, and spectrum efficiency has been analyzed through simulation derived from MATLAB. Furthermore, the simulation statistics has been compared with other related techniques.

Keywords: 802.16e, OFDM, PAPR, clipping, TR, amplitude scale factor.

1 Introduction

Performing well in anti-multipath fading and spectrum utilization, Orthogonal Frequency Division Multiplexing (OFDM) has become a kind of technology widely used in various high speed wireless communication systems [1-3], including IEEE 802.16e system. Yet there are still several critical problems waiting to be solved. One major drawback is the high peak-to-average power ratio (PAPR) of the transmit signal. Thus the power amplifier in the transmitter requires a wide dynamic range or to be backed off, to prevent spectrum spreading issued from nonlinear distortion and BER rising issued from in-band distortion. But that will increase the system cost or lead to low power efficiency.

In order to address the PAPR problem, a number of corresponding techniques have been proposed [4, 5]. These techniques include clipping [6, 7], clipping and filtering

Q. Zu, B. Hu, and A. Elçi (Eds.): ICPCA-SWS 2012, LNCS 7719, pp. 339–349, 2013.

[8, 9], coding [10, 11], tone reservation (TR) [12, 13], active constellation extension (ACE) [14], selected mapping (SLM) [15], using pilot tones and unused carriers [16], and so on. The simplest approach is to clip the high amplitude peaks, but it will cause both in-band and out-of-band distortion [6]. Clipping and filtering won't cause out-of-band distortion but can lead to serious degradation in BER [8]. Coding can also effectively reduce the PAPR, but it is limited to multicarrier systems with a small number of subcarriers and requires exhaustive search for a good code [10, 11].

TR is another efficient technique to reduce the PAPR of OFDM signals by adding a data-block-dependent time domain signal to the original multicarrier signal to reduce its peaks. But these causes a reduction in data through-put for a set of subcarriers must be reserved [12].

For IEEE 802.16e system, TR method can be utilized to reduce PAPR. And the researcher in [13] has analyzed the lower bound in worst-case of TR for WiMAX and proposed a calculation method to decide whether the transmitter should use TR. As 802.16e system has more subcarriers, finding out an effective method which not only has good PAPR performance but also can reduce the computation cost for searching the best subset of subcarriers is exigent.

In this paper a new PAPR reduction technique for 802.16e Wireless OFDM physical layer is proposed through combining Clipping and TR. This scheme has a very low out-of-band distortion, requires no side information and gains better PAPR performance by sacrificing fewer sub-carriers. Moreover, it makes the system only need iterative processing once by using the amplitude scale factor algorithm which greatly reduces the computation cost. Therefore, this technique is more applicable to 802.16e system.

2 System Overview

For an OFDM system with N sub-carriers, the baseband signal in discrete form can be written as:

$$x(t) = \frac{1}{\sqrt{N}} \sum_{n=0}^{N-1} X_n e^{j2\pi f_n t} \qquad 1 \le t \le NT \tag{1}$$

Where Xn is the symbol carried by the nth sub-carrier, fn is the frequency of the nth sub-carrier, and T is the OFDM symbol duration. The PAPR of the transmitted signal can be expressed as:

$$PAPR = 10\log_{10} \frac{\max\left|x(t)\right|^2}{E\left[\left|x(t)\right|^2\right]} \tag{2}$$

Where denotes the expectation operation. In the OFDM system, not all the sub-carriers are used to transmit data information; a number of sub-carriers are set to "0" to prevent out-of-band distortions. In EEE802.16d system, there are 256 sub-carriers,

in which two hundred are used to transmit data, eight are used to transmit pilot information, one is used as a DC sub-carrier and the remaining 55 sub-carriers are used to protect the band. Because the remaining 55 sub-carriers are not used in the transmission process and don't affect the orthogonality between the data sub-carriers, they can be used to reduce the PAPR. PAPR Reduction Technique for OFDM Using Pilot Tones and Unused Carriers [16] not only use the free sub-carriers, but also use the pilots' phase information. Comparing with this method, the technique proposed in this paper does not need to use the pilots but can achieve the similar PAPR performance. Then the pilots can be used in channel estimation [17].

3 New PAPR Reduction Techniques

In this paper a new PAPR reduction technique for 802.16e Wireless OFDM physical layer is proposed through using Clipping and TR, and also considering the amplitude scale factor. This technique has the similar basic idea with the traditional TR method. The idea is that the best signal C with special structure in frequency domain is found to reduce the PAPR of OFDM systems. In the traditional TR technique, the signal C with special structure in frequency domain is selected by traversing search. The sub-carriers with non-zero value of the special signal in frequency domain are defined as the reducing peak carriers whose amount is L. In theory, the amplitude and phase of the reducing peak carriers are advisable of any value. But this will make the system's calculation complexity very high. Therefore, in order to reduce the calculation complexity, the reducing peak carriers are usually restricted to a specific area. That is, the amplitude and phase of each reducing peak carrier have K kinds (including zero) of possible values. By searching combinations of amplitude and phase of reducing peak carriers, select an optimal combination which makes the PAPR smallest. Take QAM as an example, the specific areais generally selected.

The block diagram of the traditional TR technique is shown in Figure 1:

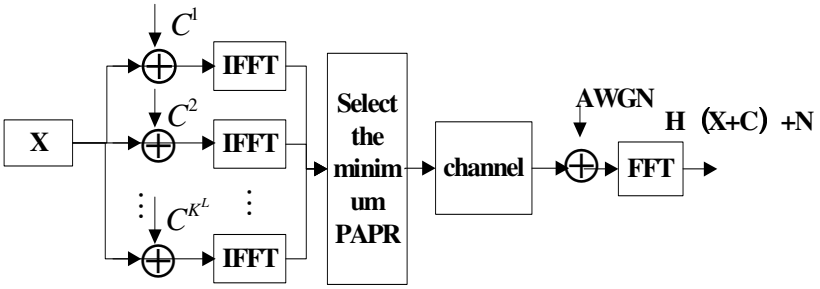

Fig. 1. The block diagram of the traditional TR technique

Define as the location sequence of all sub-carriers in OFDM system, as the location sequence of the reducing peak carriers, R as the complement collection of. That is. The signal X and C in frequency domain satisfy the principle: at the sub-carriers that

the values of signal C are zero, the values of original signal X are non-zero; at the sub-carriers that the values of signal C are non-zero, the values of original signal X are zero. That is:

$$X_k = \begin{cases} X_k & k \in R \\ 0 & k \in R^c \end{cases} \quad C_k = \begin{cases} 0 & k \in R \\ C_k & k \in R^c \end{cases} \tag{3}$$

The Tone Reservation Ratio (TRR) is defined as: TRR=L/N.

Where L is the amount of reducing peak carriers and N is the amount of all carriers. In order to reduce PAPR of the OFDM system more effectively, the TRR is need to be increased, that is, increase the amount of reducing peak carriers L. This means the amount of sub-carriers used to transmit useful information is reduced. It also means the spectral efficiency and the energy for the useful information transmission is reduced. In addition, times of IFFT operations need to be done in the traditional TR technique. And with the increase of the amount of sub-carriers and the reducing peak carriers, the times of IFFT operations needs to be increased observably. So the complexity of TR technique will be very high.

In this paper, aiming at alleviating the deficiency of the TR technique, the advantages of clipping and traditional TR algorithm are combined and the amplitude scale factor is used to find the optimal signal C in frequency domain. Finally a clipping-TR technique based on amplitude scale factor is proposed. In this technique, fewer sub-carriers (5~10 in 256) are sacrificed as reducing peak carriers so that the spectrum utilization of the system can be significantly improved. Besides, using the amplitude scale factor algorithm makes the technique only need iterative processing once rather than times. Therefore the computation cost of this technique is low.

The block diagram of this technique is shown in figure 2:

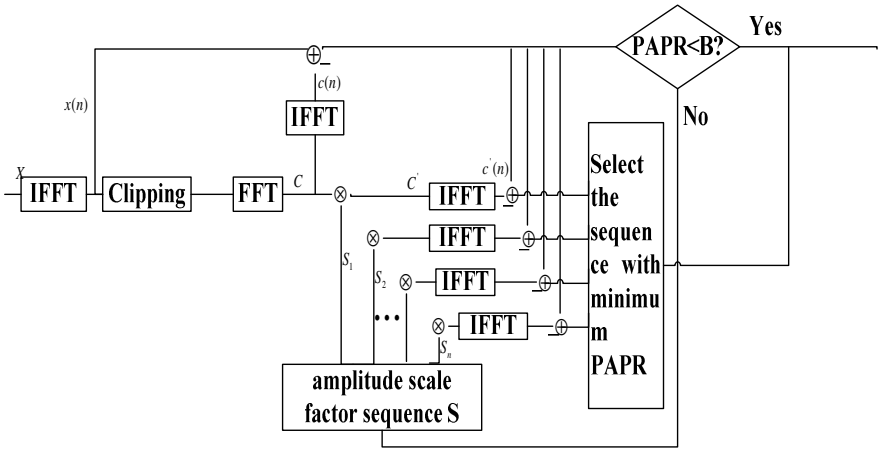

Fig. 2. The block diagram of the proposed technique

1. According to the parameters of OFDM system, the amount of reserved sub-carriers "L" and their location is set, the PAPR threshold "B" and the amplitude scale factor "S". In theory, the more sub-carriers are reserved, the more information of ideal eliminating peak sequence can be retained, and the better the effect of PAPR reduction will be. However, because the reserved sub-carriers don't carry useful information, the more sub-carriers reserved, the lower the system's spectral efficiency will be. The technique proposed in this paper only need 5~10 (2%~4%) reserved sub-carriers. When receiver received the data, it can discard the data at the reserved sub-carriers directly.
2. Get the eliminating peak signal in time-domain. In order to reduce system complexity further, IFFT operation to the data sequence *X* and eliminating peak sequences *C* are carry out respectively and the signals $x(n)$ and $c(n)$ are obtained in time-domain. Thus, the data sequence only needs IFFT operation once, so the computation cost has reduced times. In order to obtain eliminating peak sequences C, clipping to $x(n)$ through comparing with thresholds need to be carried out. Then the signal $x^{'}(n)$ with ideal PAPR performance will be obtained after clipping.

$$x^{'}(n)=\begin{cases}|x|e^{j\phi}, |x|\le A\\ Ae^{j\phi}, |x|>A\end{cases} \tag{4}$$

So the ideal eliminating peak signal $d(n)$ in time-domain can be obtained by the follows:

$$d(n)=x(n)-c(n) \tag{5}$$

Through carrying out the FFT transform to $d(n)$, the ideal eliminating peak sequences D will be obtained in frequency domain. Then the eliminating peak sequences C will also be obtained in frequency domain through retaining the values of L reserved sub-carriers and assigning "0" to the other N-L sub-carriers. And then, after IFFT transform to C, the eliminating peak signal $c(n)$ is got in time-domain, and $z(n)$ will be achieved as follows through subtracting $c(n)$ from $x(n)$:

$$z(n)=x(n)-c(n)=IFFT(X)-IFFT(C) \tag{6}$$

Calculate the PAPR value of $z(n)$.If the value is less than the threshold B, $z(n)$ will be transmitted as the final signal. If the value is greater than the threshold B, step 3 will be carried out. That is, the amplitude scale factor will be used to find the eliminating peak sequences $c(n)$ which can make the PAPR of $z(n)$ minimum.

3. First of all, a collection of amplitude scale factors is generated which conclude n amplitude scale factor sequences *S*. *S* is defined as:

$$S_i = [s_1, s_2, ..., s_r], r = 1, 2, ..., N, i = 1, 2, ..., n$$
$$s_r = \begin{cases} f, r \in R^c \\ 0, r \in R \end{cases} \quad (7)$$

Where f is the factor generated randomly in the range of 5~45.

Multiplications cross is carried out to eliminating peak sequences *C* and amplitude scale factor sequences *S*, n new eliminating peak sequences will be obtained. IFFT is done to these *n* sequences, and n eliminating peak signals $c^{'}(n)$ will be obtained in time-domain. And then, *n* sequences $z^{'}(n)$ will be obtained through subtracting $c^{'}(n)$ from $x(n)$. Then the PAPR value of $z^{'}(n)$ is calculated and the sequence $z^{'}(n)$ with the smallest PAPR value is selected as the final transmitted signal.

4 Performance Analyses

In order to verify the PAPR performance of the proposed technique, this paper has done large numbers of simulations and compared with the PAPR reduction technique for 802.16e Wireless OFDM physical layer using pilot tones and unused carriers [16] and traditional TR technique [12]. The results are shown as Fig. 3 for an IEEE802.16d system employing 6 free sub-carriers and 6 amplitude scale factor sequences for PAPR reduction.

It's evident that the new technique can significantly improve the PAPR performance of OFDM systems. When the PAPR value is greater than 8dB, the original signal's Complementary Cumulative Distribution Function (CCDF) value is about 70%. While the technique proposed in this paper is employed, it's only 0.5%. That means this technique can be very effective in reducing PAPR of OFDM systems.

Fig. 4 shows the results of the comparison of the proposed technique with the PAPR reduction technique using pilot tones and unused carriers and the traditional TR technique. The traditional TR uses 16 free sub-carriers, the technique using pilot tones and unused carriers uses 5 free sub-carriers and the proposed technique employs 6 free sub-carriers, 6 amplitude scale factor sequences. As shown in Fig. 4, when the CCDF is 10^{-3}, the traditional TR can reduce the PAPR values about 1dB, the technique using pilot tones and unused carriers can reduce the PAPR values about 2dB, and the new technique can reduce the PAPR value about 2.3dB. We can easily see that the last one has a better PAPR performance.

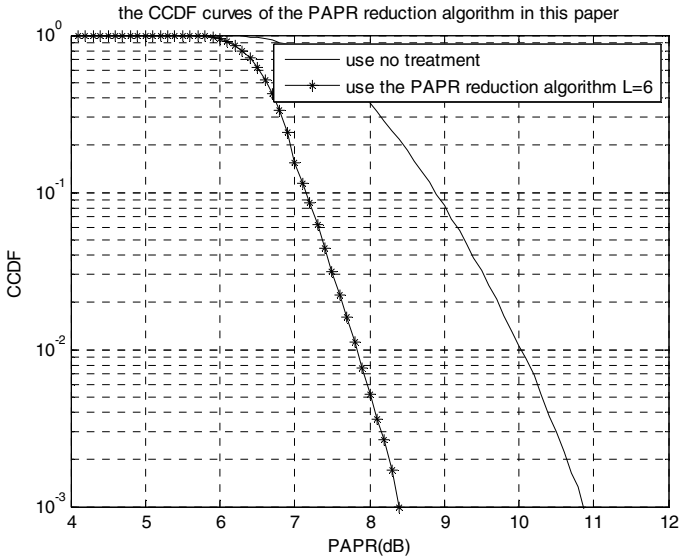

Fig. 3. The CCDF curves of the proposed technique

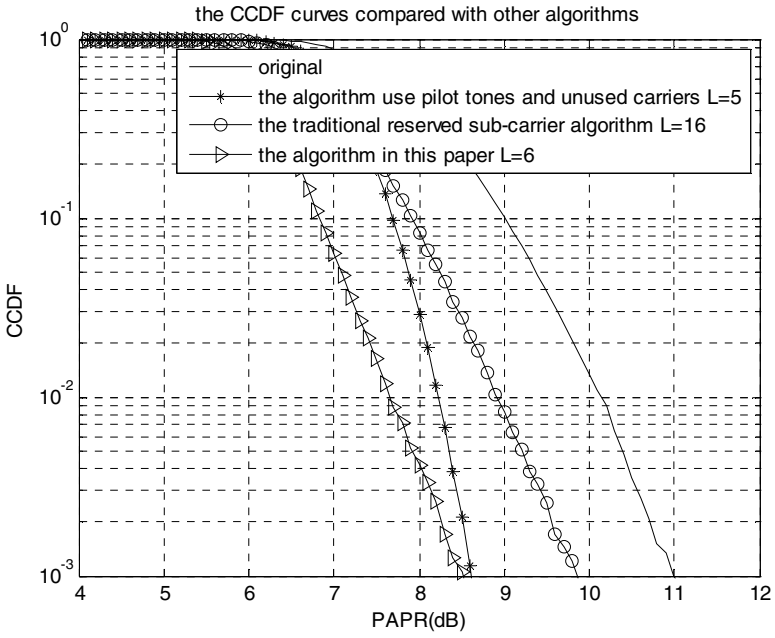

Fig. 4. The CCDF curves compared with other algorithms

Fig. 5 shows the comparison of the proposed technique with the technique using pilot tones and unused carriers on BER performance. It can be easily found that the technique proposed in this paper has a similar BER performance with the other one. The BER is about 10^{-5}~10^{-6} when SNR is 10dB, which can satisfy the BER requirement of the 802.16e system.

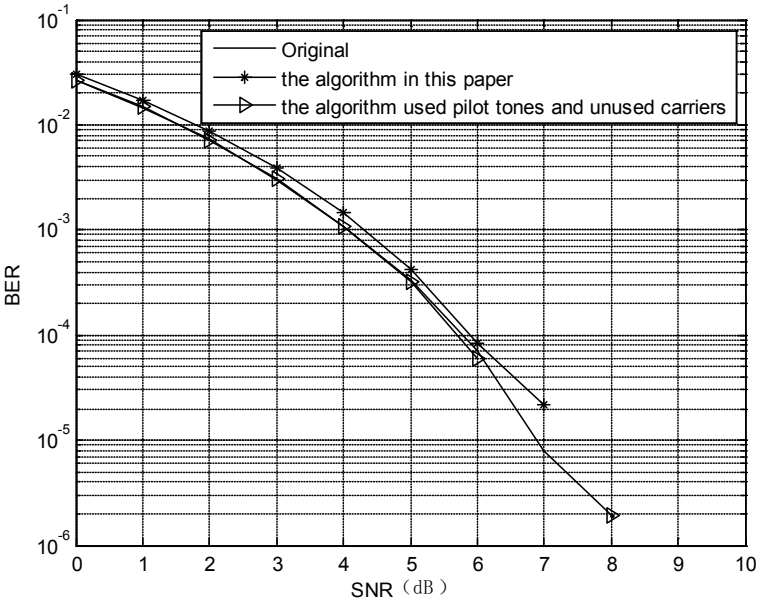

Fig. 5. The BER curves of the new technique and the one using pilot tones and unused carriers

The new technique can greatly reduce the system's computation complexity compared with other popular PAPR reduction method applicable to 802.16e. The technique using pilot tones and unused carriers has low computation complexity and has been verified in the 802.16e system. But it still needs to use three iterations at least. In order to get better PAPR performance, it will need more iteration. The proposed technique only needs iteration once due to using the amplitude scale factor algorithm. Moreover, it can achieve better PAPR performance, and meet the BER requirement of the 802.16e system at the same time. So it's more suitable for the 802.16e system.

In addition to above, this new technique an also greatly improve the spectral efficiency compared with the traditional TR technique. Fig. 6 is the frequency spectrums of OFDM symbol under the case that use no free sub-carriers, Fig. 7 is the frequency spectrums of OFDM symbol under the case that use the TR technique and Fig. 8 is the frequency spectrums of OFDM symbol under the case that use the new technique. In Fig. 6, OFDM symbols occupy spectrum width about 3.2MHz, in Fig. 7, OFDM symbols occupy spectrum width about 4.5MHz and in Fig. 8, OFDM symbols occupy spectrum width about 4MHz. From the result it can be seen the great improvement on the spectral efficiency.

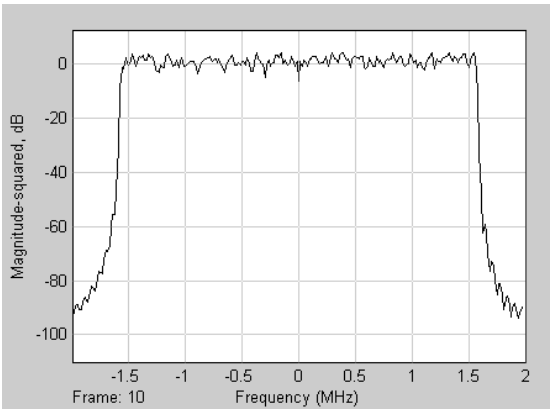

Fig. 6. The OFDM symbol frequency spectrums of not using the free sub-carrier

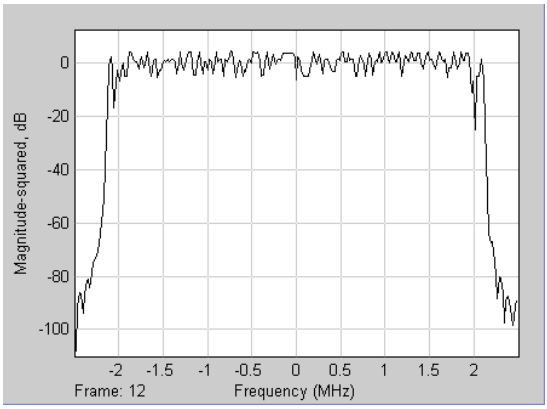

Fig. 7. The OFDM symbol frequency spectrums of using the traditional reserved sub-carriers algorithm

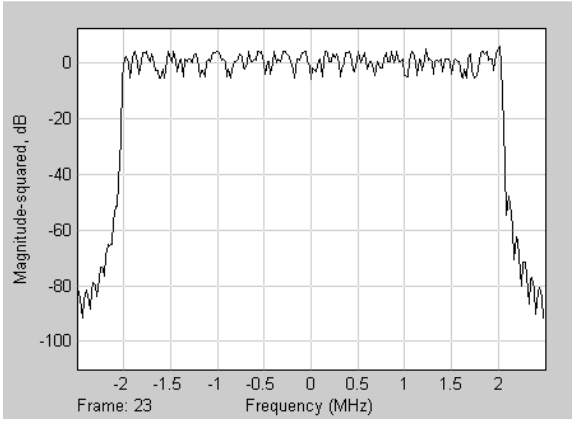

Fig. 8. The OFDM symbol frequency spectrums of using the technique in this paper

5 Conclusions

Considering to the deficiencies about complexity of the PAPR reduction technique proposed at present for 802.16e OFDM physical layer, we propose a new PAPR reduction technique through using Clipping and TR based on the amplitude scale factor in this paper, which combines the advantages of clipping and the traditional TR method and uses the amplitude scale factor algorithm. Through simulation, we may conclude that this technique not only has a good PAPR performance, but also greatly reduces the system complexity and improves the spectrum utilization. Furthermore, it can meet the BER requirements of 802.16e. Therefore, this new technique proposed in this paper is more applicable to 802.16e.

Acknowledgment. The authors would like to express their many thanks to the supports from the Independent Research Topic of State Key Lab. of Rail Traffic Control and Safety under grantNo.RCS2009ZT005, the Program for Changjiang Scholars and Innovative Research Team in University under Grant No.IRT0949, the NSFC (National Natural Science Foundation of China) No. 61172130.

References

1. Nee, R.V., Prasad, R.: OFDM Wireless Multimedia Communications. Artech House (2000)
2. Cimini Jr., L.J.: Analysis and Simulation of a Digital Mobile Channel using Orthogonal Frequency Division Multiplexing. IEEE Trans. Commun. 33(7), 665–675 (1985)
3. Chang, R.W., Gibby, R.A.: A Theoretical Study of Performance of an Orthogonal Multiplexing Data Transmission Scheme. IEEE Trans. Commun. 16(4), 529–540 (1968)
4. Han, S.H., Lee, J.H.: An overview of peak-to average power ratio reduction techniques for multicarrier transmission. IEEE Wireless Communications 12(2), 56–65 (2005)
5. Jiang, T., Wu, Y.: An Overview: Peak-to-Average Power Ratio Reduction Techniques for OFDM Signals. IEEE Transactions on Broadcasting 54(2), 257–268 (2008)
6. O'Neill, R., Lopes, L.B.: Envelope Variations and Spectral Splatter in Clipped Multicarrier Signals. In: Proc. IEEE PIMRC 1995, Toronto, Canada, pp. 71–75 (September 1995)
7. Ochiai, H., Imai, H.: Performance of the deliberate clipping with adaptive symbol selection for strictly band-limited OFDM systems. IEEE Journal on Selected Areas in Communications 18(11), 2270–2277 (2000)
8. Armstrong, J.: Peak-to-Average Power Reduction for OFDM by Repeated Clipping and Frequency Domain Filtering. Elect. Lett. 38(8), 246–247 (2002)
9. Li, X., Cimini Jr., L.J.: Effect of Clipping and Filtering on the Performance of OFDM. IEEE Commun. Lett. 2(5), 131–133 (1998)
10. Jones, A.E., Wilkinson, T.A., Barton, S.K.: Block Coding Scheme for Reduction of Peak to Mean Envelope Power Ratio of Multicarrier Transmission Scheme. Elect. Lett. 30(22), 2098–2099 (1994)
11. Jones, A.E., Wilkinson, T.A.: Combined Coding for Error Control and Increased Robustness to System Nonlinearities in OFDM. In: Proc. IEEE VTC 1996, Atlanta, GA, pp. 904–908 (April-May 1996)
12. Tellado, J.: Peak to Average Power Reduction for Multicarrier Modulation. Ph.D. dissertation, Stanford Univ. (2000)

13. Hu, S., Wu, G., Guan, Y.L., Law, C.L., Li, S.: Analysis of tone reservation method for WiMAX system. In: Intl. Symp. on Commun. and Inform. Tech., ISCIT 2006, September 18- October 20, pp. 498–502 (2006)
14. Krongold, B.S., Jones, D.L.: PAR Reduction in OFDM via Active Constellation Extension. IEEE Trans. Broadcast. 49(3), 258–268 (2003)
15. Bäuml, R.W., Fisher, R.F.H., Huber, J.B.: Reducing the Peak-to-Average Power Ratio of Multicarrier Modulation by Selected Mapping. Elect. Lett. 32(22), 2056–2057 (1996)
16. Devlin, C.A., Zhu, A., Brazil, T.J.: Peak to Average Power Ratio Reduction Technique for OFDM Using Pilot Tones and Unused Carriers. In: RWS 2008, pp. 33–36 (2008)
17. Coleri, S., Ergen, M., Puri, A., Bahai, A.: Channel Estimation Techniques Based on Pilot Arrangement in OFDM Systems. IEEE Transactions on Broadcasting 48(3), 223–229 (2002)

A DCaaS Model of DNA Computing for Solving a Class of Nonlinear Problems

Xiyu Liu, Laisheng Xiang, and Xiaolin Yu

Shandong Normal University, Jinan Shandong 250014, China
{sdxyliu,xLs3366}@163.com, yuxL1212@126.com

Abstract. A class of new cloud computing model DCaaS is proposed. This model combines traditional DNA computing with SaaS model. The main advantage of DCaaS model is to separate biological experiments with DNA computing, and obtain biological operations as a service via DNA programs. As application frame, approximate solution of a class of nonlinear problems is presented.

Keywords: DNA computing, cloud computing, nonlinear problems.

1 Introduction

Deoxyribonucleic acid computing, or DNA computing in short, has become a new technique in soft computing and has been attracted wide focus recently. Basically DNA computing is inspired by the similarity between the way DNA stores and manipulates information with traditional Turing machine. The main advantage of DNA computing is, among others, its super parallel ability. Since the original work of Adleman's experiment (Adleman [1]), and its early generalizations of Lipton [9] to the satisfiability problem, DNA computing has been applied to many computationally hard problems especially combinatorially complex problems such as factorization, graph theory, control and has been a new and important technique in computational intelligence, see [11][13][7][8][14][4][5][12] and the references therein.

Adelman's original work includes a basic computing model. Later generalizations include the sticker model, the splicing model, and the insertion deletion model, etc [14]. Among all these models, biological experiments are key factors for an algorithm to implement. These experiments include preparation of strands, or DNA soups, various enzymes, and biology operations, such as merging, amplifying, and so on. All these experiments are hard to implement and they have much similarity for different DNA algorithms. Therefore, to propose a general solution to solve this problem is useful.

The purpose of this paper is to propose a DCaaS model for DNA computing which works in a similar way as SaaS model. Our main focus is to separate experiment from DNA computing and put these experiments into the cloud. To our knowledge, there is seldom research which join the idea of cloud computing with DNA computing. Clearly this idea is new and will have wide potential applications.

Q. Zu, B. Hu, and A. Elçi (Eds.): ICPCA-SWS 2012, LNCS 7719, pp. 350–363, 2013.

Finally, we present an application framework in boundary value problems. Boundary value problems are important area nonlinear analysis. Typical theoretic approach to boundary value problems are topological methods such as indices and variational methods, together with cone methods. Although there are extensive researches in this area, the computing models are rarely found in the literature [3]. Hence our research provide a new methodology to this classical problem.

2 The DNA Computational Model

2.1 The Computational Model

In DNA, the nucleotides are the purines adenine (A), guanine (G), the pyrimidines thymine (T) and cytosine (C). Single-stranded DNA molecules are formed by connecting the nucleotides together with phosphodiester bonds. The single strands of DNA can form a double-stranded molecule when the nucleotides hydrogen bond to their Watson-Crick complements, $\overline{A} = T$ and $\overline{G} = C$. Each strand has a $5'-$ end and a $3'-$ end. The pairs (A, T) and (G, C) are called complementary base pairs. There is another structure of DNA molecules called the hairpin structure. This happens in a long single strand DNA where part of its nucleotides hydrogen bond to itself by the Watson-Crick rule. Then the DNA forms a partial double strand in hairpin formation [7].

The cutting of certain strands of a DNA molecule is performed by the so-called restriction enzymes. These enzymes catalyze the cutting operations at very specific DNA base sequences which are called recognition sites. Recognition sites are typically 4-8 DNA base pairs long. A restriction enzyme cuts DNA into pieces with sticky ends. On the other hand, sticky ends will match and attach to other sticky ends of any other DNA that has been cut with the same enzyme. DNA ligase joins the matching sticky ends of the DNA pieces from different sources that have been cut by the same restriction enzyme.

The basic operations performed by enzymes are denaturing, replicating, merging, detecting etc. Some of these operations are similar to simulated genetic operations. Biologically, the basic DNA operations available on DNA are mainly:

- Merge $m(N_1, N_2) \triangleq N_1 \cup N_2 = N$.
- Amplify $duplicate(N_1) = N$.
- $Detect(N)$.
- Separate or extract. Given a word w consisting of strings from $\Sigma = \{A, G, C, T\}$ and a tube N, generate two tubes $+(N, w)$ and $-(N, w)$ which contains and does not contains the string w: $N \leftarrow +(N, w), N \leftarrow -(N, w)$.
- Length separate. Given a tube N and an integer n, generate a tube containing stands with length less or equal to n: $N \leftarrow (N, \leq n)$.
- Position separate. Given a tube and word generate a tube with stands beginning (ending) with the word: $N \leftarrow B(N_1, w), N \leftarrow E(N_1, w)$.

Tom Head [5] proposed a splicing model $S=(A,L,B,C)$ consisting of a finite alphabet A, a finite set I of initial strings in A^* (language over A), and finite sets B and C of triples (c,x,d) with $c,d,x\in A^*$. Each such triple in B or C is called a pattern. For each such triple the string cxd is called a site and the string x is called a crossing. Patterns in B are called left patterns and patterns in C are called right patterns. The language $L=L(S)$ generated by S consists of the strings in I and all strings that can be obtained by adjoining to $Lucxfq$ and $pexdv$ whenever $ucsdv$ and $pexfq$ are in L and (c,x,d) and (e,x,f) are patterns of the same hand. A language L is a splicing language if there exists a splicing system S for which $L=L(S)$.

The $k-$armed model is based on some more complicated molecule structures which have three-dimensional DNA architecture ([6]). Although the armed molecules are relatively less well known, they have been found existed in real molecules and researches on the construction and stability have begun.

2.2 Evolutionary DNA Program

Since the original work of Adelman and Lipton, nearly all the current DNA computing strategies are based on enumerating all candidate solutions, and then using some selection process to choose the correct DNA. This technique requires that the size of the initial data pool increases exponentially with the number of variables in the calculation. In this subsection, we will propose an evolutionary splicing model based on the work of Tom Head [5]. In order to simplify the symbols, we will use the lower case letters a; c; g; t to represent the four deoxyribonucleotides that incorporate adenine, cytosine, guanine and thymine respectively. Then the alphabet is defined by

$$\begin{cases}\Sigma=\{A,C,G,T\}\\ A=\begin{bmatrix}a\\ t\end{bmatrix},T=\begin{bmatrix}t\\ a\end{bmatrix},G=\begin{bmatrix}g\\ c\end{bmatrix},C=\begin{bmatrix}c\\ g\end{bmatrix}\end{cases} \tag{1}$$

Let Σ^* be the set of all finite strings consisting of symbols from the alphabet. Then a member of Σ^* is a double stranded DNA which will be denoted by lower case Greek letters later. The natural involution operator on Σ^* is defined by

$$\begin{cases}f(A)=T, & f(G)=C\\ f(f(\alpha))=\alpha, & f(\alpha\beta)=f(\beta)f(\alpha)\end{cases} \tag{2}$$

A subset $P\subset\Sigma^*$ is called a population. We now define evolutionary operators on the population, that is, crossover, mutation, and selection. We use the symbol S_{ez} to represent a restriction enzyme in the form of $\pm(\alpha,\beta,\gamma)$ where α and γ are the cutting sites and β is the cleavage sequence. The symbol $\pm$ indicates that the left cutting is at the top strand (5'–) end, or the bottom strand (3'–) end. In Table 1 there are some examples of restriction enzymes. The set of all possible restriction enzymes are denoted by $S=\{S_{ez}\}$.

First we consider crossover performed by a restriction enzyme. According to the number of crossover points, there are one-point crossover and multiple point crossovers. For one-point crossover, let $\alpha, \beta \in P$ be two strands. Each of them is cut into two strands with sticky ends by certain restriction enzymes, that is, $\alpha = \alpha_L \oplus \alpha_R, \beta = \beta_L \oplus \beta_R$. Suppose the sticky ends of α_L, β_R are matching, then the crossover operation will result two new strands $\alpha_L \oplus \beta_R$ and $\beta_L \oplus \alpha_R$. Since in fact multiple crossovers can be treated as combinations of successive one-point crossovers, we only use one-point crossover in the sequel.

Table 1. Examples of restriction enzymes

Enzyme	**Representation**	**Cutting example**
*Eco*RI	+(*G, AATT, C*)	*xxxxxg* *aattcxxxxx* *xxxxxcttaa* *gxxxxx*
*Taq*I	+(*T, CG, A*)	*xxxxxt* *ggaxxxxx* *xxxxxagc* *txxxxx*
*Sci*NI	+(*G, CG, C*)	*xxxxxg* *cgcxxxxx* *xxxxxcgc* *gxxxxx*
*Hha*I	-(*G, CG, C*)	*xxxxxgcg* *cxxxxx* *xxxxxc* *gcgxxxxx*

Mutation will randomly select one or several successive bases and replace them with other bases. For example, we can choose a base A and change it into G. The operation of mutation is carried out by insertion and deletion technique. First we can locate the DNA subsequence and delete sequence by melting and annealing. Then we can insert a new sequence by PCR and ligation operations.

From the above discussion, we propose the DNA evolution procedure as in Table 2. Notice that we are not using full amount of DNA which contains all the possibilities corresponding to the problem solution. Rather we are using a relatively small amount of DNA sequences and evolve them to get the desired solution.

Table 2. DNA Evolution Procedure

1. Generate suitable amount of DNA sequences and place them in a test tube.
2. Generate enough DNA complements and mutation sequences as desired. Prepare desired enzymes.
3. Perform crossover and mutation operations.
4. Perform selection and fitness computation.
5. Eliminate a number of worst DNAs and substitute with new DNA sequences.
6. Check best one by DNA length to determine if it is the desired solution.
7. Loop.
8. The final obtained DNA sequence shows the solution.

3 DNA Computing as a Service: A DCaaS Model

One of the main problems and difficulties of DNA computing is biology experiment. This is partly due to the inadequate of large expensive of biological devices. On the other hand, DNA experiments have intensive similarities in many experiments. Hence we propose a service model for DNA experiments which will solve this problem in some extents. We call this service model the DNA computing model, or the DCaaS model.

Traditional SaaS model changes the rule of a software vendor, who should be equally concerned with operating and managing the environment that supports all their customers. By extending this idea to DNA computing we have the DCaaS model which use similar concepts. The structure of a DCaaS model is shown in Fig 1. There are five layers in this model. They are the user layer, the application layer, the DNA engine layer, and the DNA source layer.

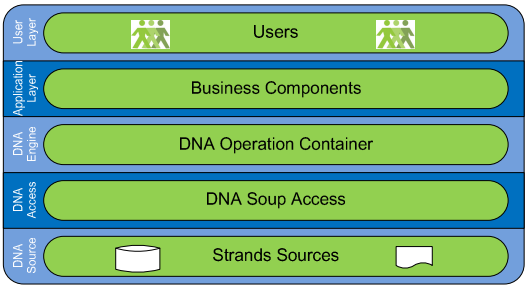

Fig. 1. A DCaaS model

— The User Layer
The user layer consists of thin client applications, typically the Web browser. The main functionality of this layer is to handle input from the user and output from the server where most of the processing and the business logic resided.

— The Application Layer
DCaaS applications supplied by bioengineering vendors keep in contact with each other in this layer by service description and service integration, and so on. This layer provides web service applications by DCaaS platform. The application layer also manipulates the issues of administration and monitoring as components that operate across layers.

— The DNA Engine Layer
In this layer, various DNA operations are performed such as merging, amplifying, detecting, separating, and so on. Usually this layer will be located physically at the same place with the DNA source.

— The DNA Access Layer
The DNA access layer handled the processing of all requests for stands. According to the requirements of DNA engine, the DNA access engine will spread tasks into small units. Each unit will perform operations in a source.

— The DNA Source Layer

The DNA source storage layer was used for the physical storage of strands. In layer, PCR equipments are necessary for generating new strands. The DNA source may be stored in multiple storage.

4 DCaaS Model Implementation

In this section we will present an implementation for the DCaaS model. The execution of a DNA program in the DCaaS model is like the execution of scripts. The user poses DNA program using data structure as shown below to the server. The server executes the program by constructing tubes and perform operations.

4.1 Data Structure

The basic data type in DCaaS model is object. Objects of same type is described in classes. A class contains attributes and operations which is derived class of four base classes as CAdleman, CSticker, CInsertionDeletion, CSplicing. These four DNA computing models are basic models as shown in Paun [11]. A basic data class is CStrand which contains two strings, the single strands and double strands. Elements of single strands are {A,G,T,C}. Elements of double strands are pairs $\alpha, \beta, \hat{\alpha}, \hat{\beta}, a, g, t, c, \hat{a}, \hat{g}, \hat{t}, \hat{c}$ as follows (including incomplete double strings)

$$\alpha = \begin{bmatrix} A \\ T \end{bmatrix}, \beta = \begin{bmatrix} G \\ C \end{bmatrix}, \hat{\alpha} = \begin{bmatrix} T \\ A \end{bmatrix}, \hat{\beta} = \begin{bmatrix} C \\ G \end{bmatrix} \tag{3}$$

$$a = \begin{bmatrix} A \\ \end{bmatrix}, g = \begin{bmatrix} G \\ \end{bmatrix}, g = \begin{bmatrix} T \\ \end{bmatrix}, c = \begin{bmatrix} C \\ \end{bmatrix} \tag{4}$$

$$\hat{a} = \begin{bmatrix} A \\ \end{bmatrix}, \hat{g} = \begin{bmatrix} G \\ \end{bmatrix}, \hat{t} = \begin{bmatrix} T \\ \end{bmatrix}, \hat{c} = \begin{bmatrix} C \\ \end{bmatrix} \tag{5}$$

Basic operations are defined in base classes. For example, there are eight functions in CSticker as shown below with their function declarations and descriptions.

- The merge function returns an reference of an object T where T contains the data of T1 and T2 for two objects T1 and T2.

```
CSticker& CSticker::merge(CSticker& T1, CSticker& T2)
```

- The amplify function copies the object T to T1 and T2.

```
void CSticker::amplify(CSticker& T, CSticker T1, CSticker
T2)
```

- The detect function returns true if T contains the word *w*. Otherwise it returns false.

```
bool CSticker::detect(CSticker& T, CStrand& w)
```

- The separate function generates two new objects T1 and T2 with the strands in T which contain *w* as s substring (resp. do not contain) for an object T.

```
void CSticker::separate(CSticker& T, CStrand& w, CStrand
T1, CStrand T2)
```

- The append function affixes *w* at the end of each sequence in T.

```
void CSticker::append(CSticker& T, CStrand& w)
```

- Function SeparatePlus and SeparateMinus returns a new object which contains data where its i-th bit is on (resp. off).

```
CSticker CSticker::SeparetePlus(CSticker& T, int i)
CSticker CSticker::SeparateMinus(CSticker& T, int i)
```

- The Set function turns the i-th bit on. The Clear function turns the i-th bit off.

```
void CSticker::Set(CSticker& T, int i)
void CSticker::Clear(CSticker& T, int i)
```

- The detect function returns true if the object contains nonempty data and false otherwise.

```
bool CSticker::Set(CSticker& T)
```

Now we propose a description for tubes, i.e., the class CTube. As described above, single strand can be coded as strings of {A,G,T,C} while double strands are coded as strings of {a,g,t,c,b,h,u,d,w,x,y,z} where

$$w = \alpha, x = \beta, y = \hat{\alpha}, z = \hat{\beta}, b = \hat{a}, h = \hat{g}, u = \hat{t}, d = \hat{c} \tag{6}$$

```
class CTube
{
  protected:
    int nSize; int* pLength;
    string* sStrands;
  public:
    CTube(int size);
    string* CreateStrands(int size);
};
```

4.2 DNA Program Executions

Following is an example of a DNA program in sticker model with the functions described above.

Algorithm 1. A DNA program in sticker model

```
weigh(T, b, d, T1, Tg, Te)
{
  i=1; T1=0; Tg=0;
  repeat
    T0 = SepareteMinus(T, b + i); T1 = SeparatePlus(T,
b+i);
    if di=0 then
      Tg = merge(Tg, T1); T= T0;
    else
      T1 = merge(T1, T1); T = T1;
    endif
    i =  i + 1;
  until(i = q + 1) or (detect(T)==NULL)
    Te = T;
}
```

4.3 Results of Computations

The result of a computation is often a Boolean value returned by a function as in sticker model. In other cases it may return an object containing the best solutions of the problem. Below there is an example of the find function.

Algorithm 2. Algorithm of find function in a sticker model

```
bool find(T)
{
  T0=0; T1=0;
  for(i=1;i<=q;i++)
  {
    T0=SeparateMinus(T,  q(N + 2k + 1) + i);
    T1=SeparatePlus(T, q(N+2k+1)+i);
    if(detect(T0) = false)
      T =  T1;
    else
      T = T0;
    return detect(T);
  }
}
```

5 A Class of Nonlinear Problems

The deformations of an elastic beam in equilibrium state can be described by a fourth-order boundary value problem of the following type (where $f \in C(R,R)$):

$$\begin{cases} x^{(4)}(t) = f(x(t)),\ 0 < t < 1 \\ x(0) = x(1) = x''(0) = x''(1) = 1 \end{cases} \tag{7}$$

Owing to its importance, the existence of solutions to this problem has been studied by many authors, see for example [10][14][2]. Most of these researches explore techniques of existence from nonlinear analysis, critical point theory, etc. However, there is no information about the location of these solutions, and how to find them.

In [10], Pang studies the boundary problem (3) of fourth order. Under certain conditions, he obtained the existence of 6 or 8 distinct solutions. His main conditions are listed as follows.

(**H1**) $f(0)=0$, and for $u\in R$ we have $uf(u)\geq 0$.

(**H2**) $f(u)$ is continuously differentiable at $u=0$ and there exists a positive integer n_0 such that

$$(2n_0)^4\pi^4<\alpha_0<(2n_0+1)^4\pi^4,\ \alpha_0=\lim_{u\to 0}\frac{f(u)}{u} \tag{8}$$

(**H3**) There exist n_1 such that

$$(2n_1)^4\pi^4<\alpha_0<(2n_1+1)^4\pi^4,\alpha_1=\lim_{u\to\infty}\frac{f(u)}{u} \tag{9}$$

(**H4**) There exists a constant $T>0$ such that

$$|f(u)|<2T,\ \forall 0<|u|\leq T \tag{10}$$

The main results of Pang [1] are as follows.

Theorem 1. Suppose hypotheses (H1)-(H4) hold. Then problem (3) has at least 6 distinct nontrivial solutions with 2 positive solutions, 2 negative solutions and 2 nodal solutions.

Theorem 2. Suppose hypotheses (H1)-(H4) hold and f(u) is an odd function, that is, $f(-u)=-f(u)$. Then problem (3) has at least 8 distinct nontrivial solutions.

If we denote $[x]$ the largest integer not exceeding x. Then it is straight forward that condition (4) is equivalent to the following.

$$0<\frac{\sqrt[4]{\alpha_0}}{2\pi}-\left[\frac{\sqrt[4]{\alpha_0}}{2\pi}\right]<\frac{1}{2} \tag{11}$$

And (5) is equivalent to the following.

$$0<\frac{\sqrt[4]{\alpha_1}}{2\pi}-\left[\frac{\sqrt[4]{\alpha_1}}{2\pi}\right]<\frac{1}{2} \tag{12}$$

Now we present some examples. Let the function $f(u)$ be as follows.

$$\begin{cases} f(u)=h(u)+g(u) \\ h(u)=\alpha_0 ue^{-u},\ g(u)=\alpha_1 ue^{-A/u^2} \end{cases} \tag{13}$$

Then it is direct to get

$$M_T = \max_{|u|\le T} | f(u) | \le \frac{\alpha_0}{\sqrt{2}} e^{-\frac{1}{2}} + \alpha_1 T e^{-\frac{A}{T^2}} \tag{14}$$

We now suppose α_0, α_1 are positive constants. First choose T and A such that

$$T = \frac{\alpha_0}{\sqrt{2}} e^{-\frac{1}{2}},\ A = T^2 \log 2\alpha_1 \tag{15}$$

Then it is clearly that (H4) holds from the fact that

$$M_T = \frac{3}{2} T < 2T \tag{16}$$

To give concrete examples, we now choose two positive integers n, m and let

$$\begin{cases} \alpha_0 = \left(2n + \dfrac{1}{2}\right)^4 \pi^4,\ \alpha_1 = \left(2m + \dfrac{1}{2}\right)^4 \pi^4 \\ T = \dfrac{\alpha_0}{\sqrt{2}} e^{-\frac{1}{2}},\ A = T^2 \log 2\alpha_1 \\ f(u) = \alpha_0 u e^{-u^2} + \alpha_1 u e^{-\frac{A}{u^2}} \end{cases} \tag{17}$$

Then the function $f(u)$ is odd and satisfies all the hypotheses (H1)-(H4). Figure 2 shows the image of the function with $n = 1, m = 3$.

By similar arguments we can now give a variant example (14). The image is shown in Figure 11 with $n = 1, m = 3$ and $\lambda = 0.0001$.

$$\begin{cases} \alpha_0 = \left(2n + \dfrac{1}{2}\right)^4 \pi^4,\ \alpha_1 = \left(2m + \dfrac{1}{2}\right)^4 \pi^4 \\ T = \dfrac{\alpha_0}{\sqrt{2}} e^{-\frac{1}{2}},\ A = (T^2 + 1) \log 2\alpha_1 \\ f(u) = \alpha_0 u e^{-u^2} + \alpha_1 u h(u) e^{-\frac{A}{u^2+1}} \\ h(u) = \dfrac{| e^{\lambda u} - e^{-\lambda u} |}{e^{\lambda u} + e^{-\lambda u}} \end{cases} \tag{18}$$

From [10] we know that the solutions of (3) correspond to the following problem.

$$\begin{cases} x(t) = \int_0^1 \int_0^1 G(t,s) G(s,r) f(x(r)) dr ds \triangleq Ax(t) \\ x \in P \triangleq \{ x \in C[0,1] \mid x(t) > 0, t \in (0,1) \} \end{cases} \tag{19}$$

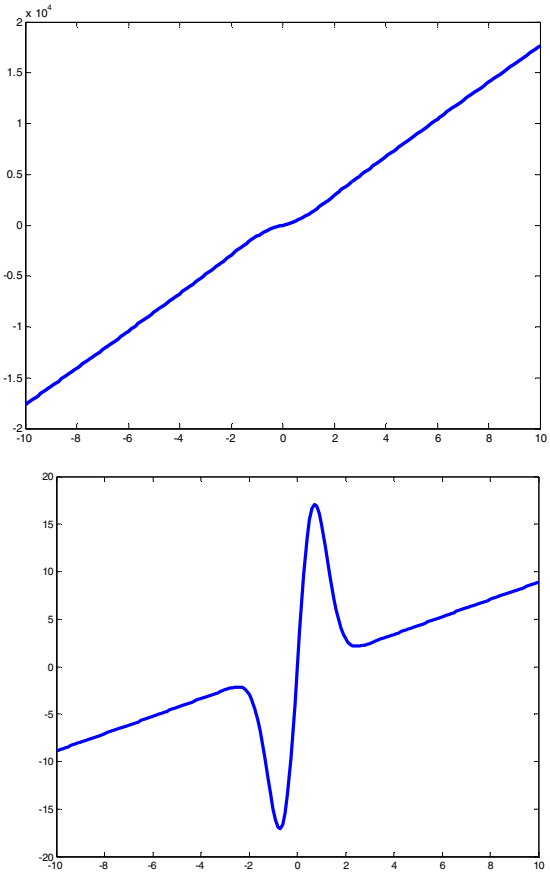

Fig. 2. Function image with $n=1, m=3$ of (13). The second image is the image with $n=1, m=3$, $\lambda=0.0001$ of (14). In this example, the parameters are $\alpha_0=39.0625, \alpha_1=1785.1, T=16.7532, A=2304.2$.

Where $\|x\|=\max|x(t)|$ and

$$G(t,s)=\begin{cases} t(1-s), & 0\le t\le s\le 1 \\ s(1-t), & 0\le s\le t\le 1 \end{cases} \tag{20}$$

It is easy to get another form of the operator $Ax(t)$.

$$Ax(t)=\frac{t(1-t)}{6}\left[3+3t+t^2\right]\int_0^t rf(x(r))dr \tag{21}$$

$$+\frac{1}{6}(1-t)\int_0^t r^3(2r-3)f(x(r))dr \tag{22}$$

$$+\frac{1}{3}t\int_t^1 r(1-r)^3 f(x(r))dr \tag{23}$$

$$+\frac{1}{3}(1-t)\int_0^t r^3(1-r)f(x(r))dr \tag{24}$$

$$-\frac{1}{6}t^3\int_t^1 r(1-r)f(x(r))dr \tag{25}$$

$$+\frac{1}{6}t\int_t^1 (3-2r)(1-r)f(x(r))dr \tag{26}$$

6 The DNA Encoding Scheme for BVP

From the above discussion we know that if there exists $x\in P$ such that $x=Ax$, then is a solution to the problem. In order to apply the DNA computing technique, we need to get a discretized representation of $x\in P$. Suppose $n>1$ is an integer, say $n=100$ for example. For $x\in P$ let $\delta=1/n$ and $X=[x(0),x(\delta),x(2\delta),\cdots,x(1)]^T\in R_{n+1}^+$. Then the vector X is an approximation of x. Define the searching space by

$$\Omega_0=\{X\in R_{n+1}^+\}, R_{n+1}^+=\{(x_0,\cdots,x_n)\mid x_i\geq 0,\forall i\} \tag{27}$$

For a specific point we now compute the image under the operator A. Let. Then we have

$$y_i=\frac{t_i(1-t_i)}{6\delta}\left[3+3t_i+t_i^2\right]\sum_{r=1}^{i}t_r f(x_r)+\frac{1-t_i}{6\delta}\sum_{r=1}^{i}t_r^3(2t_r-3)f(x_r) \tag{28}$$

$$+\frac{t_i}{3\delta}\sum_{r=i+1}^{n}t_r(1-t_r)^3 f(x_r)+\frac{1-t_i}{3\delta}\sum_{r=1}^{i}t_r^3(1-t_r)f(x_r) \tag{29}$$

$$-\frac{t_i^3}{6\delta}\sum_{r=i+1}^{n}(1-t_r)f(x_r)+\frac{1}{6\delta}t_i\sum_{r=i+1}^{n}t_r^2(3-2t_r)(1-t_r)f(x_r) \tag{30}$$

Next we consider the energy function of the problem. For $x\in\Omega_0$ and $Y=AX$ define $e(X)=\frac{1}{n+1}\sum_{r=0}^{n+1}|x_r-y_r|$. Then the problem is expressed in an optimization form as

$$\min e(x),\ X\in\Omega_0 \tag{31}$$

Next we define the data set as $\Omega=\{(X,e(X))\mid X\in\Omega_0\}\subset\Omega_0\times R^+$. In order to design a coding scheme we suppose that the set is bounded by a constant $M>0$. Therefore for each point $\xi\in\Omega$ the estimate $\|\xi\|\leq M$ holds. A point in the data set will be denoted by the lower case Greek letters.

First we give the encoding of the distances. In order to do this, we assume a large integer $\mathcal{N}$ to describe the grid size of observation, and let $\varepsilon = M / N$. Let $\xi = (X, e) \in \Omega$ be a data point. Then the energy e is encoded by the sequence $E(e) = XXXX \cdots XXXX$ with $i(e) = [e / \varepsilon]$ number of groups of $\mathcal{XXXX}$s as follows where the total number of bases are $4i(e)$. Here we use a four string to represent one bit.

$$E(e) = \overbrace{AAAA\,GGGG \cdots TTTT}^{i(e) \text{ number of } XXXXs} \tag{32}$$

By this encoding if we know the length of the DNA as L then we can easily know the energy is $e = L\varepsilon$. Next we present the encoding of a data point $\xi = (X, e) \in \Omega$. Since points are vector in the $(n+1)-$dimensional real space, we first encode a real number in single stranded DNA sequences. Let $-M \le x \le M$, then we will use the approximate integer $m(x) = [(x + M) / \varepsilon]$ to represent the original value. Evidently $0 \le m(x) \le 2N$. Let $L = 2 + \left[\frac{1}{4} \log_2 N \right]$. Then we can use a $4L$ bit binary string to represent $m(x)$. By the above discussion this is encoded as a string consisting of the four bases by letters A, T, G, C . Thus for $X \in \Omega_0$ its data DNA sequence is as follows

$$E(X) = \underbrace{\overbrace{AGTC \cdots TC}^{2L \text{ number of bases}} \cdots \overbrace{TAGA \cdots GT}^{2L \text{ number of bases}}}_{n+1 \text{ groups total}} \tag{33}$$

Then the encoding of ξ is $E(\xi) = E(X) \oplus E(e)$. By this encoding scheme the DNA sequence with shortest length will correspond to the solution of the problem. There is one final problem, that is, the generation of DNA sequences. The main difficulty lies in the generating of the energy sequences.

In fact, upon detailed analysis we find that the generation of energy is a composite of five basic operations. They are the addition, subtraction, multiplication, division and exponent. For fixed length DNA sequences, these operations are standard and can be fulfilled by standard biological techniques except the exponent operation.

First the general exponent operation e^x can be transformed into the special operation 2^x . Let x be a binary sequence of fixed length, say L for example. Then it is clear that 2^x is a standard bit-operation of left movement. This is easy to find biological implementation. Suppose x is the following string.

$$x = TTTTTTTTAGTCAGTCGGGGGGGG \tag{34}$$

Then clearly we know that

$$x << 8 = AGTCAGTCAAAAAAAA \tag{35}$$

Thus it is easy to implement the exponent operations.

Acknowledgments. This research is supported by the Natural Science Foundation of China (No. 61170038, 71071090), Humanities and Social Sciences Project of the Ministry of Education of China (No. 12YJA630152), the Natural Science Foundation of Shandong Province (No.ZR2011FM001), the Shandong Soft Science Major Project (No.2010RKMA2005).

References

1. Adleman, L.M.: Molecular computation of solutions to combinatorial problems. Science 266, 1021–1023 (1994)
2. Bai, Z.B., Ge, W.G., Wang, Y.F.: The method of lower and upper solution for some fourth-order equations. J. Inequalities in Pure and Applied Math. 5, 1–17 (2004)
3. Guo, D.: Nonlinear functional analysis. Shandong Science and Technology Press, Jinan (1985)
4. Hao, Y., Zhang, X.P., Shen, Z.Y., Seeman, N.C.: A robust DNA mechanical device controlled by hybridization topology. Nature 415, 62–65 (2002)
5. Tom, H.: Formal language theory and DNA: an analysis of the generative capacity of specific recombinant behaviors. Bulletin of Mathematical Biology 49, 737–759 (1987)
6. Jonoska, N., Karl, S.A., Saito, M.: Three dimensional DNA structures in computing. Biosystems 52, 143–153 (1999)
7. Sakamoto, K., Sakamoto, K., Gouzu, H., Komiya, K., Kiga, D., Yokoyama, S., Yokomori, T., Hagiya, M.: Molecular computation by DNA hairpin formation. Science 288, 1223–1226 (2000)
8. Li, R.-H., Yu, W.: An exploration of the principles of DNA computation. Chinese J. Computers 24, 972–978 (2001)
9. Lipton, R.J.: DNA solution of hard computational problems. Science 268, 542–545 (1995)
10. Pang, C., Dong, W., Wei, Z.: Multiple solutions for fourth-order boundary value problem. J. Math. Anal. Appl. 314, 464–476 (2006)
11. Paun, G., Rozenberg, G., Salomaa, A.: DNA computing, new computing paradigms. Springer, Heidelberg (2010)
12. Abu Bakar, R.B., Watada, J., Pedrycz, W.: DNA approach to solve clustering problem based on a mutual order. BioSystems 91, 1–12 (2008)
13. Deaton, R., Garzon, M., Rose, J., Franceschetti, D.R., Stevens Jr., S.E.: DNA computing: a Review. Fundamenta Informaticae 30, 23–41 (1997)
14. Xu, J., Zhang, S.-M., Fan, Y.-K., Guo, Y.-A.: DNA computer principle, advances and difficulties (III): the structure and character of “data” in DNA computing. Chinese Journal of Computers 30, 869–880 (2007)

How to Dynamically Protect Data in Mobile Cloud Computing?

Hongliang Lu, Xiao Xia, and Xiaodong Wang

National University of Defense Technology, Changsha, Hunan, China
honglianglu@nudt.edu.cn

Abstract. Mobile cloud computing (MCC) is introduced as a supporting architecture for mitigating the resources and energy limitations of mobile devices. And security is considered as a key factor which significantly affects MCC's widely deployment. Thus data protection methods such as encryption were applied to ensure the security of data. However, the complexity increased by data protection methods brings down the performance of transaction processing in MCC. In order to reduce the hurts brought to users' satisfactory by data protection methods, we firstly carried out some experiments based on the Hadoop cloud computing platform for quantitative analysis. We used the two popular encryption algorithms DES and AES(512), simulated the transaction processing, measured the time consumption, and logged the battery voltage change of mobile terminals. Results show that data protection methods have significance effects on the efficiency of transaction processing and the energy consumption of mobile devices. Furthermore, the degree of these effects is closely related to the complexity of protection methods. Based on the analysis, this paper proposed a framework for dynamic data protection, expecting to balance the security and resource consumption in MCC.

Keywords: Mobile Cloud Computing, Security, Transaction Processing Performance, Dynamic Data Protection.

1 Introduction

Recently, we have witnessed the rapid growth of mobile applications as the increasing popularity of smart phones and ubiquity of wireless access. But mobile devices have intrinsic storage, process, and battery power constraints, so mobile applications often hit a performance wall. Unlimited computing and storage resources offered by cloud computing can help break through this wall [1]. Mobile Cloud Computing (MCC) is a well accepted concept that could help to storage and process data on mobile devices, thereby reduce the devices' limitations [2]. For mobile devices there are amount of security problems. Such as authorization while link is setting up, data and link protection during the actual operation logic process and so on. Here the protection includes preventing from tampering, hijacking, replaying and other vicious attacks. All of these are exigent tasks to be solved [2][3].

One of the familiar measurement solving these security problems is applying security protocols, e.g. security socket layer (SSL) [4]. Another is encryption technology.

Q. Zu, B. Hu, and A. Elçi (Eds.): ICPCA-SWS 2012, LNCS 7719, pp. 364–371, 2013.

We name these operations data protection (DP). In most cases, the operations are computing intensive, so it will bring significance effects to transaction processing. Meanwhile the effects to the terminal's energy consumption cannot be neglected. Basing on the cognition of security problems, and the significance effects brought by data protection to transaction processing performance, we deployed an experiment to validate the effects. Then we proposed a framework for dynamically changing the policy of data protection in different transactions and under different context, intending to balance the security and resource consumption.

The rest of the paper is organized as follows: Section 2 describes the security problems and data protection in MCC; Section 3 measured the delay and energy consumption. Section 4 introduced the framework for dynamically changing data protection policy and analyzed the feasibility. Section 5 concludes the paper.

2 Security Problems and Data Protection in MCC

As a new computing framework, the security problem in mobile cloud computing cannot be neglected. Stressing these problems, the directly way is data protection.

2.1 Security Problems in MCC

The security problem in mobile cloud computing includes following aspects:

Security of Mobile Client. Protection for mobile client primarily lies on system and control right. If a vicious user accesses the rights of the system and control, a large amount of resource consumption may be resulted. Another scenario happens during the migration of mobile client [5][6]. In such condition, the info change of client's battery, load and so on will result the system cannot divide tasks properly, and will introduce serious communication expenses [7].

Threaten to the MCC Structure and Resource Pool. Info tampering at the server side could result the client to face the threat of plenty of resource consumption and unnecessary data transmit. The directly result is the performance of the wireless channel declined, and meanwhile the fee for user hiring the resources rise greatly.

Security Problem of the Channel for Data Transmitting. Protecting the transition channel is an urgent task either. Because when hijacking or middle person attack happens, additional spending and charge will be resulted [8].

Anyway, regardless of which security aspects, the data's usability, secrecy, integrality and non-repudiation will be affected [9]. Ensuring the data's properties as mentioned above, protection is eagerly.

2.2 Data Protection in MCC

Despite of using the applications of cloud or enjoying the services offered by the cloud under MCC environment, data transmission is indispensable. Some cases, the key point of data protection is a guarantee for achieving the purpose of the application or service. So data protection is very important.

Regularly data protection method could be referred as three techs, controlling, encryption and filtering technology. Controlling technology controls and manages data in centralization through configuring access rights, checking and auditing the data periodically, thus prevent from leakage. Encryption technology refers to data encryption in file level, disk level, hardware level and network level. Setting content filtering devices at the gateway point is the filtering technology's main threads, and the devices could analyze the datagram of the protocols HTTP, POP3, FTP, in time communication and so on. Besides, datagram could be filtered due to content either [9].

Though mobile devices appear to be limited resources in complex Apps, their computing ability has been distinctly improved and the reconfigurable and programmable abilities have also been extended. To prevent and detect vicious crab, analysis the program on devices is the regular approach. Scanning for certain resource usage and access and judging for the validity due to the rights while the program run is the common character of these programs. Thus additional computing and processing is needed, and as a result waste energy. Though protecting the cloud platform and resource pool would not introduce additional compute to devices directly, to the user any examine mode will unavoidably reduce the respond time.

Preventing the data from wire-tapping and tampering while transferring over the wireless channel, data encryption is the customary protection scheme. When a wire-tapper gets a datagram, he could not identify and change it. But the encryption operates on mobile device are CPU intensive. So to protect data security, additional computing cannot be avoided. We introduce the test in the following to prove this.

3 Consumption of Data Protection in MCC

In this section we study the effect of data protection to transaction performance via an experiment.

3.1 Experiment Design

There are three technologies related to data protection [9] as described above. We know encryption tech processes data on client over the whole transaction process and is familiar to the common users. And encryption tech has a certain request for terminal's resources and thus easy the measurement. So we choose it for experiment.

Scenario Choose. Referring to data encryption, mixed data encryption algorithms are put forwarded. We choose DES, AES(512) and compare with not encrypted data transmission each others.

Parameters Choose. There are many measurable elements of transaction performance in mobile cloud computing, such as delay, energy consumption, throughput and so on. Because we carry out our work under wireless environment and the terminal is smart-phone, we choose time and energy consumption as the measure. And the detail parameters of the experiment take out as table 1 shows.

Table 1. The experiment parameters

Items	Elements
terminal	Minestone2, Android 2.2
server	Hadoop, five nodes
transferring channel	Wiffi channel
NameNode	Intel(R) Core(TM) i3, 2.27GHz, 2.00G RAM

3.2 Results

We obtained the time consumption and battery voltage change over three different way of data process and transmission, encrypting data with DES, AES(512) and no encryption to data. The result listed in table 2 and 3.

Table 2. The time consumption for certain size package under different situation

Data size (MB)	201.4	402.8	604.2	805.6	1007
None (second)	248.8	525.4	771.6	1027.2	1396.5
DES (second)	273.4	567.6	817.2	1104.4	1453.0
SSL (second)	292.9	590.3	843.5	1197.6	1527.5

Table 3. The change of the battery under different situation

Data size (MB)	201.4	402.8	604.2	805.6	1007
None (milli volt)	43	57	75	86	103
DES (milli volt)	47	59	79	93	114
SSL (milli volt)	49	65	84	102	121

Transmitting different amount of data under different process, the time consumption's compare shows in figure 1(a) and the battery voltage change's compare in figure 1(b).

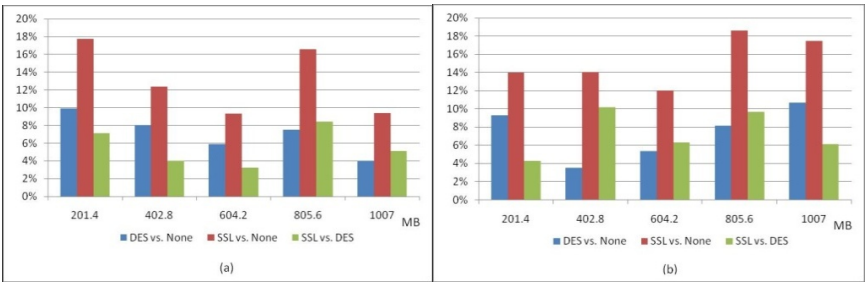

Fig. 1. Relative increase between different encryption methods

We can see that data protection have significant effects on the efficiency of transaction processing and the energy consumption of mobile devices.

3.3 Result Analysis

Over table 2, we can find that using AES algorithm consumes more time than DES, this suggests that the complexity of data protection is closely related to the performance of data transmission. The maximum increase of time consumption comparing DES with no encryption reached 9.8% transmitting the same amount of data. And the increase using AES will reach 17.7% even. Meanwhile, comparing AES and DES algorithm the increase will reach 8.4%, the compare showing in figure 1(a).

In table 3, we just measured the change of battery voltage, and let the initial voltage to be closely each time. But even in such condition, the more data is the more energy consumption is. Besides, complexity of the encryption algorithm has significant effect to the energy consumption, and comparing AES with DES the increase reached to 10.2%, the other compare show in figure 1(b). As a result, we can conclude that data protection methods have significant effects on the efficiency of transaction processing and the energy consumption of mobile devices. Furthermore, the magnitude of this effect depends on the complexity of protection methods.

4 System Design

As mentioned above, the data protection has significant effect on transaction processing. To provide better service and bring high quality applying experience, we propose a new framework for dynamically data protection basing on the environment info, aiming at balancing security and resource consumption.

4.1 Framework of the System

Data protection is inevitable when a mobile terminal accesses cloud service via AP. Generally, only the user actively chooses different policy due to the type of data he wishes to access. For example, in the stage of authentication may deploy a more complex encryption algorithm than in the stage of accessing a video. Such data protection policy cannot adjust to the user's actual application environment to change the protection method. So in some severe cases, such as the environment, including terminal's usable resources and network conditions and so on, exacerbated seriously but the data protection policy remains in the state of some complex level. Then high delay and serious energy consumption to terminal will be brought. If we can consider the user's transaction processing, data requesting, remaining compute and storage resources, the remaining energy resource and the current network condition including delay, throughput and bandwidth synthetically, and get a quantitative level of environment parameters, basing on the level choosing the proper data protection policy dynamically will save resources and improve the user experience significantly. We design a framework for such purpose as figure 2 shows.

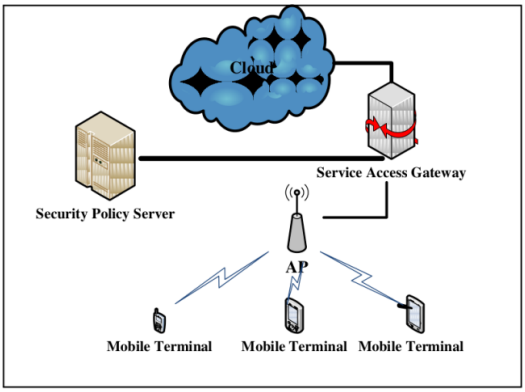

Fig. 2. The framework of dynamically data protection

In figure 2, when a mobile terminal request for the service and resources in cloud, firstly is the right check. Until this is done, the normal transaction processing will not begin. And at the beginning there are two way to start the data protection policy. The first one is specified by the terminal, sending the data protection policy to service access gateway, and the other one is determined by the server, in which the terminal send its resource consumption and the network condition info to the gateway, and the gateway will request security policy server to make certain data protection policy. Under the first condition, when the service access gateway obtained the protection policy from a terminal, it submits the info to security policy server, and the server manages a database for terminal's security policy. In the other case, after a first turn communicate, the terminal send its resource status and network condition info to SAP periodically, and the gateway will send these info to security policy server directly. Obtaining the info the security policy server will quantify the info due to the strategy made previously. When the server calculated the level and got the security parameters, it sends back to the gateway. The gateway will apply these parameters during the data transmitting. The clear interaction process shows in figure 3.

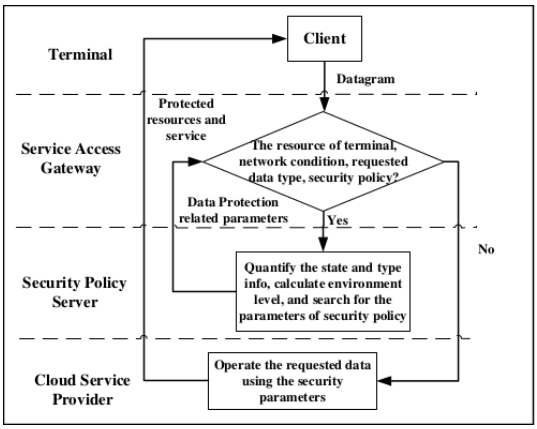

Fig. 3. Information Exchange Flow

4.2 Feasibility Analysis

There are three key items relating to the efficiency of the system. They are service access gateway (SAG), security policy server (SPS) and the need for uploading the status info. The performance of the front two will affect the system's performance directly, so they are in some aspect the bottle-neck of the system. Following is the analysis.

First of all, the SAG is the data stream passage. The capability of processing datagram determines the system's performance in some level. Datagram processing here includes data packet decomposition and analysis, by analyzing a specific field or the entire content of a data packet to obtain the terminal's request data stream type, and such prepare for subsequent data processing. The performance issues in the process could be reduced through a multi-gateway technology. That is, setting up multiple gateways and then through the load balancing of data packet processing to achieve balance. Besides, we can also set some bit of the datagram to assist for data packet type judging. Only the certain bit set to be true, the packet is needed to be analyzed and the gateway is often efficient to determine a particular bit. Therefore, reasonable policy settings will effectively reduce the gateway out of the performance limits.

Besides, the SPS is not an ignorable factor affecting the performance, when the user substantial scale, this centralized SPS access will be a performance bottleneck either. But we can distribute the centralized into semi-centralized, and full use the performance advantages of distribution and making such a restriction to a minimum. Meanwhile, we can module the service and data of the system to reduce the visits of safety-related parameters when processing for categories' determine and data processing, thus, to some extent reduce the pressure of the server. From the above we can see that all processes in the system architecture is feasible.

4.3 Key Issues Remaining

In the framework, to balance the security and terminal's resource consumption, The remaining problems to be solved in the future include:

- Quantify the terminal's state and network condition in reason. For these variables are the most important elements, so properly quantify is eagerly needed.
- Determine the contribution for each parameter to the environment level properly. Different weight distribution will determine the reasonableness of environmental classification and affect the performance at last.
- Environment level's classification. The level's grading is the key of system's complexity and efficiency.
- Security policy's study and accumulate as time goes on.

5 Conclusion

In order to solve the problem of limited resources of mobile terminals, cloud computing is introduced as a support structure to mobile computing and brought out the

mobile cloud computing. As a new mobile computing architecture, mobile cloud computing provides users with scalable, dynamic storage, computing, software, services and other variety of new applications, allowing users to rent resources according to their own needs, avoiding waste of resources resulted by meeting the peak demand. Applications in mobile cloud computing are also facing a variety of security issues, in order to ensure data security needs for data protection. But resource consumption introduced by applying encryption technology to data protection cannot be ignored.

In order to quantify study the impact of data protection to transaction processing performance in MCC, we transmitted different size data encrypted using different encryption algorithms and measured the time consumption and the battery voltage change to reflect the effect brought by data protection. We get the conclusion that data protection has significance impact on transaction processing. Basing on the conclusion, we proposed a framework for dynamically protecting data considering the environment condition and transaction type synthetically, expecting to balance the security request and terminal's resource consumption.

Besides, efficient data protection method's study is necessary in mobile cloud computing. These studies will accelerate the progress of adopting application and service in cloud for user. And the dynamic adjustment of data protection policy is a good way for reducing the security cost. Apart from that, how to quantify the network condition and classify the level properly, and how to make the strategy's accumulate while transaction processing goes on will be the future study focus.

References

1. Xu, C.: Mobile Cloud Computing and Applications. ZTE Communications 9(1), 3 (2011)
2. Chetan, S., Gautam Kumar, K., Dinesh, M.K., Abhimanyu, M.A.: Cloud Computing for Mobile World, chetan.ueuo.com (2010)
3. Yue, L.: Reviews of Cloud Computing and Research on the Application of Mobile Cloud Computing. Information and Communications Technologies 4(2) (2010)
4. Wagner, D., Schneier, B.: Analysis of the SSL 3.0 protocol. In: 2nd USENIX Workshop on Electronic Commerce (1996), `http://www.cs.berkeley.edu/~daw/ssl3.0.ps` (revised version of November 19, 1996)
5. Chun, B.-G., Maniatis, P.: Augmented Smartphone Applications Through Clone Cloud Execution. In: Proc. of the 8th Workshop on Hot Topics in Operating Systems (HotOS), Monte Verita, Switzerland (May 2009)
6. Chun, B.-G., Ihm, S., Maniatis, P., Naik, M.: CloneCloud: Boosting Mobile Device Applications Through Cloud Clone Execution (2009)
7. Cuervo, E., Balasubramanian, A., Cho, D.-K., Wolman, A., Saroiu, S., Chandra, R., Bahl, P.: MAUI: Making Smartphones Last Longer with Code Offload, mobisys (2010)
8. Cremers, C., Rasmussen, K.B., Capkun, S.: Distance hijacking attacks on distance bounding protocols (2011)
9. Yang, G.H.: Analysis of Security for Mobile Internet. In: Confernce on Global Mobile Internet 2011 (2011)

Enriching Context-Oriented Programming with Structured Context Representation

Jun Ma[1], Xianping Tao[1], Tao Zheng[2], and Jian Lu[1]

[1] State Key Laboratory for Novel Software Technology, Nanjing University
NO. 22 Han Kou Road, Nanjing, China 210093
{majun,txp,lj}@nju.edu.cn
[2] Software Institute, Nanjing University, NO. 22 Han Kou Road,
Nanjing, China 210093
zt@software.nju.edu.cn

Abstract. Context-oriented Programming (COP) has been proposed as a new promising paradigm for programming context-aware applications in pervasive environments. However, the expressive power of the layer abstraction in current COP extensions is limited, as layers are only suitable for expressing context with boolean or nominal values and lack support for describing temporal property of context. Besides, partial methods of COP are defined only on top of each single layer but not on a combination of layers, and the behavior of an invoked method is unpredictable as it is determined by the layer activation order. In this paper, we enriches COP by replacing layers with well-structured *context entries*. Each *context entry* specifies a piece of context information as well as its temporal property, and a *context* is represented as a set of many *context entries*. Many new *operations* are introduced to manipulate *context* more conveniently. Furthermore, partial methods are now defined on the notion of *situation* which is expressed as a combination of multiple *context entries*, and the evaluation order of multiple active partial methods can be explicitly specified so that the behavior of an invoked method becomes predictable. An implementation on top of $ContextJ*$ and experiments for evaluating it in term of time overhead are also presented in this paper.

Keywords: pervasive computing, programming language, context awareness.

1 Introduction

Context awareness[1][2] is one of the key characteristics of pervasive computing. However, programming support for context aware applications remains to be a challenging task. One crucial problem is the lack of an appropriate programming paradigm and supporting programming languages which treat context and context-dependent concerns as fundamental elements of programming. Context-oriented Programming (COP) has recently been proposed as a new promising paradigm for the task[3]. Layers, as the basic concepts in COP, are declared and can be activated (or deactivated) to specify the context for a method invocation.

Q. Zu, B. Hu, and A. Elçi (Eds.): ICPCA-SWS 2012, LNCS 7719, pp. 372–388, 2013.

```
public class Test implements I_Test {
    public Test() {
    }

    public void print(String s) {
        layers.select().print(s);
    }

    private LayerDefinitions<I_Test> layers = new LayerDefinitions<I_Test>(
    // root method implementation
            new I_Test() {
                public void print(String s) {
                    System.out.print(s);
                }
            });
    // partial methods definitions
    {
        layers.define(Layers.Log, new I_Test() {
            public void print(String s) {
                System.out.println("[Log]'print(String)'  invoked!");
                layers.next(this).print(s);
                System.out.println();
                System.out.print("[Log]'print(String)'  finished!");
            }
        });
        layers.define(Layers.Block, new I_Test() {
            public void print(String s) {
                System.out.println("================================");
                layers.next(this).print(s);
                System.out.println();
                System.out.print("================================");
            }
        });
    }
}
```

(a) class `Test`

```
public interface I_Test {
    public void print(String s);
}
```

(b) interface `I_Test`

```
import be.ac.vub.prog.contextj.ContextJ.Layer;

class Layers {
    public static final Layer Log = new Layer();
    public static final Layer Block = new Layer();
}
```

(c) layer declaration

```
final Test atest = new Test();
with(Layers.Log, Layers.Block).eval(new Block() {
    public void eval() {
        atest.print("Hello World!");
    }
});
```

(d) invocation with layers

```
================================
[Log]'print(String)'  invoked!
Hello World!
[Log]'print(String)'  finished!
================================
```

(e) output (Log activated first)

```
[Log]'print(String)'  invoked!
================================
Hello World!
================================
[Log]'print(String)'  finished!
```

(f) output (Block activated first)

Fig. 1. An example written in *ContextJ∗*

The behavior of an invoked method is assembled (from many partial methods) at runtime based on activated layers to archive context-dependent behaviors. However, current COP extensions are not powerful enough in following aspects:

- Limitations in expressive power of layers.
  - As layers can be only activated or deactivated, they are suitable for describing contexts with boolean (e.g., whether the light of a room is on or off) or nominal values(e.g., the hair color of a person)[4],[1] but not suitable for describing those with ordinal, interval or ratio values(e.g., the height, weight of an object, the luminance of a room, etc.).
  - With structureless layers, the meaning of a layer is subjective to the definition given by the programmer.
  - There is no direct support for expressing the temporal property of context so that historical context is hard to specified.
- Limitation in partial method definition and evaluation.
  - Partial methods are defined only on top of each single layer but not on a combination of layers.

[1] Stevens classified four different scales of measurements: *nominal, ordinal, interval* and *ratio* in [4].

  - The behavior of a invoked method is unpredictable and depends on the order of layer activations, so programmers have to pay more attention on the order when activating layers.

To address the mentioned problems, in this paper, we introduce a formal context model which enriches COP with a well-structured context representation. In the model a *context* is represented as a set of many *context entries*, each of which specifies a piece of context information as well as its temporal aspect. More specifically, the main contributions of this paper are:

- We have introduced an enhanced formal context model to COP.
  - The meaning of each *context entry* is embedded in its structure (as explained in Sec.3);
  - *Duration* is introduced to depict the temporal aspect of context so that the model can be used to describe historical context;
  - New operations are introduced to manipulate context;
- We have introduced the concept of *situation* (see Sec.3.4), which can be specified as a combination of multiple *context entry*.[2]
  - Partial methods are now defined on top of different *situation*s as well as their (logical) combinations;
  - Evaluation order of multiple active partial methods can be explicitly specified so that the behavior of an invoked method becomes predictable.
- We extended the COP language *ContextJ∗*[3] with the proposed scheme and carried out experiments to evaluate it in term of time overhead.

The rest of this paper is organized as follows: Section 2 gives a brief introduction to Context-oriented Programming(COP) and related works. Section 3 shows the formal model of the proposed context representation. Section 4 presents how the formal model can be introduced to COP by showing an implementation on top of the COP language *ContextJ∗*[3]. In Section 5, we first discuss the pros and cons of our implementation and show the results of two experiments for evaluating it in term of time overhead. We conclude this paper and discuss future works in Section 6.

2 Related Works

Context-oriented Programming[3] is generally considered as an extension of Object-oriented Programming (OOP) and has been proposed as a promising paradigm for programming context aware applications in a pervasive computing environment. In COP, a *layer* is an abstraction to group context-dependent behaviors, each of which is specified by a *partial method* defined in the layer. Layers can be activated (or deactivated) to specify the context for a method invocation, and the actually behavior of the invoked method is composed from partial methods of activated layers. Many COP extensions (e.g.,*ContextL*[5] *ContextJ∗*[3], *ContextJ*[6] and its successor *JCop*[7], etc.) have been implemented, a detailed comparison among most of the current COP extensions is provided in the paper[8]. Despite of the differences, these COP extensions share

[2] Specifically, a single *context entry* is also considered as a situation.

the common limitations as mentioned in Sec.1 and the same goal of separating context-aware concerns from the base program's logics so as to ease the development of context-aware applications. Therefore, we just take *ContextJ∗* as a representative of COP in this paper.

ContextJ∗[3] is a implementation of COP based on Java. In *ContextJ∗*, each layer is pre-declared as a globally accessible object of the `Layer` class and a static list activeLayers is introduced for each thread to record current active layers for the corresponding thread. Once upon a method is invoked, its behavior is composed from a set of partial methods defined (for behavior variations) on top of the activated layers.

Take Fig.1 for instance, two layers Log, Block are pre-defined (as instance of `Layer` class)as shown in Fig.1(c); `Test` class implements `I_Test` interface.[3] The private field layers is used to keep a map between layers and corresponding partial methods. Two partial methods are defined on each single layer (i.e.,Log and Block) correspondingly (Fig.1(a) lines 17-34.) The method for layer Log adds log information[4] once print(String) is invoked while the method for layer Block tries to add two lines blocking the output of print(String). As shown in Fig.1(d), the method print(String) is invoked with Log and Block activated orderly by using with statement, which is actually a static function provided by *ContextJ∗*; [5]in Fig.1(e) and 1(f) show the outputs for invocations where both Block and Log activated (with different activating order). It is clear to see that the behavior of each invocation varies with the activated layers as well as the activating order.

Lucx[9][10] introduced context as first-class objects in an intensional programming language Lucid. A collection of context calculus operators were introduce for formally manipulation of contexts. In the calculus, two categories of contexts are classified: *simple context* and *context set*. A *simple context* is represented by a collection of $\langle d : t\rangle$ pairs(i.e., $[d_1 : t_1, d_2 : t_2, ..., d_m : t_m]$), where d_i is a *dimension* and t_i is a valid tag of the *dimension* represent by d_i (see [9] for detailed descriptions); while a *context set* is a set of simple contexts(i.e., $\{[d_1^1 : t_1^1, d_2^1 : t_2^1, ..., d_m^1 : t_m^2], [d_1^2 : t_1^2, d_2^2 : t_2^2, ..., d_m^2 : t_m^2], ..., [d_1^k : t_1^k, d_2^k : t_2^k, ..., d_m^k : t_m^k]\}$). Based on the context definitions, a set of operations (e.g., isSubContext, union, difference, projection, intersection,.etc) were introduced for manipulating contextual information in a uniformed way.

We borrowed the context calculus from Lucx[9][10] as the base of our context model and extended it with the capability of specifying temporal aspect of context; finally, we introduced the enhanced context model into Context-oriented Programming paradigm and implemented it on top of a Java base COP extension *ContextJ∗*. We first show the enhanced context model in the following section.

[3] *ContextJ∗* requires the code for implementing the interface to be of the form as shown in Fig.1(a) lines 5-7; and the real implementation of the interface is archived by a special root method as shown in Fig.1(a) lines 10-14.

[4] Here, we just print out the log information through the standard output stream for demonstration

[5] Implemented by a WithEvaluator class , while without is implemented by a WithoutEvaluator.

3 Context Model

In this section, we introduce the basic ideas of the proposed context model.

3.1 Duration

In this subsection, we introduce the definition and operations of *Duration* and *DurationSet* used in this paper.

Definition 1 (Duration). *A duration is a period (or a point) of time and is denoted as a interval of real numbers (i.e [b,e], [b,e), (b,e] or (b,e)).*

Actually, a duration stands for a non-empty (generally infinite) set of continuous real numbers, and we denote $r \in d$ if and only if the real number r is in the set represented by the duration d. Especially, we let $d^U = (-\infty, +\infty)$ denote the universal duration which stands for the set of all real numbers.

Given two durations d_1, d_2, we could define many relationships between them:

- equals: $d_1 = d_2$ iff $\forall r, r \in d_1 \Leftrightarrow r \in d_2$;
- before (after): $d_1 \rhd d_2$ ($d_2 \lhd d_1$) iff $\forall r \in d_1, \forall r' \in d_2,\ r < r'$;
- within (contains): $d_1 \subset d_2$ ($d_2 \supset d_1$) iff $(\forall r, r \in d_1 \Rightarrow r \in d_2) \wedge (\exists r' \in d_2, r' \notin d_1)$;
- pre-overlay (suc-overlay): $d_1 \overleftarrow{\Diamond} d_2$ ($d_2 \overrightarrow{\Diamond} d_1$) iff $(\exists r, r \in d_1, r \in d_2) \wedge (\exists d' \subset d_1, d' \rhd d_2) \wedge (\exists r', r' \in d_2, r' \notin d_1)$;
- overlay: $d_1 \Diamond d_2$ iff $d_1 \overleftarrow{\Diamond} d_2$ or $d_1 \overrightarrow{\Diamond} d_2$
- direct connected: $d_1 \blacklozenge d_2$ iff : (a) $d_1 \not\rhd d_2 \wedge d_2 \not\rhd d_1$, or (b)$(d_1 \rhd d_2) \wedge \nexists d'(d_1 \rhd d' \rhd d_2)$, or (c) $(d_2 \rhd d_1) \wedge \nexists d'(d_2 \rhd d' \rhd d_1)$.

Given a set of real numbers R, two real number r_1, r_2 is said to be connected in R(denoted as $r_1 \bowtie r_2$) if and only if $r_1 \in R \wedge r_2 \in R \wedge (\forall r',\ r_1 < r' < r_2 \Rightarrow r' \in R)$. Obviously, the relation '$\bowtie$' is an equivalence relation, so a partition of R based on '$\bowtie$' can be obtained; as each element of the partition is actually a duration, we call the partition "the duration set covered by R" (denoted as $\mathfrak{dur}(R)$).

Let $\mathbb{D}$ denote the set of all durations, then we define a set of functions of the form $\mathbb{D} \times \mathbb{D} \to 2^{\mathbb{D}}$:

$$d_1 \ominus d_2 \triangleq \mathfrak{dur}(R), R \triangleq d_1 - d_2 = \{r | r \in d_1 \wedge r \notin d_2\} \tag{1}$$

$$d_1 \otimes d_2 \triangleq \mathfrak{dur}(R), R \triangleq d_1 \cap d_2 = \{r | r \in d_1 \wedge r \in d_2\} \tag{2}$$

$$d_1 \oplus d_2 \triangleq \mathfrak{dur}(R), R \triangleq d_1 \cup d_2 = \{r | r \in d_1 \vee r \in d_2\} \tag{3}$$

Specially, $\forall d \neq d^U$, we have $d \subset d^U$, $d \ominus d^U = \phi$, $d \otimes d^U = \{d\}$, $d \oplus d^U = \{d^U\}$. Let $d_1 = [2,5], d_2 = [0,2]$, then $d_1 \overleftarrow{\Diamond} d_2$, $d_1 \blacklozenge d_2$,and $d_1 \ominus d_2 = \{(2,5]\}$,$d_1 \otimes d_2 = \{[2,2]\}$,$d_1 \oplus d_2 = \{[0,5]\}$.

Definition 2 (Duration Set and Normal Formed Duration Set, NFDS). *A set of durations is called a duration set. A normal formed duration set D is such a duration set that neither two of its elements are connected with each other.*

For example,the empty set ϕ and one element set $\{d\}$ are both normal-formed.

Let $\Re(D)$ denote the set of all real numbers covered by all durations in the duration set D (i.e.$\Re(D) \triangleq \{r|r \in d, d \in D\}$), and we call it the *coverage* of D.

Given a duration set D we could build a NFDS as $\mathfrak{dur}(\Re(D))$. We further call this NFDS the *normal form* of D, and denote it as $NF(D)$. Then, it is obvious that $\Re(D) = \Re(NF(D))$.

Given two durations sets $D_1, D_2 \in 2^{\mathbb{D}}$, we could further define operations($2^{\mathbb{D}} \times 2^{\mathbb{D}} \to 2^{\mathbb{D}}$) on duration sets as follows:

$$D_1 \ominus D_2 \triangleq \mathfrak{dur}(R), R \triangleq \Re(D_1) - \Re(D_2) = \{r|r \in \Re(D_1) \wedge r \notin \Re(D_2) \tag{4}$$

$$D_1 \otimes D_2 \triangleq \mathfrak{dur}(R), R \triangleq \Re(D_1) \cap \Re(D_2) = \{r|r \in \Re(D_1) \wedge r \in \Re(D_2) \tag{5}$$

$$D_1 \oplus D_2 \triangleq \mathfrak{dur}(R), R \triangleq \Re(D_1) \cup \Re(D_2) = \{r|r \in \Re(D_1) \vee r \in \Re(D_2) \tag{6}$$

For example, let $D_1 = \{[0,3],[5,9]\}$ $D_2 = \{(2,6),[7,11]\}$, then we have: $D_1 \ominus D_2 = \{[0,2],[6,7)\}$, $D_2 \ominus D_1 = \{(3,5),(9,11]\}$, $D_1 \otimes D_2 = D_2 \otimes D_1 = \{(2,3],[5,6),[7,9]\}$, $D_1 \oplus D_2 = D_2 \oplus D_1 = \{[0,11]\}$.

For any two duration sets D_1, D_2, it is easy to see that $D_1 \ominus D_2$,$D_1 \otimes D_2$ and $D_1 \oplus D_2$ are still NFDSs.

3.2 Context

A pervasive computing system may consist of many entities (e.g. a people or a device) interacting with one another. We denote an entity as e_i and the set of all entities of a pervasive computing system as $\mathbb{E}$.

An entity may have many state dimensions (sd) whose values are used to describe the state of the entity. For example, the height, weight, friends of a people are sds of the people. Let $SD(e_i)$ denote the set of all state dimensions of the entity e_i and $\mathbb{S}$ stand for the union set of all $SD(e_i)$ for a given system as:

$$\mathbb{S} \triangleq \bigcup_{e_i \in \mathbb{E}} SD(e_i) \tag{7}$$

Given any $sd_k^i \in SD(e_i)$, let $Dom(sd_k^i)$ denote the set of all possible values for sd_k^i; and finally we denote $\mathbb{V}$ as the union set of all $Dom(sd_k^i)$ for all sd_k^i of every e_i of a system as below:

$$\mathbb{V} \triangleq \bigcup_{sd_k^i \in SD(e_i), e_i \in \mathbb{E}} Dom(sd_k^i) \tag{8}$$

Definition 3 (Context Statement). *A tuple $\langle e, sd, v\rangle$ ($e \in \mathbb{E}, sd \in SD(e), v \in Dom(sd)$) is called a context statement. The set of all context statements is denoted as $\mathbb{Q}$.*

Definition 4 (Context). *A context C is subset of the relation $\mathbb{Q} \times \mathbb{D}$, and the set of all contexts is denoted as $\mathbb{C}$.*

We call each element of a context (i.e., a tuple of the form $\langle cs, d\rangle$) a *context entry*(or entry for short) and denote the set of all context entries as $\mathbb{K}$. A context entry is used to specify a piece of context information as well as its temporal

aspect and the meaning of a entry is embedded in its structure ($\langle cs, d\rangle$ stands for that the value of the state dimension(specified by $cs.sd$) of the entity (specified by $cs.e$) is $cs.v$ during the duration of d). In the rest of this paper, we use $ce.e$ (as well as $ce.sd$, $ce.v$) and $ce.cs.e$ (as well as $ce.cs.sd$, $ce.cs.v$) interchangeablely for convenience.

Given a context C, we denote $\kappa(C) = \{ce.cs | ce \in C\}$ and $\delta(C, cs) = \{ce.d | ce \in C\}$. For example, let $C_1 = \{ce_1, ce_2, ce_3\}$, where $ce_1 = \langle\langle e_1, sd_1, v_1\rangle, [8, 10]\rangle$, $ce_2 = \langle\langle e_2, sd_2, v_2\rangle, [9, 10)\rangle$ and $ce_3 = \langle\langle e_1, sd_1, v_1\rangle, [9, 11]\rangle$. Then $\kappa(C_1) = \{cs_1, cs_2\}$: $cs_1 = \langle e_1, sd_1, v_1\rangle$, $cs_2 = \langle e_2, sd_2, v_2\rangle$; $\delta(C_1, cs_1) = \{[8,\ 10],\ [9, 11]\}$; $\delta(C_1, cs_2) = \{[9, 10)\}$.

Based on the definition of normal-formed duration set, we could similarly define the Normal-Formed Context as shown in Def.5.

Definition 5 (Normal-Formed Context,NFC). *A context C is a* normal-formed context *(*NFC*) if and only if for any $cs \in \kappa(C)$, the corresponding duration set $D = \delta(C, cs)$ is a NFDS; otherwise, we say that C is* non-normal-formed.

For example, the above context C_1 is a non-normal-formed context, as $\delta(C_1, cs_1)$ is not a NDFS.

We further define two basic relationships between two contexts $C_1, C_2 \in \mathbb{C}$:

- $C_1 = C_2$ iff $\forall ce, ce \in C_1 \Leftrightarrow ce \in C_2$;
- $C_1 \subset C_2$ iff both following conditions hold: (a)$\forall ce \in C_1,\ \exists ce' \in C_2$, such that $ce.cs = ce'.cs$, $ce.d \subseteq ce'.d$; (b) $C_1 \neq C_2$.

we further denote $C \subseteq C'$ if and only if $C \subset C'$ or $C = C'$. In case $C \subseteq C'$, we call C a sub-context of C', and call C' a sup-context of C.

Definition 6 (Normal Form of a Context). *The normal form of a given context C is the smallest normal-formed context C' satisfies $C \subseteq C'$. Here "smallest" means that if there is another normal-formed context C'' satisfying the requirements(i.e.,$C \subseteq C''$), then $C' \subseteq C''$.*

We denote $NF(C)$ as the normal form of the given context C. Actually, $NF(C) = \bigcup_{cs \in \kappa(C)} (\{cs\} \times NF(ds(C, cs)))$. For example, the normal form of the context C_1 is $NF(C_1) = \{\langle\langle e_1, sd_1, v_1\rangle, [8, 11]\rangle,\ \langle\langle e_2, sd_2, v_2\rangle, [9, 10)\rangle\}$.

3.3 Context Operations

In this subsection we introduce the basic operations for manipulating contexts. As each context can be normal-formed, here we only consider operations on **NFC**s.

Union of contexts($C_1 \hat{\cup} C_2$) Normally, the union of two contexts (i.e. $C_1 \hat{\cup} C_2$) generates the smallest common sup-context (normal-formed) of two given contexts, i.e. the *normal form* of the context that consists of all context entries of the two contexts:

$$C_1 \hat{\cup} C_2 \triangleq NF(C),\ \text{where } C = \{ce | ce \in C_1 \vee ce \in C_2\} \tag{9}$$

Intersection of contexts($C_1 \hat{\cap} C_2$) The intersection of two contexts($C_1 \hat{\cap} C_2$) is the maximum normal-formed context C, such that $C \subseteq C_1 \wedge C \subseteq C_2$. Here "maximum" means if there is another normal-formed context C' and $C' \subseteq C_1 \wedge C' \subseteq C_2$, then $C' \subseteq C$. Generally, this operation can be used to find the common context information shared by two contexts.

$$C_1 \hat{\cap} C_2 \triangleq \bigcup_{cs \in \kappa(C_1) \cap \kappa(C_2)} (\{cs\} \times (\delta(C_1, cs) \otimes \delta(C_2, cs))) \tag{10}$$

Difference of contexts($C_1 \hat{-} C_2$) The difference of two contexts (i.e. $C_1 \hat{-} C_2$) is the maximum normal-formed context C, such that $C \subseteq C_1 \wedge C \hat{\cap} C_2 = \phi$.

$$\begin{aligned} C_1 \hat{-} C_2 &\triangleq C' \cup C'' \\ C' &\triangleq \{ce | ce \in C_1, ce.cs \in (\kappa(C_1) - \kappa(C_2))\} \\ C'' &\triangleq \bigcup_{cs \in \kappa(C_1) \cap \kappa(C_2)} (\{cs\} \times (\delta(C_1, cs) \ominus \delta(C_2, cs))) \end{aligned} \tag{11}$$

Update one context with another($C_1 \Uparrow C_2$) $C_1 \Uparrow C_2$ generates a normal-formed context by updating $ce \in C_1$ with $ce' \in C_2$. To specify the semantics of update operation, we first define another function sub as follows:

Given a context C, and a context statement cs, let $sub(C, cs)$ denote the context by substituting $ce.cs$ with cs for every $ce \in C$, where $ce.cs.e = cs.e, ce.cs.sd = ce.sd$.

$$sub(C, cs) \triangleq \{\langle cs, ce.d \rangle | cs.e = ce.cs.e, cs.sd = ce.cs.sd, ce \in C\} \tag{12}$$

With $sub(C, cs)$, we could further define the semantics of $C_1 \Uparrow C_2$ as:

$$C_1 \Uparrow C_2 \triangleq C_2 \hat{\cup} (C_1 \hat{-} \hat{\bigcup_{cs \in \kappa(C_1)}} sub(C_2, cs)) \tag{13}$$

Projection of context ($C \downarrow \mathfrak{p}$) Projection of context provides a way for constructing a sub-context of a given context by matching each ce with a pre-defined context pattern.

Definition 7 (Context Pattern). *A context pattern (pattern for short), $\mathfrak{p}$, is defined by a tuple $\langle \Pi_{\mathbb{E}}, \Pi_{\mathbb{S}}, \Pi_{\mathbb{V}}, \Pi_{\mathbb{D}} \rangle$. Here $\Pi_{\mathbb{E}} \subseteq \mathbb{E}$, $\Pi_{\mathbb{S}} \subseteq \mathbb{S}$, $\Pi_{\mathbb{V}} \subseteq \mathbb{V}$, $\Pi_{\mathbb{D}} \subseteq \mathbb{D}$, and $\Pi_{\mathbb{D}}$ is a NFDS.*

Then the projection of a context C with respects to a pattern $\mathfrak{p}$ is to find the maximum normal-formed context C', such that $C' \subseteq C$ and that $\forall ce', ce' \in C' \Rightarrow ce'.cs.e \in \mathfrak{p}.\Pi_{\mathbb{E}} \wedge ce'.cs.sd \in \mathfrak{p}.\Pi_{\mathbb{S}} \wedge ce'.cs.v \in \mathfrak{p}.\Pi_{\mathbb{V}} \wedge (\exists d \in \mathfrak{p}.\Pi_{\mathbb{D}}, ce'.d \subseteq d)$. Furthermore, $C \downarrow \mathfrak{p}$ can be described as follows:

$$C \downarrow \mathfrak{p} \triangleq \bigcup_{\substack{cs \in \kappa(C), \\ cs.e \in \mathfrak{p}.\Pi_{\mathbb{E}}, \\ cs.sd \in \mathfrak{p}.\Pi_{\mathbb{S}}, \\ cs.v \in \mathfrak{p}.\Pi_{\mathbb{V}}}} (\{cs\} \times (\delta(C_1, cs) \otimes \Pi_{\mathbb{D}})) \tag{14}$$

3.4 Situation

In previous subsections, we have shown how context is modeled and manipulated. In this subsection, we try to show how a *Situation*, a high level abstraction for describing the state of a system (or an instance of a system), can be defined

based on these single context entries. A situation can be represented formally as follows:

$$\begin{aligned} SIT &:= ce|SIT_{and}|SIT_{or}|SIT_{not} \\ SIT_{and} &:= SIT \wedge SIT \\ SIT_{or} &:= SIT \vee SIT \\ SIT_{not} &:= !SIT \end{aligned} \tag{15}$$

As shown in the equation, a situation can be a single context entry or a set of context entries combined by the logic operators $(\wedge, \vee, !)$. Furthermore, given a normal formed context C, and a situation SIT, we say SIT holds in the context C (denoted as $C \vdash SIT$) by applying following rules:

$$R_{ce} : \frac{SIT := ce, \exists ce' \in C, ce.cs = ce'.cs, ce.d \subseteq ce'.d}{C \vdash SIT} \tag{16}$$

$$R_{and} : \frac{C \vdash SIT_L \&\& C \vdash SIT_R}{C \vdash SIT_L \wedge SIT_R} \tag{17}$$

$$R_{or} : \frac{C \vdash SIT_L || C \vdash SIT_R}{C \vdash SIT_L \vee SIT_R} \tag{18}$$

$$R_{not} : \frac{C \nvdash SIT}{C \vdash !SIT} \tag{19}$$

As shown in the rules, a situation consisting of only one single context entry holds in the context C if the context entry is covered[6] a SIT_{and} holds in C if both its sub-situations hold (in C); a SIT_{or} holds if either of its sub-situations holds (in C); while a SIT_{not} holds if the base situation (i.e., the one following '!') does not hold (in C).

4 Extension on *ContextJ∗*

In section 3, we have shown the formal model of our enhanced context representation. In this section we show how this model can be used to enhance COP by giving a example implementation on a Context-oriented Programming language, *ContextJ∗*[3], and here we call it *ContextJ+* for convenience.

4.1 Implementation of the Enhanced Context Model

Fig.2 shows the class graph for implementing our context model. Currently, `ContextStatement` implementation restricts the `e` and `sd` fields of being the type `String` while the type of `v` can be any `Object`. `Duration` class consists of two fields, begin and end, for specifying the start time and end time of a duration; while the being_icl and end_icl are used to indicate whether the duration interval is open or not (either at begin or end). Methods like equals(), before(), after(),

[6] A context entry by C;ce is covered by a context C if $\exists ce' \in C, ce.cs = ce'.cs, ce.d \subseteq ce'.d$.

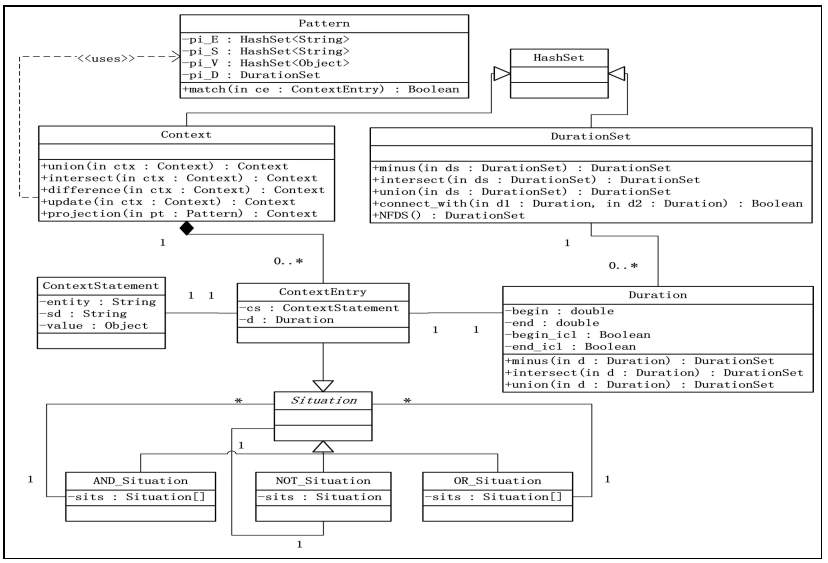

Fig. 2. Class graph of the enhanced context model

within(), contains(), pre_overlay(), suc_overlay(), overlay(), dir_connect() are also introduced to reveal the relationships between durations shown in Sec.3.1.[7]

`DurationSet` is implemented as a subclass of `HashSet`. The static method connect_with () verifies if two `Duration` instances are connected within the `DurationSet` object; while the method NFDS() returns the normal form of the `DurationSet` object.

`Context` is also a subclass of `HashSet` for hosting a set of `ContextEntry` instances. The `ContextEntry` itself is a subclass of the abstract class `Situation`. Three other subclasses (i.e., `AND_Situation`, `OR_Situation` and `NOT_Situation`) of `Situation` are introduced as well for implementing the situation abstraction mentioned in Sec.3.4.

4.2 Modify *ContextJ∗*

A layer in *ContextJ∗* is declared as a globally accessible instance of the `Layer` class. The layer can then be activated/deactivated by applying with/without statements (functions) to the corresponding layer object. As mentioned in Sec.1, the simple layer model is limited in expressive power. So, we replace the simple layer based model of *ContextJ∗* with the proposed context based model (see Sec.3 and 4.1). To archive this, a lot of work needs to be done:

First, replace activeLayers (see [3] for details) with activeContext. In *ContextJ∗*, a static ThreadLocal field activeLayers (of the type `LinkedList<Layer>`) is introduced per each thread to record activated layers for that thread. We replace it with

[7] These methods are not shown in Fig.2 for saving space.

another static ThreadLocal field activeContext (an instance of `Context` class) which records current activated context entries for the thread.

Second, replace layer manipulating statements with those for manipulating `Context`. with, without are the only two statements (functions archived by the `WithEvaluator` and `WithoutEvaluator`[3]) in *ContextJ∗* for manipulating the activeLayers field. In our *ContextJ+* enhancement, they are removed and new union, intersect, difference, update and projection statements (also as static functions) are introduced (by adding new `Evaluators` correspondingly) for manipulating the activeContext field. For example, Fig.3 shows the code of the `UnionEvaluator`, which implements the function of union statement. Once using the union(Context...ctxs) statement, an instance of `UnionEvaluator` is created and the filed theContext is initiated with the parameter ctxs; then the eval(Block b) of the new created `UnionEvaluator` is invoked to archive context-dependent behavior defined in b (which usually contains a method invocation). It first keeps a snapshot of activeContext before the invocation (lines 12-13), and updates the current active context with the theContext filed (line 14); after invoking b.eval(), it finally resets the activeContext back to the snapshot taken beforehand (lines 17-19).

```
1  private static class UnionEvaluator implements Evaluator {
2      private Context theContext;
3
4      private UnionEvaluator(Context[] ctxs) {
5          this.theContext = new Context();
6          for (Context c : ctxs) {
7              this.theContext = Context.union(theContext, c);
8          }
9      }
10
11     public void eval(Block b) {
12         Context currentActiveCTX = activeContext.get();
13         Context clonedActiveCTX = (Context) currentActiveCTX.clone();
14         activeContext.set(currentActiveCTX.union(theContext));
15         try {
16             b.eval();
17         } finally {
18             activeContext.set(clonedActiveCTX);
19         }
20     }
21 }
```

Fig. 3. The UnionEvaluator

Third, modify partial method definition. As we mentioned in Sec.1, a partial method of *ContextJ∗* can be defined only based on a single layer, but not on a combination of different layers. We address this problem by enabling defining a partial method on top of a `Situation`, which is a higher abstraction for specifying the program's status(see Sec.3.4). Fig.4(a) shows the signature of the define() method for defining partial methods, where sit specifies the situation on which the partial method is defined, definition holds the implementing codes of the defined method, priority defines the method's priority and blockinglist contains a list of situations. priority and blockinglist are optional and they are specified for controlling the evaluation process. Briefly, the higher the priority is, the earlier the defined method (if activated) is invoked and partial methods with the same priority are invoked randomly (one after another). Once the defined method is

invoked, other partial methods (of the same root method) defined on situations listed in blockinglist would be blocked.[8] For example, Fig.4(b) shows three partial methods defined on top of $(sit1 \wedge sit2)$, $(sit1 \vee sit2)$, and $(!sit1)$ respectively.[9] Here the method defined on $(sit1 \wedge sit2)$ has a priority of 9 and blocks the second method defined on $(sit1 \vee sit2)$, which has a priority of 5 without blocking other methods.

```
1 public void define(Situation sit, Definition definition,
2         Integer priority, Situation... blocklist)
```

(a)

```
1 layers.define(and(sit1, sit2), new I_Test() {
2     public void m1() {
3         System.out
4                 .println("Invoked when both sit1 and sit2 are activated!");
5         layers.proceed();
6     }
7 }, 9, or(sit1, sit2));
8
9 layers.define(or(sit1, sit2), new I_Test() {
10    public void m1() {
11        System.out
12                .println("Invoked when either sit1 or sit2 is activated!");
13        layers.proceed();
14    }
15 }, 5);
16
17 layers.define(not(sit1), new I_Test() {
18    public void m1() {
19        System.out.println("Invoked when sit1 is deactivated!");
20        layers.proceed();
21    }
22 });
```

(b)

Fig. 4. Partial methods defined on situations

Fourth, change the evaluation process of a method invocation. In $ContextJ*$, as there is direct mapping between a layer and the partial method defined on it, the evaluation process is quite simple. As shown in Fig.5(a), layers in the activeLayers list are checked one by one to see if there are partial methods defined on them. Specifically, if a partial method is found for a active layer, the method is invoked and the process goes on to the next layer; otherwise the layer is skipped. When all the activated partial methods are invoked (with respects to the order of the activeLayers list), the root method (see line 12-17 of Fig.1(a)) invoked.[10]

Unlike $ContextJ*$ keeping a mapping between each single layer and its corresponding partial method, $ContextJ+$ defines partial methods on top of situations and keeps a mapping between situations and partial methods. Once a method is invoked, related partial methods can not be directly selected from current activated context entries (kept in the activeContext field), and another step to evaluate activated situations is needed. Situations with higher methods'

[8] A partial method can only block methods with priorities lower than that of itself.

[9] Here,and, or, not are static functions provided for constructing situations; the method proceed() equals to layers.next(this).m1() in functionality.

[10] Here in Fig.5, we assume that each partial method implementation proceeds to the next layer and none of them override the root method.

priorities are evaluated first (assuming the PM_Map in Fig.5(b) is sorted in a descending order with respects to priorities). Partial method defined on an situation (which is evaluated to be active) is put into a list (see $activePM$ in Fig.5(b)); and finally, the behavior of the invoked method is composed by invoking all the activated partial methods in $activePM$ (as well as the root method) one after another.

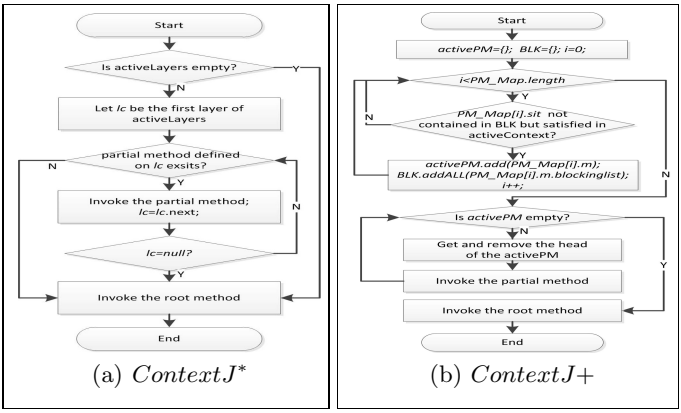

Fig. 5. Evaluation processes

5 Discussion and Evaluation

In previous sections we have introduced our enhanced context model and an implementation on top of $ContextJ*$. When compared with $ContextJ*$ and other existing COP extensions[8], our proposed scheme has advantages in the following respects: context entries are more powerful in expressing context information than layers as they can represent not only context with boolean or nominal values but also those with ordinal, interval or ratio values. Besides, with the introduction of *duration*, temporal aspect of context can be described. Furthermore, unlike isolated layers, context entries could share some relationships as they may describe the same *entity* or *state dimension* and the meaning of each entry is embedded in its structure. With the new introduced operations (and their corresponding statements), the activeContext field can be manipulated more flexibly.

More importantly, defining partial methods on top of situations is more powerful than on top of single layers. On one hand, *it is easier to refine context-dependent behaviors*. For example, two partial methods PM_1, PM_2 are pre-defined on top of two different situations S_1, S_2 (in the definition of a class), and the programmer wants to introduce some additional processing logics in the case that both S_1 and S_2 are activated. This is not a trivial work if he/she programs with $ContextJ*$, but, with our extension, this can be easily archived by defining a

new partial method PM_3 (implementing the additional processing logics) on top of the composed situation $(S_1 \wedge S_2)$. On the other hand, it also provides a way for reducing duplicated code. Given a case to define partial methods with the same processing logics on top of many different situations $S_1, S_2, ..., S_k$, we can define just one partial method on top of the composed situation $(S_1 \vee S_2 \vee ... \vee S_k)$.

As mentioned in Sec.4.2, the process of determining the behavior of an invoked method in our extension is different from that of *ContextJ∗* and other existing COP extensions. *ContextJ∗* manages the activeLayers field in a stack-like way, the latest activated layer is (re-)placed into the head of the list of activeLayers. Then the behavior of the invoked method is archived by invoking the partial methods (whose corresponding layer is in the activeLayers field) with respect to the order in the activeLayers list. For example, the outputs shown in Fig.1(e) and Fig.1(f) are affected by the activation order of the two layers Log, Block. This process is not good enough as it forces programmers to pay scrupulous attention to the activation order, otherwise the result might vary far away from the expectation. In *ContextJ+*, the activeContext field structure is flat, and all context entries in the field are equal and orderless. Two parameters priority and blockinglist are introduced when a partial method is defined, and they provide programmers with flexible and explicit ways for specifying how to select and order multiple activated partial methods so that the assembled behavior of the invoked method is more predictable.

In *ContextJ+*, the same as in most COP implementations, context activation (or deactivation) can be only achieved by explicitly using operations (i.e., union(), intersect(), difference(), update() and projection()) in the base program. As pointed out in[11], this is not suitable for systems where changes of context and executions of context-dependent behaviors happen at different points in a program and/or in different threads of execution. Currently, very few COP implementations, such as *JCop*[7] and *EventCJ*[11], provide event-based context(layer) activation/deactivation mechanisms which separat layer activation from the base program. We are now working on adopting the idea of event-based context(layer) (de-)activation to our current implementation.

Context conflicts are very common in pervasive computing and they may result from failures of underlying sensors, careless designed context processing logics or latencies in disseminating context information, etc. It is possible for the activeContext field contains two context entries conflicting with each other (e.g., $ce_1 = \langle\langle Bob, location, Beijing\rangle, [8am\ dayA, 7pm\ dayA]\rangle$ may conflicts with $ce_2 = \langle\langle Bob, location, Hongkong\rangle, [10am\ dayA, 7pm\ dayA]\rangle$ but not with $ce_3 = \langle\langle Bob, location, China\rangle, [10am\ dayA, 8pm\ dayA]\rangle$). However, our current context representation and related manipulations do not provide any support for handling such conflicts and the problem is left to the programmer. Some mechanisms such as ontology may be introduced to describe properties of (and relationships among) different entities as well as state dimensions to address this problem.

Last but not the least, apart from the benefits obtained, extra processing overheads are introduced as well by the extension of the well-structured context representation. In the following of this section, we show two experiments we have

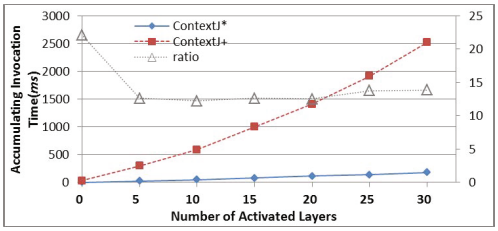

Fig. 6. Comparison between $ContextJ*$ and $ContextJ+$. The invocation times for both $ContextJ*$ and $ContextJ+$ are near linear with respects to the number of activated layers; $ContextJ+$ takes more time than $ContextJ*$ does.

done to evaluate our work. All the experiments are evaluated on a Intel Core i5 (2.53 GHz) with 4GB memory running Window7 professional. In the first experiment we try to show how many extra overheads are introduced by $ContextJ+$ when compared with $ContextJ*$. We implemented a class with only one *int* field f1 and a root method m1() which just increases f1 by one in both $ContextJ*$ and $ContextJ+$; thirty different layers $(L_1, L_2, ..., L_{30})$ were predefined for the $ContextJ*$ version (while thirty different context entries $ce_1, ce_2, ..., ce_{30}$ were predefined for the $ContextJ+$ version[11]). On each layer L_i (or context entry $ce_i)(i = 1 - 30)$ we defined an partial method pm_i which contains the same code $layers.next(this).m1()$ (i.e., pm_i directly proceed to the next activated partial method).

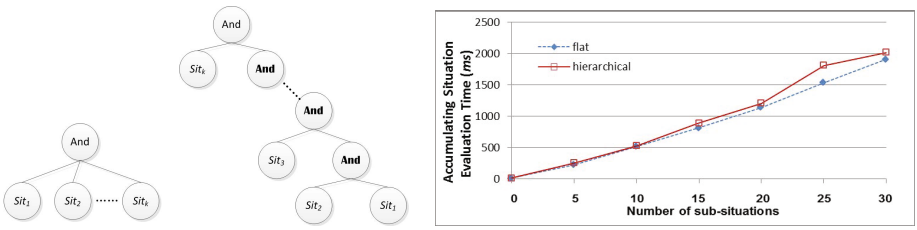

(a) Flat (b) Hierarchical (c) Evaluation times

Fig. 7. Situation evaluation in $ContextJ+$. It is clear that: (1)for both the styles, the evaluation time grows linearly with respects to the number of simple sub-situations; (2) the height of the hierarchy of a situation does not increase the evaluation time very much, only a little more time is introduced to evaluate a situation defined in hierarchical style.

Then, in both versions, we invoked m1() 10000 times with $k(k = 5i, i = 0 \sim 6)$ activated layers (or union a context containing k different context entries for the $ContextJ+$ version), and recorded the accumulating invocation time

[11] $ce_i = \langle\langle \text{“}e1\text{”}, \text{“}sd\text{”}+i, i\rangle, d^U\rangle (i = 1 \sim 30)$.

as shown in Fig.6. We can easily find that:(1) the invocation times for both *ContextJ∗* and *ContextJ+* (as well as their difference) are near linear with respects to the number of activated layers; (2) our current implementation of *ContextJ+* requires more time (with a ratio around 13 times) than *ContextJ∗* does. This extra overhead mainly comes following aspects:(a) the evaluation process of *ContextJ+* requires a extra step to evaluate all situations on which partial methods are defined. (b) the structure of `ContextEntry` as well as its operations are more complex and time consuming. From the figure we could also found that *ContextJ+* consumes over 20 times more time than *ContextJ∗* does for $k = 0$, which is much higher than the average ratio (13 for $k > 0$). This is caused by the fact that our current implementation would go through all situations even if the activeContext is empty (as shown in Fig.5(b)).

In the second experiment we try to show how the number of sub-situations and the structure of a situation would affect the evaluation process of *ContextJ+* in term of situation evaluation time. Like in the first experiment, we implemented (in *ContextJ+*) a class with one *int* field f1 and a root method m1() which just increases f1 by one; the same thirty different context entries $ce_1, ce_2, ..., ce_{30}$ (simple situations) were predefined as well. Unlike in the first experiment, this time we only defined one partial methods on top of a single `And_Situation`. Two styles of `And_Situation` (as shown in Fig.7(a)and Fig.7(b)) were evaluated. In the flat style, the `And_Situation` was built directly on top of k sub-situations; while the hierarchical style built the `And_Situation` in a layered way where each leaf node is one of the provided simple situations. We built classes for $k = 0, 5, 10, 15, 20, 25, 30$ and for each k we invoked m1() 10000 times and recorded corresponding accumulating situation evaluation times as shown in Fig.7(c).

6 Conclusion and Future Work

In this paper, we introduced a formal context model which enriches Context-oriented Programming with a well-structured context representation. Also, we showed the implementation details of the model in *ContextJ+*. With the enhanced context model, programmers can describe contexts with different types of values and specify the temporal aspect of context. We further replaced with and without of COP with new and more powerful operations, which provided programmers with more flexibilities to manage activated context (i.e., the activeContext field). In *ContextJ+*, partial methods are not defined on each single layer but on many different situations and their combinations; and the evaluation order of multiple active partial methods can be explicitly specified so that the behavior of an invoked method becomes predictable.

In the near future, our works will focus on following aspects: first, as mentioned in in Sec.5, we will adopt the idea of event-based context(layer) (de-)activation proposed by *JCop*[7] and *EventCJ*[11] to our current implementation; second, we will also explore the mechanism for specifying and detecting conflicts based on our context model; in addition, we will try to implement a new COP language enhanced with our proposed context model by introducing new concise language syntaxes as well as its own compiler or runtime-environment.

Acknowledgment. This work was supported by the 973 Foundation of China under Grant No. 2009CB320702; the 863 Hi-Tech Research and Development Program of China under Grant No.2012AA011205; the National Natural Science Foundation of China under Grant 61073031,61021062.

References

1. Dey, A.K.: Understanding and using context. Personal Ubiquitous Computing 5, 4–7 (2001)
2. Schmidt, A.: Ubiquitous Computing - Computing in Context. PhD thesis, Lancaster University (2003)
3. Hirschfeld, R., Costanza, P., Nierstrasz, O.: Context-oriented programming. Journal of Object Technology 7, 125–151 (2008)
4. Stevens, S.S.: On the theory of scales of measurement. Science 103, 677–680 (1946)
5. Desmet, B., Vallejos, J., Costanza, P.: Layered design approach for context-aware systems. In: 1st VaMoS 2007 (2007)
6. Appeltauer, M., Hirschfeld, R., Haupt, M., Masuhara, H.: Contextj: Context-oriented programming with java. Information and Media Technologies 6, 399–419 (2011)
7. Appeltauer, M., Hirschfeld, R., Masuhara, H., Haupt, M., Kawauchi, K.: Event-Specific Software Composition in Context-Oriented Programming. In: Baudry, B., Wohlstadter, E. (eds.) SC 2010. LNCS, vol. 6144, pp. 50–65. Springer, Heidelberg (2010)
8. Appeltauer, M., Hirschfeld, R., Haupt, M., Lincke, J., Perscheid, M.: A comparison of context-oriented programming languages. In: International Workshop on Context-Oriented Programming, COP 2009, pp. 6:1–6:6. ACM, New York (2009)
9. Wan, K., Alagar, V.S., Paquet, J.: Lucx: Lucid enriched with context. In: PLC, pp. 48–56 (2005)
10. Tong, X., Paquet, J., Mokhov, S.A.: Complete context calculus design and implementation in gipsy. CoRR abs/1002.4392 (2010)
11. Kamina, T., Aotani, T., Masuhara, H.: Eventcj: a context-oriented programming language with declarative event-based context transition. In: Proceedings of the Tenth International Conference on Aspect-Oriented Software Development, AOSD 2011, pp. 253–264. ACM, New York (2011)

Analysis of the Square Pillar Electromagnetic Scattering under the PML Absorbing Boundary Condition

Xiangfang Mao, Jie Jin, and Jinsheng Yang

School of Electronic Information Engineering, Tianjin University, Tianjin, 300072, China
{maoxiangfang,jinjie,jsyang}@tju.edu.cn

Abstract. When solving the electromagnetic issues, the Finite Difference Time Domain method is proposed. It is a simple and effective solution to calculating the dispersion and radiation of the electromagnetic wave in time domain. However, it only could be used in the limited space area as the capacity of computer memory has limitation. Thus, the perfectly matched layer absorbing boundary condition is necessary to simulate the open areas electromagnetic issues. Avoiding the human error accumulation, the numerical stability conditions should also be introduced in the electromagnetic scattering simulation. When the researchers is considering the above mentioned factors, the simulation results must be get faster and also be more accurate.

This study is based on the principle of the finite difference time do-main method (FDTD), which is widely applied in the electromagnetic calculation, on the conditions of reasonable the appropriate baseband Gaussian pulse excitation source choice and also setting a Perfectly matched layer (PML) absorbing boundary conditions. Give full consideration to the numerical stability conditions, it should select the appropriate time step and space step. This paper simulates the TM wave scattering in the two-dimensional space by Matlab, bring out the electromagnetic wave scattering situation of square cylindrical.

Keywords: PML Absorbing Boundary Condition, FDTD, Scattering, Numerical Stability.

1 Introduction

When solving the electromagnetic issues, Finite Difference Time Domain method is first proposed by K. S. Yee in 1966 [1]. It gets the explicit electromagnetic field recurrence equation by central difference discretizing the Maxwell's curl equations, which are following the Faraday's electromagnetic induction theorem and Ampere circuital theorem, in space and time. FDTD method should also be noted that in addition to taking into account the application of the method, a key problem is that it sets termination of the problem in the propagating space by absorbing boundary conditions. J. P. Berenger proposed perfectly matched layer (referred to as PML), which has also been widely used in the calculation of the time-domain finite difference method in 1994 [2–4]. The basic idea is to split the field components in the absorbing boundary area, and each split field components assigned to different loss, so that the

Q. Zu, B. Hu, and A. Elçi (Eds.): ICPCA-SWS 2012, LNCS 7719, pp. 389–395, 2013.

boundary of FDTD grid to get a non-physical consumption absorbing medium. Under certain conditions, simulated area and fully matching layer can completely match as well as matching layer internal. In the simulation area, external electromagnetic waves can get in lossy media without reflection, attenuate during propagation. Thereby effectively absorb the external wave that is transmitted from the simulation area. Reference 5 compared the PML absorbing boundary conditions with Mur absorbing boundary conditions to get the conclusion is that the latter runs faster while has a relatively simple program and cost less memory. But its absorption characteristics and algorithm accuracy is poor [6]. It is suitable for less demanding system, for example, waveguides, microstrip antennas and microwave circuits, etc. In reference 7, we could obtain the FDTD grid of cylindrical and spherical formula derivation under PML conditions. It applied complex coordinate stretching methods and extended to two-dimensional and three-dimensional grid.

This paper chooses a simple square cylindrical as an example, when calculating electromagnetic problems in the application of finite difference time domain method. It fully considers the numerical stability, with setting reasonable time step and space step of the grid, simulates scattering of TM electromagnetic waves in two-dimensional free space under simulation. It shows that the PML absorbing boundary conditions can prevent the electromagnetic waves reflection phenomenon occurs on simulation grid boundary, and will not affect the propagation of electromagnetic waves in the mesh inside also. It provides a guarantee to get an accurate result in electromagnetic research.

2 Excitation Source

As using FDTD method to solve electromagnetic problems, both medium scattering, absorption and coupling problems, it is concerned about the simulation of the studied medium in enough grids. Moreover, it has another important factor is that simulate the appropriate incident wave function introduced for the application of the FDTD method.

The excitation source signal functions divide into two categories based on their change over time: one is that the source changes with time called as time-harmonic field sources; the other is pulse source that is pulse form with time changed.

Commonly used time-harmonic field sources are:

Sinusoidal excitation source

$$g(t)=\begin{cases}\sin(\omega t) & t\geq 0\\ 0 & t<0\end{cases} \tag{1}$$

Cosine excitation source

$$g(t)=\begin{cases}\cos(\omega t) & t\geq 0\\ 0 & t<0\end{cases} \tag{2}$$

Commonly used pulse source are:

Baseband Gaussian pulse source

$$g(t) = \exp\left[-\frac{4\pi(t-t_0)^2}{\tau^2}\right] \tag{3}$$

Modulated Gaussian pulse source

$$g(t) = -\cos(\omega t)\exp\left[-\frac{4\pi(t-t_0)^2}{\tau^2}\right] \tag{4}$$

Differential Gaussian pulse source

$$g(t) = (t-t_0)\exp\left[-\frac{4\pi(t-t_0)^2}{\tau^2}\right] \tag{5}$$

Raised cosine pulse source

$$g(t) = \begin{cases} 0.5\times\left[1-\cos\left(\frac{2\pi t}{\tau}\right)\right] & 0 \le t \le \tau \\ 0 & other \end{cases} \tag{6}$$

This paper chooses a baseband Gaussian pulse source as the excitation source to simulate PML absorbing boundary conditions.

3 Numerical Stability Conditions

FDTD is an explicit format differential algorithm. It is to calculate the variation of the electromagnetic field within the grid space by the time step, so the time step Δt and the space step Δx, Δy and Δz should follow certain rules, or stability problems will occur. It not caused by error accumulation, but it's due to the destruction of electromagnetic wave propagation causality as artificially setting time step and space step. In 1975, Taflove and others discussed the numerical stability of the Yee difference scheme and deduced the courant stability conditions, called as numerically stability conditions. The conditions gave the relationship between the time step and space step, its three-dimensional form is as follows:

$$\Delta t \le \frac{1}{v\sqrt{\left(\frac{1}{\Delta x}\right)^2+\left(\frac{1}{\Delta y}\right)^2+\left(\frac{1}{\Delta z}\right)^2}} \tag{7}$$

The formula can reflect the physical meaning of the stability condition that the time step size shall not be longer than the time that electromagnetic wave propagate one space step cost, otherwise it will destroy the causality.

If uniform cubic grid was chosen, in the n ($n \geq 1$) dimensional space, the numerical stability condition is,

$$\Delta t \leq \frac{\Delta s}{v\sqrt{n}} \tag{8}$$

4 PML Absorbing Boundary Condition

As finite difference time domain method is applied, it proposed absorbing boundary conditions to solve the contradiction between the finite capacity of computer memory and the unlimited extending physical space as well as the accuracy requirements. It is because that too high-accuracy absorbing boundary conditions will reduce the efficiency of FDTD. However, low-accuracy absorbing boundary conditions will reduce the FDTD accuracy and the authenticity of results. Therefore, it is one of the key points to select the absorbing boundary conditions accurately and properly for FDTD application. Absorbing boundary conditions must do some special processing to the limited space boundary, so keep the electromagnetic waves traveling at the boundary, with no reflection phenomenon. It seems to be totally absorbed by the border and will not affect the distribution of the internal field [8].

In order to overcome the limitations of the actual medium, Berenger constituted the matching layer with non-physical medium, so that the matching characteristics are independent of the frequency and angle of incidence. Assuming that the electrical conductivity and the magnetic permeability of the medium are σ and σ^* respectively, the parameter (σ_x, σ_x^*, σ_y, σ_y^*) are isotropic conductivity and magnetic permeability. When the conductivity and magnetic permeability of the medium parameters (σ_x, σ_x^*, *0, 0*) and (*0, 0,* σ_y, σ_y^*) are able to satisfy the following conditions, which makes the medium impedance and vacuum impedance matching, there will be no reflection phenomenon on the plane. It is perpendicular to the x-axis and y axis that the electromagnetic wave incident to. The boundary medium parameters of four corners area is (σ_x, σ_x^*, *0, 0*) and (*0, 0,* σ_y, σ_y^*), so that the plane wave can also be non-reflective traveling on the boundary.

5 Simulation Result

The study is using Matlab to simulate propagation of TM wave in 2D free space [9]. Given full consideration to the PML absorbing boundary conditions, choose the baseband Gaussian pulse source as the excitation source, which is shown in equation(3). Set t0 = 25s, τ = 8s, simulate the distribution of electric field Ez.

Mathematical modeling: number of the grid is 100*100. The space step is 0.005m which is defined as 1/20 of the wavelength. Time step is 8.33ps, which is satisfied with courant stability conditions. The actual pulse wave propagating space is 0.5m * 0.5m. And the pulse source position is setting on the grid coordinate (50, 50).

Analyze simulation results:
When time step T = 350,

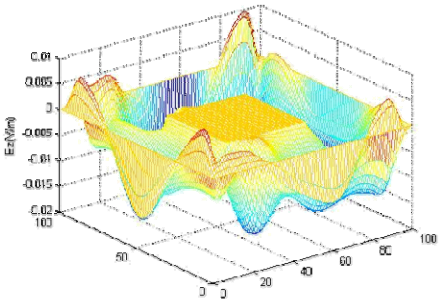

Fig. 1. T=350, Electric field distribution

When time step T = 400,

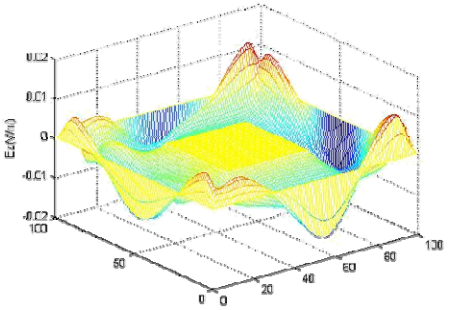

Fig. 2. T=400, Electric field distribution

When time step T = 680,

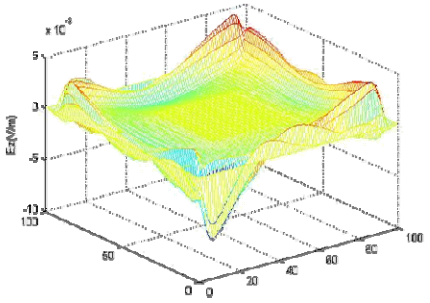

Fig. 3. T=680, Electric field distribution

When time step T = 700,

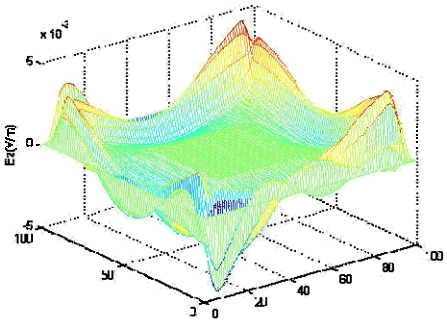

Fig. 4. T=700, Electric field distribution

When time step T = 750,

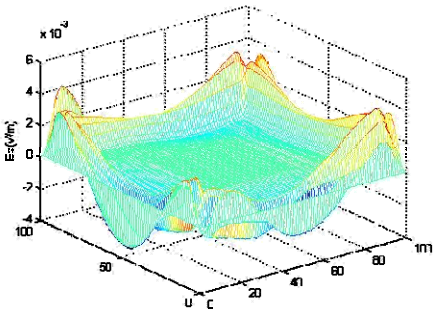

Fig. 5. T=750, Electric field distribution

The conclusions can be got from Figures 1 to 5 that the electromagnetic waves have been gradually absorbed by boundary with the time step increases. Only in four corners of the space, the electromagnetic wave is not completely absorbed.

6 Conclusion

When study the electromagnetic scattering calculation, we use the finite difference time domain method (FDTD). Taking perfectly matched layer (PML) absorbing boundary conditions into account, the contradictory, which is caused by the finite capacity of computer memory and the unlimited extending physical space as well as the accuracy requirements, is effectively solved. As simulating the electromagnetic wave scattering, setting the PML absorbing boundary conditions can control the electromagnetic wave absorption of the grid boundary. Thus, it will get the desired effect

that it is neither affect the grid internal propagation of electromagnetic waves, nor propagate to the boundary.

In order to verify the effectiveness of this approach, the baseband Gaussian pulse source is as the excitation source, with a square cylindrical scatterer, which is placed in the free space simulation environment. Fully considering the numerical stability conditions for grid constraints, we use Matlab to simulate the two-dimensional TM wave scattering. The results can adequately reflect that the electromagnetic waves in the grid can be completely absorbed by boundary with non-reflection, and the boundary does not affect the propagation of electromagnetic waves in the internal space.

Acknowledgement. This work is supported by National Science and Technology Major Project (No. 2010ZX03005-001).

References

1. Yee, K.S.: Numerical solution of initial boundary value problems involving Maxwell's equations in isotropic media. IEEE Trans. Antennas Propagation 3(14), 302–307 (1966)
2. Berenger, J.P.: A perfectly match layer for the absorption of electromagnetic waves. Journal of Computational Physics 114, 185–200 (1994)
3. Berenger, J.P.: Three-dimensional perfectly matched layer for the absorption of electromagnetic waves. Journal of Computational Physics 127, 363–379 (1996)
4. Yang, X.D., Bai, Y., Feng, L.L., Li, Z.N.: Mend on the Implementation of PML-FDTD Using Z-transform. Microwave Journal 8, 36–39 (2010)
5. Mur, G.: Absorbing boundary conditions for the finite-difference approximation of the time-domain electromagnetic-field equations. IEEE Trans. Electromagnetic Compatibility 23(4), 377–382 (1981)
6. Xu, H., Huang, H.L., Chen, Y.Q.: Comparison of Absorbing Boundary Conditions of FDTD in High Frequency Electromagnetic Field Simulation. In: The Ninth International Conference on Electronic Measurement & Instruments, ICEMI 2009, vol. 1, pp. 128–131 (2009)
7. Teixeira, F.L., Chew, W.C.: PML-FDTD in Cylindrical and Spherical Grids. IEEE Microwave and Guided Wave Letters 7, 285–287 (1997)
8. Yi, Y., Chen, B., Chen, H.L., Fang, D.G.: TF/SF Boundary and PML–ABC for an Unconditionally Stable FDTD Method. IEEE Microwave and Guided Wave Letters 17, 91–93 (2007)
9. Tian, T.: FDTD Arithmetic Programming in Electromagnetic Field using Matlab Language. Radio Engineering of China 6(38), 38–46 (2008)

A Framework Based on Grid for Large-Scale Risk Files Analysis

Jiarui Niu, Bin Gong, and Song Li

School of Computer Science and Technology, Shandong University, Jinan, China
{Karryniu1990,lisong.cruise}@gmail.com, gb@sdu.edu.cn

Abstract. With the development of the internet, the number of malicious programs rises observably, which has become one of the main threats to national basic network, information system and so on. Besides, the analysis of malicious programs has a sharp contradiction between accuracy and speed, and how to analyze malicious programs quickly and efficiently has become a popular research direction in safety field. This paper proposes an analysis framework that applies grid technology, the core of the framework is to design an optimized system architecture and an efficient scheduling algorithm to be able to quickly scheduling and analyze risk files in parallel to improve the efficiency of risk files analysis greatly. In order to exhibit the framework better, we develop a set of portlets to present analysis framework into the web portal framework.

Keywords: malicious program, risk file, grid technology, optimization scheduling.

1 Introduction

The rapid and thriving development of the internet has changed the mode of people's work and life little by little. But malicious code as a program has ensued and has brought a lot of unsafe factors to people's digital life. In addition, the growth rate of the malicious programs is amazing, according to incompletely statistics, the kind of networks malicious programs has exceeded 33 million in 2009. So the detection and prevention of malicious programs becomes more and more meaningful.

"Grid" computing has emerged as an important new field, distinguished from conventional distributed computing by its focus on large-scale resource sharing, and, in some cases, high performance orientation [1]. Grid Computing aims to "enable resource sharing and coordinated problem solving in dynamic, multi-institutional virtual organizations" [2].

2 System Architecture

The risk files analysis framework based on grid applies the classic distributed parallel B/S structure, it enables users to visit portal through browser to submit suspicious files to servers at any time and any place. The layout of the servers in the framework applies the grid structure which can analyze files efficiently in parallel. The overall structure of the framework is as follows (see Fig.1).

Q. Zu, B. Hu, and A. Elçi (Eds.): ICPCA-SWS 2012, LNCS 7719, pp. 396–399, 2013.

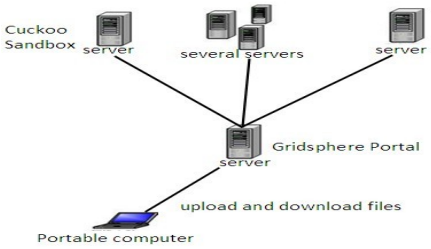

Fig. 1. Overall Structure of System

On the basis of the overall structure, we designed the realization architecture of the analysis framework. According to the realization architecture, the analysis framework consists of four modules, such as portal module、distribution module、sandbox module and collection module. These four modules contact with each other through the Network File System to realize the corresponding function and constitute a unified whole (see Fig.2).

A. The Portal Module

The portal module is mainly designed as a communication bridge to transfer information between the user and the other parts (see Fig.3). The key functions of the portal module are described as follows:

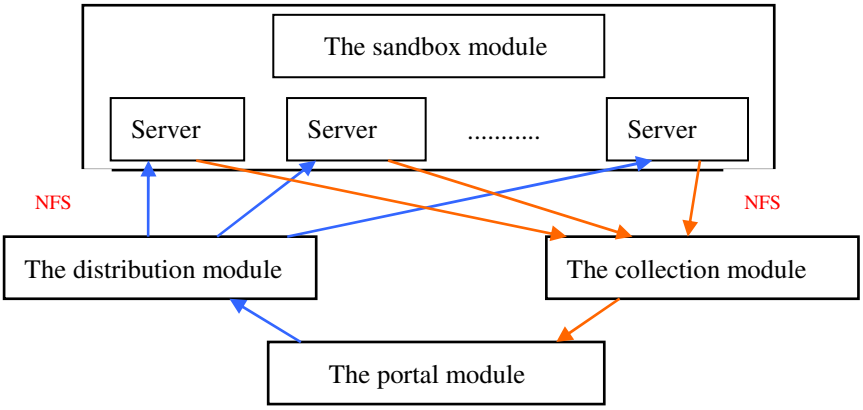

Fig. 2. System Architecture

It can receive the suspicious files and upload these files to a corresponding folder that can make these files to be obtained by the distribution module easily, and at the same time register these files by the md5 value in a XML file. In addition, it provides a platform that users can view the safety information of related files, and provide a way to download analysis results of these files from a designated folder.

In this module, the key point of the design is that different files have different MD5 values, and every suspicious file applies the MD5 value to register and as the index in the course of file analysis.

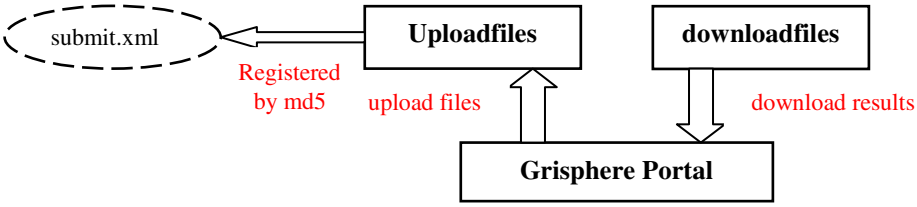

Fig. 3. The Portal Module

B. The Distribution Module

For all the suspicious files that are submitted to the portal module, we should rely on a kind of scheduling mechanism to distribute them to every application server reasonably and effectively in order to analyze them quickly to improve the efficiency of the whole system. So the emphasis of this distribution module is to design and develop an efficient scheduling algorithm.

In this module, we write a script as a distribution engine to realize this algorithm, the scheduling benchmark that we designed is described here:

In a single application server, the files that are waiting to be analyzed in the designated folder will form a queue, and the number of the files will be displayed in the log file of Cuckoo. The script will view the number of every cuckoo first before distributing files. The number of the files in the queue is to be the main basis of scheduling. In addition, we also use the CPU number of the machine、the number of the windows sandbox engine and memory size as the weighted factors in order to get the optimal allocation strategies.

C. The Sandbox Module

The sandbox module is mainly responsible for analyzing suspicious files that are distributed by the distribution module. This module consists of several servers and applies the grid structure. Also we should develop several scripts to assist in analyzing. These scripts in every server of the sandbox module execute every once in a while. The suspicious files are shared between the distribution module and the sandbox module through the way of NFS (Network File System).

A single server in the sandbox module must be a physical server. Sandbox as a scheduling engine of sandbox analysis, calls VirtualBox to control the open and close of windows virtual machines in order to automatically analyze malicious files, and the malicious files and relevant results in the virtual machines is shared between virtual machines and the core part through Samba(see Fig.4).

D. The Collection Module

The collection module is designed to collect all the analysis results from every server in the sandbox module to a designated folder in the collection module through the execution of the script. The analysis results are shared between the collection module and the sandbox module through the way of NFS (Network File System). At the same time, every analysis result will be registered in a file by the MD5 value in order to produce the corresponding download link according to the MD5 value to allow users to download related analysis results (see Fig.5).

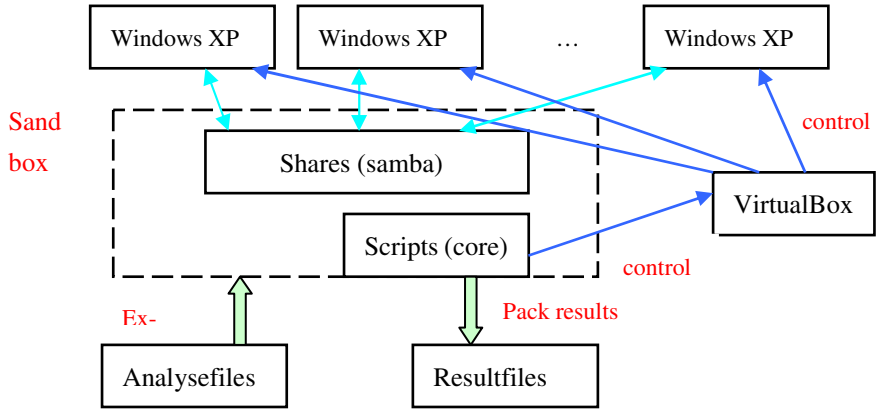

Fig. 4. The Sandbox Module

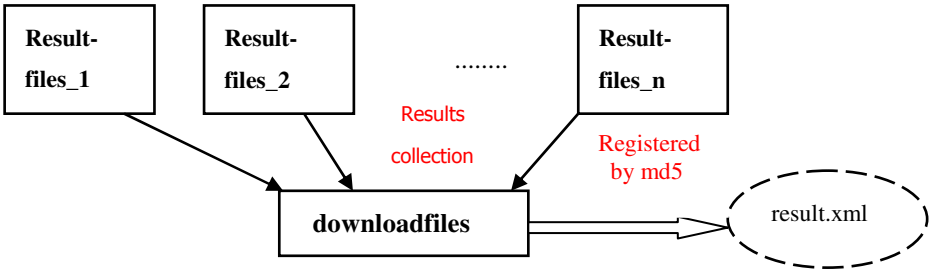

Fig. 5. The Collection Module

3 Conclusion

The purpose of the design and development of the analysis framework is to detect and analyze suspicious files efficiently, realize the effective prevention and control of suspicious files and reduce the adverse influence to users. In this paper, we concentrated on building a analysis framework that adopted the grid structure, and developed a collection of portlets based on the framework to control the analysis framework. In a word, the analysis framework is efficient、flexible and extensible.

References

1. Foster, I., Kesselman, C., Tuecke, S.: The Anatomy of the Grid: Enabling Scalable Virtual Organizations. International Journal of High Performance Computing Applications 15(3), 200–222 (2001)
2. Foster, I., Kesselman, C., Nick, J., Tuecke, S.: The Physiology of the Grid: An Open Grid Services Architecture for Distributed Systems Integration. Globus Project (2002)

A Cache-Sensitive Hash Indexing Structure for Main Memory Database

Xiaoqing Niu[1], Xiaojia Jin[2], Jing Han[1], Haihong E[1], and Xiaosu Zhan[1]

[1] Computer Department, Beijing University of Posts and Telecommunications, Beijing, China
[2] China Mobile Group Hebel Co., Ltd.

Abstract. To satisfy the need of data processing speed, and increase cache hit rate of traditional hash indexing structure in Main Memory Database (MMDB), a page-based cache-sensitive hash indexing structure is proposed in this article. While maintaining the processing speed, storage efficiency, this structure greatly enhances the processor cache hit rate. This article describes the design and implementation of this cache-sensitive hash indexing structure in detail. After that, theoretical analysis and simulation experiments are performed. We come to a conclusion that for real MMDB, this new hash structure improves cache hit rate greatly and the whole database becomes more effective than traditional ones.

Keywords: cache-sensitive, MMDB, hash indexing, page mapping, cache hit rate.

1 Introduction

As many applications require much higher data operation speed, traditional Data Resident Databases(DRDBS) such as SQL Server, Oracle become outdated gradually because they have low I/O read and write speed and can not reach satisfactory operation efficiency. Difference of read and write speed between memory and disk is very large, so since 1980s, people have tried to move the whole database from disk into main memory to satisfy new applications. This kind of databases are called Main Memory Databases(MMDBs).

To satisfy the demand for real time processing of huge amounts of data [1,2], people have to try to use a faster and more efficient storage medium. Cache is the low-latency memory storage medium between the processor and main memory, and it can automatically store recently accessed memory data. Speed of access to cache is two orders of magnitude faster than the speed of access to main memory. How to design a indexing structure suitable to cache and to make cache miss rate low become the key problems to improve database operation efficiency [3,4].

The query and update performance of MMDBs varies from different data structures in main memory. A good data structure needs concerns to system usage, main memory capacity and cache property. Nowadays many existing works achieve higher performance for specific applications by using approximate data structures, including region-area structure, shadow memory structure, sequence list structure, search tree

Q. Zu, B. Hu, and A. Elçi (Eds.): ICPCA-SWS 2012, LNCS 7719, pp. 400–404, 2013.

structure [5,6] and hash table structure [7,8]. Among them, hash indexing structure become the first choice of many lightweight databases because of its flexible memory footprint, fast access speed and less additional space allocation. Among real database queries over a small period of time, queries to the same data element or data elements with nearby key values(nearby queries) are very common. Many works propose corresponding methods to improve cache hit rate of databases based on different basic memory structures, including CST-tree [9] and HT-tree [10]. In this paper, we combine this feature of real MMDB queries with hashing structure, and propose a new page-based hash indexing structure. While maintaining the advantages of hash indexing structure in processing speed and storage space, this new structure improves processor cache hit rate a lot.

2 Design of Hash Structure for Cache-Sensitive MMDB

2.1 Problem of Traditional Hash Structures

Traditional hash table indexing utilizes a fixed hash function to distribute data elements into different buckets averagely. Data elements inside each bucket are arranged by sequence lists. When indexing, key value of a data element is transferred to Hash Function to get the bucket number which contains this data element. The actual address of the data element is obtained after searching sequence list of that bucket. Operations like insertion, deletion, modification and query can be executed directly after that.

Traditional hash structure doesn't work well in handling nearby queries, since traditional hash structure distributes data elements with nearby key values into different buckets to the greatest extent, in order to make data elements distribute averagely in different buckets, thus ensures high query performance. Because data elements with nearby key values are distributed in different memory cells, they can not be well cached by processors in traditional hash structure. What processors cache is just some data elements in the same bucket, these cached data are useless in improving cache-hit rate of nearby queries.

2.2 Page-Based Hash Indexing

Based on the characteristics of our Cache-Sensitive MMDB, we propose a new hash structure that makes cache miss rate decease a lot. Fig.1 illustrated this new Page-based hash table indexing structure. The main idea of this new structure is that firstly do page mapping to the main database and ensure most nearby data elements are mapped into the same page. This new hash structure uses pages as hash indexing unit instead of data elements, so data elements of the same page are indexed into the same bucket and then data elements of the same page are distributed continuously in main memory.

To better utilize cache of the database to improve query efficiency, we try to cache data elements with nearby key values when a data element is queried. It will gain high performance acceleration in our Cache-Sensitive MMDB. Taken into consideration

that we can traverse data elements in the same bucket easily when a data element is queried, the most directly way is to redefine Hash Function that distribute data elements with nearby key values into the same bucket. But this solution is quite bad, because it loses hash structure's advantage that all data distribute averagely between buckets. In our implementation, it may cause very large data burden in several buckets and make the whole system much less efficient. Here we propose a new page-based hash table structure. The basic idea of the new structure is to map data elements with nearby key values into the same bucket along with to ensure data's average distribution. We firstly build pages for all legal data elements (no matter whether they already have legal values). In this step we map some data elements with nearby key values into the same page, and the relative address of each data element in the page is linear to its key value. When building hash indexing structure, we use the page number and its physical pointer instead of original key value and data element. Thus when query data elements with nearby key values, data can be directly found in cache, these queries acquire higher speed.

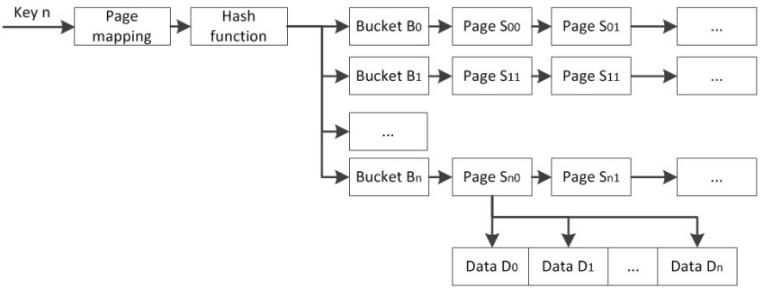

Fig. 1. Page-based hash table indexing structure

The purpose of paging is to distribute data elements with nearby key values into the same bucket to facilitate data caching. We divide all legal data elements into pages based on their key values. Each page contains a fixed amount of data elements, and the size of each page is smaller than but close to the processor cache size to the greatest extent. This property ensures that each page can be moved into cache freely. We use pages as our basic processing unit. When the indexing system acquires the queried key value n, corresponding page number sn is firstly computed by page mapping function. This function is predefined in the paging process and would a very simple piecewise function. After that, new Hash Function maps the page number into corresponding bucket number bn where the actual physical address of that page is stored. We can get actual physical address s of page sn in the sequence list of the bucket. This process is efficient than traditional hash indexing, because pages are much less than key values. After all of that, actual data element can be queried by the relationship of relative address offset to that page and key value.

The new hash structure uses pages as basic processing unit of the system. Operations like insertion, deletion and modification will firstly find corresponding page number, and then do these operations inside that page. In page mapping process correspondence between key value and page number is determined, but there is no memory allocation. In other words, if a page has no meaningful data elements, it's only a

logic concept and doesn't have actual physical address. Once an insertion operation is executed in a new page, we allocate memory for the whole page directly while in traditional hash structures, we only allocate memory for the data element. Meanwhile, after deletion operator is performed to a data element, we check whether there are any meaningful data elements in that page. If no meaningful data element is found, we free the whole page from memory. Note here in a single query process, our new page-based hash structure needs extra operations, thus has no advantage against traditional method. But for amounts of queries in many real MMDBs, it would achieve good performance.

3 Experimental Results

To verify the advantage of our page-based hash table structure, we do simulation in our Cache-Sensitive MMDB. At first, we build a database with 1,000,000 data elements, and then we build traditional hash indexing structure and our page-based hash indexing structure. In the experiment, we use two different types of query sequence: random query sequence and our real database query sequence (based on our real system). To generate random query sequence we use query to random data element in the database at any time point. And for real database query sequence, we use the record of real queries in our system over a very long time. In each group of the experiment, we record the time costs of the two hash structures to handle at most 500,000 queries. Experiment results are showed in Fig.2.

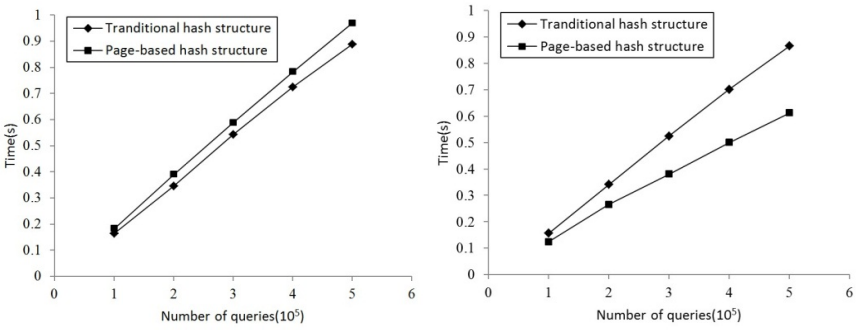

Fig. 2. Performance comparison between traditional hash structure and page-based hash structure for (left) random query sequence and (right) real database query sequence

We can see from these results that in random query sequence handling, page-based hash structure is slightly less efficient than traditional hash structure. This is because the process to handle a single query in page-based hash structure is more complicated. Extra works in paging and cache management decrease the query efficiency. But to handle real database query sequence, the efficiency of page-based hash structure is 1.1-1.4 times that of traditional hash structure. This finding implies that for our real database query sequence, page-based hash structure uses cache more efficiently, and this agrees with our theoretical analysis.

4 Conclusion

This paper introduces storage and data structure of MMDB, and proposes a new page-based hash table indexing structure based on traditional one. It achieves better performance in our real MMDB. We use simulation experiments to verify our assumption. We come to a conclusion that for random query sequence, page-based hash structure is slightly less efficient than traditional hash structure. However, in our real MMDB, page-based hash structure improves cache hit rate a lot, thus improves the whole performance. This strategy can be directly combined with any existing hash indexing based structure, and we are approaching to plant it into other indexing structures(like HT-tree). Distributed Cache-Sensitive hash indexing structure is also a very important future work.

Acknowledgment. This work is supported by the National Key project of Scientific and Technical Supporting Programs of China (Grant No. 2009BAH39B03, 2012BAH01F02); the National Natural Science Foundation of China(Grant No.61072060); the National High Technology Research and Development Program of China Grant No. 2011AA100706);the Research Fund for the Doctoral Program of Higher Education (Grant No. 20110005120007); the Fundamental Research Funds for the Central Universities(2012RC0205, 2012RC0206); the Co-construction Program with Beijing Municipal Commission of Education; Engineering Research Center of Information Networks, Ministry of Education.

References

1. Lu, H.: A approach for distrubuted realtime main memory database. Dalian University of Technology (2008)
2. Zhang, Q.: Design and Implementation of realtime main memory database. Wuhan University of Science and Technology (2008)
3. Hu, J.: Design and Implementation of a main memory database spatial indexing. Huazhong University of Science and Technology (2009)
4. Sheng, Y., Lu, Y.: A data management method for cache-sensitive main memory database. Approaches of Computer Technology and Application 08 (2007)
5. Xu, Y., Li, J.: Organization optimization of realtime memory database. Taiyuan University of Science and Technology (2008)
6. Oyang, W., Li, C., Zhong, S.: Memory database indexing technology research. Science and Technology Innovation Herald 29 (2008)
7. Luo, Q., Luo, L.: Orgnization method for main memory database. Computer Applications 28 (2008)
8. Yuan, P., Pi, D.: Design and Implementation of Hash Index Used in Main Memory Database. Computer Engineering 18 (2007)
9. Lee, I.-h., Shim, J., Lee, S.-g., Chun, J.H.: CST-Trees: Cache Sensitive T-Trees. In: Kotagiri, R., Radha Krishna, P., Mohania, M., Nantajeewarawat, E. (eds.) DASFAA 2007. LNCS, vol. 4443, pp. 398–409. Springer, Heidelberg (2007)
10. Wang, C., Chen, G., Dong, J.: Study of improved cache sensitive B+-tree. Computer Measurement & Control 11 (2006)

SCADA System Security, Complexity, and Security Proof

Reda Shbib, Shikun Zhou, and Khalil Alkadhimi

School of Engineering, University of Portsmouth, Portsmouth, UK
{reda.shbib,shikun.zhou,khalil.alkadhimi}@port.ac.uk

Abstract. Modern Critical infrastructures have command and control systems. These command and control systems are commonly called supervisory control and data acquisition (SCADA). In the past, SCADA system has a closed operational environment, so these systems were designed without security functionality. Nowadays, as a demand for connecting the SCADA system to the open network growths, the study of SCADA system security is an issue. A key-management scheme is critical for securing SCADA communications. Numerous key-management structures for SCADA also have been suggested. 11770-2 Mechanism 9 Key establishment Protocol has been used in SCADA communication however a security proof for the 11770-2 Mechanism 9 protocol is needed. The purpose of this paper is to provide a general overview about SCADA system, and its related security issues. Furthermore, we try to investigate the importance of key management protocol and the need of formal security poof.

Keywords: SCADA, key management, 11770-2 Mechanism 9, Formal security poof.

1 Introduction

SCADA systems are used to control and monitor assets where central data acquisition is as important as control[1, 2] .These systems are used in distribution systems such as water distribution and wastewater collection systems, oil and gas pipelines, electrical utility transmission and distribution systems, and rail and other public transportation systems. SCADA systems integrate data acquisition systems with data transmission systems and HMI software to provide a centralized monitoring and control system for numerous process inputs and outputs. SCADA systems are designed to collect field information, transfer it to a central computer facility, and display the information to the operator graphically or textually, thereby allowing the operator to monitor or control an entire system from a central location in real time. Based on the sophistication and setup of the individual system, control of any individual system, operation, or task can be automatic, or it can be performed by operator commands [1, 3].

Q. Zu, B. Hu, and A. Elçi (Eds.): ICPCA-SWS 2012, LNCS 7719, pp. 405–410, 2013.

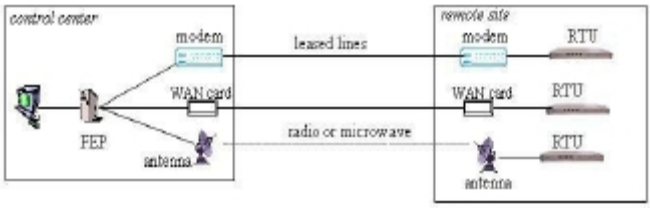

Fig. 1. Simple SCADA System

2 SCADA Vulnerabilities

2.1 SCADA System Vulnerabilities

Critical infrastructures are facing important threats as the development in the use of SCADA systems and the integrated networks. In addition, the complicated infrastructure offers huge capabilities for operation, control, and analysis; it also increases the security risks due to cyber vulnerabilities The Development of SCADA systems have also attract-ed some issues about cyber-attacks. The SCADA industry is transitioning from a legacy environment, in which systems were isolated from the Internet and focused on reliability instead of security, to a modern environment where networks are being leveraged to help improve efficiency. In addition the connectivity of SCADA networks with outside net-works will continue to grow, leading to an increasing risk of attacks and the significant need to advance the security of these networks [4, 5].

Furthermore, open communication protocols such as Modbus and DNP3 are increasingly used to achieve interoperability, exposing SCADA systems to the same vulnerabilities that threaten general purpose IT systems[6]. The integration of SCADA networks with other networks has made SCADA vulnerable to various threats [5]. Many SCADA protocols use TCP/IP (Transmission Control Protocol/Internet Protocol) and provide no additional protection. Vulnerabilities in the TCP/IP protocol include IP spoofing and man-in-the middle attacks. Additionally, the standardization of software and hardware used in SCADA systems potentially makes it easier to mount SCADA-specific attacks, as was evident in thecae of Stuxnet. Stuxnet was a piece of malware created to specifically target control systems [6, 7].

2.2 Security Concerns

Most of Countries are becoming significantly reliant on automated Supervisory Control and Data Acquisition (SCADA) systems to support deliver critical services. SCADA systems, which once used proprietary communication mechanisms, are using standard protocols, such as DNP3 [8]. Security incidents have significantly increased since 1988 and recorded by CERT to 137.529 incidents in 2003 (CERT/CC Statistics 1988-2005).The necessity to make SCADA systems more secure has therefore been classified as a significant field of research. One of the most important security

requirements for SCADA systems is that communication channels must be more secured. Secure keys need to be established before cryptographic techniques can be used to secure communications [9].

3 Formal Security Proof

3.1 Security Proofs

Security proofs were major concerns of many of research in last few years. To ensure that a protocol or a software have a certain requested properties, is an important issue. This task has to be done by formal reasoning instead of examinations and simulations, as the latter approach is not as comprehensive as the formal one [10].

Security proofs are methods to validate the security of a protocol. A reductionist security proof of a protocol helps to show that the security in the proof model is related to the cryptographic primitives used. A security proof attempt to show that a protocol meets the defined goals for the protocol in the security model used [11].

3.2 Protocols Verification Approaches

Protocol verification has mainly two possible approaches: The formal model and the computational model

- In the first model, we are in a very idealized setting; thus this can be efficiently implemented in completely automated protocol verifiers.
- The second model inspires ideas from complexity theory and needs more human interference in proofs, and it is being automated only in very recent times [12].

These verification methods let us to discover and uncover design faults that can stay hidden for years. The purpose of the present paper is to investigate a proof of security on the 11770-2 Mechanism 9 protocol in the formal model.

The purpose of this protocol 11770-2 mechanisms 9 (ISO 1996) is to establish a long-term key shared between the nodes.

4 Protocol Description

The ISO 11770-2 standard has been published in 1996, and specifies a series of protcols for establishing shared secret keys using symmetric cryptographic techniques. The protocols in this standard use a many of different mechanism in order to ensure the freshness of the established keys, and offer several cryptographic assurances techniques of the established keys. [13]

We are mainly concerned about ISO 11770-2 mechanism 9 which used as a basis for the node-node key establishment protocol. This mechanism has chosen, as it is the best fit for SCADA systems. In the case of SCADA, it is more appropriate for the generation of keys to be performed by the external device, and not have keys generated by the nodes in the systems.

1. $B \rightarrow A:\ N_B$
2. $A \rightarrow S:\ N_A, N_B, B$
3. $S \rightarrow A:\ \{N_A, K_{AB}, B, Text1\}_{K_{AS}}$
   $\{N_B, K_{AB}, A, Text2\}_{K_{BS}}$
4. $A \rightarrow B:\ \{N_B, K_{AB}, A, Text2\}_{K_{BS}}$
   $\{N'_A, N_B, B, Text3\}_{K_{AB}}$
5. $B \rightarrow A:\ \{N_B, N'_A, Text4\}_{K_{AB}}$

Fig. 2. ISO 11770-2 Mechanism 9

Where, A and B are nodes that need to establish a key; NA is a nonce that is created by node A; NA′ is a second nonce created by node A; S is the server (representing the Key Distribution Centre); A → B is message sent from node A to node B; KAB is the shared key between node A and B ; {Text} KAB is the encryption of the message text, using the key KAB; Strings Text1 to Text4 are text messages.

5 Security Proof

The fact that a security proof depends on the model used. The security model will outline the aims for security, and the controls given to the opponent. The selection of the accurate model has the impact on the value of the security proof. In this section we try to investigate a security proof of 11770-2 mechanisms 9 protocol, it is assumed to use Bellare Rogaway model. Bellare Rogaway model has been developed and refined over many years, with some different versions, which has been used for different proofs. It is very important in any security proof to specify the adversarial model and a clear definition of security. We will follow in our developing the proof of Boyd, Choo and Mathuria.

5.1 Reductionist Security Proofs

Reductionist security proofs are a significant part of generating valuable and safe cryptographic protocols. The aim of provable security is to demonstrate that a protocol will meet the security goals .The final outcome will be to say that breaking any of security properties will require an attacker to have broken a fundamental security primitive [14].

Several number models for security proofs performance of protocols have been pro-posed. The model that will be used as the starting point for the security proof of 11770-2 mechanisms 9, is the Bellare Rogaway model.

Cryptographic community is essential to validate security proofs. Many proofs have been found to have flaws, and it is necessary to be validated before it is established. Although the use of provable security techniques is not perfect, and does not promise a full security, they do offer important tools for helping to validate the security of a protocol [15].

6 Proposed Bellare Rogaway Model

Bellare Rogaway model permits the development of reductionist security proofs in order to validate that the desired protocol is secure, meeting the specified goals. The reductionist security proof will demonstrate that in order to breakdown the protocol, an adversary must attack the encryption function, which the protocol depends on. Thus by implementing the protocol using strong encryption algorithm the protocol will be more secure.

The security is defined as the advantage of the adversary in distinguishing session keys from random strings and is used to define the security of the protocol. Furthermore, a secure protocol must complete successfully with the principals accepting the session key if the adversary does nothing to interrupt the protocol.[16]

The Bellare Rogaway model has a strict definition of security (in distinguish ability of established keys from random keys). Protocol is supposed to be insecure if it employs the new key to encrypt any messages.As the entity authentication messages that form a part of the 11770-2 protocol use the established key, it will be classified as insecure in the Bellare Rogaway model, since the adversary can check whether authentication works for the string it has been given, if the string is the session key then the authentication check will work but if the string is a random string then the authentication will fail [16].

In this section we have introduced the Bellare Rogaway model for developing reduc-tionist security proofs. This model is a well-established approach for verifying security. We are going to use Bellare Rogaway model to create a reductionist security proof, which proves the security of the key establishment protocol 11770-2.

7 Conclusion

This paper provided a detailed discussion on critical infrastructures and the role crytographic mechanism protocol plays in their protection. We examined one of current protocol 11770-2 mechanisms and determined that the solutions are not sufficient for such an interconnected infrastructure. We provided our initial framework design for the security proofing of this protocol following the 'model' those we will use in the future.

Our future work will focus on the introducing the Bellare Rogaway Model for developing a reductionist security proofs. This model has been well established for verifying security .Next step is to show how the security goals in this model meet the set of security aims of 11770-2 mechanisms 9. We will use Bellare Rogaway model to create a reductionist proof which proves the security of the key establishment protocol.

References

1. Ning, C., et al.: SCADA system security: Complexity, history and new developments. In: 6th IEEE International Conference on Industrial Informatics, INDIN 2008, pp. 569–574 (2008)
2. Gold, S.: The SCADA challenge: securing critical infrastructure. Network Security 2009, 18–20 (2009)

3. Johnson, R.E.: Survey of SCADA security challenges and potential attack vectors. In: 2010 International Conference for Internet Technology and Secured Transactions (ICITST), pp. 1–5 (2010)
4. Donghyun, C., et al.: Efficient Secure Group Communications for SCADA. IEEE Transactions on Power Delivery 25, 714–722 (2010)
5. Rautmare, S.: SCADA system security: Challenges and recommendations. In: 2011 Annual IEEE India Conference (INDICON), pp. 1–4 (2011)
6. Stouffer, K., et al.: Guide to Supervisory Control and Data Acquisition (SCADA) and Industrial Control Systems Security. In: The National Institute of Standards and Technology, NIST (2006)
7. C. Office, The UK Cyber Security Strategy Protecting and promoting the UK in a digital world (2011)
8. Brewer, R.: Protecting critical control systems. Network Security 2012, 7–10 (2012)
9. Igure, V.M., et al.: Security issues in SCADA networks. Computers & Security 25, 498–506 (2006)
10. Goubault-Larrecq, J.: Towards Producing Formally Checkable Security Proofs, Automatically. In: IEEE 21st Computer Security Foundations Symposium, CSF 2008, pp. 224–238 (2008)
11. Carcano, A., Fovino, I.N., Masera, M., Trombetta, A.: Scada Malware, a Proof of Concept. In: Setola, R., Geretshuber, S. (eds.) CRITIS 2008. LNCS, vol. 5508, pp. 211–222. Springer, Heidelberg (2009)
12. Bresciani, R., Butterfield, A.: A formal security proof for the ZRTP Protocol. In: International Conference for Internet Technology and Secured Transactions, ICITST 2009, pp. 1–6 (2009)
13. ISO, Information technology — Security techniques — Key management, ISO/IEC (2008)
14. Stolbunov, A.: Reductionist Security Arguments for Public-KeyCryptographic Schemes Based on Group Action. Presented at the NISK (2009)
15. Koblitz, N.: Another Look of Provable Security. Journal of Cryptography 20, 37 (2007)
16. Dawson, R.: Secure Scada Communication (2008)

Cranduler: A Dynamic and Reusable Scheduler for Cloud Infrastructure Service

Xuanhua Shi, Bo Xie, Song Wu, Hai Jin, and Hongqing Zhu

Services Computing Technology and System Lab
Cluster and Grid Computing Lab
School of Computer Science and Technology
Huazhong University of Science and Technology, Wuhan, 430074, China
{xhshi,wusong,hjin}@hust.edu.cn,
{bxiecgcl,zhuhongqing1203}@gmail.com

Abstract. As an import trend of cyberspace in the future, cloud computing has attracted much attention from the IT industry. Many research institutions and companies have launched their own cloud platforms, which have virtual machine schedulers to manage the infrastructure resource pool. The virtual machine scheduling modules in these platforms are built in the platform and it is hard for developers to re-program. Since developers cannot design and implement special policies in the platform, the flexibility of the virtual machine scheduler is poor. Furthermore, the schedule architecture which has a firm and unchangeable interface is designed and customized for one kind of cloud platform. It leads to poor portability. To target the problems above, this paper presents a dynamic and reusable scheduling system for cloud infrastructure service, called Cranduler, which introduces the advantages of cluster schedulers to the virtual machine scheduling in cloud infrastructure. The scheduling policies of Cranduler could be dynamically configured by developers. Developers can easily insert the custom policy. In addition, Cranduler provides a set of unified interfaces to the cloud platform, which make the system easily access resources from different cloud platforms and be reused in different cloud platforms.

Keywords: cloud computing, virtual machine scheduler, dynamic policy, reusable.

1 Introduction

With the rapid development of cloud computing technology and virtualization technology [20], many IT enterprises have launched their own cloud platforms, such as Amazon EC2, IBM's blue cloud, and Microsoft's azure. Infrastructure service is the basic cloud service of other cloud services. Cloud infrastructure services deliver computer infrastructure, typically a platform virtualization environment, as a service, along with raw storage and networking. Rather than purchasing servers, software, datacenter space or network equipment, clients instead buy those resources as a fully outsourced service. From the service providers' point of view, the management of

Q. Zu, B. Hu, and A. Elçi (Eds.): ICPCA-SWS 2012, LNCS 7719, pp. 411–425, 2013.

virtual machines is an important part in cloud infrastructure. The infrastructure service platform assigns CPU resources, memory resources, and IO resources to virtual machines and deploys the virtual machines on the specific physical machine. These VMs assignments are implemented by the scheduling module in the cloud platform.

Nowadays the main infrastructure of cloud platforms have their own scheduling modules and strategies to schedule virtual machines, such as the round-robin scheduling of Eucalyptus [7][8], the rank scheduling of OpenNebula [3][6], the equilibrium scheduling rating service request of Microsoft Azure [21], energy scheduling of IBM Blue Cloud, Amazon EC2's elastic scheduling [9][10]. The scheduling module which allocates and deploys virtual machines used by the cloud platform is built in the system, and the flexibility of the scheduling module is poor. The users and the developers are not able to customize a suitable policy for their own services according the features of the applications. All the virtual machines with different applications are scheduled in a changeless strategy which may lead to poor performance and low resource utilization, and some services and applications require a specific scheduling strategy for virtual machines' placement in a cloud center, for example, virtual machines used for WEB services should be placed in different physical machines in order to improve the service performance and the service reliability, however, the virtual machines with communication-intensive application should be put on the same physical machine to make full use of physical machine resources. Furthermore, the scheduling modules in varied cloud platforms have a lot of common parts, but the modules cannot be reusable, e.g., the scheduling module in OpenNebula can not schedule virtual machines for Eucalyptus, and vice verse, which leads the lock-in problem more serious in cloud computing.

To target the problems above, we develop a system, called Cranduler, which provides virtual machine scheduling strategies to cloud infrastructure. In Cranduler, we use plug-in technology to make the strategies easily to be managed and maintained in IaaS. The developers can implement a new strategy conveniently, and the new strategy can be integrated into the system flexibly. Furthermore, the Cranduler can manage the virtual resources in a variety of different cloud platforms, such as Eucalyptus, OpenNebula and CRANE [4]. CRANE is a cloud computing platform developed by us, which provides IaaS with virtual machine (Xen, and KVM). Compared with the existing technology, the scheme presented in this paper is more extensible, more reconfigurable and more portable.

The rest of this paper is organized as follows. Section 2 discusses the related work. Section 3 describes the system architecture. Section 4 presents the design and implementation of the system, and section 5 presents performance evaluation. We conclude our work in section 6.

2 Related Work

Job scheduling have been intensively studied in cluster/grid computing [4][5][19], and several research groups have explored the use of virtual machines as a mechanism to allocate and manage computational resources, addressing a variety of issues such as job scheduling on virtual clusters [13][20], VM consolidation [14][17], virtual

networking and load balancing between multiple physical clusters [13], and automatic configuration and creation of virtual machines [12]. However, most of these researches focus on meeting the requirement of either immediate virtual machines or best effort virtual machines, and do not support the suspending/resuming of virtual machines to improve utilization of physical resources.

Several solutions have emerged, both in industry and academia, to manage virtual infrastructures, allowing dynamic deployment of virtual machines in a pool of physical servers. Datacenter-based solutions include commercial products such as VMware VirtualCenter [22] and Amazon EC2, and open-source projects such as OpenNebula. Amazon EC2 and Eucalyptus are examples of clouds that provide infrastructure-as-a-service using virtual machines. However, all these solutions use an immediate provisioning model where virtual machines must be allocated right away, or not at all, with no support for advanced reservation virtual machines. As such, they do not support resource preemption and thus have no need to model suspension/resumption in virtual machines to improve utilization of physical resources.

Usher [14] is a virtual machine management system designed to impose few constraints upon the computing environment under its management. Usher enables administrators to choose how their virtual machine environment will be configured and the policies under which they will be managed. The modular design of Usher allows for alternate implementations for authentication, authorization, infrastructure handling, logging, and virtual machine scheduling.

Entropy [10] is a resource manager for homogeneous clusters, which performs dynamic consolidation based on constraint programming and takes migration overhead into account. The use of constraint programming allows Entropy to find mappings of tasks to nodes better than those found by heuristics based on local optimizations, and that are frequently globally optimal in the number of nodes. Because migration overhead is taken into account, Entropy chooses migrations that can be implemented efficiently, incurring a low performance overhead.

Haizea [1] is relevant to use cases where advanced reservation of virtual machines and the ability to support them efficiently are desirable. Service provisioning clouds, such as the one being built by the RESERVOIR project, have requirements that cannot be supported with only an immediate provisioning model, including the need for capacity reservations at specific times to meet service-level agreements or peak capacity requirements. Additionally, smaller clouds with limited resources, where not all requests may be satisfied immediately because of lack of resources, stand to benefit from sophisticated virtual machines placement strategies supporting queues, priorities, and advanced virtual machines. On the other hand, Haizea does not support customizable strategies for scheduling of virtual machines. To improve the performance, the applications may require a different scheduling strategy. Sometimes Load-aware Policy may works well, but sometimes using Packing Policy to save energy may be better. Although Haizea can be used as a standalone component or as a scheduling backend for a virtual infrastructure manager, it is only suitable for OpenNebula, but could not be used in other cloud platforms such as Eucalyptus, Amazon EC2, and CRANE.

3 System Architecture

The dynamic and reusable scheduler for cloud infrastructure service can be used in a variety of cloud platforms, such as Amazon EC2, OpenNebula and Eucalyptus. It can be directly used in various cloud platforms with a very simple configuration, no need to modify the platform configuration and the codes. The scheduler receives the request of virtual machines from the cloud platform, does preceding operations on the virtual machines according to predefined scheduling strategy in the system, makes a decision of placement for the virtual machines, and suspends the virtual machines that have lower priority, finally gives the final operations list to the cloud platform.

From a hierarchical viewpoint, the Cranduler architecture can be divided into three layers (see Fig. 1): system interface layer, system core layer and virtual machine platform layer. In this layered architecture, each layer has its own services and interfaces which are invoked by its upper layer, layers are flexible and independent between each other. This makes the system easy for implementation and maintenance.

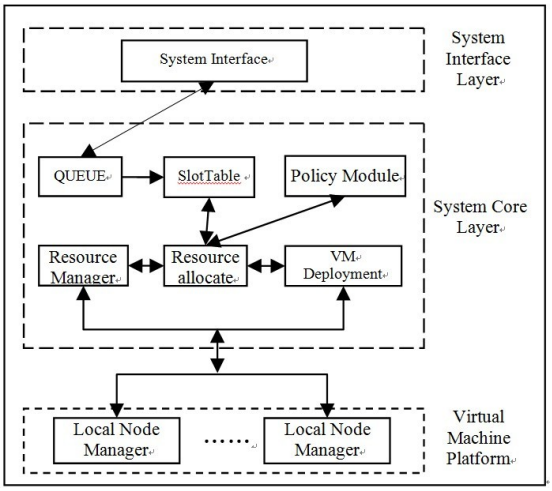

Fig. 1. Architecture of Cranduler

3.1 System Interface

To make this system be easily reused in different cloud platform, a friendly system interface is indispensable. It should be easy for different cloud platform to submit the request for virtual machines and delete the virtual machines. In Cranduler, the requests for virtual machine is formalized, and the requests can be transformed to the requests for different platforms, such as EC2, OpenNebula, and CRANE, based on the CPU, memory, and disk IO information, which make Cranduler reusable for different platforms. The requests for virtual machines in Cranduler includes starting time, time for running, resources for virtual machines, types of jobs, priority of jobs, etc.

3.2 System Core

The system core layer provides the core functions for resource allocation in the cloud. In order to give the mapping list of the virtual machines to physical nodes, a mapping policy should be chosen. To make the allocation policy flexible, the system core provides the customization strategy which can be configured by the developers. The modules in the layer are as follows.

3.3 QUEUE Module

The queue module pre-processes the requests for virtual machines from the cloud platform. It determines whether a given request for virtual machines should be accepted or not. The module interacts with the Policy Module, and makes decision according to the job admission strategy.

Pre-processing the requests is not about whether the request can be scheduled or not (although this could certainly be a part of the policy), the policy simply decides whether the request can be considered for scheduling or not. For example, a user can submit an AR (Advanced Reservation) VM request that must start in 1 hour, but the policy can dictate that all AR VMs must be notified at least 2 hours in advance, and the request can be rejected, regardless of whether there was resource available for it in 1 hour. Similarly, an AR VM request is requested 4 hours in advance, and can be accepted by the VM pre-process strategy, then it can be rejected by the scheduler if there are no resources available at that time.

Another function of the module is making the request for VMs line up in queues. The module manages several queues with different weights. As the priority of VMs is various, VMs are put in different queues and are scheduled separately.

3.4 SlotTable Module

The slot table is one of the main modules in Cranduler. It tracks the capacity of the physical nodes on which virtual machines can be scheduled. This module contains the resource requests of all the jobs including running jobs and waiting jobs, and allows efficient access to them. When resource allocate module maps virtual machines to physical nodes, most read-only interactions with the slot table are executed rapidly through the interface of slot table module.

3.5 Policy Module

The policy module offers the strategy of mapping the virtual machines to physical nodes for resource allocate module. It maintains several strategies for Cranduler to choose. In order to make the system dynamic and flexible, the module offers a set of parameters which defines the platform and job environment for developers. With the parameters and the expression of parameters, the developers could customize special strategy to meet the special requirement for the applications and services.

The general function for the policy module is to decide which physical node the virtual machines should be scheduled to be deployed. When virtual machines will be mapped to physical nodes, the policy determines which hosts are more desirable. Given a virtual machines request and a time which the Cranduler will be scheduled, the module would return a score indicating how desirable that the hosts is for that request at that moment. The score can be between 0.0 and 1.0. The higher the score is, the more desirable the physical node is. Based on the score, the final decision for the VM mapping to physical node will be made.

Different purpose will lead to different policy for VM scheduling, e.g., an energy-saving policy might give higher score to the hosts that already have virtual machines running, and leave empty physical nodes as many as possible, which will make the number of running physical node smaller and the physical nodes without VMs can be turned off to save energy. QoS guarantee policy will give higher score for low workload physical nodes or nodes without VMs, which makes that virtual machines are deployed on more physical nodes, and reaches load balancing among all the nodes.

3.6 Resource Manager Module

The resource manager module maintains a global resource list of the platform. The list records all the attributes and status of the resource. The module automatically detects the physical nodes that join in the resource pool, and this automatic detection mechanism makes Cranduler more flexible and scalable.

Resources in a 'capacity' object can be multi-instance, which means that several instances of the same type of resources can be specified. For example, if a virtual machine requires '2 CPUs', which means that two instances of the same type of resource 'CPU' are required. Most resources, however, will be *single instance* with some parameters (e.g., a physical node only has *one* memory with specific number of memory space).

With this module, the resource status will be transferred to the resource allocation module for allocating resource to virtual machines, and the allocation will base on the strategy that the policy modules offered via analyzing these resources status data.

3.7 Resource Allocate Module

The resource allocate module pre-allocates resource to jobs requesting for virtual machines. It assigns the resource logically, and does not deploy virtual machines on physical nodes. When the resource is allocated to jobs, the status of the resource in the slot table is changed.

The module gets the status of jobs from the slot table, and obtains the global resource list from the resource manager module. It calculates the amount of available resources currently, and maps the virtual machines to physical nodes that satisfy the request based on the strategy the policy module offers. The problem of the allocation scheme is a NP-hard 2-dimensional bin packing problem [15], where the dimensions in Cranduler are corresponding to the amount of memory and number of CPU processing units.

3.8 VM Deployment Module

The VM deployment module executes the actual allocation of physical resources that have been pre-allocated logically to virtual machines, and deploys the virtual machines on the nodes based on the allocation list that the resource allocate module has calculated.

The VM deployment module interacts with the physical nodes and starts virtual machines on the nodes. Before deploying the virtual machines, the virtual machines can be suspended or be migrated, and the image templates have to be transferred to target nodes ahead of the job start time. All these work is scheduled as prologue-job, and the prologue-jobs are completed beforehand. Correspondingly, when it comes to the end of the virtual machine‘s life cycle, all the post-processing work is scheduled as epilogue-job.

3.9 Virtual Machine Platform

The virtual machine platform layer is deployed on the physical nodes and carries out the real deployment process. *Local Node Manager* (LNM) module is located on all the nodes. It provides the concrete realization of the deployment service, including extracting information of the nodes, the creation and launching of the virtual machines.

In order to make the system support heterogeneous cloud platforms and to make the system reusable in different cloud platforms, LNM encapsulates the interfaces of the virtual machine operations. LNM on each node provides a remote API to the core layer for managing local virtual machines and reports local events to the core layer. Upon invoking an API method, LNM translates the operation into the equivalent operation of the VM management API exposed by the VMM running on the node. To make the system scalable, the LNM API methods are asynchronous so that the system does not block waiting for the VMM operation to complete.

4 System Design

In this section, we present the design of Cranduler, which targets the major challenges, such as how to develop configurable scheduling strategies dynamically, how to choose the proper physical nodes for virtual machines, and how to make the system reusable in different cloud platforms.

4.1 Dynamic Configuration

In order to make the system dynamic and capable to customize special policies in different services, Cranduler takes a pluggable module to customize the strategy which guides the resource allocate module for VM deployment and VM migration.

Due to cost and QoS issues, the scheduling policies of VM placement are strict in cloud computing platform. To enforce these policies in Cranduler, the policy is a plug-in type, which is capable to be written or configured to schedule virtual

machines. The plug-in policy gets registered for the events of scheduling virtual machines by specifying these registrations in the system's configuration file. Once registered, subsequent scheduling of virtual machines is passed to the plug-in policy. When a request for virtual machine is submitted to the cloud computing platform, the plug-in policy can approve, approve with modification, or simply reject the request according to the policies. After the plug-in policy module accepts the request, the virtual machine request will be passed on to be scheduled. The plug-in policy which implements the method of sorting nodes, selecting nodes and getting node scores, is used to apply placement of virtual machines.

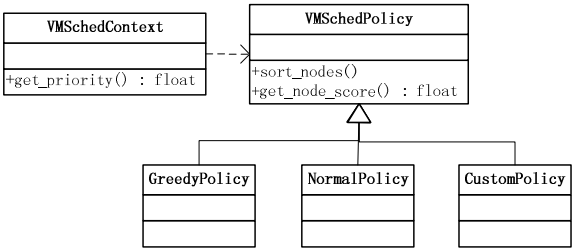

Fig. 2. Plugins for policies

The policy in Cranduler is implemented as abstract method. As shown in Fig. 2, the system provides several abstract methods, such as sorting nodes and getting the score of each virtual machine. To make new customized policies, the developers need to implement the plug-in policy which inherits from the base methods, and configure the methods according to their own requirements. The module *VMSchedContext* maintains a list of available polices, and selects the policy to control resource scheduling when the system initializes.

The new policy development is shown in Fig. 3. In Fig. 3, a new scheduling policy called my-policy will be developed. First, the developer inherits *VMSchedPolicy* to make my-policy. Then, the developer adds the name of the policy to module *VMSchedContext* which records all the file path of policies. With these two steps, my-policy can be used in the cloud platform by setting the content of configure file. When the system initializes, it reads the configuration file, gets the file of the policy, and sets the scheduling policy in use.

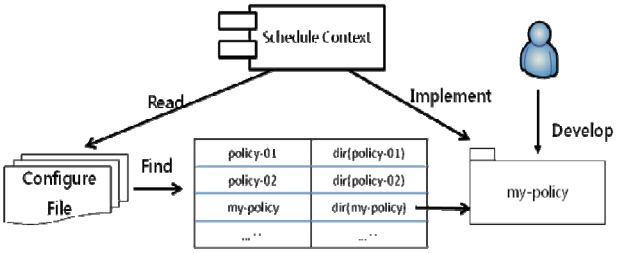

Fig. 3. Development of new policies

4.2 Greedy Mapping Algorithm

Cranduler uses a greedy algorithm to determine how virtual machines are mapped to physical resources at a specific point in time when the scores of all nodes are got according to the schedule policy.

Table 1 presents the basic mapping algorithm. Before describing the algorithm, we illustrate some parameters and variables. The parameter *J* is the job to be scheduled, and it contains a set of virtual machine requirements. *S* is the time when the job is going to start. *T* is the slot table which contains all of the resource in the system.

First, the algorithm greedily orders the physical nodes from the most desirable to the least desirable. For example, a physical node with no virtual machines scheduled on it now or in the future is preferable to one with virtual machines if the system works in the load balancing strategy. This ordering is done by the policy engine.

Then, the algorithm traverses the list of nodes and tries to map as many virtual machines into each physical node before moving on to the next node. If the list of physical nodes is exhausted without finding a mapping for all the virtual machines of a job, then the algorithm tries to find a mapping by suspending or migrating other virtual machines that have lower priority.

Table 1. The algorithm MapJobToNode (*J*, *T*, *S*)

```
1:  pnodes=get available nodes at time  T from S
2:  sort pnodes according to the policy
3:  mapping = {};
4:  done=false;
5:  while not done do
6:  cur_vm=J.firstVM
7:  add cur_vm to need_to_map
8:  for p in pnodes do
9:      avail=available_source(p)
10:         while  p has resources do
11:             if avail>need_to_map then
12:                 mapping[cur_vm]=p
13:                 if J.nextVM exits then
14:                     add J.nextVM to need_to_map
15:                 else
16:                     done=true
17:                     return mapping
18:             end if
19:         else
20:             suspend vms on p
21:         end if
22:     end while
23: end for
24:  end while
```

Before suspending virtual machines, the algorithm has to determine what virtual machines could be preempted first. This decision is delegated to the strategy, which returns a list of virtual machines ordered from the most preempted one to the least preempted one. The algorithm attempts a mapping assuming that the first virtual machine is going to be suspended, then assuming the first and the second until there is enough resource for new virtual machines.

If no mapping is found with preemption, then there is no mapping at the requested time. The job will be delayed until there are enough resources if the job could be delayed.

4.3 Reusable Interfaces

Cranduler can be used in different cloud platforms such as Amazon EC2, OpenNebula and Eucalyptus to deal with the placement, scheduling and migration of virtual machines. In order to support these platforms, the system provides an interface adapter to extend the system.

As these cloud platforms use different virtual machine schedulers and the formats of virtual machine requests are different from each other, the interface module packs the requests to a capacity object used in the system.

Cranduler uses remote procedure call to insert the system into different cloud platforms. The RPC interface is the primary interface of the system, and it exposes all the functionality of cloud interface module to the system. Through the RPC interface, developers can control and manage the resource in system, such as virtual machines and physical nodes.

When the scheduling module calls a method to interact with the cloud platform, it invokes the RPC server which transforms the interface of scheduling module to the interface of the cloud platform, as shown in Fig. 4. The RPC server maintains a list of interface pairs. The fist key of the pair is the interface of the scheduling module, and the second key of the pair is the interface of the cloud interface module. The interface of scheduling module creates a method handle which invokes a system call. The system call of the client interacts with the kernel of server through network. Then

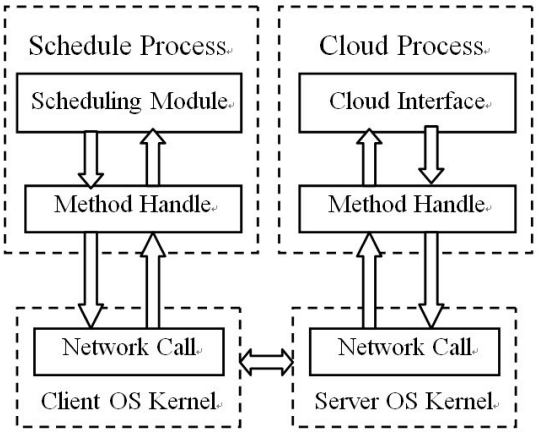

Fig. 4. The transformation of the interfaces

the kernel of server calls the interface of cloud interface module with a method handle. With a series of processes, the interface of the scheduling module is transformed to the interface of cloud interface module.

The system provides several remote procedure call functions, including getting the pending virtual machines, getting the running virtual machines, getting the nodes information, and operating virtual machines, etc. Through these RPC interfaces, the system masks the differences of programming language and processes the request in the uniform interface. The only thing the developers have to do is to match the remote procedure call interfaces to the interfaces of various cloud platforms.

5 Performance Evaluation

In this section, we evaluate the system with a series of experiments. Two sets of experiments are performed to test the VM running time with different strategies. The VM running time is the total time from the point at which the first VM starts running, to the point at which the last VM stops running on the server. Our results show that the mechanism based on VM priority reduces the VM running time, improves the resource utilization.

5.1 Experiment Environments

We conduct our performance evaluations on a cluster. The cluster consists of a front-end node and 3 target nodes. The front-end node is equipped with two Intel Xeon 4 core 2.40GHz CPUS, 4GB memory and 500GB storage, the target nodes in the cluster are equipped with four Intel Xeon 6 core 2.67GHz CPUS, 16GB memory and 500GB storage. The cluster systems are in the VM-based environment, Xen-4.0.0 [3] with the 2.6.32 kernel is used on all target nodes. The Xen domain0 hosts SUSE Linux Enterprise Server 11 with 1GB memory. All user domains are running with a single virtual CPU. The guest OS in DomU used to evaluate the running time uses the Redhat Enterprise Linux 5 templates.

5.2 Running Time Evaluation

The virtual machines are generated by a module called VM generator. When the VM is submitted, it would be queued, waiting resource become available, then starting to run. The VM generator works an hour in each test.

The number of virtual machines submitted per minute follows the Poisson distribution [21]. The Poisson distribution is a discrete probability distribution that expresses the probability of a given number of events occurring in a fixed interval of time if these events occur with a known average rate and independently of the time since the last event. The quantity of memory that each virtual machine demands obeys the Poisson distribution, too.

The mathematical expectation of the memory quantity for virtual machines is labeled as *r1*. The mathematical expectation of the virtual machines number per minute is labeled as *r2*. In order to build model conveniently, we suppose that the variable *r1* expresses the number of 128MB memory.

We assume that each VM runs for half an hour. The VM running time we test is the duration from the point at which the first VM starts running, to the point at which the last VM stops running. We compare the VM running time with two policies. One policy is the round-robin policy (RR policy) used in Eucalyptus cloud platform. The other policy is greedy policy based on VM priority (PG policy). It is used in Cranduler which is integrated in Eucalyptus in the evaluation. In Cranduler, we assume that the virtual machines with large memory could suspend the virtual machines with small memory and grab the resource. The method of getting node scores in PG policy mentioned above is guided with formula (1). The variable *CPU* in (1) expresses the utilization of CPU on the physical node, the variable *MEM* expresses the utilization of the memory of the node, and the variable *VMs* expresses the number of virtual machines that run on the physical node. The variable *Priority* expresses the priority of the physical node. The larger the value of priority is, the more possible the virtual machine would run on.

$$\frac{1}{Priority} = \frac{1}{1-CPU} \times \frac{1}{1-MEM} \times \frac{1}{1-VMs} \tag{1}$$

As shown in Fig.5, the running time changes along with *r2* (the mathematical expectation of VM number per minute) in the case of *r1* (the average quantity of 128MB memory for virtual machines) assigned as 1 and 4. The x-axis expresses *r2*, and the y-axis expresses the VM running time. When *r1* is a constant, the running time of using PG policy is less than the running time of using RR policy. When the number of virtual machines is small, the difference of the two policies is not obvious. When the number of virtual machines increases, PG policy is much better than RR policy in terms of the running time, which shows that Cranduler performs better for large scale VM scheduling compared with the scheduler module in Eucalyptus.

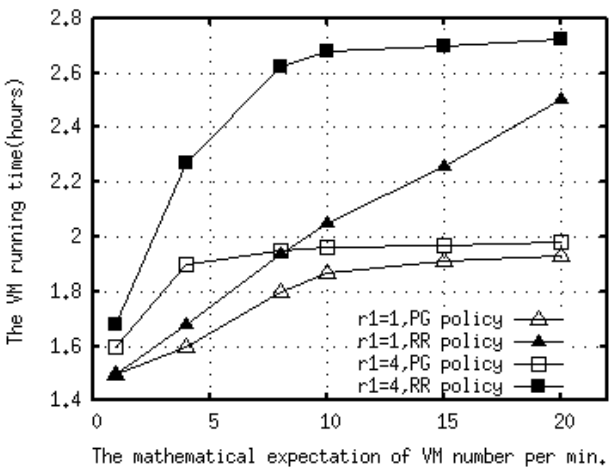

Fig. 5. Test result when *r1* is a constant

In Fig.6, the running time changes along with *r1* with *r2* = 8. The x-axis expresses the mathematical expectation of the memory quantity for virtual machines (*r1*), and the y-axis expresses the VM running time. When the memory demanded by the virtual machines is small, the running time of two policies are close. As the value of *r1* increases, the memory of virtual machines increases. It leads to many resource fragments in the cloud infrastructure when RR policy is used. There is no suspending/resuming in RR policy, so the running time increases largely. Since the virtual machine with small memory can be suspended and release memory to the virtual machine with large memory in PG policy, it will reduce the number of fragments, and enhances the resource utilization.

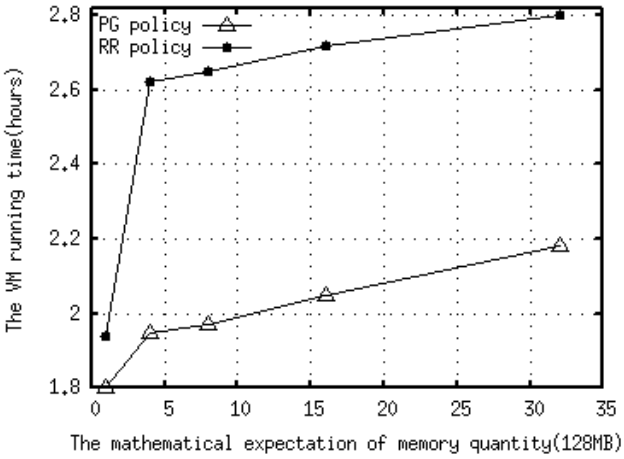

Fig. 6. Test result with *r2* = 8

Fig.7 shows the resource utilization of all the physical nodes in case of *r1* = 8. When the value of *r2* is 1, 4, 8, 10, 15, and 20, the resource utilization of PG policy is 4.60%, 17.10%, 33.90%, 42.02%, 60.98%, 78.74%, respectively, and the resource utilization of RR policy is 4.30%, 12.82%, 25.16%, 31.06%, 46.30%, and 61.73%,

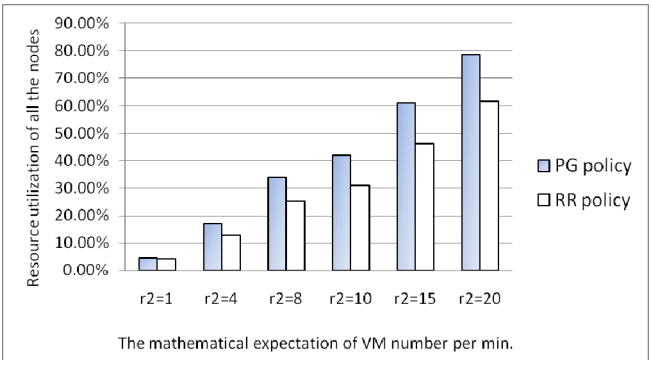

Fig. 7. The resource utilization

respectively. It can be seen from Fig. 7 that when the number of virtual machines is larger, PG policy could enhance the resource utilization much better because the system could suspend virtual machines that have lower priority in order to use the resource fragment.

6 Conclusion

This paper presents Cranduler, a dynamic and reusable scheduling mechanism for cloud infrastructure service. Cranduler introduces the advantages of cluster schedulers to the virtual machine scheduling in clouds. The schedule policies of the system could be dynamically configured by developers. Developers can easily insert the custom policy for different applications. In addition, the present system provides a group of unified interfaces to the cloud platform, which make the system easily access different cloud platforms and be reused in different cloud platforms. The performance evaluation demonstrate that the new polices in Cranduler could improve the system utilization in cloud computing environments. In future, we plan to develop new policies that provide accurate and fine-grained use of other resources, such as network bandwidth and disk.

Acknowledgments. This paper is partly supported by the NSFC under grant No.61133008, National Science and Technology Pillar Program of China under grant No.2012BAH14F02, MOE-Intel Special Research Fund of Information Technology under grant MOE-INTEL-2012-01, and Chinese Universities Scientific Fund under grant No.2012TS046.

References

1. Lindsay, A.M., Galloway-Carson, M., Johnson, C.R., Bunde, D.P., Leung, V.J.: Backfilling with Guarantees Granted upon Job Submission. In: Jeannot, E., Namyst, R., Roman, J. (eds.) Euro-Par 2011, Part I. LNCS, vol. 6852, pp. 142–153. Springer, Heidelberg (2011)
2. Amazon Elastic Compute Cloud, `http://aws.amazon.com/ec2/`
3. Barham, P., Dragovic, B., Fraser, K., Hand, S., Harris, T., Ho, A., Neugebauer, R., Pratt, I., Warfield, A.: Xen and the Art of Virtualization. In: Proceedings of 19th the ACM Symposium on Operating Systems, pp. 164–177. ACM Press, New York (2003)
4. Crane project, `http://crane.hustcloud.com`
5. Claris, C., George, N., Khaled, H.: Resource co-allocation for large-scale distributed environments. In: Proceedings of the 18th ACM International Symposium on High Performance Distributed Computing (HPDC 2009), pp. 131–140. ACM Press, New York (2009)
6. Daniel, N., Wolski, R., Grzegorczyk, C., Obertelli, G., Soman, S., Youseff, L., Zagorodnov, D.: Eucalyptus: A Technical Report on an Elastic Utility Computing Architecture Linking Your Programs to Useful Systems. UCSB Computer Science Technical Report, Number 2008-10

7. Emeneker, W., Stanzione, D.: Efficient Virtual Machine Caching in Dynamic Virtual Clusters. In: Proceedings of SRMPDS Workshop at ICAPDS 2007 Conference (December 2007)
8. Cloud Computing Software from Eucalyptus, http://www.eucalyptus.com/
9. Fabien, H., Xavier, L., Jean-Marc, M., Gilles, M., Julia, L.: Entropy: a Consolidation Manager for clusters. In: Proceedings of the 2009 ACM SIGPLAN/SIGOPS International Conference on Virtual Execution Environments, VEE 2009 (2009)
10. Gmach, D., Rolia, J., Cherkasova, L., Belrose, G., Turicchi, T., Kemper, A.: An Integrated Approach to Resource Pool Management: Policies, Efficiency and Quality. In: Proceedings of IEEE International Conference on Dependable Systems and Networks, DSN 2008 (2008)
11. Ahrens, J.H., Dieter, U.: Computer Generation of Poisson Deviates from Modified Normal Distributions. ACM Transactions on Mathematical Software 8(2), 163–179
12. Murty, J.: Programming amazon web services, 1st edn., pp. 62–108. O'Reilly & Associates, Inc., Sebastopol (2008)
13. McNett, M., Gupta, D., Vahdat, A., Voelker, G.M.: Usher: An Extensible Framework for Managing Clusters of Virtual Machines. In: Proceedings of the 21st Large Installation System Administration Conference (LISA 2007), pp. 167–181 (November 2007)
14. Milojicic, D.S., Llorente, I.M., Montero, R.S.: OpenNebula: A Cloud Management Tool. IEEE Internet Computing 15(2), 11–14 (2011)
15. Maui project, http://www.supercluster.org/
16. OpenNebula: The Open Source Solution for Data Center Virtualization, http://www.opennebula.org/
17. OpenPBS project, http://www.openpbs.org/
18. Shaw, P.: A Constraint for Bin Packing. In: Wallace, M. (ed.) CP 2004. LNCS, vol. 3258, pp. 648–662. Springer, Heidelberg (2004)
19. Sotomayor, B., Keahey, K., Foster, I.: Combining Batch Execution and Leasing Using Virtual Machines. In: Proceedings of the 17th International Symposium on High Performance Distributed Computing, HPDC 2008 (June 2008)
20. Sotomayor, B., Santiago, R., Martín, I.L., Foster, I.: Resource Leasing and the Art of Suspending Virtual Machines. In: Proceedings of the 11th IEEE International Conference on High Performance Computing and Communications, HPCC 2009, June 25-27 (2009)
21. Sotomayor, B., Montero, R.S., Liorente, I.M., Foster, I.: An Open Source Solution for Virtual Infrastructure Management in Private and Hybrid Clouds. IEEE Internet Computing 13(5), 14–22 (2009)
22. Wood, T., Shenoy, P., Venkataramani, A., Yousif, M.: Black-box and gray-box strategies for virtual machine migration. In: Proceedings of the 4th USENIX Conference on Networked Systems Design & Implementation (April 2007)

Multi-objective Virtual Machine Selection for Migrating in Virtualized Data Centers

Aibo Song[1], Wei Fan[1], Wei Wang[1], Junzhou Luo[1], and Yuchang Mo[2]

[1] School of Computer Science and Engineering, Southeast University, Nanjing, P.R. China
[2] Department of Computer Science, Zhejiang Normal University, Jinhua, P.R. China
{absong,fanwei,wangweing,jluo,myc}@seu.edu.cn

Abstract. With the increasing deployment of large-scale virtualized data centers, using virtual machine (VM) migration technology to consolidate VMs is becoming very important for improving the efficiency of data center. The primary prerequisite for VM consolidation is to determine the best candidate VM for migration, and the most previous work targets only on optimizing single objective in VM selection. In this paper, we first propose a multi-objective optimization model based on detailed analysis of the impact of CPU temperature, resource usage and power consumption in VM selection. We then develop a VM selection algorithm to optimize the synthesized effect of VM migration, which will ultimately improve the system performance of physical machines (PMs). We further evaluate our algorithm by comprehensive experiments based on VM monitor Xen, and the results show that it can achieve the best tradeoffs among the resource usage, CPU temperature and power consumption of data center.

Keywords: VM Migration, VM Selection, Multi-objective, Data Center.

1 Introduction

Many cloud providers, such as Google and Amazon, are building their data centers using virtualization technology to provide a variety of cloud storage or computing services. Data center virtualization can improve resource utilization, reduce power consumption, simplify management and assure application performance, etc. From fine-grained point of view, VM consolidation allows the resource of a PM, such as CPU, memory, disk IO and network, to be sliced into multiple isolated execution environments deployed on VMs. The net effect is to run fewer PMs with much higher utilization, and this will remarkably reduce hardware costs and operational expenses related to power, cooling, etc. Although VM consolidation may significantly improve the operational efficiency of data center, it also results in a large quantity of VM migrations.

VM migration has attracted considerable attention of data center managers in recent years. Industry products including XenMotion [1] and VMotion [2] have been implemented as build-in tools in their virtualization platforms. VM migration mainly involves three key issues of when, which and where a VM should be migrated

Q. Zu, B. Hu, and A. Elçi (Eds.): ICPCA-SWS 2012, LNCS 7719, pp. 426–438, 2013.

[3][4][14]. The primary prerequisite for migration is to identify which VM should be moved away from an overloaded PM. It may result in different degrees of impact on the system performance of the overloaded PM. For example, migrating a light-load VM may maintain the service performance of the light-load VM, but can't alleviate the loads of the overloaded PM well. The result is that the PM will keep full-load for a long time, which may significantly degrade its system performance. In contrast, migrating a full-load VM can effectively alleviate the loads of the overloaded PM. But it could generate high migration cost, including migration time and energy cost. Migration cost significantly influences the applications running on VMs and PMs, so we should reduce the number of VM migration as much as possible.

A great amount of work has been devoted to decide which VM needs to be migrated. Bobroff et al. [3] and Wood et al. [4] studied the dynamic VM migration mechanism, which mainly solved the problem of identifying movable VMs and appropriate destination hosts. The goal was to improve resource utilization while maintaining application performance. Hot spots could result in heat imbalances, which may increase cooling costs and degrade system performance [6][7][8]. In order to effectively eliminate the hot spots of data center, Tang et al. [7] proposed a temperature-aware VM selection algorithm. Power consumption was a significant contributor to the operational costs of data center [9][10][12]. Using VM migration to consolidate VMs and turning off the idle PMs was proposed to save considerable power in [9][10], which mainly focused on determining which and where VM should be migrated. The above research works about VM selection only concerned one objective of maximizing resource usage, eliminating hot spots and minimizing power consumption, rather than considered them together. We comprehensively take these criteria into account to keep data center running at high resource utilization, well-balanced thermal dissipation and low energy cost. However, conflicts always occur if these objectives are considered together. For example, Consolidating movable VMs on fewer PMs can improve resource utilization and save large power. However, it may cause resource competition and hot spots. An effective algorithm should consider tradeoffs among all of those objectives.

In this paper, we design a multi-objective VM selection algorithm based on theoretical analysis and empirical studies on Xen platform. Our algorithm aims at achieving the best tradeoffs among resource usage, CPU temperature and power consumption while guaranteeing application performance. To achieve the above objective, the design of VM selection algorithm faces the following challenges: (1) It is difficult to consider the resource usage, CPU temperature and power consumption together and balance their effects on VM selection; (2) Migration cost needs to be carefully considered while selecting a movable VM, as VM migration brings power consumption to PM.

To address these issues, we consider resource usage, CPU temperature and power consumption together, and design a multi-objective VM selection algorithm based on their unified optimization model. Firstly, we construct the unified model of resource, temperature and power, and calculate their efficiencies. Then, we find out the key factors in determination of migration cost and construct the computing model based on large experiments. In addition, other two computing models are built to estimate the power consumption and CPU temperature of VM. Finally, we design a multi-objective VM selection function based on the above achievements.

The rest of the paper is organized as follows. We discuss related work about VM migration in Section 2. Then, Section 3 in detail presents the multi-objective VM selection algorithm. The performance evaluation and experimental results are shown in Section 4. Finally, we conclude our work in Section 5.

2 Related Work

Currently, works about VM migration mostly focus on improving resource usage, eliminating hot spots and reducing power consumption. This section will discuss VM migration expanding from the above three aspects.

Because of expensive hardware costs, the size of data center is often limited. Therefore, how to improve its resource utilization and maintain the application performance guarantees is always being a hot topic. Many cloud application services, such as Amazon EC2 [22] and IBM Blue Cloud [23], focused on efficient management of VMs while meeting the performance requirements of users, aiming at achieving the flexible service of data center. A new dynamic VM placement algorithm [3] was introduced for resource reallocation in virtualized server environments. The goal of the algorithm was to reduce the amount of physical capacity required to support a specified rate of SLA violations by computing the minimum number of running hosts. Sandpiper proposed both gray-box and black-box approaches to automatically migrate VMs by employing the facility of VM live migration [4]. Sandpiper implemented a detection algorithm that determined when to migrate VMs, and a mitigation scheme that used a greedy algorithm to determine which and where to migrate and how much resource to allocate after the migration. A scheduling algorithm for VM migration was presented in [21] based on fuzzy decision making. They employed TOPSIS algorithm to find the most loaded servers and make more effective migration decision when the decision making conditions vague or uncertain, aiming at maintaining application performance guarantees. Hermenier et al. [13] proposed a new approach to consolidation in a homogeneous cluster environment. It considered both the problem of allocating VMs to the available nodes and the problem of how to migrate VMs to these nodes. Its consolidation manager, Entropy, worked in two phases. Firstly, based on constraints describing the set of VMs and their CPU and memory requirements, computed a placement using the minimum number of nodes. Then, proposed a tentative reconfiguration plan to achieve that placement. Finally, based on a refined set of constraints that took feasible migrations into account, tried to improve the plan to reduce the number of VM migration required. In summary, the above VM migration strategies concentrated on improving resource utilization while maintaining application performance, but didn't take hot spots and power consumption into account.

In recent years, hot spots have attracted the attention of many researchers. Fast growth of the compute-intensive applications induces a higher temperature of servers, which decreases the reliability of the affected components to the point that they start to behave unpredictably or fail altogether. To effectively eliminate the hot spots of data centers, Ramos et al. [8] proposed three thermal management policies including turning hot servers off, Freon, and LiquidN2. The first strategy simply turned off any server in which CPU had reached its red-line temperature. Freon reduced much heat

of the hot server by migrating VMs. Compared with Freon, LiquidN2 used voltage/frequency to scale hot servers down, then moved few VMs away from them. Some work investigated the placement of VMs on thermal-efficient locations. A temperature-aware workload placement algorithm in [6][11] aimed at reducing the peak temperature of data center to maintain the system performance. Tang et al. [7] addressed the similar thermal problem and proposed to measure thermal emergency so as to guide the VM migration. In order to eliminate the hot spots, the above work devoted to solve the problem of when and where VMs should be migrated. However, they didn't consider the VM selection.

Keeping running the large-scale data center consumes a large amount of power, and power consumption is a critical issue for IT organizations. For example, in 2006, data centers consumed about 4.5 billion kWh, equaling roughly 1.5% of the total U.S. electricity consumption, and trends showed that power consumption kept growing at 18% annually [12]. Lim et al. [18] presented a strategy of VM consolidation to save power in a virtualized environment. Large power could be saved by dynamically migrating VMs and packing them onto fewer PMs. It focused on the VM placement algorithm to minimize the total energy while avoiding SLA violation. Hu et al. [10] implemented an energy-aware approach that used live migration to transfer workload among the server nodes. It mainly addressed the following two aspects: (1) turning off the redundant nodes to save energy when the system is in non-intensive computing state; (2) transferring violating jobs or big jobs to the idle nodes to obtain performance gains when the system is in compute-intensive state. Liu et al. [14] concerned the performance penalty and energy cost during VM migration, and designed two application-oblivious models for the prediction of migration cost to determine which VM was the desirable candidate for migration. However, the above work only concentrated on energy consumption and application performance, ignored the resource usage and hot spots.

Although some work [16][17] considered resource usage, temperature and power consumption together, they only focused on where VM should be migrated and also didn't take migration cost into account. Xu et al. [15] designed the corresponding VM selection strategy according to the different trigger factor of VM migration. But it never considered tradeoffs among them. While Fortes et al. [5] proposed a VM selection strategy based on multi-objective optimization, they didn't build a unified model of resource, temperature and power. Differently from the above work, VM selection for migration in our work considers not only improving the system performance, but also reducing the migration cost. We construct a unified optimization model among different optimization criteria, and propose a multi-objective VM selection algorithm, aiming at balancing the resource usage, CPU temperature and power consumption of data center while maintaining its application performance.

3 Multi-objective VM Selection Algorithm

In this section, VM selection is modeled as a multi-objective optimization problem. We propose a multi-objective VM selection algorithm named MVMSA. MVMSA mainly includes the following three features: (1) Because of different units and ranges, temperature, resource and power are processed based on a unified model. (2) Because migration

cost significantly influences the system performance of PM, it is carefully considered while selecting the movable VM. (3) In order to achieve an effective balance among these criteria, a multi-objective VM selection function is designed.

3.1 Temperature Model

Temperature efficiency is an effective measure of CPU temperature of VM. To keep CPU temperature within the safe range, its metric function should reflect the following properties: Efficiency changes slowly when temperature is far below the safe threshold, and drops rapidly when approaching or exceeding the threshold.

Based on the above analysis, we define the metric function as shown in formula (1). In formula (2), U_{T_i} is the current temperature of VM i. $U_{T_{low}}$ and $U_{T_{high}}$ respectively denote the virtual temperature of VM when it runs at idle and full-load.

$$V_i(temp) = 1 - \delta_T^{\,m+\delta_T}, m \geq 2 \tag{1}$$

$$\delta_T = \frac{U_{T_{high}} - U_{T_i}}{U_{T_{high}} - U_{T_{low}}} \tag{2}$$

δ_T represents the ratio of remaining temperature of VM i to its range of variation. The temperature efficiency $V_i(temp)$ is within [0~1], and the default value of m is set as 2. m can be adjusted according to the feedback of model effects. Migrating VMs with large $V_i(temp)$ may significantly lower the temperature of hot hosts.

3.2 Resource Model

Resource efficiency well reflects the usage of multi-dimensional resources and is an effective measure of VM performance. The metric function should have the similar properties described in temperature model.

In formula (3), U_{CPU_i} is the CPU utilization of VM i, $U_{CPU_{low}}$ and $U_{CPU_{high}}$ respectively represent the CPU utilization of VM when it runs at idle and full-load. δ_C represents the ratio of remaining CPU of VM i to its range of variation. As shown in formulas (4), (5) and (6), the definitions of U_{Mem_i}, $U_{Mem_{low}}$, $U_{Mem_{high}}$, δ_M, U_{IO_i}, $U_{IO_{low}}$, $U_{IO_{high}}$, δ_I, U_{Net_i}, $U_{Net_{low}}$, $U_{Net_{high}}$ and δ_N are similar with the CPU.

$$\delta_C = \frac{U_{CPU_{high}} - U_{CPU_i}}{U_{CPU_{high}} - U_{CPU_{low}}} \tag{3}$$

$$\delta_M = \frac{U_{Mem_{high}} - U_{Mem_i}}{U_{Mem_{high}} - U_{Mem_{low}}} \tag{4}$$

$$\delta_I = \frac{U_{IO_{high}} - U_{IO_i}}{U_{IO_{high}} - U_{IO_{low}}} \tag{5}$$

$$\delta_N = \frac{U_{Net_{high}} - U_{Net_i}}{U_{Net_{high}} - U_{Net_{low}}} \tag{6}$$

Then, the metric functions of CPU, memory, disk and network IO are shown in formulas (7), (8), (9) and (10).

$$V_i(CPU) = 1 - \delta_C^{\,m+\delta_C} \tag{7}$$

$$V_i(Mem) = 1 - \delta_M^{\,m+\delta_M} \tag{8}$$

$$V_i(IO) = 1 - \delta_I^{\,m+\delta_I} \tag{9}$$

$$V_i(Net) = 1 - \delta_N^{\,m+\delta_N} \tag{10}$$

Any resource may be the bottleneck of the system performance of server. Therefore, in formula (11), we define the resource efficiency of VM as the maximum efficiency

$$V_i(res) = \max\{V_i(CPU), V_i(Mem), V_i(IO), V_i(Net)\} \tag{11}$$

of multi-dimensional resources. Migrating VMs with large efficiency $V_i(res)$ may effectively avoid the resource bottleneck of server.

3.3 Power Model

Power efficiency is an effective measure of power consumption of VM. U_{Pow_i} is the power consumption of VM i, $U_{Pow_{low}}$ and $U_{Pow_{high}}$ respectively represent the power consumption of VM when it runs at idle and full-load. δ_P in formula (12) represents the ratio of remaining power of VM to its range of variation. Similarly to temperature model, we define the metric function as shown in formula (13).

$$\delta_P = \frac{U_{Pow_{high}} - U_{Pow_i}}{U_{Pow_{high}} - U_{Pow_{low}}} \tag{12}$$

$$V_i(power) = 1 - \delta_P^{\,m+\delta_P} \tag{13}$$

VM with large efficiency $V_i(power)$ should be migrated to effectively reduce the power consumption of server.

3.4 VM Selection Function

Based on the unified model of temperature, resource and power, the VM efficiency is defined as the weighted sum of the above three efficiencies. That is

$$Vol_i = a \cdot V_i(temp) + b \cdot V_i(res) + c \cdot V_i(power) \tag{14}$$

where $a+b+c=1$, a, b and c are the weights.

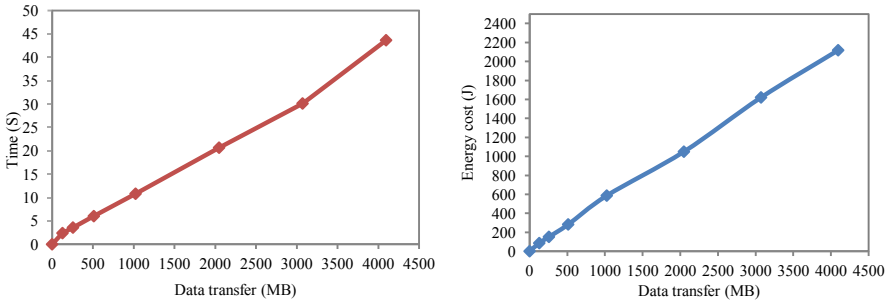

(a) (b)

Fig. 1. The (a) time and (b) power consumption due to VM migration with different data transfer

VM migration could generate migration cost. Migration cost should be carefully taken into account when data center needs to migrate numerous VMs. In order to effectively estimate the migration cost, we conduct a large number of experiments based on Xen platform, and the network bandwidth is 1000Mb/s. By carefully analyzing the experimental results, we conclude the relationship between migration cost and data transfer as shown in Fig. 1. We can see that the power consumption in VM migration is linearly related to the data transfer, and only determined by it. Migration time also increases linearly with data transfer when PMs have stable loads. Results also show that the data transfer is mainly determined by the memory size of movable VM. In order to effectively reflect the impact of migration cost on VM selection, we define the VM selection function as follows,

$$VKS_i = Vol_i \cdot K / S_i \tag{15}$$

where S_i represents the memory size of VM i. Constant K is used to enlarge the VM efficiency Vol_i. The larger the memory size of a VM, the smaller the VKS.

3.5 Migration Phase

The condition for VM migration includes the following three trigger factors. (1) Hotspots: If the CPU temperature of a server exceeds 55°C, a hotspot will occur. (2) Resource contention: Multiple VMs may compete for limited physical resources, such as CPU, memory, network and disk IO. We define the threshold of any physical resource utilization as 80%. (3) Low power consumption: We simply consider it to be in low-power if the CPU utilization of PM is lower than 10%. Large power savings can result from moving VMs away from the low-power host and turning off it.

To determine which VMs to migrate, MVMSA orders the VMs on source host in decreasing order of *VKS* . Then, it attempts to select the VM with the maximum *VKS* for migration until the source host recovers its efficient system state.

4 Experimental Analysis

In this section, we first introduce how to obtain the resource utilization, temperature and power consumption from our Dell Blade Center. Then, the MVMSA is evaluated using a set of experiments and compared with an improved single-objective VM selection algorithm (SVMSA) to show its performance.

4.1 The Methods of Data Acquisition

Our Dell Blade Center has 32 PE1855 blades, and each blade is configured with two Xeon 3.2GHz processors with 2MB L2 cache, 6GB RAM, 80GB SAS disk, 64-bit CentOS 5.6 and Gigabit Ethernet. In Blade Center, the data collected includes the resource utilization, temperature and power consumption of blade servers and VMs.

It's important for VM migration to accurately obtain the resource utilization. Physical resource utilization can be determined from the Xen hypervisor or by monitoring events within the Domain0 of Xen. Domain0 is a distinguished VM in Xen that is responsible for I/O processing. It's relatively easy to get the virtual resource utilization. By querying *top* and *iperf* , the real-time performance statistics of each VM can be obtained.

There are two methods of measuring the temperature and power of blade server. The first method is to measure them using Dell DRAC module [22]. In addition, we could also measure them using the following computing method. We use the model in [19] to estimate the power consumption of blade server, where power consumption is linearly related to the CPU utilization while neglecting the effect of heat generated by other servers nearby. The model is presented as follows, where p_1 is the power consumption of the idle PM, and p_2 represents the difference in power consumption

$$P = p_1 + p_2 \cdot U_{CPU} \tag{16}$$

between the full-load PM and idle PM. Similarly to power, we use the model in [20] to estimate the steady CPU temperature, which is shown in formula (17). R denotes the thermal resistance and T_{amb} is the ambient temperature. Using the relationship between power consumption and CPU utilization, we conclude the equation presented in formula (18).

$$T = P \cdot R + T_{amb} \tag{17}$$

$$T = (p_2 \cdot R) \cdot U_{CPU} + (p_1 \cdot R + T_{amb}) \tag{18}$$

Because p_1 and p_2 depend on the type of server, so we conduct several groups of experiments to calculate the coefficients of formulas (16) and (18) on June 15

between 11:00 am to 2:00 pm. We use Dell DRAC to measure the temperature and power consumption of a blade server, which keeps running the varying applications. As shown in Fig. 2, we can see that the temperature and power consumption are both approximately linear functions of the CPU utilization. We may get the following computing formulas using fitting method.

$$T = 36 \cdot U_{CPU} + 27 \tag{19}$$

$$P = 80 \cdot U_{CPU} + 130 \tag{20}$$

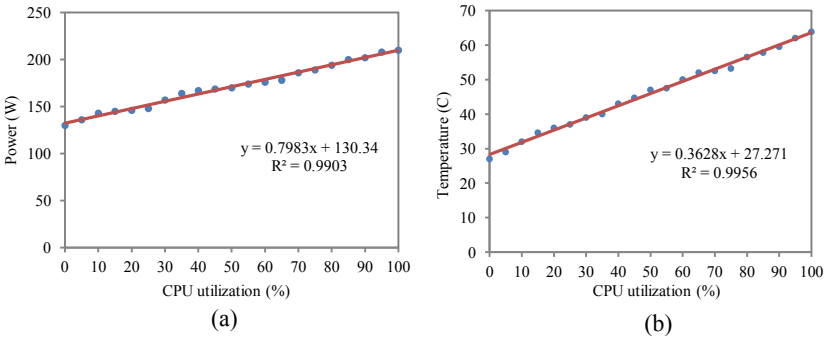

Fig. 2. The (a) power consumption and (b) CPU temperature of the blade server with varying CPU utilization

We use the Dell DRAC to accurately measure the temperature and power consumption of blade server. However, the virtual temperature and power consumption of VM can't be directly measured. In our experiments, we effectively measure them using formulas (19) and (20).

4.2 Evaluation of MVMSA

In order to evaluate the performance of MVMSA, we compare it with an improved SVMSA proposed in [15]. Based on different trigger factor, the improved SVMSA selects the movable VM which has the maximum utilization of single resource, while the MVMSA selects the movable VM using a unified multi-objective VM selection function. For the sake of fairness, MVMSA and the improved SVMSA are used for VM migration based on the same threshold conditions.

To better balance the resource usage, temperature and power consumption, we set $a = b = c = 1/3$ in formula (14). K in formula (15) is simply set as 2048 with respect to the maximum memory size of VM. We choose two blade servers as the experimental hosts. The one running 5 VMs is regarded as the source host, and the other keeping idle is the destination host. The resource usage of 5 VMs are shown in table I. Each VM runs CPU-intensive or disk-intensive applications that are implemented as Linux shell scripts.

Table 1. The resource usage of VMs on source host

	Mem(MB)	CPU (%)	Disk IO (%)
VM1	1024	74.6	79.5
VM2	1024	28.7	94.6
VM3	1024	87.2	91.5
VM4	1024	78.6	74.9
VM5	2048	89.3	23.8

Fig. 3 shows that the physical CPU and disk IO utilization of source host are both exceed the predefined threshold 80%. On the other hand, high CPU utilization will cause high temperature and power consumption. This is precisely the moment that VM migration will occur. MVMSA selects the VM3 to migrate, while the improved SVMSA first migrates the VM5 and then migrate the VM2. The details of VM migration based on the improved SVMSA and MVMSA are shown in Fig. 4.

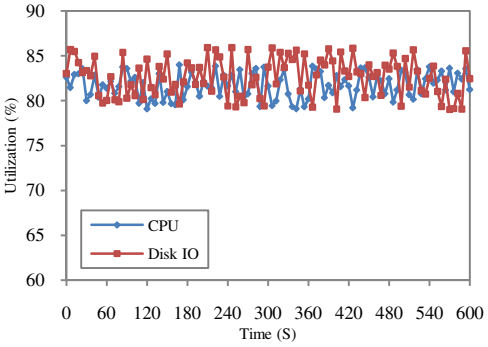

Fig. 3. The variation in CPU and disk IO utilization of source host during ten minutes

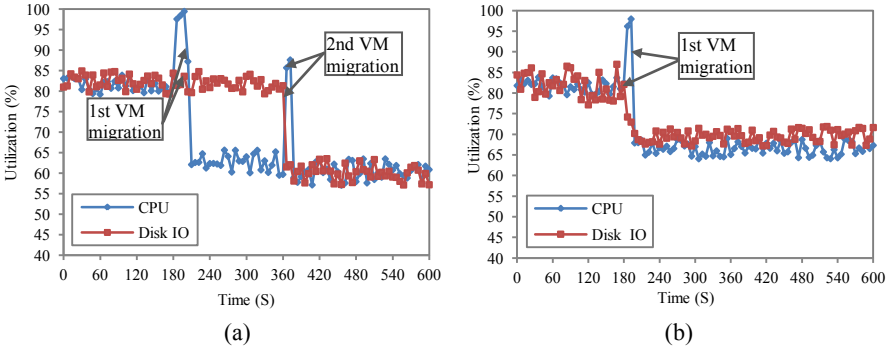

Fig. 4. The variation in CPU and disk IO utilization of source host during VM migration based on (a) the improved SVMSA and (b) MVMSA

As shown in Fig. 4, we can see the variation in resource utilization during VM migration respectively based on the improved SVMSA and MVMSA. The two algorithms can both effectively alleviate the competition of CPU and disk IO of source host. However, the improved SVMSA needs two VM migrations. The first migration only benefits for alleviating the CPU competition and the second migration only alleviates the disk IO competition. Compared with the improved SVMSA, our MVMSA needs only one VM migration.

Fig. 5 shows the variation in CPU temperature and power consumption of the source host during VM migration based on different algorithms. No-control denotes that VMs on source host never move away from it. Compared with No-control, the improved SVMSA and MVMSA can both reduce the CPU temperature and power consumption of source host. However, compared with our MVMSA, the improved SVMSA with two VM migrations may bring a larger overhead of CPU temperature and power to source host and destination host when migrating VMs.

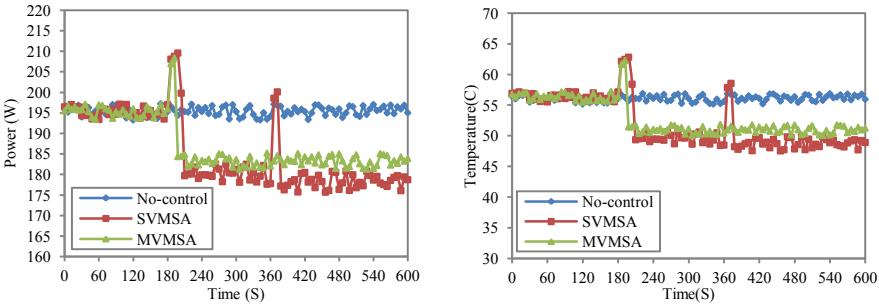

Fig. 5. The variation in (a) power consumption and (b) CPU temperature of source host during VM migration based on different algorithms

The migration costs of the improved SVMSA and MVMSA are presented in table 2. We can see that the time and the power consumption in migration caused by the improved SVMSA are much more than our algorithm. The improved SVMSA needs two VM migrations to improve the system performance of the source host. In contrast, MVMSA only needs one migration, which could effectively reduce the migration time and power consumption. When large-scale data center needs to dynamically migrate numerous VMs among different PMs, MVMSA will behave much better than the improved SVMSA.

Table 2. The comparison of the migration cost between the improved SVMSA and MVMSA

Migration cost	SVMSA	MVMSA
Number of migration	2	1
Time (S)	56	22
Power (J)	1697	586

5 Conclusion

In this paper, the problem of VM selection for migration is formulated as a multi-objective optimization problem. The goal is to collaboratively optimize possibly conflicting objectives, including making efficient usage of multi-dimensional resources, eliminating hot spots, and reducing power consumption.

First of all, a unified model of different optimization criteria is presented to combine the conflicting goals. Then, several groups of experiments are conducted to study the migration cost of VM. The results show that energy cost is only determined by the data transfer, and migration time is also only determined when PMs have stable loads. In addition, the data obtained from measurements of a Dell Blade Center are used for building the models of CPU temperature and power consumption. What's more, we design a multi-objective VM selection function to determine the movable VM for the temperature/resource/energy-efficient migration. Finally, we evaluate our MVMSA compared with an improved SVMSA. The results show that our MVMSA has better performance.

Acknowledgments. This work is supported by National Natural Science Foundation of China under Grants No. 61070161, No. 61070158, No. 61003257 and No. 90912002, National Key Basic Research program of China under Grants No. 2010CB328104, China National Key Technology R&D Program under Grants No. 2010BAI88B03, China Specialized Research Fund for the Doctoral Program of Higher Education under Grants No. 200802860031, Jiangsu Provincial Natural Science Foundation of China under Grants No. BK2008030, China National S&T Major Project under Grants No. 2009ZX03004-004-04, Opening Fund of Top Key Discipline of Computer Software and Theory in Zhejiang Provincial Colleges at Zhejiang Normal University, Supporting technology deepen research in smart grid scheduling technical support system, State Key Laboratory of Information Security, Jiangsu Provincial Key Laboratory of Network and Information Security under Grants No. BM2003201, and Key Laboratory of Computer Network and Information Integration of Ministry of Education of China under Grants No. 93K-9.

References

1. Clark, C., et al.: Live Migration of Virtual Machines. In: Proc. of the 2nd Symposium Networked Systems Design and Implementation, CA, pp. 273–286 (2005)
2. Nelson, M., et al.: Fast Transparent Migration for Virtual Machines. In: Proc. of USENIX Annual Technical Conference, CA, pp. 391–394 (2005)
3. Bobroff, N., et al.: Dynamic placement of virtual machines for managing SLA violations. In: Proc. of 10th IFIP/IEEE International Symposium on Integrated Network Management, NY, pp. 119–128 (2007)
4. Wood, T., et al.: Black-box and Gray-box Strategies for Virtual Machine Migration. In: Proc. of 4th USENIX Symposium on Networked Systems Design and Implementation, MA, pp. 229–242 (2007)

5. Xu, J., Fortes, J.: Multi-objective Virtual Machine Placement in Virtualized Data Center Environments. In: IEEE/ACM International Conference on Green Computing and Communications, FL, pp. 179–188 (2010)
6. Moore, J., et al.: Making Scheduling Cool: Temperature-Aware Resource Assignment in Data Centers. In: Proc. of USENIX Annual Technical Conference, CA, pp. 10–15 (2005)
7. Tang, Q., et al.: Energy-Efficient, Thermal-Aware Task Scheduling for Homogeneous, High Performance Computing Data Centers: A Cyber-Physical Approach. IEEE Transactions On Parallel and Distributed Systems 19(11), 1458–1472 (2008)
8. Ramos, L., Bianchini, R.: C-Oracle: Predictive Thermal Management for Data Centers. In: Proc. of the 14th International Symposium on High Performance Computer Architecture, SL, pp. 111–122 (2008)
9. Cardosa, M., et al.: Shares and Utilities Based Power Consolidation in Virtualized Server Environments. In: Proc. of the 11th IFIP/IEEE International Conference on Symposium on Integrated Network Management, NY, pp. 327–334 (2009)
10. Hu, L., et al.: Magnet: A Novel Scheduling Policy for Power Reduction in Cluster with Virtual Machines. In: Proc. of IEEE International Conference on Cluster Computing, Tsukuba, pp. 13–22 (2008)
11. Sharma, R., et al.: Balance of Power: Dynamic Thermal Management for Internet Data Centers. IEEE Internet Computing 9(1), 42–49 (2005)
12. Report to Congress on Server and Data Center Energy Efficiency, U.S. Environmental Protection Agency ENERGY STAR Program, http://www.energystar.gov/ia/partners/Prod_development/downloads
13. Hermenier, I., et al.: Entropy: a consolidation manager for clusters. In: Proc. of the ACM SIGPLAN/SIGOPS International Conference on Virtual Execution Environments, NY, pp. 41–50 (2009)
14. Liu, H.-K., et al.: Performance and energy modeling for live migration of virtual machines. In: Proc. of the 20th International Symposium on High Performance Distributed Computing, San Jose, CA, pp. 171–182 (2011)
15. Xu, J., Fortes, J.: A Multi-objective Approach to Virtual Machine Management in Datacenters. In: Proc. of the 8th ACM International Conference on Autonomic Computing, NY, pp. 225–234 (2011)
16. Chen, Y., et al.: Integrated Management of Application Performance, Power and Cooling in Data Centers. In: Proc. of IEEE/IFIP Network Operations and Management Symposium, Osaka, pp. 615–622 (2010)
17. Jung, G., et al.: Mistral: Dynamically Managing Power, Performance, and Adaptation Cost in Cloud Infrastructures. In: Proc. of the 30th IEEE International Conference on Distributed Computing Systems, Atlanta, GA, pp. 62–73 (2010)
18. Lim, M.Y., et al.: PADD: Power-Aware Domain Distribution. In: Proc. of the 29th International Conference on Distributed Computing Systems, Montreal, QC, pp. 239–247 (2009)
19. Lien, C., et al.: Estimation by Software for the Power Consumption of Streaming-Media Servers. IEEE Transactions on Instrumentation and Measurement 56(5), 1859–1870 (2007)
20. Krum, A.: Thermal Management. In: The CRC Handbook of Thermal Engineering, pp. 2.1–2.92. CRC Press, Boca Raton (2000)
21. Tarighi, M., et al.: A New Model for Virtual Machine Migration in Virtualized Cluster Server Based on Fuzzy Decision Making. Journal of Telecommunications 1(1), 40–51 (2010)
22. Dell DRAC, http://en.wikipedia.org/wiki/Dell_DRAC
23. The Amazon Elastic Compute Cloud (Amazon EC2), http://aws.amazon.com/ec2/
24. IBM Blue Cloud, http://www.ibm.com/ibm/cloud/

Study on Virtual Simulation of the New Screw Pile Hammers Based on a Combination of Multi-software Platforms

Yangyang Su, Li Bo, and Dingfang Chen

Research Institute of Intelligent Manufacture & Control, Wuhan University of Technology, Hubei, P.R.China,430063
{suyangyangwhut,whlibo163}@163.com
dfchen@whut.edu.cn

Abstract. This thesis uses the virtual simulation of the new screw pile hammers as an example, and puts forward a virtual simulation method based on a combination of multi-software platforms. It simply introduces how to design the size of the machine, and check the strength of each part with the help of ANSYS. Then focuses on the introduction to the working process of this virtual simulation method, achieves the goal of seamless connection of different software, the build of 3d model of the pile hammer, and the production of the virtual pile hammer. Meanwhile, the virtual simulation of four processes demonstrates the functions of the new screw pile machine in different stages and the principle of piling. Compared with the traditional method which stimulates and analyzes with a single software, the practical applications demonstrate that, the virtual stimulation method based on a combination of multi-software platforms is easier to operate, more flexible to modify and more authentic.

Keywords: multi-software platforms, virtual simulation, pile hammers.

1 Introduction

With the rapid development of mechanical manufacturing industry, machinery is more and more powerful in function and the parts of the machine are more and more complex. Therefore, new requires on virtual simulation are unavoidable. Nowadays, there are various kinds of software in the world, which have disadvantages and advantages[1,2,3]. We face the problem how to combine different kinds of virtual simulation software effectively to achieve the virtual simulation, which gives birth to a virtual simulation method based on a combination of multi-software platforms.

2 Background

The new screw pile machine structure design adopts advanced floating technology, planet gear load uniform and reasonable, gear carrying capacity is high, long service life, economical.

Q. Zu, B. Hu, and A. Elçi (Eds.): ICPCA-SWS 2012, LNCS 7719, pp. 439–446, 2013.

According to the demand of customer, we need to do the following two points:

- Calculate a series of data (especially the spindle size of reducer).
- Make the virtual prototype of the pile hammer and its videos.

It is of great importance to research on the virtual simulation of the new screw pile hammers. The prototype can promote the interaction between manufacturer and client (especially the non-technical staff). Through the video of the prototype, clients can learn about the new type of the machine such as its advantages, structure and principle without going out, which contributes to the promotion of the products as well.

3 Calculation and Analysis

3.1 Calculate the Power and Torque of the Output Shaft

Given conditions :

The output torque of the reducer is $\mathrm{T} = 25\mathrm{T} \times \mathrm{m}$;
The output speed of the reducer is $\mathrm{N} = 3.981\mathrm{r/min}$;

- **Calculate the output power.**
- The input power of the reducer is:

$$\mathrm{P}_1 = \frac{\mathrm{T} \times \mathrm{N}}{9549} = \frac{25 \times 10^3 \times 9.8 \times 3.981}{9549} = 102.141\mathrm{kw}$$

In the above formula:

Efficiency of the bearing[4] η_1—we can check the value of $\eta_1$is 0.98~0.99,than take 0.98 as η_1.

Efficiency of the gear[5] η_2—we can check the value of η_2 is 0.98~0.995,than take 0.99 as η_2.

Efficiency of the planetary gear[5] η_3 —we can check the value of η_3 is 0.97~0.99,than take 0.98 as η_3.

Efficiency of the gear coupling[6] η_4—we can check the value of η_4 is 0.99.

- The output power of the reducer is:

$$\mathrm{P}_2 = \frac{\mathrm{P}_1}{2{\eta_1}^2{\eta_2}^2} = \frac{102.141}{2 \times 0.98^2 \times 0.99^2} = 54.256\mathrm{kw}$$

- The input power of the motor:

$$\mathrm{P}_3 = \frac{\mathrm{P}_2}{\eta_1\eta_2\eta_3\eta_2\eta_3\eta_4} = \frac{54.256}{0.98 \times 0.99 \times 0.98 \times 0.99 \times 0.98 \times 0.99} = 59.411\mathrm{kw}$$

Conclusion: we can calculate the output power is 59.411kw based on the given condition ($\mathrm{T} = 25\mathrm{T} \times \mathrm{m}$), which is less than the rated power (75kw)of the motor, that means the maximum output torque of the pile hammers can be achieved to 25 $\mathrm{T} \times \mathrm{m}$.

- **Calculate the output torque**.
- Input torque of the gear:

$$T_1 = \frac{9549 \times P_3}{n_2} = \frac{9549 \times 59.411}{1000} = 569.096N \times m$$

In the above formula:

$$n_2 — \text{rated speed of the motor},1000r/min$$

- Input torque of the reducer:

$$T_2 = \frac{9549P_3\eta_4}{n_2} = \frac{9549 \times 59.411 \times 0.99}{1000} = 561.639N \times m$$

- Input torque of the gear shaft(high-speed shaft):

$$T_3 = \frac{9549P_3\eta_3\eta_4\eta_3\eta_2\eta_3\eta_2}{n_3} = 26270.32N \times m$$

In the above formula:

$$n_3 — \text{rated speed of the gear shaft}$$

$$n_3 = \frac{n_2}{\tau_1\tau_2} = \frac{1000}{8.7692 \times 5.6667} = 20.124r/min$$

In the above formula:

The first level ratio of the planetary gearbox:$\tau_1 = 8.7692$

The second level ratio of the planetary gearbox:$\tau_2 = 5.6667$

- Output torque of the gear shaft (high-speed shaft):

$$T_4 = \frac{9549P_3\eta_4\eta_3\eta_2\eta_3\eta_2\eta_1}{n_3} = 2.627\ T \times m$$

- Input torque of the gear shaft (low-speed shaft):

$$T_5 = 2 \times \frac{9549P_4\eta_2\eta_2}{n_4} = 2 \times \frac{9549 \times 54.256 \times 0.99 \times 0.99}{3.981} = 26.031\ N \times m$$

In the above formula:

$$P_4 — \text{stands for the output power of the planetray gearbox}$$

- Output torque of the gear shaft (low-speed shaft):

$$T_6 = \frac{9549P_5}{n_4} = \frac{9549 \times 102.141}{3.981} = 24.500\ T \times m$$

Conclusion: T_6 is less than the given torque ($T = 25T \times m$).

3.2 Finite Element Analysis

Output shaft, planet carrier (low-speed), planet carrier (high-speed) and the support body are the key components of the reducer. Their mechanical properties directly affect the reliability of the gear reducer safety work and performance. We need to analyze their mechanical properties using the ANSYS software.

- Calculate the allowable stress [σ]

According to the material mechanics knowledge, we can calculate the material allowable stress:

$$[\sigma] = \frac{\sigma_s}{n}$$

In the above formula:

σ_s— stands for the allowable stress of the material

n— stands for the safety factor

The allowable stress of the key mechanical components of the new screw pile hammers are shown in table1.

Table 1. Allowable stress of the key mechanical components

Name of each component	Material	Yield limit (MPa)	Safety factor n	Allowable stress (MPa)
Output shaft	42CrMo	930	2	465
planet carrier (low-speed)	ZG42CrMo	490	2	245
planet carrier (high-speed)	ZG42CrMo	490	2	245
Support body	QT600-3	370	1.33	278
Reducer housing	Q235-A	235	1.33	177

- Check the strength of the output shaft

Build the three-dimensional finite element model of the output shaft using the solid45 as element type and analyze the force of it. The stress drawing and displacement drawing are shown in figure1 and figure2.

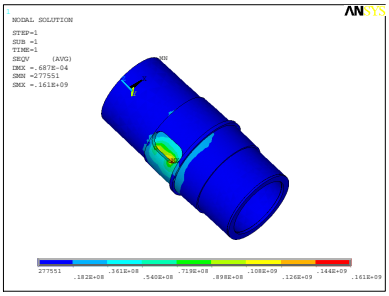

Fig. 1. Stress drawing of the output shaft

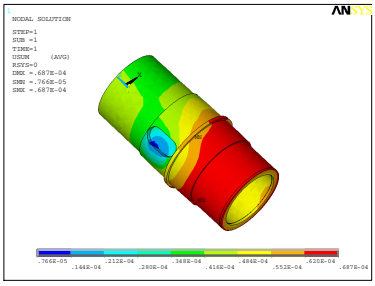

Fig. 2. Displacement drawing of the output shaft

Conclusion:$\sigma_{max} = 161\text{MPa} < [\sigma] = 465\text{MPa}$, strength meet the requirements.

Use the same methods to check other components' stress and make sure their strength meet the requirements.

4 Introduce of the Working Process of the Virtual Simulation Method Based on a Combination of Multi-software Platforms

Take the virtual simulation of the new screw pile hammers as an example. The flow chart of the virtual simulation method is as follows in figure3:

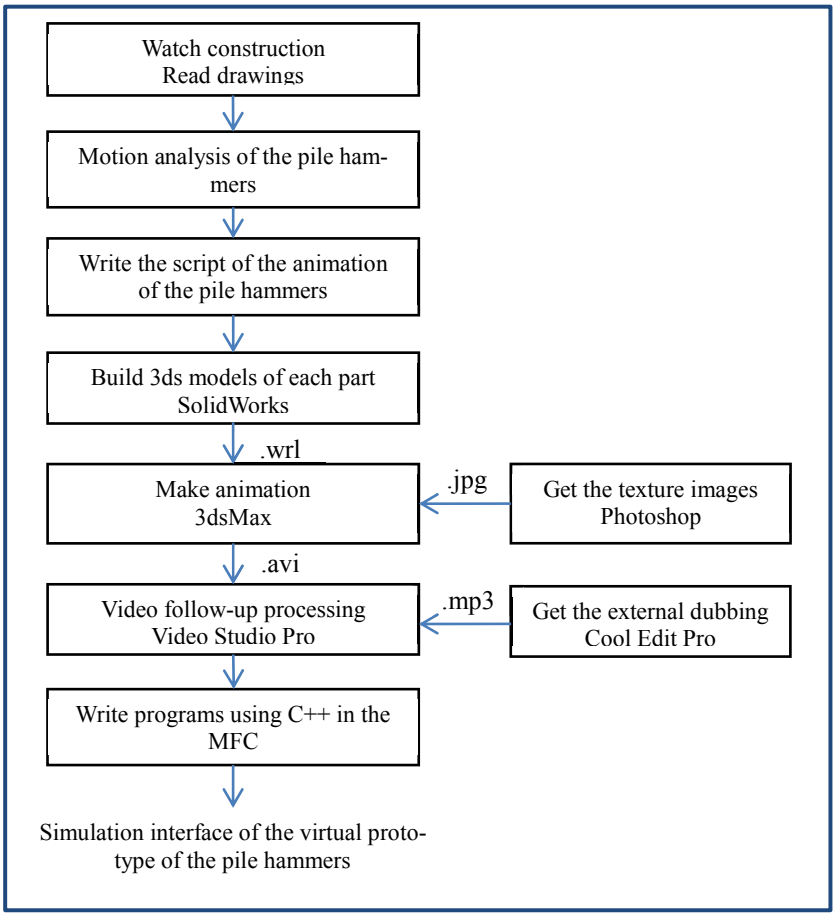

Fig. 3. Working process

1. Analyzes the state of function in all stages, and takes down the scripts which are required for the making of virtual simulation video.
2. Establish the 3d models of the parts in the environment of SolidWorks software based on the calculation, then save them as wrl format.

3. Deal with the pictures of screw pile hammers and other relative pictures with the help of Photoshop, then get the required texture maps in the jpg format.
4. Import the wrl files into 3dsMax, map and render the 3d models of the parts of the new screw pile hammers, then make the video and save it in the avi format.
5. Record the sound that requires when the machine works in the environment of Cool Edit Pro and save it in the mp3 format.
6. Import the video and the sounds into Video Studio Pro and approach them further and save the final video in the flv format.
7. Use C++ language program in MFC framework to make the simulation interface.

4.1 Analyzes the Motion State of the New Screw Pile Hammers

Observe and analyze the whole process in which the pile machine is transported, assembled, constructed, disassembled and transported. At the same time, read the drawings of the machine, learn about the joint state of each part, and especially take down the notes on their relative motion in different stages. After that, make a form. In order to help clients learn about the new type of machine directly and clearly, the function of the machine in reality is divided into four stages: assembly-pile-transposed construction-disassembly. Organize the notes carefully and write the script of the simulation flash.

4.2 Build the 3D Models of the New Screw Pile Hammers Base on SolidWorks

In the environment of SolidWorks, establish the 3d models of the parts of new screw pile hammers based on the calculation.

There are two ways to establish the model-top to the bottom and bottom to the top. The aim here is to make simulation animation and the assembly process of some parts need to be done in 3dsMax, therefore we adopt the bottom to the top way to establish the models. That is to say, we disassemble the machine into individuals and establish them one by one. The newly-built 3d models should be imported to 3dsMax, so the models of the parts should be saved in the format of wrl.

The models of those parts which need to be assembled in the 3dsMax should be saved in the format of wrl. Others can be assembled in the environment of SolidWorks, the assembly models should be saved in the format of wrl.

4.3 Make the Simulation Videos of Virtual Prototype Base on 3DsMax

According to the written script, import the models into the environment of 3dsMax to make simulation animation.3dsMax is a commonly used software to make 3d video. During the process of virtual simulation, it is used to do the followings:

- Set the working scene of the new screw pile hammers

In order to achieve a convincing effect, we can set the working scene of the new screw pile hammers in the environment of 3dsMax, such as the ground with yellow soil, the street behind the site, the trees and the buildings in the city. Schematic diagram is shown in figure4.

Fig. 4. Interface of 3ds Max software

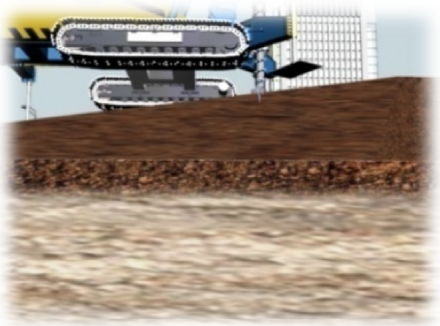

Fig. 5. The new screw pile hammers

- Map and render the models

The models established in SolidWorks are colorless, so there is need to render texture. The final models are shown as the figure4, which has strong visual impact.

- Make the virtual simulation video files of the new screw pile hammers

Import the rendered models into the working scene and achieve the relative motion between each part and between the pile machine and the working site according to the working principle of the machine in reality. Figure5 shows the relative rotation of the hammers under the construction site. Debug the related motion parameter, and export the video in the avi format.

4.4 Post Processing of Animated Video

Corel Video Studio Pro software is a video processing software, through which we can put static pictures and dynamic video files together to create a new video file. We mainly do the following treatment to the avi format video files in the environment of the Corel Video Studio Pro software: the treatment of color brightness; adding the suitable background music, associated subtitles and dubbing commentary. Through this way we can get a new video file with strong impact both in visual and hearing. The audiences especially the non-technical staff can easily have knowledge of the characteristics and advantages of the new screw pile hammers through watching the video file.

4.5 Make the Simulation Interface

According to the needs, use C++ language program in MFC framework to make the simulation interface. Virtual simulation interface as shown in figure6, there are four buttons in the top right corner of interface which mean the machine assembly, piling, transposed construction and pile hammer removal. Click on the buttons to play the corresponding video animation.

Fig. 6. Virtual simulation interface

5 Conclusion

This thesis uses the virtual simulation of the new screw pile hammers as an example, and puts forward a virtual simulation method based on a combination of multi-software platforms. It focuses on the introduction to the working process of this virtual simulation method, achieves the goal of seamless connection of different software, the build of 3d model of the pile hammer, and the production of the virtual pile hammer. Meanwhile, the virtual simulation of four processes demonstrates the functions of the new screw pile machine in different stages and the principle of piling. Compared with the traditional method, the new method is more flexible to modify and more authentic.

References

1. Yan, Y., Shi, G.: Virtual simulation method and its application research based on a combination of multi-software platforms, 3rd phase, vol. 23 (March 2006)
2. Xiao, Z., Zheng, R.: A joint simulation analysis method based on multi-software. Machine and Hydraulic, 6rd phase, vol. 38 (March 2010)
3. Cai, W., Chen, G.: Design of the virtual simulation system for mine based on 3DMax and Virtools. Coal Engineering, 1st phase (2011)
4. Gong, Y.: Course Exercise in Mechanical Design. Science Press, Beijing, TH122-41 (2008)
5. Wu, Z.: Manual of the Mechanical Designer. China Machine Press, Beijing, TH122-62
6. Wang, W., Wang, J.: Mechanical Design. Huazhong University of Science and Technology Press, Wuhan, TH122 (2007)

The Interference Effect of Group Diversity on Social Information Foraging

Guichuan Sun, Wenjun Hou, and Yu Cui

Beijing Key Laboratory of Network System and Network Culture
Automation School, Beijing University of Posts and Telecommunications
No.10, Xi Tu Cheng Road, Beijing, 100876
Wenjunh2113@263.com

Abstract. In order to find useful information efficiently among vast amounts of information, Pirolli built the basic social information foraging (SIF) model (basic SIF model) and proposed related theories. Traditional information foraging theory proposed that information foraging process is divided into within-patch and between-patch. This paper focused on the interference effect between patches in the social information foraging environment, which has not been covered by the SIF model. Then this paper proposed that group diversity play an important role in this process and built the interference cost model of this process to improve the social information foraging model. Experimental results show the correctness and practical value of this model.

Keywords: social information foraging, group diversity, interference effect.

1 Introduction

Technology progress and rapid development of Internet make people have to face the huge amounts of information. It is a problem to find useful information efficiently among these vast amounts of information. Against this background，in order to obtain more information foraging gains，Pirolli built the basic social information foraging (SIF) model(basic SIF model) [3],which derives from the quantitative theory of cooperative problem solving developed by Clearwater, Hogg, and Huberman [1]and is consistent with the theory of social structural holes (structural holes theory) proposed by Ronald S. Burt[2]. The basic SIF model also incorporates some simple general assumptions about the nature of interference costs that arise in cooperation，based on the computational ecology studies of group foraging by Seth[4]. Traditional information foraging theory proposed that information foraging process is divided into within-patch and between-patch. Analysis of the reasoning process of the model found that Pirolli only consider the individuals foraging interference costs of information search and decision-making in within-patch process，but not the between-patch process.

Through the analysis of the problem mentioned above, we found that inspired and prompted by the group members will be impossible to share and transfer completely

Q. Zu, B. Hu, and A. Elçi (Eds.): ICPCA-SWS 2012, LNCS 7719, pp. 447–453, 2013.

in group synergy, because the diversity of the group will inevitably reduce the efficiency and energy of the group synergy. Then, analyze the causes of interference effects based on the group diversity. We are trying to identify the logical relationship between group diversity and interference effects through the analysis of diversity theory, and propose the information foraging interference cost model of between-patches combined with the knowledge of social psychology, organizational behavior and related disciplines, thereby improving the social information foraging model.

2 Interference Effects of the Group Diversity on Social Information Foraging

According to the Structural Holes Theory [2], we can summarize:

1. Group members distribute in the physical space and cognitive space in accordance with the model of structural holes, because of different physical and cognitive distance.
2. Middleman in the structural holes model would be a corresponding role with different background, age, gender, education level and interpersonal relationship, which lead to different network constraints in the social network.
3. Different physical and cognitive properties are also the reason of asymmetric information transmission in social networks.
4. The group diversity is defined as the performance of the individual attribute differences in the group.

These factors will be the key factors of the overall behavior of the affected groups. Based on the above analysis, we propose the following assumptions:

There will be interference effects in the process that individuals search for information between patches, caused by group diversity.

2.1 Attributes of Group Diversity

There are many classification of the group diversity. Based on the difficulty to identify, classic diversity model [5] will be divided into Group Surface-Diversity and Group Deep-Diversity.

Group surface-diversity mainly refers to the demographic characteristics of the group members. Borrowed from the research of Neal M. Ashkanasy about organizational behavior[6], this paper select nine main features of surface diversity that directly relate to the deep-diversity ,which are Gender, age, race, geographical categories, education, occupational categories, professional level, length of service in the organization and economic conditions. According to the mathematical properties of these demographic attributes, these nine surface characteristics can be divided into two categories. Among them, age, length of service in the organization, and economic conditions are numeric attributes; gender, race, geographical categories, education, occupational categories, professional level are categorical attributes.

The numerical diversity property can be performed by the coefficient of variation, which is the percentage of the expectation of the numerical standard deviation. It can measure the dispersion degree of the data. The greater the difference coefficient is, the more obvious dispersion degree of data is. The coefficient of variation is usually expressed as V_s, which is calculated as follows:

$$V_s = \frac{\sqrt{\frac{\sum_j^n (y_i - \overline{y})^2}{N}}}{\bar{y}} \tag{1}$$

The categorical attribute property can be calculated by the difference formula proposed by Teachman [7]. Normalized difference coefficient $V_i$can be expressed as:

$$V_i = \frac{-\sum_{i=1}^{I} P_i (ln\, P_i)}{lnI} \tag{2}$$

I is the number of Category attribute variables, Pi is the percentage of each category in the total members of the group.

In this paper, the numeric attributes is positive integers, then V_i and V_s belong into the numerical range of 0 to 1. The closer it is to 0, the smaller the difference coefficient is.

It is difficult to study the deep-diversity because it has complex content and is difficult to be observed. Therefore, according to the basic theory of the group diversity, the scholars divided the deep-diversity into cognitive diversity and relational diversity [8].

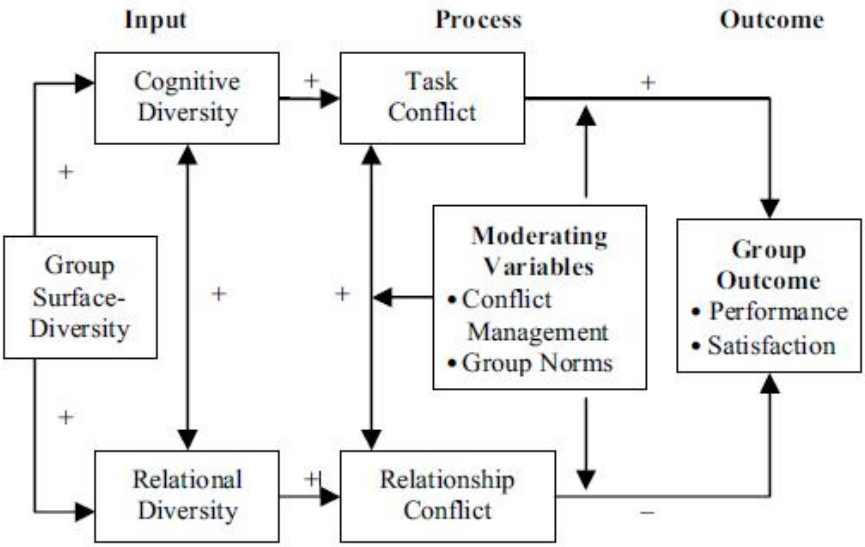

Fig. 1. The Integrated model of group diversity, conflict and group outcomes

The group diversity also concentrates on the costs and benefits of group behavior. In order to understand the input and output "black box" model of the group diversity

more easily, group diversity has been summarized as IPO (Input-Process-Outcome) model, shown in Figure 1[9].

Research has shown that correlation between the properties of diversity is complex and multidimensional. At the highest level, group surface-diversity and deep-diversity are positively correlated. Further, the properties of the deep-diversity in cognitive diversity and relational diversity will influence each other [10].

Under the hypothesis that deep-diversity is determined by the properties of all surface-diversity directly, we propose the mapping between the group deep-diversity D_d and group surface-diversityD_s, shown as

$$D_d = \sum_{i=1}^{N} w_i D_{si} \tag{3}$$

N is the total number of categories of surface-diversity and w_i is the impact factor of the i-th surface-diversity properties.

2.2 Mechanism of Interference Effects with Group Diversity

In the basic SIF model, group synergy plays a role through the heuristic or hints between the members and the number of distinct effective hints, H. And H is assumed to be linear correlation of the group size, N [3].

But in fact, due to the selectively of structural holes distribution of the group members and transmission of information, the group synergies will be significantly affected. The main effect is to reduce the quantity and quality of hints that the individuals can receive from other members in the group.

According to the deduction method proposed by Huberman, the quality of hints will follow a lognormal distribution related to H. Therefore, H can reflect the role of interference effects. So we need to research the relationship between properties of diversity and H.

Based on the behavior of group synergy, we summarize them as a few key steps

1. Individuals receive information for the first time
2. Individuals share information to the group space
3. Form an independent prompt information cloud in Group
4. Individuals receive the prompt information

This paper defines n as the total amount information that group members received for the first time. In the basic SIF model assumptions, individual foraging heuristic or hints make sense only in the situation that information is not repeated. Therefore, we define η as the repetition rate that individuals contact information for the first time in the group environment ($0<\eta<1$). Social information foraging related theory mention that the distribution of the individual members of the social information foraging environment is consistent with the structural holes model. Individual has a different role and influence on the social network constituted by group members, because of background attributes and location differences. This paper assumes that this influence embodied in the

collaborative process through information-sharing behavior. Therefore, we define μ_i as the information sharing rate of individual i in the group environment ($0 < \mu_i < 1$).

On the basis of above definitions, we can express the number of distinct effective hints of group as $n(1-\eta)$. We motioned above that individual information needs to release into the community environment to be received by the other members. Under the assumption of individual undifferentiated, we assume that the group members have homogenization behaviors in this collaborative process Model of interference cost with group diversity. Therefore, this paper expresses the group sharing rate as the expectation of individual sharing rate, $E\mu$.

Then we can express the max number of distinct effective hints, H_D

$$H_D = n(1-\eta)E\mu \tag{4}$$

Based on the above，we can make use of the empirical and computer model to build the mathematical model of the role of deep-diversity played on the synergistic effect.

According to the assumptions of basic SIF model, there is no difference between individuals in the social information foraging. Therefore, we assume

$$n = aN \tag{5}$$

a is the total amount of useful information individual received in information foraging between patches when $N = 1$.

Individuals with different cognitive has different perspectives and solutions facing the same problem. They prefer to contact with information associated with the individual cognitive domains in social information foraging. In this situation, the same cognitive part will guide the individual using the same approach. Therefore, we assume

$$\eta = b(1 - D_{d-c}) \tag{6}$$

b is the conversion rate between the cognitive and information, which belongs into the numerical range of 0 to 1.

Related study pointed out that different backgrounds and experiences between individuals is easy to interfere with communication and cohesion among group members, which means that relational diversity have affected the individual information-sharing. According to the structural holes theory [2] and the empirical model, we propose that it is consistent with the power-law, which can be expressed as

$$E\mu = cN^{-D_{d-r}} \tag{7}$$

c is the share constant, that is, when N = 1, the individual's share rate.

Finally, we can obtain the formula 8 putting the formula 5,6and7 into formula 4:

$$H_D = ac(bD_{d-c} + 1 - b)N^{(1-D_{d-r})} \tag{8}$$

That is the interference cost model expressed by deep-diversity ($D_{d-\mathrm{r}}$,D_{d-c})).

3 Model Validation

In micro-blogging, information arranged in reverse chronological order in the individual's Timeline. This information is produced by the individual concerning crowd and relate to all users of the micro-blogging. Therefore, we treat the whole micro-blogging environment as the social information foraging environment. We treat each individual's concerning crowd as an information foraging group. The information in the individual Timeline is received from the other members of the groups. Therefore, amounts of non-duplication information can be considered as the max number of distinct effective hints, H_D

This paper randomly selects 50 of the Sina micro-blogging female artist users as the research individuals and analyzes micro-blogging information from May 1 to June 1, 2012 through the Web crawler tools to verify the theory proposed in this paper.

We select the female artist from concerning crowd of these individuals as a sample for data collection to ensure that the group has a similar diversity. We import the data into the Origin data analysis tools. Data collection results, fitting curves and evaluation are as follows:

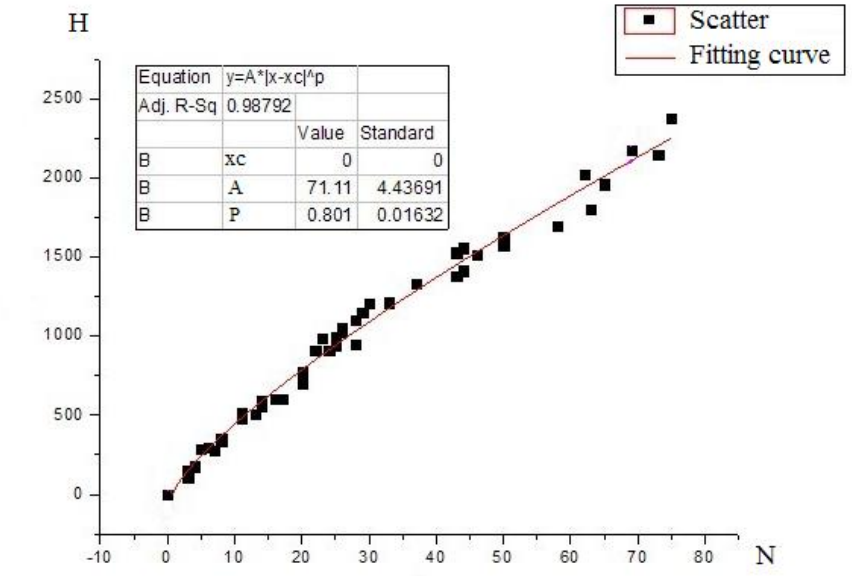

Fig. 2. Data collection results, fitting curves and evaluation

The analysis shows that the curve can well fit the sample data. P stands for the value of $1 - D_{d-\mathrm{r}}$. Then we know that the value of relational diversity ($D_{d-\mathrm{r}}$) is 0.199, which shows that the selected sample has a low relational diversity.

4 Summary

In this paper, we research the interference effect of group diversity on social information foraging and convert these effects to the relationship between group di-versity and the number of distinct effective hints, H. Then we build the interference cost model of information foraging between patches, and amend the basic SIF model, which make the social information foraging gains closer to the real situation. Then we take micro-blogging for example and preliminary verify the interference cost model. Experimental results show the correctness and practical value of the interference cost model of information foraging between patches.

However, because the related theory is built on interdisciplinary, which com-bines the knowledge of sociology, psychology, biology, behavior and others, throughout the study, there are some idealized assumptions. In addition, the interference cost model is built on the basis of the empirical model. Social information foraging environment shows a wide variety and analysis of individual behavior in the group environment requires a large number of observations. Therefore, it needs multi-dimensional experiments to improve the theories and models proposed in this paper. These will be the focus of future research.

References

1. Huberman, B.A.: The performance of cooperative processes. Physica D (42), 38–47 (1990)
2. Burt, R.S.: Structural Holes-The Social Structure of Competition, 18 (1922)
3. Pirolli, P.: An elementary social information foraging model. In: Proceedings of the 27th International Conference on Human Factors in Computing Systems, pp. 605–614 (2009)
4. Seth, A.K.: Modeling group foraging: Individual suboptimality, interference, and a kind of matching. Adaptive Behavior (9), 67–90 (2002)
5. Jehn, K.A.: A multimethod examination of the benefits and determinants of intragroup conflict. Administrative Science Quarterly (40), 256–282 (1995)
6. Ashkanasy, N.M., Hartel, C.E.J., Daus, C.S.: Diversity and emotion:the new frontiers in organizational behavior research. Journal of Management 28(3), 307–338 (2002)
7. Teachman, J.D.: Analysis of Population Diversity. Sociological Methods 8(3), 341–362 (1980)
8. Harrison, D.A., Price, K.H., Bell, M.P.: Beyond relational demography: time and the effects of surface- and deep-level diversity on work group cohesion. Academy of Management Journal (41), 96–107 (1998)
9. Liu, Y., Wei, X., Luo, M., Hu, Z.: An Integrated Model of Group Diversity, Conflict and Outcomes: A Process-based Perspective. In: 4th International Conference on Wireless Communications, Networking and Mobile Computing, WiCOM 2008, pp. 1–4 (2008)
10. Miller, C.C., Burke, L.M., Glick, W.H.: Cognitive diversity among upper-echelon executives: implications for strategic decision processes. Strategic Management Journal (19), 39–58 (1998)

Hierarchical Clustering with Improved P System*

Jie Sun and Xiyu Liu**

School of Management Science and Engineering, Shandong Normal University, Jinan 250014, China
{sdxyliu,sjiezz}@163.com

Abstract. Membrane computing has a characteristic of great parallelism, so it has been applied in broad fields such as Biological modeling, NPC problems and combinatorial problems by reducing the computational time complexity greatly. In this paper we approach the problem of hierarchical clustering with a new method of membrane computing. An improved P system with external output is designed for finite set individuals with nonnegative integer variables. In the process of hierarchical clustering, the clustering is obtained depending on the dissimilarity between individuals or groups, so the less dissimilar two individuals are, the more similar they are. For an arbitrary matrix P_{Nk} representing the values of N individuals, one possible hierarchy with clusters can be obtained by this improved P system in a non-deterministic way. The time complexity is polynomial in the number of individuals, the number of variables and the certain maximum value A^* without increasing the complexity of the classical clustering algorithms. At the end of this paper, we cluster an example of dataset to obtain the final results. Through example test, we verify the feasibility and effectiveness of this improved P system to solve hierarchical clustering problems. A greater range of hierarchical clustering problems will be solved with this improved P system.

Keywords: Membrane computing, P system, Hierarchical clustering.

1 Introduction

Hierarchical clustering, as an important method of clustering, obtains clusters successively by separating individuals hierarchically. In this paper the problem of hierarchical clustering is approached with membrane computing. An improved P system with improved rules based on the P system in [1] is designed to solve hierarchical clustering of individuals with nonnegative integer variables. The amount of used resources is polynomial. More hierarchical clustering problems will be solved with this new model of computation.

* This work is supported by the Natural Science Foundation of China(No.61170038), Natural Science Foundation of Shandong Province, China (No.ZR2011FM001), Humanities and Social Sciences Project of Ministry of Education, China (No.12YJA630152), Social Science Fund of Shandong Province, China (No.11CGLJ22), Science-Technology Program of the Higher Education Institutions of Shandong Province, China (No.J12LN22).

** Corresponding author.

Q. Zu, B. Hu, and A. Elçi (Eds.): ICPCA-SWS 2012, LNCS 7719, pp. 454–460, 2013.

2 Hierarchical Clustering

In the case of the hierarchical clustering, we need to group the individuals in similar groups whose members are all similar. The grouping follows a hierarchy formed by the partitions $P_0, P_1, \cdots, P_m$ of the individuals. At first, the partition P_0 consists of N groups. The groups join progressively until arriving at the last partition P_m that contains one group formed by all individuals.

The k-set $\Omega = \{w_1, \cdots, w_N\}$ is the dataset in hierarchical clustering. The values of the individuals can be represented in matrix form and w_{ij} is the value of the j-th variable of the individual i :

$$P_{Nk} = \begin{pmatrix} w_{11} & w_{12} & \cdots & w_{1k} \\ w_{21} & w_{22} & \cdots & w_{2k} \\ & & \cdots & \\ w_{N1} & w_{N2} & \cdots & w_{Nk} \end{pmatrix}$$

In the process of obtaining clusters, we choose the minimum dissimilarity successively to obtain the result. The less dissimilar two individuals are, the more similar they are, and so the individuals with low degree of dissimilarity will be grouped in similar groups. We work with nonnegative integer variables, so the dissimilarity we used is the Manhattan Distance [2] and it is defined as follows:

(1) Dissimilarity between individuals:

$$\forall w_i, w_j \in \Omega: \quad d(w_i, w_j) = \sum_{r=1}^{k} \left(\left| w_{ir} - w_{jr} \right| \right), \; w_i = \{w_{i1}, \cdots, w_{ik}\} \tag{1}$$

(2) Dissimilarity between groups:

$$d(h_1, h_2) = \max\left\{ d(w_i, w_j) \middle| \; w_i \in h_1, w_j \in h_2 \right\} \tag{2}$$

For a given dataset Ω, hierarchical clustering algorithm is used to obtain a hierarchy H whose elements are classified clusters. Therefore the input of this algorithm is the k-set Ω, and the output is a hierarchy H. The procedure is as follows.

(1) Put each individual of Ω in its own cluster, creating the first partition of clusters.

$$P_0 = \{D_1 = \{w_1\}, D_2 = \{w_2\}, \cdots, D_N = \{w_N\}\}$$

(2) Calculate the dissimilarities, by equation (1) and (2), between all the pair of clusters, and find the two closest clusters D_i, D_j $(1 \le i < j \le N)$ with the lowest dissimilarity, then group them and form a new cluster $D_i = D_i \cup D_j$.

(3) Remove D_j from the partition and obtain next partition P_i , $1 \le i \le N-1$.

(4) Go to step 2 until there is only one cluster remaining.

Remark: Because of the non-determinacy, if there is more than one possibility at step 2, one of them is chosen at random. Therefore the hierarchy *H* obtained is not unique.

3 Hierarchical Clustering with Membrane Computing

3.1 Designing a P System

Firstly we presume that the maximum value in Ω is A^*, $\max_{i=1,j=1}^{i=N,j=k}(w_{ij}) = A^*$, So $\Omega \in \{0,1,2,3,4,5;\cdot\cdot\}^k$ .The P system associated with the matrix P_{Nk} for clustering is defined as follows:

$$\prod(P_{Nk}) = (\Gamma(P_{Nk}), \mu(P_{Nk}), \tau, \omega_1, \omega_2, \ldots, \omega_{N-1}, \omega_N, R, \rho)$$

Where

$$\Gamma(P_{Nk}) = \{a_{js},\ b_{js} : 1 \le s \le k \wedge 1 \le j \le N\} \cup \{D_{ij},\ C_{ij} : 1 \le i < j \le N\} \cup \{\#\} \cup$$
$$\{\beta_i : 0 \le i \le A^*k-2\} \cup \{\alpha_{(ij)^t},\ X_{(ij)^t} : 1 \le i < j \le N, 1 \le t \le A^*k-1\} \cup \{\phi\} \cup$$
$$\{h_i : 1 \le i \le N\} \cup \{\varepsilon_i : 0 \le i \le 3A^*k-2\} \cup \{\eta_i : 0 \le i \le (N-1)(3A^*k-1)\}$$

Membrane structure: $\mu(P_{Nk}) = [_N\ [_1]_1\ [_2]_2 \cdots [_{N-1}]_{N-1}\ ]_N$

External output: $\tau = \{X_{(ij)^t}\},\ 1 \le i < j \le N, 1 \le t \le A^*k$

Initial multisets: $\omega_i = \{a_{js}^{w_{is}} : 1 \le s \le k \wedge 1 \le i \le N-1 \wedge i+1 \le j \le N\} \cup$
$$\{b_{js}^{w_{js}} : 1 \le s \le k \wedge 1 \le i \le N-1 \wedge i+1 \le j \le N\};$$

$$\omega_N = \{h_N,\ \varepsilon_0,\ \eta_0\};$$

Rules in the skin membrane labeled N:

$$r_0 = \{\varepsilon_0 \to \varepsilon_1\beta_0\} \cup \{\varepsilon_i \to \varepsilon_{i+1} : 1 \le i \le 3A^*k-2 \wedge i \ne A^*k\} \cup$$
$$\{\eta_i \to \eta_{i+1} : 0 \le i \le (N-1)(3A^*k-1)-1\}$$

$$r_u = \{\beta_{u-1}D_{ij}^u \to \alpha_{(ij)^u} : 1 \le i < j \le N\}\ \ 1 \le u \le A^*k-1$$

$$r_u' = \{\beta_{u-1} \to \beta_u\}\ \ 1 \le u \le A^*k-1$$

$$r'_{A^*k-1}=\left\{\eta_{(N-1)(3A^*k-1)}\to(\#,out)\right\}$$

$$r_{A^*k}=\left\{\varepsilon_{A^*k}h_q\alpha_{(ij)^t}\to\varepsilon_{A^*k+1}X_{(ij)^t}^{A^*k}h_{q-1}\left(X_{(ij)^t},out\right):2\le q\le N,\right.$$
$$\left.1\le i<j\le N,\ 1\le t\le A^*k-1\right\}$$

$$r'_{A^*k}=\left\{\varepsilon_{A^*k}\to\varepsilon_{A^*k-1}\right\}$$

$$r_{A^*k+1}=\left\{X_{(ij)^t}D_{ip}D_{jp}\to C_{ip}X_{(ij)^t}:1\le i<j<p\le N,1\le t\le A^*k-1\right\}$$

$$r'_{A^*k+1}=\left\{X_{(ij)^t}D_{ip}\to C_{ip}X_{(ij)^t}:1\le i<j<p\le N,1\le t\le A^*k-1\right\}\cup$$
$$\left\{X_{(ij)^t}D_{jp}\to C_{ip}X_{(ij)^t}:1\le i<j<p\le N,1\le t\le A^*k-1\right\}$$

$$r_{A^*k+2}=\left\{X_{(ij)^t}D_{ip}D_{pj}\to C_{ip}X_{(ij)^t}:1\le i<p<j\le N,1\le t\le A^*k-1\right\}$$

$$r'_{A^*k+2}=\left\{X_{(ij)^t}D_{ip}\to C_{ip}X_{(ij)^t}:1\le i<p<j\le N,1\le t\le A^*k-1\right\}\cup$$
$$\left\{X_{(ij)^t}D_{pj}\to C_{ip}X_{(ij)^t}:1\le i<p<j\le N,1\le t\le A^*k-1\right\}$$

$$r_{A^*k+3}=\left\{X_{(ij)^t}D_{pi}D_{pj}\to C_{pi}X_{(ij)^t}:1\le p<i<j\le N,1\le t\le A^*k-1\right\}$$

$$r'_{A^*k+3}=\left\{X_{(ij)^t}D_{pi}\to C_{pi}X_{(ij)^t}:1\le p<i<j\le N,1\le t\le A^*k-1\right\}\cup$$
$$\left\{X_{(ij)^t}D_{pj}\to C_{pi}X_{(ij)^t}:1\le p<i<j\le N,1\le t\le A^*k-1\right\}$$

$$r_{A^*k+4}=\left\{X_{(ij)^t}^{A^*k}\to X_{(ij)^t}^{q-2}:1\le i<j\le N,1\le t\le A^*k-1,2\le q\le N\right\}$$

$$r_{A^*k+5}=\left\{C_{ij}\to D_{ij}:1\le i<j\le N\right\}\cup$$
$$\left\{\varepsilon_{3A^*k-1}X_{(ij)^t}^{q-2}h_{q-1}\to\varepsilon_1\beta_0h_{q-1}:1\le i<j\le N,1\le t\le A^*k-1\right\}$$

$$r'_{A^*k+5}=\left\{\varepsilon_{3A^*k-1}\to\varepsilon_1\beta_0\right\}$$

Rules in the skin membrane labeled i:

$$r_{A^*k+6}=\left\{a_{js}b_{js}\to\phi:1\le s\le k,i+1\le j\le N\right\}$$

$$r'_{A^*k+6}=\left\{a_{js}\to(D_{ij},out):1\le s\le k,i+1\le j\le N\right\}\cup$$
$$\left\{b_{js}\to(D_{ij},out):1\le s\le k,i+1\le j\le N\right\}$$

Priority relation on the membrane labeled i: $\rho_i=\left\{r_{A^*k+6}>r'_{A^*k+6}\right\}$

Priority relation on the skin membrane labeled N:

$$\rho_N=\left\{r_1>r'_1>r_2>r'_2>\ldots r_{A^*k-1}>r'_{A^*k-1}\right\}\cup\left\{r_{A^*k}>r'_{A^*k}\right\}\cup$$
$$\left\{r_{A^*k+i}>r'_{A^*k+i}:1\le i\le3\right\}\cup\left\{r_{A^*k+1}=r_{A^*k+2}=r_{A^*k+3}>r_{A^*k+4}>r_{A^*k+5}>r'_{A^*k+5}\right\}$$

3.2 The Computations and Performance Analysis in P System

At the beginning of a computation the membrane labeled i contains the object $a_{js}^{w_{is}}$, $b_{js}^{w_{js}}$. The number of $a_{js}^{w_{is}}$, $b_{js}^{w_{js}}$ is equal to w_{is} , w_{js} . The skin membrane firstly contains the objects $h_N, \varepsilon_0, \eta_0$. The object h_N indicates the number of clusters. The object ε_0 used to synchronize the loop. The object η_0 is a counter used to stop the P system after $(N-1)(3A^*k-1)$ steps and the system send the object # into the environment.

The rules r_{A^*k+6}, r'_{A^*k+6}, are initially applied in membrane labeled i to send the object D_{ij} to the skin membrane. The multiplicity of D_{ij} represents the dissimilarity between individuals. The rules in membrane labeled i were modified to obtain the number of D_{ij} by eliminating the same parts of the individual i and j and transforming the different parts into D_{ij} [3].

In the membrane labeled N, the rules are applied by loops of $3A^*k-1$ steps. Each one of these loops is formed by two stages. The first stage is formed by A^*k steps, the rule r_0 is firstly applied to obtain ε_1 and β_0, then transform the object ε_1 until we obtain the object ε_{A^*k}. The rules r_u and r'_u are applied to select the object D_{ij} with minimum multiplicity. In the k-th step of the loop, the rule r_{A^*k} produces the objects $X_{(ij)^t}$ and sends a copy to the environment. The objects $X_{(ij)^t}$ represent that the clusters with lowest dissimilarity can be united to form a new cluster. What's More, in rule r_{A^*k} the object h_q is transformed in the object h_{q-1} which indicates the fact that two clusters have been united and the number of the clusters has decreased by one. In this stage the rule r_u was modified to select the object D_{ij} with minimum dissimilarity between the clusters i and j.

In the second stage, the rules $r_{A^*k+1}, r'_{A^*k+1}, r_{A^*k+2}, r'_{A^*k+2}, r_{A^*k+3}, r'_{A^*k+3}$ calculate the dissimilarities between new cluster i and the other clusters. After the rules r_{A^*k+4} and r_{A^*k+5}, this information is kept in the objects D_{ip}. In the $(3A^*k-1)$-th step of the loop, the rule r_{A^*k+4} transforms the object ε_{3A^*k-1} in the objects β_0 and ε_1 to continue the loop. The improvement in this stage is the modification of the rules r_{A^*k+1}, r'_{A^*k+1}, r_{A^*k+2}, $r'_{A^*k+2}, r_{A^*k+3}, r'_{A^*k+3}$. Because of the definition of dissimilarity between groups, equation (2), the rules calculating the dissimilarities between new cluster and the previous clusters need to obtain the maximum

differentiation between two clusters, thus the rules $r'_{A^*k+1}, r'_{A^*k+2}, r'_{A^*k+3}$ was created to make it certain. When there is no object of D_{ij} in membrane N, the rule r'_{A^*k-1} is applied to stop the P system.

3.3 Performance Analysis of the P System

Considering the powerful storage capacity of cellular membranes in biological system, we merely analyzed the time complexity of the P system. As we analyzed above, there are N clusters at first and in each loop two clusters are united so we need N-1 loops to obtain the last cluster. So a hierarchy with clusters is obtained with $(N-1)(3A^*k-1)$ steps and the time complexity is polynomial. Consequently it is possible to construct the system $\prod(P_{Nk})$ from the matrix P_{Nk} by means of a Turing machine working in polynomial time.

4 Example and Illustration

In order to verify the feasibility and effectiveness of the improved P system, we cluster an example to obtain the final results. In the example, N =6, k=5, $A^* = 9$, and the matrix form is as follows.

$$P_{65} = \begin{pmatrix} 0 & 0 & 0 & 0 & 1 \\ 1 & 3 & 5 & 7 & 8 \\ 5 & 6 & 9 & 4 & 3 \\ 7 & 8 & 2 & 3 & 1 \\ 6 & 9 & 5 & 2 & 3 \\ 2 & 4 & 3 & 5 & 7 \end{pmatrix}$$

(1) Create the first partition of clusters firstly and design a P system for this matrix P_{65}.

$$P_0 = \{D_1 = \{w_1\}, D_2 = \{w_2\}, \cdots, D_6 = \{w_6\}\}$$

(2) Calculate the dissimilarities, group two closest clusters D_i, D_j and form a new cluster $D_i = D_i \cup D_j$. The objects D_{ij} produced in this example are as follows:

$$D_{12}^{23}, D_{13}^{26}, D_{14}^{20}, D_{15}^{24}, D_{16}^{20},$$
$$D_{23}^{19}, D_{24}^{25}, D_{25}^{21}, D_{26}^{7},$$
$$D_{34}^{14}, D_{35}^{10}, D_{36}^{16},$$
$$D_{45}^{8}, D_{46}^{18},$$
$$D_{56}^{18}.$$

The rules r_u and $r_u^{'}$ is applied to select the object D_{26}^7 with minimum multiplicity. After that, the rule r_{A^*k} is applied to produce the object $X_{(26)^7}$ which represents that a new cluster $D_2 = D_2 \cup D_6$ is formed.

(3) A new cluster D_2 is formed, and then D_6 is removed.

$$P_1 = \{D_1 = \{w_1\}, D_2 = \{w_2\ ,\ w_6\}, \cdots, D_5 = \{w_5\}\}$$

(4) Go to step (2) until there is only one cluster remaining.

After operating in P system with hierarchical clustering algorithm, we can get the results.

The output of this P system:

$$X_{(26)^7}, X_{(45)^8}, X_{(34)^{14}}, X_{(12)^{23}}, X_{(13)^{26}}$$

The partitions we obtained are as follows:

$$P_0 = \{\ D_1 = \{w_1\}, D_2 = \{w_2\}, D_3 = \{w_3\}, D_4 = \{w_4\}, D_5 = \{w_5\}, D_6 = \{w_6\}\ \}$$
$$P_1 = \{\ D_1 = \{w_1\}, D_2 = \{w_2\ ,\ w_6\}, D_3 = \{w_3\}, D_4 = \{w_4\}, D_5 = \{w_5\}\ \}$$
$$P_2 = \{\ D_1 = \{w_1\}, D_2 = \{w_2\ ,\ w_6\}, D_3 = \{w_3\}, D_4 = \{w_4\ ,\ w_5\}\ \}$$
$$P_3 = \{\ D_1 = \{w_1\}, D_2 = \{w_2\ ,\ w_6\}, D_3 = \{w_3\ ,\ w_4\ ,\ w_5\}\ \}$$
$$P_4 = \{\ D_1 = \{w_1\ ,\ w_2\ ,\ w_6\}, D_3 = \{w_3\ ,\ w_4\ ,\ w_5\}\ \}$$
$$P_5 = \{\ D_1 = \{w_1\ ,\ w_2\ ,\ w_6\ ,\ w_3\ ,\ w_4\ ,\ w_5\}\ \}$$

5 Conclusions

In this paper, we propose an improved P system with improved rules based on the P system in [1] to solve hierarchical clustering of individuals with nonnegative integer variables. The time complexity is polynomial. So this improved P system is feasible and effective to solve a greater range of hierarchical clustering problems. In future, we will continue to research how to using membrane computing techniques to cluster the individuals with more clustering algorithms, such as Chameleon, CURE and ROCK.

References

1. Cardona, M., Angels Colomer, M., Perez-Jimenez, M.J., Zaragoza, A.: Hierarchical Clustering with Membrane Computing. Computing and Informatics 27, 497–513 (2008)
2. Jia, Z.W., Cui, J., Yu, H.J.: Graph-Clustering Method Based on the Dissimilarity. Journal of Shanxi Agricultural University 29(3), 284–288 (2009)
3. Huang, C.Y., Dong, X.J., Long, H.: Solving Sorting Problem by P System. Journal of Shanghai Jiaotong University 42(2), 206–208 (2008)

A New Positioning Algorithm in Mobile Network

Shaohua Teng[1], Shiyao Huang[1], Yingxiang Huo[1], Luyao Teng[2], and Wei Zhang[1]

[1] School of Computer, Guangdong University of Technology,
Guangzhou 510006, China
shteng@gdut.edu.cn, {420996162,369867128}@qq.com,
weizhang@gdut.edu.cn
[2] Monash University, Melbourne, Australia
180885094@qq.com

Abstract. In face of an increasingly competitive mobile communications market, how to keep the customers is the most important factor for operators and enterprises. The development of enterprise cannot be separated from customers. In general, clients always require more stable and better quality of network services, and more rapid response to their demand. The operators keep of making customers' more satisfactory by a deal of services. In this paper, we study how to position the mobile terminal by analyzing user communication data which includes the base stations, the communication signal data, user information, and so on. The text shows the reasons that affect the positioning accuracy of mobile network. At last we propose a fast locating algorithm about the mobile terminals based on multiple base stations. The experimental results of current mobile network data show the efficiency of our method.

Keywords: locating algorithm, mobile client, client behavior, client analysis.

1 Introduction

China Mobile's strategy is: "Becoming world-class enterprises, achieving new spans from excellent to outstanding". So they have paid an attention to realize the overall, balanced, sustainable development for enterprise's economics, community and environment. It's mainly engaged in mobile voice, data, IP telephone and multimedia services, and it owns many well-known brands such as "global ", "Shenzhou Xing ", " M-Zone " and so on. China Mobile has more than 360 thousands base stations and more than 450 million households, and is the largest telecom company. It has the largest network and clients in the world [1]. Along with the mobile applications into people's work and life, the customers require more and better network services. The management of Mobile Operator is becoming more scientific day by day. Mobile Operators pay more attention to analyze clients' data. Specially, the analysis of user behavior is very important. It is used to setting base stations, improving communication signal, loading balancing, deciding business planning and markets, detecting fraud of illegal users, and improving service quality.

Q. Zu, B. Hu, and A. Elçi (Eds.): ICPCA-SWS 2012, LNCS 7719, pp. 461–476, 2013.

2 Related Work

The positioning technology of the wireless network is the key technology, which is used to explore the wireless coverage, optimize network, analyze user behavior, and develop new user. Without the help of the GPS, many methods to improve positioning accuracy and minimize positioning overhead are proposed. The data that is used to locate mobile users includes social behavior data, communication data, business position, and business type. The business time and type can be determined by time stamp and flag data, but user position information is difficult to determine. It is a bottleneck of analyzing user behavior. Many positioning methods are proposed, but positioning accuracy is low. The method of comparing time is a common method. The general rules of normal client behavior are extracted by analyzing a deal of historic data that is composed of delaying time of communication, starting time, times, and so on. In general, wireless location methods can be divided into the following categories.

2.1 Common Wireless Terminal Location Methods

(1)Mobile Station Signal Strength of Arrival (SSOA)
The field strength arriving mobile station signal is used to locate. Specific methods are as follows [2]: the distance between the base station and the mobile node is calculated according to the radio wave propagation model and these parameters. They are field strength measuring or receiving by mobile node, field strength values of nearby base stations, and collecting transmit power. The location of the mobile node is approximated and estimated according to the latitude and longitude of the adjacent base stations, and distance between base station and the mobile node. The positioning accuracy depends on matching measure between radio wave propagation model and environment. Okumura model, Hata model, and the Okumura-Hata model were often used, but it cannot be guaranteed that these models match well with the environment. The SSOA method may exist much deviation.

(2)Time of Arrival (TOA)
The propagation time of TOA [3] scheme is defined by delaying of radio propagation signal from base stations to mobile. The TOA scheme calculates distance between mobile and base station by propagation delay of signal. This method needs arrival time values from 3 base stations to mobile and synchronous accuracy. It is difficult and error for the method, because propagation delay of signal is unknown. Propagation delay of signal needs to be measured. This method has a large overhead.

(3)Time Difference of Arrival (TDOA)
TDOA [4] is an improved algorithm of a TOA. Because the signal propagation delay calculating accurately is difficult in TOA method, the signal delay difference spreading from two base stations to mobile terminal is used to position a mobile terminal. TDOA's error is less than TOA, since it is calculated by differential. Although this method is used in positioning GPS or radar, it still needs propagation delays of three base stations in cellular mobile communication system. The method also has a large

overhead [2]. The time-based location estimation algorithms can be categorized into the time-of-arrival (TOA) and the time difference-of-arrival (TDOA) techniques. The TOA scheme measures the arrival time of the radio signals from different wireless base stations, while the TDOA [5] scheme measures the time difference between the radios signals.

(4)Angle of Arrival (AOA)

The basic idea is to steer in space a directional antenna beam until the direction of maximum signal strength is detected. In terrestrial mobile systems, the directivity required to achieve accurate measurements is obtained by means of antenna arrays (Sakagami et al.1994). Basically, a single measurement produces a straight-line locus from the base station to the mobile phone. Another AOA measurement will yield a second straight line, and the intersection of the two lines gives the position fix for this system [6]. Because AOA depends on antenna direction, the little deviation of antenna angle may lead to large deviation of positioning mobile. Along with intelligent antenna is used in TD-SCDMA and LTE networks, AOA technology becomes practical.

2.2 Other Location Methods

In addition to the common positioning methods, there are some mixed positioning methods and technologies based on data fusion, which are composed by combining with several basic positioning methods. These methods aim to improve positioning accuracy, or expand the service. Such as the circumference and a straight line method is, it determines the mobile station location coordinates by solving the intersection of circles and straight lines. It can remove the fuzzy solution according to the serving cell or cell sector information. The advantage of this method is that only needs one base station to participate in orientation. Thus the computational complexity of this method is low, its' positioning accuracy is poor.

The main problem of the positioning methods aforementioned is unable to adapt to the demand for large-scale real-time positioning. The large amount of system overhead is needed, and the accuracy of positioning cannot guarantee. Because the base station locate on information is known, a new method is proposed in the text. It is as follows: (1) calculating two Euclidean distances. The first is the distance between the main service area and the adjacent base station center. The second distance is calculated by radio wave propagation model, and parameters, level values received. (2)comparing two distance values. When the difference of two distances is very large, the coordinates of the vector of the user is adjusted. (3)pre-calculating the first distances. The calculation result is stored in a database. When it is needed, the first distance extracting directly from the database compares the second distance. The experimental results show the efficiency of our method. In this paper, we achieve fast and accurate positioning by using our positioning method. In general, mutual positioning services can be realized to meet the user's needs in the absence of satellite network coverage .

3 Client Behavior Analysis Model of Mobile

Mobile user behavior analysis aims at classify the user groups. The trajectory of the mobile user location is established through the geographic information of user, mobile data, and mobile user information. In modeling, the first step is to collect the data of the mobile communication. Nonlinear model parameters are used to model the social attributes of the mobile user groups by using the data regions, network status, and user groups. Finally a certain algorithm of analyzing mobile user behavior is used to model.

3.1 Analysis Model Architecture

The model is composed of data acquisition, data preprocessing, and analysis algorithm, and display module [7]. Data acquisition: collect data that should be analyzed; Data preprocessing: transform the collected data into a standardized, uniform data format; Analysis algorithm is the core of the model, which is used to model mobile user behavior; Display module displays analyzing results according to the mobile operator requirements. The model architecture is shown in Fig. 1.

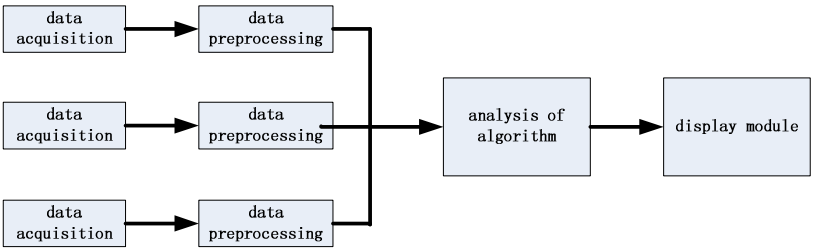

Fig. 1. Mobile user behavior model

3.2 Data Acquisition

The accuracy of the data analysis is guaranteed by collecting the mobile network traffic data and mobile user data, extracting the relevant social attributes, and exploiting social relationships among users. Because the GSM system is the main mobile communication network, analyzing data in this paper comes from the GSM data of mobile communication company in a province. The measurement report (MR) is mobile terminals in the real-time measurement of current network state. Partial lists of the MR data format are as shown in Table 1.

Table 1. MR data format

definition	declare	definition	declare
MR timestamp reported	the time of MR report	rxlev_dl_sub	Download Level SUB
Cell_identification	Lac/CI in the service area of the MR	rxqual_dl_ful	Download quality FUL
Carrier_frequency	Indicates MR carrier frequency	rxqual_dl_sub	Download quality SUB
Channel	channel types of MR reports	BS_ power	Base station power
TS	the number of the MR channel	MS_power	Mobile terminal power
MR _effective_ flag	The effectiveness of current MR	TA	Time advanced quantity
MSC	Mobile switch center	BA	ba_used
rxlev_dl_ful	Download Level FUL	CI_BSC	BSC belongs to Cell
N_n	ncell_num	LAC	location area code
CI_station	Station belongs to Cell		

3.3 Data Preprocessing

Firstly, extract location information of wireless from the MR data and the base station data, especially receiving level values of six adjacent areas base stations near mobile user, which are used to form the regional signal fingerprint vector. Cell LAC and cell CI may correspond to base station information. Main carrier wave of China's GSM network is 900MHz when 1800MHz is auxiliary. Data source in this paper comes from these parties. The first step, we get the latitude and longitude of the base station from the public parameter list. The second step, the intrinsic properties of the parameters of the mobile users can be extracted from MR frame. At last, we extract the boundary tag of the cell of mobile clients. So we can gain the social properties which affect user's behavior. These data are the resource of our model.

Secondly, because each attributes data is stored in the string type, data reading will take a very amount of calculation time even if the speed being 80-100Mb per second. Because position calculation needs numeric types, string type participating calculation is converted into numeric type. Converting data work can be completed in advance. That reduce calculating time of loop, and makes position arithmetic fast. That reduces storage space and shortens computing time and space.

The atoi function in the VC environment is used to make specific conversion functions, as follows:

```
#include <stdlib>              //Header files
int atoi(const char *nptr)     // defined function
```

Function Description: Parameters nptr is a string. When the first non-space character of nptr is absent, or is not a number, or is not signed, function returns zero; otherwise, do type conversion. When non-numeric (including the end character "\ 0") character is detected, stop conversion, returns an integer.

3.4 Mobile Communication User Location Algorithm

In this paper, the location algorithm we propose is RIFMA (Regional sIgnal Fingerprint Matching Arithmetic). Its detail is in paragraph 4.

3.5 Displaying Result

Appling graphical tools, the user's location [8] is shown in Fig. 2.

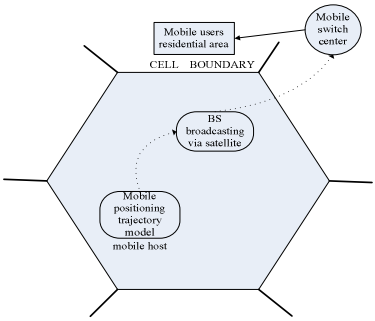

Fig. 2. Mobile users positioning display

4 RIFMA

RIFMA is Regional sIgnal Fingerprint Matching Arithmetic. Fingerprint matching location technology first needs to abstract and formalize the specific position circumstances. The information of various positions is described by specific, quantitative parameters. The information is integrated in the database. When positioning with MR, we need to use these receiving Level of the current channel in main service district, as well as strong BCCH Level information from the most adjacent 6 areas.

It, formalizing and quantifying the characteristics of the location information, is known as "fingerprint" in the industry. Positioning, the "fingerprint" characteristic of the specific object is used to location the database. Specific matching rules in the database are used to determine the location of the object. The core of the positioning technology is the location feature database and matching rules. Essentially that is a pattern recognition method.

4.1 Positioning Steps and Euclidean Distance Calculation

Positioning method mainly includes the following two stages:

(1) Establish the fingerprint database. Establish signal characteristics querying database;
(2) Positioning. Specific observation signal, using the pattern matching algorithm, is used to position.

The specific implementation steps are as follows in this paper:

(1) Divide the whole communication area into several grid;
(2) Use road test equipment for long call dial, and record the location information in each grid, service district Level, and adjacent area Level;
(3) Adjust COST 231-Walfisch-Ikegami model, and access signal signature of the failed test grid outdoor.
(4) Establish a signal fingerprint database. Build a feature vector by main service district and N adjacent areas' Level. Let the feature vectors of the grid be
$$V_S = (\text{sig } s_1, \text{sig } s_2, \ldots\ldots, \text{sig } s_n).$$
(5) Calculate the Euclidean distance between observed MR data eigenvectors V_S and fingerprint database feature vector, assuming that the observation data vector is (sig m_1, sig m_2, ……, sig m_n), the Euclidean distance to the grid s is
$$ds = \sqrt{\sum_{i=1}^{n} (sig\ m_i - sig\ s_i)}.$$
(6) Get the minimum value of the ds, the minimum value of the grid is the MR location.

4.2 Mobile Terminal Positioning Algorithm Based on Multi-base Station

The specific location algorithm is proposed as follows:

(1) Use a path loss of signal to calculate propagation distance. According to radio wave propagation model, use time difference between adjacent areas station and mobile station Level to calculate the distance from adjacent station to mobile station.
(2) Position the area from the base station to the mobile terminal. Chose a base station as the center, radius is distance between the mobile terminal and the base station, and make a circular;
(3) Location the mobile terminal with multiple base stations. Intersection of circulars is known as the area of mobile terminal;
(4) Correct Position. The smallest ds, which meets steps mentioned above and match with the fingerprint algorithm, is mobile terminal location.

The positioning method that is proposed based on multiple base stations in the paper is used to correct the error in the signal fingerprint positioning method, as well as it can also be used to correct the deviation of signal in the fingerprint database. For example, if we only calculate the values of spreading model in three base stations, the junction of three circulars is the mobile station location [9]. It is shown in Fig. 3.

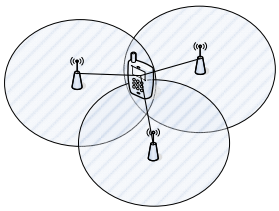

Fig. 3. Positioning algorithm based on multi-base stations

4.3 Factors Affecting the Precision and Processing

Obviously, the main factors affecting the positioning accuracy are the parameters of the radio wave propagation model and the time-varying error of receiving Level. As the measurement report only includes downloading data, we deal with the relationship of downloading data between the propagation loss and the distance.

The following factors need to be considered in downlink computing function:

(1) EIRP (Effective Isotropic Radiated Power)

EIRP(dBm) = high power transmitter(dBm) - feeder loss(dB) + antenna gain(dB) (1)

Note: Usually take as 5 dB

(2) Pathloss
Free space propagation loss

$$\text{Pathloss} = 32.45+20 \lg f + a * 10 \lg d \quad (2)$$

Note: f: Radio Frequency(MHz); d: Free-space propagation distance(KM); a: propagation coefficient, According to different geographical and feature of environment, more complex of geographical and environment, the greater the coefficient. Experience value: rural = 2; suburbs = 3; city = 3.5; dense urban areas = 4

(3) Body Loss: Usually take as 3 dB

(4) Penetration Loss, It is the difference of field Level between outside and inside of the building. Usually set parameters be as follows for different urban and building:

a) 900M: city = 25dB; suburbs = 20dB
b) 1800M: city = 30dB; suburbs = 25dB

Rxlev(Received Signal Level)(dBm)

Value is measured in a period of time. It has eliminated the impact of fast fading.

After the path loss, penetration loss, and body loss, EIRP converts to Rxlev in the mobile station side, which was shown in Fig.4

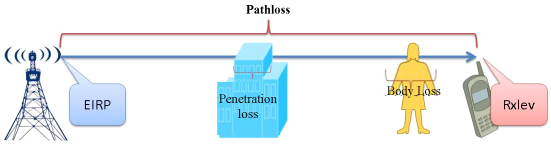

Fig. 4. Rxlev

Thus a function is as follows:

Rxlev = EIRP - Pathloss - Penetration Loss - Body Loss

= high power transmitter - feeder loss + antenna gain -（32.45+20lgf+a*lgd)- Penetration Loss - Body Loss

Let b = Feed loss + 32.45 + (59 or 65) + penetration loss + body loss

Here, the range of b is: 99dB~ 135dB. Lower limit of the range is : 900M without the penetration loss, the maximum is: 1800M with 30dB penetration loss.

The above formula is transformed into:

$$\text{Rxlev} = \text{high power transmitter} + \text{antenna gain} - b - a * 10 \lg d \quad (3)$$

According to above formula, spreading distance can be calculated by the measurement report (MR). In above formula, a and b are the regression coefficients, which can be derived according to regression equation by the road test data, the location of mobile station, and base station. Because Rxlev, transmitter power, antenna gain, a, and b are known, d can be calculated.

4.4 Ending Conditions

Specific calculation is done by using a loop approximation, and the iterative ending condition can be taken as the number of loop iterations or accuracy of position. As follows:

(1) When the distance values of some continuous iterations did not change, we can terminate loop;

(2) Or iteration belongs to disjoint areas, we will terminate loop, because we can determine that the mobile terminal is not in the intersection region;

(3) Or the iteration belongs to the areas, the smallest distance ds is calculated by the fingerprint method, we will terminate loop.

In above conditions, we can find that the smaller intersection region, the more successful positioning. When the number of iterations is too small, the results are not reliable, and if too many, not efficiency. The number of iterations is dynamic. When intersection region is absent, we should retry by removing some base stations. In the case, most likely, the data of the base station is mistake or a base station signal is drifted [10]. These conditions must be considered in calculation process, which are density of the base station, distance weighs, and mistake data. That is reason to remove some base stations and foundation to improve the positioning accuracy.

4.5 Acceleration Method

Calculating the Euclidean distance, the value of square root can be pre-computed method. We have computed the value of square root from number 0 to 2^{32}, which are stored in a database. When needed, it can simply be obtained from the database. Because data is too huge, it requires a lot of storage space. So we define a new floating-point type, propose and design a fast integer square root method. Experiments show our method has efficient. Specific prescribing function is defined as follows:

```
inline unsigned int qsqrtUL(unsigned int sq)
   // Fast integer square root (error less than 0.5%)
{
    unsigned int h=((sq>>24==0?(sq>>16>0):2));
       // sq is the value before prescribe
    unsigned int h3=(h<<3);
    #if def QSQRTLUL_PRECISE2
    reurn(psqUL[(h<<16)+(sq>>h3)+((sq&psqUlround[h])>0
    )]);
       // return the value after mapping
    #else
        return(psqUL[(h<<16)+(sq>>h3)]);
    #endif
}
```

Here: a large number is expressed by a multiple and a base; Binary shift is used to simplify computing and to improve efficiency, and while it is used to replace decimal multiplication and division. So the whole calculation is converted to a binary operator, bit computing. As a result, the numbers of 2^{32} can be mapped to 2^{18} ranges, and data is expressed in the form of the exponent and mantissa. At the same time, according to type of data column, a function of an array fun([n])() is defined. According to type of different data columns, different functions are analogously defined. Firstly, all default data length is 10. The three arrays defined below are used for expanding:

```
void genBinBSLst(TCHAR* filePath,TCHAR* outPath)
{
     // read the base station data csv, output in
     // binary format: accepts input
     //LAC,CI,BSIC(6bit),BCCH(10bit?),x,y,pwrcomplex
   int len;
   static  void (*func[10])(char*,byte*,int)
  {
      NULL,NULL,NULL,NULL,NULL,NULL,NULL,NULL,NULL,NULL
      } ;
      if(!func[0]){
      func[0] = convLac;
      func[1] = convCi;
```

```
        func[2] = convBsic;
        func[3] = convBcch;
        func[4] = convX;
        func[5] = convY;
        func[6] = convPwr;
        func[7] = convNULL;
        func[8] = convNULL;
        func[9] = convNULL;
    }
}
```

In order to calculate the location of the user, we define a base station information node StationInfElem as follows:

```
struct StationInfElem
{           // Base station information node
    int pow;
           // Pre-treatment emission signal strength
    int x;     //x coordinate
    int y;     //y coordinate
    float a;   //a parameter (backfill, unknown)
    char b;    //b parameter (backfill, unknown)
};
```

Then define user information record node UseInfElem as follow:

```
struct UsrInfElem
{             // User information record node
    unsigned int srvGlobal;
       //4-byte service station global positioning
    unsigned short NBNo[STATION_LIMIT];
       //2 * 6 bytes ,neighbor station bsic,bcch
       //char srvrx;//1
    char rx[STATION_LIMIT+1];
       //all rxlev [0] is service rxlev
       //4+12+7=23
    char ex0;       // Byte aligned, blank
};
```

4.6 Determining the Main Service

Calculating a data core functions:

```
void calLocateCore(UsrInfElem* dat, int ret[3], int
maxStation)
```

When user is in the service area, the strongest signal is often from a primary service station. But it is not only a primary service station to provide services, at the same time the adjacent station signals are also received around. When the user is not in the main service area, main station will automatically switch to the station of strongest signal.

In the paper, we denote the main service station with NLAC and NCI, while denote adjacent base station with BSIC and BCCH. The main service station is known as normal service station. These distances which are calculated by rxlev between client and base stations are stored in a array dst[STATION-LIMIT+1]. If you cannot find a service station, the corresponding data is not recorded; If you find that the location of base station is overlaps, robust information of the base station is removed. The density of each base station location is calculated, the greater the density, the higher the weight value.

The base station is calculated as follows:

```
for(k=0;k<maxStation;k++)
{
       // Obtain the relative density of
       //each base station location
       //get the relative density of
       //each base station location
    st=sts[k];
    for(i=0;i<maxStation;i++)
    {
        if(i==k)  {continue;}
        dx=st->x-sts[i]->x;
        dy=st->y-sts[i]->y;
        dx=dx<0?-dx:dx;
        dy=dy<0?-dy:dy;
        if(dx+dy==0)  {continue;}
        mul[k]+=1.0f/qsqrtUL(dx*dx+dy*dy);
            // The denser the higher weights
    }
}
```

4.7 The Steps of Positioning Algorithm

The steps of positioning algorithm are as follows:

1. Convert the base station data by function genBinBSLst;
2. Rapidly sort the data by sortBinBSLst() and newhBlst();
3. Calculate the location of the user by RIFMA. When the calculated location information is different with location information calculated by the propagation model, adjust the position vector;
4. Come to the positioning accuracy defined ahead by iteration of the loop,.

5 Experimental Results and Analysis

5.1 Data Sets

The experimental data of the table 2 comes from a mobile company. In the table 2, the format of the data set is as follows: time (A), GPRS longitude (B), GPRS latitude (C). After preprocessing, X, Y coordinates are used. X coordinate is (D), Y coordinates is (E); the computation result of X coordinate is (F); the computation result of Y coordinates for (G). After removing outliers, the computation result of X coordinate is (H); the computation result of Y coordinates is (I); (J) is used to label these distances between the data point and the corresponding GPRS road test points. Under remaining the outlier, (M) is used to label the result that is difference of two time values, which come from successor record and current record; when the time difference is less than 3 seconds, (N) is marked up adding a point to the next line as the motion compensation; when time difference is greater than 3 seconds, let (N) be 1. The other columns of data are not described in the texts. The specific data shown in Table 2:

Table 2. Experimental data format

	A	B	C	D	E	F	G	H	I	J	K	L	M	N
1	43:49.0	102.7300833	25.031905	3922.066394	0	0	0	0	0				3.00	1
2	43:51.9	102.72999	25.031805	3912.703603	956.3042458	0	0	0	0				5.00	1
3	43:57.2	102.7298467	25.03165833	3898.323238	940.004287	0	0	0	0				14.00	1
4	44:11.4	102.7288317	25.03096167	3796.466501	862.5819841	4025	969	4025	969	252.0959	252.095922	252.0959224	1.00	3
5	44:12.0	102.7287483	25.03090167	3788.097189	855.9139708	4025	969	4025	969	262.5098	262.509794	262.5097936	1.00	2
6	44:12.9	102.7286633	25.03084	3779.567315	849.0603644	4018	982	4018	982	272.9892	272.989179	272.9891794	3.00	1
7	44:15.8	102.7283833	25.03065667	3751.468905	826.6862497	0	0	0	0				1.00	2
8	44:17.2	102.7282867	25.03059167	3741.774953	821.4625686	0	0	0	0				9.00	1
9	44:25.9	102.7273283	25.029925	3645.59811	747.3731611	0	0	0	0				15.00	1
10	44:40.9	102.7258833	25.029005	3500.590243	645.13029	0	0	0	0				12.00	1
11	44:53.2	102.7250633	25.02845833	3418.302042	584.3760092	3833	446	3833	446	437.1757	437.175668	437.1756684	51.00	1
12	45:43.7	102.7241983	25.02792333	3331.498026	524.920457	3312	540	3312	540	24.64885	24.6488462	24.64884622	0.00	19
13	45:44.2	102.7241567	25.02790333	3327.323405	522.6977859	3312	540	3312	540	23.11219	23.1121904	23.11219039	2.00	18
14	45:45.7	102.7241133	25.02788	3322.966151	520.10504	3312	519	3312	519	11.02368	11.0236769	11.02367687	0.00	17
15	45:46.1	102.7240733	25.02765833	3318.954093	517.6967759	3259	493	3259	493	64.84153	64.8415295	64.84152949	1.00	16
16	45:47.1	102.7240367	25.027845	3315.281229	516.2153658	3312	535	3312	535	19.06906	19.0690575	19.06905751	2.00	15
17	45:48.9	102.7240083	25.027835	3312.431247	515.10403	3312	544	3312	544	28.89919	28.8991878	28.89918782	1.00	14
18	45:50.0	102.7239817	25.027825	3309.761898	513.9926944	3312	530	3312	530	16.16301	16.1630112	16.16301117	0.00	13
19	45:50.5	102.7239583	25.027815	3307.413674	512.8813588	3312	530	3312	530	17.72237	17.7223661	17.72236606	0.00	12
20	45:51.0	102.723935	25.027805	3305.075485	511.7700233	3312	544	3312	544	32.96544	32.9654411	32.96544106	1.00	11
21	45:52.0	102.72391	25.02790167	3302.566698	511.3999488	3312	517	3312	517	10.97031	10.9703125	10.97031247	1.00	10
22	45:53.0	102.7238833	25.02779333	3299.887314	510.4730947	3312	452	3312	452	59.71449	59.7144871	59.71448706	1.00	9
23	45:54.4	102.7238567	25.02778333	3297.217965	509.3617592	3182	446	3182	446	131.491	131.491034	131.4910341	2.00	8
24	45:56.0	102.723825	25.02777833	3294.036824	508.8060914	3212	434	3212	434	111.0225	111.022483	111.0224832	0.00	7
25	45:56.3	102.72379	25.02776667	3290.524523	507.5102741	3204	437	3204	437	111.6163	111.61627	111.6162702	1.00	6
26	45:57.3	102.72375	25.027755	3286.510464	506.2133458	3186	444	3186	444	118.2068	118.206828	118.2068261	1.00	5
27	45:58.3	102.723715	25.02774167	3282.996163	504.7319353	3312	459	3312	459	54.15271	54.1527143	54.1527143	1.00	4
28	45:59.3	102.7236783	25.02773333	3279.315264	503.8050814	3312	450	3312	450	62.95458	62.9545769	62.95457689	2.00	3
29	46:00.8	102.72364	25.027725	3275.471803	502.8793389	3177	448	3177	448	112.7317	112.731707	112.7317072	2.00	2
30	46:02.6	102.7235617	25.02770833	3267.614283	501.0267425	3190	444	3190	444	96.31213	96.3121297	96.3121297	4.00	1

5.2 Experimental Results

GPRS data converted is shown in Fig. 5. In order to test the algorithm effect, GPRS data converted is compared with the experimental results. We have the results by experiments. When data is less than 2000 records, computation results of user's behavior are very close to road test results. It's shown in Fig. 6. When the user data is up to 5000 records, the calculated results exists litter different with road test data. It is shown in Fig. 7. This shows that deviations of data are accumulated. The more the data is, the more necessary the data is sophisticatedly preprocessed.

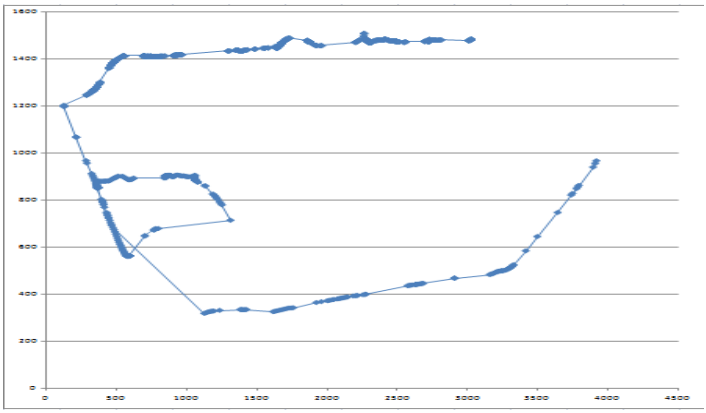

Fig. 5. GPS road test data

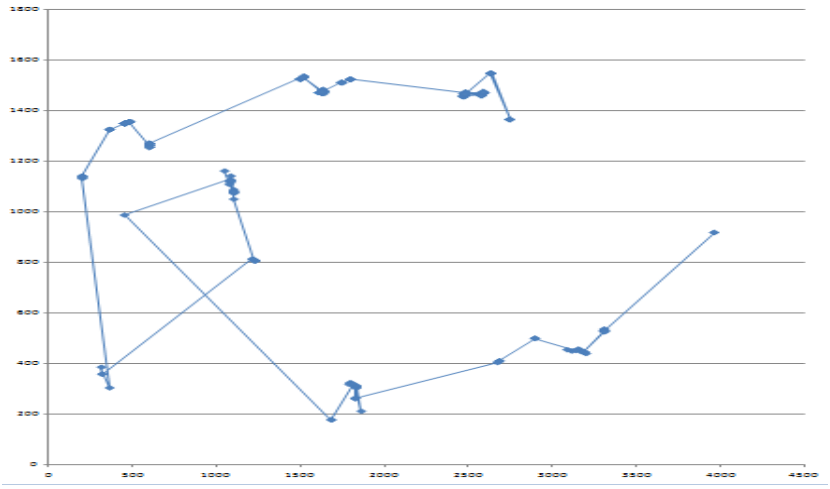

Fig. 6. Records less than 2000

5.1 Algorithm Analysis

The user location information method is calculated with single TA value in the MR and receiving Level. This paper proposes a new regional fingerprint algorithm, and corrects calculation results by combing with a radio propagation model. Exponent and mantissa are used to data expression and processing. A new method of fast integer square root is used to calculate the Euclidean distance, which avoids the fault accumulation of the algorithm. So our algorithm has robust function and work well. Double buffering technique is used to design parallel algorithm in the text, and the overall efficiency of the algorithm is raised. X and Y coordinates pre-calculated are separately reversed into the user's longitude and latitude, then they are used to analyze mobile user behavior by combining with the time change of the user moving.

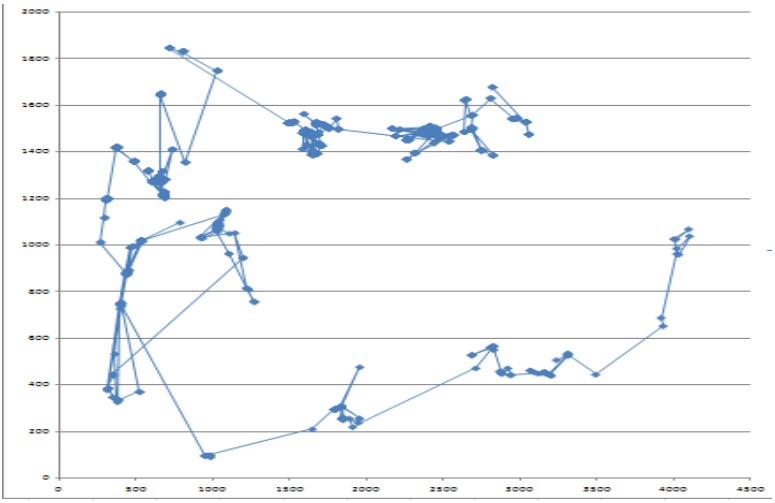

Fig. 7. Records less than 5000

6 Conclusions

With increasing mobile clients and data type, the mobile user behavior analysis has become enormous challenges and problems. The complexity of arithmetical time and space grows in exponential. That may lead to that it is very difficult to exhibit user behavior orbit. Analyzing user behavior is more difficult than that. We propose a new method in the paper. Firstly, the weight of the site is determined by calculating the site density. Related data of the base station and fingerprint data are preprocessed. Combining with the base station and the adjacent station information, the positioning algorithm is designed. Pre-computing greatly improves the speed of the positioning algorithm. Experimental results show that our method is better than others. Using MR receiving Level positioning method, positioning can reach about 550 meters or so, but our method can reach about 90 meters.

Acknowledgements. This work was supported by Guangdong Provincial Natural Science Foundation (Grant No. 9151009001000007, 10451009001004804), and Key Laboratory of the Ministry of Education project (Grant No. 110411).

References

1. http://www.miit.gov.cn/n11293472/n11505629/n11506554/n1151748 6/n11919487/n11920090/12031345.html
2. Wanghao: Research on Social Behavior Model and Optimization Algorithms for Mobile Communication Networks. Huazhong University of Science & Technology, Wuhan 430074, P.R China (2010)

3. Yibo: Cluster analysis and applied research in the mobile communications business data mining analysis. Hunan University 3 (2008)
4. Hybrid TOA/TDOA Based Unified Kalman Tracking Algorithm for Wireless Networks. Department of Electrical Engineering National Chiao Tung University Hsinchu. IEEE, Taiwan (2010)
5. Lee, J.: Tracking Algorithm for Wireless Networks, Mixed-integer nonlinear Programming: some modeling and solution issues. IBM Journal of Research and Develop 51(3/4), 489–497 (2007)
6. Giaglis, G.M.: Mobile Location Service Category. Mobile & Wireless Computing, 2590–2594 (2009)
7. Han, J., Kamber, M.: Data Mining Concepts and Techniques, 2nd edn. China Machine Press (2008)
8. Chakraborty, G., Bista, B.B., Chakrabort, D., et al.: Location management in PCN by movement prediction of the mobile host. In: Proc. of IEEE International Symposium on Industrial Electronics, ISIE 2002, vol. 1, pp. 78–83 (2002)
9. Lee, J.-K., Hou, J.C.: Modeling Steady-state and Transient Behaviors of User Mobility: Formulation, Analysis, and Application. In: Mobihoc 2006, pp. 202–211 (2006)
10. Borrel, V., de Amirim, M.D., et al.: A Preferential Attachment Gathering Mobility Model. IEEE Communications Letters 10(1), 900–902 (2005)

Performance Analysis with Different Sensing Results in the Cognitive Radio Networks

Yinglei Teng, Yanan Xiao, Gang Cheng, Yong Zhang, and Mei Song

Beijing University of Posts and Telecommunications, Beijing, China
lilytengtt@gmail.com

Abstract. In this paper, we provide capacity and outage probability analysis with different sensing results for three different transmission scenarios in the cognitive radio networks, i.e., overlay, underlay, and cooperative transmission of secondary users (SUs) relaying for primary users(PUs) (CToSP) according to [1]. Numerical results show that CToSP model achieves better performance under given situations, and different sensing results impact much.

Keywords: overlay, underlay, capacity, outage probability, cognitive radio.

1 Introduction

There are mainly three different transmission scenarios in the cognitive radio network, i.e., overlay, underlay, CToSP. In overlay mode, SU and PU share the spectrum in an opportunistic way, while in the underlay, SU works under constraints for interference temperature in [2] and has its own SINR requirement for transmission. We make a comparison for three different CR strategies with different sensing results. We investigate CToSP in which SU plays a double role in [1]: the source and the relay. Acting as a relay, the cognitive user can adopt amplify and forward (AF) and decode and forward (DF) forwarding techniques. Each slot is divided into two parts. During phase 1, PU broadcasts data. The relay re-transmits it in phase 2 (together with its own data).With different sensing results, we make a comparison for the three transmission mode of performance metrics of system capacity and outage probability.

2 Transmission Model with Different Sensing Results

There are four cases with different sensing results by hard detection: (1) PU absence/PU absence; (2) PU presence/PU absence; (3) PU presence/PU presence; (4) PU absence/PU presence. The former is sensing result and the latter is actual fact. Consider one PU and M SUs pairs (SU sender (SS), SU receiver (SR)) to share N orthogonal subchannels. Assume that channel gain from SS m to SR m, from PS to SR m, from PS to PR, from SS m to PR, from PS to SS m on subchannel n are $\left|g_{m,n}^{ss}\right|^2$, $\left|g_{m,n}^{ps}\right|^2$, $\left|g^{pp}\right|^2$, $\left|g_{m,n}^{sp}\right|^2$, $\left|g_{m,n}^{pr}\right|^2$ which are Rayleigh distributed and independent. There are zero-mean complex variables of symmetric Gaussian distribution with variance σ^2 on all links. Corresponding transmission process is described in Fig.1.

Q. Zu, B. Hu, and A. Elçi (Eds.): ICPCA-SWS 2012, LNCS 7719, pp. 477–481, 2013.

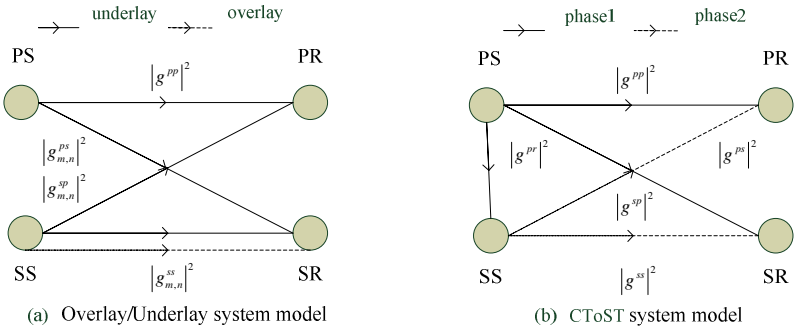

(a) Overlay/Underlay system model (b) CToST system model

Fig. 1. Transmission description of three models

3 Information Theoretic Analysis: Capacity and Outage Probability

We define system capacity as $R = r_p + r_s = r_s$ and outage probability as $P^{out} = P_p^{out} \bullet P_s^{out}$.

3.1 Capacity Analysis

Overlay/ Underlay Model

For the overlay spectrum access, we define $r_p = 0$ $P_p = 0$. When in case (1), we get (2). The capacity of PU/SU are r_p r_s, B is bandwidth, $p_{m,n}$ is power for the SU m on subcarrier n. When in case (2), we get the same expression except (1) from [2].

$$\sum_{m}^{M} \left| g_{m,n}^{ps} \right|^2 p_{m,n} \le TkB \tag{1}$$

For the underlay spectrum access, when in case (3), we get the capacity (2) (3) subjecting to (1) (4). p_p is the PU's power and $SINR_0$ is the min-SINR of SU:

$$r_s = \sum_{m}^{M} \sum_{n}^{N} B \log(1 + \frac{\left| g_{m,n}^{ss} \right|^2 p_{m,n}}{B\sigma^2 + \left| g_{m,n}^{ps} \right|^2 p_p}) \tag{2}$$

$$r_p = B \log(1 + \frac{\left| g^{pp} \right|^2 p_p}{B\sigma^2 + \sum_{m}^{M} \sum_{n}^{N} \left| g_{m,n}^{sp} \right|^2 p_{m,n}}) \tag{3}$$

$$SINR_{m,n} = \frac{\left| g_{m,n}^{ss} \right|^2 p_{m,n}}{\left| g_{m,n}^{ps} \right|^2 p_p + B\sigma^2} \ge SINR_0 \tag{4}$$

When in case (4), we get the expressions as (2) (3) with subjecting to (4).

Cooperative Transmission of Secondary Users Relaying for Primary Users

From [3] in case (2), we define $r_p = 0$ $P_p = 0$, and we can get (6) with subjecting to (5):

$$\left|g^{sp}\right|^2 p_{s2} \le TkB \tag{5}$$

In case (3) for DF model, expressions are (6) (7). P_{s1} P_{s2} are power of PU/ SU.

$$r_s = B\log_2\left(1+\frac{\left|g^{ss}\right|^2 P_{s2}}{B\sigma^2 + P_p\left|g^{ps}\right|^2 + \left|g^{ss}\right|^2 P_{s1}}\right) \tag{6}$$

$$r_p = B\min\left[\log_2\left(1+\frac{P_p\left|g^{pr}\right|^2}{B\sigma^2}\right), \log_2\left(1+\frac{P_p\left|g^{pp}\right|^2}{B\sigma^2}+\frac{P_{s1}\left|g^{sp}\right|^2}{B\sigma^2+P_{s2}\left|g^{sp}\right|^2}\right)\right] \tag{7}$$

In the AF model, we introduce an amplification parameter $\beta = \sqrt{\frac{P_{s1}}{P_p\left|g^{ps}\right|^2 + B\sigma^2}}$.

We get (6) (8) in AF model. To note that, in AF and DF, the system capacity is achieved subjecting to the same constraints (5) and (9).

$$r_p = B\min\left[\log_2\left(1+\frac{P_p\left|g^{pr}\right|^2}{B\sigma^2}\right), \log_2\left(1+\frac{P_p\left|g^{pp}\right|^2}{B\sigma^2}+\frac{\frac{P_{s1}P_p\left|g^{pr}\right|^2\left|g^{sp}\right|^2}{P_p\left|g^{pr}\right|^2+B\sigma^2}}{B\sigma^2(1+\frac{P_{s1}\left|g^{sp}\right|^2}{P_p\left|g^{pr}\right|^2+B\sigma^2})+P_{s2}\left|g^{sp}\right|^2}\right)\right] \tag{8}$$

$$SINR = \frac{\left|g^{ss}\right|^2 p_{s2}}{B\sigma^2 + P_p\left|g^{ps}\right|^2 + \left|g^{ss}\right|^2 p_{s1}} \ge SINR_0 \tag{9}$$

3.2 Outage Probability Analysis

Overlay/ Underlay Model.

For overlay model, $P_p^{out} = 1$, $P_p = 0$, the expression is (10) for case (1). r^+ is target rate. $\left|K^{ss}\right|^2$ $\left|K^{pp}\right|^2$ are Rayleigh parameters of channels gain. In case (2), we get same expression except (1).

For underlay model in case (3), we get the expressions below subjecting to (1) (4):

$$P_s^{out} = \prod_m^M \prod_n^N 1 - e^{-\frac{(2^{r^+/B}-1)^2(p_p\left|g_{m,n}^{ps}\right|^2 + B\cdot\sigma^2)^2}{2p_{m,n}{}^2\left|K^{ss}\right|^4}} \tag{10}$$

$$P_p^{out} = 1 - e^{-\frac{(2^{r^+/B}-1)^2 (\sum_m^M \sum_n^N p_{m,n} \left| g_{m,n}^{ps} \right|^2 + B\sigma^2)^2}{2 p_p^2 \left| K^{pp} \right|^4}} \tag{11}$$

When in case (4), we get the same expressions as (10) (11) with subjecting to (4).

Cooperative Transmission of Secondary Users Relaying for Primary Users

When in case (2), we define $P_p^{out} = 1$ $P_p = 0$, and we can get (12) subjecting to (5).When in case (3) and the DF model, we get (12) subjecting to (5) (9):

$$P_s^{out} = 1 - e^{-\frac{(B\sigma^2 + P_p \left| g^{ps} \right|^2)^2}{2\left(\frac{p_{s2}}{2^{r^+/B}-1} - p_{s1}\right)^2 \left| K^{ss} \right|^4}} \tag{12}$$

$$P_p^{out} = 1 - e^{-\frac{\left(2^{r^+/B} - A\right)^2 B^2 \sigma^4}{2 p_p^2 \left| K^{pr} \right|^4}} \tag{13}$$

$$A = \left(1, when r_p = B \log_2 \left(1 + \frac{P_p \left| g^{pr} \right|^2}{B\sigma^2} \right); 1 + \frac{P_{s1} \left| g^{sp} \right|^2}{B\sigma^2 + P_{s2} \left| g^{sp} \right|^2}, when r_p = B \log_2 \left(1 + \frac{P_p \left| g^{pp} \right|^2}{B\sigma^2} + \frac{P_{s1} \left| g^{sp} \right|^2}{B\sigma^2 + P_{s2} \left| g^{sp} \right|^2} \right) \right) \tag{14}$$

In the AF model, the expressions are same subjecting to (5) (9) with variable A.

$$A = \left(1, r_p = B \log_2 \left(1 + \frac{P_p \left| g^{pr} \right|^2}{B\sigma^2} \right); 1 + \frac{\frac{P_{s1} P_p \left| g^{pr} \right|^2 \left| g^{sp} \right|^2}{P_p \left| g^{pr} \right|^2 + B\sigma^2}}{B\sigma^2 (1 + \frac{P_{s1} \left| g^{sp} \right|^2}{P_p \left| g^{pr} \right|^2 + B\sigma^2}) + P_{s2} \left| g^{sp} \right|^2}, r_p = B \log_2 \left(1 + \frac{P_p \left| g^{pp} \right|^2}{B\sigma^2} + \frac{\frac{P_{s1} P_p \left| g^{pr} \right|^2 \left| g^{sp} \right|^2}{P_p \left| g^{pr} \right|^2 + B\sigma^2}}{B\sigma^2 (1 + \frac{P_{s1} \left| g^{sp} \right|^2}{P_p \left| g^{pr} \right|^2 + B\sigma^2}) + P_{s2} \left| g^{sp} \right|^2} \right) \right) \tag{15}$$

4 Simulation Results

From the results, we can know that under the given situation, CToSP achieves better performance than Overlay/Underlay. Meanwhile, DF model shows advantages than AF. In fact, different sensing results bring different requirements to the system, when the SNR of SUs is lower, the system is first to make sure QoS of PU. Simultaneously, according to the outcomes of Fig 2 and Fig 3, the sensing results impact the capacity or outage probability much, and when the state of PU is sensed mistakenly, we set different transmission power of SUs to cater for different rate requirement.

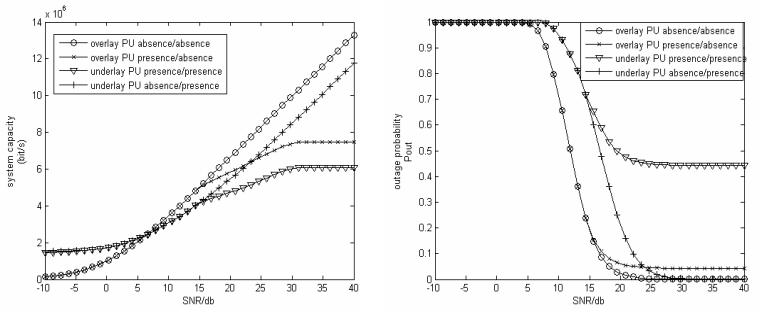

a Capacity with variance of SNR of SUs for Overlay/ Underlay b Outage probability with variance of SNR of SUs for Overlay/Underlay

Fig. 2. Capacity and outage probability with variance of SNR of SUs for Overlay/ Underlay

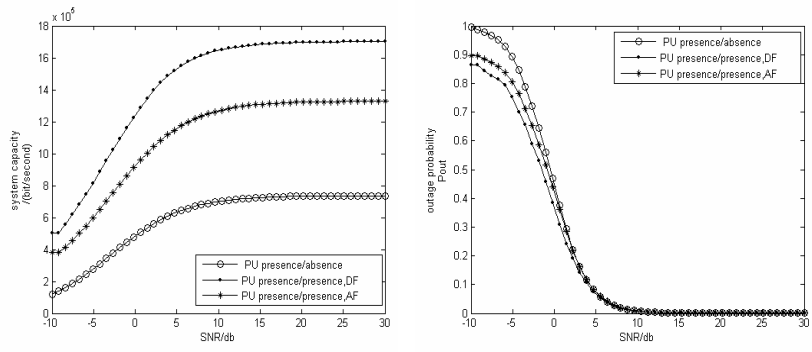

a Capacity with variance of SNR of SUs for CToSP b Outage probability with variance of SNR of SUs for CToSP

Fig. 3. Capacity and outage probability with variance of SNR of SUs for CToSP

5 Conclusions

We analyze two performance metrics with different sensing results. Simulation results show advantages of CToSP over the conventional methods.

Acknowledgement. This work is supported by the State Major Science and Technology Special Projects under (Grant No. 2011ZX03003-002-01) and Chinese Universities Scientific Fund (Grant NO.2012RC0306).

References

1. Giorgetti, A., et al.: Analysis and Performance Comparison of Different Cognitive Radio Algorithm. In: CogART, pp. 127–131 (2009)
2. Clancy, T.: Formalizing the interference temperature model. Wiley Journal on Wireless Communications and Mobile Computing 7(9), 1077–1086 (2007)
3. Ng, T.C.-Y., et al.: Joint Optimization of Relay Strategies and Resource Allocations in Cooperative Cellular Networks. IEEE J. Sel. Areas Communications 25(2) (February 2007)

QoS Routing for LEO Satellite Networks

Aida Nathalie Urquizo Medina and Gao Qiang

School of Electronic and Information Engineering, BeiHang University,
XueYuan Road No.37, HaiDian District, Beijing, China
u_nathalie@hotmail.com, gaoqiang@buaa.edu.cn

Abstract. Since the population distribution on the earth surface is highly non-uniform, the traffic requirements are unbalanced in LEO (Low Earth Orbit) satellite networks, some ISLs(Inter-Satellite Link) of satellite networks are congested while others are underutilized.This work proposes a QoS routing protocol for LEO satellite networks called BQR (Balanced QoS Routing) on the Iridium Constellation that implements a balanced mechanism based on the population density. The occupancy factor has a classification by location of the satellite and changes according the countries where the satellite is flying above. The countries with high population will receive high value of occupancy factor that will help to calculate the ISL cost based on a combination of propagation and queuing delay. The routing table maintains many entrieswith different ISL cost for the same destination, a path with high ISL cost has less probability to be selected that will balance the satellite network traffic.The integration between OPNET and STK is used to simulate the proposed BQR routing protocol. The simulation results show that our protocol can achieve a better traffic load balancing that leads to minimize the end to end delay and optimize the throughput.

Keywords: LEO Satellite Networks, QoS Routing, Iridium Constellation.

1 Introduction

Satellite networks providing a global coverage area are an effective solution to provide ubiquitous network access services all over the world[1].Low earth orbit (LEO) satellite networks with their potential for global coverage and high bandwidth availability are an attractive option for establishing “Internet in the sky” and it’s becoming increasingly important for global communications. LEO satellite communications network provide worldwide multicasting coverage to users in remote locations with limited or no network connectivity such as network systems in rural areas, the sea and disaster-stricken areas[2]. To carry real-time multimedia trafficwith specific time-delay requirements, the LEO satellite networks must support quality of service (QoS), based on parameters like package loss rate, throughput, end to end delay and also QoS routing because it is the key to support QoS [3].

As a result of population dispersion, economic flourish and the diversity in technology penetration, satellite systems have to face a challenging scenario of unfair

Q. Zu, B. Hu, and A. Elçi (Eds.): ICPCA-SWS 2012, LNCS 7719, pp. 482–494, 2013.

distribution of network traffic. Thus, without an efficient routing algorithm,this unbalanced traffic will lead to significant queuing delays and large number of packet drops at the high traffic concentration areas.

This work proposes the BQR protocol for the Iridium Constellation. BQR's main aim is to achieve better loading balancing over the entire satellite system. Because of this, it introduces a mechanism that calculates the ISL cost factor according the geographic position, which is evaluated in the routing path cost to select the most efficient way to route.

2 Balanced QoS Routing Protocol

The most general way to detect network congestion is to monitor the changes in the incoming traffic rate, and regard the measurements of higher rates exceeding a predefined or dynamically adjusted threshold as an occurrence of network congestion[4]. This serves as the motivation behind our work. Since it is possible in mesh constellations of LEO satellites to know which LEO satellite is going toward the congested area, in the proposed scheme, the satellite above the congested area preliminarily informs the neighboring satellite following itself with the coordinates of the congested area. The congested area can be defined as a circle with its center at the informed coordinate. The radius of the circular field needs to be determined according to the configuration of the satellite constellation and the LEO satellites coverage area. In the proposed scheme, the congested state implies that the corresponding LEO satellite has low and high probability of the occurrence of congestion, respectively. During this state where there is a threat of the cause of congestion, not only the monitoring of the traffic but also traffic distribution and the information exchange for congestion prediction are performed according to whether it exists in congested or non-congested areas. The status transition from no congested area occurs when observing a higher incoming traffic rate than the threshold so it will be denoted by, or entering into the congested area. On the other hand, each LEO satellite returns its status from the actual network congestion events.

When a LEO satellite moves from a non-congested area to the congested area by detecting a growing incoming traffic rate, it begins detouring traffic, and declares the area as a congested area and notifies the neighboring LEO satellites [5]. In contrast, after a LEO satellite transitions to the warning state by entering the congested area, it begins the traffic detouring when the incoming traffic rate exceeds the threshold. Since the probability of network congestion is relatively higher than the non-congested area, we use a balanced technique to invoke traffic detouring to the non-congested area. If the LEO satellite decides to detour traffic due to a high incoming traffic rate, it informs its neighbors that the area is congested. In contrast, if the traffic detouring was never carried out while the LEO satellite flies over the congested area, the area is regarded as being non-congested, and the handover of the information on the congested area will be terminated.

2.1 ISL Cost Modification Mechanism

Since the satellite networks are expected to provide continuously seamless global coverage, it means that the access of users satellite networks are distributed geographically evenly as it is shown in the Figure 1, the estimated distribution of zones, the more dense color means high populated zones with high probability of users to access to the satellite network in 2010 thus those zones will be denoted as hotspot zones.

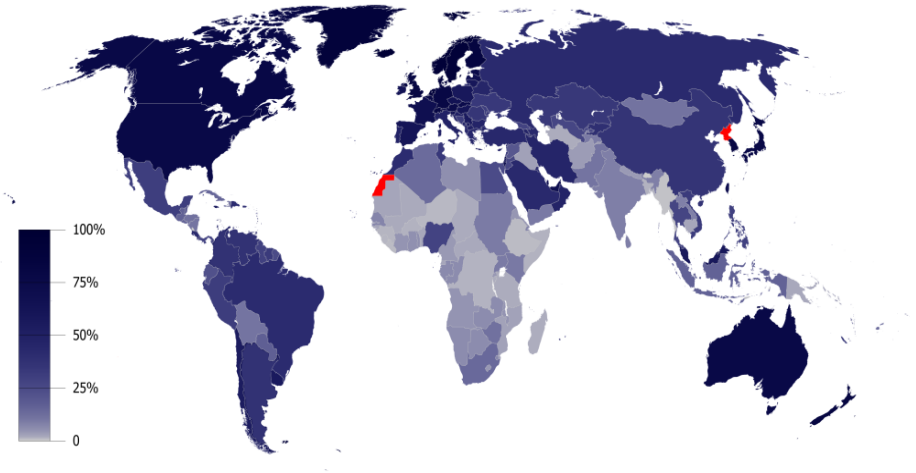

Fig. 1. World Internet users estimated distribution of zones 2010 - Source: Internet World Stats

Table 1shows that the distribution intensity levels of users on the planisphere are diverse at different areas. The majority of users and traffics are distributed within and alongside the continents that leads the BQR protocol development to classify to determine an occupancy factor according the number of users in every country.

Table 1. List of countries by number of Internet users in 2010 - Source: International Telecommunications Union.b

.#	Country or Region	Population, 2011 Est.	Internet Users Latest Data	Penetration % Population	World % Users
1	China	1,336,718,015	485,000,000	36.3 %	23.0 %
2	United States	313,232,044	245,000,000	78.2 %	11.6 %
3	India	1,189,172,906	100,000,000	8.4 %	4.7 %
4	Japan	126,475,664	99,182,000	78.4 %	4.7 %
5	Brazil	203,429,773	75,982,000	37.4 %	3.6 %
6	Germany	81,471,834	65,125,000	79.9 %	3.1 %
7	Russia	138,739,892	59,700,000	43.0 %	2.8 %
8	United Kingdom	62,698,362	51,442,100	82.0 %	2.4 %
9	France	65,102,719	45,262,000	69.5 %	2.1 %

Table 1. (*Continued*)

10	Nigeria	155,215,573	43,982,200	28.3 %	2.1 %
11	Indonesia	245,613,043	39,600,000	16.1 %	1.9 %
12	Korea	48,754,657	39,440,000	80.9 %	1.9 %
13	Iran	77,891,220	36,500,000	46.9 %	1.7 %
14	Turkey	78,785,548	35,000,000	44.4 %	1.7 %
15	Mexico	113,724,226	34,900,000	30.7 %	1.7 %
16	Italy	61,016,804	30,026,400	49.2 %	1.4 %
17	Philippines	101,833,938	29,700,000	29.2 %	1.4 %
18	Spain	46,754,784	29,093,984	62.2 %	1.4 %
19	Vietnam	90,549,390	29,268,606	32.3 %	1.4 %
20	Argentina	41,769,726	27,568,000	66.0 %	1.3 %
TOP 20 Countries		4,578,950,118	1,601,772,290	35.0 %	75.9 %
Rest of the World		2,351,105,036	508,993,520	21.6 %	24.1 %
Total World - Users		6,930,055,154	2,110,765,810	30.5 %	100.0 %

2.2 ISL Factor of Occupancy

Since the population density and the number of internet users reflect an even growing behavior this work will use the list of the Countries by number of Internet Users shown in Table 1 to classify into four classes, the Table 2 presents the parameters criteria to determine the occupancy factor.

Table 2. Parameters that define the occupancy factor. After define the occupancy factor usage percentage we have used the exponential function e^{ofp} to assign the real value of the occupancy factor *of*.

Internet Users (Million)	Class	Occupancy Factor Probability % Ofp	Occupancy Factor of
> 100	A	0.50	1.648721
50 - 100	B	0.25	1.284025
27 – 50	C	0.15	1.161834
< 27	D	0.10	1.105171

The orbit of each Iridium Satellite contains the latitude and longitude during the motion around the earth globe determining the exact position of the satellite. The BQR protocol implement a balanced mechanism based on the population density introducing the factor of occupancy that has a classification by location of the satellite and it change according the countries where the satellite is flying above so countries with high population will receive high value of occupancy's factor as it is shown in Table 2.

2.3 ISL Path Cost

In order to obtain the total ISL path cost, the Satellite congestion index and the queuing delay are consider. Let Q_{total} and $Q_{occupancy}(t)$ denote the total length of its queue and the predicted occupancy of its queue at time t on a given satellite u, respectively. The congestion at a time t can be expressed as in equation (1).

$$QD_i(t) = \frac{Q_{occupancy}(t)}{Q_{total}} \tag{1}$$

Where:

$$Q_{occupancy}(t) = \sum_j \left(\frac{1}{\Delta t} \int_{t-\Delta t}^{t} q_j(i) * delay_i\right) \tag{2}$$

$q_j(i)$ denotes the instant occupancy of the ISL queue at time i.

The path connecting source satellite *s* and destination *d* comprises many satellites and ISLs. So the cost path can be evaluated as the total sum of ISL cost. The ISL factor of occupancy is also taken account to adjust the path cost.

$$ISLCost(t) = QD(t) + PD(t) \tag{3}$$

Where: *QD=Queuing Delay*

PD=Propagation Delay

Suppose the path from satellite to node s to node d can be expressed as (4)

$$s \to v_1 \to .... \to v_n \to d \tag{4}$$

Let the path cost equation (5)

$$PathCost_{s,d}^{v_1}(t) = ISL\cos t_{s,v_1}(t) + \sum_{i=1}^{n-1} of_{v_i} ISL\cos t_{v_i,v_{i+1}}(t) + of_{v_n} ISL\cos t_{v_n,f}(t) \tag{5}$$

2.4 QoS Routing Mechanism

The routing table is validated whenever the network topology changes, each satellite delete the routing entities that include disabled ISLs. At a specified time interval, delay query messages are sent to investigate delay along routes. If delay satisfies required QoS delay, the entity's timer is reset. Otherwise, the routing entry will be deleted. Evaluation of weight value of routes is based on end-to-end delay along routes. Weight values ω_i are calculated by the equations (6) and (7) respectively [10].

$$w_i = \frac{\frac{1}{d_i}}{\sum_{j \in S} \frac{1}{d_j}} \tag{6}$$

Where:

$$d_i = \frac{Path\cos t_i}{\sum_{j \in S} \frac{1}{Path\cos t_j}} \tag{7}$$

Where d_i is the delay for i-th route, and s is a set of routes of the same destination. In the above equations, first we normalize the delay valuesd_i by dividing by the total sum of them to have the delay normalization value $\eta_i$and second we calculate the reciprocal number of η_i and normalize them to have a weight value.

The above equations implies that a smaller d_i value of generates a larger ω_i, so it will let the BQR protocol choose the smallest end-to-end delay when a new call arrives.

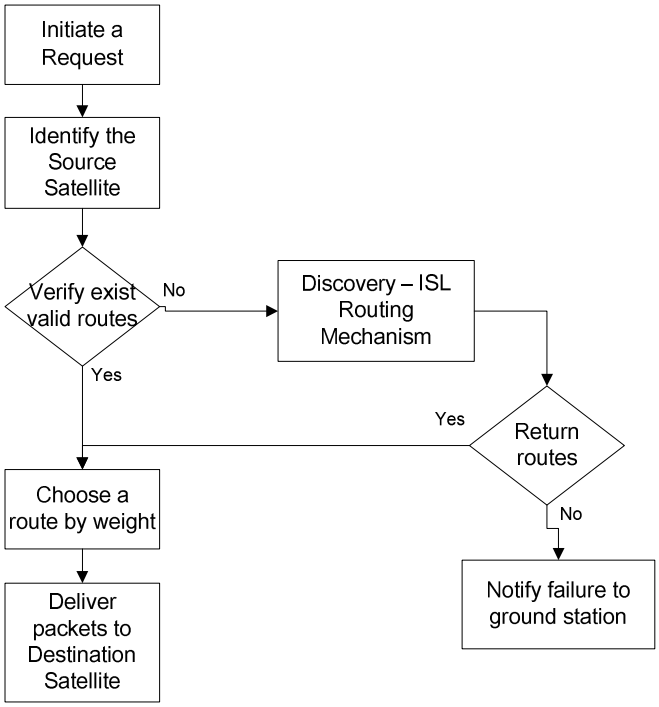

Fig. 2. BQR Workflow chart

3 Simulation

In the simulation, the Network is made up of sixty-six Iridium Satellites, two earth stations, the low-flying satellites travel at approximately 17,000 miles per hour, completing an orbit of the Earth in about 100 minutes. The software used for the simulation is the STK- Satellite Tool Kit integration with OPNET [12].

The tool OPNET has been used mainly for network-performance modeling and simulation. However, it fails to represent dynamic nodes in the mobile network. In contrast, STK is strong in mobile platform modeling and analysis but lacks a network-performance analyzed mechanism. Therefore, combining these two tools should illustrate the behavior of the dynamic node in the mobile network with sufficient network-performance support.

The STK orbit file can be added into OPNET simulation environment, which makes the accurate location information on the satellite. The Schema Design of the simulation is shown in the Figure 3.

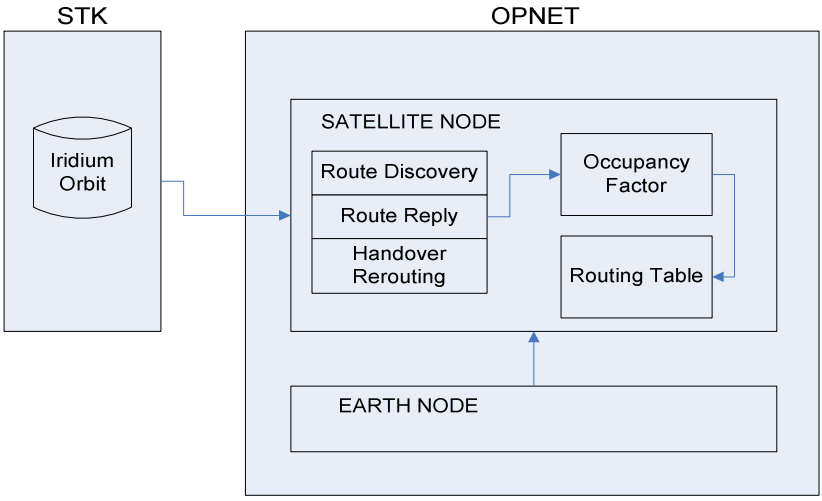

Fig. 3. BQR Routing Protocol Schema Simulation Design

3.1 Simulation Configuration

The orbits of Iridium satellites are created by STK and the network topology. Pinpointing a place is extremely easy on the world map if we exactly know the latitude and longitude geographical coordinates of the country and with the help of STK ephemeris file of each satellite we can know the exact location of the satellite. When a Satellite is over the hotspot zones the cost factor will be updated into the routing table and will set a congested value so the path that contain that satellite will have less probability to be selected with this mechanism we will balance the load and move the traffic to the none hotspot zones.

Table 3. OPNET Modeling Domains.The remaining specification corresponds to particular modeling domain since OPNET mainly support the three principal domains.

Domain	Editor	Modeling Focus	Description
Network	Project	Network Topology Links Geographical Context	Iridium Constellation ISL Earth Globe (World Map)
Node	Node	Node Internal Architecture	Earth Station Node Satellite Node
Process	Process	Protocol	BQR-Routing Protocol

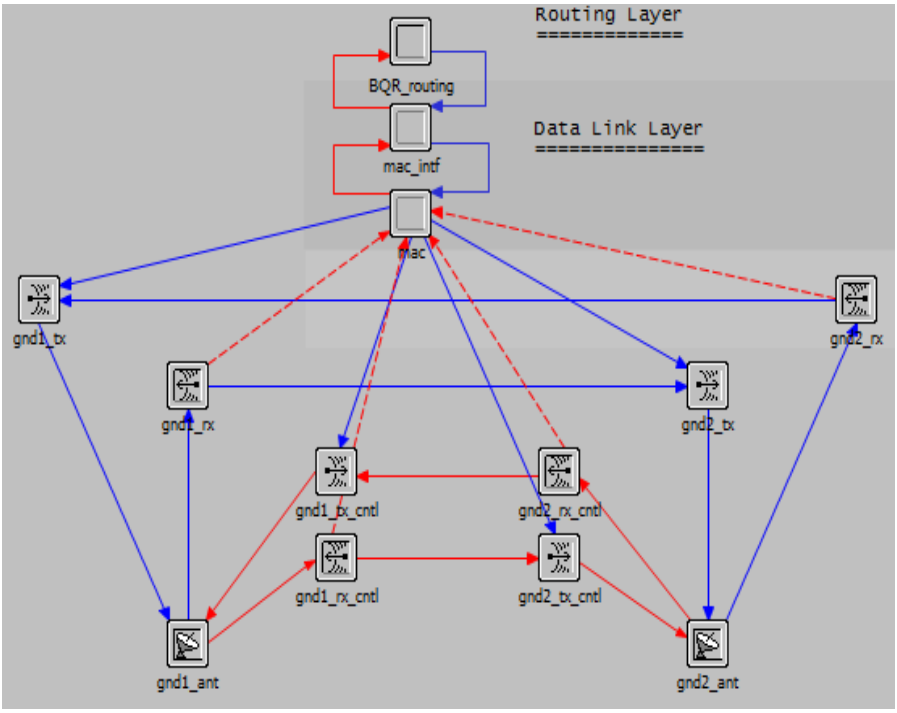

Fig. 4. Iridium Satellite Node Configuration (OPNET Configuration)

In this work, the buildup Iridium constellation is simulated in OPNET. The simulation system adopts a multilayer topology structure. The world map is placed as the simulation background. The scenario topology is depicted in Figure 5 and the

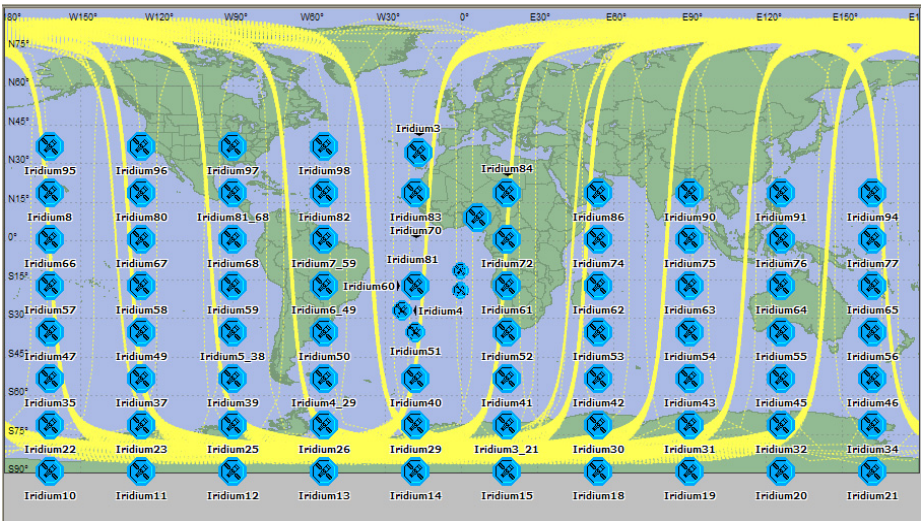

Fig. 5. Iridium Satellite Constellation (OPNET Configuration)

satellite node configuration is shown in Figure 4, during the simulation, each satellite moves in its own orbit.

LEO (Low-Earth Orbit) satellites have periods that depend on their orbital altitudes. The higher the orbit, the longer it takes. At the lowest stable orbits, the orbital period is around 100 minutes.

Table 4. Simulation Parameters in OPNET - Iridium Constellation, Satellite Node &Earth Node

Attributes	Iridium	Earth Station
Transmitting Power [dBW]	13	10
Frequency [GHz]	1.62125	20
Data Transfer rate [b/s]	1024	1024
Transmitting Antenna gain [dB]	Adaptive	1
Bean Attenuation	3 dB	
Receiving Antenna gain/dB	1	Adaptive
Noise Temperature	14 K	290 K
Height of Station		8.9 m
Latitude and longitude of station		31N, 121E
Elevation Satellite		8.3 -56.83 deg
Rain Height		3.245 Km

4 Results

The Balanced QoS Routing Protocol implemented in the Iridium Constellation can provide an outperforming result in throughput compared with the rest of ad-hoc protocols applied in LEO satellite networks.The Figure 6 shows the throughput in the system with a stunning amelioration, the maximum data transfer ratefor Iridium Constellation is 1.5 Mbps with the BQR protocol and its balanced mechanism the throughput obtained is 1.41 Mbps the curves in the figure shows a high call arrival rate as a result of more available routes.

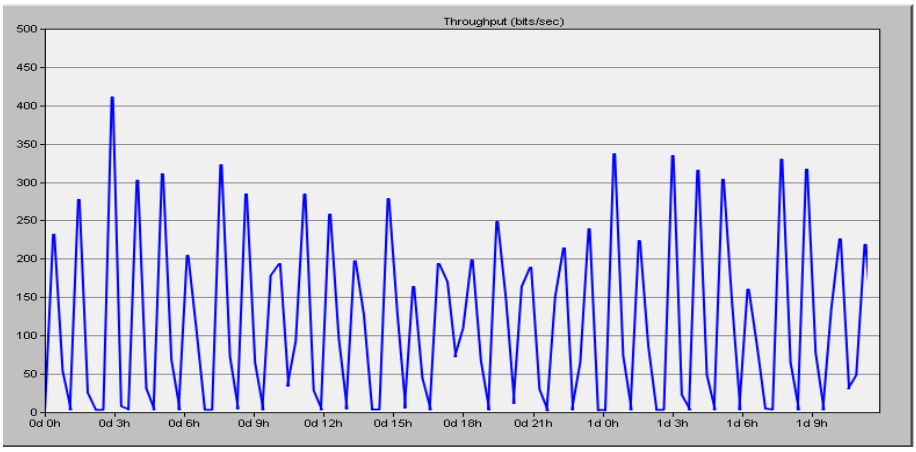

Counter	Range	Min	Max	Avg
Throughput (bits/sec)	+1000	1000	1410	1250

Fig. 6. Iridium Satellite Network Throughput (BQR Protocol Simulation)

This results are attributable to the balanced mechanism based in the population density applied that lead to an ISL routing success as a result of that the system provide a better performance in view of the fact that the performance of routing schemes the most important condition is high call arrival rate since in each system is desired to maximize the throughput.

Figure 7displays the throughput using DSR (Dynamic Source Routing Protocol) the results shows that 1.2 Mbps is the maximum throughput obtained and if we compare with the results obtained using the BQR so it is been proved that our BQR routing protocol outperform the DSR protocolshowing 22% of better performance. In addition BQR exhibits much smoother curves than DSR, which indicates BQR achieve better load balancing that DSR.

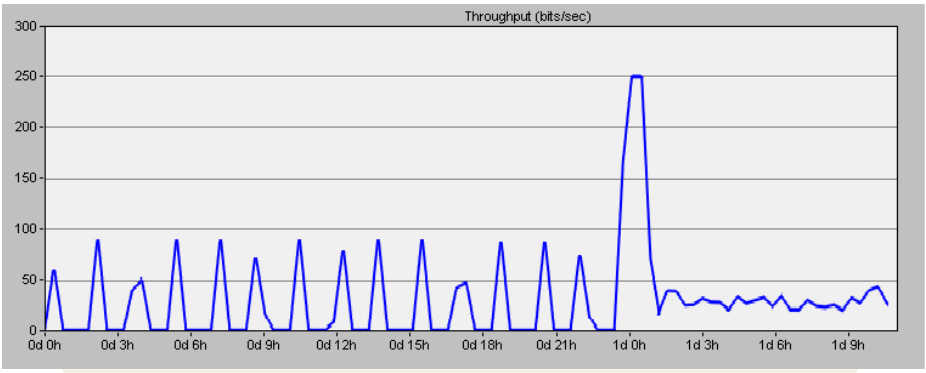

Counter	Range	Min	Max	Avg
Throughput (bits/sec)	+1000	1000	1250	1100

Fig. 7. Iridium Satellite Network Throughput (DSR Protocol Simulation)

The end to end delay for the Iridium system obtained is between 200ms and 300ms, this is results is well below compared with the required 400ms delay for real-time voice applications; which indicates that Iridium is capable of providing voice service.

5 Conclusions

The BQR routing protocol is implemented into inter-satellite networks for the Iridium Constellation, the routing algorithm designed provide and efficient load balancing mechanism that improves the performance for multimedia applications and minimizes the congestion providing scalability and capable to meet QoS specifications.

The simulation results prove the feasibility and the performance of the proposed BQR routing protocol. The BQR protocol offers better throughput and delay which is particularly lower and more stable so it's been demonstrated that BQR outperform in 22% to the other Ad hoc protocols implemented in the Iridium Constellation by accomplishing a balanced distribution of traffic over the entire network. The end to end delay analysis showed that the system is able to meet the standard minimum of 400 ms end to end delay. The congestion prediction achieved by the load balancing mechanism will avoid network congestion in the incoming traffic rate.

The number of users for the Iridium System is growing considerably faster with a highly non-uniform distribution as evidenced by the recent advent in the use of its systems in both commercial and military. Thus for the characteristics of our BQR routing protocol with the balanced mechanism based in the population density using the geographic location of the satellite it is perfectly suitable to face this effect and show traffic optimization in the network.

The proposed BQR routing protocol simulated for the Iridium Constellation also can be applied to other LEO satellite networks. According to the characteristics of Iridium Constellation System this routing model can also be applied for the Iridium NEXT that will be launched in 2015.

The simulation of the BQR protocol based on OPNET and the ephemeris extracted from STK helps to have an accurate result close to real scenario. The Integration between OPNET and STK simulation software for Satellite network can be an important reference for the actualizing of the LEO satellite communication system.

Acknowledgments. This work is supported by the Program for New Century Excellent Talents in University and the National Basic Research Program (973 Program) under Grant No. 2010CB731800.

References

1. Choi, K.S., You, J.H., Lee, S.P.: Utilization Plans for Ka Band Satellite Communication System using COMS. In: The 12th International Conference on Advanced Communication Technology, Gangwon-do Korea (February 2010)
2. Hubenko Jr., V.P., Raines, R.A., Baldwin, R.O., Mullins, B.E., Mills, R.F., Grimaila, M.R.: Improving Satellite Multicast Security Scalability by Reducing Rekeying Requirements. IEEE Journal Network 21, 51–56 (2007)
3. Yang, Z., Long, F., Sun, F., Wang, D.: A Dynamic QoS Routing Mechanism based on Steiner Trees for LEO Satellite network. In: 2010 International Conference on Networking, Sensing and Control (2010)
4. Feng, S., Geng, X., Li, G., Jiang, Y.: Low Earth Orbit Satellite Constellation Topology Design and Analysis for a Special Case. In: 2010 International Conference on Computer Application and System Modeling (2010)
5. Nishiyama, H., Kudoh, D., Kato, N., Kadowaki, N.: Load balancing and QoS Provisioning Based on Congestion Prediction for GEO/LEO Hybrid Satellite Networks. Proceedings of the IEEE 199, 1998–2007 (2011)
6. Berson, S., Jin, Y.: Effect of mobility on Future Satellite Packet Networks routing protocols. In: IEEE Aerospace Conference (2009)
7. Kucukates, R., Ersoy, C.: High performance routing in a LEO satellite network. In: Proceedings Eighth IEEE International Symposium Computers and Communication (2003)
8. Rao, Y., Wang, R.-C.: Performance of QoS routing using generic algorithm for Polar-orbit LEO satellite networks. Journal of Electronics and Communications 65(6), 530–538 (2011)
9. De Sanctis, M., Cianca, E., Ruggieri, M.: Improved algorithms for Internet routing in Low Earth Orbit satellite networks. Space Communications Journal 20(3-4) (2005)
10. Zhang, X., Ding, L., Rao, Y.: QoS Routing by Genetic Algorithm for LEO Satellite Networks. In: 2009 Second International Symposium on Computational Intelligence and Design (2009)
11. Rao, Y., Wang, R.-C.: Agent-based load balancing routing for LEO Satellite Networks. Journal ELSIEVER Science Direct 2010 Computer Networks 54, 3187–3195 (2010)
12. Wang, X., Zong, P., Yu, J.: Link Analyzing and Simulation of TDRSS Based on OPNET. In: 2010 International Conference on Communications and Mobile Computing (2010)

13. Mohorcic, M., Svigelj, A., Kandus, G.: Democraphically weighted traffic flow models for adaptive routing in packet-switched non-geostationary satellite meshed networks. Computer Networks 2002 Journal 2002(43), 113–131 (2002)
14. Tarik, T., Daisuke, M., Jamalipour, A.: Explicit load balancing technique for NGEO satellite IP networks with onboard processing capabilities. IEEE/ACT Transactions on Networking 17, 281–293 (2009)
15. Karapantazis, S., Papapetrou, E., Pavlidou, F.-N.: Multiservice On-Demand Routing in LEO Satellite Networks. IEEE Transactions on Wireless Communications 8(1), 107–112 (2009)

A Slot Assignment Algorithm Based on Nodes' Residual Energy*

Qianping Wang, Xiang Xu, Jin Liu, and Liangyin Wang

School of Computer Science and Technology,
China University of Mining and Technology, Xuzhou, 221116, China
qpwang@cumt.edu.cn

Abstract. Aiming to extend the network lifespan through balancing the energy consumption, an EDRAND (Enhanced DRAND) algorithm based on the node's residual energy is presented in this paper. The EDRAND can be considered as an improved DRAND in which slot sizes are determined by the residual energy of sensor nodes. By taking into account of the nodes' residual energy and the network traffic, an E-ZMAC (Energy-ZMAC) protocol which employs energy control and traffic adaptive mechanism in the Z-MAC protocol, is introduced. In the presented protocol, a node in the network will switch to sleep mode for a while within its slot to reduce power consumption and network traffic. The time span in the sleep mode of a node will be shortened with the growth of the network traffic. A node will switch to TDMA mode when the network traffic reaches a certain upper bound. By doing so, the channel access mode is enabled to transit smoothly from competition-based to scheduling-based. In the presented methodology, the contention window size will be increased with the growth of the network traffic, and the backoff span will be negatively related to the amount of residual energy. To validate the presented approach, a group of simulations are conducted in NS2 under different scenarios. The simulation results have demonstrated that the proposed E-ZMAC protocol outperforms Z-MAC protocol in terms of network lifespan, throughput and energy consumption.

Keywords. Wireless Sensor Networks (WSNs), hybrid MAC protocol, node's residual energy, traffic adaptive protocol, EDRAND Slot Assignment algorithm, E-ZMAC protocol.

1 Introduction

1.1 Network Model

In the TDMA mechanism, time is organized in frames which are non-overlapping equal slices. When the frame is divided into finer time intervals, we call it slot. Slot assignment is regarded as assigning a slot for each node, and the possible collision

* This paper is supported by part of NSFC(51134023/E0422).

Q. Zu, B. Hu, and A. Elçi (Eds.): ICPCA-SWS 2012, LNCS 7719, pp. 495–512, 2013.

nodes are assigned different slots. With such a different slot assignment for each node, nodes will send and receive data in a slot, and sleep in another slot. Crosstalk and interference issues can then be avoided. As a result, it can reduce the control overhead, and also can effectively reduce the energy loss caused by channel contention and collision retransmission. But due to the complex of the time frame management, and slot assignment algorithm scalability is poor, which is one of the major contributors that undermine the performance of the overall network.

In order to describe the problem better, we first give a description of the topology of wireless sensor networks. Assuming that the network G = (V, E), in which V represents the set of nodes, E denotes the set of edges. When and only when u and v are in V and the signal noise ratio (SNR)between u and v is greater than a threshold (Formula (1)), the two nodes are considered to be within the scope of their communication and exists interference relations, and the edge e = (u, v) ∈ E exists (edges are bidirectional). Definition that node u and v are one-hop neighbors and the distance between them is 1. There will be collisions, if u and v send data at the same time. If there are nodes i and j, but i and j is not one-hop neighbors, and there is an intermediate node k , (i, k) ∈ E , (k, j) ∈ E, we regard the distance between node i and j as 2. If the two-hop nodes transmit data at the same time, it will give rise to conflicts in the common neighbor nodes within one hop. In broadcast scheduling mode, the nodes within two hops are likely to conflict, and in unicast mode, sending and receiving nodes within one hop may conflict.

$$SNR(u,v) = \frac{Pu}{L_b(u,v)N_r} \geq \gamma_0 \tag{1}$$

Where Pu is the transmit power of node u, Nr is the impact of white noise, Lb (u, v) is the path loss factor between node u and node v. In the network we discussed, assuming that the transmit power of all nodes are consistently and the path loss factor between two points is symmetrical.

1.2 Centralized and Distributed Slot Assignment

The most common wireless network based on the slot assignment is GSM (Global System of Mobile Communication) network. In the time division multiplexing mechanism of GSM, each frame contains eight consecutive slots (T_{S0}-T_{S7}). And these slots are assigned dynamically by a central node, i.e., the sink node. The sink node assigns a unique slot for the node which requested for slot. Due to that there must be one central node which is responsible for slot management, slot assignment method is also known as a kind of centralized algorithms.

The central control node of centralized algorithm can acquire global topology information of the network, so the algorithm based on centralized slot assignment usually take the performance of the entire network as the optimization objective. Centralized assignment algorithm includes RAND algorithm, uniform slot assignment algorithm USAP and adaptive frame length slot assignment algorithm ASAP[1]. Another type of slot assignment algorithm is the distributed slot assignment

algorithm, which does not require central control node. An ant-based distributed assignment algorithm which regards all nodes within two hops as a collision domain was presented in [2]. The algorithm aims at assigning different slot for all nodes within a collision domain. At present, most of assignment algorithms apply distributed algorithms. They exchange control information between the neighbors, resolve the slot assignment and slot reservation within a collision domain. The advantages of the centralized assignment are that it can get better results of the indicators, such as the overall channel utilization of the network and frame size. The drawback is that the dynamic collection of network topology information brings some overhead, the scalability is poor, and when the network topology changes, it need to re-gather the global slot assignment information. Distributed assignment algorithm has good scalability, easy and convenient, but it only consider the local optimum, so it needs to combine with other control techniques to optimize overall network performance. At present, distributed slot assignment algorithm is in prevail in wireless sensor networks.

Distributed slot assignment algorithm performance is determined by three points:

(1) The maximum number of slots: Slot assignment problem is the expansion of the graph coloring problem. The goal is to color the vertices of the graph with the least color, and any two adjacent vertices should color different colors. The graph coloring problem has proven to be the NP-Hard problem. Generally, we use the heuristic algorithm to solve the graph coloring problem. The maximum number of slots $Max_{(slot)}$ in the slot assignment problem is equivalent to the minimum number of colors in the graph coloring problem, determining the frame size.

(2) the time complexity of algorithm: The key of measuring an algorithm is the time that ban algorithm spent to solve the problem, and the spent time should be in the acceptable range.

(3) the control overhead of the algorithm: In wireless sensor network, the node was powered by the battery, and during the vast majority of occasions, the battery can not be replaced, while the energy consumed by the node to send information is most, so we should minimize the messages transmitted between nodes.

A distributed slot assignment algorithm DRAND[3] was proposed based on a centralized slot assignment algorithm RAND. DRAND algorithm, a scalable slot assignment algorithm, applies to the wireless sensor network with stationary nodes. The algorithm works according to the "round", and the time of each round is decided by the network delay adaptively. Assuming that Ci is the number of the nodes which may request slot assignment during the i-th round, and Pi is the probability of the node making the request, so probability of the successful request P（Success）=CiPi（1-Pi）Ci-1. After slot assignment in accordance with the DRAND algorithm, each node in its own slot can communicate interference-free. The next section of this paper will detail the algorithm.

It proposed a distributed dynamic slot assignment algorithm[4]. The algorithm divides slot into guide slot, broadcast slot, and appointment slot. A new network node chooses a slot in four steps: (1) request the slot assignment information in the competitive domain, (2) set the frame length and acquire slot assignment information,

(3) select an unassigned slot, (4) inform the neighbors of its own slot information. It proposed a scalable slot assignment algorithm for distributed wireless sensor network [5]. The algorithm uses the grid-based Latin square scheduling access (GLASS). When the data load of the data-intensive sensor network increases, it is able to maintain a slow performance with low overhead, high scalability, and a higher robustness when moving.

In wireless sensor networks, a TDMA-based MAC protocol should do the assignments of the nodes, and Z-MAC protocol used in an efficient distributed slot assignment algorithm DRAND. This paper introduces the DRAND algorithm, and improves the algorithm according to the residual energy. Then, EDRAND algorithm (Enhanced DRAND) has been proposed.

2 DRAND Algorithm

DRAND algorithm is a distributed slot assignment algorithm, and the Z-MAC[6] protocol described in the next section uses this algorithm to assign slots. Before the slot assignment, the algorithm performs a simple neighbor discovery protocol, and each node gets one-hop neighbor list and two-hop neighbor list. Then, it regards the

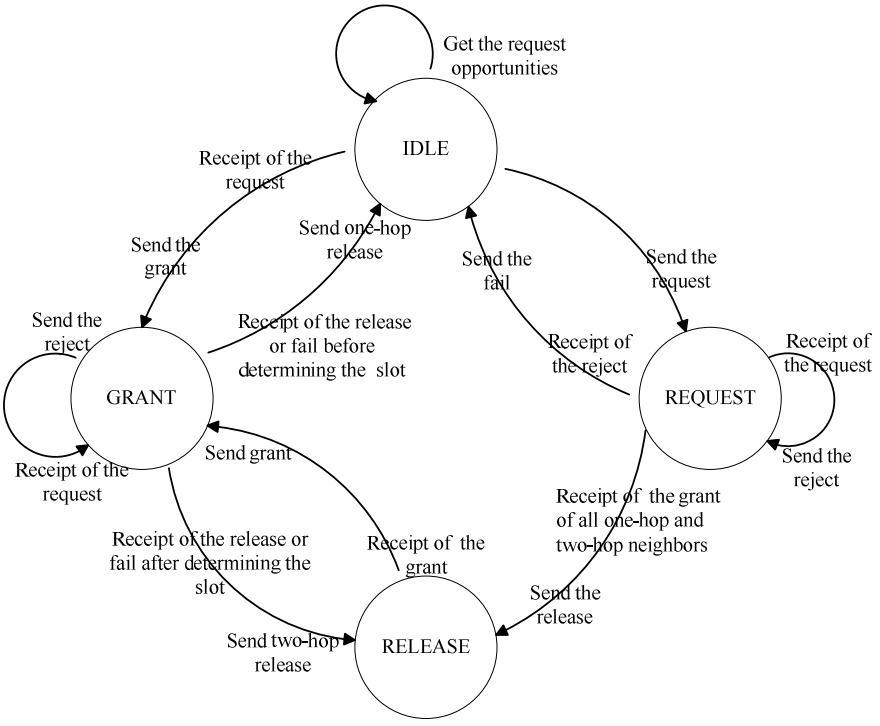

Fig. 1. Node states transformation of DRAND

nodes in the two-hop neighbor list as the input parameters of DRAND algorithms. In DRAND algorithm, the node has four states, IDLE, GRANT, RELEASE, REQUEST. The transitions of a node's state show as in Fig.1. The type of the information exchanged between nodes has request, grant, reject, fail and release.

Node A initiates a slot request with P_i probability every T_A time. The slot request results of node A may be a failure (not be assigned a slot) or may be successful (be assigned a slot). If a failure, it initiates a request again. Fig.2 (a) is a successful slot assignment request process, but Fig.2 (b) is a failure of the slot assignment request process.

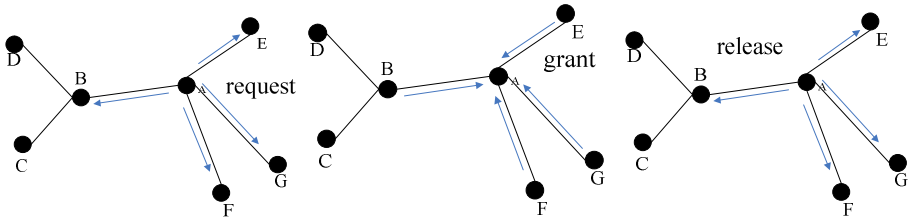

(a) A successful slot assignment request process

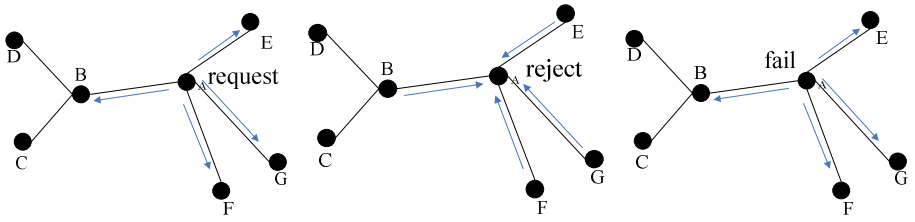

(b) A failure of the slot assignment request process

Fig. 2. A round of slot assignment

The $grant_i$ information sent by node B contains the one-hop neighbors' slot information of node B. If the node B is in the REQUEST or GRANT state, B will send $reject_i$ message to A. After receiving $reject_i$ message, node A will send a fail message to all of its one-hop node, and the state of node A is set to the IDLE. When B receives this fail message, if B has not yet be assigned a slot, it will be set to GRANT, or if B has, then it will be set to RELEASE.

Assuming that node A initiates the i-th round request and broadcast request message to its one-hop neighbors. When a neighbor node B receives the request information from node A, if B is in the IDLE or RELEASE state, it turns into the GRANT state immediately, and sends a granti information to A. The conditions that B is in the IDLE and the RELEASE state: (1) B's other neighbors are not send request message to it (taking into account A and B are not synchronized, node B may be in

the other round of the slot assignment); (2) B has not sent a grant message to any node so far, (3) If B has sent grant information to other node but not A, and it received the fail or release information from the node.

Compared with the existing slot assignment algorithms, there are four distinct advantages of the proposed approach which is listed as the followings:

(1) there is no need for precise time synchronization within the whole network;

(2) the effects of topology changes of the network is restricted within two-hop range, which makes the proposed approach scalable.

(3) low time complexity and space complexity. The time complexity is O (n), and the space complexity of the algorithm is O (n) when it is set to some network delay.

(4) compared with clustering slot assignment mechanisms of cluster protocols, there is no interference between clusters[7].

Weak points of using DRAND algorithm in the MAC protocol lie in that there are large overhead, and the node must execute slot assignment in the initialization phase, which consumes some energy other than the part of the implementation of an effective data transfer. The efficient data transfer rules of Z-MAC protocol makes up for the energy consumed by the slot assignment. Though DRAND slot assignment performs complex and consumes energy, we can optimize the network further to prolong the network lifetime in this process. The next section, we add energy balance strategy into DRAND algorithm, and propose a slot assignment EDRAND based on the node's residual energy.

3 Design of the EDRAND Algorithm

3.1 Slot Assignment based on the Residual Energy

In wireless sensor networks, the nodes close to the sink node often die prematurely due to the non-equilibrium of energy consumption, thus produces the energy hole [8], which directly affects the channel utilization, network throughput and delay. Other nodes with special location are prone to assume too much data to send and also die prematurely, such as the node closest to the incident, then the energy hole is formed in the incident. Energy balancing technology tries its best to average the energy consumption of the entire network to all sensor nodes and prolong the lifetime of the network. Energy balancing strategy optimizes the network energy consumption further on the basis of energy conservation. The common method of energy balancing is that according to the residual energy of nodes, it does channel access, route and data fusion [9] [10] [11] . Usually, adding the node's residual energy into the classic protocol, the communication protocol of energy balancing is formed.

In order to prolong the network's lifetime, in addition to the periodic listen/sleep, low-power listening, traffic adaptive and other energy-saving mechanisms, making the nodes with more residual energy to send and receive data to balance energy consumption of the whole network is a feasible method. In Fig.3, node A collects data and sends to the sink node. Nodes B, C and D are within the communication range of

node A, node B, C, and D are in the communication within the interference range of each other, and node D has the most remaining energy. If the node D is assigned the longest slot, for the probability of receiving data sent by node A, node D is greater than node B and C (the sleep time of node B and C are more). This process makes the nodes with more residual energy to forward data. In Fig.3, the thick dotted line path represents the data dissemination process.

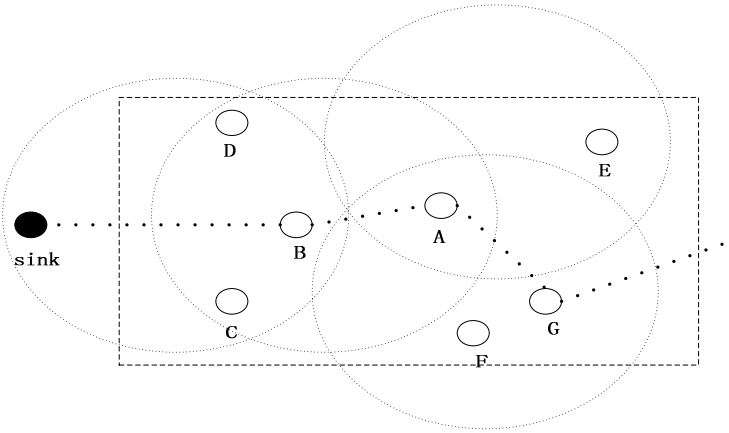

Fig. 3. Nodes with more residual energy have priority to transmit data

In the Z-MAC protocol, DRAND algorithm does the slot assignment. When the initialization of the network, it performs slot assignment one time, and only until the network topology changes greatly (nodes died or new node joined), it do the re-assignment slots within the local two-hop neighbors. In key business areas, the nodes with heavier data acquisition task consume energy relatively fast. In the subsequent slot assignment, if these nodes are assigned a shorter slot, it can prolong the lifetime of these nodes.

EDRAND algorithm decides the slot size based on the residual energy of nodes, which can be directly read out by the energy module of the sensor nodes, and the key is how to determine the relationship between the slot size and the node's residual energy. A seemingly simple method is that exchanging the information about residual energy between the nodes, sorting the residual energy values descending, and sorting the slot sizes as same as the order of the residual energy. The size of the slot assigned by the above method is reasonable, but the overhead is too high. In order to sort the residual energy values, each node must save residual energy values of nodes within two hops and perform the sorting algorithm. Moreover, the sorting process of the residual energy values and the slot assignment process (DRAND algorithm process) can not be carried out simultaneously, and the whole algorithm is complex, which significantly increase the control overhead.

Another method is that the node with the most or the second most residual energy is assigned a longer time slot. In this method, each node only needs save two

additional energy values. The process of selecting the nodes with the most and the second most residual energy can be piggybacked in the slot assignment process, so it increases control overhead rarely. Implementation of the slot assignment requires energy consumption, so it can not be executed many times. Therefore slot assignment results affect the network a long time. Simply assigning a longer slot assignment for the node with the most or the second most residual energy, which consumes energy much faster than other nodes in the next period, may cause the unbalance of energy consumption. The next section proposes the concept of micro-slot, and the slot is divided into smaller micro-slot which solves the problems of the fairness about the length of slot assignment and the control overhead.

3.2 Micro-slot

This section presents the concept of micro-slot. The Micro-slot is a time unit, which is smaller than the slot, shown in Fig.4. In the traditional TDMA mechanism, the smallest time unit is slot, and the slot forms the frame. In EDRAND algorithm, the smallest time unit is micro-slot, which forms slot and then shot forms frame. When deciding the slot's length of the node, if the slot is regarded as a unit, so the size of the node's slot is $i \times slot(i = 1, 2, 3 \cdots m)$. If the slot is too large, it will increase the network's latency. If the slot's length is reduced, then it will have an impact on the follow-up operations which regard the slot as the time unit. Micro-slot is transparent to the follow-up operations of MAC protocol, and the follow-up operations still regard slot as the smallest time unit.

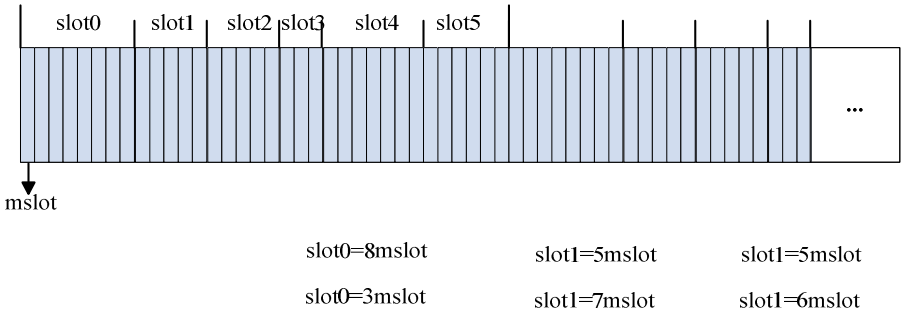

Fig. 4. Micro-slot

Assuming that each slot is composed of micro-slot whose number is up to M, the node's initial energy is the E_{max}, and the node's real-time residual energy is E_{now}. According to the following formula, n, the micro-slot number of each node can be determined:

$$n = \begin{cases} 1 & \frac{E_{now}}{E_{\max}} \times M \le 1 \\ \left\lceil \frac{E_{now}}{E_{\max}} \times M \right\rceil & \frac{E_{now}}{E_{\max}} \times M > 1 \end{cases} \quad (2)$$

M, the maximum micro-slot number, can be set freely, and the general value is about 8. The M is smaller, the gap of the slot is smaller, on the contrary, the M is greater, the gap of the slot is greater.

In the network topology shown in Fig.2, assuming that the initial energy of each node in the wireless sensor network is 100J. When the local network topology changes, node G stops working, and runs the slot assignment algorithm again. At this very moment, the residual energy of node A, B, C, D, E, F is respectively81J, 47J, 73J, 76J, 53J, 66J. The results of slot assignment in accordance with the DRAND is show in Fig.5(a). When M = 8, according to Formula (2), the micro-slot number obtained in the slots of A, B, C, D, E is respectively 7,4,6,6,5,6, and the node's slot number remains same, which is shown in Fig.5(b).

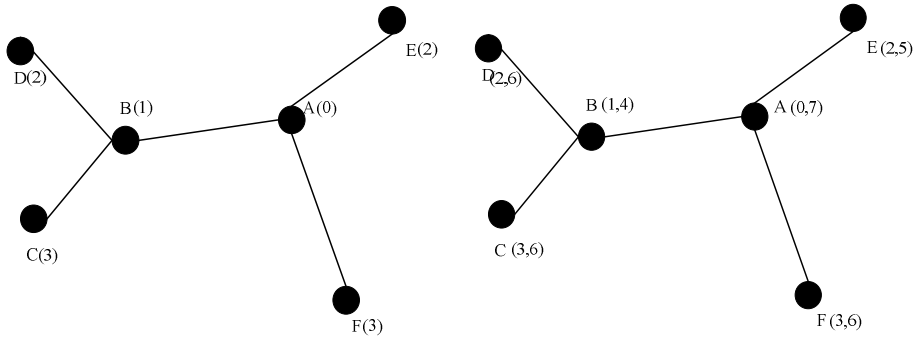

(a)DRAND slot assignment results (b)EDRAND slot assignment results

Fig. 5. An example of slot assignment

When a node's residual energy becomes very small, the value of $\frac{E_{now}}{E_{\max}} \times M$ may be less than 1. In the above example, the residual energy of node A, B, C, D, E, and F is 8.1J, 4.7J, 7.3J , 7.6J, 5.3J, 6.6J. Nodes' energy are very small, so there is no need to distinguish priority. However, if the node's initial energy is 1000J, when the remaining energy is less than 100J, the value of $\frac{E_{now}}{E_{\max}} \times M$ will be less than 1.

There is need to perform further calculations, and n, within two hops, calculates according to Formula (3):

$$n=\begin{cases}1 & (1) \quad \frac{E_{now}}{E_{\max}}\times M\le 0.1\\ \left\lceil \frac{E_{now}}{E_{\max}}\times M \right\rceil \times 10 & (2) \quad 0.1<\frac{E_{now}}{E_{\max}}\times M<1\\ \left\lceil \frac{E_{now}}{E_{\max}}\times M \right\rceil & (3) \quad \frac{E_{now}}{E_{\max}}\times M\ge 1\end{cases} \tag{3}$$

In the network, where the gap between node's energy consumption is small, the results of the above formula are reasonable. However, if the node's energy consumption is seriously uneven, within two hops, there may have nodes with 700J residual energy and 70J at the same time. In accordance with Formula (4), the two nodes are assigned a slot with the same micro-slot number. However, the micro-slot number of the node with 70J residual energy is greater than the node with 500J residual energy, resulting in the node with 70J residual energy consumes more energy. The reason lies in that in order to reduce overhead, the nodes are only aware of their own value of residual energy, without any awareness of the values of other nodes.

The solution is that the node within two hops can not both use (2) and (3) of the formula (3) and they must use the same calculation method. Therefore the formula (3) should split into formula (2) and formulas (4). A node within two hops can use the formula (2) and (4) at the same time to calculate the micro-slot number for each node.

$$n=\begin{cases}1 & \frac{E_{now}}{E_{\max}}\times M\le 0.1\\ \left\lceil \frac{E_{now}}{E_{\max}}\times M \right\rceil \times 10 & 0.1<\frac{E_{now}}{E_{\max}}\times M<1\\ M & \frac{E_{now}}{E_{\max}}\times M\ge 1\end{cases} \tag{4}$$

The conditions about node's energy consumption uneven within two hops previously mentioned exists the following three detailed case: the first case, nodes' residual energy is mostly about 700J, only one or two nodes' residual energy is less than 100J; The second case is the residual energy of nodes is mostly about 70J, and less than 100J, only relatively few nodes' residual energy is about 700J; The third case has a considerable number nodes with 700J and 70J residual energy. Under the premise of the nodes within two hops can only use the same formula to calculate the slot size, the first case uses the formula (2), so few nodes with relatively low residual energy are assigned one micro-slot, and micro-slot number of the majority of nodes changes as the node's residual energy changes; the second case uses the formula (4), and the slot

number of a small number of nodes with relatively high residual energy is M; the third case, the number of nodes with the calculated residual energy less than 100J is Sl and greater than 100J is Sm. When Sl <=Sm, we calculate in accordance with the formula (2), and when Sl > Sm, we calculate in accordance with the formula (4).

We defined that the number of alternative formulas within two hops is the energy level of the network. In the example described above, the initial energy is 100J, the energy level of the network is 1, and when the initial energy is the 1000J, the energy level of the network is 2(less than 100J is Level1, and greater than 100J is Level 2). The energy level of the network is higher, the effect of energy balance is longer, and the overhead about computational and storage is also correspondingly larger.

3.3 Process of the Algorithm

In the algorithm proposed in this paper, the nodes need to save their residual energy. Before the slot assignment, it calculates micro-slot number about the node's slot, and after acquiring the slot number successful, the node will put its own slot number and the micro- slot number into the release message, and broadcast it to its one-hop neighbors .

By using micro-slot, there is no need to transmit and compare the residual energy values between the neighbor nodes to determine the slot size. When the energy level is 1, you only need to notify the slot size as well as the slot number at the same time, which only increases the storage and transmission of a variable. The list of the new neighbor nodes includes the ID of the neighbor nodes, the slot number and the slot size (the contained micro-slot number) of the nodes. When the energy level is k, the node needs to store the value of its own residual energy and k variables (represent the number of nodes in each energy level). During the neighbor discovery phase, nodes exchange their residual energy level, come out statistics about the values of k variables according to the records in the two-hop neighbors list, and choose its own slot formula according to the energy level corresponding to the maximum variable to achieve the reunification about the slot size calculation within two hops. In the example of above section, where the network energy level is 2, the number of nodes whose calculated energy level is 2 (the value of residual energy is less than 100J) within two hops is k2 and the number of nodes whose calculated energy level is 1 (the value of residual energy is more than 100J) is k1.When k1 is greater than or equal to k2, we calculate in accordance with the formula (2), otherwise we calculate in accordance with the formula (4).

```
84  typedef struct releaseMsg{
85    uint8_t sendID;
86    uint8_t myState;
87    uint8_t lastRequestID;
88    uint8_t roundNum;
89    uint8_t slot;
90    uint8_t localC;
91    unit8_t slotSize;
92  } releaseMsg;
```

Fig. 6. Data structure of release packet

This article only discusses the execution of the algorithm when the network energy level is 1. It increases the variable about slot size in the releaseMsg structure of DrandConst.H header files, which is shown in Fig.6:

After adding slot length which is assigned in accordance with the nodes' residual energy into the original DRAND algorithm, the pseudo code of slot assignment for each round is shown as follows:

```
If (stateX = IDLE)
{
 send request message to its one-hop neighbors;
        // stateX is the state of X
        stateX = REQUEST;
}
When (Y receives the request)
   If (stateY=IDLE or stateY=RELEASE)
{
stateY=GRANT;
Node Y sends grant message to node X;
When (nodes X receives the grant message from all of one-
hop neighbors)
{
   assign an unused smallest slot tmin within two-hop
neighbors to node X;
   calculate the number of micro-slot which the slot
contains,n;
  send the release message with slot number tmin and slot
size n to one -hop neighbors;
   stateX=RELEASE;
   When (Y received the release)
  {
   If (Y haven't be assigned slots)
       StateY = IDLE;
     Else stateY=RELEASE ;
        Node Y forwards this release message to one-hop
neighbors;
  }
}
}
If (stateY=REQUEST or stateY=GRANT)
{
Node Y sent reject message to the node X;
    When (node X receives the reject)
   {
      Node X sends fail message to one-hop neighbors;
      stateX=IDLE•
     // the slot assignment of Node X fails, and wait for
sending the request of the next round again
      If (stateY receives a fail message || stateY=GRANT)
         IF (node Y haven't be assigned slots)
```

```
                StateY =IDLE ;
Else stateY=RELEASE;
    }
}
```

The improved slot assignment algorithm doesn't increase too much control messages and achieves the energy balance for the slot assignment, so the slots with more residual energy has more opportunity to access the channel to send and receive data, which prolong the effective work time of the network.

4 Simulations and Analysis

This section briefly describes the NS2 network simulation software and its energy mechanism. We use NS2 to simulate EDRAND and DRAND, and compare the performance of Z-MAC protocol when it uses the two time slot assignment algorithm.

4.1 NS2 and Energy Model

After from NS2.26 version, NS2 starts to support the energy model. Energy model is for wireless networks, such as Ad-hoc networks and wireless sensor networks. Energy model implements in the file ~ns/mobility/energy- model.h/cc, and is referenced in ~/ns/mac/wireless-phy.h/cc at the same time, which is used to control energy, such as sending energy and receiving energy. By default, NS2 does not enable the energy model. Energy is the node's attribute and when using the energy model, nodes' configuration shows as in the following parameters:

$ Ns_ node-config-energyModel "EnergyModel" \
The-initialEnergy (J) ---------- (node initial energy)
The-rxPower (w) --------------- (receiving state power)
The-txPower (w) --------------- (sending state power)
The-idlePower (w) ------------- (idle listening state power)
The-sleepPower (w) ------------ (sleep state power)
-SleepTime ----------------- (the time that a node needs to wait before the beginning of sleep, in seconds)
The-transitionPower ---------- (the power required to switch between sleep and idle states, in W)
-TransitionTime ------------ (the time required to switch between sleep and idle states, in seconds).

In the trace file, the part format of the energy model shows as in follow:

energy [total remaining energy] ei [idle consumption] es [sleep consumption] et [transmition consumption] er [receiving consumption].

The following code can obtain the node's residual energy values in each protocol or functional modules: iEnergy = iNode->energy_model()->energy().

4.2 Simulations and Analysis

DRAND and Z-MAC have been achieved in NS2 and TinyOS system[14]. In this section, simulation is carried in NS2.34, and we compare the effects which DRAND and EDRAND algorithm play on Z-MAC protocol. The implementations of DRAND and Z-MAC in NS2 do not consider the energy problem, so we need to add energy model in the code first. The simulation scenario is that 50 nodes are randomly distributed in the range of network topology within the region of 300m × 300m. Fig.7 is the simulation scenario, and Table 1 is part of the simulation parameters. In the DRAND algorithm, the size of T_0 is set to eight slots, the size of T_{n0} is set to 32 slots, the initial T_0 of EDRAND is set to 4M micro-slot size, the initial T_{n0} is set to 16M micro-slot size, and M = 8.

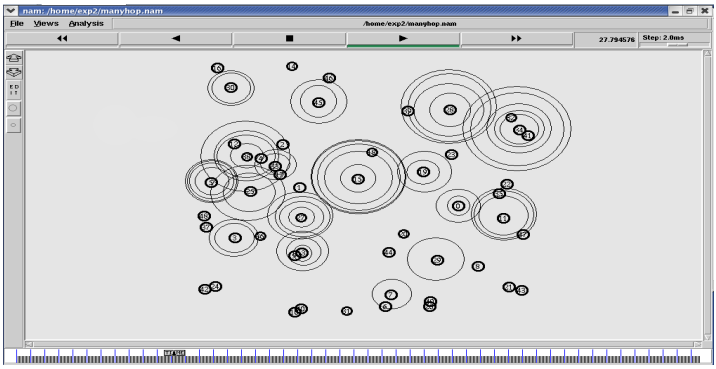

Fig. 7. Simulation scene

Table 1. Simulation parameters

Parameter name	Parameter value
Interference range / m	50
Upper layer routing protocol	AODV
ECN effective time T_{ECN}/s	10
Micro-slot size /us	400
Communication bandwidth /kbps	20
Packet length /Byte	256
Transmit power /mW	24.75
Receiver (listener) Power /mW	13.5
Sleep power consumption /uW	15
Node initial energy /J	1
The rate of sending data /	1 packet/s

In the same simulation scenario, we simulate the original protocol and improvement of the protocol separately, and we compare the lifetime and throughput performance of the network of the Z-MAC protocol which use DRAND algorithm and EDRAND algorithm separately.

Fig.8 is the trace file when you run the EDRAND algorithm, and we use the awk script to analyze the trace file obtained by the simulation. If the initial energy is equal, the results of slot assignment which are performed by DRAND algorithm and EDRAND algorithm are the same, shown in Fig.9 (a), the first number represents the node number and after the "SLOTINFO" is slot number. Fig.9 (b) is the slot assignment results about the simulation with EDRAND algorithm which runs to 350s and the network topology changes, the first number represents the node number, and after the "SLOTINFO" is slot number and the micro-slot number.

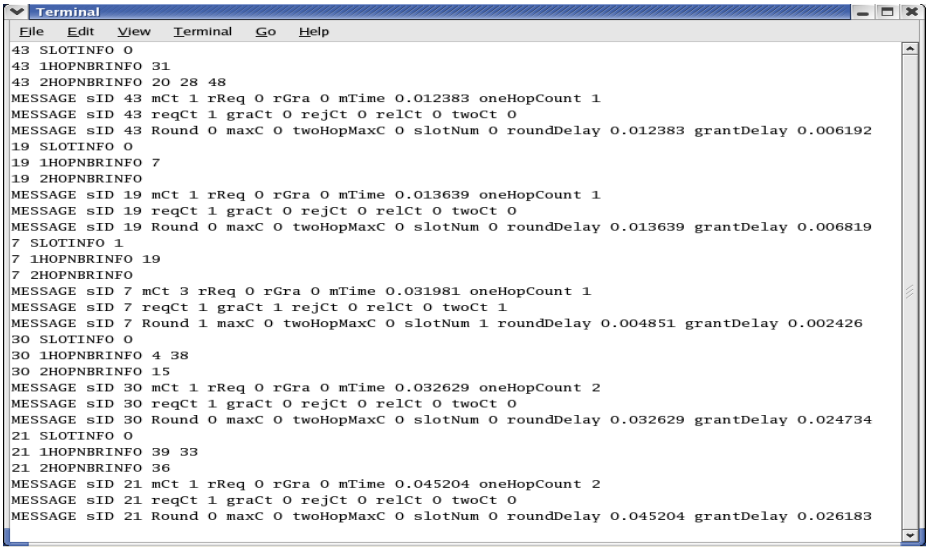

Fig. 8. The content of trace file

```
43 SLOTINFO 0    44 SLOTINFO 1    17 SLOTINFO 2
19 SLOTINFO 0    42 SLOTINFO 0    20 SLOTINFO 5
7 SLOTINFO 1     5 SLOTINFO 0     46 SLOTINFO 3
30 SLOTINFO 0    47 SLOTINFO 1    6 SLOTINFO 2
21 SLOTINFO 0    33 SLOTINFO 2    26 SLOTINFO 6
39 SLOTINFO 1    13 SLOTINFO 1    8 SLOTINFO 7
36 SLOTINFO 2    27 SLOTINFO 0    0 SLOTINFO 8
10 SLOTINFO 0    49 SLOTINFO 1    9 SLOTINFO 4
25 SLOTINFO 1    45 SLOTINFO 2    23 SLOTINFO 5
14 SLOTINFO 0    3 SLOTINFO 0     28 SLOTINFO 3
41 SLOTINFO 1    31 SLOTINFO 2    48 SLOTINFO 9
24 SLOTINFO 0    1 SLOTINFO 3     37 SLOTINFO 6
15 SLOTINFO 1    2 SLOTINFO 4     12 SLOTINFO 10
4 SLOTINFO 2     18 SLOTINFO 1    34 SLOTINFO 2
38 SLOTINFO 3    32 SLOTINFO 2    16 SLOTINFO 6
40 SLOTINFO 0    35 SLOTINFO 2
```

(a) The DRAND slot assignment results

```
34 SLOTINFO 0  3    39 SLOTINFO 1 2
18 SLOTINFO 1  2    41 SLOTINFO 2 8
7 SLOTINFO 3   1    16 SLOTINFO 0 1
36 SLOTINFO 2  6    5 SLOTINFO 2 6
20 SLOTINFO 0  5    14 SLOTINFO 4 2
21 SLOTINFO 1  4    15 SLOTINFO 5 5
23 SLOTINFO 2  1    27 SLOTINFO 7 4
2 SLOTINFO 4  8     35 SLOTINFO 1 3
19 SLOTINFO 1  2    20 SLOTINFO 6  6
12 SLOTINFO 0  4    6 SLOTINFO 2 4
22 SLOTINFO 1  3    26 SLOTINFO 3 8
26 SLOTINFO 0  2    8 SLOTINFO 1 5
13 SLOTINFO 3  8    11 SLOTINFO 3 3
4 SLOTINFO 3 6      0 SLOTINFO 2 4
8 SLOTINFO 0 3      9 SLOTINFO 0 2
47 SLOTINFO 1 1     24 SLOTINFO 0 7
```

(b)EDRAND slot assignment results

Fig. 9. Slot assignment result

When wireless sensor networks run for some time, some nodes begin to run out of energy, namely the death of nodes. Node's death rate follows a normal distribution roughly, 10% to 80% of the nodes have died within a relatively short time. The first node's death does not mean the end of the network lifetime, as long as the majority nodes of the regional with monitoring tasks are not death and can complete the tasks about data acquisition, and we still think that the network is working properly. Therefore, to prolong the network lifetime is to maximize the nodes' survival time in a normal distribution. Fig.10 shows the number of the survival nodes in the network over the simulation time.

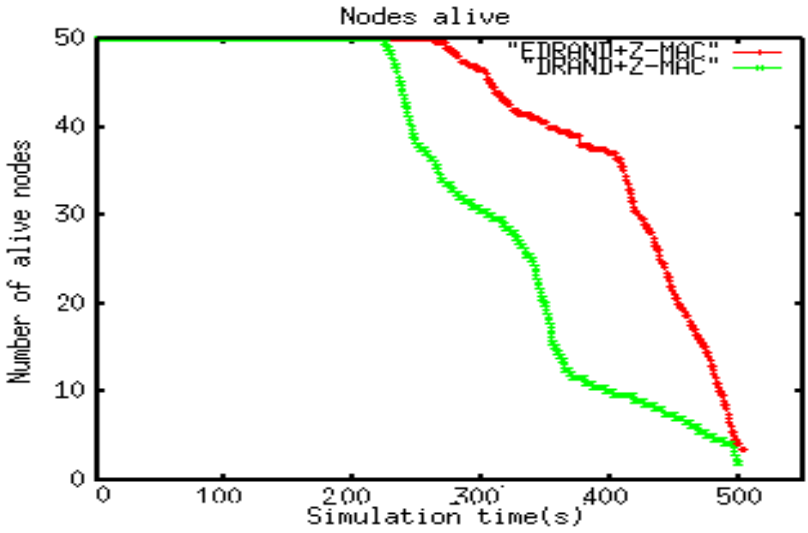

Fig. 10. Node alive comparison

It can be seen from the figure, using EDRAND algorithm for slot assignment has effectively improve the overall survival time of the nodes, and previous node's death is more slowly which maintains the connectivity of the network. During the two experiments, the death of the first node in the network happens about in 220 seconds. This is because that before the death of the first node, the network topology does not change, and it doesn't implement the strategy of the slot assignment in accordance with the residual energy of EDRAND algorithm. In the networks using EDRAND algorithm in 230 seconds to 250 seconds, the death rate of nodes slows down, and after 400 seconds, node's death speed in EDRAND network increases dramatically, because the nodes with more residual energy consumed more energy in the former period and in fact, the network can no longer perform normal tasks in this phase, so the death rate of the nodes has no influence on the network.

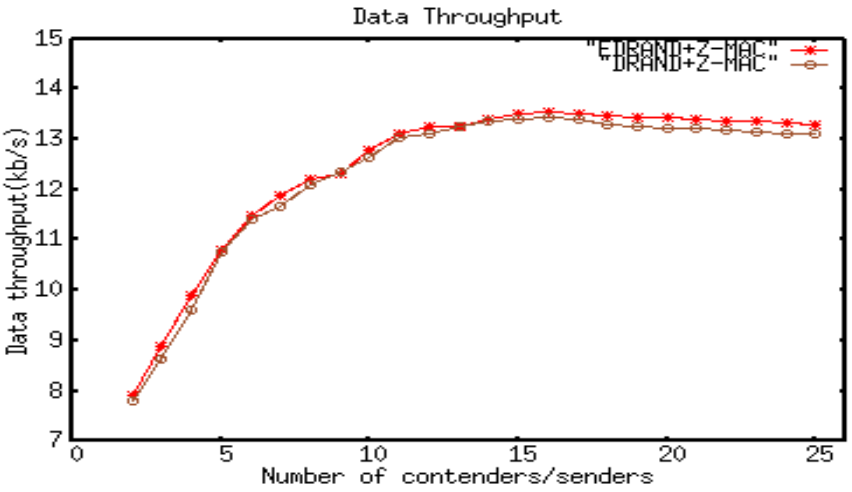

Fig. 11. Network throughput comparison

Fig.11 is the comparison of network throughput, the two curves almost overlap, and with the minimal gap, it shows the additional control overhead of EDRAND is very small, and has no impact on network throughput.

5 Conclusions

This paper firstly presented a brief introduction of the slot assignment algorithm which is used in the MAC protocols based on TDMA mechanism. A network model of slot assignment was presented thereafter and the advantages and disadvantages of centralized algorithms and distributed algorithms were compared. Followed by, we analyzed the efficient and scalable distributed slot assignment algorithm DRAND used in Z-MAC protocol in detail, and proposed a slot assignment algorithm EDRAND based on node's residual energy. In the EDRAND algorithm, the node decides the number of micro-slot covered by its own slot and the slot information includes the slot number and the number of micro-slot according to its residual energy. The simulation results of NS2 show that by using DRAND algorithm l, death time is delayed compared with that by using DRAND algorithm in the Z-MAC protocol and the effective working time of the network can be extended.

References

1. Yu, S.: Research on Slot Assignment Technology of Wireless Dynamic TDMA Network. Xi'an University of Electronic Science and Technology, Xi'an (2009)
2. Li, Y.: Research on Time Synchronization and Slot Assignment Algorithm for Wireless Sensor Networks. Zhejiang University, Hangzhou (2011)

3. Liu, L., Shi, Y., Chen, K.: Adaptive Backoff Algorithm for Wireless Sensor Networks. Computer Applications and Software 28(10), 1930–1934 (2006)
4. Dou, W., Jia, Z., Wu, L., Zhang, W.: TDMA-based Distributed Dynamic Slot Assignment Algorithm for Ad Hoc Networks. Computer Engineering and Design 28(19), 4667–4712 (2007)
5. Lin, C.-K., Zadorozhny, V.I., Krishnamurthy, P.V., Park, H.-H., Lee, C.-G.: A distributed and scalable time slot allocation protocol for wireless sensor networks. IEEE Transcation on Mobile Computing 10(5), 505–518 (2011)
6. Polastre, J., Hill, J., Culler, D.: Versatile low power media access for wireless sensor networks. In: Proc. of the 2nd ACM Conf. on Embedded Networked Sensor Systems (SenSys), Baltimore, pp. 95–107 (2004)
7. Liu, Z.-X., Zheng, Q.-C., Xue, L.: Energy and node degree synthesized clustering algorithm for wireless sensor networks. Journal of Software 20(9), 250–256 (2009)
8. Matrouk, K., Landfeldt, B.: RETT-gen: a globally efficient routing protocol for wireless sensor networks by equalising sensor energy and avoiding energy holes. Ad Hoc Networks 7(3), 514–536 (2009)
9. Anastasi, G., Conti, M., Di Francesco, M., Passarella, A.: Energy conservation in wireless sensor networks: A survey[J]. Ad Hoc Networks (7), 537–568 (2009)
10. Fu, J., Qi, X.: Clustering Algorithm based on Residual Energy and Node Degree for WSNs. Application Research of Computers 28(1), 250–252 (2011)
11. Cheng, X., Deng, Z.: Constructing a large scale wireless sensors network and resources scheduling among multiple personal area networks. International Journal of Distributed Sensor Networks (IJDSN) 5(1), 76–79 (2009)
12. Yu, B., Sun, B., Wen, N., Wang, H., Chen, J.: NS2 and Network Simulation. People's Posts & Telecom Press, Beijing (2007)
13. Ke, Z., Cheng, R., Deng, D.: NS2 Simulation Experiments——Multimedia and Wireless Network Communication. Electronic Industry Press, Beijing (2009)
14. DRAND and Z-MAC Coding, `http://research.csc.ncsu.edu/netsrv/?q=content/drand-ns-2`

Heterogeneity-Aware Optimal Power Allocation in Data Center Environments

Wei Wang, Junzhou Luo, Aibo Song, and Fang Dong

School of Computer Science and Engineering, Southeast University, Nanjing, P.R. China
{wangweing,jluo,absong,fdong}@seu.edu.cn

Abstract. Data centers generally consume an enormous amount of energy, which not only increases the running cost but also simultaneously enhances their greenhouse gas emissions. Given the rising costs of power, many companies are looking for the solutions of best usage of the available power. However, most of the previous works only address this problem in the homogeneous environments. Considering the increasing popularity of heterogeneous data centers, this paper investigates how to distribute limited power among multiple heterogeneous servers in a data center so as to maximize performance. Specifically, we optimize the power allocation in two case: single-class service case and multiple-class service case. In each case, we develop an algorithm to find the optimal solution and demonstrate numerical data of the analytical method respectively. The simulation results show that our proposed approach is efficient and accurate for the performance optimization problem at the data center level.

Keywords: power allocation, performance optimization, heterogeneous servers, data center.

1 Introduction

The cloud provider giants often build huge data centers in order to provide services. A typical data center usually consists of hundreds to thousands of servers, which consume an enormous amount of electric power for operating and cooling [1]. The power consumption of data centers is expected to double every five years which is a huge cost to both environment and service providers all over the world. No longer is faster necessarily better; both performance and power consumption must be considered in the operation of current cloud systems. Hence the emphasis is on providing good service while maintaining power efficiency. In a data center for cloud computing, there are typically multiple heterogeneous servers which provide services in different application domains. Data center are inherently heterogeneous due to upgrading cycles and replacing of failed components. In addition, new processor and memory architectures appear every few years and this trend has driven update cycles in large data centers to less than two years [2].

Fig. 1 illustrates the heterogeneous data center architecture we considered in this paper. It consists of with k heterogeneous servers. In such a data center, a user

Q. Zu, B. Hu, and A. Elçi (Eds.): ICPCA-SWS 2012, LNCS 7719, pp. 513–528, 2013.

typically requires a certain service with a certain quality requirement defined in service level agreement (SLA), which is a contract agreed between a user and the data center service provider. If the provider cannot meet deadline defined in the SLA, s/he has to pay for the penalty according to the clauses defined in the SLA. Thus, it is important for service providers to meet users' requirements on service response time. The mean response time can be improved by increasing the CPU's power level of each server. That is to say, by varying the power allocated to a server, one can dynamically change the server's mean response time. However, increasing the CPU speed of a server implies more power consumption of the server. Hence, given a data center with a fixed power budget, there is a problem of how to distribute available power among servers, such that the overall quality of service of the servers in the data center is optimized [4-5]. Note that the power allocated to a server is controlled via the CPU's voltage and frequency settings. Thus, our objective is to maximize the overall performance of the data center by using a fixed power budget and our control knob is the amount of power we allocate to each server.

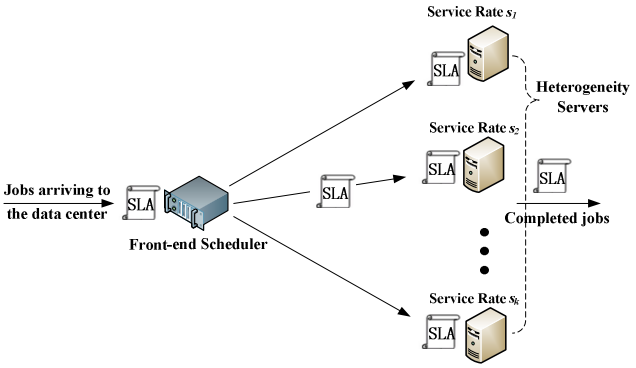

Fig. 1. A heterogeneity data center model

To fully understand the relationship between power allocation and jobs' mean response time, we introduce a queuing theoretic model, which allows us to predict the optimal power allocation in a variety of scenarios. We model each server as a queuing system and the job mean response time is formulated as a function of power allocations to the servers.

We distinguish the data center service in two cases; single-class service and multiple-class service. Single-class service means there is only one kind of application service provided by the data center service provider. Thus, all data center users request for the same kind of service which has the same processing procedure. The multiple-class service means there are multiple kinds of application services. Each kind of service has a different processing procedure at the computing server, a different requirement on the service response time and so on. Increasingly, data centers are being used to serve multiple classes of jobs. Large corporations like Google and Amazon use the same data center for serving multiple jobs: answering search queries,

mail, instant messaging and other research problems. However, it is notable hard to analysis the performance optimization problem for the multiple-class service.

In order to find the optimal solution of the power allocation problems for the above two cases, we first model the service process of a data center system as a queuing network, and derive the formulation of the mean response time and the total power consumption. Then, we derive a theoretically optimal solution for the single class service case. For the multi-class service case, it is hard to obtain the theoretically optimal solution, thus we propose a modified Lagrange Multiplier method to obtain an approximate optimal solution. The correctness and effectiveness of our approach will be verified via extensive simulations using Cloudsim tool[18].

The rest of the paper is organized as follows. In Section 2, we introduce the related work. In Section 3, we discuss system models. The optimization analysis of mean response time with power constrained is presented in Section 4. In Section 5, we present the simulation results. And in the last section, we conclude this paper and discuss future works.

2 Related Work

Efficient power management and performance optimization in large-scale data centers or server farms has gained much attention in the research literature in recent years. The most similar related work has been done in [6-10]. In [6], the authors proposed a novel, system-level power management technique called "Power Shifting" for increasing performance under constrained power budgets. "Power Shifting" employs activity monitoring and power estimation techniques to predict future power consumption, dynamic power allocation among the system components, and mechanisms to regulate component level activity to enforce the desired power allocation. Their evaluations show that (1) Dynamic power budgeting performs better than static budgeting (2) Inaccuracies in utilization or power requirement estimates can be effectively combated with the sliding window to the basic proportional-last-interval policy. In [7], the authors proposed a coordination solution to address the enterprise power management problem. They found that for current systems with high baseline idle power consumptions, VM consolidation can be a more effective way to save power in spite of its additional overhead. They also found that the redundancy in power optimization across multiple levels can enable systems to be much simpler by supporting a few widely separated power states spectrum. In [8], the authors studied DMA-aware techniques for memory energy management in data servers. They proposed two novel performance-directed energy management techniques that maximize the utilization of memory devices by increasing the level of concurrency between multiple DMA transfers from different I/O buses to the same memory device. In [9], the authors allocate peak power so as to maximize throughput in a data center while simultaneously attempting to satisfy certain operating constraints such as load-balancing the available power among the servers. Chase et al. [10] present an auction-based architecture for improving the energy efficiency of data centers while achieving some performance specifications.

Gandhi et al. [11] study the performance of some simple allocation strategies aiming at reducing the Energy-Response time Product (ERT). However, while the authors consider the fact that servers consume energy but do not serve any job when system in the setup/off states. Since running too many servers increases the energy consumption while having too few servers turned on requires running those servers' processors at higher frequencies, some hybrid approaches have been proposed (see, for example, [12]). Sangyeun Cho et al. [13] developed an analytical framework to study the trade-off between program performance, parallelization and energy consumption. Although their framework is based on many simplifying assumptions, some of which are inherited from Amdahl's law and some of which are specific to variable-speed processors, it provides interesting insights on these trade-off.

3 System Model

3.1 System Modeling and Notations

The system under study is a distributed data center consisting of k heterogeneous servers (As shown in figure 1). The speed of these corresponding servers is denoted by s_i (i=1,…,k). When allocating power to a server i, there is a minimum level of power consumption (l_i) needed to operate the CPU at the lowest allowable frequency and a maximum level of power consumption (m_i) needed to operate the CPU at the highest allowable frequency. Thus, by varying the power allocated to a server, one can dynamically change the server's mean response time. Each server has its own computation queue to store job requests waiting for processing. The architecture of the data center designs as two levels of schedulers, a global scheduler and local schedulers. The global scheduler has no waiting queue and therefore incoming jobs are immediately dispatched to individual servers. The local servers schedule the jobs based on a non-preemptive and First-In-First-Out policy. We assume all the incoming jobs are CPU bounded, in other words, CPU speed is the bottleneck of performance. This is reasonable because Bohrer[15] pointed out that CPU is the largest consuming component for typical web server configuration. The jobs are online and have exponentially distributed inter-arrival and execution times. A job submitted to a server must be serviced on that server and job mitigation/migration/rejection is not allowed. We assume the total arrival rate is λ (for the multi-class service case, the total arrive rate is the sum of the arrival rate of each service class).We employ possibility random generation method as scheduling scheme, which means the possibility q_i of job requests sent to server i is randomly generated. Thus, the arrival rate of jobs to server i is $q_i\lambda$, denoted by λ_i. According to the decomposition property of Poisson Process, the arrivals of jobs at server i follow a Poisson Process with arrival rate λ_i. At last, after computation phase, the final result will be sent back to the users.

3.2 Power-to-Frequency Relationship Model

To understand the power-to-frequency relationship of a single server is crucial to the power aware data center design. In [4], researchers found that that the power-to-frequency relationship for DVFS looks like a linear plot. There are two reasons to explain this relationship. Firstly, manufacturers usually settle on a limited number of allowed voltage levels, which results in less-than-ideal relationship between power and frequency in practice. Secondly, DVFS is not applied to many components at the system level.

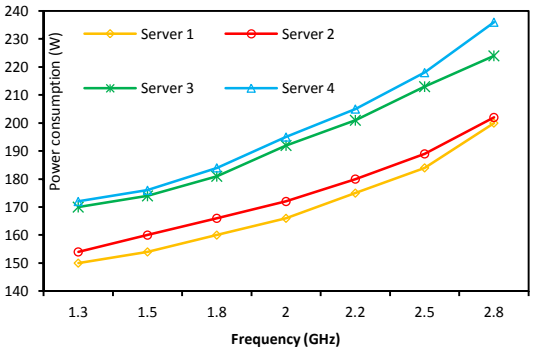

Fig. 2. Power-to-frequency Relationship Model

In linear model, the power consumption P is set as a function of server frequency, as: $f = f_l + \beta(P\text{-}l)$. in which l is the minimum power consumed by a running server over the allowable range of processor frequency; f_l is the speed (or frequency) of a fully utilized server running at l Watts; Coefficient β is the slope of the power-to-frequency curve. In this paper, we use linear model in our theoretical framework. Figure 2 plots the average power consumption of the four servers used in our experiments. The power consumption of the four servers are at six available CPU frequency levels, which correspond to effective frequencies of 12.5%, 25%, 50%, 75%, 87.5% and 100% of the maximum server frequency. From the figure, we can figure out that the linear model fits well for the four servers. Thus, the power-to-frequency curve for DVFS can be approximated as a linear function.

4 Power Allocation Problem Formulation

In this section, we use the proposed system model in section 3 to study the power allocation problem in data center.

4.1 Single-Class Service Case

In this subsection, we study the optimal power allocation in single-class service case, in which there is only one kind of service provided in the data center. As shown in figure 3, we assume the jobs' arrival process is Poisson with average rate λ. Each server receives a fraction q_i of the total workload. Thus, corresponding to any vector of workload allocation (λ_1, . . . , λ_k), there exists an optimal power allocation vector (p^*_1, . . . , p^*_k).

We model each server i as an M/M/1 queuing system (i.e. Poisson arrivals and exponentially distributed processing times) and is characterized by its average service rate μ_i. According to the power-to-frequency relationship model discussed in section 3, we have $\mu_i = f_{li} + \beta_i(p_i - l_i)$. To maintain a stable queue, the constraint $\lambda_i < f_{li} + \beta_i(p_i - l_i)$ should be satisfied. The mean response time of server i is given by $\frac{1}{\mu_i - \lambda_i}$, and the mean response time of all k servers can be computed as:

$$E(T_{single}) = \sum_{i=1}^{k} \frac{\lambda_i}{\mu_i - \lambda_i} \tag{1}$$

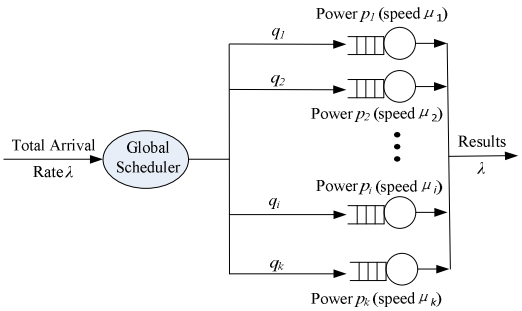

Fig. 3. Queuing model for single service case

The optimization problem consider here is to find the optimal power allocation (p^*_1, . . . , p^*_k), which minimizes the mean response time $E(T_{single})$, given the fixed power budget P. As stated earlier, each server i should be allocated at least power l_i. Thus, the amount of power can be allocated flexibly among the heterogeneity servers is $P' = P - \sum_{i=1}^{k} l_i$. Then our optimization problem can be reduced to find the optimal power allocation (p'_1,..., p'_k), ($0 \le p'_i \le m_i - l_i$, $i=1,\ldots,k$) to minimize the overall mean response time $E(T_{single})$. We assume m_i is the maximum level of power consumption needed to operate the CPU of server i at the highest allowable frequency. Let $m'_i = m_i - l_i$, then the optimization problem can be formulated as

$$\begin{aligned} P1: \quad & \textit{minimize} \quad E(T_{single}) \\ \textit{subject to} \quad & \lambda_i < f_{li} + \beta_i p'_i,\ i=1,\ldots,k \\ & \textstyle\sum_{i=1}^{k} p'_i \le P' \\ & 0 \le p'_i \le m'_i,\ i=1,\ldots,k \end{aligned}$$

In order to determine the optimal solution of problem *P1*, we prove the following theorem.

Theorem 1. The objective function $E(T_{single})$ is minimized when

$$p_i^{'} = \sqrt{\lambda_i / \beta_i} * (P^{'} + \sum_{i=1}^{k} (f_{li}/\beta_i - \lambda_i/\beta_i)) \Big/ \sum_{i=1}^{k} \sqrt{\lambda_i/\beta_i} - (f_{li}/\beta_i - \lambda_i/\beta_i) \tag{2}$$

***Proof*:** This is a constrained-minimum problem and can be solved using the Lagrange multiplier method. Let $\alpha \geqslant 0$, $\eta_{1i} \geqslant 0$, $\eta_{2i} \geqslant 0$ and $\eta_{3i} \geqslant 0$, i=1,…,*k*, denote the Lagrange multipliers. The Lagrangian is

$$\begin{aligned} &L(p_1^{'},...,p_k^{'},\alpha,\eta_{11},...,\eta_{1k},\eta_{21},...,\eta_{2k},\eta_{31},...,\eta_{3k}) \\ &= E(T_{single}) - \alpha(P^{'} - \sum_{i=1}^{k} p_i^{'}) - \sum_{i=1}^{k} \eta_{1i} p_i^{'} - \sum_{i=1}^{k} \eta_{2i} (p_i^{'} - (\lambda_i - f_{li})/\beta_i) - \sum_{i=1}^{k} \eta_{3i} (m_i^{'} - p_i^{'}) \end{aligned}$$

The Kuhn-Tucker conditions imply that $p^{'}_i$, $i = 1, ..., k$ is the optimal solution if and only if there exists $\alpha \geqslant 0$, $\eta_{1i} \geqslant 0$, $\eta_{2i} \geqslant 0$ and $\eta_{3i} \geqslant 0$, i=1,…,*k*, such that:

$$\begin{aligned} &\partial L/\partial p_i^{'} = 0, \partial L/\partial \alpha = 0, \eta_{1i} p_i^{'} = 0, \eta_{2i} (p_i^{'} - (\lambda_i - f_{li})/\beta_i) = 0, \\ &\eta_{3i} (m_i^{'} - p_i^{'}) = 0, \sum_{i=1}^{k} p_i^{'} \leq P^{'}, \lambda_i < f_{li} + \beta_i p_i^{'}, 0 \leq p_i^{'} \leq m_i^{'}, i = 1,...,k. \end{aligned}$$

The conditions become :

$$\begin{aligned} &\frac{-\lambda_i \beta_i}{(f_{li} + \beta_i p_i^{'} - \lambda_i)^2} + \alpha - \eta_{1i} + \eta_{3i} = 0, P^{'} = \sum_{i=1}^{k} p_i^{'}, \eta_{2i} = 0, \\ &\eta_{1i} p_i^{'} = 0, \eta_{3i} (m_i^{'} - p_i^{'}) = 0, \sum_{i=1}^{k} p_i^{'} \leq P^{'}, 0 \leq p_i^{'} \leq m_i^{'} \end{aligned}$$

We consider the case of $0 < p_i^{'} < m_i^{'}$, then, we obtain $\alpha = \frac{\lambda_i \beta_i}{(f_{li} + \beta_i p_i^{'} - \lambda_i)^2}$, if combined with $P^{'} = \sum_{i=1}^{k} p_i^{'}$, we obtain

$$p_i^{'} = \sqrt{\lambda_i/\beta_i} * (P^{'} + \sum_{i=1}^{k} (f_{li}/\beta_i - \lambda_i/\beta_i)) \Big/ \sum_{i=1}^{k} \sqrt{\lambda_i/\beta_i} - (f_{li}/\beta_i - \lambda_i/\beta_i)$$

This completes the proof.

The power allocation specified by Theorem 1 may not always be practical since $p_i^{'}$ is not guaranteed to be non-negative. $p_i^{'}$ is negative if

$$(P^{'} + \sum_{i=1}^{k} (f_{li}/\beta_i - \lambda_i/\beta_i)) \Big/ \sum_{i=1}^{k} \sqrt{\lambda_i/\beta_i} \leq f_{li} \Big/ \sqrt{\lambda_i \beta_i} - \sqrt{\lambda_i/\beta_i} \tag{3}$$

When $p_i^{'}$ is negative, an intuitive method to make the solution feasible is to set $p_i^{'}$ to 0 and recalculate power for other servers according to Theorem 1. Based on this institution, we propose the following algorithm which describes how to assign power to all servers.

Algorithm 1. The optimal power allocation algorithm for single class service

Input: Power budget P, the minimum speed vector $\boldsymbol{f_l}$, coefficient vector $\boldsymbol{\beta}$, total arrival rate λ.

Output: optimal power allocation solution $\boldsymbol{p}^*$.

Step 0: Sort the servers in non-decreasing order of their $f_{li}/\sqrt{\lambda_i\beta_i} - \sqrt{\lambda_i/\beta_i}$ values.

Step 1: Set with $n_1 = 1$ and $n_2 = k$.

Step 2: while $n_1 \leq n_2$

(a) Set $n_3 = (n_1 + n_2)/2$.

(b) Evaluate expression (3) for $i = n_3$.

(c) If it is satisfied, then $n_1 = n_3 + 1$.

(d) Else $n_2 = n_3 - 1$.

Step 3: $s = n_2 + 1$.

Step 4: For server i in the list after and including s, $p_i = 0$.

All other servers are assigned power according to Eq. 2.

Step 6: **Output** $\boldsymbol{p}^*$.

Algorithm 1 uses a binary search to determine the maximum i that satisfies expression (3), then all servers after this server in the list should not be allocated any power (i.e. running at the minimum power consumption level).

Here we give a simple example to illustrate the correctness of theorem 1. In this example, we do not need to run the power reallocation process as describe in algorithm 1.

Example 1. The example data set as follows. There are three servers in the data center. The minimum speed vector is $\boldsymbol{f_l}$ =(2,2.4,2.5), coefficient vector $\boldsymbol{\beta}$ = (0.008,0.005,0.006). The arrival rate to each server is λ_1=2.0, λ_2=2.5, λ_3=2.5, respectively. Power budget P is 150. According to Theorem 1, we calculate the optimal power allocation vector is <35.08,69.61,45.29>, and the corresponding minimum mean response time is 26.40. Figure 4 illustrates the location of the optimal solution in a three-dimensional diagram, which can clearly explain the optimality of our solution.

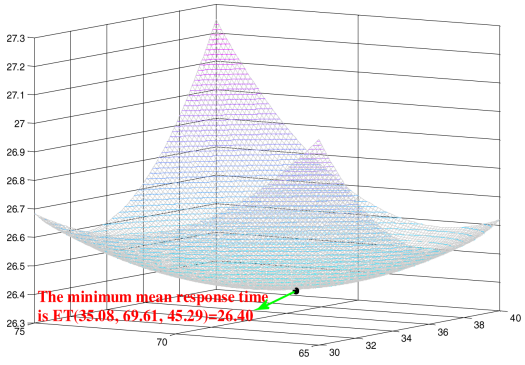

Fig. 4. The three-dimensional graph of mean response time

4.2 Multi-class Service Case

The queuing model for scheduling multiple class jobs in data center is shown in Figure 5. More precisely, we assume that there are J different classes of jobs in the system. For each class j, $1 \le j \le J$, it generates a stream of jobs follows the Poisson distribution with a rate ψ_j. Each incoming job is dispatched to one of the servers according to a probability matrix $\boldsymbol{Q}=[p_{ji}]_{1\le j\le J,\ 1\le i\le k}$. The arrival and service processes of different classes of jobs are mutually independent, so the arriving rate to server i is

$$\lambda_i = \sum_{j=1}^{J} \psi_j p_{ji} = \sum_{j=1}^{J} \psi_{ji} \tag{3}$$

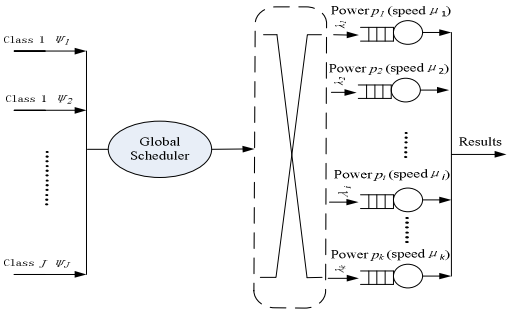

Fig. 5. Queuing model for multi service case

We assume that each class of service has a different size of service result. The average size of result for class-j service is denoted by S_j. The service time for the class-j service result at server i is exponentially distributed with mean service time $\mu_{ji}^{-1} = S_j/\mu_i$, where μ_i is the service rate of the server i. Therefore, the server queue can be viewed as a queuing system in which jobs are grouped into a single arrival stream and the service distribution is a mixture of J exponential distributions. The service queue is actually an M/HK/1 queuing system, where HK represents a Hyperexponential-K distribution. And the response time of the M/HK/1 queuing system can be deduced from M/G/1 queuing system [16]. Therefore the response time of service queue is given as

$$E(T_{multi}) = \sum_{i=1}^{k} \frac{\lambda_i}{\sum_{j=1}^{J} \psi_j} \left(\frac{\sum_{j=1}^{J} \psi_{ji} S_j^2}{\mu_i^2 - \mu_i \sum_{j=1}^{J} \psi_{ji} S_j} + \frac{\sum_{j=1}^{J} \psi_{ji} S_j}{\lambda_i \mu_i} \right) \tag{4}$$

The response time minimization problem can be stated as: to minimize the total service response time in data center by optimizing the server rates of the different servers, subject to the queuing stability constraint in each queuing system and the power constraint. Mathematically, the problem can be formulated as:

$$P2: \quad \begin{array}{ll} \textit{minimize} & E(T_{multi}) \\ \textit{subject to} & \lambda_i < f_{bi} + \beta_i p'_i,\ i=1,\ldots,k \\ & \sum_{i=1}^{k} p'_i \le P' \\ & 0 \le p'_i \le m'_i,\ i=1,\ldots,k \end{array}$$

The response time minimization problem is actually a convex optimization problem. In this paper, we extend the Augmented Lagrange Multiplier Method developed in [17] to solve this optimization problem. The method developed in [17] adds slack variables to the original formulation of the problem to convert the inequalities to equalities. It may increases the dimension of the problem, so it is not suitable to solve the large-scale optimization problem in data centers. To this end, we introduce the function $\varphi(x)=max\{g(x),-\eta/r\}$ to deal with inequality constraints. In each iteration, it only needs to compute the local minimum point of the corresponding Lagrangian penalty function approximately. Any accumulation point generated by the algorithm is the KKT point of problem *P2*.

Let $\boldsymbol{p}'=(p'_1,\ldots, p'_k)$, $\boldsymbol{\beta}=(\beta_1,\ldots, \beta_k)$, $\boldsymbol{\lambda}=(\lambda_1,\ldots, \lambda_k)$, $\boldsymbol{f}_b=(f_{b1},\ldots,f_{bk})$, $\boldsymbol{m}'=(m'_1,\ldots, m'_k)$, then we can rewrite the constraints as:

$g_1(\boldsymbol{p}') = \sum_{i=1}^{k} p'_i - P' \le 0$, $g_2(\boldsymbol{p}') = -\boldsymbol{\beta}\boldsymbol{p}'^{\mathrm{T}} + \boldsymbol{\lambda} - \boldsymbol{f}_b \le 0$, $g_3(\boldsymbol{p}') = -\boldsymbol{p}' \le 0$, $g_4(\boldsymbol{p}') = \boldsymbol{p}' - \boldsymbol{m}' \le 0$

then the augmented Lagrangian function of problem *P2* is

$$\phi(\boldsymbol{p}', \boldsymbol{\eta}, r) = E(T_{multi}) + \sum_{l=1}^{4} (\eta_l \varphi_l(\boldsymbol{p}') + \frac{r}{2}\varphi_l(\boldsymbol{p}')^2) \tag{5}$$

in which $\boldsymbol{\eta} = (\eta_1,\ldots, \eta_k)$ is the Lagrange multiplier vector, r is the penalty parameter, $\varphi_i(x)=max\{g_i(x),-\eta_i/r\}$, $i=1,\ldots,k$. Then, we have

$$\nabla\phi(\boldsymbol{p}', \boldsymbol{\eta}, r) = \nabla E(T_{multi}) + \sum_{l=1}^{4} \begin{cases} (\eta_l + r g_l(\boldsymbol{p}'))\nabla g_l(\boldsymbol{p}'), \eta_l + r g_l(\boldsymbol{p}') \ge 0 \\ 0, \quad otherwise. \end{cases}$$

Let $c(\boldsymbol{p}')=(g_1(\boldsymbol{p}'), g_2(\boldsymbol{p}'), g_3(\boldsymbol{p}'), g_4(\boldsymbol{p}'))^T$, $\boldsymbol{\eta}'(\boldsymbol{p}', \boldsymbol{\eta}, r) = \boldsymbol{\eta} + rc(\boldsymbol{p}')$, then the Extended Augmented Lagrange Multiplier Algorithm (E-ALMA) is given as follows.

Algorithm 2. E-ALMA Algorithm

Input: performance metric function F(σ,μ,N), N, λ, θ, initial point $[\sigma_0,\mu_0]^T$ and a positive tolerance Δ.
Output: approximate solution $[\sigma^*,\mu^*]^T$.
Step 0: Giving initial Lagrange multiplier vector $\boldsymbol{\eta}^{(0)} \ge \boldsymbol{0}$, control error $0<\varepsilon_1<1$, $0<\varepsilon_2<1$, initial penalty parameter $r^{(0)}>0$, $0<\gamma<1$, $a^{(0)}= \min\{1/r^{(0)}, \gamma\}$, $\omega^{(0)}= a^{(0)}$,$\sigma^{(0)}=(a^{(0)})^{0.1}$. Set *h* to 0.
Step 1: Solving the unconstrained problem $\min \phi(\boldsymbol{p}', \boldsymbol{\eta}^{(h)}, r^{(h)})$, and getting a solution $\boldsymbol{p}'^{(h)}$, satisfy $\left\|\nabla\phi(\boldsymbol{p}'^{(h)}, \boldsymbol{\eta}^{(h)}, r^{(h)})\right\| \le \omega^{(h)}$ If $\left\|c(\boldsymbol{p}'^{(h)})\right\|_\infty \le \sigma^{(h)}$, go to step 2. Else, go to step 3.
Step 2: If $\left\|\nabla\phi(\boldsymbol{p}'^{(h)}, \boldsymbol{\eta}^{(h)}, r^{(h)})\right\| \le \varepsilon_1$ and $\left\|c(\boldsymbol{p}'^{(h)})\right\|_\infty \le \varepsilon_2$, then stop, else compute $\boldsymbol{\eta}^{(h+1)} = \boldsymbol{\eta}'(\boldsymbol{p}', \boldsymbol{\eta}^{(h)}, r^{(h)})$; $r^{(h+1)}= r^{(h)}$; $a^{(h+1)} = \min\{1/r^{(h+1)}, \gamma\}$;$\omega^{(h+1)}=\omega^{(h)}$ $a^{(h)}$; $\sigma^{(h+1)} =\sigma^{(h)}(a^{(h+1)})^{0.9}$.
Step 3: Compute $\boldsymbol{\eta}^{(h+1)} =\boldsymbol{\eta}^{(h)}$; $r^{(h+1)}=10r^{(h)}$; $a^{(h+1)} = \min\{1/r^{(h+1)}, \gamma\}$; $\omega^{(h+1)}=\omega^{(h+1)}$; $\sigma^{(h+1)} = (a^{(h+1)})^{0.1}$;
Step 4: $h= h+1$, and then go back to Step 1.

This algorithm consists of three programs: Al_obj, Al_com and Al_main. Al_obj converts the optimization problem into an unconstrained minimization problem by adding a penalty function. Al_com is a discriminant function, its role is to determine whether the constraints are satisfied. Al_main is the main program.

5 Performance Evaluation

In this section, we use CloudSim[18] to simulate the heterogeneous data center environment to present our simulation results. We build a simulator which consists of a job generator, a job scheduler, and several number of servers. Each application receives requests exogenously according to a random arrival process of rate ψ_j (j=1,…,6, for the multi service case). Each server has N =6 levels adjustable frequency. The simulations were run over 100,000 jobs and with different random number sequences at each run. In order to obtain stable and accurate results with a confidence of 95%, each of our experiments was repeated 25 times and an average measure was taken. Note that we also have conducted simulations on 10 and 100 groups each with 80 or 800 computers and with different parameter settings. Similar trends on performance have been observed and hence they are not shown in this paper.

5.1 Simulations for Single-Class Service Case

Firstly, we perform simulations to evaluate the proposed algorithms in the single-class service case. We choose the system parameters as follows. $\boldsymbol{f_b}$ = {2.1,2.2,2.1,2,2.6}. $\boldsymbol{\beta}$ = {0.008,0.002,0.005,0.006,0.004}. The routing probability vector is <0.15,0.25,0.2, 0.15,0.25>. One larger instance server is deployed as scheduler server and five medium instance servers are deployed as service servers to process job requests.

We evaluate the performance of our algorithm by comparing with the other two heuristic allocation schemes. The first one is MEC scheme, in which the power is allocated proportionally according to the minimum value of energy consumption. The second one is RPV scheme, in which the power is allocated proportionally according to the job routing vector.

Fig. 6 plots the average response time as a function of the arrival rate with a power budget of P = 300W. We observe that when arrival rate increases, the average response time increase sharply for MEC and RPV while they increase smoothly for our algorithm. Obviously, for the average response time metric, our algorithm performs better than MEC and RPV.

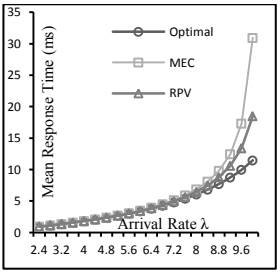

Fig. 6. The effect of λ on $E(T_{single})$

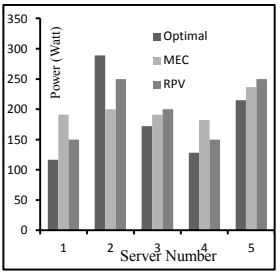

Fig. 7. The comparison of the allocated power to different servers

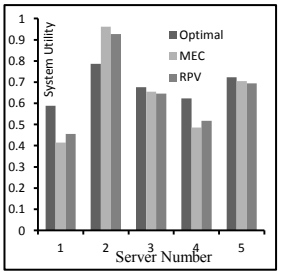

Fig. 8. The comparison of the system utilization of different servers

Note that the improvement in mean response time afforded by our algorithm over MEC and RPV is huge at the latter half of the Fig.6, ranging from a factor of 1-1.2 at low arrival rates ($\lambda \approx 5$) to as much as a factor of 2-3 at high arrival rates ($\lambda \approx 10$). The fact proofs that our algorithm optimize the average response time while allocating the power, which is not guaranteed by MEC or RPV.

Fig. 7 shows the detailed information of the allocated power to different servers when λ is set to 8 requests/s. As shown in Fig.7, our allocation scheme allocates a smaller portion of power to server 1, 4 and allocates excess power to server 2. MEC and RPV allocate less power to server 2. Due to the fact that the behavior of the average response time deteriorates so badly as $\rho \rightarrow 1$.thus the MEC and RPV pay an extreme penalty when they run the server 2 near its capacity, which leading to a much higher average response time.

Secondly, we evaluate the utilization of servers between our proposed optimal allocation scheme with the MEC and RPV allocation schemes. The values are averaged over a sufficient period of time when λ is set to 8 requests/s. It can be observed from fig.8 that our optimal allocation scheme has the best balanced utility value by optimizing power allocation among heavily-loaded and lightly- loaded servers.

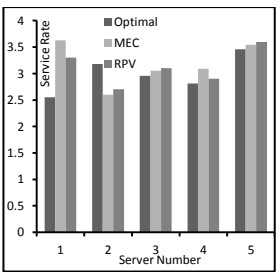

Fig. 9. The comparison of the server rates of different server

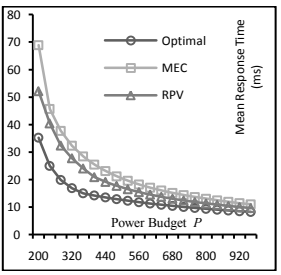

Fig. 10. The effect of P on $E(T_{single})$

Fig. 9 shows the comparison of the service rate of different servers. As the same with figure 8, our optimal allocation scheme has the best balanced service rate value by optimizing power allocation among heterogeneity servers. This balance can be reflected by the standard deviation of the server rate. The standard deviation of the three allocation schemes (Optimal, MEC and RPV) is 0.3105, 0.3590 and 0.3324 respectively. Thus, the optimal allocation scheme has the minimum standard deviation and the best balanced service rate value.

Figure 10 shows the influence of power budget P on the mean response time $E(T_{single})$. In figure 10, we observe that the expected response time $E(T_{single})$ decreases as a function of the power budget P. We find that the expected response time $E(T_{single})$ of our allocation scheme does not drop too much when $P > 600$, which means that providing a much higher power budget is not necessarily useful if the jobs' expected response time is high enough. This observation is very useful if we want to optimize the power consumption with the constraints of the response time for the data centers.

5.2 Simulations for Multi-class Service Case

We present the simulation results for the multi-class service case in this subsection. The detailed information of the system parameters is set as follows. The arrival rate vector of different service class is $\boldsymbol{\psi}$=(2,2.5,2.5,2.2,2), the configuration of different heterogeneity servers is $\boldsymbol{f}_b$={2.1,2.2,2.1,2,2.6}, $\boldsymbol{\beta}$ = {0.008,0.002,0.005,0.006,0.004}, $\boldsymbol{S}$=(0.2,0.4,0.5,0.5,0.4) and the routing matrix is

$$Q = \begin{pmatrix} p_{11}, p_{12}, p_{13}, p_{14}, p_{15} \\ p_{21}, p_{22}, p_{23}, p_{24}, p_{25} \\ p_{31}, p_{32}, p_{33}, p_{34}, p_{35} \\ p_{41}, p_{42}, p_{43}, p_{44}, p_{45} \\ p_{51}, p_{52}, p_{53}, p_{54}, p_{55} \end{pmatrix} = \begin{pmatrix} 0.3,0.2,0.1,0.2,0.2 \\ 0.2,0.1,0.2,0.2,0.3 \\ 0.1,0.3,0.2,0.2,0.2 \\ 0.2,0.2,0.3,0.1,0.2 \\ 0.2,0.2,0.2,0.3,0.1 \end{pmatrix}$$

According to the formula (3), the arrival rate vector to different servers is $\boldsymbol{\lambda}$ = (λ_1, λ_2, λ_3, λ_4, λ_5) = (2.25,2.28,2.28,2.26,2.33).

Firstly, we compare the mean response time between the three proposed allocation schemes. Fig. 11 shows the comparison of the mean service response time. From Fig. 11, we find that if we increase the total arrival rate $\boldsymbol{\lambda}$ (in the experiment, we increase the arrival rate of each service class simultaneously), and the mean response time will increase correspondingly. We also can see that the proposed optimal allocation scheme takes less response time than the other two allocation schemes under the same budget constraint.

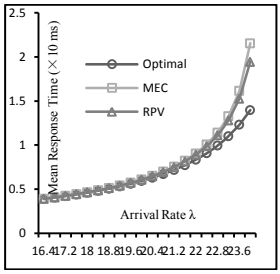

Fig. 11. The effect of λ on $E(T_{multi})$

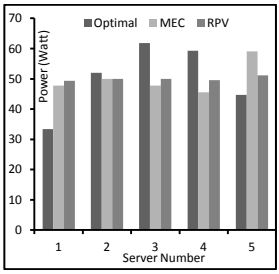

Fig. 12. The comparison of the allocated power to different servers

Fig. 12 shows the detailed information of the allocated power to different servers when the arrival rate vector is fixed. The server 1 and 5 is allocated too much power in the MEC and RPV allocation scheme, which results in the less power allocated to server 3, 4 and causes power unbalance. As stated earlier, due to the fact that the behavior of the average response time deteriorates so badly as $\rho \rightarrow 1$.thus the MEC and RPV run the server 3 and 4 near its capacity, which degrades the system performance.

We also evaluate the utilization and the server rates for different servers among the three allocation schemes. The simulation results are shown in figure 13 and 14. As the same in single class service case, we also use the standard deviation to reflect the load balance and the power balance. In figure 13, we obtain the standard deviation is 0.4203(Optimal), 0.4952(MEC) and 0.4868 (RPV) respectively. In figure 14, we obtain the standard deviation is 0.2901(Optimal), 0.3854(MEC) and 0.3259 (RPV) respectively. Thus, our optimal allocation distributes the power much even than the other two allocation schemes, no matter on the metric of server utilization or the server rate.

Figure 15 reflects the influence of power budget P on the mean response time $E(T_{multi})$. Fig.15 reveals that $E(T_{multi})$ decreases quickly as P increases at the beginning of the horizon. That means providing a higher power budget is useful to reduce the response time. But the downward trend is getting slower with the increase of power budget P. At the latter half of the figure, providing a higher power budget has a little help on the mean response time.

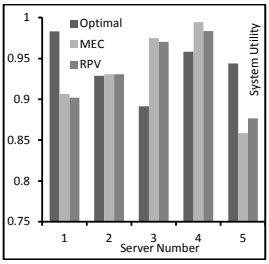

Fig. 13. The comparison of the system utilization of different servers

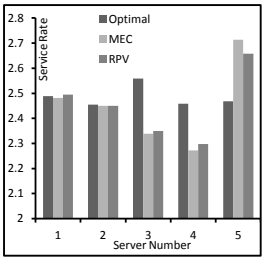

Fig. 14. The comparison of the system rates of different servers

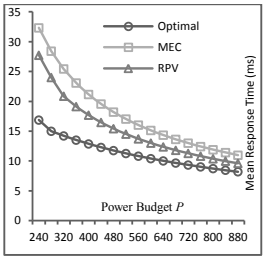

Fig. 15. The influence of power budget P on the mean response time $E(T_{multi})$

6 Conclusion

We studied the problem of optimal power allocation among multiple heterogeneous servers of a data center in this paper. The objective of this study is to minimize the mean response time using a fixed peak power budget. We first measure the power-to-frequency relationship within a single server and then model a single server as an M/M/1 queuing system. We use the queuing theory to capture the relationship between the power budget and the service response time. We study the power allocation problem in both single class service case and multiple-class service case, respectively. For the single class service case, we derive theorem 1 to determine the optimal power vector. For the multiple-class service case, we develop an algorithm to find the optimal solution numerically. Our approach provides an analytical way of studying the power-performance tradeoff at the data center level. To verify our theoretical predictions, we conduct extensive experiments to demonstrate that our proposed optimal allocation scheme can improve the performance significantly. In our future work, we plan to use real trace to conduct the simulation study. This will enable us to provide illustrative case studies highlighting the factors that affect the feasibility and effectiveness of our analysis results in various real-life conditions. Another direction worth of further investigation is to extend our work to more general queuing system such as G/G/1 model, which can be applied to more data centers and cloud computing environments.

Acknowledgement. This work is supported by National Key Basic Research Program of China under Grants No. 2010CB328104, National Natural Science Foundation of China under Grants No. 60903161, No. 60903162, No. 61003257, No. 61070161, China National Key Technology R&D Program under Grants No. 2010BAI88B03 and No. 2011BAK21B02, China National Science and Technology Major Project under grants 2010ZX01044-001-001, China Specialized Research Fund for the Doctoral Program of Higher Education under Grants No. 20110092130002, Jiangsu Provincial Natural Science Foundation of China under Grants No. BK2008030, Jiangsu Provincial Key Laboratory of Network and Information Security under Grants No. BM2003201, and Key Laboratory of Computer Network and Information Integration of Ministry of Education of China under Grants No. 93K-9, Shanghai Key Laboratory of Scalable Computing and Systems.

References

1. Barroso, L.A., Holzle, U.: The case for energy-proportional computing. Computer, 33–37 (2007)
2. Heath, T., Diniz, B., Carrera, E.V., Meira Jr., W., Bianchini, R.: Energy conservation in heterogeneous server clusters. In: Proceedings of the 10th Symposium on Principles and Practice of Parallel Programming, PPoPP (2005)
3. Xiong, K.: Power-aware resource provisioning in cluster computing. In: IEEE International Symposium on Parallel&Distributed Processing (IPDPS), pp. 1–11 (2010)

4. Gandhi, A., Balter, M.H., Das, R., Lefurgy, C.: Optimal power allocation in server farms. In: Proceedings of the Eleventh International Joint Conference on Measurement and Modeling of Computer Systems, pp. 157–168 (2009)
5. Li, K.: Optimal power allocation among multiple heterogeneous servers in a data center. Sustainable Computing: Informatics and Systems, 13–22 (2012)
6. Felter, W., Rajamani, K., Keller, T., Rusu, C.: A performance-conserving approach for reducing peak power consumption in server systems. In: Proceedings of the 19th Annual International Conference on Supercomputing, pp. 293–302 (2005)
7. Raghavendra, R., Ranganathan, P., Talwar, V.: No "Power" Struggles: Coordinated Multi-level Power Management for the Data Center. Architectural Support for Programming Languages and Operating Systems (2008)
8. Vivek, P., Jiang, W., Zhou, Y., Bianchini, R.: DMA-Aware Memory Energy Management. In: HPCA, pp. 133–144. IEEE Computer Society Press (2006)
9. Femal, M.E., Freeh, V.W.: Boosting Data Center Performance Through Non-Uniform Power Allocation. In: Proceedings of the Second International Conference on Automatic Computing, Washington, DC, pp. 250–261 (2005)
10. Chase, J.S., Anderson, D.C., Thakar, P.N., Vahdat, A.M.: Managing energy and server resources in hosting centers. In: Proceedings of the Eighteenth ACM Symposium on Operating Systems Principles (SOSP), pp. 103–116 (2001)
11. Gandhi, A., Gupta, V., Harchol-Balter, M., Kozuch, M.: Optimality analysis of energy-performance trade-off for server farm management. In: Proceedings of the 28th Performance (2010)
12. Elnozahy, E.M., Kistler, M., Rajamony, R.: Energy-efficient server clusters. In: Proceedings of the 2nd Workshop on Power-Aware Computing Systems, pp. 179–196 (2002)
13. Cho, S., Melhem, R.G.: On the interplay of parallelization, program performance, and energy consumption. IEEE Transactions on Parallel and Distributed Systems, 342–353 (2010)
14. Lee, Y.C., Zomaya, A.Y.: Energy conscious scheduling for distributed computing systems under different operating conditions. IEEE Transactions on Parallel and Distributed Systems, 1374–1381 (2011)
15. Bohrer, P., Elnozahy, E., Keller, T., Kistler, M.: The case for power management in web servers (2002)
16. Gross, D., Shortle, J.F., Thompson, J.M., Harris, C.M.: Fundamentals of Queuing Theory. John Wiley and Sons Inc. (2008)
17. Boyd, S., Vandenberghe, L.: Convex Optimization. Cambridge University (2004)
18. Calheiros, R.N., Ranjan, R., Beloglazov, A., De Rose, C.A.F., Buyya, R.: CloudSim: A Toolkit for Modeling and Simulation of Cloud Computing Environments and Evaluation of Resource Provisioning Algorithms. Software: Practice and Experience 41(1), 23–50 (2011)

A Discussion on Intelligent Management System for Centralized Plotting and Filing of Railway Design Institute

Xiangqing Wang[1,2], Dingfang Chen[1], and QiaoHong Zu[1]

[1] Wuhan University of Technology,
Wuhan 430063, Hubei, China
[2] China Railway Siyuan Survey and Design Group Co., Ltd.
Wuhan 430063, Hubei, China

Abstract. This paper enumerates and analyzes problems existing in the process of printing and filing engineering and architectural drawings/records used in railway design. An archiving and processing system is proposed that can plot and file drawings centrally and intelligently based on the requirements of integrating information systems in railway survey and railway design hereinafter. Technical difficulties of designing and implementing such a system are discussed. These include auto detection and extraction of PLT drafting zone size, plotter load balancing strategy based on entropy, consistency of paper documents and the respective electronic documents, and etc. The initial and preliminary evaluation of the proposed approach is promising and showed the feasibility in real-life settings.

Keywords: PLT file, centralized plotting, plotting area, load balancing, pre-filing.

1 Introduction

Drawings play a vital role in any engineering projects. Even though electronic copies are expected to become dominant and to replace paper copies in many areas, drawing print-outs are still widely used for archiving purposes and for settings that are not suitable for electronic drawings (e.g. harsh environment and/or places where access to electricity is restricted). Railway survey and engineering is an exemplar domain wherein printed drawings are necessary and desired to complement electronic copies.

In practice, printing drawings is performed at the last stage of a railway survey and design achievements. It is also an important part of integrated system of railway survey and design. As railway projects have become more complicated with involvement from multiple public sector and private sector organizations (most likely from different regions and even different countries), it becomes increasingly important to satisfy the requirements from all participating organizations. As part of our project, we have carried out case studies with real-users of railway design information systems (being stated-owned and private design institutes, survey organizations, and engineering companies). In the paper we concentrate mainly on the printing and filing design

Q. Zu, B. Hu, and A. Elçi (Eds.): ICPCA-SWS 2012, LNCS 7719, pp. 529–540, 2013.

drawings. We have identified the following problems and shortcomings of existing systems.

Firstly, waste of printing papers. Green legislation has been promoted and put into place by China's central government. Reducing the production of unnecessary paper copies is considered an important measure. Based on our observation, waste of papers is caused by either using papers that are of larger size than the actual drawings during printing or ineffective overall control that leads in too many waste plots or lacking bases when checking staff performance. Secondly, delivery status of drawings cannot be controlled effectively. For the coordinator of major survey and engineering projects, information about whether all the drawings of the relevant projects have been printed is not normally available and the printing is not guaranteed after authorizing to print them. Meanwhile for design companies and institutes, it is hard to know whether their delivered drawings have been printed. Thirdly, it's hard to maintain a uniform standard of drawings. Due to the conventions and the habits obtained through years of working experience, different designers, especially designers with different backgrounds, tend to exercise very different drawing and annotating styles, e.g. with different fonts, line styles, drawing frames and corner marks. Even though there are organization and/or community standards and agreements, they cannot be effectively reinforced due to a lack of transparency and a lack of means for quality control. The situation is aggravated because of the discrepancies of software printer drivers used by different organizations. Printer drivers can sometimes produce idiosyncratic style of drawings increasing inconsistencies. Fourthly, as drawings are delivered disruptively, even if the plotting is centralized, the actual quantity of prints of projects in different types and scales is hard to be monitored due to the lack of scientific methods and statistical basis. And it is hard to put a real sense of project management into effect as well. Finally, there is often an inconformity problem between filed paper documents and the corresponding electronic documents. After the design of a railway project is completed, engineering and technical companies/contractors have to spend a large amount of time reviewing and setting the list of pre-filing electronic files to complete the filing of electronic files, which, however, results in an inconformity problem between filed paper documents and the corresponding electronic documents and the loss of electronic files that should be filed.

Current IT support for design data management normally targets at generic domains. Though some plotter venders provide the management systems of plotting, they do not take into account the special requirements of railway projects, in particular are not compatible with the standards issued by the governing body, the Chinese Design Institute of Railway. Furthermore, existing systems suffer from limited management function, the intransparency of application programming interfaces, the restricted user access to the source code, and a lack of extensibility.

The inefficiency of existing systems has inspired us to develop a drawing printing and filing system that suits particular the needs of our customers. The remainder of the paper is organized as follows. We first look into the needs of end users and present the system architecture in Section 2. We then inspect and contemplate on technical difficulties of implement the system to satisfy end users' needs (Section 3). We conclude the paper in Section 4 and listed things that can be further improved.

2 Centralized Drawing Printing and Filing System

The proposed system is based on client-server model. Characteristics that we have elicited from the end users and that we will be implemented include centralized drawing management, intelligent paper selection, and xxx.

2.1 System Architecture

The framework of the proposed system is shown in Figure 1.

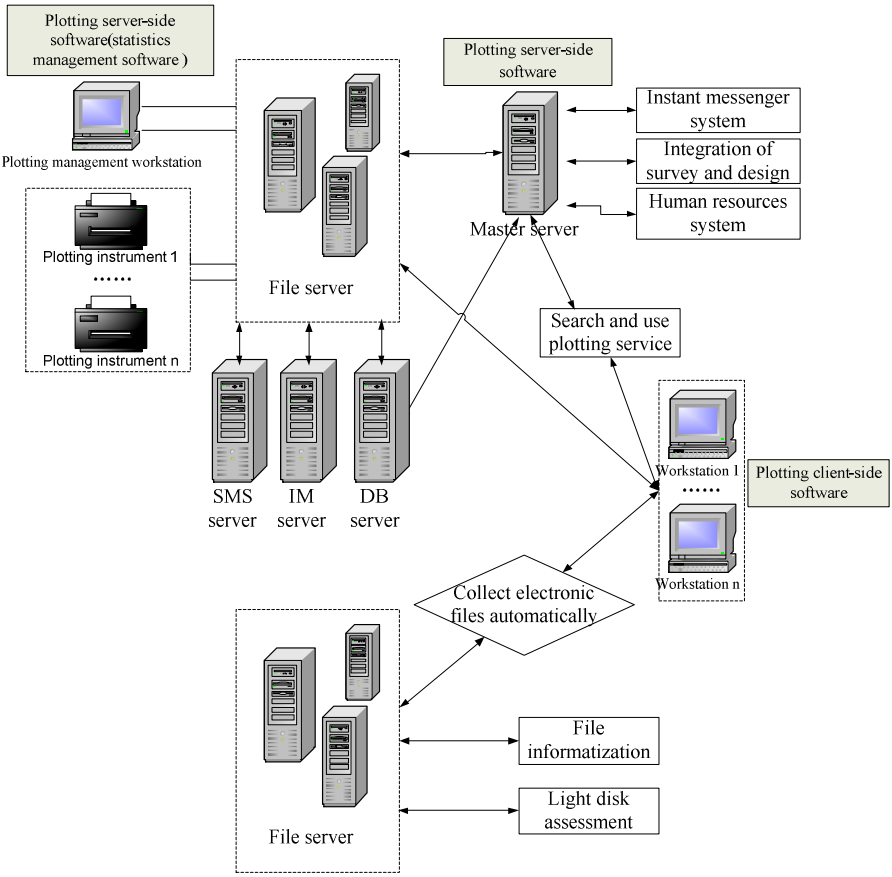

Fig. 1. The architecture of intelligent printing/filing management system

2.2 Implementation Scheme and the Function of the Study

The proposed system is based on client/server model, its programs on both client-side and server-side are implemented using Visual C#2008, its database is created using SQL Server 2008, and all plug-in units needed by AutoCAD environment are implemented using Visual C++.

To solve the problems above, this system needs to achieve the following functions automatically: calculate the precise sizes of drawings, select proper drafting instruments, select proper paper feeder according to the actual size of drawing area and the needed paper type, provide plotting statistics and pre-filing information, etc. These functions are allocated to the system as follows.

2.2.1 Server Side

Server-side functions include FTP file server and master server. FTP file server is used to save the uploaded plotting files such as PLT, PDF files. It also keeps the load balance to a certain level, to guarantee that the system can endure the peak pressure of centralized plotting. Master server is mainly used for calculations and decision-making of load balancing, generation and optimization of printing strategy, plotting management and statistics, and responding queries on the above information. In detail, server-side software can: a) Divides all the output devices, like plotters, into resource pools and group them, set different plotting strategy for every group based on their attributes, such as using papers of the most fitting size for plotting, or allowing small drawings to be plotted on big papers. b) Detects all the plotting instruments in the printing pool, and set the relevant attributes, such as the size of paper, black-and-white or color drawings, and type of papers (e.g. vegetable parchment or plain paper) etc. c) Users can adopt automatic dispatch mode or manual intervention dispatch mode, thus appoint a certain plotter group or a certain plotter and the corresponding paper feeder for plotting conveniently. d) Sets operations such as printing in prior, canceling printing, for the files waiting to be plotted according to dispatch orders. e) Gives relevant statistics and generate expenses statements automatically based on requirements. f) Automatically generates messages such as printing finished, out of paper, out of printing ink, and inform the relevant staff through SMS or instant messengers. g) Maintains load balance between plotter groups according to the outcome of the load balance decision matrix.

2.2.2 Client Side

The main functions of client-side software are as following: a) Basic information settings for operators, including ID, password, name, departments, room number, etc. which is convenient for auditing and process tracking. b) Automatically detects necessary factors of the files uploaded for printing, such factors include length and width of the actual plotting area for PLT file, or size and number of papers for PDF files, and so on. c) Chooses proper papers, like plain paper, vegetable parchment or developing paper, and set other parameters like black-and-white or color drawings, for printing. d) Sets drawings' properties, like projects they belong to (can be obtained from databases about projects-operators relationship). Such information automatically goes to pre-filing pool along with corresponding electronic documents, and helps to classify files to be printed before handle them. e) Uploads the files to be printed in batches and automatically solve filename conflicts. f) Has abundant search and statistical functions, including checking current queue of printing, querying whether a printing task has been finished, or count number of drawings that have been plotted according to any combination of conditions (which offers evidence for cost accounting). g) Add tags to PLT files according to requirements of delivery.

2.2.3 AutoCAD Plug-in

AutoCAD plug-in unit is integrated in the environment of AutoCAD; therefore it can be loaded and updated automatically when AutoCAD is activated. This module mainly has the following functions: a) Recognizes and reads key words in drawings, including the project's name, drawing number, designer, and examinant, etc. b) Generates and uploads barcodes, ensures the consistency of the drawings and the corresponding archived electronic documents. c) Uploads seal information (including the operator's name, department, room number, etc.), to help technicians to know where to get the drawings. d) Separates drawings. E.g., if a file contains more than one design drawings, they will be separated and named by their drawing number when plotting. e) Functions related to pre-filing, like to upload DWG electronic files going to be plotted to the pre-filing server, to help the archivists receive and file them directly after the project is finished.

2.2.4 Centralized Control

Control the standard of drafting and execute the function module compulsively. Because of the lack of effective controlling methods, it is hard to put the drafting standard into effect, which is a consistent problem hard to tackle. Adopt the method of centralized plotting as well as flexible and effective controlling tools, to solve the problem about unifying the standard of drafting. Of course, the standard established should reflect the necessary factors accurately during the design of different majors, and define the standard drafting as meta-graph, whose line type, font, the size of drawing borders, the size of drawing angle scale, location and so on are regarded as metadata. This function module can be placed in either the server side or the client side, which contains the following functions: a) Check the electronic files to be drafted according to the standard metadata, if not compatible, refuse to print and reflect the incompatible parts to users precisely. b) Control the levels of standardization in different major design dynamically. Taking the characteristics of some majors into account, it may be unnecessary to check regarding to some parts of standard metadata and need to expand the number of metadata. As for these problems, we should provide the personnel with the access to the corresponding interfaces.

The function module of drafting approval process controlling sets privileges of drafting approval according to the demand. Regarding to the drafting of high cost, it can only be printed by the personnel with the corresponding authority, e.g., the larger drawing should be signed by the director before printing, the color printing should be signed by the section chief before printing, the responsible person decides whether the normal drawings should be printed.

In addition, the plotters can be placed in two methods, one is to place them in the same sector or department, and the other one is to place them in different sectors or departments according the demand. The key is that all the plotters should be controlled by the same centralized plotting system.

2.3 Technical Difficulties

1. Detection and Extraction of Drawing Size

A critical question to answer so as to enhance the "green" aspect of the system (in terms of paper-consumption reduction) is how to detect the specification of printing

papers. Having knowledge of such specifications, the system can automatically selects printers and paper feeders that meet the specific requirements. This will also provide accurate calculations of the printing cost. The auto-selection is achieved in multiple steps.

As the first step, we have to solve the detection and extraction of the size of the visible drawing area. Hereinafter, we will use AutoCAD as an example. Generally speaking, in the AutoCAD environment, engineers and technicians first transform drawings into PLT files for the convenient of batch plotting. PLT is a print data file style with formats specific to print drivers.

Different print drivers therefore generate different PLT file formats, though the main frame of all PLT files are built using HPGL/2 languages. For the purpose of scoping drawing area, the system needs to precisely analyze PLT files in accordance with HPGL/2 instructions, to detect the drawing length and width.

```
INTPUT F
F=F*3.33
F=INT(F)
A=F
IF F>=0 THEN F=2*F ELSE F=2*ABS(F)+1
WHILE C>=BASE
OUTPUT CHR$(63+(C MOD 64))
C=C DIV 64
END
IF BASE=64 THEN N=191+N
IF BASE=32 THEN N=95+N

   OUTPUT CHR$(N)
```

Fig. 2. Algorithm for drawing size detection

A typical HPGL/2 file consists of a large number of ASCII characters and a few control codes. In text form, their presentations are as follows:

- IN; SC; PU; PU; SPI; LT; RO; BP; PS; (Drawing initial data)
- PAl2345; 4567; PD; PA-2345; 6789; PE<=eee; PE=www…(Drawing data)
- PU; PG; EC l; PM2FPPUPG; (Drawing terminate data)

By analyzing HPGL/2 instructions like PE, PS, and decoding characters following the PE instruction, we can detect the reference point coordinates of a PLT document, and thus calculate its drawing area size. The pseudo-code of this algorithm is shown in Figure 2.

2.4 Acquisition of Plotters' Working Status

In order to implement automatic management of plotters, managers must know each plotter's precise working condition in real time, so that corresponding processes can

be made in time. However, while having a plot-heavy workload and printing being required frequently, limited staff cannot constantly patrol all the plotters. Under this circumstance, how to capture working status of plotters placed at different places becomes a problem that need to be solved urgently. Generally, plotters' states are consist of preheating, printing, stopping printing, free, lack of paper, lack of printing ink, which are not hard to obtain. However, getting states, like printing process terminates suddenly, or out of paper during printing, could be a serious problem. To deal with this, there are different solutions for different types of plotters, but all solutions shares common key methods: mapping different paper feeders of each plotter into virtual printers with fixed port; and obtain the state of these virtual printers through functions like GetPrinterStat (string Printer Device). After status acquisition, system can sent the obtained states to managers by SMS.

2.5 Extraction of Drawing Tag Information

In order to alleviate staffs from the simple duplication works during delivering printed drawings and filing documents, drawings' tag information must be able to be automatically identified and extracted. In order to achieve this, firstly , all kinds of sample drawings used in actual designing must be analyzed, sorted and summarized to form a common designing standard frame, which include detailed definition of drawing frame, corner mark, angle signature and their coordinates(e.g., the meta-graph and metadata mentioned above), as well as handles of these properties. After that, system will automatically extract information such as project name, design phase, professional, designers, reviewer from the design electronic documents according to needs, thus generates delivery notices and filing information. Request to print drawings that did not follow the standard frame will be refused, to ensure the implementation of the unity designing standard.

2.6 Load Balance

It is completely transparent to users which plotters will be used to export the drawing files. It is impossible for system administrators to choose plotter for every file. Therefore, system has to select plotter for every mission automatically. To avoid too many missions to be clustered in one plotter, there must be a good load balancing strategy, to make sure every plotter can achieve its best efficiency. Load balance affects the system in two aspects. One is, when users upload documents going be printed, system needs to decide which file server will be used. The other one is, according to the completion situation of printing tasks on each file server, system should perform reasonable dispatch, and transfer tasks from overloaded server to more free file server in time, to ensure plotters load equilibrium. Therefore, the proposed system built a load balancing strategy according to an entropy based multi-attribute fuzzy decision-making method.

Generally speaking, the greater the variation of an attribute's value is, the smaller its information entropy is, and the more information that attribute can provide, which means the more important that attribute will be in decision making, the higher its weight should be, vice versa.

Let u be the attribute factor set, if there are enough factors in u, they can be grouped according certain rules (usually by similarity).

Assume that factors in u are grouped into I groups:

$$U = (\mathrm{u}_1, \mathrm{u}_2, \cdots, \mathrm{u}_I) \tag{1}$$

and satisfy:

$$U = \bigcup_{\mathrm{i}=1}^{I} \mathrm{u}_{\mathrm{i}}, \quad (\text{if and only if } \mathrm{i} \neq \mathrm{j}, \ \mathrm{u}_{\mathrm{i}} \cap u_j = \Phi) \tag{2}$$

For every u_{i}:

$$\mathrm{u}_{\mathrm{i}} = \{u_{\mathrm{i}1}, u_{\mathrm{i}2}, \cdots, u_{\mathrm{i}n(\mathrm{i})}\}, \tag{3}$$

Where $\mathrm{n(i)}$ is the number of factors of group i.

It is clear that factor set is divided in to layers, where U is the high layer factor set, and $u_{\mathrm{i}} (i = 1,2, \cdots, n)$ is the low layer factor set.

Let $V_I = \{V_{\mathrm{i}1}, V_{\mathrm{i}2}, \cdots, V_{\mathrm{in(i)}}\}$ to be the ranking level set, it affects every factor of every layer. Using multi-layer ranking model, system makes evaluation from bottom to top. That is, for $\forall \mathrm{i} \in \{1,2, \cdots, I\}$, it evaluates each ranking space $(u_{\mathrm{i}}, V_{\mathrm{i}}, R_{\mathrm{i}})$, where R_{i} is a single factor evaluation to matrix u_{i}:. Given the weights of factors in u_{i}: as:

$$A_{\mathrm{i}} = (\mathrm{a}_{\mathrm{i}1}, \mathrm{a}_{\mathrm{i}2}, \cdots, \mathrm{a}_{\mathrm{in(i)}}), \tag{4}$$

Then the evaluation can be expressed as:

$$B_{\mathrm{i}} = A_{\mathrm{i}} R_{\mathrm{i}}. \tag{5}$$

A 2-level fuzzy ranking model is shown in figure 2.

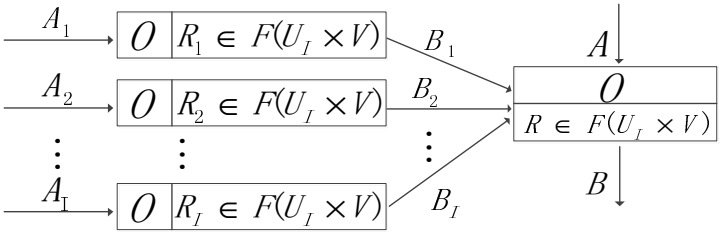

Fig. 3. 2-level fuzzy ranking model

But in reality there are often much more factors need to be consider, all of which could be fuzzy and in different layers, therefore multi-level fuzzy ranking model, as shown in Figure 3 and (5), is needed.

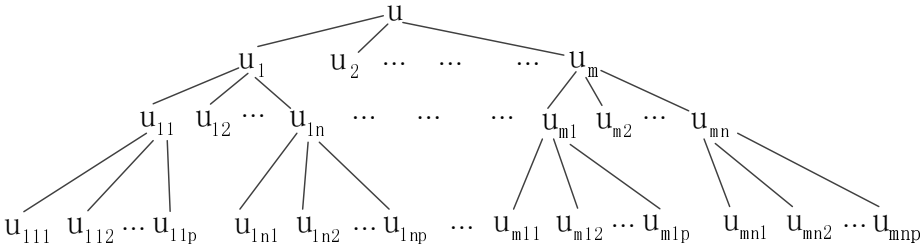

Fig. 4. Multi-layer factor model

$$B = AR = A\left[A_1\begin{bmatrix} A_{11}R_{11} \\ A_{12}R_{12} \\ \vdots \\ A_{1n}R_{1n} \end{bmatrix} \quad A_2\begin{bmatrix} A_{21}R_{21} \\ A_{22}R_{22} \\ \vdots \\ A_{2n}R_{2n} \end{bmatrix} \quad \cdots \quad A_m\begin{bmatrix} A_{m1}R_{m1} \\ A_{m2}R_{m2} \\ \vdots \\ A_{mn}R_{mn} \end{bmatrix}\right]^T \tag{6}$$

In order to eliminate the influence of different physical dimensions on the resultant decisions, we propose the following formulas. Equation 7 computes where is the *efficiency index*:

$$r_{ij} = \frac{a_{ij}}{p_j}, \; i \in M, j \in N \tag{7}$$

Equation 8 gives where is the *cost index*:

$$r_{ij} = \frac{p_j - a_{ij}}{p_j}, \; i \in M, j \in N \tag{8}$$

are used to transform fuzzy decision matrix $A = [a_{ij}]_{m\times n}$ into standardization matrix $R = [r_{ij}]_{m\times n}$,

where:

$$P_j = \max\{a_{ij}, i \in M\}, \; P_j = \max\{P_j - a_{ij}, i \in M\} \tag{9}$$

Let *CU* to be the server CPU utilization measurement:

$$CU\% = 100 - (CC * 100),$$

and *CC* be the free CPU utilization rate, we calculate *CC* as:

CC=SysPerInfo.liIdleTime/SysTimaInfo.liKeSystemTime,

Where T_{idle} is … and T_{sys} is…

Measurement of ram usage is *MU*, which can be obtained through correlation function. Free disk occupy ratio measurement DFE is the ratio of size of free disk and the entire disk, both of which can be obtained directly using API functions. The size of free disk is DF. Delay of disk is IO. Delay of network is ND (it is that how much time each back-end node spend on executing a query). Having the above parameters, we can get the load decision matrix A (assume there are 3 servers):

Table 1. Data of three exemplar servers

	CU	*MU*	*DFE*	*DF*	*IO*	*ND*
*sever*1	1	52	45	19100	9	12
*sever*2	4	46	4	15678	5	9
*sever*3	3	39	5	14689	4	6

Load balancing is achieved as follows:

1) According to (6) and (7), fuzzy decision matrix $A = [a_{ij}]_{m\times n}$ is transferred into standardization matrix $R = [r_{ij}]_{m\times n}$.

2) Calculate the information entropy outputted from attribute u_j :

$$E_j = \frac{1}{\ln m}\sum_{i=1}^{m} r_{ij} \ln r_{ij}, j \in N \text{ if } r_{ij} = 0, \text{define } r_{ij} \ln r_{ij} = 0. \quad (10)$$

3) Calculate attribute weight vector $w = (w_1, w_2, \cdots, w_n)$, where:

$$w_j = \frac{1 - E_j}{\sum_{k=1}^{n} 1 - E_k}, j \in N. \quad (11)$$

4) Calculate fuzzy utility values z_i at every node using:

$$z_i = \sum_{j=1}^{n} r_{ij} w_j, i \in M \quad (12)$$

5) According to $z_i (i \in M)$, nodes can sorted, and the node which has the biggest z_i value is the best node according to evaluation. Each time a task assignment happens, it should be assigned to the best node.

3 Conclusion

The achievement of this research has been successfully used in centralized design and filing management system of Railway Siyuan Survey and Design Group Co., LTD. It changed the traditional design drawing plotting from distributed plotting to centralized plotting, reduced the cost, and improved the management elaboration level of designing outcomes. It thoroughly solved the inconsistent of paper documents and the corresponding electronic documents, and unified design drawings standard. At the same time, since all print information is centralized managed and published, in the designing process, the number of drafts plotted reduced significantly. Also, it provides scientific basis for staff working performance assessment.

Further research can be conducted about the assessment of work load of drafting operating managers, the statistics of drafting workload of different types and scales, and so on.

References

1. China Railway Siyuan Survey & Design Group Co.,Ltd. Railway Design Institute survey and design integration management system. In: Gang, L., Rui, Z., et al. (eds.) 17th The National Enterprise Management Monetization Innovation Achievement, pp. 633–644. Enterprise Management Press, Beijing (2011)
2. Zhou, X.: HPGL description language in the application of spot-gluing machine. CNC Machine Tool Market (12), 106–108 (2006)
3. Tang, Y.: Hewlett-Packard Company. The Application of HPGL Description Language in dispensing machine. Tsinghua University Press, Beijing (1995)
4. Gao, X., Zhang, W., Li, H.: Load Balancing Technologies and Applications. Computer Engineering and Science 25(3), 11–13 (2003)
5. He, J., Xiong, W., Chen, L., Yin, J.: Study and Implementation of Dynamic Load Balancing Based on Database Cluster. Microcomputer and ITS Applications 30(2), 68–71 (2011)
6. Yang, D.: The design and implementation of an object-oriented Chinese PDF reader. Computer Applications 19(6), 1–4 (1999)
7. Zhang, H.: The Theory of Software Engineering. Tsinghua University Press, Beijing (2008)
8. Wang, X., Wei, R.: A Discussion on Railway Survey and Design Integration Substructure Specialty Interface System. Computer and Communications (04), 84–86 (2005)
9. Wang, X.: Cooperative Design in Railway Survey and Design Institute. Computer and Communications (01), 77–79 (2008)
10. Ma, H., Li, J.: Enterprise Application Integration System Based on SOA. Computing Technology and Automation 24(4), 87–89 (2005)
11. Zeng, G., Sun, H.: Research on a component based software development method. Journal of Computer Research and Development 35(11), 991–995 (1998)
12. Dai, J.: The research and development of integration system in railway survey and design. Zhongnan University, Changsha (2007)

13. Xu, R.: The research of the development of CAD application system. Heilongjiang Science and Technology Information (10), 69–69 (2010)
14. Chen, K.: The requirements of standardization adapt to the railway crossing development situation. Railway Technical Supervision (6), 1–2 (2004)
15. Lei, H.: The research of standard specifications in enterprises informatization. Equipment Manufacturing Technology (1), 95–97 (2008)
16. Ding, Y.: The research of enterprise design management present situation in China. Scientific and Technical Information (24), 170–171 (2009)
17. Li, X.: The research of reconfigurable information system model oriented business component. Nanjing University of Aeronautics and Astronautics, Nanjing (2002)

Optimizing Interactive Performance for Desktop-Virtualization Environment

Xiaolin Wang[1,3], Binbin Zhang[2], and Yingwei Luo[1,3]

[1] Dept. of Computer Science and Technology, Peking University, Beijing, China, 100871
[2] Dept. of Computer Science and Engineering, Yunnan University, Yunnan, China, 650091
[3] The Shenzhen Key Lab for Cloud Computing Technology and Applications, Peking University Shenzhen Graduate School, Guangdong, China, 518055

Abstract. Full virtualization is vastly applied in desktop virtualization. Although hardware-assisted virtualization greatly improves the performance, the interactive performance is still a bottleneck for full virtualization. Interactive performance is mainly influenced by I/O devices. In one hand, I/O devices are slow device. In another hand, they are often shared by multiple virtual machines through simulation. Our study focuses on the interactive performance optimization, and can mainly be classified into three categories: (1) Targeting multi-core system, we investigate virtual machine deployment to ensure stable performance of the whole system and individual virtual machine. (2) Dynamically adjust the resource among virtual machines based on the individual machine's interactive behavior. (3) Optimize the I/O request scheduler in term of the virtualization implementation.

Keywords: Multi-core, Desktop-virtualization, Interactive Performance, Collaborative Scheduler.

1 Introduction

The performance of computer hardware is continuously improving. Because virtualization technology can enhance the utilization of physical resources, it is widely used. The advantages of virtualization technology, such as isolation, scalability, easy-to-migrate, snapshot and cloning, accelerate the virtualization technology to be used in both enterprise and personal applications.

Network classroom is an application based on virtualization technology (Figure 1). In this scenario, multiple virtual machines run on the server. Each virtual machine is remote connected by a thin client to provide students with an individual environment. This application has three characteristics: 1. Virtual machines are similar to each other because the students using the network classroom often use a similar environment; 2. Many similar virtual machines should be deployed on a server with limited capability; 3. These virtual machines provide desktop applications, so good user experience must be promised; 4. User access the virtual machine through a remote connection, so network I/O performance is a key factor affecting the user experience. There are quite a few researches on improving interactive performance. But most of the current

Q. Zu, B. Hu, and A. Elçi (Eds.): ICPCA-SWS 2012, LNCS 7719, pp. 541–555, 2013.

researches focus on physical environment. They study how to distinguish the interactive process and make them high priority. The virtual environment is different from physical environment. The applications in virtual machine are not visible from VMM perspective. So only the overall performance of virtual machine can be improved to improve the interactive performance of the applications.

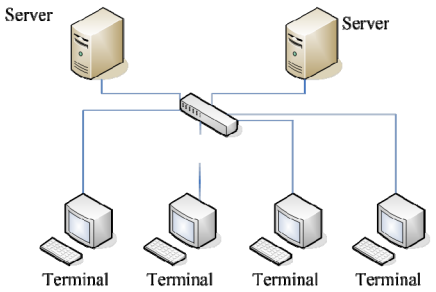

Fig. 1. Network Classroom

Our work is based on Xen HVM virtual machine. We propose three optimized methods aimed at multi-core and virtualization environment to improve interactive performance of virtual machine: 1. Static bind virtual CPU (VCPU) to the core to balance loads among multi cores; 2. Adjust the disk I/O queue to optimize disk I/O performance; 3. Collaborate VCPU and QEMU scheduling to reduce the waiting latency to ensure the timely response. The paper is structured as follows: Section 2 describes the research background, analyzes interactive performance in desktop virtualization and multi-core environment, Section 3 propose resource allocation scheme, including static VCPU-core binding, collaborative scheduling, and receive queue adjusting. Section 4 gives the results of experimental evaluation. Section 5 presents related work, and finally is the conclusion.

2 Background

2.1 Xen HVM

Xen currently supports two modes of virtualization, para-virtualization and hardware-assisted virtualization (HVM). The operating system must be modified if it used on Xen's para-virtualized virtual machines. But the HVM supports unmodified operating systems run directly. So Windows can be used. In the virtual classroom scenarios, Windows applications are very common, so our work based on the Xen HVM mode.

Hardware-assisted virtualization technology (e.g. Intel VT-x, AMD SVM) extends the instruction set to support Guest OS instructions directly running on the hardware. The technology divides the CPU's operating environment into two levels, non-root and root. Virtual machines run in non-root environment, while VMM run in the root environment. When sensitive instructions in the Guest OS occur, VMExit happens and the VMM continues to run. The VMM tries to complete a cause analysis and the corresponding emulation. And then return to the virtual machine by VMEntry and the

Guest OS continues to run. The context switches are completed by the hardware when VMExit and VMEntry happen. The emulation is completed by the Qemu-dm[3] in Dom0 in Xen. The process simulates most devices used in virtual machines. Figure 2 illustrates the details of the I/O processing in virtual machine: (1) A VMExit occurs when I/O request submitted by virtual machine. Then the VMExit handler (*vmx_vmexit_handler* for Intel VT-x) will be called. (2) VMM writes the I/O information into a page shared by virtual machine and QEMU. Then Dom0 is informed through an event channel. VMM will block the virtual machine raised the I/O request and then schedule. (3) Dom0 resume to work by the scheduling. (4) *hypervisor_callback* is called and in which *evtchn_do_upcall* will be called. (5) All the I/O requests are collected by *cpu_get_ioreq* in *evtchn_do_upcall*. (6) QEMU is scheduled to work. *select* will be called to wait for I/O request. (7) Read the shared page. QEMU will identify which device will be accessed. Call the callback functions registered when device initiates. For disk I/O, the callback functions are *ide_ioport_read* and *ide_ioport_write*. (8) The callback function writes the virtual device states into the shared page, or does a real data copy. In general emulated DMA is used for data read/write (*ide_sector_read/write_dma*). QEMU informs the VMM that the I/O processing is completed through the event channel. (9) After VMM is informed, the blocked virtual machine is unblocked. Meanwhile the virtual machine is informed for the follow processing by setting a virtual interrupt.

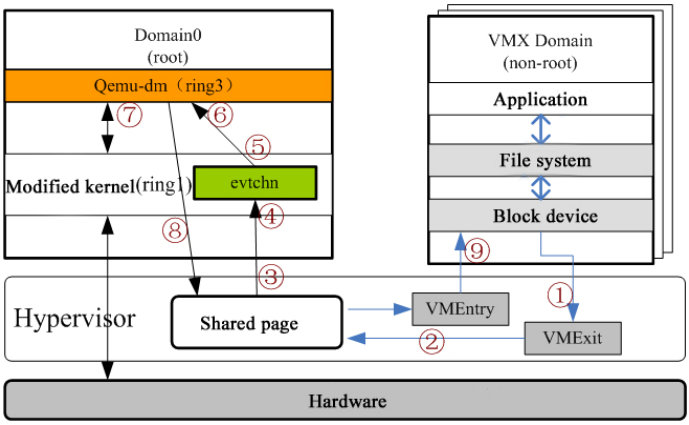

Fig. 2. I/O processing in Xen HVM

2.2 Virtualization in Multi-core Environment

Dom0 manages hardware resources to simulate other virtual machines' I/O requests. So it requires more CPU resources. I/O data must be exchanged between DomU and Dom0, which brings more context switches overhead, including cache miss overhead.

With the development of the CPU, multi-core technology dramatically increases the computing power of a single computer. However, in the actual implementation, there are different structures in multi-core. Figure 3 shows two typical implementations. (1) Each core has its own independent on-chip L1 Cache. But they share L2 Cache; (2) Each core has a separate on-chip Cache, only shared front-side bus.

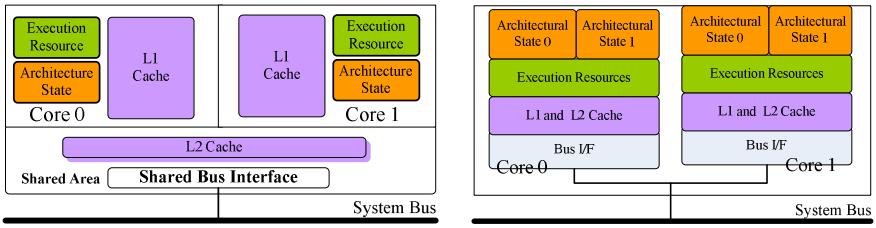

Fig. 3. Two different structures in multi-core

Xen manages multi-core in a manner similar to SMP (Symmetrical Multi-Processing). A virtual machine has one or more VCPU. A VCPU can be located on different physical CPU (PCPU). A PCPU maintains a VCPU queue. The VMM is responsible for VCPU scheduling. In Xen, the scheduler is aimed at full use of processor resources. When a PCPU is idle, a VCPU can be transferred from other PCPUs to use the idle PCPU. However, VCPU switches bring large overhead. The reason lies in two aspects. Firstly VCPU has much status information to be maintained. Secondly when a VCPU switches to another PCPU, it will lead to DTLB miss, ITLB miss and Cache miss. If the switch happens during the handling of the virtual machine I/O requests, the I/O performance must be affected.

3 Performance Issues When Virtual Machines Deployed in Multi-core Environments

Combination of the specific characteristics of virtualization and multi-core architecture to achieve the different virtual machine deployment, performance differences can be quantitatively analyzed and compared.

Experimental environment: Core i7 CPU, containing 4 cores, which can be extended to 8 processing threads through Hyper-Threading technology. Each core has separate 32KB instruction cache, 32KB data cache, and 256KB L2 cache. Meanwhile, the four cores share 8MB L3 cache. Xen-3.3.1 is deployed, using HVM mode.

The privileged Dom0 uses one VCPU, and start a DomU using one VCPU. We deploy VCPUs in the three modes illustrated in Table 1. Run netperf [10] on DomU for network bandwidth testing. Experiments show that the network throughput is almost the same in the three different deployments, but there is a big difference in CPU utilization (Figure 4).

In the I/O-intensive test, Dom0 and DomU are running alternately. When they share a thread, fewer context switches occur, and cache miss overhead is low. So in Figure 4, CPU utilization is the lowest in mode I. When Dom0 and DomU are running on different cores (mode III), the I/O data needs to transfer from one core to the other, bringing more cache miss. So Dom0 will use more CPU resources. In mode II, Dom0 and DomU are running on different processing threads, but sharing a same core, that is, sharing L1 and L2 Cache. As the inconsistent scheduling, there are two levels of VCPU scheduling involved in the processing of virtual machine I/O requests, one scheduler in Dom0, and the other in QEMU. It will lead to cache Ping-Pang phenomenon occurs, which eventually makes the two domain very high CPU utilization.

Table 1. Different VCPU deployments

	VCPU Deployment in Dom0 and DomU	Experiment results
Mode I	Share a thread in a same core	CPU utilization = 87%, which means the CPU is not the bound in network applications
Mode II	Share a same core, but different threads	The CPU utilization is arise compared to Mode I
Mode III	On Different cores	The highest CPU utilizations

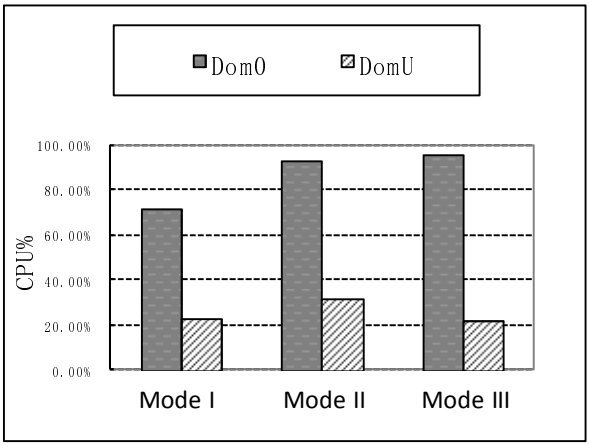

Fig. 4. Netperf test – CPU utilization in different VCPU deployments

In order to further analysis the overhead brought by the context switches between different cores, we carry out these experiments: Dom0 and DomU each uses one VCPU. The first deployment is to keep Dom0 running on Core 0 while DomU running on Core 1 (Mode I). The second deployment is to bind Dom0 to Core 0, but DomU run on Core 0 and Core 1 alternatively. The switch happens every second. Run netperf test in DomU and count the L2 cache miss in Core 0 and Core 1. The results are illustrated in Table 2. The cache miss is measured in mpkc (miss per 1000 cycles).

The results show that the virtual machines are not equal. The Dom0 will use more CPU resources. And in multi-core environment, different VCPU deployments will lead to different I/O performance.

Table 2. Cache misses

Deployment	L2 Cache Miss (mpkc)
Mode I: VCPU-core binding	6.8
Mode II: Alternatively using PCPUs	10.91

Xen hypervisor is based on the Linux operating system, which is mainly used in server scenarios. Credit algorithm is used to schedule VCPU in Xen. This algorithm focuses on equity. But it is not very friendly for interactive applications. We carry out experiments according to the deployments in Table 3. Four virtual machines (DomU1, DomU2, DomU3, DomU4) run simultaneously. Only one VCPU is assigned to each virtual machine, and each VCPU is bound on a PCPU. Four virtual machines run different types of loads, including CPU-intensive tests (PI calculation) and I/O-intensive tests (netperf bandwidth test). CPU utilization is measured. And the results are shown in Figure 5.

Table 3. Different Benchmarks Deployments

	Mode I	Mode II	Mode III	Mode IV
Applications	DomU1: netperf Others: idle	DomU1: netperf DomU2: PI Others: idle	DomU1: netperf DomU2: PI DomU3: PI DomU4: idle	DomU1: netperf DomU2: PI DomU3: PI DomU4: PI

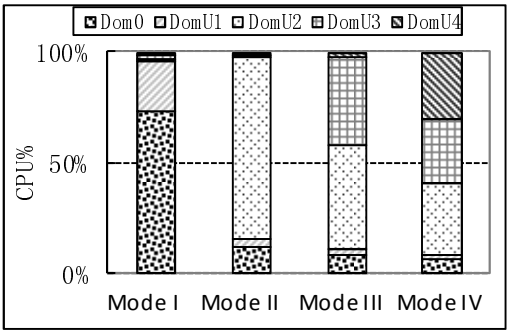

Fig. 5. CPU utilization in different benchmark deployments

In Figure 5, we can see that with the virtual machine CPU-intensive workloads increase, I/O-intensive virtual machine's CPU utilization is reduced, and ultimately close to "suspended animation." This means that the CPU-intensive virtual machines seize too much CPU resources, making the I/O-intensive virtual machines not work properly. The main reason is that the VCPU scheduler and I/O devices emulation process scheduler are inconsistencies. When both CPU-intensive and I/O-intensive virtual machines exist, the I/O-intensive virtual machine will be blocked waiting for the virtual I/O request emulated. Meanwhile CPU-intensive virtual machine keeps running by the Credit scheduler. And it will over-occupy more CPU resources, affecting the normal operation of Dom0, keeping Dom0 from handling I/O requests in time, and resulting in I/O-intensive virtual machine "starve to death." This effect is more prominent in virtual classroom environment for all the virtual machines are accessed from remote desktop connections. By Xentrace statistics we find that remote desktop connections produce large amounts of network external interrupts. These interrupts bring amounts of VMexit, accounted for 15.13% of total. The VMexit

processing time is as high as 93.02% of total processing time. This shows that the I/O performance make a great impact on virtual desktop performance.

These experiments illustrate that different VCPU deployment will result in different virtual machine performance. And also the scheduler affects the interactive performance of virtual machine. Therefore, we propose static VCPU-core binding and dynamic allocating resources to achieve load balance. And we try to improve the scheduler in Xen to optimize interactive performance.

4 Interactive Performance Optimization

We propose the following three improvements to optimize the interactive performance for Xen virtual machines: 1. Static VCPU-core binding: bind VCPU to the core in order to avoid VCPU migration across cores and reduce the cost of cache miss. Further, bind each virtual machine's network receive queue to the corresponding core. When a network packet is received, it will be distributed directly to the receive queue of the virtual machine. And we complete parallel processing soft interrupts; 2. Dynamic cooperative scheduling: according to the load of the virtual machine, dynamically adjust the VCPU and QEMU process scheduling priority thereby reduce the latency caused by waiting for CPU resources to response I/O requests in time; 3. Adjust disk I/O scheduler queue to reduce disk seek time overhead.

4.1 Static VCPU-Core Binding

By default, VCPUs are scheduled by Credit algorithm. The credit of current running VCPU is reduced by 100 every 10ms, while the credit of the VCPUs in waiting queue is increased every 30ms. If there is an idle PCPU, migrate waiting VCPU to the idle PCPU to run. However, Dom0 takes up more resources than DomUs. And I/O data should be transferred between different virtual machines. Frequent VCPUs switches will lead to cache Ping-Pang, resulting in a waste of CPU resources and a decrease in the virtual machine performance. Based on these considerations, we propose VCPU-core binding.

In Xen, the number of VCPU virtual machine using can be set by a HyperCall. And also the VCPU's affinity with PCPU can be set. In usual applications, allocating sufficient VCPU resources to Dom0 can ensure other virtual machines' I/O performance. Device emulation (QEMU)'s affinity with PCPU can also be set by system calls. As the analysis in the previous section, different VCPU-core bindings will bring different performance. Considering multi-core's characteristics, we design more efficient ways to bind VCPU to core. Let Dom0 use the same number of VCPUs as the actual number of cores, which can take advantage of the processor and other device resources and thereby more virtual machines can be run simultaneously. Let the same number of VCPUs run on each core, which can balance the load among processors. Let VCPU and the corresponding QEMU run on the same core, which can improve the cache hit rate and reduce the data transferring between the cores. Static VCPU-core binding can be deployed either before the virtual machine run or while it is running. In Dom0 user mode, you can use the HyperCall and system call to implement the binding.

We can further optimize the network I/O. In the multi-core system, each core maintains a network data queue. When the NIC receives a network packet, it will insert the packet into a queue at random. When multiple virtual machines run simultaneously, packets dispatched to multi-queue maintained by multi-core will easily lead to cache Ping-Pang. To avoid this overhead, the packet can be dispatched in order to enhance cache hit rate.

The method is to associate the packets with the receive queue maintained by the core which used by the virtual machine. We implement it by modifying the network receive interrupt processing. Firstly, we get the running status of each virtual machine, including the core binding to its VCPU and its MAC address. Secondly, we build a table recording the mappings from MAC address to the core. Then the packets can be dispatched to the certain queue according to the destination MAC address and the mappings. The modification mainly located in the function *netif_receive_skb* and *netif_rx*. Due to the virtual machine receives the network packet by the QEMU process, so we make the QEMU process and the corresponding virtual machine run on the same core (Figure 6).

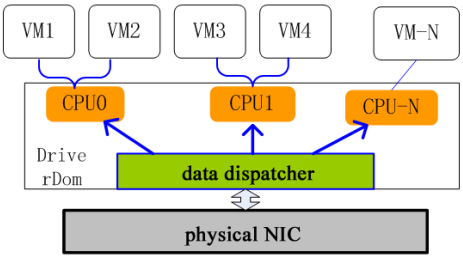

Fig. 6. Dispatch the received packets to the queue binding to the core

Further we parallelize the processing of the soft interrupt to make the receive queue work simultaneously. The parallelized soft interrupt handling can be implemented by IPI (Inter-Process Interrupt).

4.2 Dynamic Collaborative Scheduler

Three schedulers are involved during virtual machine I/O requests processing: (1) When VMexit occurs because of I/O requests, VCPU scheduler is needed. It will block the virtual machine which request I/O and schedule Dom0 to run; (2) Dom0 analysis of I/O requests. And the request will be emulated by QEMU. So only when the QEMU is scheduled, the request can be processed; (3) After QEMU completes I/O request and returns results, Xen will set virtual interrupt to notify the virtual machine for further processing. Only when the virtual machine can be scheduled to run, the interrupt can be responded and the I/O processing can be completed.

As long as any scheduling is not in time, it will affect the I/O response time. The latest Credit scheduler in Xen has been optimized and a BOOST state added to prioritize I/O-intensive applications. But the premise is that the VCPU has been triggered

by I/O events. If the QEMU is delayed or blocked, it will affect the VCPU scheduler and easily lead to reversal of priority, that is high priority task must wait for low priority tasks completed, so the sub-priority task to seize it.

In order to solve the inconsistency of scheduler's problem, we add a collaborative scheduling controller in the QEMU. There are two advantages to add collaborative controller in the QEMU: (1) It is easy to implement and control. And the configuration can be dynamically adjusted according to user requests. (2) In the QEMU, I/O requests information can be intercepted. The information can be used to predict the virtual machine's behavior. (3) In the QEMU, actual resource usage and also the overall load of the virtual machine can be collected. It can be used to adjust virtual machine resource allocation. Collaborative controller is mainly composed of three parts: I/O requests monitoring and analysis module, collaborative scheduling module, the feedback control module.

(1) I/O requests Monitoring and Analysis Module. It monitors virtual machine disk I/O requests and network I/O requests. The virtual machine usually uses QCOW file as its disk. The two functions *qcow_aio_read* and *qcow_aio_write* are modified for monitoring disk read and write. The functions *tap_send* and *tap_receive* are modified for monitoring network traffic. The network packets for remote interaction are extracted for monitoring interactive requests. RDP and VNC are commonly used in remote connection. Both of them are based on TCP connection. So we need to distinguish between the request packets and the ACK packets during the monitoring.

(2) Collaborative Scheduling Module. It dynamically adjusts the priority of the VCPU and corresponding QEMU process according to the virtual machine I/O requests. By setting the timer (qemu_new_timer) for intermittent adjustments, the resources can be reallocated in time according to the actual resource usage. PCPU utilization by VCPU can be adjusted using HyperCall *xc_sched_credit_domain_set*. The priority of the QEMU process can be adjusted by a system call *setpriority* which can change the CPU time slice used by QEMU. In the cooperative scheduling module, not only CPU processing time allocation can be adjusted, but also the disk I/O queue can be optimized (see Section 4.3). Table 4 is a rules table instance for reallocating the resources based on network data transmission rate in remote connections.

The network transmission rate of remote connection can reflect how the user is busy. The transmission rate is counted every second. Different transmission rates correspond to different priorities. The transmission rate increasing indicates user requests frequency and also the requirement for response latency increasing. At this time enhancing the CPU utilization and the priority of the QEMU process can timely meet users' requirement. When the transmission rate drops, considering the latency of I/O request processing, we cannot immediately adjust the priority, but to make an additional attenuation factor to ensure the I/O requests can be effectively completed. In Table 4, "VCPU Capability" can keep these compute-intensive virtual machines from excessively occupying CPU resources and affecting other virtual machines' normal interaction.

Table 4. A rules table for reallocating the resources based on network data transmission rate

Network data transmission rate	QEMU Priority	VCPU Capability	VCPU Weight	Attenuation factor
0	10	20	32	10
20	0	50	256	10
50	-5	75	1024	10
100	-7	100	2048	10
200	-8	0	3072	10
400	-10	0	4096	10
1000	-15	0	8192	10
2000	-15	0	16384	10

(3) The Feedback Control Module. It keeps monitoring the load of the whole physical machine and the actual resources used by each virtual machine. In Dom0 through the proc file system, we can get the overall memory usage (including cache, buffer, and swap memory usage), CPU utilization, interrupt handling frequency, the frequency of context switches, and network/disk loads. Through the interface provided by Xen we can get the actual CPU utilization and network/disk throughputs in each virtual machine. This information can direct the resource reallocation among virtual machines and collaborating VCPU scheduler with QEMU.

4.3 Adjust the Disk I/O Schedule Queue

Disk I/O scheduler in Dom0 uses the CFQ (complete fair queue) algorithm by default. With CFQ, the disk I/O requests of each process are organized as a red-black tree. Meanwhile, in order to ensure I/O requests completed in time, these requests are maintained in a FIFO queue. When selecting a pending I/O request, the FIFO queue is first checked to see if there is an expired request. If there is no expired request, a closer request is selected from the red-black tree and submitted. This algorithm ensures fairness between processes, and also effective in reducing the overhead of disk seeks.

However, in a virtualization environment, each virtual machine has its own disk file. With the increase in the number of virtual machines, on the one hand, simulation overhead increase the disk request processing cycles; on the other hand, the different virtual machine disk files occupy different contiguous disk sectors. When several virtual machines simultaneously submit I/O requests, disk accesses become very frequent and discrete. Considering these two practical factors, the existing CFQ algorithm should be modified to adapt to the characteristics of virtualization. Depending on disk request statistics in collaborative scheduling module, the time slice used by QEMU to process I/O requests can be adjusted in time. By increasing the processing time slice used by QEMU process, not only the I/O requests can be completed on time to improve interactive response, but also the overhead of disk seeks can be reduced to improve the overall performance of the disk. Four parameters should be adjusted. They are *fifo_sync_expire, fifo_async_expire*, *slice_async*, *slice_sync*. Using the proc file system, these parameters can be changed from a user mode.

5 Evaluations

Experiment environment: Intel Core i7 processors (4 cores, 8 threads, shared 8MB L3 cache), 8GB memory. The operating system is CentOS 5.0 (Linux 2.6.18-x86_64). Xen3.3.1 is used. Each virtual machine is configured with one VCPU, 320MB memory, running CentOS 5.0 operating system (Linux 2.6.18-x86_32).

Experiment I. Evaluate static VCPU-core binding. Considering in virtual classroom application browser is used frequently, we use Sunspider as a benchmark. It tests firefox browser with JavaScript operations, including String, regular expressions, math, 3D and so on. In this experiment four guest virtual machines run simultaneously for testing, named as DomU1, DomU2, DomU3, DomU4. Four VCPUs is assigned to Dom0. Two deployments are evaluated. 1. Four VCPUs (0, 1, 2, 3) used by Dom0 are bound to CPU (0, 2, 4, 6) while the VCPUs used by DomU1, DomU2, DomU3, and DomU4 are bound to CPU (1, 3, 5, 7). 2. Four VCPUs (0, 1, 2, 3) used by Dom0 are bound to CPU (0, 1, 2, 3) while the VCPUs used by DomU1, DomU2, DomU3, and DomU4 are bound to CPU (4, 5, 6, 7). Note: CPU 0-4, 1-5, 2-6, 3-7 are two threads on a same core sharing L1 and L2 cache.

Figure 7 illustrates the experimental results. It shows that due to the differences in the physical structure of the processor, performance is different in different bindings. When the default scheduler is used, VCPU switches between the cores will bring additional overhead. By static binding, cache hit rate can be improved, and the computing performance of the virtual machine is optimized.

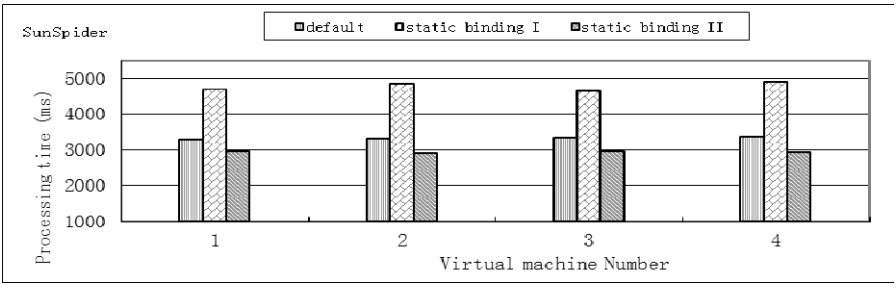

Fig. 7. Evaluating static VCPU-core binding

Further, to evaluate the optimization of the network receive performance, four virtual machines start. Each of them is assigned with 320MB memory, a simulated rtl8139 NIC using tap. Four VCPUs used by four DomUs are bound to CPU (0, 1, 2, 3) while four VCPUs used by Dom0 are bound to the other cores. Each DomU runs netperf, keeps receiving 16KB sized packets and sending 1KB sized packets for 60 seconds. The throughputs are shown in Figure 8.

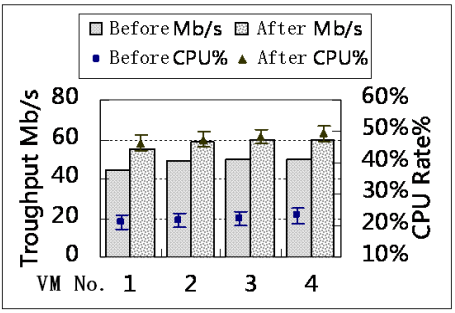

Fig. 8. Throughputs after queue-core binding

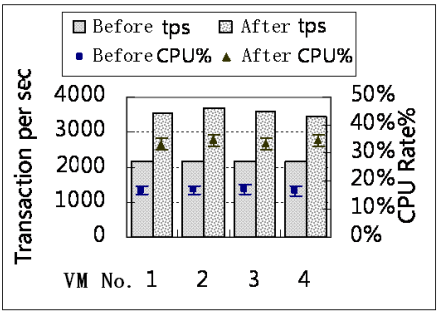

Fig. 9. Latency after queue-core binding

Each DomU keeps receiving 1B sized packets and sending 1B sized packets for 60 seconds. The latency is shown in Figure 9.

Experiment II. Evaluate collaborative scheduling. Start 20 virtual machines. One of them does netperf bandwidth test, and the others browse the webs simultaneously. To make the virtual machines browse web synchronously, a background control process is needed. This process interacts with the remote control process through a socket. When it receives an open browser command, it begins to browse the webs. We chose *www.sina.com.cn* to visit because there are many flash refresh operations which are I/O-intensive. The network throughput and CPU utilization of the netperf virtual machine are evaluated. We change its message size configuration and repeat this test. The results are shown in Figure 10.

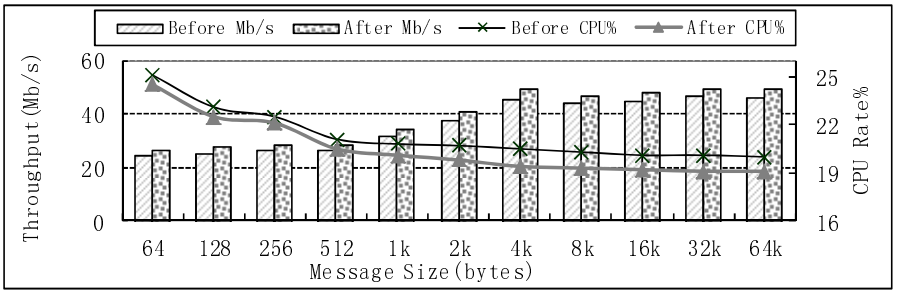

Fig. 10. Evaluating the collaborative scheduling optimization

In this experiment, after the collaborative scheduling optimization, the virtual machine doing the netperf test will be allocated more resources. So the network throughput is improved (an average of 7%), and the CPU utilization is reduced.

Experiment III. Evaluate disk I/O queue optimization. Make the time slice used by I/O processing in QEMU become 1.5 times the original. Meanwhile, dynamic adjust the time slice according to the data amount read and written. We start 3 virtual machines for testing. In order to better reflect the users' interactive usage, OpenOffice

Word editing and saving is used as a load generator. During the OpenOffice is used, we use Blktrace [11] for collecting the physical disk sector read/write records. The results are shown in Table 5, 6.

Table 5. Sector read/write statistics before optimization

VM number	QEMUPid	Number of continuous submission	Number of sectors accessed/submission	Total number of sectors accessed
1	22099	715	294.42	210512
	22037	360	71.18	25624
2	21925	579	226.50	131144
	22411	273	75.02	20480
3	22547	535	171.77	91896
	21868	338	82.93	28032

Table 6. Sector read/write statistics after optimization

VM number	QEMUPid	Number of continuous submission	Number of sectors accessed/submission	Total number of sectors accessed
1	25239	510	360.22	183712
	25385	235	73.12	17184
2	25212	391	309.18	120888
	25093	201	77.17	15512
3	25399	428	272.43	116600
	25229	241	77.94	18784

In these tables, we can see that by optimizing the disk queue, more continuous sectors are submitted. It will reduce the number of disk seeks. The disk read-write throughputs are also improved. The results are shown in Table 7.

Table 7. Throughput optimized by adjusting disk queue

Throughput KB/s	Before optimization	After optimization
Read	1159	1644
Write	293	398

These three experiments evaluate the CPU computing, network performance, disk performance during interactive applications before and after our optimization. Experimental results show that our optimization to improve interactive performance can work well.

6 Related Work

Multi-core technology greatly improves the efficiency of parallel processing. It provides virtualization technology a good hardware platform. The design of Intel

Core i7 can enhance the interaction performance between the virtual machines. In addition to hardware performance improvements, Guangdeng Liao et al. [7] enhance I/O performance in multi-core systems by a software scheme. They proposed a cache-aware scheduling for VCPU. When a VCPU migrates between cores, make it migrate to a core sharing the same cache. They also increase the credit value for the VCPU doing I/O processing in the driver domain, reduce the latency to exchange the network packets in the virtual bridge, and adjust the length of the transmit queue to improve network performance.

Diego Ongaro et al. [8] study the impact on performance when different types of virtual machines run simultaneously. They proposed to add a BOOST state to improve the performance of I/O-intensive virtual machine. They make the Domain submit an I/O request to a BOOST state. It will be scheduled prior to reduce I/O response latency. To prevent Driver Domain be seized by other Domains at a BOOST state during it processes network packets, they proposed to allow the scheduler to be wake up by Driver Domain. Meanwhile, according to credit algorithm, I/O-intensive virtual machine consumes credit slower than CPU-intensive virtual machine, which will reduce I/O latency.

Menon et al. [9] improve the virtual NIC to optimize the network performance in Xen. They make the virtual NIC simulate TSO (TCP Segment Offload), Checksum Offload, and gather/scatter I/O already supported in the existing physical NIC. Herbert et al. proposed RPS (Receive Packet Steering) to dispatch received packets to multi cores by a hash function. So the soft interrupt can be processed in parallel. And the cache hit rate will be high.

7 Conclusion

This paper discusses how to optimize interactive performance of virtual machine in multi-core environment. We analyze the I/O performance of Xen HVM virtual machine. Considering the physical characteristics of multi-core, we propose static VCPU-core binding and further QEMU-core to balance the load and enhance shared cache hit rate to improve I/O performance. And we further propose to dispatch network packets directly to the queue managed by the corresponding core to avoid the data transmission between the cores and frequent cache miss. It can also make soft interrupt processed in parallel. We also propose to collaborate VCPU scheduling with QEMU scheduling. Real-time monitoring I/O requests in virtual machine can help dynamical resource reallocation. According to the application of the virtual machine environment, I/O scheduling algorithm CFQ has been modified to reduce the physical disk seek time and improve the virtual machine's disk I/O response time. These improvements can be applied to virtual network environment in the classroom.

References

1. Barham, P., Dragovic, B., Fraser, K., Hand, S., Harris, T., Ho, A., Neugebauer, R., Pratt, I., Warfield, A.: Xen and the art of virtualization. In: Proceedings of the Symposium on Operating Systems Principles, SOSP (2003)

2. Kivity, A., Kamay, Y., Laor, D.: KVM: the Linux Virtual Machine Monitor. In: Ottawa Linux Symposium (2007)
3. Bellard, F.Q.: A Fast and Portable Dynamic Translator. In: Proceedings of the Usenix Annual Technical Conference (2005)
4. Credit scheduler, http://xen.org/files/summit_3/sched.pdf
5. SunSpider, http://www.webkit.org/perf/sunspider/sunspider.html
6. Jens Axboe, git://git.kernel.dk/blktrace.git
7. Liao, G., Guo, D., Bhuyan, L., King, S.R.: Software Techniques to Improve Virtualized I/O Performance on Multi-core Systems. In: 4th ACM/IEEE Symposium on Architectures for Networking and Communication Systems (2008)
8. Ongaro, D., Cox, A.L., Rixner, S.: Scheduling I/O in Virtual Machine Monitors. In: Proceedings of the Fourth ACM SIGPLAN/SIGOPS International Conference on Virtual Execution Environments (2008)
9. Menon, A., Cox, A.L., Zwaenepoel, W.: Optimizing Network Virtualization in Xen. In: Proceedings of the Usenix Annual Technical Conference (2006)
10. Netperf, http://www.netperf.org/netperf
11. Jens Axboe. Git://git.kernel.dk/blktrace.git

Design and Implementation of Clusters Monitor System Based on Android

Yan Wang, Bin Gong, and Song Li

School of Computer Science and Technology, Shandong University, Jinan, China
{Wangyan2010sdu,lisong.cruise}@gmail.com, gb@sdu.edu.cn

Abstract. With the development of high performance computing (HPC), clusters play a more and more important role in a lot of scientific fields such as graphics, biology, physics, and climatology etc. Therefore, monitoring becomes more critical for sufficient utilization of clusters considering the limited availability of HPC resources. However, the traditional clusters monitoring systems have a common disadvantage of poor mobility which limits the efficiency of cluster management. For this reason, the mobile clusters monitoring system designed on Android platform is presented in this paper that will make it possible to monitor the whole cluster anywhere and anytime to allow administrators to manage, diagnose, and troubleshoot cluster issues more accurately and promptly. The monitoring system is developed on the popular monitoring tools, Ganglia and Nagios, to collect required information from server and display on client – mobile phone. The remote monitoring system also provides the communication module and the other applications such as instant messaging, global positioning and shift changing notice. This system makes clusters monitoring more flexible, efficient, and convenient. Most importantly, the method described in this paper can provide a possibility to customize and extend functions based on user requirements.

Keywords: Android, Ganglia, Nagios, Cluster, remote monitoring.

1 Introduction

Due to the rapid growth of the HPC center and quick expanding of the cluster scale, the diversification of devices and range of the geographical distribution become more complicated which result in increase of expenses and human resources on cluster monitoring. Fortunately, the wireless networks and mobile devices are becoming more common which could be far more efficient tools on cluster monitoring. In this way, the system administrators will easily get the critical alarms and detail information of clusters via smart mobile phones. It will make management of clusters more flexible in any place and any time which overcomes the weakness of traditional monitoring methods and greatly decreases dedicated resources used on system monitoring.

This paper presents a method which is concentrated on building a cluster monitoring system that will provide comprehensive monitoring details to administrator who is frequently out of monitoring office. This method not only integrates information getting from Ganglia and Nagios [1], but also monitors the status of computing

Q. Zu, B. Hu, and A. Elçi (Eds.): ICPCA-SWS 2012, LNCS 7719, pp. 556–561, 2013.

environment. Moreover, it provides a function of real time visualized view which can realize unattended operation. As smart phones become more popular in the field of office automation, the mobile monitoring is the direction of clusters monitoring development in future.

2 Related Work

The system is based on Android platform launched by Google, and built on Ganglia and Nagios which are popular open source monitoring software.

Android platform [2] is free and open platform providing an easy-to-use development kit which is containing flexible displays and functions. Android architecture is comprised of four layers, which are called application, application framework, systems runtime libraries and Linux kernel, from higher to lower respectively.

Ganglia is a scalable distributed monitoring system designed for large localized clusters, provides a PHP Web front-end for administrator to view real time cluster status information including certain metrics such as the number of processor/core, the load of processor, the free/total size of memory, and the usage of disk [3], [4].

Nagios [5] developed by Ethan Galstad is another free, web-based network monitoring tool which can monitor the status of host systems, network services and most of common protocols such as HTTP, FTP, ICMP and SMTP. Nagios is also used for diagnosing, preventing, dealing with network problems and notifying the user.

3 System Design

The concept of our Android-based system is to improve flexibility of monitor system and enhance the communication between administrators. This system is divided into two levels, server and client. First of all, the server probes the data via monitoring tools, and then the server produces a visualized global view based on the data. After that, the mobile client gets the monitoring packages by Socket. At last, the data is shown on the Android application.

- Server: The server should run the web service (Apache), mail service, database (RRDtool), clusters monitoring tool – Ganglia, and network monitoring tool – Nagios.
- Client: By the coverage of wireless network, remote administrators receive the clusters status through the mobile client. For providing a friendly interface, the administrator can choose the way of implement and the content of information.

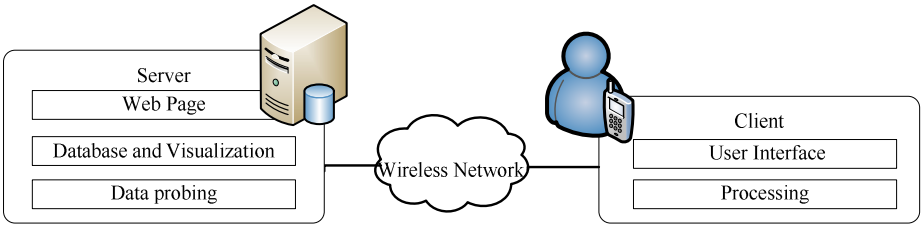

Fig. 1. The system structure

Monitoring tools deployment: the Ganglia monitoring daemon (gmond) runs on Linux hosts of clusters; the Ganglia Meta daemon (gmetad) runs on Server and aggregates data from multiple gmonds [3]. Ganglia can monitor some main metric and extend easily to monitor additional properties by providing a script. Nagios need only run at Server, and it can be used to monitor network services due to a snmp interface. Nagios can transform the metric from Ganglia into its own format [6], and also monitor Windows hosts in which NSClient++ should be installed. The deployment of monitoring tools is shown on Fig. 2. Nagios can monitor some infrastructure which Ganglia can not do, and importantly it provides the good alarm mechanism. Nagios can alter administrators for any metric which hits threshold. The metric's threshold can be configured through Nagios configuration file. The final purpose is to get the comprehensive details of entire HPC center for realizing seamless monitoring and using less overhead.

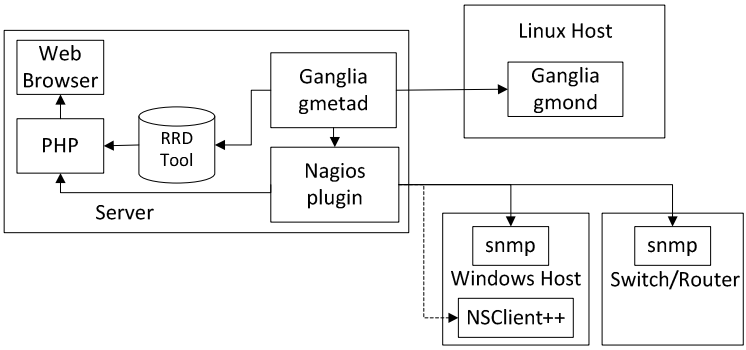

Fig. 2. The deployment of monitoring tools

The existing open resource technologies are integrated and improved to manage and monitor clusters on Android platform. So that, the system is easy for administrator to develop in order to meet the ever-changing nature of clusters. The structure of client is shown in Fig.3.

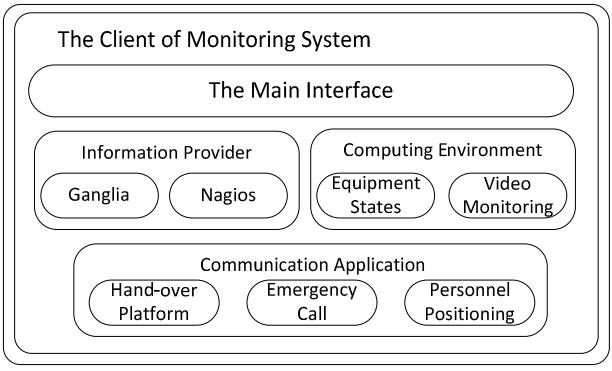

Fig. 3. The structure of client

4 Implementation

Android program is generally composed of four components: Activity, Intent, Content Provider and Service. For main interface with button mode, the system provides a user-friendly GUI to administrators. There are seven buttons: get monitoring information from Ganglia; get monitoring information from Nagios; states of external equipment; video; hand-over platform; emergency call; personnel positioning.

Ganglia mobile interface runs on Android system by WebView. WebView is a very powerful application platform with touch screen, graphic display and internet access. First, add WebView control into this layout document by defining an XML document. Then, load this control in Ganglia Activity, set the Ganglia address which the current WebView link to by loadUrl method. At last, set WebView related properties according to actual requirement. The whole process of creating Ganglia Activity shows as Fig. 4. Finally, Ganglia mobile web shows two-dimensional graphs of main metrics: CPU, load, memory, process, etc [7].

Considering compatibility and complement of the integrated software, Nagios provides the alarm system which Ganglia could not. Administrators learn the state of changes or a problem of the clusters via E-mail and Short Message Service (SMS). Nagios monitoring alerts indicate the problems caused by over a certain threshold in memory usage, processor load and so on.

Authenticating before login Nagios, now WebView can not solve this problem. So browse pages at this module by calling the Android built-in browser. The states of hosts and services can be display real-time on the Nagios mobile interface [8].

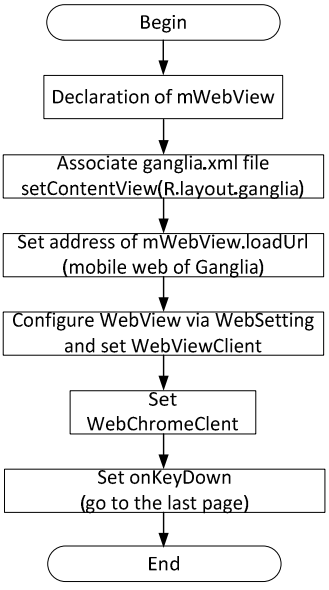

Fig. 4. The flowchart of creating Activity

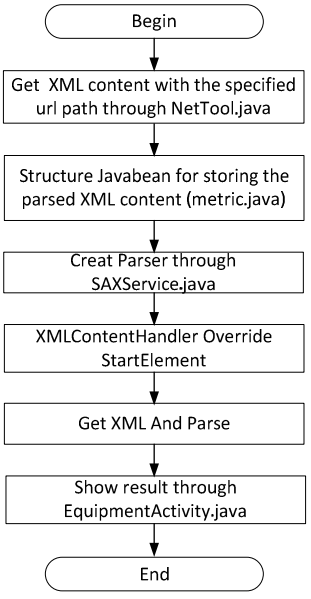

Fig. 5. The process of creating SAX parser

Stable power and constant temperature are the premise for the clusters normal operating. If the power supply interrupts or the cooling system breaks down, the node will not be running as well as expected. So the voltage/current of UPS, the temperature of cabinet, and other important information should be added into this system. These data display in real time updating XML and translate to readable format. Due to the limited space, the details of the XML generation algorithms are not presented in this paper. Get data from XML through the internet and then parse to show on Android. We parse XML files by using SAX for its minimal memory-usage. The process of creating SAX parser shows in Fig. 5.

The positioning module is responsible for finding the closest administrator by calculating the coordinate's difference between the administrator's current location and HPC center. The process of realization: first get the object of LocationManager, and then bind LocationListener. For providing the Location-based service by GPS, set parameters: updated time is 5000 milliseconds; updated minimum distance is 3000 meters. Finally, display the latitude/longitude and the difference by calling a comparison operation.

After the stage of design, development and debug test we run the monitoring application on an Android emulator with 256Mbytes memory executing Linux2.6. Some pictures are illustrated in Fig. 6. Administrators can view the detailed information of nodes on Android mobile phone that is helpful for dealing with fault point events accurately.

a. The main interface of monitoring system
b. The real-time graph of nodes, captured by Ganglia
c. The states of hosts and services, captured by Nagios

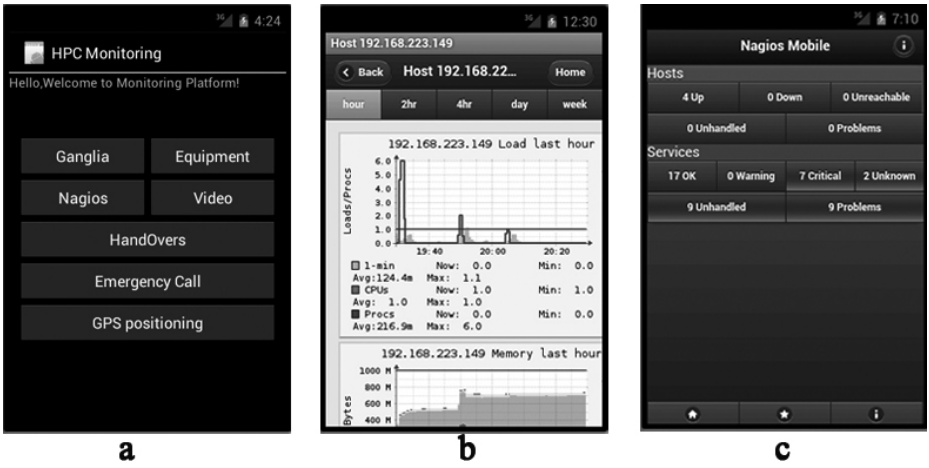

Fig. 6. Interface display

Positioning module shows in Fig.7. On the emulator, the DDMS tool in Android SDK sends geographical coordinates by manual input, and administrators get the following data. In practice, this module obtains the precise longitude and latitude through GPS, and gets the value – the difference from the HPC center at same time.

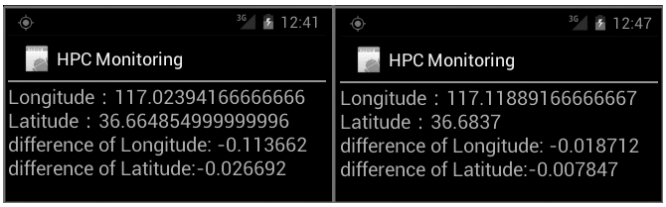

Fig. 7. The positioning information of administrator A and B

5 Conclusions

The cluster monitoring system designed on Android mobile phone can easily collect the cluster status information such as disks, memory, services, UPS, and cooling system, etc and provide better alarming mechanism which can help administrator make decision on time and provide prompt maintenance appropriately. It will ensure the better operation of HPC center and maximize the usage of clusters. The applicability and capability of the system were proved by the test on Android emulator. The methods described in this paper can provide a possibility to customize and extend functions of mobile clusters monitoring system according to user requirements in the future such as integrating with IPMI (Intelligent Platform Management Interface) to provide more basic metrics of Server and enhancing functionalities of this system to provide the retrieval, database management and remote-control services.

References

1. Ganglia and Nagios, http://www.ibm.com/developerworks/cn/linux/l-ganglia-nagios-1/
2. Fengsheng, Y.: Android Unlashed. China Machine Press, Beijing (2010)
3. Matthew, L.M., Brent, N.C., David, E.C.: The ganglia distributed monitoring system: design, implementation, and experience. Parallel Computing 30, 817–840 (2004)
4. Ganglia Monitoring System, http://ganglia.info/
5. Nagios, http://www.nagios.org/
6. Ganglia Nagios Integration, http://sourceforge.net/apps/trac/ganglia/wiki/ganglia_nagios_integration
7. Ganglia Web “2.0” Documentation, http://sourceforge.net/apps/trac/ganglia/wiki/gangliaweb-2
8. Installing Nagios Mobile, http://assets.nagios.com/downloads/exchange/nagiosmobile/Installing_Nagios_Mobile.pdf

An Empirical Comparative Study of Decentralized Load Balancing Algorithms in Clustered Storage Environment

Yun Wang, Xiangyu Luo, Feifei Yuan, and Cong Li

School of Computer Science & Engineering
Key Lab of CNII, MOE
Southeast University, 211189 Nanjing, China
{yunwang,luoxiangyu,yuanfeifei,congli}@seu.edu.cn

Abstract. Load balance is critical for large-scale storage systems to produce high I/O performance. Decentralized solutions are especially preferred for no single point of bottleneck. We implement four typical hypercube-based decentralized load balancing algorithms in a prototype storage system, and conduct extensive experiments with the system running on a testbed comprising 32 nodes. We compare the efficiency and scalability of the four algorithms through the experiments. The comparison results lead to the following new observations contrary to the conclusions obtained in previous simulation studies. Firstly, algorithms with no redundant load migration do not actually achieve savings of migration costs. Secondly, algorithms tolerating a certain degree of redundancy in load migration may achieve improvements in scalability. The two observations provide new insights into the design of load balancing algorithms in distributed storage systems.

Keywords: load balance, storage system, skewed popularity, hypercube, distributed computing.

1 Introduction

Load balance is critical for large-scale storage systems to produce high I/O performance. In a poorly balanced system where some nodes are idle or lightly loaded while others are heavily loaded, the whole performance will be severely affected [1]. Load imbalance could be caused by many factors, such as system expansion, different types of failures, etc. Among the factors, the most significant one is the highly-skewed distribution of request rates for different files. Popular files are frequently requested while unpopular ones are seldom accessed. Consequently, some nodes may be overloaded by massive requests for popular files, while others storing unpopular files may be idle, leaving their I/O resources wasted. Besides, even if the system is balanced at the moment, it cannot always be balanced without proper measures, for the popularities of files dynamically change [2].

To keep long-term load balance in a distributed storage system, there needs to be a proper algorithm constantly migrating files from overloaded nodes to lightly loaded ones as file popularities change. Decentralized algorithms will be especially preferred

Q. Zu, B. Hu, and A. Elçi (Eds.): ICPCA-SWS 2012, LNCS 7719, pp. 562–574, 2013.

for no single point of bottleneck. However, such a satisfactory algorithm is still under explored. Existing decentralized solutions either require each node to communicate with a great number of nodes [17] or adopt a random strategy [4]. In the former case, the system still suffers from poor scalability. In the latter case, each node compares itself with a number of randomly selected nodes to judge whether it needs to migrate load to others. The destination nodes will also come from these randomly selected nodes according to their load values. With the random strategy, the system is not ensured of a load balanced state within a definite number of steps. Moreover, the system suffers from poor efficiency, since the migration costs (measured with the amount of data migrated and the time consumed) are far from optimal.

Contributions of the paper are summarized as follows.

Firstly, we apply hypercube-based decentralized load balancing algorithms [5-8] traditionally used in other fields such as parallel computing to a distributed storage system. To the best of our knowledge, it is the first attempt to do so. The feasibility and efficiency of this kind of algorithm used in storage environments are confirmed by experimental results.

Secondly, instead of simulations as in previous studies [6-8], we compare the efficiency and scalability of four typical hypercube-based algorithms through extensive experiments which have been conducted in a storage cluster comprising 32 nodes.

Lastly and most importantly, our comparison results lead to new observations contrary to the conclusions obtained in previous simulation studies. On one hand, algorithms with no redundant load migration do not actually achieve savings of migration costs. On the other hand, algorithms tolerating a certain degree of redundancy in load migration may achieve improvements in scalability. The observations provide new insights into the design of load balancing algorithms.

The rest of the paper is organized as follows. Section 2 gives a review of the related work. Section 3 states the problem, while Section 4 briefly describes the four typical hypercube-based algorithms. Details of the experimental results are discussed in Section 5. Finally, Section 6 concludes the whole paper.

2 Related Work

In a large-scale distributed storage system, the highly-skewed distribution of request rates for different files yields a high probability of imbalanced usage of I/O resources. Moreover, as time passes by, the popularity of each file dynamically changes, so that even a balanced system could become unbalanced later. Besides, the extremely large scale, the heterogeneities among different devices and the frequent failures also bring great challenges on load balance. Load balancing algorithms for large-scale storage systems have been extensively studied in the literature.

In earlier studies, the problem was stated as FAP (File Assignment Problem). The system is composed of a collection of nodes and is to be assigned with a set of files. Each node N_j is represented as a tuple (c_j, t_j). The two elements respectively represent storage capacity and I/O bandwidth. Each file f_i is represented as a tuple (s_i, λ_i). s_i represents the size of the file while λ_i represents the arrival rate of requests for the file. FAP means to figure out a mapping of files to nodes so that each node bears I/O load and storage consumption proportionate to their I/O bandwidth and storage

capacity. FAP has been intensively studied [9-12]. But it is assumed that the request rate for each file is available in advance and seldom changes within the whole life period.

To handle the circumstance that the popularity of each file may not be known in advance and may even change as time passes by, dynamic request dispatching among multiple replicas is proposed to realize load balance. By replicating each file on several distinct nodes, the system obtains a certain degree of freedom in choosing the service provider when a request arrives. Without replication, each request is statically assigned to the unique server that stores the required file. While with replication, the request could be dispatched to the least loaded server among several replicas. D-SPTF [13] and Kinesis [1] are two representative studies.

In D-SPTF, the request is sent to all the replica servers. Each replica server firstly checks whether the requested file data are in its memory. If so, it immediately sends the data to the requester and notifies other replicas to delete the request from their queues. Otherwise, it puts the request into its queue. Whenever some replica takes out a request from its queue, it immediately notifies others to delete the same request from their queues.

In Kinesis, the requester firstly queries the load status of each replica server. Then it takes the least loaded one as the service provider. Moreover, Kinesis discusses the placement of replicas. It aims to minimize the intersection of arbitrary two nodes regarding the files assigned, thus the probability is low that popular files are replicated on the same set of nodes.

Although replication ensures a certain degree of load balance, a static replication strategy, in which both the number of replicas for each file and the replica locations are statically determined, still has many limitations. Either a more skewed distribution of file popularities or a larger system scale could lead to the dropping of load balance.

Data migration is the popular solution to load balance at present. The system collects popularity information of the files and monitors the load status of each node. Whenever the system becomes highly unbalanced, some files are selected to migrate from one node to another so that load balance can be kept. Load balancing algorithms relying on data migration could be further divided into two categories: centralized and decentralized. Centralized algorithms have been investigated sufficiently [3, 14, 15]. But since this kind of algorithms depend on a central node collecting global information and making system wide decisions, the system suffers from a single point of bottleneck and failure. Decentralized algorithms are proposed to overcome the drawback [17, 4].

In [17], the central node is removed while each node itself is responsible for migration decision making. However, each node needs to communicate with a great number of nodes, so the system still suffers from poor scalability. In [4], a random strategy is adopted which cannot ensure a load balanced state in a definite number of steps. Moreover, the migration costs cannot be optimized.

Therefore, an ideal decentralized solution to load balance, i.e. both scalable and efficient, is still under explored. Besides, load migration depends on correct estimates for workload characteristics. How to effectively discover relevant knowledge from massive log data also attracts many researchers' attention [16].

Lastly, load balancing algorithms have been extensively studied in other fields such as parallel computing. Hypercube-based algorithms [5-8] are representative studies, in which load balance can be achieved in a decentralized manner.

3 Problem Statement

We concentrate on the systems with 'write-once-read-many' workload, in which the load is mainly caused by reading requests. We assume that there are n nodes. Each node N_j is represented as a tuple (c_j, t_j). The two elements respectively represent the storage capacity and I/O bandwidth of the node. There are m files. Each file f_i is represented as a tuple (s_i, λ_i). The two elements respectively represent the size and popularity of the file. The load caused by the file f_i is computed as $s_i * \lambda_i$. Here λ_i is not a constant, but a variable dynamically changing with time. It expresses the expected number of requests for the file in a given time interval such as one hour. Its value is not exact but estimated through history information and periodically updated. The changes of file popularities may occasionally lead to a highly unbalanced usage of I/O resources.

The problem is how to migrate some files from one node to another in a decentralized manner, so that the load assigned to each node is proportionate to its I/O bandwidth subject to the constraints of storage capacity. Furthermore, data traffics and time consumed in the migration process should be reduced. On one hand, load balancing is a background activity and should not cause high data traffics that compete for I/O bandwidth with user requests. On the other hand, a balanced state should be attained as quickly as possible to improve system performance.

File popularities may even change during the migration process, resulting that the load distribution among the nodes is not ideally balanced when the migration finishes. We do not address the problem in this paper. We assume that although file popularities dynamically change in the long term, they are relatively stable in a certain period (several days or weeks) which is much longer than the time spent in migration (several seconds or minutes).

4 Algorithm Descriptions

Hypercube-based load balancing algorithms were used for task migration in parallel computing when first proposed. Since it is difficult to correctly estimate how many CPU cycles each computation task will consume, a static task allocation among different processors is not sufficient to achieve load balance. Tasks should be dynamically migrated from overloaded nodes to lightly loaded ones at run time.

Although hypercube-based algorithms have already been widely used for balancing the computational load, to the best of our knowledge, it is the first attempt to apply this kind of algorithm to a distributed storage system for I/O workload balance. This section will give a brief introduction to hypercube, and review four typical algorithms based on it.

4.1 Hypercube Introduction

Hypercube is a kind of topology under which the system totally accommodates 2^d nodes, with each of them having d neighbors. Here d is called the number of dimensions of the hypercube. Each node is identified with a sequence of d bits $(b_d,\cdots,b_1)$.

Two nodes are neighbors if their sequences differ in just one bit. The neighbor that differs in the bit b_i is called the ith dimensional neighbor. Two nodes are in the same j-dimensional space if their highest (d-j) bits are the same. All nodes that share the same sequence prefix containing (d-j) bits form a j-dimensional space which totally accommodates 2^j nodes. We can obtain that two nodes in the same j-dimensional space are also in the same k-dimensional space for each k satisfied $j \leqslant k \leqslant d$. All the nodes are in the same d-dimensional space. If two nodes are in the same j-dimensional space but different (j-1)-dimensional space, we say that their space distance is j.

Fig. 1 shows a hypercube with d equaling 3. The node denoted as (0,0,0) has three neighbors, with the 1st dimensional neighbor (0,0,1), the 2nd dimensional neighbor (0,1,0) and the 3rd dimensional neighbor (1,0,0). The two nodes denoted as (0,0,0) and (0,0,1) are in the same 1-dimensional space. The four nodes denoted as (0,0,0), (0,0,1), (0,1,0) and (0,1,1) are in the same 2-dimensionl space. All nodes in the figure are in the same 3-dimensional space. The space distance between the nodes denoted as (0,0,0) and (0,0,1) is 1, while that between the nodes denoted as (0,0,0) and (0,1,1) is 2.

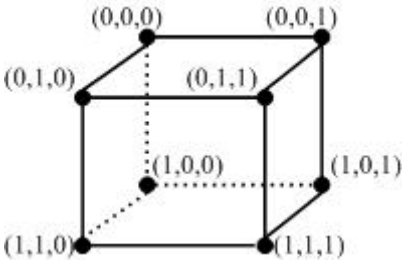

Fig. 1. Hypercube with d equaling 3

The hypercube topology could be either physical or logical. As to physical, each node is directly connected with its neighbors. Communications between two nodes that are not neighbors depend on multi-hop forwarding. As to logical, all nodes are connected by LAN or WAN. But two nodes do not know each other's network identity such as IP address unless they are neighbors. Each node makes decision only through message exchanging with its neighbors. Only log$n$ messages are required for each node to get the average load of the system (n is the total number of nodes in the system). In the storage environment, hypercube is a logical topology.

4.2 Typical Hypercube-Based Algorithms Review

For simplicity, this section only describes the main ideas of the algorithms applied in a homogeneous system where each node is equipped with the same storage capacity and I/O bandwidth, etc. The algorithms are easy to extend in a heterogeneous system [7].

DEM (Dimension Exchange Method). The main idea of DEM is to balance the system dimension by dimension. Firstly, each node communicates with its 1st dimensional neighbor to exchange the load value. Then the heavier one is required to push some load that equals half of the difference to the lighter one. After this step, each

1-dimensional space is balanced ('A j-dimensional space is balanced' means that all of the 2^j nodes in the space are equally loaded). Secondly, each node communicates with its 2nd dimensional neighbor. After the second round, each 2-dimensinal space becomes balanced. The process continues until the whole system or the d-dimensional space is balanced.

DEM belongs to the algorithm type 'with redundant load migration', meaning that an overloaded node may still pull load in (resulting in pushing out more after) while a lightly loaded one may even push load out (resulting in pulling in more after) during the load balancing process. Since nodes initially make decisions only relying on the information of load distribution in a relatively small area, migration could occur between two nodes that are both heavier or both lighter compared to the average load of the whole system.

DirectMap. DirectMap was proposed to eliminate redundant load migration. Each node firstly obtains the average load value of the system in a dimension by dimension manner. Through the load value exchange with the 1st dimensional neighbor, each node obtains the average load value of its 1-dimensional space. Then through the exchange of the average load value of 1-dimensional space with the 2nd dimensional neighbor, each node obtains the average load value of its 2-dimensional space. After d rounds, the average load of the whole system is figured out. According to the average load, each node could judge whether itself is overloaded or not. Moreover, it knows the difference δ between itself and the average. δ is positive for overloaded nodes while negative for lightly loaded ones. It is convenient to think of the node as having δ 'peg' units or $-\delta$ 'hole' units depending on whether $\delta > 0$ or $\delta < 0$. If $\delta = 0$, the node has no 'peg' or 'hole'. The total number of 'peg' units equals that of 'hole' in the whole system. The main idea of DirectMap is to map each 'peg' unit to a 'hole' unit. In this kind of mapping based algorithms, overloaded nodes never pull load in while lightly loaded ones never push load out.

The working process of DirectMap is divided into four phases: 'peg' balancing, 'hole' balancing, local 'peg-hole' mapping and result notifying. Firstly, 'peg' units are balanced in a dimension by dimension manner. For each round i, each node exchanges 'peg' information (including the number of 'peg' units and the original owners' identifiers) with its ith dimensional neighbor. The one that possesses more 'peg' units will migrate half the difference to the other. After d rounds, each node possesses the same number of 'peg' units. To differentiate the 'peg' units owned by the node itself and those migrated from others, 'peg' units are initially marked with the original owner's network identifier such as IP address. Note that in this phase, only the descriptive information about 'peg' units is migrated, while no actual load migration occurs. Secondly, 'hole' units are balanced in the same manner. When the second phase finishes, the number of 'peg' units equals that of 'hole' units on each node, and both 'peg' units and 'hole' units may be marked with identifiers of different original owners. Thirdly, each node independently maps the 'peg' units and 'hole' units on itself. Each of the generated mapping item means that a unit of load should be migrated from the original owner of the 'peg' to that of the 'hole'. Since the node itself may not be the original 'peg' owner, in the last phase, each mapping item obtained in the third phase is sent to the original 'peg' owner, so that overloaded nodes figure out where the excessive load should be migrated.

DBDS (Dimension By Dimension Spreading). DBDS is also a kind of mapping. For the given distribution of 'peg' units and 'hole' units among the nodes, there could be multiple mapping results. Although DirectMap correctly obtains a kind of mapping, it does not care whether the mapping result is efficient for later load migration. For example, migration could occur between two nodes that are far away from each other. DBDS is a kind of cost-aware mapping. A 'peg' unit owned by node N_1 will never be mapped to a 'hole' unit that owned by a node N_2 which is not in the same j-dimensional space unless the total amount of load in the j-dimensional space is initially excessive. So DBDS is a mapping of 'Shortest Space Distance First'. With a careful construction of the hypercube topology, the space distance between two nodes that are in the same switch or cabinet could be smaller than that between two nodes connected through multi-hop switches or routers. So DBDS reduces communication costs compared to DirectMap. To avoid conflicts with others that push load to the same node, DBDS adopts a proportion-based strategy. Each overloaded node independently figures out its mapping share in the 'hole' units on every lightly loaded node. More details of the algorithm could be found in [7].

CWA (CubeWalk Algorithm). Opposite to DEM, CWA balances the system from the highest dimension to the lowest one. Firstly, it brings the system into two (d-1)-dimensional spaces that share the same total amount of load through load migration from the nodes in the initially heavier (d-1)-dimensional space to their dth dimensional neighbors in the other (d-1)-dimensional space. The total amount of load migration in this round equals half the difference between the two spaces. The details of how to decide the migration quantity of each node could be found in [8]. After this round, there will be no load migration between the two spaces. Secondly, each (d-1)-dimensional space is divided into two equally loaded (d-2)-dimensional spaces in the same way. The process continues until each 1-dimensional space is divided into two equally loaded 0-dimensional spaces (0-dimensional space only contains the node itself), so that the whole system is balanced. CWA is a heuristic algorithm. In each round, the load migration is minimized for equally partitioning the load into two spaces. However, redundant load migration still exists, because a node in the less loaded (j-1)-dimensional space may be overloaded itself which may still receive load from its jth dimensional neighbor in the heavier (j-1)-dimensional space.

5 Empirical Study

In this section, through extensive experiments, we investigate the following two problems. Firstly, in the storage environment, does the conclusion still hold that the algorithms with no redundant load migration save migration costs, as shown in previous simulation studies? Secondly, are the hypercube-based algorithms easy to expand as the system grows?

5.1 The Setup

Our testbed for the experiments consists of 32 storage nodes, each equipped with Intel Core2 Quad CPU, 2.96GB of RAM and two SATA disks. The interconnectors are two Ethernet switches of Cisco Catalyst 2960 series. Each of them contains 24 ports

of 10/100Mbits/s and 2 ports of 10/100/1000Mbits/s. Each node is connected to a switch port of 10/100Mbits/s, satisfying the condition that each switch contains 16 nodes. The two switches are directly connected through a port of 10/100/1000Mbits/s.

The Zipf distribution, which properly describes the skewed distribution of request rates for different files, is used to generate file popularities. In the Zipf distribution, the file ranking ith takes a fraction proportionate to $1/i^{\alpha}$. The parameter α reflects the skew degree and the bigger α the more skewed distribution.

5.2 Results and Analysis

What's the Difference in Clustered Storage Environment? In this experiment, the storage system is deployed on 16 nodes. Each node stores 1,000 files randomly selected from a total of 16,000 files whose popularities subject to the Zipf distribution with the skew degree parameter α assigned to 1.0. All of the files are 10MB sized. Fig. 2 shows the initial load distribution among the 16 nodes. The horizontal axis represents node identifiers which are decimal numbers converted from binary sequences. For example, the binary sequence (1,1,0,1) is substituted by a decimal number 13. The vertical axis represents the ratio of the amount of load on each node to that in the whole system.

The four algorithms have been respectively used to bring the system into a balanced state. The migration costs are shown with the full lines in Fig. 3. The horizontal axis represents the four algorithms DEM, DirectMap, DBDS and CWA, while the vertical axis represents the ratio of the cost (either the amount of time or data) consumed by each algorithm to the total amount of the four algorithms. The figure shows that both the amount of the migrated data and the time spent in CWA (an algorithm tolerating a certain degree of redundancy in load migration) are far less than those in the other three algorithms. This is contrary to the conclusion obtained in previous simulation studies, in which algorithms without redundant migration such as DirectMap and DBDS achieve savings of migration costs compared to CWA.

To find out the reason behind, we conduct another experiment as comparison, in which the load distribution among the nodes is the same to that shown in Fig. 2. However, the unbalanced state is not caused by the skewed distribution of popularities but the different numbers of files stored in the nodes. Each file is assumed to have the same popularity (this assumption rarely exists in real applications, and we use it only to reproduce the results similar to previous simulation studies). The four algorithms have also been respectively used to balance the system and the results are shown with the dotted lines in Fig. 3, indicating that DBDS and DirectMap consume the smallest cost, similar to the conclusion obtained in previous simulation studies.

Two opposite comparison results (respectively shown in full lines and dotted lines in Fig. 3) indicate that the highly skewed distribution of file popularities should be carefully considered in the design of load balancing algorithms. Under the influence of this factor, simply minimizing the load migration which means that overloaded nodes never pull load in while lightly loaded ones never push load out will not necessarily achieve savings of migration costs. Because of the highly skewed distribution of popularities, the amount of the migrated data is no longer simply proportionate to the amount of the migrated load. Quite different amounts of load could be generated by the same sized files.

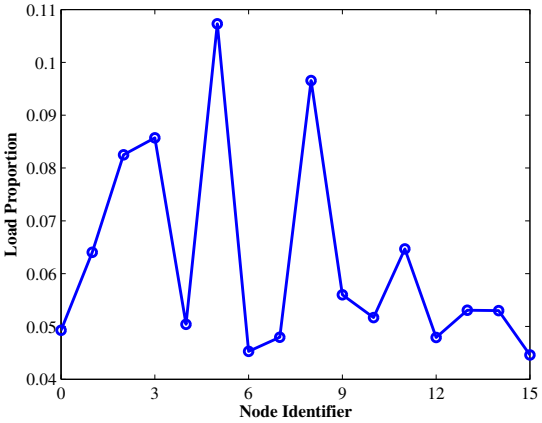

Fig. 2. Load distribution among 16 nodes

To further indicate why CWA (an algorithm with redundant load migration) consumes a smaller migration cost than the algorithms without redundant load migration such as DBDS, we draw the data migration relationships among the nodes in Fig. 4 and Fig. 5. The figures show that the number of node pairs that have migration relationships is much smaller in CWA than in DBDS. Although CWA may cause redundant load migration (e.g. the node numbered 11 pulls load from the node numbered 3 while pushes load to the node numbered 15 in Fig. 4), only two nodes that are dimensional neighbors may have a migration relationship. While in DBDS, overloaded nodes never pull in load (they only have outgoing edges such as the node numbered 2 in Fig. 5) and lightly loaded nodes never push out load (they only have incoming edges such as the node numbered 10 in Fig. 5), but an overloaded node may has migration relationships with a great number of lightly loaded nodes and vice verse. Therefore, in DBDS, an overloaded node may divide a large amount of load for migration into many small parts to migrate to different nodes. However, even a very small amount of load migration requires

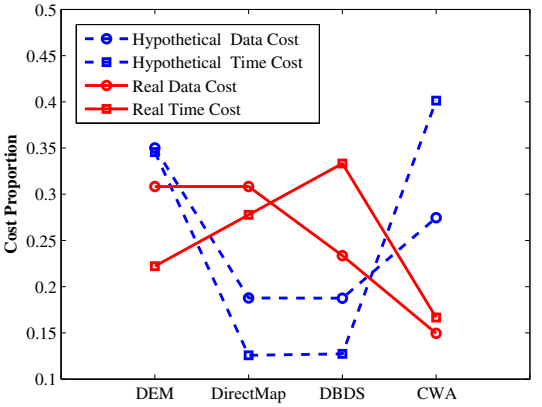

Fig. 3. Comparisons of the four algorithms under two cases

migrating at least one file. While even a large quantity of load migration may also be realized through moving a few files, for heavy overloads are usually caused by several extremely popular files. Not the amount of load migration but the number of migration pairs greatly determines the migration costs.

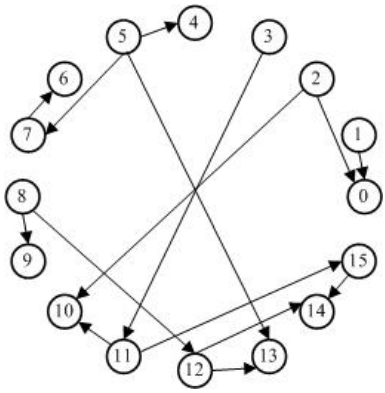

Fig. 4. Migration pairs in CWA

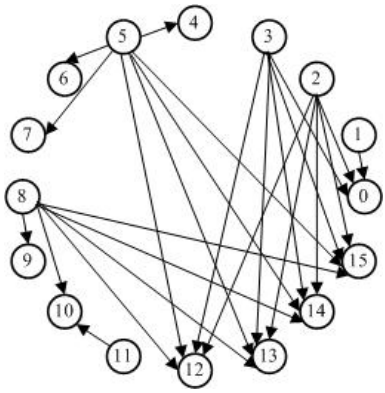

Fig. 5. Migration pairs in DBDS

Are the Algorithms Scalable? In this experiment, the skew degree parameter α, the number of files each node contains and the size of each file are all the same to those in the first experiment, while the number of nodes respectively equals 4, 8, 16 and 32. The four algorithms are respectively studied, and the results are shown in Fig. 6 and Fig. 7.

Fig. 6 shows the relationships between the total amount of data migrated and the system scale under the four algorithms. It indicates that the amount of data migrated approximately linearly increases with the system scale in all of the four algorithms. DEM increases fastest, DirectMap and DBDS are in the middle, while CWA has a smallest growing speed.

Fig. 7 shows the relationships between the time to finish the migration and the system scale. It indicates that in both DBDS and DirectMap, the time consumed almost linearly increases with the system scale, while in DEM and CWA, the time almost stays the same as the system scale expands. The reason behind is that in DEM and CWA, the variance of the data migration quantity is small among different nodes, while in DBDS and DirectMap, nodes have quite different migration tasks. The heaviest node needs to split the overloads into more parts to migrate to more nodes as the system scale expands and takes more time to finish the migration process.

In this experiment, all of the four algorithms can balance the system in a short time (no more than 30 seconds), but as the system expands, CWA is the most adaptive solution which enjoys perfect scalability and high efficiency.

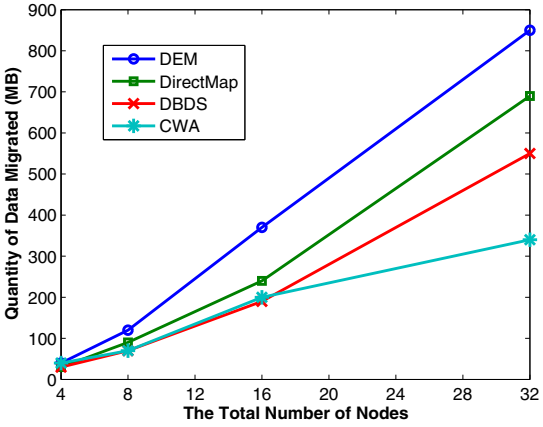

Fig. 6. Effects of system scale on data migration quantity

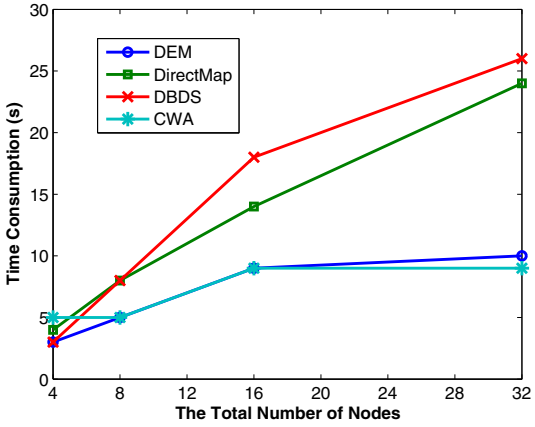

Fig. 7. Effects of system scale on time consumption

6 Conclusion

In this paper, we investigate decentralized load balancing algorithms for clustered storage systems. We make the first attempt to apply hypercube-based algorithms traditionally used in other fields to the storage environment, implement four typical such algorithms in a prototype system, and conduct extensive experiments. The experimental results confirm the feasibility and efficiency of the algorithms. Furthermore, we compare the efficiency and scalability of the four algorithms through experiments, leading to new observations that are contrary to the conclusions obtained in previous simulations studies. The reason behind the observations is that the amount of data migrated (which actually leads to migration costs) is disproportionate to the amount of load migration due to the highly skewed distribution of data popularities in real applications. The observations provide new insights into the design of load balancing algorithms for distributed storage systems. Firstly, purely minimizing the amount of load migration does not necessarily achieve savings of migration costs. Secondly, tolerating a certain degree of redundancy in load migration may gain improvements in scalability.

Our prototype system only considers the ideal situation. For example, we do not consider the situation in which the number of nodes is not the power of 2. We do not consider heterogeneities and failures, either. In fact, hypercube-based algorithms could be easily extended to the situations. For heterogeneities, the nodes exchange their load values together with their capacities. Failed nodes and those nonexistent node identifiers could be regarded as virtual nodes with capacity equaling 0. We will realize the idea in our prototype system in future work.

Acknowledgment. This research work is partially supported by the Natural Science Foundation of China under grant No. 60973122, the 973 Program in China under grant No. 2009CB320705, and 863 Hi- Tech Program in China under grant No. 2011AA040502.

References

1. Maccormick, J., Murphy, N., Ramasubramanian, V., Wieder, U., Yang, J., Zhou, L.: Kinesis: A New Approach to Replica Placement in Distributed Storage Systems. ACM Transactions on Storage 4(4), 11:1–11:28 (2009)
2. Kari, C., Kim, Y.A., Russell, A.: Data Migration in Heterogeneous Storage Systems. In: 31st IEEE International Conference on Distributed Computing Systems, pp. 143–150. IEEE Computer Society, Minneapolis (2011)
3. Wei, Q.: CDRM: a Cost-effective Dynamic Replication Management Scheme for Cloud Storage Cluster. In: IEEE International Conference on Cluster Computing, pp. 188–196. IEEE Computer Society, Heraklion (2010)
4. Xie, C., Cai, B.: A Decentralized Storage Cluster with High Reliability and flexibility. In: 14th Euromicro International Conference on Parallel, Distributed, and Network-Based Processing, IEEE Computer Society, Montbeliard-Sochaux (2006)

5. Ranka, S., Won, Y., Sahni, S.: Programming a hypercube multicomputer. IEEE Software 5(5), 69–77 (1998)
6. Nicol, D.M.: Communication efficient global load balancing. In: International Conference on Scalable High Performance Computing, pp. 292–299. IEEE (1992)
7. Luo, X., Wang, Y.: DBDS: a Fully Distributed Algorithm for Data Migration. Computer Applications and Software 28(11), 45–48 (2011) (in China)
8. Wu, M.Y., Shu, W.: A Load-Balancing Algorithm for n-cubes. In: International Conference on Parallel Processing, pp. 148–155. IEEE (1996)
9. Dowdy, W., Foster, D.: Comparative Models of the File Assignment Problem. ACM Computing Surveys 14(2), 287–313 (1982)
10. Graham, R.L.: Bounds on Multiprocessing Timing Anomalies. SIAM Journal on Applied Mathematics 17(2), 416–429 (1969)
11. Lee, L.W., Scheuermann, P., Vingralek, R.: File Assignment in Parallel I/O Systems with Minimal Variance of Service Time. IEEE Transactions on Computers 49(2), 127–140 (2000)
12. Madathil, D.K., Thota, R.B., Paul, P., Xie, T.: A Static Data Placement Strategy towards Perfect Load-Balancing for Distributed Storage Clusters. In: International Symposium on Parallel and Distributed Processing, pp. 1–8. IEEE Computer Society, Miami (2008)
13. Lumb, C.R., Golding, R., Ganger, G.R.: D-SPTF: Decentralized Request Distribution in Brick based Storage Systems. In: the 11th International Conference on Architectural Support for Programming Languages and Operating, pp. 37–47. ACM, Boston (2004)
14. Ghemawat, S., Gobioff, H., Leung, S.T.: The Google File System. In: 19th ACM Symposium on Operating Systems Principles, pp. 29–43. ACM, Bolton Landing (2003)
15. Hall, J., Hartline, J., Karlin, A.R., Saia, J., Wilkes, J.: On Algorithms for Efficient Data Migration. In: 12th Annual ACM-SIAM Symposium on Discrete Algorithms, pp. 620–629. ACM, Washington, DC (2001)
16. Bodik, P.: Automating Datacenter Operations Using Machine Learning. Doctoral Dissertation, University of California, Berkeley (2010)
17. Wang, W., Zhao, Y.: A Novel Network Storage Scheme: Intelligent Network Disk Storage Cluster. In: 5th International Conference on Networking, Sensing and Control, pp. 142–147. IEEE Computer Society, Sanya (2008)

A Contact-History Based Routing for Publish-Subscribe Scheme in Hierarchical Opportunistic Networks

Zhen Wang[1], Yong Zhang[1], Mei Song[1], Yinglei Teng[1], and Baoling Liu[2]

[1] ICN&CAD Center,
Beijing University of Posts and Telecommunications, Beijing, P.R.C.
wangzhen1948@gmail.com, {yongzhang,songm,lilytengtt}@bupt.edu.cn
[2] Universal Wireless Communication Lab,
Beijing University of Posts and Telecommunications, Beijing, P.R.C.
blliu@bupt.edu.cn

Abstract. Opportunistic networks is aimed to provide a solution for communication in disrupt tolerate networks, which has attracted lots of researches. However, for reasons such as finite buffer size and energy of nodes in opportunistic networks, the further improvement of network performance is limited. Therefore, we set powerful cluster nodes in the network to form hierarchical opportunistic networks. In this paper, a publish/subscribe scheme in hierarchical opportunistic networks is put forward. The object of publish/subscribe scheme is to realize the sharing of resources between nodes. In our scheme, nodes disseminate their data requests with a TTL value to limit their flooding and after receiving the subscribed data items, an ACK will be flooded to delete the useless data packets in the network. To choose appropriate relays for data packets, a utility function to estimate the relay ability of nodes is designed, what's more, cluster nodes are brought in as relay nodes too. Simulations are given to demonstrate the performance improvement of our scheme.

Keywords: Hierarchical Opportunistic Networks, cluster nodes, publish/subscribe scheme, utility function.

1 Introduction

With the spreading of intelligent devices equipped with the capability of short-range wireless communications, a new type of network called opportunistic networks [1], composed of intelligent mobile devices, come into being. Due to nodal mobility, low density or lossy link, there may not exist an end-to-end path between source and destination in general in opportunistic networks. Therefore, opportunistic networks have to utilize the communication opportunities arising from node movement to forward messages, and implement communications between nodes based on the "store-carry-forward" routing pattern.

In opportunistic networks, the probability of direct encounter between source and destination is very poor and communication paths usually consist of opportunistic

Q. Zu, B. Hu, and A. Elçi (Eds.): ICPCA-SWS 2012, LNCS 7719, pp. 575–585, 2013.

contacts between nodes. When the scale of the network expands and the number of transferred messages increases, transmission efficiency becomes very low, meanwhile, the overhead of control information and the consumption of power and storage space turns high, resulting in a sharp decline in the network performance such as network throughput and transmission delay. To avoid this, we set some static or mobile cluster nodes to transform the current architecture of opportunistic networks to a novel hierarchical one. In general, these cluster nodes have larger storage space, enhanced computation ability and more power, making these nodes be powerful storage nodes or forwarding nodes. A set of cluster nodes can form a group, together with the group of common nodes, constituting the hierarchical networks. Hierarchical opportunistic networks can significantly improve the scalability and throughput of networks, and achieve a better performance.

Nodes in opportunistic networks, which are intelligent mobile devices, usually carry abundant multi-media data (created by themselves or downloading from the Internet), which might be of interest to other nodes. So designing efficient publish/subscribe scheme to achieve the sharing of content becomes a necessity for users in the network. Data dissemination research in opportunistic networks has gained some achievements [2-7], however, the proposal of hierarchical opportunistic networks brings new opportunities and challenges. In this paper, we aim to design a novel publish/subscribe scheme in hierarchical opportunistic networks. In this scheme, we launch a resource retrieval procedure by flooding the user interests in a controlled way. Then the contact history of the nodes and the powerful relay and storage capability of cluster nodes is made full use of to devise our relay selection strategy. We also take nodes' buffer usage into consideration in our scheme. Simulation indicates that our approach can significantly improve the performance of data dissemination scheme.

2 Related Works

The research of data dissemination in opportunistic networks has attracted more and more attention. Current work can be divided into two categories. One is based on content characteristics, i.e., popularity and availability of the data, to select cashing content, while the other exploits the social or movement characteristics of nodes to choose appropriate relay nodes.

Epidemic scheme [8] is a simple protocol, in which nodes exchange data items that they have no matter whether they are interested in these data items when meet. This flooding strategy apparently will waste too many resources. Reference [2] replicates subscription requests to improve the successful ratio of resources discovery and responds events according to the communication frequency between different nodes adaptively, but this mechanism doesn't consider how to select reasonable relays to convey data objects. ContenPlace [3] supposes that users belong to social communities. The authors use Future policy to assign weights to different communities to compute the utility of data and according to the rank of the utility nodes store the data in their buffers. Yet for the disconnected topology of network, nodes are hard to have a global knowledge of the network state, making it a difficult task to compute the utility of data.

In the research of relay selection algorithm，PROPHET [9] exploits nodes' contact history to estimate the probability of encountering, according to which to make forwarding decisions. HiBOp [10] is designed to manage and exploit context information of nodes, such as users' working address, the probability of visiting particular places and so on, to select the next hop. Nodes similar to destination in contexts or often in touch with nodes similar to destination will be selected to be forwarders.

Evolved from reference [2], in our scheme we flood acknowledgements after receiving requesting content to delete useless packets in the network. We use PROPHET and HiBOp for reference to design our relay selection algorithm, nodes have higher probability of encountering destination will have priority over other nodes to be selected as forwarding nodes. Different from them, nodes' buffer usage is considered as an important factor when choosing relays. What's more, we bring in cluster nodes as the complementary relays to take advantage of the hierarchical opportunistic networks.

The rest of paper is organized as follows: in section three, we describe our system model. In section four, we present our relay selection algorithm. We simulate our scheme in section five, followed by a conclusion in section six.

3 System Model

In opportunistic networking scenario, nodes are equipped with the ability of short-range wireless communication. When two nodes come into communication range, they exchange the data cashed in their buffer. We assume that every node in the network has a unique ID, additionally, cluster nodes have different IDs from the common ones and their IDs can be recognized by arbitrary nodes. We assume that the wireless bandwidth is sufficiently large to complete data items exchange in the contact duration. Nodes in the network are cooperative in default, so every node can forward data for others selflessly.

Data dissemination is a many-to-many communication protocol, the process of which can be described as follows: when a node is interested to some data items, it disseminates the requests for them. Then nodes have corresponding data items will send the data to the node after receiving the requests. In our scheme, requesting nodes can gain their interested data items in two ways. Firstly, nodes can obtain the data directly when they encounter the publisher. Secondly, the publisher that receives the request will push the data to the subscriber through an opportunistic route. In either way, after getting their interested data, nodes will produce an ACK message to be propagated network-wide in order to remove the subscription requests and data packets generated during this procedure.

In our scheme, a subscription request is composed of four parts: the ID of the subscriber, the description of the interesting data object, creating time of the packet and TTL value. The node ID and the creating time can uniquely identify a subscription request. Corresponding to the subscription request, the ACK message consists of the cryptographic hash of the content and the ID of the subscriber. Compared to data packets, the overhead resulting from the flooding of the two types of packets mentioned above is very low.

Data delivery in opportunistic networks is accomplished through data exchange of the encountering nodes. In our scheme, nodes exchange the lists of subscription requests and data items stored in their buffer when meet. Subscriptions that are not stored in the opposite peer and whose TTL values are beyond zero will be transferred to each other. If the encountering node has the data items that are of interest to the local node, the node will obtain them directly, however, we mainly discuss how to assist to transfer the data items that are interested to other nodes in the next section.

4 Algorithm Description

4.1 Transmission Delay Estimation

The movement of nodes in opportunistic networks is not completely random, especially in human-contact based networks. In real life, it is probable for a user to visit a place again if it has visited it before. On the basis of this, we exploit the contact history of nodes to design our relay selection algorithm.

In this approach, every node maintains a table to record its contact history, which is shown in Table 1. In this table, the Meeting Times has two values, the first one called the real value represents the real times of encountering with this node, which is used to calculate the Average Meeting Time, while the value in the bracket called the virtual value is equal to the real value at the beginning but will be updated by setting the expiration time, which is used to deleted useless records.

Table 1. History Table

Node ID	Meeting Times	Latest Meeting Time	Average Meeting Interval(min)
N054	6(4)	17:33	124

We set expiration time to remove outdated records. If nodes didn't encounter each other during a period of expiration time, the virtual value of their meeting times will be decreased by one. The record will be deleted if the virtual value drops to zero. We compute the expiration time as follows:

$$T_e = \lambda e^{-in} + \kappa \tag{1}$$

Where n is the virtual value of the meeting times and i is a constant value. When n is equal to one, $T_e = \lambda e^{-i} + \kappa$, which is the value of the maximum delay that users can tolerate; When n is infinite, $T_e = \kappa$, which is the value of the expected delay of the users. (Here the delay means the time that is taken for the data to transmit from the publisher to the subscriber) From the equation we can see that with the increase of meeting times, expiration time turns shorter and tends to be κ at last. In this way, we can remove these records without usage effectively.

Using this table, we can predict the next meeting time:

$$\begin{cases} t_p = t_l + T_e & (n=1) \\ t_p = t_l + \overline{T} & (n>1) \end{cases} \tag{2}$$

In this formulation, t_p is the predicted time of the next meeting, t_l is the time of the last meeting, T_e is the expiration time and $\overline{T}$ is the average meeting interval. From Eq.2, we can estimate the transmission delay:

$$t_d = t_p - t_c \tag{3}$$

Where t_c indicates the current time.

4.2 Utility Function

Nodes in opportunistic networks usually have very limited buffer, when data packets carried increase, their buffer decreases sharply and sometimes even exhausts, so that these nodes are no longer considered as good relay candidates. Therefore when selecting relays, we have to consider the remaining buffer of the nodes. So we define the utility function as follows both considering transmission delay and buffer usage:

$$U = \frac{t_d}{e^{\theta}} \tag{4}$$

In this formulation, θ represents the ratio between remaining buffer and the buffer sum of the node. We use the utility value as the criterion of relay selection. The utility value is inversely proportional to the rate of the remaining buffer and proportional to the transmission delay. The less the latency and the more the remaining buffer is, the less the utility value is, and the node will act as a better relay node.

4.3 Relay Selection Algorithm

When a publisher has received a subscription request, the corresponding data will be disseminated to the subscriber according to the ID contained in the request. To make the dissemination procedure more efficient, we optimize the relay selection algorithm, in which we attend to choose a reasonable path computed according to the utility value computed by the Eq.3. Specifically speaking, we choose two types of nodes as relays, that is, nodes have contact history with the destination (For simplification, we call them the C-nodes in the rest of the paper) and cluster nodes.

We set cluster nodes to form hierarchical opportunistic networks, which can be arranged at a certain place or selected dynamically from the common nodes. Cluster nodes usually appear at the places where node density is high or that joint two adjacent communities. Compared to common nodes, cluster nodes have advantage in many aspects such as storage space, computing capability and energy reserves. By making full use of cluster nodes we could reduce the traffic of common nodes and improve the disseminating efficiency of data items.

Communication process when nodes meet can be described as follows. At the first beginning, nodes exchange ID and the list of their cashed data packets. For data packets not buffered in the peer, If the peer is a cluster node, then the local node replicates the being transferred packet and forwards the copy to it, as well as the utility value (U_1) of the packet estimated by the local node. If the cluster nodes encounter the C-node in the future whose utility value for this packet is U_2, the data items will be forwarded to the C-node without local replication as long as $U_2(1+\varepsilon)<U_1$ (ε is a constant value between 0 and 1), otherwise the data items will be carried until the nodes encounter the destination or the data is expired. If it's not the cluster node, the local node transmits the destination IDs contained in the packets to the peer. If the IDs exist in the history table, the peer calculates the utility U. If $U(1+\varepsilon)<U_1$, the packet will be forwarded to the peer. The detailed version of our algorithm is illustrated in Fig. 1.

****

When node i encounters node j, the following routine is executed to determine whether the data packets should pass to node j. Node j will perform the same action. In this description U represents the utility value for data item d computed by the local node, and for a cluster node it is U_1.

1. **while** i encounters j
2. Exchange Node ID and the data packets list;
3. **for** each data packet d not buffered in j
4. **if** (j is a cluster node)
5. i replicates the data item d ;
6. i forwards the copy of d and the utility value for d , i.e., U_1;
7. **else**
8. i forwards the destination ID of d to j ;
9. **if** (the history table of j contains the records of the relevant ID)
10. j computes the utility value U_2 ;
11. j sends the value of U_2 to i ;
12. **if** ($U_2(1+\varepsilon)<U$)
13. i forwards the data item d to j ;
14. **end if**
15. **end if**
16. **end if**
17. **end for**
18. **end while**

****

Fig. 1. Relay Selection Algorithm

5 Performance Evaluation

In this section, we present the results of our simulation of the proposed scheme.

5.1 Simulation Configuration

We choose ONE simulator [11] in the simulation of the mechanism. For the map of Helsinki, capital of Finland, we use 126 Normal Nodes and 5 Cluster Nodes. The shortest path algorithm based on the Map Movement Model is adopted to simulate Normal Nodes and the Fixed Station Movement Model for Cluster Nodes. The detailed simulation parameters are showed in Table 2.

Through Area Heat we can set the Cluster Node. Area Heat means the probability of the node appeared in the area. By using this parameter we can fix the location of 5 cluster nodes.

Table 2. Parameters Used for Simulation

Parameters	**Value**
Speed of Normal Nodes	0.5 m/s-13.92 m/s
Transmission range	10m
Transmission speed	10Mbps
Buffer size of normal node	50M
Buffer size of cluster node	500M
Size of files	500K-5M

Before simulation, we set 200 different files, each has 1 to 20 copies, distributed in the total 131 nodes randomly. When the simulation begins, the Normal Node will produce a Request for interested Packet randomly in 15 to 20 minutes. Because the data packets have expiration time, so the nodes will delete the data in buffer periodically. We set the expiration time as 6hours. And then we verify the protocol in the following there parts: the Data request success rate, delay and network traffic.

5.2 Simulation Results

Successful Delivery Rate VS TTL of Requests

Firstly, we test the functional relationship between the data request success rate and the TTL of the requests. The simulation time is 12 hours. We can see in the Fig. 2 that at first when the TTL increases, the success rate increases remarkably. While the TTL

come to the value of 4 hours, the success rate increases to the peak value, and has little change afterwards. The reason for this is that with the growth of TTL, the requests are spread in a larger scope, so the probability for retrieving the data increases, and when come to the 4 hours, almost all the area and all nodes can be covered, so later when the TTL increases, the retrieving scope doesn't expand any more, so the success rate comes to the peak value. The success rate cannot approach 1, that's because the environment of opportunistic networks is poor, which lead to severe loss of packets. In the following simulations, we set the TTL value as 4 hours.

Successful Delivery Rate

Secondly we simulate the properties of our scheme in the network with and without Cluster Nodes, and then compared these results with the Epidemic Scheme. We can see form Fig.3 that even without the Cluster Nodes, the performance of our mechanism is better than the Epidemic scheme, the Data Request Success Rate nearly doubles. And when with Cluster Nodes, the rate has a further improvement. As the time increases, the success rate maintains at a stable level, which proves the robustness of our mechanism.

Average Latency

Delay defines the interval between the time Node sends the Requests and the time the corresponding data is sent to the Node. As shown in Fig.4, compared to Epidemic mechanism, delay in our mechanism has a 1000 seconds increasement. As the time increases, delay in the Epidemic scheme increases rapidly, however the improvement in our mechanism is little. That's because the Epidemic scheme is a kind of Flooding Mechanism, for which as the time increases, traffic in the network increases straightly and the buffer resource of some nodes in network even exhausts. This will leads to the algorithm performance reduction. Compared to no Cluster Nodes, the delay of our mechanism is larger in the hierarchical opportunistic networks, for the buffering of the packets in Cluster nodes during the forwarding process increases the delay of data transmission.

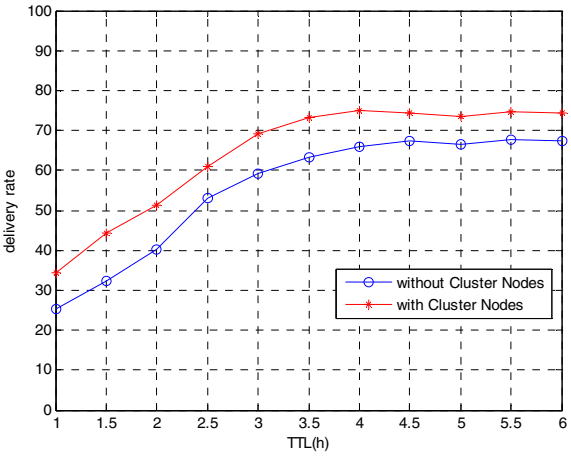

Fig. 2. Delivery Rate VS TTL

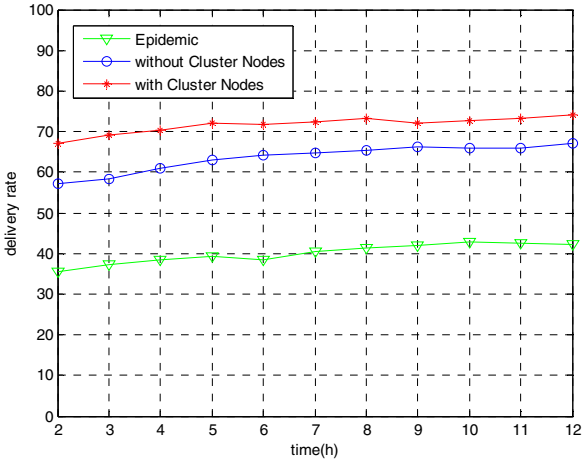

Fig. 3. Delivery Rate

Network Traffic

We define the network traffic as the average buffer occupation ratio of the nodes in the network. From the Fig. 5 we can see that, compared to Epidemic scheme, the network traffic of our scheme reduces largely, for we take some methods to control it. Firstly, for the size of the Requests and ACK is very small, flooding them in the net work will not lead to a big increase in traffic load. Secondly, after receiving the requesting data items, nodes flood ACK immediately to delete the useless packets. Thirdly, we only choose good candidates as our relays. Buffer resources are very precious for nodes in opportunistic networks, so limiting the consumption of them is essential to guarantee the performance of the scheme.

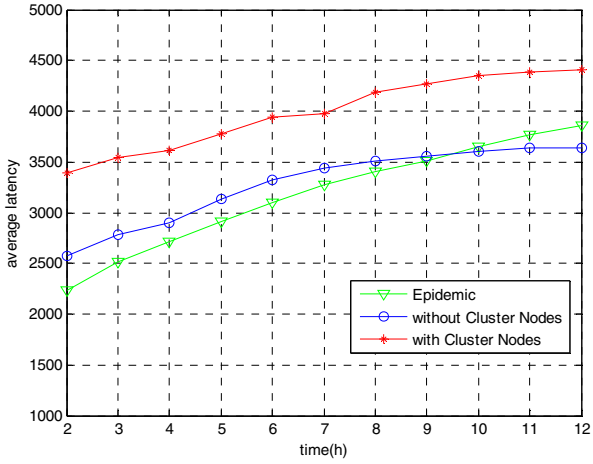

Fig. 4. Average Latency

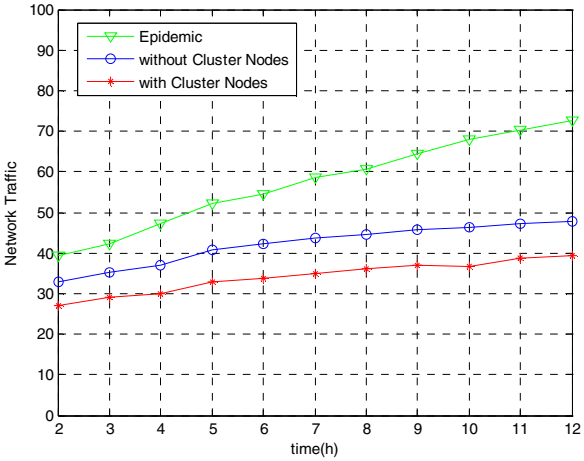

Fig. 5. Network Traffic

In a word, our approach apparently improves the performance of publish/subscribe scheme in terms of successful delivery rate and traffic load. Though the latency increases, but for opportunistic networks, a delay-tolerate network, a little increase of latency will not result in a severe impact on users' satisfaction feeling. The most important factor to estimate the performance of a data dissemination scheme is successful delivery rate, which is significantly improved by our scheme with network traffic controlling in a lower level.

6 Conclusions

Hierarchical opportunistic networks are an evolution from current opportunistic networks. Based on the research results of data dissemination in opportunistic networks, we propose a novel publish/subscribe scheme for hierarchical opportunistic networks. In our scheme, we set TTL of the subscription requests to limit its flooding and by transmitting acknowledgements network-wide we remove the useless packets; considering the contact history and the buffer consumption of the nodes, we design our relay selection algorithm, additionally, we treat cluster nodes as good forwarders and cashing nodes to make advantage of the hierarchical architecture. The simulation indicates that our scheme can achieve a better performance.

Acknowledgements. This work is supported by the National Natural Science Foundation of China under Grant No.61171097, the International Scientific and Technological Cooperation Program (2010DFA11060), and the State Major Science and Technology Special Projects(Grant No. 2011ZX03003-002-01).

References

1. Pelusi, L., Passarella, A., Conti, M.: Opportunistic networking: data forwarding in disconnected mobile ad hoc networks. J. Communications Magazine 44(11), 134–141 (2006)
2. Niu, J., Wu, F., Huo, D., Hu, K.: Message publish/subscribe scheme based on opportunistic network. In: The 7th International Conference on Ubiquitous Intelligence & Computing and 7th International Conference on Autonomic & Trusted Computing (UIC/ATC), Xi'an, China, pp. 180–184 (2010)
3. Boldrini, C., Conti, M., Passarella, A.: Design and Performance Evaluation of ContentPlace, a Social-Aware Data Dissemination System for Opportunistic Networks. J. Computer Networks 54(4), 589–604 (2010)
4. Conti, M., Mordacchini, M., Passarella, A.: Data Dissemination in Opportunistic Networks using Cognitive Heuristics. In: IEEE International Symposium on a World of Wireless, Mobile and Multimedia Networks (WoWMoM), Lucca, Italy, pp. 1–6 (2011)
5. Mascolo, C., Musolesi, M., Picco, G.P.: Socially-aware routing for publish-subscribe in delay-tolerant mobile ad hoc networks. J. IEEE Journal on Selected Areas in Communications, 748–760 (2008)
6. Gao, W., Cao, G.: User-Centric Data Dissemination in Disruption Tolerant Networks. In: INFOCOM, Shanghai, China, pp. 3119–3127 (2011)
7. Chuah, M., Yang, P., Hui, P.: Cooperative User Centric Information Dissemination In Human Contact-Based Networks. In: IEEE 16th International Conference on Parallel and Distributed Systems (ICPADS), Shanghai, China, pp. 794–799 (2010)
8. Becker, V.D.: Epidemic routing for partially connected ad hoc networks. Technical report, CS-2000-06, Department of Computer Science, Duke University, Durham, NC (2000)
9. Lindgren, A., Doria, A., Schelén, O.: Probabilistic routing in intermittently connected networks. ACM SIGMOBILE Mobile Computing and Communications Review 7(3), 19–20 (2003)
10. Boldrini, C., Conti, M., Passarella, A.: Exploiting Users' Social Relations to Forward Data in Opportunistic Networks: The HiBOp Solution. J. Pervasive Mobile Comp. 4(5), 633–657 (2008)
11. Keronen, A., Ott, J.: The ONE Simulator for DTN Protocol Evaluation. In: SIMUTools, Rome, Italy (2009)

Study of E-commerce-Based Third-Party Logistics Alliance System*

Zhengguo Wang, Guoqian Jiang, and Hanbin Xiao

School of Logistics Engineering, Wuhan University of Technology,
Wuhan, 430063, P.R.C
zgwang@whut.edu.cn

Abstract. Alliance is the trend of third party logistics's development, the management of third party logistics can be improved by the advantage of e-commerce information technology. This paper discusses the development status of third party logistics enterprise, analyzes the characteristic of the third party logistics alliance. A third party logistics alliances system based on e-commerce is established , the logistics alliance composition, structure and operation processes of the system are determined, then a system platform of a third party logistics alliance based on e-commerce is built. The result provides a theory reference for the development of the third-party logistics enterprise and e-commerce logistics.

Keywords: e-commerce, third party logistics, logistics alliance.

1 Introduction

With the IT acceleration and gaining ground rapidly, the whole conventional economy activities are intrinsically changed. Under this background, the e-commerce emerged as the times require, at the same time the new logistics mode came into being. The combination of e-commerce and modern logistics produces the bran-new logistics mode, namely the e-commerce logistics mode[1][2].But the logistics is also the direct factor of restricting the development of our country e-commerce development, currently the third party logistics(3PL) enterprises in China generally have small scale with backward infrastructure and low level of management, and can not satisfy the demand of e-commerce. In order to solve this problem, a new organization – the 3PL alliance – begins to be drawn attention[1-6].

Currently there isn't uniform definition about the 3PL alliance, commonly the 3PL alliance is deemed to be the enterprise alliance based on logistics cooperation, which is a loose network organization forming complementary advantage, risk mutual bearing, benefit sharing through agreement or contract. The 3PL enterprise should use the limit resource to exert the maximal function and create the maximal benefit, so each 3PL enterprise should use the limit resource to its own core business, which requires

* Supported by the "Fundamental Research Funds for the Central Universities" 2011-IV-061.

Q. Zu, B. Hu, and A. Elçi (Eds.): ICPCA-SWS 2012, LNCS 7719, pp. 586–591, 2013.

that the 3PL enterprise should conform and compose the 3PL strategic alliance. At the same time, a platform of information exchanging and sharing is built among the 3PL alliance, so this alliance should be based on the e-commerce.

2 The Characteristic of the 3PL Alliance

The 3PL alliance can be treated as the collaborative network of the 3PL enterprises, the main members are three parts. One is the demand party of logistics service, who is mostly industry enterprise, the industry enterprises usually outsource the logistics to the 3PL enterprise in order to exert the core advantage. The second is the supply party of logistics service. The third is the end customer, they are the final service users, who may be industry enterprise, or the individual consumer.

The following is the characteristics of the 3PL alliance:

- The study objects of the 3PL alliance system are extend to every nodes of supply chain network.
- These nodes maybe the core enterprise of supply chain, or one underlying section of manufacturer(e.g. procurement section).
- Every node may represent the supplier or the 3PL logistics enterprise, or the customer, also have several roles simultaneously.
- The suppliers and customers can together look for some carriers for long term cooperation, the three parties can entirely share their information, and build the e-commerce platform with information sharing, and become the long term cooperative partners.

The physical flow and the information flow are depicted in figure 1.

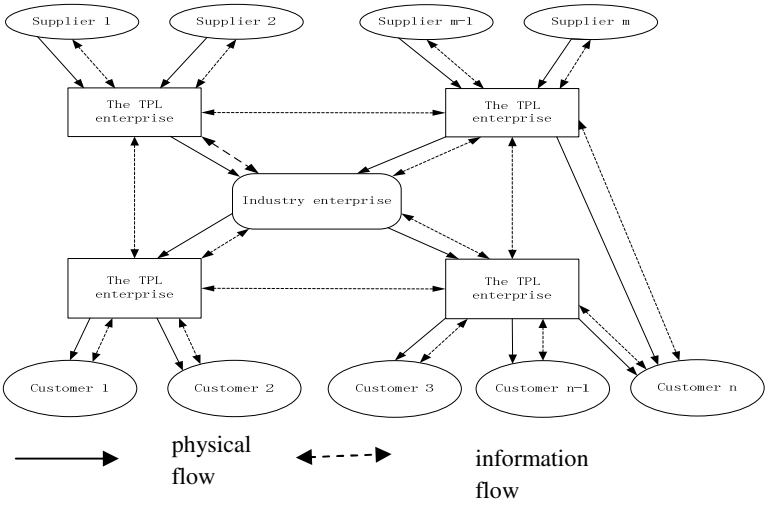

Fig. 1. Physical flow and information flow in logistics alliance

3 The Building Process of the 3PL Alliance

Every node in the supply chain can be treated as the united body of correlated supplier、the 3PL enterprise and customer, the close supplier and customer will together look for the 3PL enterprise to provide the logistics service. The 3PL enterprise will aperiodically release their logistics information on the platform, the supplier and customer can make decision by getting the 3PL enterprise's logistics information. The information sharing platform which are together developed by suppliers, the 3PL enterprise and customer is called an information unit, the whole 3PL alliance supply chain network is made up of n units.

From the systemic point the multilayer supplier, the 3PL enterprise and customer can be integrated in the 3PL alliance of supply chain network, so the collaborative management and the high effective joint of business flow and material control are realized through building information platform.

4 The Constructing Scheme of the 3PL Alliance

The constructing scheme of the 3PL alliance maybe define two types: (1)supplier and customer commonly seek for the 3PL enterprise. After long term cooperation with the supplier and customer, these 3PL enterprises can compose the 3PL alliance, who can share their information with the suppliers and customers , then establish e-commerce information sharing platform and become long term cooperation partners; (2)when the capability of the 3PL alliance's transportation is not enough, the supplier and customer can seek for the 3PL enterprise who provides temporal logistics service through restricting invite public bidding, this 3PL enterprise becomes short term cooperation partner through temporal joining in the alliance and enhancing the capability of the alliance, the temporal leaguing enterprise can also share their logistics information by using the e-commerce platform, so during the short term cooperation the two parties can sign long term cooperation agreement and become long term league if they have the long term cooperation will.

4.1 The Implementing Process of Scheme One

(1) The 3PL enterprise selects collaboration partner(or production logistics sector within the enterprise).
(2) Discuss every party's right and obligation during the cooperation.
(3) Establish the relation, sign the cooperation agreement.
(4) Three parties join in the information platform by one unit, implementing the information sharing in the prescribing range of the agreement.
(5) Establish the total goal, sharing each demand information, together forecast and decide the order and the plan of shipment, and adjust the logistics facilities at the right time and right capacity to respond the demand plan according to the shipment plan by the member logistics enterprise.
(6) Through monitoring, locating and tracking of logistics process, every party will realize the visualization of business process.

(7) Finding the supplier, customer, and member logistics enterprise's deficiency and exceptive instance during the operating process, solving with cooperation.
(8) Distinguishing the problem existing in the information sharing and operation with cooperation, improving continuously and pursuing the seamless connection.

4.2 The Implementing Process of Scheme Two

(1) The 3PL enterprise with capability of transportation endorses agreement with the alliance and joins in the 3PL alliance with the league member and makes use of the e-commerce platform.
(2) Every unit in the supply chain establishes the whole goal, shares each demand information, together forecasts the order and shipment plan, publishes them on the e-commerce information platform of the 3PL alliance.
(3) Other 3PL enterprise can see all kinds of freight demand and requirement of the whole supply chain from logistics invite public bidding, according to self carrying capacity, and bid premising that can respond to the requirement rapidly and effectively.
(4) Related supplier and customer together choose the bidder and cooperate with them, then they form short term or long term cooperation fellowship and realize the information sharing.
(5) According to the shipment plan the logistics alliances the 3PL enterprise adjusts the logistics facility and responds to demand plan at right time, right place and right capacity.
(6) Every party in the league realizes the visualization of business process through monitoring, locating and tracking of logistics process.
(7) Finding the supplier, and member logistics enterprise's deficiency and exceptive instance during the operating process , solving with cooperation.
(8) Discovering and distinguishing existing problem during information sharing and operation with cooperation, improving in time, evaluating the short term leaguing 3PL enterprise by logistics alliance, and deciding to whether continue long term cooperation or not.

5 The Structure of the 3PL Alliance System Platform Based on e-Commerce

The system's platform structure is shown as figure 3:

The e-commerce platform begins to arrange distribution according to contract parties' agreement, the place of picking up the goods is arranged according to both claims and optimization scheme, the distribution route and the member enterprise of delivery are chosed. A whole distribution scheme is coming into being, then the distribution scheme is submitted to the contract parties as soon as possible, after the contract parties accept it, the distribution center is notified to pickup and delivery according to the distribution scheme, the deal is completed.

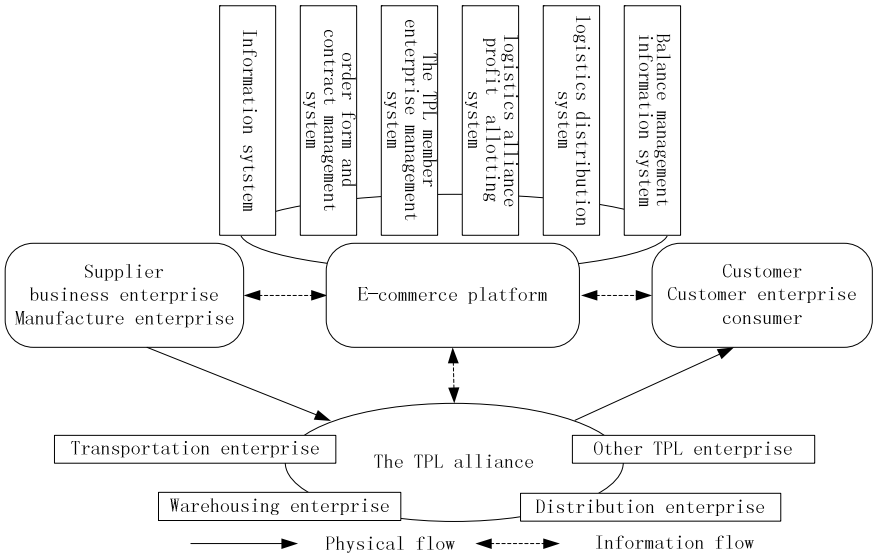

Fig. 2. The structure of the system platform

The module of e-commerce platform system and function are shown as follow:

(1) information system

Information system is the window that the 3PL member enterprises enter into e-commerce system and make e-commerce business, which includes page layout, page content maintenance, client register, client submitting order form and etc. Member enterprise and ordinary trade customer can both browse the web, enter into the e-commerce system and make business.

(2) order form and contract management system

Order system has the function of receiving the order form, checking, processing, feedback and other business activities, which has the section of physical distribution order comparing with the ordinary order dealing process. Client contract is the gist of business process and fare settlement, the system reasonably allots the implementing scheme and charge standard of logistics service through the contract's standardization, patternization and process standardization.

(3) The 3PL member enterprise management system

The 3PL member enterprise management system is a system that fully manages the 3PL distribution member enterprise distributing every where. Besides the customer register, customer authentication, credit management in general customer management system, there should add a management system evaluating the competence of logistics enterprise.

(4) logistics alliance profit allotting system

This system synthetically assesses the 3PL alliance member by multi-factors and makes the profit allotting according the contribution during the collaborating. The profit allotting model considers not only the investment and risk profit, but also the member enterprise's workload and technique value with it's comprehensive strength.

(5)logistics distribution system

Logistics distribution system is the core of system, which includes: Distribution system management, distribution routing optimization management, transportation management system, dispatching management information system, GPS tracing system.

(6)Balance management information system

This system's main function include: toll rate and price management, fare maintenance and balance, fare statistic and apportion, budget management, account receivable/account payable management, verification management, invoice management, account aging analysis, cost benefit analysis, balance management.

6 Conclusion

At present the 3PL market share is small in our country, the overall scale of the 3PL enterprise is relatively limited, and the management level is rather low, the service function is single, the level of information level is backward. After making up of the 3PL alliance, the basic resource with the advantage of e-commerce informationization is extended at crossing domain or crossing regional. The soft resource is getting perfect, the predominant resource is complementary, each resource is expanded to some extent, the effect is obtained that logistics market is commonly developed, the logistics cost is reduced and the logistics benefit is improved. This study will have significantly realistic meaning for our country's e-commerce and the 3PL development.

References

1. Liu, H.: E-commerce Logistics Mode and its Development Trend. China Economist (8) (2009)
2. Wei, S.: Research on the Logistics Model under the E-business Environment. Wuhan University of Technology master degree thesis (2006)
3. Wang, P.: Logistics Stratagem Alliance Stability Analysis. Comprehensive Transportation 3 (2004)
4. Xie, H.: Development of the 3PL Alliance Information System Based on B/S Structure. Logistics Technology (4), 123 (2010)
5. Yang, H.: Study on the Establishment of the Third Party Logistics Enterprise's Dynamic Alliance. Changan University Master degree's thesis (2007)
6. Peng, B., Gu, X., Hu, R.: Study on Network Collaborative Mode of Third Party Logistics Alliance. Commercial Research (4), 165–167 (2006)

A Fast Indexing Algorithm Optimization with User Behavior Pattern

Zhu Wang, Tiejian Luo*, Yanxiang Xu, Fuxing Cheng, Xin Zhang, and Xiang Wang

Graduate University of Chinese Academy of Sciences (GUCAS)
19(A) Yuquan Rd., Beijing 100049, China
wangzhubj@gmail.com, {tjluo,xuyanxiang}@gucas.ac.cn,
chengfuxing07@mails.gucas.ac.cn, zhx040688@163.com,
wangxiang1124@foxmail.com

Abstract. Internet users' access pattern for objects has been observed to follow Zipf's law. The preference for network resource is showing strong influence on real-time lookup performance in large-scale distributed systems. In order to guarantee search response rate with limited memory space, we develop a new object indexing and locating algorithm called Bloom filter Arrays based on Zipf's-distributed user Preference (ZPBA). The algorithm uses a compact data structure to achieve high accuracy in item lookup. We give the theoretical analysis of ZPBA and then conduct experiments with one million item corpus and 100,000 queries to validate our design. Comparison shows that our solution can be 77% more space efficient than traditional bloom filter based index approaches for applications of concentrated user access preference. The algorithm demonstrates practical application potential in fault tolerant large-scale distributed indexing and item lookup.

Keywords: bloom filter, Zipf's law, object locating, indexing, ZPBA.

1 Introduction

The rapid Internet growth in recent years leads to the fact that many applications are supported by distributed systems. Those systems contain a large number of objects and require fast item lookup. The goal of efficient and effective object locating in large-scale distributed online systems brings about challenges for object indexing and retrieval, which are the key technique in content management. Therefore, how to design an efficient object indexing and lookup algorithm which is scalable and assures the high performance is the fundamental issue in modern online systems.

The differentiated user preference complicates the problem as well. User preference for objects and the likelihood that a user requests a certain item varies from case to case. The phenomenon can lead to problems, such as the imbalance in index workload, etc.

Bloom filter is a data structure proposed for representing a set of objects and for supporting membership queries at a low cost rate of false positive probability [13].

* Corresponding author.

Q. Zu, B. Hu, and A. Elçi (Eds.): ICPCA-SWS 2012, LNCS 7719, pp. 592–605, 2013.

The simple mathematical format offers a high item indexing and lookup performance while requiring a small storage resource. Actually, many online systems, which emphasize fast item retrieval and can tolerate a small false rate, are now using bloom filters as their key object management component. Standard bloom filter, however, does not suit for the differentiated user query pattern in many Internet applications. The algorithm treats items equally, regardless of their popularity. That causes a waste of indexing space for "cold" items and affects system performance. In this paper, we present a new algorithm, the Bloom filter Arrays based on Zipf's-distributed user Preference (ZPBA), to handle the object indexing and locating problem. The algorithm utilizes the differentiated query frequency in indexing and locating objects. We establish a compact data structure (HBF) for indexing "hot" items and maintain a larger data structure (HBF) for the entire corpus. The HBF is adjusted to be very precise with low false positive rate while the CBF is relatively less precise. The index building procedure is completed with the accomplishment of HBF and CBF. In lookup procedure, all queries are first directed to HBF. Since all "hot" items are indexed by HBF, according to Zipf's law, a large proportion of them will be hit(find a match in HBF) and the lookup procedure ends successfully. The remaining unmatched items will then be redirected to CBF for a second look up. Because of the compact size, high accuracy and high hit rate of HBF, the overall system accuracy will rise and total space usage will drop down. In that way, ZPBA ensures a satisfactory performance compared to the standard bloom filter technique.

The rest of the paper is organized as follows: In section two we present the related work of our research. Section three describes our algorithm and corresponding data structure. We also analyze the theoretical performance of the method. In section four we use experiments to examine the performance of the proposed algorithm. Finally, section five concludes the paper with some future work.

2 Related Work

We first introduce Zipf's law on the Internet and then describe some standard indexing techniques.

2.1 Zipf's Distribution and Zipf-Like Distribution

The basic user activity in Internet system is to send a content query and receive response. The user requests in many online systems are observed to be differentiated between identical objects. That is to say, the frequency of user request for different objects varies from one item to another. The phenomenon is reported in many independent research papers. Work of [1] claims that user requests for terms in information retrieval system follow Zipf's law. Researchers in [2] find term frequency follows the Zipf's distribution. In Zipf's distribution [3], the top twenty percent of ranked items account for a major part of the total query probability. Zipf's law states that the probability of a ranked object is inversely proportional to its rank.

$$P_i = C \cdot i^{-1} \tag{1}$$

Here C is a constant. i is the rank of the object. P_i is the probability of the item occurrence.

[4] [5] [6] [7] discover that Internet applications like web cache do not follow Zipf's law but has a Zipf-like distribution instead. The Zipf-like distribution can be described as

$$P_i = C' \cdot i^{-\alpha}, \alpha < 1 \tag{2}$$

Total number of items is N, which is very large. Using normalization condition and conclusions in [8] we have

$$C = \frac{1}{\ln N}, C' = \frac{1-\alpha}{N^{1-\alpha}-1} \tag{3}$$

Bring C and C' into the original probability description, we have

$$P_i(\alpha) = \begin{cases} \frac{1}{i^{\alpha} \cdot \ln N} & \alpha = 1 \\ \frac{1-\alpha}{i^{\alpha}(N^{1-\alpha}-1)} & \alpha < 1 \end{cases} \tag{4}$$

Here we regard the Zipf's distribution as a special case of Zipf-like distributions. The fact that many applications have differentiated user requests can have a notable impact on Internet system performance, especially on object indexing and lookup. A "hot" item which arouses many query requests can cause workload imbalance while a "cold" item may be wasting its allocated resource if both items are treated equally in an indexing system. Therefore, the differentiated query frequency for items complicates the indexing design. On the other hand, it may provide an opportunity for system architects to improve performance by using the observed rule.

2.2 Indexing Technique on the Internet

Before ZPBA, there are several indexing and locating techniques that deal with the object lookup task.

2.2.1 Database

Traditional database [9] stores the object as an entry in a table and performs item lookup by searching the item key in the table. The database offers a straightforward way to store the item itself and its metadata and receives a widespread usage on the Internet. Until now, database is still an irreplaceable storage method in most of the online applications. However, owing to the linearity nature of tables, database suffers from low lookup pace and large storage cost.

2.2.2 Hash Table

Hash table [10] [11] transforms object lookup into calculation by mapping the item onto a hash value, and replaces the traditional metadata table with a hash table. In this

way, the storage space is reduced and item lookup is accelerated. However, in order to maintain the consistency of hash functions, the data structure restricts the freedom of content placement and requires the object migration when storage nodes are inserted or deleted.

2.2.3 Tree-Based Index

Tree-based index [12] stores table contents into a tree structure and performs item insertion and lookup along the path of the index tree. The data structure accelerates the item lookup by using a binary search but requires a large scale content migration to maintain load balance.

2.2.4 Bloom Filter

Bloom filter [13] works as an index which records all elements of a set. We may assume that set $S=\{x_1,x_2,\ldots,x_n\}$, which consists of n elements. A Bloom Filter vector (BFV), which consists of m bits, is used to represent elements of set S. All bits of the vector are set to zero initially. For each element, the algorithm uses k hash functions $\{h_i\}_{i=1\ldots k}$ to map the element onto k positions of the vector and set the bit on the position to 1. The k functions ranging from 1 to m are independent from each other and can map elements of the set S to a random place on the vector. During the insertion period, the algorithm maps all elements of the set to load the BFV with all the information of the elements. Figure 1 shows the element insertion.

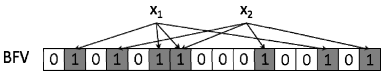

Fig. 1. Element Insertion

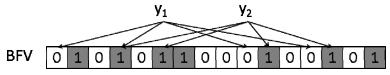

Fig. 2. y2∈S, y_1 doesn't

In lookup procedure which we want to check whether an element y belongs to the set S, the algorithm uses the same hash functions to map y onto k locations and check whether all $h_i(y)$ equal to 1. If the answer is no, we conclude that y doesn't belong to S, otherwise, we say y belongs to S. Figure 2 shows the look up procedure.

It needs to be mentioned that there is a probability that elements don't belong to S be judged as inside S by BF. That is to say, BF has a false positive rate. [13] shows that the false positive rate can be represented as follows:

$$f_{FP} = \left(1 - e^{-\frac{kn}{m}}\right)^k \tag{5}$$

f_{FP} reaches minimal value when

$$k = \frac{m}{n}\ln 2 \tag{6}$$

Due to its simple structure and smooth integration characteristic, the mathematical format allows considerable potential improvement for system designers to develop new variations for their identical application requirement [14] [15]. Counting bloom filters [16] [17] [18] can be used to improve network router performance [19]. Other variations are adopted in state machines [20], IP trace back [21] and publish/subscribe networks [22]. In this paper, we focus on fast object lookup in distributed systems. There are also many algorithms designed to deal with that problem.

2.2.4.1 Pure Bloom filter Array. Pure Bloom filter Array (PBA) [23] [24] uses one standard bloom filter to represent items on one node and performs lookup operation in the bloom filter arrays. The method achieves a high performance in nondiscriminatory object queries but doesn't handle well the popularity-biased requests.

2.2.4.2 Weighted Bloom Filter. Weighted Bloom Filter (WBF) [25] takes the query frequency and object popularity into consideration. The data structure uses different numbers of hashes for different object popularity level. "Hot" items are calculated with more hash functions and "cold" ones use less hashes. In that way, the false positive rate of "hot" items decreases and the overall system performance increases. However, Weighted Bloom Filter needs to obtain the prior distribution of each queried item and calculate proper hash number in real time before each insertion and lookup procedure. That increases time complexity and degrades system response.

2.2.4.3 Hierarchical Bloom filter Array. Hierarchical Bloom filter Array (HBA) [23] uses two bloom filters to store items, one for least recently used objects and one for entire objects. When a query arrives, the first bloom filter is checked and if there is a miss, the second one is examined. Since the first bloom filter stores much fewer objects than the second one, the overall system performance can be improved. That approach, however, uses only bloom filters to judge the item existence and lacks the real object locating mechanism. The result is correct only with a certain probability. Moreover, if more than one node in the system reports a positive response for one query, the system cannot judge which one is the correct one. The more the nodes, the larger probability two nodes conflicts in, and the more likely the search fails. From that aspect, the scalability of the algorithm needs to be carefully evaluated.

In this paper, we present a new algorithm called Bloom filter Arrays based on Zipf's-distributed user Preference (ZPBA). The method takes the imbalanced item popularity into consideration and optimizes the lookup performance by handling "hot" items and "cold" items separately. The algorithm chooses a certain number of "hot" items according to a threshold and stores them in a more reliable, efficient bloom filter. After each bloom filter search, the algorithm checks the result immediately. If there is a true positive response, the search procedure stops and the result is returned to the user directly. In that way, the algorithm obtains a satisfactory performance for the Zipf's and Zipf-like distributed objects queries.

3 ZPBA Design

In this section we describe the design of our ZPBA algorithm. ZPBA is used to set up an index structure for items in large-scale distributed systems and perform fast item lookup. For comparison, we first present the traditional Pure Bloom filter Array (PBA) design and then show our own design. At last, the performance analysis is provided.

3.1 Pure Bloom Filter Array (PBA) Design [23] [24]

3.1.1 System Environment

We first consider a simple use case. The distributed system consists of s nodes; each node stores approximately n unique objects, so the entire system holds ns unique objects. We further assume that those objects' distribution on the nodes is in uniform distribution, so the probability of one object occurring on a node is 1/s.

3.1.2 Index Building

For one node, we insert all of its elements into a bloom filter. We repeat the process in the distributed system and establish a bloom filter for each node. These bloom filters (also referred to as Pure Bloom filter Arrays) are then loaded with all the items in the entire system and can now act as an indexing system.

3.1.3 Object Locating

The system first checks whether the object exists in node 1. It first looks the object up in the BFV, if the answer is no, it goes on to look up in node 2; if the answer is yes, it means that the object possibly exists in node 1, but with a small probability that the real situation is not, so the system has to search in the real node to actually find the object. If it does find the object, the locating process finishes; if not, which means the Bloom Filter raises a false negative case and the object doesn't exist in node 1, system will have to continue searching for node 2 until it finally finds the object.

3.2 Bloom Filter Arrays Based on Zipf's-Distributed User Preference (ZPBA)

The Zipf's law implies that the top twenty percent of all ranked items account for a majority of user queries. That phenomenon inspires us to improve the PBA design. Unlike the basic PBA which treats each item equally, we try to bias better "service" for "hot" items and comparatively poor "service" for "cold" items in ZPBA.

3.2.1 System Environment

The environment of ZPBA is mostly the same as that in PBA. All items are distributed uniformly among nodes and the system parameters, n and s remain unchanged for easy comparison. The only difference is that user requests in ZPBA use case follow the Zipf-like law while PBA does not take the user preference into consideration.

3.2.2 Index Building

PBA puts all elements into a single bloom filter, regardless of the elements' popularity. According to the Zipf's law, however, a small portion of items (i.e., "hot" items) attracts a majority of user requests. These items are then considered to be important and deserve the better treatment. Thus, in ZPBA, we keep the common bloom filter (CBF) for storing the entire elements of the node and add an additional bloom filter, the "hot" item bloom filter (HBF), to store "hot" items of the node. "Hot" item bloom filters are adjusted to perform more accurately in finding the requested item (with lower false positive rate) than the common bloom filter, so the overall false positive rate will be reduced. Since the volume of "hot" items is quite small in comparison with the whole item set, the size of "hot" item bloom filter can be compact as well. In that way, we achieve a much lower system false positive rate just with a small increase in storage space.

3.2.3 Object Locating

Like PBA, ZPBA system also tries to find the answer for a query through two steps, namely the approximate search with bloom filter and by-node validation. The main difference is that ZPBA first looks up the item in the "hot" item bloom filter layer, one HBF by one HBF. If a match reports in HBFs, the system directly checks the matched node to find the real answer. If the item does exist in the node, the lookup procedure stops and the item is returned to the user. If none of the HBFs finds the requested item, the system goes down to search the CBF layer until it identifies a match. The lookup algorithm can be described as follows:

```
Input: ObjectID
Output: NodeID
for NodeID=1:s
    Calculate hash positions {P_H} in HBF with HBF hash functions {hash_H}
    if all positions HBF{P_H}==true
        Search for object in the node
        if searchinnode(NodeID, ObjectID)==false    continue;
        else    return NodeID;
end;
for NodeID=1:s
    Calculate hash positions {P_C} in CBF with CBF hash functions {hash_C}
    if all positions CBF{P_C}==true
        Search for object in the node
        if searchinnode(NodeID, ObjectID)==false    continue;
        else    return NodeID;
end;
```

Given s, the time complexity of the lookup algorithm is O(s).

3.3 System Performance Analysis

We first look into PBA as a baseline of the new algorithm. Then we analyze the false positive rate of ZPBA.

3.3.1 PBA

All items in PBA are stored in common bloom filters (CBF). Let Q be the total number of queries. From (5) the false positive rate for each bloom filter is

$$f_{CBF} = \left(1 - e^{-\frac{k_C n}{m_C}}\right)^{k_C} \tag{7}$$

Here m_C is the BF vector length, and k_C is the hash number of CBF.

For the ith common bloom filter on ith node, the number of queries that can cause false positives is

$$q_f(i) = Q - i\frac{Q}{s} \tag{8}$$

Average false positive number per query is

$$F_{PBA}/Q = \frac{\sum_{i=1}^{s} q_f(i) \cdot f_{CBF}}{Q} = \frac{s-1}{2} f_{CBF} \tag{9}$$

3.3.2 ZPBA

ZPBA has two layers of bloom filters: "hot" item bloom filter (HBF) and common bloom filter (CBF). The CBF still stores all the elements on a node, so we just need to investigate the false positive rate of HBF. Let β be the ratio of elements in HBF to elements in CBF. From (5) we have

$$f_{HBF} = \left(1 - e^{-\frac{k_H n \beta}{m_H}}\right)^{k_H} \tag{10}$$

Here m_H is the BF vector length, and k_H is the hash number of HBF.

Let Q be the total number of queries, r the ratio that the number of queries the HBF layer can absorb. The number of queries that can cause false positives with ith HBF on ith node is

$$q_{fH}(i) = q_H(i) - \frac{rQ}{s} = Q - \frac{i}{s} rQ \tag{11}$$

When it comes to lookup the CBF layer, there are only Q(1-r) queries remaining. The number of queries that can cause false positives in ith HBF on ith node is

$$q_{fC}(i) = q_C(i) - \frac{(1-r)Q}{s} = Q(1-r) - \frac{i}{s} Q(1-r) \tag{12}$$

Average false positive number per query is

$$F_{ZPBA}/Q = \frac{\sum_{i=1}^{s} q_{fH}(i) \cdot f_{HBF} + \sum_{i=1}^{s} q_{fC}(i) \cdot f_{CBF}}{Q} = \left(s - \frac{s+1}{2} r\right) f_{HBF} + \frac{s-1}{2}(1-r) f_{CBF} \tag{13}$$

4 Experimental Evaluation

We perform experiments to simulate real online applications. Then we make comparison between the experimental result and the theoretical analysis. In all experiments we set node number s=100, the total number of items $N=10^6$. The items are scattered randomly among s nodes, so each node has approximately $n=10^4$ items. The probability that an object be allocated in one node is identical among all servers. The total query number $Q=10^5$.

4.1 PBA Approach

We first use the PBA approach as a baseline of our new approach. Figure 3 shows the result.

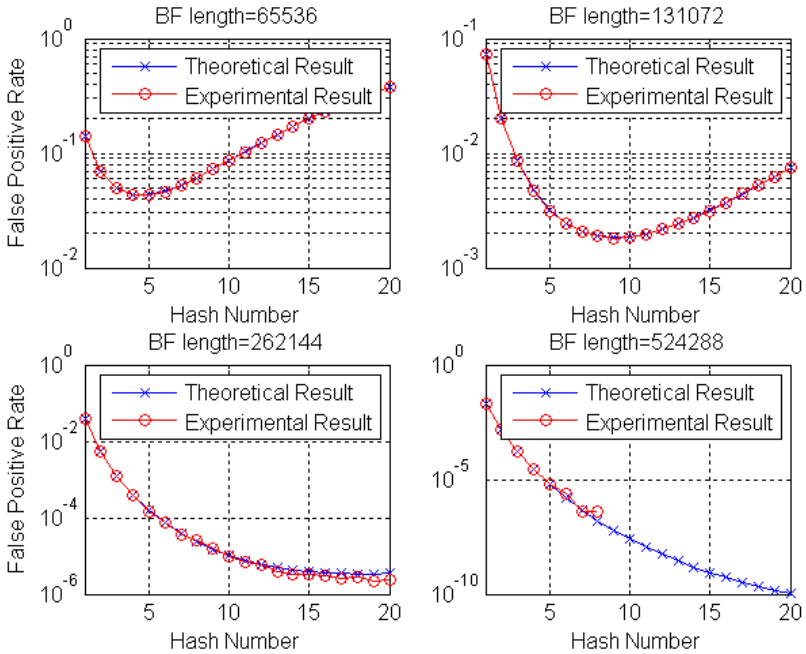

Fig. 3. PBA approach

From the figure we can see that the experimental result is very close to the theoretical result. The latter separation of the two in the third and fourth figure is caused by the small number of experimental observations. Thus we can have a basic understanding of bloom filters that it is more practical when its size is larger.

4.2 Basic Experiments with α=1 and β=0.1

We consider a simple situation. The entire corpus follows the standard Zipf's law (α=1) with total number $N=10^6$. The queries reflect the real popularity of the corpus, so the queries follow the same distribution as the corpus. Actually, queries are formed as a sampling set of Zipf's law with parameter $N=10^6$, not the query number 10^5.

In each node, as stated above, there are approximately $n=10^4$ items. All items are stored in CBF. We set β=0.1, meaning one tenth of the items of a node are stored both in HBF and in CBF. In actually processing, we first order all items in a node by the popularity rank and pick the first "hot" βn items. Then we construct the HBF for those "hot" objects. By then the ZPBA construction is finished. All hash numbers satisfy the optimal value in (6). The ratio that a queried item exists in HBF is

$$r = \sum_{i=1}^{N\beta} P_i = \sum_{i=1}^{N\beta} \frac{1}{i \ln N} \approx \frac{\ln(N\beta)}{\ln N} = 0.833 \tag{14}$$

After index construction we perform query lookup in the system. Every query returns a result. We then count the false positives. We set m_C to be 2^{16}, 2^{17} and 2^{18}. For each m_C we choose m_H to run from $m_C/8$, $m_C/4$ to $m_C/2$. The experimental result of false positives per query is given in Figure 4, where the theoretical result is calculated by (12).

False positive number per query is a key performance indicator in indexing systems. It reflects the average false positive rate occurring in one query lookup. From the figure we see that false positive per query is very low in some situations, around 3×10^{-5}, which means there will be only one false positive every 30,000 queries. All ZPBAs perform better than PBAs and the performance improves with the increase of m_C and m_H, as expected. Furthermore, the experimental result of ZPBA merges well with our theoretical analysis.

4.3 Experiments with α=1 and Varying β

We want to analyze the impact of β. We set β values to be 0.05, 0.1 and 0.2 and rebuild the index with each identical β. Then we repeat the query lookup. The change of average false positives per query is given in Figure 5.

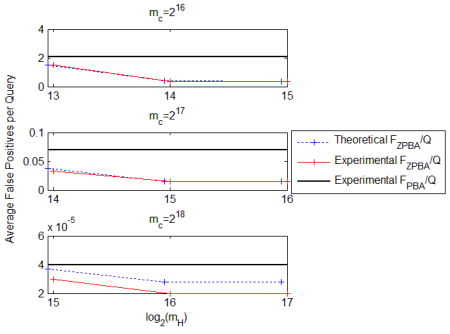

Fig. 4. FZPBA/Q of ZPBA and PBA

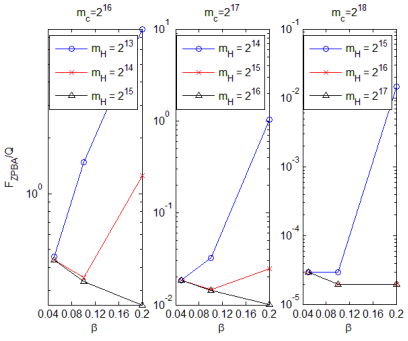

Fig. 5. False positive per query with β

We can see that when m_H is relatively small, the average false positive rate per query increases with the raise of β. That is interpreted by the heavier load in HBF and the higher false positive rate. When m_H is large, the average false positive rate may decrease with the increase of β. The reason for that is when there are more items in HBF, the hit rate of HBF becomes higher, resulting in the increase of system performance. However, since the hit rate gain is relatively small compared with the increase of β, the system performance just has a limited improvement.

4.4 Experiments with Varying α

In further experiment we want to investigate the effect of α. For each β, we use different α (0.7, 0.8, 0.9 and 1) to run the experiment. The result is given below.

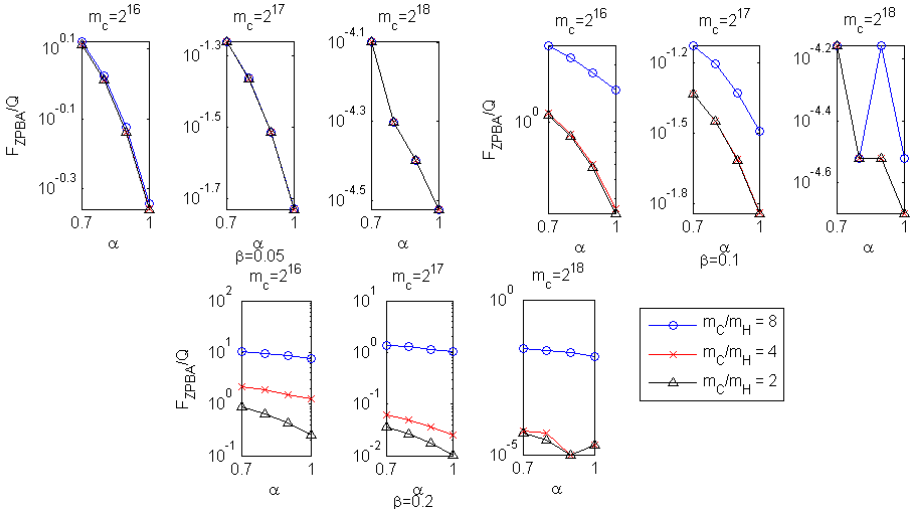

Fig. 6. The effect of α in ZPBA

We can see that in most circumstances, the system performance increases with α (the exceptions are caused by low experiment dataset where false positive rate per query is very low - less than 10^{-4}). Actually, α is the symbol indicating the concentration of user queries. Larger α and bigger hit rate on HBF results in the better system performance.

4.5 System Performance Evaluation

Now we show the performance of our algorithm. We set $m_C=2^{15}$ and observe the false positive rate per query with different α, β and m_H. The result is given in Figure 7.

We can see when α and β are large enough, our algorithm can achieve a lower false positive rate per query than PBA with the same space consumption (when $m_H=m_C=2^{15}$ and $m_{PBA}=2^{16}$). That reveals the advantage of our algorithm: higher space efficiency than standard PBA. We define a new evaluation metric

$$SE \equiv \frac{1}{M \cdot F/Q} \tag{15}$$

Here M is total space used; F/Q is false positive per query. The smaller the F/Q, the smaller the space usage, the larger the SE, and the larger the space efficiency is. So SE is an indicator that reflects the space efficiency of the data structure. The comparison of ZPBA space efficiency and that of PBA is given below in figure 8:

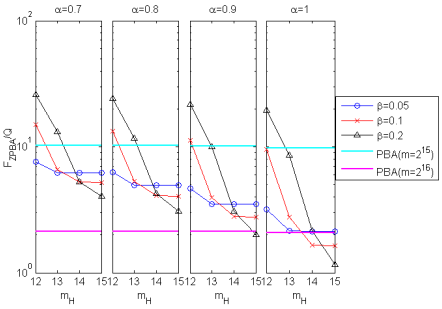

Fig. 7. FZPBA/Q when $m_C=2^{15}$

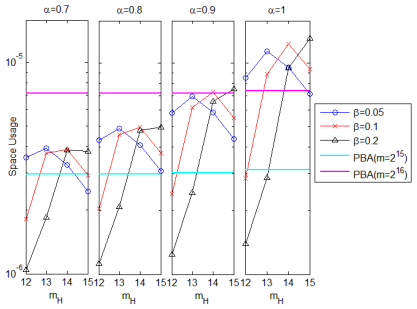

Fig. 8. Space efficiency comparison

We can see that our algorithm achieves a better performance when α is large enough. The space efficiency can be improved by 77%. That is to say, ZPBA performs well in the concentrated user preference system, where it can outperforms standard PBAs in terms of space efficiency.

5 Conclusion and Future Work

In this paper we first survey the user behavior pattern on the Internet. We find that user queries in many applications follow the Zipf's or Zipf-like distribution. Inspired by that phenomenon, we develop a novel indexing and lookup algorithm, ZPBA. We compare our method with traditional PBAs and show that our algorithm can achieve similar performance with the traditional one but is more space-efficient when user preference for objects is concentrated.

Zipf's law is one of the many rules used to describe Internet user behavior. Other descriptions such as step distribution, Benford's law and Long Tail distribution need also to be considered in our algorithm in future work. The design of the data structure has to be adjusted to fit new distributions and their combinations.

The proposal in the paper is an ideal solution in a near-perfect scenario. In real applications, system function requirement may differ from case to case. For example, it may be necessary to consider whether to find all copies of a given item; whether to allow item deletion in bloom filter structure; whether to support approximate lookup, etc. We need to keep improving our algorithm to satisfy user needs in actual environment.

Moreover, the synchronization mechanism and communication method of ZPBA need further attention as well. In design, we will consider the prior knowledge of the item distribution, query distribution and their internal dependency. The usage pattern such as update rate and query frequency will have impacts on the algorithm.

References

1. Chierichetti, F., Kumar, R., Raghavan, P.: Compressed Web Indexes. In: 18th International Conference on World Wide Web, pp. 451–460. Association for Computing Machinery, New York (2009)
2. Sato, I., Nakagawa, H.: Topic Models with Power-law using Pitman-Yor Process. In: 16th ACM SIGKDD International Conference on Knowledge Discovery and Data Mining, pp. 673–682. Association for Computing Machinery, New York (2010)
3. Zipf, G.K.: The Psychobiology of Language. Houghton-Mifflin, Boston (1935)
4. Breslau, L., Pei, C., Li, F., Phillips, G., Shenker, S.: Web Caching and Zipf-like Distributions: Evidence and Implications. In: IEEE Annual Joint Conference of the IEEE Computer and Communications Societies, pp. 126–134. IEEE Press, New York (1999)
5. Rodriguez, P., Spanner, C., Biersack, E.W.: Analysis of Web Caching Architectures: Hierarchical and Distributed Caching. IEEE/ACM Transactions on Networking 9(4), 404–418 (2001)
6. Kotera, I., Egawa, R., Takizawa, H., Kobayashi, H.: Modeling of Cache Access Behavior Based on Zipf's Law. In: 9th Workshop on Memory Performance: Dealing with Applications, Systems and Architecture, pp. 9–15. Association for Computing Machinery, New York (2008)
7. Jelenković, P.R., Kang, X.: Characterizing the Miss Sequence of the LRU Cache. ACM SIGMETRICS Performance Evaluation Review 36(2), 119–121 (2008)
8. Zorich, V.A., Cooke, R.: Mathematical Analysis. Springer, Berlin (2004)
9. Ozsu, M.T., Valduriez, P.: Principles of Distributed Database Systems, 3rd edn. Springer, Berlin (2011)
10. Stoica, I., Morris, R., Karger, D., Kaashoek, M., Balakrishnan, H.: Chord: A Scalable Peer-to-peer Lookup Service for Internet Applications. In: 2001 Conference on Applications, Technologies, Architectures, and Protocols for Computer Communications, pp. 149–160. Association for Computing Machinery, New York (2001)
11. Ratnasamy, S., Francis, P., Handley, M., Karp, R., Shenker, S.: A Scalable Content-Addressable Network. In: 2001 Conference on Applications, Technologies, Architectures, and Protocols for Computer Communications, pp. 161–172. Association for Computing Machinery, New York (2001)
12. Weil, S.A., Pollack, K.T., Brandt, S.A., Miller, E.L.: Dynamic Metadata Management for Petabyte-Scale File Systems. In: 2004 ACM/IEEE Conference on Supercomputing, p. 4. IEEE Computer Society, Washington, DC (2004)
13. Bloom, B.: Space/time Trade-offs in Hash Coding with Allowable Errors. Communications of the ACM 13(7), 422–426 (1970)
14. Tarkoma, S.C., Rothenberg, E., Lagerspetz, E.: Theory and Practice of Bloom Filters for Distributed Systems. IEEE Communications Surveys & Tutorials 14(1), 131–155 (2004)
15. Wang, Z., Luo, T.-J.: Intelligent Video Content Routing in a Direct Access Network. In: 3rd Symposium on Web Society, pp. 147–152. IEEE Press, New York (2011)
16. Fan, L., Cao, P., Almeida, J., Broder, A.Z.: Summary Cache: A Scalable Wide-Area Web Cache Sharing Protocol. IEEE/ACM Transactions on Networking 8(3), 281–293 (2000)

17. Bonomi, F., Mitzenmacher, M., Panigrahy, R., Singh, S., Varghese, G.: An Improved Construction for Counting Bloom Filters. In: Azar, Y., Erlebach, T. (eds.) ESA 2006. LNCS, vol. 4168, pp. 684–695. Springer, Heidelberg (2006)
18. Ficara, D., Giordano, S., Procissi, G., Vitucci, F.: Multilayer Compressed Counting Bloom Filters. In: 27th Annual Joint Conference of the IEEE Computer and Communications Societies, pp. 311–315. IEEE Press, New York (2008)
19. Song, H., Dharmapurikar, S., Turner, J., Lockwood, J.: Fast Hash Table Lookup using Extended Bloom Filter: an Aid to Network Processing. In: 2005 Conference on Applications, Technologies, Architectures, and Protocols for Computer Communications, pp. 181–192. Association for Computing Machinery, New York (2005)
20. Bonomi, F., Mitzenmacher, M., Panigrah, R., Singh, S., Varghese, G.: Beyond Bloom Filters: from Approximate Membership Checks to Approximate State Machines. In: 2006 Conference on Applications, Technologies, Architectures, and Protocols for Computer Communications, pp. 315–326. Association for Computing Machinery, New York (2006)
21. Sung, M., Xu, J., Li, J., Li, L.: Large-scale IP Traceback in Highspeed Internet: Practical Techniques and Information-theoretic Foundation. IEEE/ACM Transaction on Networking 16(6), 1253–1266 (2008)
22. Jokela, P., Zahemszky, A., Esteve, C., Arianfar, S., Nikander, P.: LIPSIN: Line Speed Publish/Subscribe Inter-Networking. In: 2009 ACM SIGCOMM 2009 Conference on Data Communication, pp. 195–206. Association for Computing Machinery, New York (2009)
23. Zhu, Y., Jiang, H., Wang, J., Xian, F.: HBA: Distributed Metadata Management for Large Cluster-Based Storage Systems. IEEE Transactions on Parallel and Distributed Systems 19(6), 750–763 (2008)
24. Wang, Z., Luo, T.: Optimizing Hash Function Number for BF-Based Object Locating Algorithm. In: Tan, Y., Shi, Y., Ji, Z. (eds.) ICSI 2012, Part II. LNCS, vol. 7332, pp. 543–552. Springer, Heidelberg (2012)
25. Bruck, J., Gao, J., Jiang, A.: Weighted Bloom Filter. In: 2006 IEEE International Symposium on Information Theory, pp. 2304–2308. IEEE Press, New York (2006)

An FPGA Real-Time Spectrum Sensing for Cognitive Radio in Very High Throughput WLAN

Zhigang Wen, Zibo Meng, Qing Wang, Lihua Liu, Junwei Zou, and Li Wang

School of Electronic Engineering
Beijing University of Posts and Telecommunications
Beijing, P.R. China, 100876
zwen@bupt.edu.cn, llhbupt@sina.com

Abstract. In this paper, a spectrum sensing module of cognitive radio for a high speed WLAN is proposed, which aims at a G-bit data transmission rate. Energy detection for spectrum sensing is selected due to its needless of knowledge of PU signal. Also, a new method of adaptive threshold generation mechanism is introduced and accomplished. Both simulation and implementation are done and the performance is analyzed. With all the above work completed, this potential application may be used for the future WLAN to achieve higher performance. In addition, the aspects of potential methods to improve the performance of this module are provided for further study.

Keywords: high Throughput WLAN, cognitive radio, spectrum sensing, energy detection, threshold, FPGA.

1 Introduction

Wireless communications has become ubiquitous in today's society and leading to a dense allocation of relevant frequency bands. Actual measurements [1], however, reflect that most of these frequency bands are vastly underutilized because they are assigned to a single licensed user which cannot be used all the time and stay vacant, while some other wireless users are starving for spectrum resources. The resulting scarcity of the available frequency bands confines many consumer applications to the unlicensed ISM bands which in turn are becoming increasingly crowded. Wireless communications like WLAN in these bands is often limited by mutual interference. However, the need for higher speed WLAN is increasingly fierce.

1.1 WLAN

WLAN (Wireless Local Area Network) has enjoyed a long term evolution from 802.11a, 802.11b, 802.11d, 802.11e, 802.11g, 802.11h, 802.11i, 802.11j, to 802.11n[2] in both capacity and compatibility since the brought out of the first IEEE 802.11 standard which worked at 2.4G and applied FHSS (Frequency-Hopping Spread Spectrum) and DSSS (Direct Sequence Spread Spectrum) to reach up to

Q. Zu, B. Hu, and A. Elçi (Eds.): ICPCA-SWS 2012, LNCS 7719, pp. 606–616, 2013.

2Mbps. And in the year 2008, new amendments are called to improve the performance of 802.11a, in order to form a new standard, that is, 802.11ac which has a high data throughput down to 1Gbps, means a great challenge to the limited spectrum resources.

2 Cognitive Radio and Energy Detection

Cognitive radio (CR), as an agile radio technology, has been proposed to promote the efficient use of the spectrum [3]. By sensing and adapting to the environment, a CR is able to fill in spectrum holes and serve its users without harmful interference to the licensed user. To do so, the CR must continuously sense the spectrum it is using in order to detect the reappearance of the PU (Primary User or Licensed User). Once the PU is detected, the CR should withdraw from the spectrum so as to minimize the interference which may be caused. This is a very difficult task, as various PUs will employ different modulation schemes, data rates, and transmission powers in the presence of variable propagation environments and interference generated by other secondary users. There are 4 methods concerned which will be introduced for spectrum sensing, and they are summarized from both advantages and disadvantages into Table 1 [4]:

Table 1. Methods for Energy Detection

Methods	**Advantages**	**Disadvantages**
Matched Filter Detection	less time to achieve high processing gain	Need prior knowledge of PU; Require dedicate sensing receiver for all primary using signal types
Energy Detection	Needless of prior knowledge of PU	poor performance with low SNR ; threshold used in energy selection depend on noise condition;
Cyclostationary Detection	PU with strong cyclostationary can be detected at very low SNR sensitive to distinct PU &SU cyclostationary characteristics	the auto correlation of signal is required to be a periodic function of time t with some period
Wavelet Detection	Implementation costs Flexibility in adapting to the dynamic spectrum	High sampling rates for characterizing the large bandwidth.

The WLAN system runs at 5.75GHz ~ 5.85GHz, and within it, there are totally 5 channels each has a bandwidth of less than 20MHz, the spectrum allocation is demonstrated in figure 1:

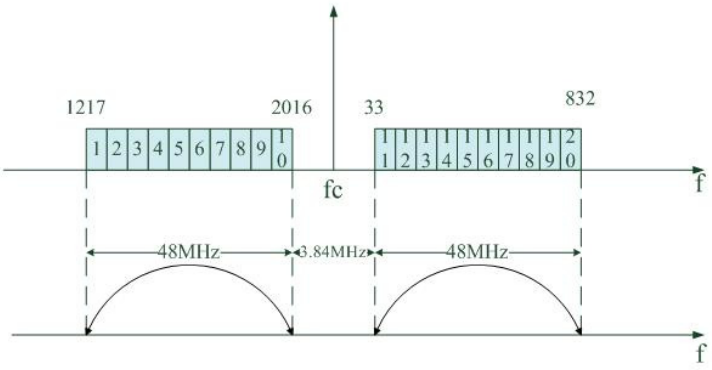

Fig. 1. The spectrum allocation

The "fc" is the frequency center (5.8GHz), and the numbers in the rectangular on the x-axis implies the sub-carriers of the channel (OFDM modulation) and they are grouped as physical-channels of the system, the details are presented in Table2:

Table 2. The correspondence of sub-carriers and physical-channels

Sub-carriers	Physical-channel
1,2,19,20	Channel 1
3,4,17,18	Channel 2
5,6,15,16	Channel 3
7,8,13,14	Channel 4
9,10,11,12	Channel 5

Our sensing goal is to denote an output of 5bits, each of which represents the state of one channel (1 for occupied, and 0 for vacant), for the MAC (Media Access Control layer) to schedule the data streams. The correlations are shown in Table 3 below:

Table 3. The correlations of output and channel states

Output	Channel States
00000	All channels vacant
00001	Channel 1 occupied
00010	Channel 2 occupied
00100	Channel 3 occupied
01000	Channel 4 occupied
10000	Channel 5 occupied

In order to achieve higher data transmission rate, we apply enhanced physical layer technology and enhanced MAC layer technology, MIMO, OFDM, multi-channel CSMA and etc. Considering the universal utilization of WLAN, and knowing little about the PU signals, together with the advance of FFT (Fast Fourier Transformation) algorithm which makes it possible to do FFT on FPGA, energy detection based on FFT is selected as the suitable solution for this system.

2.1 System Structure

With spectrum sensing module inside, the system can get the information of the available channels and decide which channel to use and schedule to achieve the highest efficiency. The structure of MAC layer with energy detection module is illustrated in Figure 2 below:

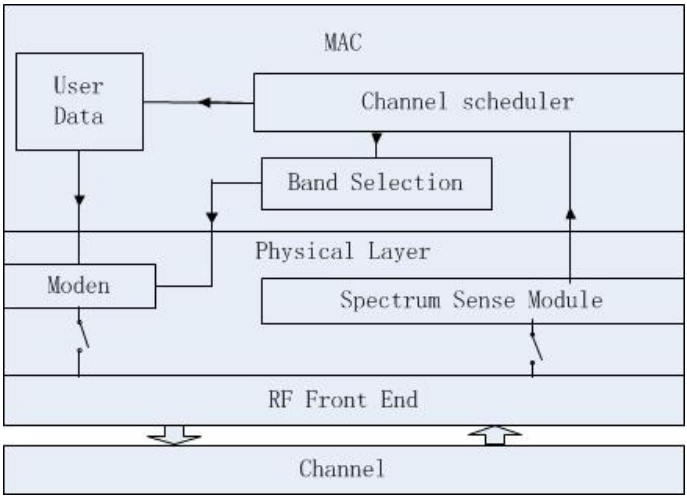

Fig. 2. The structure of system structure

The spectrum sensing module acquires the information of the channels, and sends 5 bits of channel states to the channel scheduler which decides the transmission channel and tells the Band Selector to change the Modern configuration and simultaneously selects the proper user data to the Modern. By all above steps, channels are efficiently utilized.

The rest of this paper is organized as follows: section 1 introduces WLAN, Cognitive Radio and other basic concepts and ideas; section 2 introduces the concrete FPGA implementation of the energy detection module; section 3 analyzes the performance of this module; and section 4 gives the final conclusion of this paper and the future work.

3 Design Implementation

In this section, the design of spectrum sensing module based on FFT algorithm is presented in this section.

3.1 Energy Detection Module

Knowing little of PU signals, we choose energy detection as our main method. Considering that DFT (Discrete Fourier Transformation) which can reveal the features of frequency spectrum as well as power of a signal, FFT is a fast algorithm of DFT, Which is revised for computer computing. The outcome of FFT algorithm is discrete complex points, each of which represents a discrete frequency point, where the first point is 0-frequency-point (or DC component) with its amplitude modulus N times the DC component of the signal, and other frequency points have modulus values of N/2 times the peak of that signal frequency. And the energy of a certain-bandwidth signal is the sum of energy of each frequency point within it, and this can be calculated out by the sum of squares of the amplitudes of the frequency points. OFDM modulation applied to reach a higher efficiency, the signal has a high energy due to multi-carrier modulation, and it is good for energy detection to achieve a precision result (When occupied, the energy in the sub-channel is vastly bigger than that of a vacant one).

FFT is a fast algorithm for DFT. In complex computing, a N points FFT, needs to do $(N-1)^2$ complex multiplies, so the larger N (for example >1000) is, the longer time it will consume that it cannot possibly be done real-timely. There are several methods of improved algorithms, namely Cooley-Turkey's 2-Radixed or 4-Radixed algorithm, which takes advantages of the periodicity and symmetry of the phase factor of DFT. Some other method like split-radix algorithm is not good enough for VLSI implementation. What we apply here is 2-Radix algorithm, which can easily form a pipeline to improve performance.

We can implement these methods in FPGA using Xilinx IP core, which has already developed several versions of FFT IP core. Xilinx LogiCORE IP Fast Fourier Transformation v7.0[5] is an configurable IP core to compute an N-point forward DFT or inverse DFT (IDFT) where N can be , m = 3~16.The principle is Cooley-Turkey's 2-Radixed and 4-Radixed algorithm. Pipeline Streaming I/O mode is our best choice to achieve good time response.

With FFT calculated out, what we should do is to accumulate the proper points of FFT which is a sequence related to the frequencies from 0 to Fs (the AD sampling rate) - yet according to Nyquist Sampling Theorem which said the sampling rate of a signal must be more than 2 times the frequency of the signal sampled-and only 0~Fs/2 is the effective data, and the last Fs/2~Fs is the mirror of the former half about Fs/2.After accumulation, a comparison is needed to decide if the channel is occupied, that is, if the accumulation result is greater than the threshold which is the minimum energy of an occupied channel, the output comparison bit should be registered with the label of the specific channel. Wait until the comparison results of all the channels come out, the final channel state is send to the output port.

3.2 Sub-system Structure

In order to implement the above method, we design the following module as shown in Figure 3:

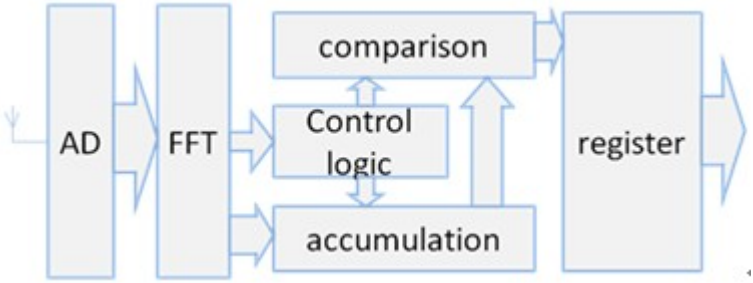

Fig. 3. The structure of spectrum sensing module

From Figure 3, it can be noticed that wireless signals are bandpass-sampled by AD (Analog to Digital) which can cover all the bands of the channel, and with the output data transmitted to FFT IP core, after a certain period of processing time, the outcome of FFT begins to be send to accumulation module, then with enough points calculated, the cumulative results are send to comparison part, and all of the operation after FFT is controlled by a Control Logic module. At last, all the comparison results are registered to form a whole channel state output. This is the main idea of this module, and now comes the solid implementation in Figure 4 below:

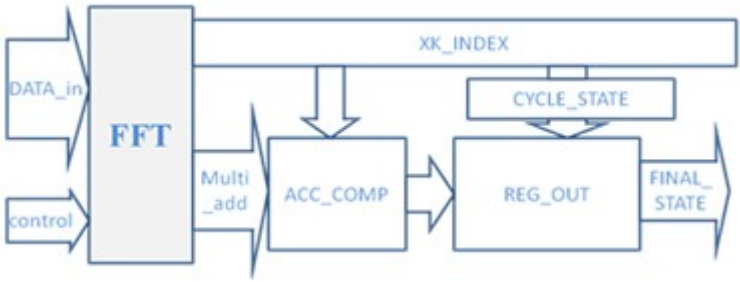

Fig. 4. Sub-modules of implementation

In Figure 4, there are some differences from Figure 3. Initially, some control signals are needed for the initialization of FFT IP core, so a control block is presented, then notice the XK_INDEX signal, that is an output bus of FFT IP, which is used to index each outputs from 0 to 511(if a 512-point FFT is calculated), and by taking advantage of this signal, we can precisely control the accumulation and comparison parts to gain the desire results. For example, the point 0 to 30 is within the first channel, and we want to accumulate the energy of these points, we can tell the

accumulation block to do accumulating when 0<=XK_INDEX<=30, and make the comparison if the comparison block knows XK_INDEX is equal to 31, however, we should consider the delay of the calculation, it is easy to accommodate by just add the number of delay to the XK_INDEX each block referred to, for instance, in the above example, if energy calculation delay is 6 clocks' time, the first XK_INDEX mentioned will be set to 6~36, and the second 37.

There is a CYCLE_STATE module here, and it controls the system to do N cycles of FFT, and then give a mean result for higher stability.

REG_OUT, is the register of the whole system, it accepts every comparison result of the former block and registers the data for each channel, until the whole N cycles FFTs are done, the final mean result is given out with a DONE signal pulse indicates that the final sensing outcome is ready for the next block.

4 Performance Analysis

In this section, two test methods are presented and analyzed, and the result comes out to be acceptable for system requirement. ModelSim® is a product of Mentor Graphics, which has a single kernel simulator (SKS) technology with a unified debug environment for Verilog, VHDL and System C. The combination of industry-leading, native SKS performance with the best integrated debug and analysis environment make ModelSim® the simulator of choice for our design (including Behavioral simulation, Post-translate simulation, Post-map simulation and Post-route simulation).

Xilinx Chipscope Pro® is a kind of real-time system debugging and verification tool, which can enable user to capture and view signal activities inside any of Xilinx® FPGAs through JTAG port.

Tested data should be prepared for the system, and now we use Matlab to generate a controllable data stream instead of AD outputs, which is compound of a DC signal and a signal with the frequency of 500Hz, as shown in the Figure 5.

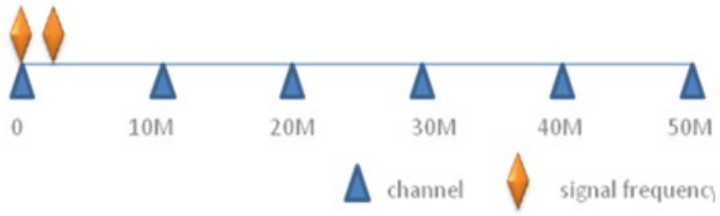

Fig. 5. The spectrum of the tested signal

The result can be predicted to be 10000 referred to the channel allocation in the 2nd section of this paper, only the 5th channel is occupied. It is easy to do Post-Route simulation which can mostly show the real performance of the module, but to run this module on board need all the tested data downloaded into the on-board memory, so a ROM is designed for the verification to store the tested data, the ModelSim® simulation result and chipscope result is shown in Figure 6 and Figure 7 below:

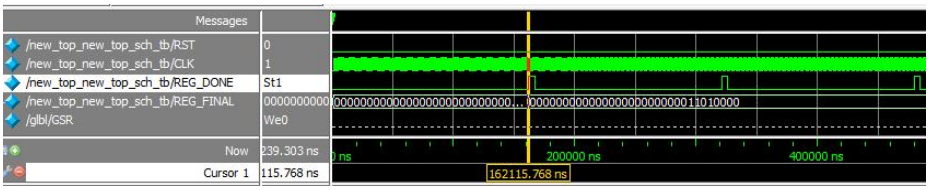

Fig. 6. ModelSim® Post-Route Simulation Result

In Figure 6, RST is the global reset signal, and CLK is the 100MHz clock, REG_DONE, indicates that the output of channel states is coming, and REG_FINAL is the output of the final state of spectrum sensing. The Tested data is stored in the ROM of the project.

With ROM of the tested data generated for this project, bit file is created for downloading to the FPGA through JTAG chain. The real clock of the system on board is 4 times the frequency of the crystal (about 128.88MHz), the output is shown in Figure 7 below.

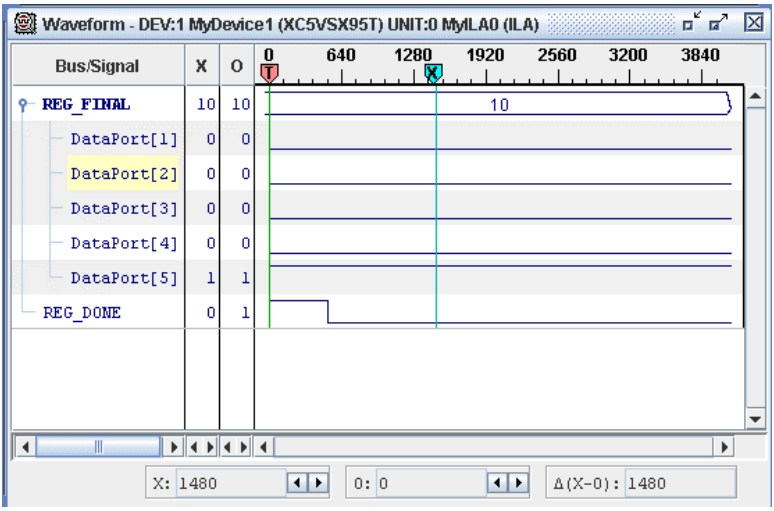

Fig. 7. Xilinx Chipscope Pro® Waveform

In Figure 7, REG_DONE is the indicator of REG_FINAL which is the final sensing state of the channel. The system is designed to hold the value of REG_FINAL until it changed, but REG_DONE is defined as an impulse to show the coming of the final result, for it can provide long-time-valid data for the next block which maybe the scheduler of the channels. That is why REG_DONE turns low, while REG_FINAL stills shows the channel state.

From above, we can know that, first of all, this module can export the right result of the spectrum sensing. Then the deviation will be analyzed.

As we know, the definition of FFT IP is the key factor of the sensing accuracy. Now, look at the following chart of FFT results with the same input from both Matlab and FFT IP.

	fft_mtlab <512x1 double>	fft_ip <512x1 double>
	1	1
1	2.0480e+03 + 0.0000e+00i	2.0480e+03 + 0.0000e+00i
2	0.0498 - 4.0600i	-60.0000 - 63.0000i
3	0.0000 + 0.0000i	0.0000 + 0.0000i
4	-0.1322 + 3.5885i	-63.0000 - 59.0000i
5	0.0000 + 0.0000i	0.0000 + 0.0000i
6	-0.2431 + 3.9566i	-13.0000 - 7.0000i
7	0.0000 + 0.0000i	0.0000 + 0.0000i
8	-0.5801 + 6.7360i	-12.0000 - 7.0000i
9	0.0000 + 0.0000i	0.0000 + 0.0000i
10	-0.4673 + 4.2141i	-11.0000 - 4.0000i
11	0.0000 + 0.0000i	0.0000 + 0.0000i
12	0.8484 - 6.2464i	-9.0000 - 19.0000i
13	0.0000 + 0.0000i	0.0000 + 0.0000i
14	-0.1729 + 1.0746i	-15.0000 - 18.0000i
15	0.0000 + 0.0000i	0.0000 + 0.0000i
16	-1.1814 + 6.3454i	-17.0000 - 4.0000i
17	0.0000 + 0.0000i	0.0000 + 0.0000i
18	1.6229 - 7.6660i	1.0000 - 8.0000i
19	0.0000 + 0.0000i	0.0000 + 0.0000i
20	-2.2490 + 9.4701i	-7.0000 + 1.0000i
21	0.0000 + 0.0000i	0.0000 + 0.0000i
22	0.3730 - 1.4152i	-6.0000 + 1.0000i
23	0.0000 + 0.0000i	0.0000 + 0.0000i
24	0.7742 - 2.6697i	1.0000 - 5.0000i
25	0.0000 + 0.0000i	0.0000 + 0.0000i
26	-0.6138 + 1.9374i	-8.0000 - 3.0000i
27	0.0000 + 0.0000i	0.0000 + 0.0000i
28	0.2293 - 0.6666i	-6.0000 - 1.0000i
29	0.0000 + 0.0000i	0.0000 + 0.0000i
30	-4.2877 + 11.5350i	-17.0000 + 11.0000i
31	0.0000 + 0.0000i	0.0000 + 0.0000i
32	-3.9866 + 9.9688i	0.0000 + 3.0000i
33	0.0000 + 0.0000i	0.0000 + 0.0000i
34	0.4600 - 1.0731i	0.0000 - 1.0000i
35	0.0000 + 0.0000i	0.0000 + 0.0000i
36	-0.0212 + 0.0463i	-3.0000 - 2.0000i
37	0.0000 + 0.0000i	0.0000 + 0.0000i
38	1.1671 - 2.3913i	-8.0000 - 3.0000i
39	0.0000 + 0.0000i	0.0000 + 0.0000i
40	-2.2974 + 4.4280i	-1.0000 - 4.0000i

Fig. 8. FFT results of Matlab and FFT IP

The reader may be amazed at the outcome of the different calculations: except the first pair of numbers, there is almost no pairs of numbers that are close to each other, it seems error. However it is undeniable that the output of the system is the predicted

result in both simulation and on-board testing. What is the problem? Bear this in mind, I record the results of FFT IP to Matlab, and make a comparison with the Matlab results,and plot them in two figures as it shows in Figure 9:

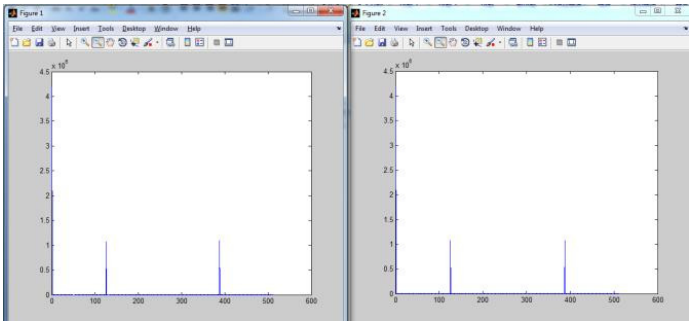

Fig. 9. The comparison of Results Matlab® FFT and IP core FFT

It showed the almost the same frequency spectrum features, and we need a closer view, maybe Figure 10 is good enough:

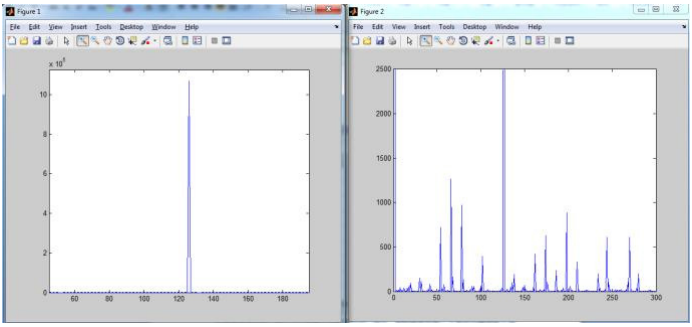

Fig. 10. A closer view of Figure 9

Figure 10 revealed the secret, in Matlab, all above data is processed in double float, a data type which has a really high precision. But in FFT IP it is a 14-bit fixed point precision, and after FFT, a truncation is launched to maintain a fixed-point data type.

Consider the glitch of the max amplitude, the value is 1250, and the amplitude of the point which is the center frequency of the tested signal, the value is 1100000, and the ratio is 1250/1100000= 0.001136, which is less than thousandth. So it is acceptable for us, that's because even we do a 512-point FFT, which has a frequency definition of 0.1882, and at most we need to do 40 times accumulation to get the energy of a sub-channel, the ratio could be 1250*40/1100000=0.045. That could be accommodated by threshold setup. Yet, we could know that with the increase of FFT points, and sub-channel bandwidth, the deviation of such kind, to a certain degree, cannot be neglected anymore.

In this section, the performance of the implementation is presented. The test work is conducted in two methods due to the different tools used, and the result together with the accuracy is analyzed. The next section will give a summary of my research work and the entire paper.

5 Conclusion

This paper systematically presents the design and implementation of the spectrum sensing module using energy detection method. The spectrum sensing module applied in the WLAN MAC layer to make a better use of the limited spectrum resources, and achieve a Giga-byte data rate in WLAN. And the authors hope this paper can make contribute to the new 802.11 standards.

Acknowledgements. The work presented in this paper was supported by the National Natural Science Foundation of China (Grants No. NSFC-61170176), National Great Science Specific Project (2010ZX03005-001-03), (2012ZX03003006), Beijing Municipal Commission of Education Build Together Project.

References

1. Cabrić, D., Mishra, S.M., Willkomm, D., Broderson, R., Wolisz, A.: A Cognitive Radio Approach for Usage of Virtual Unlicensed Spectrum. In: Proc. IST Mobile Wireless Communications Summit (2005)
2. IEEE Std 802.11u™-2011
3. Mitola, J., Maguire, G.Q.: Cognitive radio: Making software radios more personal. IEEE Pers. Commun. 6, 13–18 (1999)
4. Letaief, K.B., Zhang, W.: Cooperative communications for cognitive radio networks. Proceedings of the IEEE 97(5), 878–893 (2009)
5. Xilinx, LogiCORE IP Fast Fourier Transform v7.1, DS260 (April 19, 2010)

Trust Services-Oriented Multi-Objects Workflow Scheduling Model for Cloud Computing*

Wenan Tan[1,2], Yong Sun[1], Guangzhen Lu[1], Anqiong Tang[2], and LinShan Cui[1]

[1] School of Computer Sci. and Tech., Nanjing University of Aeronautics and Astronautics
[2] School of Computer and Information, Shanghai Second Polytechnic University
wenantan@it.sspu.cn, syong@nuaa.edu.cn

Abstract. Cloud Computing is promising as a new style of collaborative environment. Efficient Workflow Scheduling is crucial for achieving high performance in Cloud Computing environment. In spite of workflow scheduling has been widely studied. And various algorithms have been proposed to optimize execution time and cost. However the existing cloud services are owned and operated by third-party organizations or enterprises in a closed network. The uncertainty and unreliability existed in the network has caused great threat to the applications. Therefore trust services-oriented strategies must also be considered in workflow scheduling. This paper proposes a *Trust services-oriented multi-objectives Workflow Scheduling (TMOWS)* model. And a case study has been given to explain the proposed model.

Keywords: Trust, Multi-Objective, Workflow scheduling, Cloud Computing.

1 Introduction

Cloud Computing is defined as a new style of collaborative environment in which dynamically scalable and often virtualized resources are provided as a service over the Internet. Almost everything can be offered as a service which is integrated into a composite service for users. Cloud services are typically exploited by a pay-per-use model in which guarantees are offered by the cloud provider [1]. They have become a key technology to support collaboration.

However, the existing commercial cloud services are owned and operated by individual organizations or enterprises in a closed network, which is expensive to maintain. While Cloud Computing provide enormous services, uncertainty and unreliability existed in the larger-scale distribute system has caused great threat to the applications [2-4].

Scheduling complex tasks on trustworthy services has become even more important. Usually the workflow system is deployed as the aggregation of cloud services to facilitate the automation of distributed large-scale applications in the cloud

* This paper was supported in part by the National Natural Science Foundation of China under Grant no. 61272036, and Innovation Program of Shanghai Municipal Education Commission under Grant no.11ZZ188.

Q. Zu, B. Hu, and A. Elçi (Eds.): ICPCA-SWS 2012, LNCS 7719, pp. 617–630, 2013.

or grid environment. These workflows consist of multiple tasks provided by cloud providers that offer similar service at different levels of quality. WFS is defined as the allocation of workflow tasks to distributed services which is considered as NP-Complete problems.

A number of scheduling algorithms have been developed to satisfy users' requirements in many large-scale applications. Many algorithms focus on minimizing their execution time or cost on the commercial cloud platform. An effective and efficient trust workflow system is highly desirable in cloud environment. The scheduling of workflow must also account for reliability as well as time and cost. Trust must been considered as a crucial concept in large-scale networks [5].

Instead of focusing on cost or time objectives, we endeavor to develop the scheduling strategies which require striking a balance for the different and conflicting requirements such as time, cost, and trust. Overall aim is to find the schedule that reaches a compromise to satisfy all requirements for users. To address the scheduling problem, a trust multi-objective workflow scheduling, denoted as TMOWS, is proposed to balance the factors while meeting user's requirements or constraints.

The rest of the paper is organized as follows. In section 2, we discuss the related works. Fuzzy Multi-Objective Workflow Scheduling Model is presented in section 3. In Section 4, Model algorithm is proposed. Numerical examples have been given to explain the proposed algorithm in section 5. Finally, we summarize the conclusions and point out our future work.

2 Related Works

Services users can give feedback with a rating to the service provider after each transaction. Then eBay [6] calculates the positive feedback rate $R = p/p+n$ to display on web, where p is the number of positive ratings and n is the number of negative ratings from the buyers. They consider a central authority model where ratings are supplied by different users.

Powertrust model proposed by Zhao and Hwang computes the local trust value based on the feedback of successful transactions [7]. *EigenTrust* computes the global trust value of a given peer based on the trust value of local successful transactions by using binary rating model [8]. A trust model proposed in [9] calculates subjective rating by using Dempster-Shafer belief theory. The WFS model has been proposed to optimizing execution time and reliability on heterogeneous systems [10].

With increasing presence of services on Internet, Zheng et al. have developed a collaborative filtering model for predicting QoS values to make service recommendation [11-13]. Recommendation is the strategy which makes a prediction of user's needs or interests. A user is given recommendations based on the ratings by other users who are similar to the given user. Recommend system has been helpful and successful for service composition and selection [14-16].

There are only limited numbers of research works considering the trustworthy in workflow applications. Fierce competition on cloud services may result in failures from time to time. Trust is an important element for dependable workflow application in Cloud Computing environment.

A Cloud Computing system has a cost benefit in various aspects. Workflow execution cost must be considered while scheduling based on user's QoS constraints. In [17], scheduling workflow model with budget, denoted as constraints LOSS and GAIN strategy proposed by Sakellariou, is studied from an assignment which has good performance under one of two optimization criterions, and then swaps tasks between services trying to optimize as much as possible for the other criterion.

A cost-based WFS algorithm, denoted as *Deadline-MDP*, is proposed by Yu and Buyya to minimize the execution cost while meeting the deadline by distributing the deadline over each task partition [18, 19]. *Deadline-MDP* has been developed by Yuan and Li to use a backward method to create a new algorithm called *Deadline Bottom Level (DBL)* [20]. The workflow deadline is segmented into the time intervals of all tasks. All tasks in each bottom level have the same sub-dead-line, but the starting time of a task in each level is determined by the maximum finishing time of its predecessors, rather than the finishing time of its parent group which is adopted by DTL. The DBL algorithm can considerably improve the average performance of DTL.

The WFS algorithms mentioned above have focused on minimizing execution time or cost. They all ignore the critical influence of uncertainty and unreliability in the large scale distributed systems. Unfortunately, in the Cloud Computing environment, many discrete malicious events lead to failures of a workflow application. From this sense, we endeavor to develop a trust Services-Oriented workflow scheduling model that can strike a balance in different and conflicting requirements.

3 Multi-Objectives Workflow Scheduling Model

In this section, we provide a brief overview of basic terms related to the scope of this paper including WFS Model, fuzzy modeling and multi-objectives modeling. In addition, we discuss the problem related to the trust Services-Oriented workflow scheduling model.

3.1 Workflow Scheduling Model

If users submit their requirements for integration with the workflow application requiring maximum QoS constraints, the WFS planner will return the results to users, and allow users to choose the most suitable schedule and confirm the information. Finally, systems start to execute the workflow according to the conventional information. In the context of cloud computing, a wide range of integrated systems can be represented as workflows which can be modeled as *Directed Acyclic Graphs* (*DAGs*) [21]. The following model provides an effective way to map the node (or task) to service.

Definition 1. Let $W=\{T,E\}$ denote a workflow which consists of a set of tasks, $T=\{T_1,\cdots,T_i,\cdots,T_n\}$, and a set of dependencies among the tasks. Tasks sometimes also called nodes. $E=\{<T_1,T_2>,\cdots,<T_i,T_j>,\cdots,<T_{n-1},T_n>\}$, T_i is the parent task of T_j, where T_j, $T_j \in T$. A child task cannot be executed until all of its parent tasks have been completed.

Definition 2. In a workflow DAG, we call a task which does not has any parent tasks an entry task and denote it as T_{entry}, while a task which does not has any child tasks an exit task, denoted as T_{exit}.

Definition 3. Let m be the total number of candidate services. There are a set of s_j^i (where $1 \le i \le n,\ 1 \le j \le m_i$) which are available for the task. Services have varied processing capability delivered at different prices and time. We denote t_j^i as the sum of processing time and data transmission time, and c_j^i as the sum of service price and data transmission cost for processing t_i on the service s_j^i.

Definition 4. The minimum time to complete the schedule is the length of the critical path from the entry node of workflow to the exit node. In symbols,

$$EF = ES + D_i \tag{1a}$$

$$LS = LF + D_i \tag{1b}$$

$$Slack = LF - EF \tag{1c}$$

Where ES represents the earliest start time, *EF* is the earliest finish time, *LS* denotes the latest start time, *LF* is the latest finish time, the slack for a task is the difference between its latest finish time and its earliest finish time, D_i is the estimated duration of the task T_i. Each task with *zero slack* is on a critical path through the workflow *DAGs*.

3.2 Multi-Objective Model

The workflow planning problem is a multi-objectives optimization problem (MOP) in which a group of conflicting objective are simultaneously optimized.

Definition 5. In order to formulate this model, the notations are defined as follows.

D	time constraint (deadline)
B	cost constraint (budget)
Tr	trust constraint
t_j^i	time of the *j-th* service assigned for the *i-th* task
x_j^i	if the *j-th* service is assigned for the *i-th* task then $x_j^i = 1$, else $x_j^i = 0$
n	number of all tasks
m_i	number of services available for the *i-th* task

Definition 6. Mathematically, a typical model for workflow scheduling in the service cloud can be described as follows.

$$Minimize: \quad Z_1 = \sum_{i=1}^{n} \sum_{j=1}^{m_i} x_j^i c_j^i \tag{2a}$$

$$Minimize: \quad Z_2 = \sum_{i=1}^{n} \sum_{j=1}^{m_i} x_j^i t_j^i \tag{2b}$$

$$Maximize: \quad Z_3 = \sum_{i=1}^{n}\sum_{j=1}^{m_i} x_j^i tr_j^i \tag{2c}$$

$$subject\ to: \quad Z_1 \le B \tag{2d}$$
$$Z_2 \le D$$
$$Z_3 \ge Tr$$

where Z_i is the object or criteria such as time, cost, and trust for minimization; X_d is the set of feasible solutions that satisfy the set of system and policy constraints. The optimization of the workflow is to map every T_i onto some S_j^i in order to achieve minimum execution cost and time while meeting the constraints of trust.

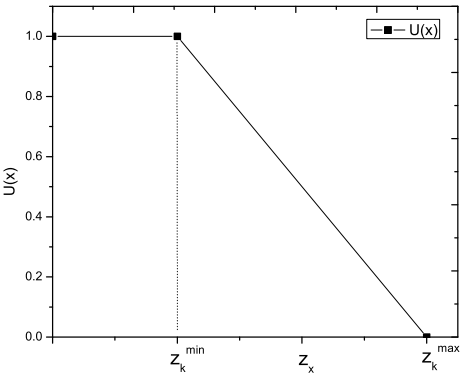

Fig. 1. Membership function for objective

3.3 Fuzzy Model

Using max-min as the operator [22, 23], the membership function of objectives is formulated by separating every objective into its maximum and minimum values [24]. The linear membership functions for optimization goal (Z_k, Z_l) are given as follows.

$$u(x) = \begin{cases} 1, & z_k \le z_k^{\min} \\ \dfrac{z_k^{\max} - z_k(x)}{z_k^{\max} - z_k^{\min}}, & z_k^{\min} \le z_k \le z_k^{\max} \\ 0, & z_k^{\max} \le z_k \end{cases} \tag{3}$$

$$u(x) = \begin{cases} 0, & z_l \le z_l^{\min} \\ \dfrac{z_l(x) - z_l^{\min}}{z_l^{\max} - z_l^{\min}}, & z_l^{\min} \le z_l \le z_l^{\max} \\ 1, & z_l^{\max} \le z_l \end{cases} \tag{4}$$

where $z_k^{\max}$ and $z_k^{\min}$ can be computed through solving the multi-objective problem as a single objective in each time. $z_k^{\max}$ is the maximum value of $z_k^{\max}$, and $z_k^{\min}$ is the minimum value of $z_k(x)$, as shown in Fig.1.

3.4 Trust Services-Oriented Workflow Scheduling Model

The present work considers the WFS problem as multiple objectives problem subjected to time and cost constraints. The problem formulation proposed here considers three different objectives related to trust, time and cost.

Member Function for Trust Evaluation

In a large-scale distributed system, many discrete events could lead to the failures of a workflow application. Therefore, we present a trust service-oriented scheduling algorithm which considers the reliability of a service for workflow execution. A general trust metric that combines direct and recommendation trust is defined as follows.

$$Tr(S_i) = w_i * DT(S_i) + (1 - w_i) * RT(S_i) \tag{5}$$

where $DT(S_i)$ is a direct trust of the *i-th* service by the experiences which is based on the history of using the service by the users. $RT(S_i)$ is a recommendation trust of the *i-th* service by other users. w_i is the weight of direct trust and recommendation trust for the *i-th* service, which can be computed as follows.

$$w_i = 1 - \frac{1}{e^k} \tag{6}$$

where k is the times of the *i-th* service used by service client, w_i is adaptively changing with the value of k. For a more frequently used service, higher weights should be assigned for the direct trust evaluation. For example, if $w_i = 0$, it means the client never uses the *i-th* service, so $Tr(S_i)$ depends completely on the recommendation trust evaluation.

$DT(S_i)$ is established through observations on whether the previous interactions among the services are successful used. The observation is often described by two variables: n_i, denoting the number of successful interactions, and N_i, denoting the total number of interactions for the *i-th* service. The direct trust value can be calculated as:

$$DT\left(S_i\right) = \frac{n_i + 1}{N_i + 2} \tag{7}$$

where the trust value of a service is initialized to 1/2.

$RT(S_i)$ is recommendation trust value of the *i-th* service. $RT(S_i)$ is the weighted sum of ratings by others, where the weight corresponds to the similarity between the active user and each of the other users.

To describe the prediction algorithm formally, let S be the set of services being rated, n be the number of users, S_i be the set of services rated by user i, and v_{ij} be the rating given by user i to the *j-th* service. Next, let average v_i be the average rating by user i as given by

$$avg(v_i) = \frac{1}{|S_i|} * \sum_{j \in S_i} v_{ij} \tag{8}$$

Based on Collaborative filtering model [11-13], we can define the predicted rating of the active user a for service j as (n is the number of users):

$$RT(S_j) = avg(v_a) + \frac{\sum_{i=1}^{n} w_{ai}(v_{ij} - \bar{v}_i)}{\sum_{i=1}^{n} | w_{ai} |} \tag{9}$$

The weight w_{ai} reflects similarity between user a and user i. The weights for the users are calculated by *Pearson Correlation Coefficient* (*PCC*) which is widely used to compute the degree of similar relationship between two variables. The similarity between user a and i would be computed as follows.

$$w_{ai} = \frac{\sum_{j \in S}(v_{aj} - \bar{v}_a)(v_{ij} - \bar{v}_i)}{\sqrt{\sum_{j \in S}(v_{aj} - \bar{v}_a)^2 (v_{ij} - \bar{v}_i)^2}} \tag{10}$$

where $S = S_a \cap S_b$ is the subset of services which have been used by both user a and i.

Using max-min as the operator, the membership function for trust evaluation of the service is formulated as follows.

$$U_{T_i}(tr_x) = \frac{tr_x^i - tr_{\min}^i}{tr_{\max}^i - tr_{\min}^i},\ if\ tr_{\min}^i \le tr_x^i \le tr_{\max}^i \tag{11a}$$

$$U_{T_i}(tr_x) = 0,\ if\ tr_{\min}^i = tr_x^i \tag{11b}$$

$$U_{T_i}(tr_x) = 1,\ if\ tr_{max}^i = tr_x^i \tag{11c}$$

where tr_x^i is the trust value for the service selected for the *i-th* task, tr_{max}^i is the max value of trust for the service available for the *i-th* task, and $tr_{\min}^i$ is the min value of trust for the service.

Member Function for Execution Time

There are a set of services in which s_j^i (where $1 \le i \le n$, $1 \le j \le m_i$) is capable of executing the task. The linked list data structure is employed to solve the problem of mapping task T_i to s_j^i, as shown in Fig.2.

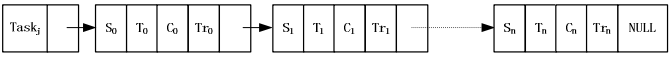

Fig. 2. Data structure of mapping tasks

In the linked list, we store each service in a node that contains three elements such as time, cost, feedback value and a reference to next node in the list, and the list of services are sorted in a descending way based on value of time.

Using max-min as the operator, the membership function for execution time is formulated as follows.

$$U_{T_i}(t_x) = \frac{t_{\max}^i - t_x^i}{t_{\max}^i - t_{\min}^i},\ if\ t_{\min}^i \le t_x^i \le t_{\max}^i \tag{12a}$$

$$U_{T_i}(t_x) = 0, \ if \ t^i_{\max} = t^i_x \tag{12b}$$

$$U_{T_i}(c_x) = 1, \ if \ t^i_{\min} = t^i_x \tag{12c}$$

where t^i_x is the time for the service selected for the *i-th* task, $t^i_{\max}$ is the max value of time for the service available for the *i-th* task, and $t^i_{\min}$ is the min value of time for the service available for the *i-th* task.

Member function indicates that the closer the value of t^i_x is to $t^i_{\min}$, the better the selected service is, and the more the objective is satisfied.

Membership Function for Execution Cost

Similar to membership function of execution time, the membership function for execution cost of the *i-th* task can be defined as follows.

$$U_{T_i}(c_x) = \frac{c^i_{\max} - c^i_x}{c^i_{\max} - c^i_{\min}}, \ if \ c^i_{\min} \le c^i_x \le c^i_{\max} \tag{13a}$$

$$U_{T_i}(c_x) = 0, \ if \ c^i_{\max} = c^i_x \tag{13b}$$

$$U_{T_i}(c_x) = 1, \ if \ c^i_{\min} = c^i_x \tag{13c}$$

where c^i_x is the cost for the service selected for the *i-th* task, $c^i_{\max}$ is the max value of cost for the service available for the *i-th* task, and $c^i_{\min}$ is the min value of cost for the service available for the *i-th* task.

The time and cost are conflicting requirements. According to the analysis of membership function for execution cost, the list of services is stored in a descending order based on the time. In contrast, the list is in an ascending order based on the cost.

The equation of membership function for cost indicates that if the value of c^i_x is high, the membership value is low. On the other hand, if the value of $c^i_{\min}$ is low, the higher membership value is assigned, the better the selected service is, and the more the objective is satisfied.

WFS require policies to strike a balance for the different requirements. For example, enterprise may expect to save budget but have longer time, or aim to minimize the execution time of schedule. In order to satisfy the multiple criteria simultaneously, a compromise should be made to find a suitable solution.

Using max-min as the operator, the above fuzzy model can be converted to the following crisp model as:

$$Maxmize \ \lambda_i \tag{14a}$$

$$U_{T_i}(t_x) \ge \lambda_i \tag{14b}$$

$$U_{T_i}(c_x) \ge \lambda_i \tag{14c}$$

$$U_{T_i}(tr_x) \ge \lambda_i \tag{14d}$$

$$t_x \ge 0, c_x \ge 0, tr_x \ge 0 \tag{14e}$$

$$\lambda_i \in [0,1], \ i = 1, \cdots, n \tag{14f}$$

The degree of overall satisfaction is the minimum of all the above membership values. The fuzzy decision may be considered as the choice that satisfies all of the objectives. Therefore, the fuzzy decision for overall satisfaction is given as follows.

$$U_{T_i}^{*} = min\{U_{T_i}(t_x), U_{T_i}(c_x), U_{T_i}(tr_x)\} \tag{15}$$

The selection of services for WFS is the maximum of all degrees of satisfaction. We define the selection decision as follows.

$$\lambda_{T_i}^{x} = max\{U_{T_i}^{1}, U_{T_i}^{2}, \cdots, U_{T_i}^{m_i}\} \tag{16}$$

where *k* means the *k-th* service which has the maximum of degrees of satisfaction for the *i-th* task, so the *k-th* service is mapping on the *i-th* task. U_T is the vector of services membership including $U_{T_i}(t_x), U_{T_i}(c_x)$, and $U_{T_i}(tr_x)$ values.

From the above analysis, the trust Services-Oriented workflow scheduling model is stated in Algorithm 1:

Algorithm 1 Trust Services-Oriented Multi-Objects Workflow Scheduling

```
A schedule for all workflow tasks (Output)
A workflow graph(Input)
request processing time, cost and trust from available service.
Var
    iTask: 0..TaskNumber;
    jService: 0..ServiceNumberOfTask
    max,minUtility fTime, fCost, fTrust: Real;
begin
  repeat
    compute the in degrees for the i-th Task;
    insert no incoming i-th Task into stack;
    while(!stack.isEmpty())
      for each service in available services of the i-th task;
        minUtiity(jService)=minimum(fTime,fCost,fTrust)
        max = maximum(minUtility(jService))
      endfor
      if the Utility of the k-th service is max then
          Mapping the k-th service onto the i-th task.
      end if
      for each edge e in adjacent vertices of ith task
           vertex w = e.dest
               if w.indegree == 0 then
                 insert w into stack
               end if
      end for
    end while
  until all tasks have been scheduled
end.
```

4 Case Study

In this section, a case study is used to illustrate the value of the proposed algorithm. The algorithm is explained using an example of workflow applications described in Fig.3.

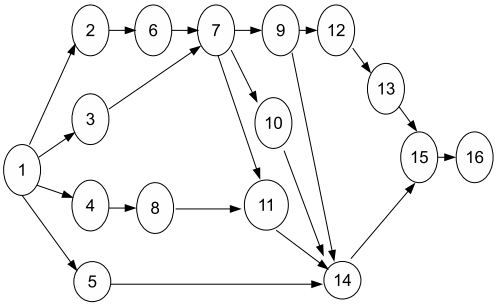

Fig. 3. Sample DAG of the workflow application

4.1 Trust Evaluation for Candidate Services

To illustrate the value of trust evaluation, we consider the following example based on the ratings of Table 1. Example: A user needs to evaluate the candidate service A for the *i-th* tasks in the example workflow application that the user has not yet used. The blank in Table means that users' ratings are missing and they are treated as if it equals that users' average rating.

Table 1. Sample of the ratings of cloud services

	A	**B**	**C**	**D**	**E**
User 1	?	3	4	5	5
User 2	4	3	5	5	
User 3	2	5		3	3
User 4	5	3	4	3	5

The similarities between the pairs of users in the example are computed via PCC. The results are shown in Table 2.

Table 2. User-based Pearson Correlation

	User 1	**User 2**	**User 3**	**User 4**
User 1	1.00	0.866	-1	0.455
User 2	0.866	1.00	-0.646	-0.866
User 3	-1	-0.646	1.00	-0.688
User 4	0.455	-0.866	-0.688	1.00

The predicted rating would be calculated as following.

$$RT(S_j) = avg(v_a) + \frac{\sum_{i=1}^{n} w_{ai}(v_{ij} - \bar{v_i})}{\sum_{i=1}^{n} | w_{ai} |} = 4.25 + \frac{0.866*(4-4.25)+(-1)*(2-3.25)+0.455*(5-4)}{0.866-1+0.455} \approx 4.6 \quad (18)$$

4.2 Mapping Task onto Suitable Services

Each task in the workflow can be executed by a series of similar cloud services at different levels of quality. All candidate cloud services are in the service list of the *i-th* task. For example, {(5,3,3),(10,2,4),(20,1,5)} is a candidate service list for the *6-th* task. Table 3 shows the service list of each task for this workflow example.

Table 3. Sample of services list

Task Id	Service List	Service Number
2	(4,12,2), (6,10,3), (8,8,4), (13,4,5)	**4**
3	(8,6,3), (10,5,4.5), (12,4,4)	**3**
4	(4,7,3), (5,6,4), (6,5,5), (7,4,4.6)	**4**
5	(10,4,3), (12,3,4.5), (15,2,4)	**3**
6	(5,3,3),(10,2,5),(20,1,4)	**3**
7	(15,20,3), (25,15,4), (30,10,4.7)	**3**
8	(20,4,3),(30,3,4.5),(45,2,5)	**3**
9	(10,9,3.5),(12,8,4),(18,5,4.9)	**3**
10	(10,30,3.5),(15,20,4.0),(20,15,4.2)	**3**
11	(40,12,3),(50,10,4.8),(80,6,4.6)	**3**
12	(12,13,3),(18,9,4),(20,8,4.2)	**3**
13	(40,25,2),(50,20,3.5),(60,16,4.1)	**3**
14	(80,30,5),(120,20,4),(150,15,4.5)	**3**
15	(50,13,4),(60,10,4.8),(70,9,4.5)	**3**

Service selection and service ranking are based on the objective functions for cost, time and trust respectively. The steps of service selection are described in the following steps.

Step 1: Using Max-Min operator, compute the vectors of $\left(U_{T_i}(t_x), U_{T_i}(c_x), U_{T_i}(tr_x)\right)$ for the *i-th* task.

$$t^6_{\max}=3, t^6_{\min}=3;\ c^6_{\max}=20, c^6_{\min}=5;\ tr^6_{\max}=5, tr^6_{\min}=3;$$

$$U^1_{T_6}=min\left\{\frac{20-5}{20-5}\ \frac{3-3}{3-1}\ \frac{3-3}{5-3}\right\}=min\{1\ 0\ 0\}=0$$

$$U^2_{T_6}=min\left\{\frac{20-10}{20-5}\ \frac{3-2}{3-1}\ \frac{5-3}{5-3}\right\}=min\left\{\frac{2}{3}\ \frac{1}{2}\ 1\right\}=\frac{1}{2}$$

$$U^3_{T_6}=min\left\{\frac{20-20}{20-5}\ \frac{3-1}{3-1}\ \frac{4-3}{5-3}\right\}=min\left\{0\ 1\ \frac{1}{2}\right\}=0$$

Step 2: Compute max of U of execution time and cost for the *i-th* task.

$$\because\ \lambda^x_6=max\left\{U^1_{T_6}\ U^2_{T_6}\ U^3_{T_6}\right\}=max\{0\ \frac{1}{2}\ 0\}$$

$$\therefore i=6, x=2$$

Step 3: λ^2_6 is max, then the s^6_2 is selected, so mapping the *6-th* task onto the *2-th* service.

The other tasks in the workflow are scheduled by the same way as the *6-th* task. The solution for the example workflow scheduling is shown in Table 4.

Table 4. The optimum solution for the workflow

Task Id	Service selected	Time	Cost	Trust
2	s^3_2	8	8	4
3	s^2_3	5	10	4.5
4	s^3_4	5	6	5.0
5	s^2_5	3	12	4.5
6	s^2_6	2	10	4.6
7	s^2_7	15	25	4.0
8	s^2_8	3	20	4.0
9	s^2_9	8	12	4.8
10	s^2_{10}	20	15	4.0
11	s^2_{11}	10	50	4.8
12	s^2_{12}	9	18	4.2
13	s^3_{13}	16	60	4.1
14	s^2_{14}	20	120	4.0
15	s^2_{15}	10	60	4.8

By performing the topological sorting, we can get the sequence order list as follows: 1 5 4 8 3 2 6 7 11 10 9 14 12 13 15 16; the critical path is 1 2 6 7 10 14 15 16; and the execution time of the WFS is 76.

5 Conclusions

A trust service-oriented workflow scheduling strategy is proposed for cloud applications. The contribution of this work is three-fold: First, we define the problem description with regards to the multi-objectives-oriented workflow scheduling; second, the proposed scheduling algorithm adopts a general trust metric that combines direct trust and recommendation trust; third, for *TMOWS* model, the cloud service criterion of execution time, cost and trust are considered simultaneously to yield a genuinely optimal solution. Limited work still exists in trying to understand how dynamic. Run time changes usually affect the statically predetermined schedule. One planned future research is to extend *TMOWS* algorithm for rescheduling tasks in response to changes in Cloud Computing.

References

1. Buyya, R., Yeo, C.S., Venugopal, S., Broberg, J., Brandic, I.: Cloud computing and emerging IT platforms: Vision, hype, and reality for delivering computing as the 5th utility. Future Generation Computer Systems 25(6), 599–616 (2009)
2. Wang, X., Yeo, C.S., Buyya, R., Su, J.: Optimizing the makespan and reliability for workflow applications with reputation and a look-ahead genetic algorithm. Future Generation Computer Systems 27(8), 1124–1134 (2011)
3. Sebastian, S., Terry, R.P., Nicholas, R.J.: Flexible, Provisioning of Web Service Workflows. ACM Transactions on Internet Technology 9(1), 1–45 (2009)
4. Rahman, M., Ranjan, R., Buyya, R.: Reputation-based dependable scheduling of workflow applications in Peer-to-Peer Grids. Computer Networks 54, 3341–3359 (2010)
5. Hwang, K., Li, D.: Trusted Cloud Computing with Secure Resources and Data Coloring. IEEE Internet Computing 14(5), 14–22 (2010)
6. eBay.com, `http://www.eBay.com`
7. Zhou, R., Hwang, K.: Powertrust: A robust and scalable reputation system for trusted peer-to-peer computing. IEEE Transaction Parallel Distribute System 18(4), 460–473 (2007)
8. Kamvar, S.D., Schlosser, M.T., Garcia-Molina, H.: The Eigentrust Algorithm for Reputation Management in P2P Networks. In: Proceeding Intelligent Conference on World Wide Web, pp. 640–651 (2003)
9. Jφsang, A., Ismail, R., Boyd, C.: A Survey of Trust and Reputation Systems for Online Service Provision. Decision Support Systems 43(2), 618–644 (2007)
10. Dongarra, J.J., Jeannot, E., Saule, E., Shi, Z.: Bi-objective scheduling algorithms for optimizing makespan and reliability on heterogeneous systems. In: SPAA 2007: Proceedings of the Nineteenth Annual ACM Symposium on Parallel Algorithms and Architectures, pp. 280–288 (2007)
11. Resnick, P., et al.: Grouplens: An Open Architecture for Collaborative Filtering of Netnews. In: ACM Conference on Computer Supported Cooperative Work, pp. 175–186 (1994)
12. Herlocker, J., et al.: Evaluating Collaborative Filtering Recommender Systems. ACM Transaction Information Systems 22(1), 5–53 (2004)
13. Zheng, Z.B., Ma, H., Lyu, M.R., King, I.: QoS-Aware Web Service Recommendation by Collaborative Filtering. IEEE Transactions on Services Computing 4(2), 140–152 (2011)

14. Adomavicius, G., Tuzhilin, A.: Toward the Next Generation of Recommender Systems: A Survey of State-of-the-Art and Possible Extensions. IEEE Transaction Knowledge and Data Engineering 17(6), 734–749 (2005)
15. Massa, P., Avesani, P.: Trust Metrics in Recommender Systems. In: Computing with Social Trust, pp. 259–285. Springer (2009)
16. Patricia, V., Chris, C., Martine, D.C., Ankur, M.T.: Trust- and Distrust-Based Recommendations for Controversial Reviews. IEEE Intelligent Systems 26(1), 48–54 (2011)
17. Sakellariou, R., Zhao, H., Tsiakkouri, E., Dikaiakos, M.D.: Scheduling workflows with budget constraints. In: Proceedings of the Workshop on Integrated Research in Grid Computing, Pisa, Italy, pp. 347–357 (November 2005)
18. Yu, J., Buyya, R.: A taxonomy of workflow management systems for grid computing. Journal of Grid Computing 33(4), 171–201 (2005)
19. Yu, J., Buyya, R., Tham, C.K.: Cost-based scheduling of workflow applications on utility Grids. In: Proceedings of the First IEEE International Conference on e-Science and Grid Computing, Melbourne, Australia, pp. 140–147 (2005)
20. Yuan, Y., Li, X., Wang, Q., Zhang, Y.: Bottom Level based heuristic for scheduling workflows in Grids. Chinese Journal of Computers 31(2), 282–290 (2008)
21. Zhou, M., Guo, W., Xiao, S., Wei, A., Jin, Y., Hu, W., Geller, G.: Availability-driven scheduling for real-time directed acyclic graph applications in optical grids. IEEE/OSA Journal of Optical Communications and Networking 2(7), 469–480 (2010)
22. Zadeh, L.: Fuzzy sets. Information and Control 8(3), 338–353 (1965)
23. Zimmermann, H.J.: Fuzzy programming and linear programming with several objective function. Fuzzy Sets and Systems 1(1), 45–55 (1978)
24. Lin, C.: A weighted max-min model for fuzzy goal programming. Fuzzy Sets and Systems 142(3), 407–420 (2004)

Scalable SAPRQL Querying Processing on Large RDF Data in Cloud Computing Environment

Buwen Wu, Hai Jin, and Pingpeng Yuan

Services Computing Technology and System Lab, Cluster and Grid Computing Lab
School of Computer Science and Technology
Huazhong University of Science and Technology, Wuhan, 430074, China
hjin@hust.edu.cn

Abstract. Recently the flexibility of RDF data model makes increasing number of organizations and communities keep their data available in the RDF format. There is a growing need for querying these data in scalable and efficient way. MapReduce is a parallel data processing solution for processing large data-intensive workloads, which is not supported directly for join-intensive workloads. In this paper, we present a schema based hybrid partitioning technique for RDF triples placement according to the relationships between them, and reduce the necessary number of MR cycles in each SAPRQL query job. Then we propose a lightweight sideways information passing techniques which pass the join information across MR jobs to decrease the intermediate results involved in join operations. The experimental results show that our approaches achieve a substantial performance improvement, and outperform the previous system by a factor of 2-20 using LUBM benchmark.

Keywords: RDF Data, Partitioning, MapReduce, Cloud Computing.

1 Introduction

The foundation of the semantic web is RDF (*Resource Description Framework*) [5], a flexible and extensible way to represent information about WWW resources, represented as triple (*S, P, O*) consisting of three parts, subject (*S*), object (*O*), and property (*P*). SPARQL [6], a W3C standard query language similar to SQL for databases, can extract RDF sub-graphs based on information in query graphs from a triple store. An example is shown in Fig. 1(a), which retrieves the information of students whose supervisor is the teacher of Java lessons.

Due to flexibility of RDF data model, it is widely accepted as a description framework of data. Community driven projects such as Wikipedia and science commons including social network [1] and bioinformatics [7] have exported RDF data. Linked Open Data Project announced more than 31 billion triples were published till Sept. 2011 [2]. Many RDF engines [9, 12, 24] running on single machine were well developed in past decades. Because of the limitations of single machine, few of them can answer the complex queries over massive RDF data set. Hence, it is highly desired to develop a high performance system for processing RDF data.

Q. Zu, B. Hu, and A. Elçi (Eds.): ICPCA-SWS 2012, LNCS 7719, pp. 631–646, 2013.

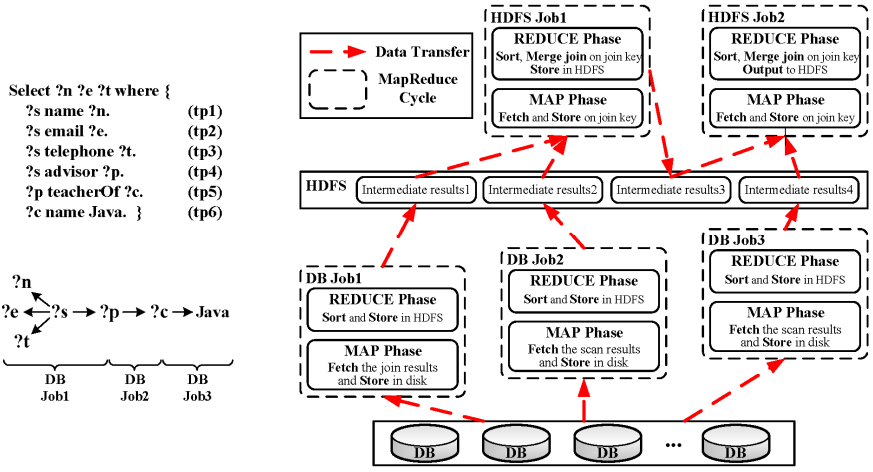

(a) SPARQL Query (b) Query Processing in HadoopDB

Fig. 1. SPARQL Querying Processing using MapReduce

The emergence of MapReduce [14] framework and its open source implementation Hadoop, provide a scalable and cost-efficient solution for processing large data intensive applications on heterogeneous clusters. Hence, recent researches also employ Hadoop as the basic infrastructure to process large scale RDF data [15, 20, 26–28, 30]. These researches mainly concentrate on extending HDFS to store RDF data and executing SPARQL queries using high level dataflow languages. In furtherance of benefiting index and query optimization techniques from DBMS, a hybrid solution called HadoopDB [10] has been developed which utilizes the merits of both MapReduce and DBMS. However, queries that have much complex structure will add more MR cycles which lead to non-trivial overhead in I/O and communication. Therefore, an appropriate RDF data partitioning approach which can push more joins into one MR cycle will be the first problem. In addition, during the query processing, a non-selective sub-query will produce a large number of intermediate results, even if the final output is small [23]. As the data set grows, the hard disk I/O, communication and sort overhead incurred by these intermediate results become the bottleneck. As a concrete example, consider the query shown in Fig. 1(a). Suppose that RDF data is split using hash partitioning, and accordingly the query is decomposed into three parts as Fig. 1(a) shown. The MR cycles answering this query are divided into two types: DB job is to perform the sub-queries, and HDFS job is to join two results of DB job on the join key. Therefore, the query in Fig. 1(a) is performed as shown in Fig. 1(b).

In this paper, we address the described problems above by two approaches. First, we propose a RDF schema based hybrid partitioning technique to guarantee that related triples can be gathered at one computing node in order to push as much join processing as possible in computing node, to avoid unnecessary remote I/O. Second, we introduce a light-weight sideways information passing technique for passing join information across MR cycles. The filter operations will be added into each MR job

(including DB job and HDFS job) according to information of previous finished MR jobs. This provides much more accurate information for joining key or scanning operations before MR job to skip large unnecessary intermediate results by the filter.

In summary, the primary contributions of our work are the following, and we implement all these approaches in the open-source system HadoopDB.

- We propose a RDF schema based hybrid partitioning, using vertical partitioning and horizontal partitioning to store related triples into the same machine.
- We describe the implementation of SPARQL query decomposition upon the schema based hybrid partitioning technique, and establish a left-deep tree for optimal execution order.
- We provide a light-weight sideways information passing technique for passing information across MR jobs.

2 Related Work

The major partitioning approach for RDF data is hash partitioning, which is used in the recent researches towards clustered RDF data systems, such as 4store [17], YARS2 [18], Atlas [22]. This technique has proven to work well for simple query patterns, but for more complicated queries, the performance is inefficient [19]. Huang et al. [19] attempted to address the complex queries problem by partitioning the data in a graph oriented scheme which gathers the vertices by the hops between them.

Hadoop based RDF data systems [15, 20, 26–28, 30] directly store RDF data in HDFS files and process the SPARQL queries using the high level dataflow languages on Hadoop such as Pig [25] and Hive [31]. However, the significant problems in I/O cost, communication overhead and intermediate results incurred by MapReduce jobs are still existing. Moreover, without indexes, MapReduce has only brute force as a processing option [3], which will lead to far more useless intermediate results when answering large join. HadoopDB [10] is a hybrid of MapReduce and DBMS technologies for analytical workloads, which benefits from both of the performance and efficiency of DBMS and scalability, fault tolerance and flexibility of MapReduce.

Horizontal and vertical partitioning techniques that are important aspects of physical design in relational database [11] are also used in RDF data systems. Ceri et al. [13] provided a horizontal partitioning algorithm using directed links between relations that are related to each other by an equi-join operation. Abadi et al. [8] implemented vertical partitioning on RDF data. By this means, triples are mapped to multiple 2-column tables instead of a long table as row stores do, which avoid much more self-joins over universal triples table.

Although join order can be optimized in optimal or suboptimal ways, join remains a costly operation. Sideways information passing [21, 23] across operations in execution tree can reduce the cardinality involved in joins substantially. Sideways information passing is a general model for passing filer information between separate joins according to the query execution tree at run-time, which provides significant benefits in intermediate results size and query execution time.

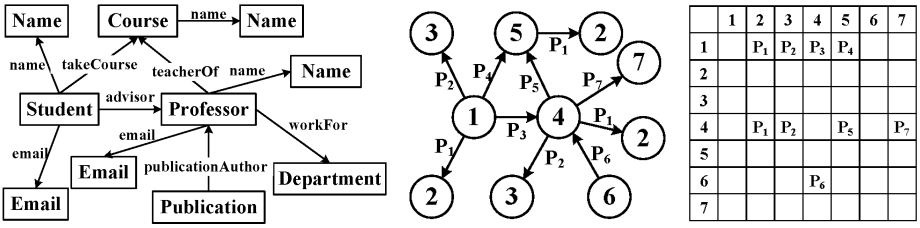

	1	2	3	4	5	6	7
1		P_1	P_2	P_3	P_4		
2							
3							
4		P_1	P_2		P_5		P_7
5							
6				P_6			
7							

(a) Schema Graph (b) Simplified Graph (c) Adjacency Matrix

Fig. 2. Schema Graph and Adjacency Matrix

3 Schema Based Hybrid Partitioning

RDF data partitioning is one of the most important steps of SPARQL query processing in clustered system. We now look at a hybrid partitioning solution to decompose the entire RDF data set upon the schema of them. The global conceptual schema is important to note how the triples are connected to one another, especially with joins. Since the RDF provides no mechanisms for describing relationships between properties and other resource, first we discuss the schema extracting approach to obtain the relationships between resources in RDF data set. Then we consider the hybrid vertical and horizontal partitioning method for RDF data set upon the schema.

3.1 RDF Schema Extracting

For each RDF data set, there is a schema to specify the relationships between resources hidden in RDF vocabulary description language or potential information need to be explored. These schemas provide the facilities needed to describe classes and properties, and to indicate which classes and properties are expected to be used together. With these schemas, we can clearly realize the possibility of joins between classes and properties, and keep the related classes and properties in one partition for joining efficiently. Fig. 2(a) shows a part of the LUBM benchmark schema, extracting from the benchmark ontology named Univ-Bench. In this schema, we know that triples with property *workFor* will never join with the triples with property *takeCourse*, but may join with triples with property *teacherOf*. Therefore, we can maintain the triples with property *workFor* and *teacherOf* in one computing node when partitioning the RDF data set.

Here, the problem is how to acquire the schema. We provide two different approaches to extract schema in different scenarios. First, we can analyze the schema of RDF data via the ontology file endorsed by the W3C Recommendation of RDF vocabulary description language and ontology language which provides mechanisms for describing hierarchical resource groups using classes (is similar to object-oriented programming languages) and the relationships between classes using properties. In this file, a property is defined by *rdfs:domain* and *rdfs:range*, to assert that the subject and object of such property statements must belong to the indicate class description.

For example, in Univ-Bench, the *rdfs:domain* and *rdfs:range* of property *teacherOf* are *Faculty* and *Course*, which means the subject and object of triples with property *teacherOf* are instance of class *Faculty* and *Course*. Then, the next step is to explore the hierarchy between classes by *rdfs:subClassOf*. We find that *Professor* is the sub class of *Faculty* and deduce that *Professor* can be the subject of property *teacherOf* as shown in Fig. 2(a).

However, not all RDF data sets have the ontology file to describe the relationships between properties and classes. In this situation, we have to explore the potential information hidden in RDF data. The official W3C Recommendation defines that property *rdf:type* used to state that a resource is an instance of a class. Therefore, given a triple *t*, we can state *t* by the classes of subject and object. If a resource does not have *rdf:type* property statement, this resource is denoted as the instance of string class. Based on these concepts, we also can explore the *domain* and *range* (multiple) of a property by analyzing all triples with this property using the characteristic of property *rdf:type*. This algorithm is implemented simply using MapReduce programming model as shown in Algorithm 1. In this algorithm, we replace the subject of each triple with classes. In the same way, objects also can be replaced with classes. Then the relationships between different classes can be collected from the results.

Algorithm 1. Extracting Schema

```
Input: RDF triples
  map(key, value):      //key: line number   value: triples
    emit(triple.subject, triple)
  reduce(key, iterator value)
    class := "string"
    for triple in value do
      if triple.property = "rdf:type" then
        class := triple.subject
    for triple in value do
      if triple.property != "rdf:type" then
        emit(null, class+triple.property+triple.object)
      else
        emit(null, triple)
```

3.2 Hybrid Partitioning

After generating schema of RDF data set and obtaining the relationships between resources, the next step is to decompose the entire RDF data into multiple partitions maintaining related triples in the same partition. We propose a hybrid vertical and horizontal partitioning method considering the relationships in schema.

We represent the schema as a direct graph $G = (V, E)$. The elements of V (vertex) are the classes in RDF data set and the elements of E (edge) are properties. Examples are given in Fig. 2(a) and Fig. 2(b) (we use IDs instead of classes and properties for

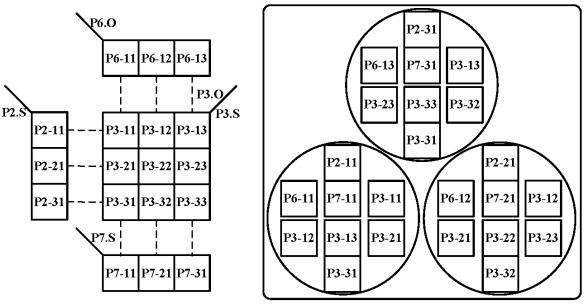

Fig. 3. Hybrid Partitioning and Placement

simplicity). The adjacency matrix A of graph G is shown in Fig. 2(c), rows and columns of A labeled with the classes. The non-diagonal entry in this matrix in row i and columns j is the edge (property) connecting vertices i, j and from i to j. In matrix A, the properties in the same row indicate that these properties share with common subject, which means there may be joins occurred between the triples with these properties formed S-S join. In the same way, the properties in the same columns shows that there will be O-O join occurred between triples shared with common object. Moreover, the multiplication of matrix A is to record the paths in RDF data. Suppose that multiplying pairwise the entries in row r by the entries in column c is: $(0\ 0\ 0\ P_6\ 0\ 0\ 0)\ (0\ 0\ 0\ P_7\ 0\ 0\ 0)^T = P_6\text{-}P_7$, it means there is a 2-hop path connecting classes r and c, P_6 to P_7, where there may be S-O joins existed between P_6 and P_7. If A is the adjacency matrix of ontology graph G, A^1, A^2, ... , A^i with power i is means of representation of i-hop paths between classes. Consequently, according to the adjacency matrix of schema represented in Fig. 2(c), $\{P_1, P_2, P_3, P_4\}$ may join on class "1", and $\{P_3, P_6\}$ may join on class "4", etc. Then the 2-hop path can be shown by the multiplication of this adjacency matrix, and the join will be occurred between the object of first property and subject of second property.

Note that, all possible joins mentioned above are on the basis of properties. Therefore, first we group the triples with common property into a two column tables, whose first column contains the subjects and second column contains the objects [8]. The relations are the basic unit of the next step: horizontal partitioning, and represented as P_i. Given a relation P_i and the number of computing nodes N, for each triple t in P_i, the horizontal partitioning is computed such that

$$P_i\text{-}nm \begin{cases} hash(t.s) \bmod N = n \text{ and } m = 1 \text{ (on subject)} \\ hash(t.o) \bmod N = m \text{ and } n = 1 \text{ (on object)} \end{cases}$$

where the hash function ensures partitions are of a uniform size for better load balancing. Note that, the relations are not independent, we also have to consider the relationship links between them [13]. The link between two relations is defined as an equijoin. Accordingly, given two relations P_i, P_j and a link on their subject, the horizontal partitioning can be implemented on subject of each relation. Since hash function ensures the same subject or object in the common partition, the hash on the linked columns can be seen as the equi-join on them. However, a relation maybe

linked with others both on subject and object, then for each triple t the horizontal partitioning is computed such that

$$P_i\text{-}nm = hash(t.s) \bmod N = n \text{ and } hash(t.o) \bmod N = m$$

According to the partitioning approach, P_i-nm is partitioned only on object or subject, P_i-$1m$ places on node m, P_i-$n1$ places on node n. If P_i-nm is partitioned both on subject and object, P_i-nm places on nodes n and m. Consider links between P_2, P_3, P_6, P_7 in Fig.2, where P_2 and P_3 are linked on subject, and subject of P_7 is linked with object of P_3 and P_6. Then we show the horizontal partitioning results according to the links in Fig. 3 with the assumption that there are 3 nodes. The placement of relations is shown in Fig. 3.

4 Query Processing and Optimization

Reducing the number of MR cycles in SPARQL query execution is far more efficient, since this can avoid the unnecessary overhead. Therefore, we group as much triple patterns as possible into sub-query which can be performed in one MR cycle. The optimal situation is that the query can be executed in one MR cycle entirely. However, in some cases the queries have to be decomposed. In this section, we discuss a query decomposed method based on the principle that groups as much triple patterns as possible. A light-weight sideways information passing technique for passing join information across MR cycles will be introduced.

4.1 Query Decomposition and Optimization

We propose a query decomposition approach corresponding to schema based hybrid partitioning algorithm, a performance enhancing technique that group the triple patterns of SPARQL queries into sub-queries orderly and efficiently. The SPARQL query consisting of multiple triple patterns shown in Fig. 1(a) can be redrawn as a query graph shown in Fig. 4(a), where triples patterns are denoted as vertices and edges connect two vertices by the common join variables between them. The *SQ* is a sub-query (conjunction of triple patterns) that can be performed in one MR cycle. When finishing the triple patterns grouping, we will reverse the orders between sub-queries to establish a left-deep tree for optimal execution ordering using the selectivity estimation strategies in [29]. We later will discuss how to utilize the optimal join ordering for sideways information passing to reduce intermediate results (section 4.2).

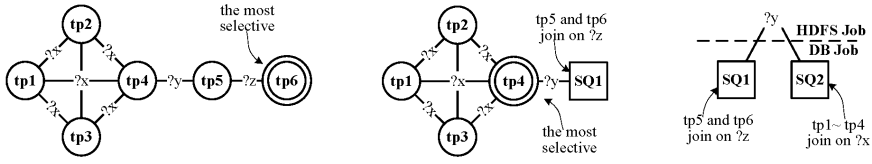

(a) Selectivity (b) Sub Query Grouped (c) Execution Tree

Fig. 4. SPARQL Query Decomposition and Optimization

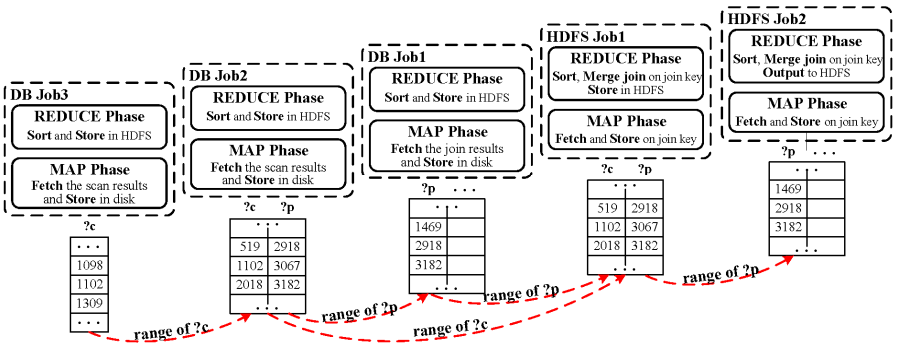

Fig. 5. Example of Sideways Information Passing between MR Jobs

The SPARQL query decomposition and optimization algorithm works as follows. Initially, each node in the query graph is assigned with the selectivity of the corresponding triple pattern. The algorithm first selects the most selective vertex in query graph and groups this vertex with the adjective vertices as much as possible according to the data partitioning algorithm (i.e. 2-hop S-O join or S-S, O-O join). After grouping triples patterns, a new sub-query graph is generated. Then the algorithm iteratively chooses the vertex with the most selectivity in the remaining triple patterns and groups the adjective vertices. Finally, the algorithm terminates when no vertex remains in the query graph. Then we calculate the selectivity of each sub-query and establish the left-deep tree to display the execution order between these sub-queries. Fig. 4 shows an example execution of this algorithm. *tp6* is the most selective, and then we group *tp5* and *tp6* into *SQ1* by 2-hop chain join in Fig. 4(a). Then in the remaining triple patterns, *tp4* is the most selective one, we group all star triple patterns into *SQ2* in Fig. 4(b). Via computing the selectivity of *SQ1* and *SQ2*, the left-deep tree is built shown in Fig. 4(c), where each *SQ* is executed in one MR cycle and the joins between *SQ* are executed in one MR cycle.

4.2 Sideways Information Passing

Although data partitioning and the query decomposition upon it can reduce the MR cycles for the certain SPARQL queries, the non-selective sub-queries will also lead to large number of intermediate results to transfer and write to HDFS, such as (*?x P ?y*) where relation *P* contains large number of triples. To alleviate the impact of this situation, we propose a light-weight sideways information passing mechanism to pass the information of join variables between MR jobs. In general, there are two capabilities have to be followed: (1) to obtain the knowledge about which channel has to be chosen to pass the information of variables between different MR jobs, and this is prepared at query compile-time, (2) to compute and pass the information of variables to next MR job needed in an efficient-cost way, and this is implemented at run-time.

Now we would like to discuss the channel of variables' information passing between all MR jobs. For each MR job, a collection of information for each join

variable *v* is denoted as $V_n(v)$, and this MR job is *nth* executed MR job. In the execution tree, each MR job will receive the information of join variables from the MR jobs that have been executed, i.e. the information of $V_n(v)$ will be update by $V_i(v)$ where $i < n$. For example, the channel in query execution in Fig. 1(b) is illustrated in Fig. 5, supposing that DB job3 → DB job2 → DB job1 → HDFS job1 → HDFS job2 is the optimal order. Note that, DB job3 is the most selective sub-query, and produces the precise information of join variable *?c*. Then the information of *?c* will be passed to DB job2 as a filter condition to reduce the intermediate results and produce more precise information of *?c* and *?p*. Iteratively, information of join variables are passed to next MR job until MR jobs are completed.

At run-time, the information has to be stored and fetched in an efficient-cost way. In DB jobs, the SPARQL sub-queries are converted into SQL expressions. While in HDFS jobs, the joins are executed using reduce-side join method which uses the join key as map output key and performs joins as merge join in reducer over the inputs which ordered on join key. Therefore, information of all join variables in the DB jobs and HDFS jobs can merely contain the range of each join variable to allow the operations of sideways information passing in a simple and light-weight way. To pass the information to each MR job, there are two main operations: store and fetch. When a MR job finishes, the range of join variables involved in this MR job will be stored in HDFS shared by all MR jobs. Then the fetch operation can obtain the needed HDFS files according to the channel of variables' information passing and compute the range for each join variable. In DB jobs, the information is represented into a *$where$* clause to specify the range of join variables added to the original SQL statement, such as "*subject* <= *max and subject* >= *min*". However, in HDFS jobs, the range of join variables is used in map phase to filter the inputs to reduce the number of triples involved in sort and reduce phase.

5 Performance Evaluation

In this section, we evaluate our methods over LUBM [16]. We measure the performance of Hive, a simple hash partitioning version of base system (HadoopDB [10]), and the enhanced system that contains our methods in various types of query.

All experiments are performed on a 15-nodes cluster. Each node of this cluster has two processors at 2.4GHz, 4GB RAM, 12GB disk swap space and 150GB hard disks. The network speed is approximately 25MB/s. We have prototyped all these techniques in the HadoopDB with the well-known column database MonetDB [4]. For our experiments, we choose Hive version 0.6.0, HadoopDB version 0.1.1.0, Hadoop version 0.19.2, and MonetDB version 11.5.7.

5.1 Benchmark

LUBM [16] data set is widely used in semantic web fields for the RDF data management system evaluation. In our experiment, we generate LUBM data sets contains 100, 500, 1000, 2000, 5000 universities respectively shown in Table 1.

Table 1. LUBM Data Set

Data Set	#Triples	#Entity(S ⋃ O)	#P
LUBM-100	13,409,395	3,303,742	18
LUBM-500	69,099,760	16,439,334	18
LUBM-1000	138,318,414	32,905,171	18
LUBM-2000	276,425,052	65,764,622	18
LUBM-5000	667,592,614	146,246,363	18

Table 2. Benckmark Queries

	#triple patterns	#S-S joins	#O-O joins	#S-O joins	Hash		Hybrid		#Hive jobs
					#DB jobs	#HDFS jobs	#DB jobs	#HDFS jobs	
Q1	5	4	0	0	1	0	1	0	1
Q2	3	0	1	1	3	2	1	0	1
Q3	2	0	0	1	2	1	1	0	1
Q4	3	0	0	2	3	2	2	1	2
Q5	4	1	0	2	3	2	2	1	2
Q6	6	3	0	2	3	2	3	2	4
Q7	6	3	0	2	3	2	2	1	3
Q8	4	1	0	2	3	2	2	1	2

Our experiments choose eight queries that need to be executed on each comparison system through the LUBM data sets. Most of these queries are the benchmark queries in LUBM; others are typical queries for different feature of systems. The queries are provided in full in the appendix as SPARQL triple patterns format. Table 2 shows the number of triple patterns, subject-subject joins, object-object joins, subject-object joins, the number of DB jobs and HDFS jobs corresponding to simple hash partitioning, schema based hybrid partitioning and the number of MR jobs in Hive in each queries. The number of DB jobs in simple hash is only related to the number of S-S joins, while the schema based hybrid partitioning can also handle the S-O joins and O-O joins. In this table, we can understand the obvious improvement of schema based hybrid partitioning in reducing the number of MR cycles.

5.2 Data Distribution

First, we investigate the impact of schema based hybrid partitioning algorithm on data distribution. While RawHadoop, Hive and Hash partitioning try to evenly distribute the RDF data on the cluster, schema based hybrid partitioning algorithm additionally tries to group the related data as much as possible. Fig. 6 shows the data distribution results over cluster. The x-axis stands for the cluster nodes and y-axis shows the ratio of data size in this node to the total data size. As Fig. 6 shows, in contrast to hash partitioning, schema based hybrid partitioning only slightly disturbs the distribution of the data over cluster. However, RawHadoop and Hive show the worse results, there are some spots a little far from the average line.

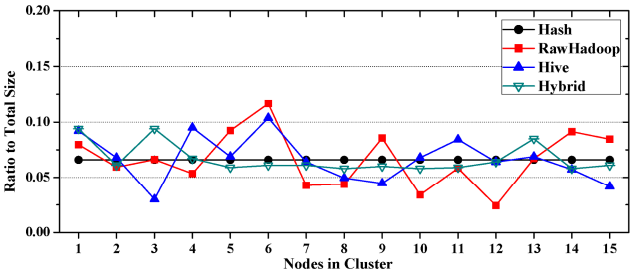

Fig. 6. Data Distribution over the Cluster

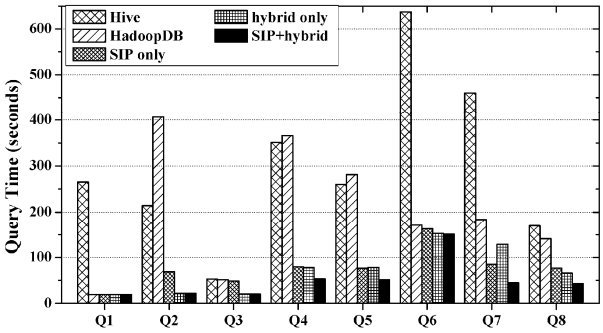

Fig. 7. Query Performance on LUBM-5000

5.3 Performance Comparison

The performances of eight queries are shown in Fig. 7. To measure the effects of our individual technique, we run all experiments on different techniques where only enable our method for sideways information passing (**SIP only**) and replace the hash partitioning with the schema based hybrid partitioning (**hybrid only**), and enable both approaches (**SIP+hybrid**). All times presented in this paper are the averages of four runs. The sizes of intermediate results of each technique are shown in Table 3.

Obviously, the results show that the techniques described in this paper achieve an excellent improvement on performance, and combination of two methods (*SIP+hybrid*) achieves the best performance in every benchmark query. Although HiveQL uses query compiler and optimizer to build the efficient query plans for each benchmark queries as Table 2 shows, without indexes Hive has only brute force as a processing option which lead to much more costly operations. As shown in Table 3, the sizes of intermediate results in *SIP+hybrid* are reduced even more than three-four orders of magnitude than original HadoopDB. Our methods deployed on HadoopDB perform a factor of 2-20 faster than the original HadoopDB and Hive. To better analyze the reasons, we discuss each query separately.

Table 3. Intermediate Results Size (LUBM-5000)

	Q1	Q2	Q3	Q4	Q5	Q6	Q7	Q8
HadoopDB	0.04MB	2905.43MB	71.02MB	1856.18MB	1061.07MB	829.41MB	616.91MB	319.15MB
SIP only	0.04MB	0.21MB	0.14MB	0.23MB	0.22MB	829.40MB	1.86MB	0.23MB
hybrid only	0.04MB	0.04MB	0.05MB	264.25MB	160.21MB	827.71MB	404.2MB	71.01MB
SIP+hybrid	0.04MB	0.04MB	0.05MB	0.15MB	0.15MB	827.69MB	1.22MB	0.14MB

For Q1, simple hash partitioning and schema based hybrid partitioning group all SPARQL triple patterns into one sub-query, which means all five systems with different approaches are performed in the same way. Therefore, the performances and the size of intermediate results are almost unanimously except Hive.

For Q2 and Q3, the schema based hybrid partitioning is more important. Since in simple hash partitioning, there are 5 and 3 MR cycles to be executed, while in schema based hybrid partitioning, the number is merely 1. These lead to more MR cycles overhead including the Hadoop start-up time and communication cost. Moreover, the overhead of transferring and storing the intermediate results affects the key impact on the performance, because the sizes of intermediate results using simple hash partitioning are much larger as shown in Table3. The query time of sideways information passing in Q2 and Q3 are slower than schema based hybrid partitioning because of the number of MR cycles. The performance of combination method equals to schema based hybrid partitioning, since one MR cycle does not need sideways information passing.

For Q4, Q5, Q7, and Q8, the sideways information passing plays more significant role. Although schema based hybrid partitioning reduces the number of MR cycles needed to be performed, there are far more intermediate results than using sideways information passing. The combination of both methods achieves major benefits from two methods, performs the best performance. All triples patterns are non-selective in Q6. Therefore, the effect of sideways information passing is trivial for Q6, shown in Table 3. The schema based hybrid partitioning does not reduce the MR cycles in Q6, only regroups the sub-queries in Q6 and optimizes the sequence of sub-queries performing. Since the size of intermediate results is not reduced obviously, the performance is improved rarely.

5.4 Varying the Data Set

Although the query performance on certain benchmark is important, an arguably factor to explore the performance of clustered system is the scalability. In this part, we study the performance when varying the size of data sets. The results of Q2, Q5 and Q8 on different data sets are shown in Fig. 8, to illustrate the impacts on different approaches when data set size changes (hence we do not compare with Hive).

With the growth of data set size, the original approaches in HadoopDB induce much more intermediate results, which have a significant impact on query performance. We observe clearly that the combination of two approaches which benefit from each optimized approach, achieves the best performance by dramatically reducing the I/O cost and communication overhead. In details, for Q2, since the schema

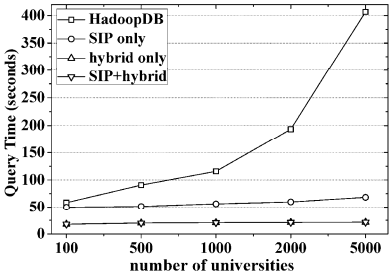

(a) Varying Data Set Size for Q2

Data Set	HadoopDB	SIP only	hybrid only	SIP+hybrid
LUBM-100	49.26MB	0.21MB	0.04MB	0.04MB
LUBM-500	262.77MB	0.21MB	0.04MB	0.04MB
LUBM-1000	544.48MB	0.21MB	0.04MB	0.04MB
LUBM-2000	1107.02MB	0.21MB	0.04MB	0.04MB
LUBM-5000	2905.43MB	0.21MB	0.04MB	0.04MB

(b) Intermediate Results Size of Q2

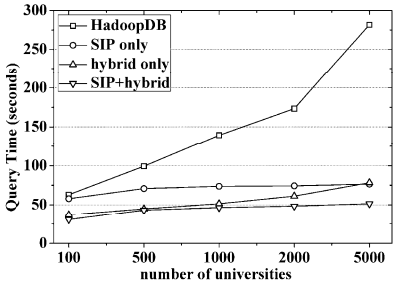

(c) Varying Data Set Size for Q5

Data Set	HadoopDB	SIP only	hybrid only	SIP+hybrid
LUBM-100	18.15MB	0.22MB	2.95MB	0.15MB
LUBM-500	96.23MB	0.22MB	14.95MB	0.15MB
LUBM-1000	199.43MB	0.22MB	30.61MB	0.15MB
LUBM-2000	404.62MB	0.22MB	61.79MB	0.15MB
LUBM-5000	1061.07MB	0.22MB	160.21MB	0.15MB

(d) Intermediate Results Size of Q5

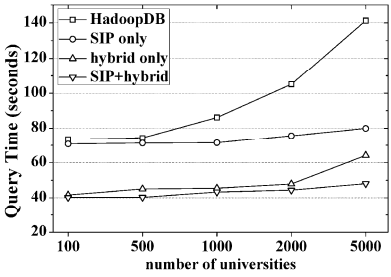

(e) Varying Data Set Size for Q8

Data Set	HadoopDB	SIP only	hybrid only	SIP+hybrid
LUBM-100	5.60MB	0.23MB	1.34MB	0.14MB
LUBM-500	29.03MB	0.23MB	6.54MB	0.14MB
LUBM-1000	60.00MB	0.23MB	13.42MB	0.14MB
LUBM-2000	121.69MB	0.23MB	27.14MB	0.14MB
LUBM-5000	319.15MB	0.23MB	71.01MB	0.14MB

(f) Intermediate Results Size of Q8

Fig. 8. Varying Data Set Size

based hybrid partitioning approach can reduce the number of MR cycle to one, the query execution time in *hybrid only* and *SIP+hybrid* is merely related to the query time in each DBMS deployed on computing node. Although the intermediate results size in *SIP only* is rarely small, more MR cycles will bring in the more Hadoop start-time. For Q5 and Q8, as expected, query execution time in *SIP only* and *SIP+hybrid* do not increase as the number of triples stored in cluster grows, and the intermediate result sizes in different data sets almost unchanged. These are caused by the factor that the passed information is quite accurate to avoid most unnecessary join cardinality involved in join processing. Although *hybrid only* can reduce the number of MR cycle included in Q5 and Q8, as Fig. 8(d) and Fig. 8(f) show, the intermediate results increasing also affect the query execution time. In Fig. 8(c), the speedup of *hybrid*

only exceeds that of *SIP only*, and these two curves intersect when answering the query in LUBM-5000 benchmark. In Fig. 8(e), although the performances of *hybrid only* are better than that of *SIP only*, with the growth of data sets, *hybrid only* will also achieve the poorer performance by increased intermediate results.

6 Conclusion

In this paper, we propose a schema based hybrid partitioning technique for RDF data placement. Our approach provides a mechanism to extract the global conceptual schema of RDF data set for describing the relationships between properties and resources. Corresponding to the schema, the hybrid of vertical and horizontal partitioning methods is presented, which addresses the challenge of reducing the number of MR cycles when answering the queries. Further, by carefully designing the SPARQL query decomposition and join ordering approaches, we present a light-weight sideways information passing techniques, to provide highly effective filters on each input streams of MR jobs. The experimental results show that our approaches achieve a substantial performance improvement.

Acknowledgement. The research is supported by National High Technology Research and Development Program of China (863 Program) under grant No.2012AA011003 and National Science Foundation of China (61073096).

References

1. The Friend of a Friend (FOAF) project, `http://www.foaf-project.org/`
2. Linking open data on the Semantic Web, `http://www.w3.org/wiki/SweoIG/Task-Forces/CommunityProjects/LinkingOpenData`
3. MapReduce, A.: major step backwards, `http://databasecolumn.vertica.com/database-innovation/mapreduce-a-major-step-backwards/`
4. MonetDB, `http://www.monetdb.org/`
5. Resource Description Framework (RDF), `http://www.w3.org/TR/rdf-concepts/`
6. SPARQL query language for RDF, `http://www.w3.org/TR/rdf-sparql-query/`
7. The universal protein resource (Uniprot), `http://www.uniprot.org/`
8. Abadi, D., Marcus, A., Madden, S., Hollenbach, K.: Scalable semantic web data management using vertical partitioning. In: Proc. VLDB, pp. 411–422 (2007)
9. Abadi, D., Marcus, A., Madden, S., Hollenbach, K.: SW-Store: a vertically partitioned DBMS for Semantic Web data management. The VLDB Journal 18(2), 385–406 (2009)
10. Abouzeid, A., Bajda-Pawlikowski, K., Abadi, D., Silberschatz, A., Rasin, A.: HadoopDB: An architectural hybrid of MapReduce and DBMS technologies for analytical workloads. In: Proc. VLDB, pp. 922–933 (2009)
11. Agrawal, S., Narasayya, V., Yang, B.: Integrating vertical and horizontal partitioning into automated physical database design. In: Proc. SIGMOD, pp. 359–370 (2004)
12. Atre, M., Chaoji, V., Zaki, M., Hendler, J.: Matrix Bit loaded: a scalable lightweight join query processor for RDF data. In: Proc. WWW, pp. 41–50 (2010)

13. Ceri, S., Navathe, S., Wiederhold, G.: Distribution design of logical database schemas. IEEE Transactions on Software Engineering (4), 487–504 (1983)
14. Dean, J., Ghemawat, S.: Mapreduce: Simplified data processing on large clusters. Communications of the ACM 51(1), 107–113 (2008)
15. Erling, O., Mikhailov, I.: Towards web scale RDF. In: Proc. SSWS (2008)
16. Guo, Y., Pan, Z., Heflin, J.: LUBM: A benchmark for OWL knowledge base systems. Web Semantics: Science, Services and Agents on the World Wide Web 3(2), 158–182 (2005)
17. Harris, S., Lamb, N., Shadbolt, N.: 4store: The design and implementation of a clustered RDF store. In: Proc. SSWS, pp. 94–109 (2009)
18. Harth, A., Umbrich, J., Hogan, A., Decker, S.: YARS2: A Federated Repository for Querying Graph Structured Data from the Web. In: Aberer, K., Choi, K.-S., Noy, N., Allemang, D., Lee, K.-I., Nixon, L.J.B., Golbeck, J., Mika, P., Maynard, D., Mizoguchi, R., Schreiber, G., Cudré-Mauroux, P. (eds.) ASWC 2007 and ISWC 2007. LNCS, vol. 4825, pp. 211–224. Springer, Heidelberg (2007)
19. Huang, J., Abadi, D., Ren, K.: Scalable sparql querying of large rdf graphs. In: Proc. VLDB (2011)
20. Husain, M., McGlothlin, J., Masud, M., Khan, L., Thuraisingham, B.: Heuristics based query processing for large RDF graphs using cloud computing. IEEE Transactions on Knowledge and Data Engineering 23(9), 1312–1327 (2011)
21. Ives, Z., Taylor, N.: Sideways information passing for push-style query processing. In: Proc. ICDE, pp. 774–783 (2008)
22. Kaoudi, Z., Kyzirakos, K., Koubarakis, M.: SPARQL Query Optimization on Top of DHTs. In: Patel-Schneider, P.F., Pan, Y., Hitzler, P., Mika, P., Zhang, L., Pan, J.Z., Horrocks, I., Glimm, B. (eds.) ISWC 2010, Part I. LNCS, vol. 6496, pp. 418–435. Springer, Heidelberg (2010)
23. Neumann, T., Weikum, G.: Scalable join processing on very large RDF graphs. In: Proc. SIGMOD, pp. 627–640 (2009)
24. Neumann, T., Weikum, G.: The RDF-3X engine for scalable management of RDF data. The VLDB Journal 19(1), 91–113 (2010)
25. Olston, C., Reed, B., Srivastava, U., Kumar, R., Tomkins, A.: Pig latin: a not-so-foreign language for data processing. In: Proc. SIGMOD, pp. 1099–1110 (2008)
26. Ravindra, P., Hong, S., Kim, H., Anyanwu, K.: Efficient processing of rdf graph pattern matching on mapreduce platforms. In: Proc. International Workshop on Data Intensive Computing in the Clouds, pp. 13–20 (2011)
27. Rohloff, K., Schantz, R.: High-performance, massively scalable distributed systems using the MapReduce software framework: the SHARD triple-store. In: Proc. Programming Support Innovations for Emerging Distributed Applications (2010)
28. Sridhar, R., Ravindra, P., Anyanwu, K.: RAPID: Enabling Scalable Ad-Hoc Analytics on the Semantic Web. In: Bernstein, A., Karger, D.R., Heath, T., Feigenbaum, L., Maynard, D., Motta, E., Thirunarayan, K. (eds.) ISWC 2009. LNCS, vol. 5823, pp. 715–730. Springer, Heidelberg (2009)
29. Stocker, M., Seaborne, A., Bernstein, A., Kiefer, C., Reynolds, D.: SPARQL basic graph pattern optimization using selectivity estimation. In: Proc. WWW (2008)
30. Tanimura, Y., Matono, A., Lynden, S., Kojima, I.: Extensions to the Pig data processing platform for scalable RDF data processing using Hadoop. In: Proc. IEEE 26th International Conference on Data Engineering Workshops (ICDEW), pp. 251–256 (2010)
31. Thusoo, A., Sarma, J., Jain, N., Shao, Z., Chakka, P., Zhang, N., Antony, S., Liu, H., Murthy, R.: Hive-a petabyte scale data warehouse using hadoop. In: Proc. ICDE (2010)

Appendix: LUBM Queries

Q1: SELECT ?x WHERE {?x ub:name ?y1. ?x ub:telephone ?y3. ?x ub:emailAddress ?y2. ?x ub:worksFor <http://www.Department0.University0.edu>. ?x rdf:type ub:FullProfessor.}
Q2: SELECT ?x, ?y WHERE {?y rdf:type ub:Course. ?x ub:takesCourse ?y. <http://www.Department0.University0.edu/AssociateProfessor0> ub:teacherOf ?y.}
Q3: SELECT ?x, ?y WHERE {?x ub:worksFor ?y. ?u ub:subOrganizationOf <http://www.University0.edu>.}
Q4: SELECT ?x, ?y, ?z WHERE { ?x ub:teacherof ?y. ?y ub:name ?z. <http://www.Department0.University0.edu/FullProfessor2/Publication13> ud:publicationAuthor ?x.}
Q5: SELECT ?x ?y WHERE {?x rdf:type ub:GraduateStudent. ?y rdf:type ub:GraduateCourse. ?x ub:takesCourse ?y. <http://www.Department0.University0.edu/AssociateProfessor0> ub:teacherOf ?y.}
Q6: SELECT ?x ?y ?z WHERE {?y ub:teacherOf ?z. ?x ub:advisor ?y. ?z rdf:type ub:Course. ?x ub:takesCourse ?z. ?x rdf:type ub:UndergraduateStudent. ?y rdf:type ub:FullProfessor.}
Q7: SELECT ?s ?p WHERE { ?s name ?n. ?s email ?e. ?s telephone ?t. ?s advisor ?p. ?p teacherOf ?c. ?c name "Course72".}
Q8:SELECT ?x ?z WHERE
{ <http://www.Department0.University0.edu/FullProfessor0/Publication0> ub:publicationAuthor ?x. ?x ub:advisor ?y. ?y ub:worksFor ?z. ?x rdf:type ub:GraduateStudent.}

Iterative Receiver with Joint Channel Estimation and Decoding in LTE Downlink

Weijie Xiao[1, 2], Qiong Li[2], Xinxue Zhao[1], and Qiang Gao[1]

[1] School of Electronic and Information Engineering, Beihang University, Beijing, China
{xiaoweijie,zhaoxinxue}@ee.buaa.edu.cn, gaoqiang@buaa.edu.cn
[2] State Key Laboratory of Wireless Mobile Communications (CATT), Beijing, China
liqiong@catt.cn

Abstract. In this paper, an iterative receiver using joint channel estimation and channel decoding is proposed for LTE downlink. In each iterative process, a modified LMMSE estimator is adopted to estimate the channel gain based on pilots as well as signals fed back from Turbo decoder. In contrast to a traditional LMMSE estimator, the modified estimator can make more precise channel estimation because a smaller spacing interpolation is performed with the help of feedback signals. The estimator and the decoder provide each other more accurate information in an iterative way, thus the performance of the receiver is improved. Three distribution patterns of the signals fed back from Turbo decoder with different density is compared, and the one with medium density is demonstrated to be the best by simulation results. To reduce the computational complexity of the receiver, cyclic redundancy check (CRC) is used to early stop the iteration. Simulation is done according to LTE physical layer specifications and the results show that the iterative receiver can provide about 50% accuracy improvement compared with a non-iterative receiver when SNR is 10dB. At the same time, the iterative receiver's computational complexity is in the same order of magnitude as the non-iterative receiver.

Keywords: LTE, iterative receiver, channel estimation.

1 Introduction

Recently, iterative signal processing becomes an attractive idea in the field of wireless communications. It is realized that Turbo principle can be applied to the design of iterative receivers. Now, there exist several schemes applying iterative signal processing in wireless communications such as Turbo equalization [1], iterative joint channel estimation and decoding [2], iterative multiuser detection [3].

In an iterative receiver in LTE downlink, channel estimator is a crucial module. Now, there are several channel estimation methods, such as LS (Least Square), LMMSE (Linear Minimum Mean Square Error) [4] and DFT-based (Discrete Fourier Transform based) [5]. LS is the fundamental channel estimation method which neglects the effect of noise so that its accuracy is low. LMMSE is a de-noising channel estimation method which takes advantage of channel correlation, and it is widely used for its high accuracy.

Q. Zu, B. Hu, and A. Elçi (Eds.): ICPCA-SWS 2012, LNCS 7719, pp. 647–652, 2013.

In this paper, we present an iterative receiver with joint channel estimation and decoding. The receiver's performance is improved through iterations because the channel estimator and the decoder can provide each other more accurate information.

Iteration stopping criterion is an important issue in iterative receivers. Usually, iteration stops when it reaches a maximum iteration number, which has a high computational complexity. An iteration early stopping criterion is present in this paper to reduce the complexity.

The rest of the paper is organized as follows: in section 2, the considered system is described. Section 3 discusses the proposed iterative receiver. The receiver's performance is evaluated in section 4 and the conclusion is made in section 5.

2 System Description

In LTE systems, pilot assisted channel estimation is employed. According to 3GPP specifications [6], pilots locate at the 0th and the 5th OFDM symbols in time domain and every sixth carrier in frequency domain. In this paper, we denote complex symbols at each resource element (RE) by $X_{l,k}$, where l represents the OFDM symbol index and k represents the subcarrier index($l \in \{0,...,L-1\}, k \in \{0,...,K-1\}$).

After being generated, the signal is transmitted over a wireless multipath Rayleigh fading channel whose channel impulse response is:

$$h(\tau,t) = \sum_{i=0}^{M-1} \alpha_i(t)\delta(\tau - \tau_i) \tag{1}$$

In (1), $h(\tau,t)$ is the response measured at time t to an impulse input at time delay τ, $\alpha_i(t)$ is wide-sense stationary complex Gaussian random process, representing the ith propagation path gain at time t, obeying Rayleigh distribution. M denotes the total number of resolvable paths. For the convenience of analysis, without a loss of generality, we assume that:

1. The wireless channel is static within an OFDM symbol but varies for different OFDM symbols;
2. Timing and frequency offsets are completely eliminated.

At the receiver, the received signal of the lth OFDM block and kth carrier after Fast Fourier Transform (FFT) is:

$$Y_{l,k} = X_{l,k} \cdot H_{l,k} + W_{l,k} \tag{2}$$

In (2), $W_{l,k}$ is fast Fourier transformed zero-mean complex additive white Gaussian noise. In the following-up modules, $Y_{l,k}$, combined with estimation of $H_{l,k}$, is used to calculate the original signal.

3 Design of Iterative Receiver with Joint Channel Estimation and Decoding

In this section, an iterative receiver with joint channel estimation and decoding in LTE downlink is proposed. We first describe the structure of the iterative receiver and analyze the iterative process. Since the traditional LMMSE estimator is based on pilots, in order to apply it to iterative process, we use a simply modified LMMSE estimator based on both pilots and feedback data. For the sake of reducing the receiver's complexity, we propose an iteration early stopping criterion, which imposes CRC.

3.1 Iterative Receiver and Iterative Process

The block diagram of the proposed iterative receiver is depicted in Fig.1. Code block is detected in an iterative way. At the *i*th iteration, the iterative process is performed as follows:

First, estimated channel gain { $\hat{H}^{(i)}$ }is obtained using LMMSE algorithm and time and frequency interpolation. In the initial stage (i=0), LMMSE estimation is performed based on pilots, from the first iteration on (i>0), it is performed based on both pilots and data fed back from Turbo decoder. Second, QPSK symbols { $\hat{X}^{(i)}$ } are detected using estimated channel gain and received signal { $\hat{Y}^{(i)}$ }. Then, { $\hat{X}^{(i)}$ } are converted to bit stream { $\hat{C}^{(i)}$ } by QPSK demodulation and RE demapping (pilots are also discarded in RE demapping module). { $\hat{C}^{(i)}$ } is decoded in Turbo decoder, generating { $\hat{D}^{(i)}$ }. Errors are corrected completely or partly in this step. At last, a judgment is made to determine whether the iterative process goes on or not. If the process goes on, transmitted signal { $\tilde{X}^{(i+1)}$ } is reconstructed by Turbo coding, QPSK modulation, and RE mapping.

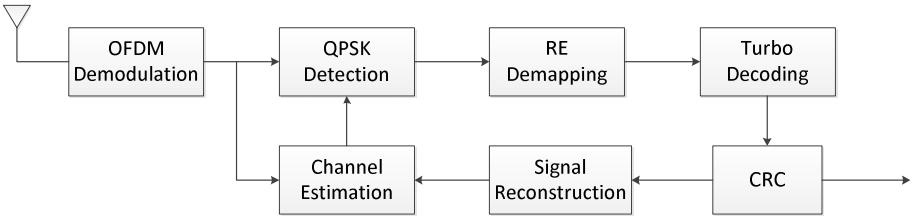

Fig. 1. Block diagram of the proposed iterative receiver

Through the iteration goes on, the receiver's performance is improved because the channel estimator and the decoder tend to provide each other more accurate information. For a non-iterative receiver, channel estimation is made just based on pilots and its accuracy is limited. However, for the proposed iterative receiver, channel estimation is made not only based on pilots but also based on error corrected symbols

fed back from Turbo decoder, so it can achieve more accurate channel estimation. Also, the Turbo decoder can provide more reliable error corrected results because its input coded bits are produced using more accurate channel estimation.

3.2 Channel Estimator in the Iterative Process

Since the traditional LMMSE estimator is based on pilots, in order to apply it to iterative process, we use a simply modified LMMSE estimator based on both pilots and data fed back from Turbo decoder:

$$\hat{\boldsymbol{H}}_s^{(i)} = \mathbf{R}_{H_s H_s} (\mathbf{R}_{H_s H_s} + \frac{\beta}{SNR}\mathbf{I})^{-1} \tilde{\boldsymbol{H}}_s^{(i)} \tag{3}$$

where subscript s denotes both pilot and reconstructed signal. $\hat{\boldsymbol{H}}_s^{(i)}$ denotes LMMSE channel estimation results. $\mathbf{R}_{H_s H_s} = E\{\boldsymbol{H}_s \boldsymbol{H}_s^H\}$ is channel autocorrelation matrix. $\tilde{\boldsymbol{H}}_s^{(i)}$ is the LS channel estimation.

We consider three reconstructed data distribution patterns fed back to the modified estimator, which is shown in Fig.2.

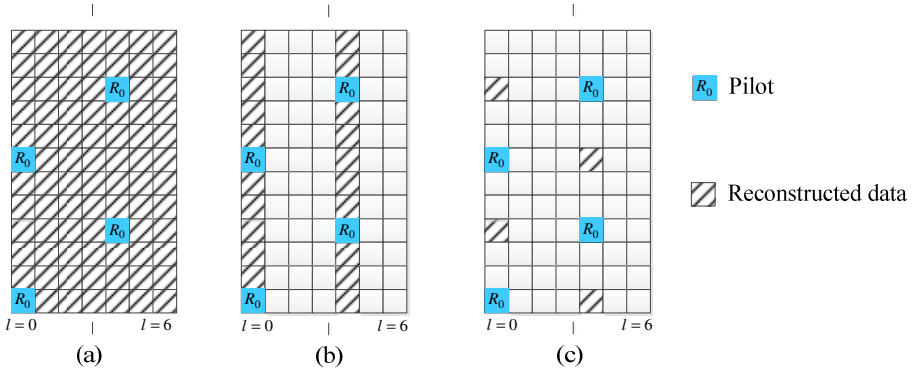

Fig. 2. Reconstructed signal distribution pattern

The pilots and reconstructed data distribution pattern shown in Fig.2 has different density. In the modified estimator, after LMMSE estimation, frequency and time interpolation is made respectively when we consider pattern (c). When we come to pattern (b), only time interpolation is needed, while in pattern (a), no interpolation is needed.

3.3 Iteration Early Stopping Criterion

For an iterative receiver, iteration stopping criterion is an important issue. Usually, a fixed number *N* is given and the iteration stops when it is processed *N* times. However, as the computational complexity of each iterative process is in the same order of

magnitude, if the iteration goes on N times, the computational complexity is almost N times as the non-iterative receiver, resulting in a large processing delay.

In LTE specification [7], CRC parity bits are added to the tails of a code block for error detection. In the proposed iterative receiver, we also apply CRC to the iterative process. CRC checksum is calculated in each iterative process, if the checksum is right, the iteration early stops regardless of whether the receiver reaches the maximum iteration time N, because the correctly received code block doesn't need to be calculated again in an iterative manner any more. So, by applying early stopping criterion, the receiver's complexity can be reduced without accuracy reduction.

4 Performance Evaluation

To assess the performance of the proposed LTE downlink receiver, link level simulation is conducted. The transmitted signal is generated according to LTE specification [6]. We choose simulation scenario to be wireless PedB channel, with a 5Hz Doppler frequency and a 1/3 channel coding rate.

Fig.3 shows BLER over Signal to Noise Ratio (SNR). We can see that: the iterative receivers outperform non-iterative receiver. When the maximum iteration time N is set to 3, the receiver performs better than the case that N=1. This result confirms that the iterations provide accuracy improvement. It can be also seen that reconstructed data distribution pattern also affects the receiver performance: receiver with pattern (b) has a higher accuracy than pattern (a) and pattern (c). So the receiver should apply pattern (b) and the BLER will drops about 50% through the iterations when SNR is 10dB.

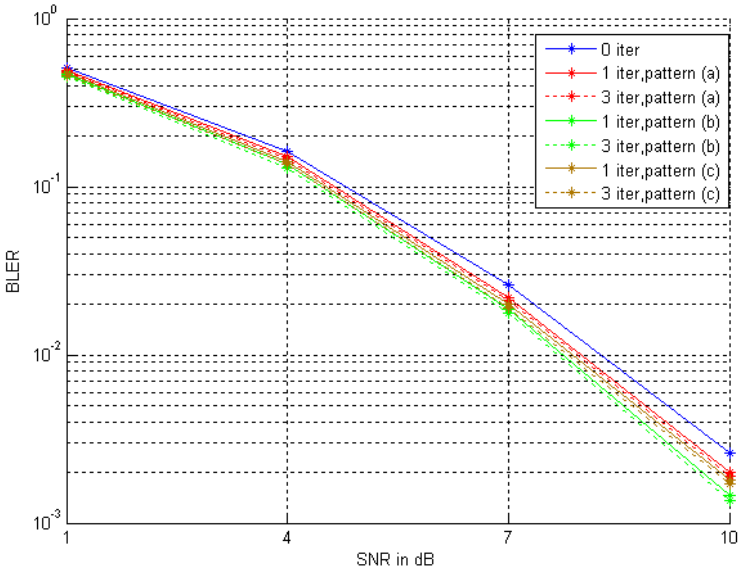

Fig. 3. BLER performance with varying SNR

Now, the computational complexity is discussed. We can see in Fig.3 that BLER is about 0.003 in the initial stage (SNR=10dB), meaning about 99.7% of the code blocks can early stop the iteration in the initial stage. For the remaining 0.3% of the code blocks, iteration is performed. However, these blocks cannot strongly affect the overall computational complexity of the iterative receiver because their proportion is too small. So, compared to non-iterative receiver, there is not an obvious computational complexity increase in the proposed iterative receiver.

5 Conclusion

In this paper, an iterative receiver with joint channel estimation and decoding in LTE downlink is proposed. The simulation results show that, in contrast to a non-iterative receiver, the iterative receiver can achieve about 50% accuracy improvement when SNR is 10dB. At the same time, the iterative receiver's computational complexity is in the same order of magnitude as the non-iterative receiver.

Acknowledgement. This work is supported by the State Key Laboratory of Wireless Mobile Communications (CATT), Program for New Century Excellent Talents in University, and the National Basic Research Program (973 Program) under Grant No. 2010CB731800.

References

1. Douillard, C., Picart, A., Jezequel, M., et al.: Iterative Correction of IntersymbolInterference: Turbo-equalization. Europe Trans. on Communications 6, 507–511 (1995)
2. Valenti, M.C.: Iterative Channel Estimation for Turbo Codes over Fading Channels. In: WCNC, pp. 1019–1024. IEEE Press, Chicago (2000)
3. Teh, K.C., Gunawan, E.: Iterative multiuser detection for asynchronous CDMA with concatenated convolutional coding. JSAC 19, 1784–1792 (2001)
4. Edfors, O., Sandell, M., Wilson, S.K., Borjesson, P.O.: On Channel Estimation in OFDM Systems. In: IEEE 45th Vehicular Technology Conference, vol. 2, pp. 815–819. IEEE Press (1995)
5. Fernandez-Getino Garcia, M.J., Paez-Borrallo, J.M., Zazo, S.: DFT-based channel estimation in 2D-pilot-symbol-aided OFDM wireless systems. In: IEEE 53rd Vehicular Technology Conference, vol. 2, pp. 810–814. IEEE Press (2001)
6. 3GPP: Evolved Universal Terrestrial Radio Access (E-UTRA). Physical Channels and Modulations, TS36.211 (2010)
7. 3GPP: Evolved Universal Terrestrial Radio Access (E-UTRA). Multiplexing and Channel Coding. TS36.212 (2011)

The Research and Design of an Applied Electronic Lottery System

Yuhong Xing

Shandong Jiaotong University, Jinan China 2500023
sd_xingyuhong@163.com

Abstract. An applied electronic lottery system is designed and constructed in this paper. In the system, electronic lottery has all characteristics which lottery based on paper has. It is a simple, facilitate, shortcut lottery sales system. Lottery buyer can buy lottery by Internet; it is impossible to counterfeit a lottery; the Personal information who win a prize in the lottery system should be protected privacy; if a person lost his lottery, he can find it back in the lottery number database which is convenience to inquire about; it can reduce the cost of lottery. It will help the players develop electronic lottery system with safety.

Keywords: Electronic Lottery, digital signature, RSA, Hash Function.

1 Introduction

Recently, people are paying more and more attention to lottery which is still an emerging industry in China. Along with the development of science and technology, players put forward much higher request to the quality and function of lottery service, at the same time, many problems like the current lottery operation mode does not adapt to lottery scientific development have been highlighted, mainly reflected in the following respects.

Firstly, the paper lottery is not safe enough to solve the "forsaken award" problem. On the one hand, paper lottery is easy to damage and lose. It can reflect from the lottery expiry date situation, there are about 300 million Yuan of winning tickets unable to turn in cash and abandon the award each year.

Secondly, players can only get the winning information from passive query. After buying lottery tickets, players can only be sure of winning or not through inquires. Thirdly, the waste of resources is serious. The paper, consumables quantity for national lottery is very large every year.

After the promulgating of "electronic signature law" in our country, the electronic commerce has got a rapid development, investing in stocks on the net and electronic payments have already gone deeply into thousands of households. In this background, a simple, effective, practical and safe electronic lottery system is constructed in this paper, which can make the whole process electronic from buying lottery tickets to the expiry date. The system can solve the following problems, 1) the players can purchase online lottery tickets at home; 2) effectively prevent the forgery of lottery; 3) protect the winners' personal privacy and security effectively; 4) prevent the loss of the

Q. Zu, B. Hu, and A. Elçi (Eds.): ICPCA-SWS 2012, LNCS 7719, pp. 653–658, 2013.

lottery effectively; 5) players can inquire the winning information timely and conveniently; 6) reduce lottery circulation link, thus decrease the cost.

In the lottery system design, these principles should be obeyed: Safty: To ensure that either the betting or lottery claiming process be accurate and the use r account cannot be stolen;

Openess: the variety of the lottery types has been taken into account while desiging the system, making it convenient to increase various kinds of new lotteries in the basis of actual requirements with minimum changes.

Usibiity: making the process of betting, inquiring and cashing the winning lottery as simple as possible.

2 Electronic Lottery System

2.1 System Design

This system mainly includes the following four parts: banks, the trusted third party (CA), lottery center (C) and players (A), they can connect with each other through Internet. Banks, lottery center, the players need to register from a trusted third party first.

The structure of the electronic lottery system is as following

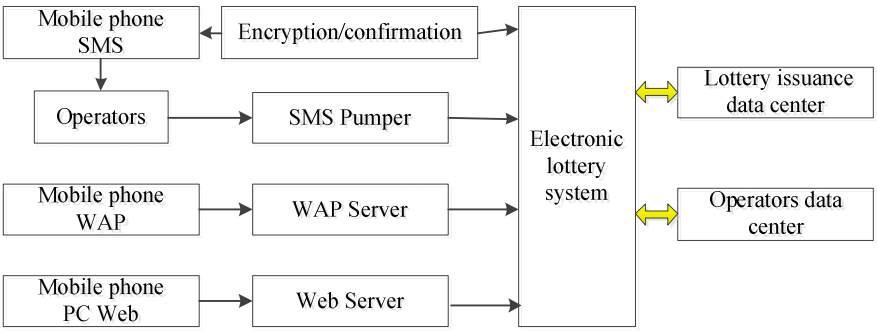

Fig. 1. The structure of the electronic lottery system

The initialization of the trusted third party (CA): Choose a signature system (such as RSA), publish the signature verification public key PKCA, Select a safe Hash function such as SHA[1].

The initialization of the lottery center(C): Lottery center can register in a trusted third party and keep its identity information stored in the trusted third party, at the same time generate its own public or private key, keep public key PKC in trusted third party for releasing. Open an account in the bank.

The initialization of bank (B) : Banking institutions can register in a trusted third party and keep their identity information stored in the trusted third party, at the same

time generate its own public or private key, keep public key PKC in trusted third party for releasing

The initialization of the players(A) :

1) The players register in the trusted third party, put its own identity information stored in the trusted third party, and at the same time generate their own public or private key, stay public key PKa in trusted third party for release

2) The players choose two big prime number p, q, these two numbers must satisfy the equation p = 2q + 1, and p in the discrete logarithm Zp is difficult to hander. A chooses the original α of Zp, and secretly chooses a α, α meets the limit of 1≤a≤q - 1, then use A to calculate the equation β = α a mod p .[2]

3) Open a deposit account in the bank.

2.2 Describing the Basic Protocol

The concrete protocol is described as following:

- Purchase agreement:

1) players choose the lottery number to buy, and calculate the cost m, then combine bank account c, withdrawing amount m with time t to form a message, the message will be signature and encrypted with a bank public key, namely to compute the function Z = EPKb (ID||c||m||t||sign(c||m||t)),the calculated results Z will be sent back to the bank.

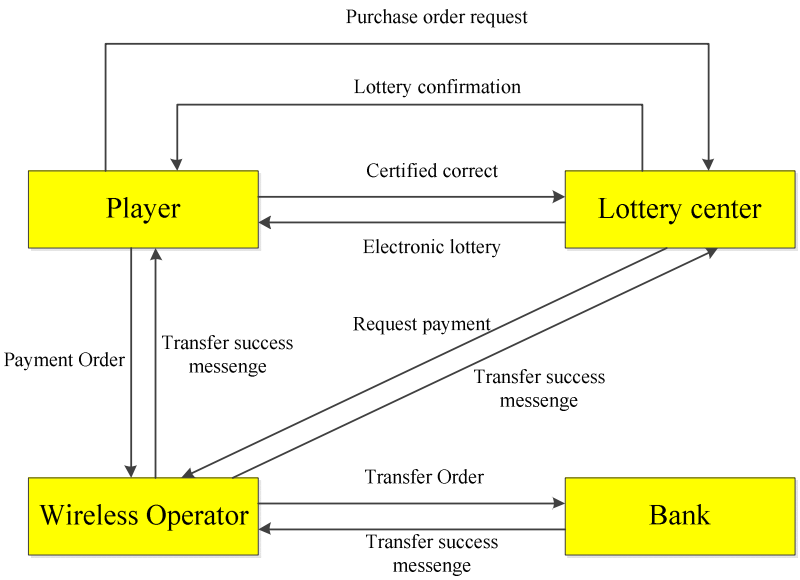

Fig. 2. The process of the lottery purchase

2）After receiving the Z, the bank will decrypt player's ID as well as the message c||m||t through the private key, then use the corresponding public key to verify the signature of the player, then form a message including the bank ID、the message c||m||t sent by the player, player's ID and so forth to do hash operation to get a value u with a length of 160. The number u is the only serial number to withdraw, the bank will calculate the function Y = Epka (u||c||m||sign B(u||c||m)), and the result y will be sent to player A.

3.） The player decrypts the result y with his private key. After verifying the received news with bank public key, the player will form a message M with the selected number、 issue、 time 、 u||c||m||sign b (u||c.||m) and the initial choosed p, α, β, then calculate the function S = Mα mod p, finally encrypt M and S with the public key of lottery center, after calculating the equation x = Epkc(m||S), the player will send the calculated results x to the lottery center c.

4） As long as lottery center has received this news, it will calculate Dpvc (x), and check the consistence between note number and the amount of money to make sure if the amount has been repeated spent, then deposit in the bank. Successfully passing the checking, lottery center will calculate Hash (M) and save M, Hash (M) and Signpva (M) to the lottery number database (this database will be regularly updated). In addition, the M, Hash (M) will be signatured by private key of lottery center and encrypted by player 's public key, and the value v will be transferred to the player by computing the function v = Epka(M||Hash(M)|| signpvc (M||Hash(M))). However, if the checking process encounters some problems, the agreement will terminate immediately and must inform player of the reasons.

5） After receiving the message v and verifying the message is really coming from lottery center, the player will save this lottery.

- Deposit agreement:

（1） Lottery center will put u||c||m with the private key signature and bank public key encryption, then calculate the function n =Epkb (u||c||m||sign (u||c||m)), the results will be sent to the bank.

（2） When the bank receives the message n, it will be decrypted by the private key and verified by the public verification of lottery center to check whether the amount of money has been repeated spent. If not, it will automatically generate a bill t and the bill will be sent to lottery center. At the same time a log will be formed for further inspection use. Otherwise, if the amount has been repeated spent, the agreement will be terminated, and will inform the lottery center of the specific reasons.[3]

- Rewarding agreement:

If the player win the number, he will encrypt the lottery with the public key of lottery player and pass it back to lottery center, after decrypting, the lottery center will verify this lottery with its private key to ensure the lottery is indeed issued by the lottery center, and the signature of the lottery owner will be checked as followings: C selects e1 randomly and e2∈Zp; Calculating f = Se1βe2, and sending f to A;

A calculates the function d = fa-1 mod q mod p, and sends d to C;

C verifies whether d is equal to Me1 β e2, if it is, then A will considered to be the legal ticket holders. [4]

Lottery center will deposit the bonus in an account offered by the customer and at the same time gets signed receipt from the bank.

- Tracking agreement:

Once a link has problems, the whole transaction process is traceable. Different business between players and lottery center are concerned with banks, and banks will generate log for each transaction, so once appearing dispute, the log can be checked with the authorization of relevant departments.

2.3 System Characteristics and Safety Analysis

2.3.1 This System Has the Following Characteristics

1) Electronic lottery not only owns all functions which paper lottery bears, but also easily solves the lost and fake problems with paper lottery.

2) Players can inquire the winning information much more conveniently and timely.

3) Player is anonymous in the buying and rewarding process, it can effectively protect the winners' personal privacy and security.

4) The whole process is realized by toolkit, the operator just needs to click on the selection box, which is simple and timesaving. [5]

2.3.2 The Analysis of System Safety

1) All data transmission in the process of withdrawing money from the bank is encrypted. The difficulty of modifying the data is equivalent to the difficulty of breaking the RSA or other public-key cryptosystem. The time information is contained in the withdrawal information, so the reproduction of the message can be prevented.

2) The electronic cash that lottery players applied for comes with a unique serial number to prevent double-spending. The serial number is created by hashing the teller information. If the 160 bit one-way hash function is used to compute the serial numbers, according to the "birthday paradox", the probability of the two same serial numbers coming out is less than 1/280.[6]

3) Lottery players have used the undeniable digital signature when buying lottery tickets.

The probability of a person pretends to be the signer to deceive the lottery center is 1 / q, q is a large prime number, so the probability is very small.

4) It cannot be denied when lottery center received the lottery numbers and e-cash. When lottery center deposits money in the bank, each item of business is recorded in its log. At the same time, each electronic has a unique serial number. So arbitration institutions can inquiry to the bank, once the disputes between lottery center and lottery players come out.[7]

5) With the participation of CA, each public key corresponds to the identity information, thus can prevent the attacker from using its public key to replace the legitimate public key.

2.4 System Complexity Analysis

In order to prevent winner's loss caused by lottery lost, a lottery number database was increased in the system.The complexity of the data transmission is equivalent to that of RSA public key encryption, Hash function and SHA. All of these arithmetic are divided into two kinds of circumstances, for lottery center and bank, adopting high speed encryption machine to operate, the single-shot process need no more than 1/100 seconds; For the player, using smart IC card or software package, an operation process is less than 1 second in most cases.

3 Conclusion

A practical electronic lottery system is introduced in this paper, which can realize the electronic process from buying the lottery to the expiry date. Compared with traditional lottery、network purchasing and consignment, electronic lottery is safer, more convenient and standardized. It will benefit the players to develop electronic lottery as well as to improve the service functions. The model can be applied to the electronic government affairs in other systems.

References

1. Feng, D., Pei, D.: The cryptography guidance. Science press
2. Stallings, W.: Translated by Xiao Xiang studio. Network security elements - application and standard
3. Liu, Y., Hu, L.: Using an efficient hash chain and delaying function to improve an e-lottery scheme (07) (2007)
4. Yevgeniy, D., Aleksandr, Y.: A verifiable random function with short proof and keys (2005)
5. Lee, J.-S., Chang, C.-C.: Design of electronic t-out-of-n lotteries on the Internet (02) (2009), doi:10.1016/j.csi.2008.05.004
6. Yang, Y.: The network security theory and technology. The People's Posts and Telecommunications Press
7. Chaum, D., van Antwerpen, H.: Undeniable Signatures. In: Brassard, G. (ed.) CRYPTO 1989. LNCS, vol. 435, pp. 212–216. Springer, Heidelberg (1990)

Scheme of Cognitive Channel Allocation for Multiple Services without Spectrum Handover

Haoman Xu, Yinglei Teng, Mei Song, Yifei Wei, and Yong Zhang

ICN&CAD Center, Beijing University of Posts and Telecommunications, Beijing, P.R.C.
vicky87126@yeah.net,
{lilytengtt,songm,weiyifei,yongzhang}@bupt.edu.cn

Abstract. In the system of primary users and cognitive users sharing spectrum resource, dynamic spectrum allocation becomes a key issue to face with, especially when the services are various. A cognitive channel allocation scheme is put forward to maximize the throughput and to reduce the blocking rate of multiple services in the premise of not increasing the interruption probability. In the scheme, cognitive users do not need the capability of spectrum handover, and just by adjusting the index of channels timely, the allocation becomes orderly and simple. Markov chain is used to analyze the performance of the proposed allocation scheme. The numerical results show that the proposed scheme can achieve better performances.

Keywords: Cognitive Radio, Primary User, Cognitive User, Channel Allocation, Markov Chain, Spectrum Handover.

1 Introduction

In cognitive radio system, the idea of open spectrum sharing is widely accepted, that is, cognitive users is allowed to access the primary spectrum while not interfering primary user's service. Channel allocation is one of the key issues that face big challenges for these reasons: a) Users, including primary users and cognitive users, are selfish. They are uncooperative and may cheat to win more resource in the competition of spectrum. It not only makes channel allocation unreasonable but also reduces the utilization of spectrum. b) In resource allocation of multi-users, the informational constrains and the distributed nature should be recognized, that is, the private information of users is not known by the system or other users. As to reduce communication overhead of interaction, information exchange among users should be limited.

Researchers have widely investigated the multi-user channel allocation in cognitive radio and some centralized and distributed methods are used to solve the allocation problem or competition problem among cognitive users. The allocation methods mainly used include approaches based on list coloring[1,2], optimization theory[3], game theory[4,5], and auction bidding[6]. The former two are centralized methods, and the complexity is a bottleneck. The latter two are distributed methods, while the

Q. Zu, B. Hu, and A. Elçi (Eds.): ICPCA-SWS 2012, LNCS 7719, pp. 659–671, 2013.

convergence should be seriously considered, so the algorithm must be designed carefully. [7] put forward a channel allocation method with reserved channels and gives much analysis, while [8,9] amended several mistakes in [7] and simulated again giving the right results. In [10], an optimal channel allocation is proposed to share time resource among primary users and cognitive users. In the allocation scheme, time-slots are assigned in a centralized way. However, these solutions are all for single service. Approaches or analysis of multiple services is rarely considered.

In the paper, a centralized channel allocation scheme is proposed to maximum the throughput and to reduce the blocking rate of multiple services, while not increasing the interruption probability at the same time. In the scheme, cognitive users do not need the capability of spectrum handover and the interaction among them is reduced. By adjusting the index of channels in the proposed scheme, the allocation is simple and ordered. To analyze the performance of the scheme, Markov chain is used to model the allocation and service process.

The rest of the paper is organized as follow. Section 2 describes the system model and some assumptions. Section 3 and 4 are the proposed allocation scheme and performance analysis, respectively. Section 5 gives the simulation and results. Finally, section 6 concludes the paper.

2 System Model and Assumptions

Suppose that there are two kinds of radio users, Primary Users (PU) and Cognitive Users (CU). Different services need different bandwidth guaranteed. In the paper, two types of service are considered in cognitive radio system:

- BroadBand Service(BBS), which is critical in bandwidth or delay sensitive, like stream service.
- NarrowBand Service(NBS), which is a kind of undemanding service in transmission rate and delay time, just like Best Effort(BE) service.

The services in PU system are the broadband ones that request N channels each. The N channels is called ***channel block*** for simplify. In CU system, except for BBS, there are also NBS which only need one channel to communicate. PUs and CUs operate in the same spectrum bands, which include M (M is a multiple of N) channels as shown in Fig. 1.

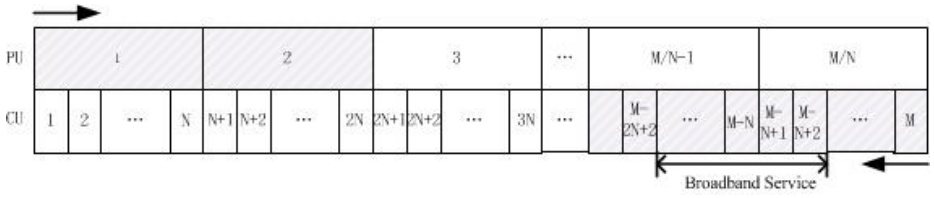

Fig. 1. Channels used by PUs and CUs

It is assumed that the arrivals of PU services and CU services are Poisson process with arrival rate λ_P and λ_C, respectively. The corresponding service time is exponentially distributed with rates μ_P and μ_C. Since there are two kinds of services for CU, when a CU service arrives, it has the probability of P_{c1} to be NBS, and the probability of BBS is P_{c2}=1-P_{c1}. Note that cognitive services can be preempted by primary users since they have priority to obtain resource.

3 Channel Allocation Scheme

The allocation scheme is for cognitive radio system without spectrum handover capability. Each channel is indexed by two contemporary numbers, one aims at PUs and delegates in which channel block it is by index k, and the other directs against CUs and represents the index number for CU numbered by l. For the same channel, there is a relationship between l and k, that is $l^- = \lceil k^- / N \rceil$ (where N is the number of channels needed for BBS, i.e., the size of one channel block.) to assure that the Uniformity of channel index for PUs and CUs.

Numbered channels are allocated in quite a different order to PUs and CUs. PUs' are assigned in an ascending way and channel reassignments are made to select vacant channels immediately after occupied PU channels. CUs' are assigned in a descending way and channel reassignments are made to select vacant channels that are immediately before the occupied CU channels. As shown in Figure 1, the dash area indicates channels that are occupied and the blank space indicates the vacant ones. In the situation of figure 1, when there is new PU service coming, No. 3 channel will be allocated to it. However, if there is CU service, the index less than $M - 2N + 1$ will be allocated.

Note that the index of the channels is not fixed. In order to ensure the channels that are already allocated to the users sequential and avoid the spectrum handover, the index of the bands may need to be adjusted in case that PUs or SUs vacate the channel. More details will be described in the following statements.

The process of channel allocation is described as a continuous Markov chain. It is characterized by states and transition rates. M channels are shared by PUs' services and CUs'. In this case, states are described by an integer pair (i, j), in which $i(1 \le i \le M/N)$ denotes the number of channel blocks allocated to PUs, while $j(1 \le j \le M - i*N)$ denotes the number of bands assigned to CUs.

At time slot t, let $S_P(k,t)$ indicates the state function of PU at channel block k. It is computed based on:

$$\begin{cases} S_P(k,t) = 1 & \text{if the } k\text{th channel block is} \\ & \quad \text{allocated to PU service} \\ S_P(k,t) = 0 & \text{else} \end{cases}$$

Similarly, let $S_C(l,t)$ indicates the state function of CU at channel l. It is computed base on:

$$\begin{cases} S_C(l,t)=1 & \text{if the } l\text{th channel is} \\ & \text{allocated to CU service} \\ S_C(l,t)=0 & \text{else} \end{cases}$$

From the equation above, state (i, j) at time t can be easily computed:

$$i(t)=\sum_{k=1}^{M/N} \mathrm{S}_P(k,t);\ j(t)=\sum_{l=1}^{M} \mathrm{S}_C(l,t) \tag{1}$$

The allocation scheme is described in details:

Initialize: Set $i=0$ and $j=0$ because all the channels are vacant. At the initial time, there is also

$$\mathrm{S}_P=\{\mathrm{S}_P(k)=0 \mid 1\le k\le M/N\};$$
$$\mathrm{S}_C=\{\mathrm{S}_C(l)=0 \mid 1\le l\le M\}$$

Main Part (State Transition): At time t, compute i and j based on (1). State transition will happen in any of the following cases.

(A). A PU service arrival:
Since we suppose the services of PU are all BBS, one of the channel blocks will be allocated to a PU service if resource is sufficient. Only if there is no channel left, the PU service would be blocked. Therefore, the state function $S_P(k)$ of PU channel blocks will change based on:

$$\begin{cases} blocked & \text{if } i=M/N \\ S_P(k\_\min)=1 & \text{else} \end{cases}$$

where $k\_\min=\min\{S_p(k)=0 \mid \forall k\}$. Accordingly, if $Ni(t)+j(t)>M$ at this time, some of the CU service will be preempted out by PU service because of their lower priority. The state function $S_C(l)$ of CU will change based on:

Loop if $Ni+j>M$

$S_C(l\_\mathrm{int}errupt)=0$ and $j=\sum_{l=1}^{M}\mathrm{S}_C(l)$

End

where $l\_\mathrm{int}errupt=\min\{S_C(l)=1 \mid \forall l\}$.

*(B).*A CU narrowband service(NBS) arrival:
If and only if the channels are all occupied, the CU service were blocked, Otherwise the max indexed idle channel would be allocated to the service. The state function $S_C(l)$ of CU will be:

$$\begin{cases} blocked & \text{if } Ni+j=M \\ S_C(l\_\max)=1 & \text{else} \end{cases}$$

where $l\_\max=\max\{S_C(l)=0 \mid \forall l\}$.

*(C).*A CU broadband service(BBS) arrival:
When the vacant channels are not able to make up a channel block, the CU BBS will be blocked. Otherwise, the max N indexed idle channels will be allocated to the service. State function $S_C(l)$ of CU is computed as followed:

$$\begin{cases} blocked & \text{if } Ni+j>M-N \\ S_C(l\_allo)=1 & \text{else} \end{cases}$$

where l_allo is a set of channels' index which can be allocated to the new arrived service. It is determined by the function $l\_allo=\{l\_\max \sim l\_\max-N+1\}$, where the definition of $l\_\max$ is same with that in section B.

*(D).*A PU service over:
When a PU service is over, the channel block which is vacated moves to the largest index that is allocated as shown in Fig. 2. Suppose that it occupied the k_vacate^{th} channel block, the index of channel will be adjusted based on the following rules:

$$\text{For } k: \begin{cases} \text{Unjusted} & \text{if } k<k\_vacate \,\|\, k>k\_\max \\ \text{Take } k \text{ to be } k-1 & \text{if } k\_vacate<k<k\_\max \\ \text{Take } k \text{ to be } k\_\max & \text{if } k=k\_vacate \end{cases}$$

where $k\_\max=\max\{S_P(k)=1 \mid \forall k\}$.

Note that the index l should be adjusted correspondingly to guarantee the uniformity of the channel index.

$$\text{For } l: \begin{cases} \text{Unjusted} & \text{if } l \le N*(k\_vacate-1) \,\|\, l>N*k\_\max \\ \text{Take } l \text{ to be } l-N & \\ & \text{if } N*k\_vacate<l\le N*k\_\max \\ \text{Take } l \text{ to be } (N*k\_\max-1)+l & \\ & \text{if } N*(k\_vacate-1)<l\le N*k\_vacate \end{cases}$$

The state function $S_P(k)$ of PU is computed based on: $S_P(k\_\max)=0$.

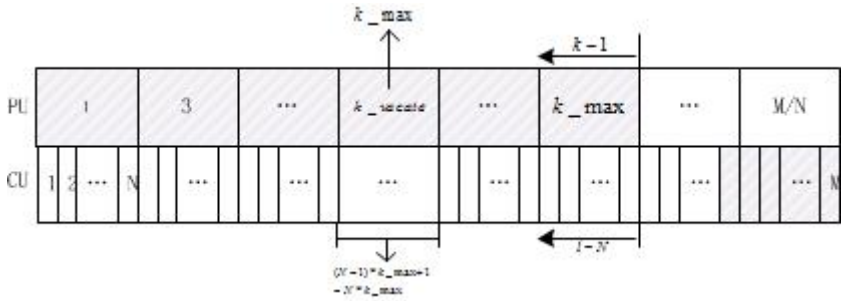

Fig. 2. Schematic diagram of the adjustment in channel index(1)

*(E).*A CU Narrowband Service (NBS) over:
When a CU narrowband service vacates a channel and the index of the channel is l_vacate. The index of channels will be adjusted based on the following rules:

$$\text{For } l: \begin{cases} \text{Unjusted} & \text{if } l > l\_vacate \,\|\, l < l\_\min \\ \text{Take } l \text{ to be } l-1 & \text{if } l\_vacate > l > l\_\min \\ \text{Take } l \text{ to be } l\_\min & \text{if } l = l\_vacate \end{cases}$$

where $l\_\min = \min\{S_C(l) = 1 \mid \forall l\}$.

Correspondingly, the index k should be adjusted, too. Rules are as following:

1)If $\lceil l\_vacate/N \rceil = \lceil l\_\min/N \rceil$, that is, the index of the vacant channel belongs to the last channel block whose channels are occupied by CU services, index k remains unchanged.

2)If condition 1) is not satisfied, the index of the vacant channel and the last channel of each channel block before the vacant channel should be changed based on:

$$\text{For } k: \begin{cases} \text{Take } k \text{ to be } k+1, & \text{if } \lceil l\_vacate/N \rceil > k > \lceil l\_\min/N \rceil - 1 \;\&\; (l^k \bmod N) = 0 \\ \text{Take } k \text{ to be } \lceil l\_\min/N \rceil, & \text{if } l^k = l\_vacate \\ \text{Unjusted}, & \text{else} \end{cases}$$

Where l^k denotes index l which corresponds to index k, that is, $k = \lceil l/N \rceil$.

The state function $S_C(l)$ of CU is computed based on: $S_C(l\_\min) = 0$

*(F).*A CU Broadband Service(BBS) over:
When a CU broadband service vacates a channel block, adjust the index of channels just in the same way described in the former part if necessary and compute the state function $S_C(l)$ of CU based on:

$initial: Count = 0$

Loop if $N - Count > 0$

$S_C(l\_\min) = 0$ and $Count = Count + 1$;

End

The proposed channel allocation scheme well copes with the problem of spectrum handover. By adjusting the contemporary channel index, the occupied channels and vacant channels are ordered throughout. When there is new service arrives, the centralized channel allocation is very simple.

4 Analysis of System Performance

As it is described above, Markov chain is used to analyze the proposed allocation scheme, which has been used in literature [10] to analyze time-slot allocation in cognitive radio. Fig. 3-5 shows the Markov transition process of the scheme, where $r = P_{c1} / (P_{c1} + NP_{c2})$.

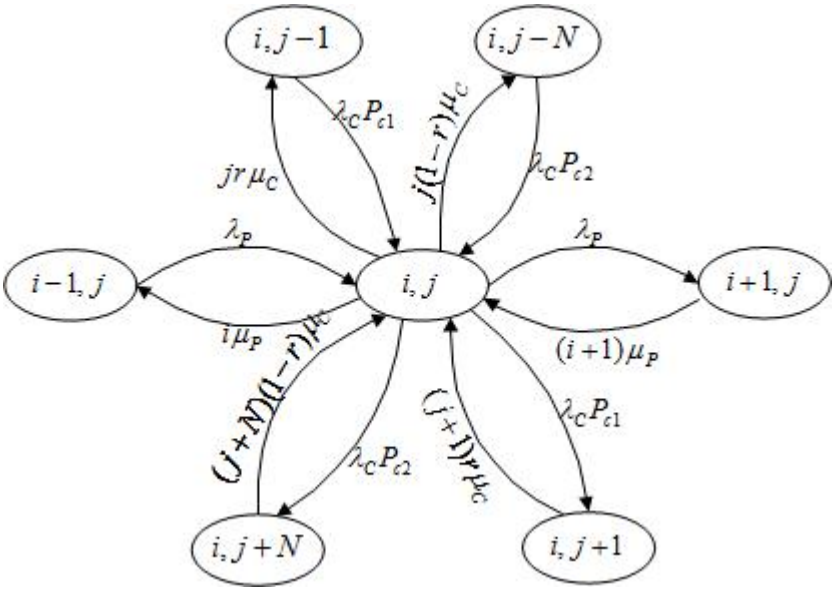

Fig. 3. Markov chain of the proposed scheme ($Ni + j \le M - N$)

When $Ni + j \le M - N$, as shown in Fig. 3),the state transition includes scenarios as follows:

1)During time $(t,t+\Delta t)$, the transition probability of system from state (i, j) to state $(i+1, j)$ is λ_P, where λ_P is the arrival rate of PU service.

2)During time $(t,t+\Delta t)$, the transition probability from state (i, j) to state $(i\text{-}1, j)$ is $i\mu_P$, where μ_P is the departure rate of PU service.

3)During time $(t,t+\Delta t)$, the transition probability from state (i, j) to state $(i, j+1)$ is $\lambda_C P_{c1}$, where λ_C is the arrival rate of CU service and P_{c1} is the probability of CU NBS.

4) During time $(t,t+\Delta t)$, the transition probability from state (i, j) to state $(i, j\text{-}1)$ is $jr\mu_C$, where μ_C is the leaving rate of CU service and r is the probability of that the service in the current channel is NBS.

5) During time $(t,t+\Delta t)$, the transition probability from state (i, j) to state $(i, j+N)$ is $\lambda_C P_{c2}$.

6) During time $(t,t+\Delta t)$, the transition probability from state (i, j) to state $(i, j\text{-}N)$ is $j(1\text{-}r)\mu_C$.

The balance equation for $Ni + j \le M - N$ is:

$$\begin{aligned}
&[jr\mu_C\kappa(i, j-1) + j(1-r)\kappa(i, j-N) + \lambda_P\kappa(i+1, j) + \lambda_C P_{c1}\kappa(i, j+1) \\
&+\lambda_C P_{c2}\kappa(i, j+N) + i\mu_P\kappa(i-1, j)]P(i, j)\kappa(i, j) = \\
&\lambda_C P_{c1}P(i, j-1)\kappa(i, j-1) + \lambda_C P_{c2}P(i, j-N)\kappa(i, j-N) + \\
&(i+1)\mu_P P(i+1, j)\kappa(i+1, j) + (j+1)r\mu_C P(i, j+1)\kappa(i, j+1) + \\
&(j+N)(1-r)\mu_C P(i, j+N)\kappa(i, j+N) + \lambda_P P(i-1, j)\kappa(i-1, j)
\end{aligned} \tag{2}$$

Where $\kappa(i, j)$ is an indication function that equals 1 only if state (i, j) is a feasible state of the Markov chain and 0 otherwise.

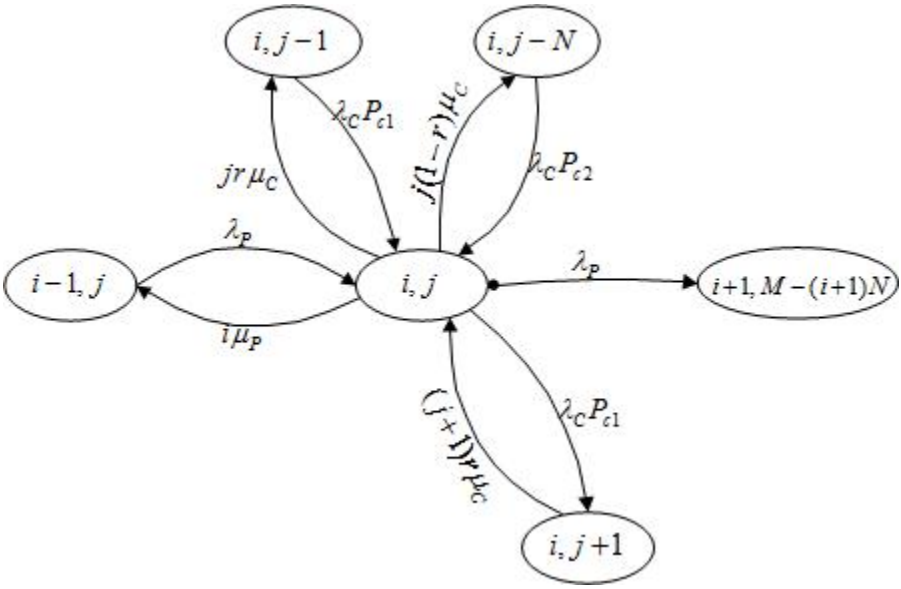

Fig. 4. Markov chain of the proposed scheme ($M - N < Ni + j < M$)

For $M-N<Ni+j<M$, specially, if there is PU service arrives, the CU services will be preempted out and interruption occurs and there is no state of CU BBS to be served. The balance equation is(as represented in Fig. 4):

$$\begin{aligned}&[jr\mu_C\kappa(i,j-1)+j(1-r)\kappa(i,j-N)+\lambda_P\kappa(i+1,M-Ni-N)\\&+\lambda_C P_{c1}\kappa(i,j+1)+i\mu_P\kappa(i-1,j)]P(i,j)\kappa(i,j)=\\&\lambda_C P_{c1}P(i,j-1)\kappa(i,j-1)+\lambda_C P_{c2}P(i,j-N)\kappa(i,j-N)+\\&(j+1)r\mu_C P(i,j+1)\kappa(i,j+1)+\lambda_P P(i-1,j)\kappa(i-1,j)\end{aligned} \tag{3}$$

It is worth noting that there is no state transition from state $(i+1,M-(i+1)N)$ to state (i,j), because system can not dispose more than one services request at one time.

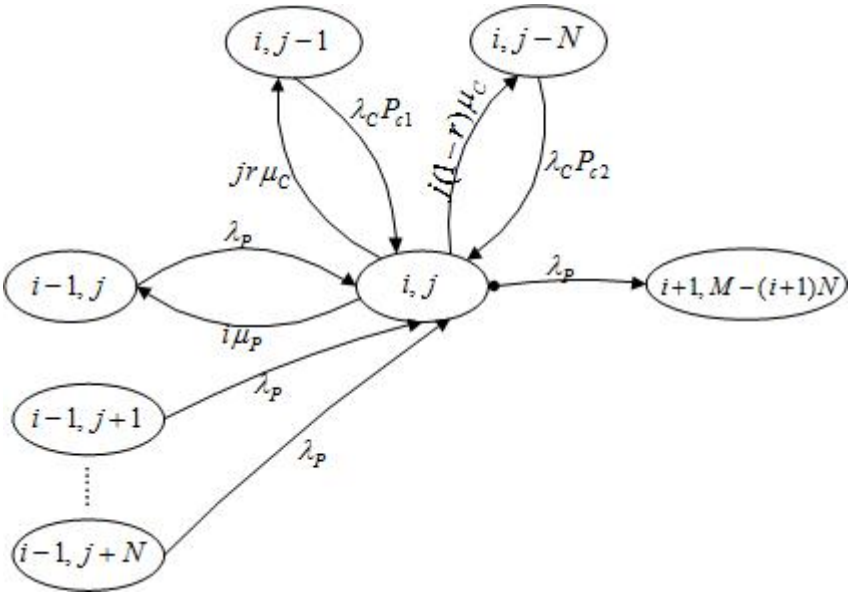

Fig. 5. Markov chain of the proposed scheme ($Ni+j=M$)

In the case $Ni+j=M$, any new CU service will be blocked. As represented in Fig. 5, the balance equation is:

$$\begin{aligned}&[jr\mu_C\kappa(i,j-1)+j(1-r)\kappa(i,j-N)+\lambda_P\kappa(i+1,M-Ni-N)\\&+i\mu_P\kappa(i-1,j)]P(i,j)\kappa(i,j)=\lambda_C P_{c1}P(i,j-1)\kappa(i,j-1)\\&+\lambda_C P_{c2}P(i,j-N)\kappa(i,j-N)+\sum_{\nu=0}^{N}\lambda_P P(i-1,j-\nu)\kappa(i-1,j-\nu)\end{aligned} \tag{4}$$

4.1 Analysis of Blocking Probability

Blocking of CU services occurs in two circumstances: 1) when $Ni+j=M$, a CU narrowband service arrives; and 2) when $Ni+j>M-N$, a CU broadband service

arrives. Denote the blocking rate in the first circumstances is P_{B1}, and the second one is P_{B2}, the blocking rate of the two kinds of service will be:

$$P_{B1} = \sum_{i=0}^{M/N} \sum_{j=0}^{M} \delta(Ni + j = M) P(i, j)$$
$$P_{B2} = \sum_{i=0}^{M/N} \sum_{j=0}^{M} \delta(Ni + j > M - N) P(i, j) \tag{5}$$

Where $\delta(\bullet)$ specifies the condition of states.

4.2 Analysis of Interruption Probability

The definition of interrupt rate is given as follows:

$$P_{in} = \frac{\text{Total CU interrupt rate}}{\text{Total CU connection rate}} \tag{6}$$

Interruption occurs in two circumstances when an additional PU service arrives: 1) when $Ni + j > M - N$, $d(1 \le d \le N(i+1) + j - M)$ CU narrowband services will be preempted; and 2) in the special moment when $Ni + j = M$, a CU broadband service may be preempted. For each state (i, j), the number of two kinds of interrupted CU services per unit time is given respectively by $\sum_{m=1}^{N} \sum_{d=1}^{m} dP_{c1}^{d} \gamma_{(i+1, j-m)}^{(i,j)}$ and $P_{c2} \gamma_{(i+1, j-N)}^{(i,j)}$, where $\gamma_{(i+1, j-m)}^{(i,j)}$ is the transition probability from state (i, j) to state $(i+1, j-m)$. $\gamma_{(i+1, j-m)}^{(i,j)}$ is given by

$$\gamma_{(i+1, j-m)}^{(i,j)} = \frac{\begin{bmatrix} N \\ m \end{bmatrix} \begin{bmatrix} M - (i+1)N \\ j - m \end{bmatrix}}{\begin{bmatrix} M - Ni \\ j \end{bmatrix}} \lambda_P, (m = 1, 2, \ldots, N) \tag{7}$$

The total CU interruption rate over all feasible states, with the probability $P(i, j)$, can be written as $\sum_{i=0}^{M/N-1} \sum_{j=0}^{M} \left(\sum_{m=1}^{N} \sum_{d=1}^{m} dP_{c1}^{d} \gamma_{(i+1, j-m)}^{(i,j)} + P_{c2} \gamma_{(i+1, j-N)}^{(i,j)} \right) P(i, j)$. Therefore, the expression of the interruption probability is given by

$$P_{in} = \frac{\sum_{i=0}^{M/N} \sum_{j=0}^{M} \left(\sum_{m=1}^{N} \sum_{d=1}^{m} dP_{c1}^{d} \gamma_{(i+1, j-m)}^{(i,j)} + P_{c2} \gamma_{(i+1, j-N)}^{(i,j)} \right) P(i, j)}{\lambda_c [P_{c1}(1 - P_{B1}) + P_{c2}(1 - P_{B2})]} \tag{8}$$

4.3 Analysis of Throughput

According to the analysis of blocking probability and interruption probability, the throughput per time unit is calculated by

$$\rho_1 = \lambda_c P_{c1}(1-P_{B1})(1-P_{in1})\left(\frac{\mu_C}{(1-P_{in1})}\right)^{-1}$$
$$\rho_2 = N\lambda_c P_{c2}(1-P_{B2})(1-P_{in2})\left(\frac{\mu_C}{(1-P_{in2})}\right)^{-1} \quad (9)$$

where $\lambda_c P_{c*}(1-P_{B*})(1-P_{in*})$ is the connection completion rate and $\mu_C/(1-P_{in*})$ is the average service time of the completed connections. The total throughput of CU services per time unit is $\rho = \rho_1 + \rho_2$.

5 Simulation and Results

In this section, we simulated the blocking probability, interruption probability and throughput of services use these parameters: $M = 18, N = 3;$ $\mu_p = 0.06; \mu_c = 0.6; P_{c1} = P_{c2} = 0.5$. In the simulation, Monte Carlo method is applied to statistic the average performance characters.

In the simulation, the proposed scheme is compared to the scheme with spectrum handover in literature [7], in order to exhibit the performance of it.

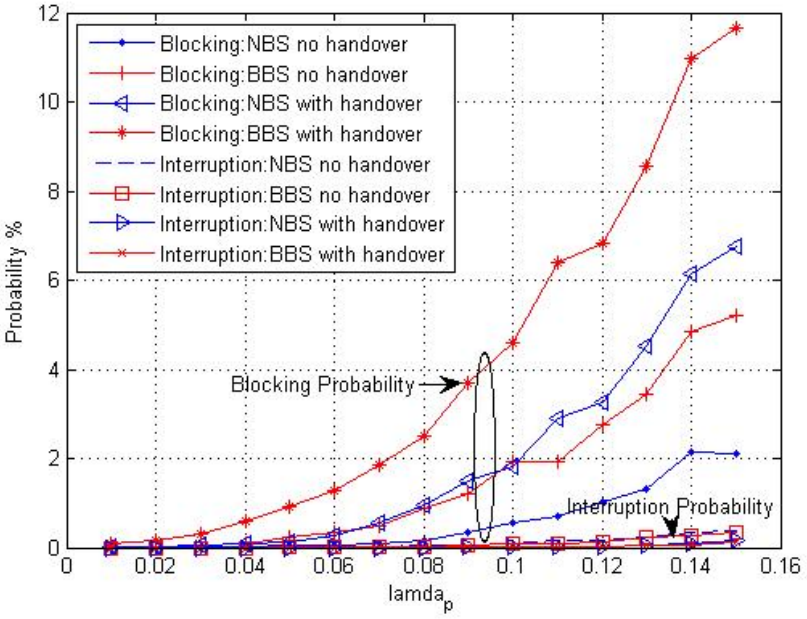

Fig. 6. Simulation results （P_B & P_{in} vs λ_p）

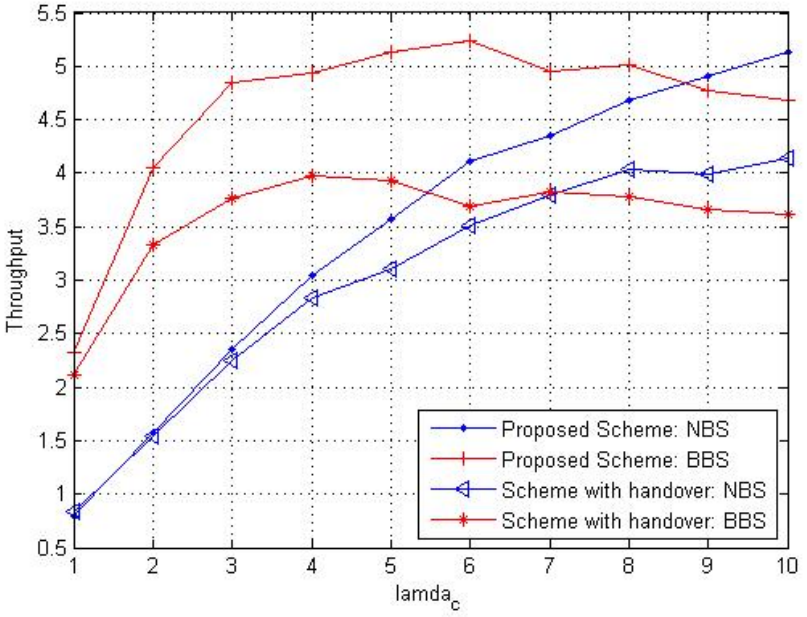

Fig. 7. Simulation results （Throughput vs λ_c）

Fig. 6 shows the blocking probability and interruption probability of multiple services changing with λ_p when $\lambda_c = 2$. The blocking rate of both the two services in the proposed scheme is much lower than the scheme with handover and the interruption probability is almost the same and keeps in a very low level(10^{-3}). It is also shown that the blocking probability of narrowband service is lower than the broadband ones. This is reasonable in the simulation since the service arriving probability is assumed to be $P_{c1} = P_{c2} = 0.5$ and the broadband service will more likely to be blocked when there is few channels left. While the narrowband ones will obtain the resource even if there is only one channel left.

Fig. 7 shows the throughput of the two services in the proposed allocation scheme compared to the scheme with handover when $\lambda_p = 0.08$. It is obvious that the proposed scheme achieves higher throughput because channel utilization becomes higher when all the channels are allocated.

6 Conclusion

In the paper, a channel allocation scheme is proposed to solve the multiple service access problem of cognitive radio without spectrum handover ability. By adjusting the index of channels continuously in the allocation process, the assignment action becomes ordered and simple. Markov chain is put forward to analyze the performance of the scheme. The simulation results show that the proposed scheme not only

improves the throughput but also reduces the blocking probability at the same time. It keeps the interruption probability at a very low level meanwhile.

Acknowledgement. This work is supported by the National Natural Science Foundation of China under Grant No. 60971083, 61101107, and the State Major Science and Technology Special Projects (Grant No. 2011ZX03003-002-01).

References

1. Lin, Y., Zhu, Q., Cai, L.: An Improved Channel Allocation Algorithm Based on List-coloring. In: IEEE WiCOM, pp. 1–4 (2010)
2. Bai, B., Chen, W., Cao, Z.: Low-complexity Hierarchical Spectrum Sharing Scheme in Cognitive Radio Networks. IEEE Communications Letters 13(10), 770–772 (2009)
3. Bai, Y., Chen, L.: Flexible Spectrum Allocation Methods for Wireless Network Providers. In: Proc. IEEE PIMRC, pp. 1–5 (September 2006)
4. Niyato, D., Hossain, E.: Competitive Pricing for Spectrum Sharing in Cognitive Radio Networks: Dynamic Game, Inefficiency of Nash Equilibrium, and Collusion. IEEE Journal on selected Areas in Communications 6(1), 192–202 (2008)
5. Zhu, J., Ray Liu, K.J.: Multi-Stage Pricing Game for Collusion-Resistant Dynamic Spectrum Allocation. IEEE Journal on Selected Areas in Communications 26(1), 182–191 (2008)
6. Huang, J., Han, Z., Chiang, M., Poor, H.V.: Auction-Based Resource Allocation for Cooperative Communications. IEEE Journal on Selected Areas in Communications 26(7), 1226–1237 (2008)
7. Zhu, X., Shen, L., Yum, T.-S.P.: Analysis of Cognitive Radio Spectrum Access with Optimal Channel Reservation. IEEE Communication Letters 11(4), 304–306 (2007)
8. Ahmed, W., Gao, J., Suraweera, H.A., Faulkner, M.: Comments on Analysis of Cognitive Radio Spectrum Access with Optimal Channel Reservation. IEEE Transactions on Wireless Communications 8(9), 4488–4491 (2009)
9. Martinez-Bauset, J., Pla, V., Pacheco-Paramo, D.: Comments on Analysis of Cognitive Radio Spectrum Access with Optimal Channel Reservation. IEEE Communications Letters 13(10), 739 (2009)
10. Kim, C.H., Chung, J.-M., Choi, S.: Analysis of Optimal Cognitive Radio Channel Allocation with Finite User Population. In: ICTC 2010, International Conference on Digital Object Identifier, pp. 241–242 (2010)

A Content Aware and Name Based Routing Network Speed Up System*

Ke Xu, Hui Zhang, Meina Song, and Junde Song

Department of Computer Science, Beijing University of Posts and Telecommunications, China
National Computer Network Emergency Response Technical Team/
Coordination Center of China
{xu_ke,mnsong,jdsong}@bupt.edu.cn, zhanghui@isc.org.cn

Abstract. The enormous increase in Internet traffic usage has been leading to problems such as increased complexity of routing topology, explosion in routing table entries, provider-dependent addressing, which reduce the speed of network service. The emerging new techniques such as CDN, P2P, VPN, etc. speed up the network from different perspectives. A new speed up system called CANR, content aware and name based routing, is proposed in this paper, which integrates benefits of several existing mehanisms. CANR consists of a cluster of proxy peers deployed in different network domains, which can work as collaborative routers, forwarding requests to each other to speed up the cross-domain visits. CANR can automatically aware the changes of network and re-construct name-based routing table based on a new multi objectie k shortest algoritm by itself, finding a set of cheapest and most fast k routing paths, which is different from current static preconfigured systems.

Keywords: speed up, content aware, name-based routing, k short path.

1 Introduction

With the development of network service and explosion of data transaction, the speed of network is still a bottle neck which troubles both industry and academia. As Andy Beal's Law, no matter how fast the network hardware develops, the new emerging software service will consume it. Therefore, more and more new techniques are continuously proposed to speed up the network from the birth of internet. In this paper, summarized the main ideas of different network acceleration strategies, we propose a new one, content aware and name-based routing network system (CANR) which integrates multi-benefits of current speedup technique and has good compatibility with the existing systems.

* This work is financially supported by the National Natural Science Foundation of China(Grant No.61072060); the National Key project of Scientific and Technical Supporting Programs of China under Grant No.2009BAH39B03,2012BAH01F02; the National High Technology Research and Development Program of China Grant No.2011AA010601, 2011AA100706; the Research Fund for the Doctoral Program of Higher Education (Grant No. 20110005120007).

Q. Zu, B. Hu, and A. Elçi (Eds.): ICPCA-SWS 2012, LNCS 7719, pp. 672–688, 2013.

The rest of the paper is organized as follows. We make a study of speed up related works in Section 2. In Section 3 the proposed CANR is explained. In section 4, we give a multi-objective k shortest path algorithm to find routing path, then Section 5 make a simulation to verify the performance of CANR. Finally, we conclude in Section 6.

2 Related Works

Most of current speed up technology can be classified into three types. The first can be called topology optimization which shortens the hop path from sender to receiver by adjusting the nethwork routing, such as VPN and proxy. The second is called replication which duplicates resource to the area near the requester, speeding up the network visiting and reducing the burden of original servers. These systems are always resource oriented and name based, such as CDN[1], P2P[2][3] and data grid[4][5][6] systems. The third is about data compression protocol which speeds up the network service by reducing the transfer data amount, such as video and audio stream technique, MP3, MPEG, .etc.

The focused of this paper is about routing improvement to name based replica network. The proposed system CANR can integrate the benefits of the first two strategies, topology optimization and replica collaboration, fully compatible with existing network resources.

In addition to bandwidth limit, the long path of cross-domain transmission is one of the main factors which cause the network delay in practical. As Internet is composed by different network domain, the entry gateway between different regions is not that broad as inside. Usually, a proxy, as a bridge, between different network domains is used to penetrate a fast channel for cross domain visit. Figure 1 gives an example.

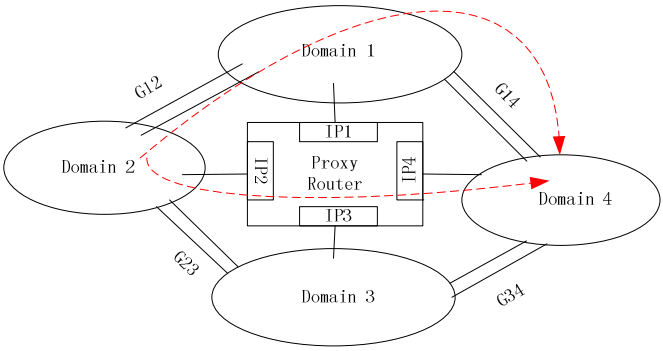

Fig. 1. Cross Domain Visit by Proxy

The proxy in the middle bridged four different domains which are separated. Since the proxy has four IP addresses assigned by four domains, it can forward data directly between domains beyond gateway. In the example from Figure 1, if a data package will be transformed from Domain 2 to Domain 4, without the proxy, it will pass gateway G12 and gateway G24, going through Domain 1 which never needs the data.

But the proxy can forward the data from Domains 2 to 4 directly, speeding up the visit. However, the proxy is usually pre-configured with the maps of host addresses and domain, if a proxy receives a new request, it must know which domain to forward that request. With the large amount of increasing data blocks and its replicas are distributed everywhere in the multi-domain networks, the static configured, host-based proxy mechanism will be hard to extend. Furthermore, the traditional proxy usually works separately, and it is difficult to make them large-scale cooperate.

2.1 About Name Based Routing

We introduce name-based routing to realize CANR system of this paper, which may be a trends in the future. A lot of projects named as ICN[7]、CON[8]、CCN[9]、NDN[10] and software system as CCN[11], DONA[12], PSIRP[13], TRIAD[14], CBCB[15] are essentially name-based content oriented network. Different with traditional host based routing protocol as TCP/IP, a name based system is content oriented. A requester just cares the meaningful description of a content file, such as file name, URL, .etc. The name based system can auto locate the request to the resource, no matter original or replica, which provides a more flexibility to application and content oriented data storage [16]. However, current name-based systems should give a mechanism for content provider to register its resource, manually or automatically, so that the system can recognize where the content is. This may affect the compatibility of the new name-based systems with the existing resource. Furthermore, the existing name-based system's speedup policies are usually preconfigured by parameters, seldom care about the circumstance of network in practice, which is often changed dynamically. Those shortcomings may affect the new name-based system to be commercialized and productize. The system of CANR proposed in this paper is trying to overcome the issues.

3 Content Aware and Name-Based Routing Speed Up System

3.1 Design Conception

A content aware and name based routing system is composed of a cluster of proxies which can be deployed in different domains. The proxy routers will not be pre-configured with routing table, but can aware information by itself. The example architecture of CANR is shown in Figure 2.

In the figure above we can see, there are several proxy routers deployed in different domains and the routers can directly link with each other. A domain may have several routers while a router may bridges multi-domains. If the cluster of routers can work together, they may high speed link many domains. Initially, a proxy router may not know what resource or host a domain has, it just forward all the requests received, such as URL, to the original server by the traditional locate protocol, as DNS. But it can log and analyze the request history, communicate with other neighbors in the cluster, then constructing a routing table. At last, it will know how to forward a request to the most suitable domain where has the resource or its replica, or to the best neighbor router which can be the fastest next hop to the object. In the following section, the detailed will be explained.

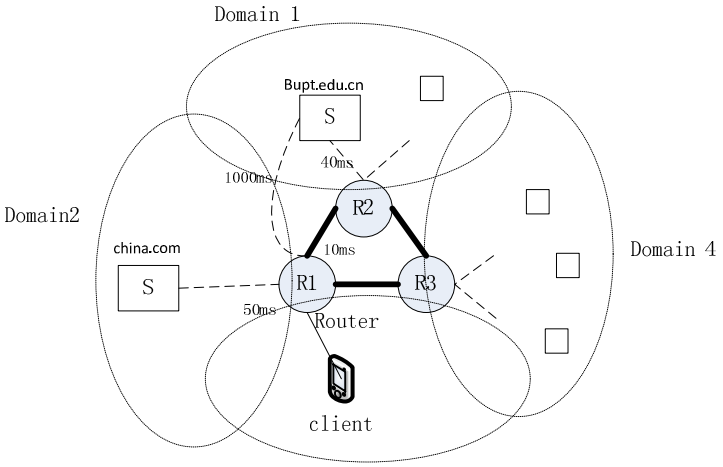

Fig. 2. Example Architecture of CANR

3.2 Data Definition

In order to explain the algorithm, some definitions are present first.

1. R: proxy router peer, the *i*th router is named R_i
2. S: server host which contains the requested data , no matter original or replicas
3. RTT: round trip time which represent the time from a request sent to a response received
4. $Route\_table_{Ri}$: the routing table on router R_i, the data structure is as table 1.

Table 1. Data Structure of $Route\_table_{R1}$

Name	Next Hop	Path	RTT_{cur}	RTT_{Dir}	Neighbor
Bu.edu.cn	R_2	R_1-R_2-S	50ms	1000ms	
China.com	S	R_1-S	50ms	50ms	

The columns of the above table are explained as follow:

a) Name: The target name. All the routing line is name based index. A new line will be initialized when a new target name is first requested and logged.
b) Next Hop: The next hop to forward the request of the name. Initialized by S, which mean R_1 will directly visit the resource server by DNS. May be adjusted to R_i, $0<i\leq n$.

c) Path: The current routing path in the R cluster before S, which should be the shortest path to another R. If the link is current R to S directly, which is the initial value, the path will be current R itself. If the Next Hop is filled with some R, the Path will be filled by Path_tableRi which will be illustrated later.
d) RTT_{cur}: The RTT by "Path" to visit "Name"
e) RTT_{Dir}: The RTT to visit "Name" directly
f) $Neighbors_{Name}$: The neighbor's information about connection to the resource of the "name" of the line, which maintains the direct link RTT to the target from different Neighbor router peers which are the entries of different domain. The data structure of $Neighbors_{Name}$ is as table 2

Table 2. Neighbors"$_{Bupt.edu.cn}$"

Neighbor ID	RTT_{Dir}
R2	40ms
R3	2000ms

g) Path_tableRi: The shortest route table from Ri to Rk, $0<k\leq n$. The shortest route table can be calculated by the Dijkstra's algorithm for the Single Source Shortest Path or some other improved one. The example of this table structure is as following:

Table 3. Path_tableRi

Neighbor ID	Shortest Path	RTT
R2	R1R2	10ms
R3	R1R3	10ms

3.3 Routing Protocol

Based on the data definition above, the main algorithms will be explained in this section.

3.3.1 Aware Network

Collect RTT_{cur} and RTT_{Dir} when forwarding request

```
//When R_i receives a request of "Name", the procedure of "ForwardRequest"will be called:
PROCEDURE ForwardRequest
{
Lookup the "Name" in Route_table_Ri;
    If "Name" exist in Route_table_Ri
send request to "Next Hop";
Else
    Find host of "Name" by DNS;
    send request to the host;
}

//When R_i receives the response corresponded to previous forwarded "Name", the procedure of "CollectRTT" will be called
PROCEDURE CollectRTT
{
  If previous request is direct to "Name" host
Record RTT_Dir;
initialize a new line in Route_table_Ri;
  Else
        Record RTT_cur in Route_table_Ri;
}
```

3.3.2 Update Path Table

R_i will try to probe all the neighbors, R_k, $0<k\leq n$, in the cluster periodically by some way, for example send ICMP package to the peers. So it can maintain a list of the valued path to every other peer, which is the basic to calculate the $Path\_table_{Ri}$ by the Shortest Path Algorithm as the Dijkstra's. The $Path\_table_{Ri}$ will be refreshed periodically (or event triggered) for the distance between routers may change, although they are usually relatively stable.

However, in practice the weight of a path is always multiple and the result of shortest path is not only one for backup. The multi-objective k shortest path should be taken into account, as described in Section 4.

3.3.3 Update Route Table

```
PROCEDURE UpdateRoute
{
Condition1 := Path_table_Ri has any change;
Condition2 := RTT_cur has any change;
If Condition1 or Condition2
        Call PROCEDURE UpdateNextHop
}
```

```
PROCEDURE UpdateNextHop(name)
{
  //Lookup "name" in Path_table_Ri
  RTT_cur := value from Route_table_Ri by "name"
  For R_k  in Neighbors_Name
{
    RTT_Dir := value from table Neighbors_Name by R_k;
    RTT_Rk-Ri := value from table Path_table_Ri by R_k;
    RTT_Evalued  := RTT_Dir + RTT_Rk-Ri;
      If RTT_Evalued < RTT_cur
          Next Hop _name ,Ri := R_k
}
}
```

3.3.4 Synchronization

```
PPRCEDURE SyncInfo
{
   Condition := RTT_dir of R_i to "name" has some change; //from algorithm 3.3.1
   If Condition
      Send mapping data (R_i , "name", RTT_dir) to peers in Path_table_Ri
}
```

4 Multi Objective k Shortest Path Algorithm

4.1 About Shortest Path Problem

From the routing algorithm of the system above, we can see that the request will be forwarded among Rs before it is sent to source server. So the routing selection between each R to R in the cluster will have an important affect to the speed at last. In chapter 3.3, a simple policy was given, which first gets direct connection weights between linked Rs, then generated the shortest path based on Dijkstra algorithm.[16] For example, if time delay is used as weights, the time shortest path between each Rs will be get, which can be filled in Path_tableRi.

However, the classic shortest path policy which has been researched deeply can only get one optimized line based on one type of weight. [17-20] .There will be two problems in practice, one is about multi-objective decision, and the other is about multi alternative paths selection.

4.1.1 About Multi-objective Decision

A single target policy is difficult to accurately describe the problem in real life, for example, when choosing the path in the transport network, it is necessary to take into account a number of targets simultaneously, such as cost, time, risk and security, which requires the multi-objective optimization method.

A multi objective policy is not simply an extension of a single one, for there may be conflicts among different Goals and an advantageous solution for a target may not be the best for another. Moreover, a multi-objective shortest path problem generally may not have an optimized solution, but a satisfactory solution which is known as the Pareto solution. Major policies can be classified into 3 types: Utility function method[21], Interactive method[22] and Production methods including Dynamic programming method[23], Pareto labeling method[24] and Pareto ranking methods[25]. For multi-objective shortest path algorithm, the usual approach is linear weighting of different target or making certain objectives into constraints. However, it is difficult to determine the weight for the linear weighting method and the second method is proved an NP hard problem.

4.1.2 About K Shortest Path

Another problem of routing is about the Fault-tolerant backup. In practice, one optimized path may be not enough, it is also need that more than one sub-optimal path can be used as backup, which introduce the k shortest path problem. The K shortest path problem is first proposed by Hoffman and Pavley in 1959 [26]. In 1973, Fox proposed a time complexity of O (m + knlogn) serial algorithm [27]. Then Eppstein achieved a good serial algorithm with the complexity of O(m+nlogn+k) in 1999 [28]. E.Ruppert parallelized Eppstein's algorithm in 2000 [29] with the time complexity of O (logk + logn). In this paper, a distributed algorithm is proposed.

4.2 Design Idea

In this paper, although the CNBR system proposed can speedup network transaction by penetrate different network area, different telecom operators may require CNBR to pay for the usage of their network. So the algorithm of routing selection must take the cost into account beside the time delay. Furthermore, in real application, a set of sub-optimal path should be prepared as backup for the system can work stably no matter what happen. So an algorithm of multi-objective k shortest path (MO-K as abbreviation) is proposed in this paper to resolve the problem in practice, by which the CNBR can select the cheapest and near most fast k sub optimize paths.

The algorithm MO-K includes two steps. The k shortest paths based on weight of c (cost) will be get first, then the k paths will be resorted by another weight t (time). After eliminating the over threshold of t paths, the first k elements in the reordered queue will be the answer to fill the Path_table_{Ri}. So the k shortest paths selecting is important.

When initialing, each peer in the network, R, has no idea of any remote nodes but only neighbors. Its Path_table_{Ri} just records the direct link weight with other peers. When the algorithm starts, every the peer will continuously collect information from its neighbors and refresh its local Path_table_{Ri} if needs. The updating is an interactive process. The idea of the step i to the next step i+1 is shown in the following figure 3 which describes how to create the k shortest paths between peer A and B. Figure 3.a shows the i th step of the interaction. In this stage, there are k paths have been found

between peer A and B, and the peer v is beyond any path of which. That is mean all the path haven't pass peer v currently. But in this step, there already exists k shortest path between A and v. The focus is on the impact to the existing k path from A to B when adding a direct edge between v and B. The Figure 3.b shows the step i+1. When peer v informs all its neighbors there is a new edge between v and B. All its neighbor, such as peer A, will start the (i+1)th step to update its new k shortest paths to B by resorting the k paths with v and without v. In this step, the initiator is peer v and the affected peer is A which will update its $\text{Path\_table}_{\text{Ri}}$. Peer v just need inform its direct previous neighbors, instead of all the peers in the system. The updating can be forwarded iteratively by its previous neighbor. Each update will get a smaller result, so the algorithm is one-way convergent. Different with the existing algorithms, all the peers will share the complexity of the computing, and when the k shortest path assorting, two types of weight including cost and time should be concerned together. In the following chapter, the detail of the algorithm will be described.

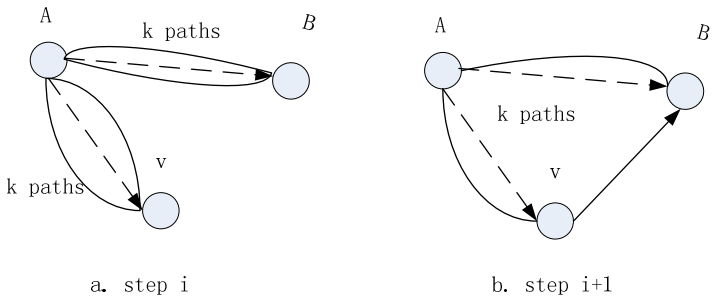

Fig. 3. k short paths selection

4.3 The Distributed Multi-objective k Shortest Path Selection

In order to describe the algorithm clearly, we must give some data and calculate symbols first. Then the algorithm and program working flow detail will be given.

4.3.1 Symbols Definition

- weight value

  $c_{uv.i}, 1 \le i \le k$ means the cost weight of the i th path from the k shortest paths of u to v;

  $t_{uv.i}$, $1 \le i \le k$ means the time weight of the i th one in cost weight 's k shortest paths;

  $c_{uv.0}$, means the cost weight of the edge direct linked between u and v;

  $t_{uv.0}$, means the time weight of the edge direct linked between u and v;

- path vector

  $C_{uv}^{k} = (c_{uv.1}, c_{uv.2}, ..., c_{uv.k}), c_i < c_j, 1 \le i < j \le k$. This vector represents the weights of the k short paths from peer u to v. The weights of a path $c_{uv.i}$ are sorted in the vector.

  $T_{uv}^{k} = (t_{uv.1}, t_{uv.2}, ..., t_{uv.k})$, the element $t_{uv.i}$ means the delay value of path correspond to $c_{uv.i}$

  $C_{uv}^{0} = (c_{uv.0}, c_{uv.0}, ..., c_{uv.0})$, means the direct link cost weight vector from u to v, which will be used as a computing param, and the same as the vector $T_{uv}^{0} = (t_{uv.0}, t_{uv.0}, ..., t_{uv.0})$.

- matrix D^k and T^k

  $D^{k} = \begin{bmatrix} C_{11}^{k} & ... & C_{1n}^{k} \\ ... & ... & ... \\ C_{n1}^{k} & ... & C_{nn}^{k} \end{bmatrix}$, n is the numbers of all of the peers in the system. D^k uses C_{uv}^{k} vector as its elements, so it contains all of the k shortest paths of all the peers to each other.

  $T^{k} = \begin{bmatrix} T_{11}^{k} & ... & T_{1n}^{k} \\ ... & ... & ... \\ T_{n1}^{k} & ... & T_{nn}^{k} \end{bmatrix}$, is the correspond time delay matrix of D^k

- matrix D_v^k and T_{uv}^k

  $D_{v}^{k} = \begin{bmatrix} & C_{1v}^{k} & \\ & ... & \\ C_{v1}^{k} & ... \; C_{vv}^{k} \; ... & C_{vn}^{k} \\ & ... & \\ & C_{nv}^{k} & \end{bmatrix}$, D_v^k is a sub matrix from D_v^k, which represents the k short path to peer v (the column) and from v (the row).

  T_{uv}^{k} is the correspond time delay matrix.

  D_v^0 means the initialized D_v^k while T_{uv}^0 means the correspond T_{uv}^k

- vector D^k_{*v} and D^k_{v*}

  $D^k_{*v} = \begin{pmatrix} C^k_{1v} \\ ... \\ C^k_{nv} \end{pmatrix}$ is the available line of matrix D^k_v, which represents all of the k shortest paths from any peer to v; $D^k_{v*} = \begin{pmatrix} C^k_{v1} & ... & C^k_{vn} \end{pmatrix}$ is the row from D^k_v which record the shortest k paths from v to any other peer.

- vector $\Delta C^k_{u.xv}$

  $\Delta C^k_{u.xv}$ is the vector with the restrictions that all paths must have the edge xv, and $\Delta T^k_{u.xv}$ is the correspond T^k_{uv}

- Extended Computing symbol

  Assume $A = (a_1, a_2, ..., a_k), a_i < a_j$ and $B = (b_1, b_2, ..., b_k), b_i < b_j$, where $1 \le i < j \le k$,

  Define function $\min_k\{V\}$ can get the first k minimum elements from vector V, then

  (1)Extended plus

  $A \oplus B = \min_k\{a_i, b_i : 1 \le i \le k\}$, means merging and resorting the elements from A and B, then return the first k ones.

  (2)Extended multiply

  $A \otimes B = \min_k\{a_i + b_j : 1 \le i \le k, 1 \le j \le k\}$, means combining the elements from A and B, then resorting and return the first k shortest elements. Combining here means link the two edges.

  (3)Extended compare

  In this paper, there are two weights should be concerned when resorting. So the comparing rule for sorting is a multi-dimensional one. Assume the extended compare is about c (cost) and t(time), so the element of k vector above is also another vector, for example $d_i=(c_i, t_i)$. The comparing rule of $d_i=(c_i, t_i)$ and $d_j=(c_j, t_j)$ is defined as following:

  (i) Cost is the first that is c values will be compared first, if c values equal, then compare t. For example:
  if $c_i < c_j$ and $t_i < T_{max}$, $t_j < T_{max}$,then $d_i < d_j$
  if $c_i = c_j$ and $t_i < t_j < T_{max}$, then $d_i < d_j$

  (ii) If t is over limit, the path is invalid.
  For example:
  if $t_i > T_{max}$ and $t_j < T_{max}$, then $d_i > d_j$ (no matter what is c_i and c_j)
  if $t_i > T_{max}$ and $t_j > T_{max}$, then $d_i = d_j = \infty$ (no matter what is c_i and c_j)

4.3.2 Algorithm Description

Each peer maintains a matrix D_{vi}^{k} which initially records only direct neighbors, then will be updated interactively.

- Initializing

Initially, all the peers have no idea of other peers, all the link between each other is the direct edge. If a $t_{uv.0}$ is too long, it means there is no good edge between u and v, then we deem it as ∞. That is if $t_{uv.0} > t_{max}$, then $t_{uv.0} = \infty$, $T_{uv}^{0} = (\infty, \infty, ..., \infty) = V_{\infty}$. If there is no direct link between u and v, the $c_{uv.0}$ can also be set to ∞, that is $C_{uv}^{0} = (\infty, \infty, ..., \infty) = V_{\infty}$.After initializing, the D^{k} will record the path weight vector of edge if the two peers can link directly or V_{∞} if there is no direct link. For example, $D_{v_i}^{k} = \begin{bmatrix} & C_{1v_i}^{k} & \\ & \infty & \\ \infty & C_{v_i 2}^{k} \quad \ldots \quad \infty & C_{v_i n}^{k} \\ & \infty & \\ & C_{nv_i}^{k} & \end{bmatrix}$ means there is direct edges from v_i to peer 2 and to peer n, and edges from 1 to v_i and n to v_i

- Updating

In order to facilitate the description, assume peer V_i has Predecessor peers V_{i-1} and Successors V_{i+1}, which is shown in figure 4. V_{i-1} or V_{i+1} here names a multiple of peers with the same logic relation with V_i.

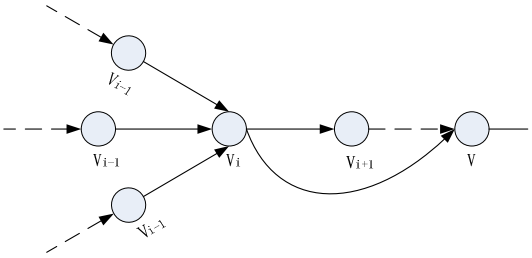

Fig. 4. Routing Update

The updating of V_i has two cases. The first is when V_i finds a new direct neighbor, it will refresh its local table and initiate the updating to all other related ones such as V_{i-1}, it is an active process. The first case is called “Original Updating”. The second is

when V_i receive the "Original Updating" from others such as V_{i+1}, V_i will refresh its local table and then forward the updating, which is called "Forwarded Updating" and will be flooded in the network until the end condition.

(1) Original Updating

V_i periodicity checks its neighbors, when it finds a new V_{i+1}, this updating will be triggered. Assuming V_i has already get a $D^k_{v_i}$ without path through V_i to V_{i+1} in the previous steps, in this step , the new path will be tried to used beyond the existing ones. We use $\Delta C^k_{\overline{v_i v_{i+1}}*}$ to represent the changed vector when the new path of V_i to V_{i+1} has been used. The character * represents all of the peers in the system. The formula is

$$\Delta C^k_{\overline{v_i v_{i+1}}*} = C^k_{v_i*} \oplus c_{\overline{v_i v_{i+1}}} \otimes C^k_{v_{i+1}*} \tag{1}$$

$c_{\overline{v_i v_{i+1}}}$ means the direct edge weight from V_i to V_{i+1}. And $\Delta D^k_{\overline{v_i v_{i+1}}*}$ is the unit matrix from $\Delta C^k_{\overline{v_i v_{i+1}}*}$, to different peer *, which will be sent to V_i's predecessor peers, V_{i-1}.

(2)Forwarded Updating

When a V_{i-1} receives its successors' $\Delta D^k_{\overline{v_i v_{i+1}}*}$, it will first check its forward path (the subscript $\overline{v_i v_{i+1}}$) whether there is any circulation path. If none, it will start its "Forwarded Updating". The formula is

$$\Delta C^k_{\overrightarrow{v_{i-1} v_i v_{i+1}}*} = C^k_{v_{i-1}*} \oplus C^k_{v_{i-1} v_i} \otimes \Delta C^k_{\overline{v_i v_{i+1}}*} \tag{2}$$

The matrix $\Delta D^k_{\overrightarrow{v_{i-1} v_i v_{i+1}}*}$ is composed by $\Delta C^k_{\overrightarrow{v_{i-1} v_i v_{i+1}}*}$ of different peer *. After updating, V_{i-1} will check that if there is anything different between $\Delta D^k_{\overrightarrow{v_{i-1} v_i v_{i+1}}*}$ and $D^k_{v_{i-1}}$, the $\Delta D^k_{\overrightarrow{v_{i-1} v_i v_{i+1}}*}$ will be forwarded to its predecessor V_{i-2} and the forward will be passed down. A general description of the forward is as the formula 3:

$$\Delta C^k_{\overrightarrow{v_{i-x} \cdots v_i v_{i+1}}*} = C^k_{v_{i-x}*} \oplus C^k_{v_{i-x} v_{i-x+1}} \otimes \Delta C^k_{\overrightarrow{v_{i-x+1} \cdots v_i v_{i+1}}*} \tag{3}$$

The forward will be flooded in the network until one of the two conditions happen: a) A circulation path. b) There is no different between $\Delta D^k_{\overrightarrow{v_{i-x} \cdots v_i v_{i+1}}*}$ and $\Delta D^k_{v_{i-x}}$. So the forwarding will be stopped finally. Since every updating will cause a shorter path or remain unchanged, so the algorithm is one-way convergence.

From the descriptions above we can see, the updating is originated from peer V_i and forwarded to all the peers in the system which will affect their path to V_{i+1}. This like put a stone in the water, causing the wave diffusion from that center (V_i) and calming down at last.

(3)The complexity of the Updating

Assuming there are m peers, n edges in the system, and peer V_i's neighbors count is q_i. The k shortest path proposed in this paper can be analyzed as following. Every "Original Updating" may cause m*n times "Forwarded Updating", to a peer V_i, the "Forwarded Updating" time is m* q_i. In each updating, the comparing time will be m*k (by insert sorting). So the comparing time in each peer will be (m* q_i + 1)*m*k. If the value of q_i is very much, that means V_i has a lot of neighbors, so Vi can directly reach most of the target peer, so the "Original Updating" may get the finally result, "Forwarded Updating" may end here for stop reason (2). If the value of q_i is little, although the totally computing is complex, the distributed task apportioned to each peer is acceptable. Furthermore, every times of updating can achieve a more optimal result which can be used in practice.

- Sorting

D_{u*}^k is a vector in each peer u describe the current k short paths from u to all other peers. However, it should be resorted by another weight before it is used for routing. For example, $C_{uv}^k = (c_{uv.1}, c_{uv.2}, ..., c_{uv.k})$ is a k short paths vector from u to v, the weight is cost, which means the system tend to choose a cheaper route. But for a speedup system, time is also very important. So the $T_{uv}^k = (t_{uv.1}, t_{uv.2}, ..., t_{uv.k})$ will be used to eliminate and re-arrange the elements in C_{uv}^k.

The rule of resorting is that:

if $t_{uv.i} > t_{max}$, then $c_{uv.i} = \infty$, setting the element to the tail of C_{uv}^k;

if $c_{uv.i} = c_{uv.j}$ and $t_{uv.i} < t_{uv.j}$, then set $c_{uv.i}$ before $c_{uv.j}$ in vector C_{uv}^k;

The result of resorting is described as $C_{uv}'^k$

- Creating $Path\_table_{Ri}$

Select the first element in $C_{uv}'^k$ as a cheapest and near most fast path from u to v, fill the correspond path to $Path\_table_{Ri}$

5 Evaluation

We developed the CANR system based on squid, famous open source proxy software. The main part of the work is to add name-based routing functions, including history request record and analyzes, RTT collecting, next hop calculating and synchronizing

with neighbors. In order to evaluate the effect of CANR's main algorithm, a simulation environment is built on ns2. The network topology is shown as Figure 5. There are six Routers and six Domains which contain a tree of content servers. Domain 6 gives the content servers' detail topology, and others are the same as it. In order to simulate, it is assumed that all the network delay between two direct link peers are 50ms, and each transmission cross domains' Gateway will get a delay of 1000ms. Each R_i, proxy router, belongs to at least one domain, so it direct link an in-domain peers will cost 50ms. The six routers units to work together, some of them may belong to a same domain, because a router may have multiple addresses to several domains. The delays between routers are signed in the figure. In the experiment, a client from Domain1 will send a request randomly to different contents.

Considering the average delay as output, comparing with the internet request without and optimization, we get the result as following Figure 5. The evaluation is focused on the speed weight of a path. The cost of pay from CANR speed up system is naturally higher than the one without it so that we deem it no need to compare the cost between them. A request simply forwarded by internet is naturally cheaper, for an internet user just should pay for one network access operator while the CANR penetrate different telecom operators' area, so it must pay for multiple network supporters. In chapter 4, a cheapest path algorithm is proposed making the CANR reduce the cost as much as possible while speeding up.

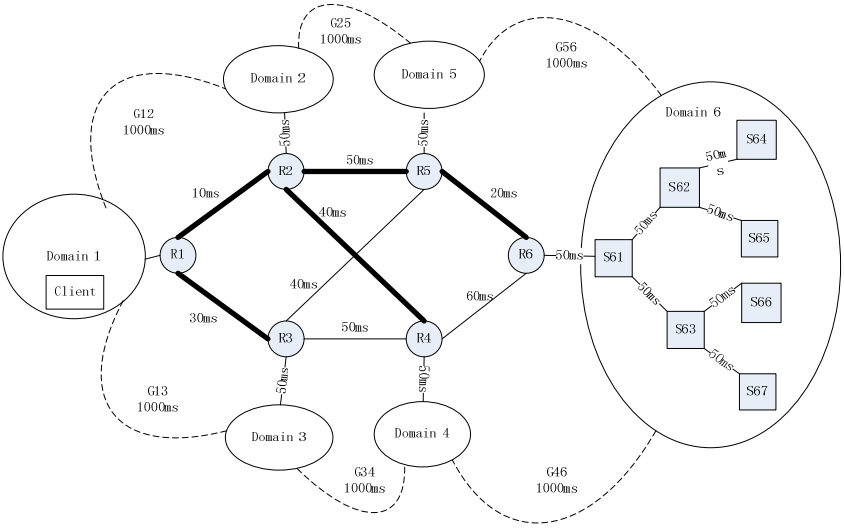

Fig. 5. Topology of Simulation

In the result Figure, we can see that, at the beginning, the average delays of requests are similar between two lines for the CANR initially has no idea of the network, it need time to aware and learn. After some time passed, when the CANR becomes steady, the result shows that the CANR has the significant improvement.

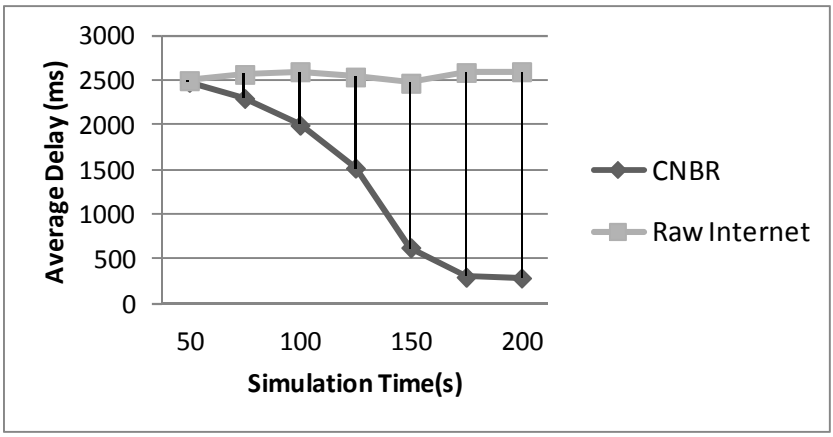

Fig. 6. Simulation Result

6 Conclusion and Future Work

In this paper, we propose a content aware and name-based routing speed up network systems, CANR, which can automatically aware the changes of topology and bandwidth, and then construct name-based routing table by a new multi-objective k shortest algorithm. The CANR works as a collaborative cluster of proxies which can bridge different domains and try to find the cheapest and shortest path when routing. The system is self-managed and self-evolution. The evaluation result proved the system has the better performance in speed. In the future, we will do more evaluations of CANR about two weights of cost and delay with large data.

References

1. Pallis, G., Vakali, A.: Insight and Perspectives for Content Delivery Networks. Communications of the ACM 49(1), 101–106 (2006)
2. Lei, M., Vrbsky, S.V., Hong, X.: An on-line replication strategy to increase availability in Data Grids. Future Generation Computer Systems 24(2), 85–98 (2008)
3. Pérez, J., García-Carballeira, F., Carretero, J., Calderón, A., Fernández, J.: Branch Replication Scheme: A New Model for Data Replication in Large Scale Data Grids. Future Generation Computer Systems 26(1), 12–20 (2010)
4. Tu, M., Li, P., Yen, I.-L., Thuraisingham, B., Khan, L.: Secure Data Objects Replication in Data Grid. IEEE Transactions on Dependable and Secure Computing 7(1), 50–64 (2010)
5. Furfaro, F., Mazzeo, G.M., Pugliese, A.: Managing Multi-dimensional Historical Aggregate Data in Unstructured P2P Networks. IEEE Transactions on Knowledge and Data Engineering 22(9), 1313–1330 (2010)
6. Agneeswaran, V.S., Janakiram, D.: Node-Capability-Aware Replica Management for Peer-to-Peer Grids. IEEE Transactions on Systems, Man, and Cybernetics—PART A: Systems and Humans 39(4), 807–818 (2009)

7. Ahlgren, et al.: A survey of information-centric networking. IEEE Communications Magazine, 26–36 (July 2012)
8. Choi, J., et al.: A Survey on content-oriented networking for efficient content delivery. IEEE Communications Magazine 49(3), 121–127
9. Jacobson, V., et al.: Networking Named Content. In: Proc. CoNEXT, Rome, Italy, pp. 1–12 (2009), http://doi.acm.org/10.1145/1658939.1658941
10. http://www.named-data.org
11. Jacobson, V., et al.: Networking Named Content. In: CoNEXT 2009, New York, NY, pp. 1–12 (2009)
12. Koponen, T., et al.: A Data-Oriented (and Beyond) Network Architecture. In: SIGCOMM 2007, pp. 181–192 (2007)
13. Visala, K., et al.: An Inter-Domain Data-Oriented Routing Architecture. In: ReArch 2009: Proc. 2009 Wksp. Rearchitecting the Internet, New York, NY, pp. 55–60. PSIRP (2009)
14. Gritter, M., Cheriton, D.R.: An Architecture for Content Routing Support in the Internet. In: 3rd Usenix
15. Carzaniga, A., et al.: A Routing Scheme for Content-Based Networking. In: IEEE INFOCOM 2004, Hong Kong (2004)
16. Hwang, H., Ata, S., Murata, M.: A Feasibility Evaluation on Name-Based Routing. In: Nunzi, G., Scoglio, C., Li, X. (eds.) IPOM 2009. LNCS, vol. 5843, pp. 130–142. Springer, Heidelberg (2009)
17. Dijkstra, E.W.: A note on two problems in connection with graphs. Number Math. 1, 269–271 (1959)
18. Cai, X., et al.: Time varying shortest path problems algorithm for problems with constraints. Networks 31, 193–204 (1998)
19. Mirchandani, P.: A simple O(n2) algorithm for the all-pairs shortest path problem on an interval graph. Networks 27, 215–217 (1996)
20. Burton, D., et al.: On an instance of the inverse shortest pairs problem. Mathematical Programming 53, 45–61 (1992)
21. Brumbaugh, S.J., et al.: An empirical investigation of some bicriterion shortest path algorithms. European Journal of Operational Research 43, 216–224 (1989)
22. Granata, J., et al.: The interactive analysis of the multi criteria shortest path problem by the reference point method. European Journal of Operational Research 151, 103–118 (2003)
23. Martins, E.Q.V.: On a multicriteria shortest path problem. European Journal of Operational Research 16, 236–245 (1984)
24. Azvedo, J., et al.: An algorithm for the multiobjective shortest path problem on acyclic networks. Investigacao Operational 11, 52–69 (1991)
25. Martins, E.Q.V., et al.: The labeling algorithm for the multiobjective shortest path problem. Coimbra, Portugal: CISUC Technical Report TR99/005, University of Coimbra (1999)
26. Hoffman, W., Pavley, R.: A method of solution of the Nth best path problem. Journal of the ACM 6, 506–514 (1959)
27. Fox, B.L.: Calculating kth shortest paths. INFOR; Canadian Journal of Operational Research 11(1), 66–70 (1973)
28. Eppstein, D.: Finding the k shortest paths. SIAM Journal on Computing 28(2), 652–673 (1999)

Solving Directed Hamilton Path Problem in Parallel by Improved SN P System

Jie Xue and Xiyu Liu

School of Management Science and Engineering
Shandong Normal University Shandong,
Jinan, 250014
China
{xiaozhuzhu1113,sdxyliu}@163.com

Abstract. The directed Hamiltonian path (DHP) problem is one of the hard computational problems for which there is no practical algorithm on conventional computer available. Many problems, including the traveling sales person problem and the longest path problem, can be translated into DHP problems. Inspired by the biological neurons, priority of rules in membrane computing, we introduce spiking neural P systems with priority and multiple output neurons into the application of DHP problems. In this paper, a new SN P System based algorithm is presented. We use neurons to stand for all the possible path and filter out the DHP we want automatically, all the processes will implement in the new SN P system. Instances indicate that the proposed SN P system based algorithm reduces the time complexity efficiently by huge parallelism.

Keywords: DHP problems, improved SN P System, priority, multiple outputs.

1 Introduction

Membrane computing is a new branch of natural computing which is initiated by Păun at the end of 1998[1] ,it abstracts computing models from the function of living cells, just like DNA computing coming from gene, particle swarm optimization from biomes, etc. The advantages of these methods are huge inherent parallelism, membrane computing has drawn great attention from the scientific community so far. The obtained computing systems proved to be so powerful that it is equivalent with Turing machines[2] even when using restricted combinations of features, and also computationally efficient. From now on, a number of applications were reported in several areas: biology, bio-medicine, linguistics, computer graphics, economics, approximate optimization, cryptography, etc.[3]

There has been three main types of P systems: cell-like P systems, tissue-like P systems, and neural-like P systems[4].

SN P systems are a variant of tissue-like and neural-like P systems from membrane computing, which are a class of distributed parallel computing devices inspired

Q. Zu, B. Hu, and A. Elçi (Eds.): ICPCA-SWS 2012, LNCS 7719, pp. 689–696, 2013.

from the way neurons communicate by means of spikes. An SN P system consists of a set of neurons placed in the nodes of a directed graph, sending spikes along synapses (edges of the graph)[5]. Each neuron contains a number of spikes, who are moved, created, or deleted by a number of firing and forgetting rules within the system. The computational efficiency of SN P systems has been recently investigated in a series of works .It has been used in the solution of NP problems, especially the SAT issues.

William Rowan Hamilton was Astronomer Royal of Ireland in the mid-19th century, the problem that has come to bear his name .A Hamiltonian path is a path that visits each vertex exactly once, given starting and ending vertex beforehand. The Hamiltonian path problem is to decide for any given graph with specified start and end vertices whether a Hamiltonian path exists or not. So it is a decision problem.

There have been many algorithms to deal with the Hamiltonian path problem, just like greedy algorithm, dynamic planning algorithm, divide and conquer algorithm .However, it seemed that there were any efficient methods in solving it. In the early 1970s, it was shown to be NP complete. Until 1994, Adleman used DNA computation to find the Hamilton path in a seven vertex directed graph, which proved to be a much powerful algorithm. But there have not been any- body using other efficient algorithm--membrane computing solving this problem. Up to the authors knowledge the combination of membrane computing and Hamilton path problem is found in a few researches just as Pan linqiang etc.[8].

Inspired by the research of Pan linqiang etc. [8], this paper focuses on the joint study of membrane computing with DHP problems. We propose an improved SN P system with the idea of constructing all the possible paths by neurons which can solve DHP efficiently. Different with other researches, this can reduce the complexity of the work significantly by the huge parallelism of P systems. Finally we present two examples to show the details of our technique.

2 Improved SN P System

2.1 Basic SN P System

We start by introducing the basic class of SN P systems .A spiking neural P system of degree m≥ 1 is a construct of the form[6][7]:

$$\prod = (O, \sigma_1, \sigma_2, ..., \sigma_m, syn, in, out)$$

Where O = {a} is the singleton alphabet (a is called spike); $\sigma_1, \sigma_2, ..., \sigma_m$ are neurons, of the form $\sigma_i = (n_i, R_i)$ $1 \le i \le m$; $n_i \ge 0$ is the initial number of spikes contained in σ_i; R_i is a finite set of rules of the following two forms:(1) $E / a^c \to a^p; d$, where E is a regular expression over a, and $c \ge 1$, $d \ge 0$,$p \ge 1$, with the restriction $c \ge p$;(2) $a^s \to \lambda$ for $s \ge 1$; $syn \in \{1,2,...,m\} \times \{1,2,...,m\}$ with $i \ne j$ for each $(i, j) \in syn$, $1 \ge i, j \ge m$(synapses between neurons); $in, outs \in \{1,2,...,m\}$ indicates the input and the output neurons.

The rules of type (1) are firing rules. If the neuron σ¡contains k spikes, and $a^k \in L(E), k \geq c$, then the rule $E / a^c \rightarrow a^p; d$ can be applied. This means consuming c spikes, the neuron is fired, and it produces p spikes after d time units.If d = 0, then these spikes are emitted immediately, if d = 1, then these spikes are emitted in the next step, etc. If the rule is used in step t and d≥1, then in steps t, t + 1,…, t + d-1 the neuron is closed, so that it cannot receive new spikes and spikes being sent to it are lost. In the step t + d, the neuron spikes and becomes again open, so that it can receive spikes.

The rules of type (2) are forgetting rules. if the neuron σ_i contains exactly s spikes, then the rule $a^s \rightarrow \lambda$ removed from σ_i from R_i can be used, meaning that all spikes are removed from σ_i.

In each time unit, if a neuron σ_i can use one of its rules, then a rule from R_i must be used. Sometimes, it is possible that two or more rules can be applied in a neuron, and in this case, only one of them is chose non-deterministically. Note however that, by definition, if a firing rule is applicable, then no forgetting rule is applicable. Thus, the rules are used in the sequential manner in each neuron, at most one in each step, but neurons function in parallel with each other. It is worth to say that the applicability of a rule is established based on the total number of spikes contained in the neuron.

Using the rules as described above, one can define transitions among configurations. Any sequence of transitions starting in the initial configuration is called a computation. A computation halts if it reaches a configuration where all neurons are open and no rule can be used. In order to computing a function among configurations. Any sequence of transitions starting in the initial configuration is called a computation. A computation halts if it reaches a configuration where all neurons are open and no rule can be used. In order to computing a function $f : N^k \rightarrow N$,we introduce k natural numbers $n_1, n_2, ..., n_k$ in the system by “reading” from the environment a binary sequence $z = 10^{n_1 - 1}10^{n_2 - 1}...10^{n_k - 1}$ This means that the input neuron of $\prod$ receives a spike in each step corresponding to a digit 1 from the string z and no spike otherwise. Note that we input exactly k +1 spikes, i.e., after the last spike we assume that no further spike is coming to the input neuron. The result of the computation is also encoded in the distance between two spikes: we impose the restriction that the system outputs exactly two spikes and halts(immediately after the second spike), hence it produces a spike train of the form $0^b 10^{r-1}1$ for some b ≥ 0 and with $r = f(n_1, \ldots, n_k)$ (the system outputs no spike for a non-specified number of steps from the beginning of the computation until the first spike).

2.2 SN P System with Priority and Multiple Output Neurons

SN P systems with priority of rules and multiple output neurons have the same components and the similar way of working as the above basic SN P systems except for the parts of the rules and the number of outputs.

Ri is the finite set of rules of the following three forms :

(1) $E/a^c \to a^p;d$, where E is a regular expression over a, $E \neq a^c$ and c≥ 1, d ≥ 0,

p ≥ 1, with the restriction c ≥ p;

(2) $a^c \to a^p, d$,c≥ 1, d ≥ 0, p ≥1, with the restriction c ≥p;

(3) $a^s \to \lambda$, for s ≥ 1

In this system, we divide the initial firing rules into two forms according to E and ac, when $E \neq a^c$,we define them as the first class of firing rules $E/a^c \to a^p;d$, and when $E = a^c$,they are the second class of firing rules $a^c \to a^p, d$

We also define the priority of rules(1)>(2)>(3),which means that in each time unit, if a neuron σ_i can use one of its rules, then a rule from R_i must be used, but the use of these rules have a sequence, rules (1) will work firstly ,rules(2)will work only after rules(1) can not be used any more, rules(3)will work only after rules(1)and (3)are useless.

Besides, we expand the number of output neuron, in SN P systems with priority of rules and multiple output neurons, every neuron can be used as an output if it is necessary .One SN P system will have multiple outputs.

3 Solving DHP by SN P System

3.1 SN P Systems Design for DHP

The purpose of this paper is to obtain all the Hamilton path by means of the improved SN P system. An improved spiking neural P system of degree $K = [(n-2)!+1] \times (n-1)$ is a construct of the form:

$\prod = (V, \sigma_{001}, \sigma_{112}, ..., \sigma_{(n-1)(n-2)t_n}, \sigma_1, ..., \sigma_{n-2}, syn, in, outs)$,where V = {a} is the singleton alphabet; t_i is a random member in one array of the full array; $\sigma_1, \sigma_2, ..., \sigma_m$ are neurons with (n_i, R_i) , here we divide σ_i into two sorts:

a) $\sigma_{001}, \sigma_{112}, ..., \sigma_{(n-1)(n-2)t_n}$,there exist 2 situations :

for any two vertexes i and j, i?j, if there is an edge e_{ij} from i to j, $n_j = a^j, R_j = a^i a^j \to a^j$ $_{j,}$ else if there is not an edge e_{ij} from i to j, $n_j = \varnothing, R_j = a^i \to \lambda$

b) (n_i, R_i) in $\sigma_1, \sigma_2, ..., \sigma_{n-2}$, $n_i = n - t_i$, $a^{t_i} a^{n-t_i} \to a^n$

(3) $syn \in \{1,2,...,m\} \times \{1,2,...,m\}$ with i≠ j for each $(i, j) \in syn$, 1 ≥ i, j ≥ m(synapses between neurons); $in, outs \in \{1,2,...,m\}$ indicates the input and the output neurons. here, the synapses are all the possible path between the start vertex 1 and the ending vertex n, and for our algorithm ,we design another (n-2) synapses between $\sigma_1, ..., \sigma_{n-2}$ and outputs, in this paper, we do not consider synapses 1-n and any other vertex to the start node 1.

(4)In1 is the input neuron and output belongs to the set $\{O_i \mid 1 \le i \le (n-2)!\}$

Rules in output neurons Oi are as follows, there are n rules contained in $O_i : a^n / a \to a; 1, a^{n-1} / a \to a; t_i (2 \le i \le n-1), a \to a; 5$

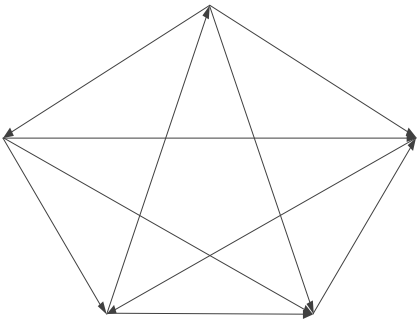

Fig. 1. An directed graph of 5 vertex

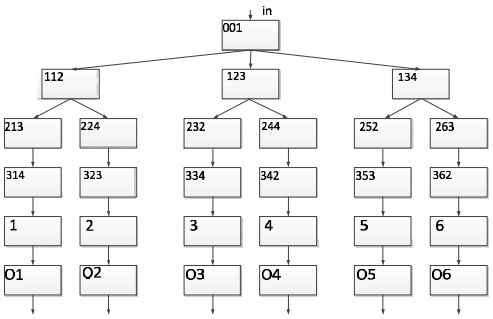

Fig. 2. The SN P system design for the 5 node directed graph

3.2 An Overview of Computations

In this section, we use a simple instance with 5 patterns as Fig1. to illustrate our algorithm clearly.

At first, we construct the SN P systems for it, the construction is shown in Fig.2

A spiking neural P system as Fig.5 of degree m=28 is a construct of the form $\prod = (V, \sigma_{001}, \sigma_{112}, ..., \sigma_{362}, \sigma_1, ..., \sigma_6, syn, in, outs)$

O = {a} is the singleton alphabet (a is called spike);

Neuron001: $a \to a$, a^2,a^3 in neuron 112,123 respectively: $aa^2 \to a^2$, $aa^3 \to a^3$,neuron134: $a \to \lambda$,a^3 in neuron 213,353 respectively: $a^2 a^3 \to a^3$,a^4 in neuron 224,334 respectively: $a^2 a^4 \to a^4$, neuron232,362: $a^3 \to \lambda$, a^4 in neuron 244,314 respectively: $a^4 a^3 \to a^4$, neuron252,263,323,342: $a^4 \to \lambda$.

1,3: $a^4 a \to a^5$ 2,5: $a^3 a^2 \to a^5$ 4,6: $a^2 a^3 \to a^5$

O1: $a^5 / a \to a; 1, a^4 / a \to a; 2, a^3 / a \to a; 3, a^2 / a \to a; 4, a \to a; 5$

O2: $a^5 / a \to a; 1, a^4 / a \to a; 2, a^3 / a \to a; 4, a^2 / a \to a; 3, a \to a; 5$

O3: $a^5 / a \to a;1, a^4 / a \to a;3, a^3 / a \to a;2, a^2 / a \to a;4, a \to a;5$

O4: $a^5 / a \to a;1, a^4 / a \to a;3, a^3 / a \to a;4, a^2 / a \to a;2, a \to a;5$

O5: $a^5 / a \to a;1, a^4 / a \to a;4, a^3 / a \to a;2, a^2 / a \to a;3, a \to a;5$

O6: $a^5 / a \to a;1, a^4 / a \to a;4, a^3 / a \to a;3, a^2 / a \to a;2, a \to a;5$

(3)syn $\subseteq$ {1, 2, . . . ,28} × {1, 2, . . . 28} with i≠ j for each $(i, j) \in \text{syn}$, 1 ≤ i, j ≤28

The synapses are as Fig.2.

(4)In_1 is the input neuron and output belongs to the set{O_i|1≤i≤6}.

The input neuron is 001,every path has their own output neuron {Oi|1≤i≤6} and neurons with different initial symbols and rules which are as above.

In this instance, one spike activates the rule $a \to a$, 001 send one a to 112,123,134 at the same time and they deal with this symbol in parallel. In 112, $aa^2 \to a^2$ works and send a^2 to 213 and 224, $aa^3 \to a^3$ in 123 send a^3 to 232,244, $a \to \lambda$ makes neuron 134 become empty and all the computation in 134 and neurons linked with it halt. There are four paths remain.

$a^2a^3 \to a^3$, $a^2a^4 \to a^4$ and $a^4a^3 \to a^4$ in 213,224,244 will be active and deliver a^3 and a^4 to 314,323,342 . Meanwhile, $a^3 \to \lambda$ let neuron 232 become empty and all the computation in 232 and neurons linked with it halt. There are three paths remain.

$a^4a^3 \to a^4$ will be active by a^4 in 314 and deliver a^4 to neuron1, $a^4 \to \lambda$ will make 323 and 342 empty and all the computation in 323,342 and neurons linked with it halt. There is only one path remain.

In neuron 1, $a^4a \to a^5$ will send a^5 to O_1,a^5 will activate rules in O_1,at last, there are 101001000100001 being outputted from O_1 to the environment ,we get the result of HPP by reading 101001000100001 out ,it is 12345.

3.3 Example and Discussion

In the instance above, we show the process of our algorithm in the 5 patterns directed graph, all the computation occur in P system and in parallel, we just use 5+15=20 steps to find the Hamilton path. The membrane computing method proposed in this study was applied to the 9 points directed graph for another instance, which is as Fig.3 We use 40328 neurons to implement our algorithm, there are 5040 ways work at the same time ,the time complexity of this instance is equal to the traverse from 1 to 9,it is 9 steps and in neurons we will use 45 steps to read out the result. 126485379 ,so the total steps is 9+45=54.which is O(n).

Our algorithm is different with other algorithms carrying out by silicon computers, we introduce the biology thought to find Hamilton path .,we use the improved SN P system to propose a new solution to an NP-complete problem, the directed Hamilton path problem, According to the parallelism of membrane computing ,we reduce the time complexity and get all the possible Hamilton path simultaneously. The time complexity is O(n).

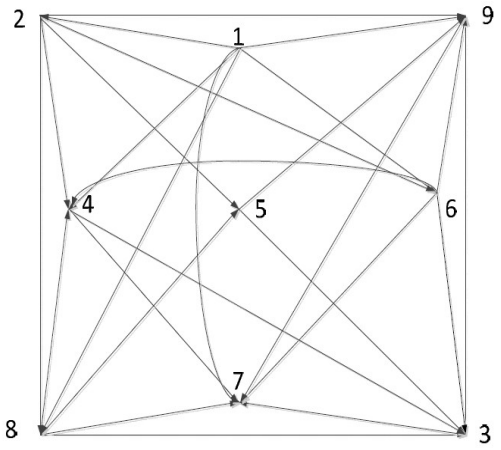

Fig. 3. An directed graph with 9 points and 26 edges

This algorithm based on bio-computing technique has the advantages of the conventional algorithm and membrane computing, which is suitable for the complicated graph. It also can be used as a scheme for designing solutions to other NP-complete problems from graph theory such as the vertex-cover problem, the clique problem, etc.

4 Conclusion

In this paper we presented a new membrane computing based technique for DHP problems. An example is given to show the effect of our algorithm. By the SN P system we can implement the automatic selection of the path in the process of finding possible Hamilton path significantly. This is especially useful for complicated graph since membrane computing has large parallel ability. Up to the authors knowledge, this is the first research in DHP problems by membrane computing. It provides an alternative solution for this traditional knowledge engineering. However, we need to say that in this research ,there are many problems waiting to be solved, just as we use a little more neurons ,we should reduce the number of neurons that are consumed in our future work.

Reference

1. Păun, G.: A quick introduction to membrane computing. The Journal of Logic and Algebraic Programming 79, 291–294 (2010)
2. Día-Pernil, D., Gutirúez-Naranjo, M.A., Peréz-Jiménz, M.J., Riscos-Núnez, A.: A Linear-time Tissue P System Based Solution for the 3-coloring Problem. Electronic Notes in Theoretical Computer Science 171, 81–89 (2007)

3. Ionescu, M., Păun, G., Yokomori, T.: Spiking neural P systems. Fundamenta Informaticae 71(2-3), 279–308 (2006)
4. Pan, L., Alhazov, A.: Solving HPP and SAT by P systems with active membranes and separation rules. Acta Informatica 43, 131–145 (2006)
5. Leporati, A., Mauri, G., Zandron, C., Păun, G., Pérez-Jiménez, M.J.: Uniform solutions to sat and Subset Sum by spiking neural P systems. Natural Computing 8(4), 681–702 (2009)
6. Leporati, A., Zandron, C., Ferretti, C., Mauri, G.: Solving Numerical NP-Complete Problems with Spiking Neural P Systems. In: Eleftherakis, G., Kefalas, P., Păun, G., Rozenberg, G., Salomaa, A. (eds.) WMC 2007. LNCS, vol. 4860, pp. 336–352. Springer, Heidelberg (2007)
7. Leporati, A., Zandron, C., Ferretti, C., Mauri, G.: On the computational power of spiking neural P systems. International Journal of Unconventional Computing 5(5), 459–473 (2009)
8. Pan, L., Zeng, X., Zhang, X., Jiang, Y.: Spiking Neural P Systems with Weighted Synapses. Neural Process. Lett. 35, 13–27 (2012)

Application of TDMI in Government Informatization

Liyou Yang[1], Hongyu Zhao[1], and Yongqiang Wang[2]

[1] Network Center of Logistics Academy, Beijing,100858
[2] Network Center of CESEC, Beijing ,100840
mytbaby@sohu.com, {zhaohy_web,yqw323}@sina.com

Abstract. The main goal of informatization top-level design is to reduce appearance of new isolated information islands. To find a kind of methods which restrains isolated information islands in informatization areas is our common goal recent years. TDMI as a sort of methods is a new type of methods for informatization top-level design. It aims at solving the isolated information islands problems from multi-level, such as informatization architecture framework, system architecture framework, data architecture framework. In this paper we discuss informatization top-level design for government areas using TDMI. The method firstly requires to describe the status and goals in government areas. Then we build the information architecture framework, systems architecture framework and data architecture framework. After that ,it starts into developing phrase. Lastly, they are integrated testing, testing run, run and maintenance phrase. The core of TDMI is to plan and restrain information systems design under the center for data.

Keywords: government informatization, TDMI, informatization systems integrated.

1 Introduction

1.1 The Current Status of Informatization Top-Level Design

In the past, we did not pay more attention to the methodology about integrated design in informatization areas and current popular top-level design aspects. One design resolution only fits one specific system. There was no a set of directive, regular and restrain provisions that abstracts from the position of methodology. Informatization for government or huge informatization areas is a long period and developing process. Under the government guidance we should regulate a set of directive, regular and restrain rules which direct, regulate and restrain information systems design and implementation. Since 80's late in 20st century, the design concept of the Enterprise Architecture[1] and TOGAF(The Open Group Architecture Framework)[2] were put

[1] EA:http://msdn.microsoft.com/en-us/library/bb466232.aspx
[2] TOGAF: http://www.opengroup.org/togaf/

Q. Zu, B. Hu, and A. Elçi (Eds.): ICPCA-SWS 2012, LNCS 7719, pp. 697–710, 2013.

forward in the United States. Those methods form a lot of informatization architectures design methods which aims at solving the government informatization problems. But at the beginning of 21st century, it was found that they still stayed in the design concept of single big system. They still continued to make the new isolated informatization islands. Until the middle of first 10 years in 21st century, they change the center of products or information systems into center of data. It commences to solve the architecture design for complicated huge system from the position of methodology. It smoothes out the road for the interconnection and inter-access among the systems in United States government and US military.

China Government Informatization still stays in the design concept of single big system so far. There was no methodology such as informatization architecture methods for government There are a lot of standards which apply to government informatization areas, but they are only some technical standards for designs process, there were no use for interconnect and inter-access. The more systems developed, the more isolated informatization islands appear.

In order to build the environments in which the data and information can be shared. We should regulate the sharing data models in which do not include the PDM(Physical Data Model), but it should contain the PES (Physical Exchange Specifications). This kind of design methods solve the data exchange for variety of information systems using PES, and solves the PDM's separately design for variety of information systems which realize the character of each information system.

This paper we aim at solving the integrated design methodology, also called Top-level Design Methods for Informatization, not face the single information system design issue. If we restrain all information systems developing with the mode of sharing data and information, which would guarantee the information systems that would not become the new isolated information islands. To solve the data and information sharing is the big problem in government informatization areas, also big problem in other informatization areas.

1.2 Thought about TDMI Method

TDMI was created according to following thought: First of all, the core thought of TDMI must focus on the sharing of mass data and information, not focus on the interoperations between application systems. In the past, it was right to emphasize the interconnection, intercommunication and interoperations between different systems or heterogeneous systems. But its implication of interoperations among three elements was not clear so far. The super huge systems are also hardly to complete according to interoperation between systems. The interconnection is precondition, the intercommunication is supporting, and the inter operations is goal, but the inter operations are not all focused on the application systems, they should focus on the sharing data and information. One system accesses the other system, the other system accesses previous system or next system, or all systems access the centric system, the result like doing will bring a lot of access rights to set up. If we start at beginning of

sharing data and information to design our systems, let the different or heterogeneous system rapidly provide decision-making or service information according to demanding, The complement of huge systems will be much easy. That is the basic implication of sharing data or information. So that we can reduce the amount of analysis working of systems, largely enhance the efficiency of systems too. The next core thought of TDMI must be openness designing based on web model, not the close designing or nonexpanding. These idea is to build the model of plug-in and plug-out based on web platform.

The top-level design based on web is the best designing model which concentrates the advancement, stability, openness, flexibility and expansion all together. It fits the design demanding that is the Boundaryless Information Flow[3] for super huge systems. Therefore the TDMI's informatization architecture framework was built according to the openness framework based on web, which idea is needless to argue for top-level design. We mentioned in previous discussion that the connotation of interoperations are not very clear, in a contrary, the sharing data and information are not only very clear on the content and concept, it also is the highest goal for informatization designing.

In the top-level design for government informatization, another difficulty problem that we face is how to let all layers of staffs and leaders to understand the work what we are doing. Therefore the other goal of sharing data and information designing still need to take the measures of multi-presentation for understanding and visibility for all layers of staffs and leaders. So we face a lot of presentations of sharing data and information to do, such as the unification of standards and regulations, integrating and confirmation of basic data and so on. Those are the foundational work of technical aspects, but there are numerous amount of work to do. But the decision-makers and business men often seldom think of them. In DoDAF's[4] designing, in which good idea and measures are provided. There are 8 types of Viewpoints[5] which are consisted of various views, such as consistent view, bar view, convergence view, figure view and reference view etc. The viewpoint refers to all-viewpoint, capability viewpoint, data and information viewpoints, operation viewpoints, project viewpoints, services viewpoints, standard viewpoints and system viewpoints and so forth. These designing of view and viewpoints enhance and rich the presentation of sharing data and information, they are the one of important elements in TDMI's methodology thought.

---

[3] Boundaryless Information Flow was proposed by The Open Group in TOGAF's standard organization, which was put forward according to the concept of the Boundaryless Management Model, which was proposed by the president Welch in GM Company. The boundaryless is not really no boundary, neither need not organizations or institutions. That means the departments or organizations do not become the obstacle of information flow, that also implicate that informatization infrastructure should support the business expansion and workflow improvement, That is to say, which should support the breakthrough of ranges and boundary.

[4] DoDAF means Department of Defense Architecture Framework.

[5] The presentation or modle were presented by multi-media form, such as files, electronic form, abstract data, or figure. Collect all these data into some figure which is called view, the collection of organized view is called viewpoints.

1.3 TDMI Method

The TDMI is a kind of top-level design method for informatization which aims at avoiding appearance of new isolated informatization islands. There are 8 steps including in the TDMI. First step, the current status were described in some informatization areas; Second step, expecting goals were considered and set; Third step, informatization architecture framework was planned and plotted; Fourth step, system architecture framework was worked out; Fifth step, data architecture framework was built; Sixth step, system developing, such as coding, interface standards and so on could be commenced; Seventh step, systems integrating, including interconnecting, data transferring and so forth have to be done; Eighth step, performance testing, it prepares for system normal running.

Step1-2: Description of current status and expecting goals, they are the beginning of informatization in some areas. The main objective is to analyze the status and goal position for the informatization areas. The analysis objects include informatization infrastructure, information resources, information systems, information security and managements, informatization facilities and informatization supporting environment. It is necessary to fill in the forms according to the analysis results of current status and the future objectives or goals. Take the informatization infrastructure for an example, its contents of forms at least includes types of communications, bandwidth, transmitting speed, information load, system quantities, security level, facilities type, and description of standard specifications etc.. Only we are clear of these status, we can get the connect informatization construction plan. Those are the foundation of all that we are going to do.

Step-3: informatization architecture framework, it indicates the framework structure in which we should do in the informatization areas. It includes five layers which are the network infrastructure layer, common supporting layer, data resources layer, application services layer and user access layer. Security and management layer in the framework, including their strategies and measures are needed for all layers in the informatization areas. They are in charge of security and managements in whole informatization areas. The security and managements are the most important element for any informatization areas and must be done well, otherwise the informatization only bring us a lot of troubles and disasters. The common informatization architecture framework for informatization areas is represented in figure-1.

Security and Management	Information portal	User access layer
	Shared applications, Special applications	Application services layer
	Shared data, Special data, Exchange data	Data resources layer
	Data center, Computing services	Common support layer
	Satellite, Wire, Wireless, Mobile	Network infrastructure layer

Fig. 1. The common informatization architecture framework for informatization areas

Network infrastructure layer in the figure is a must-have for all informatization areas, whether it is the government, the military or a huge system. For a large informatization areas, satellite communications are needed to support transmissions from space to ground, while wired, wireless and mobile supporting are require for the ground or non-distance. Meanwhile they are necessary to get the interconnections between multi-systems. Specific parameters or standards are determined according to the requirements in the informatization areas.

Common support layer includes data center and data center operation management system, strategies configuration and their computing services. Data center can be distributed, centralized combined with distributed or centralized, but the majority is the centralized mode combined with distributed one, which is more in line with the modern models of cloud computing or grid computing. This layer mainly provides storage and computing services for the upper layer. It also could combine with its upper layer, which is common support layer.

Data resource layer consists of the shared data in the informatization areas, the special data in the business fields, and the data needed to be exchanged between the old and new systems. This is not only the most unique part of the informatization architecture framework, but also the core of dealing with system integrating. Extraction of shared data must be based on informatization standards in the informatization areas and in all crossed areas. For example, the shared data for human resources includes name, gender, date of birth, place of birth, place of origin and ID number, those are the common information that all people are born with and will remain unchanged in their life. They are also the basic sharing information differentiating those with the same names and the same gender who are in the different units.

Application service layer contains several elements, one is the shared applications for all business areas, the other is special applications in specific business area. Shared applications contain e-mail system, file transfer system, domain name system, office platform, forum, blog and so on. Special applications can be in various forms and different functions whose quantities are determined by the requirements in the informatization areas. The numbers even can be up to several dozen. Special applications are finally integrated and coordinated effectively through common interface and information portal.

User access layer is used so that users can access with confirmed identity and authentication, through the information portal, various types of authorized resources, application systems and information services provided by the portal. The future developing trend in informatization is the providing information services, providing demanded services are more important than inter-operation between systems.

Step-4: system architecture framework. It refers to the best set of information systems in the informatization areas which is used to meet the needs of informatization applications and development. All information systems registered in the system architecture framework must take the shared data as the shared foundation and combine it with the special data in the systems to form special systems. The special data should also be in conformity with the regulated informatization standards.

Step-5: data architecture framework. Here it in fact refers to the design principles of the data structure described in the data resources layer. Any fields of informatization will involve human resources, financial resources, assets resources, facilities resources and information resources. Extraction of shared resources and the adoption of standards

is the core in TDMI. Therefore, the construction of the data architecture framework, though which will take a long time to complete, is worth to effort. Otherwise, the result will be more isolated information islands.

Step-6: systems development. The concept needs not to explain more, but here the systems are not only refering to the information systems, it exactly refers to informatization projects development. It also contains systems deployment and information support environments which are done under the regulation of informatization architecture framework, system architecture framework, and data architecture framework. No informatization contents in all field is the same. What can be identified are the unified standards, unified practices, and unified data sharing structure. With these regulatory constraints, the development process should be conducted separately. The task of the decision-making teams is to monitor the implementation and control quality of informatization process. The information systems developed in this way can meet not only the requirements of system integrating, but also the special needs of individualized systems.

Step-7: system integration. It refers to integrating of information systems developed in various phrase separately, or integrating between old and new systems. Recently, there has been a growing trend with integrating between complex systems. At the same time, performance optimization, robustness, and reliability among heterogeneous systems to realize a common goal have become the focus of various information systems integration. With using TDMI, the development of individualized systems is done under the constraints of top-level design specifications, the workload of system integration will be greatly reduced. An informatization area is equivalent to a wide areas network in the network age, which is also a huge system. For example, informatization in taxation area in government departments is really a huge information system. Therefore integration of various huge systems has become feasible under the constraints of the top-level design in government informatization.

Step-8: performance testing. It is to test all kinds of pre-set indicators, information system performance, supporting environments, security and management factors. This is a necessary step, because only when the performance tests of the systems are able to meet the requirements and operate normally, can the system capacity is fully developed. After this step, the system will enter the operation and maintenance phase.

The 21st century informatization is witnessing a rapidly change in the way we face. Many of the underlying the traditional systems engineering strategies are no longer valid. The traditional systems engineering has been focusing on developing stand-alone systems under the stable architecture and less changing technology base[6]. The TDMI is put forward according to weakness above and new demands. The eight steps in TDMI should be implemented in order, but there might be cases of localized crossing or synchronization, which needs the art of organization and leadership.

[6] Mo Jamshidi, System of Systems Engineering: Innovations for the 21st Century,2009, Printed in USA and Canada,p21-21.

2 Top-Level Design for Government Informatization

The main tasks of government informatization are to provide common informatization infrastructure by the government, which services the public. The common informatization infrastructure includes network infrastructure, information infrastructure, and varieties of electronic administration information systems, later contains human resources, finances, taxation, commerce and land resources management information systems etc.. As a government, it is usual to manage a huge affairs and areas. Therefore, the top-level design is very important for government informatization. The areas here refer to management range which has clear boundary and management business. Specific design contents need to describe separately for government informatization according to TDMI.

Step 1-2: Description of current status and expecting goals. To analyze the current status for government informatization first, then set the goal position according to current status and future demands goals. The analysis objects include network infrastructure, information infrastructure, information resources, information systems, information security and managements, informatization facilities and informatization supporting environment. It is necessary to fill in the unified forms according to the analysis results of current status. The contents of forms include types of communications, bandwidth, transmit speed, information load, system numbers, security level, facility type, and description of parameter specifications etc.. The descriptions of expecting goals need to embed in specific data. That is to describe goals through regular form according to expecting objectives. Take the government network infrastructure, for example, it involves satellite communication, IP network, wireless

Table 1. The table of current status and demand goals for government informatization

Category 1	Category 2	Current status	Expecting goals
Satellites	GPS Sensor Satellite, mobile communication Multimedia data transmission		
IP	Network technology WAN bandwidth LAN bandwidth User access ports number Terminal bandwidth		
Wireless	Mobil internet channel Special wireless channel Wi-Fi channel		
Information management centers	User registration center Network management center Network running center Security control center		

network, and their government institutes and regulations. The form of current status and demand goals for government informatization are given in table-1. The descriptions of other item's current status and goals demands can refer to the table-1. They are very important for later design.

Step 3: Informatization architecture framework building, Here we need to construct realistic framework for specific areas of government informatization. This framework involves the network infrastructure layer, common support layer, the data resources layer, application service layer and user access layer, as well as the security and management of the government informatization areas. The common informatization architecture framework for government informatization areas is represented in figure-2.

Gov. Security and Management	Gov. information portal	User access layer
	Gov. shared applications, Gov. special application IS	Application service layer
	Gov. shared data, Gov. special data, Gov. exchange data	Data resources layer
	Gov. data center, computing services	Common support layer
	Satellite,Wire, Wireless, Mobile	Network infrastructure layer

Fig. 2. The common informatization architecture framework for goverment informatization areas

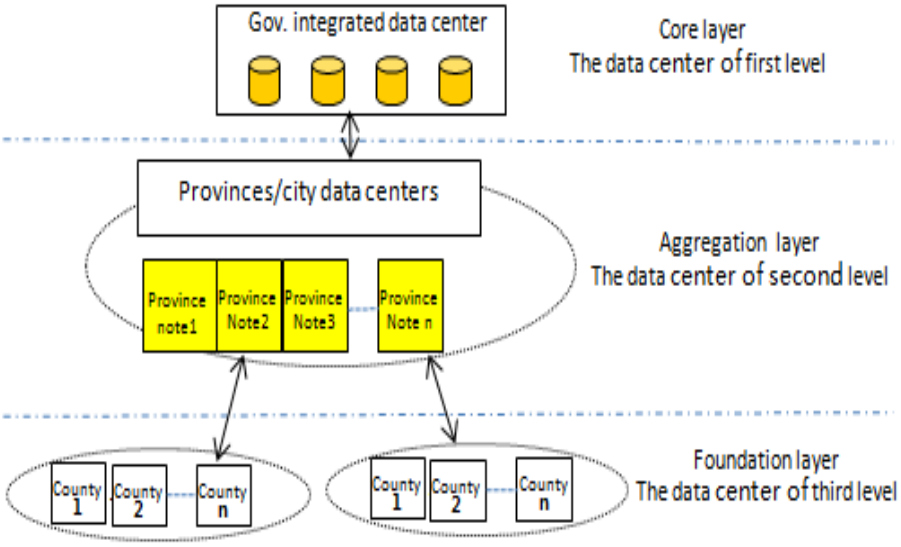

Fig. 3. The deployed framework for the data center of the government common support layer

In this framework, we take the data center and common computer services in common support layer as an example. It includes government integrated data center, province integrated data center and foundation data center in which they separately provides storage facilities, dictionary services, search services, management systems, rules configuration, and computing services etc.. The centralized data center for each level can combine with distributed one, which work well with the modern models of cloud computing and grid computing. Each level can also provide storage and computing services for the upper layer. The three layer data center in the government common support layer can be deployed as above figure-3.

Integrated data center is not only the environments for sharing data collection, data storage, disaster backup, data recovery and security managements, at same time, they are also the center providing sharing data, data exchange, data analysis, data backup and information services. Only to make the common supporting layer done well, the convergence between systems can be acted smoothly.

Step-4: The systems architecture framework building, In this step we first plan the best set of information systems in government informatization areas which is used to meet the needs of government information applications and development. All information systems registered in the government systems architecture framework must take the shared data as the integrated core and combine it with the special business data in the specific systems to form specific business systems. The special business data should also be in conformity with the government informatization standards. The best set of information systems in government informatization areas or the systems architecture framework, which can certainly be changed when it needs, is showed in following figure-4.

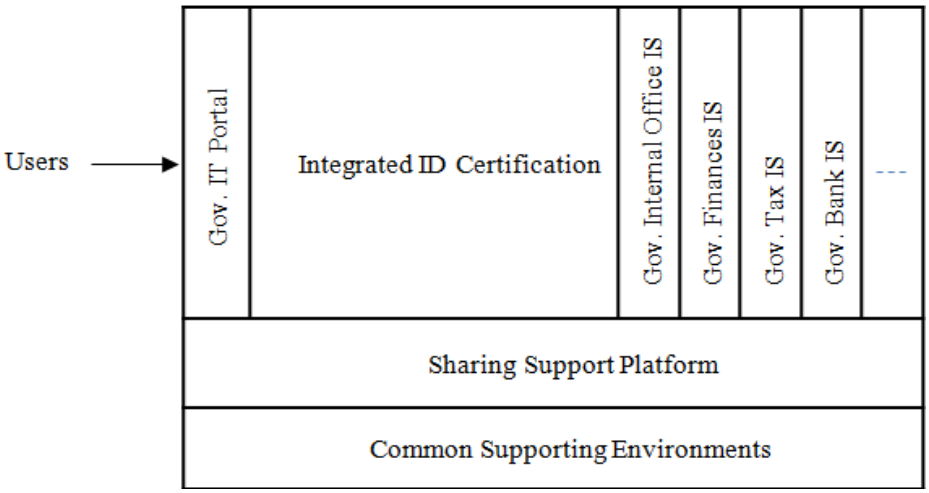

Fig. 4. The systems architecture framework for Government Informatization

The integrity and expansion of this framework need to be confirmed. Therefore numbers of information systems could only maintain to not change in the period of several years. Here the specific business information systems are developed through professional software enterprise, which is explained later.

Step-5: Data architecture framework building. First of all in this step what we do is to formulate the regulations for storage, adoption and deploy of sharing data, special data and exchange data. Those data and information will involve government human resources, financial resources, assets resources, facility resources and information resources and so on. All data and information will be inter-accessed shared, exchanged between areas or departments, for instance, the interoperation between new and old systems, between different departments. The following figure-5 is the sharing data architecture framework.

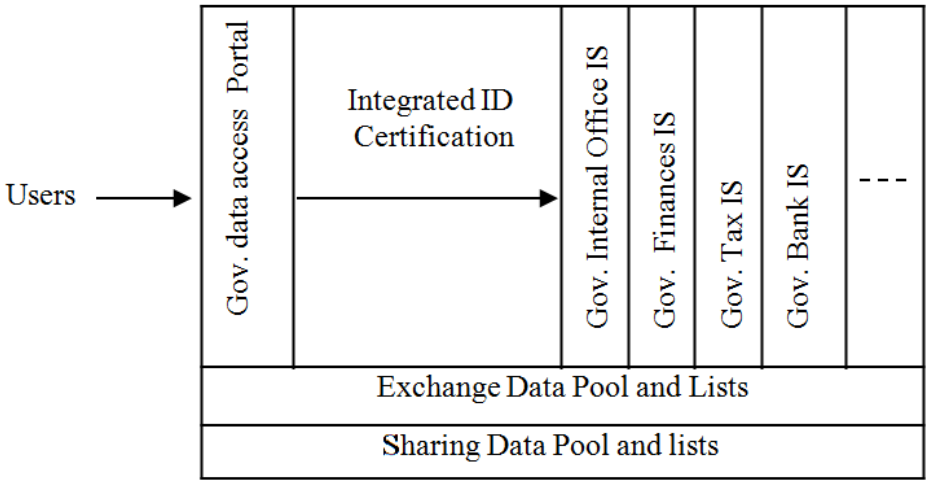

Fig. 5. The data architecture framework for Government Informatization

The gov. data access portal refers to the website which provides platform for the users who access sharing database or data pools. And identity of those users must be confirmed before the access requirements, here we call the Integrated ID Certification. The upper right columns of the figure-5 refer to the planning information systems from the framework. The contents of the exchange data and the sharing data were described depending on various business systems. The pool here means related database and their access lists. All of these consist of the integrated data environment in which provides the translation, routing, business rules management, and data access etc.

Step-6: Systems development. Firstly all departments in government must be aware of that information systems development, system deployment and information support environment building are curried out under the restrains of government informatization architecture framework, system architecture framework and data architecture framework, and they also need to know that no one informatization process in any fields is the same, especially in systems development phrase. Secondly specific

standards, practice methods, data sharing structures should unify by the government. With these regulatory constraints, the systems development process should be conducted separately through the qualified enterprises. Thirdly the decision-making teams in government departments monitor the informatization implementation and guarantee the process of projects smoothly. Lastly government audit agency should audit the investment according to contracts every year.

Step-7: systems integration. In this step, we start to the integrating of information systems developed in the various phrase separately, or integrating between old and new systems. Although the development of individualized systems is done under the constraints of top-level design specifications, the coordinating work between systems must be tested together. Firstly we should guarantee the all individual information systems run and effect correctly, and output the parameters into layer systems or next layer systems or same layer systems normally, and get the expected results which they are integrated in one wide-areas network. Secondly we should test the interconnection and intercommunication between different integrated information systems within wide areas network. After that, integration of various huge systems should become feasible under the constraints of the top-level design of the government informatization.

Step-8: performance testing. This is the last step which is the traditional step and an important one. First of all we need to test all kinds of specifications, parameters or indicators before deployment. And then evaluate information systems performance, supporting environments, security and management factors. In this step we can judge if the integrated huge systems are to meet expecting performances, because, only when the performance testing of the systems is able to meet the requirements and operate normally, can the integrated system be vitality. And until now, the system can enter the operation and maintenance phase in which the business staffs need to collect and change the data or information everyday for the applied information systems, guarantee them provide services to public normally.

3 The Application Thinking of TDMI in Government Informatization Areas

The descriptions and structure models for government informatization are given above according to TDMI are just the partly concept models and design thoughts from the perspective of top-level design, but we could see the TDMI's building ideals from previous discusses. It stresses on the information systems as backbone and treats the sharing data as core for government informatization, because any informatization fields have the information systems as main applications. As for information security, informatization management, informatization supporting environments etc., they must be designed around the secure running for information systems. The design of sharing data architecture framework aims at solving the inter-access and inter-operations between information systems. The goals of design try to converge between information systems. In addition to above we still need to pay attention to following several points using the TDMI in government informatization areas.

3.1 The Unity and Confirmation of Government Informatization Architecture Framework

There are a lot of forms or types describing the informatization architecture framework, but the basic structure and concepts must be unity. Three layers or five layers structures are both allowed to describe the framework, but the contents and concepts must be identified. In previous section, for example, we mentioned the informatization infrastructure which contains two parts, the one is the network infrastructure, and the other is the information infrastructure. And information infrastructure consists of integrated information portal, integrated data standards, integrated identity confirmation and integrated the management of sharing data. This idea will not have a consistent understanding within peers. Whatever we describe, these concepts must be unified. Otherwise it will be confused in description of informatization architecture framework.

3.2 The Organization and Implementation for Government Informatization

It refers to the model for organizing and informatization process for currying out for government informatization. For instance, the network infrastructure we pointed in previous, which should be planned and designed and organized by government's related departments, not allowed to do those projects through the subordinate departments separately. The sub-departments can take part in the discussion and regulation for their demanding and goals. The market bidding must be used with government informatization projects, projects process were curried out through qualified enterprises. Government departments just take part in to test the wanted standards according to the previous signed contracts.

3.3 The Risk Evaluation and Supervision for Government Informatization

It is necessary step to promote the transformation of existing government into service type governments. The Government informatization is the key elements for enhancing the service capability of government departments. The informatization construction in government departments involves the whole processes for capability enhancements, but those processes face a lot of risks, such as fickle technologies, the policy adjustment, regulation supporting, management models changing and staffs qualification etc. The government departments are full of aware of their capability level and adopted regulation after government informatization. The government departments need to evaluate status and quality level of the projects process in time. This will promote deep changing of the development strategy, administration policy and managements mechanism through risk evaluation. At the same time, it will help government find problems with informatization process, regulate new measurements, optimized service models. It will get the goal of modernization service government done, and go along the healthy road for government informatization.

4 Conclusion

The main idea of TDMI is to reduce appearance of new isolated information islands, which we mentioned in whole paper. Firstly it emphasizes the key role of the information systems and treats the sharing data and information as core for government informatization. It also emphasize the different or heterogeneous system rapidly provide decision-making or service information according to demanding, that is the basic implication of sharing data or information. Therefore the entirely new meaning is given to the interconnection, intercommunication and interoperations between different systems or heterogeneous systems. Doing like that, we can not only reduce the numerous amount of analysis working of systems, but also largely enhance the efficiency of systems. Secondly, that is the next core thought of TDMI which is TDMI must be openness designing based on the web model, not the close designing or nonexpanding. The top-level design based on web concentrates the advancement, stability, openness, flexibility and expansion all together. It fits the design demanding that is the Boundaryless Information Flow for super huge systems. Therefore the TDMI's informatization architecture framework, system architecture framework and data arzhitecture framework all were built according to the openness framework based on web.

We hope this kind of method will be applied to the government informatization areas, so that we can prevent isolated information islands from appearance. And we also mentioned, TDMI are just the partly concept models and design thoughts from the perspective of top-level design, but we could see the TDMI's building ideas from author's discusses. They are the excellent ideas for solving isolated informatization islands. The unfortunately thing is that TDMI still seldom apply to some huge areas, but the author are sure that they will be applied to the fields of government informatization, military informatization, and international cooperation enterprises along with demanding of mass data sharing.

At the same time, there are a lot of problems remained for us to study, such as understanding of informatization architecture frammework, the model of mass data sharing, model of inter-access between different or heterogeneous systems, cloud computing, introduced, management and registration of information systems and so on. We hope that these problems will be solved with the applications in the future.

References

[1] Yang, L., Zhao, H.: The Top-level Design Method on Informatization. In: ICPCA6//SWS3 2011, pp. 127–132 (2011)
[2] Zhao, H.: Grid computing and web education. Educational Technology (April 2007)
[3] http://msdn.microsoft.com/en-us/library/bb466232.aspx
[4] http://www.opengroup.org/togaf/
[5] Jamshidi, M.: System of Systems Engineering: Innovations for the 21st Century, Printed in USA and Canada, p. 21 (2009)
[6] House of Commons Public Accounts Committee, Defense Information Infrastructure, First Report of Session 2008-09 (December 15, 2008)

[7] The Data Archiving and Access Requirements Working Group (DAARWG), Global Earth Observation Integrated Data Environment (GEO-IDE) Architecture Team Proposal (January 31, 2008)
[8] Perry, W., et al.: Exploring Information Superiority: A Methodology for measuring the Quality of Information and Its Impact on Shared Awareness (2003)
[9] Levine, L.F.: Model and Data Interchange at Object Management Group (OMG) (June 29, 2010)
[10] Department of Defense, Capstone Concept for Joint Operations Version 3.0 (January 15, 2009)
[11] Sommervile, I.: Software Engineering, 7th edn. China Machine Press (2004)
[12] Wennergren, D.M.: The Department of Defense Architecture Framework (DoDAF) Version 2.0. (May 28, 2009)
[13] Barnett, J.A., et al.: Network & Information Integration. In: DoD Spectrum Symposium (2009)
[14] Deputy Secretary of Defense, Implementation of the Department of Defense Information Sharing Strategy (August 29, 2007)
[15] Grimes, J.G.: Department of Defense. Information Sharing Strategy (May 04, 2007)
[16] Morris, E., et al.: System of Systems Interoperability (SOSI): Final Report (April 2004)
[17] Freeman, G.R.: Integrating Humans into Systems and Systems of Systems—A New Approach (August 2008)
[18] Morel, G., et al.: System of Enterprise—Systems Integration Issues: An Engineering Perspective (2007)
[19] Clark, J.O., et al.: System of Systems Engineering and Family of Systems Engineering, From a Standards, V-Model, and Dual-V-Model Perspective (2009)
[20] Lane, J.A., et al.: Accelerating System of Systems Engineering Understanding and Optimization through Lean Enterprise Principles (July 27, 2010)
[21] Dahmann, J., et al.: System Engineering for Systems of Systems Experience, Issues and Next Steps (May 3, 2006)
[22] KM Center, WEB services and grid convergence is the future trend. SAN (April 05, 2006)
[23] CVSIN Guide to Top-Level Design, http://cvisn.fmcsa.dot.gov/downdocs/guide
[24] Developing Applications for HUE (EB/OL) (September 27, 2010)
[25] KM Center, WEB services and grid convergence is the future trend, SAN (April 05, 2006)
[26] Commander in chief, U.S. Joint Forces Command, Global Information Grid, JROCM, P2-2 (August 30, 2001)
[27] http://baike.baidu.com/view/169819.html
[28] A Comparism of the top four enterprise architecture methodologies, http://msdn.microsoft.com/en-us/library/bb466232.aspx
[29] Department of Defense Architecture Framework, http://en.wikipedia.org/wiki/Department_of_Defense_Architecture_Framework
[30] Department of Defense Architecture Framework 2.0, http://cio-nii.defense.gov/sites/dodaf20
[31] Hadooop Cluster Setup (September 26, 2010)
[32] Hu, X.: The wonderful picture of grid era. China Distance Education Information (5) (2005)
[33] Developing Applications for HUE (EB/OL) (September 27, 2010)
[34] KM Center, WEB services and grid convergence is the future trend, SAN (April 05, 2006)

Design of Control System for Hydraulic Lifting Platform with Jack-Up Wind-Power Installation Vessel

Xuejin Yang, Dingfang Chen, Mingwang Dong, and Taotao Li

Research Institute of Intelligent Manufacture & Control,
Wuhan University of Technology, Hubei, China
{yangxuejin.2007,taotaoliwhut}@163.com, cadcs@126.com

Abstract. Jack-up wind-power installation vessel is the most important tool in construction of wind farm. And the control system for hydraulic lifting platform is the key point of jack-up wind-power installation vessel. Therefore the design of the control system for hydraulic lifting platform with jack-up wind-power installation vessel is a basic and formidable problem. This article provides an integrated solution to the design of control system. Firstly, on the base of actual working condition, we introduce the control principle and basic requirements of the hydraulic lifting platform, such as the structure of leg, vessel gradient, alarm, calibration. Secondly we introduce the design solution of PLC (Programmable Logic Controller) control system, which includes the design solution of hardware as well as software for the hydraulic control system. In this part, we introduce the basic components and main function of hydraulic control system, hardware scheme, software design project. Then we introduce a good human-machine interface. Finally we do the work of program design according to the process of lifting unit. By using wincc-flexible and PLCSIM, we can layout the control module well and realize the man-machine interaction. At last, we can obtain a viable hydraulic control system and verify feasibility of the hydraulic control system by simulation software. At the same time, we obtain the working parameters of the lifting unit from the simulation.

Keywords: hydraulic control, Programmable Logic Controller, wind-power, hydraulic lifting platform.

1 Introduction

As renewable energy, wind energy is attracting more and more attention. With the development of science and technology, increasing wind farms are under building. As the main component of wind farm, offshore turbine is very huge and hard to be installed. So we should use an important tool-- jack-up wind-power installation vessel to finish the installation. As an important component of jack-up wind-power installation vessel, the control system of hydraulic lifting platform is a guarantee for the normal work of it. For the vessel is very huge, we must guarantee the precision and stability of hydraulic lifting platform. PLC control system is widely used because of its high precision and good stability. So in this article, we design a PLC control system of hydraulic lifting platform based on modular design.

Q. Zu, B. Hu, and A. Elçi (Eds.): ICPCA-SWS 2012, LNCS 7719, pp. 711–718, 2013.

2 The Control Principle of Hydraulic Lifting Platform

The Jack-up wind-power installation vessel includes four legs, and each leg contains two groups of hydraulic cylinders. The first group of hydraulic cylinders is known as the secondary cylinders, another group is called the primary cylinders. Three-dimensional model of lifting unit for the Jack-up wind-power installation vessel is shown in Figure 1.

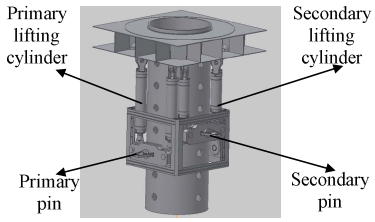

Fig. 1. Lifting unit of one leg

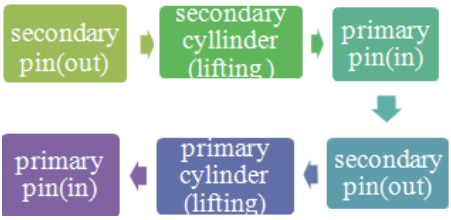

Fig. 2. Process of one stroke for the lifting unit

Figure 2 shows the process of one stroke: secondary pin is pulled out, then the secondary cylinders rise up; then secondary pin is pulled back and primary pin is pulled out, finally primary cylinders rise up, then primary pin is pulled back. And the lifting process of hydraulic lifting platform can be divided into four parts: leg lifting, leg lowering, platform lifting, platform lowering. In this article, we only introduce the process of leg lowering.

3 The Design Process of Hydraulic Lifting Platform

3.1 The Basic Requirements and Components of the Hydraulic Control System

Based on the actual working condition, the hydraulic control system must meet the following requirements:

(1) Function of vessel gradient display and its alarm.
(2) Function of status display for lifting device and its alarm.
(3) Function of display for hydraulic system parameters in real time and its alarm.

In Figure 3, the hydraulic control system includes central console and local control center. The central console can realize the function of overall control for the system. Local control center can communicate with the central console, which is equipped with a local control cabinet. In the condition of leg's individual operation, the local control center works by the central/local switch.

The layout of hardware for the PLC control system includes three parts: central console, local console, and actuator. And each part also contains many elements.

Central console: it includes IPC (industrial personal computer) and main PLC.IPC is used for controlling the whole action of the hydraulic lifting platform. At the same time, it is connected with the main PLC by MPI communication.

Local console: local console is laid near the leg, whose main function is to control the lifting of leg separately. Here we choose the distributed I/O site-ET200M, which is used in the condition that the number of the remote site's I/O points is huge. Meanwhile, we should provide the power for ET200M.

Actuator: this part includes motor, hydraulic pump, solenoid valve, and sensor. Some are used to provide status information, and some are used to realize the action or provide the power.

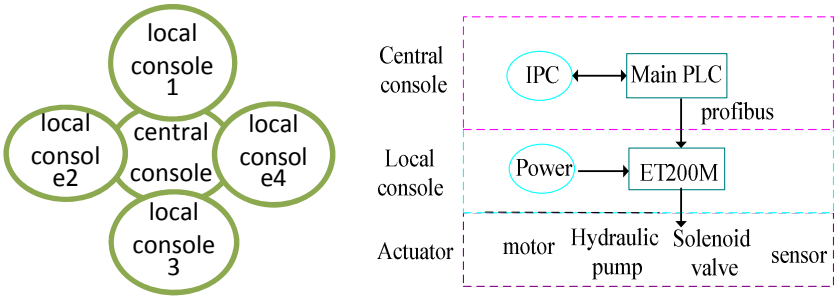

Fig. 3. Layout of hardware for the PLC control

3.2 Structure Design of Software

Through the design of the software program, the hydraulic control system can complete the intended action with the input signal. We use the thought of modular design. And the master control program can be divided into four modules, as in Figure 4.

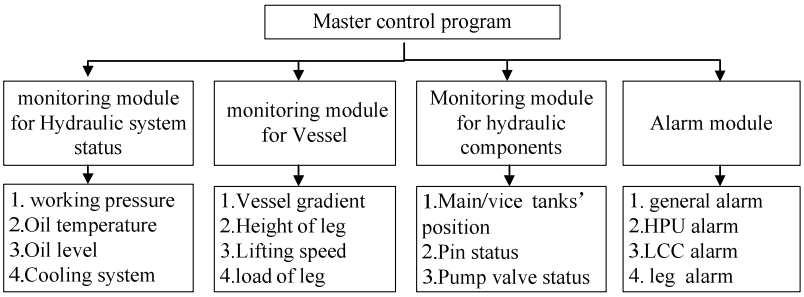

Fig. 4. Design of software for hydraulic control system

The monitoring module for hydraulic system status: its main function is to monitor the working status of the hydraulic system in real time, including hydraulic system pressure, oil level, oil temperature and oil cooling system. Pressure screen displays the pressure values of hydraulic cylinders. And oil level is divided into three levels:

high, low, the lower. Oil temperature is shown directly on the screen in numerical form. The status of the cooling system is also displayed on the screen.

The monitoring module for vessel: this module's main function is to monitor the working status of vessel's components in real time, including legs' height, legs' load, lifting speed of hydraulic cylinders and vessel's gradient.

The Monitoring module for hydraulic components: this module includes the location of lifting cylinder, pin's status and pump's valve. The screen shows the outstretched distance of 32 lifting cylinders, 8 secondary pin cylinders and 8 primary pin cylinders. Meanwhile, the screen displays the pump's valves.

Alarm module: it includes main general alarm, HPU alarm, LCC alarm, legs' alarm.

3.3 Program Design

For leg lowering, the whole working process can be divided into 6 phases in figure 5.

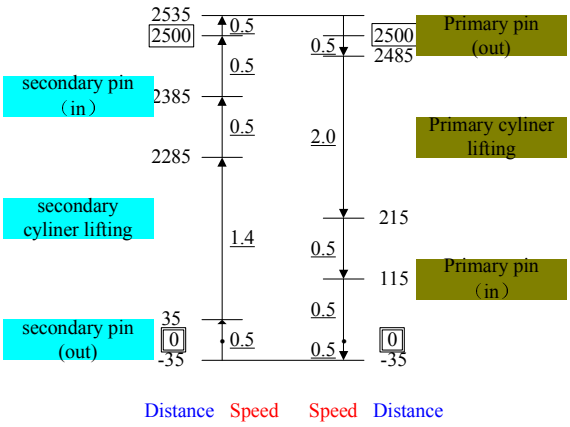

Fig. 5. Working process of leg lowering

(1) Secondary pin pulling out

In this phase, secondary cylinder lifts at a speed of 0.5m/min. at the same time, secondary pin is pulled out, and travel switch will limit the maximum distance of the secondary pin.

(2) Secondary cylinder lifting

Here secondary cylinder lifts at a speed of 1.4m/min. when the distance of the cylinder reach the number of 2285mm, the sensor sends a signal and the speed decreases.

(3) Secondary pin putting in

When the speed of secondary cylinder becomes 0.5m/min, secondary pin is put in. after engaging, the sensor sends the signal, and next phase starts.

(4) Primary pin pulling out

In this phase, primary cylinder lifts at a speed of 0.5m/min. at the same time, primary pin is pulled out, and travel switch will limit the maximum distance of the secondary pin.

(5) Primary cylinder lifting

Primary cylinder lifts at a speed of 2.0m/min. when the distance of the cylinder reaches 2485mm, the sensor sends a signal and the speed decreases.

(6) Primary pin putting in

When the speed of primary cylinder becomes 0.5m/min, primary pin is putted in. After engaging, the sensor sends the signal. A stroke ends.

3.4 Synchronization Control of Cylinder

As the platform is sensitive to the gradient, we must guarantee the synchronization of cylinder. Using the height difference as the feedback control signal, we can control the height difference by adjusting the rotational speed of motor. And through this method, we can realize the synchronization of cylinder. The control algorithm is showed as follow.

When the cylinder lifts, we choose "-". If the cylinder lowers, we choose "+".

$$v = \left(1 \mp \frac{h}{a}\right) v_0 \quad h < b \tag{1}$$

$$v = \left(1 \mp \frac{c \times \sqrt{|h|}}{a}\right) v_0 \quad h \geq b, c = \frac{h}{|h|} \tag{2}$$

h—height difference
a—control factor
b—control inflexion
v_0—set speed
v—actual speed of cylinder

On the other hand, the flow rate of cylinder is related to the speed. And the formula is show as follow.

$$Q = \frac{A \cdot v}{\eta_v} = \frac{\pi}{4\eta_v}(D^2 - d^2) \times v \times 10^3 \tag{3}$$

Q—flow rate of cylinder
A—the effective action area of cylinder
η_v— volumetric efficiency of hydraulic cylinder,
v—lifting speed of cylinder
d—diameter of rod chamber
D—diameter of non-rod chamber

3.5 Design for HMI

When the hydraulic lifting platform works, we should keep watching the working status of the vessel. And HMI (human-machine interface) can provide us the convenience. So the design of HMI is an essential aspect for hydraulic control system.

HMI can be divided into two parts: central console interface and local console interface.

(1) The design of the central console interface

The central console interface is divided into four sections: basic startup information block, HPU control block, pin control block, display screen.

Basic startup information block includes switches (CCD switch, central/local switch, and manual/semi B automatic switch) and buttons (leg lifting, platform lifting, support model, pre-loaded, half-brake, speed change and fixed detachment). According to different needs, we can make appropriate choice.

HPU control block is used for HPU's control, including start and stop of HPU, status display of LCC, emergency stop.

Pin control block is used for the control of leg's pins, including status display of pin system, reset, and testing.

(2) The design of the local console interface

Local operation is adopted especially in the process of legs' lifting. Local console interface includes two parts: pressure display and buttons (local/central switch, leg lifting, platform lifting, pre-loading, fixing, local control and alarm).

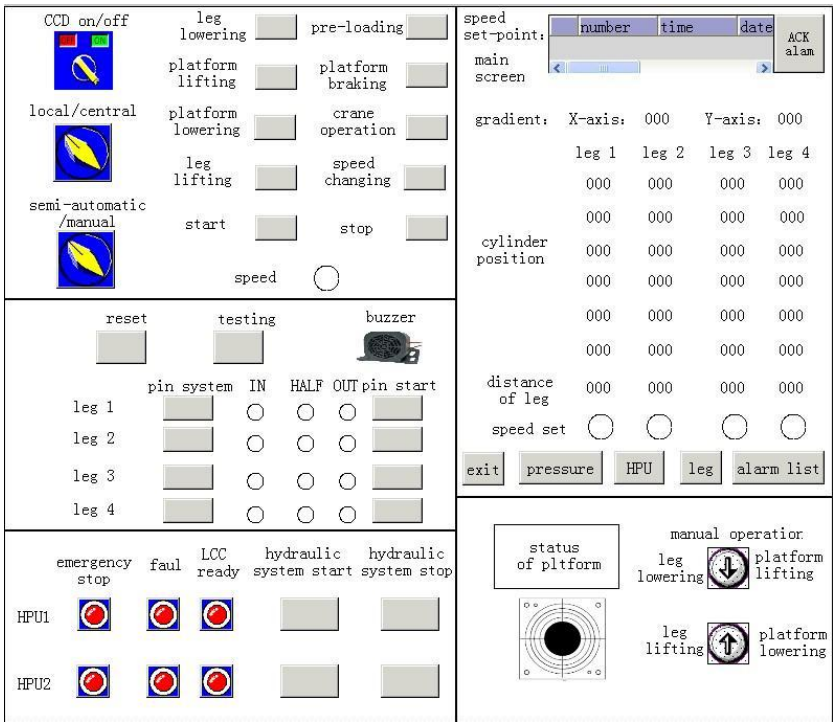

Fig. 6. Central control interface

4 Simulation

When we complete the above design work, we will obtain a whole PLC control system of hydraulic lifting platform with jack-up wind-power installation vessel. Due to the limitation of actual condition, we have to use the software to verify our design. In this article, we choose the PLCSIM and wincc-flexible.

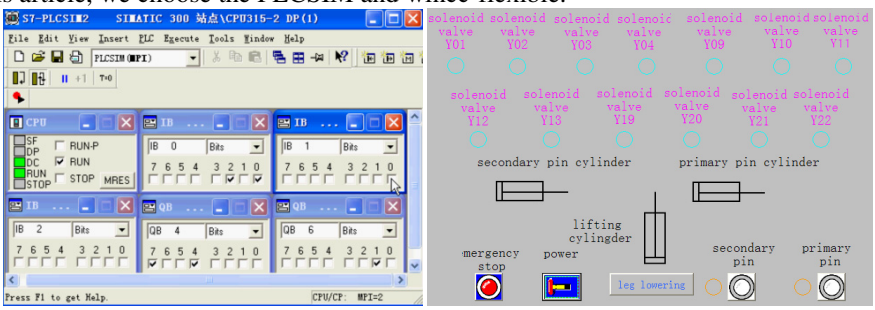

Fig. 7. Interface of simulation

In figure 6, we verify the correctness of the program. At the same time we know the working status from the interface. We also can realize the switch of different working module.

We can obtain the actual numerical valves of working pressure, and speed from the control system. And the actual valves are shown in table 1.

Table 1. Actual working status of leg lifting

action	working pressure of system (Mpa)	Flow rate of the main line (L/min)	Speed of cylinder(m/min)
Secondary pin out	5.75	328.74	0.5
Secondary cylinder lifting	5.75	647.76 328.74	1.4 0.5
Secondary pin engaging	5.75	328.74	0.5
Primary pin out	0.65	328.74	0.5
Primary cylinder lifting	0.65	1004.84 251.2	2.0 0.5
Primary pin engaging	0.65	251.2	0.5

5 Conclusion

Based on the actual analysis of working condition for hydraulic lifting platform, we obtain the control principle of the hydraulic lifting system and the structure of lifting unit. At the same time, we complete the design of control system for hydraulic lifting platform according to the actual requirements, including the design of hardware and

software for PLC control system, the design of good human-machine interface by using wincc- flexible. By and large, this article completes the design of control system of hydraulic lifting platform with jack-up wind-power installation vessel. Meanwhile it can do well for the development of wind farm.

Acknowledgment. This research was supported by "the Fundamental Research Funds for the Central Universities".

References

1. Zhan, Y., Zhang, X.: PLC Control of Pin Climbing-rod Hydraulic Self-lift Ocean Oil Boring Platform. Machine Tool & Hydraulics (2000)
2. Zhao, Y.-N., Hao, J.: Current Situation and Development Trend of the Legs of the Self-elevating Offshore Wind Power Installation Vessels. Marine Engineering (2010)
3. Li, W.-H., Zhang, Y.-D.: Analysis of the Hydraulic Elevating Systems of the Self-elevating Offshore Platform. Chinese Hydraulics & Pneumatics (2006)
4. Liu, H., He, W.: PLC Programming and application of Siemens S7-300/400. China Machine Press, Beijing (2011)
5. Che, C.: The Hydraulic and Control System's Design of The Bolt Climb Rod Wind Power Installation Vessel's Lifting Devices. Wuhan University of Technology, Wuhan (2012)
6. Zhou, K., Chen, B., Feng, Y.: Hydraulic Synchronous Lift System. Machine Tool & Hydraulics (2007)

Research on Motion Control Technology for Virtual Assembly Platform

Yanfang Yang[1], Wengeng Guo[1], Jia Li[2], and Dingfang Chen[1]

[1] Research Institute of Intelligent Manufacture & Control Wuhan University of Technology, Hubei Wuhan 430063
[2] Navy Submarine Academy, Shandong Qingdao 266042

Abstract. This article mainly focused on interactive virtual assembly platform with interactive technology and motion control technology. Basing on the physical properties of the object, the authors put forward a method that combines dynamics and particle spring principle to realize the interactive motion control of flexible object on the virtual assembly platform. It adopts the node matrix operation method to realize the real-time assembly and disassembly. A 3D graphics engine tool Open Scene Graph (OSG) is used to complete the development of interactive virtual assembly and virtual disassembly platform of a crane. It realize the select, drag, assembly and disassembly of interactive parts. The physical properties of the object is displayed by physics engine It realizes the motion control of flexible object. The automatic assembly and roam of parts in the scene can be realized by using the function of event callback and update callback.

Keywords: Interactive technology, Particle dynamics, Virtual Assembly Platform, Motion Control, Crane.

1 Introduction

The virtual assembly of mechanical equipment which can simulate the process of 3D virtual assembly parts can be realized according to the shape and precision of parts. And it allows the user to control the process of 3D virtual reality assembly with a interactive method. It is also a process which repositions, determines the process of assembling parts whether is a process of optimal assembly or not, disassembly and reconstruct according to the constraint relationship of model to test the assembling products at the same time. This definition is based on the simulated process of physical assembling products. It also can verify assembling design and operation whether they are correct or not to find problem in the assembly early at the same time, realize the parametric modification of model and display assembly process. The virtual assembling simulation can produce the most suitable process for assembly parts; reduce the time of physical prototype design process which is expensive and time-consuming.

Q. Zu, B. Hu, and A. Elçi (Eds.): ICPCA-SWS 2012, LNCS 7719, pp. 719–727, 2013.

At present, the CAD system provides the function of virtual assembly. However, the CAD system uses interface of 2D, such as the keyboard and mouse, allows the user to choose matching surface, the axis, boundary to assembly these components according to the constraint information (relationship) manually. Therefore, these interfaces cannot reflect the complex parts of human-computer interaction. So it will be difficult to foresee the problem appeared in the process of assembly. For example, the feasibility of replacement part in the process of maintenance and the effect of change assembling sequence are ensured. This computer system lacks the ability of solve problems which is relevant to ergonomics, such as, it is difficult to achieve the operation process of human-machine.

This article mainly focused on platform of interactive virtual assembly with interactive technology and motion control technology. Setting simulated platform of virtual assembly up for a crane by using a 3D graphics engine of OSG and the software of Visual Basic to realize the typical simulation of interactive virtual assembly and disassembly.

2 The General Idea of Platform of Interactive Virtual Assembly

The platform of interactive virtual assembly mainly realizes interactive assembly and disassembly of parts, according to (the function which the platform of assembly must realize) the needs which realizes the platform's function. It is divided into the following four modules.

(1) Interactive module: mainly realizes the operation of interactive platform, such as: selection, towing, scaling, rotating, switching angle.

(2) Module of parts management: mainly realizes the parts management of layering and classification;

(3) Module of motion control: mainly realizes the motion control of rigid body and flexible object, considering the different physical properties of parts in order to realize the movement of objects with different control;

(4) Module of conflicting detection: avoids the interference and collision happened between parts and institutions, makes the simulated process more authentic.

3 The Motion Control of Object

In the constructive process of virtual assembly platform, the movement of object is mainly the movement of rigid parts and flexible objects, the movement of rigid parts can be controlled by the program, this paper adopts the method of physics engine to deal with the motion control of flexible object (for example: the lifting rope of crane). The physics engine mainly adopts the method of particle dynamics model not considering rotation of rigid body, not setting joint types, using method of particle spring to realize the motion control of wire rope.

3.1 The Motion Control of Flexible Object

3.1.1 The Principle of Particle Dynamics

Particle has a certain quality but no size. In a three-dimensional space, it can only be translated without rotation. Newton's law $F = ma$ will describe the relationship of particle force and acceleration.

In 3D space, the acceleration is described by a three dimensional vector a, the received force described by a three dimensional vector F, the vector form of Newton's law is:

$$F = ma \tag{1}$$

If the displacement of particle is a three dimensional vector x, it will have motion differential equations:

$$\begin{aligned} \frac{dx}{dt} &= v \\ \frac{dv}{dt} &= a = F / m \end{aligned} \tag{2}$$

In the particle dynamics, it often needs two kinds of force: elastic force and resistance force.

$$f_s(t) = kx(t) \tag{3}$$

$$f_d(t) = hv(t) = h\frac{dx(t)}{dt} \tag{4}$$

K indicates elastic coefficient in the formula 3, it is generally positive. The elastic force and displacement have a direct proportional relationship in the formula 3. In the formula 4, h indicates damping coefficient, it is generally positive. From the formula 4, we can see that the resistances of particles and the speed have a directly proportional relationship.

3.1.2 Method of Mass-Spring

The object is simulated into the system which is consisted of a large number of particles and spring by the method of particle spring [11] and the particle is connected by the spring. The physical model of object can be built by this method. It needs to consider the displacement of particle when the object is conducting defoemate simulation. Discretize the simulation object into particles and connect the particles which spring which comply with linear elastic (" Hooke's law "). As shown in figure 1.

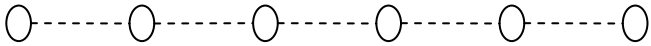

"O" indicates particle , "—"indicates spring which connects particle

Fig. 1. Simplified schematic diagram of spring particle

The particle force is given by:

$$F_i = \sum_j^n g_{ij} - d_i v_i + f_{exti} \tag{5}$$

Where,

v_i represents the velocity of particle;

d_i represents the coefficient of particle;

f_{exti} represents the external force of particle;

g_{ij} The spring stress between particle i and particle j on particle i

In the interactive virtual assembly platform of a crane, in simulation of a wire rope, we use a series of points which is connected with interactional spring. If the number of simulated spring particle is larger, the precision of simulation will be higher. Physical model is showed in figure 2.

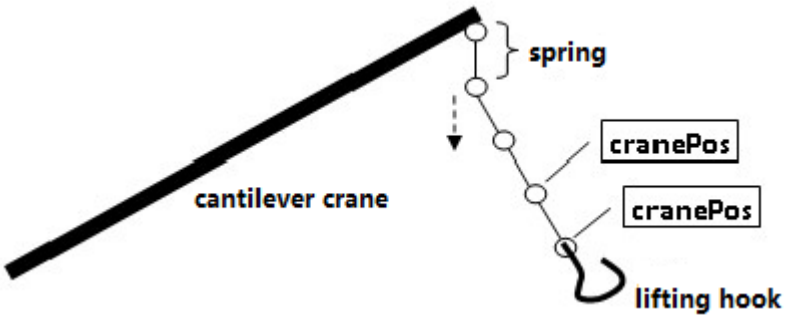

Fig. 2. Physical model diagram of rope

Gravitation and air friction will be joined into the simulation of wire rope. Universal gravitation and air friction will be focused on each particle. In our model, it also needs to consider the friction between the rope and ground, the upward force that ground give to the rope.

3.2 Dynamics of Rigid Body

Dynamics of rigid body which is focused on the motion law of rigid body under external force is a branch of general mechanics. The difference between rigid motion and particle motion is that rigid motion has a rotary motion. Rigid motion includes translation and rotation. When the rigid body is translated, the track, speed and acceleration of each particle are the same and rigid motion can be represented by the movement of centroid.

When the force which is focused on the rigid body is not in line with the center of mass, it not only makes centroid accelerate translation, but also produces moment that makes rigid body accelerate rotation. The rotation of the rigid body relates to inertia. Inertia and quality is the basic quantity which is used to describe the inertia of rigid body, quality is used to describe the extent of the acceleration of translation of rigid body and if we want to promote the object of more quality, we need more force apparently. And the moment which makes the rigid body rotates up is measured by the moment of rigid body inertia.

The rotary inertia is used to measure the rotational inertia of shaft and it is defined as sum of products which is quality ($\mathbf{m_i}$) of each particle multiplies the square of the distance ($\mathbf{r_i}$) from the axis, the rotary inertia is given by:

$$I_z = \sum m_i r_i^2 \tag{6}$$

Obviously, if the distance distributed from shaft of particle is larger, the inertial moment of rigid body will be larger. For the rigid body whose distribution of quality is continuous, the type will be changed into the following formula:

$$I_z = \int r^2 dm \tag{7}$$

In the rotation of rigid body, the rotation of fixed axis only has one degree of freedom, so it is simpler; the law of rotation is shown as the following:

$$M = I_z a \tag{8}$$

M represents the sum of moment of rigid body;

I_z represents rotational inertia of fixed axis;

a represents the acceleration of rotation in the type.

It provides the basic equation which solves the problem of rotation around a fixed axis.

4 The Realization of Interactive Technique

A basic characteristics of virtual environment is interactivity with user, therefore, when a user want to model the dynamic behavior of object, he must use the mouse, keyboard and other input devices to interact the object which locates in the virtual environment to increase the presence of virtual environment.

4.1 Interaction of the Flexible Objects

The basic realized process can be divided into three process according to the interactive system of a mass-spring: picking object with mouse, using the spring to link the object which has be picked up and the point which is correspondent to the mouse in the 3D space (this spring is called the mouse spring), using the mouse to control the object which has been looted.

1) Picking object with mouse

This operation is a complex and key step, involves many complex operations, such as change the conversion of screen coordinates into the 3D world coordinates, the comparison of cache data, the feedback of picked results. And the operation can be realized through the corresponding function in the interface of advanced computer graphics software (such as OSG, Direct3D.).

2) The mouse spring

The simplest method which controls the object of virtual environment is that uses the mouse to drag the object directly. However, the fast motion of mouse often leads to the problem of stability of system. This is mainly due to the location of the objects in virtual environment is determined by solving a series of ordinary differential equations, especially for the object which uses the mass-spring system to model. Like the position of particle, the speed of particle must keep the correct number. When we choose the object correctly, and add the appropriate mouse spring, normally, it will not bring problem if we set the stationary length that is added by mouse spring at zero. The distance of mouse moving is the elongation of mouse spring, using this elongation multiplies the elastic coefficient is the force which user aims at the object.

4.2 Realization of Interactive Control

The core of interactive technology is the interactive control of platform and the object in the platform, namely the controlling scene. There is a class of viewer which is the core of the scene class in OSG. There is a method of add Event Handler in the class of viewer and it can be realized increase in an event handler. Because the interface is osg GA: GUI Event Handler, so we can write class A which is derived out from the public, namely: class A: public osgGA: GUI Event Handler. We add all kinds of operations that have been dealt well to the viewer, namely: viewer. Add Event Handler (new A (It has parameter inside)). Through this method, we can realize interaction between different peripherals (mouse, keyboard, etc.) and scene constantly. The process of response of events is showed in figure 3.

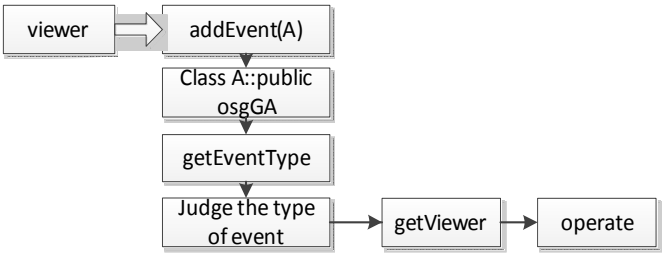

Fig. 3. Flow chart of interactive event processing

According to the interactive process between the mouse picks object up and interactive movement, the towing device is used in OSG. The device of TabBoxDragger(TBD), TabPlaneDragger(TPD), TabBoxTrackballDragger(TBTD), TranslateAxisDragger(TAD) is used commonly. The towing device of TranslateAxisDragger is used in this system. It can be translated at three directions in the XYZ axis. The drag of components will be realized when the apparatus of drag and node of parts is added to the father node. As shown in figure 4.

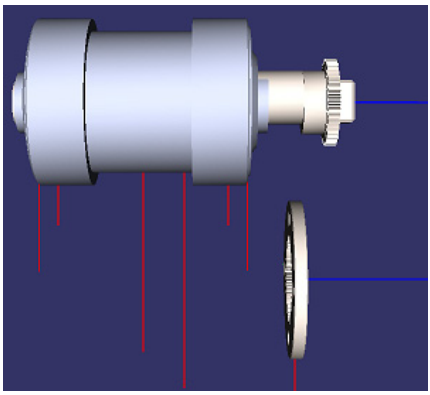

Fig. 4. Realization of interactive dismantling process by the towing device

5 Realization of Interactive Virtual Assembly Platform

The development of ideas of interactive virtual assembly platform is showed in figure 5. The main process is showed as follows:

Constructing a three dimensional model in Solidworks, and save model in WRL format. Importing the model which is saved in WRL format into the software of 3D Max, then the model will be exported in 3ds format, and then take this file into the folders of data which is located in the installation directory of OSG.

We Use official format conversion of OSG and condensed program of osgConv to convert this file into that model which is saved in IVE format. The system deals with the compatible relationship that is based on geometric surface constraint of parts and the operational relationship of artificial input constantly, so as to establish the virtual assembling scene, realizing the visualization of virtual assembly [15,16].

The virtual assembly system realizes the technology of path animation, towing, stereo display and so on. In the virtual assembly platform, planning personnel can choose parts and remove them through 3D operation directly, the system can ensure the effectiveness of disassembling process constantly through the collision detection mechanism automatically, it can simulate the process of disassembly by the guide removal of user to get disassembling sequence of parts and disassembling path, thus determining assembling sequence of products. At the same time, the system displays disassembling sequence of various parts through the playback function of animation. User can observe the movement of the assembling parts from different angle at the same time, as shown in figure 6.

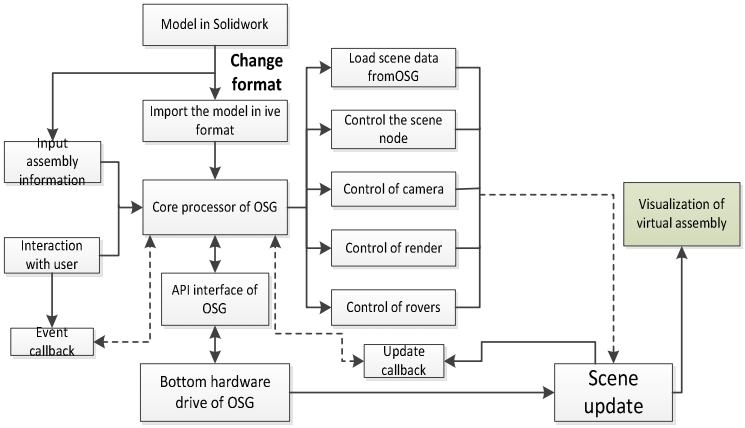

Fig. 5. The development of idea based on virtual scene platform in OSG

Fig. 6. Some operation effect of interactive virtual assembly platform

Acknowledgement. This work is supported by the Fundamental Research Funds for the Central Universities（2011-IV-079).

References

1. Liu, F., Yan, Q., Yao, S.: Research on virtual assembly platform realization technology of vehicle transmission system. In: Applied Mechanics and Materials. Advances in Science and Engineering II, vol. 135-136, pp. 856–861 (2012)
2. Lian, J., Yin, Y., Yang, X., Zhai, X.: Research on the Visual System of Semi-submersible Heavy Lift Vessel Handling Simulator Based on OSG. IEEE (2010) 978-1-4244-5858-5/10
3. Yuan, P., Wang, S., Zhang, J., Liu, H.: Virtual Reality Platform Based on Open Sourced Graphics Toolkit Open Scene Graph. IEEE (2007) 978-1-4244-1579-3/07
4. Meng, X.-K., Hua, Z.X.: Explosive Discharge Visual Simulation and Corresponding key technology based on OSG. Computer Simulation 27(7), 234–238 (2010)
5. Howard, B.M., Vance, J.M.: Desktop haptic virtual assembly using physically based modeling. Virtual Reality 11(4), 207–215 (2007)
6. Wang, X., Wang, H., Wu, D.: Interactive Simulation of Crawler Crane's Lifting Based on OpenGL. In: Proceedings of the ASME 2008 IDETC/CIE, New York, USA, pp. 1533–1540 (2008)

7. Yang, J.-J., Zang, S.-Y., Jiang, M.-F.: Discussion on the Combination of Open Dynamics Engine and Open Scene Graph in Virtual Reality System. Geomatics
8. Cha, J.-H., Lee, K.-Y., Roh, M.-I., Park, K., Phil, S.-H.: Discrete event/discrete time simulation of block erection by a floating crane based on multibody system dynamics. In: Proceedings of the 19th International Offshore and Polar Engineering Conference, pp. 678–685 (2009)
9. Ajmal Deen Ali, M.S., Ramesh Babth, N., Varghese, K.: Collision free path planning of cooperative crane manipulators using genetic algorithm. Journal of Computing in Civil Engineering 19(2), 182–193 (2005)
10. Wang, Q.-H., Li, J.-R.: Interactive visualization of complex dynamic virtual environments for industrial assemblies. Computer in Industry 57, 366–377 (2006)
11. Witkin, A., Baraff, D.: Physically Based Modeling: Principles and Practice. Siggraph 1997 Course Notes (1997)
12. Fu, Y., Wang, Z., Tan, J., Wan, C.: Positioning and driving virtual prototyping with metaphors in dynamic analysis. Simulation Modeling Practice and Theory 14, 527–540 (2006)
13. Yang, Y., Zhu, X., Mei, J., Chen, D.: Design and Real-time Simulation of Rain and Snow based on LOD and Fuzzy Motion. In: Proceeding of the 3rd ICPCA, vol. 10, pp. 510–513 (2008)
14. Wan, D., Xu, L.: Development and Application of Three-dimensional Visualization system for Hydraulic Engineering Based on OSG. Computer & Digital Engineering, 135–138 (2009)
15. Mike, W.: GLSL Shading with OpenSceneGraph (EB/OL), Los Angeles (2005), http://mew.cx/osg_glsl_july2005.pdf
16. Sauer, J., Schömer, E.: A Constraint-Based Approach to Rigid Body Dynamics for Virtual Reality Applications. In: Proceedings of the ACM Symposium on Virtual Reality Software and Technology, pp. 153–162 (1998)
17. Liu, G.-W., Jia, Q.-X., Sun, H.-X.: Model Database Construction for Virtual Assembly System. Journal of Engineering Graphics (1), 48–53 (2010)
18. Li, F., Sun, J., Yang, Q.: Design and Research of Virtual Assembly System Based on OSG. In: 2011 Second International Conference on Digital Manufacturing & Automation (2011)

Efficient Data Collection with Spatial Clustering in Time Constraint WSN Applications

Zhimin Yang[1], Kaijun Ren[2], and Chang Liu[3]

[1] Department of Computer, Shandong University at Weihai, Weihai, 264209, P.R. China
[2] College of Computer, National University of Defense Technology, Changsha, Hunan, 410073, P.R. China
[3] Faculty of Engineering and Information Technology, University of Technology, Sydney, Australia
yangzhimin@sdu.edu.cn, renkaijun@nudt.edu.cn, changliu.it@gmail.com

Abstract. With the development of wireless sensor networks, more and more applications require the high data rate and real time decision making based on sensing data. In this paper, to achieve energy efficiency and quick reaction to real time event monitoring, a novel algorithms for collecting WSN data based on clustering is proposed. The algorithm depends on the similarity to cluster sensor nodes. In every cluster, only one representative node needs to report its data. Hence, the time slots of other nodes can be saved. When there is an event monitoring query offered by users, the query evaluation can return a query answer as soon as possible. Significant reaction time then can be saved. Furthermore, with the reduced reaction time, less sensor nodes are involved in the data communication, the energy efficiency can also be achieved in terms of transmission because of longer sleeping time can be guaranteed.

Keywords: wireless sensor networks, clustering algorithm, event monitoring, real time applications, query evaluation, reaction time, energy efficiency.

1 Introduction

In event monitoring wireless sensor networks (WSN), reaction time or query evaluation speed has a vital influence to the application success. Most of the previous WSN data processing techniques and protocols aims to save the data transmission size and energy cost. Energy and time efficiency are the requirement from real applications. Because most of real world sensor networks are inaccessible after their first deployment, energy saving and prove to be critical to WSN working life time [4, 22]. In order to achieve energy efficiency, hence the in WSN, data transmission reduction techniques have been developed at different layers of WSN, such as radio signal, links quality, MAC, network routing and application requirement [3, 11-12, 23]. At application and network layers, to efficiently process data sampled by sensor nodes, different techniques can be found in literature, including sensing data

Q. Zu, B. Hu, and A. Elçi (Eds.): ICPCA-SWS 2012, LNCS 7719, pp. 728–742, 2013.

compression, sensor nodes clustering, WSN query optimizations efficient data routing topology, temporal/spatial data prediction. Those techniques for efficient data processing can be classified into two types. (1) At data sampling stage, techniques are developed to compress the data collected by each node. (2) At data reporting stage, techniques are developed to carry out in-network data reusing, approximation, sharing, predicting etc. To offer an efficient data aggregation framework, the data reduction techniques at the above two stages should be both considered.

1.1 Motivation

Under the theme of energy efficiency and real time performance of WSN data collecting, the spatial clustering can be used to save the energy. How to effectively use them for energy savings is our main research interest in this paper.

To effectively and accurately carry out the data aggregation over WSN and reduce the time for collecting sensor data, some clustering based algorithms are proposed. The clustering algorithms based on connections between time series are developed to save the data transmission energy [1-2]. However, for most of current clustering algorithms, the distribution of data sets has decisive influence to the performance of data reduction and energy saving. Specifically, for a given clustering algorithm, it can achieve significant transmission reduction over certain data distributions, but less transmission reduction over others. So, as the first important motivation of this paper, we aim to design and implement a sensor clustering algorithm to only work on effective data segments with specific distribution features. In other words, with the knowledge of sensing data set distribution, we can deploy the proposed clustering algorithm to the most suitable segments to achieve effective transmission reduction. It will not be deployed over data segments where trivial transmission reduction can be yielded. Because frequent re-clustering will bring energy cost, avoiding unnecessary re-clustering over unsuitable data segments can save more cost. However, other technique should be deployed over the data segments which our proposed clustering algorithm has less effect on. Furthermore, the time duration for collecting data can be too long. It has big influence to the performance of WSN. The shorter data collection time normally indicates better performance in event detecting application. So, reaction time saving is anther important research aspect. The above problems motivate our second research in this paper.

1.2 Organization of the Paper

Our solutions for the research based on the above research motivation will be introduced and organized in the rest of the paper as follows. In Section 2, we give the analysis and comparison for the current work on clustering based data aggregation and event monitoring applications which require real time data collection. In Section 3, a sensor nodes clustering technique for data transmission reduction is introduced. In Section 4, we introduce how to deploy our clustering strategy based on data changes. In Section 5, a novel WSN data clustering algorithm based on the calculation of similarity is introduced. In Section 6, Experiments are designed and implemented

to verify the algorithms in terms of absolute size of transmitted data in bytes, the time cost for data collection and fidelity loss during data sampling, transmitting process. In section 7, the conclusion is offered.

2 Related Work

In this section, we give a review for current energy-saving and efficient data processing techniques in WSN. Based on the requirement for energy saving and time efficiency, the comparison is carried out between those data processing techniques, such as clustering, aggregation, approximation, data reusing and sharing in WSN.

2.1 Clustering and Data Collection

Currently data clustering and aggregation techniques [1-3, 5-10, 13-16] are prosperous in terms of data reduction and energy saving. Specifically, the work of CAG [1] presented an updated CAG algorithm that forms clusters of nodes sensing similar values within a given threshold (spatial correlations). The formed clusters remain unchanged as long as the sensor values stay within the given threshold (temporal correlations) over time. With the clustering technique, every time, there is only one sensor data being transmitted; whereas the data aggregation algorithm without clustering requires all sensors to transmit. Low Energy Adaptive Clustering Hierarchy ("LEACH") [2] is a TDMA-based MAC protocol which is integrated with clustering and a simple routing protocol in wireless sensor networks (WSN). The goal of LEACH is to provide data aggregation for sensor networks while providing energy efficient communication that does not predictably deplete some nodes more than others. LEACH is a hierarchical protocol in which most nodes transmit to cluster-heads, and the cluster-heads aggregate and compress the data and forward it to the base station. Each node uses a stochastic algorithm at each round to determine whether it will become a cluster-head in this round. Nodes that have been selected as cluster-heads cannot become cluster-heads again for next k rounds in LEACH, where k is the desired percentage of cluster heads. Hence, each node has a 1/ k probability of becoming a cluster-head in each round. At the end of each round, each node that is not a cluster head selects the closest cluster-head to join a cluster. Finally, all nodes that are not cluster-heads only communicate with the cluster head in a TDMA fashion, according to the schedule created by the cluster-head. LEACH offers an approach to automatically select suitable cluster-heads in terms of energy situation and radio coverage. It solves the technical issues such as topology construction and routing table maintenance. Random Walk techniques [6] are proposed for data aggregation. It only needs a connected neighbor to keep moving. There is no critical point. All the nodes are unimportant at all time. It dose not consult all the nodes in a WSN to for queries and reduces the Cover Time from n (whole graph) to log(n) (partial graph). Under the random walk data aggregation technique, only a sub-set of nodes are required to produce the aggregate result as in a cluster, only cluster-head reports its data. Work in [7] studies the problem of aggregating data from a sparse set

of nodes in a wireless sensor network. In sparse aggregation, each node that should participate in the aggregation knows this fact based on its own sensor readings, but there is no overall knowledge in the network of where all these interesting nodes are located. Sparse aggregation shows how the interesting nodes can autonomously detect each other in a distributed way to form an ad-hoc aggregation architecture. Paper [15] proposes a semi-structured approach that benefits from the strengths of the structured and the structure-less approaches. The main challenge in designing such a protocol in this paper is to determine the packet forwarding strategy in absence of a pre-constructed global structure to achieve early aggregation. Paper [23] offers Two-Tier Multiple Query Optimization technique which can also benefit to the data aggregation. Specifically, when there are multiple queries posed to a resource constrained wireless sensor network, it is critical to process them efficiently. In this paper, a Two-Tier Multiple Query Optimization (TTMQO) scheme is proposed. The first tier, called base station optimization, adopts a cost-based approach to rewrite a set of queries into an optimized set that shares the commonality and eliminates the redundancy among the queries in the original set. The optimized queries are then injected into the wireless sensor network. In the second tier, called in-network optimization, the scheme efficiently delivers query results by taking advantage of the broadcast nature of the radio channel and sharing the sensor readings among similar queries over time and space at a finer granularity [23].

2.2 Event Detection Applications

Event detection, as an important real world application of WSN, is based on sensing data collecting and analyzing. It has been discussed from different aspects [17-22].

Paper [17] proposed a light-weight and accurate event detection approach for in-network decentralized event detection. This approach used decision trees for distributed event detection. Furthermore a novel reputation-based voting method for aggregating the detection results of individual sensor nodes and reaching a consensus among different decisions was developed. It shows that despite their simplicity, decision trees are highly accurate. At the same time, their simplicity fulfills the WSN application requirements. The performance of the proposed approach is measured in terms of detection accuracy and time complexity. But, this work has no discussion about the using spatial feature of sensing data to reduce the time for data collection and event detection.

Paper [16] discussed the important applications of wireless sensor networks in event monitoring. Based on the fact that sensor readings do not always represent the true attribute values, some research work suggested threshold-based voting mechanism which involves collecting votes of all neighbors to disambiguate node failures from events, instead of reporting an event directly based on the decision of single sensor node. Although such mechanism significantly reduces false positives, it inevitably introduces false negatives which lead to a detection delay under the scenario of gradual events. With the above technique, a new detection method called the “bit-string match voting” (BMV) was developed in paper [16]. It provides a response time close to that of the direct reporting method and a false positive rate even lower than

that of the threshold-based voting method. Furthermore, BMV is able to avoid repeated and redundant reports of the same event, thus prolongs the life of the network. However, paper [16] neglects the data layer reaction time reduction for data collection and the spatial data correlation which can be used as opportunities for time saving.

3 Clustering with Time Series Difference

In Section 2, some typical data clustering algorithms and techniques have been introduced. In this section, we will introduce a novel regression algorithm based on temporal changes to compute the similarity of time series. Particularly, the analysis for the algorithm efficiency will be offered over different data distribution features.

3.1 Scenario for Sensor Clustering

As shown by the example in Fig.1, there are several time series collected by the real world noisy sensor nodes deployed in a public transportation area. The sound is measured in standard Decibel (dB).

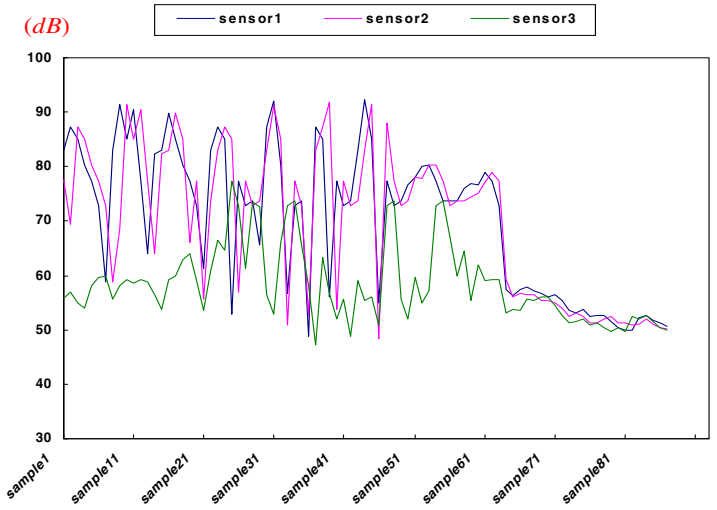

Fig. 1. Clustering Sensors based on Time Series Difference

Specifically, data time series 1 and 2 are quite similar to each other according to the whole sampling period from sample 1 to 90. In other words, time series 1 or 2 can be used to approximately represent each other, which is used by most of current clustering algorithms to reduce the data size. However, they neglected the opportunity that the data collection time can be greatly reduced.

For example, to report the three time series 1, 2 and 3, previous clustering algorithms can divide three time series into 2 time series groups A and B. In group A,

there are time series 1 and 2 from sensor 1 and sensor 2. In group B, there is time series of sensor 3. However, there is one problem in the previous clustering algorithms. The timing of re-clustering for time series is not optimal. Because the re-clustering frequency also waste the precious, for a given data series set, we want to do the minimum re-clustering to capture the maximum time series difference. In Fig. 1, it can be observed that, from sample 65, the data feature of time series 1, 2 and 3 changes. The time series before sample 65 is very bumpy. It means that, the difference between time series 1, 2 and 3 can change quickly. To capture that changing, more clustering operation is required. But after sample 65, time series 1, 2 and 3 become relatively smooth and static. It means that with less re-clustering operation, the partition of time series groups can be done with the satisfaction to accuracy requirement. In order to capture these attributes of three time series and carry out effective clustering, different method can be adopted. For example, if the data window with of each node can be maintained by the cluster-head, we can use normal regression to predict the data trend of each time series. Hence, that data trend can be used as a criterion for sensor nodes partition in each cluster. Furthermore, how to choose an optimal time frequency of re-clustering according to the feed back of analysis of data history raises an interesting research topic. In this paper, we develop a clustering algorithm with improved data aggregation which in stead of carrying out regression over a set of historical data directly, it carries out data aggregation over a consecutively series of weighted data changes. For example, in Fig. 1, to predict the changing trend after sample 65, the prediction regression model will not directly work on the data samples before time stamp 65. In stead, a series of data trends with time stamp from 1 to 64 will be calculated for regression. In addition, with our proposed method, the problem of how to choose an optimal timing for re-clustering will also be discussed. We will give an approach to choose what kind of data distribution is suitable to deploy our proposed clustering. Hence, over the unsuitable data distributions, the clustering can be terminated to avoid the cost of frequent clustering operations.

3.2 Similarity and Error Model Influence to Clustering

Our clustering algorithm based on weighted data changes conducts its decision making for node sets partitioning according to whether two time series being similar enough. So, firstly, it is important to define the similarities of two time series. Popular and direct similarity definition can be based on some average distance of sets of previous data belonging to different time series. To calculate that distance as a similarity and to predicate the future similarity of two time series, temporal prediction models should be developed. Current work can be found for temporal prediction based data regression [9]. However, there is a main disadvantage for this prediction model if applying it for clustering. When two time series have shape similar to "*cos()*" and "*sin()*" functions, though the regression results of two time series can be of high level similarity, the true situation of two time series can be totally different.

To overcome the above in-accuracy brought by normal regression model based on historical temporal data, we develop a novel regression based data prediction model. Suppose that there are two time series, denoted as $X_1\{x_{11}, x_{12}, \ldots, x_{1m}\}$, and $X_2\{x_{21}, x_{22},$

…, x_{2m}}. m is the time tamp for each data collection rounds. We aim to predict the average dissimilarity of data trend for X_1 and X_2 in future m rounds. Based on X and Y, we can calculate a dissimilarity vector $D(d_1, d_2, …, d_m)$, where $d_i=x_i-y_i$. With the data trends vector D, we develop a weighted data regression model to calculate the average dissimilarity of data changes between time series X_1 and time series X_2. The specific regression model is as follows.

$$X=\begin{bmatrix} x_{11} & x_{12} & \dots & \dots & x_{1m} \\ x_{21} & x_{22} & \dots & \dots & x_{2m} \\ x_{31} & x_{32} & \dots & \dots & x_{3m} \\ \vdots & \vdots & \vdots & \vdots & \vdots \\ x_{n1} & x_{n2} & \dots & \dots & x_{nm} \end{bmatrix} \quad (1)$$

X is data a data value set with temporal and spatial formed by n sensor vectors. In the matrix (1), the values collected buy sensor nodes 1 to n during m data collection rounds is described. Then we assign a weight vector for the changing slopes of each X_i, denoted as $W\{w_1, w_2, …, w_{m-1}\}$ which means that according to a specific time stamp, the weight for carrying out regression is different. Then the matrix (1) can be changed to a data changing matrix, X' in (2). With $W \times X'$, we can calculate a weighted data changing value matrix $V= W \times X'$ in (3). The weights vector is generated with the assumption that the importance is of variation of Gaussian distribution with the changing of different stamps.

$$X'=\begin{bmatrix} (x_{12}-x_{11})^2 & (x_{13}-x_{12})^2 & \dots & \dots & (x_{1m}-x_{1(m-1)})^2 \\ (x_{22}-x_{21})^2 & (x_{23}-x_{22})^2 & \dots & \dots & (x_{2m}-x_{2(m-1)})^2 \\ (x_{32}-x_{31})^2 & (x_{33}-x_{32})^2 & \dots & \dots & (x_{3m}-x_{3(m-1)})^2 \\ \vdots & \vdots & \vdots & \vdots & \vdots \\ (x_{n2}-x_{n1})^2 & (x_{n3}-x_{n2})^2 & \dots & \dots & (x_{nm}-x_{n(m-1)})^2 \end{bmatrix} \quad (2)$$

$$V=\begin{bmatrix} X_1' \\ \dots \\ \dots \\ X_n' \end{bmatrix} \times \begin{bmatrix} w_1 \\ \dots \\ \dots \\ w_n \end{bmatrix} \quad (3)$$

In order to calculate the W for a time flow, the probability density function of normal distribution should be configured to describe a time series in which a data with newer time stamp should have higher importance. According to $3\times\sigma$ principle, in Gaussian distribution, we only use the domain between [0, $3\times\sigma$] to calculate the final weight vector W, and it is enough to guarantee that $\sum_{k=1}^{m-1} w_k \approx 1$ because more according more than 97% data will be within this [$-3\times\sigma$, $-3\times\sigma$]. However, the time stamp

for sensing data changes from [0, $+\infty$] which is not between the domain of [$-3\times\sigma$, $-3\times\sigma$]. So in our work, we change the standard normal distribution as follows in (4).

$$\sum_{k=1}^{m-1} w_k = \int_0^{3\sigma} \frac{2}{\sigma\sqrt{2\pi}} e^{(-\frac{(x-\mu)^2}{2\sigma^2})} \tag{4}$$

Because we assume that the starting time for data collection is 0, we can get μ =0. So the summary value of the whole weights domain is calculated with (5)

$$\sum_{k=1}^{m-1} w_k = \int_0^{3\sigma} \frac{2}{\sigma\sqrt{2\pi}} e^{(-\frac{x^2}{2\sigma^2})} \tag{5}$$

As a result, for a data history window with m items or a vector X_i, we can distribute *m-1* consecutive to the domain calculated with formula (5). Specifically, the data range between [0, 3] is divided into *m-1* fragments as 0 to $3\times\sigma/m-1$, $3\times\sigma/m-1$ to $6\times\sigma/m-1$ until to the final fragment, [$(m-2)\times3\times\sigma/m-1$, $6\times\sigma/m-1$]. Then any item w_k in the weight vector W can be calculated as following (6). With the above W, the regression matrix V can be evaluated.

$$w_k = \int_{\frac{(k-1)\times3\sigma}{m-1}}^{\frac{k\times3\sigma}{m-1}} \frac{2}{\sigma\sqrt{2\pi}} e^{(-\frac{x^2}{2\sigma^2})} \tag{6}$$

To compare the similarity of any two time series X_i and X_j based on our data changing regression model, we only need to compute the summary difference of corresponding V_i and V_j. If $|V_i - V_j,|$<Threshold (threshold is a given error bound from application requirement), time series X_i and X_j will be judged as similar enough and allocated into the same cluster.

4 Deploying Clustering by Exploiting Data Changing

In Section 3.2, we introduced our approach for computing the similarity between any two time series X_i an X_j. With that similarity, the clustering process can be carried out. In this section, we will specify what kind of data distribution is suitable our clustering algorithm. As shown in Fig. 2 (a), under a certain data distribution, if the similarity of time series is of high level, with the time stamp changing from T1 to T2, the clustering algorithm does reduce the number of reporting node. Specifically, in Fig. 2 (a), at T1, only 3 nodes are selected as cluster-heads and at T2, only 2 nodes are selected as cluster-heads. However, under some high variation data distribution, the effectiveness of clustering algorithm can be not good. In Fig. 2 (b), at time stamp T1, the data variation is relative steady. However, when it comes to time stamp T2, sensing data set is of high volatile and it makes the clustering algorithm divide more cluster-head.

Under some extreme conditions, it can make all the leaf nodes become cluster-heads as shown in Fig. 2 (b) when time stamp is equal to T1. So under this scenario, when do not want to use the clustering algorithm because the clustering brings no transmission reduction for data gathering, and introduce further energy cost for computing and clustering propagation from cluster-heads to leaf nodes. Hence, we develop a method which exploits the trade-off between cost and gains brought by clustering algorithm to adaptively deploy our clustering algorithm according to underlining data changes. This method is based on the energy consumption model which decomposes and analyzes the energy cost of different activities and operation over wireless sensor network data processing.

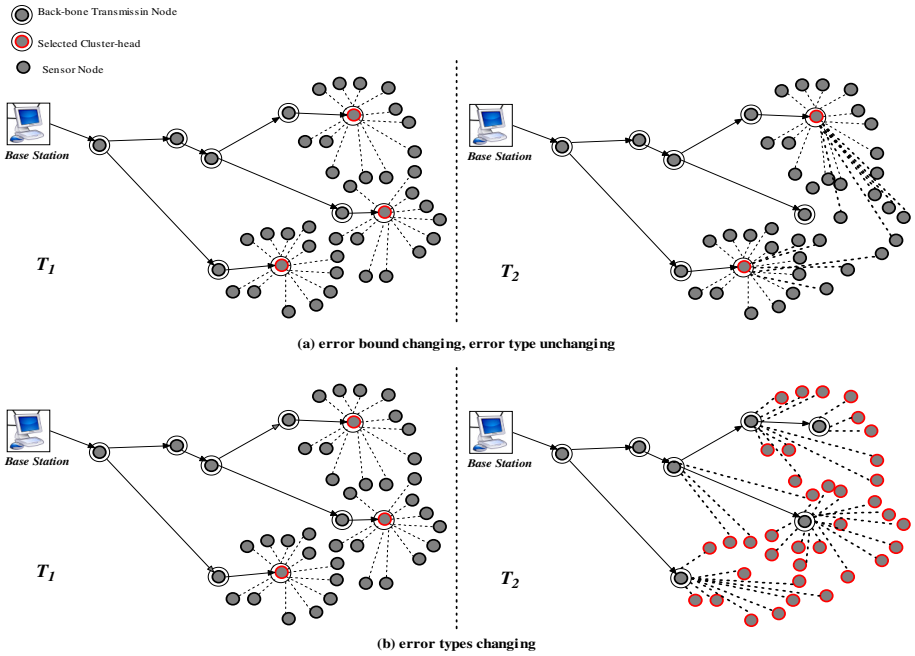

Fig. 2. Influence of Data Changes to a Clustering Algorithm

- Q_s: the size of the new clustering message to be propagated
- T_{node}: the time slot scheduled for each sensor
- E_b: the energy used to broadcast 1 bit of data
- E_r: the energy used to receive 1 bit of data
- P_s: the size of data pacakge
- $h(O, nodeID)$: the jumps from base station to leaf nodes
- E_{instr}: energy cost for executing instructions for clustering
- D: duration
- t: time stamp

In every data gathering round, suppose that there are n different nodes. To clustering them, the energy cost for the clustering is E_{instr}. Suppose that totally the clustering

algorithm selects x cluster-heads and n-x leaf nodes. Then for k rounds of data gathering, the data receiving cost should be $Ps \times k \times t \times (x) \times E_r$. The data sending cost should be $Ps \times k \times t \times (x) \times E_b$. However, the energy for propagating the new clustering should be counted. The cost of receiving and sending are $Qs \times k \times t \times (x) \times E_r$ and $Qs \times k \times t \times (x) \times E_b$ respectively. There also is some cost for clustering algorithm at base station, E_{instr}. If $k \approx n$, it can be observed that no energy will be saved and it also brings new clustering energy cost. At the same time, if there are m nodes selected for report, the reporting time of each data collection round is $T_{node} \times m$. So, $(1-m/n) \times 100\%$ of total reaction time of data collection can be achieved.

5 Clustering Algorithm

The clustering algorithm is on the cluster-head. It takes time series set X and similarity threshold d as inputs. The output is a clustering result which specifying each cluster-head node and its related leaf nodes.

Clustering Algorithm with Data Trend Similarity

Input: a vector set $X = \{x_1, x_2, \ldots x_n\}$, $(v_i = \{v_{i1}, v_{i2}, \ldots, v_{im}\})$,
x_i is a time series of node i,
disimilarity threshold: d, clustering round: k, $i \in [1, n]$, $j \in [1, m]$;
Output: cluster-head nodes set S *and cluster information*;

```
(1)  While (time stamp j<=k)
(2)     if(j%R = = 0 && R ! = 0) // R is for reclustering and not the first round
(3)        Normalize X to V; V=X × W;
(4)     select ∀ unselected v_i from set V;
(5)     initialize a cluster C_i with v_i; record v_i in S;
(6)     While(existing unselected element in S)
(7)        select ∀ unselected x_i from set X; transform x_i to v_i;
(8)        comparesimilarity(v_j, S) ;
(9)        if(complaresimilarity(v_j, S)>d)
(10)          initialize C_j with v_j; record v_j in S_j;
(11)       else
(12)          adding v_i into the C_l with minimum similarity;
(13) if (all nodes have been traversed)
(14)    resturen S;
```

As shown in the clustering algorithm, in Line (1), the data collection time stamp j is counted from 1 to the data collection application duration, k. In line (2), if the j is the time stamp for re-clustering, the clustering process will be executed. In line (3), the algorithm changes the computation of Matrix X to data change matrix V with the technique introduced in Section 3.2. From line (4) to (5), the algorithm selects any vector from V to form the first cluster C_i and node x_i will be used as the cluster-head of C_i. From Line (6), the algorithm will carry out the selection of a new vector until

all the vectors are clustered. Specifically, it selects a vector x_j from X and transforms it into v_j in line (6) to line (7). In line(8), for each newly selected v_j, it will be compare to previous clustered vectors, if the similarity between the is within the given threshold d, v_i and x_i will be added into a previous cluster line (11) to line (12). If the similarity exceeds the given threshold d, a new cluster C_j will be initialized with v_j or x_j as its cluster-head as shown in line (9) to line (10). Finally, it all the nodes have been compared and clustered, the algorithm will return the final clustered nodes set and clustering information S which is a partition plan for X.

6 Empirical Study

To verify the effectiveness of the proposed clustering algorithms for WSN data, experiments are conducted with the real sound and light data sets collected by Mica2 motes. In the experiment, 50 time series are used under a tiered tree network topology. The data sets time duration is 720 minutes with their data gathering interval as 2 seconds (with the increased collection intervals, reaction time becomes more critical). The purpose of the empirical study is to demonstrate both energy saving and time efficiency.

To compare the light and sound raw data and time series, the normalization is conducted first. The normalization is based on the data changing rate of light and sound data. As shown in Fig. 3, it can be observed that the under most of time, the time series of sound data changes much more dramatically than the time series of light data. In this experiment, in each data set (light and sound), around 2.5 MB data is collected and used.

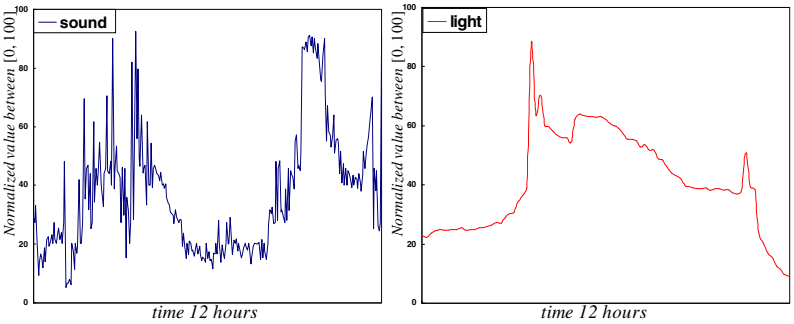

Fig. 3. Plot of Experiment Data Sets

6.1 Energy Cost

Firstly, we test the clustering algorithm over light data set. As shown in Fig. 4 (1), the clustering based algorithm can save more than half of total data size for light data set. At the end of 720 minutes data collection, around 60% of total energy for data transmission can be saved.

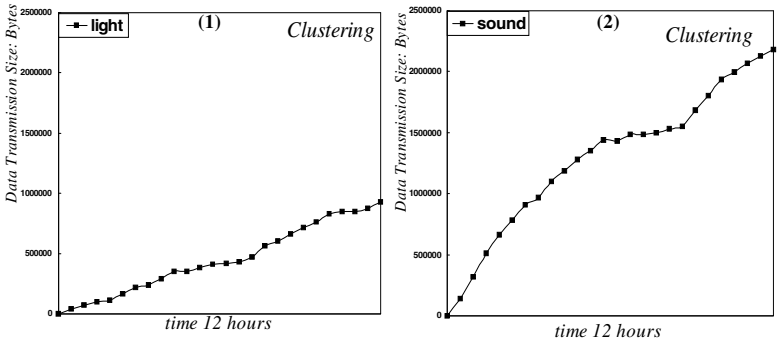

Fig. 4. Energy Cost for Data Collection

Secondly, we test the clustering algorithm and compression algorithm over sound data set. Because the sound data set changes more frequently and dramatically, it can cause the clustering algorithm lose effect in terms of data size reduction as shown in Fig. 4 (2). At the end of 720 minutes data collection, around 20% of total energy for data transmission can be saved through the experiment over the sound data set.

6.2 Data Collection Time Duration

Except for the energy saving, the proposed algorithm can significantly improve the data collection speed for event monitoring applications. As shown in Fig. 5, for the experiment over light sensors, on average, the proposed clustering algorithm can save as much as 70% data collection time. For the sound data, the proposed algorithm can save around 15% data collection time. In other words, for event monitoring application, our developed algorithm can efficiently reduce the waiting time which can be critical.

Finally, we compare the fidelity loss before and after deploying our proposed clustering algorithm. It is clear that to achieve the time saving and energy efficiency, we have to sacrifice the data collection accuracy within an acceptable level. Through the experiments over different data sets, it shows that the fidelity loss is around a small percentage value, which comes to the requirement of most applications.

The light and sound data are all normalized to standard value between 0 and 100. we define fidelity loss as (realvalue-generatedvalue)/100$\times$100%. Then, the average accuracy of data collection fidelity is shown in Fig. 6. Specifically, the average accuracy for our proposed clustering data gathering algorithm is quite close to 100%. Compared to the original data collection which is used as standard data of 100% accuracy, the average fidelity loss of our proposed data gathering approach is around 5%. For the data collection of ordinary WSN applications, it can guarantee the data quality.

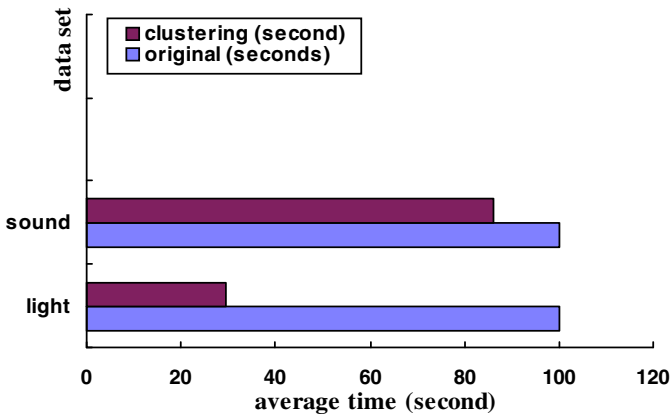

Fig. 5. Data Collection Time Duration

6.3 Fidelity Loss

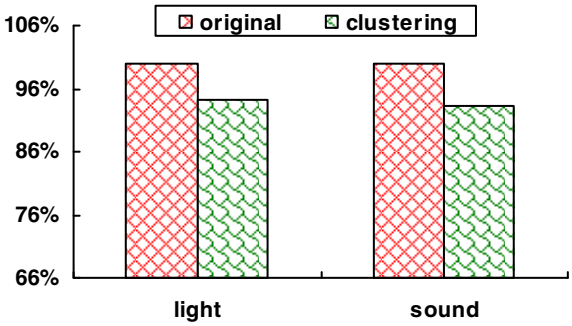

Fig. 6. Fidelity Loss

7 Conclusion

In this paper we introduced an approach with clustering algorithm to effectively reduce the data collection energy and time in WSN. We demonstrated that under different data distributions, the clustering algorithm has different performance gains in terms of transmission reduction and time cost. Through the experiments over real light and sound data collected with Mica2 motes, we demonstrated that (1) Using our proposed clustering algorithm can significantly save the data transmission and improve event monitoring reaction speed which are important performance gains over changing distribution data sets. (2) Our proposed technique limits the average fidelity loss within 5% which is acceptable for most of WSN application requirements. With respect to achieved energy saving, time saving, the trade-off between transmission size and fidelity loss is acceptable for normal WSN applications.

Acknowledgments. The work described in this paper was partially supported by grants from the National Nature Science Foundation of China (Grant No. 60903042, 60736013) and National 863 plans projects, China (Grant No.863-2010AA012404).

References

1. Yoon, S.H., Shahabi, C.: An Experimental Study of the Effectiveness of Clustered Aggregation (CAG) Leveraging Spatial and Temporal Correlations in Wireless Sensor Networks. ACM Transactions on Sensor Networks, 1–36
2. Handy, M.J., Haase, M., Timmermann, D.: An Low Energy Adaptive Clustering Hierarchy with Deterministic Cluster-Head Selection. In: Proc. 4th International Workshop on Mobile and Wireless Communications Network (MWCN), pp. 368–372
3. Gehrke, J., Madden, S.: Querying Processing in Sensor Networks. IEEE Pervasive Computing (March 2004)
4. Sugihara, R., Gupta, R. K.: Programming Models for Sensor Networks: A Survey. ACM Transactions; Franklin, M., Hellerstein, J., Hong, W.: TinyDB: An Acquisitional Query Processing System for Sensor Networks. ACM Transactions on Database Systems (TODS) 30(1), 122–173 (2005)
5. Xiang, S., Lim, H.B., Tan, K., Zhou, Y.: Two-Tier Multiple Query Optimization for Sensor Networks. In: Proc. of 27th International Conference on Distributed Computing Systems, ICDCS 2007 (2007)
6. Chen, Y., Carlos, B.: Efficient and Robust Query Processing in Dynamic Environments Using Random Walk Techniques. In: Proc. of ACM/IEEE International Conference on Information Processing in Sensor Networks (IPSN 2004), pp. 277–286 (April 2004)
7. Gao, J., Guibas, L., Hershberger, J.: Sparse Data Aggregation in Sensor Networks. In: Proc. of the 6th International Conference on Information Processing in Sensor Neworks (ACM IPSN 2007), pp. 430–439 (2007)
8. Benson, J., O'Donovan, T., Raoedig, U., Screenan, C.J.: Opportunistic Aggregate over Duty Cycled Communications in Wireless Sensor Networks. In: Proc. of the 7th International Conference on Information Processing in Sensor Neworks (ACM IPSN 2008), pp. 307–318 (2008)
9. Edara, P., Limaye, A., Ramamritham, K.: Asynchronous In-network Prediction: Efficient Aggregation in Sensor Networks. ACM Transacations on Sensor Network 4(4), article 25 (2008)
10. Liu, M., Cao, J., Zheng, Y., Gong, H., Wang, X.: An Energy-efficient Protocol for Data Gathering and Aggregation in Wireless Sensor Networks. Journal of Supercomputing 43(2), 107–125 (2008)
11. Yang, C., Cardell-Oliver, R.: An Efficient Approach Using Domain Knowledge for Evaluating Aggregate Queries in WSN. In: Proc. of 5th International Conference on Intelligent Sensors, Sensor Networks and Information Processing (ISSNIP 2009), pp. 427–432 (December 2009)
12. Yang, C., Cardell-Oliver, R., Mcdonald, C.: Combining Temporal and Spatial Data Suppression for Accuracy and Efficiency. In: Proc. 7th International Conference on Intelligent Sensors, Sensor Networks and Information Processing (ISSNIP 2011), Adelaide, Australia, pp. 347–352 (December 2011)
13. Yao, Y., Gehrke, J.: Query Processing for Sensor Networks. In: Proc. of Conference on Innovative Data Systems Research, CIDR (January 2003)

14. Romer, K., Renner, B.C.: Aggregating sensor data from overlapping multi-hop network neighborhoods: Push or pull. In: Proc. of 5th International Conference on Networked Sensing Systems, pp. 107–110 (2008)
15. Fan, K., Liu, S., Sinha, P.: Scalable Data Aggregation for Dynamic Events in Sensor Networks. In: Proc. of ACM, SenSys 2006 (November 2006)
16. Watfa, M., Daher, W., Al Azar, H.: EEIA: Energy Efficient Indexed Aggregation in Smart Wireless Sensor Networks. International Journal of Computer Science, 234–245 (2008)
17. Peng, L., Gao, H., Li, J., Shi, S., Li, B.: Reliable and Fast Detection of Gradual Events in Wireless Sensor Networks. In: Li, Y., Huynh, D.T., Das, S.K., Du, D.-Z. (eds.) WASA 2008. LNCS, vol. 5258, pp. 261–273. Springer, Heidelberg (2008)
18. Bahrepour, M., Meratnia, N., Poel, M., Taghikhaki, Z., Havinga, P.: Distributed Event Detection in Wireless Sensor Networks for Disaster Management. In: Proc. IEEE International Conference on Intelligent Networking and Collaborative Systems, pp. 507–512 (2010)
19. Abadi, D.J., Madden, S.: REED on Sensor Networks 4(2) (March 2008)
20. Madden, S.: Robust, Efficient Filtering and Event Detection in Sensor Networks. In: Proc. of 31st International Conference on Very Large Data Bases (VLDB 2005), pp. 769–780 (2005)
21. Xue, W., Luo, Q., Chen, L., Liu, Y.: Contour Map Matching for Event Detection in Sensor Networks. In: Proc. of ACM SIGMOD International Conference on Management of Data (SIGMOD 2006), pp. 145–156 (June 2006)
22. Chong, C.Y., Kumar, S.P.: Sensor networks: evolution, opportunities, and challenges. Proc. of the IEEE 91(8), 1247–1256
23. Xiang, S., Lim, H.B., Tan, K., Zhou, Y.: Two-Tier Multiple Query Optimization for Sensor Networks. In: Proc. of 27th International Conference on Distributed Computing Systems, ICDCS 2007 (2007)

The Effect of Critical Transmission Range in Epidemic Data Propagation for Mobile Ad-hoc Social Network

Hong Yao, Huawei Huang, Qingzhong Liang, Chengyu Hu, and Xuesong Yan

School of Computer, China University of Geosciences, Wuhan, China
yaohong@cug.edu.cn

Abstract. In this paper, we study the information dissemination in mobile ad-hoc network, where mobile nodes are randomly and independently distributed with a given density on a square. Nodes in network move following a random direction mobility (RDM) model. One piece of information is disseminated from source to all other nodes in the network, utilizing the basic epidemic routing protocol. We develop an analytical model based on Ordinary Differential Equation (ODE) approach, in which we take the transmission range as the critical and intuitive system parameter instead of pair-wise meeting rate. Typically, we proceed to study the impacts of overlap among the moving informed nodes on the percolation ratio and the delivery delay. The analytical mode is verified by simulations. This research captures the characteristics of information disseminated in mobile ad-hoc network.

Keywords: mobile ad-hoc network, epidemic routing, overlap, percolation ratio, delivery delay.

1 Introduction

The mobile ad-hoc network (MANET) is a self-organizing network which is composed of several kinds of wireless mobile devices, including smart phones, PADs, laptops, and other personal mobile digital devices. The users of these devices may share content to their interest. Therefore, they tend to form a mobile ad-hoc network in a MANET within a limited area, e.g., in a university campus. In such a mobile ad-hoc network, members move and meet each other. Due to the wireless devices are governed by their human owners, so that, just as humans could only transit infection to others in their vicinities, they could only communicate with other wireless devices when they are in the small transmission range of each other, but not via the assistance of base stations. Consequently, the wireless devices link between two devices is intermittent due to the mobility of the mobile users. Thus there may not be a path between two wireless devices at any time instant usually. Therefore, many ad-hoc data routing algorithms for MANETs have been widely studied [1-4].

In this paper, we are especially interested in the scenario where a message is disseminated from a source node to the whole network. Many practical applications fall into such scenario, e.g., advertisement distributed in a vehicular ad hoc network, message sharing in a pocket switched network in a campus, and information dissemination in a battle field as fast as possible, due to the temporal effectiveness of the information.

Q. Zu, B. Hu, and A. Elçi (Eds.): ICPCA-SWS 2012, LNCS 7719, pp. 743–756, 2013.

Two important metrics to evaluate the system performance are percolation ratio [5] and delivery delay. The former is defined as the ratio of mobile nodes that have successfully received the information at a given time instant and the later as the duration from the generation time of a message at the source until its final reception at a destination. A flooding broadcast algorithm [6] in the wireless mobile network is an alternative common method. However, the message sender may not meet all peers within a short period due to the limitations of his transmission range and his moving area. If other peers broadcast the new message without any control when they just receive it immediately, it may issue the broadcast storm problem [7]. Therefore, we adopt the epidemic routing [8-13] for disseminating information in the view of the similarity between MANET and human network. Epidemic routing has been proved as an efficient way to achieve high percolation ratio and low average delivery delay [9], [13] due to its greedy message forwarding approach. It adopts the so-called "store-carry-forward" paradigm, with which a node stores and carries the received packet and then pass the packet to new nodes that it encounters. The epidemic routing well leverages the nodes' mobility and efficiency of disseminating information in MANETs.

It is believed that the information propagation process is determined by various parameters such as node density, mobility, transmission range, etc [11]. Based on an extensive survey on related work, we notice that most current studies assume that the intermittent connections (i.e., transmission opportunities) can be described by an empirical exponential distribution of pair-wise meeting interval between mobile devices [9-13]. However, this assumption has the following limitations: 1) the pair-wise meeting rate is often unknown priori and its accurate value is hard to obtain, 2) while the meeting rate could be estimated under certain mobility model, the analytical result is applicable only when the transmission range of a node is much smaller than the whole network region (Lemma 4 in [18]), and 3) the analytical results can hardly be utilized by network planners because the pair-wise meeting rate cannot be controlled directly.

This motivates us to investigate the delivery performance of epidemic routing in MANETs as a function of parameter that can be adjusted directly and accurately. One such parameter is the transmission range. An intuitive example is illustrated in Fig. 1, where no transmission is possible when node *a* and node *b* pass by under a setting shown in Fig. 1(a) while a transmission opportunity can be seen in Fig. 1(b).

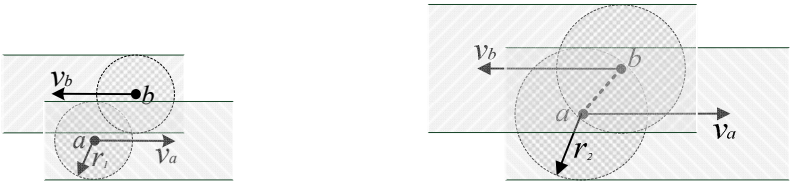

(a) With a smaller transmission (b) With a bigger transmission range

Fig. 1. The effect of the transmission range on the transmission opportunity

Therefore, we apply an ODE based model to investigate the how does this parameter affect the performance: 1) what is the percolation ratio at any time instant? 2) what is the expected delivery delay to a specific destination in the network?

The major contributions of this paper are summarized as follows.

Under RDM [14] mobility model, we develop an analytical method that is the first to deal with the effect of coverage areas of mobile nodes to the delivery performance by taking transmission range as an intuitive and critical system parameter, instead of the pair-wise meeting rate. And typically, we proceed to study the impact of overlap among moving nodes' tracks in our ODE based analytical model.

We organize the rest of the paper into the following sections. In Section 2, we present a brief description of existing related research works. In Section 3, we describe the network model, mobility model and the epidemic routing utilized in this paper. The analytical results are derived in Section 4. Extensive simulation has been performed to validate our analysis is elaborated in Section 5. The conclusion and future work will be given in Section 6.

2 Related Work

Many previous researches have investigated on data dissemination for mobile ad hoc networks. As a result, a handful of data dissemination schemes and theoretical models have been proposed in literatures.

Such as, Wang *et al.* [15] investigate the effect of mobility on the critical transmission range for asymptotic connectivity in *k*-hop clustered wireless ad hoc networks where all nodes move under either the random walk mobility (RWM) model with non-trivial velocity [14] or the i.i.d. mobility model. Similarly, we also study the effects of critical transmission range on the expected fraction of nodes who receive the information at any time instant, and on the delivery delay of a specific destination when it receives the information. One identical point to Wang's work, we either consider the significant impact of the potential coverage overlap of nodes' tracks while they are moving.

Lately, in [16], Keung *et al.* studied an important problem, the Target Tracking in mobile sensor networks. They derived the inherent relationship between the tracking resolution and a set of crucial system parameters including sensor density, sensing range, sensor and target mobility. The sensor range is same meaning with the transmission range in this paper. As we can see, the transmission range of the sensor to the target tracking problem also has a definitive effect in the mobile sensor network.

Recently, Islam *et al.* [17] construct an analytical model based on Markov chain to calculate the expected delay of information diffusion in a mobile network. In their work, they also use the epidemic model of disease spreading to analyze the probabilities of transmitting information from one node to multiple nodes. The epidemic model they use is similar with our work, but the difference is that we utilize ODE approach.

About the ODE approach, Zhang *et al.* [9] develop a rigorous, unified framework based on ODE to study epidemic routing and its numerical variations. In fact, the authors give the closed-form expressions for expected fraction of infected nodes at any time instant and the average delivery delay under epidemic routing as what we study in this paper. Later on, Lin *et al.* [13] either introduce an analytical framework utilizing ODE to study the performance of epidemic routing using network coding in opportunistic networks. However, on the analytical models in [9] and [13], authors simply

import a pair-wise meeting rate [18] to describe the meeting rate between a pair of nodes. But the pair-wise meeting rate is not applicable when the transmission range is large. However, we believe that the meeting rate between an informed node and an uninformed one has the determinative relationship with moving node's transmission range in mobile ad hoc network. Accordingly, we derive the effect of the critical transmission range in mobile wireless ad-hoc network using ODE based approach.

The most related recent work with ours is [11], in which Zhang *et al.* studied the definitive parameters for the information propagation process in a MANET, which include node density, mobility, radio range, etc. They propose a single metric, the *reproductive rate* R_0, to capture the impacts of various parameters. They utilize the radio range to express the definitive metric R_0. However, this R_0 is an upper bound. Further, it is a time-varying parameter. In their analytical tractability, maybe it is not suitable that they use the upper bound all the time to derive their lemmas and theorems. In our theoretical model, we derive our analytical results via utilizing the exact value of the crucial parameter transmission range directly. And the utmost different point to distinguish our analytical model from theirs is that we take the impact of overlap among the moving informed nodes into consideration.

3 System Model

In this section, we introduce the system mode, which consists of network model, mobility model and epidemic routing scheme.

3.1 Network Model

In our analytical model, we consider a mobile wireless ad-hoc network where nodes are randomly and independently distributed on an $L*L$ (width*height) square area following a Poisson point process with density ρ_0, i.e., $\rho_0=N/(L*L)$. Without loss of generality, we assume that all nodes have the same transmission range denoted by r. Then, two nodes can directly connected only if their Euclidean distance is smaller than or equal to the transmission range.

The RDM [6] model is adopted in our paper since it has been widely accepted as a classical and accurate human mobility model [11], [17-19]. In RDM, at the beginning, each node chooses its direction independently and uniformly in $[0, 2\pi)$, and then moves at a constant velocity v common to all nodes. When a node reaches to the border of network topology, it pauses for a little while, then chooses its next direction in $[0, \pi)$ and proceeds to move to the other border of the network topology. The impact on the information dissemination process under other mobility models, e.g. Random Walk Mobility Model, Random Waypoint Mobility Model, Gauss-Markov Mobility Model and City Section Mobility Model, etc shown in [14] is left as our future work.

3.2 Basic Epidemic Routing

We consider a set of N nodes (N-1 uninformed nodes and one source), each with a finite transmission range, moving within a closed square area. Two nodes "meet" when they enter into transmission range of each other, where they can exchange packets. We

focus on a single piece of information's propagation in this paper. Further, we assume that the information can be forwarded within meeting duration. Proceed to describe the basic disease spreading style epidemic routing we use. The source node can be viewed as the first carrier of a new disease, i.e., the first infected node, which infects (copies the packet to) every susceptible node (i.e., node without a copy of the packet) it meets. These new infected nodes become infectious and act in the same way. Once a node is infected, it can't receive the information again. As a result, the population of susceptible nodes decreases over time. The destination node can be selected from all susceptible nodes randomly and independently at the beginning. If an infected node meets the destination, it forwards the packet to the destination. Then it deletes the packet from its buffer, but retains "packet-delivered" information which will prevent it from receiving another copy of this packet in the future. We say that this node is recovered from the disease. Here the recovery process simply relies on meeting with the destination. We will consider more sophisticated recovery schemes in the future work. The percolation ratio will approximate to 1 over time. That is, the destination will definitely receive the information which is from source. Thus, the moment when destination receives the information is delivery delay.

Let $S(t)$ ($s(t)$) and $I(t)$ ($i(t)$) denote the number (fraction) of susceptible and infectious nodes at time t, respectively, where $s(t)=S(t)/N$ and $i(t)=I(t)/N$. We notice that $S(0)=N$-1and $I(0)=1$. Further, there is always $s(t)+i(t) \equiv 1$, $t \geq 0$.

4 Stochastic Analysis on the Information Propagation Process

The information dissemination process in a mobile wireless ad-hoc network is determined by various parameters such as node density, mobility and the critical transmission range. In this section, we introduce our stochastic analytical model utilizing ODE approach. Through the paper we show that ODE is a valid tool for investigating the percolation ratio at any time instant under epidemic style routing, because it allows us to derive closed-form formulas for the percolation ratio and proceed to derive the expected delay for one specific node in the mobile wireless ad-hoc network. Typically, we could further model the effects of coverage overlap among the moving infected nodes' tracks to the percolation ratio and delivery delay.

4.1 Percolation Ratio

Notice that every node can has only one copy of the information, thus the percolation ratio at time t is the fraction of infectious nodes in fact. Hence, the percolation ratio $\phi(t)$ can be expressed as a time-varying function as:

$$\phi(t) = \frac{I(t)}{N} = i(t), \ t \geq 0. \tag{1}$$

Therefore, to obtain the percolation ratio $\phi(t)$, it is required to derive $i(t)$, or equivalently $I(t)$.

Given N nodes roaming in the network, the scanned area of one moving infectious node during *K-time-slot* is shown as Fig. 2.

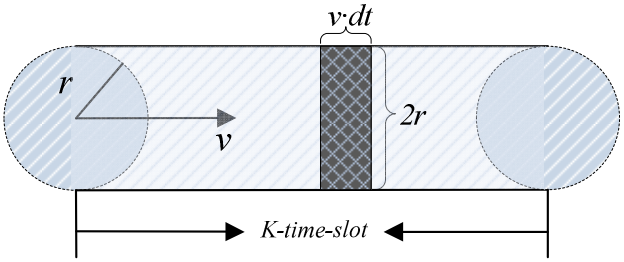

Fig. 2. The scanned area of one moving infectious node

In this way, the size of the area scanned by the transmission range of the infectious node during a tiny period [t, t+dt] is:

$$dS = 2r \cdot v \cdot dt. \tag{2}$$

We call the incremental scanned area dS as "*infectious area*". Accordingly, during this tiny period, the incremental number of infectious nodes is dI, which is the expected number of susceptible nodes those inside all infectious nodes' infectious area. Therefore, the number of infectious nodes, i.e., the I(i), is the solution of the following equation:

$$\frac{dI(t)}{dt} = \frac{\rho_{S(t)} \cdot I(t) \cdot dS}{dt}, \tag{3}$$

where $\rho_{S(t)} = \rho_0 (N\text{-}I(t))/N$, is the susceptible nodes' density at time t in the whole network. With the initial condition $I(0) = 1$, we could solve the ODE and obtain $I(t)$:

$$I(t) = \frac{N}{1 + (N-1) \cdot e^{-2rv\rho_0 t}}. \tag{4}$$

Thereafter, the percolation ratio at time t, can be calculated as:

$$\phi(t) = \frac{I(t)}{N} = \frac{1}{1 + (N-1) \cdot e^{-2rv\rho_0 t}}. \tag{5}$$

4.2 Impact of Overlap

Although we obtain the closed-form solution of percolation ratio at time t, we should not ignore one significant problem, the impact of infectious nodes' tracks overlap while transmission range becomes larger. In fact, this problem will cause quite a large deviation to the $\phi(t)$ and delivery delay, which will be illustrated in Section 5.

Proceed to study how to eliminate the impact of tracks overlap to $\phi(t)$. In the analysis above, during a tiny period [t, t+dt], there may be the same type of infectious

nodes are inside the scanned area of a moving infectious node's track. In that case, the total size of all infectious nodes' scanned area is overestimated. Therefore, we need to minus the size of overlapped area in ODE.

The Overlapped Area between Two Meeting Infectious Nodes. During the tiny period [t, t+dt], the overlapped area between two infectious nodes' incremental infectious area (denoted by S_{IA}) is illustrated as Fig. 3. There are kinds of irregular shapes of the overlapped incremental infectious area. However, they are all in the overlapped area of the two meeting infectious nodes' traveling tracks, which is shown as Fig. 4. Furthermore, the average percentage of the overlapped incremental infectious area takes in the overlapped tracks' area can be calculated.

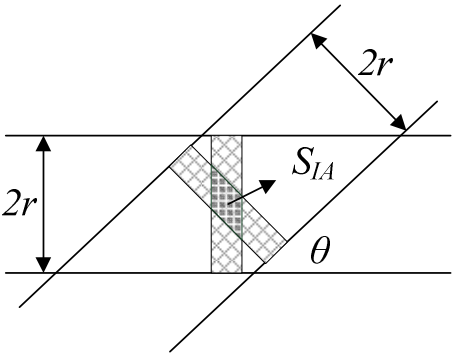

Fig. 3. The overlap of the incremental infectious areas

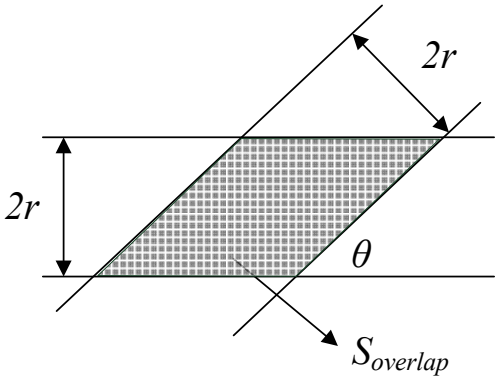

Fig. 4. The overlap of two meeting infectious nodes' tracks

We first to evaluate the average overlapped area of two meeting infectious nodes' tracks, as shown in Fig. 4. Assume two infectious nodes meet each other with an angle between their moving directions θ ($0<\theta\leq\pi/2$). Let S_{AOL} denotes the average

overlapped area of the two meeting infectious nodes' tracks, and considering the symmetry we have:

$$\begin{aligned} S_{AOL} &= \int_{\varepsilon}^{\pi/2} \frac{(2r)^2}{\sin\theta} \cdot \frac{1}{\pi/2-\varepsilon} d\theta, \\ &= \frac{4r^2}{\pi/2-\varepsilon} \cdot \ln(\tan\frac{\theta}{2}) \Big|_{\varepsilon}^{\pi/2}, \ (\varepsilon > 0), \end{aligned} \tag{6}$$

where, the ε is the lower bound of the integration. The value of S_{AOL} will be infinite if ε approaches 0, wherefore we need to find an appropriate value for it. The detail of deriving the value of ε is elaborated at Appendix A.

The Expected Percentage. Let *EP* denotes the expected average percentage of the overlapped incremental infectious area takes in the overlapped tracks' area during a tiny period [*t*, *t*+*dt*]. Due to the intermeeting time between two infectious nodes is uniformly distributed, *EP* equals to the probability of one infectious node is in the incremental infectious area of another infectious node. Then we have:

$$\begin{aligned} EP &= \rho_{I(t)} \cdot I(t) \cdot dS, \\ &= I(t)(2rvdt) \cdot \frac{I(t)}{N} \rho_0, \end{aligned} \tag{7}$$

where the $\rho_{I(t)} = \rho_0 \cdot I(t)/N$, is the infectious nodes' density at time *t*.

Adjust the Percolation Ratio. Then we adjust the percolation ratio with consideration of the total overlapped area. Let S_{OA} denote the sum of total overestimated overlapped infectious area at time *t*, we have:

$$S_{OA} = EP \cdot S_{AOL}. \tag{8}$$

As a result, the increase rate of infectious nodes during the tiny period [*t*, *t*+*dt*] should be rewritten as:

$$\frac{dI(t)}{dt} = \frac{\rho_{S(t)} \cdot [I(t) \cdot dS - S_{OA}]}{dt}. \tag{9}$$

The percolation ratio $\phi(t)$ should be re-calculated relying on the new solution ofEq. (9) correspondingly.

4.3 Delivery Delay

Let T_d denote the information delivery delay, which is the duration from when the information is first generated at the source to the time when it is first received by the

destination. And let $F(t)=\Pr(T_d<t)$ denote Cumulative Distribution Function (CDF) of T_d. To obtain the $F(t)$, we need to get the probability of the destination meets an infectious node in the tiny period $[t, t+dt]$ firstly:

$$\begin{aligned}
&\Pr\{dest \text{ meets an infectious node in } [t, t+dt]\ \} \\
&= \Pr\{dest \text{ is in the infectious area of all } I(t) \text{ moving nodes in } [t, t+dt]\}, \\
&= \frac{\binom{N_s}{1}}{\binom{S(t)}{1}}, \\
&= \frac{N_S}{N-I(t)},
\end{aligned}$$

$N_S=\rho_{S(t)}\cdot I(t)\cdot dS$ means the number of susceptible nodes those are inside the coverage of the moving $I(t)$ infectious nodes during the tiny period. Then we derive $F(t)$, the CDF of T_d. When destination receives the information, there is:

$$\begin{aligned}
&F(t+dt)-F(t) \\
&= \Pr(t <= T_d < t+dt), \\
&= \Pr\{dest \text{ meets an infectious node in } [t, t+dt]\ \}\cdot \Pr\{T_d > t\}, \\
&= \Pr\{dest \text{ is in the coverage of } I(t) \text{ nodes}\}\cdot(1-F(t)), \\
&= [\frac{N_S}{N-I(t)}]\cdot(1-F(t)), \\
&= [2rv\rho_0\frac{I(t)}{N}](1-F(t))dt.
\end{aligned}$$

Correspondingly, the following equation holds for $F(t)$:

$$\frac{dF}{dt} = [2rv\rho_0\frac{I(t)}{N}](1-F(t)). \tag{10}$$

It is worth noting that, the $I(t)$ is the solution of Eq.(9). Solving Eq.(10) with initial condition $F(0) = 0$ yields:

$$F(t) = 1-e^{\frac{-2rv\rho_0 I(t)t}{N}}. \tag{11}$$

Form $F(t)$, the expected delivery delay can be expressed like this:

$$\mathrm{E}[T_d] = \int_0^\infty (1-F(t))dt. \tag{12}$$

5 Simulation Results

We report on simulations to validate the accuracy of the analytical results in this section. The simulations are conducted utilizing a MANET simulator developed in C++. In simulations, nodes are randomly and independently deployed initially on a square area which has a size of 600m*600m. And we control the number of nodes N =200, 500, or 1000, in the network. Hence, different scales of network can be estimated, the density varies correspondingly. After deployment of nodes, they start to move according to RDM mobility model. The velocity is set to be 2m/s (approx. human walking speed) or 10m/s (approx. vehicle's velocity in mobile ad-hoc network). To evaluate the impact of critical parameter transmission range, we set it varying from 1 meter to 5 meters. Note that, the results of nodes moving in 2m/s have the same trend and accuracy as those with a velocity of 10m/s, so that we just show the results with a velocity of 10m/s in the following.

Fig. 5 shows the percolation ratio as a function of transmission range r. The subfigures (a), (b) and (c) estimate the $\phi(t)$ under N=200, 500 and 1000, respectively. It is worth noting that, there are two kinds of analytical results. They are obtained without consideration of the overlap (Ana.w/o.OL) of moving nodes and with considering it (Ana.w.OL), respectively. When transmission range is small, say r=1, these two analytical results are almost same, but when transmission range grows larger, their discrepancy shows up gradually, which can be seen in Fig. 5. And the simulation results have more approximate trends to the analytical results that consider the impact of overlap, which proves that our further analytical model is more accurate than the previous one. The discrepancy between analytical result and simulation result shown in Fig. 5 is caused by the random distribution of nodes at the beginning of simulation. However, the discrepancy can be weaken follows the running of simulation with high probability. And the simulation result fairly matches the analytical result in the end.

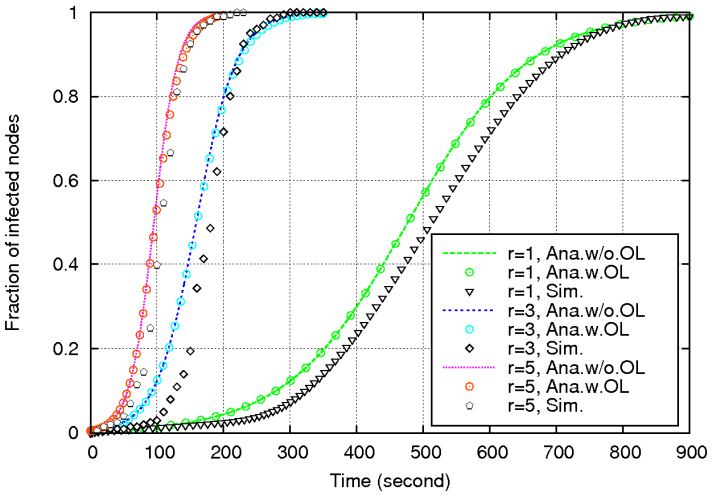

(a) N=200

Fig. 5. The percolation ratio of analysis and simulation

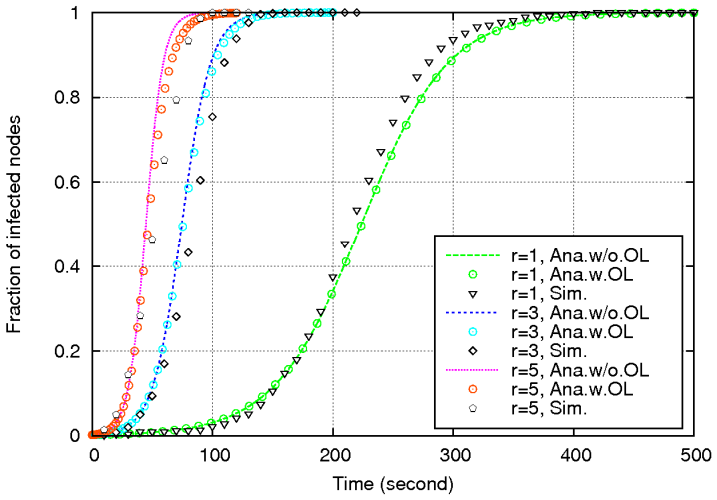

(b) N =500

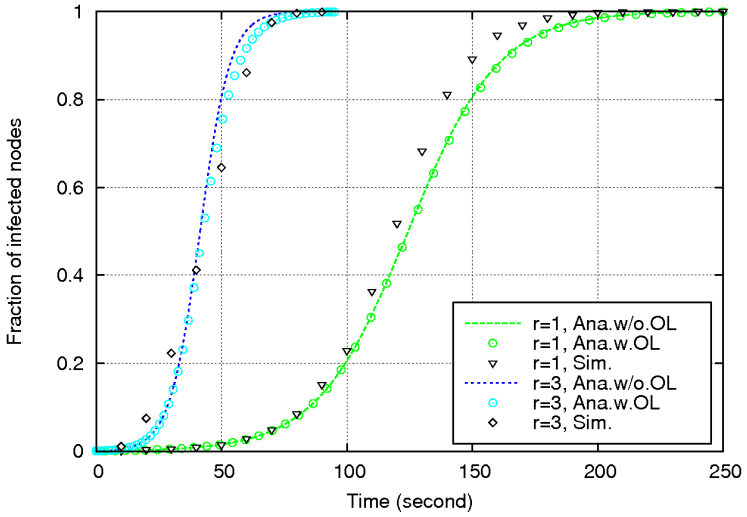

(c) N =1000

Fig. 5. (*Continued.*)

Fig. 6 shows the expected delivery delay under various scales of the network and different transmission ranges. The analytical result in the figure is the solution of Eq.(11). From the figure, we can see that the delivery delay has degradation while transmission range increases, and it has the similar trend to different scales of network in which the total number of nodes N=200, 500 and 1000, respectively. It is reasonable that, the delivery delay reduces following the number of nodes increases in the network, because the probability of meeting the destination is large when nodes'

number grows. And in Fig. 6, it shows the simulation results are fairly accurate to the analytical ones.

In the discussion above, Fig. 5 and Fig. 6 validates that the transmission range is the definitive metric for the percolation ratio in the mobile ad-hoc network. Especially, the impact of overlap among the moving informed nodes' tracks is notable.

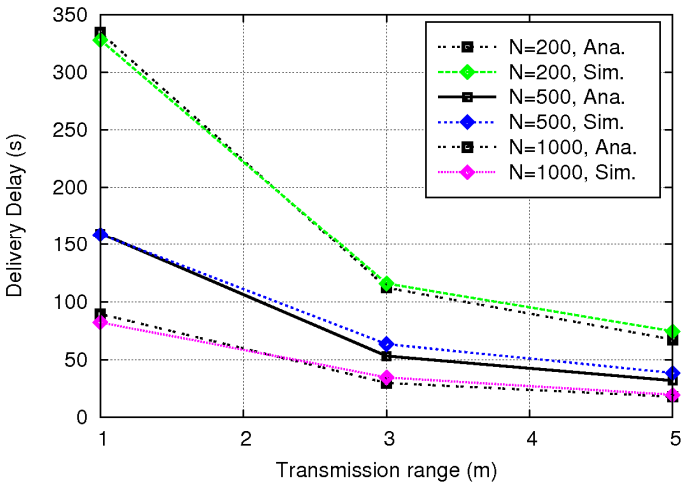

Fig. 6. Delivery delay of analysis and simulation

6 Conclusion and Future Work

In this paper, we investigate propagation of one piece of information in mobile ad-hoc network. We first develop an analytical model utilizing ODE approach, in which we take the transmission range as the critical and intuitive system parameter. Typically, we proceed to study the impacts of the moving informed nodes' overlap on the percolation ratio and the delivery delay. Extensive simulations show our analytical model is fairly accurate to capture the characteristics of information dissemination process in mobile ad-hoc network. In the future work, we plan to study our ODE model under some other mobility models as aforementioned in Section 3, and proceed to explore the effects to the other metrics mentioned in this paper, considering more variants of epidemic routing.

Acknowledgement. The work was partially supported by Project 61272470 supported by National Natural Science Foundation of China; Natural Science Foundation of Hubei Province of China.(No.2011CDB346, NO.2011CDB334); and the Fundamental Research Funds for the Central Universities, China University of Geosciences (Wuhan). (No.CUGL100232).

References

1. Daly, E.M., Haahr, M.: Social network analysis for routing in disconnected delay-tolerant MANETs. In: MobiHoc, pp. 32–40 (2007)
2. Zeng, D.Z., Cong, L., Huang, H., Guo, S., Yao, H.: Deadline Constrained Content Distribu-tion in Vehicular Delay Tolerant Networks. In: IEEE International Wireless Communications and Mobile Computing Conference (IWCMC), pp. 994–999 (2012)
3. Zeng, D.Z., Guo, S., Jin, H., Leung, V.C.: Dynamic Segmented Network Coding for Reliable Data Dissemination in Delay Tolerant Networks. In: IEEE International Communications Conference (ICC), pp. 1–5 (2012)
4. Zeng, D.Z., Guo, S., Jin, H., Leung, V.C.: Segmented Network Coding for Stream-like Applications in Delay Tolerant Networks. In: IEEE GLOBECOM, pp. 1–5 (2011)
5. Stauffer, D., Aharony, A.: Introduction To Percolation Theory, 2nd edn. CRC Press (1994)
6. Williams, B., Camp, T.: Comparison of broadcasting techniques for mobile ad hoc networks. In: MobiHoc, pp. 194–205 (2002)
7. Tonguz, O.K., Wisitpongphan, N., Parikh, J.S., Bai, F., Mudalige, P., Sadekar, V.K.: On the Broadcast Storm Problem in Ad hoc Wireless Networks. In: BROADNETS, pp. 1–11 (2006)
8. Vahdat, A., Becker, D.: Epidemic routing for partially connected ad hoc networks. In: Technical Report CS-200006, Duke University (2000)
9. Zhang, X., Neglia, G., Kurose, J.F., Towsley, D.F.: Performance modeling of epidemic routing. Computer Networks, 2867–2891 (2007)
10. Abdulla, M., Simon, R.: Controlled Epidemic Routing for Multicasting in Delay Tolerant Networks. In: IEEE International Symposium on Modeling, Analysis and Simulation of Computers and Telecommunication Systems (MASCOTS), pp. 1–10 (2008)
11. Zhang, Z., Mao, G., Anderson, B.D.O.: On the Information Propagation in Mobile Ad-Hoc Networks Using Epidemic Routing. In: GLOBECOM, pp. 1–6 (2011)
12. Khouzani, M., Eshghi, S., Sarkar, S., Shroff, N., Venkatesh, S.: Potimal energy-aware epidemic routing in DTNs. In: 13th ACM International Symposium on Mobile Ad Hoc Networking and Computing (Mobihoc), pp. 175–182 (2012)
13. Lin, Y., Li, B., Liang, B.: Stochastic analysis of network coding in epidemic routing. IEEE Journal on Selected Areas in Communications, 794–808 (2008)
14. Camp, T., Boleng, J., Davies, V.: A survey of mobility models for ad hoc network research. Wireless Communications and Mobile Computing, 483–502 (2002)
15. Wang, Q., Wang, X., Lin, X.: Mobility increases the connectivity of K-hop clustered wireless networks. In: MOBICOM, pp. 121–132 (2009)
16. Keung, G.Y., Li, B., Zhang, Q., Yang, H.: The Target Tracking in Mobile Sensor Networks. In: GLOBECOM, pp. 1–5 (2011)
17. Islam, M.T., Akon, M.M., Abdrabou, A.L., Shen, X.: Modeling Epidemic Data Diffusion for Wireless Mobile Networks. In: GLOBECOM, pp. 1–5 (2011)
18. Groenevelt, R., Nain, P., Koole, G.: The message delay in mobile ad hoc networks. In: Perform. Eval., pp. 210–228 (2005)
19. Zhang, Z., Mao, G., Anderson, B.D.O.: On information dissemination in infrastructure-based mobile ad-hoc networks. In: IEEE Wireless Communications and Networking Conference (WCNC), pp. 1743–1748 (2012)

Appendix A: Derivation of Lower Bound of ε

In this section, we derive the approximate value of ε when we calculate the average overlapped area between two meeting infectious nodes' tracks in Section 4, part A. From the Eq.(6), we find that the result of the integration will be infinite if ε approaches 0, therefore we need to find an appropriate value to calculate S_{AOL}. In fact, if two moving nodes' tracks almost coincide, the total overlap area is a rectangle which has a size of $L \cdot 2r$. In this way, we could obtain the appropriate value of ε. First, if the angle between two moving nodes' tracks is θ, the overlapped area size $S_{overlap}$ is:

$$S_{overlap} = \frac{(2r)^2}{\sin\theta}, \tag{A. 1}$$

Then, the maximal overlap area (denoted by $S_{max\text{-}overlap}$) between two moving nodes' tracks is:

$$S_{\max-overlap} = (2r) \cdot L = \frac{(2r)^2}{\sin(\varepsilon)},$$

So that, ε can be calculated as:

$$\begin{aligned} \varepsilon &= \arcsin\left(\frac{(2r)^2}{(2r) \cdot L}\right), \\ &= \arcsin\left(\frac{2r}{L}\right). \end{aligned} \tag{A. 2}$$

Waveform Decreasing Multi-copy Based Routing in Low Node Density DTNs

Chen Yu, Longbo Zhang, and Hai Jin

Services Computing Technology and System Lab
Cluster and Grid Computing Lab
School of Computer Science and Technology
Huazhong University of Science and Technology, Wuhan, 430074, China
yuchen@hust.edu.cn

Abstract. *Delay Tolerant Networks* (DTN) is one of the mobile wireless networks that topology logic may change frequently. Variable topology logic characteristics lead to several low efficiency routing problems, and in which how to increase the routing efficiency in low node density is an important issue that must be solved. The mainstream DTN routing strategy is multi-copy based routing and in order to solve the problem of flooding scale, the routing strategy always makes the messages flooding scale change under specific conditions called *Waveform Decreasing Multi-copy* (WDM) routing strategy: the flooding scale could increase or decrease. In this paper, we propose an improved routing strategy named WDM routing strategy aimed to improve the routing efficiency under low node density in DTN environment. Using several special mechanisms, the improved WDM routing strategy can obtain good performance in the case of low node density: transfer new messages first, special message transfer list, and the way of flooding scale changed. The simulation results show the WDM routing significantly improve the performance than the two mainstream routing: the Spray and Wait routing and the MaxProp routing.

Keywords: Delay Tolerant Network, Low Node Density, Waveform Decreasing, Spray and Wait routing, MaxProp routing.

1 Introduction

Delay Tolerant Networks (DTN) [1] often refer to sparse mobile ad-hoc network, where topology logic changes frequently. Many emerging communication networks fall into this paradigm including wildlife tracking and habitat monitoring sensor networks [2], *vehicular sensor network* (VSN), *inter-planetary networks* (IPN) [3], nomadic communities networks etc. Because of the changing topology caused by: the node moving out of the area, the node switching to the sleep state when the energy descent or the node being damaged physically, the network faces the problem that the node density decreases frequently.

As DTN's differences from the traditional network, the routing strategy is a major challenge. The most popular routing strategies are divided into two categories: single-copy strategy [4] and multi-copy strategy [5]. The single-copy strategy is mainly

Q. Zu, B. Hu, and A. Elçi (Eds.): ICPCA-SWS 2012, LNCS 7719, pp. 757–768, 2013.

predict the topology and transfer the messages through the prediction, this strategy applies only to the specific network and the delivery ratio is low; the multi-copy strategy is based on random flooding, by using the messages copies increase the messages delivery ratio and decrease the delay, it applies to all DTN networks and it can achieve better performance on delivery ratio and delay at the expense of memory consumption. Multi-copy strategy is considered to be more efficient than the single-copy strategy, and the most common routings in DTNs are multi-copy based. The traditional routings deal with the low node density situation by increasing the flooding scale; this is a simple and direct method, but the result is not satisfactory. The routing strategy has to consider the situation of low node density; however the existing strategies have problems in this regard.

Waveform decreasing multi-copy is a special multi-copy strategy, it is used to describe the changeable flooding scale, and it will increase or decrease when the messages subject to certain conditions. Waveform decreasing multi-copy is a good method to deal with the DTNs routing problems. In this paper, we try to find ways to improve the routing efficiency in the low node density based on waveform decreasing multi-copy strategy. First, we study the common DTN routing strategies and their routing efficiency under different node density, and analyze the advantages and disadvantages of different routing strategies. Then, we give our method to increase the routing efficiency by estimating the transmitted bytes of the node to decide the hop-count threshold, and make the message flooding increase linearly decrease exponentially. The simulation results show our method can get better efficiency in low node density.

The rest of the paper is organized as follows. Section 2 presents the state of the art for DTN routing protocol and presents their routing efficiency under different node density. Section 3 gives our method to increase the routing efficiency and the WDM routing protocol. Section 4 provides the simulation results of WDM routing protocol and related discussion. Finally, section 5 concludes the paper.

2 Related Works

In DTN networks, different from traditional network, the node density is a very important parameter, if it is too low, the routing efficiency will face great challenges such as low nodes connection probability, network congestion. In general, the node transmit range is l, the network area is S, the node number is N, if $(2\times l)^2\times N/S<0.5$, we call the node density is low [6]. Although several multi-copy based routing strategies have been proposed for DTNs, the routing efficiency is not satisfactory. In general, these algorithms are based on deciding which messages to forward during a meeting with a given peer and which messages to drop when buffers reach capacity. The most common routing protocols are Spray & Wait protocol [7] and Maxprop protocol [8].

Spray & Wait routing protocol is an improved method for unlimited flooding routing by fixing the number of copies. In Spray & Wait routing, there are two phases: spray phase and wait phase. In spray phase, the source node of a message initially starts with L copies of this message related to the number of nodes and the requirements for delay. Any node **A** that has $n>1$ message copies (source or relayed), when it encounters another node **B** with no copies, it hands over to $B^{\lfloor n/2 \rfloor}$ copies and keeps

$B^{\lceil n/2 \rceil}$ copies for itself. When **A** is left with only one copy, it switches to direct transmission. In wait phase, each of the nodes carrying one message copy performs direct transmission. There will be L nodes each carrying one message, because the Binary Spray phase runs time until there is no node holding more than 1 message copy. L can be calculated from:

$$\left(H_M^3 - 1.2\right)L^3 + \left(H_M^2 - \frac{\pi^2}{6}\right)L^2 + \left(a + \frac{2M-1}{M(M-1)}\right)L = \frac{M}{M-1}$$

M is the number of nodes; α is multiples of the time units; $H_n^\tau = \sum_{i=1}^{n} \frac{1}{i^\tau}$ is the n^{th} Harmonic number of order of τ.

The flooding based multi-copy routing protocol can achieve good performance. However, this strategy will increase the overhead ratio and cost much energy. Spray & Wait routing protocol to a certain extent solves the above problems.

MaxProp is an effective routing protocol based on prioritizing both the schedule of packets transmitted to other peers and the schedule of packets to be dropped. These priorities are based on the path likelihoods to peers according to historical data and also on several complementary mechanisms, including acknowledgements, a head-start for new packets, and lists of previous intermediaries. The core of the MaxProp protocol is a ranked list of the peer stored packets based on a cost assigned to each destination. The cost is an estimate of delivery likelihood.

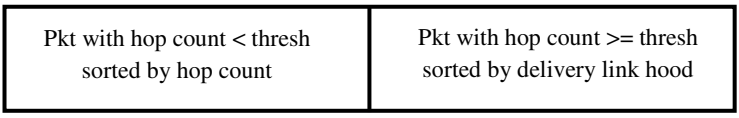

Fig. 1. MaxProp routing strategy

As shown in Figure 1, MaxProp logically splits the buffer in two phases according to whether the packets have a hop count less than a threshold t hops. Packets below the threshold are sorted by hop count; packets above the threshold are sorted by the scoring by cost. In environments where the average number of bytes transferred per transfer opportunity, x, is much smaller than the byte size of buffer, b, we prioritize low-hop count packets. As x grows, we slowly reduce the threshold to the difference between the two values. When x is larger than the buffer size, then we remove the threshold completely, it is no longer needed. Specifically, after each transfer opportunity, the routing protocol reevaluates the threshold by first choosing a portion of the buffer p as follows:

(a): if $x<b/2$, then $p=x$
(b): if $b/2 \leq x \leq b$, then $p=\min(x, b-x)$
(c): if $b<x$, then $p=0$

In this following part, we will analyze the efficiency of these routing protocols and discuss the advantages and disadvantages of them. In order to observe their performance, we simulate with different number of nodes in the area of 400 km^2. The nodes both have 250kbps transmission speed, 500m transmission range, 2km/h move speed, and 20MB memory. Table 1 and 2 are the comparison of their performance.

From Tables 1, we can find that when the node density is less than 0.5 per km^2, the message delivery ratios are below 0.4, the routing efficiency is seriously affected; even increase to 0.75, the delivery ratios are about 0.5. So, when the node density is lower than 0.5, the routing efficiency faces challenges. It is obvious that with the node density gets low, the routing efficiencies have decreased. However, we can find that Spray & Wait protocol and MaxProp protocol are significantly different: MaxProp protocol is better than Spray & Wait protocol in the situation of 100 nodes; with the increasing of node density, Spray & Wait protocol performance increases greatly, when the node density is 0.75, its performance is better than MaxProp protocol.

Table 1. Delivery Ratio Comparation

Routing Protocol	Number of Nodes		
	100	200	300
Spray & Wait	0.2267	0.3610	0.5186
MaxProp	0.2533	0.3806	0.4897

The main difference of the two protocols is the way to deliver the message copies. Spray & Wait protocol is totally random; MaxProp protocol is base on the path likelihoods to peers. In detail, Spray & Wait protocol sends messages to connected nodes without chosen, it is typical of random routing; MaxProp protocol sends messages based on destination cost estimation, it preferential transmits new messages and messages have a high delivery likelihood. As we analyze the estimation algorithm of MaxProp protocol, the nodes have to keep two maps to estimate the delivery likelihood: the map of meeting probabilities of all hosts from this host's point, the map of current costs for all messages to their destination. When the node density is low, the estimation algorithm can help message transfer more exactly; but when the node density is high, the data scale need to maintain will increase, it will occupy the limited memory, leading to the node prematurely discard the messages and has a negative impact on delivery ratio.

As we calculate, the maps' size growth is about the number of nodes squared; when there are 300 nodes, the maps occupy about 10% memory of nodes. In order to validate our assumptions, we increase the node memory about 10% and test the performance of MaxProp protocol, the delivery ratio increases about 0.6 as we expect and is much better than Spray & Wait protocol. However, the problem of memory waste is an important issue: if we can not reduce the date scale, it will bring troubles at a certain time and make it a bad performance compared with Spray & Wait protocol.

On the delay, from Tables 2, we can find that the performance of Spray & Wait protocol is stable, it changes little with the increasing of node density. MaxProp

protocol performance is much better when the node density is 0.75; when the node density is lower, it will sharply increase. One mechanism of MaxProp protocol is a ranked list of the peer stored packets. The important points are packets below the threshold are sorted by hop count aiming at improving the delivery ratio of new messages, the other messages are sorted by the cost aiming at priority to transfer messages to destination quickly. These two points affect each other: with the priority of new messages, the other messages' transmission delay will be affected. If we remove the mechanism of priority transfer of new messages, the simulate result shows that the delay is reduce and the delivery ratio increases. Spray & Wait protocol performs much stable, in general the efficiency is base on the flooding scale: *L*. It is clear that when the node density is lower than 0.5, the delay of Spray & Wait protocol is better than that of MaxProp protocol.

Table 2. Delay Comparation

Routing Protocol	Number of Nodes		
	100	200	300
Spray & Wait	1782.1353 s	1721.7113 s	1686.0742 s
MaxProp	1942.0316 s	1778.2161 s	1494.2651 s

The main reason is that the low node density makes the estimation unreliable, as the node density increases, the delay decreases significantly. So, with a certain size of estimation data, the estimate strategy can achieve an excellent performance. However when the node density is not high enough, a random transfer strategy is better than the estimate strategy.

As analyzed, the two traditional routing strategies have different problems in low node density situation, we try to find ways to solve these problems and design a more efficient routing strategy. Considering the generic and efficiency of multi-copy strategy and the waveform decreasing multi-copy, we aim to design the strategy base on the waveform decreasing multi-copy strategy to improve the routing efficacy in low node density DTNs.

3 WDM Routing Strategy

In the section, we will present our assumptions, and the details of our routing strategy. As we analyze these two protocols, we find the advantages and disadvantages of them. In order to solve these problems, we propose our special mechanisms combining their strengths and show the pseudo code of the core WDM routing strategy.

As DTN's particularity, it always faces the problem of changing topology. Node density is an important parameter of the network topology to describe the proportion of the transfer area which the nodes cover and the network coverage area. In general, when the transmission range of the node is l, the coverage area of the network is S, the total number of the nodes is N, the node density can be formalized as: $(2\times l)^2\times N/S$. If the value of $(2\times l)^2\times N/S$ is smaller than 0.5, we can define the network as a low node density network. In this case, the DTN faces a series of challenges in general, such as

time cost on setting up connections, low connectivity probability , network congestion and long transfer delay.

The traditional multi-copy routing strategy is based on random flooding, by spreading the message copies to increase the delivery ratio and to decrease the delay. Especially, when the flooding scale increases and decreases in certain tendency, we call this as Waveform Decreasing Multi-copy.

As the analysis in section 2, the main ideas of the traditional routing strategy concentrate on the flowing points: whether the random transmission is better than the chosen transmission; how to get the utmost of the limited memory of node; how to handle with the new messages; and how to define the priority of the message transmission.

In the previous works, we can find that pre-estimating the network topology can optimize the network delay in some cases, but it can only get better performance in the high node density situation, while the delivery ratio may decrease dramatically. To improve the efficiency in low node density network, we focus on the random transmission when design the routing strategy in this paper.

Due to hardware cost, the physical memory of the nodes in DTN is always limited, so that, to get the utmost of the limited memory of node is another important issue in the routing strategy design. The memory of the node is occupied in two aspects: store the messages to transfer; store the topology information of the network to guide the message transmission. Thus, the more memory sizes are occupied by the topology storage, the less memory sizes are for the message storage. If the memory sizes for storing the messages are very limited, the node will drop many messages and lead to very low delivery ratio, very long delay and heavy network congestion. The comparison between Spray & Wait routing and MaxProp routing indicates the interrelationship of the two storages. In this paper, we assume the node memory be used for message storage as much as possible.

In MaxProp routing, the latest messages have the highest transmission priority, so the new arrival message always has high delivery probability. This mechanism is well for improving the routing efficiency, but in the low node density DTN, it will increase the delay dramatically. The messages buffered in the memory will be affected and miss their connecting node when there is a new arrival message with higher transmission priority. Thus, it is important to optimize the transmission priority for the new arrival message and other messages in the memory.

We summarize these common problems in the traditional routing strategies into three phases as following:

(1) Randomly choose the transferring node is a better way to increase the delivery ratio and the topology information of the network is not necessary to be stored in every node. Even though the complete topology information can accelerate the transmission, the memory cost of the topology information leads to the lower delivery ratio.
(2) The traditional transmission priority can dramatically increase the delivery probability of the latest message. However, this priority can cause negative impact on the network delay because the size of the stored messages in the memory is generally larger than the latest one.
(3) The transmission of the messages should be in a certain order. As in the MaxProp routing, the transmission priority on lower transferring cost leads to the higher transmission speed.

In order to solve the above problems, we choose the random transmission strategy to control the messages' delivery because it has the same performance as the pre-estimation routing strategy in low node density DTN. And the random transmission strategy is the best way to solve the memory problem: the storage of the topology information is no longer needed. Thus, the remained problem is to order the messages. The node is randomly chose, but the messages should be in a certain order to be transferred, so our designed routing strategy should have a parameter to describe the messages delivery probability. Our solution is to order the messages by the remained number of copies: the less copies left, the higher probability to transfer the messages to the destination. As the feature of flooding, the less copies of a message left, the more nodes carry this message and the message can reach the destination more easily, no matter a node can transfer this message in a high probability or not.

Thus, the most important step to design our strategy is to confirm the transmission priority of the latest arrival messages. From the previous analysis, transferring the latest arrival message in the highest transmission priority causes negative impact on the delay, but this can increase the delivery ratio of the latest arrival message.

We propose the solution to balance the above contradiction: the latest arrival message which can reach the hop count threshold faster has the higher transmission priority; for the messages have already reached the hop count threshold, transfer them in the order of remained number of copies. In the design, the node can transfer the messages which below the hop count threshold first and the number of this kind of messages can decrease quickly. Then, the latest arrival messages are in the middle of the buffer storage as shown in Figure 1, the transmission priority of these messages can be in a certain extent. To complete our solution, we need further to ensure the messages which can reach the hop count threshold faster, have more copies. Thus, we revise the traditional Spray & Wait routing during the message transferring: if the message hop count is smaller than the threshold, then the number of copies left plus 1, the node delivers all the copies to the next connecting node and keep the message without any change; if the message hop count is larger than the threshold, the node delivers half number of copies to the next connecting node and keep the other half as the traditional Spray & Wait routing.

Figure 2 shows the example of Waveform Decreasing Multi-copy in which the number of copies changes decreasingly in the waveform.

Our designed routing strategy works in the following steps: when a new connection is setting up, the node updates the hop count threshold, then collects the messages which have copies left in the memory and ensure the messages which hop count is smaller than the threshold, plus 1 to the number of copies left in the memory, and then order the messages by the number of copies. During transferring the message, if the message hop count is smaller than the threshold, the node delivers all the copies of the message to the next connecting node and keep the message without any change, else the node delivers half number of copies to the next connecting node and keep the other half without any change. When there are no more copies of the message, the routing strategy turn to the wait phase, till the messages reach the destination. The pseudo code algorithm shows the core WDM routing strategy.

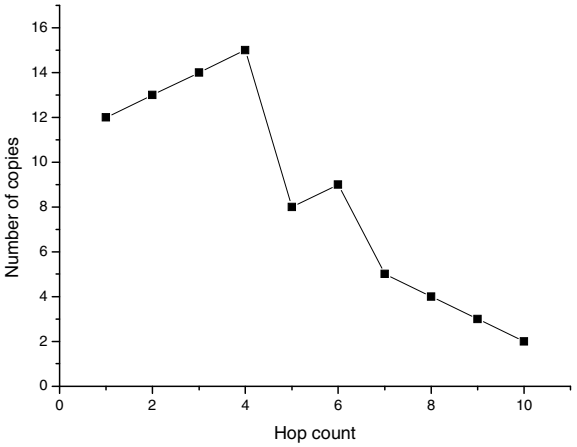

Fig. 2. Waveform Decreasing changes of the number of copies

```
Algorithm of strategy
if connect then
updatethreshold();
while messageCollection()! =NULL do
if message.hopcount<threshold
message.copyleft++;
end if
if message.copyleft>1 then
addlist(message);
end if
end while
queen messages by number of copies;
while list! =NULL do
if message.hopcount<threshold then
sendmessageto(otherhost, copyleft);
messageupdate(copyleft);
else
sendmessageto(otherhost, copyleft/2);
messageupdate(copyleft/2);
end if
end while
end if
```

4 Performance Evaluation

To demonstrate and evaluate the performance of WDM routing strategy, we use ONE1.4.1 [9], an Opportunistic Network Environment simulator which can provide a powerful tool for generating mobility traces, running DTN messaging simulations with different routing protocols, and visualizing both simulated results in real-time

and after computation interactively. We use the ONE1.4.1 to simulate the environment of Helsinki, capital of Finland, in the area of 448 km^2. In this environment, we run our simulation with different numbers of nodes. The nodes are divided into four groups. The nodes in group 1 and 4 simulate as the pedestrians nodes, each of them has 10MB memory, with 2Km/h moving speed, with 100m transmit range, but move in different area; the nodes in group 2 and 3 simulate as the cars nodes, each of them has 15MB memory, with 150m transmit range, but move limited on the road of the city, and group 2 and group 3 have different speeds on 10Km/h and 30Km/h. The flowing figures show the performance comparison of three routing protocols.

Figure 3 and Figure 4 show the delivery ratio comparison of three routing strategies. We can see from the figures that the WDM strategy performs better results on the delivery ratio than the Spray & Wait routing strategy and the MaxProp routing strategy.

Figure 3 and 4 indicate that the WDM routing strategy has a significant improvement on delivery ratio than the Spray & Wait routing strategy especially in the low node density situation: the delivery ratio increases (0.29-0.23)/0.23≈26% when the node density is 0.25, and increases (0.43-0.4)/0.4≈7.5% when the node density is 0.5. And the WDM routing strategy has a indistinctive improvement on delivery ratio than the MaxProp routing strategy in the low node density situation: the delivery ratio increases (0.29-0.26)/0.26≈11.5% when the node density is 0.25, and increases (0.43-0.41)≈4.8% when the node density is 0.5.

The WDM routing strategy can reach better performance than the random Spray & Wait routing strategy in terms of delivery ratio because it employs the transmission priority that the messages have high priority which have higher delivery probability and the new arrival messages have the secondary priority to a certain extent.

The WDM routing strategy can reach better performance than the MaxProp routing strategy in terms of delivery ratio because the information of pre-estimating the network topology is not complete enough. And in the high node density situation, the next connecting node cannot be chosen accurately. When the node density increases, the improvement of the WDM routing strategy is indistinct because randomly choose the next connecting node cannot reach better performance than the pre-estimating the network topology method even though the optimization of the memory can increase the delivery ratio, the results of the MaxProp routing strategy and WDM routing strategy are similar. The node do not need to maintain the network acknowledgements any longer..

Figure 5 and Figure 6 show the delay comparison of three routing strategies. We can see from the figures that the WDM routing strategy perform better results than the MaxProp routing strategy but similar results as the Spray & Wait routing strategy.

Figure 5 and 6 indicate that the WDM routing strategy has a significant improvement on network delay than the MaxProp routing strategy especially in the low node density situation: the network delay decrease (1920-1790)/1790≈7.3% when the node density is 0.25, and decrease (1750-1670)/1670≈4.8% when the node density is 0.5.

In the case of low node density, the acknowledgements of the network are incomplete and are not reliable enough. Thus, transferring the latest arrival messages in the first priority increases the heavy delay of the other messages stored in the memory. But the WDM routing strategy can solve this problem to a certain extent: in the low density situation, the latest arrival messages are stored in the middle of the memory buffer, the messages with first priority are sorted by the hop count, which is similar to the Spray & Wait routing strategy, the impact between latest arrival messages and

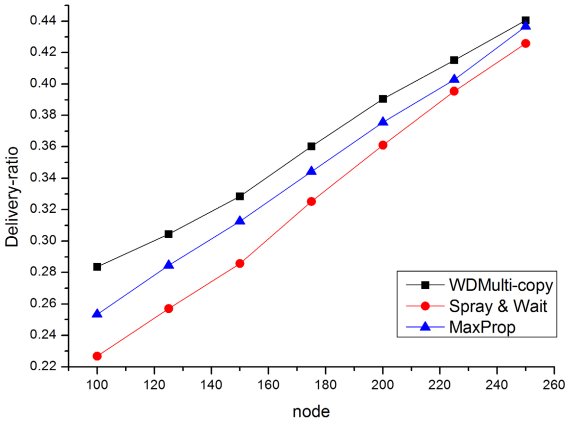

Fig. 3. Delivery-ratio comparison in different network sizes

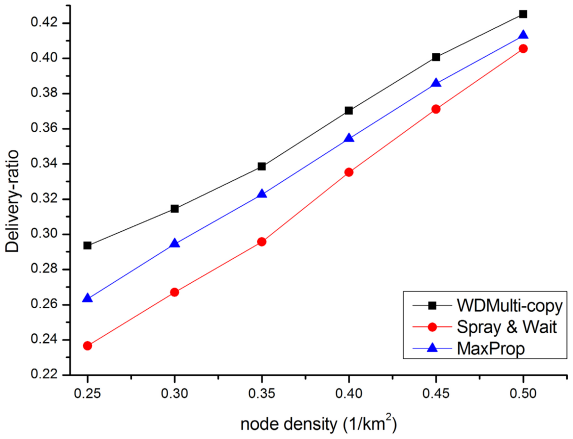

Fig. 4. Delivery-ratio comparison in different nodes densities situation

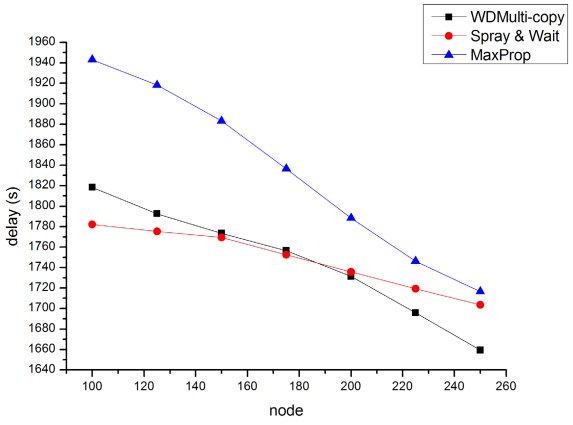

Fig. 5. Delay comparison in different network sizes

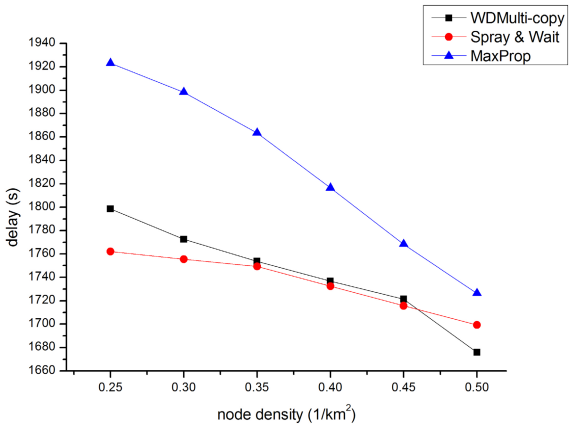

Fig. 6. Delay comparison in different nodes densities

other stored messages can be minimized. Thus, the WDM routing strategy can achieve the better performance on network delay than MaxProp routing strategy, but achieve the similar performance on network delay to Spray & Wait routing strategy.

From the numerical results on comparison these three routing strategy, we can find that the WDM routing strategy can achieve much better performance on delivery ratio than both Spray & Wait routing strategy and MaxProp routing strategy, and can achieve much better performance on network delay than MaxProp routing strategy but similar to Spray & Wait routing strategy.

Strategy to deal with the low node density situation than the traditional Spray & Wait routing and MaxProp routing. It shows a good performance on the delivery ratio: it increased at least about 8% delivery ratios when the node density is 0.5, and in extreme cases, it increased about 25% when the node density is 0.25 compare with the Spray & Wait routing; it increased at least about 5% delivery ratios when the node density is 0.5, and it increased about 13% in extreme cases when the node density is 0.25 compare with the MaxProp routing. The delay performance is also satisfactory: it reduced at least about 5% delay when the node density is 0.5, and in extreme cases, it reduced about 9% delay when the node density is 0.25 compare with the MaxProp routing; it performed quite similar with the Spray & Wait protocol, the difference of delay is not exceeding 2%.

5 Conclusions

In this paper, we propose an optimized routing strategy, named as WDM strategy, which is aimed to solve the routing efficiency problems in the low node density DTNs. With several improved mechanisms, WDM routing strategy works very well in the low node density DTNs. The simulation results show that the WDM strategy is better than the traditional Spray & Wait routing and MaxProp routing on both delivery ratio and network delay. For the future work, we commit to adopt our strategy suitable for general DTNs in different node density situations.

Acknowledgement. The work is partly supported by National Natural Science Foundation of China (No.61003220), Research Fund for the Doctoral Program of Higher Education of China (No.20090142120025), Fundamental Research Funds for the Central Universities (HUST:2010QN051) and Natural Science Foundation of Hubei Province of China (No.2010CDB02302).

References

1. Delay tolerant networking research group, `http://www.dtnrg.org`
2. Juang, P., Oki, H., Wang, Y., Martonosi, M., Peh, L.S., Rubenstein, D.: Energy-efficient Computing for Wildlife Tracking: Design Tradeoffs and Early Experiences with Zebranet. In: Proceedings of 10th International Conference on Architectural Support for Programming Languages and Operating Systems, pp. 96–107. ACM Press, California (2002)
3. F.K.A.: Delay-Tolerant Network Architecture for Challenged Internet. In: Proceedings of the 2003 Conference on Applications, Technologies, Architectures, and Protocols for Computer Communications, pp. 27–34. ACM Press, Karlsruhe (2003)
4. Spyropoulos, T., Psounis, K., Raghavendra, C.S.: Single-copy Routing in Intermittently Connected Mobile Networks. In: Proc. of IEEE Secon., pp. 235–244 (2004)
5. Spyropoulos, T., Psounis, K., Raghavendra, C.S.: Multiple-copy Routing in Intermittently Connected Mobile Networks. Technical Report CENG-2004-12, USC (2004)
6. McMahon, A., Farrell, S.: Delay and Disruption-Tolerant Networking. In: IEEE Internet Computing, vol. 13(6), pp. 82–87. IEEE Press (2009)
7. Spyropoulos, T., Psounis, K., Raghavendra, C.S.: Spray and Wait: An Efficient Routing Scheme for Intermittently Connected Mobile Networks. In: Proceedings of the 2005 ACM SIGCOMM Workshop on Delay-Tolerant Networking, pp. 252–259. ACM Press, New York (2005)
8. Burgess, J., Gallagher, B., Jensen, D., Levine, B.N.: MaxProp: Routing for Vehicle-Based Disruption-Tolerant Networking. In: Proceedings of 2006 IEEE INFOCOM. IEEE Press, Barcelona (2006)
9. The Opportunistic Network Environment simulator (ONE), `http://www.netlab.tkk.fi/tutkimus/dtn/theone/`

Research on Cooperative Scheduling at Container Terminal under Uncertainties

Meng Yu[1], Yun Cai[2], and Zhangye Zhao[1]

[1]School of Logistics Engineering, Wuhan University of Technology, Wuhan, P.R. China
ymmona@126.com, zzy63277@163.com
[2]School of Machinery and Automation, Wuhan University of Science and Technology, Wuhan, China
yuncai@126.com

Abstract. Collaborative scheduling problem of container terminal is one of multi-objective, multi-restraint, multi-resources, dynamic NP-combination optimization problems. This problem is made more difficult by some uncertain factors, such as equipment failure, changeable climate and so on. It is difficult for General analytical method to solve it, so the mobile Agent system can intelligently percept sudden changes of environment in real time and then make intelligent decisions during the rapid development of wireless communication network.

In this paper, to reduce interfering of uncertain factors and coordinate the conflict of optimization purposes, based on analyzing and coupling uncertain factors, a hybrid distributed model of cooperative scheduling system is established through adopting computer architecture-based Agent by the bottom-up modeling approach combined with the central processor and bus technology.

Keywords: Cooperative Schedule, Uncertainties, Container Terminal, Multi-Agent System.

1 Introduction

At container terminal, operative objects include arrived ships, import containers and export containers, whose loading and unloading process can be described respectively as location changes from the ship to the yard and verse vice. Container terminal is generally operated with three types of equipments, namely Quayside Cranes(QC) with limited range of motion, Yard Cranes(YC) and Container Trucks(CT) which are horizontal transport, linking the two kinds of Cranes. Furthermore, there are some hardware facilities such as berths, yards and so on.

To increase the productivity of the terminal and the utilization of equipments, some advanced scheduling strategies are adopted, such as simultaneous loading and unloading, simultaneous scheduling of multiple cranes in loading/unloading operations and dynamical scheduling of CTs shared by all cranes, etc... However, these strategies will lead to complexity of scheduling. Moreover, the scheduling process can be obstructed by some uncertain events that are equipment failure, container information missing, shipping delaying, container ships suddenly arriving or being cancelled,

Q. Zu, B. Hu, and A. Elçi (Eds.): ICPCA-SWS 2012, LNCS 7719, pp. 769–774, 2013.

changeable climate, which further increase the difficulty of the operation. Therefore, terminal scheduling problem is uncertain and complex, which is one of multi-objective, multi-restraint, multi-resources, dynamic NP-combination optimization problems. Furthermore, it is need for potential interferences between cranes to be considered and for the cooperation between different types of equipments to be improved[1-5].

Since it is difficult for General analytical method to solve it, Multi Agents are adopted, which can intelligently percept sudden changes of environment in real time and then make intelligent decisions during the rapid development of wireless communication network. Moreover, the Agent has some intelligence to fulfill tasks in an automatic way, to receive information, to negotiate about affair and to confederate with other ones to solve complex problem, so it can reduce manual workforce and information burden[6-10].

In this paper, to reduce interfering of uncertain factors and coordinate the conflict of optimization purposes, based on analysing uncertain factors, a hybrid distributed model of cooperative scheduling system is established, through adopting computer architecture-based Agent by the bottom-up modeling approach combined with the central processor and bus technology.

2 Analysis of Factors Effecting Scheduling at Container Terminal

2.1 Main Factors

In this section, main factors and their existing forms will be analyzed, which are involved in Collaborative scheduling problems.

Time Factors. It is vital to analyze constraints in operation time of container ship and handling time of Quay Crane, Yard Crane and Container Truck. The main time factors including: Berthing time, handling operations, block time, idle time of equipments, interactive operation time among equipments and so on.

Space Factors. Internal operation at terminal is essentially two dimension space-time transformation process of container between container ship and storage yard. The main space factors include: Terminal layout, position of import and export, plan of shipping stockpiling, Operation position of equipment, traveling route of equipment, order of container handling and so on.

Resources Factors. Since resources of container terminal are limited, which would cause resources conflict in the process of handling, it became the focus of research how allocating resource of equipments effects operation time, space, and efficiency of operation assignments effect the optimization of scheduling decision-making and improve stevedoring efficiency.

2.2 Uncertainties

Main uncertainties come from outside of the system (such as ships arriving time), daily operation (such as traffic congestion) and discrete anomalies (such as equipment failure). Even more, a part or all of time factors, space factors and resources factors will become uncertain randomly.

According to the characteristics of uncertain factors, these factors can be classified into three major types, uncertainties meeting statistical properties, uncertainties meeting the fuzzy characteristics, uncertainties meeting neither statistical properties nor the fuzzy characteristics.

3 MAS Framework of Container Terminal Scheduling

In this paper, to allocate operative jobs properbly, coordinate the conflict of resouce allocation and reduce interfering of uncertain factors, a hybrid distributed model of cooperative scheduling system is established, adopting computer architecture-based Agent by the bottom-up modeling approach combined with the central processor and bus technology, followed by establishment of individual models.

According to horizontal and vertical relationships of the subsystems in the scheduling system that are the command and obedience relationships among superior and subordinate subsystems, and collaboration, consultation, competitive relationships among parallel subsystems, three types of individual Agents are established, namely, Control Agent (fixed), Execution Agent (moving with wireless mobile terminal) and Operation (Mobile) Agent (dynamically generated).

Based on architecture of computer, Controlling Agents and Execution Agents having relationship between superior and subordinate are assembled into the entire scheduling system model. Operation Agents are created dynamically and freely throughout the whole system just like computer software, whose life cycle includes creating instructions, being assigned by control Agent, and performing on a different Execution Agent, finally confirming and returning to instructions.

3.1 Establishment of Individual Agent

- Controlling Agents include Central Processing Agent, Berth Schedule Agent, Quayside Crane (QC) Schedule Agent, Yard Crane (YC) Schedule Agent and Container Truck (CT) Schedule Agent, Berth Assigning Agent, Yard Allocating Agent. The structure of Control Agent is described by Berths Assigned Agent as an example shown in Figure 1.
- Execution Agents include Yard Agent, Yard Crane Agent, Quay Crane Agent, Container Truck Agent, Berth Agent and Yard Agent.
- Operation Agents include Unloading operation Agent, Loading operation Agent, Accepting Containers Operation Agent and Picking-up Containers Agent.

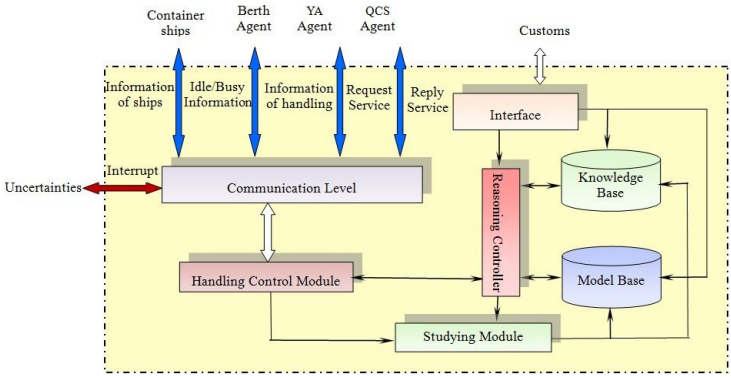

Fig. 1. Structure of Berth Allocation Agent

An Operation Agent is created by the Central Processing Agent, assigned job by the Control Agent, implemented by Execution Agent. As a case, the implementation process of Loading Operation Agent is shown in Figure 2.

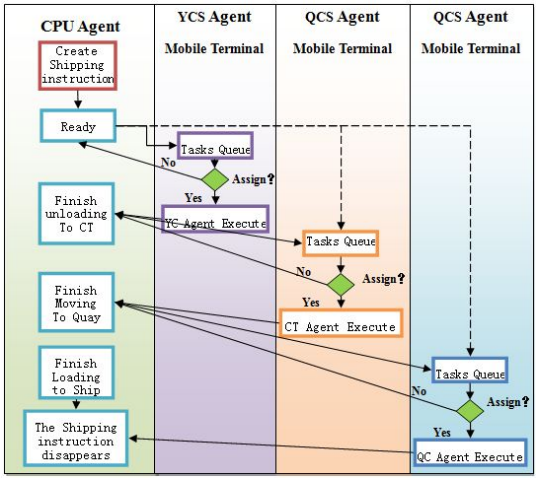

Fig. 2. Life cycle and moving paths of Loading Operation Agent

3.2 Collaboration of Agents in System

Through researching on factors effecting operation at main domestic container terminals and their business process, appropriate model framework based on Multi-Agent System (MAS) is proposed. The article will analyze the architecture of MAS.

Figure 3 shows the whole system hierarchical structure, in which the problem is divided into several sub-problems and every sub-problem has a specific Agent to solve. These Agents have horizontal and vertical relationships with another.

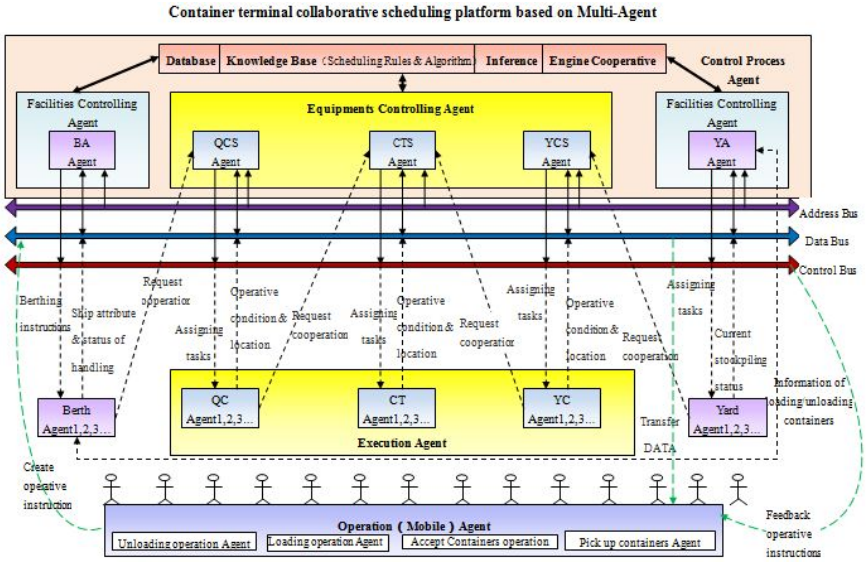

BA-Berth Assigning; QCS- Quay Cranes Scheduling; CTS- Container Trucks Scheduling; YCS-Yard Cranes Scheduling; YA- Yard Allocating

Fig. 3. Framework of container terminal schedule system based Multi-Agent

4 Conclusion

By research on container terminal scheduling system and analysis of Multi-Agent technology applied in container terminal scheduling, this article proposes a model of container terminal scheduling system based on Multi-Agent including three types of Agents. Each Agent mainly consists of Knowledge Database, Reasoning Machine, Study Module, Task Controller and Communicator, etc... The structure of Agents is explained by Berth Schedule Agent in detail. In the cooperation process of Multi-Agent-based terminal schedule System, the scheduling task is divided and cooperated by BCPN negotiation, which can avoid resource contest in scheduling, retrieve real-time scheduling information, and finally optimize the utilization of equipments at terminal.

The next task is to consider more practical factors, research on reasoning method, introduce optimization algorithm into reasoning and negotiating and simulate the Multi-Agent-based terminal scheduling in order to further optimize the system.

References

1. Bierwirth, C., Meisel, F.: A survey of berth allocation and quay crane scheduling problems in container terminals. European Journal of Operational Research 202(3), 615–627 (2010)
2. Chang, D.F., Jiang, Z.H., et al.: Integrating berth allocation and quay crane assignments. Transportation Research Part E-Logistics and Transportation Review 46, 975–990 (2010)

3. Jun, H.A.N., Xiao-na, S.U.N., Zhi-hong, J.I.N.: Coordinated optimization method for berth and quay crane allocation in container terminal. Journal of Dalian Maritime University 34, 117–121 (2008)
4. Zeng, Q.-C., Yang, Z.-Z.: Integrating scheduling model and hybrid optimization algorithm for container terminals. Journal of Systems Engineering 25, 264–270 (2010)
5. Serrano, D., Gossard, D.: Tools and techniques for conceptual design. In: Artificial Intelligence in Engineering Design, pp. 71–116. Academic Press, New York (1992)
6. Lewis, K., Mistree, F.: Modeling interactions in multidisciplinary design: A game theoretic approach. AIAA Journal 35, 1387–1392 (1997)
7. Lokuge, P., Alahakoon, D.: Improving the adaptability in automated vessel scheduling in container ports using intelligent software agents. European Journal of Operational Research 177, 1985–2015 (2007)
8. Yu, M., Wang, S.: Study on Scheduling System Based on Multi-Agent of Container Terminal. In: Proceedings 2006 10th International Conference on Computer Supported Cooperative Work in Design, Nanjing, China, pp. 579–584 (2006)
9. Li, B., Li, W.: Container terminal logistics systems collaborative scheduling based on multi-agent systems. Computer Integrated Manufacturing Systems 17, 2502–2513 (2011)
10. Xu, B., Yang, D.-L.: Application of mobile Agent in the real-time scheduling at container wharf. Information Technology 13, 13–18 (2010)

A New Hyper-parameters Selection Approach for Support Vector Machines to Predict Time Series

Yanhua Yu*, Junde Song, and Zhijun Ren

PCN&CAD Center, School of Computer,
Beijing University of Posts and Telecommunications, Beijing China
{yuyanhua,jdsong,renzj}@bupt.edu.cn

Abstract. The selection of hyper-parameters is a crucial challenge in Support Vector Machine modeling. Differed from using basic statistics of residuals in previous method, the new approach selects hyper-parameters by checking whether or not there is information redundancy in residual sequence. Furthermore, Omni-Directional Correlation Function (ODCF) is applied to test redundancy in residual, and the proof of the accuracy of the methodology is given in terms of numerical demonstration. Experiments conducted on benchmark time series, annual sunspot number and Mackey-Glass time series; indicate that the proposed method has better performance than the recorded in previous literatures.

Keywords: Support Vector Machines, Hyper-parameter, Residual, ODCF.

1 Introduction

As one branch of data mining technology, time series prediction techniques have been widely used in many applications. Although SVM time series prediction has been applied in wide spectrum of applications, there appears to be several challenges associated with using SVM. Selection of hyper-parameters is one of the issues. Hyper-parameters include kernel parameter, the regularization parameter C and ε-insensitive zone which determines the number of support vectors. Finding the optimal hyper-parameters is crucial for a SVM model with good generalization performance. But till now there is no optimal method for selection of SVM hyper-parameter.

Some researches have been done with respect to changing hyper-parameters associated with SVM training to improve prediction results[1-7]. Below is a summary of the investigations:

- Schölkopf [1] proposed $\upsilon - SVM$ to use parameter υ rather than ε. The value of υ ranges from 0 to 1 which indicates the upper bound of proportion of support vectors to the whole training set and lower bound of fraction of points

* Corresopnding author.

Q. Zu, B. Hu, and A. Elçi (Eds.): ICPCA-SWS 2012, LNCS 7719, pp. 775–787, 2013.

outside ε-tube. After υ is set, the value of parameter ε can be calculated automatically.

- Kwok [2] and Smola et al [3] proposed asymptotically optimal ε-values proportional to noise variance.
- In [4] regularization parameter C is selected equal to the range of output values.
- Reference [5] used K-fold Cross Validation (KCV) for parameter choice.
- Reference [6] proposed Leave One Out (LOO).
- Reference [7] presented improved hyper-parameter selection approach using statistical theory based on [2]-[4].

All of these recommendations are with no consideration on particular properties of time series. This paper presents a novel approach to selecting hyper-parameters based on information redundancy test.

This contribution is organized as follows. Section 2 presents the novel approach to selecting SVM regression hyper-parameters based on information redundancy test. The selection methodology and the numerical proof are also described in this section. Section 3 conducts experiments applying the proposed approach in two benchmark time series: annual sunspot number and Mackey-Glass. The empirical comparison demonstrates the advantages of the proposed approach. Finally, conclusion is drawn in section 4.

2 Redundancy-Test-Based Hyper-Parameter Selection Approach

There are three steps in using SVM for time series prediction. Firstly, phase space is reconstructed and two key parameters, the embedding dimension and delay, are determined. Secondly, hyper-parameters are properly selected so that the optimal SVM model is constructed accordingly. Here we use the redundancy-test-based approach for hyper-parameters selection. Finally, prediction is made through the model and generalization performance is evaluated.

2.1 The Proposal of Hyper-Parameters Selection Approach Based on Redundancy Test

SVM can automatically determine on network structure and find the global minimum. But the hyper-parameters have to be selected manually. There is still no 'optimal' method in the field [1]-[7]. So far, most of methods only check the goodness of hyper-parameters using statistics (Mean Squared Error, MSE) of residuals on training set or validation set, e.g., cross-validation approach applied in most applications only used MSE on validation set.

There is a significant difference between time series prediction and other regression problem: the observations in a time series have inherent correlations with each other, while in common regression problem the samples are assumed to be independent with each other. Based on this characteristic, time series prediction technique can construct auto-regression (AR) model to predict proceeding data by using previous data.

Therefore, if a model is valid, the residuals should be reduced to containing no information redundancy and uncorrelated to delayed outputs. A novel redundancy-test-based hyper-parameter selection approach is proposed in this paper through checking the adequacy of the identified SVM model using ODCF.

In fact, time series is a special kind of dynamical system without input information. Selection of hyper-parameter for SVM can be regarded as the same to dynamical system identification, since different settings of hyper-parameters will directly result in different support vectors acquired, which constitutes the model in turn. In dynamical system identification, validation is an important step to check the adequacy of the identified model. For nonlinear system identification, Zhang [8], Ljung [9] and Billings [10] developed validation procedure to check the quality of identified neural network based on correlation test. By using this procedure, neural network structure can be determined automatically rather than manually. Up to now, no research on parameter selection using residual redundancy test has been done for SVM time series prediction.

Yu and Song [11] proposed to select hyper-parameters by checking the whiteness of residual sequence, and a good performance has been achieved for traffic volume prediction in mobile network. But when extending this approach to nonlinear time series such as annual sunspot number and Mackey-Glass, the prediction performance is poor. After deep analysis, the reason appears to be that the traffic volume series in mobile network is linear series, in which linear un-correlation in residual is equivalent to complete un-correlation whereas in nonlinear time series, it is not sure. In other words, even if no linear correlation exists, there is still nonlinear correlation available in the residual [12]. Hence, this paper proposes to use ODCF to check the redundancy of residual, and develops a validation procedure how to use ODCF whose effectiveness is proven in terms of theoretical analysis and experiment in following sections.

2.2 Introduction of ODCF

The ODCF statistics, which was proposed by L. F. Zhang, Q. M Zhu and Longden in [13-14] based on autocorrelation function (ACF) and cross-correlation function (CCF), is proved to be appropriate for checking correlations whatever linear or nonlinear.

ODCF can be categorized into omni-directional cross-correlation function (ODCCF) and omni-directional autocorrelation function (ODACF). The latter can be viewed as a special case of the former when the two series are identical. Next the computation equations for ODCCF are listed. Assume $a(t)$, $b(t)$ are two time series data, let

$$\begin{aligned} \alpha(t) &= \left|a^{'}(t)\right| = \left|a(t) - \frac{1}{N}\sum_{t=1}^{N} a(t)\right| \\ \beta(t) &= \left|b^{'}(t)\right| = \left|b(t) - \frac{1}{N}\sum_{t=1}^{N} b(t)\right| \end{aligned} \tag{1}$$

Then four correlation coefficient functions can be calculated as follows where τ denotes time delay.

$$r_{\alpha\beta}(\tau)=\frac{\sum_{t=\tau+1}^{N}(\alpha(t-\tau)\beta(t))}{\sqrt{\sum_{t=1}^{N}(\alpha(t))^2\sum_{t=1}^{N}(\beta(t))^2}} \tag{2}$$

$$r_{\alpha b'}(\tau)=\frac{\sum_{t=\tau+1}^{N}(\alpha(t-\tau)b'(t))}{\sqrt{\sum_{t=1}^{N}(\alpha(t))^2\sum_{t=1}^{N}(b'(t))^2}} \tag{3}$$

$$r_{a'b'}(\tau)=\frac{\sum_{t=\tau+1}^{N}(a'(t-\tau)b'(t))}{\sqrt{\sum_{t=1}^{N}(a'(t))^2\sum_{t=1}^{N}(b'(t))^2}} \tag{4}$$

$$r_{a'\beta}(\tau)=\frac{\sum_{t=\tau+1}^{N}(a'(t-\tau)\beta(t))}{\sqrt{\sum_{t=1}^{N}(a'(t))^2\sum_{t=1}^{N}(\beta(t))^2}} \tag{5}$$

By combining the above four coefficients, a statistic called ODCCF denoted by $\rho_{ab}(\tau)$ can be acquired as follows.

If

$$\left|\max(r_{\alpha\beta}(\tau),r_{\alpha b'}(\tau),r_{a'b'}(\tau),r_{a'\beta}(\tau))\right|>\left|\min(r_{\alpha\beta}(\tau),r_{\alpha b'}(\tau),r_{a'b'}(\tau),r_{a'\beta}(\tau))\right|$$

Then

$$\rho_{ab}(\tau)=\max(r_{\alpha\beta}(\tau),r_{\alpha b'}(\tau),r_{a'b'}(\tau),r_{a'\beta}(\tau)) \tag{6}$$

Else

$$\rho_{ab}(\tau)=\min(r_{\alpha\beta}(\tau),r_{\alpha b'}(\tau),r_{a'b'}(\tau),r_{a'\beta}(\tau)) \tag{7}$$

When $a(t)=b(t)$, $\rho_{ab}(\tau)$ is referred to as ODACF.

For time series data, when the model is proper, the following two equations hold according to central limit theorem.

$$\begin{cases} \rho_{\varepsilon\varepsilon}(\tau) = 1, \tau = 0 \\ \rho_{\varepsilon\varepsilon}(\tau) \sim N(0, \frac{1}{N}), \text{ otherwise} \end{cases} \tag{8}$$

$$\begin{cases} \rho_{y\varepsilon}(\tau) \neq 0, \tau = 0 \\ \rho_{y\varepsilon}(\tau) \sim N(0, \frac{1}{N}), \text{ otherwise} \end{cases} \tag{9}$$

2.3 Redundancy-Test-Based Validation Based on ODCF and Its Proof

As a special form of dynamical system, time series model can be mathematically stated as

$$\begin{aligned} y(t) &= f(\boldsymbol{y}^{t-1}) + e(t) \\ &= f(y(t-1), \cdots, y(t-t_y)) + e(t) \end{aligned} \tag{10}$$

The estimated function $\hat{f}(.)$ can be acquired after model identification is performed. Output value $y(t)$ can be predicted by using function $\hat{f}(.)$.

$$\hat{y}(t) = \hat{f}(\boldsymbol{y}^{t-1}) \tag{11}$$

$$\varepsilon(t) = y(t) - \hat{y}(t) \tag{12}$$

$\varepsilon(t)$ is the prediction error referred to as residual at time point t. An adequate model should get all information about the dynamical system the model tries to approximate, so that the training should go until no information redundancy left in the residual. If the residual contains autocorrelation or has correlation with delayed output, it can be concluded that the acquired model is not appropriate for the data and further training is needed. In this case, the residual can be expressed as follows:

$$\varepsilon(t) = \hat{g}(\boldsymbol{y}^{t-1}) + e(t) \tag{13}$$

where $\hat{g}(.)$ can be linear or nonlinear. From (10) and (13), we can get the equation below:

$$\begin{aligned} \varepsilon(t) &= \hat{g}(\cdots, y(t-p), \cdots) + e(t) \\ &= \hat{g}(\cdots, \hat{f}(y(t-i-p)) + \varepsilon(t-p), \cdots) + e(t) \end{aligned} \tag{14}$$

From (14) we can see that if residual is correlated with delayed output, residual will be auto-correlated. So $\rho_{\varepsilon\varepsilon}(\tau)$ can also be used to indicate the correlation between $\varepsilon(t)$ and $y(t-p)$.

However, $\rho_{\varepsilon\varepsilon}(\tau)$ may display less detection power, practically, when the variance of $\hat{g}(.)$ is much smaller than the variance of $e(t)$.

Here is the numerical demonstration. Consider a nonlinear system expressed as

$$y(t) = 0.8\,y(t-1) + 0.8\,y^2(t-1) + e(t) \tag{15}$$

In (15), $\{e(t)\}$ was the normally distributed random noise sequence with zero mean and variance 0.001.

The following three residual equations are possibly resulted from ill hyper-parameter selection:

$$\begin{cases} \varepsilon_1(t) = e(t) \\ \varepsilon_2(t) = 0.1\,y(t-1) + e(t) \\ \varepsilon_3(t) = 0.02\,y(t-1) + e(t) \end{cases} \tag{16}$$

All these data sequences have length of 1000. Compute the ODACF and ODCCF for the above three residual sequences in (16), and the results are depicted in Fig. 1-3. In each figure, the dash lines indicate the confidence interval calculated using significance level of 5%. In Fig. 1, no correlation function exceeds confidence limits so $\varepsilon_1(t)$ contains no information redundancy. This validity test result is accordant with the true. In Fig. 2-3, the correlations lie outside confidence interval, so $\varepsilon_2(t)$ to $\varepsilon_3(t)$ are residuals containing information redundancy. As indicated in (16), both these two residual sequences include omitted predictable terms.

The validation results can be extensively analyzed as follows. In Fig. 2, both $\rho_{\varepsilon\varepsilon}$ and $\rho_{y\varepsilon}$ lie outside confidence interval. We can deduce that in this case, redundancy can be detected by only using $\rho_{\varepsilon\varepsilon}$. Fig. 3 clearly suggests that only $\rho_{y\varepsilon}$ lies outside confidence interval. The expressions for $\varepsilon_2(t)$ and $\varepsilon_3(t)$ are similar, the only difference is that the parameter decreases from 0.1 in $\varepsilon_2(t)$ to 0.02 in $\varepsilon_3(t)$. $\rho_{\varepsilon\varepsilon}$ in $\varepsilon_3(t)$ displays less detection power than $\rho_{y\varepsilon}$ since the variance of $g(t) = 0.02\,y(t-1)$ is much smaller than the variance of $e(t)$: $\frac{\mathrm{var}(e(t))}{\mathrm{var}(g(t))} = 781$.

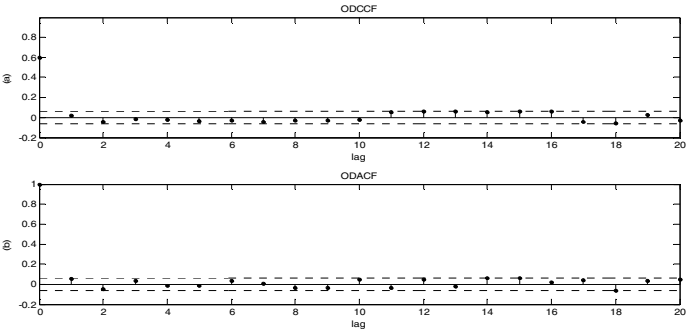

Fig. 1. Validity test for ε_1 ((a) $\rho_{y\varepsilon}(\tau)$ (b) $\rho_{\varepsilon\varepsilon}(\tau)$)

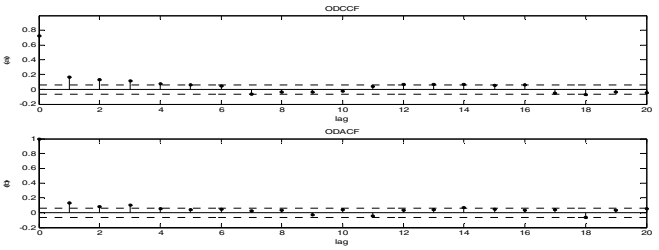

Fig. 2. Validity test for ε_3 ((a) $\rho_{y\varepsilon}(\tau)$ (b) $\rho_{\varepsilon\varepsilon}(\tau)$)

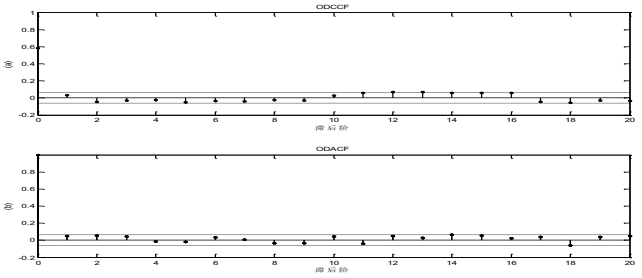

Fig. 3. Validity test for ε_4 ((a) $\rho_{y\varepsilon}(\tau)$ (b) $\rho_{\varepsilon\varepsilon}(\tau)$

Therefore, besides ODACF of $\varepsilon(t)$, i.e., $\rho_{\varepsilon\varepsilon}(\tau)$, ODCCF between residual and delayed output, i.e., $\rho_{y\varepsilon}(\tau)$ has also to be involved in the model validation test.

3 Experiments

Next, we describe experimental procedure and then apply the procedure on annual sunspot number series and Mackey-Glass series respectively.

There are several commonly used kernels for SVM, and the most commonly used is Gaussian kernel function. In this paper this kernel function is adopted and its expression is described as follows.

$$K(x,x^{'}) = \exp(-\gamma \left\| x - x^{'} \right\|^2) \tag{17}$$

or

$$K(x,x^{'}) = \exp(-\frac{\left\| x - x^{'} \right\|^2}{2p^2}) \tag{18}$$

The procedure for selection of optimal hyper-parameters ε, γ and C is as follows. Firstly, let us consider the value of ε. According to [7], when using RBF kernel, ε has little impact on the model. nd also, according to [1], the value of parameter ε can be automatically computed given the value of parameter ν ranging from 0 to 1. This means if the value of ν is determined, ε will be selected accordingly. Here we let ν=0.1.

With respect to parameter γ in (17), we can get its value by calculating kernel width parameter p in (18) and then transforming it. According to [7], the kernel width parameter should reflect the input range of training data. The RBF width parameter should be set to $p \sim (0.2 - 0.5) * range(x)$. For higher m-dimensional problem where all m input variables are pre-scaled to [0, 1], the RBF width parameter is set up according to the following formulation:

$$p^m \sim (0.2 - 0.5) \tag{19}$$

Finally, we come to the determination on the value of parameter C. This can be done by adaptively changing the parameter C until no information redundancy is detected by ODCF in residual.

The followings are experiments using the procedure described above.

3.1 Annual Sunspot Number

Annual sunspot number is a classic nonlinear time series which has long served as a benchmark to assess statistical model and prediction method. To make results comparable, this study uses the same experimental setup as [15-17].The only difference is that in our experiment, the annual sunspot numbers from 1700 to 1955 are used as training data.

1. Reconstructing phase space from original time series. Many studies reveal that annual sunspot number shows some chaotic behavior. The correlation dimension D of its strange attractor is calculated as $D < 2$ .By Takens theorem $m \geq 2D + 1$, we use embedding dimension $m = 5$.
2. Constructing the optimal model and selecting optimal hyper-parameters based on redundancy test on residual.
   (a) Set $\upsilon = 0.1$.
   (b) Calculate the value range of parameter γ associated with kernel width. Using (19) to calculate parameter p , and then transform it to γ in (17) .The result is $\gamma = 0.5 \sim 0.8$. With γ increasing, the complexity of SVM model increases accordingly.
   (c) Get the value of parameter C given the value of υ and γ .Set $\gamma = 0.5$ .Let the initial value $C = 1$. Iterate C with pace 1 and check the redundancy in residual until the value of C passes the correlation test. There is a problem that with different confidence interval we have different range of C value obtained. When we use the confidence interval of 2 times standard deviation, there is not any value of C can pass the correlation test while the confidence interval of 3 times standard deviation is employed, a large amount of values of C can pass the correlation test. In order to obtain the optimal C value, we decrease the range of confidence interval with pace 0.05 until there is no C value can pass the correlation test. By this approach, the confidence interval of 2.65 times standard deviation is selected and the value of C is taken up finally with 1589.
   (d) Change the value of parameter γ in the range of $0.5 \sim 0.8$ with increment pace 0.1 and repeat step c). For $\gamma = 0.6$, the appropriate confidence interval is 2.85 times standard deviation. For $\gamma = 0.7$ it is 2.8 times' and for $\gamma = 0.8$ it is 2.85 times'. So it can be concluded that hyper-parameters with $\gamma = 0.5$, C=1589, $\upsilon = 0.1$ are the optimal which make the residual sequence least correlated.
3. Apply the identified SVM model to predict annual sunspot number from 1956 to 1979. Evaluate the performance of the proposed approach using metric NMSE (Normalized Mean Squared Error).

$$\mathrm{NMSE} = \frac{1}{\delta^2 l}\left(\sum_{i=1}^{l} (y_i - \hat{y}_i)^2\right)$$

$$\delta^2 = \frac{1}{l-1}\left(\sum_{i=1}^{l} (y_i - \bar{y})^2\right) \tag{20}$$

Table 1. shows that the performance of the proposed approach based on redundancy test is better than that reported in [15]-[17]. The metric NMSE indicates the overall deviation of predicted from the actual.

Table 1. NMSE of sunspot number in 1956 TO 1979

Methods	NMSE
SVM based on redundancy-test	13.5%
Benchmark[15]	15.4%
Benchmark[16]	35.0%
Benchmark[17]	28.0%

3.2 Mackey-Glass

Mackey-Glass time series comes from the modeling of blood cells production evolution. It is a nonlinear time series determined by:

$$\frac{dx(t)}{dt} = -0.1x(t) + \frac{0.2x(t-t_d)}{1+x(t-t_d)^{10}} \tag{21}$$

which, for values of t_d greater than 16:8, shows some highly nonlinear chaotic behavior. Mackey-Glass is often used for artificial forecasting benchmark.

1. To make prediction result comparable, we use the same experimental setup as [18] in constructing phase space: embedding dimension $m=6$ and delay $\tau=6$. So $\mathbf{X}(t)$ is used to predict $x(t+\tau)$, and the whole dataset can be split into 6 independent datasets, the first one S_1 containing $x_{1+(d-1)\tau}$, the second one S_2, $x_{2+(d-1)\tau}$, $\cdots$, and the sixth one S_6, $x_{d\tau}$. In [18], the first 100 points of S_1 are used as training set, while the first 100 points of S_2 serve as the validation set to choose hyper-parameters. In this paper, hyper-parameters are selected by checking redundancy in residual sequences.
2. Apply redundancy-test-based validation approach to select optimal hyper-parameters
   (a) Set $\upsilon = 0.1$.
   (b) Calculate the value range of parameter γ associated with kernel width.

   Using (19) to calculate parameter p, and then transform it to γ in (17). The result is $\gamma = 0.5 \sim 0.7$. With γ increasing, the complexity of SVM model increases accordingly.
   (c) Get the value of parameter C given the value of υ and γ. Set $\gamma = 0.5$. Let the initial value $C=1$. Iterate C with pace 1 and check the redundancy in residual until the value of C passes the correlation test. The first value of C that passes the correlation test is $C = 32$ under the confidence interval of 2 times standard deviation. So it can be concluded that hyper-parameters with $\gamma = 0.5$, C=32, $\upsilon = 0.1$.

3. Apply the identified SVM model to predict the points in S_1 from data point number 101 to number 200. Evaluate the performance using RMSE with formulation

$$RMSE = \sqrt{\frac{1}{l}\left(\sum_{i=1}^{l}(y_i - \hat{y}_i)^2\right)} \tag{22}$$

It can be seen from Table 2 that the performance of redundancy-test-based approach is better than that based on validation set and the recorded in [18]. RMSE indicates the overall deviation of prediction from the actual.

Fig.4 depicts the cause of the difference in performance between the proposed approach and the one based on validation set. Fig. 7 shows that as the value of C increases from 1 to 100, MSE on test set initially decreases but subsequently increases. On the other hand, it also can be observed from Fig. 7 that as the value of C increases MSE on validation set decreases monotonically until $C = 78$, and then converges to a fixed value. This figure reveals that the change pattern of MSE on validation set and test set are different. When MSE on test set is minimal, MSE on validation set remains decrease; when MSE on validation set converges, MSE on test set increases. This problem can be avoided when using proposed redundancy-test-based approach, by which we can get the C=32 at which the MSE on test set is minimal.

Table 2. Comparison of Mse on Test Set between Validation Based and The New Approach

Item	Proposed approach	Approach with validation
RMSE of test set(101-200 of S1)	0.016	0.018

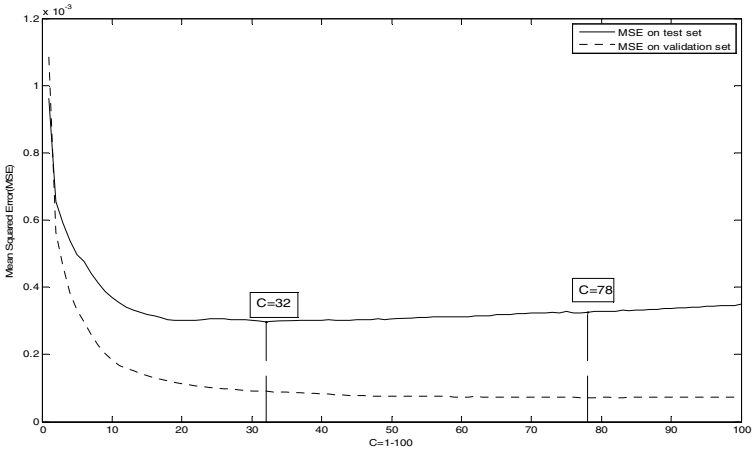

Fig. 4. MSE on test set and validation set with hyper-parameter C from 1 to 100

4 Conclusion

In this study, a novel hyper-parameters selection approach based on redundancy test is proposed. This new algorithm selects the optimal parameters by checking whether or not the residual sequence contains information redundancy. This approach is derived from the characteristic of time series that the time series observations have inherent correlations with each other. This is different from other regressions in which the samples in training set are independent. The method based on redundancy test is developed by using ODCF, and the proof has been given in the study from theoretical analysis and numerical simulation. Experiments conducted on two typical nonlinear time series, annual sunspot number and Mackey-Glass, demonstrate the advantage of the proposed approach.

Acknowledgment. This work is supported by the National Natural Science Foundation of China (Grant No.61072060); the National High Technology Research and Development Program of China (Grant No. 2011AA100706); the Research Fund for the Doctoral Program of Higher Education(Grant No. 20110005120007); the Co-construction Program with Beijing Municipal Commission of Education; Engineering Research Center of Information Networks, Ministry of Education.

References

1. Schölkopf, B., Bartlett, P., Smola, A., Williamson, R.: Support Vector Regression with Automatic Accuracy Control. In: Niklasson, L., Bodén, M., Ziemke, T. (eds.) Proceedings of ICANN 1998, Perspectives in Neural Computing, pp. 111–116. Springer, Berlin (1998)
2. Kwok, J.T.: Linear Dependency between ε and the Input Noise in ε-Support Vector Regression. In: Dorffner, G., Bischof, H., Hornik, K. (eds.) ICANN 2001. LNCS, vol. 2130, pp. 405–410. Springer, Heidelberg (2001)
3. Smola, A., Murata, N., Schölkopf, B., Muller, K.: Asymptotically Optimal Choice of ε–loss for Support Vector Machines. In: Proceeding of ICANN (1998)
4. Mattera, D., Haykin, S.: Support Vector Machines for Dynamic Reconstruction of a Chaotic System. In: Schölkopf, B., Burges, J., Smola, A. (eds.) Advances in Kernel Methods: Support Vector Machine, MIT Press (1999)
5. Cherkassky, V., Mulier, F.: Learning from Data: Concepts, Theory, and Methods. John-Wiley & Sons (1998)
6. Scholkopf, B., Burges, J., Smola, A.: Advances in Kernel Methods: Support Vector Machine. MIT Press (1999)
7. Cherkassky, V., Ma, Y.Q.: Practical Selection of SVM Parameters and Noise Estimation for SVM Regression. Neural Networks, 113–134 (2004)
8. Zhang, L.F., Zhu, Q.M., Longden, A.: A Correlation-test-based Validation Procedure for Identified Neural Networks. IEEE Transaction on Neural Network 20(1), 1–13 (2009)
9. Ljung, L.: System Identification-Theory for the User. Prentice-Hall Inc. (1999)
10. Mao, K.Z., Billings, S.A.: Multi-directional Model Validity Tests for Non-linear System Identification. International Journal of Control 73(1) (2000)
11. Yu, Y.H., Song, J.D.: A Mechanism of Telecommunication Network Performance Monitoring Based on Anomaly Detection. Journal of Electronics & Information Technology 31(9), 2220–2225 (2009)

12. Billings, S.A., Zhu, Q.M.: Nonlinear Model Validation Using Correlation Tests. International Journal of Control 60, 1107–1120 (1994)
13. Zhang, L.F., Zhu, Q.M., Longden, A.: A Set of Novel Correlation Tests for Nonlinear System Variables. International Journal of System Science 38(47), 47–60 (2007)
14. Zhu, Q.M., Zhang, L.F., Longden, A.: Development of Omni-directional Correlation Functions for Nonlinear Model Validation. Automatica 43, 1519–1531 (2007)
15. Cao, L.J.: Support Vector Machines Experts for Time Series Forecasting. Neurocomputing 51, 321–339 (2003)
16. Weigend, A.S., Huberman, B.A., Rumelhart, D.E.: Predicting the Future: a Connectionist Approach. International Journal of Neural Systems 1, 193–209 (1990)
17. Tong, H., Lim, K.S.: Threshold Autoregressive, Limit Cycles and Cyclical Data. Journal of Royal Statistic Society 42(3), 245–292 (1980)
18. Ralavola, L., d'Alche-Buc, F.: Dynamical Modeling with Kernels for Nonlinear Time Series Prediction. In: Proc. NIPS, vol. 13, pp. 981–987 (2001)

Location Context Aware Collective Filtering Algorithm

Wenjun Yue, Meina Song, Jing Han, and Haihong E

School of Computer, Beijing University of Posts and Telecommunications, Beijing, China
yuewenjun@gmail.com, {mnsong,ehaihong}@bupt.edu.cn,
babyblue110128@hotmail.com

Abstract. To improve the quality of the recommendation of the recommendation system, a distance-interest affective model is proposed to combine user location context on the preferences of user interests. Based on the model and user-based collaborative filtering algorithm, the location context aware collective filtering algorithm is designed. Firstly, measure the location-similarity between users through the user's location context information. Second, calculate the origin user-similarity from the user-item rating matrix. Then, gain the location-similarity as a weight of final user similarity, calculate the final similarity. Finally, recommendation is supplied by top-N recommendation. The simulation results were compared with the traditional algorithm to prove the precision and recall rate of the proposed algorithm is superior to traditional algorithms.

Keywords: recommender system, collaborative filtering, similarity measure, location context.

1 Introduction

The advent of the Internet and the popularity has brought a lot of information to users, meeting the need of information in the information era for the user. In the other side, the sharp increase of online information brought in by the rapid development of the network leads to a situation that user in the face of a large number of information can't get to that part of the really useful information and reduced the information efficiency. This problem is the so-called “information overload” problem.

Currently, search engine (such as Google, Bing, Baidu, etc.) is the most useful tool for people to obtain information, which retrieve information with key words supply by users and return information relativity. As information and communication is diversified, and the demand of the users for information is diversification and individuation, the results obtained by search engines as a representative of information retrieval system still can’t satisfy people’s different information demand as they from different backgrounds, having different purposes and in different periods. The problem of "information overload" is more and more serious.

To solve the "information overload" problem, personalized service proposed to meet different needs for different people. Recommender system [3-6] is an important branch of the personalized service research field, which recommends information and products

Q. Zu, B. Hu, and A. Elçi (Eds.): ICPCA-SWS 2012, LNCS 7719, pp. 788–800, 2013.

that users are interested in. Through mining user behavior, recommender system generates recommendations helping users to find items (such as movies, music, books, Web information, etc.) that they might probably interested in from a large number of data to satisfy user's personalized demand. Currently, recommender system have made great progress in e-commerce (such as Amazon, Alibaba, watercress network, Dangdang, etc.), information retrieval (such as iGoogle, MyYahoo, etc.), as well as Internet advertising and many other areas.

Recommend system works in two steps: first the analysis user's interest bias through the user behavior history, and then get users' potential interested products or services according to the interest bias. Usually, we get user's interest bias by analyze items which users have behaviors on. In the research of recommender systems, we usually concern on mining relationship between user and items, generally from the user-item rating data.

We are paying few attentions to the context (such as time, location, mood, devices, network conditions, etc.) of user and items while lots of efforts have made to the binary relationship in user and items. However, according to the study, context does impact on the interest of users. In many situation, effective recommend cannot be supplied by merely discuss on the relationship between the user and items. By taking contextual factors into account, it is possible to improve the recommendation precision at some degree.

Based on the existing research of collaborative filter recommender systems and contextual aware recommender systems, a location context-aware collaborative filtering algorithm (the Location Context Aware Collective Filtering Algorithm LCACF) is proposed to combine user location context on the preferences of user interests. Experiment shows that the feasibility and effective of the algorithm. Section 2 introduces related works about collaborative filtering and context-aware recommender systems. Section 3 discusses the Location Context Aware Collective Filtering Algorithm. Section 4 analysis the LCACF algorithm through experiment results and section 5 makes a conclusion of the paper.

2 Related Works

Recommender systems are usually classified into the following categories, based on how recommendations are made [8]:

- Content-based recommendations: The user will be recommended items similar to the ones the user preferred in the past;
- Collaborative filtering recommendations: The user will be recommended items that people with similar tastes and preferences liked in the past;
- Hybrid approaches: These methods combine collaborative and content-based methods.

Collaborative filtering recommendation algorithm is the most studied and widely used personalized recommendation algorithm. Recommender system uses preference of user to generate personalized recommendation. The biggest advantage of collaborative filtering recommendation system is that they can handle music, movies, and other things which are difficult to structure representation.

Collaborative filtering recommendations can be divided into two categories: user-based collaborative filtering algorithms and item-based collaborative filtering algorithms. The main idea of user-based collaborative filtering algorithms can be defined as two steps: first, calculate the similarity between users based on user history behavior; second, predict the interest of target user by analyze ratings from people who have the same interests. The idea of item-based collaborative filtering algorithms is similar with user-based collaborative filtering algorithms, which calculate the similarity of items and based on the item similarity to obtain user interest. In this paper, we focus on combining location context with user-based collaborative filtering algorithm.

Currently, studies around collaborative filtering algorithm mostly focused on how to improve and combination the algorithms of user-based recommendation and items-based recommendation. [7] proposed collaborative filtering algorithm based on the field nearest neighbor, using user rated items as the basic of similarity calculation. The algorithm divides non-target users into categories, and makes recommendations by categories. [8] come up with an uncertain nearest neighbor collaborative filtering recommendation algorithm UNCF. The algorithm is based on the similarity of the user and item calculated, adaptively selecting a prediction target nearest neighbor objects as recommended group. [9] proposed a collaborative filtering algorithm based on items attributes and cloud filled. Recommendations are supposed by filled matrix which is filled by cloud model computing. All these algorithms concentrate on the link between the user and items, but do not care about the context information.

In recent years, the academic community for context-aware recommendation system is gradually increased. [10] extends the recommendation from two-dimensional recommendation to a multi-dimensional one based on the context information. Combining the ability of multi-dimensional information handle of OLAP applications, the article proposes a multidimensional recommendation model. [11] according to the context information in the recommended process of different position, summarizes the context awareness recommend system of three kinds of models: preliminary context filtering, after-context filtering and context model. [12] proposes a trust forecasting model based on entity context and time stamp, established trust grade space with 8 granularity and introduced multi-dimensional measurement standard to more scientific and accurate measure of interaction satisfaction degree.

To location context in recommendation system, there are some researches on it now. Research in [13] shows that users from different place are having interests with very big difference. Users of different countries and regions exists certain differences in their interest. Researchers at the university of Minnesota through the statistical on MovieLens data set on the user E-mail data statistics found that Florida users like

movies and Wisconsin users like all types of movies is put in very big difference. The table below shows the result:

Table 1. Movielens preference locality

U.S State	Top Movie Genres	Avg. Rating
Minnesota	Film-Noir	3.8
	War	3.7
	Drama	3.6
	Documentary	3.6
Wisconsin	War	4.0
	Film-Noir	4.0
	Mystery	3.9
	Romance	3.8
Florida	Fantasy	4.3
	Animation	4.1
	War	4.0
	Musical	4.0

Based on the result of research, they proposed LARS Algorithm which partitioon users into small subsets by location information and recommended by users in the same subsets.

3 Location Context Aware Collective Filtering Algorithm

3.1 Data Model

Formally, the recommendation problem can be formulated as follows: Let C be the set of all users and let S be the set of all possible items that can be recommended, such as books, movies, or restaurants. Let u be a utility function that measures the usefulness of item s to user c, i.e.,$u: C \times S \to R$, where R is a totally ordered set (e.g., nonnegative integers or real numbers within a certain range). Then, for each user $c \in C$, we want to choose such item $s \in S$ that maximizes the user's utility.

$$\forall\, c \in C, \qquad S = \arg\max_{s \in S} u(c, s)$$

Each element of the user space C can be defined with a profile that includes various user characteristics. In the simplest case, the profile can contain only a single (unique) element, such as User ID. Similarly, each element of the item space S is defined with a set of characteristics. For example, in a movie recommendation application, where S is a collection of movies, each movie can be represented not only by its ID, but also by its title, genre, director, year of release, leading actors, etc.

In recommender systems, the utility of an item is usually represented by a *rating*, which indicates how a particular user liked a particular item. However, as indicated earlier, in general, utility can be an arbitrary function, including a profit function.

Depending on the application, utility u can either be specified by the user, as is often done for the user-defined ratings, or is computed by the application, as can be the case for a profit-based utility function[18].

In a typical collaborative filtering recommendation system, the input data is represented as a $m \times n$ user-item rating matrix $R(m, n)$, m is the number of users, n is number of items. User rating data can be used to represent the user interests. A line of the matrix represents a user, and the column on behalf of an item. The user-item rating data matrix is shown as in Table 2.

Table 2. User-item rating matrix

	Item1	…	Itemj	…	Itemn
User1	$R_{1,1}$	…	$R_{1,j}$	…	…
…	…	…	…	…	/
Userj	$R_{j,1}$	…	$R_{i,j}$	…	$R_{j,n}$
…	…	…	…	…	…
Userm	/	…	$R_{m,i}$	…	$R_{m,n}$

In the paper, we use vector model to represent the user Context of attribute, expand the traditional "user-item" two-dimensional rating model to multidimensional rating model including a variety of Context information. The utility function that measures the usefulness of item s to user c changed into $u: C \times S \times D \rightarrow R$. So for each er $c \in C$, we want to choose such item $s \in S$ that maximizes the user's utility.

$$\forall\, c \in C, \qquad S = \arg\max_{s \in S} u(c, s, d)$$

3.2 Algorithm Design

Through analyze of user data of the MovieLens data set, it can be found that users from different areas are having very big difference in the favor of different types of movies. As interest of user from different countries and regions exist significant differences, it is necessary to consider the location context information when doing recommendations to user. The location context information of user can be used to enhance the recommendation quality of recommender system. LCACF algorithm put forward by this paper will process the user location context information into the collaborative filtering recommendation.

LCACF algorithm enhances user-based collaborative filtering algorithm and mainly compound by two steps:

(1) Calculate user-set having similar interest to target user;

(2) Select items that are liked by the user-set from step (1) and the target user have no comment with, and recommend to user.

The key to Step (1) is calculating the interest similarity between two users. If the similarity is higher, the users will be defined as closer, and they will probably like a thing more. Collaborative filtering algorithm mainly uses user behavior in similarity

calculation. Given user u and user v, the similarity between them defined as $m(u,v)$. The item's score that each user rated can be treated as a n-d vector, a measure of similarity between users can be the same as similarity between different n-d vector.

In LCACF algorithm, firstly using cosine similarity or Pearson correlation to calculation initial interest similarity of user i and user j:

$$sim(i,j) = \cos(\mathbf{i},\mathbf{j}) = \frac{\mathbf{i}\cdot\mathbf{j}}{\mathbf{i}*\mathbf{j}} \tag{1}$$

$$sim(i,j) = \frac{\sum_{c\in I_{i,j}} (R_{i,c} - \overline{R}_i)(R_{j,c} - \overline{R}_j)}{\sqrt{\sum_{c\in I_{i,j}} (R_{i,c} - \overline{R}_i)^2}\sqrt{\sum_{c\in I_{i,j}} (R_{j,c} - \overline{R}_j)^2}} \tag{2}$$

Among them, set the item set that user i and user j both rated R. Ri,c represents the rating from user i to item c. Ri and Rj respectively represent average score of user i and user j. Secondly, process the user's location attenuation according to the user's location context information. For a given user u and user v, D (u, v) means the distance between user u and user v, using Euclidean distance to measure. On the basis of user distance, add location attenuation factor to user similarity. For users to u and user v, the location similarity Luv can be defined as:

$$L_{uv} = \frac{1}{1+\alpha * D(u,v)} \tag{3}$$

The formula shows that when giving recommendations for user u, the closer between user u and v, the high ranking will be for items that user v interested in. Among them, a is the location attenuation factor, its value in different system is different according to the different data sets. If the influence of location factor for user interest is bigger in a system, it should take a bigger one. Otherwise choose a smaller one. By adding location attenuation factor into algorithm, we integrate the user location context information into the recommender system. At the same time, we can also avoid data sparseness cause by divide data set according to location context classification. The improved user similarity can be achieved by following code:

```
def LocateSimilarity(train):
#Caclulate distance effect between users
    for i in train.keys():
        for j in train.keys():
            if i == j:
                continue
            C[i][j] = Distance(i,j)
    for i, related_items in C.items():
        for j, cij in related_items.items():
            L[i][j] = 1 / (1 + alpha * cij)
#caculate similarity matrix W
    W = dict()
    for i in train.keys():
```

```
        for j in train.keys():
            if i == j:
                continue
            W[i][j]=Simi(train,i, j) * L[i][j]
    return W
```

After complete step (1) getting interest similarity between user, step (2) will recommend K items from the rating that users having a most close interest. The interest of user u to item i as $p(u,i)$ used to recommendation is as follow:

$$p(u,i) = \sum_{v \in S(u,K) \bigcap N(i)} w_{uv} r_{vi} \tag{4}$$

The $S(u, k)$ contains the interest nearest k user to user u , $N(i)$ is users set of who had rating for the item, w_{uv} is the interest similarity of user u and user v. r_{vi} on behalf of interest of user v to item i, in the user-item rating matrix, it's the rating of user v to item i. The code above achieves the algorithm:

```
def Recommend(user, train, W, K):
    rank = dict()
    interacted_items = train[user]
    for v, wuv in top(sort(W[user].items(),K):
        for i, rvi in train[v].items():
            if i in interacted_items:
                continue
            rank[i] += wuv * rvi
    return rank
```

Among them, train is the user-item rating matrix, W is the user similarity calculated including the location context. Algorithm result set rank contains the most interesting items to user predict by algorithm. At last, recommend items of top N ranking to the user.

4 Experiment and Analysis

4.1 Dataset

In this paper data set provided by MovieLens site (http://movielens.umn.edu/) is used. MovieLens is a recommender system based on Web receives the user rating to the film and provides corresponding film recommended list. At present, the Web site has more than 43000 users, films rated by user more than 3500 department.

We choose 100000 rating data from the user dataset as experimental data set; the experiment data set contains 943 users and 1682 movie, of which each user rated at least 20 films.

4.2 Metrics

Use LCACF algorithm to recommend items for user by behavior of users in training set, define recommendation set which contains N items produce by the algorithm as R(u), and item-set that the user likes in the test set as T(u). By calculating the precision

and recall of the recommendation, we can evaluate the accuracy of recommendation algorithm.

Define recommendation precision as:

$$\Pr ecision = \frac{\sum_{u} \left| R(u) \bigcap T(u) \right|}{\sum_{u} \left| R(u) \right|} \tag{5}$$

Define recommendation recall as:

$$\mathrm{Re} call = \frac{\sum_{u} \left| R(u) \bigcap T(u) \right|}{\sum_{u} \left| T(u) \right|} \tag{6}$$

The code above calculates the precision and recall of an algorithm[3]:

```
def PrecisionRecall(test, N):
    hit = 0
    n_recall = 0
    n_precision = 0
    for user, items in test.items():
       rank = Recommend(user, N)
       hit += len (rank & items)
       n_recall += len(items)
       n_precision += N
   return [hit / (1.0 * n_recall), hit / (1.0 * n_precision)]
```

4.3 Results

The aim of this experiment is to measure the effect of proposed location context aware collaborative filtering algorithm; experiments use same data set and evaluation standard to compare the new algorithm and the traditional collaborative filtering algorithms. First of all, divide user behavior data set into N copies (this paper take N = 5) according to the uniform distribution randomly, choose one as a test set, the rest of the N - 1 as the training set. Build up user interest model in the training set, and forecast user behavior on the test set, then statistics according to the metrics.

1) Different Effect of Location Attenuation Factora

The value of location factor chooses according to different data set. In the experiment, in order to verify the quality of recommendation, we calculate the precision under different a. Test results are shown below. It can be seen that value of a does impact to the recommendation quality. With the increase of a, the influence decreases gradually. But overall, the LCACF algorithm having a predict precision and recall higher than traditional collaborative filtering algorithm.

Table 3. The affect of different a

K=25	Precision		Recall	
	traditional	LCACF	traditional	LCACF
a=0.001	0.05779	0.08017	0.01189	0.01650
a=0.01	0.05779	0.09936	0.01189	0.02045
a=0.1	0.05779	0.12566	0.01189	0.02586
a=1	0.05779	0.13065	0.01189	0.02689
a=10	0.05779	0.13150	0.01189	0.02706
a=100	0.05779	0.13107	0.01189	0.02697

Set the number of neighbor K=25, predict precision in different value of a is shown as the following table:

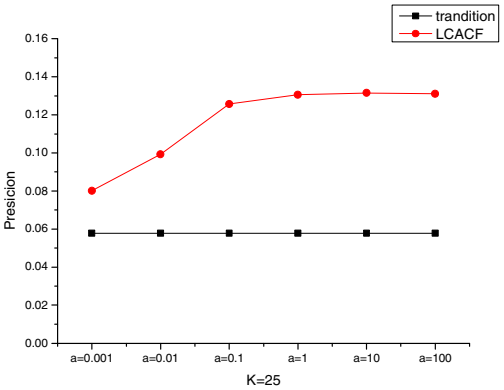

Fig. 1. The affect of different a to presision

Set the number of neighbor K=25, predict recall in different value of a is shown as the following table:

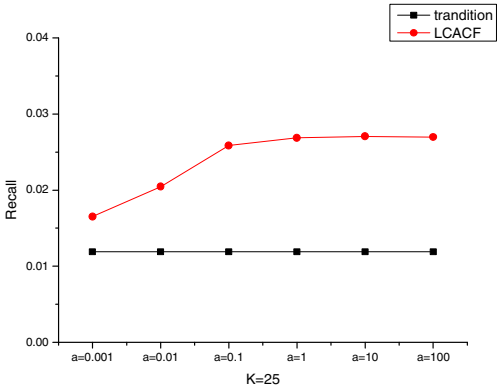

Fig. 2. The affect of different a to recall

2) The Different Effect of Nearest Neighbors Set Size

The size of neighbors set has a great influence to the quality of prediction. To verify the quality of recommendation, experimental calculated accuracy of recommendation in different neighbor set size

A. Precision

Set location attenuation factor a = 0.01, precision under cosine similarity and location aware cosine similarity in different K shown as graph below:

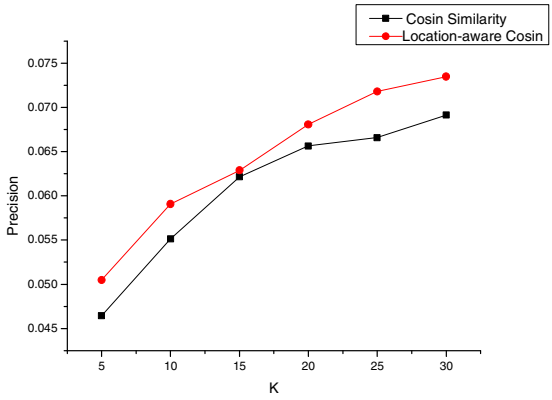

Fig. 3. The affect of different a

Set location attenuation factor a = 0.01, precision under Pearson similarity and location aware cosine similarity in different K shown as graph below:

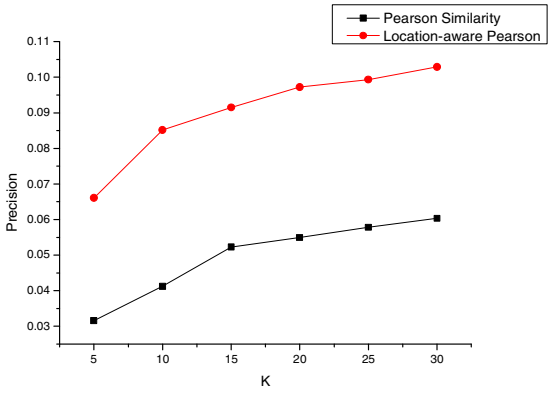

Fig. 4. Precision under Pearson similarity

B. Recall

Set location attenuation factor a = 0.01, recall under cosine similarity and location aware cosine similarity in different K shown as graph below:

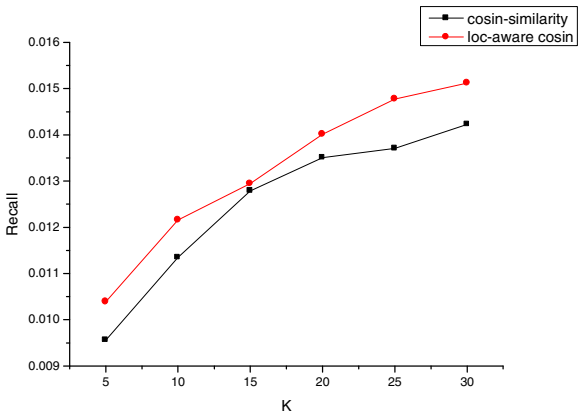

Fig. 5. Recall under Pearson similarity

Set location attenuation factor a = 0.01, recall under Pearson similarity and location aware cosine similarity in different K shown as graph below:

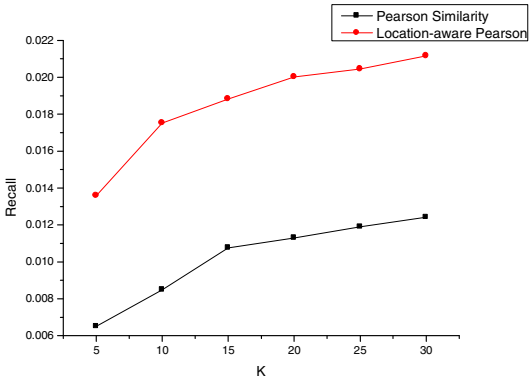

Fig. 6. Recall under cosine similarity

Test results as shown. From the result we find that with the increase of neighbor set size, precision and recall rate are increased gradually for both of the algorithms. In comparison, the improved algorithm's prediction quality has always been better than traditional collaborative filtering recommendation algorithm. From the experimental results it can be seen that LCACF algorithm has higher precision and recall rate, it can be concluded that the proposed recommendation algorithm have better recommendation than traditional algorithm.

5 Conclusion

The paper first analyzes the traditional similarity calculation method in collaborative filtering system which only considers user-item rating score, regardless of user interests based on the different location context.

In view of the above problems, this paper puts forward a location context aware collaborative filtering recommendation algorithm; this algorithm can make up the defect effectively. The experimental result shows that, the collaborative filtering recommendation algorithm based on the location context can effectively improve the precision of recommendation, significantly improve the quality of recommendation.

In the paper, Euclidean distance is used to calculate of location attenuation. For the Euclidean distance simply calculate linear distance, the algorithm should be improved. How to use location context information to retrieve the user similarity better still needs further research.

Furthermore, this paper considers the affect of long term location factor and does not conclude the mobile location, how to integrate the instant location factor into recommendation needs more efforts.

Acknowledgements. This work is supported by the National Key project of Scientific and Technical Supporting Programs of China (Grant No. 2009BAH39B03); the National Natural Science Foundation of China(Grant No.61072060); the National High Technology Research and Development Program of China Grant No. 2011AA100706);the Research Fund for the Doctoral Program of Higher Education (Grant No. 20110005120007); the Fundamental Research Funds for the Central Universities(2012RC0205); the Co-construction Program with Beijing Municipal Commission of Education; Engineering Research Center of Information Networks, Ministry of Education.

References

1. Liu, J.-G., Zhou, T., Wang, B.-H.: The research progress of personalized recommendation system. J. Progress in Natural Science 19(1) (2009)
2. Wang, G.-X., Liu, H.-P.: Survey of personalized recommendation system. Computer Engineering and Applications 48(7), 66–76 (2012)
3. Xiang, L.: Recommend system practice. People's post and telecommunications university press (2012)
4. Deng, A.-L., Zhu, Y.-Y., Shi, B.-L.: A Collaborative Filtering Recommendation Algorithm Based on Item Rating Prediction. Journal of Software 14(9), 1621–1628 (2003)
5. Wang, J., Yin, J., Zheng, L.-R.: Collaborative Filtering Recommendation Algorithm Based on Co-ratings and Similarity Weight. Computer Science 37(2), 99–104 (2010)
6. Wang, L., Meng, X., Zhang, Y.: Context-Aware Recommender Systems. Journal of Software 23(1), 1–20 (2012)
7. Li, C., Liang, C., Ma, L.: A Collaborative Filtering Recommendation Algorithm Based on Domain Nearest Neighbor. Journal of Computer Research and Development 45(9) (2008)

8. Huang, C., Yin, J., Wang, J.: Uncertain Neighbors' Collaborative Filtering Recommendation Algorithm. Chinese Journal of Computers 33(8) (2010)
9. Sun, J.-G., Ai, L.-R.: Collaborative filtering recommendation algorithm based on item attribute and cloud model filing. Journal of Computer Applications 32(2) (2012)
10. Adomavieius, G., Sankaranarayanan, R., Sen, S., et al.: Incorporating contextual information in recommender systems using a multidimensional approach. ACM Transactions on Information Systems 23(1), 103–145 (2005)
11. Wang, L.C., Meng, X.W., Zhang, Y.: Context-Aware recommender systems. Journal of Software 23(1), 1–20 (2012)
12. Li, F., Shen, L.-M., Si, Y.-L.: A Trust Forecasting Model Based on Entity Context and Time Stamp. Journal of Electronics & Information Technology 33(5) (2011)
13. Levandoski, J.J., Sarwat, M.: LARS: A Location-Aware Recommender System. In: 2012 IEEE 28th International Conference on Data Engineering (ICDE), pp. 450–461 (2012)
14. Woerndl, W., Groh, G.: Utilizing Physical and Social Context to Improve Recommender Systems. In: 2007 IEEE/WIC/ACM International Conferences on Web Intelligence and Intelligent Agent Technology Workshops, pp. 123–128 (2007)
15. Adomavicius, G., Tuzhilin, A.: Context-Aware Recommender Systems. In: Recommender Systems Handbook (2011)
16. Waga, K., Tabarcea, A., Franti, P.: Context Aware Recommendation of Location-based Data. In: 2011 15th International Conference on System Theory, Control, and Computing (ICSTCC), pp. 1–6 (2011)
17. Adomavicius, G., Tuzhilin, A.: Context Aware Recommender Systems. In: Recommender Systems Handbook, pp. 217–253. Springer Press, New York (2011)
18. Adomavicius, G., Tuzhilin, A.: Toward the next generation of recommender systems: A survey of the state-of-the-art and possible extensions. IEEE Trans. on Knowledge and Data Engingeering 17(6), 734–749 (2005)
19. Waga, K., Tabarcea, A., Fränti, P.: Context Aware Recommendation of Location-based Data. In: 2011 15th International Conference on System Theory, Control, and Computing, ICSTCC (2011)

Clustering Analysis Research Based on DNA Genetic Algorithm

Wenke Zang[1], Xiyu Liu[1], and Yanlong Wang[2]

[1]School of Management Science and Engineering, Shandong Normal University, China
{Zwker,xyliu}@163.com
[2] College of Information Technical Science, Nankai University, Tianjin, China
ruoshuiwyl@163.com

Abstract. This article proposes a fuzzy C-means clustering analysis method, which is based on DNA genetic algorithm. DNA encoding is used to analyze the center of the cluster and the quality of clustering is judged by eigenvectors and the sum of Euclidean distance of the corresponding cluster center. Through selection, crossover, mutation and inversion operation the encoding of cluster centers can be optimized, thus to get the best cluster center of cluster division. According to the simulation results the effect of this method is superior to the genetic algorithm of fuzzy C-means clustering analysis.

Keywords: DNA genetic algorithm, Fuzzy C-means, clustering analysis, DNA computing.

1 Introduction

The clustering analysis method is a new multivariate statistical method, which aggregates things into categories in accordance with certain properties of them. It makes the similarity in the class as small as possible but between the classes as large as possible, which leads to the analysis of the data. Clustering analysis is widely used in data mining and pattern recognition. Fuzzy C-Means clustering in the fuzzy clustering analysis is the most widely used and the most sensitive algorithm. In clustering analysis, each clustering algorithm has its own shortcomings, such as, being easy to fall into local optimum, sensitive to the initial cluster center, the high complexity, and so on.

According to the disadvantage of the clustering algorithm, the researchers combine clustering algorithm together with the genetic algorithm, which is a widely used global optimization method. Its main advantage is that it is simple, generally used, robust strong and suitable for parallel processing. Its efficiency is higher than that of the blind search, and more universal than those specialized algorithms for specific problems. It is a solving model that has nothing to do with problems. Therefore, the combination of genetic algorithm and FCM can not only play a genetic algorithm (GA) global search capability, but also take into account the FCM local optimization ability. However, the genetic algorithm still has low efficiency in the case of late search,

Q. Zu, B. Hu, and A. Elçi (Eds.): ICPCA-SWS 2012, LNCS 7719, pp. 801–813, 2013.

the weak ability of local optimization, and it is easy to be precocious and so on. Common binary code cannot express the wealth of genetic information.

In recent years, with the advent and development of DNA computing, it has been discovered that DNA-based intelligent system is able to present the genetic information of organisms. DNA computing is conducive to the development of more powerful intelligent behavior to solve more complex problems. Researchers put forward the DNA genetic algorithm (DNA-GA), which enriches the traditional genetic algorithm, and makes the method of operation more abundant.

In the research that combines DNA genetic algorithm and clustering analysis, DNA genetic algorithm is used to enrich the operator, and fewer iterations are used. Then it is more effective to identify the cluster centers. According to the characteristics of the DNA genetic algorithms and fuzzy C-means clustering analysis, this article puts forward a fuzzy C-means clustering algorithm which is based on DNA genetic algorithm.

2 Related Knowledge

2.1 Fuzzy C-Means Algorithm

Fuzzy C-Means algorithm is one of the most popular clustering techniques, in which categories can be pre-defined and no similarity measure of data points is expressed with the Euclidean distance. It is minimized as much as possible. Fuzzy C-Means algorithm is an iterative algorithm, and cluster centers and data points on the types of membership values are updated to minimize the dissimilarity measure.

Suppose there are N L-dimensional data points, which are expressed as $x_i, i = 1, 2, \cdots, N$ for the clustering problem. Each data point $x_i, i = 1, 2, \cdots, N$ is characterized by a vector of L values. That is $x_{i1}, x_{i2}, \cdots, x_{iL}$, Assuming that the above data are be divided into Class C, $2 \le C \le N$, and g is the weighting factor of the level of ambiguity in a display category, we expressed the attached matrix as $[\mu]$ and the dimension as $N \times C$. Therefore, the membership value of the i-th data point and j th category is expressed with μ_{ij}. μ_{ij} is in the range of $(0.0, 1.0)$ and satisfies the following conditions: $\sum_{j=1}^{C} \mu_{ij} = 1.0$. The objective function of the optimization problem is $F(\mu, C) = \sum_{j=1}^{C} \sum_{i=1}^{N} \mu_{ij}^{g} d_{ij}^{2}$, Where d_{ij}^{2} is the Euclidean distance of the ith point and the jth class. It is calculated by $d_{ij} = \| C_j - x_i \|$. The criteria of clustering minimize the objective function $F(\mu, C)$. Lagrange multiplication is used to solve it and get the following results.

$$\begin{cases} \mu_{ij} = \dfrac{1}{\sum_{m=1}^{C} \left(\dfrac{d_{ij}}{d_{im}}\right)^{\frac{2}{g-1}}} \cdots\cdots\cdots\cdots \text{when } I_k \neq \varnothing \\ \mu_{ij} = 0, \forall i \in \overline{I}_k, \sum_{i \in I_k} u_{ik} = 1 \quad \text{when } I_k = \varnothing \end{cases} \tag{1}$$

Cluster centers:

$$CC_i = \frac{\sum_{i=1}^{N} \mu_{ij}^{g} x_i}{\sum_{i=1}^{N} \mu_{ij}^{g}} \tag{2}$$

Cluster centers and membership values can be updated according to the above equation (1) and (2). This algorithm can find all kinds of corresponding cluster centers. However, this algorithm is sensitive to initialization, and is easy to fall into local optimal.

2.2 Traditional Genetic Algorithm

Genetic algorithm (GA) was proposed in 1965 by Professor Holland from University of Michigan. It is a population-based probabilistic search and optimization technique, and works on the basis of natural genetic mechanisms and the principles of Darwin's natural selection.

Genetic algorithm has the following principles:

(i) It begins with a population composed of random initial solutions.
(ii) Calculate the fitness of each solution in the population.
(iii) Use a different operator such as reproduction, crossover, and mutation to improve the solution of population.
(iv) The solution quality of a population cannot be the same. The role of the copy of the operator is to choose a good solution according to their fitness. Therefore, a good composition of the mating pool will be formed at random. There are copy ratio selection, tournament selection, and sorting selection, etc.
(v) Randomly select mates from the above mating pool, which is known as the paternal individuals. They may be involved in the cross depending on the crossover probability. At the intersection, an exchange of property between the paternal individuals will generate new individual solutions. There are such crossover operators as single-point crossover, two point crossover, multi-point crossover and uniform crossover.
(vi) In biology, variability refers to the sudden change of parameters. While in GA search, the variation is used to obtain a local change that is close to the current solution. Therefore, if a solution is the local minimum, this operator is expected to help it out of this dilemma, but it is also possible to jump into the global trap.

(vii) After the application of copy, crossover and mutation to the entire population, a generation the GA is completed. Different criteria can be used to terminate the program, such as the maximum algebraic, and the ideal accuracy of the solution.

The work flow chart of the genetic algorithm is as flowing:

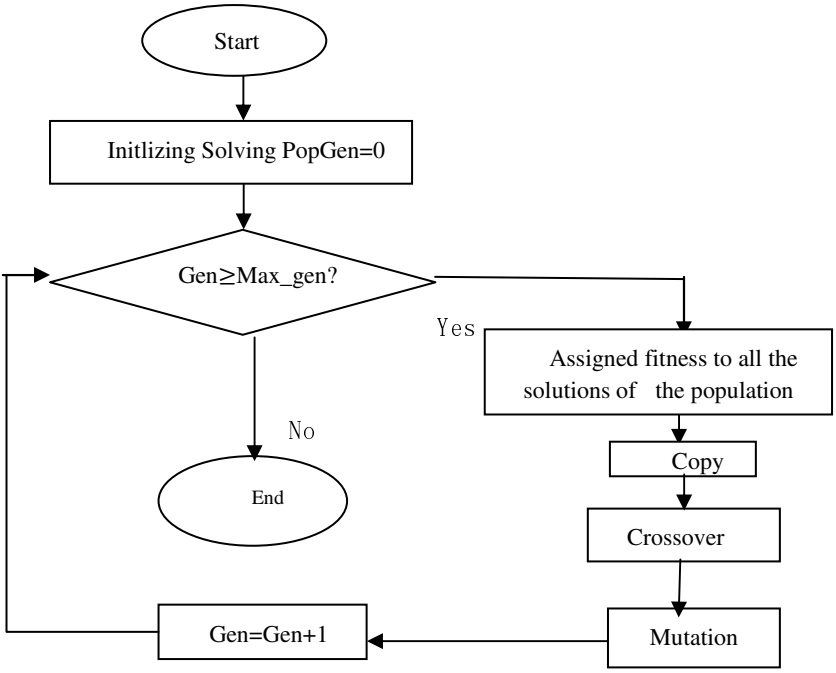

Fig. 1. GA Work Flow Chart

2.3 DNA Computing

DNA computing is a new intelligent computing method with DNA and relevant bio-enzymes as its basic materials. The method uses the double-helix structure of DNA and base pairing rules to code, mapping the objects to be operated in a DNA molecular chain. Data pool is generated with the biological role of the enzyme, and then the original data is mapped into the DNA molecule chain according to certain rules, and finally molecular biological techniques are used for the testing of the result.

The biggest advantage of DNA computing is that it takes full advantage of the mass genetic code of DNA molecule, as well as a huge amount of parallelism. Since Adleman successfully applied DNA computing methods to a 7-vertex Hamiltonian path problem, researchers try to use DNA computing to solve more problems, hoping to fully exploit the potential of DNA computing and have successfully solved the NP problems such as Hamilton path, maximum Clique.

From a mathematical perspective, the single-stranded DNA can be viewed as a string of symbols ACGT, just like computer coded 0 and 1, which can be represented as a collection of four letters to decode the information. Specific enzyme can act as a

"software" to complete the processing of the necessary information, and different enzymes used for different operators.

With the deepening of the exploration, the researchers find that the development of DNA computing, there are many difficulties. DNA computing is mostly achieved through biochemical tests. Although from the accuracy point of view biological operations have reached a high level, it have not yet reached the accuracy of the mathematical problem solving. DNA computing is still stuck in the level of biological experiments, limiting its application in engineering fields.

The researchers find that genetic algorithm also uses chromosome to mean individual, and evolves through individual's genetic manipulation, and there are a lot of similarities between the algorithm ideology and DNA computing. Therefore, inspired by the biological context of DNA computing, researchers believe that the wealth of genetic information of DNA operations can promote the expression mechanism of genetic algorithm to further simulate the biological genetic information, thereby improving the performance of GA. Scholars have carried out the study of the DNA genetic algorithm.

2.4 DNA Genetic Algorithm

In the traditional genetic algorithm, the binary encoding is the most common one, which cannot express the wealth of genetic information and the computational model does not reflect the effect of genetic information for organism growth and development, especially the key role of DNA encoding mechanism. With the advent and development of DNA computing, some scholars link DNA with genetic algorithm to form the DNA genetic algorithm (DNAGA). The basic structure of DNAGA is similar with the traditional genetic algorithm, except that the DNA genetic algorithm uses the DNA encoding, and gets the solution to the problem based on the encoding genetic manipulation to the individual. DNAGA evolves from the traditional genetic algorithm, and in addition to the advantages of traditional genetic algorithm, the DNA genetic algorithm has the following advantages:

i. Compared with traditional binary encoding, its encoding has greater improvement, suitable to express complex knowledge and flexible for encoding with high precision.
ii. Because of the diversity of decoding and the richness of coding, it allows the population to maintain a certain level of diversity in the case of low mutation probability.
iii. It introduces complex gene-level operations, develops more effective genetic operators, such as inversion, separation, ectopic, etc., and enriches evolutionary means.

DNA genetic algorithm uses the form of DNA encoding and the base string composed of four bases ACGT to represent the candidate solutions to the problem. The specific encoding and decoding methods are different. An encoding is to mimic the process of biological genetic base codon determines the amino acid. In this algorithm, if a problem self-variable have three nucleotides encoding, we can get the codon corresponding to amino acid through codon and amino acid table(as table 1). Different amino acids may correspond to an integer of between [-9,9], and then mapped to the interval of the independent variable changes by this integer, thereby obtaining the argument corresponding real digital.

Table 1. Codon and amino acid comparison table

First Nucleotide5′	Second Nucleotide				Third Nucleotide 3′
	U	C	A	G	
U	Phenylalanine	Serine	Tyrosine	Cysteine	U
	Phenylalanine	Serine	Tyrosine	Cysteine	C
	Leucine	Serine	Termination codon	Termination codon	A
	Leucine	Serine	Termination codon	Tryptophan	G
C	Leucine	Proline	Histidine	Arginine	U
	Leucine	Proline	Histidine	Arginine	C
	Leucine	Proline	Glutamine	Arginine	A
	Leucine	Proline	Glutamine	Arginine	G
A	Isoleucine	Threonine	Asparagine	Serine	U
	Isoleucine	Threonine	Asparagine	Serine	C
	Isoleucine	Threonine	Lysine	Arginine	A
	Methionine	Threonine	Lysine	Arginine	G
G	Valine	Alanine	Aspartate	Glycine	U
	Valine	Alanine	Aspartate	Glycine	C
	Valine	Alanine	Glutamate	Glycine	A
	Valine	Alanine	Glutamate	Glycine	G

The other encoding is using the base string of a certain length to represent one independent variable of the problem, then accordingly changing the four bases into four numbers, namely 0, 1, 2, 3, thus turning a base string into a quaternary numeric string. First calculating the bit weighting of the individual genes, and weights for the four hex, and then mapped to the interval of the independent variable changes resulting integer .The accuracy of this encoding is determined by the length of the base string corresponding to each independent variable. When the same coding length is higher than the accuracy of the binary encoding, with the introduction of complex genetic operation, it is more suitable for solving optimization problems. Most of the DNA genetic algorithm operators are still simple crossover operators, mutation operators and inversion operators.

Based on the above analysis, DNA genetic of algorithm is studied and applied to clustering analysis, and fuzzy C-means clustering algorithm of DNA genetic algorithm is put forward.

Crossover operator: For each selected for breeding, which part of the DNA strand interchangeable, to produce a new strand of DNA through the cross, the cross-way single-point crossover and multi-point crossover.

Single point crossover: For example1: ACGTGTTGAAC CCGGTAACGA 2: CGTAGCTGGA GGTACCCTGA

Sequences 1 and 2 cross-operation: 1’ ACGTGTTGAAC GGTACCCTGA 2’ CGTAGCTGGA CCGGTAACGA

Mutation operator: selected DNA chain base in the position of a gene mutation for another base.

For example: the sequence ACGTGTTGAAC CCGGTAACGA mutation operation ACATGTCGAAC CGCGTACCGA

Inversion operator: the inversion of the order of a certain period of the nucleotide sequence in the individual.

For example: ACGTGTTGAAC GGTACCCTGA inversion operation CAGTGTTGAAC GGTACCCTGA

3 Fuzzy C-Means Clustering Algorithm of DNA Genetic Algorithm

3.1 The Basic Algorithm Flow

(1) Fitness Function

The fitness function is used to evaluate the fitness of individuals, and distinguish the pros and cons of the individuals of the populations. For the fuzzy clustering of objective function, the smaller the objective function is, the better the effect of clustering is. The DNA genetic algorithm clustering analysis of fitness should be at maximum. So you can use the objective function to define the fitness function.

$$F(\mu, C) = \left(\sum_{j=1}^{C}\sum_{i=1}^{N}\mu_{ij}^{g} d_{ij}^{2}\right)^{1}. \tag{3}$$

Here g is the given constant, and μ_{ij} is indicated that as:

$$\begin{cases} \mu_{ij} = \dfrac{1}{\sum_{m=1}^{C}\left(\dfrac{d_{ij}}{d_{im}}\right)^{\frac{2}{g-1}}} \cdots\cdots\cdots \text{when} \quad I_k \neq \varnothing \\ \mu_{ij} = 0, \forall i \in \overline{I}_k, \sum_{i \in I_k} u_{ik} = 1 \quad \text{when} \quad I_k = \varnothing \end{cases} \tag{4}$$

(2) DNA Encoding and Decoding

In this paper, the DNA encoding is used in the DNA genetic clustering. The cluster center is considered as the chromosomal DNA encoding, and a chromosome is considered as a string that consists of C cluster centers. As for Class C clustering analysis for the L-dimensional sample data, the chromosome structure that is based on the cluster center of the chromosome is:

$$S = \{x_{11}, x_{12}, \cdots, x_{1L}, x_{21}, x_{22}, \cdots, x_{2L}, x_{C1}, x_{C2}, \cdots, x_{CL}\}.$$

Every chromosome is a DNA encoding with the length $C \times L$.

(3) Population Initialization
After determining the encoding, population initialization should get started, and the maximum iteration algebra is set. The initialization process is to randomly generate an initial population. Select from the sample space of k individuals, whose values are determined by the users. Each individual means an initial cluster center. Repeat Size chromosome initialization process (Size for population size) until the initial population is generated.

(4) Selection Operation
In the process of biological evolution, the species that have the strong ability to adapt to the living environment will have more opportunities to pass on to the next generation, while the opportunity for those species with poor ability is relatively small. Choices of operation are built on the evaluation of individual fitness, and its purpose is to avoid gene deletion and to improve the global convergence and computational efficiency. This article will take the optimal retention policy.

(5) Crossover Operation
The crossover operation is to sufficiently replace the individual part of the structure of the two paternal, to generate new individuals operating. Its purpose is to produce new individuals for the next generation, and the crossover operation is a key part of the genetic algorithm. Chromosome takes cluster center matrix as the gene, which results in the disorder of the gene string. The information between the two chromosomal alleles are not necessarily related, so if you are using the traditional crossover operator to cross, resulting in chromosomal crossover, the adaptive value of individuals of the next generation is generally poor. It will affect the efficiency of the algorithm. This article takes a randomized crossover method.

(6) Mutation Operation and the Inversion Operation
Mutation operation is the locus of the gene values in the individual chromosome encoded string with the locus of certain allelic replacement to form a new individual. It has two purposes: First, the enhancement of local search ability of the algorithm; the second, the increase of the diversity of the population in order to change the performance of the algorithm and to avoid premature convergence. The mutation operator can produce populations of new genes. This is random mutation operation. Inversion operation and mutation operators can generate new gene-rich genetic diversity and is more effective in preventing the genetic algorithm from the local optimum.

(7) Evolutionary Process
Evolutionary process includes the selection, crossover, mutation and inversion operation of chromosomes of the populations, and then calculates the fitness of each individual, and finds the corresponding fitness. And find the individual of the best fitness to replace the individual of the worst fitness in the last evolutionary process, in order to achieve the survival of the fittest.

(8) Clustering Based on DNA Genetic Algorithm to Identify the Cluster Center
After the evolution of the maximum number of iterations, the chromosome of the best fitness in the population can be calculated. Decode the cluster center, divide the clustering and output of the clustering results.

4 Algorithm for the Simulation Experiment

In order to verify the validity of the above algorithm, we use the matlab simulation experiment. For example, we use the fix (rand (100, 2) * 100), and randomly generate 100 two-dimensional coordinates of range of [0,100].

The data distribution is shown in Figure 2:

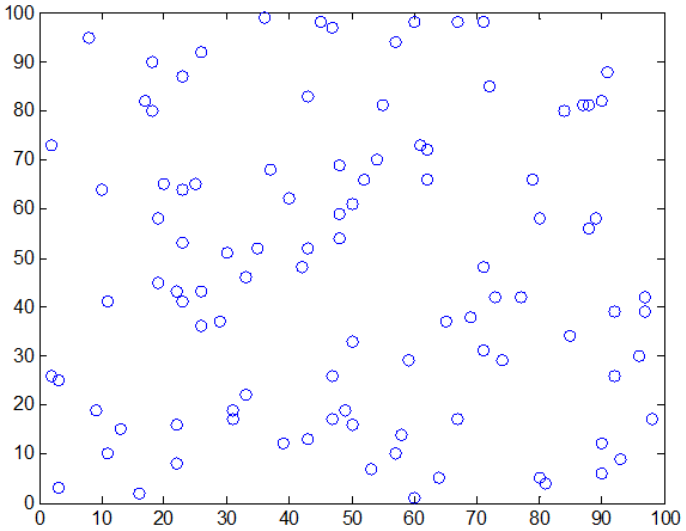

Fig. 2. Random data distribution map

Use the fuzzy C-means clustering analysis of DNA genetic algorithm and divide the sample into three categories. The accuracy of the cluster center is assumed to be $\Delta=0.0001$, g = 2.

4.1 Using Matlab for Fuzzy C-means Clustering Analysis Based on DNA Genetic Algorithm

(1) Initial Data

Suppose the population size is 20, the maximum iterative algebra is 300, and crossover probability is 0.9 (the general election in [0.8, 1]). The mutation probability is 0.1 and the inversion probability is 0.1.

(2) DNA Encoding and Population Initialization

The mapping used in this paper is 0123/CGAT. We use (3.3) to calculate the weight of a vector is 11, so the length of the chromosome is 66. We may randomly set up a DNA sequence: ACTGCTAGCTC GAGCGAGCTGT CGAGAGTGAGT AGTCGATGTAA GTTGAGGTTAC GTTGGGCCAAG, which corresponds to the cluster center $(x_{11,}, x_{12}, x_{21}, x_{22}, x_{31}, x_{32})$.

(3) Selection, Crossover, Mutation and Inversion Operation

Based on chromosome sequence of DNA, we can calculate the value of the fitness of each chromosome according to the fitness function

$$F(\mu, C) = \left(\sum_{j=1}^{C} \sum_{i=1}^{N} \mu_{ij}^{g} d_{ij}^{2} \right)^{1} \tag{5}$$

Use elitist to reserve the best fitness value to the next, and roulette wheel selection method to select the operation, and then have cross-operation. Cross option is to use a randomized crossover to retain the best individual. Then have the mutation operation, with the random mutation operator. The last is the inversion operation, which changes the richness of the chromosome. And then we have the next generation of choice until you reach the maximum number of iterations.

(4) Matlab Simulation Results

The output cluster centers is (81.6149, 34.0188;45.9856, 76.7724; 32.0342, 24.6727) and the changes of optimal fitness function is shown in Figure 3:

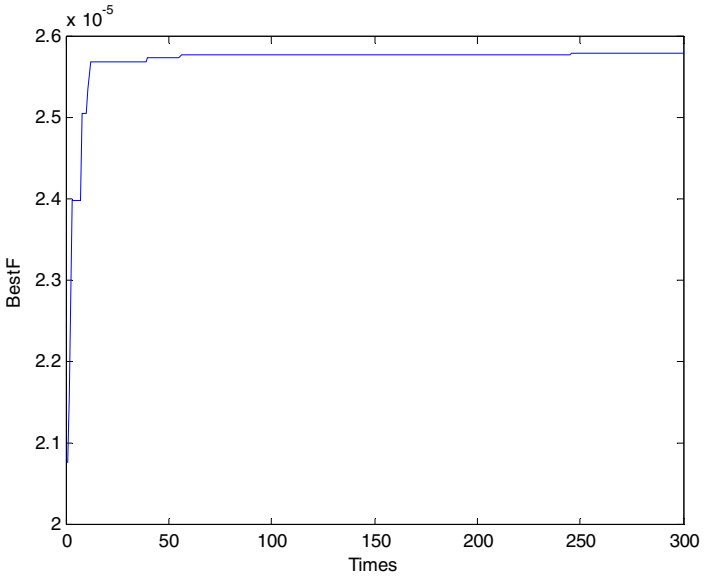

Fig. 3. The optimal fitness function

4.2 Fuzzy C-Means Clustering Analysis Using Matlab Genetic Algorithm

Matlab is used to analyze fuzzy C-means clustering (GAFCM) of genetic algorithm. After 300 iteration, the cluster centers are (56.4638,74.1085; 71.9277,20.7768; 25.5475,27.1473), and the best fitness function changes are shown in Figure 4 shows:

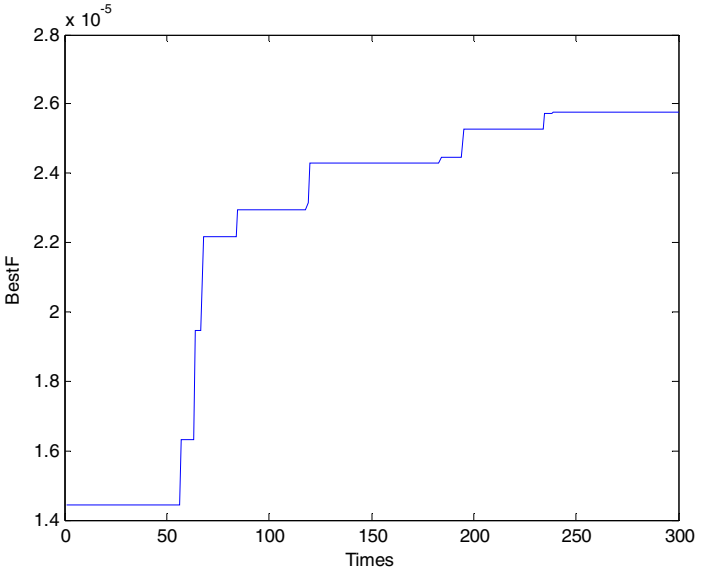

Fig. 4. GAFCM modest function changes

We have simulation, and comparison between genetic algorithm fuzzy C-means clustering analysis (GAFCM) and DNA genetic algorithm, fuzzy C-means clustering analysis. Simulate at random for 10 times, 20 times, 30 times respectively, and calculate the average number of iterations to achieve the fitness function 2.55e-5, FCM and DNAGAFCM. They are shown in Table 3:

Table 2. GAFCM and DNAGAFCM average number

	GAFCM	DNAGAFCM
10	243	101
20	221	109
30	228	111

We can know from the table the average number of iterations when DNAGAFCM algorithms achieve the optimal solution, and compare with GAFCM algorithm. There is a large reduction in the number of iterations of the DNAGAFCM algorithm. The simulation does not show the powerful parallel computing capabilities of DNA computing. At the same time, we find through experiments that the change of population size, mutation probability, crossover probability will have a great impact on algorithm iterations. As the data dimension and the raw data increase, we find that the DNA genetic algorithm will have better performance.

5 Conclusion

This paper presents a combination of DNA genetic algorithms and clustering analysis algorithm, which overcomes the slow convergence characteristics of local clustering analysis. The experiments show that the algorithm has its advantage of reducing the number of iterations and improving the clustering performance in solving the problem of clustering. The algorithm actually combines the DNA genetic algorithm and clustering analysis and takes advantage of the advantages of both. With the development of DNA computing, parallelism of DNA computing is brought into full play, which will be more conducive to use this method. The algorithm proposed in this paper provides a good reference when deal with the issue of large data clustering analysis. However, DNA genetic algorithm has some limitations, namely, whether it is the operating change in the approach, or the change of mutation probability or population size, the number of iterations of the algorithm will be influenced. It needs our further exploration to overcome this limitation.

Acknowledgment. The research is supported by the National Science Foundation of China (No: 61170038, No.60873058, No: 11171193), the Natural Science Foundation of Shandong Province (No:ZR2011FM001) and College Science and Technology Project of Shandong Province(No:J12LN65).

References

1. Lu, H., Fang, W.: Join transmit/receive antenna selection in MIMO systems based on the Priority-based genetic algorithm. IEEE Antennas and Wireless ProPagation Letters 6, 588–591 (2007)
2. Ranagou, E.Z., Kodogiannis, V.S.: Application of neural networks as a non-linear modeling technique in food mycology. Expert Systems with Applications 36(l), 121–131 (2009)
3. Fernanoez, A., Jesus, M., Herra, F.: On the 2-tuples based genetic tuning Performance for fuzzy rule based classifications systems in imbalanced data-sets. Information Sciences 180(8), 1268–1291 (2010)
4. Chen, X., Wang, N.: A DNA based genetic algorithm for parameter estimation in the hydrogenation reaction. Chemical Engineering Journal 150, 527–535 (2009)
5. Yongjie, L., Jie, L.: A feasible solution to the beam-angle-optimization problem in radiotherapy planning with a DNA-based genetic algorithm. IEEE Transactions on Biomedical Engineering 57, 499–508 (2010)
6. Zhao, Y.-Q., Jin, X.-H., Liu, Y.: The preemptive EDF optimization based on DNA-genetic algorithm. In: 2010 2nd Conference on Environmental Science and Information Application Technology, ESIAT 2010, vol. 2, pp. 121–124 (2010)
7. Xu, G., Yu, J.: Optimal Design of TS Fuzzy Control System Based on DNA-GA and Its Application. In: Li, K., Fei, M., Irwin, G.W., Ma, S. (eds.) LSMS 2007. LNCS, vol. 4688, pp. 326–334. Springer, Heidelberg (2007)
8. Wang, K., Wang, N.: A protein inspired RNA genetic algorithm for parameter estimation in hydrocracking of heavy oil. Chem. Eng. J. 167, 228–239 (2011)
9. Zhou, K., et al.: Closed circle DNA algorithm of eight queens problem. Computer Engineering and Application 43(4), 4–6 (2007)

10. Zhou, K., et al.: Algorithm of maximum independent set problem based on closed circle DNA computing. Computing Engineering 34(4), 40–44 (2008)
11. Zhang, L., Wang, N.: A modified DNA genetic algorithm for parameter estimation of the 2-Chlorophenoloxidation in supercritical water. Appl. Math. Modell. (2012)
12. Zhao, J., Wang, N.: A bio-inspired algorithm based on membrane computing and its application to gasoline blending scheduling. Comput. Chem. Eng. 35, 272–283 (2011)
13. Wang, K., Wang, N.: A novel RNA genetic algorithm for parameter estimation of dynamic systems. Chem. Eng. Res. Des. 88, 1485–1493 (2010)
14. Bakar, R.A., Watada, J.: A Biologically Inspired Computing Approach to Solve Cluster-Based Determination of Logistic Problem. Biomedical Soft Computing and Human Sciences 13(2), 59–66 (2008)
15. Bakar, R.A., Watada, J., Pedrycz, W.: DNA approach to solve clustering problem based on a mutual order. Biosystems, 1–12 (2008)

Massive Electronic Records Processing for Digital Archives in Cloud

Zhang Guigang[1], Xue Sixin[2,3], Feng Huiling[2], Li Chao[1], Liu Yuenan[2], Yong Zhang[1], and Chunxiao Xing[1]

[1] Research Institute of Information Technology, Tsinghua University, Beijing 100084, China
[2] School of Information Resource Management, Renmin University of China, Beijing, 100872, China
[3] Archives of Tsinghua University, Tsinghua University, Beijing, 100084, China
guigang@tsinghua.edu.cn

Abstract. With the development of cloud technologies, more and more electronic records will be stored and processed in the cloud. In order to manage massive electronic records, a kind of storage system named CloudDA is proposed in cloud environment in our paper. In the CloudDA, the HUABASE database and the THCFS file system are designed. HUABASE is used to store all kinds of structured data such as the metadata and index information. And the THCFS is used to store massive archives files. Finally, we design a kind of massive electronic records processing prototype system for digital archives in the cloud.

Keywords: Cloud computing, Electronic commerce, Data storage.

1 Introduction

Cloud computing is playing a more and more important role in the data intensive applications such as massive data processing, massive data storage and massive data analysis etc. As the other data intensive applications, the traditional archive management system is not suit for the requirements of Web users. In order to address massive digital records management and provide services better, the traditional archives management systems, such as the digital library and digital archives applications, are suggested to transplant into the cloud environment. As we know, the big challenges of the digital archives management applications can be summarized into the following several aspects:

(1) How to store and preserve massive electronic records in digital archives? In order to store these massive data through the data intensive applications, lots of distributed files systems and cloud databases are developed. Such as the Google's GFS [1], Hadoop HDFS [2], Haystack [3], Hypertable[4] and Taobao FS etc. HDFS and Hypertable are the variants of GFS. They use the single metadata node and their replicas are 3. They provide the API interface for other applications to access them. HDFS is the open source version of GFS. And now, lots of applications use the HDFS

Q. Zu, B. Hu, and A. Elçi (Eds.): ICPCA-SWS 2012, LNCS 7719, pp. 814–829, 2013.

to deploy their storage cluster. Hypertable is used by Baidu. Baidu Company uses it to store massive digital files. Haystack is used to store massive photos in the Facebook. Taobao FS is developed by Taobao Company. All these non-structured data can be stored by distributed file systems. However, there are still some structured data need to store into databases. Google's BitTable[5], Hadoop Hbase[6] ,Cassandra[7] , Megastore[8] ,Dynamo[9] and HadoopDB[10] are some famous cloud databases.

(2) How to process data intensive computing tasks in the digital archives system? According to the international standard of OAIS [11], the massive records or archives' metadata and entities need to be processed by several steps. First, SIP should be created (Submission information package). Second, archives administrators need to add some new information and metadata based on the SIP and inform an AIP (archives information package). Finally, these AIP package should be packaged into the DIP (Dissemination information package) package according user's individual demand. All these DIP packages can be utilized by all kinds of end-users. According the OAIS model, the process from the original digital information into the SIP package, from the SIP package into the AIP package and from the AIP package into the DIP package need to use a data packaging standard such as VERS2.0[12] or "Onion" model. From the former description, it is found that computing tasks (packaging all kinds of information of electronic records entity and metadata) is very big. So it needs to improve the processing speed using the cloud technologies such as the computing resources virtualization by the VMware Vsphere4 [13], OpenStack[14] or eucalyptus[15] etc.

(3) How to ensure the security of electronic records in digital archives system? Massive records' data security is very important in the cloud environment. In order to ensure the cloud electronic records' security and evidence, the PKI security technologies and framework are suggested to adopt.

All these challenges will become more and more salient with the appearance of massive electronic records, especially the requirements of transferring these large numbers of electronic records into the digital archives for long-term preservation. Fortunately, the cloud computing technology can provide the relevant solutions for these challenges. In this paper, a digital archives system framework in the cloud, named CloudDA, is designed. CloudDA is composed of massive electronic records storage, electronic records processing workflow and massive electronic records security assurance. The THCFS cloud file system based on the Hadoop DFS and a relational database HUABASE are and applied to store massive records. HUABASE is used to store the structured data such as the metadata information and some index information of massive records.

The rest of this paper is arranged as follows, section 2 begins with the designing of CloudDA framework based on the software engineering approach. Section 3 introduces the HUABASE and THCFS (Tsing Hua Cloud File System) to address the emerging massive records storage problems. Finally section 5 concludes this paper with a discussion of its contribution and future work.

2 Framework of CloudDA

Figure 1 illustrates the framework of CloudDA. CloudDA can be processed by three roles: Records creator, Records manager and Records user. And In the CloudDA

framework, OAIS model is abided and it involves three kinds of important information packages, which are the SIP (Submission Information Package), AIP (Archive Information Package) and DIP(Distributed Information Package) packages.

- Part 1: Records creator. Creators or filing people firstly capture, extract and arrange each electronic records and its metadata according to the OAIS and others standards from the business system. Secondly, creators make or computer digital abstract for the big records using a hash function. （Records creator compute the digital archives and its metadata's）. Then the records creator package the electronic records entity, metadata and digital abstract of records into a SIP package using related standard, such as VERS2.0, "Onion" model or the others methods(this paper using DA/T48-2009, a archives industry standard in china).
- Part 2: Records manager. When SIP packages are received by archives department, records managers working in archives should first un-package the SIP, and verify the integrity of SIP packages. Usually, managers need to add some new archival information such as transferring records and file number etc. And then, managers create AIP package for long-term preservation according to the DA/T48. Sure of course, the AIP package maybe update or migrate in the future, and so AIP need to be verified itself by the archive managers at some time. For example, when AIP package is published into the DIP package, the archive manager needs to verify the AIP. From the figure 1, in the part 2, all data storage and processing are based on the cloud environment. In order to store PB, even EB records, this paper designs a cloud file system, named THCFS (Tsing Hua Cloud File System) and introduce it in section 3. At the same time, in order to execute very big computing tasks, all computing resources are virtualized using the open source tool OpenStack.
- Part 3: User. If the user wants to utilize the records in digital archives, the DIP package is created and distributed. All of users maybe the personnel user (public person) or institutional users and they are granted various access rights by system specification or legal permission

From the part 1 to part 2 and from the part 2 to the part 3, it needs to ensure their security transport because transmission usually crosses networks between units. So the VPN technology is suggested to use.

In order to store massive electronic records, a database is needed to store the massive electronic records' metadata and a cloud file system (distributed file system) is needed to store massive electronic records' entity. In this paper, HUABASE, a kind of column-based database developed by Tsinghua University is applied and THCFS, a kind of cloud file system is introduced. THCFS is designed based on the Hadoop distributed file system.

The virtualization of PaaS layer (storage layer) can be solved by the cloud file system THCFS and the virtualization of IaaS lay (computing layer) can be solved by the open source tools OpenStack.

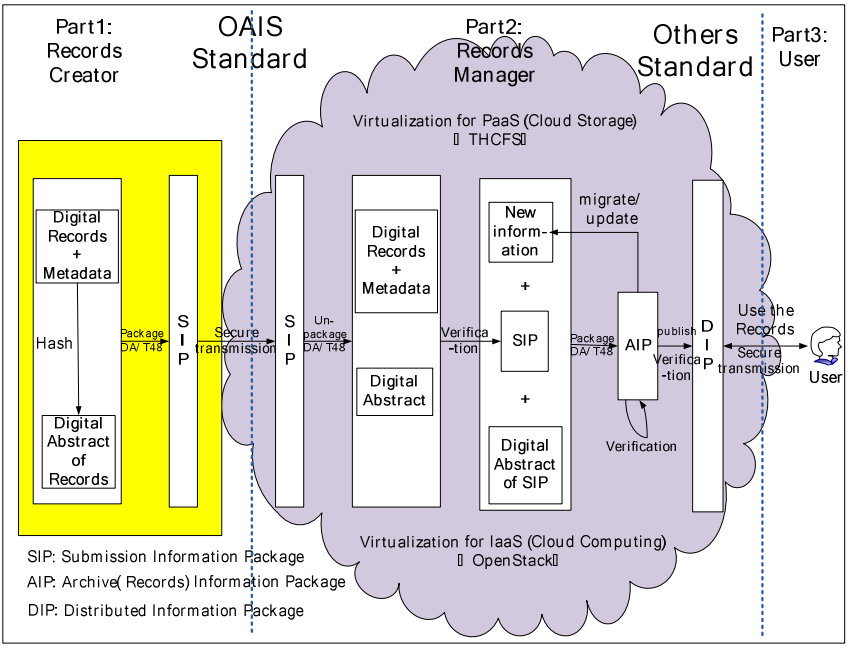

Fig. 1. Framework of CloudDA

3 Cloud Storage of Massive Electronic Records

To store the massive electronic records is a very important part in CloudDA. As introduced in the section 2, HUABASE is used to store the structured data such as the records' metadata and their massive index information..And THFS cloud file system is designed based on the Hadoop DFS,but different from the Hadoop DFS, to cooperate with HUABASE.

Distributed file systems are used to store massive data files and records in the cloud. The most important distributed file systems have GFS, HDFS and KFS etc. Unlike the Hadoop DFS and Google's GFS, the THCFS has not metadata node but design some supercomputing nodes. The supercomputing nodes can help the query requests to find the data's storage locations and arrange the new storage locations when some new records data arrived.

3.1 HUABASE

HUABASE [16] is a relational database based on the column-based storage. Tsinghua University has developed the first version of HUABASE in 2010 and 2011.Now, the second version is published and it can run on top of THCFS file system. HUABASE has a good feature at some analysis applications. For example, it can improve the processing speed a lot when executing some complex query processing. This research uses HUABASE database to store the massive archives metadata and all files' index information.

3.2 THCFS

Although the Google's GFS and Hadoop's HDFS has gained a very big successful, however they can't process the users' large numbers of ad hoc queries as soon as possible. In order to satisfy the users' ad hoc queries requirements, this paper designed a kind of new cloud file system, named THCFS. THCFS is composed by the following three parts.

- Electronic records storage path judgments algorithm. It is the key part of THCFS. The records entities' storage locations are decided by this algorithm.
- Super nodes. They will store all electronic records' metadata information and storage entities' locations in the data nodes.
- Data nodes. All the electronic records entities are stored in these data nodes include the word, Jpeg, video and audio files formats and so on.

(1) The Writing Process of THCFS

Figure 2 shows the writing process of THCFS.

- Step 1: Input massive electronic records into the path judgment algorithm.
- Step 2: Update the Records-SuperNode Mapping table.
- Step 3: The super node cluster response the storage locations of electronic records' metadata.

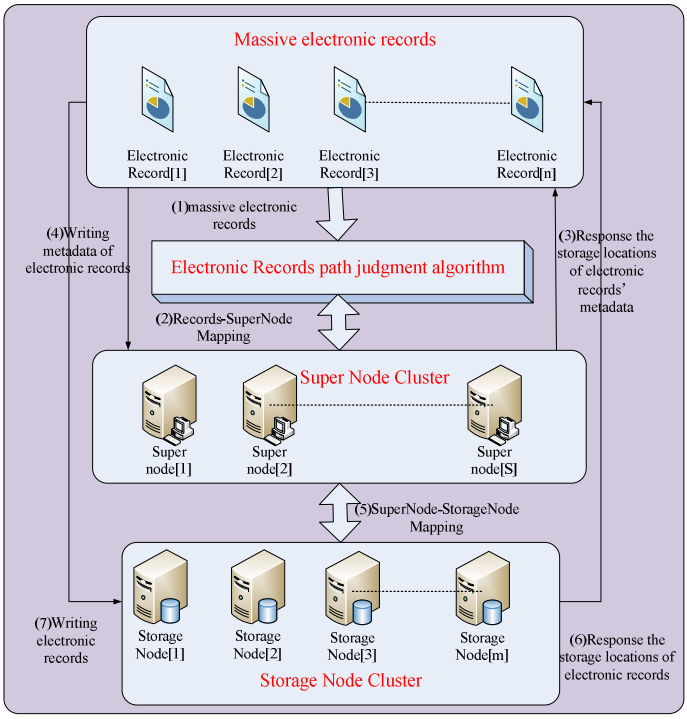

Fig. 2. Writing process of THCFS

- Step 4: Every one of the electronic records' metadatas are written into one of the processors in the super node cluster.
- Step 5: Update the SuperNode-StorageNode Mapping table.
- Step 6: The storage node cluster response the storage locations of electronic records entities.
- Step 4: every one of the electronic records' entities are written into one of the processors in the storage node cluster.

(2) The Query Process of THCFS

The figure 3 shows the query process of THCFS. It includes five steps as following.

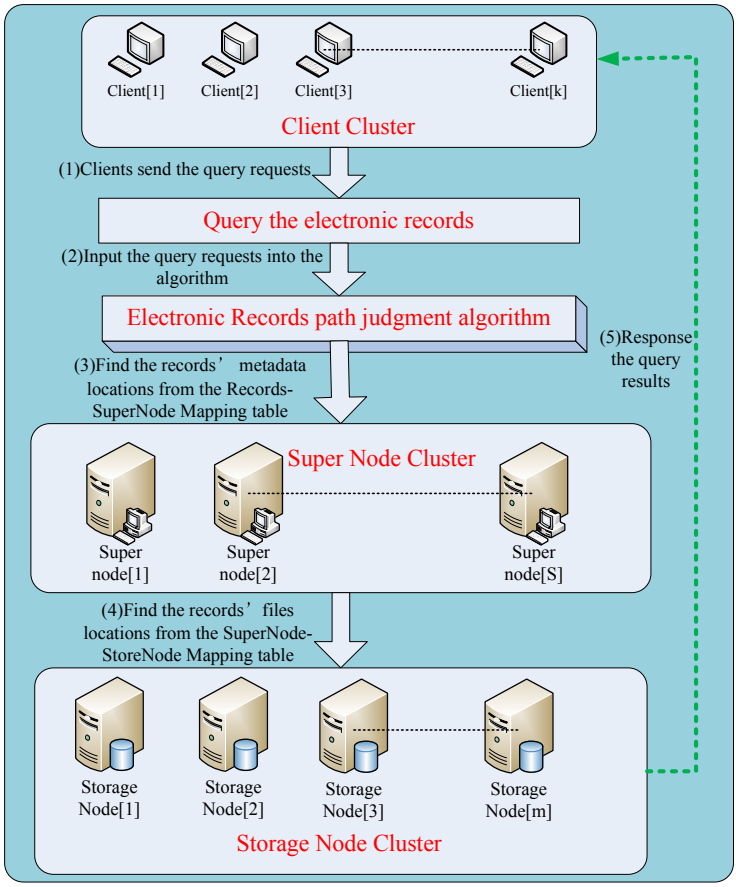

Fig. 3. Query process of THCFS

- Step 1: Clients send the users' query requests. Lots of query requests are the ad hoc queries, and so it need the THCFS can process these requests speedily.
- Step 2: The query requests will be processed by the electronic records path judgment algorithm.

- Step 3: Find the electronic records' metadata locations from the Records-SuperNode Mapping table.
- Step 4: Find the electronic records' entity locations from the SuperNode-StoreNode Mapping table.
- Step 5: Response the query results to the clients (users).

3.3 Electronic Records' Entity Name

In order to improve the processing speed, Electronic records entity is specified according the following rules.

Rule 1: [The Name Rule of Electronic Records Entity]
[Type][Year][Month][Day][Hour][Minute][Second][Serial number].[File extension name]

(1) Type include {P, E,……, M}
- P: political type;
- E: education type;
- M: military type.

(2) Year. It indicates the created year of the electronic records entity.
(3) Month. It indicates the created month of the electronic records entity.
(4) Day. It indicates the created day of the electronic records entity.
(5) Hour. It indicates the created hour of the electronic records entity.
(6) Minute. It indicates the created minute of the electronic records entity.
(7) Second. It indicates the created second of the electronic records entity.
(8) Serial number. It indicates the created serial number of the electronic records entity.
(9) File extension name. It indicates the created file extension name of the electronic records entity.

For example, the following two items are two electronic records' entities name.

File 1: P20120330180808123456.pdf
File 2: E20120331200855000008.doc

3.4 Three Key Algorithms of THFS

In figure2 and figure3, there are three key algorithms in the THCFS cloud file system. These three algorithms can be described as the follows. Electronic records judgment algorithm, the assignment algorithm between the massive electronic records' metadata and the super node cluster and the assignment algorithm between the massive electronic records entity and storage node cluster.

(1) [Algorithm 1] Electronic Records Judgment Algorithm

The objective of this algorithm is to find the classification for every electronic record which will be input into the cloud environment.

The figure 4 shows the basic principle of algorithm 1. There are n numbers of electronic records need to be classify into p groups according to our classification rules designed before. The algorithm displays the classification method.

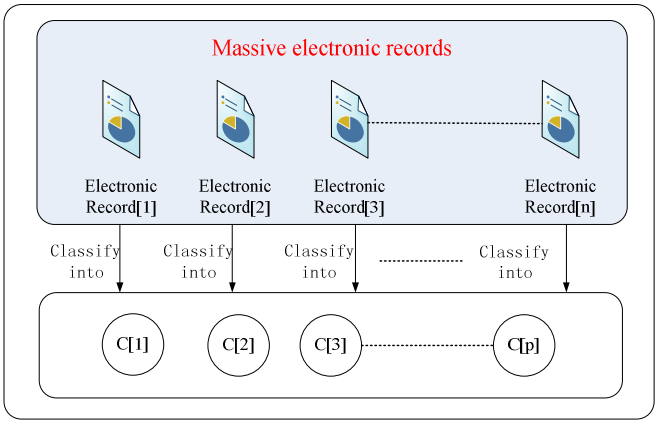

Fig. 4. Principle of Algorithm 1

Input: Massive electronic records.

Output: The classification of massive electronic records.

[1] Start

[2] For (i=0; i<MassiveElectronicRecords.Number; i++) // construct the loop of massive electronic records.

[3] For (j=0; j<ElectronicRecordsType.Number; j++) // construct the loop of massive electronic records' file classification.

[4] {

[5] If (ElectronicRecords[i] is belong to the Classfication[j])

[6] System.Out.println("The electronic"+ ElectronicRecords[i]+ " is belong to the classification"+ Classfication[j]);

[7] j++; // loop for the electronic records classification.

[8] }

[9] i++; // loop for the electronic records entity.

[10] }

[11] End //every electronic record file have been assigned the file classification and end the program.

(2) [Algorithm 2] The Assignment Algorithm between the Massive Electronic Records' Metadata and the Super Node Cluster

The objective of this algorithm is to find the mapping relationships between the massive electronic records' metadata and the super node cluster. And this algorithm

will assign the massive electronic records' metadata into the super node cluster according to the relationship.

(1) There are p groups, they are the $\{C[1], C[2], \ldots\ldots, C[p]\}$

(2) The electronic records 'metadata numbers of Group $\{C[1], C[2], \ldots\ldots, C[p]\}$ are $\{P[1], P[2], \ldots\ldots, P[p]\}$.

(3) There are S numbers of super nodes, they are the $\{SuperNode[1], SuperNode[2], \ldots\ldots, SuperNode[S]\}$

(4) The objective of this algorithm is to assign all the electronic records' metadata into the super node cluster $\{SuperNode[1], SuperNode[2], \ldots\ldots, SuperNode[S]\}$.

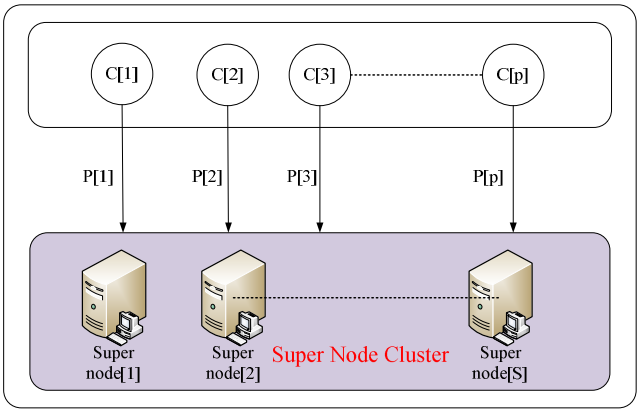

Fig. 5. Principle of Algorithm 2

Input: $\{C[1], C[2], \ldots\ldots, C[p]\}$, $\{P[1], P[2], \ldots\ldots, P[p]\}$ and $\{SuperNode[1], SuperNode[2], \ldots\ldots, SuperNode[S]\}$.

Output: The assignment result.

[1] Start

[2] For (p=0; p<ClassificationNumber.Length; p++)//construct the loop for the classification numbers.

[3] For (S=0; S<SuperNode.Lengteh; S++0)//construct the loop for the super nodes' numbers.

[4] {

[5] If (S==p)//if the numbers of super nodes is equal to the numbers of groups, then assign every group electronic records' metadata are assigned into every super node.

[6] {

$C[1]$—>Super Nbde[1] ;

$C[2]$—>Super Nbde[2] ;

[7] ……

$C[p]$—>Super Nbde[S] ; (p==S)

[8] }

If (S>p) // if the numbers of super nodes is more than the numbers of groups, then assign every group electronic records' metadata are assigned into every super node according to the order.

[9] {

$C[1]$—>Super Nbde[1] ;

$C[2]$—>Super Nbde[2] ;

[10] ……

$C[p]$—>Super Nbde[p] ; (p<S)

[11] }

[12] If (S<p)// if the numbers of super nodes is less than the numbers of groups, it will be the most complex assignment method.

[13] {

[14] ElectronicRecordsTotalNumber=

$Electronic\,\mathrm{Re}\,cordsNumber = \sum_{i=1}^{p} p[i];$ //computing the whole numbers of electronic records.

[15] $A\mathrm{v}erageNumber = Electronic\,\mathrm{Re}\,cordsNumber / S;$ //compute the ideal average workload numbers of every super node.

[16] Find all these groups $\{G(1), G(2), \ldots\ldots, \mathrm{G(g)}\}$, which electronic records numbers is more than $A\mathrm{v}erageNumber$;

$G[1]$—>Super Nbde[1] ;

$G[2]$—>Super Nbde[2] ;

[17] ……

$G[g]$—>Super Nbde[g] ; (g<S)

//assign all groups a super node for every group that satisfies the condition in the step 16.

[18] LeftClassificationGroup=p-g;//compute the groups' numbers which still not be assigned.

[19] LeftSuperNodeNumber=S-g; //compute the super nodes' numbers which still not be assigned the workload.

[20] Complete the assignment that according to the step 13 to step 19;

[21] }

[22] }

[23] End //every electronic record file have been assigned the file classification and end the program.

(3) [Algorithm 3] The Assignment Algorithm between the Massive Electronic Records entity and Storage Node Cluster

The objective of this algorithm is to find the mapping relationships between the massive electronic records and the storage node cluster. And this algorithm will assign the massive electronic records' entity into the storage node cluster according to the relationship.

(1) There are p groups, they are the $\{C[1], C[2], \ldots\ldots, C[p]\}$

(2) The electronic records ' metadata numbers of Group $\{C[1], C[2], \ldots\ldots, C[p]\}$ are $\{P[1], P[2], \ldots\ldots, P[p]\}$.

(3) There are S numbers of super nodes, they are the $\{StorageNode[1], StorageNode[2], \ldots\ldots, StorageNode[m]\}$

The objective of this algorithm is to assign all the electronic records' entity into the super node cluster $\{StorageNode[1], StorageNode[2], \ldots\ldots, StorageNode[m]\}$.

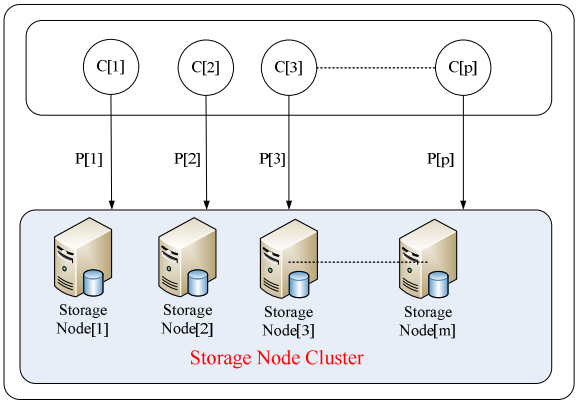

Fig. 6. Principle of Algorithm 3

Input: $\{C[1], C[2], \ldots\ldots, C[p]\}$, $\{P[1], P[2], \ldots\ldots, P[p]\}$ and $\{StorageNode[1], StorageNode[2], \ldots\ldots, StorageNode[m]\}$.

Output: The assignment result.

[1] Start

[2] For (p=0; p<ClassificationNumber.Length; p++)//construct the loop for the classification numbers.

[3] For (m=0; m<StorageNode.Lengteh; m++0)// //construct the loop for the super nodes' numbers.

[4] {

[5] If (m==p)// if the numbers of storage nodes is equal to the numbers of groups, then assign every group electronic records' data are assigned into every storage node.

[6] {

[7] $C[1]\text{—>}StorageNode[1];$
$C[2]\text{—>}StorageNode[2];$
……
$C[p]\text{—>}StorageNode[m];\ (p==m)$

[8] }

If (m>p) // if the numbers of storage nodes is more than the numbers of groups. It has very big difference with the algorithm 2.

[9] {

[10] ElectronicRecordsTotalNumber=
$ElectronicRecordsNumber = \sum_{i=1}^{p} p[i];$ //compute the whole numbers of the electronic records.

[11] $AverageNumber = ElectronicRecordsNumber / S;$ // compute the ideal average workload numbers of every storage node.

[12] Find all these groups $\{Q(1), Q(2), \ldots\ldots, Q(q)\}$, which electronic records numbers is less than $AverageNumber$.

[13] $Q[1]\text{—>}StorageNode[1];$
$Q[2]\text{—>}StorageNode[2];$ // assign all groups a storage node
……
$Q[q]\text{—>}StorageNode[q];\ (q<m)$
for every group that satisfies the condition in the step 12.

[14] LeftClassificationGroup=p-t;// compute the groups' numbers which still not be assigned.

[15] $ElectronicRecordsNumber1 = \sum_{i=1}^{p-t} p[i]$; Compute the electronic records entity numbers of the left p-t groups;

[16] LeftStorageNodeNumber=m-q; // compute the storage nodes' numbers which still not be assigned.

[17] $AverageNumber1 = ElectronicRecordsNumber1 / m - q$; // compute the ideal average workload numbers of every storage node.

[18] For (r=0;r<p-t;r++)

[19] {

[20] P[r]/ $AverageNumber1$>w;//w is a integer ;

[21] Assign w+1 storage nodes to C[r]; //assign w+1 numbers storage nodes to the group c[r].

[22] }

[23] Complete all the assignment that according to the step 18 to step 22;

[24] }

[25] If (m<p)// if the numbers of storage nodes is less than the numbers of groups, the method like the algorithm 2 is used.

[26] {

[27] ElectronicRecordsTotalNumber=

$ElectronicRecordsNumber2 = \sum_{i=1}^{p} p[i]$; //compute the numbers of electronic records.

[28] $AverageNumber2 = ElectronicRecordsNumber / S$; // compute the ideal average workload numbers of every storage node.

[29] Find all these groups $\{T(1), T(2), \ldots\ldots, T(t)\}$, which electronic records numbers is more than $AverageNumber$;

[30]
$T[1]$—>StorageNode[1];
$T[2]$—>StorageNode[2];
……
$T[t]$—>StorageNode[t]; (t<S)
// assign all groups a storage node for every group that satisfies the condition in the step 29

[31] LeftClassificationGroup=p-t;// Compute the groups' numbers which still not assign the workload.

[32] LeftStorageNodeNumber=m-t; // compute the storage nodes' numbers which still not be assigned.

[33] Complete the assignment that according to the step 27 to step 32

[34] }

[35] }

[36] End //every electronic record file have been assigned the file classification and end the program.

4 Case Study of Massive Electronic Records Processing in Digital Archives

In order to verify CloudDA system, a basic experiment environment is assembled and a cloud data center is constructed. And the solution is used by Bejing Archives, which will be applied into the electronic records' management of 17 traditional archives in the Beijing.

4.1 Deployment of Infrastructure

The experiment environment has been installed in the Tsinghua University Library. According to the preliminary requirements of Beijing Digital Archives, our prototype system can implement the each step's security verification for the electronic records. And a basic experiment environment is selected to verify the availability of our method.

(1) Hardware

- IBM X3850X5 core servers, 2 devices
- IBM X3650M3 Cloud Servers, 8 devices
- IBM DS5020 storage device, 1device
- Brocade BR-360-0008 Optical switches, 1 devices
- RG-S5750-28GT-L Network switches, 2 devices

(2) Software

- IBM X3850X5 core server, 2device
  - Ubuntu 10.04
  - HUABASE
  - OpenStack Controller Node
- IBM X3650M3 Cloud Environment Servers, 8 devices
  - Ubuntu 10.04
  - OpenStack Compute Node

4.2 The Implementation of Beijing Digital Archives Prototype System

The figure 7 shows the main interface of digital archives prototype system.

Fig. 7. The main interface of Beijing digital archives prototype system

The Beijing archives prototype system mainly includes six parts in the function. They are:

(1) Electronic records submission platform. It takes charge of all electronic records' submission.
(2) Electronic records transmission platform (sender). It takes charge of all electronic records' transmission to receiver.
(3) Electronic records transmission platform (receiver). It takes charge of all electronic records' transmission from sender.
(4) The receiver platform of all electronic recorders in the Beijing digital archives. All electronic recorders will be stored here, including more than 2 millions electronic records' files and 2TB-size electronic records files.
(5) Electronic records management platform. It includes the certification management, user management, system management and electronic records transmission management. The electronic records transmission includes: from the electronic records to the SIP packages, from the SIP packages to the AIP packages and from the AIP packages to the DIP packages.
(6) DIP utilization platform. All authorized users can browser the electronic records.

4.3 The Utilization Effect of the Digital Archives

Our method has been used in the construction of Beijing Digital Archives, 2TB size electronic records and more than 2 million numbers' metadata records of electronic records have been uploaded into our experiment. Our experiment shows that our method is efficient. The verification results can be summarized as the follows. CloudDA framework is running in Tsinghua University Library, it can satisfy the requirements for our experiment for 2TB size electronic records and more than 2 million numbers' metadata records of electronic records. In order to improve the processing efficiency for massive electronic records' encryption computing and decryption computing so on, the cloud technologies are used in our paper. More computers are used to process the massive electronic records' encryption computing and decryption computing. It will improve the processing speed more than 400% than using only one processor to process.

5 Conclusions and Future Work

In this paper, a digital archives system framework (CloudDA) in the cloud is designed. In the CloudDA, the HUABASE database and the THCFS file system are integrated. HUABASE is used to store all kinds of structured data such as the metadata and index information. And the THCFS is used to store massive archives files. In the future, the THCFS's replica strategy research will be focused on. If some records are accessed frequently, some replicas are added and if some records are accessed little, their replicas are reduced.

Acknowledgments. This research was supported by: 1) National Basic Research Program of China (973 Program) No.2011CB302302; 2) The National Natural Science Foundation of China under Grant Nos.61170061.3) Beijing Science and Technology Program "development and application of electronic records evidence protection core technologies based on the heterogeneous systems" No. Z111100075011001.

References

1. Ghemawat, S., Gobioff, H., Leung, S.-T.: The Google File System. In: Proc. of the 19th ACM Symposium on Operating Systems Principles (SOSP 2003), pp. 29–43 (2003)
2. Borthakur, D.: HDFS Architecture (April 2009), http://hadoop.apache.org/common/docs/r0.20.0/hdfs_design.html
3. Beaver, D., Kumar, S., Li, H.C., Sobel, J., Vajgel, P.: Finding a needle in Haystack: Facebook's photo storage. In: OSDI 2010 (2010)
4. [2012-7-20] (July 20, 2012), http://hypertable.org/
5. Chang, F., Dean, J., Ghemawat, S., et al.: Bigtable: A Distributed Storage System for Structured Data. In: Proceedings of OSDI 2006: Seventh Symposium on Operating System Design and Implementation, pp. 205–218 (2006)
6. Sun, J., Jin, Q.: Scalable RDF store based on HBase and MapReduce. In: Advanced Computer Theory and Engineering (ICACTE), pp. 633–636 (2010)
7. Lakshman, A., Malik, P.: Cassandra - A Decentralized Structured Storage System. ACM SIGOPS Operating Systems Review Archive 44(2), 35–40 (2010)
8. Baker, J., Bond, C., Corbett, J.C., Furman, J.J.: Megastore: Providing Scalable, Highly Available Storage for Interactive Services. In: 5th Biennial Conference on Innovative Data Systems Research (CIDR), pp. 223–234 (2011)
9. DeCandia, G., Hastorun, D., Jampani, M., et al.: Dynamo: amazon's highly available key-value store. In: ACM SIGOPS Symposium on Operating Systems Principles, New York, pp. 205–220 (2007)
10. Abouzeid, A., et al.: HadoopDB: an architectural hybrid of MapReduce and DBMS technologies for analytical workloads. In: Proceedings of the VLDB 2009, pp. 922–933 (2009)
11. Reference Model for an Open Archival Information System (OAIS). Recommendation for Space Data System Standards 1, 1–148 (2002)
12. http://prov.vic.gov.au/wp-content/uploads/2012/01/VERS_Advice12.pdf
13. https://www.vmware.com/
14. http://openstack.org/
15. http://www.eucalyptus.com
16. http://www.huabase.cn/product.jsp

Research and Analysis of Method of Ranking Micro-blog Search Results Based on Binary Logistic Model

Jing Zhang[1,2] and Wen-jun Hou[1,2]

[1] Beijing Key Laboratory of Network System and Network Culture
[2] Beijing University of Posts and Telecommunications, Beijing, China
buptzhangjing@gmail.com, wenjunh2113@263.net

Abstract. Ranking results in micro-blog search as user's interests is challenging because of the special form of micro-blog search results. To attempt to solve the problem, in this paper, we summarize the characteristics of micro-blog search results, propose a method using a sort of decision model- binary logistic model, test the confidence level of the model and estimate the weight of the variable in the model collecting the real samples. The result shows the relation between user's decision and the factors from each individual micro-blog search result as well as the feasibility of ranking using the model. We also analyze the model.

Keywords: micro-blog search, binary logistic model, ranking, utility.

1 Introduction

Social search has been the focus of the third-generation search engine and micro-blog search. As a form of social search engine, micro-blog search is considered as the most suitable for the third-generation search engine platform both in the field of research and commercial areas. For now, micro-blog search has played an important role in the local business service and micro-blog marketing. However, at present, a simple search for micro-blogs always returns huge information that cause foraging overload. Therefore to solve the problem, a method of ranking results for web-blog search should be carried out.

The research on ranking search results is mainly focused on two aspects: one is based on the analysis of the links and the other is based on the analysis of the contents. In the research on link analysis, combined with some specific needs for search, large amount of improved algorithms based on PageRank, HITS algorithm are presented: Wang et al. have developed a ranking algorithm implemented to web2.0 community search model[1], and Cheng has proposed a search sorting algorithm based on personalized information model and the PageRank value[2]. Meanwhile, in the research on content analysis, Walisa et al. have studied user behavior patterns in social search, and reordered the search results according to the relation of the user labels and the contents[3], Fan ranks the search results from the blog search by building user interest vectors and comparing the vectors and the contents of the blog articles[4], Li Jing et al. rank the results for the music search on the basis of the

Q. Zu, B. Hu, and A. Elçi (Eds.): ICPCA-SWS 2012, LNCS 7719, pp. 830–842, 2013.

correlation between the user emotional labels and music[5] . From the results of previous studies above, we can conclude that whether link analysis or content analysis, the research on ranking results for search are essentially in terms of the quality of the contents in pages, that is, the results which are considered containing high qualities of the contents by machines or most users are ranked near the top. Besides, almost all the researchers take the traditional Web search engine as their object of research. However as the large differences of the user's backgrounds and preferences, different users tend to choose different results as their best decisions although the queries are the same. So it is unreasonable that the results ranking search only are based on the machine or most of users. Moreover, at present, as there are few researches which are from the point of the view of the individual users' decision on selecting the results for search, such researches are worthy of further exploration.

In this paper, first, we analyzed the characteristics of micro-blog search results. Then with both the users' features and search results considered, a method of ranking results for micro-blog search was proposed based on the utility the results bring to the users, using a typical discrete decision model - binary logistic model. After that, we tested the confidence level of the model which the proposed method had applied and estimated the weight of the variable in the model. Next, we analyzed the model and it was proved to be practical. The final section provides a conclusion and ideas for future work.

2 Analysis of Characteristics of Micro-blog Search Results

Firstly, searching in a particular area, micro-blog search essentially is a kind of vertical search. Unlike traditional web search, the objectives and results of micro-blog search are the micro-blogs sent by the users. Due to being in real-time and containing a large amount of data, micro-blog has a huge advantage and good performance in the aspect of foraging the information of local business service and the public comments and tracking emergency.

Secondly, the results for micro-blog search are presented in a special form. With the limit of a single micro-blog containing only 140 words, an individual search result which itself is a micro-blog carries less information than a traditional Web search result, so all the contents of the micro-blogs can be shown completely, while the results for traditional web search only show the title links and the snippets of the webpages. It is because of the characteristic of the micro-blog search that it cannot be studied with the methods (such as user implicit feedback) applied to the research on the traditional Web search results. Besides, the information about authors of the micro-blogs is available. So any user in the micro-blog community can obtain or estimate the information about the attributes of the authors in micro-blog community (such as the time of joining in the micro-blog community, the number of micro-blogs, the number of following and the number of followers, etc.). In addition to the qualities of the contents of the micro-blogs itself, the information about the attributes of the authors in micro-blog community is the important factors affecting users' decisions on the results.

Thirdly, with the limit of 140 words, the effects of the queries in the micro-blogs on semantic expression of whole contents are remarkable. So there is a strong correlation between the queries and results for micro-blog search, that is, the search results are mostly the information users want to forage.

Fourthly, micro-blogs are self-correcting. In the micro-blog community, anyone having read some micro-blog has the right to examine the micro-blog and to make comments according to the utility users have received. Then as new micro-blogs, the comments are examined by other users in turn. Socialization is thus reflected in the way. Besides, the function of posting and reposting being more easy to use, the data about users' behaviors can be mined more directly.

In addition, every micro-blog user owns specific community attributes that are different from others in the community, so this feature of the micro-blog users makes personalized search possible.

3 Proposed Method of Users' Decision Model for Micro-blog Search with Binary Logistic Model

3.1 Development of Binary Logistic Model

The theoretical basis of the binary logistic model includes Random Utility Model (RUM) and maximum utility theory.

If the decision makers select alternative i from the set A of choices ($i \in A$), the utility function U_i is the utility produced by alternative i. This is a simple statement of Random Utility Model (RUM). The utility function U_i is composed of a deterministic component V_i and a random component ε_i, and they are assumed to have a linear relationship. So U_i can be expressed as:

$$U_i = V_i + \varepsilon_i \tag{1}$$

where V_i is the deterministic component in RUM, and ε_i is the random component in RUM.

Facing a large number of search results, different alternatives (the categories of result selected) bring to users different utility, and RUMs assume the utility brought to the users is maximum (maximization utility theory). Therefore, we can rank the results according to the utility the results bring to users.

Based on the discussion above, the users will select alternative i if and only if the utility of alternative i is greater than all the other alternatives in the choice set A. This can be as follows:

$$U_i > U_j, i \neq j, \forall j \in A \tag{2}$$

The probability $P(i)$ of users have selected alternative i is

$$\begin{aligned} P(i) &= P(U_i > U_j, i \neq j, j \in A) \\ &= P(V_i + \varepsilon_i > V_j + \varepsilon_j, i \neq j, j \in A) = P(\varepsilon_j < V_i - V_j + \varepsilon_i, i \neq j, j \in A) \end{aligned} \tag{3}$$

The total number of the alternatives in the choice set is n , and the joint probability density function of the random component $\varepsilon_1,\varepsilon_2,...,\varepsilon_n$ is presented as $f(x_1, x_2, ..., x_n)$. So the equation (3) is as follows:

$$P(i) = \int_{-\infty}^{+\infty}[\int_{-\infty}^{V_i-V_1+\varepsilon_i}\int_{-\infty}^{V_i-V_2+\varepsilon_i}\cdots\int_{-\infty}^{V_i-V_{i-1}+\varepsilon_i}\int_{-\infty}^{V_i-V_{i+1}+\varepsilon_i}\cdots \int_{-\infty}^{V_i-V_n+\varepsilon_i} f(x_1,x_2,...\varepsilon_i,...,x_n)dx_1dx_2\cdots dx_{i-1}dx_{i+1}\cdots dx_n]d\varepsilon_i \tag{4}$$

It is typical to assume that the distributions of the random component ε_i are independent identically distributed Gumbel distributions, and the location parameter is 0 and the scale parameter 1 [7], so the probability density function of ε_i can be expressed as follows:

$$f(\varepsilon) = \exp(-\varepsilon)\exp[-\exp(-\varepsilon)] \tag{5}$$

We can get the probability $P(i)$ of users have selected alternative i by substituting equation (5) into equation (4):

$$P(i) = \frac{\exp(V_i)}{\sum_{j=1}^{n}\exp(V_j)}, (i \neq j, \forall j \in A) \tag{6}$$

According to whether the author of the result for micro-blog search is followed by the users, the results for micro-blog search can be classified into two categories: followed results and not-followed results. To the users, the alternative is selecting either the followed results or not-followed results. Users selecting the followed results is presented as Y=1 and not-followed results as Y=0. The equation (6) is transformed as follows:

$$P(Y=1) = \frac{\exp(V)}{\exp(V)+1} \tag{7}$$

The equation (7) is the binary logistic model. The model suggests that with personal preferences and following maximum utility theory the users select a search result (followed result or not-followed) which can bring certain utility with a probability $P(i)$, so for ranking, calculating the utility U_i is switched to computing the value of the probability $P(i)$.

The equation (7) can be transformed as follows:

$$\text{logit } P = V \tag{8}$$

where $\text{logit } P = \ln\frac{P}{1-P}$.

As the deterministic component V of the utility function has the same monotonicity as the probability $P(i)$, we can compare the values of V instead of comparing the values of the probability $P(i)$ ranking the search results.

3.2 Quantification and Analysis of Variables in Binary Logistic Model for Micro-blog Search

Creating the binary logistic model for micro-blog search mainly consists of the following steps: to define the characteristic variables of the deterministic component V, to discretize the characteristic variables, and to define the utility function.

Definition of Characteristic Variables of Deterministic Component. According to the characteristics of micro-blog search, the characteristic variables were defined as follows (see Table 1):

Table 1. The characteristic variables of the deterministic component

	Names of variables	variables
User information	Joining time	X_1
	Follow number	X_2
	Follower number	X_3
	Micro-blog number	X_4
	User level	X_5
Author information	Joining time	X_6
	Follow number	X_7
	Follower number	X_8
	Micro-blog number	X_9
	Author level	X_{10}
Micro-blog information	Reposted number	X_{11}
	Replied number	X_{12}

Discretization and Analyze on Characteristic Variables. There being large differences between each characteristic of micro-blog search and others, the real values of the characteristic variables are diverse and complex, and binary logistic model cannot work well. So it's necessary to discretize the characteristic variables.

Follower Number. We take Sina Weibo as example. The numbers of followers exist as power exponent distribution or long-trailed distribution, that is, only less than 1% of the total users have more than 1,000 followers, while the vast majority of the users have only tens or hundreds of followers. Besides, considering the social responsibilities and reputations, the Sina Weibo users who have more than 1,000 followers hardly post information about the local business service. So we can only focus on the users who have only tens or hundreds of followers. From all this, follower number is discretized as follows (see Table 2):

Table 2. The discretized follower number

Real value	0-100	101-200	201-400	401-600	601-800	801-1,000	>1,000
Discrete value	1	2	3	4	5	6	7

Follow Number. In 1992 Oxford University anthropologist Professor Robin Dunbar found that the human brain cannot accommodate more than 148 people with stable relationships. According to this conclusion and the survey and analysis of Sina Weibo users, the majority of the users are not able to follow more than 150 authors. And Sina Weibo has the limit to the number of the users following, less than 2,000. Therefore, follow number is set as follows (see Table 3):

Table 3. The discretized follow number

Real value	0-100	101-200	201-400	401-600	601-800	801-1,000	1,001-2,000
Discrete value	1	2	3	4	5	6	7

Micro-blog Number. According to the distribution of the numbers of the micro-blogs the ordinary user post per day and the users' joining time, micro-blog number of ordinary users are set as follows (see Table 4):

Table 4. The discretized micro-blog number of users

Real value	0-100	101-200	201-400	401-600	601-800	801-1,000	>1,000
Discrete value	1	2	3	4	5	6	7

The survey found that the selected micro-blog authors' micro-blog number mostly distributed in 1,000 to 2,000, so micro-blog number of the authors are set as follows (see Table 5):

Table 5. The discretized micro-blog number of authors

Real value	0-1000	1001-2000	2001-4000	4001-6000	6001-8000	8001-10000	>10000
Discrete value	1	2	3	4	5	6	7

Joining Time. As the discretized follower number, joining time is discretized as follows (see Table 6):

Table 6. The discretized joining time

Real value	0-100	101-200	201-300	301-400	401-600	601-800	801-1,000	>1,000
Discrete value	1	2	3	4	5	6	7	8

User/Author Level. According to the levels Sina Weibo sets for users, user/author level can be set as follows (see Table 7):

Table 7. The discretized user/author level

Real level	Ordinary	Weibo expert	Authentication
Discrete value	1	2	3

Posted/Replied Number. According to the statistics on the distribution of posted number and replied number, we can discretize the two characteristic variables as follows (see Table 8):

Table 8. The discretized posted/replied number

Real value	0-10	11-50	51-100	>100
Discrete value	1	2	3	4

Definition of Utility Function. We define that the vector of the characteristic variables is $X=[X_1,X_2,...,X_{12}]$, and the coefficient vector of the characteristic variables is $\theta=[\theta_1,\theta_2,...,\theta_{12}]$. Then the utility function can be expressed as follows:

$$V = f(\theta, X) \tag{9}$$

This function can be in a linear form, a log linear form or CES (Constant Elasticity Substitution) form. Because linear form simplifying the definition of the model is widely used, we select the linear form for the function as follows:

$$V = \theta_0 + \sum_{i=1}^{12} \theta_i X_i = \theta_0 + \theta_1 X_1 + \theta_2 X_2 + \cdots + \theta_{12} X_{12} \tag{10}$$

4 Verification of Model

To estimate coefficients and verify the confidence level of the characteristic variables in the binary logistic model for micro-blog search, we carried out an experiment collecting the related data of users selecting the results for micro-blog search and processing the data with statistical software SPSS (Statistical Product and Service Solutions).

4.1 Experimental Design

Subjects. As subjects 100 students regularly using Sina Weibo (post or read the Weibo at least one time per day) were asked to participate in the experiment. A reward was paid when they finished our experiment.

Materials and Equipment. With the largest number of users, active users and posts daily, Sina Weibo is typical of the domestic micro-blogs. So Sina Weibo was selected as the network platform in the experiment. The experiment was carried out on the specific PC, and the network environment is stable.

Procedure. To avoid others' affects, each subject was asked to complete the tasks alone. First, the subject need to log in his or her Sina Weibo and click the search icon in the top of the page to enter the page for micro-blog search. Second, the subject was asked to enter the queries (ie. a new restaurant, a recent released movie, etc.) to search, and ensured that there were at least 3 results in the result page, otherwise the subject need to change the queries, and search again. Third, the subject was asked to scan the results for less than 2 minutes and select one result which was considered to bring the most utility (useful or trusted information) to the subject. Finally, the information about the values of characteristic variables in Table 1 and whether the author of the result was followed by the subject were recorded as one set of data.

4.2 Result

We randomly selected 40 sets of data (20 sets selecting followed author and 20 sets selecting not-followed author) as samples for statistical analysis. When filtering the characteristic variables in the model our strategy was based on forward stepwise regression of the maximum likelihood estimation (Forward: LR). In this way, the variables and their coefficients were shown as below (see Table 9 and Table 10):

Table 9. Iteration History

Iteration		-2 Log likelihood	Coefficients									
			Constant	X1	X3	X4	X5	X6	X7	X9	X10	X12
Step 1	1	33.466	.252	-.438	.104	-.182	-.451	-.178	.009	.322	.947	1.397
	2	33.293	.032	-.469	.115	-.182	-.498	-.210	.028	.306	1.051	1.734
	3	33.282	-.095	-.465	.114	-.175	-.507	-.215	.036	.290	1.057	1.831
	4	33.282	-.106	-.465	.114	-.174	-.508	-.215	.036	.288	1.058	1.840
	5	33.282	-.106	-.465	.114	-.174	-.508	-.215	.036	.288	1.058	1.840

Table 10. Coefficients of the variables in the Equation

		B	S.E.	Wald	df	Sig.	Exp(B)
Step 1	X1	-.465	.841	.306	1	.058	.628
	X3	.114	.580	.039	1	.084	1.121
	X4	-.174	.281	.385	1	.053	.840
	X5	-.508	.931	.297	1	.059	.602
	X6	-.215	.381	.319	1	.057	.806
	X7	.036	.305	.014	1	.090	1.037
	X9	.288	.474	.370	1	.054	1.334
	X10	1.058	.806	1.721	1	.019	2.880
	X12	1.840	1.199	2.355	1	.012	6.298
	Constant	-.106	4.194	.001	1	.098	.899

As can be seen from Table 9, when estimating the coefficients in the model with the maximum likelihood estimation, the coefficients became convergent after 5 iterations. In the 5 iterations, the values of the logarithm of maximum likelihood function (LL) were -33.466, -33.293, -33.282, -33.282, -33.282. That indicated that the explanation of the model was gradually enhanced.

As can be seen from Table 10, follow number of user, follower number of author and reposted number were excluded from the model. The significant test on the regression coefficients of remaining variables showed that the values of the probability-P were less than the significant level of 0.1, and this meant that there was actually a significant linear relationship between $\text{logit}\,P$ and the remaining variables. So the remaining variables should be included in the model.

Therefore, the model can reflect the relation between the characteristic variables and $\text{logit}\,P$. The decision model for users selecting the results by followed author can be expressed as follow:

$$V_1 = -0.106 - 0.465X_1 + 0.114X_3 - 0.174X_4 - 0.508X_5 - 0.215X_6 + 0.036X_7 + 0.288X_9 + 1.058X_{10} + 1.840X_{12} \tag{11}$$

Where what $X_1, X_2, ..., X_{12}$ presents is explained in Table 1.

As

$$\text{logit}\,(1-P) = \ln\frac{1-P}{P} = -\text{logit}\,P = -V \tag{12}$$

So the decision model for users selecting the results by not-followed author can be expressed as follow:

$$V_2 = 0.106 + 0.465X_1 - 0.114X_3 + 0.174X_4 + 0.508X_5 + 0.215X_6 - 0.036X_7 - 0.288X_9 - 1.058X_{10} - 1.840X_{12} \tag{13}$$

We can substitute the values of the results' characteristic variables into the equitation (11) or (13) to ranking the results by the calculated values of the deterministic component in the model.

5 Analysis of Model

Comparing equitation (11) and (13), we can see that the users take completely different strategies for the results by followed authors and not-followed authors when making decisions on the results for micro-blog search. In the Micro-blog community, a user following an author from hundreds of millions of users means that the author attracts the user and the author's micro-blogs interest the user and bring certain utility to him. So whether the user following the author reflects whether the author interesting the user and that is the essential reason for users taking two different strategies. Besides, the coefficients of the characteristic variables in the model also reflect the weights of characteristic variables.

The first four variables in the model describe the user profiles.

To the users, the longer they have joined in the micro-blog community, the more deeply they understand the micro-blog community. So they are glad to receive the messages out of their circles and joining time of a user has a positive influence on his selecting the results by not-followed authors. On the contrary, with following for a long time, the users' interests to the messages by followed authors begin to fall. So joining time of a user has a negative influence on selecting followed authors' results.

The users with a larger numbers of micro-blogs always obtain the more attention and are considered to be more active in their circles where they have a higher probability to become the leaders. As the messages in their circles are the same as the users' knowledge, the users tend to ignore the massage in the circles and receive the message out of the circles, that is, micro-blog number have a positive influence on selecting not-followed authors' results, while a negative influence on selecting followed authors' results.

The users with more followers have greater influences in the micro-blog community. And the authors followed by such users have the equal influences usually. So the users tend to select the results by followed authors. Otherwise the authors followed by the users with fewer followers have fewer influences, and the users prefer to believe the not-followed authors who may be more influential.

The absolute value of coefficient of user level is the biggest in the four characteristic variables about user profiles, and it means user level have a larger effect on the users' making decisions. The users with higher levels have longer joining time, stronger abilities of processing the messages, and stronger desires of keeping up with the messages out of their circles. So they prefer to select the results by not-followed authors. To not-followed authors, user level has a positive influence, while to followed authors, a negative influence.

The four coefficients of the variables above also explain the behavior of long-term micro-blog users regularly changing their following authors.

The next four variables in the model are about the micro-blog author.

The users without the ability of getting the information about joining time of authors only from the search results, joining time of authors belongs to a kind of implicit variable. Therefore, the analysis of the variable's effect on decision-making should focus on the relationship between authors and users. The longer authors join in the micro-blog community, the larger opportunities they are invited by marketers to be promoters with, and the objectives of the authors as promoters are the users following the authors. Currently the main form of marketing in micro-blog is advertising, and the users bored to the advertisements which are always overblown. So the users are not willing to select such results by followed authors and joining time of authors has a negative influence on the users' selecting the search results by followed authors. Otherwise, as the micro-blogs by not-followed authors having joined a long time cannot be considered as advertisements for the users, they are easier to be believed by the users. So joining time of authors has a positive influence on the users' selecting the search results by not-followed authors.

Besides, the absolute value of the coefficient is smaller, the influences of joining time of authors are limited.

Follow number reflects the range of knowledge of the authors. 50 authors were selected randomly and the numbers of their follows and the fields they focused on are recorded and analyzed. The correlations between the numbers of their follows and the

fields they focused on are illustrated as fig. 1. From fig. 1, we can conclude that the more follows the authors have, the wider range of knowledge they cover. As it was considered that a man with a wide range of knowledge cannot master the knowledge deep enough, the not-followed authors with wider range of knowledge can cause more distrusts of the users. While to the followed authors whose knowledge was wider, the users believed them more with the belief and the interest to them before. Therefore, follow number of the not-followed authors has a negative influence, while the followed authors has a positive influence.

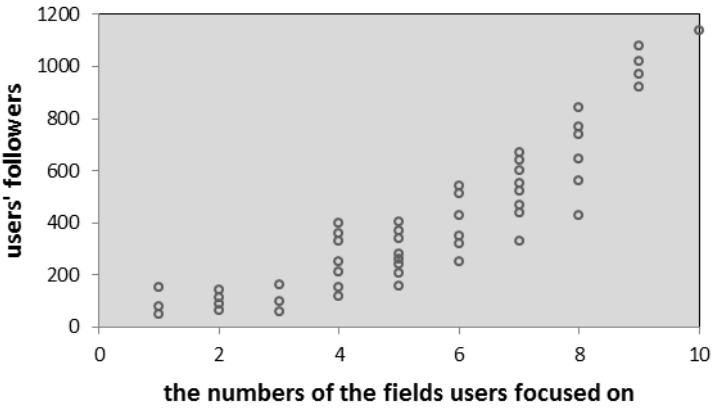

Fig. 1. The relation between the users' follows and the numbers of the fields they focused on

Micro-blog number of the authors reflects the activity of the authors. A author being more active can effect on his followers continuously, so the search results the author post can interest the users. However, as the users' lack of the interest to the not-followed authors, the users tended to suspect the authors, so the authors were considered to have more differences with the users if the authors appearing more active so that the search results by not-followed authors were ignored more easily.

The absolute value of the coefficient of author level is bigger than most of coefficients, so author level has a significant effect on making decisions. we selected 20 users randomly, and asked them to search with the same queries. Then the users were asked to rate the search results (including the results by different levels of followed and not-followed authors) using the 5-point Likert scales (the higher the scores were, the greater the users' utility is). The result was illustrated as fig. 2.

From fig. 2, we can see that the higher the followed authors' levels were, the more utility the users can be brought to, while the higher the not-followed authors' levels were, the more utility the users can be brought to. That is because that to the search results for local business services, the high leveled authors were very likely to be the owners or operators of the things described by the queries (ie. a restaurant, a product, a film, a book, etc.), and the results by the not-followed authors were treated as advertisements. While the low leveled authors were believed as they were more objective. Therefore author level of the not-followed authors has a positive influence on the users' making decisions, while the followed authors, a negative influence.

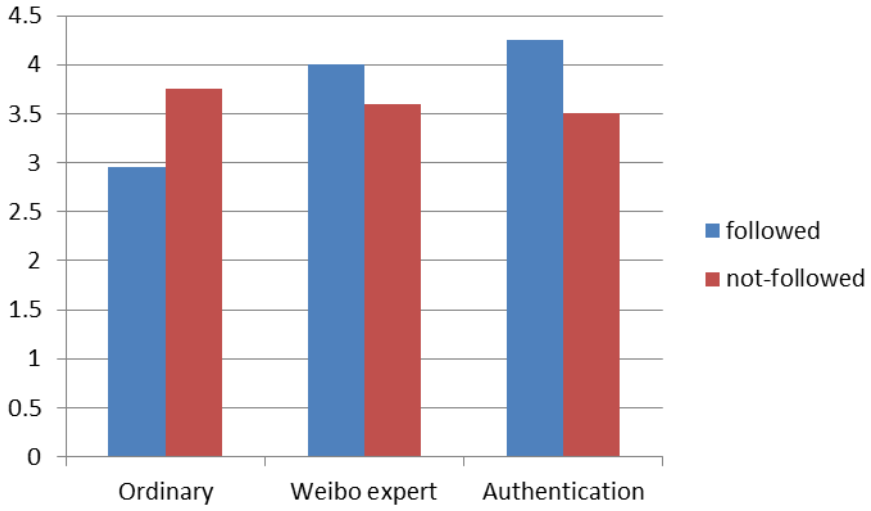

Fig. 2. Points users rate to the results

Replied number is the attribute of micro-blog. In the ideal micro-blog community, replied number is one of the key factors that reflect the qualities of the contents of micro-blogs. The absolute value of the coefficient of replied number is the biggest in the proposed users' decision model for micro-blog search, and that means replied number should have a significant effect on users' making decisions. We selected 10 users randomly to search for 10 different queries belonging to local business services. The distribution of the replied numbers of the search results was shown in fig. 3.

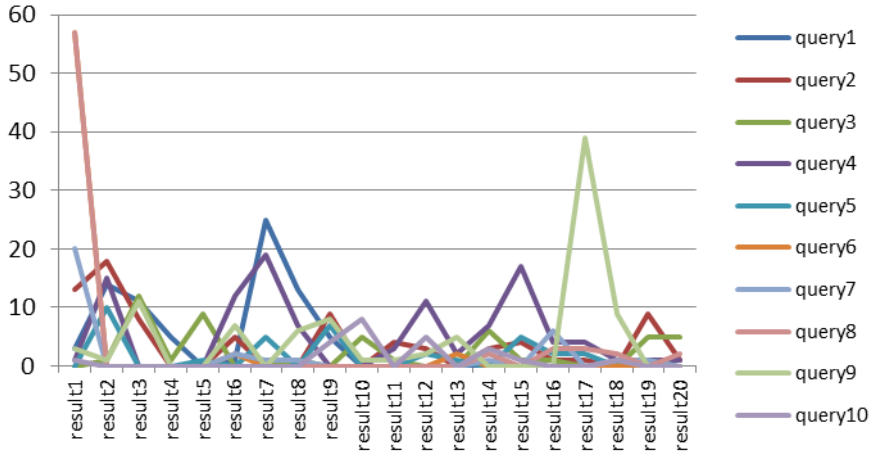

Fig. 3. The distribution of the replied numbers of the search results for different queries

As can be seen in fig. 3, more than 90% of the search results for local business services had less than 10 replies. Users' being not very fond of replying to a micro-blog for local business services, in the majority of cases, the values of replied number were 1. That limited the influence of replied number on users' making decisions. So replied number is not the critical variable. The more the replies were, the more attentions | the micro-blog received. So the users obtained more utility from the micro-blogs by followed authors. As lack of belief to the not-followed authors, the replies were considered negative. So replied number of the not-followed authors has a negative influence on the users' making decisions, while the followed authors, a positive influence.

6 Conclusion

In conclusion, based on the analysis of the micro-blog search and the binary logistic model, we can apply the user decision model to the ranking the results for micro-blog search. The proposed method of analyzing the results for micro-blog search using the user decision model is proved valid and practicable.

In addition, the methods of ranking micro-blog search results mentioned in this paper can also be extended to study. User decision model is on the basis of the large amount of data, so the future work will focus on the following. A research with a large number of real-time dynamic data and iterative calculation to ensure the accuracy of the coefficient of each variable will be conducted.

Acknowledgements. The research is supported by Specialized Research Fund for the Doctoral Program of Higher Education (No. 20110005110016).

References

1. Wang, F., Wu, Q.-B., Yang, S.-Z.: Design and Implementation of Web2.0 Community Search Module Ranking Algorithm. Computer Engineering (2009)
2. Cheng, Z.-H.: Research on Information Model and Sort Algorithms for Personalized Search. Southeast University, China (in Chinese)
3. Walisa, R., Wichian, P.: Exploring Web Search Behavior Patterns to Personalize the Search Results. In: 2011 Third International Conference on Intelligent Networking and Collaborative Systems (2011)
4. Hui, F.: Research on Personalized Search Based on Contents in Blogs. Huazhong University of Science and Technology (in Chinese)
5. Li, J., Lin, H.-F.: Emotion Tag Based Music Retrieval Algorithm. In: The Proceedings of 6th Chinese Conference on Information Retrieval (CCIR 2010) (2010)
6. Guo, T.-Y.: Research on Traffic Survey and Method of Analyzing Data Based on Disaggregate Model. Southeast University, China
7. Pirolli, P.: Information Foraging Theory. Oxford University Press

A Kinect Based Golf Swing Reorganization and Segmentation System

Lichao Zhang[1,2], Jui-Chien Hsieh[2], and Shaozi Li[1]

[1] Dept. Cognitive Science, Xiamen University, Xiamen , China
Zhanglichao0420@gmail.com Szlig@mail.xmu.edu.cn
[2] Dept. Information Management, Yuan-Ze University, Chung-Li, Taiwan
yzuhsieh@gmail.com

Abstract. This study displays a method to recognize and segment the time-sequential postures of golf swing. It's crucial to develop a system that can effectively recognize the steps of golf swing and facilitate self-learning of correct golf swing. First, a game controller, Kinect, is used to capture the 3D skeleton coordination of a golfer while performing swing. Second, a Hidden Markov Model (HMM) is applied onto the symbol sequence to recognize and segment the postures of golf swing. Results indicate that the proposed methods can effectively identify and categorize golf swing into 5 stages In conclusions, this developed golf swing training system is cost-effective as compared to traditional camera based golf swing trainer.

Keywords: HMM, Kinect, Golf Swing.

1 Introduction

Human posture recognition is an essential topic in computer vision area; it can be used in automatic monitoring, and human interaction with computer. The human's posture is so complicated, it is important that we should reduce the algorithm complexity if we want to recognize the posture in real time [1]. Pellegrini and locchi [2] used stereo vision to achieve humans' 3D features and skeleton features, and to judge their behavior made by the HMMs with these features. Kellokumpu, Pietikainen et al. [3] developed a system with SVM and Discrete HMMs to identify and cluster the 15 gesture timely.

Golf is a kind of sports which shot the balls into the hole with the golf clubs. The perfect swing is the first and most important skill. But the price of training golf equipment is expensive and the coaches are not enough to train the student. Therefore, the automatic Golf swing analysis and correct system have wide prospect of the market, and vast of manufactures and investigator have carried on some beneficial researches in this fields [4]. But these devices are so professional that need volume of space to set up or much of money to purchase. The Kinect have a RGB color to obtain the normal image, and 2 infrared devices, include an infrared emission device and an infrared CMOS camera to constitute a 3D depth inductor. the device can obtain the human skeleton framework and joints location [5].

Q. Zu, B. Hu, and A. Elçi (Eds.): ICPCA-SWS 2012, LNCS 7719, pp. 843–847, 2013.

Because of the Golf swing process is time-sequentially and similar with the posture recognize. We propose a system which based on Hidden Markov Models and use the Kinect device to recognize the state of a Golf swing. It obtained the skeleton and joints position by the Kinect, extract the features from these data, to train the Hidden Markov Models and recognize. The result shows that our system is feasibility and reliability.

In our paper, section 2 details the Hidden Markov Models and the way to recognize and learning. Section 3 illustrates how a set of time-sequential image data are converted into the symbols sequences and how the system work. Section 4 gives experimental results, and discusses some relative phenomenon in our paper. The last section we will summarizes our system and looking to the future work.

2 Method

The Hidden Markov Model is a kind of relative mature matching algorithm. HMMs make it possible to deal with time sequential data and can provide time-scale invariability in recognition like speech recognition, intellective Chinese Pinyin IME and gesture recognition. Moreover, HMMs are strongly at the learning ability which is achieved by presenting time-sequential data and automatically optimizing the model with the data. Because of these advantages, HMMs was widely used in Human posture recognition.

The way to train the HMMs parameters means that we use the observe sequences which we need to train, adjust the parameters when the $P(O|\{p_i,A,B\})$ likelihood maximum with some algorithms. For HMMs, the most frequently used algorithm is Baum-Welch algorithm. Although Baum-Welch algorithm is a very efficient tool for training, but the algorithm has weakness, it is easy to get into the local optimums because the algorithm defects. So we should prudent to choose the parameters initial value. It is stated that[6] the parameters Π and A is less important when we evaluate and training the HMMs, but the parameter B is an effective variable. Most of the systems would calculate the initial B parameter.

3 System Detail

3.1 Feature Extraction

To apply HMMs to time-sequential images $I=\{I_1,I_2,\ldots I_T\}$, the images must be transformed into symbol sequence O in learning and recognition phases. From each frame Ii of an image sequence, a feature vector fi∈Rn is extracted and fi is assigned to a symbol v_j chosen from the symbol set V. It is necessary to associate the symbol set V with the feature space R_n. For this, the feature space is divided into clusters by a pattern classification technique, and the symbols are assigned to the clusters. We used vector quantization here, as is usual in HMM applications. For vector quantization, codewords $g_j \in R_n$, which represent the centers of the clusters in the feature R_n space,

are needed. Codeword g_j is assigned to symbol v_j, Consequently, the size of the code book equals the number of HMM output symbols.

Our system uses the Kinect and the supporting SDK to update the 20 skeleton positions. As the experiment result, we choose the highest dividing feature, the right hand position (x_{ht},y_{ht},z_{ht}), spine position (x_{st},y_{st},z_{st}) in each frame. The usual code methods include Rubine features[7], speed[8],or angel[9]. In our experiment we use these angels to get the codes. The posture could be described as the orientation features sequence. We developed a 12 orientation code method to obtain the obscure sequence. The algorithm we can describe like that:

(a) Code 1 means the region from $-\pi/12$ to $\pi/12$
(b) Code 2 means the region from $\pi/12$ to $3*\pi/12$, the rest can be done in the same manner until Code 12

3.2 Trainning the HMM and Improvement

As described in Section 2, the symbol sequences obtained from the above procedures are used for both the recognition and learning phases. First of all, we choose the initial HMM parameters. In the absence of supervision conditions, the states can free to jump. But it is not correspond with the time sequence in swing action; even we use a large database, it does not promote the segmentation accuracy rate. Combined with the actual situation, we choose the single-track state HMM to train, as the equation (1)-(2), each state can only jump to the next state except the initial state and the halted state.

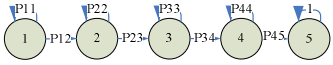

Fig. 1. The structure of forehead HMM

At the same time, we can evaluate the parameters A,B with the most likelihood method because we have known all of the observe sequences. When we confirm the initial models, the HMM parameters will use the Baum-Welch algorithm to train with the discrete sequence loop. Until the trained models apply the probability of the observe sequence convergence, we can obtain the new trained HMM.

Based on the foregoing HMMs, we can use the Viterbi algorithm to find the optimum sequence and to separate the continuous actions. However, there are some obvious mistakes in the result of the sequence. We need to add some revise rules to correct the result with the Hand position movement features. The method can be described like that:

(a) Using HMMs to preliminary estimate the 5 subsection
(b) With these subsection, we use some obvious evidence to correct mistakes, such as during the subsection 1 and 2, if we find one frame that the right hand y axis value is minimum, we can deem it is the break point of subsection 1 and subsection2. We can find other 3 break points similarity.

4 Experiments

We tested our algorithm with the Discrete HMM method to recognize and classify the Golf swing action. In our experiment, we choose Matlab 2010b and the HMM toolbox code by Kevin Murphy to train and test. Our HMM classifier will separate the consistent action to 5 steps automatically because of the procedures of swing consist of 5 steps, include pre-swing, back swing, swing, to send the ball, and finish work.

4.1 Experiment 1

According to our method, we choose 6 people as subjects, each person collect 20 swing sample. We collect 120 Golf swing samples with the speed about 28 26 24 22 frames per second to extract features and the observe sequence totalize. With these sequence, we adopt 5 steps single-track discrete HMM to train the parameter. Then we use the cycling test to measure the rate of identification. Table 1 shows the result of the test and the rate.

Table 1. The Accuracy rate in Different Frames per Second

F/S	28	25	22	20
Accuracy	0.820	0.803	0.770	0.705

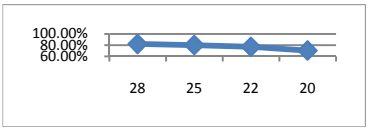

Fig. 2. The Accuracy rate in Different Frames per Second

As the chart shown, the recognize accuracy rate about gradually descend with the sampling frame frequency decrease. This is because that if we choose the low test pattern subject sample frequency, we will miss or blurred some key frames when the steps transferring, and influence the recognition rate of the systems.

4.2 Experiment 2

In these experiments, we use the 3 of the 6 research subjects' samples to test. The sampling frequency is 30 frames per second. We train the data A, B and C independently, use these samples to test the HMMs. Next we were training the HMMs with the data set B, C, B+C, use the A data set as the test samples. The test result we will show in the Table2:

Table 2. The Accuracy rate in Different Trainning Data

	Training Data player			
Test Player	B	C	B+C	A
A	0.6712	0.7023	0.7887	0.8753

In experiment (2), as shown in Table3, the recognition rates of the HMMs were not as good as experiment (1). We hold the option that test pattern subject and training pattern subjects were different. Each person has some specialty in his/her action, but the variance range is limited such that humans can recognize. We can improve the rate if we mixed the train dataset, as we seen the rate with B+C HMMs improve to 78.87%. Thus point out that the more subject training patterns which we collected, the higher separate accuracy we can get.

5 Conclusion

In this paper we present a golf swing recognition and segmentation system based on the Hidden Markov Models. In addition, this system completes the segment mission. The main experimental results show that our method is promising to realize human action recognition. To improve our current implementation , we will try a large scale experiment and further refine feature extraction. We will continue our work to optimize the segmentation way, give a score about the segment data to estimate the subjects' swings veracity. In the future we would like the system could apply to the medical rehabilitation area.

References

1. Yamato, J., Ohya, J., Ishii, K.: Recognizing Human action in time-sequential images using Hidden Markov Model. In: CVPR 1992, Champaign, IL, pp. 379–385 (1992)
2. Pellegrin, S., Iocchi, L.: Human Posture Tracking and Classification through Stereo Vision and 3D Model Matching. EURASIP Journal on Image and Processing 2008 (April 2008)
3. Kellokumpu, V., Pietikainen, M., Heikkila, J.: Human Activity Recognition Using Sequences of Posture. In: Proceedings of IAPR 2005, Tsukuba City, pp. 570–573 (2005)
4. Gulgin, H., Armstrong, C., Gribble, P.: Hip rotational velocities during the full golf swing. Journal of Sports Science and Machine 8, 296–299 (2009)
5. Xia, L., Chen, C.: Human Detection Using Depth Information by Kinect. In: CVPRW 2011, CO, pp. 15–22 (2011)
6. Kale, A., Rajagopalan, A., Cuntoor, N., Kruger, V.: Gait-based recognition of human using continuous HMMs. Automatic Face and Gesture Recognition, 336–341 (2002)
7. Rubine, D.: Specifying gesture by example. Computer Graphics 21(4), 329–337 (1991)
8. Sun, Z., Liu, W., Peng, B., Zhang, B., Sun, J.: User Adaptation for Online Sketchy Shape Recognition. In: Lladós, J., Kwon, Y.-B. (eds.) GREC 2003. LNCS, vol. 3088, pp. 305–316. Springer, Heidelberg (2004)
9. Derk, A., Craig, B.: Hidden Markov Model symbol recognition for sketch-based interfaces. In: Proc. of AAAI Fall Symposium, Arlington, Virginia, pp. 15–21 (2004)

An EEG Based Pervasive Depression Detection for Females

Xiaowei Zhang[1], Bin Hu[1,*], Lin Zhou[1], Philip Moore[2], and Jing Chen[1]

[1] The School of Information Science and Engineering,
Lanzhou University, Lanzhou 730000, China
{zhangxw,bh,zhoulin11,jchen10}@lzu.edu.cn
[2] The School of Computing, Telecommunications and Networks,
Birmingham City University, Birmingham B42 2SU, UK
Philip.Moore@bcu.ac.uk

Abstract. Recently, depression detection is mainly completed by some rating scales. This procedure requires attendance of physicians and the results may be more subjective. To meet emergent needs of objective and pervasive depression detection, we propose an EEG based approach for females. In the experiment, EEG of 13 depressed females and 12 age matched controls were collected in a resting state with eyes closed. Linear and nonlinear features extracted from artifact-free EEG epochs were subjected to statistical analysis to examine the significance of differences. Results showed that differences were significant for some EEG features between two groups (p<0.05) and the classification rates reached up to 92.9% and 94.2% with KNN and BPNN respectively. Our methods suggest that the discrimination of depressed females from controls is possible. We expect that our EEG based approach could be a pervasive assistant diagnosis tool for psychiatrists and health care specialists.

Keywords: Depression, EEG, Pervasive computing.

1 Introduction

Depression, generally considered to be the most prevalent of all diagnosed mental disorders, is a state of low mood involving sadness, discouragement, despair, or hopelessness lasting for weeks, months, or even longer. Recent findings show that without treatment, depression can impair functioning and well-being to levels comparable with or worse than chronic medical conditions such as hypertension, diabetes, angina and gastrointestinal disorders [1]. Both the World Health Organization (WHO) and the World Bank identified depression as the leading cause of disability worldwide [2]. Today depression is being diagnosed in increasing numbers in various segments of the population over the world [2]. Females, from early adolescence through adulthood, especially, have a higher rate, which is one-and-a-half to three times, to have recurring depressive episodes than males [3-5]. The disproportionately large number of females compared to males among those identified as victims of depression presents a serious social problem.

* Corresponding author.

Q. Zu, B. Hu, and A. Elçi (Eds.): ICPCA-SWS 2012, LNCS 7719, pp. 848–861, 2013.

Delayed depression detection escalates the risk of females experiencing serious mental health problems. Detecting depressed states in an early stage can lead to effective prevention and management [6]. Currently, subjective rating scales, such as Diagnostic and Statistical Manual of Mental Disorders-fourth edition (DSM-IV), Hamilton Depression Rating Scale (HAM-D) and Beck Depression Inventory (BDI) are common methods of detecting depression by psychiatrists and health care specialists. While the efficiency of these scales has been proven in detecting depression, they have some drawbacks as they all are a potential source of subjectivity in the detection as well as the fact that the detection procedure requires the attendance of a physician, implying that these scales can not meet the needs of pervasive or home use [6]. Therefore, there is an emergency need for the development of some objective and pervasive measures to help detect depression. Given the ratios for depression in females and males, gender is an important variable in cross-culturally conceptualizing, assessing, and treating depression [3].

The goal of pervasive computing is to provide people with a more natural way to interact with information and services by embedding computation into the environment as unobtrusively as possible [7]. The range of use of pervasive computing is very large. Emerging pervasive computing technologies are applicable in many areas of life such as healthcare. Given recent advances in wearable physiological sensor and EEG techniques, there is now a chance to quantitatively, accurately and pervasively access how the physiology of individuals, such as EEG is correlated to changes in depression. EEG is a record of the oscillations of brain electric potential recorded from electrodes on human scalp [8]. Since Dr. Hans Berger, a German neuropsychiatrist, published the earliest research on human EEG in 1929, EEG has been motivated by the need to study the mental (psychiatric) state and disease diagnosis [9]. EEG was the main useful tool in this area until brain-imaging techniques, such as MRI and fMRI became available. The Online Predictive Tools for Intervention in Mental Illness (OPTIMI), which is funded by European Union's 7th Framework Programme Personal Health Systems aiming to improve the health of European citizens as well as address global health issues, tries to develop a pervasive behavioral and physiological monitoring technologies by EEG, ECG, activity monitoring and electronic diaries, with the potential to detect early signs of stress and depression and then develop a database and a data mining system making it possible to correlate these measurements with assessments by experienced therapists using gold standard diagnostics [10].

Given the possibility that the EEG findings may only pertain to depressed state in males or females separately, research should take the gender into consideration when study depression [11-13]. This study, taking advantage of a sample of females participated in the OPTIMI, aimed to develop a pervasively depression detection approach by EEG for females. The remainder of this paper is organized as follows: Section 2 sets out an overview of related research with the focus on EEG analysis in depression. In Section 3, we give information about our participants, EEG recording procedure and pre-processing of raw EEG data. The theory and algorithm of linear and nonlinear EEG features and classification applied in this study are also briefly introduced. Section 4 presents results based on statistical analysis and classification. In Section 5, we discuss our results. The conclusion is given in Section 6.

2 Related Work

Recent studies have indicated that quantitative EEG analysis has the potential to provide meaningful contributions to the understanding of cortical disturbances in depression. These studies have analyzed EEG features derived from epochs of artifact-free data and investigated the EEG disturbance in depressed subjects as compared with controls [13-16]. Quantitative EEG methods are generally classified into linear and nonlinear approaches.

Traditionally, EEG approach is based on spectrum analysis, which hypothesizes that the EEG is a linear stationary process. Power spectral analysis is one of the first applications of linear EEG analysis. The basic idea of power spectral analysis is that EEG can be divided into several classic non-overlapping frequency bands: Delta wave (0.5~4 Hz), Theta wave (4~8 Hz), Alpha wave (8~13 Hz), Beta wave (13 ~30 Hz) and Gamma wave (> 30Hz). During the past years, absolute and relative power and center frequency of EEG have been widely used in studies related to depression. In cases characterized by resting with eyes-closed, the EEG measurements of depressed patients have shown elevated Alpha and Beta frequency bands activity compared with controls [14]. Knott et al. reported absolute and relative power in the Beta frequency band, but not in the Delta, Theta or Alpha frequency bands, differentiated depressed patients and controls, with the former group exhibiting more power than the latter group [13].

During past decades, nonlinear dynamic theory has been applied to the analysis of EEG signals generated by people with psychiatric disorders including depression. Nonlinear EEG analysis is predicated on the mathematical theory of nonlinear dynamical systems [17]. Stam reported that the application of nonlinear dynamics to EEG has opened up a range of new perspectives for the study of normal and disturbed brain function and is developing toward a new interdisciplinary field of nonlinear brain dynamics [17]. Nonlinear methods, such as correlation dimension, the largest Lyapunov exponent and Lempel-Ziv complexity have been found to be useful to detect EEG changes in different psychological states. Nandrino et al. reported a link between reduced correlation dimension and the symptoms of depression [18]. Rochke et al. computed the largest Lyapunov exponent of EEG segments corresponding to different sleep stages. They found the largest Lyapunov exponent significant decreased during some sleep stages in depressive patients compared with controls [19]. Li et al. have used the Lempel-Ziv complexity to characterize EEG disturbances in the subjects with depression at resting state; their results showed increased Lempel-Ziv complexity in depressive subjects [16]. These studies have implied that nonlinear EEG analysis represents a useful approach to the study of depression.

Results reported in the researches support the conclusion that the utility of computer-analyzed EEG features can be a valuable and investigational tool when analyzing depressed groups. Currently there is little research in pervasive application of depression detection, although so many results based on EEG investigation in depression have been found. Given the above, a preliminary study in EEG based pervasive depression detection for females is proposed.

3 Experimental Approach

3.1 Subjects

25 right-hand volunteer mothers, aged from 30 to 42, were recruited in this study. They were free of any medications interfering with sleep, any medications interfering with cardiovascular function, any medications interfering with cortisol regulation, any medications interfering with psychotropic and exhibited no concomitant psychiatric (including alcohol/drug abuse) disorders. The volunteers were selected to participate in OPTIMI. Firstly, all subjects completed the Beck Depression Inventory II (BDI-II). The Depressed group (DG) was created by using the traditional cut-off score of 14 or higher on the BDI-II, which is indicative of at least mild depression [20], and the Control group (CG) was created with a score of less or equal to 13. Finally, 12 females were classified into controls and 13 age matched females were classified into DG. In fact, the range of BDI-II scores in the DG was 17-36 (M=24.23, S.D. =6.33), and the range of BDI-II scores in the CG was 0-13 (M=7.58, S.D. =3.78). All subjects were informed of the aims and protocols of the experiment and then signed a consent form. After the experiments, all the subjects were financially compensated.

3.2 EEG Recording

The experiment was conducted in an acoustically shielded room. Subjects were seated in a comfortable chair for the application of electrodes. After some time adapting the device, the subjects were monitored (EEG data recording) for one minute in a resting state with their eyes closed. The subjects were told to try not to move during the EEG recording procedure. The experimental period was one month during which one trial for each subject was collected every day. For the pervasive use, we developed a mobile EEG belt, a wireless EEG collection device that sends raw EEG data to a computer (see Fig. 1). Compared to existing EEG commercial caps, our mobile EEG belt uses a limited number of electrodes on the forehead so that users will not be disturbed by adhesive conductive gel on their hair or an inconvenient multichannel EEG cap, which enhances its pervasive application. The performance and practice use of our EEG belt had been rigorously demonstrated in previous study [10]. EEG signals were recorded from three electrodes-Fp1, Fp2 and Fpz complying with the international 10-20 system with reference to linked earlobes. EEG data were sampled at 256 Hz, low pass filtered at 50 Hz and digitized to 24 bits per sample.

3.3 Data Preprocessing

The raw EEG data was contaminated by artifacts such as electrooculography (EOG) and electromyography (EMG). We carried out some pre-processing prior further analysis. Firstly, raw EEG data was processed by low-pass filtered with 40Hz cutoff frequency, which can eliminate EEG signals drifting and EMG disturbances. Secondly, EOG disturbances were eliminated using algorithm proposed in [21].

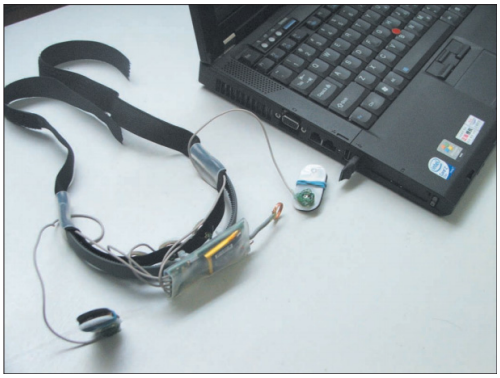

Fig. 1. The prototype of mobile EEG belt. Three recording electrodes (Fp1, Fp2 and Fpz) are placed on the forehead complying with the international 10-20 system, with the reference and ground electrodes on the ear lobes.

3.4 EEG Features

Artifact-free EEG epochs of 4s with continuous epochs overlapping by 50% were extracted and both linear and nonlinear EEG features were calculated from these epochs.

Artifact-free epochs were subjected to a Fast Fourier Transform (FFT) algorithm for calculation of absolute (μV2) power (Abs_Pow), relative (%) power (Rel_Pow) and center frequency (Hz) (F0) in Theta (4~8 Hz), Alpha (8~13 Hz) and Beta (13 ~20 Hz) for each electrode. Relative power indices for each band were derived by expressing absolute power as a percent of the total power in each separate frequency band. Center frequency was also derived from each separate frequency band.

Four nonlinear EEG features were adopted in our study: C0-complexity, correlation dimension (D2), the largest Lyapunov exponent (LLE) and Lempel-Ziv complexity (LZC). They were all derived from a whole band of 4 ~20 Hz.

C0-complexity (C0): C0 is a description of time sequences randomness [22]. By assuming that complexity time series could be divided into two parts: regular and random components. C0 is defined as the ratio of the square of the difference between random part and time axis to square of the whole time sequences and time axis. C0 is mainly derived through an FFT calculation. As once an estimation of C0 has been produced, it only requires one further recalculation, so it has the advantage of saving a part of the computational effort. C0 is defined as:

$$C0 = \frac{\sum_{t=0}^{N-1} \left| x(t) - \tilde{x}(t) \right|^2}{\sum_{t=0}^{N-1} \left| x(t) \right|^2} \tag{1}$$

where $\tilde{x}(t)$ is regular component of time sequences, and $x(t) - \tilde{x}(t)$ is random component of time sequences. If $x(t), t = 0,1,2....,N-1$ is constant or periodic

and $r>1$, $\lim_{N\to\infty} C0=0$; otherwise if $r>1, 0<C0<1$. Hence, the more random the time sequence, the larger value of C0.

Correlation Dimension (D2): D2 can well indicate dynamics of EEG signal. In general, the larger D2, the more complex the EEG time series are. The EEG signal can be defined as a time sequences $X(t), t=1,2,3,...,N$, which can be reconstructed into a *m*-dimensional vector $Y_j, j=1,2,3...M \quad (M=N-(m-1)*time-delay)$ with time-delay embedding as given in Grassberger and Procaccia [23]. Before calculating D2, the correlation integral function should be estimated:

$$C_m(r)=\frac{2}{(M-1)\times M\sum_{i=1}^{M-1}\sum_{j=i+1}^{M}\left(\theta-\left(r_{ij}\right)\right)} \tag{2}$$

Here, $C_m(r)\propto r^D$ is the Heaviside unit function. The Heaviside function is 0 if the distance between the vectors is greater than r, and 1 if the distance between the vectors is less than or equal to r. In theory, if the m is sufficiently large and the r is sufficiently small, the following relation is assumed to hold: $C_m(r)\propto r^D$. Then D2 is defined as:

$$D2=\lim_{r\to 0}\frac{\partial\log(C_m(r))}{\partial\log r} \tag{3}$$

The dimension of the attractor is estimated from the slope of a linear scaling region in the $\log(C_m(r))-\log r$ plot.

Largest Lyapunov Exponent (LLE): Lyapunov exponents measure the exponential rates of divergence or convergence of nearby trajectories in state space, which are generally calculated to characterize the chaotic process. If the largest value of Lyapunov exponents is positive, it means that the system is chaotic. The largest value equal to zero indicates periodic or quasi-periodic dynamics. If all Lyapunov exponents are negative, the stable critical point is an attractor. Among all the Lyapunov exponents, the LLE has aroused considerable interest for its significant practical applications. We calculated LLE applying the method proposed by Rosenstein [24].

Lempel-Ziv complexity (LZC): LZC measures pattern complexity for the sequences of finite length through two simple operations: copy and insert [25]. EEG signals will be transformed into binary sequences before calculating complexity measure. After the binarization, the EEG sequences are scanned from the beginning to calculate the LZC. More details of easily LZC calculation can be found in previous work [26].

Finally, a total of 13 EEG features from each electrode were extracted in this study.

3.5 Statistical Analysis

Statistical approaches were applied to select which EEG feature could well differentiate depressed females from controls. Statistical analysis of the data was done by using the SPSS 15.0 software (SPSS Inc., Chicago, Ill). We applied *t*-test to investigate whether the mean value differences of EEG features were significant between two groups.

3.6 Classification

Previous studies have indicated different psychological states could produce different EEG patterns. So we can use classification algorithms to identify these psychological states based on different EEG patterns. In this study, both Back Propagation Neural Network (BPNN) and *k*-nearest neighbor (KNN, k=1) were employed to classify the depressed females from the controls. These two classifier algorithms were found to be efficient in classification of EEG signals derived from persons with psychological disorders [22, 27, 28].

4 Results

The experimental results include both statistical and classification results. The group averaged values of each feature across Fp1, Fp2 and Fpz electrodes between the Control group and the Depressed group were calculated. The averaged results of linear EEG features are shown in Fig. 2 and nonlinear EEG features are shown in Fig. 3. From these results, it was identified that there were differences for each feature between two groups (DG vs. CG). The significance of the differences is currently unclear and ascertaining the relative significance requires further investigation. Results of *t*-test showed significant group differences (p<0.001) by BDI-II scores while no significant group differences by age (p>0.05).

4.1 Statistical Results

The results of *t*-test for linear and nonlinear EEG features were showed in Table 2 and Table 3 respectively. As can be seen in Table 2, in Fp1, Theta_Abs_Pow, Alpha_Abs_Pow and Beta_Abs_Pow showed significant differences between two groups. And the averaged value difference between two groups in Fpz was significant for Theta_Abs_Pow, Alpha_Abs_Pow, and Beta_Abs_Pow. Finally, in Fp2, the difference was significant for Theta_Abs_Pow, Alpha_Abs_Pow and Beta_Abs_Pow. Results revealed that Depressed group had larger absolute power in the whole band.

As to nonlinear EEG features, C0, LLE and LZC all showed significant differences between two groups except for D2. Specifically, the Depressed group showed increased C0 and LZC while decreased LLE at all three electrodes.

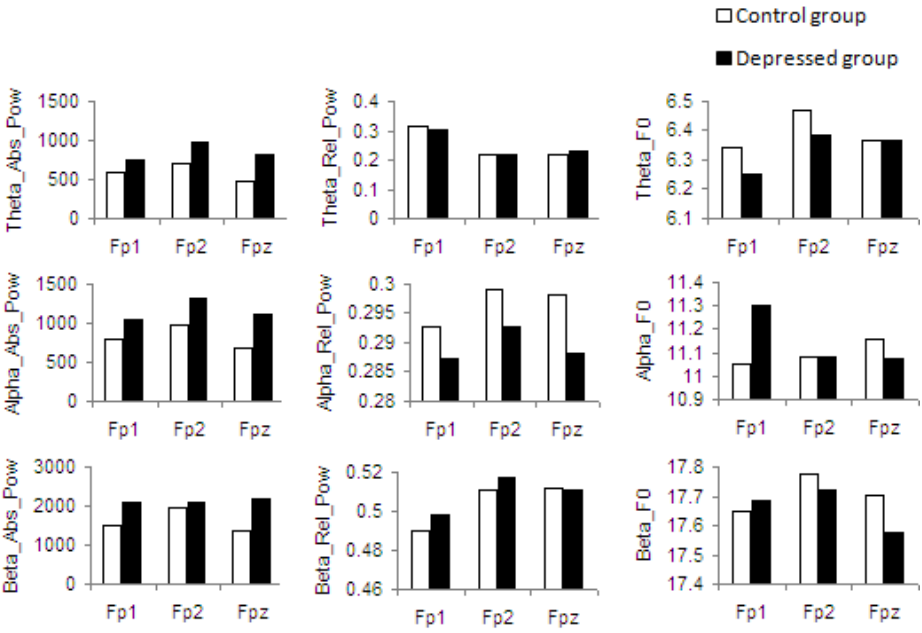

Fig. 2. Group averaged values of linear EEG features across Fp1, Fp2 and Fpz electrodes

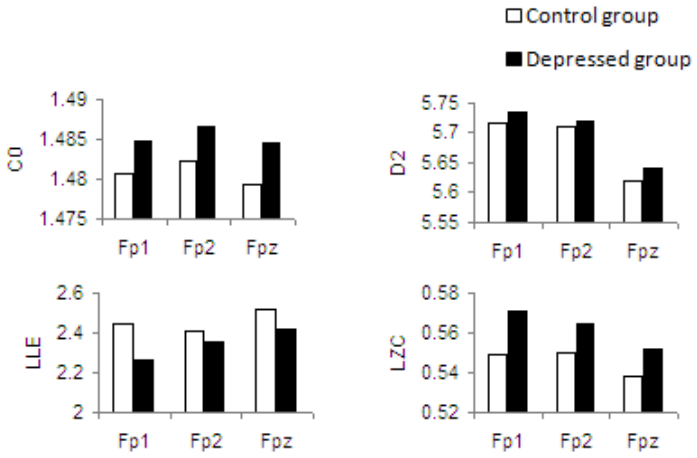

Fig. 3. Group averaged values of nonlinear EEG features across Fp1, Fp2 and Fpz electrodes

4.2 Classification Results

With respect to classification, all dataset were randomly divided into a training set (accounting for 2/3) and a testing set (accounting for 1/3). A 3-cross validation was applied to reach a more reliable and stable classification accuracy. According to

statistical results, Theta_Abs_Pow, Alpha_Abs_Pow, Beta_Abs_Pow, C0, LLE and LZC could significantly discriminate the Depressed group relative to the Control group. So they were taken into consideration and applied as the feature vector for the classifier. A mean classification rate of 94.2% by BPNN and 92.9% by KNN was achieved, meaning that our approach can accurately detect depression in females.

Table 1. Results of *t*-test for linear EEG feature, a significant difference with $p<0.05$

Feature	Theta_Abs_Pow			Theta_Rel_Pow			Theta_F0		
	DG	CG	*p*	DG	CG	*p*	DG	CG	*p*
Fp1	750	586	0.000	0.302	0.314	0.288	6.253	6.340	0.218
Fpz	828	484	0.000	0.228	0.218	0.104	6.366	6.366	0.987
Fp2	969	696	0.000	0.218	0.218	0.992	6.384	6.472	0.207
Feature	Alpha_Abs_Pow			Alpha_Rel_Pow			Alpha_F0		
	DG	CG	*P*	DG	CG	*p*	DG	CG	*p*
Fp1	1051	785	0.000	0.287	0.293	0.123	11.30	11.05	0.426
Fpz	1107	977	0.000	0.288	0.298	0.055	11.08	11.16	0.319
Fp2	1318	675	0.000	0.293	0.299	0.08	11.08	11.09	0.987
Feature	Beta_Abs_Pow			Beta_Rel_Pow			Beta_F0		
	DG	CG	*P*	DG	CG	*p*	DG	CG	*p*
Fp1	2075	1489	0.000	0.498	0.490	0.641	17.68	17.65	0.739
Fpz	2182	1358	0.002	0.511	0.511	0.927	17.58	17.70	0.229
Fp2	2110	1971	0.000	0.518	0.511	0.224	17.72	17.77	0.59

Table 2. Results of *t*-test for nonlinear EEG feature, a significant difference with $p<0.05$

Feature	C0			D2		
	DG	CG	*p*	DG	CG	*p*
Fp1	0.307	0.287	0.000	5.734	5.716	0.644
Fpz	0.287	0.276	0.001	5.640	5.620	0.073
Fp2	0.301	0.295	0.018	5.721	5.710	0.802
Feature	LLE			LZC		
	DG	CG	*p*	DG	CG	*p*
Fp1	2.264	2.444	0.000	0.571	0.549	0.000
Fpz	2.419	2.523	0.002	0.552	0.538	0.000
Fp2	2.350	2.405	0.015	0.565	0.550	0.000

5 Discussion

Our study was motivated by the emergency need of developing a pervasive depression detecting approach for females. In this study, we proposed a depression detecting approach for females by some analysis of EEG. From the above results, it can be seen that depressed females show abnormal EEG when compared with healthy females.

When compared with controls, we found that depressed females had more absolute EEG power in all three frequency bands. Buchsbaum et al. had stated that subjects

with depressive disorders had a significantly higher global cerebral metabolism to exhibit higher metabolism ratios than controls [29]. And Nagata et al. had reported that beta activity to be positively correlated with brain metabolism [30]. Our observation of more cerebrally activated in depressed females was in line with these findings. However, contrasts with our findings, Knott et al. reported the significant differences did not exist in the theta and alpha frequency bands in male depression [13]. These inconsistencies may due to gender differences in neuroendocrinological systems and more work is required to clarify these phenomena [11]. Different findings between these studies further indicate that future research of depression should note that gender form an important consideration in the design of such investigations.

EEG has already been recognized to results from a dynamical system. LZC is a nonlinear dynamical measure which can indicate the probability of generating new patterns in a time series. Larger LZC imply a greater chance of the occurrence of new sequential patterns and thus a more complex dynamical behavior [16]. In our study, the depressed females had a significant larger LZC in all three electrodes compared with those of the controls. Our results are consistent with findings given in, which confirm that depressed subjects present increased LZC than controls. The reason why increased complexity of EEG in the depressed group is that EEG complexity is closely related to the integrity of inter neuronal connectivity; it increases with the number of different oscillatory systems active at the same time. Previous study has described increased functional connectivity in depression by using other methods. Greicius et al. reported an increased functional connectivity using fMRI in depressed patients [31]. Additionally, Fingelkurts et al. also described 'strengthened' functional connectivity using EEG structural synchrony in depression group during a resting condition [32].

C0 was proposed to solve the problem of over-coarse graining preprocessing in LZC. Previous research has reported that C0 is a good indicator of EEG complexity [22]. A novel feature of our study is applying C0 to the analysis of EEG in depressed subjects. Our results showed the depressed females had significant lager C0 than controls, which is similar to our findings of LZC. Therefore, we can infer that increased C0 and LZC of EEG may be markers of depressed subjects.

As to D2, the depressed females showed higher values than of controls. However, all these differences were not significant. The reason is that D2 is a measure of dimensional complexity of a dynamical system, while LZC and C0 represent the sequence pattern complexity of a dynamic system. A higher D2 may not be due to the occurrence of new patterns in the system. D2 and LZC or C0 are the descriptors of dynamical system from two different aspects. Our finding of higher D2 in depressed females is inconstant with findings by [18]. This may be due to our short data sets because the reliable estimation of D2 requires amount of EEG which is beyond the range of most laboratory recordings [33].

Lyapunov Exponent measures the sensitive dependence on the initial conditions. It defines the average rate of divergence of two neighboring trajectories. Traditionally, the LLE was mainly evaluated from sleep EEG in depression. In their study, they found statistically significant decreased values of LLE during some sleep stages in depressives compared with a healthy control group [19]. While in this study, LLE was calculated from resting waking EEG of depressed subjects. Our results showed that

the controls were found to have significant increased LLE in a resting waking state. Under the view that the central nervous system is a complex dynamical system, altered LLE of EEG can be regarded as an expression of disturbed information processing in depression [19].

Various forms of psychopathology have influence on patterns of resting EEG, so it is possible to differentiate depressed subjects from controls on the basis of EEG. To the best of our knowledge, previous studies used either linear or nonlinear EEG features as the input of classifiers [13, 27, 34]. For example, in Knott et al.' work, Delta and Beta inter-hemispheric coherence, beta intra-hemispheric coherence and alpha intra-hemispheric power asymmetry contributed to discriminant analysis and they got overall classification of 91.3% in males [13]. Nonlinear EEG features were also have been used in depression discrimination. Fan et al. applied LZC to get the feature vectors for BPNN and achieved classification accuracies of 60~80% [27]. In our study, feature vectors combining both linear and nonlinear EEG features whose group averaged value differences were significant between two groups, and various classification were implemented. Compared with previous study, although the number of our EEG recording electrodes was relatively limited for the sake of pervasive application, relatively higher classification rates were achieved. Therefore, combining both linear and nonlinear EEG features may be more effective in depression discrimination. Furthermore, classification results show that our pervasive EEG based approach is an effective discriminator for depressed females.

6 Conclusion and Future Work

Although there have been a number of documented research projects investigating depression, relatively few investigations have tried to integrate their findings into a depression detecting approach, especially for pervasive application. In order to meet the needs of emergent mental care for females, we proposed an efficient EEG based approach which could objectively and pervasively detect depression.

By linear and nonlinear analysis of EEG, we've seen that depressed females exhibited abnormal EEG when compared with controls, which were consistent with previous research. This phenomenon may be due to neuropsychological deficit in attention, memory, psychomotor speed, processing speed and executive function in depressed subjects [35]. Depressed subjects need more neuron activities than healthy persons, resulting in more EEG activations.

As a preliminary study in pervasive depression detection, there were some limitations within our work that must be addressed in future research. Firstly, although all the features accounting for classification had significant differences between two groups, the high dimensional feature vectors not only made the classification process complicated but also affected the classification rate. Some of the features may be replaced with others with no loss in classification performance. We will make feature selection to get smaller feature vectors in future work and thus get a faster classification speed to meet the needs of real-time EEG processing in pervasive application. Secondly, we would try to improve classic classification algorithms so as to suit for

applications in pervasive environment. Thirdly, we would also investigate relations between other physiological signals, such as electrocardiograph (ECG) and electromyography (EMG) and depression and then integrate them into our approach. We also intend, furthermore, to extend this EEG based approach to males.

In summary, although EEG analysis can not be applied as a diagnostic tool in depression yet, our experiment results demonstrate that this pervasive EEG based approach could be a pervasive assistant diagnosis tool for psychiatrists and health care specialists currently.

Acknowledgement. This work was supported by the National Basic Research Program of China (973 Program) (grant No. 2011CB711001), National Natural Science Foundation of China (grant No. 60973138), the EU's Seventh Framework Programme OPTIMI (grant No. 248544), and the Fundamental Research Funds for the Central Universities (grant No. lzujbky-2011-k02, lzujbky-2011-129).

References

1. Wells, K.B., Stewart, A., Hays, R.D., Burnam, M.A., Rogers, W., Daniels, M., Berry, S., Greenfield, S., Ware, J.: The functioning and well-being of depressed patients. Results from the Medical Outcomes Study. JAMA 262, 914–919 (1989)
2. Kessler, R.C., Berglund, P., Demler, O., Jin, R., Koretz, D., Merikangas, K.R., Rush, A.J., Walters, E.E., Wang, P.S.: The epidemiology of major depressive disorder: results from the National Comorbidity Survey Replication (NCS-R). JAMA 289, 3095–3105 (2003)
3. Culbertson, F.M.: Depression and gender. An International Review. Am. Psychol. 52, 25–31 (1997)
4. Kessler, R.C.: Epidemiology of women and depression. J. Affect Disord. 74, 5–13 (2003)
5. Wetzel, J.W.: Depression: Women at risk. Social Work in Health Care 19, 85–108 (1994)
6. Michael, S., Carl, M., Pentl, Y.: Objective Physiological and Behavioral Measures for Identifying and Tracking Depression State in Clinically Depressed Patients. Massachusetts Institute of Technology Media Laboratory (2005)
7. Handte, M., Becker, C., Rothermel, K.: Peer-based automatic configuration of pervasive applications. In: Proceedings of International Conference on Pervasive Services, ICPS 2005, pp. 249–260 (2005)
8. Nunez, P.L., Srinivasan, R.: Electric Fields of the Brain: The Neurophysics of EEG. Oxford University Press (2006)
9. Thakor, N.V., Tong, S.: Advances in quantitative electroencephalogram analysis methods. Annu. Rev. Biomed. Eng. 6, 453–495 (2004)
10. Bin, H., Majoe, D., Ratcliffe, M., Yanbing, Q., Qinglin, Z., Hong, P., Dangping, F., Fang, Z., Jackson, M., Moore, P.: EEG-Based Cognitive Interfaces for Ubiquitous Applications: Developments and Challenges. IEEE Intelligent Systems 26, 46–53 (2011)
11. Kaneda, Y., Nakayama, H., Kagawa, K., Furuta, N., Ikuta, T.: Sex differences in visual evoked potential and electroencephalogram of healthy adults. Tokushima J. Exp. Med. 43, 143–157 (1996)
12. Corsi-Cabrera, M., Arce, C., Ramos, J., Guevara, M.A.: Effect of spatial ability and sex inter- and intrahemispheric correlation of EEG activity. Electroencephalography and Clinical Neurophysiology 102, 5–11 (1997)

13. Knott, V., Mahoney, C., Kennedy, S., Evans, K.: EEG power, frequency, asymmetry and coherence in male depression. Psychiatry Res. 106, 123–140 (2001)
14. Pollock, V.E., Schneidera, L.S.: Quantitative, waking EEG research on depression. Biological Psychiatry 27, 757–780 (1990)
15. Nuwer, M.R.: Quantitative EEG: II. Frequency analysis and topographic mapping in clinical settings. J. Clin. Neurophysiol. 5, 45–85 (1988)
16. Li, Y., Tong, S., Liu, D., Gai, Y., Wang, X., Wang, J., Qiu, Y., Zhu, Y.: Abnormal EEG complexity in patients with schizophrenia and depression. Clin. Neurophysiol. 119, 1232–1241 (2008)
17. Stam, C.J.: Nonlinear dynamical analysis of EEG and MEG: review of an emerging field. Clin. Neurophysiol. 116, 2266–2301 (2005)
18. Nandrino, J.L., Pezard, L., Martinerie, J.: Decrease of complexity in EEG as a symptom of depression. Neuroreport 5, 528–530 (1994)
19. Roschke, J., Fell, J., Beckmann, P.: Nonlinear analysis of sleep EEG in depression: calculation of the largest lyapunov exponent. Eur. Arch. Psychiatry Clin. Neurosci. 245, 27–35 (1995)
20. Foster, P.S., Yung, R.C., Branch, K.K., Stringer, K., Ferguson, B.J., Sullivan, W., Drago, V.: Increased spreading activation in depression. Brain Cogn. 77, 265–270 (2011)
21. Hong, P., Bin, H., Yanbing, Q., Qinglin, Z., Ratcliffe, M.: An improved EEG de-noising approach in electroencephalogram (EEG) for home care. In: 2011 5th International Conference on Pervasive Computing Technologies for Healthcare (PervasiveHealth), pp. 469–474 (2011)
22. Zhao, Q.L., Hu, B., Liu, L., Ratcliffe, M., Peng, H., Zhai, J.W., Li, L.L., Shi, Q.X., Liu, Q.Y., Qi, Y.B.: An EEG based nonlinearity analysis method for schizophrenia diagnosis. In: The Ninth IASTED International Conference on Biomedical Engineering (2012)
23. Grassberger, P., Procaccia, I.: Measuring the strangeness of strange attractors. Physica D: Nonlinear Phenomena 9, 189–208 (1983)
24. Rosenstein, M.T., Collins, J.J., De Luca, C.J.: A practical method for calculating largest Lyapunov exponents from small data sets. Physica D: Nonlinear Phenomena 65, 117–134 (1993)
25. Lempel, A., Ziv, J.: On the Complexity of Finite Sequences. IEEE Transactions on Information Theory 22, 75–81 (1976)
26. Kaspar, F., Schuster, H.G.: Easily calculable measure for the complexity of spatiotemporal patterns. Phys. Rev. A 36, 842–848 (1987)
27. Fei-Yan, F., Ying-Jie, L., Yi-Hong, Q., Yi-Sheng, Z.: Use of ANN and Complexity Measures in Cognitive EEG Discrimination. In: 27th Annual International Conference of the Engineering in Medicine and Biology Society, IEEE-EMBS 2005, pp. 4638–4641 (2005)
28. Holla, A.V.R., Aparna, P.: A nearest neighbor based approach for classifying epileptiform EEG using nonlinear DWT features. In: 2012 International Conference on Signal Processing and Communications (SPCOM), pp. 1–5 (2012)
29. Buchsbaum, M.S., Wu, J., DeLisi, L.E., Holcomb, H., Kessler, R., Johnson, J., King, A.C., Hazlett, E., Langston, K., Post, R.M.: Frontal cortex and basal ganglia metabolic rates assessed by positron emission tomography with [18F]2-deoxyglucose in affective illness. J. Affect Disord. 10, 137–152 (1986)
30. Nagata, K., Tagawa, K., Hiroi, S., Shishido, F., Uemura, K.: Electroencephalographic correlates of blood flow and oxygen metabolism provided by positron emission tomography in patients with cerebral infarction. Electroencephalogr. Clin. Neurophysiol. 72, 16–30 (1989)

31. Greicius, M.D., Flores, B.H., Menon, V., Glover, G.H., Solvason, H.B., Kenna, H., Reiss, A.L., Schatzberg, A.F.: Resting-state functional connectivity in major depression: abnormally increased contributions from subgenual cingulate cortex and thalamus. Biol. Psychiatry 62, 429–437 (2007)
32. Fingelkurts, A.A., Rytsala, H., Suominen, K., Isometsa, E., Kahkonen, S.: Impaired functional connectivity at EEG alpha and theta frequency bands in major depression. Human Brain Mapping 28, 247–261 (2007)
33. Na, S.H., Jin, S.H., Kim, S.Y., Ham, B.J.: EEG in schizophrenic patients: mutual information analysis. Clin. Neurophysiol. 113, 1954–1960 (2002)
34. Hosseinifard, B., Moradi, M.H., Rostami, R.: Classifying depression patients and normal subjects using machine learning techniques. In: 19th Iranian Conference on Electrical Engineering (ICEE), Tehran, pp. 1–4 (2011)
35. Gualtieri, C.T., Johnson, L.G., Benedict, K.B.: Neurocognition in depression: patients on and off medication versus healthy comparison subjects. J. Neuropsychiatry Clin. Neurosci. 18, 217–225 (2006)

Opportunistic Networks Architecture with Fixed Infrastructure Nodes

Yong Zhang[1,2], Zhen Wang[2], Jin Li[3], Mei Song[2], Yinglei Teng[2], and Baolin Liu[2]

[1] Beijing Key Laboratory of Work Safety Intelligent Monitoring, Beijing, P.R.C.
yongzhang@bupt.edu.cn
[2] ICN&CAD Center, Beijing University of Posts and Telecommunications, Beijing, P.R.C.
wangzhen1948@gmail.com, {songm,lilytengtt,blliu}@bupt.edu.cn
[3] Beijing Information Science & Technology University, Beijing, P.R.C.
bjlijin@126.com

Abstract. To promote the performance of Opportunistic Networks (ONs), novel network architecture with Fixed Infrastructure Nodes (FINs) is proposed. FINs have large storage capacity and short-range wireless communication ability. Two location strategies of FINs are compared in this paper including location at Points of Interest (POIs) and location at hot spots with high traffic. Routing protocol named PROPHET-F is proposed to employ the FINs' ability. The main difference between PROPHET-F and original PROPHET is that FINs own the highest message forwarding priority. FINs can collect all messages carried by the nodes passing by the FINs and transfer to other proper mobile nodes. The performance of this novel architecture is evaluated in ONE simulation platform. The simulation results indicate that Message Delivery Probability (MDP) in ONs with FINs is improved. MDP is higher while FINs are located at hot spots than at POIs. Furthermore, MDP of PROPHET-F protocol is superior to that of PROPHET.

Keywords: Opportunistic Networks, Network Architecture, Routing Protocol.

1 Introduction

Opportunistic Network (ON) is a kind of network with flat dynamic topology which only can keep intermittent connectivity in the entire network [1, 2]. Nodes in ONs communicate with each other in 'store-carry-forword' manner. The communication in ONs is based on the node mobility [1-3]. The messages sent from the source node should be carried by intermediate nodes to other geographical area and transfer to adjacent nodes until the destination node receives this message.

ON is the evolution of Ad Hoc network [2]. There are many literatures on the capacity of Ad Hoc network[4, 5]. Fixed infrastructure[4] and node mobility [5] can increase the capacity of Ad Hoc. The nodes in ONs are always mobile that is similar to the characteristic of Ad Hoc. However, the network conectivity of ONs is different from Ad Hoc. The nodes can not always keep conectivity to each node in ONs even though the Fixed Infrastructure Nodes (FINs) are set up. Intuitively, the performance of ONs with FINs will be improved. However, throughput and latency may worsen

Q. Zu, B. Hu, and A. Elçi (Eds.): ICPCA-SWS 2012, LNCS 7719, pp. 862–868, 2013.

because some messages may be entraped in some intermediate nodes and can not reach the destination node. The performance of ONs with FINs depends on the location strategy.

Reference [1] propose a hybrid ONs architecture with macro Base Stations (BSs) and Ad Hoc nodes to extend the coverage of BSs. This hybrid architecture employs macro BSs to aggregate traffic and BSs work as specfic ONs nodes which are operator-governed. BSs can keep connection directly using wired or wireless links and form backhaul network. Ad Hoc nodes conect to BSs and form some ONs which take charge of local communication connectity. This is a special application scenario in which all nodes are controlled by Cognitive Management System (CMS).

Pelusi L et al. investigated the ONs architecture and routing protocol in existing literatures [2]. The topology of Delay Tolerant Network (DTN) which is a kind of ONs is flat. Generally, ONs have the same characteristic as DTN. The routing protocols of ONs with infrastructure are discussed in reference [2]. But the routing protocol named SWIM which Pelusi L mentioned in [2] is designed for Ad Hoc network and do not discuss the location strategy of infrastructure. Currently, we do not find any literature that investigates the location strategy of FINs in ONs. Furthermore, the flat topology isn't suitable for the large-scale application. To improve the performance of ONs, we investigate the ONs architecture and propose the location strategy of FINs.

The rest of this paper is structured as follows. We propose a novel ONs architecture in section 2. And then routing protocols in ONs are discussed in section 3. We propose PROPHET-F protocol used in ONs with FINs. We evaluate our proposal in ONE (Opportunistic Networking Environment) [9] simulation platform in section 4. Finally we conclude the paper with a brief discussion.

2 Network Architecture

One of the classic application scenario is wildlife monitoring. ONs can also provide intermittent Internet connectivity to rural and developing areas. In these scenarios, wild animal, person, buses with short-range wireless devices can communicate to their neighborhood. Wireless communication devices can employ WiFi, Bluetooth or Zigbee technologies. Furthermore these nodes always move along the road from one point to another.

Node movement has regular patterns in temporal and spatial scale. Many mobility models are proposed in existing literatures, such as Random Walk Mobility Model, Random Waypoint Mobility Model and so on [6]. A mobility model should attempt to mimic the movements of real nodes, such as Map-Based Movement model (MBM). Generally, pools, holes may be some animals' interested places in wildlife monitoring scenario. The shopping malls, offices, dwelling places, gyms can be some person's frequent destination. These similar places are called POIs (Point of Interest). For more realistic analysis and simulation, Shortest Path Map-Based Movement (SPMBM) is used in this paper. Assume that the probability that node select POI i as the next destination is identical. The probability is p_i

The characteristic of node mobility heavily dependents on the road, location of POIs and nodes' behavior. Considered these factors, geographical area with high traffic flow will come into being. We call the area with high traffic flow 'hot area'.

Vice versa the area with low traffic flow is called ‘cold area‘. The coverage of ‘hot area‘ and ‘cold area‘ is the same as the radio coverage of nodes in ONs. It should be noted that the distance between two neighboring hot areas should be longer than distance of two neighbor crossroads or length of one block. This definition avoids hot areas too concentrated. For example, the radius of hot area is less than 10 meters if Bluetooth devices are equiped by nodes. But shopping malls, offices and other similar places may cover much larger than the range. So there spaces may own a large number of hot areas if we don’t define the distance of two neighbor hot areas. In deed, one hot area can represent the hot level of this place.

To represent the hot level, we give the definition ‘hot level‘ of one spot in map. It can be calculated as $h = N/T$ where N is the number of nodes which enter the coverage of this spot, T is statistics duration. This value can obtained by road testing. The spot is called hot spot if $h > h^*$, where h^* is the threshold and is appointed according to requirement to number of hot areas.

To improve the performance of ONs, extra FINs are located at specific geographical spots which have high hot level. It means that the transmission ranges of FINs can cover hot areas. These FINs have high storage capacity and hence can collect messages from many nodes passing by. But the difference between these FINs and the macro BSs in reference [1] is that these FINs can not connect to each other by direct link.

3 Routing Protocol

In the past few years, a lot of routing protocols are proposed in opportunistic network with flat topology, such as Epidemic routing[7], PROPHET[8], and so on. A few routing protocols based on fixed infrastructure are proposed [2]. As mentioned above, these protocols work in Ad Hoc network. PROPHET uses history of encounters and transitivity to decide the message forwarding strategy and has perfect performance. Herein we propose a variant protocol of PROPHET named PROPHET-F to employ FINs.

The delivery predictability calculation of PROPHET-F is same as that of PROPHET. Probabilistic metric $P_{(a,b)} \in [0,1]$ indicates delivery predictability that every node a for each destination b. When two nodes meet, they exchange the probabilistic metric and update the metric as Eq. 1. If this is their first meeting, an initial delivery probability variable $P_{init} \in [0,1]$ will be set by the two nodes. P_{init} is an initialization constant.

$$P_{(a,b)} = P_{(a,b)old} + (1 - P_{(a,b)old}) \times P_{init} \tag{1}$$

If a pair of nodes does not encounter each other in a while, the delivery predictability value must age as Eq. 2.

$$P_{(a,b)} = P_{(a,b)old} \times \gamma^k \tag{2}$$

Herein, $\gamma \in [0,1]$ is the aging constant, k is the number of elapsed time units from the last time metric was aged.

The transitive property of delivery predictability is described as Eq. 3, where $\beta \in [0,1]$ is a scaling constant.

$$P_{(a,c)} = P_{(a,c)old} + (1 - P_{(a,c)old}) \times P_{(a,b)} \times P_{(b,c)} \times \beta \tag{3}$$

The forwarding strategy of PROPHET-F is different from that of PROPHET. In PROPHET protocol, the message is transfered to the other node if the delivery predictability of the destination node is higher at the other node when two nodes meet. In PROPHET-F protocol, the messages are always transfered to the FINs when the mobile node encounter the FINs whether the delivery predictability of the destination node at the FINs is higher or not. These FINs are located at hot spots and just work as post offices. This strategy is to take full advantage of the FINs‘ high storage capacity to store and forward messages.

The main idea of PROPHET-F protocol is to improve the forwarding priority of FINs. The FINs can receive the messages from the nodes that pass by. This method can be used to extend other routing protocols.

4 Simulation and Analysis

In this section, we use ONE [9] to evaluate the performance of ONs with FINs. The experiment scenario is shown in Figure 1 which is the map of Helsinki city with the size of roughly $4500 \times 3400m$ .The evalution has two parts. Firstly, we measure the hot level to select hot spots to locate the FINs. Secondly, we set up some FINs and compare network performance with that without FINs.

The mobility model is SPMBM. The nodes in the simulation are divided into three parts, pedestrian group (80 nodes), car group (40 nodes) and tram group (6 nodes). These nodes use Bluetooth devices at 2 Mbit/s data rate with 10m radio range. The pedestrians and cars choose random destinations on the map and move there along the shortest path. Trams run along predefined routes. There are several POIs in this map. The probability that nodes go to POIs is $p_i = 0.1$. FINs do not generate messages. The detail simulation parameters are listed in Table 1.

To gather the hot level and hot spots, we locate hundreds of test nodes along the road in the Helsinki map and collect the information of hot level. The test nodes have the same communication ability with the pedestrian group. To compare the network performance, we also measure the hot level of POIs. In the next step, FINs are located in POIs, too. The locations of POIs and hot spots are shown in Figure 2 and the hot levels are listed in Table 2. It should be noted that POI 7 has high hot level. But POI 7 is omitted because it is close to FIN 1.

We compare the Message Delivery Probability (MDP) under different FINs location strategies. Firstly, we collect the MDP in the scenario without FINs using PROPHET. And then, several FINs are located at the hotest spots and the location of POIs. The number of FINs is from 1 to 10. MDPs using PROPHET and PROPHET-F are collected.

The simulation results are represented in Figure 3. From Figure 3, MDP can be improved if the FINs are deployed. Furthermore MDP is higher while FINs are located at hot spots than at the location of POIs. The improvement is more than 20% even if only one FIN are located. The performance of PROPHET-F protocol is better than that of PROPHET.

The average hop number also represents the improvement on transmission performance. We can find from Figure 4 that the average hop number is lower than 3 while FINs are located at hot spots. And the average hop number is higher while FINs are located at POIs.

To reveal why the network performance worsened while FINs are located at POIs, we measure the hot level of POIs and find that the POIs may not be the hotest spots. Some crossroads may entercounter more trafic flow. Some messages that are delivered to FINs at POIs may stay there and can not reach destination node. It is the reason that the performance is better when FINs are located at hot spots than at POIs.

Table 1. Simulation parameters

	pedestrian group	car group	tram group	FIN
Moving speed	0.5-1.5m/s	2.7-13.9m/s	7-10m/s	0
Time To Live (TTL)	4 hours	4 hours	4 hours	4 hours
Buffer space	5-50M bytes	5-50M bytes	5-50M bytes	500M bytes
Message size	500k-1M bytes	500k-1M bytes	500k-1M bytes	0
Message creation interval	25-35 seconds	25-35 seconds	25-35 seconds	0

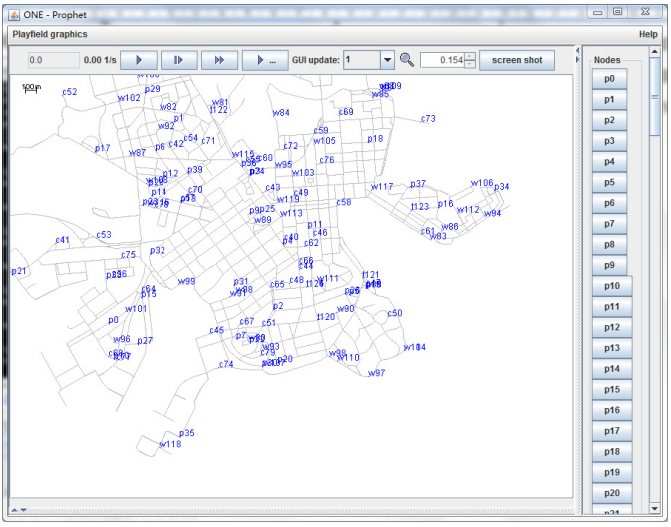

Fig. 1. Simulation scenario (Helsinki city map)

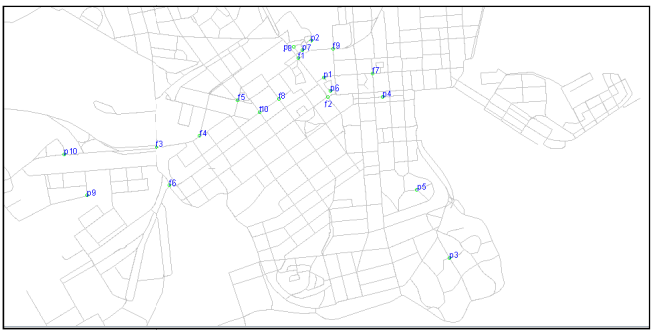

Fig. 2. Location of POIs and FINs (p: POI; f: FIN)

Table 2. Hot level of POIs and FINs (Hot level: number of encounters per hour)

No.	1	2	3	4	5	6	7	8	9	10
Hot level of PoI	17	44	6	4	2	5	91	1	25	46
Hot level of FIN	120	76	92	91	77	101	103	65	104	69

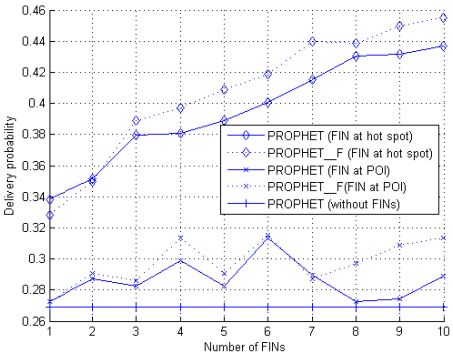

Fig. 3. Delivery probability using different FINs location strategies

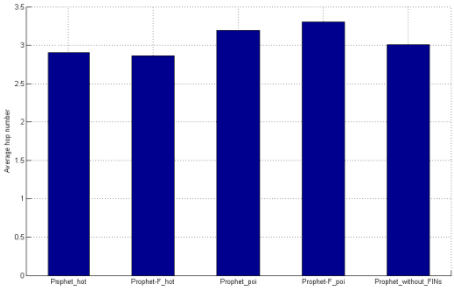

Fig. 4. Average hop number using different FINs location strategies

5 Conclusion

In this paper, we investigate the network architecture of ONs. Novel network architecture with FINs is proposed. Location stragety of FINs can improve the ONs delivery probability. The proposed routing protocol are designed based on PROPHET. But this main idea can extended to other routing protocols. The simulation results prove that the proposal can promote the performance of ONs with low cost.

Acknowledgement. This work is supported by National Natural Science Foundation of China (61171097), the State Major Science and Technology Special Projects (2011ZX03003-002-01) and International Scientific and Technological Cooperation Program (2010DFA11060).

References

1. Stavroulaki, V., Tsagkaris, K., Logothetis, M., et al.: Opportunistic networks. IEEE Vehicular Technology Magazine 6(3), 52–59 (2011)
2. Pelusi, L., Passarella, A., Conti, M.: Opportunistic Networking: Data Forwarding in Disconnected Mobile Ad Hoc Networks. IEEE Communications Magazine 44(11), 134–141 (2006)
3. Chaintreau, A., Hui, P., Crowcroft, J., et al.: Impact of human mobility on opportunistic forwarding algorithms. IEEE Transactions on Mobile Computing 6(6), 606–620 (2007)
4. Zemlianov, A., Veciana, G.D.: Capacity of Ad hoc wireless networks with infrastructure support. IEEE Journal on Selected Areas in Communications 23(3), 657–667 (2005)
5. Grossglauser, M., Tse, D.N.C.: Mobility increases the capacity of ad-hoc wireless networks. In: INFOCOM 2001. Twentieth Annual Joint Conference of the IEEE Computer and Communications Societies, vol. 3, pp. 22–26 (April 2001)
6. Karamshuk, D., Boldrini, C., Conti, M., et al.: Human mobility models for Opportunistic Networks. IEEE Communications Magazine 49(12), 157–165 (2011)
7. Vahdat, A., Becker, D.: Epidemic routing for partially connected ad hoc networks. Duke University, tech. Rep. CS-20006 (April 2000)
8. Lindgren, A., Doria, A.: Probabilistic routing in intermittently connected networks. Mobile Computing and Communication Review 7(3), 239–254 (2004)
9. Keronen, A., Ott, J.: The ONE simulator for DTN protocol evaluation. In: Proceedings of the 2nd International Conference on Simulation Tools and Techniques, Rome, Italy, pp. 1–10 (2009)

An Improved DNA Computing Method for Elevator Scheduling Problem

Hong-Chao Zhao and Xi-Yu Liu

Management Science and Engineering College, Shan Dong Normal University, Jinan, China
zhaohongchao1987@126.com

Abstract. In the paper, an algorithm based on DNA computing which can solve the elevator scheduling problem is improved. Considering the inefficiency of the existing algorithm caused by the large scale of the initial solution space, the author introduces a new conception --"connecting strand" to help produce the initial solution space in the new algorithm. “Connecting strand” can connect those rational DNA strands encoding different elevators’ running routes into one and the strand obtained just stands for the “sum-route” of the elevator system. With the help of “connecting strand”, the size of initial solution space is largely reduced and the performance of the algorithm is thus improved. In the end, the author proves the effectiveness of the algorithm by a simulation.

Keywords: DNA computing, elevator scheduling problem, connecting strand, shortest path problem, encoding.

1 Introduction

In 1994, Adleman published <<Molecular computation of solutions to combinatorial problems>> [1] on Science, in which he solved a 7-vertex instance of the Hamilton path problem by molecular biology techniques creatively. From then on, DNA computing was created and became the research focus of many subjects rapidly.

DNA computing differs from the traditional computing pattern, it uses interaction between DNA molecules to achieve parallel computing and its inherent huge parallel computing power endows itself with great potential in solving many tricky non-linear problems and NP-complete problems. Following Adleman's work, many researchers have solved a large number of hard problems using DNA computing [2-6]. Junzo Watada and his partners raised an idea of solving elevator scheduling problem by DNA computing [5,6]. In this paper, the author improves Junzo Watada's algorithm by introducing a new concept --"connecting strand" to reduce the size of the initial solution space greatly.

2 Elevator Scheduling Problem[5]

Now, elevators are widely used in skyscrapers, so efficient control of them is essential. We must confirm all the elevators in one group run reasonably to satisfy all the passengers and consume the least time at the same time.

Q. Zu, B. Hu, and A. Elçi (Eds.): ICPCA-SWS 2012, LNCS 7719, pp. 869–875, 2013.

We suppose a skyscraper with 8 floors is equipped with 2 elevators: elevator A and elevator B. At time-t, the status of the elevator system is shown by table 1

Table 1. Status of elevator system at time-*t*

Floor	Direction	Elevator A's destinations	Elevator B's destinations
8		(3,1)	
7	↓		
6			
5	↑		
4	↓		
3			
2	↑		
1			(6,8)

Here, we define two variables:

***T(i,j)*:** the time of an elevator spent running from floor *i* to floor *j*

***T_S*:** the staying time of an elevator at one floor

We suppose elevator A is on floor *i* and all its possible destination floors are the other 7 floors, the situation can be presented by Fig.1. The weights of arcs can be calculated by the sum of running time and staying time, that is:

$$\omega|j-i|=T(i,j)+Ts. \tag{1}$$

For each problem, we can construct a weighted directed graph for every elevator based on Fig.1.

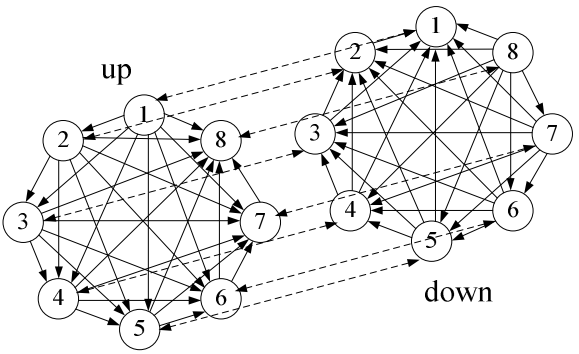

Fig. 1. Movement of an elevator

If we define 5 seconds as a unit, we get values as weights of the arcs as below:

ω1=5+15=20s=4 ω2=10+15=25s=5 ω3=15+15=30s=6 ω4=20+15=35s=7
ω5=25+15=40s=8 ω6=30+15=45s=9 ω7=35+15=50s=10.

We shall control elevator A and B to meet the requirements of the passengers inside and those on the 2nd, 4th, 5th and 7th floors and guarantee the time consumed should be the least simultaneously.

3 DNA Computing

An single strand of DNA is a polymer which is strung together from monomers called deoxyribonucleotides and there are only four kinds of deoxyribonucleotides which are adenine (abbreviated A), guanine(abbreviated G), cytosine (abbreviated C)and thymine (abbreviated T). Two single strands of DNA can form a double strand if the respective bases are the Watson–Crick complements of each other—A matches T and C matches G, also 3'-end matches 5'-end. For example, the single strands 5'-ACGGT-3' and 3'-TGCCA-5' can form a double one, we also call strand 3'-TGCCA-5' as the complementary strand of 5'-ACGGT-3'.

The procedure of DNA computing to solve problems is to map the problem to DNA fragments which are specially designed firstly, the process is called encoding, and then generate the initial solution space by biochemical reactions with the catalysis of enzymes, after that filter out the target molecules using modern molecular biology technologies and decode the molecules, finally, read out the information from the strands obtained to get the solutions.

4 DNA Algorithm for Elevator Scheduling Problem

Combined with the instance of elevator scheduling problem in part 2, we describe the procedure of the algorithm as follows:

Step 1: Construct the weighted directed graph for each elevator. The figure for elevator A and B is shown in Fig.2.

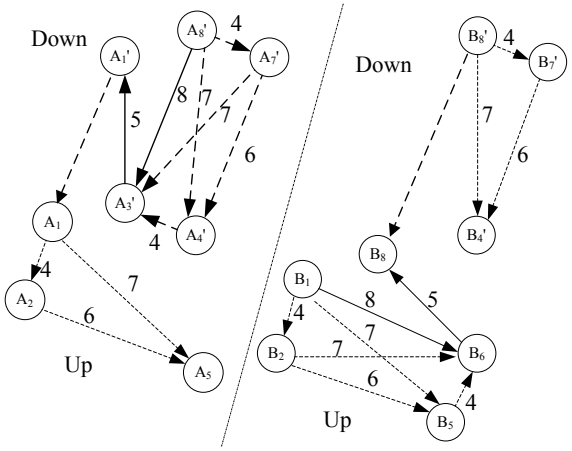

Fig. 2. The weighted directed graph for elevator A and B

Step 2: Encode the vertexes in the graph firstly. Each sequence for a vertex can be divided into two parts evenly which are represented by Via and Vib. Some encodings are listed as follows in table 2.

Table 2. Codes for the vertexes A1, B2, A8' and B8'

Up	20-mer DNA sequences(5'~3')		GC%	T_m(℃)
	V_{ia}	V_{ib}		
A_1	TACTGCGGAA	AGCAGACAGA	50	58.4
B_1	AAGCGTCTGG	CATCTCTTGA	50	55.3
Down	20-mer DNA sequences(5'~3')		GC%	T_m(℃)
	V_{ia}	V_{ib}		
A_8'	GGCAGGCGAC	CTAGACTTAT	55	60.5
B_8'	AACACGGTTA	AGATTCGCCG	50	58.4

Secondly, encode the arcs in the graph; each sequence consists of three parts: part A, B and C. For the arc e_{ij} connecting vertex Vi and Vj, part A is the complementary of the latter half of vertex Vi's encoding, part B is the complementary of the former half of vertex Vj's encoding and part C is a fixed-length DNA sequence whose length equals three times of the weight of arc e_{ij}. The structure of the sequence for arc e_{ij} is shown in Fig.3.

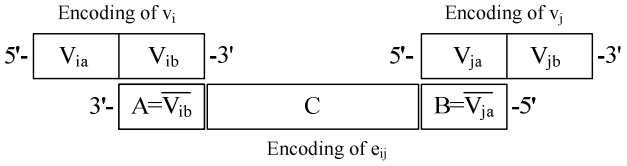

Fig. 3. Structure of the arc e_{ij}

Finally, we describe the encoding of the "connecting strand". The connecting strand consists of two parts, the former half is the complementary of the second part of encoding of terminal point of the route A and the latter half is the complementary of the first part of encoding of starting point of route B. For the instance above, the starting point of route B is vertex B1, but the destination of elevator A is uncertain which may be vertex A1', A2 or A5, so there are three connecting strands in all which are $3'-\overline{A_{1'b}}\,\overline{B_{1a}}-5'$, $3'-\overline{A_{2b}}\,\overline{B_{1a}}-5'$ and $3'-\overline{A_{5b}}\,\overline{B_{1a}}-5'$.

Step 3: Mix sufficient four kinds of nucleosides and three groups of DNA sequences together to produce the initial solution after full reaction.

Step 4: By hybridization separation, we can separate DNA strands which contain the encoding segments of two groups of vertexes-- (A8', A3', A1') and (B1, B3, B6). After that, for four groups of vertexes --(A2, B2), (A5, B5), (A4', B4') and (A7', B7'), we separate the sequences which encode only one vertex in each group. For example, for (A2, B2), we should separate the strands containing encoding of vertex A2 but not containing vertex B2 and so it is with the contrary. In this case, we can confirm that only one elevator reach a floor to take the passengers. At last, we duplicate the strands obtained by PCR as the sets of feasible solutions.

Step 5: Separate the shortest strands by gel electrophoresis as the encoding of the optimal solution.

Step 6: Check out the information of the DNA obtained in step 5 and get the optimal solution.

5 Simulation

Here, we use a java program to simulate how the algorithm works. We describe four main steps as follows.

Step 1: Based on Fig.2, generate two groups of strings. The first group includes strings for all the possible routes of elevator A which start with vertex A8' and end with A2, A5 or A1'; the second group includes those for elevator B which start with vertex B1 and ends with B8, B4' and B7'. All the strings are stored in two arrays which are listed in table 3. It is noted that the number above "-" represents the number of it, not a real number.

Table 3. The routes of elevator A and B

Routes of Elevator A	Routes of Elevator B
$A'_8 \overset{8}{-} A'_3 \overset{5}{-} A'_1$	$B_1 \overset{8}{-} B_6 \overset{5}{-} B_8$
$A'_8 \overset{4}{-} A'_7 \overset{7}{-} A'_3 \overset{5}{-} A'_1$	$B_1 \overset{4}{-} B_2 \overset{7}{-} B_6 \overset{5}{-} B_8$
$A'_8 \overset{7}{-} A'_4 \overset{4}{-} A'_3 \overset{5}{-} A'_1$	$B_1 \overset{7}{-} B_5 \overset{4}{-} B_6 \overset{5}{-} B_8$
$A'_8 \overset{4}{-} A'_7 \overset{6}{-} A'_4 \overset{4}{-} A'_3 \overset{5}{-} A'_1$	$B_1 \overset{4}{-} B_2 \overset{6}{-} B_5 \overset{4}{-} B_6 \overset{5}{-} B_8$
$A'_8 \overset{8}{-} A'_3 \overset{5}{-} A'_1 \overset{0}{-} A_1 \overset{4}{-} A_2$	$B_1 \overset{8}{-} B_6 \overset{5}{-} B_8 \overset{0}{-} B'_8 \overset{4}{-} B'_7$
$A'_8 \overset{4}{-} A'_7 \overset{7}{-} A'_3 \overset{5}{-} A'_1 \overset{0}{-} A_1 \overset{4}{-} A_2$	$B_1 \overset{4}{-} B_2 \overset{7}{-} B_6 \overset{5}{-} B_8 \overset{0}{-} B'_8 \overset{4}{-} B'_7$
$A'_8 \overset{7}{-} A'_4 \overset{4}{-} A'_3 \overset{5}{-} A'_1 \overset{0}{-} A_1 \overset{4}{-} A_2$	$B_1 \overset{7}{-} B_5 \overset{4}{-} B_6 \overset{5}{-} B_8 \overset{0}{-} B'_8 \overset{4}{-} B'_7$
$A'_8 \overset{4}{-} A'_7 \overset{6}{-} A'_4 \overset{4}{-} A'_3 \overset{5}{-} A'_1 \overset{0}{-} A_1 \overset{4}{-} A_2$	$B_1 \overset{4}{-} B_2 \overset{6}{-} B_5 \overset{4}{-} B_6 \overset{5}{-} B_8 \overset{0}{-} B'_8 \overset{4}{-} B'_7$
$A'_8 \overset{8}{-} A'_3 \overset{5}{-} A'_1 \overset{0}{-} A_1 \overset{4}{-} A_2 \overset{6}{-} A_5$	$B_1 \overset{8}{-} B_6 \overset{5}{-} B_8 \overset{0}{-} B'_8 \overset{4}{-} B'_7 \overset{6}{-} B'_4$
$A'_8 \overset{4}{-} A'_7 \overset{7}{-} A'_3 \overset{5}{-} A'_1 \overset{0}{-} A_1 \overset{4}{-} A_2 \overset{6}{-} A_5$	$B_1 \overset{4}{-} B_2 \overset{7}{-} B_6 \overset{5}{-} B_8 \overset{0}{-} B'_8 \overset{4}{-} B'_7 \overset{6}{-} B'_4$
$A'_8 \overset{7}{-} A'_4 \overset{7}{-} A'_3 \overset{5}{-} A'_1 \overset{0}{-} A_1 \overset{4}{-} A_2 \overset{6}{-} A_5$	$B_1 \overset{7}{-} B_5 \overset{4}{-} B_6 \overset{5}{-} B_8 \overset{0}{-} B'_8 \overset{4}{-} B'_7 \overset{6}{-} B'_4$
$A'_8 \overset{4}{-} A'_7 \overset{6}{-} A'_4 \overset{4}{-} A'_3 \overset{5}{-} A'_1 \overset{0}{-} A_1 \overset{4}{-} A_2 \overset{6}{-} A_5$	$B_1 \overset{4}{-} B_2 \overset{6}{-} B_5 \overset{4}{-} B_6 \overset{5}{-} B_8 \overset{0}{-} B'_8 \overset{4}{-} B'_7 \overset{6}{-} B'_4$
$A'_8 \overset{8}{-} A'_3 \overset{5}{-} A'_1 \overset{0}{-} A_1 \overset{7}{-} A_5$	$B_1 \overset{8}{-} B_6 \overset{5}{-} B_8 \overset{0}{-} B'_8 \overset{7}{-} B'_4$
$A'_8 \overset{4}{-} A'_7 \overset{7}{-} A'_3 \overset{5}{-} A'_1 \overset{0}{-} A_1 \overset{7}{-} A_5$	$B_1 \overset{4}{-} B_2 \overset{7}{-} B_6 \overset{5}{-} B_8 \overset{0}{-} B'_8 \overset{7}{-} B'_4$
$A'_8 \overset{7}{-} A'_4 \overset{4}{-} A'_3 \overset{5}{-} A'_1 \overset{0}{-} A_1 \overset{7}{-} A_5$	$B_1 \overset{7}{-} B_5 \overset{4}{-} B_6 \overset{5}{-} B_8 \overset{0}{-} B'_8 \overset{7}{-} B'_4$
$A'_8 \overset{4}{-} A'_7 \overset{6}{-} A'_4 \overset{4}{-} A'_3 \overset{5}{-} A'_1 \overset{0}{-} A_1 \overset{7}{-} A_5$	$B_1 \overset{4}{-} B_2 \overset{6}{-} B_5 \overset{4}{-} B_6 \overset{5}{-} B_8 \overset{0}{-} B'_8 \overset{7}{-} B'_4$

Step 2: Connect every string in array A with those in array B and store result strands in array C. The elements in array C just stand for the total routes of the elevator system. The array C is not list any more.

Step 3: Filter out the strings which include only one vertex in each group: (A_2, B_2)、(A_5, B_5)、(A_4', B_4') and (A_7', B_7') and store them in array D, the array D just contains the strings standing for the feasible solutions which are listed in table 4.

Table 4. Strings in array D

number	route
1	$A'_8 \overset{4}{-} A'_7 \overset{6}{-} A'_4 \overset{4}{-} A'_3 \overset{5}{-} A'_1 \overset{0}{-} A_1 \overset{4}{-} A_2 \overset{6}{-} A_5 + B_1 \overset{8}{-} B_6 \overset{5}{-} B_8$
2	$A'_8 \overset{4}{-} A'_7 \overset{6}{-} A'_4 \overset{4}{-} A'_3 \overset{5}{-} A'_1 \overset{0}{-} A_1 \overset{7}{-} A_5 + B_1 \overset{4}{-} B_2 \overset{7}{-} B_6 \overset{5}{-} B_8$
3	$A'_8 \overset{4}{-} A'_7 \overset{6}{-} A'_4 \overset{4}{-} A'_3 \overset{5}{-} A'_1 \overset{0}{-} A_1 \overset{4}{-} A_2 + B_1 \overset{7}{-} B_5 \overset{4}{-} B_6 \overset{5}{-} B_8$
4	$A'_8 \overset{4}{-} A'_7 \overset{7}{-} A'_3 \overset{5}{-} A'_1 \overset{0}{-} A_1 \overset{4}{-} A_2 \overset{6}{-} A_5 + B_1 \overset{8}{-} B_6 \overset{5}{-} B_8 \overset{0}{-} B'_8 \overset{7}{-} B'_4$
5	$A'_8 \overset{7}{-} A'_4 \overset{7}{-} A'_3 \overset{5}{-} A'_1 \overset{0}{-} A_1 \overset{4}{-} A_2 \overset{6}{-} A_5 + B_1 \overset{8}{-} B_6 \overset{5}{-} B_8 \overset{0}{-} B'_8 \overset{4}{-} B'_7$
6	$A'_8 \overset{4}{-} A'_7 \overset{6}{-} A'_4 \overset{4}{-} A'_3 \overset{5}{-} A'_1 + B_1 \overset{4}{-} B_2 \overset{6}{-} B_5 \overset{4}{-} B_6 \overset{5}{-} B_8$
7	$A'_8 \overset{4}{-} A'_7 \overset{7}{-} A'_3 \overset{5}{-} A'_1 \overset{0}{-} A_1 \overset{7}{-} A_5 + B_1 \overset{4}{-} B_2 \overset{7}{-} B_6 \overset{5}{-} B_8 \overset{0}{-} B'_8 \overset{7}{-} B'_4$
8	$A'_8 \overset{4}{-} A'_7 \overset{7}{-} A'_3 \overset{5}{-} A'_1 \overset{0}{-} A_1 \overset{4}{-} A_2 + B_1 \overset{7}{-} B_5 \overset{4}{-} B_6 \overset{5}{-} B_8 \overset{0}{-} B'_8 \overset{7}{-} B'_4$
9	$A'_8 \overset{7}{-} A'_4 \overset{4}{-} A'_3 \overset{5}{-} A'_1 \overset{0}{-} A_1 \overset{7}{-} A_5 + B_1 \overset{4}{-} B_2 \overset{7}{-} B_6 \overset{5}{-} B_8 \overset{0}{-} B'_8 \overset{4}{-} B'_7$
10	$A'_8 \overset{7}{-} A'_4 \overset{4}{-} A'_3 \overset{5}{-} A'_1 \overset{0}{-} A_1 \overset{4}{-} A_2 + B_1 \overset{7}{-} B_5 \overset{4}{-} B_6 \overset{5}{-} B_8 \overset{0}{-} B'_8 \overset{4}{-} B'_7$
11	$A'_8 \overset{8}{-} A'_3 \overset{5}{-} A'_1 \overset{0}{-} A_1 \overset{4}{-} A_2 \overset{6}{-} A_5 + B_1 \overset{8}{-} B_6 \overset{5}{-} B_8 \overset{0}{-} B'_8 \overset{4}{-} B'_7 \overset{6}{-} B'_4$
12	$A'_8 \overset{4}{-} A'_7 \overset{7}{-} A'_3 \overset{5}{-} A'_1 + B_1 \overset{4}{-} B_2 \overset{6}{-} B_5 \overset{4}{-} B_6 \overset{5}{-} B_8 \overset{0}{-} B'_8 \overset{7}{-} B'_4$
13	$A'_8 \overset{7}{-} A'_4 \overset{4}{-} A'_3 \overset{5}{-} A'_1 + B_1 \overset{4}{-} B_2 \overset{6}{-} B_5 \overset{4}{-} B_6 \overset{5}{-} B_8 \overset{0}{-} B'_8 \overset{4}{-} B'_7$
14	$A'_8 \overset{8}{-} A'_3 \overset{5}{-} A'_1 \overset{0}{-} A_1 \overset{7}{-} A_5 + B_1 \overset{4}{-} B_2 \overset{7}{-} B_6 \overset{5}{-} B_8 \overset{0}{-} B'_8 \overset{4}{-} B'_7 \overset{6}{-} B'_4$
15	$A'_8 \overset{8}{-} A'_3 \overset{5}{-} A'_1 \overset{0}{-} A_1 \overset{4}{-} A_2 + B_1 \overset{7}{-} B_5 \overset{4}{-} B_6 \overset{5}{-} B_8 \overset{0}{-} B'_8 \overset{4}{-} B'_7 \overset{6}{-} B'_4$
16	$A'_8 \overset{8}{-} A'_3 \overset{5}{-} A'_1 + B_1 \overset{4}{-} B_2 \overset{6}{-} B_5 \overset{4}{-} B_6 \overset{5}{-} B_8 \overset{0}{-} B'_8 \overset{4}{-} B'_7 \overset{6}{-} B'_4$

Step 4: Select the string with the fewest "-" in array D. Here the string $A'_8 \overset{4}{-} A'_7 \overset{6}{-} A'_4 \overset{4}{-} A'_3 \overset{5}{-} A'_1 + B_1 \overset{4}{-} B_2 \overset{6}{-} B_5 \overset{4}{-} B_6 \overset{5}{-} B_8$ is the target and it reflects that when elevator A runs in the route A'_8->A'_7-> A'_4->A'_3->A'_1 and elevator B runs in the route B_1->B_2->B_5->B_6->B_8, the elevator is the most efficient.

6 Conclusion

In Junzo Watada's work, any two sequences representing two elevators' running route can be connected, which leads that the size of the initial solution space is very large. With the help of "connecting strand", only those reasonable sequences can be connected, as a result, the size of initial solution space can be reduced by several magnitudes and the performance is thus improved.

References

1. Adleman, L.M.: Molecular Computation of Solutions to Combinatorial Problems. Science 266, 1021–1024 (1994)
2. Lipton, R.J.: DNA Solution of Hard Computational Problems. Science 268, 542–545 (1995)
3. Ouyang, Q., Kaplan, P.D., Liu, S., et al.: DNA Solution of the Maximal Clique Problem. Science 278, 446–449 (1997)
4. Sakamoto, K., Gouzu, H., Komiya, K., et al.: Molecular Computation by DNA Hairpin Formation. Science 288, 1223–1226 (2000)
5. Muhanmmad, M.S., Ueda, S., Watada, J., et al.: Solving Elevator Scheduling Problem Using DNA Computing Approach. Advances in Soft Computing 29, 359–370 (2005)
6. Watada, J.: DNA Computing and Its Applications. Studies in Computational Intelligence 115, 1065–1089 (2008)

Campus Network Operation and Maintenance Management and Service Based on ITIL Service Desk

Hong-yu Zhao[1], Yong-qiang Wang[2], Xue-yan Zhang[3], and Li-you Yang[1]

[1.] Network Center of Logistics Academy, Beijing, 100850
[2] Network Center of CESEC, Beijing, 100840
[3] Graduate School of the Academy of Medical Sciences, Beijing, 100850
{zhaohy_web,yqw323}@sina.com, zxueyan19@yahoo.com.cn,
mytbaby@sohu.com

Abstract. This paper describes the current status and requirements of Campus Network operation &maintenance management, introduces ITIL to the campus network management as a new common framework, and points out the need for building a unified operation & maintenance management system. Through the establishment of the network operation & maintenance management and service based on ITIL Service Desk, it is possible to improve business processes and gradually standardize the campus network operation & maintenance management and service.

Keywords: ITIL, Service Desk, network operation & maintenance, management and service.

1 Introduction

After more than ten years of development, the focus of information construction in colleges and universities has shifted from “sharing information, integrating and eliminating islands of information" to establishing a digital campus committed to satisfying personalized needs of teaching and research.

As the main sector of the campus information construction, Information Management Center is playing an increasingly important role. However, with the further development of information construction, Information Management Center has to bear enormous workload and face many new problems, such as the unreasonable organization of the technical service team, the vague division of functions, and the lack of practical service quality management processes and regulations. Every day network management and maintenance personnel struggle to cope with a variety of heavy workload involving maintenance, management and service, but are still not able to fully meet the needs of teaching and research.

How can we find an effective solution to the problems in network operation & maintenance management and service? The answer may lie in the development and construction of a scientific and effective network operation & maintenance

Q. Zu, B. Hu, and A. Elçi (Eds.): ICPCA-SWS 2012, LNCS 7719, pp. 876–882, 2013.

management Service Desk integrating organizations, systems, processes and technology. This may ensure the progressive realization of standardized and professional management.

2 Current Status of University Campus Network Operation and Maintenance

Lack of Standardized Management Mechanisms and Processes. At present, there is still a gap between network management awareness and the practical needs of colleges and universities. There is also a lack of management personnel. Limited staff has to deal with diverse network users and functions, making it more difficult to improve network management. In addition, there is a lack of management tools and standardized management processes.

Lack of Summary of the Service Pattern. It is necessary to set up a scientific maintenance system, supplemented by fault handling, which should serve as the guiding principle for network operation & maintenance service support. It is also important to combine this main line of thinking with practical business and tap the regularity of network management, so that network management practices and systems can be more in line with the institutional requirements.

Lack of Data Sharing Platform and Software System Support. Due to the lack of a unified sharing of fundamental data, it is difficult to associate network service support with the service, service level agreements, user and network infrastructure. Statistical analysis of service is unavailable or is merely reduced to running account. The information recorded on paper cannot support intelligent analysis and statistics, let alone provide the basis for network management and service.

3 Network Operation and Maintenance Goals

In specific, the campus network operation & maintenance process management and service is to achieve the following objectives:

- To build a centralized, unified network operation & maintenance process management platform, with all the tasks shown in one work list.
- To standardize the routine business processes, reduce exception tasks, and support a variety of daily key operations.
- To monitor all business processes to achieve closed-loop management and accurate administration.
- To adapt network operation & maintenance process management platform to the optimization of operation & maintenance processes. The changes should be flexible, configurable and scalable rather than fixed, non-extendable or impossible to use.

- To ensure that network operation & maintenance process management platform is open enough to be integrated with other systems.
- To effectively reduce the probability of network service failures and timely handle network service failures.

4 Operation and Maintenance Management Service Based on ITIL

If Service Desk can be built on common framework ITIL, and used in network operation & maintenance management and service, the construction of campus network operation & maintenance management and service platform will be promoted and the service quality of the Information Management Center will be improved.

4.1 Introduction to ITIL

ITIL, known as Information Technology Infrastructure Library, is a series of IT service management standards and best practice guides widely accepted and used in the world. ITIL emphasizes the core idea that demands for IT service should be considered not only from the perspective of IT service providers and technology, but more from that of the users and businesses. The core module of ITIL is service management. The ten core service management processes are divided into two categories: service and support. Service is composed of five processes: service level management, IT service cost management, IT service continuity management, availability management and capacity management, while support comprises five processes: incident management, problem management, configuration management, change management and release management as well as help desk function.

It can be seen that IT service management is a process-oriented and user-centered way to improve the capacity and level of support and service through the integration of IT services and organizational operations.

4.2 Specifications and Processes of ITIL-Based Network Operation and Maintenance Management and Service

ITIL-based network management and service specifications and processes can make operation and application of the application system more standardized, rational and smooth. They include incident management, problem management, change management, release management, configuration management, work order management, operational plans, duty management, assessment management, knowledge management and security management. (Figure 1)

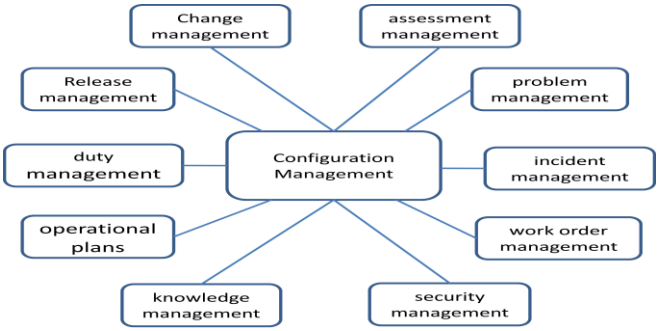

Fig. 1. ITIL-based Network Management and Service Processes

4.3 ITIL Service Desk and Construction

Service Desk usually refers to Help Desk, which serves as a service function rather than a management process in ITIL. In the network operation & maintenance management and service, Service Desk providing users with a single point of contact is the link between the user and the IT department.

Goal of Constructing Service Desk. The goal of constructing Service Desk is to provide a central point of contact to meet the needs of all users, restore service to its normal state as quickly as possible, and provide high-quality technical support so as to achieve business objectives. Service Desk should support changes, generate reports, promote network service, contact, receive, record and track all calls, support the upgrade and feedback of service calls, which plays an important role in the lifecycle management in incident management.

Service Desk Construction Methods. Service Desk is user-centered and composed of personnel with strong technical and coordinating capability. Service Desk staff not only participates in the two processes of dealing with incidents and problems, but also provides support for other processes (change, release, assets, etc.). Service Desk is also an element of the network service management as well as the maintainer of the Knowledge Base. To build ITIL Service Desk in colleges and universities and render it the main service center of the campus network, we must have incident, problem, change and configuration management in place and build the knowledge base update capability. Service Desk can focus on information from the user and process node, start the standard processes and methods to deal with all the events, and constantly improve work efficiency and quality to perfect the indicators, enhance customer satisfaction, and ultimately reduce operating costs, thus providing technical support for the development of information construction in colleges and universities.

Thus, the Center personnel no longer have to play the traditional role of the "fireman", which means a shift from working passively to working actively. For the majority of the faculty, Service Desk provides them with a single window of contact with Management Center, ensuring that they can find the technical staff to fix their

problems or respond to their requests without having to record a large number of phone numbers. That is to say, the problem can be solved as long as they find Service Desk. In addition Service Desk, as the initiator and terminator of events, also has an evaluation system to track and respond to the progress of each event.

Content and Process of Service Desk Construction. Through the construction of Service Desk, we can gradually build a network service center including people, processes and technology, which are consistent with the three core elements of ITSM: organization, practice and tools. A user-centered and service-oriented Service Desk can promote the standardization of work processes and maximize resource sharing, and is in line with the guideline of developing people-based information technology.

To construct ITIL Service Desk, we should start with developing a clear plan to determine the specific objectives and major tasks. Next, we should define assessment targets and the related business process design. Then we should properly handle relations and performance of the three core elements of ITSM in the operation of Service Desk.

Service Desk, serving one of the management functions in the construction of campus network maintenance management and service center, is mainly associated with incident management, change management, configuration and release management and a knowledge base. (Figure 2)

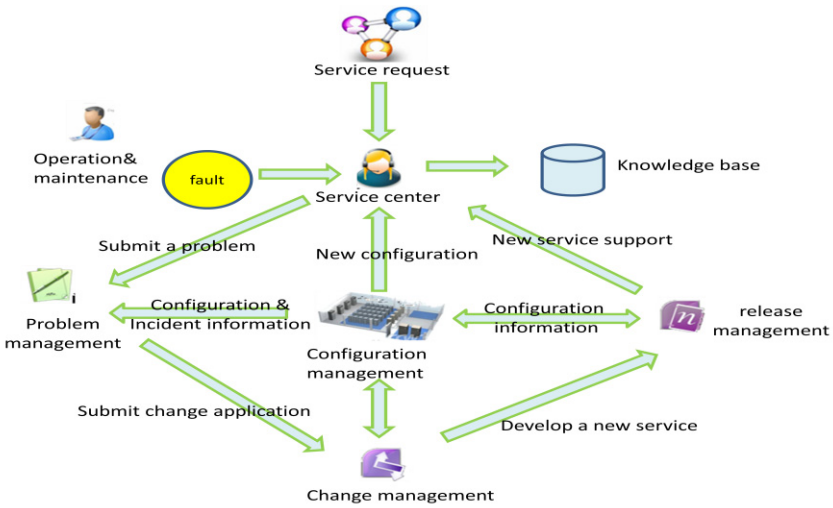

Fig. 2. Service Desk

Its main work involves: fault monitoring, service call reception, recording, tracking and prioritization, monitoring of all registered calls and upgrade of status tracking call service, call and Service Desk quality report, first-line support, timely notification of the request status and progress to customers, coordination of the second-and third-party

support teams, monitoring in the problem-solving process, and termination of emergency after getting customer acceptance.

In the construction of Service Desk, we must realize that Service Desk is not a process, but the junction point of the internal service support process and a link with the user. Through Service Desk, it is possible to reduce repetitive and passive work, to streamline processes, clarify duties, strengthen communication with the users, and improve user satisfaction. (Figure 3)

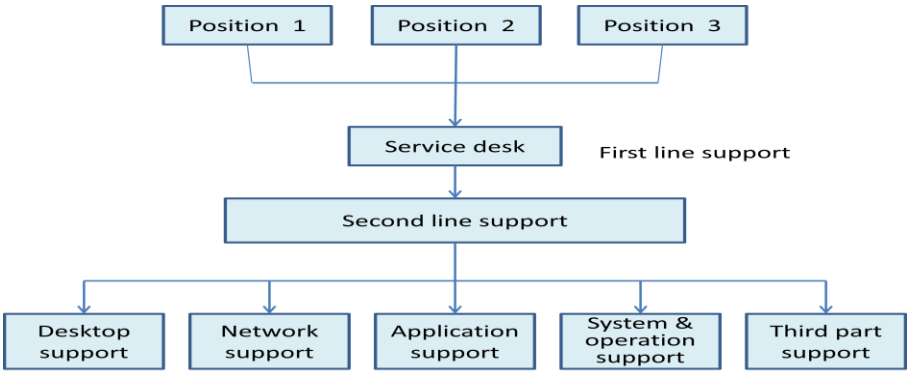

Fig. 3. Service Desk Work Setting

Through the construction of Service Desk, gradual improvement of business processes, perfection of job performance indicators, assigning of the person in charge, and development of service level priority, management and service of network operation & maintenance can be gradually quantified, job responsibilities can be clearly defined, and efficiency and customer satisfaction can be greatly improved.

When the entire Service Desk construction is finished and integration processes completed, we can build self-help desk to further improve service efficiency. However, specific attention should be paid to the coordinating relations between the "Tools" and "people". It is essential to gradually improve the process indicators and evaluation system instead of over-depending on tools or depending entirely on the operators.

5 Conclusion

Through the upgrading of existing network management and service system and the construction of a unified set of ITIL-based network management service platform and systems, we can build a maintenance and service model for operation & maintenance that aims to shift its focus from providing technical support to meeting the individual needs of teaching and research. Further, through reasonable arrangements and sharing of service resources including a variety of hardware and software within the Information Management Center, along with a performance evaluation system and better communication and collaboration in the areas of service, we will further

standardize the campus network management and service, enhance the efficiency of operation & maintenance, publish construction costs, and improve the satisfaction of the majority of faculty and staff.

References

1. Zhao, H.: Grid computing and web education. Educational Technology (April 2007)
2. KMCenter, WEB services and grid convergence is the future trend, SAN (April 05, 2006)
3. PeterBrooks, IT Service Standard. Tsinghua University Press (2008)
4. Developing Applications for HUE (EB/OL) (September 27, 2010)
5. Yang, L., Zhao, H.: The Top-level Design Method on Informatization. In: ICPCA6//SWS3 2011, pp. 127–132 (2011)
6. The Data Archiving and Access Requirements Working Group (DAARWG), Global Earth Observation Integrated Data Environment (GEO-IDE) Architecture Team Proposal (January 31, 2008)
7. Hadooop Cluster Setup (September 26, 2010)

Research on the Application of the P System with Active Membranes in Clustering*

Yuzhen Zhao, Xiyu Liu, and Jianhua Qu

School of Management Science and Engineering, Shandong Normal University, Jinan, China
zhaoyuzhen_happy@126.com, {sdxyliu,qujh1978}@163.com

Abstract. In this paper a clustering algorithm based on a P System with active membranes is proposed which provides new ideas and methods for cluster analysis. The membrane system has great parallelism. It could reduce the computational time complexity. Firstly a clustering problem is transformed into a graph theory problem by transforming the objects into graph nodes and dissimilarities into edges with weights of complete undirected graph, and then a P system with all the rules to solve the problem is constructed. The specific P system with external output is designed for the dissimilarity matrix associated with n objects. First all combinations of all nodes are listed to show all possibilities of the paths (the solution space) by using division rules of P system. Then a shortest path with the minimum sum of weights is selected. At last the path is divided into k parts from the edges with the k-1 biggest weights according to the preset number of clusters k. That is to say, all nodes are divided into k clusters. The calculation of the P system can get all the clustering results. Through example test, the proposed algorithm is appropriate for cluster analysis. This is a new attempt in applications of membrane system.

Keywords: membrane computing, P systems with active membranes, clustering algorithm.

1 Introduction

Clustering is very important [1]. A problem of clustering n objects into k clusters can be transformed into a graph theory problem by treating objects as graph nodes and dissimilarities as edges with weights. Then the work should be down is to find the shortest path that contains all nodes in the complete graph and separate the path into k

* Project supported by the Natural Science Foundation of China(No.61170038), Natural Science Foundation of Shandong Province, China (No.ZR2011FM001), Humanities and Social Sciences Project of Ministry of Education, China (No.12YJA630152), Social Science Fund of Shandong Province, China (No.11CGLJ22), Science-Technology Program of the Higher Education Institutions of Shandong Province, China (No.J12LN22), Science-Technology Program of the Higher Education Institutions of Shandong Province, China (No. J12LN65), Science-Technology Program of the Higher Education Institutions of Shandong Province, China(No.J12LN22), Research Award Foundation for Outstanding Young Scientists of Shandong Province, China (No.BS2012DX041).

Q. Zu, B. Hu, and A. Elçi (Eds.): ICPCA-SWS 2012, LNCS 7719, pp. 883–890, 2013.

parts. Through these, distant nodes belong to different clusters and near nodes belong to the same cluster [2]. While the process of finding the shortest path is actually a combinatorial problem. Membrane computing approaches are suitable used to solve combinatorial problems because of the vast parallelism (The parallelism lessens the time complexity of clustering process). This paper uses the parallelism of the membrane system based on the above conversion. This is a new application of membrane computing.

2 A Clustering Algorithm by P System with Active Membranes

2.1 Definition of Dissimilarity Based on Graph Theory

The clustering problem analyses connections among objects and clusters objects to different clusters. It can simplify the computational process followed. A general clustering problem that objects are clustered into k clusters is considered. Objects are transformed into graph nodes and dissimilarities are transformed into edges with weights of complete undirected graph. The smaller the weight is, the more similar the two objects are. Then a clustering problem transformed into a graph theory problem. First a shortest path that connects all nodes is found, then edges with the k-1 biggest weights are selected; finally the path is divided into k parts from the edges selected above. That is to say, n nodes are clustered to k clusters. The sum of all weights of edges in each cluster is smallest and among clusters is biggest. In other words, all nodes are divided into k clusters according to weights among them making distant nodes belong to different clusters and near nodes belong to the same cluster.

First of all, a dissimilarity matrix D_{nn} between any two objects is defined as follows:

$$D_{nn} = \begin{pmatrix} w_{11} & w_{12} & .. & w_{1n} \\ w_{21} & w_{22} & .. & w_{2n} \\ & & \cdots & \\ w_{n1} & w_{n2} & .. & w_{nn} \end{pmatrix} \tag{1}$$

Where, w_{ij} is the data getting by rounding the dissimilarity between the i-th object and the j-th object. Specific calculation method is selected depending on the type of object.

Secondly, the objects numbered from 1 to n can be indicated by points $a_1 \sim a_n$ because the clustering problem only uses dissimilarities among the objects.

2.2 The Structure of the P System with Active Membranes

The reader is assumed to be aware of the basic models of P systems; we especially refer to [3] [4] and [5] for more details regarding this topic.

In this section, a P system with active membranes for clustering is proposed. Its structure is as follow:

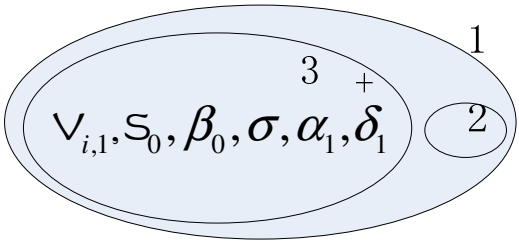

Fig. 1. The membrane computing model for clustering algorithm

The i-th object is represented by a_i. The dissimilarities among the n objects are represented by matrix D_{nn}. The sum of all dissimilarities in matrix D_{nn} is represented by Sum. The maximum in matrix D_{nn} is represented by Max.

The P system for clustering is defined as follow:

$$\prod = (O, \mu, M_1, M_2, M_3, R_1, R_2, R_3, \rho, \ i_o) \tag{2}$$

Where:

1. $O = \{\vee_{i,1}, S_0, \beta_0, \sigma, \alpha_1, \delta_1 | 1 \le i \le n\}$ O represents the set of objects in the P system. Where, $\vee_{i,j}$ indicates the i-th point of path is the j-th input object a_j. S_i indicates the sum of the all the distance in the path. β_i indicates the number of output distance.
2. $\mu = [_1[_3\ ]_3^+[_2]_2^0]_1^0$ represents the membrane structure of the P system. The subscript of membrane indicates the serial number of the membrane and the superscript indicates the electric charge of the membrane. In this structure, the membrane 3 carries a positive charge and the rest membranes carry no charge.
3. $M_1 = M_2 = \{\lambda\}, M_3 = \{\vee_{i,1}, S_0, \beta_0, \sigma, \alpha_1, \delta_1 | 1 \le i \le n\}$ M_i represents the set of initial objects in the i-th membrane. Objects only exist in membrane 3 and the rest membranes are empty (indicated by λ). There are six types of objects in membrane 3: $\vee_{i,1}, S_0, \beta_0, \sigma, \alpha_1, \delta_1$. These make up the initial state: $\vee_{i,1}$ indicates that all points that serial number from 1 to n in the path are assumed to a_1; S_0 indicates the sum of all distance of all paths are 0 because paths have not yet formed this time; β_0 indicates system output 0 distance.

The rules in R_1:

$r_1' = \{\theta^i \to \zeta_{in_3} | 1 \le i \le n!\}$

$r_2'=\{\varphi^{n!}\to\eta_{in_3}\}$

$r_3'=\{\delta_n\omega\to(\delta_n\omega)_{in_2}\mid\omega\in\{\mathrm{a}_p,0|1\le p\le n\}^*\}$

The rules in R_3 :

$r_1=\{[_3\zeta,V_{i,j},S_t,\beta_0,\sigma,\alpha_1,\delta_1]_3\to\lambda\mid1\le i,j\le n,0\le t\le Sum\}\bigcup\{[_3\zeta\varepsilon]_3\to\tau\}$

$r_2=\{[_3\tau V_{i,j},V_{i+1,p}]_3\to[_3\tau V_{i+1,p},U_{ijp}^{w_{jp}}]_3\quad 1\le i\le n-2,1\le j,p\le n\}$

$r_3=\{[_3\tau V_{n-1,j},V_{n,p}]_3\to[_3\tau U_{(n-1)jp}^{w_{jp}}]_3\quad 1\le j,p\le n\}$

$r_4=\{[_3\tau\beta_t U_{ijp}^0]_3\to[_3\tau\beta_{t+1}U_{ijp}^0V_{ijp}]_3\ 1\le i,j,p\le n,\ 0\le t<n-k\}$

$r_5=\{[_3\tau\beta_{\mathrm{t}}U_{1i_1j_1}^{p_1}U_{2i_2j_2}^{p_2}\ldots U_{(n-1)i_nj_n}^{p_{n-1}}]_3\to[_3\tau\beta_{\mathrm{t}}U_{1i_1j_1}^{p_1-1}U_{2i_2j_2}^{p_2-1}\ldots U_{(n-1)i_nj_n}^{p_{n-1}-1}]_3$
$0\le t<(n-p+1),1\le i,j\le n,\mid p\mid\le Max\}$

$r_6=\{U_{ijt}^p\to V_{i00}\mid1\le p\le Sum,1\le i\le n-1,1\le j,t\le n\}$

$r_7=\{\delta_i\omega V_{ijt}\to\delta_{i+1}\omega a_j a_t\mid1\le i\le n-1,1\le j,t\le n\}\bigcup$
$\{\delta_i\omega V_{i00}\to\delta_{i+1}\omega 0\mid1\le i\le n-1,\omega\in\{\mathrm{a}_p,0|1\le p\le n\}^*\}$

$r_8=\{\delta_n\omega\to(\delta_n\omega,out)\#\mid\omega\in\{\mathrm{a}_p,0|1\le p\le n\}^*\}$

$r_{2i+9}=\{[_3\alpha_{2i+1}V_{2i+1,j}]_3^+\to[_3\alpha_{2i+2}V_{2i+1,j}]_3^-[_3\alpha_{2i+1}V_{2i+1,j+1}]_3^+$
$0\le i\le\left\lfloor\frac{n-1}{2}\right\rfloor,1\le j\le n-2\}\bigcup$
$\{[_3\alpha_{2i+1}V_{2i+1,n-1}]_3^+\to[_3\alpha_{2i+2}V_{2i+1,n-1}]_3^-[_3\alpha_{2i+2}V_{2i+1,n}]_3^-\quad 0\le i\le\left\lfloor\frac{n-1}{2}\right\rfloor\}$

$r_{2i+8}=\{[_3\alpha_{2i}V_{2i,j}]_3^-\to[_3\alpha_{2i+1}V_{2i,j}]_3^+[_3\alpha_{2i}V_{2i,j+1}]_3^-\quad 0<i\le\left\lfloor\frac{n}{2}\right\rfloor,1\le j\le n-2\}\bigcup$
$\{[_3\alpha_{2i}V_{2i,n-1}]_3^-\to[_3\alpha_{2i+1}V_{2i,n-1}]_3^+[_3\alpha_{2i+1}V_{2i,n}]_3^+\quad 0<i\le\left\lfloor\frac{n}{2}\right\rfloor\}$

$r_{n+9}=\{[_3]_3^+\to[_3]_3^-\}$

$r_{n+10}=\{V_{i,j}\to T_{i,j}\alpha_j\quad 1\le i,j\le n\}$

$r_{n+11}=\{[_3\alpha_1\alpha_2\ldots\alpha_n]_3^-\to[_3]_3\}$

$r_{n+12}=\{[_3T_{i,j},S_0,\beta_0,\alpha_t,\sigma,\delta_1]_3^-\to\lambda\quad 1\le i,j,t\le n\}$

$r_{n+12+i}=\{[_3T_{i,j},T_{i+1,p},S_t]_3\to[_3V_{i,j},T_{i+1,p},S_{t+w_{jp}}]_3$
$1\le i\le n-2,1\le j,p\le n,0\le t\le Sum\}$

$r_{2n+11}=\{[_3T_{n-1,j},T_{n,p},S_t]_3\to[_3V_{n-1,j},V_{n,p},S_{t+w_{jp}}]_3$
$1\le j,p\le n,0\le t\le Sum\}$

$r_{2n+12}=\{\mathrm{S}_t\to\mathrm{S}_t'(\varphi,out)\#\mid0\le t\le Sum\}$

$r_{2n+13}=\{\eta\sigma S_0'\to\eta\varepsilon(\theta,out)\#\}$

$r_{2n+14}=\{\eta S_i'\to\eta S_{i-1}'\quad 1\le i\le Sum\}$

$R_2 = \{\lambda\}$ indicates there are not any rules in membrane 2.

$\rho = \{r_i > r_j \ 1 \le i < j \le (2n+14)\} \bigcup \{r_1' > r_2'\}$ indicates the priority among rules. High priority rule is executed prior.

$i_o = 2$ indicates the output membrane is membrane 2[6].

3 The Implementation Process of Rules

The idea is as follow: First all combinations of all nodes are listed to show all possibilities of the paths (the solution space) by using division rules of P system. Then a shortest path with the minimum sum of weights is selected. At last the path is divided into k parts from the edges with the k-1 biggest weights according to the preset number of clusters k. That is to say, all nodes are divided into k clusters. The process of clustering is over [7].

3.1 The Generation of All Paths

In initial state, only one membrane 3 is in this model and the objects in it are $\vee_{i,1}, S_0, \beta_0, \sigma, \alpha_1, \delta_1 (1 \le i \le n)$. That is to say, all points in path are assumed to a_1. Membrane 3 uses rules r_9 firstly according to priority and the electric charge of membrane. Membrane 3 is divided into 2 membranes with the same label 3 of different electric charge. The object $\vee_{1,1}$ is replaced by objects $\vee_{1,1}$ and $\vee_{1,2}$. $\vee_{1,1}$ and $\vee_{1,2}$ go into the membrane 3 with negative charge and positive charge respectively. Other objects are duplicated in the two new membranes. This means that the first point in path has two choices: a_1 and a_2. At this moment, only membrane 3 with $\vee_{1,2}$ has positive charge, so it uses r_9 for the second time. And so on until n membrane 3 with object $\vee_{1,1} \vee_{1,2} \ldots \vee_{1,n}$ respectively are generated. When the polarity of membrane 3 is negative, it can use rule r_{10}. This rule is similar with rule r_9 …… Finally, n^n membrane 3 are generated altogether after executing r_{n+8} .They express all possibilities that the i-th point of path takes different points of the source data. The rule r_{n+9} is set to make polarity of these membranes 3 negative in order to provide convenience for the following rules. α_j is generated to show a_j is in the path. $V_{i,j}$ is changed to $T_{i,j}$ to avoid duplication. If a membrane 3 contains all $\alpha_1\alpha_2...\alpha_n$, the polarity of it is changed to neutral. All paths that contain all $\alpha_1\alpha_2...\alpha_n$ are got by dissolving these membranes 3 with negative charges and their objects.

3.2 Finding the Shortest Path

Next, a path with minimum sum of distance will be found from above paths. The sum of all distance of each path is recorded by the subscript t of S_t. Then the subscript of

path of S_t' in each membrane 3 decreases simultaneously until S_0' appearing. The membranes 3 which do not have S_0' dissolved and objects in them disappear.

3.3 Cutting the Shortest Path to Complete the Clustering

The n points of path are divided into k parts from the edges with the k-1 biggest weights according to the preset number of clusters k. An object $U_{ijp}^{w_{jp}}$ is introduced to show that the value of the i-th distance of the path, the distance between a_j and a_p, is expressed by the superscript of $U_{ijp}^{w_{jp}}$ which has been computed by matrix D_{nn}. Then all superscripts of $U_{ijp}^{w_{jp}}$ reduce at the same time. When the superscript of $U_{ijp}^{w_{jp}}$ is 0, an object V_{ijp} is produced. The superscripts will reduce until n-k V_{ijp} are produced. These V_{ijp} show that the i-th distance of the path, the distance between a_j and a_p ,is one of the n-k shortest distance among all points. So a_j and a_p are in one cluster. Then the sequence of points in path is generated according to order. If there is the object V_{ijp}, a_j and a_p are add to the character string ω. Else it shows the distance between two points is far and the two points belong to two clusters. A char 0 is generated to separate these two clusters. The generated character string is output to membrane 1. The calculation is over. Membrane 1 put all these strings into membrane 2 which is the output membrane. The collected strings in membrane 2 are all clustering results [8].

Therefore, this P system can be used to cluster.

4 Test and Analysis

To illustrate how the membrane system shown in Fig.1 run specifically, the following simple example is considered: cluster 7 integral points (1,1), (2,1), (2,2), (3,4), (4,2), (4,3), (5,4) into two clusters. Obviously, n=7, k=2.

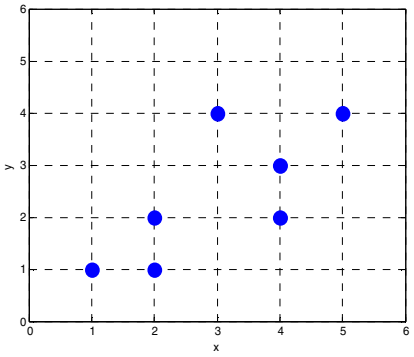

Fig. 2. The 7 points waiting for being clustered

First of all, the dissimilarity matrix D_{77} is defined. In this example, the distance between any two points is used as the dissimilarity.

$$D_{77} = \begin{pmatrix} 0 & 1 & 2 & 13 & 10 & 13 & 25 \\ 1 & 0 & 1 & 10 & 5 & 8 & 18 \\ 2 & 1 & 0 & 5 & 4 & 5 & 13 \\ 13 & 10 & 5 & 0 & 5 & 2 & 4 \\ 10 & 5 & 4 & 5 & 0 & 1 & 5 \\ 13 & 8 & 5 & 2 & 1 & 0 & 2 \\ 25 & 18 & 13 & 4 & 5 & 2 & 0 \end{pmatrix} \tag{3}$$

The membrane system clustering these seven numbers into two clusters is shown in Fig.3:

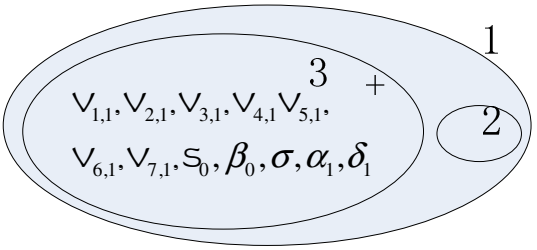

Fig. 3. The P system clustering seven numbers into two clusters

The rule r_9 is executed firstly. Membrane 3 is divided into 7 membranes with the same label 3 of negative charge. The values of $V_{1,i}$ are $V_{1,1},V_{1,2},V_{1,3},V_{1,4},V_{1,5},V_{1,6},V_{1,7}$ respectively and other objects are the same. The subscript of. adds 1. Then rule r_{10} is executed similarly in the 7 membranes 3 dependently to further divide these membranes. The values of $V_{2,i}$ have 7 choices: $V_{2,1},V_{2,2},V_{2,3},V_{2,4},V_{2,5},V_{2,6},V_{2,7}$ ……and so on. 7^7membranes 3 are generated totally after executing rule r_{15}.

Rule r_{17} r_{18} and r_{19} are executed to select the path with all 7 points. α_j is generated to show a_j is in the path. If a membrane 3 contains all $\alpha_1\alpha_2...\alpha_n$, the polarity of it is changed to neutral. The membranes 3 with negative charges and their objects are dissolved at the same time. Then the remaining 7! membranes 3 represent all permutations of the 7 points.

The sum of all distance of the path is computed and recorded by the subscript t of S_t' When accepting the object η, all 7! membranes 3 decrease the value of the subscript t until S_0'appearing. Objects σS_0 are consumed， while an object ε is generated. At the same time, one object θ is output to membrane 1, and membrane 1 input an object ζ to all membrane 3. A membrane 3 does not contain the shortest path if there is an object σ in it. It is dissolved and objects in it disappear.

The object $U_{ijp}^{w_{jp}}$ is generated in remaining membranes 3. The 5 shortest superscripts of $U_{ijp}^{w_{jp}}$ generate the corresponding V_{ijp}, and the remaining $U_{ijp}^{w_{jp}}$ generates V_{i00}. Finally, the sequence of points in path is generated according to order. The generated character string is output to membrane 1. Membrane 1 put all these strings into membrane 2 which is the output membrane. When the character strings don't increase in membrane 2 any longer, calculation is over. The result is not calculated specifically any longer here because of the high space complexity.

5 Conclusions

This paper realizes a clustering algorithm based on a P System with active membranes. The calculation of this P system can get all the clustering results. This is one of the great advantages of it. And the P system has great parallelism speaking from a theoretical point of view. So it can reduce the time complexity of computing and increases the computational efficiency. The following research work will focus on the theoretically analyze of the algorithm's time complexity.

Additionally, membrane computing is a new biological computing method. Now its theoretical research is mature, but its application is not particularly extensive. A lot of applications will emerge in various fields in the future. The application in cluster proposed in this paper is one example. There are many clustering method and this paper only use one of them. Membrane computing can be applied to a variety of other clustering methods.

References

1. Cardona, M., Colomer, M.A., Pérez-Jiménez, M.J.: Hierarchical clustering with membrane computing. Computing and Informatics 27(3), 497–513 (2008)
2. Zhang, H.Y.: The research on clustering algorithm based on DNA computing. Ph.D. dissertation, Dept. Management Science and Engineering, Shandong Normal Univ., Jinan, China (2011) (in Chinese)
3. Zhang, G.X., Pan, L.Q.: A survey of membrane computing as a new branch of natural computing. Chinese Journal of Computers 33(2), 208–214 (2010) (in Chinese)
4. Huang, L.: Research on Membrane Computing Optimization Methods. Ph.D. dissertation, Dept. Control Science and Engineering, Zhejiang Univ., Hangzhou, China (2007) (in Chinese)
5. Paun, G., Rozenberg, G., Salomaa, A.: Membrane Computing, pp. 282–301. Oxford University Press, New York (2010)
6. Marc, G.A., Daniel, M., Alfonso, R.P., Petr, S.: A P system and a constructive membrane-inspired DNA algorithm for solving the Maximum Clique Problem. BioSystems 90(3), 687–697 (2007)
7. Zhang, H.Y., Liu, X.Y.: A CLIQUE algorithm using DNA computing techniques based on closed-circle DNA sequences. Biosystems 105(1), 73–82 (2011)
8. Zhang, X.Y., Zeng, X.X., Pang, L.Q., Luo, B.: A Spiking Neural P System for Performing Multiplication of Two Arbitrary Natural Numbers. Chinese Journal of Computers 32(12), 2362–2372 (2009) (in Chinese)

Enhanced ALOHA Algorithm for Chirp Spread Spectrum Positioning

Zhengwen Yang[1], Qiang Wu[1], Yongqiang Lu[2], Pei Lu[1], Yinghong Hou[1], and Manman Peng[1]

[1] College of Information Science and Engineering, Hunan University, China
yangzhenwen2-1@163.com
[2] Department of Computer Science and Technology, Tsinghua University, China
luyq@tsinghua.edu.cn

Abstract. Location is a key context in the location-based services (LBS) which have been well studied in the domain of pervasive computing. The radio frequency (RF) based positioning plays important role in the LBS applications due to the good resolution, clear identification and low cost. However, the signal collision is a very critical issue which determines the system accuracy and throughput, especially in high-accuracy positioning such as UWB (Ultra Wide Band) and CSS (Chirp Spread Spectrum). CSS is an emerging technology which can offer highly-accurate positioning with TOA (Time-Of-Arrival) based manner similar with UWB, but is cheaper than UWB. This paper proposes a novel ALOHA-based algorithm for the signal anti-collision in CSS based positioning, which can guarantee the high throughput. Experimental results show the algorithm can maintain competitive throughput with the guaranteed accuracy in comparison with the known algorithms.

Keywords: Chirp spread spectrum (CSS) positioning, anti-collision, ALOHA, Time Of Arrival (TOA).

1 Introduction

Radio Frequency (RF) based positioning technologies have been widely used in pervasive environments, such as WiFi, Zigbee and RFID. They are low-cost to be deployed, but the positioning accuracy is relatively rough; they can only meet some average applications. In order to achieve better positioning accuracy, Ultra Wideband (UWB) [1-3] is introduced and it can gain the accuracy with the error of couple centimeters. However the chip of UWB is expensive due to the communication hardware.

Recently, researchers have introduced the Chirp signal to compromise the accuracy and cost issue, which is actually widely used in radar systems for target detection [4]. The Chirp Spread Spectrum (CSS) technology is one of the methods using such a manner; it can provide accurate ranging, high throughput and ultra low power [5].

CSS employs the Multi Dimensional Multiple Access (MDMA) to moderate the signal, which combines three well known modulation technologies, i.e. Amplitude Modulation (AM), Frequency Modulation (FM), and Phase Modulation (PM).

Q. Zu, B. Hu, and A. Elçi (Eds.): ICPCA-SWS 2012, LNCS 7719, pp. 891–903, 2013.

CSS customize the moderation method to meet the requirements of battery–powered sensor networks with high data rates, in which the reliability of the transmission as well as low power consumption are of special importance. Chirp pulses are Linear Frequency Modulated (LFM) signals with constant amplitude, which fill out the total available bandwidth over a predefined duration [6]. The following Figure 1 shows the situation that the signal of CSS transmits.

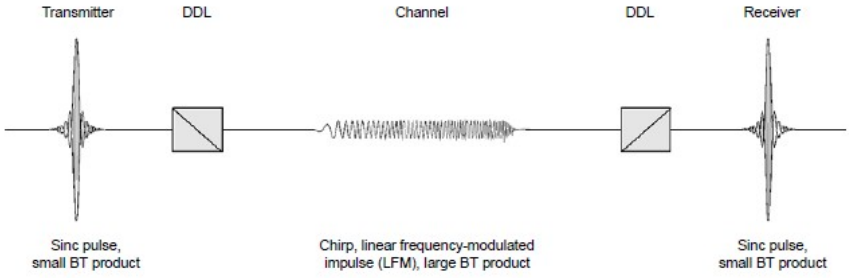

Fig. 1. Signal forms of CSS

Another reason why CSS can be used to positioning accurately is that it is very resistant against narrowband noise and also resistant against broadband disturbances. The larger is the time-bandwidth product, the more resistant the chirp pulses are against disturbances during transmission. Because CSS uses broadband chirp pulses, it is very resistant against disturbances [6].

Trilateration [7-8] is a method to determine the positioning of an object based on simultaneous range measurements from three anchors at known location. There are three methods typically used to calculate the positions using trilateration, i.e. the signal strength, time of arrival, and angle of arrival [9]. The range in IEEE 802.15.4a used in CSS is achieved by measuring the TOA. To measure the TOA between a pair of nodes, symmetric double-sided two-way ranging (SDS-TWR) is adopted. SDS-TWR does not require clock synchronization between the nodes, and it can also reduce the error of clock drift caused by the inaccuracy of crystal oscillators [10]. SDS-TWR needs double-sided range, and this will increase the expression of the communication environment, so we use two-way ranging (TWR) to range the distances.

An anchor cannot identify too many tags at one time because of the channel restrictions. When two or more tags with the same frequency respond to the same anchor simultaneously, the signal will impact each other in the air, which is called signal-collision [11]. Collision is meant here in that sense that not only the answer of a single tag is obtained as a response to the interrogation signal, but a superposition of multiple signals [12]. There are four types of solutions for the signal-collision problem: SDMA (Space Division Multiple Access), CDMA (Code Division Multiple Access), FDMA (Frequency Division Multiple Access) and TDMA (Time Division Multiple Access). As the TDMA method is simple and easy to read and write a lot of tag data, therefore it is used by the majority of anti-collision algorithm [13].

Existing anti-collision algorithms are mainly in two categories. One is the stochastic collision resolution like ALOHA and the other is the deterministic collision resolution like the binary tree [14-16]. ALOHA based algorithms suffer significant performance

degradation in case of large number of tags, and cannot avoid so-called *tag starvation*, in which a tag may not be identified for a long time due to repeated collisions [15]. The deterministic algorithm based on binary tree can solve the starvation problem, but it needs a long cycle of identification which is complex and power-consuming to run on tags, which is therefore not concerned in this paper.

Ultra-wideband (UWB) radio often uses short pulses (nanoseconds) to spread energy over at least 500 MHz of bandwidth. It is potential for anti-collision in multi-tag environments [17]. In addition, the deterministic anti-collision methods are often used in UWB positioning due to its broad bandwidth of communication, which are often called as multiple access techniques; they can fall into two main categories: centralized and distributed MAC protocols. In the centralized MAC protocols, collisions can be avoided because the central controller guarantees exclusive access to the channel [18]. It has the same shortcoming with the deterministic algorithm which mentioned above. In the centralized MAC protocols, Carrier-sense multiple access (CSMA) is used to solve the problem of collision [17].

In the stochastic collision resolution, there are several anti-collision algorithms, e.g., ALOHA, FSA (Framed Slotted Aloha) [19], DFSA (Dynamic Framed Slotted Aloha) [20-21], G-DFSA (Grouped Dynamic Framed Slotted Aloha) [22]. FSA, DFSA and G-DFSA need clock synchronization which will consume extra cost. Additionally, in ALOHA and FSA, tags absolutely do not need to receive signal in the process of ranging; in DFSA and G-DFSA, tags need to receive signal only in the process of negotiating the appropriate number of slots in a frame. However, for the TOA (Time-Of-Arrival) based positioning technique, which is also used in CSS in this paper, the tags must send and receive signals during the whole process of ranging. So, the traditional ALOHA, FSA, DFSA and G-DFSA are not suitable for CSS any longer; the anti-collision algorithm must be customized with the specific positioning techniques used.

In this paper, an enhanced ALOHA based algorithm (named CSSA) is proposed which is particularly designed for the CSS positioning technique. This proposed algorithm is used in the upper layer of the CSMA in the CSS positioning system. It can further enhance the system throughput. The feasibility of this algorithm is verified through a simulation model. Experimental results show that the system throughput can be guaranteed together with the ensured positioning accuracy contributed by the CSS technique. The throughput is defined as the ratio of the identified tags over total tags in the system.

The rest of this paper is organized as follows. The section 2 mainly introduces the mechanism of the algorithm including the power analysis of the tag, the algorithm design and the theoretical analysis of the system throughput based on the probabilistic analysis. Then, the simulation results of CSSA are explained in section 3. Finally, the conclusion of this paper is drawn in section 4.

2 Algorithm Design and Analysis

In the CSS positioning system, the range model is designed as follows. (1) The tag launches a ranging broadcast to all anchors in the region to notify all anchors to range the tag. (2) Anchors receive the broadcast and send ranging request to the tag. (3) The

tag receives ranging requests from anchors and returns ranging responses to anchors. After anchors have received the ranging responses from the tag, then distances between anchors and the tag can be calculated. This design is conducive to future system expansion. The time from the anchor sending out ranging request to the anchor receiving response data is t_1, and the time from the tag receiving ranging request to the tag sending out response data is t_2. The distance between the anchor and the tag is $((t_1 - t_2)/2) * V$, where, V is the propagation speed of the signal in the air.

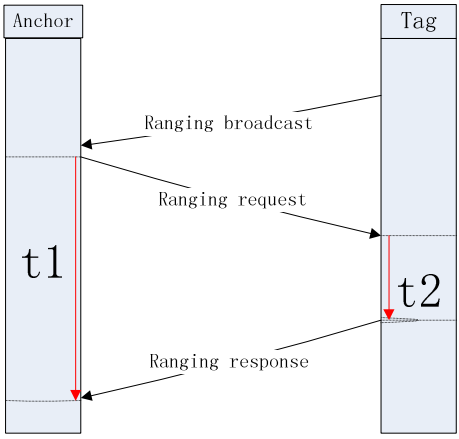

Fig. 2. The process of the range model

Actually, the calculation of distance is based on TWR. The ranging request which tags receive likes an acknowledgement of the ranging broadcast, and the ranging response likes an acknowledgement of the ranging request.

2.1 Two Phases of the Tag

Both anchors and tags need to receive data, so both anchor-sides and tag-sides are likely to generate signal collision. Therefore, both anchors and tags need the anti-collision mechanism. However, the tag should be low power consumption, while the anti-collision function will consume a lot of energy. Therefore, in order to make energy which consumed by tags more efficient, the approach we taking is: each tag has quiet state and range state. The tag is in quiet state usually; quiet state will be interrupted and the tag will go into range state when the tag needs to send ranging broadcast to anchors. Quiet state is referred to as standby model; tags don't do anything in this model, neither receiving data nor sending data; therefore, tags only need consume low energy in quiet state. Range state is referred to as active model; tags can send and receive messages in this model; tags in range state need to consume energy. If the range is successful, the tag will enter into quiet state after the end of range state. The Figure 3 shows the State transition of the tag.

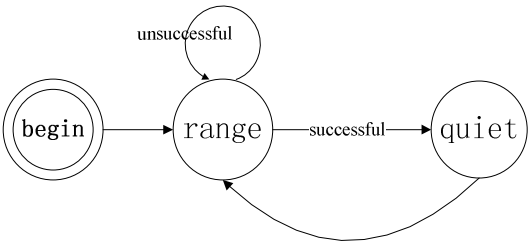

Fig. 3. The State transition of the tag

As the section 1 described, CSS positioning range is based on TWR. In the process of the TWR, the tag is always in range state. In the range state, the tag can be divided into two phases, broadcast phase and range phase. Broadcast phase is the phase between the tag sending broadcast and the anchor receiving the broadcast; the range phase is the phase between the anchor sending ranging request and the end of range state. If the anchor receives the ranging response successfully in the range phase, this indicates that the anchor ranges the tag successfully.

2.2 Anti-collision on Tag and Anchor Sides

The anchor can only judge if it receives the broadcast successfully but cannot judge if it receives the broadcast unsuccessfully. The anchor will send ranging request to the tag if the anchor has received the broadcast; the ranging request of the anchor sending to the tag likes an acknowledgement of the ranging broadcast from the tag, so if the tag receives the ranging request successfully, the anchor must have received the broadcast from the tag. If the tag does not receive ranging request before the end of range state, the anchor may not have received the broadcast. Therefore, we can conclude that the anchor successfully receives the broadcast when the tag successfully receives the ranging request, and the anchor unsuccessfully receives the broadcast while the tag unsuccessfully receives the ranging request. The tag can use whether himself receives the ranging request successfully to judge whether the anchor receives the broadcast successfully.

If the anchor does not receive ranging response from the tag within a period of time after the anchor sending out the ranging request, the anchor will regard it as occurring collision in the range phase. In the range phase, tag can't judge out whether the anchor has received the ranging response, but the anchor knows whether it has received the ranging response. Therefore, the anchor can judge out whether himself has received the ranging response.

Because the tag can judge whether the anchor has received the broadcast successfully in the broadcast phase, and the anchor can judge whether the anchor has successfully received the ranging response in the range phase, the anti-collision algorithm of CSS positioning system can be divided into two parts: anti-collision on anchor-side and anti-collision on tag-side.

2.2.1 Anti-collision on Tag-Side

The simplest case is of course one anchor working with multiple tags. Firstly, the tag will enter the ranging state with a ranging broadcast then the tag will poll whether there

is ranging request from the anchor. If the tag has received the ranging request from the anchor before the end of the range state, the tag will send ranging response to the anchor and directly goes into the quiet state which considered as the end of the tag identification cycle. If the tag has not received ranging request from the anchor before the end of the range state, which this paper call this the tag broadcast failure, this indicates that there occurs collision in the broadcast phase, then the tag will not go into the quiet state after the end of the range state but randomly delays for a short time, and re-sends a ranging broadcast; the tag will still stay in the range state. But the number of times of tag broadcast can't exceed M_b; if the number of times of tag broadcast exceeds M_b, the tag will give up sending broadcast and enter into the quiet state.

The proposed algorithm flowchart of anti-collision algorithm on the tag-side is also shown in Figure 4.

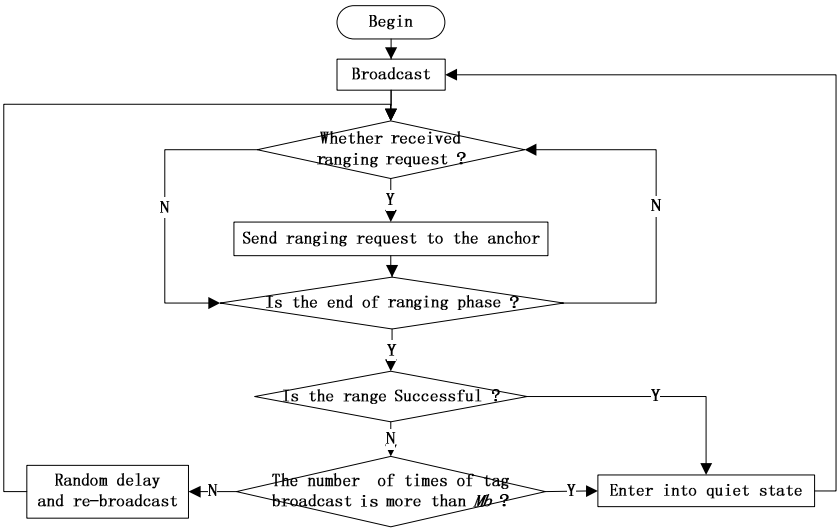

Fig. 4. The work flow of the anti-collision on the tag-side

M_b is the maximal number of times of tag broadcast. If the number of times of tag broadcast exceeds M_b, the reason may be that there are too many signals in the RF region and the wireless communication environment is bad, so the tag can give up sending broadcast to reduce the pressure of the communication environment.

The tag identification cycle is not a fixed length of time. The tag identification cycle includes several range states and a quiet state, and the number of range states can't exceed M_b. M_b is a constant which can be customized. The duration of the quiet state is t_q; the duration of the range state is t_r; the duration of the tag identification cycle t_c is:

$$t_c = n * t_r + t_q, n \in [1, M_b] \tag{1}$$

2.2.2 Anti-collision on Anchor-Side

Each anchor has A and B two queues. Queue A is a queue to be ranged which stores tags that have passed broadcast and wait for ranging. Queue B is ranged queue which

stores tags that have successfully ranged. But the tag only stays in queue B for a short time which equals the duration of the smallest tag identification cycle. If the tag stays in queue B for more than the smallest tag identification cycle, it is called the expired tag. The expired tag will be removed from queue B. The smallest tag identification cycle is consisted by a quiet state and a range state, so the duration of the smallest tag identification cycle t_s is:

$$t_s = t_q + t_r \tag{2}$$

The anchor always polls whether there are ranging broadcasts from tags. If the anchor receives a ranging broadcast, the anchor will detect queue B and queue A; the tag will be not handled if the tag is in queue B or queue A, otherwise, the tag will be added into queue A. Then the anchor detects queue A; if queue A is not empty, the anchor will range the tag. Firstly the anchor sends a ranging request to the tag; secondly if the anchor receives ranging response from the tag within a period of time after the anchor sending out the ranging request, this indicates that the range is successful; at last the anchor adds the tag into queue B and deletes the tag from queue A. If the anchor does not receive ranging response of the tag within a period of time after the anchor sending the ranging request, this indicates that signal collision occurs in the range phase, the anchor will re-send a ranging request to the tag immediately.

If the anchor does not receive ranging response of the tag within a period of time after the anchor sending out the ranging request, we call this the ranging timeout. The number of times of one tag's ranging timeout could not be more than M_r, if it exceeds M_r, then the anchor will give up ranging this tag and turn to range the next tag. M_r is a constant which can be customized.

The proposed flowchart of the anti-collision algorithm on the anchor-side can also be shown in Figure 5.

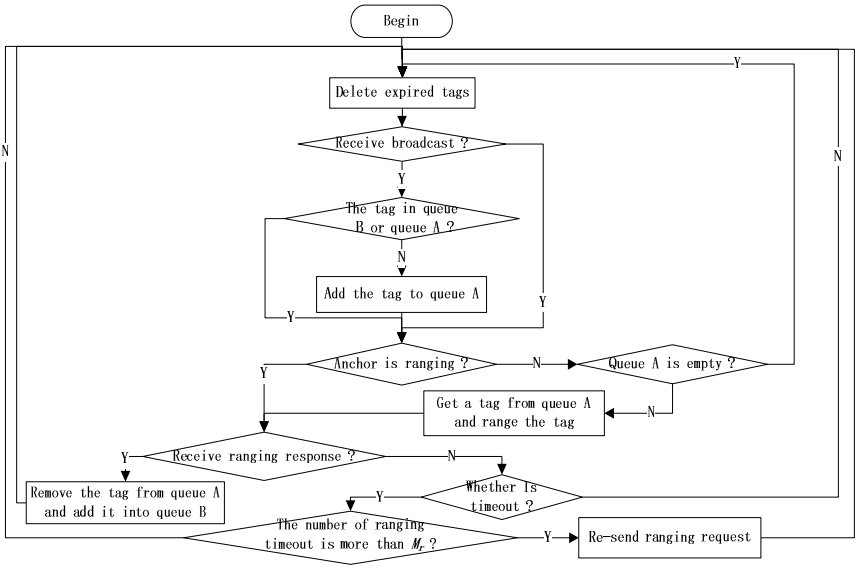

Fig. 5. The work flow of the anti-collision on the anchor-side

M_r is the maximum number of range timeouts. If the number of times of one tag's ranging timeout exceeds M_r, the reason is similar to the reason mentioned in the subsection 2.2.1.

In the case that the anchor receives the broadcast transmitted by the tag but the tag dose not successfully receive ranging request sent by the anchor, the tag will still treat as there is a collision occurring in the broadcast phase and re-send a ranging broadcast. The anchor will not handle the ranging broadcast if the anchor finds the tag already in queue A or queue B; the anchor will ignore this ranging broadcast if this happens.

2.3 Algorithm Analysis

According to the subsection 2.2 described, the tag sends a broadcast, the anchor will callback a ranging request to the tag after the anchor receives the broadcast. If the tag does not receive the ranging request before the end of range phase, the tag will re-send a broadcast. There are two situations. The first situation is that the anchor does not receive the broadcast, then, the tag re-sends a broadcast. It is just right. The second situation is that the anchor receives the broadcast but the tag does not receive the ranging request from the anchor, then, the tag re-sends a broadcast. It is superfluous. If the anchor receives the broadcast, the anchor will send ranging request to the tag. If it is ranging timeout, the anchor will re-send ranging request to the tag several times, so if the anchor receives the broadcast, the possibility of that the tag does not receive the ranging request is little. That is the possibility of the second situation is little.

The anchor sends a ranging request to the tag, the tag will callback a ranging response to the anchor. If the anchor does not receive a ranging response, the anchor will re-send a ranging request to the tag. There are also two situations. The first situation is that the tag does not receive the ranging request, then, the anchor re-sends a ranging request. It is just right. The second situation is that the tag receives the ranging request but the anchor does not receive the ranging response from the tag, then, the anchor re-sends a ranging request. If the anchor does not receive a ranging response, the range process is break, then, the range will be failing. So the second situation is necessary.

Throughput on anchor-sides is p_1; throughput on anchor-sides is defined as the ratio of identified signals over total received signals on the anchor-side. Throughput on tag-sides is p_2; throughput on tag-sides is defined as the ratio of identified signals over total received signals on the tag-side. The throughput (which defined as that in Introduction) in the condition of one anchor working with multiple tags is p_t. The probability of the anchor successfully receiving broadcast is p_b. The probability of the anchor successfully receiving ranging response is pr.

As described above, the tag will re-send a ranging broadcast if the tag does not receive the ranging request from the anchor at the end of range phase. This can increase the probability of the anchor successfully receiving the broadcast from the tag in an identification cycle. But there is only one to M_b range phases in an identification

cycle, and there is only one broadcast in a range phase, so the number of times of sending broadcast can't exceed M_b in one identification cycle. So, in theory, p_b is:

$$p_b = p_1 + p_1.(1-p_1) + p_1.(1-p_1)^2 + ... + p_1.(1-p_1)^{M_b-1} = 1-(1-p_1)^{M_b} \quad (3)$$

As described above, if anchor has received ranging response from the tag within a certain period of time after the anchor sending ranging request, the range is successful. Otherwise, the range is ranging timeout; the anchor will re-send ranging request to the tag. This can increase the probability of the anchor successfully receiving the ranging response from the tag. In theory, the probability of successful ranging (p_{rn}) until the anchor sends the n-th ranging request is:

$$\begin{aligned} p_{rn} = p_1 p_2.[&c_{n-1}^0.(1-p_1)^{n-1} + c_{n-1}^1.(1-p_1)^{(n-2)}.(p_1.(1-p_2))^1 + \\ &...c_{n-1}^i.(1-p_1)^{(n-i-1)}.(p_1.(1-p_2))^i + ... + c_{n-1}^{n-1}.(p_1.(1-p_2))^{(n-1)}] \end{aligned} \quad (4)$$

In an identification cycle of a tag, the number of times of the anchor re-sending ranging requests to the tag can't exceed M_r, so p_r is:

$$p_r = p_{r0} + p_{r1} + ... + p_{ri} + ... + p_{rn} = \sum_{i=0}^{Mr} p_{ri} \quad (5)$$

If the anchor receives broadcast successfully and receives ranging response successfully, then, the total range is successful, so p_t is:

$$p_t = p_b * p_r \quad (6)$$

3 Experimental Results

In this paper, the experiment was implemented on a PC (the configuration is Intel Core i7 processor and 4G memory) using JAVA multithread to simulate anchors and tags. Anchors and tags were communicated by static socket connection. The parameters of M_b and M_r were all set to 3 in the experiment.

The following Table 1 shows the throughput (defined as that in Introduction) in the condition of one anchor working with multiple tags in comparison with that in [22]. The first column of the Table 1 is the number of tags. The second to fourth columns show the average throughput of FFSA, DFSA, G-DFSA listed in [22], respectively; the all experimented in RFID system. The last column is the average throughput of CSSA proposed in this paper.

Table 1. Average throughput of each algorithm

tag number	FFSA	DFSA	G-DFSA	**CSSA**
100	0.132979	0.320513	0.160256	**0.357692**
200	0.197824	0.299401	0.255102	**0.376267**
300	0.235479	0.301508	0.325379	**0.335484**
400	0.253325	0.296736	0.358744	**0.211125**
500	0.257202	0.307989	0.365230	**0.184397**

When the number of tag is less than 300, the average throughput of CSSA is maintained at about 0.35. When the number of tags is more than 400, the average throughput of CSSA will decrease seriously.

It is more intuitive to show the data in a diagram. In the Figure 6, x-axis and y-axis represent the number of tags and the average throughput of several algorithms, respectively. The Figure 6 shows that the trend of throughput changes along with the number of tag changes for the different algorithms.

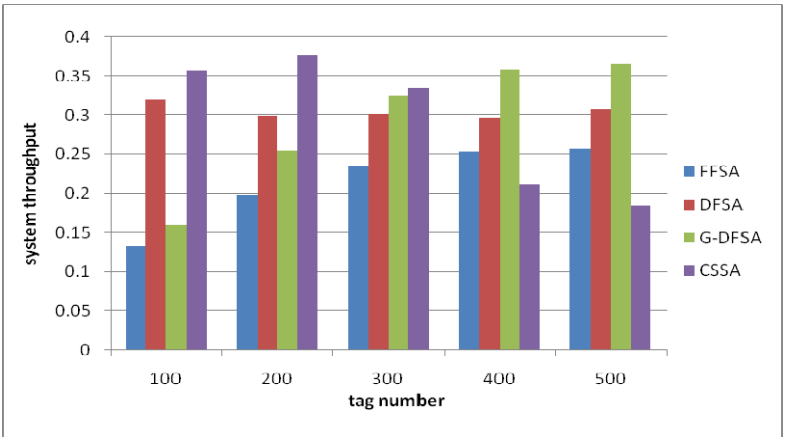

Fig. 6. The relationship between the throughput and the number of tags

It can be definitely concluded that CSSA gains much advantage when the tag number is smaller than 300; the average throughput of CSSA is maintained at about 0.35 and relatively stable; it is better than those of other algorithms. CSSA achieves the maximum throughput when the number of tags is 200. When the number of tags is more than 400, the average throughput of CSSA degrades seriously; there is no superiority compared to other algorithms.

As can be seen in the previous description, the ranging request which tags receive likes an acknowledgement of the broadcast; the ranging response likes an acknowledgement which anchors receive in the range phase. If related node does not receive the confirmation, it will retransmit related data; this mechanism can improve the throughput. But the retransmission is also increased the number of signals in the RF region, more concurrent signals impact the overall throughput. When the number of tags is low, the impact of retransmission is not obvious and it can improve the throughput; while the impact of the retransmission gets obvious and it impacts the throughput when the number of tags is high. Therefore, as can be seen from Figure 6 obtained empirically, the proposed algorithm is more suitable for that the number of tags is less than 300.

Finally the paper also gives a group of data to show the stability of CSSA and list the throughput with one anchor working with 200 tags; the algorithm runs 150

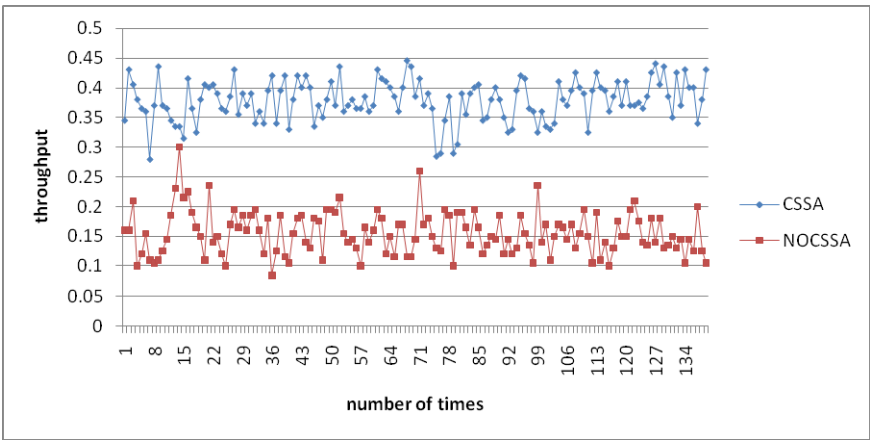

Fig. 7. The comparison of CSSA and NOCSSA

identification cycles, so there are 150 groups of throughput. In Figure 7, x-axis and y-axis represent the number of times and the throughput respectively. The legend of CSSA represents the throughput when the CSS system employs the algorithm in this paper (CSSA); NOCSSA represents the throughput when the CSS system does not use CSSA.

Tags send out broadcast stochastically rather than synchronously to notify anchors to range, so the throughput also would have a certain degree of fluctuation. But as can be seen from Figure 7, the throughput of CSSA fluctuates with the small amplitude; it is relatively stable. It also shows that the throughput of CSSA is obviously higher than that of NOCSSA, which indicates the CSSA has improved the throughput of the CSS positioning system remarkably (about 146%).

4 Conclusion

In this paper, we present an anti-collision algorithm named CSSA, which can be applied to Chirp Spread Spectrum based positioning system. The main advantage of the proposed algorithm in this paper is that it can be aware of the signal collision in a various conditions and retransmit data accordingly in the tag identification cycles to improve the throughput. It can also reduce "starve" relatively in comparison with the traditional Aloha algorithms. The performance of the proposed algorithm can also meet the application requirements of the CSS positioning system, and it is more suitable for the cases with small number of tags, say around 200 tags. The flow of the algorithm CSSA does not require complex calculation; its computation complexity is very low and suitable to be implemented on the low-power tag-side, which is particularly valuable in the applications of low-power and high-QoS pervasive computing environments.

References

1. Gezici, S., Poor, H.V.: Position Estimation via Ultra-Wide-Band Signals. Digital Object Identifier 97, 386–403 (2009)
2. Feher, G.: Ultra Wide Band (UWB) Transmitter with Configurable Design for Indoor Positioning. In: 18th International Conference on Microwave Radar and Wireless Communications (MIKON), pp. 1–4. IEEE Press, Vilnius (2010)
3. Elbahhar, F., Heddebaut, M., Rivenq, A., Rouvaen, J.M.: Positioning system using the SS-Ultra wide Band technique for transport application. In: 9th International Conference on Intelligent Transport Systems Telecommunications (ITST), pp. 663–666. IEEE Press, Lille (2009)
4. Huang, L., Lu, Y., Liu, W.: Using chirp signal for accurate RFID positioning. In: 2010 International Conference on Communications, Circuits and Systems (ICCCAS), pp. 675–679. IEEE Press, Chengdu (2010)
5. Lee, K.H., Cho, S.H.: CSS based localization system using Kalman filter for multi-cell environment. In: 2008 International Conference on Advanced Technologies for Communications (ATC), pp. 293–296. IEEE Press, Hanoi (2008)
6. Nanotron Technologies GmbH: nanoNET Chirp Based Wireless Networks (2007)
7. Hightower, J., Borriello, G.C.: Location systems for ubiquitous computing. Computer 34, 57–66 (2001)
8. Yang, Z., Liu, Y., Li, X.-Y.: Beyond Trilateration: On the Localizability of Wireless Ad-Hoc Networks. In: IEEE International Conference on INFOCOM 2009, pp. 2392–2400. IEEE Press, Rio de Janeiro (2009)
9. Vera, R., Ochoa, S.F., Aldunate, R.G.: EDIPS: an Easy to Deploy Indoor Positioning System to support loosely coupled mobile work. Personal and Ubiquitous Computing 15, 365–376 (2011); Conference on Advanced Technologies for Communications, pp. 293–296. IEEE Press, Hanoi (2008)
10. Cho, H., Lee, C.W., Ban, S.J., Kim, S.W.: An enhanced positioning scheme for chirp spread spectrum ranging. Expert Systems with Applications 37, 5728–5735 (2010)
11. Wang, C.-Y., Lee, C.-C.: A Grouping-Based Dynamic Framed Slotted ALOHA Anti-Collision Method with Fine Groups in RFID Systems. In: 5th International Conference on Future Information Technology (FutureTech), pp. 1–5. IEEE Press, Hanoi (2010)
12. Brandl, M., Schuster, S., Scheiblhofer, S., Stelzer, A.: A new anti-collision method for SAW tags using linear block codes. In: 2008 IEEE International Conference on Frequency Control Symposium, pp. 284–289. IEEE Press, Honolulu (2008)
13. Xie, X.-M., Xie, Z.-H., Lai, S.-L., Chen, P.: Dynamic adjustment algorithm for tag anti-collision. In: 2011 International Conference on Machine Learning and Cybernetics (ICMLC), pp. 443–446. IEEE Press, Guilin (2008)
14. Liu, L., Lai, S.: ALOHA-based Anti-collision Algorithms Used in RFID System. In: 2006 International Conference on Wireless Communications, Networking and Mobile Computing, WiCOM, pp. 1–4. IEEE Press, Wuhan (2006)
15. Jia, X., Feng, Q., Ma, C.: An Efficient Anti-Collision Protocol for RFID Tag Identification. Communications Letters 14, 1014–1016 (2010)
16. Choi, J.H., Lee, D., Lee, H.: Query tree-based reservation for efficient RFID tag anti-collision. Communications Letters 11, 85–87 (2007)
17. Zou, Z., Baghaei-Nejad, M., Tenhunen, H., Zheng, L.-R.: Baseband design for passive semi-UWB wireless sensor and identification systems. In: 2007 IEEE International on SOC Conference, pp. 313–316. IEEE Press, Hsin Chu (2007)

18. Zin, M.S.I.M., Hope, M.: A Review of UWB MAC Protocols. In: Sixth Advanced International Conference on Telecommunications (AICT), pp. 526–534. IEEE Press, Barcelona (2010)
19. Park, J., Chung, M.Y., Lee, T.-J.: Identification of RFID Tags in Framed-Slotted ALOHA with Robust Estimation and Binary Selection. Communications Letters 11, 452–454 (2007)
20. Eom, J.-B., Lee, T.-J.: Accurate tag estimation for dynamic framed-slotted ALOHA in RFID systems. Communications Letters 14, 60–62 (2010)
21. Bueno-Delgado, M.V., Vales-Alonso, J., Gonzalez-Castao, F.J.: Analysis of DFSA anti-collision protocols in passive RFID environments. In: 35th Annual Conference of IEEE on Industrial Electronics, IECON 2009, pp. 2610–2617. IEEE Press, Porto (2009)
22. Yu, C., Zhou, F.: A New Frame Size Adjusting Method For Framed Slotted Aloha Algorithm. In: 2009 IEEE International Conference on e-Business Engineering, ICEBE 2009, pp. 493–496. IEEE Press, Macau (2009)

A Case Study of Integrating IoT Technology in Bridge Health Monitoring

Qiaohong Zu and Xingyu Xu

School of Logistics Engineering,
Wuhan University of Technology,
Wuhan, Hubei 430063, China
{zuqiaohong,xuxingyu}@mail.whut.edu.cn

Abstract. Research on Internet of Things (IoT) and relevant applications has attracted more and more attention from both academic and industrial communities. In this paper, we focus on a particular use case of IoT, bridge health monitoring that ensures bridge health security and detects hidden defects of the infrastructure. Using total station technology, acceleration sensor technology and fiber grating technology, this application monitors a wide range of parameters, e.g. deformation of bridge structure, relative displacement of arch foot level, skewback uneven settlement, main beam distortion, suspender force, rid temperature and strain of main beam, in real time and online, so as to collect, transmit, store, statistical analyze bridge health information, and perform remote monitoring and warning timely and accurately.

Our system improves the comprehensive monitoring efficiency, assists decision-making for bridge monitoring, management and maintenance and ensures the safety of the bridge infrastructure. The paper based on real-life scenarios, offering IoT technology in the health monitoring application case study at the Yan-Cheng Century Avenue Tong-Yu River in the Jiangsu province. Our paper demonstrates how the theory is combined with practice in real-life project, that will provides useful insights and learnt lessons to projects aiming at similar applications.

1 Introduction

With the advance of Chinese economy, a huge burden has been put on road and railway networks due to increasing needs in freight and passenger transport and limited network traffic capacity across China. As a direct outcome, transport network is put constantly under test. We have witnessed multiple incidents of infrastructure failures and subsequently disasters causing human lives. For instance, on 30 August 2012, a main motorway bridge collapsed in northeast China, leading to multiple casualties and major disturbance to regional traffic as well as potentially a significant negative impact on local economy whose effect is yet to be fully appreciated. Investigations carried out after the incidents unfolded a typical scenario that is affecting many transport infrastructure assets in China. With the rapid development of the transportation industry, the

Q. Zu, B. Hu, and A. Elçi (Eds.): ICPCA-SWS 2012, LNCS 7719, pp. 904–917, 2013.

proportion of bridge construction in infrastructure construction is increasing [5]. Due to load affecting, environmental erosion, material aging and fatigue, as an important infrastructure, bridges are subject to inevitable damage every second while in use. This nature course is accelerated by overloading freight vehicles, shortening the lifespan of roads and bridges, and in the extreme cases, even leading to catastrophic incidents. Traditional bridge safety monitoring, however, is labor intensive and time consuming. Experts are expected to make physical visits periodically, set up the equipment, collect relevant data, perform off-line analysis and inform authorities accordingly. This conventional approach cannot meet the requirements of modern infrastructure management. Firstly, due to the nature of labor-intensive tasks, on-site data sampling cannot be performed in a comprehensive manner and thus do not render a complete picture of the inspected infrastructure. The missing information, sometimes, leads to major mistakes and incorrect decisions. Secondly, conventional approaches present a gap between data collection and data interpretation. Such gaps range from hours to even days. Monitoring of bridges, therefore, cannot be done in real-time and thus its efficiency is greatly reduced, resulting in potential safety risks[16].

Inefficiency in existing approaches can be remedied by adopting the Internet of Things framework. In this paper, we report a case study jointed funded by local government and infrastructure management authorities. We present the design considerations, system architecture, issues encountered in system implementation and deployment. We strongly believe our experience and learnt lessons can be helpful for organizations undergoing similar projects.

2 The Integrate of Internet of Things Technologies in Bridge Health Monitoring

In recent years the Internet of Things (IoT) technology has developed rapidly with concrete use cases and applications being developed in a variety of domains. Infrastructure health monitoring is one of areas where IoT can significantly increase the accuracy, timeliness, and accessibility that conventional approaches failed to provide [8,9,15]. New technologies such as tachometer, acceleration sensor and optical fiber grating become available at low cost with relatively low power consumption. With sensors being deployed at this inspected infrastructure, it is possible to practice continuous health "checking" and complement traditional monitoring methods with real-time and efficient data collection/analysis [3,10]. Moreover, the above modules can be integrated to build long-term health monitoring systems, which could provide bridge management, maintenance and operations with effective decisions, to ensure daily safety of infrastructure.

2.1 Internet of Things and Optical Fiber Grating Sensor Technology

IoT normally refers to interconnected and identifiable objects (also known as "things") and the networks that link the virtual presentations of such objects

together [1]. In practice, IoT is materialized as an integral framework of different sensing equipment and a variety of wireless communication technologies. IoT applications leverage Internet in order to achieve scalable interconnection be-tween "things" or human users [22]. Each sensor deployed in IoT is an independent data source; every kind of sensor captures different data with individual formats. Data obtained from these sensors will be real-time since the sensors collect environmental information periodically at a certain frequency [17]. In bridge health monitoring, acceleration sensors and optical fiber grating sensors are selected.

Acceleration sensor responses directly to acceleration vector information. It first determines the natural frequency of detected objects by picking up signal of the measured objects through environmental vibration excitation, and then deter-mines their acceleration forces according to the relationship between natural frequency and cable force [22,13].

Optical fiber grating sensor measures the parameter by detecting wavelength changes of light signal reflected by each grating [14]. Each wave crest represents an optical fiber grating sensor. These sensors can detect multi-point distributed measurement in an optical fiber. The principle of optical fiber grating sensor is illustrated in Figure 1.

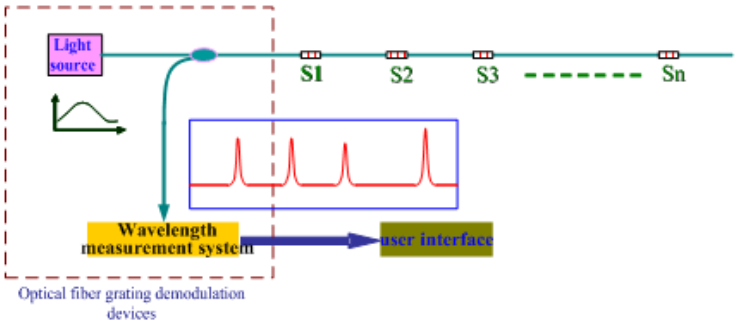

Fig. 1. Principle of optical fiber grating

The reflection wavelength of optical fiber grating change with external temperature and strain, which has a good linearity and sensitivity (temperature for $10.3pm/oC$ and strain for $1.2pm/\mu\epsilon$) [18]. Other physical quantities such as pressure, acceleration, displacement, height of water, etc. can be obtained by measuring strain conversion.

3 Components of Bridge Health Monitoring System

Bridge health monitoring system is an integrated monitoring system based on bridge structure. Using modern sensor technology, communication networks and

computer technology, it combines various functional subsystems, including optimum combination monitoring, environmental monitoring, traffic monitoring, device monitoring, integrated alarm, and network analysis of information [20]. As shown in Figure 2, the system consists of sensor module, data acquisition and processing module, data management module and the status evaluation module. Fiber optic is used to implement Bi-directional data communications between modules and ensure them to collect data over long distance transmission without being interrupted.

3.1 Sensor Module

Sensor module monitors environment changes (e.g. wind, wave and ice, vehicle load), local variables (e.g. stress, deformation, cracks, fatigue damage, reaction, etc.), and global variables (e.g. dynamic characteristics and state response) [19]. To form a sensor network, specific sensors must be arranged to monitor different data so as to maximum reduce monitoring points to capacity and the cost of inputs.

3.2 Data Collecting and Processing Module

Data collection of bridge health monitoring mainly consists of developing signal conversion interface and collection software for a variety of smart sensors [6]. The core issue of signal processing is how to extract structural damage characteristic information, and how to fully use modern signal processing methods, such as higher order spectral analysis, frequency analysis, wavelet analysis, and neural network. This module intelligently processes information of sensor transmission and characterizes structural characteristics of bridge injuries through data fusion theories to improve safety evaluation and damage assessment of bridge structure.

3.3 Data Management Module

Data management module is used to implement data fusion/integration after processing and storing bridge health monitoring data collected from each sensor, and then sends analytical reports, graphics etc., to administrator. At this moment, data storage is centralized with conventional relational databases. Data query and update is performed with standard SQL.

3.4 State Evaluation Module

The state evaluation module mainly includes damage identification, positioning, model modification, safety assessment and early warning function.

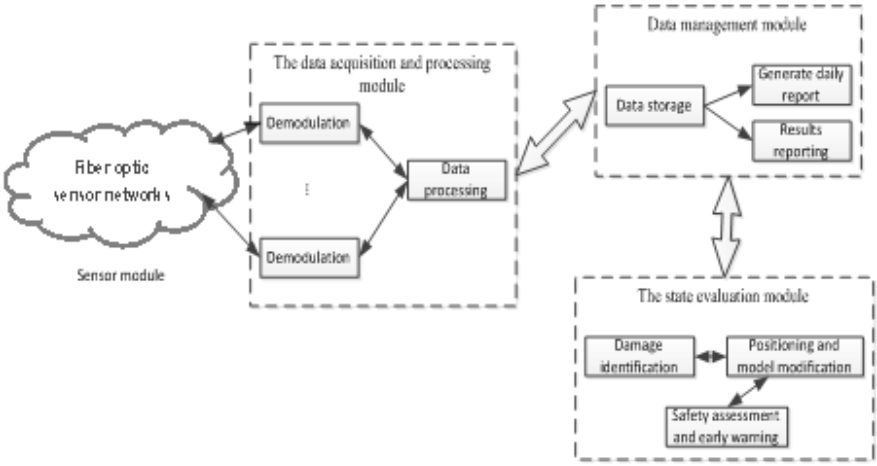

Fig. 2. Main composing modules of the bridge health monitoring system

4 IoT-Based Bridge Health Monitoring System

Tong-Yu River Bridge, which locates on the Century Avenue of Yan-Cheng City, Jiang Su Province, China, is a typical steel-concrete arch bridge. It is the largest bridge in Yan-Cheng City with a total investment of 500 million CNY. This bridge significantly improved the urban road network. The total length of the bridge is approximately 2.5 km, with 2 segments (712 meters each) and 215 meters of main bridge. Main Bridge uses steel arch concrete substructure at the lower part of bored piles. Superstructure of the approach bridges uses 30 meters box girder, their lower part are based on bored piles and column piers. Since the bridge arch consists of the live load distribution components, transmission components and load-bearing components, it is structurally more complicate. As the main load-bearing component, ribs bear the most pressure, deck, beams, stringers and other live load distribution components directly bear the traffic load. And finally, booms pass the deck load, beam weight, traffic load to the arch ribs. In practical engineering applications, due to construction, operation, maintenance and many other reasons, security problem of the bridge arch is particularly prominent. Therefore, it is very important to apply bridge health monitoring system on Tong-Yu River Bridge, to monitor its safety condition.

4.1 Design Consideration

By consulting local authorities and bridge engineering companies, we have elicited the following design considerations and requirements:

– According to the requirements of structural health and safety assessment, construction scale, budge, and geographic climate environment, a system with reliable, economic and reasonable performance should be designed to

provide a basis for curing and managing a bridge. Power consumption should be minimized and requirements for maintenance should be kept to minimum.
- The system should adopt modular design allowing easy extension. The overall design should be optimized to ensure that the system can be easily deployed while faulty components can be replaced easily with low equipment and labor costs.
- System design should be open to ensure straightforward system upgrading, remote data sharing and monitoring capabilities [21].
- The number of sensors and equipment capacity should be with moderate redundancy, balancing between system reliability and failure tolerance on the one hand and overhead and maintenance cost on the other hand. Also, the system should present enough capacity for future system improvements, expansion, and raise the requirement.
- Integrated approach of real-time monitoring and manual inspection are applied to give a comprehensive assessment of the status of the structure based on results of the two aspects. Switching entirely to IoT-based remote monitoring system is not realistic due to non-technical concerns. Manual inspection, there-fore, still plays an important rule and its results can be utilized to cross-check the outcomes of IoT-based system.
- A large quantity of data is to be collected, transported and stored by the system. The system, therefore, should be optimized to handle such data. Techniques such as data pretreatment, data filtering, data compression, and post-processing function can help to effectively dispose, analyze and manage these data. As Big Data processing is beyond the scope of this paper, existing data management algorithms will be adopted.

4.2 Selection of Bridge Monitoring Parameters

In the case of the fixed host, factors of arch bridge health status include the lines of Rib, the main beam and cable, cross-section stress (strain), cable tension and temperature, etc. Bridge health monitoring parameters are as listed in Table 1. Different sensors were used to monitor and beam different optical or electrical signal for data acquisition module processing.

Table 1. Bridge Monitoring Parameters

Parameter	Equipment
Deformation Monitoring	Leica Whole Station
Cable Force Monitoring	Acceleration Sensor
Stress Monitoring	Fiber Grating Thermometer
Temperature Monitoring	Fiber Grating Thermometer

Deformation monitoring includes the deformation of the arch ribs, arch seats shift, and the main beam distortion. Bridge arch rib is the main load-bearing component of the arch and is a key link in the load transfer path. Thrust under skewback foot arch bridge can have some arch displacement and potentially a very negative impact on the stress level of the entire bridge. Main beam deflection under traffic load and skewback uneven subsidence can produce changes that affect the structural safety. The deformation monitoring, therefore, provides a series of critical health information about a bridge. The boom in an arch bridge is an important power transmission component and can be easily damaged in the structure [7]. Therefore, it is also a vital indicator that gives hint of the health status of a bridge. In our prototypical system, such data are collected.

The destruction of the key components will affect the full-bridge force, and even cause overall damage. The strain is a direct indicator of response of the local component performance. Stress monitoring includes Rib stress and the main beam stress monitoring.

The temperature and temperature changes of the main bridge components serve as evidence of, and in many cases fine-grained adjustment to, the structural analysis results based on the load and deformation. Such values help to establish correlations between observations. In our prototypical system, temperature monitoring includes arch ribs and the main beam structure.

Structure Displacement Monitoring. Tong-Yu River Bridge is a three-span concrete-filled steel tubular arch bridge. The arch bridge girder bears the traffic load directly, while the traffic loads on the main girder and the weight of itself is transferred to the arch rib, then through the arch rib the load and its weight is transferred to abutment, eventually, abutment will transfer the loads to the foundation. It can be concluded that the main girder, boom, arch ring and abutment are the structural elements of an arch bridge according to transfer path of the load.

In such a complex system of large space structures, the deformation of structure is a comprehensive reflection of the variety of loads and structural performances. Taking into account the high cost of GPS sensor, the skewback is not suitable equipped with GPS. Instead, we use Total Station Technology to monitor the deflection of the main beam, arch rib deformation and arch seat. Although constrained by weather conditions, it is enough to meet the monitoring requirements.

When monitoring structural displacement, Total Station Technology only needs to be installed on the structure detection points with reflectors. It scans positions of the reflectors, and records three-dimensional coordinates of the center of their prisms, all of which can be finished automatically by the airborne program-driven total station motor. The advantage of this method is that as long as the conditions are met, three-dimensional coordinates of a total station can measure anywhere needed.

Total station is the center of the structural deflection monitoring subsystem, which finish the dual task of measurement and communication. For measurement, the total station's airborne program drive motor scans objects being

monitored, automatically identifies prisms laid in the monitored objects, and then measures and records their three-dimensional coordinates. In communication task, detection data can be sent to data sever or central station by wireless, then be pushed to monitoring system and analysis system.

Suspender Force Monitoring. Dead load and live load of the deck system are delivered to the arch ribs by the booms, which is an important power transmission component in arch bridge [4]. By monitoring key suspender force, the results of the state of booms can be monitored and the result of the ribs and main beam deformation can be analyzed. Accordingly, security situation of the whole bridge can be assessed. Suspender force monitoring is completed with acceleration sensors. By measuring the vibration frequency of the shortest boom and longest boom, cable force can be projected. In order to reduce the impact of the steel protective cover to the measurement, the protective cover on the ground can be fixed as appropriate, or even removed in order to avoid collision effects on the boom vibration.

The methods commonly used to measure the cable force including the (hydraulic) pressure gauge measurement method, pressure sensor (pressure ring) measurement method, the vibration frequency method and the flux method. As Tong-Yu River Bridge has been put into operation, the former two methods are not suitable for application. Vibration frequency method uses precision acceleration sensors to pick up the vibration signal stimulated in the environmental vibration. When analyzing the cable force, the natural vibration frequency should be determined by the spectrum diagram firstly, then determine cable force according to the relationship between the natural vibration frequency and cable force. As the method is simple and feasible, and the precision can meet the engineering requirements, this method is widely used in monitoring bridge health in domestic and other countries. However, there exist several difficulties when using frequency method in Tong-Yu River Bridge. First of all, the boom is constraint by uncertain elements caused by the metal protective sleeve, so the relationship between the natural vibration frequency and the cable force remains to be determined. Magnetic flux method uses a kind of small electromagnetic sensor to measure the change of magnetic flux, then according to cable force, temperature and flux change to predict the cable force. The application of this relatively novel technology cannot match up with the vibration frequency method. Ideally, flux sensor should be set to the inhaul cable before installing the anchor in the producing process, and calibrating super tensioning process one by one before they leave the factory. Using magnetic bomb instrument to measure the data during the tensioning construction, in order to check zero point of the sensor and maintain the continuity of data. The requirements and cost of the magnetic flux method is much high than that of vibration frequency method.

From the view of budget, the vibration frequency method is appropriate to predict the cable force, that is, through the acceleration sensor to measure the vibration frequency of the shortest and the longest booms.

Structural Stress/Temperature Monitoring. The internal force and stress of structure is a reflection of the components force characteristics and a direct indicator of safety condition. Therefore, it is necessary to monitor the strain of the key sections of main beam and arch ribs [11]. The measured result of strain needs to be modified according to temperature. Meantime, temperature load is also an important consideration in structure design. Therefore, Tong-Yu River Bridge Health Monitoring System also needs to monitor the temperature. The system uses fiber Bragg grating strain sensors and fiber Bragg grating temperature sensors to monitor the strain and temperature of the key sections of the arch ribs and the main beam respectively.

For the purpose of cost-saving, the system focuses on monitoring the inside of the two arch ribs, taking into account the lateral arch ribs. Sensor layout cross-section is selected in the mid-span deck section, the cross-beam cross-section, the dome section of the arch rib, 1/4 cross-section and both sides of the arch of the foot section. The deployment diagram of some sensors is illustrated in Figure 3.

4.3 System Architecture

Integrating total station instrument technology, acceleration sensor technology and fiber grating technology, Bridge Health Monitoring System monitors bridge structure deformation, relative displacement of arch foot level, skewback uneven settlement, suspender force, ribs and main beam distortion, temperature and strain in real time and online. Meanwhile, the system will work cooperatively with regular detection systems, bridge design and load test database, and other related information. The system could also gain access to bridge design and load test data, to form comprehensive electronic management for decision making of bridge management and conservation. The overall system architecture is shown in Figure 4.

5 System Implementation

As a bridge health monitoring and information exchange/management platform, application system must meet availability, practicality and reliability [12]. This system also presents good extensibility: new modules can be easily added with existing module easily upgraded through well-defined interfaces. This allows the system to be adapted as generic application platform for electronic infrastructure management. Information system can be managed and maintained validly.

The system is implemented following a client-server pattern with a thin browser-based client. It is easy to use, cost-effective and with high interoperability. The system user interface is presented in Figure 5. The landing page of the system illustrates the current status of the monitored bridge. Vital information and locations of sensors are highlighted on a 2D wireframe model of the bridge. On the right hand side of the user interface, structural evaluation outcomes and potential risks are listed in a tabular view for easy access.

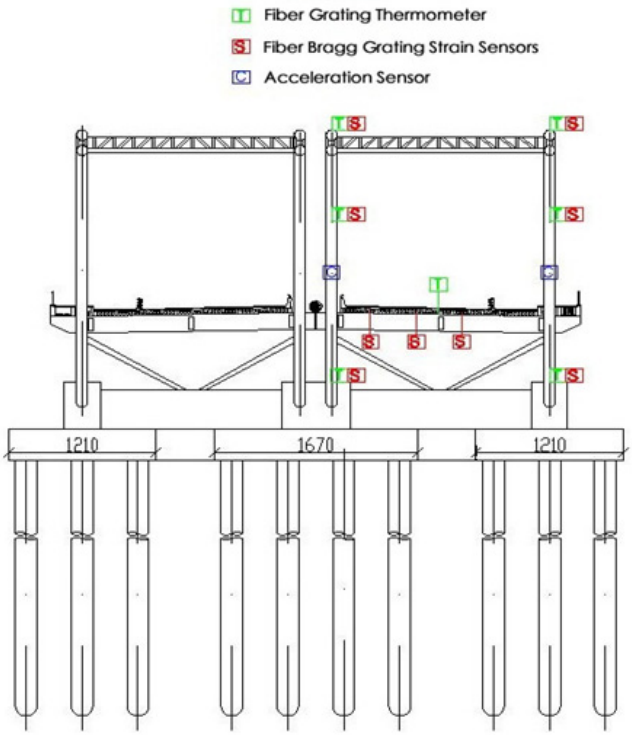

Fig. 3. Position schematic diagram of the temperature and strain measuring point

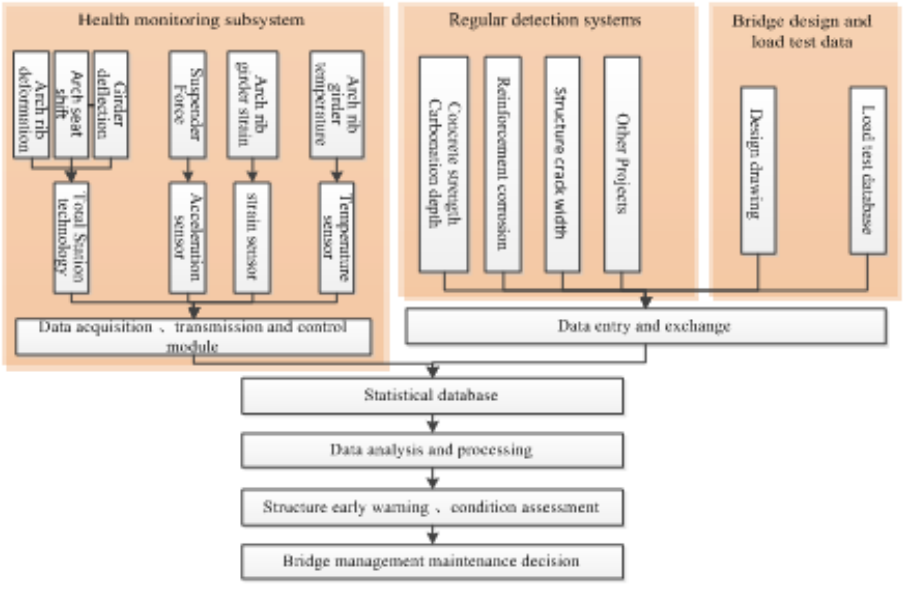

Fig. 4. The overall system architecture of the bridge monitoring system

Fig. 5. Operation interface of the system

For instance, the second row of the upper table documented a warning on 6 September 2010. The bottom table presents current and historical evaluation outcomes with a score indicating the overall status of the bridge.

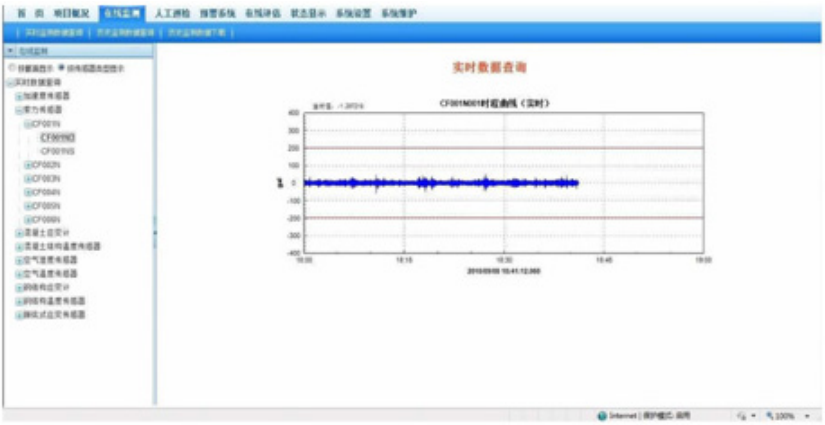

Fig. 6. User interface for bridge monitoring data analysis

Data can be queried from online monitoring in real-time and displayed on axis. Users can then drill down into particular parameters or roll-up to obtain an overall picture of the bridge. The online data management system also maintains details records of historical data for comparison and analysis. The visual monitoring chart is depicted in Figure 6.

6 Conclusions and Future Work

IoT presents a whole raft of technologies that connect objects and data consumers (being humans and services) together to form a network. IoT has gained

increasing popularity in a wide variety of domains, facilitating seamless interaction between humans and the surrounding environment. In recent years, IoT technologies have been applied to infrastructure health monitoring to perform structural data collection and interpretation in a continuous and real-time manner. In this paper, we focus on bridge health monitoring, which brings new vitality to bridge health monitoring and safety evaluation [2]. Our IoT-based bridge monitoring system exercises a modular system architecture that integrates fiber grating sensing technology and accelerometer technology. Through communication facilitated by optical fiber sensor module, data acquisition and processing module, data management module and status evaluation module, the system achieves a long-term health monitoring for bridges. We evaluated the prototypical system on a very busy bridge, the Tong-Yu River Bridge of Yan-Cheng City, using selective bridge monitoring parameters that most suit our purposes.

After carefully studying similar development from the community and comparing various monitoring techniques, our system gives high priority to the following data:

1. the bridge structure deformation,
2. relative displacement of arch foot horizon,
3. skewback uneven settlement,
4. suspender force, ribs, and main beam distortion, and
5. temperature and strains in real time

They are collected online through total station instrument technology, acceleration sensor technology, and fiber grating technology. Even though, our system presented a promising direction, at this stage we acknowledge the complexity and overhead of large scale roll-out of IoT-based infrastructure monitoring system and a lack of unreserved support and trust from infrastructure engineers, should manual and in person data collection be entirely replaced by sensing technology. It is, therefore, our contentions that the proposed remote monitoring system works best in collaboration with conventional detection approaches and methods, to complement the latter for well-grounded and well-informed decision making. Moreover, data collected through multiple sensors can also assist in bridge design and enrich load test databases. In longer term, such information provides comprehensive electronic infrastructure data for decision-making of bridge management and conservation.

The crux of our future work main lies in extended system evaluation and robustness test with an emphasis on both the sensors and the underlying decision making algorithms. For this we collaborate closely with the local authorities and bridge design, survey, and construction companies. Outcomes and feedback will be used to improve our system.

Acknowledgements. The open research project was supported by the Fundamental Research Funds for the Central Universities (Grant No. 2011-1V-084) of People's Republic of China.

References

1. Atzori, L., Iera, A., Morabito, G.: The internet of things: A survey. The Intl. J. of Computer and Telecommunications Networking 54(15), 2787–2805 (2010)
2. Bi, W., Lang, L.: An overview on fiber optic sensing technology in bridge security detection. Sensor World 06, 1–5 (2002)
3. Brownjohn, J., Magalhaes, F., Caetano, E., Cunha, A.: Ambient vibration retesting and operational modal analysis of the humber bridge. Engineering Structures 32(8), 2003–2018 (2010)
4. Chen, H., Huang, F.: The dynamometric and application of optical fiber grating. Journal of Huazhong University of Science and Technology 33(5), 58–60 (2005) (Chinese)
5. Chen, S.: The research of bridge real-time monitoring system based on the optical fiber sensing network. Highway Traffic Technology 11, 37–39 (2010)
6. Gao, Z.: Research on intelligent information acquiring and processing of health monitoring for great structure. Tech. rep., Beijing Jiaotong University (2010)
7. González, I.: Study and Application of Modern Bridge Monitoring Techniques. Ph.D. thesis, KTH (2011)
8. Kim, S., Pakzad, S., Culler, D., Demmel, J., Fenves, G., Glaser, S., Turon, M.: Health monitoring of civil infrastructures using wireless sensor networks. In: Proceedings of the 6th International Conference on Information Processing in Sensor Networks, IPSN 2007, pp. 254–263. ACM, New York (2007), http://doi.acm.org/10.1145/1236360.1236395
9. Koh, H.M., Park, W., Choo, J.F.: Achievements and challenges in bridge health monitoring systems and intelligent infrastructures in Korea. In: Proceedings of 4th Intl. Conf. on Structural Health Monitoring of Intelligent Infrastructure, pp. 1–14 (2009)
10. Koo, K.Y., Brownjohn, J.M.W., List, D.I., Cole, R.: Structural health monitoring of the tamar suspension bridge. In: Structural Control and Health Monitoring, pp. n/a–n/a (2012), http://dx.doi.org/10.1002/stc.1481
11. Fuhr, P.L., et al.: Fiber Optic sensing of a bridge in waterbury, vermont. Journal of Intelligent Material Systems and Structures 10(4), 293–303 (1999)
12. Li, H., Zhou, W., Ou, J.: The research of the integration technology for large bridge structure health monitoring intelligent system. Civil Engineering Journal 39(2), 46–52 (2006) (Chinese)
13. Li, S.: Study on remote monitoring information system based on optic fiber sensing for the tension of bridge. Tech. rep., Wuhan University of Technology (2006)
14. Liu, J.: Study on integration and design for bridge long-term health monitoring system. Tech. rep., Wuhan University of Technology (2010)
15. Liu, J., Tong, X., Liang, L.: The research of a high performance and long-term health bridge monitoring and integration system. Wuhan University of Technology Journal 31(23), 52–56 (2009)
16. Liu, S., Wei, J., Qian, Y.: The analysis of the application of optical fiber sensor in bridge monitoring. Journal of Chongqing Jiaotong University 24(3), 4–7 (2005)
17. Sha, Z.: The principle and application of Intelligent integrated temperature sensor. Press of Mechanical Industry (2002)
18. Yao, J., Jiang, D., Wei, H.: The research of optical fiber grating displacement sensor technology. Wuhan University of Technology Journal (Information and Management Engineering Edition) 28(7), 98–100 (2006)

19. Zan, Y., Xiang, S., Fang, Z.: The applications of optical fiber grating sensor. Physical 33(01), 58–61 (2004)
20. Zhao, W.: The problems in bridge health monitoring system. World Bridge 04, 75–77 (2008)
21. Zhuang, J., Zhuang, W.: The integration and modular technology of a car system. Press of Mechanical Industry (2003)
22. Zu, Q.: Logistics information system. Tech. rep., Wuhan University Press (2011)

Author Index

Alkadhimi, Khalil 405

Bachler, Martin 1
Bai, Shuotian 16
Bai, Xue 28
Bąk, Sławomir 35
Balaban, M. Erdal 57
Ben, Fei 231
Berrahal, Sarra 82
Bo, Li 439
Boudriga, Nourreddine 82
Breitwieser, Christian 50
Brunner, Clemens 50

Cai, Yun 769
Catak, F. Ozgur 57
Çelik, Duygu 165
Chai, Hualei 69
Chammem, Mhammed 82
Chen, Cheng 97, 339
Chen, Dingfang 122, 274, 332, 439, 529, 711, 719
Chen, Guohua 97, 108
Chen, Jing 848
Chen, Junren 318
Chen, Peiwen 246
Chen, Tianpei 122
Chen, Zhaocan 137
Cheng, Fuxing 150, 592
Cheng, Gang 477
Cui, LinShan 617
Cui, Shulin 339
Cui, Yu 447
Czarnecki, Radosław 35

Deniziak, Stanisław 35
Ding, Shijin 108
Dong, Fang 513
Dong, Hao 282
Dong, Mingwang 711

E, Haihong 180, 400, 788
Elçi, Atilla 165

Fan, Wei 426
Feng, Huiling 814
Fu, Xiufen 246
Fu, Yu 318

Gao, Qiang 647
Ge, CuiCui 246
Gong, Bin 396, 556
Gong, Qiyuan 194
Gu, Ning 137
Guan, Zengda 209
Guo, Wengeng 719

Hametner, Bernhard 1
Han, Jing 400, 788
He, Ben 150
He, Chaobo 108
He, Jian 216
Holzinger, Andreas 1, 50
Hou, Wenjun 447, 830
Hou, Yinghong 891
Hsieh, Jui-Chien 843
Hu, Bin 848
Hu, Cheng 231
Hu, Chengyu 743
Hu, Jiquan 332
Huang, Huawei 743
Huang, Shang 246
Huang, Shiyao 461
Huo, Yingxiang 461

Jang, Hana 259
Jang, Soonho 259
Jeong, Jongpil 259
Jiang, Guoqian 586
Jiang, Wenbin 282
Jin, Hai 282, 411, 631, 757
Jin, Jie 389
Jin, Xiaojia 180, 400

Li, Chao 814
Li, Cong 562
Li, Guojin 274
Li, Huiqin 297
Li, Jia 274, 719

Li, Jin 862
Li, Jingwen 302, 318
Li, Qiong 647
Li, Shaozi 843
Li, Song 396, 556
Li, Taotao 332, 711
Li, Wang 274
Li, Xu 339
Li, Yongzhi 122
Liang, Qingzhong 743
Liang, Yanyan 302
Liao, Xiaofei 282
Lindstaedt, Stefanie 50
Liu, Baolin 862
Liu, Baoling 575
Liu, Chang 728
Liu, Jin 495
Liu, Lihua 606
Liu, Tianjiao 339
Liu, Tiejiang 137
Liu, Xiyu 28, 350, 454, 689, 801, 869, 883
Liu, Ying 339
Liu, Yuenan 814
Long, Pengfei 332
Lu, Guangzhen 617
Lu, Hongliang 364
Lu, Jian 372
Lu, Pei 891
Lu, Tun 137
Lu, Xianqi 297
Lu, Yanling 318
Lu, Yongqiang 891
Luo, Junzhou 194, 426, 513
Luo, Tiejian 150, 592
Luo, Xiangyu 562
Luo, Yingwei 541

Ma, Jun 372
Mao, Chengjie 97
Mao, Xiangfang 389
Mayer, Christopher 1
Meng, Zibo 606
Mo, Yuchang 426
Moore, Philip 848
Müller-Putz, Gernot R. 50

Ning, Yue 16
Niu, Jiarui 396
Niu, Xiaoqing 400

Peng, Manman 891

Qiang, Gao 482
Qu, Jianhua 883

Ren, Kaijun 728
Ren, Xiaoling 28
Ren, Xiaotao 297
Ren, Zhijun 775

Shbib, Reda 405
Shi, Xuanhua 411
Song, Aibo 426, 513
Song, Junde 672, 775
Song, Mei 477, 575, 659, 862
Song, Meina 180, 672, 788
Su, Yangyang 439
Sun, Guichuan 447
Sun, Jie 454
Sun, Yong 617

Tan, Wenan 617
Tang, Anqiong 617
Tang, Feiyi 108
Tang, Yong 97, 108
Tao, Xianping 372
Teng, Luyao 461
Teng, Shaohua 246, 461
Teng, Yinglei 477, 575, 659, 862
Terbu, Oliver 50
Tong, Junjie 180

Urquizo Medina, Aida Nathalie 482

Wan, Jizheng 302, 318
Wang, Guowei 297
Wang, Li 606
Wang, Liangyin 495
Wang, Qianping 495
Wang, Qing 606
Wang, Wei 426, 513
Wang, Wenjie 150
Wang, Xiang 592
Wang, Xiangqing 529
Wang, Xiaodong 364
Wang, Xiaolin 541
Wang, Yan 556
Wang, Yanlong 801
Wang, Yong-qiang 876
Wang, Yongqiang 697
Wang, Yun 231, 562
Wang, Zhen 575, 862

Wang, Zhengguo 586
Wang, Zhu 592
Wassertheurer, Siegfried 1
Wei, Yifei 659
Wen, Hou 274
Wen, Zhigang 606
Wu, Buwen 631
Wu, Gang 69
Wu, Qiang 891
Wu, Song 411

Xia, Xiao 364
Xiang, Laisheng 350
Xiao, Hanbin 586
Xiao, Weijie 647
Xiao, Yanan 477
Xie, Bo 411
Xing, Chunxiao 814
Xing, Yuhong 653
Xu, Haoman 659
Xu, Hui 282
Xu, Ke 672
Xu, Xiang 495
Xu, Xingyu 904
Xu, Yanxiang 592
Xue, Jie 689
Xue, Sixin 814

Yan, Xuesong 743
Yang, Jinsheng 389
Yang, Li-you 876
Yang, Liyou 697
Yang, Ming 194
Yang, Xuejin 711
Yang, Yanfang 274, 719
Yang, Zhengwen 891
Yang, Zhimin 728
Yao, Hong 743
Yu, Chen 757
Yu, Fan 216
Yu, Meng 769
Yu, Xiaolin 350
Yu, Yanhua 775
Yuan, Feifei 562
Yuan, Pingpeng 631
Yuan, Sha 16
Yue, Wenjun 788

Zang, Wenke 801
Zhan, Xiaosu 400
Zhang, Binbin 541
Zhang, Guigang 814
Zhang, Hui 672
Zhang, Jing 830
Zhang, Jinghua 332
Zhang, Lichao 843
Zhang, Longbo 757
Zhang, Wei 461
Zhang, Xiaowei 848
Zhang, Xin 150, 592
Zhang, Xue-yan 876
Zhang, Yong 477, 575, 659, 814, 862
Zhang, Zhengyan 122, 332
Zhao, Hong-Chao 869
Zhao, Hong-yu 876
Zhao, Hongyu 697
Zhao, Xinxue 647
Zhao, Yuan 69
Zhao, Yuzhen 883
Zhao, Zhangye 769
Zheng, Jinjia 97
Zheng, Tao 372
Zhou, Lin 848
Zhou, Shikun 405
Zhou, Wenan 297
Zhu, Hongqing 411
Zhu, Tingshao 16, 209
Zhu, Xianzhong 180
Zou, Junwei 606
Zu, QiaoHong 529, 904